

# Next-Generation Wireless Networks (NGWN) for Autonomous Intelligent Communications

Lead Guest Editor: Shalli Rani

Guest Editors: Ali Kashif Bashir and Vinayakumar Ravi





---

**Next-Generation Wireless Networks (NGWN)  
for Autonomous Intelligent Communications**

Wireless Communications and Mobile Computing

---

**Next-Generation Wireless Networks  
(NGWN) for Autonomous Intelligent  
Communications**

Lead Guest Editor: Shalli Rani

Guest Editors: Ali Kashif Bashir and Vinayakumar  
Ravi





Copyright © 2023 Hindawi Limited. All rights reserved.

This is a special issue published in “Wireless Communications and Mobile Computing.” All articles are open access articles distributed under the Creative Commons Attribution License, which permits unrestricted use, distribution, and reproduction in any medium, provided the original work is properly cited.

# Chief Editor






















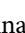

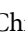


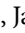





Zhipeng Cai , USA

## Associate Editors

Ke Guan , China  
Jaime Lloret , Spain  
Maode Ma , Singapore

## Academic Editors

Muhammad Inam Abbasi, Malaysia  
Ghufran Ahmed , Pakistan  
Hamza Mohammed Ridha Al-Khafaji ,  
Iraq  
Abdullah Alamoodi , Malaysia  
Marica Amadeo, Italy  
Sandhya Aneja, USA  
Mohd Dilshad Ansari, India  
Eva Antonino-Daviu , Spain  
Mehmet Emin Aydin, United Kingdom  
Parameshchhari B. D. , India  
Kalapaveen Bagadi , India  
Ashish Bagwari , India  
Dr. Abdul Basit , Pakistan  
Alessandro Bazzi , Italy  
Zdenek Becvar , Czech Republic  
Nabil Benamar , Morocco  
Olivier Berder, France  
Petros S. Bithas, Greece  
Dario Bruneo , Italy  
Jun Cai, Canada  
Xuesong Cai, Denmark  
Gerardo Canfora , Italy  
Rolando Carrasco, United Kingdom  
Vicente Casares-Giner , Spain  
Brijesh Chaurasia, India  
Lin Chen , France  
Xianfu Chen , Finland  
Hui Cheng , United Kingdom  
Hsin-Hung Cho, Taiwan  
Ernestina Cianca , Italy  
Marta Cimitile , Italy  
Riccardo Colella , Italy  
Mario Collotta , Italy  
Massimo Condoluci , Sweden  
Antonino Crivello , Italy  
Antonio De Domenico , France  
Floriano De Rango , Italy

Antonio De la Oliva , Spain  
Margot Deruyck, Belgium  
Liang Dong , USA  
Praveen Kumar Donta, Austria  
Zhuojun Duan, USA  
Mohammed El-Hajjar , United Kingdom  
Oscar Esparza , Spain  
Maria Fazio , Italy  
Mauro Femminella , Italy  
Manuel Fernandez-Veiga , Spain  
Gianluigi Ferrari , Italy  
Luca Foschini , Italy  
Alexandros G. Fragkiadakis , Greece  
Ivan Ganchev , Bulgaria  
Óscar García, Spain  
Manuel García Sánchez , Spain  
L. J. García Villalba , Spain  
Miguel Garcia-Pineda , Spain  
Piedad Garrido , Spain  
Michele Girolami, Italy  
Mariusz Glabowski , Poland  
Carles Gomez , Spain  
Antonio Guerrieri , Italy  
Barbara Guidi , Italy  
Rami Hamdi, Qatar  
Tao Han, USA  
Sherief Hashima , Egypt  
Mahmoud Hassaballah , Egypt  
Yejun He , China  
Yixin He, China  
Andrej Hrovat , Slovenia  
Chunqiang Hu , China  
Xuexian Hu , China  
Zhenghua Huang , China  
Xiaohong Jiang , Japan  
Vicente Julian , Spain  
Rajesh Kaluri , India  
Dimitrios Katsaros, Greece  
Muhammad Asghar Khan, Pakistan  
Rahim Khan , Pakistan  
Ahmed Khattab, Egypt  
Hasan Ali Khattak, Pakistan  
Mario Kolberg , United Kingdom  
Meet Kumari, India  
Wen-Cheng Lai , Taiwan

Jose M. Lanza-Gutierrez, Spain  
Pavlos I. Lazaridis , United Kingdom  
Kim-Hung Le , Vietnam  
Tuan Anh Le , United Kingdom  
Xianfu Lei, China  
Jianfeng Li , China  
Xiangxue Li , China  
Yaguang Lin , China  
Zhi Lin , China  
Liu Liu , China  
Mingqian Liu , China  
Zhi Liu, Japan  
Miguel López-Benítez , United Kingdom  
Chuanwen Luo , China  
Lu Lv, China  
Basem M. ElHalawany , Egypt  
Imadeldin Mahgoub , USA  
Rajesh Manoharan , India  
Davide Mattera , Italy  
Michael McGuire , Canada  
Weizhi Meng , Denmark  
Klaus Moessner , United Kingdom  
Simone Morosi , Italy  
Amrit Mukherjee, Czech Republic  
Shahid Mumtaz , Portugal  
Giovanni Nardini , Italy  
Tuan M. Nguyen , Vietnam  
Petros Nicolitidis , Greece  
Rajendran Parthiban , Malaysia  
Giovanni Pau , Italy  
Matteo Petracca , Italy  
Marco Picone , Italy  
Daniele Pinchera , Italy  
Giuseppe Piro , Italy  
Javier Prieto , Spain  
Umair Rafique, Finland  
Maheswar Rajagopal , India  
Sujan Rajbhandari , United Kingdom  
Rajib Rana, Australia  
Luca Reggiani , Italy  
Daniel G. Reina , Spain  
Bo Rong , Canada  
Mangal Sain , Republic of Korea  
Praneet Saurabh , India

Hans Schotten, Germany  
Patrick Seeling , USA  
Muhammad Shafiq , China  
Zaffar Ahmed Shaikh , Pakistan  
Vishal Sharma , United Kingdom  
Kaize Shi , Australia  
Chakchai So-In, Thailand  
Enrique Stevens-Navarro , Mexico  
Sangeetha Subbaraj , India  
Tien-Wen Sung, Taiwan  
Suhua Tang , Japan  
Pan Tang , China  
Pierre-Martin Tardif , Canada  
Sreenath Reddy Thummaluru, India  
Tran Trung Duy , Vietnam  
Fan-Hsun Tseng, Taiwan  
S Velliangiri , India  
Quoc-Tuan Vien , United Kingdom  
Enrico M. Vitucci , Italy  
Shaohua Wan , China  
Dawei Wang, China  
Huaqun Wang , China  
Pengfei Wang , China  
Dapeng Wu , China  
Huaming Wu , China  
Ding Xu , China  
YAN YAO , China  
Jie Yang, USA  
Long Yang , China  
Qiang Ye , Canada  
Changyan Yi , China  
Ya-Ju Yu , Taiwan  
Marat V. Yuldashev , Finland  
Sherali Zeadally, USA  
Hong-Hai Zhang, USA  
Jiliang Zhang, China  
Lei Zhang, Spain  
Wence Zhang , China  
Yushu Zhang, China  
Kechen Zheng, China  
Fuhui Zhou , USA  
Meiling Zhu, United Kingdom  
Zhengyu Zhu , China

# Contents

---

**Retracted: An Automatic Driving Control Method Based on Deep Deterministic Policy Gradient**  
Wireless Communications and Mobile Computing  
Retraction (1 page), Article ID 9896258, Volume 2023 (2023)

**Retracted: A Survey on Location Privacy Attacks and Prevention Deployed with IoT in Vehicular Networks**  
Wireless Communications and Mobile Computing  
Retraction (1 page), Article ID 9878739, Volume 2023 (2023)

**Retracted: Three-Dimensional DV-Hop Localization Algorithm Based on Hop Size Correction and Improved Sparrow Search**  
Wireless Communications and Mobile Computing  
Retraction (1 page), Article ID 9867609, Volume 2023 (2023)

**Retracted: A Novel Strategy for Waste Prediction Using Machine Learning Algorithm with IoT Based Intelligent Waste Management System**  
Wireless Communications and Mobile Computing  
Retraction (1 page), Article ID 9842608, Volume 2023 (2023)

**Retracted: An Improved Orbit Model of Space Target Radar Based on Least Square Method and Its Program Implementation**  
Wireless Communications and Mobile Computing  
Retraction (1 page), Article ID 9838626, Volume 2023 (2023)

**Retracted: Sidelobe Reduction in NC-OFDM-Based CRNs Using Differential Evolution-Assisted Generalized Sidelobe Canceller**  
Wireless Communications and Mobile Computing  
Retraction (1 page), Article ID 9814786, Volume 2023 (2023)

**Retracted: Federated Deep Learning Approaches for the Privacy and Security of IoT Systems**  
Wireless Communications and Mobile Computing  
Retraction (1 page), Article ID 9869724, Volume 2023 (2023)

**Retracted: Research on the Coupling and Coordinated Development of Sports Tourism and Cultural Industry under the Background of Artificial Intelligence Era**  
Wireless Communications and Mobile Computing  
Retraction (1 page), Article ID 9809025, Volume 2023 (2023)

**Retracted: Real Time Facial Expression Recognition for Online Lecture**  
Wireless Communications and Mobile Computing  
Retraction (1 page), Article ID 9806796, Volume 2023 (2023)

**Retracted: The Application of AI Technology in GPU Scheduling Algorithm Optimization**  
Wireless Communications and Mobile Computing  
Retraction (1 page), Article ID 9890625, Volume 2023 (2023)

**Retracted: A Novel Smart Healthcare Monitoring System Using Machine Learning and the Internet of Things**

Wireless Communications and Mobile Computing  
Retraction (1 page), Article ID 9850375, Volume 2023 (2023)

**Retracted: The Teaching Evaluation Index System and Intelligent Evaluation Methods of Vocational Undergraduate Pilot Colleges**

Wireless Communications and Mobile Computing  
Retraction (1 page), Article ID 9847372, Volume 2023 (2023)

**Retracted: Realization Path of the Social Development of Meteorological Services Based on Intelligent Data Analysis**

Wireless Communications and Mobile Computing  
Retraction (1 page), Article ID 9831460, Volume 2023 (2023)

**Retracted: Football Teaching Quality Evaluation and Promotion Strategy Based on Intelligent Algorithms in Higher Vocational Colleges**

Wireless Communications and Mobile Computing  
Retraction (1 page), Article ID 9824326, Volume 2023 (2023)

**Retracted: The Optimal Path of Cultivating and Promoting the Employment Ability of College Students Based on the Whole Process Management Mode of Construction Engineering Based on Computer Aided Technology**

Wireless Communications and Mobile Computing  
Retraction (1 page), Article ID 9812512, Volume 2023 (2023)

**Retracted: Applications of Big Data in Economic Information Analysis and Decision-Making under the Background of Wireless Communication Networks**

Wireless Communications and Mobile Computing  
Retraction (1 page), Article ID 9809037, Volume 2023 (2023)

**Retracted: Supply Chain Management System for Automobile Manufacturing Enterprises Based on SAP**

Wireless Communications and Mobile Computing  
Retraction (1 page), Article ID 9792161, Volume 2023 (2023)

**Retracted: Application Research of Time Delay System Control in Mobile Sensor Networks Based on Deep Reinforcement Learning**

Wireless Communications and Mobile Computing  
Retraction (1 page), Article ID 9785897, Volume 2023 (2023)

**Retracted: Construction of Innovation and Entrepreneurship Education Ecosystem in Higher Vocational Colleges from the Perspective of System Theory**

Wireless Communications and Mobile Computing  
Retraction (1 page), Article ID 9758107, Volume 2023 (2023)



# Contents

## **Retracted: Graph Convolutional Networks for Cross-Modal Information Retrieval**

Wireless Communications and Mobile Computing  
Retraction (1 page), Article ID 9891758, Volume 2023 (2023)

## **Retracted: Curriculum Design of College Students' English Critical Ability in the Internet Age**

Wireless Communications and Mobile Computing  
Retraction (1 page), Article ID 9851613, Volume 2023 (2023)

## **[Retracted] The Application of AI Technology in GPU Scheduling Algorithm Optimization**

Zhancai Yan , Yaqiu Liu , and Hongrun Shao  
Research Article (7 pages), Article ID 4713698, Volume 2022 (2022)

## **[Retracted] Three-Dimensional DV-Hop Localization Algorithm Based on Hop Size Correction and Improved Sparrow Search**

Pingzhang Gou , Zhaoyang Yu , Xinyue Hu , and Kai Miao   
Research Article (19 pages), Article ID 1540110, Volume 2022 (2022)


## **[Retracted] Realization Path of the Social Development of Meteorological Services Based on Intelligent Data Analysis**

Fang Guo , Yufang Feng, and Han Xiao  
Research Article (8 pages), Article ID 8904136, Volume 2022 (2022)

## **An Effective Path Planning of Intelligent Mobile Robot Using Improved Genetic Algorithm**

Zhongzhe Chen , Jianzhang Xiao, and Guifeng Wang  
Research Article (8 pages), Article ID 9590367, Volume 2022 (2022)


## **Research on Data Analysis of Digital Economic Management under the Background of Big Data**

Jie Huang   
Research Article (7 pages), Article ID 1156277, Volume 2022 (2022)


## **[Retracted] A Survey on Location Privacy Attacks and Prevention Deployed with IoT in Vehicular Networks**

Nadeem Ahmed , Zhongliang Deng, Imran Memon , Fayaz Hassan , Khalid H. Mohammadani ,  
and Rizwan Iqbal   
Review Article (15 pages), Article ID 6503299, Volume 2022 (2022)

## **[Retracted] Real Time Facial Expression Recognition for Online Lecture**

Haobang Wu   
Research Article (11 pages), Article ID 9684264, Volume 2022 (2022)


## **Optimal Recognition of Volleyball Player's Arm Movement Track Based on Embedded Microprocessor**

Ming Liu , Jingtao Wu, and Jiangang Tao  
Research Article (11 pages), Article ID 3525197, Volume 2022 (2022)






**[Retracted] Research on the Coupling and Coordinated Development of Sports Tourism and Cultural Industry under the Background of Artificial Intelligence Era**

Chao Hong, Jianmin Shi , Yan Xing, and Zejun Chang  
Research Article (6 pages), Article ID 3191655, Volume 2022 (2022)

**Course Certificate Integration Based on Wireless Communication ‘1 + X’ Intelligent Finance and Taxation**

Jing Li   
Research Article (13 pages), Article ID 2174082, Volume 2022 (2022)


**[Retracted] Sidelobe Reduction in NC-OFDM-Based CRNs Using Differential Evolution-Assisted Generalized Sidelobe Canceller**

Rashid Ahmed , Noor Gul , Saeed Ahmed, Muhammad Sajjad Khan , Su Min Kim , and Junsu Kim   
Research Article (11 pages), Article ID 9449400, Volume 2022 (2022)

**Intelligent Optimization Control Strategy for Secondary Pollution of Flue Gas in Municipal Solid Waste Incineration**

Yongsheng Ju   
Research Article (11 pages), Article ID 6125760, Volume 2022 (2022)

**Microgrid Data Security Sharing Method Based on Blockchain under Internet of Things Architecture**

Jian Shang , Runmin Guan, and Yuhao Tong  
Research Article (10 pages), Article ID 9623934, Volume 2022 (2022)







**[Retracted] Federated Deep Learning Approaches for the Privacy and Security of IoT Systems**

Malik Bader Alazzam , Fawaz Alassery , and Ahmed Almulih   
Research Article (7 pages), Article ID 1522179, Volume 2022 (2022)






**Deep Learning-Based Anomaly Traffic Detection Method in Cloud Computing Environment**

Junjie Cen  and Yongbo Li   
Research Article (8 pages), Article ID 6155925, Volume 2022 (2022)

**Behavior Dissection of NGWN Live Audio and Video Streaming Users with Enhanced and Efficient Modelling**


Asia Ali , Ihsan Ullah , Atiq Ahmed , Waheed Noor , Ahthasham Sajid , and Inam Ullah Khan   
Research Article (12 pages), Article ID 7564543, Volume 2022 (2022)

**Impact of Wireless Sensor Data Mining with Hybrid Deep Learning for Human Activity Recognition**

Rajit Nair , Mahmoud Ragab , Osama A. Mujallid, Khadijah Ahmad Mohammad , Romany F. Mansour , and G. K. Viju   
Research Article (8 pages), Article ID 9457536, Volume 2022 (2022)


# Contents

## **The Auxiliary Function of Intelligent Mobile Robot in the Standard Training of Children's Sports Movement**

Kai Liu  and Cheng Guo





Research Article (13 pages), Article ID 5157954, Volume 2022 (2022)

## **Application of Hybrid Teaching Mode in College Students' English Reading Using Intelligent Wireless Communication Multimedia**

Jiayun Yan 





Research Article (12 pages), Article ID 5828413, Volume 2022 (2022)

## **A Federated Deep Learning Empowered Resource Management Method to Optimize 5G and 6G Quality of Services (QoS)**

Hemaid Alsulami , Suhail H. Serbaya, Emad H. Abualsauod , Asem Majed Othman, Ali Rizwan , and Asadullah Jalali 


Research Article (9 pages), Article ID 1352985, Volume 2022 (2022)

## **Rating of Modern Color Image Cryptography: A Next-Generation Computing Perspective**

Muhammad Samiullah, Waqar Aslam , Muhammad Asghar Khan , Haya Mesfer Alshahrani, Hany Mahgoub, Ako Muhammad Abdullah , M. Ikram Ullah, and Chien-Ming Chen 




Review Article (20 pages), Article ID 7277992, Volume 2022 (2022)

## **[Retracted] Curriculum Design of College Students' English Critical Ability in the Internet Age**

Jie Shen, Yukun Chen, and Jiaxin Lin 


Research Article (7 pages), Article ID 5609450, Volume 2022 (2022)

## **[Retracted] Supply Chain Management System for Automobile Manufacturing Enterprises Based on SAP**

Pao-Ching Lin, Ming-Hung Shu , Bi-Min Hsu, Chien-Ming Hu , and Jui-Chan Huang 

Research Article (10 pages), Article ID 5901633, Volume 2022 (2022)

## **Optimization of Electric Automation Control Model Based on Artificial Intelligence Algorithm**

Run Ma , Shahab Wahhab Kareem , Ashima Kalra , Rumi Iqbal Doewes , Pankaj Kumar , and Shahajan Miah 

Research Article (9 pages), Article ID 7762493, Volume 2022 (2022)

## **[Retracted] Application Research of Time Delay System Control in Mobile Sensor Networks Based on Deep Reinforcement Learning**

Wenwu Zhu , Tanya Garg , Saleem Raza , Sachin Lalar , Dheer Dhvaj Barak , and Abdul Wahab Rahmani 






Research Article (7 pages), Article ID 7844719, Volume 2022 (2022)

## **Virtual Reality Primary School Mathematics Teaching System Based on GIS Data Fusion**



Yi Xie , Yaoqi Hong, and Yanni Fang

Research Article (13 pages), Article ID 7766617, Volume 2022 (2022)





### **Histogram Shifting-Based Quick Response Steganography Method for Secure Communication**

Geno Peter , Anli Sherine , Yuvaraja Teekaraman , Ramya Kuppasamy , and Arun Radhakrishnan   
Research Article (11 pages), Article ID 1505133, Volume 2022 (2022)

### **[Retracted] Construction of Innovation and Entrepreneurship Education Ecosystem in Higher Vocational Colleges from the Perspective of System Theory**

Chuanjuan Zheng , Liandong Sun, and Huifang Guo   
Research Article (8 pages), Article ID 5805056, Volume 2022 (2022)







### **Enhanced Security Against Volumetric DDoS Attacks Using Adversarial Machine Learning**

Jugal Shroff , Rahee Walambe , Sunil Kumar Singh , and Ketan Kotecha   
Research Article (10 pages), Article ID 5757164, Volume 2022 (2022)

### **Action of College Chinese Education and Information Fusion Teaching Based on the Background of Big Data**

Qiujuan Qi and Xiaoli Wang   
Research Article (14 pages), Article ID 3045608, Volume 2022 (2022)

### **Optimal Design of Intelligent Control System in the Communication Room Based on Artificial Intelligence**

Benkun Yao , Rajnish Kler , Sarfraz Fayaz Khan , Gourav Bansal , Ihtiram Raza Khan , and Bhupesh Kumar Singh   
Research Article (8 pages), Article ID 2353789, Volume 2022 (2022)

### **Architecture of Network-on-Chip (NoC) for Secure Data Routing Using 4-H Function of Improved TACIT Security Algorithm**

N. Ashok Kumar , G. Shyni , Geno Peter , Albert Alexander Stonier , and Vivekananda Ganji   
Research Article (9 pages), Article ID 4737569, Volume 2022 (2022)



### **Animation Education Innovation of Big Data in the New Media Environment**

Lu Zhang and Zhuoran Zhang   
Research Article (12 pages), Article ID 1966607, Volume 2022 (2022)

### **Power Grid Low Carbon Collaborative Planning Method Using Improved Cat Swarm Optimization Algorithm in Edge Cloud Computing Environment**


Xiang Li , Chong Guo , Chengjun Li , Tianyuan Xu , and Songyu Wu   
Research Article (11 pages), Article ID 5213270, Volume 2022 (2022)

### **KL-Detection: An Approach to Detect Network Outages Based on Key Links**

Ye Kuang , Dandan Li, and Xiaohong Huang   
Research Article (11 pages), Article ID 5099508, Volume 2022 (2022)

## Contents

### **The Role of Wireless Sensors in the Quality Monitoring of Students' Physical Fitness Tests under the Background of National Fitness**

Ruixia Xu 


Research Article (12 pages), Article ID 1769741, Volume 2022 (2022)

### **[Retracted] The Optimal Path of Cultivating and Promoting the Employment Ability of College Students Based on the Whole Process Management Mode of Construction Engineering Based on Computer Aided Technology**

Siyu Chen 


Research Article (8 pages), Article ID 4289413, Volume 2022 (2022)

### **[Retracted] The Teaching Evaluation Index System and Intelligent Evaluation Methods of Vocational Undergraduate Pilot Colleges**

Henan Wu 






Research Article (8 pages), Article ID 3485931, Volume 2022 (2022)

### **[Retracted] Football Teaching Quality Evaluation and Promotion Strategy Based on Intelligent Algorithms in Higher Vocational Colleges**

Xiance Jiao and Zefeng Li 







Research Article (7 pages), Article ID 9469553, Volume 2022 (2022)

### **A Machine Learning Centered Approach for Uncovering Excavators' Last Known Location Using Bluetooth and Underground WSN**

Sumit Kumari , Vikas Siwach , Yudhvir Singh , Dheerdhvaj Barak , and Rituraj Jain 

Research Article (11 pages), Article ID 9160031, Volume 2022 (2022)

### **A Novel Secure Authentication Protocol for IoT and Cloud Servers**

Ummer Iqbal , Aditya Tandon , Sonali Gupta , Arvind R. Yadav , Rahul Neware , and Fraol Waldamichael Gelana 


Research Article (17 pages), Article ID 7707543, Volume 2022 (2022)

### **Multiuser Computing Offload Algorithm Based on Mobile Edge Computing in the Internet of Things Environment**

Xiao Chu  and Ze Leng


Research Article (9 pages), Article ID 6107893, Volume 2022 (2022)

### **Adorno's Cultural Industry Theory in the Environment of Internet Development**

Fang Gao 

Research Article (7 pages), Article ID 2047038, Volume 2022 (2022)

### **The Influence of Wireless Network Communication and Edge Computing on the Performance of Aerobics Athletes**


Xiaoshuang Qi 

Research Article (11 pages), Article ID 1604478, Volume 2022 (2022)



**[Retracted] An Improved Orbit Model of Space Target Radar Based on Least Square Method and Its Program Implementation**

Yan Zhang , Xiao-Bin Huang , Rui Xiao, Ling Wang, and Li Lu  
Research Article (10 pages), Article ID 2341442, Volume 2022 (2022)






**Network Art Image Classification and Print Propagation Extraction Based on Depth Algorithm**

Hao Zhang, Haimin Sun, and Tianyang Yuan   
Research Article (11 pages), Article ID 2546015, Volume 2022 (2022)

**Lambertian Luminous Intensity Radiation Pattern Analysis in OLOS Indoor Propagation for Better Connectivity**

Vaishali, Sandeep Sancheti, Arvind Dhaka , Amita Nandal, Hamurabi Gamboa Rosales , Deepika Koundal, Francisco Eneldo López Monteagudo, Carlos Eric Galvan Tajada, and Arpit Kumar Sharma  
Research Article (11 pages), Article ID 3703477, Volume 2022 (2022)

**An Efficient Multidocument Blind Signcryption Scheme for Smart Grid-Enabled Industrial Internet of Things**

Ako Muhammad Abdullah , Insaf Ullah, Muhammad Asghar Khan , Mohammed H. Alsharif , Samih M. Mostafa , and Jimmy Ming-Tai Wu   
Research Article (7 pages), Article ID 7779152, Volume 2022 (2022)

**AI-Based Equipment Optimization of the Design on Intelligent Education Curriculum System**

Tu Peng, Yipin Luo, and Yanjin Liu   
Research Article (13 pages), Article ID 3614883, Volume 2022 (2022)


**[Retracted] A Novel Strategy for Waste Prediction Using Machine Learning Algorithm with IoT Based Intelligent Waste Management System**

G. Uganya, D. Rajalakshmi, Yuvaraja Teekaraman , Ramya Kuppusamy , and Arun Radhakrishnan   
Research Article (15 pages), Article ID 2063372, Volume 2022 (2022)







**An Improved Authentication Scheme for Digital Rights Management System**

Sajid Hussain , Yousaf Bin Zikria , Ghulam Ali Mallah , Chien-Ming Chen , Mohammad Dahman Alshehri , Farruh Ishmanov , and Shehzad Ashraf Chaudhry   
Research Article (11 pages), Article ID 1041880, Volume 2022 (2022)

**[Retracted] An Automatic Driving Control Method Based on Deep Deterministic Policy Gradient**



Haifei Zhang , Jian Xu, and Jianlin Qiu  
Research Article (9 pages), Article ID 7739440, Volume 2022 (2022)

**CUCKOO-ANN Based Novel Energy-Efficient Optimization Technique for IoT Sensor Node Modelling**








Deepshikha Bhargava , B. Prasanalakshmi , Thavavel Vaiyapuri , Hemaaid Alsulami , Suhail H. Serbaya , and Abdul Wahab Rahmani   
Research Article (9 pages), Article ID 8660245, Volume 2022 (2022)

# Contents

**[Retracted] Applications of Big Data in Economic Information Analysis and Decision-Making under the Background of Wireless Communication Networks**

Yaotian Deng, Han Zheng , and Jingshi Yan   
Research Article (7 pages), Article ID 7084969, Volume 2022 (2022)

**Internet of Things-Based Data Hiding Scheme for Wireless Communication**

A. Shobanadevi , G. Maragathm , Syam Machinathu Parambil Gangadharan , Mukesh Soni ,  
Rohit Kumar , Tien Anh Tran , and Bhupesh Kumar Singh   
Research Article (8 pages), Article ID 6997190, Volume 2022 (2022)








**A Novel Framework of an IOT-Blockchain-Based Intelligent System**

Aliaa M. Alabdali   
Research Article (13 pages), Article ID 4741923, Volume 2022 (2022)



**[Retracted] Graph Convolutional Networks for Cross-Modal Information Retrieval**

Xianben Yang and Wei Zhang   
Research Article (8 pages), Article ID 6133142, Volume 2022 (2022)







**New Trends and Advancement in Next Generation Mobile Wireless Communication (6G): A Survey**

Sher Ali , Muhammad Sohail , Syed Bilal Hussain Shah , Deepika Koundal , Muhammad Abul  
Hassan , Asrin Abdollahi , and Inam Ullah Khan   
Research Article (14 pages), Article ID 9614520, Volume 2021 (2021)







**[Retracted] A Novel Smart Healthcare Monitoring System Using Machine Learning and the Internet of Things**

Malik Bader Alazzam , Fawaz Alassery , and Ahmed Almulihi  
Research Article (7 pages), Article ID 5078799, Volume 2021 (2021)

**Applications of Deep Learning on Topographic Images to Improve the Diagnosis for Dynamic Systems and Unconstrained Optimization**

Gharbi Alshammari , Abdulsattar Abdullah Hamad , Zeyad M. Abdullah, Abdurhman M.  
Alshareef , Nawaf Alhebaishi , Abdullah Alshammari , and Assaye Belay   
Research Article (7 pages), Article ID 4672688, Volume 2021 (2021)





**Named Data Networking-Based On-Demand Secure Vehicle-To-Vehicle Communications**

Qudsia Saleem , Ikram Ud Din , Ahmad Almogren , Ibrahim Alkhalifa , Hasan Ali Khattak ,  
and Joel J. P. C. Rodrigues   
Research Article (15 pages), Article ID 1615015, Volume 2021 (2021)

**Augmentation of Contextualized Concatenated Word Representation and Dilated Convolution Neural Network for Sentiment Analysis**

Fazeel Abid, Ikram Ud Din , Ahmad Almogren , Hasan Ali Khattak , and Mirza Waqar Baig  
Research Article (13 pages), Article ID 1428710, Volume 2021 (2021)

**Mobile Edge Computing Enabled Efficient Communication Based on Federated Learning in Internet of Medical Things**

Xiao Zheng, Syed Bilal Hussain Shah , Xiaojun Ren, Fengqi Li, Liqaa Nawaf , Chinmay Chakraborty , and Muhammad Fayaz 

Research Article (10 pages), Article ID 4410894, Volume 2021 (2021)



## *Retraction*

# **Retracted: An Automatic Driving Control Method Based on Deep Deterministic Policy Gradient**

### **Wireless Communications and Mobile Computing**

Received 12 December 2023; Accepted 12 December 2023; Published 13 December 2023

Copyright © 2023 Wireless Communications and Mobile Computing. This is an open access article distributed under the Creative Commons Attribution License, which permits unrestricted use, distribution, and reproduction in any medium, provided the original work is properly cited.

This article has been retracted by Hindawi, as publisher, following an investigation undertaken by the publisher [1]. This investigation has uncovered evidence of systematic manipulation of the publication and peer-review process. We cannot, therefore, vouch for the reliability or integrity of this article.

Please note that this notice is intended solely to alert readers that the peer-review process of this article has been compromised.

Wiley and Hindawi regret that the usual quality checks did not identify these issues before publication and have since put additional measures in place to safeguard research integrity.

We wish to credit our Research Integrity and Research Publishing teams and anonymous and named external researchers and research integrity experts for contributing to this investigation.

The corresponding author, as the representative of all authors, has been given the opportunity to register their agreement or disagreement to this retraction. We have kept a record of any response received.

### **References**

- [1] H. Zhang, J. Xu, and J. Qiu, "An Automatic Driving Control Method Based on Deep Deterministic Policy Gradient," *Wireless Communications and Mobile Computing*, vol. 2022, Article ID 7739440, 9 pages, 2022.

## *Retraction*

# **Retracted: A Survey on Location Privacy Attacks and Prevention Deployed with IoT in Vehicular Networks**

### **Wireless Communications and Mobile Computing**

Received 12 December 2023; Accepted 12 December 2023; Published 13 December 2023

Copyright © 2023 Wireless Communications and Mobile Computing. This is an open access article distributed under the Creative Commons Attribution License, which permits unrestricted use, distribution, and reproduction in any medium, provided the original work is properly cited.

This article has been retracted by Hindawi, as publisher, following an investigation undertaken by the publisher [1]. This investigation has uncovered evidence of systematic manipulation of the publication and peer-review process. We cannot, therefore, vouch for the reliability or integrity of this article.

Please note that this notice is intended solely to alert readers that the peer-review process of this article has been compromised.

Wiley and Hindawi regret that the usual quality checks did not identify these issues before publication and have since put additional measures in place to safeguard research integrity.

We wish to credit our Research Integrity and Research Publishing teams and anonymous and named external researchers and research integrity experts for contributing to this investigation.

The corresponding author, as the representative of all authors, has been given the opportunity to register their agreement or disagreement to this retraction. We have kept a record of any response received.

### **References**

- [1] N. Ahmed, Z. Deng, I. Memon, F. Hassan, K. H. Mohammadani, and R. Iqbal, "A Survey on Location Privacy Attacks and Prevention Deployed with IoT in Vehicular Networks," *Wireless Communications and Mobile Computing*, vol. 2022, Article ID 6503299, 15 pages, 2022.

## *Retraction*

# **Retracted: Three-Dimensional DV-Hop Localization Algorithm Based on Hop Size Correction and Improved Sparrow Search**

### **Wireless Communications and Mobile Computing**

Received 12 December 2023; Accepted 12 December 2023; Published 13 December 2023

Copyright © 2023 Wireless Communications and Mobile Computing. This is an open access article distributed under the Creative Commons Attribution License, which permits unrestricted use, distribution, and reproduction in any medium, provided the original work is properly cited.

This article has been retracted by Hindawi, as publisher, following an investigation undertaken by the publisher [1]. This investigation has uncovered evidence of systematic manipulation of the publication and peer-review process. We cannot, therefore, vouch for the reliability or integrity of this article.

Please note that this notice is intended solely to alert readers that the peer-review process of this article has been compromised.

Wiley and Hindawi regret that the usual quality checks did not identify these issues before publication and have since put additional measures in place to safeguard research integrity.

We wish to credit our Research Integrity and Research Publishing teams and anonymous and named external researchers and research integrity experts for contributing to this investigation.

The corresponding author, as the representative of all authors, has been given the opportunity to register their agreement or disagreement to this retraction. We have kept a record of any response received.

### **References**

- [1] P. Gou, Z. Yu, X. Hu, and K. Miao, "Three-Dimensional DV-Hop Localization Algorithm Based on Hop Size Correction and Improved Sparrow Search," *Wireless Communications and Mobile Computing*, vol. 2022, Article ID 1540110, 19 pages, 2022.

## *Retraction*

# **Retracted: A Novel Strategy for Waste Prediction Using Machine Learning Algorithm with IoT Based Intelligent Waste Management System**

### **Wireless Communications and Mobile Computing**

Received 12 December 2023; Accepted 12 December 2023; Published 13 December 2023

Copyright © 2023 Wireless Communications and Mobile Computing. This is an open access article distributed under the Creative Commons Attribution License, which permits unrestricted use, distribution, and reproduction in any medium, provided the original work is properly cited.

This article has been retracted by Hindawi, as publisher, following an investigation undertaken by the publisher [1]. This investigation has uncovered evidence of systematic manipulation of the publication and peer-review process. We cannot, therefore, vouch for the reliability or integrity of this article.

Please note that this notice is intended solely to alert readers that the peer-review process of this article has been compromised.

Wiley and Hindawi regret that the usual quality checks did not identify these issues before publication and have since put additional measures in place to safeguard research integrity.

We wish to credit our Research Integrity and Research Publishing teams and anonymous and named external researchers and research integrity experts for contributing to this investigation.

The corresponding author, as the representative of all authors, has been given the opportunity to register their agreement or disagreement to this retraction. We have kept a record of any response received.

### **References**

- [1] G. Uganya, D. Rajalakshmi, Y. Teekaraman, R. Kuppasamy, and A. Radhakrishnan, "A Novel Strategy for Waste Prediction Using Machine Learning Algorithm with IoT Based Intelligent Waste Management System," *Wireless Communications and Mobile Computing*, vol. 2022, Article ID 2063372, 15 pages, 2022.

## *Retraction*

# **Retracted: An Improved Orbit Model of Space Target Radar Based on Least Square Method and Its Program Implementation**

### **Wireless Communications and Mobile Computing**

Received 12 December 2023; Accepted 12 December 2023; Published 13 December 2023

Copyright © 2023 Wireless Communications and Mobile Computing. This is an open access article distributed under the Creative Commons Attribution License, which permits unrestricted use, distribution, and reproduction in any medium, provided the original work is properly cited.

This article has been retracted by Hindawi, as publisher, following an investigation undertaken by the publisher [1]. This investigation has uncovered evidence of systematic manipulation of the publication and peer-review process. We cannot, therefore, vouch for the reliability or integrity of this article.

Please note that this notice is intended solely to alert readers that the peer-review process of this article has been compromised.

Wiley and Hindawi regret that the usual quality checks did not identify these issues before publication and have since put additional measures in place to safeguard research integrity.

We wish to credit our Research Integrity and Research Publishing teams and anonymous and named external researchers and research integrity experts for contributing to this investigation.

The corresponding author, as the representative of all authors, has been given the opportunity to register their agreement or disagreement to this retraction. We have kept a record of any response received.

### **References**

- [1] Y. Zhang, X.-B. Huang, R. Xiao, L. Wang, and L. Lu, "An Improved Orbit Model of Space Target Radar Based on Least Square Method and Its Program Implementation," *Wireless Communications and Mobile Computing*, vol. 2022, Article ID 2341442, 10 pages, 2022.

## *Retraction*

# **Retracted: Sidelobe Reduction in NC-OFDM-Based CRNs Using Differential Evolution-Assisted Generalized Sidelobe Canceller**

### **Wireless Communications and Mobile Computing**

Received 12 December 2023; Accepted 12 December 2023; Published 13 December 2023

Copyright © 2023 Wireless Communications and Mobile Computing. This is an open access article distributed under the Creative Commons Attribution License, which permits unrestricted use, distribution, and reproduction in any medium, provided the original work is properly cited.

This article has been retracted by Hindawi, as publisher, following an investigation undertaken by the publisher [1]. This investigation has uncovered evidence of systematic manipulation of the publication and peer-review process. We cannot, therefore, vouch for the reliability or integrity of this article.

Please note that this notice is intended solely to alert readers that the peer-review process of this article has been compromised.

Wiley and Hindawi regret that the usual quality checks did not identify these issues before publication and have since put additional measures in place to safeguard research integrity.

We wish to credit our Research Integrity and Research Publishing teams and anonymous and named external researchers and research integrity experts for contributing to this investigation.

The corresponding author, as the representative of all authors, has been given the opportunity to register their agreement or disagreement to this retraction. We have kept a record of any response received.

### **References**

- [1] R. Ahmed, N. Gul, S. Ahmed, M. S. Khan, S. M. Kim, and J. Kim, "Sidelobe Reduction in NC-OFDM-Based CRNs Using Differential Evolution-Assisted Generalized Sidelobe Canceller," *Wireless Communications and Mobile Computing*, vol. 2022, Article ID 9449400, 11 pages, 2022.

## *Retraction*

# **Retracted: Federated Deep Learning Approaches for the Privacy and Security of IoT Systems**

### **Wireless Communications and Mobile Computing**

Received 31 October 2023; Accepted 31 October 2023; Published 1 November 2023

Copyright © 2023 Wireless Communications and Mobile Computing. This is an open access article distributed under the Creative Commons Attribution License, which permits unrestricted use, distribution, and reproduction in any medium, provided the original work is properly cited.

This article has been retracted by Hindawi following an investigation undertaken by the publisher [1]. This investigation has uncovered evidence of one or more of the following indicators of systematic manipulation of the publication process:

- (1) Discrepancies in scope
- (2) Discrepancies in the description of the research reported
- (3) Discrepancies between the availability of data and the research described
- (4) Inappropriate citations
- (5) Incoherent, meaningless and/or irrelevant content included in the article
- (6) Peer-review manipulation

The presence of these indicators undermines our confidence in the integrity of the article's content and we cannot, therefore, vouch for its reliability. Please note that this notice is intended solely to alert readers that the content of this article is unreliable. We have not investigated whether authors were aware of or involved in the systematic manipulation of the publication process.

Wiley and Hindawi regrets that the usual quality checks did not identify these issues before publication and have since put additional measures in place to safeguard research integrity.

We wish to credit our own Research Integrity and Research Publishing teams and anonymous and named external researchers and research integrity experts for contributing to this investigation.

The corresponding author, as the representative of all authors, has been given the opportunity to register their agreement or disagreement to this retraction. We have kept a record of any response received.

### **References**

- [1] M. B. Alazzam, F. Alassery, and A. Almulihi, "Federated Deep Learning Approaches for the Privacy and Security of IoT Systems," *Wireless Communications and Mobile Computing*, vol. 2022, Article ID 1522179, 7 pages, 2022.

## *Retraction*

# **Retracted: Research on the Coupling and Coordinated Development of Sports Tourism and Cultural Industry under the Background of Artificial Intelligence Era**

### **Wireless Communications and Mobile Computing**

Received 26 September 2023; Accepted 26 September 2023; Published 27 September 2023

Copyright © 2023 Wireless Communications and Mobile Computing. This is an open access article distributed under the Creative Commons Attribution License, which permits unrestricted use, distribution, and reproduction in any medium, provided the original work is properly cited.

This article has been retracted by Hindawi following an investigation undertaken by the publisher [1]. This investigation has uncovered evidence of one or more of the following indicators of systematic manipulation of the publication process:

- (1) Discrepancies in scope
- (2) Discrepancies in the description of the research reported
- (3) Discrepancies between the availability of data and the research described
- (4) Inappropriate citations
- (5) Incoherent, meaningless and/or irrelevant content included in the article
- (6) Peer-review manipulation

The presence of these indicators undermines our confidence in the integrity of the article's content and we cannot, therefore, vouch for its reliability. Please note that this notice is intended solely to alert readers that the content of this article is unreliable. We have not investigated whether authors were aware of or involved in the systematic manipulation of the publication process.

Wiley and Hindawi regrets that the usual quality checks did not identify these issues before publication and have since put additional measures in place to safeguard research integrity.

We wish to credit our own Research Integrity and Research Publishing teams and anonymous and named external researchers and research integrity experts for contributing to this investigation.

The corresponding author, as the representative of all authors, has been given the opportunity to register their agreement or disagreement to this retraction. We have kept a record of any response received.

### **References**

- [1] C. Hong, J. Shi, Y. Xing, and Z. Chang, "Research on the Coupling and Coordinated Development of Sports Tourism and Cultural Industry under the Background of Artificial Intelligence Era," *Wireless Communications and Mobile Computing*, vol. 2022, Article ID 3191655, 6 pages, 2022.



## Retraction

# Retracted: Real Time Facial Expression Recognition for Online Lecture

### Wireless Communications and Mobile Computing

Received 8 August 2023; Accepted 8 August 2023; Published 9 August 2023

Copyright © 2023 Wireless Communications and Mobile Computing. This is an open access article distributed under the Creative Commons Attribution License, which permits unrestricted use, distribution, and reproduction in any medium, provided the original work is properly cited.

This article has been retracted by Hindawi following an investigation undertaken by the publisher [1]. This investigation has uncovered evidence of one or more of the following indicators of systematic manipulation of the publication process:

- (1) Discrepancies in scope
- (2) Discrepancies in the description of the research reported
- (3) Discrepancies between the availability of data and the research described
- (4) Inappropriate citations
- (5) Incoherent, meaningless and/or irrelevant content included in the article
- (6) Peer-review manipulation

The presence of these indicators undermines our confidence in the integrity of the article's content and we cannot, therefore, vouch for its reliability. Please note that this notice is intended solely to alert readers that the content of this article is unreliable. We have not investigated whether authors were aware of or involved in the systematic manipulation of the publication process.

In addition, our investigation has also shown that one or more of the following human-subject reporting requirements has not been met in this article: ethical approval by an Institutional Review Board (IRB) committee or equivalent, patient/participant consent to participate, and/or agreement to publish patient/participant details (where relevant).

Wiley and Hindawi regrets that the usual quality checks did not identify these issues before publication and have since put additional measures in place to safeguard research integrity.

We wish to credit our own Research Integrity and Research Publishing teams and anonymous and named external

researchers and research integrity experts for contributing to this investigation.

The corresponding author, as the representative of all authors, has been given the opportunity to register their agreement or disagreement to this retraction. We have kept a record of any response received.

### References

- [1] H. Wu, "Real Time Facial Expression Recognition for Online Lecture," *Wireless Communications and Mobile Computing*, vol. 2022, Article ID 9684264, 11 pages, 2022.

## *Retraction*

# **Retracted: The Application of AI Technology in GPU Scheduling Algorithm Optimization**

### **Wireless Communications and Mobile Computing**

Received 8 August 2023; Accepted 8 August 2023; Published 9 August 2023

Copyright © 2023 Wireless Communications and Mobile Computing. This is an open access article distributed under the Creative Commons Attribution License, which permits unrestricted use, distribution, and reproduction in any medium, provided the original work is properly cited.

This article has been retracted by Hindawi following an investigation undertaken by the publisher [1]. This investigation has uncovered evidence of one or more of the following indicators of systematic manipulation of the publication process:

- (1) Discrepancies in scope
- (2) Discrepancies in the description of the research reported
- (3) Discrepancies between the availability of data and the research described
- (4) Inappropriate citations
- (5) Incoherent, meaningless and/or irrelevant content included in the article
- (6) Peer-review manipulation

The presence of these indicators undermines our confidence in the integrity of the article's content and we cannot, therefore, vouch for its reliability. Please note that this notice is intended solely to alert readers that the content of this article is unreliable. We have not investigated whether authors were aware of or involved in the systematic manipulation of the publication process.

Wiley and Hindawi regrets that the usual quality checks did not identify these issues before publication and have since put additional measures in place to safeguard research integrity.

We wish to credit our own Research Integrity and Research Publishing teams and anonymous and named external researchers and research integrity experts for contributing to this investigation.

The corresponding author, as the representative of all authors, has been given the opportunity to register their agreement or disagreement to this retraction. We have kept a record of any response received.

### **References**

- [1] Z. Yan, Y. Liu, and H. Shao, "The Application of AI Technology in GPU Scheduling Algorithm Optimization," *Wireless Communications and Mobile Computing*, vol. 2022, Article ID 4713698, 7 pages, 2022.

## Retraction

# Retracted: A Novel Smart Healthcare Monitoring System Using Machine Learning and the Internet of Things

### Wireless Communications and Mobile Computing

Received 8 August 2023; Accepted 8 August 2023; Published 9 August 2023

Copyright © 2023 Wireless Communications and Mobile Computing. This is an open access article distributed under the Creative Commons Attribution License, which permits unrestricted use, distribution, and reproduction in any medium, provided the original work is properly cited.

This article has been retracted by Hindawi following an investigation undertaken by the publisher [1]. This investigation has uncovered evidence of one or more of the following indicators of systematic manipulation of the publication process:

- (1) Discrepancies in scope
- (2) Discrepancies in the description of the research reported
- (3) Discrepancies between the availability of data and the research described
- (4) Inappropriate citations
- (5) Incoherent, meaningless and/or irrelevant content included in the article
- (6) Peer-review manipulation

The presence of these indicators undermines our confidence in the integrity of the article's content and we cannot, therefore, vouch for its reliability. Please note that this notice is intended solely to alert readers that the content of this article is unreliable. We have not investigated whether authors were aware of or involved in the systematic manipulation of the publication process.

In addition, our investigation has also shown that one or more of the following human-subject reporting requirements has not been met in this article: ethical approval by an Institutional Review Board (IRB) committee or equivalent, patient/participant consent to participate, and/or agreement to publish patient/participant details (where relevant).

Wiley and Hindawi regrets that the usual quality checks did not identify these issues before publication and have since put additional measures in place to safeguard research integrity.

We wish to credit our own Research Integrity and Research Publishing teams and anonymous and named external

researchers and research integrity experts for contributing to this investigation.

The corresponding author, as the representative of all authors, has been given the opportunity to register their agreement or disagreement to this retraction. We have kept a record of any response received.

### References

- [1] M. B. Alazzam, F. Alassery, and A. Almulih, "A Novel Smart Healthcare Monitoring System Using Machine Learning and the Internet of Things," *Wireless Communications and Mobile Computing*, vol. 2021, Article ID 5078799, 7 pages, 2021.

## *Retraction*

# **Retracted: The Teaching Evaluation Index System and Intelligent Evaluation Methods of Vocational Undergraduate Pilot Colleges**

### **Wireless Communications and Mobile Computing**

Received 8 August 2023; Accepted 8 August 2023; Published 9 August 2023

Copyright © 2023 Wireless Communications and Mobile Computing. This is an open access article distributed under the Creative Commons Attribution License, which permits unrestricted use, distribution, and reproduction in any medium, provided the original work is properly cited.

This article has been retracted by Hindawi following an investigation undertaken by the publisher [1]. This investigation has uncovered evidence of one or more of the following indicators of systematic manipulation of the publication process:

- (1) Discrepancies in scope
- (2) Discrepancies in the description of the research reported
- (3) Discrepancies between the availability of data and the research described
- (4) Inappropriate citations
- (5) Incoherent, meaningless and/or irrelevant content included in the article
- (6) Peer-review manipulation

The presence of these indicators undermines our confidence in the integrity of the article's content and we cannot, therefore, vouch for its reliability. Please note that this notice is intended solely to alert readers that the content of this article is unreliable. We have not investigated whether authors were aware of or involved in the systematic manipulation of the publication process.

In addition, our investigation has also shown that one or more of the following human-subject reporting requirements has not been met in this article: ethical approval by an Institutional Review Board (IRB) committee or equivalent, patient/participant consent to participate, and/or agreement to publish patient/participant details (where relevant).

Wiley and Hindawi regrets that the usual quality checks did not identify these issues before publication and have since put additional measures in place to safeguard research integrity.

We wish to credit our own Research Integrity and Research Publishing teams and anonymous and named external researchers and research integrity experts for contributing to this investigation.

The corresponding author, as the representative of all authors, has been given the opportunity to register their agreement or disagreement to this retraction. We have kept a record of any response received.

### **References**

- [1] H. Wu, "The Teaching Evaluation Index System and Intelligent Evaluation Methods of Vocational Undergraduate Pilot Colleges," *Wireless Communications and Mobile Computing*, vol. 2022, Article ID 3485931, 8 pages, 2022.

## *Retraction*

# **Retracted: Realization Path of the Social Development of Meteorological Services Based on Intelligent Data Analysis**

### **Wireless Communications and Mobile Computing**

Received 25 July 2023; Accepted 25 July 2023; Published 26 July 2023

Copyright © 2023 Wireless Communications and Mobile Computing. This is an open access article distributed under the Creative Commons Attribution License, which permits unrestricted use, distribution, and reproduction in any medium, provided the original work is properly cited.

This article has been retracted by Hindawi following an investigation undertaken by the publisher [1]. This investigation has uncovered evidence of one or more of the following indicators of systematic manipulation of the publication process:

- (1) Discrepancies in scope
- (2) Discrepancies in the description of the research reported
- (3) Discrepancies between the availability of data and the research described
- (4) Inappropriate citations
- (5) Incoherent, meaningless and/or irrelevant content included in the article
- (6) Peer-review manipulation

The presence of these indicators undermines our confidence in the integrity of the article's content and we cannot, therefore, vouch for its reliability. Please note that this notice is intended solely to alert readers that the content of this article is unreliable. We have not investigated whether authors were aware of or involved in the systematic manipulation of the publication process.

Wiley and Hindawi regrets that the usual quality checks did not identify these issues before publication and have since put additional measures in place to safeguard research integrity.

We wish to credit our own Research Integrity and Research Publishing teams and anonymous and named external researchers and research integrity experts for contributing to this investigation.

The corresponding author, as the representative of all authors, has been given the opportunity to register their agreement or disagreement to this retraction. We have kept a record of any response received.

### **References**

- [1] F. Guo, Y. Feng, and H. Xiao, "Realization Path of the Social Development of Meteorological Services Based on Intelligent Data Analysis," *Wireless Communications and Mobile Computing*, vol. 2022, Article ID 8904136, 8 pages, 2022.

## Retraction

# Retracted: Football Teaching Quality Evaluation and Promotion Strategy Based on Intelligent Algorithms in Higher Vocational Colleges

### Wireless Communications and Mobile Computing

Received 25 July 2023; Accepted 25 July 2023; Published 26 July 2023

Copyright © 2023 Wireless Communications and Mobile Computing. This is an open access article distributed under the Creative Commons Attribution License, which permits unrestricted use, distribution, and reproduction in any medium, provided the original work is properly cited.

This article has been retracted by Hindawi following an investigation undertaken by the publisher [1]. This investigation has uncovered evidence of one or more of the following indicators of systematic manipulation of the publication process:

- (1) Discrepancies in scope
- (2) Discrepancies in the description of the research reported
- (3) Discrepancies between the availability of data and the research described
- (4) Inappropriate citations
- (5) Incoherent, meaningless and/or irrelevant content included in the article
- (6) Peer-review manipulation

The presence of these indicators undermines our confidence in the integrity of the article's content and we cannot, therefore, vouch for its reliability. Please note that this notice is intended solely to alert readers that the content of this article is unreliable. We have not investigated whether authors were aware of or involved in the systematic manipulation of the publication process.

In addition, our investigation has also shown that one or more of the following human-subject reporting requirements has not been met in this article: ethical approval by an Institutional Review Board (IRB) committee or equivalent, patient/participant consent to participate, and/or agreement to publish patient/participant details (where relevant).

Wiley and Hindawi regrets that the usual quality checks did not identify these issues before publication and have since put additional measures in place to safeguard research integrity.

We wish to credit our own Research Integrity and Research Publishing teams and anonymous and named external researchers and research integrity experts for contributing to this investigation.

The corresponding author, as the representative of all authors, has been given the opportunity to register their agreement or disagreement to this retraction. We have kept a record of any response received.

### References

- [1] X. Jiao and Z. Li, "Football Teaching Quality Evaluation and Promotion Strategy Based on Intelligent Algorithms in Higher Vocational Colleges," *Wireless Communications and Mobile Computing*, vol. 2022, Article ID 9469553, 7 pages, 2022.

## Retraction

# Retracted: The Optimal Path of Cultivating and Promoting the Employment Ability of College Students Based on the Whole Process Management Mode of Construction Engineering Based on Computer Aided Technology

### Wireless Communications and Mobile Computing

Received 25 July 2023; Accepted 25 July 2023; Published 26 July 2023

Copyright © 2023 Wireless Communications and Mobile Computing. This is an open access article distributed under the Creative Commons Attribution License, which permits unrestricted use, distribution, and reproduction in any medium, provided the original work is properly cited.

This article has been retracted by Hindawi following an investigation undertaken by the publisher [1]. This investigation has uncovered evidence of one or more of the following indicators of systematic manipulation of the publication process:

- (1) Discrepancies in scope
- (2) Discrepancies in the description of the research reported
- (3) Discrepancies between the availability of data and the research described
- (4) Inappropriate citations
- (5) Incoherent, meaningless and/or irrelevant content included in the article
- (6) Peer-review manipulation

The presence of these indicators undermines our confidence in the integrity of the article's content and we cannot, therefore, vouch for its reliability. Please note that this notice is intended solely to alert readers that the content of this article is unreliable. We have not investigated whether authors were aware of or involved in the systematic manipulation of the publication process.

In addition, our investigation has also shown that one or more of the following human-subject reporting requirements has not been met in this article: ethical approval by an Institutional Review Board (IRB) committee or equivalent, patient/participant consent to participate, and/or agreement to publish patient/participant details (where relevant).

Wiley and Hindawi regrets that the usual quality checks did not identify these issues before publication and have since put additional measures in place to safeguard research integrity.

We wish to credit our own Research Integrity and Research Publishing teams and anonymous and named external researchers and research integrity experts for contributing to this investigation.

The corresponding author, as the representative of all authors, has been given the opportunity to register their agreement or disagreement to this retraction. We have kept a record of any response received.

### References

- [1] S. Chen, "The Optimal Path of Cultivating and Promoting the Employment Ability of College Students Based on the Whole Process Management Mode of Construction Engineering Based on Computer Aided Technology," *Wireless Communications and Mobile Computing*, vol. 2022, Article ID 4289413, 8 pages, 2022.

## *Retraction*

# **Retracted: Applications of Big Data in Economic Information Analysis and Decision-Making under the Background of Wireless Communication Networks**

### **Wireless Communications and Mobile Computing**

Received 25 July 2023; Accepted 25 July 2023; Published 26 July 2023

Copyright © 2023 Wireless Communications and Mobile Computing. This is an open access article distributed under the Creative Commons Attribution License, which permits unrestricted use, distribution, and reproduction in any medium, provided the original work is properly cited.

This article has been retracted by Hindawi following an investigation undertaken by the publisher [1]. This investigation has uncovered evidence of one or more of the following indicators of systematic manipulation of the publication process:

- (1) Discrepancies in scope
- (2) Discrepancies in the description of the research reported
- (3) Discrepancies between the availability of data and the research described
- (4) Inappropriate citations
- (5) Incoherent, meaningless and/or irrelevant content included in the article
- (6) Peer-review manipulation

The presence of these indicators undermines our confidence in the integrity of the article's content and we cannot, therefore, vouch for its reliability. Please note that this notice is intended solely to alert readers that the content of this article is unreliable. We have not investigated whether authors were aware of or involved in the systematic manipulation of the publication process.

Wiley and Hindawi regrets that the usual quality checks did not identify these issues before publication and have since put additional measures in place to safeguard research integrity.

We wish to credit our own Research Integrity and Research Publishing teams and anonymous and named external researchers and research integrity experts for contributing to this investigation.

The corresponding author, as the representative of all authors, has been given the opportunity to register their

agreement or disagreement to this retraction. We have kept a record of any response received.

### **References**

- [1] Y. Deng, H. Zheng, and J. Yan, "Applications of Big Data in Economic Information Analysis and Decision-Making under the Background of Wireless Communication Networks," *Wireless Communications and Mobile Computing*, vol. 2022, Article ID 7084969, 7 pages, 2022.



## *Retraction*

# **Retracted: Supply Chain Management System for Automobile Manufacturing Enterprises Based on SAP**

### **Wireless Communications and Mobile Computing**

Received 25 July 2023; Accepted 25 July 2023; Published 26 July 2023

Copyright © 2023 Wireless Communications and Mobile Computing. This is an open access article distributed under the Creative Commons Attribution License, which permits unrestricted use, distribution, and reproduction in any medium, provided the original work is properly cited.

This article has been retracted by Hindawi following an investigation undertaken by the publisher [1]. This investigation has uncovered evidence of one or more of the following indicators of systematic manipulation of the publication process:

- (1) Discrepancies in scope
- (2) Discrepancies in the description of the research reported
- (3) Discrepancies between the availability of data and the research described
- (4) Inappropriate citations
- (5) Incoherent, meaningless and/or irrelevant content included in the article
- (6) Peer-review manipulation

The presence of these indicators undermines our confidence in the integrity of the article's content and we cannot, therefore, vouch for its reliability. Please note that this notice is intended solely to alert readers that the content of this article is unreliable. We have not investigated whether authors were aware of or involved in the systematic manipulation of the publication process.

Wiley and Hindawi regrets that the usual quality checks did not identify these issues before publication and have since put additional measures in place to safeguard research integrity.

We wish to credit our own Research Integrity and Research Publishing teams and anonymous and named external researchers and research integrity experts for contributing to this investigation.

The corresponding author, as the representative of all authors, has been given the opportunity to register their agreement or disagreement to this retraction. We have kept a record of any response received.

### **References**

- [1] P. Lin, M. Shu, B. Hsu, C. Hu, and J. Huang, "Supply Chain Management System for Automobile Manufacturing Enterprises Based on SAP," *Wireless Communications and Mobile Computing*, vol. 2022, Article ID 5901633, 10 pages, 2022.

## Retraction

# Retracted: Application Research of Time Delay System Control in Mobile Sensor Networks Based on Deep Reinforcement Learning

### Wireless Communications and Mobile Computing

Received 25 July 2023; Accepted 25 July 2023; Published 26 July 2023

Copyright © 2023 Wireless Communications and Mobile Computing. This is an open access article distributed under the Creative Commons Attribution License, which permits unrestricted use, distribution, and reproduction in any medium, provided the original work is properly cited.

This article has been retracted by Hindawi following an investigation undertaken by the publisher [1]. This investigation has uncovered evidence of one or more of the following indicators of systematic manipulation of the publication process:

- (1) Discrepancies in scope
- (2) Discrepancies in the description of the research reported
- (3) Discrepancies between the availability of data and the research described
- (4) Inappropriate citations
- (5) Incoherent, meaningless and/or irrelevant content included in the article
- (6) Peer-review manipulation

The presence of these indicators undermines our confidence in the integrity of the article's content and we cannot, therefore, vouch for its reliability. Please note that this notice is intended solely to alert readers that the content of this article is unreliable. We have not investigated whether authors were aware of or involved in the systematic manipulation of the publication process.

Wiley and Hindawi regrets that the usual quality checks did not identify these issues before publication and have since put additional measures in place to safeguard research integrity.

We wish to credit our own Research Integrity and Research Publishing teams and anonymous and named external researchers and research integrity experts for contributing to this investigation.

The corresponding author, as the representative of all authors, has been given the opportunity to register their

agreement or disagreement to this retraction. We have kept a record of any response received.

### References

- [1] W. Zhu, T. Garg, S. Raza, S. Lalar, D. D. Barak, and A. W. Rahmani, "Application Research of Time Delay System Control in Mobile Sensor Networks Based on Deep Reinforcement Learning," *Wireless Communications and Mobile Computing*, vol. 2022, Article ID 7844719, 7 pages, 2022.

## Retraction

# Retracted: Construction of Innovation and Entrepreneurship Education Ecosystem in Higher Vocational Colleges from the Perspective of System Theory

### Wireless Communications and Mobile Computing

Received 25 July 2023; Accepted 25 July 2023; Published 26 July 2023

Copyright © 2023 Wireless Communications and Mobile Computing. This is an open access article distributed under the Creative Commons Attribution License, which permits unrestricted use, distribution, and reproduction in any medium, provided the original work is properly cited.

This article has been retracted by Hindawi following an investigation undertaken by the publisher [1]. This investigation has uncovered evidence of one or more of the following indicators of systematic manipulation of the publication process:

- (1) Discrepancies in scope
- (2) Discrepancies in the description of the research reported
- (3) Discrepancies between the availability of data and the research described
- (4) Inappropriate citations
- (5) Incoherent, meaningless and/or irrelevant content included in the article
- (6) Peer-review manipulation

The presence of these indicators undermines our confidence in the integrity of the article's content and we cannot, therefore, vouch for its reliability. Please note that this notice is intended solely to alert readers that the content of this article is unreliable. We have not investigated whether authors were aware of or involved in the systematic manipulation of the publication process.

In addition, our investigation has also shown that one or more of the following human-subject reporting requirements has not been met in this article: ethical approval by an Institutional Review Board (IRB) committee or equivalent, patient/participant consent to participate, and/or agreement to publish patient/participant details (where relevant).

Wiley and Hindawi regrets that the usual quality checks did not identify these issues before publication and have since put additional measures in place to safeguard research integrity.

We wish to credit our own Research Integrity and Research Publishing teams and anonymous and named external researchers and research integrity experts for contributing to this investigation.

The corresponding author, as the representative of all authors, has been given the opportunity to register their agreement or disagreement to this retraction. We have kept a record of any response received.

### References

- [1] C. Zheng, L. Sun, and H. Guo, "Construction of Innovation and Entrepreneurship Education Ecosystem in Higher Vocational Colleges from the Perspective of System Theory," *Wireless Communications and Mobile Computing*, vol. 2022, Article ID 5805056, 8 pages, 2022.

## *Retraction*

# **Retracted: Graph Convolutional Networks for Cross-Modal Information Retrieval**

### **Wireless Communications and Mobile Computing**

Received 25 July 2023; Accepted 25 July 2023; Published 26 July 2023

Copyright © 2023 Wireless Communications and Mobile Computing. This is an open access article distributed under the Creative Commons Attribution License, which permits unrestricted use, distribution, and reproduction in any medium, provided the original work is properly cited.

This article has been retracted by Hindawi following an investigation undertaken by the publisher [1]. This investigation has uncovered evidence of one or more of the following indicators of systematic manipulation of the publication process:

- (1) Discrepancies in scope
- (2) Discrepancies in the description of the research reported
- (3) Discrepancies between the availability of data and the research described
- (4) Inappropriate citations
- (5) Incoherent, meaningless and/or irrelevant content included in the article
- (6) Peer-review manipulation

The presence of these indicators undermines our confidence in the integrity of the article's content and we cannot, therefore, vouch for its reliability. Please note that this notice is intended solely to alert readers that the content of this article is unreliable. We have not investigated whether authors were aware of or involved in the systematic manipulation of the publication process.

Wiley and Hindawi regrets that the usual quality checks did not identify these issues before publication and have since put additional measures in place to safeguard research integrity.

We wish to credit our own Research Integrity and Research Publishing teams and anonymous and named external researchers and research integrity experts for contributing to this investigation.

The corresponding author, as the representative of all authors, has been given the opportunity to register their agreement or disagreement to this retraction. We have kept a record of any response received.

### **References**

- [1] X. Yang and W. Zhang, "Graph Convolutional Networks for Cross-Modal Information Retrieval," *Wireless Communications and Mobile Computing*, vol. 2022, Article ID 6133142, 8 pages, 2022.

## Retraction

# Retracted: Curriculum Design of College Students' English Critical Ability in the Internet Age

### Wireless Communications and Mobile Computing

Received 25 July 2023; Accepted 25 July 2023; Published 26 July 2023

Copyright © 2023 Wireless Communications and Mobile Computing. This is an open access article distributed under the Creative Commons Attribution License, which permits unrestricted use, distribution, and reproduction in any medium, provided the original work is properly cited.

This article has been retracted by Hindawi following an investigation undertaken by the publisher [1]. This investigation has uncovered evidence of one or more of the following indicators of systematic manipulation of the publication process:

- (1) Discrepancies in scope
- (2) Discrepancies in the description of the research reported
- (3) Discrepancies between the availability of data and the research described
- (4) Inappropriate citations
- (5) Incoherent, meaningless and/or irrelevant content included in the article
- (6) Peer-review manipulation

The presence of these indicators undermines our confidence in the integrity of the article's content and we cannot, therefore, vouch for its reliability. Please note that this notice is intended solely to alert readers that the content of this article is unreliable. We have not investigated whether authors were aware of or involved in the systematic manipulation of the publication process.

In addition, our investigation has also shown that one or more of the following human-subject reporting requirements has not been met in this article: ethical approval by an Institutional Review Board (IRB) committee or equivalent, patient/participant consent to participate, and/or agreement to publish patient/participant details (where relevant).

Wiley and Hindawi regrets that the usual quality checks did not identify these issues before publication and have since put additional measures in place to safeguard research integrity.

We wish to credit our own Research Integrity and Research Publishing teams and anonymous and named external

researchers and research integrity experts for contributing to this investigation.

The corresponding author, as the representative of all authors, has been given the opportunity to register their agreement or disagreement to this retraction. We have kept a record of any response received.

### References

- [1] J. Shen, Y. Chen, and J. Lin, "Curriculum Design of College Students' English Critical Ability in the Internet Age," *Wireless Communications and Mobile Computing*, vol. 2022, Article ID 5609450, 7 pages, 2022.

## *Retraction*

# **Retracted: The Application of AI Technology in GPU Scheduling Algorithm Optimization**

### **Wireless Communications and Mobile Computing**

Received 8 August 2023; Accepted 8 August 2023; Published 9 August 2023

Copyright © 2023 Wireless Communications and Mobile Computing. This is an open access article distributed under the Creative Commons Attribution License, which permits unrestricted use, distribution, and reproduction in any medium, provided the original work is properly cited.

This article has been retracted by Hindawi following an investigation undertaken by the publisher [1]. This investigation has uncovered evidence of one or more of the following indicators of systematic manipulation of the publication process:

- (1) Discrepancies in scope
- (2) Discrepancies in the description of the research reported
- (3) Discrepancies between the availability of data and the research described
- (4) Inappropriate citations
- (5) Incoherent, meaningless and/or irrelevant content included in the article
- (6) Peer-review manipulation

The presence of these indicators undermines our confidence in the integrity of the article's content and we cannot, therefore, vouch for its reliability. Please note that this notice is intended solely to alert readers that the content of this article is unreliable. We have not investigated whether authors were aware of or involved in the systematic manipulation of the publication process.

Wiley and Hindawi regrets that the usual quality checks did not identify these issues before publication and have since put additional measures in place to safeguard research integrity.

We wish to credit our own Research Integrity and Research Publishing teams and anonymous and named external researchers and research integrity experts for contributing to this investigation.

The corresponding author, as the representative of all authors, has been given the opportunity to register their agreement or disagreement to this retraction. We have kept a record of any response received.

### **References**

- [1] Z. Yan, Y. Liu, and H. Shao, "The Application of AI Technology in GPU Scheduling Algorithm Optimization," *Wireless Communications and Mobile Computing*, vol. 2022, Article ID 4713698, 7 pages, 2022.

## Research Article

# The Application of AI Technology in GPU Scheduling Algorithm Optimization

Zhancai Yan , Yaqiu Liu , and Hongrun Shao

*The College of Information and Computer Engineering, Northeast Forestry University, 150000 Harbin, China*

Correspondence should be addressed to Yaqiu Liu; [darling@nefu.edu.cn](mailto:darling@nefu.edu.cn)

Received 27 January 2022; Revised 28 March 2022; Accepted 4 April 2022; Published 12 May 2022

Academic Editor: Shalli Rani

Copyright © 2022 Zhancai Yan et al. This is an open access article distributed under the Creative Commons Attribution License, which permits unrestricted use, distribution, and reproduction in any medium, provided the original work is properly cited.

With the rapid development of integrated circuit technology, GPU computing capabilities continue to improve. Due to the continuous improvement and improvement of GPU programming capabilities, functions, and performance, GPUs have been widely used in the field of high-tech general-purpose computers. This article is aimed at studying the optimization of GPU scheduling algorithm based on AI technology. Through a combination of theoretical analysis and simulation experiments, the concepts of artificial intelligence technology and GPU scheduling are explained, and the impact of GPU architecture and GPGPU load on the energy efficiency of GPGPU is explained. On the basis of comprehensive analysis of GPU cluster characteristics, a new GA-TP scheduling algorithm based on genetic algorithm was designed, and based on the energy efficiency of the cluster, a simulation verification platform was built for the accuracy of simulation. Experimental results show that the acceleration rate of the GA-TP algorithm is significantly lower than that of the HEFT algorithm, the average acceleration rate is reduced by nearly 25%, and the scheduling efficiency of the GA-TP algorithm is higher.

## 1. Introduction

Nowadays, more and more artificial intelligence products are listed and integrated into people's life. In the near future, artificial intelligence technology will have a significant impact on human society and human production and life [1, 2]. Seeing the rapid development of information industry and Internet in the past, most of the credit depends on the rapid development of integrated circuits. The rapid development of integrated circuits has changed our way of life. Among them, the difference of GPU is that it is perfect and occupies a prominent position in the established data center [3, 4].

With the emergence of GPU, there are two heterogeneous computing resources in a single system. At present, many researches and applications focus on how to give full play to the computing performance of GPU, but they do not make full use of the computing power of multicore CPU, resulting in a waste of computing power and energy. In addition, GPU technology and multicore CPU technology are developing at a high speed. GPU manufacturers have successively sold GPUs with more stream processors, and

CPU manufacturers have also launched processors with more integrated cores. The development of software has further promoted the application of GPU in various fields, such as CUDA, OpenCL, and openacc [5, 6]. Because GPU and CPU are different computing resources, the computing platform of multicore CPU-GPU can only exert its powerful computing power through effective scheduling algorithm. Therefore, it is becoming more and more important to study effective scheduling algorithms and realize load balancing, and these problems are becoming more and more obvious [7].

Recently, a new optimization method has attracted more and more researchers' interest because of its simplicity and efficiency. Jimeno-Morenilla et al. introduced their parallel algorithm based on Java GPU and analyzed the parallel performance and optimization performance using the well-known unconstrained function benchmark. The results show that the parallel Java implementation achieves significant acceleration for all benchmark functions and achieves up to 190 times acceleration without affecting the optimization performance [8]. Cao et al. proposed an artificial intelligence agent (AI agent) system. AI agents can be deployed

at different levels of SDN to realize network service prediction, resource scheduling, and other functions. A new AI agent framework is designed, which uses AI algorithm to replace the traditional service prediction and resource scheduling strategy. At the same time, the related agent deployment scheme is proposed. Finally, a resource scheduling simulation experiment based on AI agent is designed to test the accuracy of network service prediction and the rationality of resource allocation based on this framework [9]. Considering the overall impact of memory bandwidth limitation on GPU performance, the additional performance loss caused by scheduling algorithm can not be ignored when designing scheduling algorithm.

In this work, we will study parallel loop programming and propose a new scheduling method, the GA-TP algorithm. This algorithm can be applied to widely used CPU-GPU computing platforms to increase the computing power, load distribution, and programming costs of different computing sources, multicore CPUs, and GPUs. With the increasing demand for computers and the popularity of multicore CPU-GPU platforms, the application of load forecasting and scheduling algorithms plays an important role in improving the utilization of computing sources, reducing power consumption, and accelerating development speed.

## 2. Research on AI Technology in GPU Scheduling Algorithm Optimization

*2.1. Artificial Intelligence Technology.* Artificial intelligence technology is the ability of computer-based systems to replace human intelligence and physical strength in manufacturing operations and to reduce the weight of the human body [10, 11].

In terms of the vision, development, and application of artificial intelligence, its importance includes the following aspects:

- (1) Traditional intelligent technology is a technology developed from human intelligence, which is the training and imitation of human intelligence, thinking, and behavior [12]
- (2) Artificial intelligence technology is a field where computer technology is developing and growing. In addition to the main line of computer science, it also includes science, mathematics, linguistics, government, philosophy, and other fields
- (3) The development of technology is very important to the development of society. Artificial intelligence technology has also experienced innovation and optimization from laboratory research to practical application. Artificial intelligence technology has also been deeply applied in different fields such as education, medical treatment, and elderly care services

At present, the continuous transmission and exchange of information and knowledge between human beings and artificial intelligence have emerged in the application of artificial

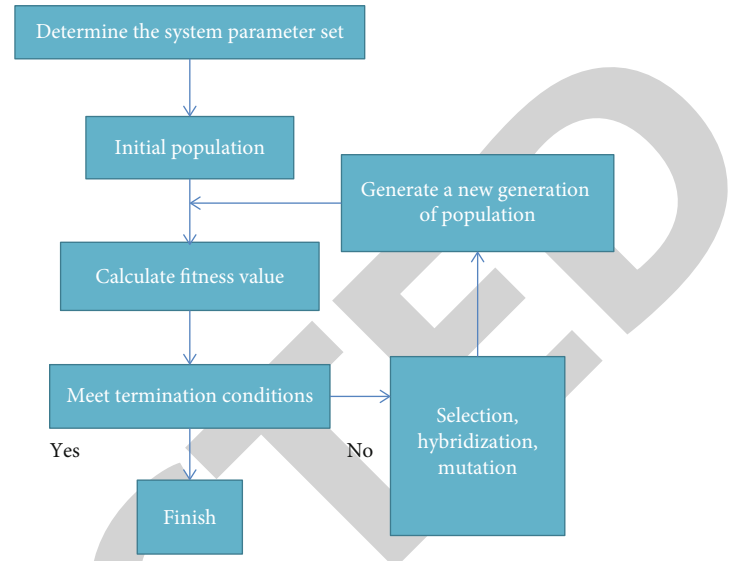


FIGURE 1: GA-TP algorithm flow chart.

intelligence in many different fields. The advantage of artificial intelligence technology is to imitate human thoughts and behaviors and analyze and study based on human characteristics identification, information storage, data analysis, and other technologies. When imitating human experience in specific fields, it is considered that the research is independent. Compared with ordinary people, the application of artificial intelligence technology can make people make more accurate and faster decisions, so as to achieve higher efficiency. When machines work better than humans, people can take artificial intelligence as a simulation object to constantly examine their behavior, expand their competition, and accelerate this new field of science.

*2.2. GPU Scheduling.* Custom scheduling methods can be divided into static scheduling and dynamic scheduling. The static system does not need to compete for sources, so the overall scheduling cost is reduced, but it is more likely to cause uneven load and reduce the amount of computing resources. Create a system with the ability to share resources, instead of operating based on processor load while the system is running. This can increase load balancing, but it also increases load settings.

When comparing the computing speed of multicore GPU with that of single core CPU, because the single core CPU processor has only one physical processor, the dual core has two processors, which can go hand in hand when processing data and process at the same time, which increases the data processing bandwidth. Therefore, the computing speed of multicore GPU is much faster than that of single core CPU, and the performance of multithreaded GPU is obviously better than that of single core. When the multicore GPU and CPU are divided into operations with higher computational sensitivity, the time of GPU multicore computing will be much shorter than that of single core CPU, resulting in longer performance of multicore GPU and reduced CPU use. GPU calculation includes data communication time and calculation time between memory



TABLE 1: Simulation parameters.

GPU parameters	Set value	SM parameter	Set value
Core frequency	1216 MHz	Register size	256 kB
Memory frequency	7 GHz	Shared memory size	96 kB
SM quantity	16	Thread limit	2048
Number of memory controllers	4 TB	Quantity limit	32

and GPU. Only tasks with long computing time and short communication time can make full use of the GPU's computing power. Therefore, GPU is suitable for computers with high attractiveness and low traffic. If the calculation sensitivity is too low, the communication and startup with the GPU will take too much time, the GPU performance is not fully utilized, and the calculation speed is even slower than the CPU core. Therefore, according to the characteristics of the CPU and GPU architecture, adding high-performance tasks to the GPU and adding small tasks to the CPU can improve the performance and efficiency of the system.

A typical GPU system has two parts: server-side code and device-side code. The code on the side device is usually called the kernel GPU. GPU systems always have many kernels. The kernel is a code base running on the GPU, and each kernel is responsible for performing certain tasks. When calling the GPU configuration, the kernel and corresponding input parameters must be passed from the CPU to the GPU. The GPU generates multiple cables to run the same code. The number of threads generated is specified by the user, so the kernel is a typical single-instruction multithreaded program.

**2.3. GA-TP Algorithm.** The working process of the GA-TP algorithm is as follows: First, it is necessary to complete the initialization of the algorithm parameters, create a "matching population" based on the relevant parameters and the initial population, and then enter the iterative algorithm loop. Assemble and then assign the set to the processor most suitable for it, calculate its applicability, modify the genome with a new genetic function, supplement the "matching population" with population information, and finally compare the default limits to determine whether the algorithm continues to be used in loops or output. Figure 1 shows the flow of the GA-TP algorithm.

The GA-TP algorithm uses a crossover operator that includes all genes. After selecting the parents, perform the tasks of AND, OR, and XOR alleles on the two genomes to complete the integration. In order to further improve the connection quality, this crossover operator also improves the choice of parents. When creating the initial population, create a "corresponding population" with fewer people in the population. In a summary of previous generations of evolution, individuals are selected for excellence (where "excellence" is defined by a person's fitness value). In the "mating" process, one parent comes from the population individual, and the other comes from the "mating population." After the completion of the "mating" process, the "corresponding population" will be updated immediately after notification, and the applicability of each generation

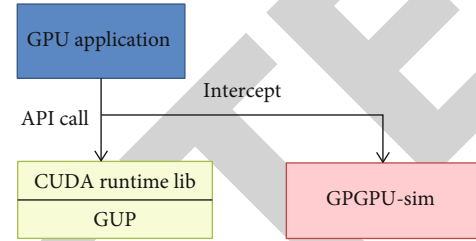


FIGURE 2: CUDA application execution path.

TABLE 2: Simulator output data.

Output data	Describe
gpu_sim_cycle	The running cycle of the current kernel
gpu_sim_nsn	The number of running instructions in the current kernel
gpu_tot_sim_cyle	Total running cycle of current kernel
gpu_tot_ipc	Number of instructions per cycle for all kernels

TABLE 3: Mean value of key parameters GA-TP and heft.

	Scheduling length	Acceleration ratio
GA-TP	109.5	0.598
HEFT	148.7	0.789

and the "breeding individual" will be compared. If the new one is higher, replace "number." Otherwise, go to the next population individual and continue the comparison.

Therefore, GA-TP algorithm is also a kind of genetic algorithm. It is an optimization calculation model of biological evolution process of genetic mechanism in the past. It is a method to simulate the natural evolution process and search and analyze the optimal solution, which can give an infinitely close to the optimal solution in a reasonable time.

### 3. Investigation and Research of AI Technology in GPU Scheduling Algorithm Optimization

**3.1. Experimental Environment.** This article uses the GPGPU-Sim simulator to implement and verify the GA-TP programming algorithm. This is a widely used GPGPU simulator with cycle-level accuracy. It can configure configuration files to simulate various popular GPUs and independently designed GPU architectures. GPGPU-Sim

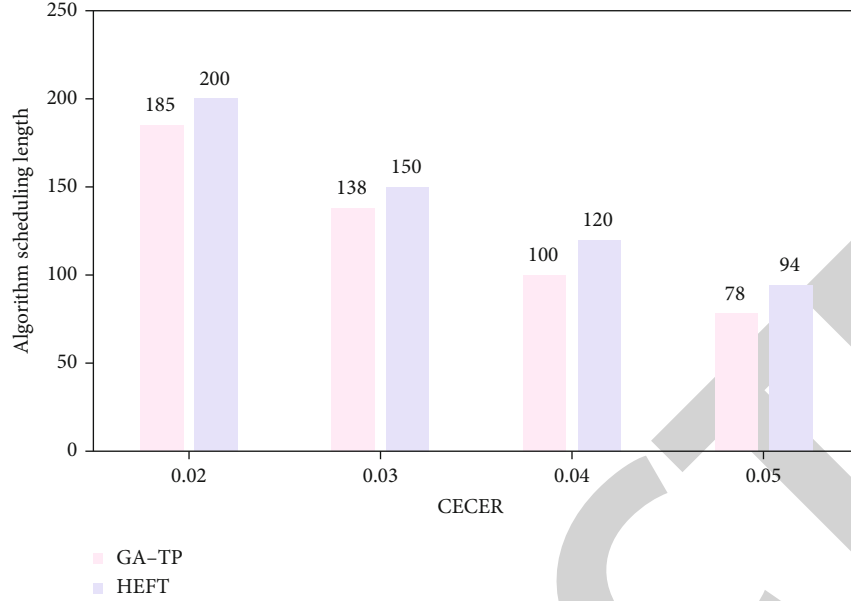


FIGURE 3: Comparison of algorithm scheduling length.

can perform CUDA and OpenCL reference tests for simulation testing. The simulation parameters are shown in Table 1.

### 3.2. Data Preprocessing

**3.2.1. Algorithm Speedup.** Algorithm acceleration is another important parameter for evaluating the performance of scheduling algorithms. All tasks in the DAG job graph are assigned to the processor with the shortest calculation time for the secondary job. This runtime is called the serial runtime load. Algorithm acceleration refers to the ratio of the charging time of parallel execution of DAG tasks to the loading time of serial execution. The calculation formula of the acceleration algorithm is shown as follows:

$$AS = \frac{AMS}{\min_{p_j \in P} \left( \sum_{T_i \in T} w(T_i, p_j) \right)}. \quad (1)$$

In the formula, AMS is the task scheduling length of the algorithm,  $P$  is the processor set, and  $T$  is the task set of the DAG graph.

**3.2.2. Than Scheduling Length.** In different application scenarios, the characteristics of DAG graphs for different computing tasks may be slightly different. Due to these differences, the experimental results of the algorithm scheduling length may have different metric scales to avoid experimental errors of different metric scales. This experiment introduces a ratio scheduling length (SLR) parameter to quantify the scheduling length and the definition of SLR as shown as follows:

$$SLR = \frac{AMS}{\sum_{T_i \in CP_{\min}} \min_{p_j \in \{w_{i,j}\}}}. \quad (2)$$

In the formula,  $w_i$  and  $j$  represent the execution time of the task  $T_i$  on the processor  $p_j$ , and the denominator represents the sum of the minimum computational overhead of all tasks on the critical path.

**3.2.3. Calculate the Toll Ratio.** For a specific task graph, the calculation ratio refers to the ratio of the average cost calculated during the execution of the task to the average cost of communication between tasks, defined as follows:

$$CECER = \frac{(1/t) \sum_{T_i \in T} w_i}{(1/e) \sum_{\text{edge}(T_i, T_j) \in E} C_{i,j}}. \quad (3)$$

In the formula,  $T$  is the set of all tasks in the task graph,  $t$  is the number of tasks included in the task set  $T$ ,  $w_i$  is the calculation cost of the task, and  $E$  is the set of edges between all task nodes in the task graph.

## 4. Investigation and Research Analysis of AI Technology in GPU Scheduling Algorithm Optimization

**4.1. The Simulator Extracts the Overall Performance Data Analysis of the GPU.** The performance of the simulation architecture is highly related to the actual hardware. When GPGPU-Sim version 3.1.0 simulates the NVIDIA Fermi architecture, the simulation accuracy rate reaches 97.35%. When simulating the NVIDIA GT200 architecture, the simulation accuracy rate reached 98.37%. The GPU performance simulated by GPGPU-Sim has been strictly confirmed to be the same as the actual GPU hardware.

Figure 2 shows the execution path of the CUDA application on the GPU hardware and the GPGPU-Sim simulator.

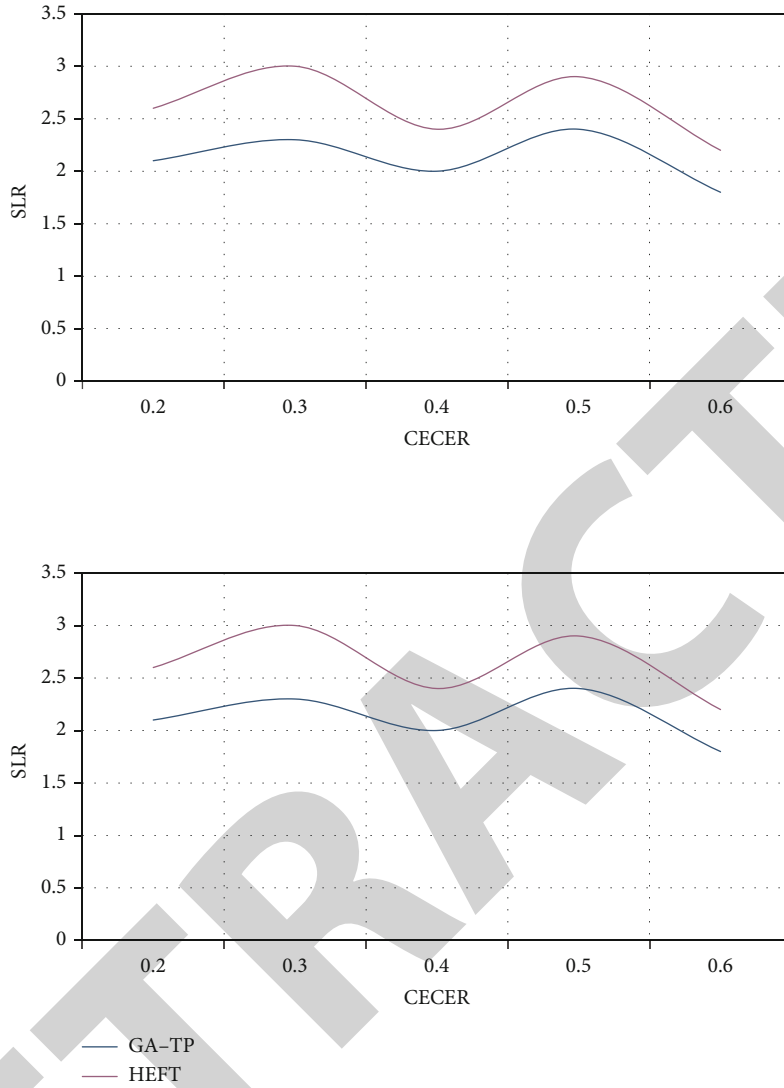


FIGURE 4: Comparison of SLR parameters of algorithm.

In a normal GPU, when the CUDA application is running, the host code is executed on the CPU, and the device code calls the API from the CUDA runtime library, and then, the CUDA runtime library sends a request to the GPU to run the code. There is a function library similar to the CUDA runtime library in GPGPU-Sim. When the CUDA program calls the API, the operating system will call the corresponding API from the GPGPU-Sim function library, and the function library will send the request to the GPGPU-Sim simulator to execute the device code in the simulator.

In the performance simulation mode, the GPGPU-Sim simulator extracts a lot of useful data to help us better understand the results of running the application. Some important output data are shown in Table 2. `Gpu_tot_ipc` describes the number of commands per application cycle. This parameter is generally used to measure the overall performance of the GPU. GPGPU-Sim can also generate performance data for various components, such as cache, memory, and network interfaces.

**4.2. GA-TP and HEFT Scheduling Algorithm Comparison.** In order to avoid errors caused by human factors such as measurement errors, the laboratory uses 10 guided acyclic graphs, and each graph is checked 3 times. All basic parameter values are the average of 3 experiments used. In order to see the improved results of the GA-TP algorithm proposed in this article more clearly, this experiment compares the GA-TP algorithm with the HEFT algorithm. The results are shown in Table 3.

Figure 3 shows the comparison diagram of the scheduling length algorithms of GA-TP and HEFT. Through the comparison results of the scheduling length of the two algorithms, it is obvious that the scheduling length of GA-TP algorithm is significantly lower than that of HEFT algorithm at different experimental values. The results show that the scheduling length of GA-TP algorithm is significantly shortened.

The GA-TP algorithm developed at this time is much smaller than the HEFT algorithm in the vertical programming algorithm, and the vertical programming algorithm is

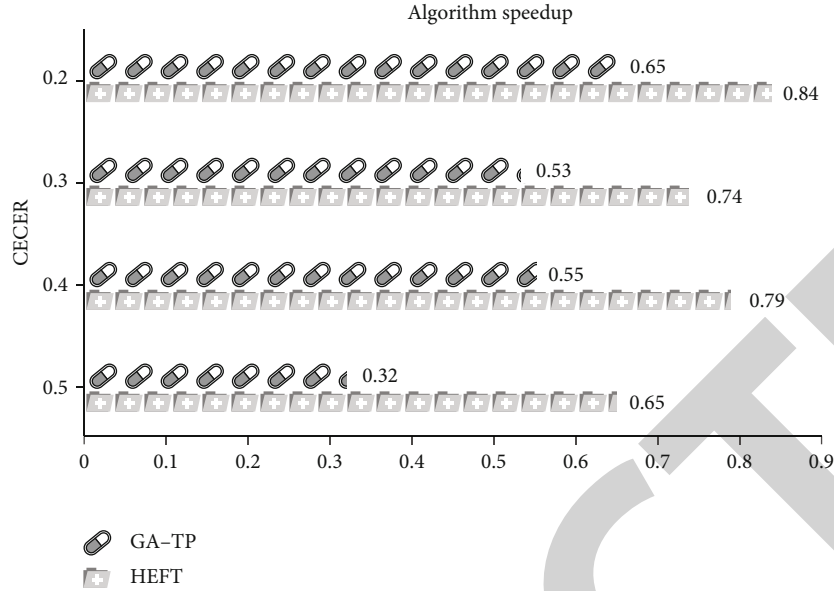


FIGURE 5: Algorithm speedup comparison.

reduced by more than 15% on average, as shown in Figure 3. This part of the performance improvement mainly comes from the workload technology. By paying attention to the adjacent work sections in the work screen, the sensitivity of work is improved, the number of work sections is reduced, and the communication cost between tasks is reduced. For the horizontal axis transmission rate, the lower the transmission rate, that is, the more frequent the interaction between functional components and the higher the communication cost, the more obvious the advantages of the GA-TP algorithm, as shown in Figure 4.

For a given DAG model, when all functions are serial, the time cost is constant; that is, the coefficient is constant, and the acceleration corresponds to the programming length of the molecular algorithm; that is, the result and the acceleration schedule of the algorithm are negatively correlated with the coefficient (0.1), because approximate acceleration of 1 will lengthen the scheduling algorithm, and the result of the scheduling algorithm will be worse. The speed-up ratio of GA-TP algorithm is significantly lower than that of HEFT algorithm, and the average speed-up ratio has dropped by about 25%, indicating that the processing effect of GA-TP algorithm is better, as shown in Figure 5. At the horizontal level, the lower the calculation rate, that is, the higher the communication load between functional components, the better the programming effect of the GA-TP algorithm.

In short, the GA-TP algorithm is more suitable for computing tasks with frequent communication between auxiliary nodes. In addition, it needs to be noted that the fluctuation of the three basic parameter values with the calculation ratio of the horizontal axis does not matter, because the 10 points on the curve correspond to 10 DAG diagrams and the horizontal comparison of the calculation amount and the communication amount of each DAG diagram are meaningless.

## 5. Conclusions

Artificial intelligence technology saves people's intellectual and physical consumption to a certain extent, improves industrial productivity, and improves human daily life. It can be said that it has made a huge contribution to the rapid development of society, and this trend will gradually strengthen over time. With the increase in the number of Internet users, the rapid expansion of data, and the introduction of new applications, different data centers are facing the challenge of improving resource utilization and providing distribution services. Therefore, the computing power of GPU has also been continuously improved under the artificial intelligence technology. Through the continuous improvement and improvement of the functional characteristics of GPU, it has been widely used in the field of intelligent computer. In order to make full use of the full range of GPU resources, this paper proposes an effective resource distribution and workflow planning framework for robust service delivery scenarios under multitask GPU distribution. Finally, the GA-TP algorithm and the HEFT algorithm are compared through the basic parameters of AMS, AS, SLR, and CECER. The result shows that the programming time of the new GA-TP programming algorithm is reduced by more than 20%.

## Data Availability

The data underlying the results presented in the study are available within the manuscript.

## Conflicts of Interest

There is no potential conflict of interest in our paper.

## *Retraction*

# **Retracted: Three-Dimensional DV-Hop Localization Algorithm Based on Hop Size Correction and Improved Sparrow Search**

### **Wireless Communications and Mobile Computing**

Received 12 December 2023; Accepted 12 December 2023; Published 13 December 2023

Copyright © 2023 Wireless Communications and Mobile Computing. This is an open access article distributed under the Creative Commons Attribution License, which permits unrestricted use, distribution, and reproduction in any medium, provided the original work is properly cited.

This article has been retracted by Hindawi, as publisher, following an investigation undertaken by the publisher [1]. This investigation has uncovered evidence of systematic manipulation of the publication and peer-review process. We cannot, therefore, vouch for the reliability or integrity of this article.

Please note that this notice is intended solely to alert readers that the peer-review process of this article has been compromised.

Wiley and Hindawi regret that the usual quality checks did not identify these issues before publication and have since put additional measures in place to safeguard research integrity.

We wish to credit our Research Integrity and Research Publishing teams and anonymous and named external researchers and research integrity experts for contributing to this investigation.

The corresponding author, as the representative of all authors, has been given the opportunity to register their agreement or disagreement to this retraction. We have kept a record of any response received.

### **References**

- [1] P. Gou, Z. Yu, X. Hu, and K. Miao, "Three-Dimensional DV-Hop Localization Algorithm Based on Hop Size Correction and Improved Sparrow Search," *Wireless Communications and Mobile Computing*, vol. 2022, Article ID 1540110, 19 pages, 2022.

## Research Article

# Three-Dimensional DV-Hop Localization Algorithm Based on Hop Size Correction and Improved Sparrow Search

Pingzhang Gou , Zhaoyang Yu , Xinyue Hu , and Kai Miao 

College of Computer Science and Engineering, Northwest Normal University, China

Correspondence should be addressed to Pingzhang Gou; [goupz@nwnu.edu.cn](mailto:goupz@nwnu.edu.cn)

Received 30 December 2021; Revised 30 March 2022; Accepted 13 April 2022; Published 11 May 2022

Academic Editor: Ali Kashif Bashir

Copyright © 2022 Pingzhang Gou et al. This is an open access article distributed under the Creative Commons Attribution License, which permits unrestricted use, distribution, and reproduction in any medium, provided the original work is properly cited.

Acquiring precise localization information of sensor nodes is very important in wireless sensor networks. The 3DDV-hop localization algorithm suffers from large localization errors and high energy consumption. In order to improve positioning accuracy and reduce energy consumption, a 3DDV-hop node localization algorithm (3D-HCSSA) based on hop size correction and improved sparrow search optimization is proposed. The algorithm redefines the amendment factor and reduces the cumulative error caused by the hop counts in the traditional algorithm. A maximum distance similar link method based on a similar path search is proposed to find the most similar known node path pair from the target node to the noncoplanar known node link and correct the hop size between multihop counts. The sparrow search algorithm is improved by using the  $k$ -means clustering and sine cosine search strategy, which solves the problem that the traditional sparrow algorithm is easy to fall into the local optimum, accelerates the convergence speed, corrects the position deviation of the target node, and improves the positioning accuracy. Experiments demonstrate that the 3D-HCSSA algorithm can improve positioning accuracy and reduce energy consumption. Compared with the 3DDV-hop algorithm, 3D-GAIDV-hop algorithm, and HCLSO-3D algorithm, the 3D-HCSSA positioning accuracy is significantly improved.

## 1. Introduction

Wireless sensor networks (WSNs) is a multihop counts wireless network that incorporates nodes to sense, collect, and process target node information, enabling access to objective physical information, extending information acquisition capabilities, and providing the most direct and accurate information in next-generation wireless networks [1]. In next-generation technology, Non-orthogonal Multiple Access (NOMA) allocates different power to known nodes (a node whose own position is known) and target nodes which have different residual energy in WSNs, saving the known node energy consumption problem by using the Successive Interference Cancellation (SIC) technique. Therefore, this technique can be extended to be used in next-generation networks for larger-scale scenarios [2]. Localization information is one of the basic elements of sensor network monitoring data and in many cases is the basis of the application. Monitoring data without localization information is often worthless, for example, monitoring events such

as forest fires and the presence of enemy vehicles on the battlefield, all of which need to determine the specific localization of the event, to achieve the localization, and to track the monitoring target. Therefore, the estimation of target node location is a key issue in wireless sensor networks [3]. It is a challenging work about how to design a localization algorithm with low hardware requirements and low communication and computing overhead. Researchers have proposed some WSNs localization algorithms, which can be broadly classified into two categories: range-based and range-free algorithms [4]. The range-based algorithm calculates the localization of target nodes by measuring the distance or angle information between nodes. Although the effect is more accurate, it requires complex and expensive hardware equipment [5]. The main algorithms based on the range-based approach are the Time of Arrival (TOA) method [6, 7], Time Difference of Arrival (TDOA) method [8], and Angle of Arrival (AOA) method [9]. The localization method based on the range-free approach does not need distance and angle information but only carries out

node localization according to some information such as network connectivity. Without additional complex equipment, the positioning accuracy is lower than that of the algorithm based on the range-based method. The typical localization methods based on the range-free algorithm include the centroid algorithm [10], approximate triangle interior point test algorithm [11, 12], and DV-hop localization algorithm [13].

The DV-hop localization algorithm was proposed by Drağoş et al. [14]. It is a localization method of WSNs that directly measures the distance among nodes without additional hardware equipment [15]. In terms of implementation, the DV-hop localization algorithm only relies on the connectivity of the whole network, so the implementation of the DV-hop localization algorithm is relatively simple and less costly to set up the network. However, cumulative errors occur during the hop size estimation stage, resulting in large errors between the expected and actual distances between the known node and the target node. In the localization stage, there is also a certain error between the actual position and the expected position of the target node. In the DV-hop localization algorithm, a swarm intelligence optimization algorithm is usually used to reduce the localization error of target nodes. Nowadays, swarm intelligence algorithms are commonly used in DV-hop localization algorithms to optimize algorithms to reduce the target node localization error; classical swarm intelligence algorithms such as particle swarm optimization algorithm (PSO) [16], genetic algorithm [17], ant colony optimization algorithm [18], grey wolf optimization algorithm [19], and bacterial foraging optimization algorithm [20]; and some novel optimization algorithms proposed in recent years, such as the sparrow search algorithm [21], the squirrel search algorithm [22], and the butterfly optimization algorithm [23]. Particle swarm optimization is a common algorithm used by researchers to optimize the DV-hop localization algorithm. In Kanwar and Kumar [24] by adjusting a few particle parameters and extending the target node to the selected known node, the objective function of the particle swarm optimization algorithm is established to provide better positioning accuracy in resource-constrained environment through iteration. However, the increase in parameters will lead to the complexity of the operation and increase the complexity of the algorithm. Singh and Sharma [25] first found the feasibility region of each target node and determined the initial position velocity of the particle in the feasibility region. Secondly, update the particles in the estimation of the particle fitness function. Finally, the optimal position of target nodes can be determined after the iteration is completed by setting the number of iterations. Singh and Sharma [26] used the PSO algorithm to further correct the proposed two-dimensional hyperbolic algorithm to determine the localization of target nodes. Firstly, find out the survival area of each target node and determine the initial position and velocity of the particles in the feasible area; secondly, estimate the fitness of each particle; and finally, obtain the optimal solution through iteration, which is the optimal position of the target node. However, this algorithm does not optimize the PSO algorithm, which will result in slow convergence; the algorithm is easy to fall into a local optimum during the solution process; and the algorithm complexity and space complexity

will also increase. In Zhang et al. [27], the PSO algorithm is used to further correct the proposed two-dimensional hyperbolic algorithm to determine the localization of unknown nodes. Firstly, find out the survival region of each unknown node, and determine the initial position and velocity of particles in the feasible region; secondly, the fitness of each particle is estimated; and finally, the optimal solution obtained through iteration is the optimal localization of unknown nodes. The algorithm improves the positioning accuracy but increases the number of operations during the iterative process, which leads to an increase in the complexity of the algorithm. Fang et al. [28] used the exponentially decreasing function to improve the inertia weights because the inertia weight values in the PSO algorithm affect the network optimization speed effect, and the improved PSO algorithm can correct the position of the target node more effectively, thus improving the positioning accuracy. However, the method only optimizes the algorithm itself, but not the global optimization of the algorithm, so the algorithm is prone to problems such as local optimization.

Other swarm intelligence algorithms optimize DV-hop localization algorithms. Cai et al. [29] proposed weight convergence analysis of the DV-hop localization algorithm based on the genetic algorithm (MW-GADV-hop). Since the traditional weight model does not analyze the convergence and ignores the relationship between weight and error, this algorithm establishes a weight model based on error variation and proves the convergence of the model, which improves the positioning accuracy. However, some results in the weight model with error variation do not converge to 1/4 communication radius, so the convergence of the model is insufficient, which will eventually affect the positioning accuracy. Kanwar and Kumar [30] proposed a DV-hop based range-free localization algorithm for WSNs using runner-root optimization (RRADV-hop). The rotary root algorithm is used to determine the fitness function, and the one with the smallest value of the fitness function through iteration is the corrected target node coordinate. The rotation root optimization algorithm is not initialized, leading to slow convergence of the algorithm and affecting the positioning accuracy. Mohanta and Das [31] proposed a class topper optimization-based improved localization algorithm in a wireless sensor network (CTODV-hop). A two-dimensional hyperbolic algorithm is used to calculate the target node localization, and by the class topper optimization approach, the efficiency and reliability of the algorithm are improved, the localization error is reduced, and the complexity of the algorithm is decreased. Jacob et al. [32] proposed a modified search and rescue optimization-based node localization technique in WSNs (MSRODV-hop). By the MSRO-NLT method, the problem of solving the target node coordinates is transformed into the problem of solving the minimum in mathematics; this method reduces the number of iterations of the algorithm. However, the algorithm only optimizes the local optimum and does not solve the problem of fast convergence, and it is difficult to cover all solution sets completely.

We combine the above studies, a 3DDV-hop localization algorithm based on hop size correction and improved sparrow

search is proposed, which further reduces the hop size and localization error and improves the positioning accuracy. The main work of this article is as follows:

- (1) The maximum distance similar link method is proposed. Based on the traditional similar path search algorithm, a pair of known node paths most similar to the link from the target node to a specific noncoplanar known node is found, and the multihop size between the known node and the target node is modified, which reduces the hop size calculation overhead and improves the positioning accuracy of the algorithm
- (2) The  $K$ -means clustering algorithm is introduced to solve the problem that the traditional sparrow search algorithm is easy to fall into the local optimum when initializing. In the optimization scrounger position update stage, in order to avoid the poor effect of the scrounger position update stage in finding the optimal, the positive cosine search strategy is introduced to enhance the convergence of the sparrow search algorithm and improve the convergence accuracy. The fitness function is redesigned so that the fitness value can correct the target node position deviation after iteration

The remainder of this article is summarized as follows. The second part summarizes the related work. The third part states the 3DDV-hop localization algorithm, the traditional sparrow search algorithm, and the improved sparrow search algorithm. The fourth part mentions the localization algorithm of 3D-HCSSA. The fifth part analyzes the experimental results. The sixth part draws conclusions.

## 2. Related Work

The 3DDV-hop algorithm mainly locates nodes by network connectivity and topology structure. It has low requirements on hardware devices and simple calculation, but nodes are distributed in different areas, resulting in different node densities. The average hop size of target nodes depends on one known node in the whole region. When there are too many known nodes in the region, the hop size of nodes will be wasted, and one known node cannot reflect the network environment of WSNs. If the known node is close to the target node and there is an error in the average hop size itself, the error will be directly transmitted to the target node; then, the error accuracy within the whole network decreases.

In the 3DDV-hop localization algorithm, various optimization algorithms and improvement methods can reduce the node localization error. Gou et al. [33] proposed a three-dimensional localization algorithm (HCLSO-3D) based on hop correction and lion swarm optimization in WSNs. The fitness function values of each type of lion are rearranged in ascending order, and the position of the lion with the smallest fitness value is the optimal position of the target node. The position of the lion king with the lowest fitness value was the optimal localization of the target node. However, this article

only improves the fitness function and does not initialize the lion swarm algorithm, which leads to problems such as local optimization and slow convergence speed. Kaushik et al. [34] proposed an improved 3DDV-hop localization algorithm (I3D-DVLAIN) based on neighbouring node information. By adopting a new method of solving the equations, subtract the last distance equation from all the other distance equations and then divide the equations by the maximum distance equation. Therefore, the error propagation is reduced, and the mathematical analysis of error propagation proves that the method can effectively improve the positioning accuracy. Due to the large number of parameters and related equations in the operation of this method, the calculation difficulty and algorithm complexity are increased during the calculation. In Kanwar and Kumar [35] firstly, the localization of the target node is corrected by the hyperbolic method. Then, the optimal target node localization was obtained by iterating through single-objective and multiobjective functions, respectively, which improved the robustness of the algorithm. However, there are many function variables and complex process in the iterative process, which increases the algorithm overhead. Cheng et al. [36] introduced that the ratio of the number of common neighbour nodes belonging to two nodes that are neighbour nodes to each other to the number of all neighbour nodes of the two nodes is used to replace the volume ratio of the area where the corresponding nodes are located, reversely solve the relation between the continuous hop count and the node ratio, and use the parameter-corrected relationship to calculate the continuous hop count, thereby reducing the distance estimation error, improving the positioning accuracy, but also increasing the algorithm complexity. Cai et al. [37] proposed a multiobjective three-dimensional DV-hop localization algorithm (N2-3DDV-hop) based on NSGA-II. Firstly, a multitarget model and NSGA-II were added to analyze the limitations of the traditional single-target localization model. Secondly, a multiobjective localization model is proposed in combination with the NSGA-II algorithm, and the target node coordinates are derived by iterating according to the model. Due to the large number of parameters and related equations in the algorithm, the calculation difficulty and algorithm complexity are increased. Sharma and Kumar [38] proposed using the genetic algorithm to improve the range-free localization of three-dimensional WSNs (3D-GAIDV-hop). Firstly, the genetic algorithm is introduced to accelerate the convergence speed. Secondly, the fitness function is redesigned; the optimal position of the target node coordinates is the one with the smallest adaptation value by iteration. The minimum fitness value is the optimal localization of the target node coordinate, and the positioning accuracy is improved. However, there is the problem that the algorithm is difficult to cover all solution sets.

Based on the above research, this article is mainly aimed at the inaccurate problem of hop count division, hop size setting, and target node coordinate calculation of the 3DDV-hop localization algorithm and proposes a 3DDV-hop localization algorithm based on hop size correction and improved sparrow search. With the HCSSA localization algorithm (3D-DV-hop based on hop size correction and improved sparrow search algorithm), this article divides the optimal hop count by redefining the amendment factor and proposes the maximum



distance similar link method to correct the multihop size between nodes.  $K$ -means clustering and sine-cosine search strategy are introduced to improve the traditional sparrow search algorithm to correct the coordinate deviation of target nodes. In conclusion, the 3D-HCSSA localization algorithm improves the node positioning accuracy and reduces the algorithm energy consumption.

### 3. 3DDV-Hop Localization Algorithm and Sparrow Search Algorithm

**3.1. 3DDV-Hop Localization Algorithm.** The 3DDV-hop (three-dimensional distance vector-hop) localization algorithm is a distributed localization algorithm based on the range-free approach [39]. The algorithm consists of three phases.

*Step 1.* Calculate the minimum hop count of the target node and each known node. The known node floods its information group to the neighbour node, including the localization information of the known node and the hop count with an initial value of zero. By receiving the minimum counts of hop for each known node, ignoring the group from the same known node with a larger count of hop, the hop count is automatically added by 1 and finally forwarded to the neighbour nodes.

*Step 2.* Calculate the distance between the target node and the known node. The known nodes calculate the average hop size by each known node based on the minimum counts of hop of other known nodes recorded in Step 1, and broadcast the average hop size information in the network to estimate the average hop size:

$$\text{AveHopsize}_I = \frac{\sum_{I \neq J} \sqrt{(x_I - X'_J)^2 + (y_I - Y'_J)^2 + (z_I - Z'_J)^2}}{\sum_{I \neq J} h_{IJ}}, \quad (1)$$

where  $(x_I, y_I, z_I), (X'_J, Y'_J, Z'_J)$  are the coordinates of known nodes  $I$  and  $J$ , respectively;  $h_{IJ}$  is the hop count between the two known nodes; and  $\text{AveHopsize}_I$  is the average hop size of known node  $I$ . Each known node uses equation (1) to estimate the average actual distance per hop based on the localization information and the number of hop counts away from other known nodes recorded in the first phase.

The distance from the known node to the target node is given by the following equation:

$$\text{HS}_{Iu} = \text{AveHopsize}_I \times \text{Hop}_{Iu}, \quad (2)$$

where  $\text{Hop}_{Iu}$  is the hop count between the known node  $I$  and the target node  $u$ .

*Step 3.* Calculate the coordinates of target nodes. After deriving the expected distances between four and more target nodes to the known node in a three-dimensional space, the

coordinates of the target nodes are calculated by the great likelihood estimation method.

**3.2. Sparrow Search Algorithm.** The sparrow search algorithm (SSA) is a swarm intelligence optimization algorithm inspired by sparrow foraging and antipredation behaviour proposed by Xue and Shin [21] in 2020. There are two roles in SSA: producer and scrounger. Producers forage and provide guidance, while the scrounger obtains food through the producer. In order to better obtain quality food, members of the population monitor each other's behaviour, and in order to increase their own predation rate, scroungers compete for food with the high intake sparrows. The localization of the sparrow population can be expressed as

$$\Pi = \begin{bmatrix} \Pi_{1,1} & \Pi_{1,2} & \cdots & \cdots & \Pi_{1,d} \\ \Pi_{2,1} & \Pi_{2,2} & \cdots & \cdots & \Pi_{2,d} \\ \vdots & \vdots & \vdots & \vdots & \vdots \\ \Pi_{n,1} & \Pi_{n,2} & \cdots & \cdots & \Pi_{n,d} \end{bmatrix}, \quad (3)$$

where  $n$  represents the number of the sparrow population and  $d$  is the optimal dimension.

The fitness of each sparrow is

$$\text{Fitness}_{\Pi} = [\zeta(\Pi_1), \zeta(\Pi_2) \cdots \zeta(\Pi_n)]^T, \quad (4)$$

where  $\zeta(\Pi_1), \zeta(\Pi_2) \cdots \zeta(\Pi_n)$  are the fitness values of each sparrow, respectively.

Define producer updated localization:

$$x_{i,j}^{t+1} = \begin{cases} x_{i,j}^t \cdot \exp\left(\frac{-i}{\alpha \cdot \text{iter}_{\max}}\right), & \text{if } R_2 < ST, \\ x_{i,j}^t + Q \cdot L, & \text{if } R_2 \geq ST, \end{cases} \quad (5)$$

where  $t$  represents the current iteration number and  $\text{iter}_{\max}$  represents a constant of the maximum iteration number.  $x_{i,j}$  represents the position information of the  $i$ th sparrow in dimension  $j$ .  $\alpha \in (0, 1]$  is a random number.  $R_2 \in [0, 1]$  and  $ST \in [0.5, 1]$  represent the warning value and the safe value, respectively.  $Q$  is a random number.  $L$  represents a  $1 \times d$  matrix. When  $R_2 < ST$ , it represents that there are no predators around the foraging environment at this time, and the producer can perform extensive search operations. When  $R_2 \geq ST$ , indicating the detection of a predator and alerting members, all sparrows fled to a safe place before foraging.

The updated localization of the scrounger is defined as follows:

$$x_{i,j}^{t+1} = \begin{cases} Q \cdot \exp\left(\frac{x_{\text{worst}}^t - x_{i,j}^t}{i^2}\right), & \text{if } i > \frac{n}{2}, \\ x_p^{t+1} + |x_{i,j}^t - x_p^{t+1}| \cdot A^+ \cdot L, & \text{otherwise,} \end{cases} \quad (6)$$

where  $X_p$  is the producer optimal localization and  $X_{\text{worst}}$  is the global worst position.  $A$  represents a matrix of  $1 \times d$ ,

where the elements have random values of  $-1$  or  $1$ , and  $A^+ = A^T(AA^T)^{-1}$ .  $i > n/2$  represents that the  $i$ th scrounger with a low fitness value has not obtained food, is in a hungry state, and needs to forage for food in order to forage for more food in other places.

SSA has strong local search ability and fast convergence speed but weak global search ability and weak operation of jumping out of the local optimum. Therefore, this article initializes the initial coordinates of known nodes and target nodes and proposes a method to further optimize the SSA when figuring out the target node coordinates.

**3.3. Improved Sparrow Search Algorithm.** This article improves the sparrow search algorithm by introducing  $K$ -means clustering and sine-cosine search strategy, using mathematical methods and clustering algorithm to optimize the sparrow search algorithm, solving the problem that the sparrow population is prone to fall into the local optimum when initializing, and improving the convergence accuracy and optimization effect of the traditional SSA. The improved SSA is applied to the third phase of the 3DDV-hop localization algorithm calculating target node coordinates. Through simulation experiments, the improved SSA accelerates the convergence speed and solves the problem that the algorithm is easy to fall into the local optimum and corrects the deviation of target node coordinates. In summary, the improved SSA can solve the problem of position deviation when calculating the target node coordinates and improve the positioning accuracy.

**3.3.1.  $K$ -means Clustering Initialization.** Since the SSA uses the random distribution principle in population initialization, the principle suffers from the problem that the sparrow population initialization cannot completely cover the solution space and there are coverage voids, which makes it difficult to traverse various cases of the solution set in the population and leads to the problem that the algorithm is prone to fall into the local optimum under complex multi-peaked functions. Therefore, in this article, the  $K$ -means clustering method is used to solve the deficiency that the algorithm is prone to fall into the local optimum when the population is initialized [40].

By choosing a similarity measurement method, the two-sample producer and scrounger are divided separately. Among them, the producer represents the known node coordinate, and the scrounger represents the target node coordinate. This partitioning makes the data within the same category as similar as possible. Using the Euclidean distance as the measurement standard, the samples with similar distances are divided into different class clusters until the set of the two samples initially divided is obtained. The mean value of each class cluster sample was taken as the centre of the next cluster, and the distance between the remaining samples and the new cluster centre was calculated and classified. Iterate repeatedly until the clustering criterion function converges or reaches the number of iterations and finally improves the global search ability of SSA.

$w = \{\Theta, \Xi\}$  is divided into two clusters:  $w_1, w_2$ , where  $w_i = (\Theta_i, \Xi_i)^T$ ,  $c_1, c_2$  are the two initial clustering centers, and the methods used in the clustering process are as follows:

Euclidean distance between samples  $\Theta, \Xi$ :

$$d(\Theta, \Xi) = \sqrt{(\Theta - \Xi)^T(\Theta - \Xi)}. \quad (7)$$

Average distance from sample  $\Theta$  to all samples:

$$m = \frac{1}{n} \sum d(\Theta, \Xi). \quad (8)$$

Sample variance:

$$\text{var} = \frac{1}{n-1} \sum [d(\Theta, \Xi) - m]^2. \quad (9)$$

Average distance of data set samples:

$$d = \frac{2}{n(n-1)} \sum \sum d(\Theta, \Xi). \quad (10)$$

Sum of squares of error:

$$S = \sum_{i=1}^2 \sum (\Theta - c_i)^2. \quad (11)$$

Assuming a population size of 100, Figures 1 and 2 are the populations initialized by random distribution and  $K$ -means clustering, respectively. After the comparison between Figures 1 and 2, it is obvious that the population distribution of the latter is more uniform than that of the former, which fully covers the knowledge space. Therefore, the algorithm has better ergodicity and improves the global search ability.

**3.3.2. Sine-Cosine Search Strategy.** The sine and cosine search strategy was proposed by Mirjalili in 2016 [41], and its main idea is to enhance the convergence of the algorithm by iteratively continuously optimizing the solution set of the objective function through the mathematical method sine and cosine function properties for the local and global search of the population. In the SSA, the scrounger position update is mainly influenced by the discoverer, which leads to the disadvantage of poor algorithm search effect, and in order to improve the convergence accuracy and search effect, this article uses an improved sine and cosine search strategy to optimize the producer position [41].

The improved sine and cosine search strategy expression can be expressed as

$$\phi(q+1) = \begin{cases} \phi(q) + r_1 \cdot \sin(r_2) \cdot D_{r_3} < 0.5, \\ \phi(q) + r_1 \cdot \cos(r_2) \cdot D_{r_3} \geq 0.5, \end{cases} \quad (12)$$

where  $r_2, r_3$  are random factors and the corresponding value ranges are  $(0, 360^\circ)$  and  $[0, 1]$ , respectively. Among them,  $r_2$  determines the moving distance in the iterative process,  $r_3$  is

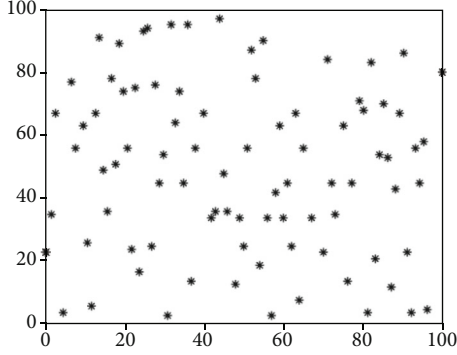


FIGURE 1: Randomly distributed initial population.

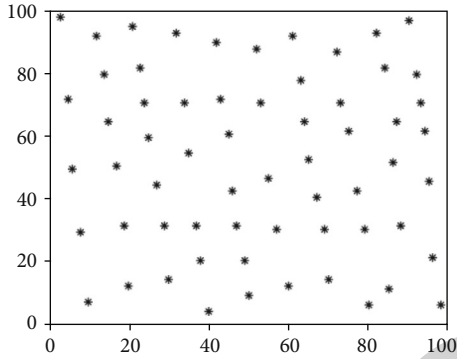


FIGURE 2: K-means cluster initialization population.

the random weight coefficient assigned to the current optimal solution to enhance (when  $r_3 > 1$ ) or weaken (when  $r_3 < 1$ ) the influence of the optimal solution on the defined distance, and  $r_1$  represents the control factor, which is a linear decreasing function that controls the fluctuation amplitude of the sine and cosine function and also determines the movement direction of the iteration. If  $r_1 < 1$ , the next solution will move from the current solution to the region of the optimal solution; if  $r_1 > 1$ , it will move in the reverse direction. The expression of the control factor is as follows:

$$r_1 = \varepsilon \left( 1 - \frac{t}{T} \right), \quad (13)$$

where  $\varepsilon$  is a constant and  $T$  represents the maximum number of iterations.

The process of seeking optimization of the sine-cosine optimization algorithm mainly includes two phases: global search and local search. As the number of iterations  $t$  increases,  $r_1$  demonstrates a linear decreasing trend. Therefore, the convergence speed of the algorithm further accelerated the convergence rate. The optimized position of the scrounger is iteratively calculated by using the sine-cosine search strategy (equation (13)) and the control factor (expressions (14) and (15)).

$$D = \{|r_4 \cdot x_i(t) - x_i(t)| i = 1, 2 \dots d\}, \quad (14)$$

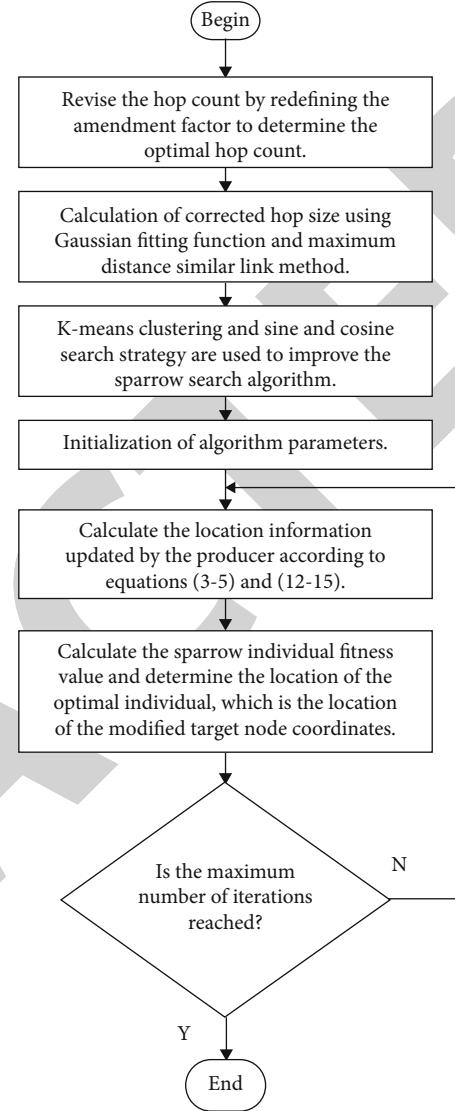


FIGURE 3: Flow chart of the 3D-HCSSA algorithm.

where  $r_4$  is the random factor on  $[0, 1]$ , which represents the switching condition of the iterative equation of the sine and cosine function.

$$r_3 = \varepsilon - \varepsilon \cdot \frac{t}{M}, \quad (15)$$

where  $M$  represents the number of iterations and  $\varepsilon$  is a constant.

#### 4. 3D-HCSSA Localization Algorithm

The 3D-HCSSA algorithm in this article is based on the hop size correction and the improved sparrow algorithm to optimize the 3DDV-hop algorithm. The 3DDV-hop algorithm is improved and optimized from three aspects: hop count division, hop size correction, and optimization of target node coordinates. The simulation results demonstrate that the improved algorithm proves that its positioning accuracy has

Algorithm 1: Finalization method to solve the sparrow optimization algorithm to solve the coordinate value  
**Input:** Known node coordinates, the distance from the target node to the corresponding known node.  
**output** Expected coordinates of target nodes.  
**Initialize a population of n sparrows and define its relevant parameters:** M, Maximum number of iterations; PD, Population Number of Producers; SD, the number of sparrows who perceive the danger; R<sub>2</sub>, Alert value; N, Total Population Quantity.  
**//Initial parameter Value Represents the initialization parameter value**  
1. **While**(t<G)**// The iteration termination condition is judged**  
2.     Sort the fitness values to find the current individual best and worst.  
3.     R<sub>2</sub>=rand (1)  
4.     **for** i=1: PD  
5.         The updated producer localization is calculated by equation (3);  
6.     **end for**  
7.     **for** i=(PD+1): N  
8.         The updated scrounger positions are calculated by equations (12-15);  
9.     **end for**  
10.     **for** i=1:SD  
11.         The sparrow position is updated by equation (6);  
12.     **end for**  
13.     Get the current latest position;  
14.     Update if the latest position is better than the previous one;  
15.     t = t +1;  
16.     **end while**  
17.     **return** X<sub>best</sub>, f<sub>g</sub>.

ALGORITHM 1: Sparrow optimization algorithm to calculate the target node coordinate value.

TABLE 1: Parameter settings.

Algorithm	Parameter
SSA	ST = 0.8 PD = 0.2SD = 0.3
LSSA	ST = 0.8 PD = 0.2SD = 0.3
HCSSA	ST = 0.8 PD = 0.2SD = 0.3

been improved from many aspects, and the node energy consumption is greatly reduced, resulting in a reduction in the overall energy consumption of the algorithm.

**4.1. Calculate the Hop Count of the Known Node.** In the 3DDV-hop algorithm, the distance between the target node within one hop of the known node and the known node in the actual network is different, which will result in lower localization accuracy. Therefore, it is necessary to optimize and improve the partition of hop count. By making a difference between the expected hop count of a known node and the perfect hop count, the ratio of the difference to the expected hop count redefines the amendment factor to reduce the cumulative error caused by hop count division. The specific steps are as follows.

**Step 1.** Set the perfect hop count. Suppose the real distance between known nodes  $i$  and  $j$  is  $d_{ij}$ ; the ratio of real distance between known nodes  $i$ ,  $j$  and the maximum communication radius  $R$  is defined as the perfect hop count  $H_{ij}$  [42]:

$$H_{ij} = \frac{d_{ij}}{R}. \quad (16)$$

**Step 2.** Set the amendment factor. The expected hop count of

a known node makes a difference with the perfect hop count, and the ratio of the difference to the expected hop count is

$$\varphi_{ij} = \frac{h_{ij} - H_{ij}}{h_{ij}}, \quad (17)$$

where  $h_{ij}$  is the expected counts of hop between known nodes  $i, j$ .  $\varphi_{ij}$  represents the amount of correction between the expected counts of hop and the perfect counts of hop which can reflect the difference between the expected counts of hop and the perfect counts of hop. Use  $\varphi_{ij}$  to redefine the amendment factor  $\omega_{ij}$  as

$$\omega_{ij} = 1 - \left( \frac{h_{ij} - H_{ij}}{h_{ij}} \right)^2. \quad (18)$$

**Step 3.** The corrected optimal hop count can be calculated by the amendment factor as

$$h'_{ij} = \omega_{ij} h_{ij}, \quad (19)$$

where  $h'_{ij}$  represents the optimal hop count.

The corrected optimal hop count obtained through the above steps can be used for the calculation of the next section.

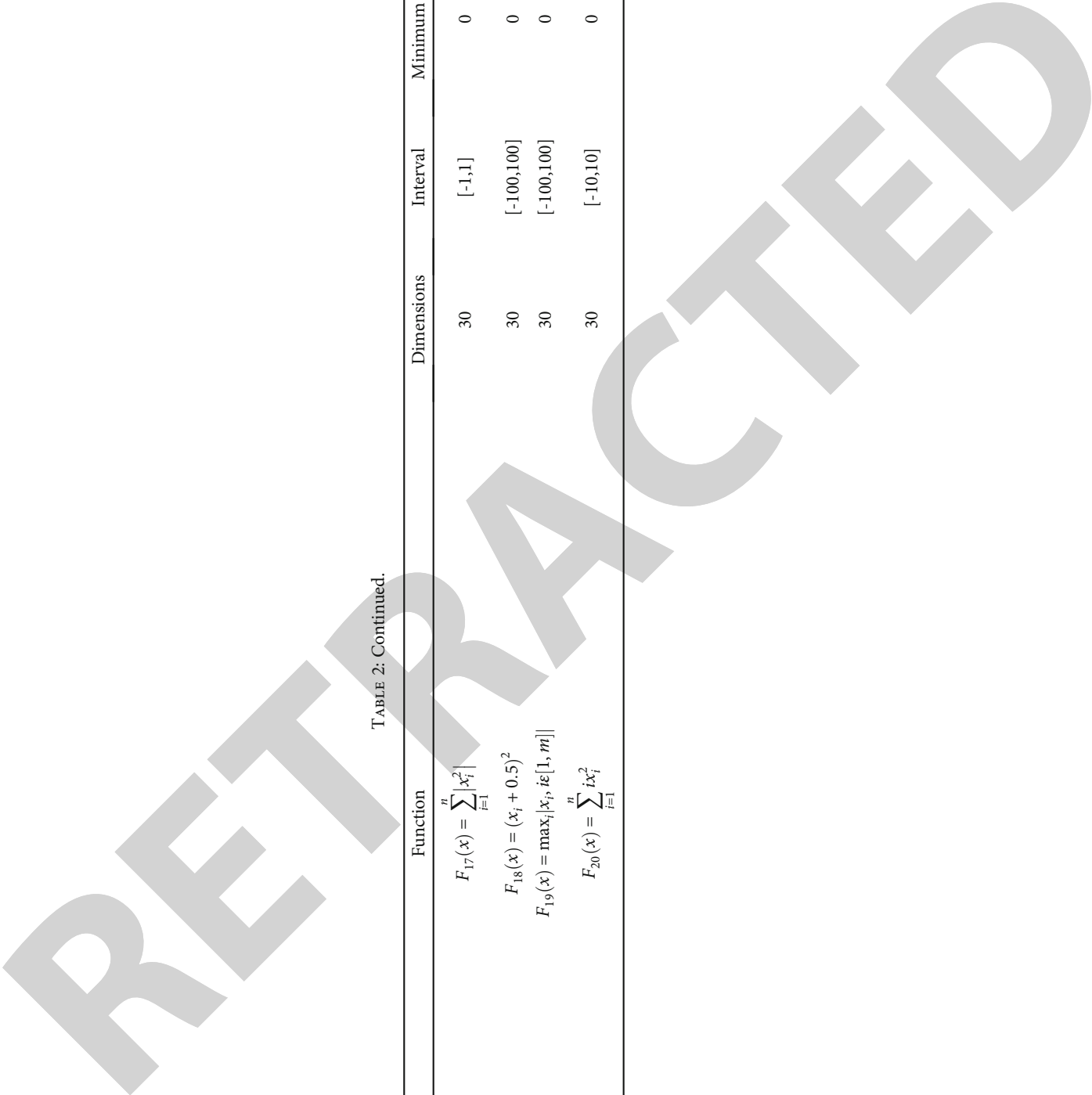
**4.2. Hop Size Correction.** This section mainly amends the one-hop size and multihop size between the known node and target node.

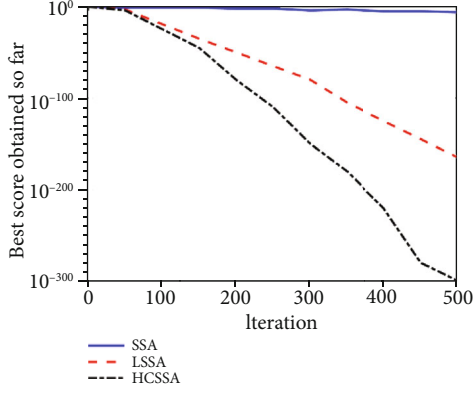
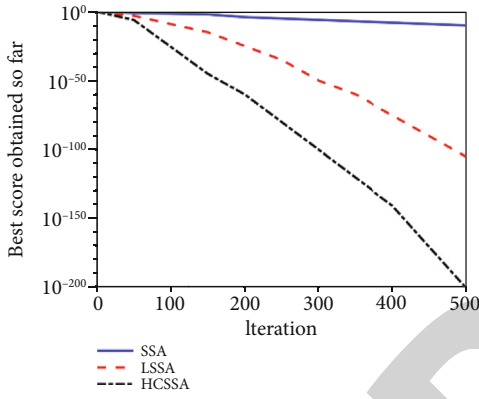
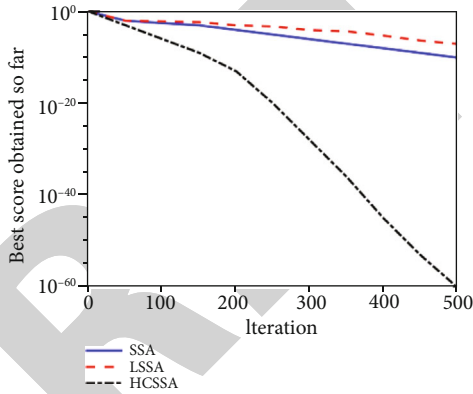
TABLE 2: 20 benchmark functions.

Number	Function	Dimensions	Interval	Minimum value
1	$F_1(x) = \sum_{i=1}^n (10^6)^{(i-1)/(n-1)} x_i^2$	30	[-100,100]	0
2	$F_2(x) = \sum_{i=1}^n \left( \sum_{j=1}^i x_j \right)^2$	30	[-100,100]	0
3	$F_3(x) = \max_i \{ x_i , 1 \leq i \leq n\}$	30	[-100,100]	0
4	$F_4(x) = \sum_{i=1}^{n-1} \left[ 100(x_{i+1} - x_i^2)^2 + (x_i - 1)^2 \right]$	30	[-30,30]	0
5	$F_5(x) = \sum_{i=1}^n ( x_i + 0.5 )^2$	30	[-100,100]	0
6	$F_6(x) = \sum_{i=1}^n ix_i^4 + \text{random}[0,1]$	30	[-1.28,1.28]	0
7	$F_7(x) = \sum_{i=1}^n ix_i^4 + r \text{and}[0,1]$	30	[-1.28, -1.28]	0
8	$F_8(x) = \sum_{i=1}^n  x_i \sin(x_i) + 0.1x_i $	30	[-100,100]	0
9	$F_9(x) = \sum_{i=1}^n x_i^2$	30	[-10,10]	0
10	$F_{10}(x) = \sum_{i=1}^n [x_i^2 - 10 \cos 2\pi x_i + 10]$	30	[-5.12,5.12]	0
11	$F_{11}(x) = \sum_{i=1}^n -x_i \sin(\sqrt{ x_i })$	30	[-500,500]	-418.9829n
12	$F_{12} = \frac{\pi}{n} \left\{ 10 \sin(\pi y_1) + \sum_{i=1}^{n-1} (y_i - 1)^2 [1 + 10 \sin^2(\pi y_{i+1})] + (y_n - 1)^2 \right\} + y_i = 1 + x_i + \frac{1}{4}$	30	[-50,50]	0
13	$F_{13} = 418.9829n - \sum_{i=1}^n x_i \sin(\sqrt{ x_i })$	30	[-500,500]	0
14	$F_{14}(x) = (1.5 - x_1 + x_1 x_2)^2 + (2.25 - x_1 + x_1 x_2^2)^2 + (2.625 - x_1 + x_1 x_2^3)^2$	30	[-4.5,4.5]	0
15	$F_{15}(x) = 100(x_1^2 - x_2)^2 + (x_1 - 1)^2 + (x_3 - 1)^2 + 90(x_3^2 - x_4)^2 + 10.1((x_2 - 1)^2 + (x_4 - 1)) + 19.8(x_2 - 1)((x_4 - 1))$	30	[-10,10]	0
16	$F_{16}(x) = \left( 0.02 + \sum_{i=1}^{25} (1/i) + (x_1 - a_{1i})^6 + (x_2 - a_{2i})^6 \right)^{-1}$ $a = \begin{pmatrix} -32 - 16.01632 - 32 \dots 0.1632 \\ -32 - 32 - 32 - 32 - 16 \dots 32.3232 \end{pmatrix}$	30	[-65.536,65.536]	0.998

TABLE 2: Continued.

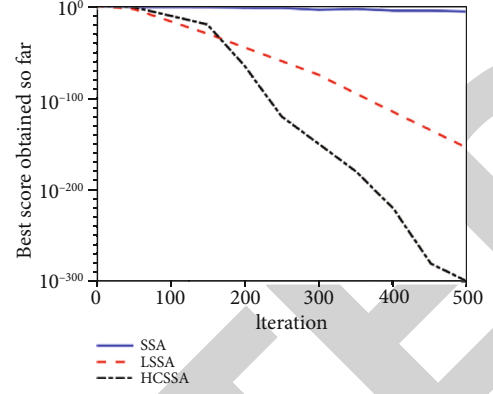
Number	Function	Dimensions	Interval	Minimum value
17	$F_{17}(x) = \sum_{i=1}^n  x_i^2 $	30	[-1,1]	0
18	$F_{18}(x) = (x_i + 0.5)^2$	30	[-100,100]	0
19	$F_{19}(x) = \max_i  x_i , i \in [1, m]$	30	[-100,100]	0
20	$F_{20}(x) = \sum_{i=1}^n ix_i^2$	30	[-10,10]	0



FIGURE 4: A roundabout way of  $F_1$ .FIGURE 5: A roundabout way of  $F_2$ .FIGURE 6: A roundabout way of  $F_3$ .

**4.2.1. Correction of One-Hop Size.** In the 3DDV-hop localization algorithm, the same average hop size is used between the known node and the target node to calculate, which not only increases the hop size error but also increases the energy cost. Therefore, in one-hop size, the distance value is derived as the hop size by proposing that through the signal strength value of the Received Signal Strength Indicator (RSSI).

Since RSSI is based on the radio wave loss between the transmitting end and the receiving end, the transmission loss is converted into distance according to a specific signal

FIGURE 7: A roundabout way of  $F_4$ .

model [43], and the most widely used logarithmic-normal distribution model is

$$\text{RSS}(d)[\text{dBm}] = P_{\text{tr}} - P_{\text{loss}}(d') - 10\alpha \log_{10} \frac{d}{d'} + x_{\xi}, \quad (20)$$

where  $\text{RSS}(d)$  represents the signal strength received by the target node from a known node,  $d$  represents the distance between the known node and the target node,  $P_{\text{tr}}$  represents the transmission signal energy,  $P_{\text{loss}}(d')$  represents the signal power loss at the reference distance  $d'$ ,  $\alpha$  represents the path loss index, whose value depends on the transmission medium, and  $d'$  represents the reference distance.  $x_{\xi}$  represents the noise, which is a Gaussian random variable with a mean of 0.  $\xi$  is the standard deviation.

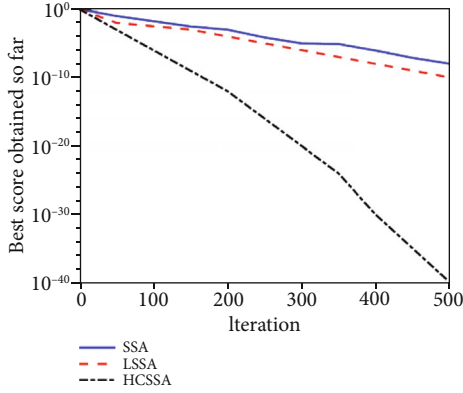
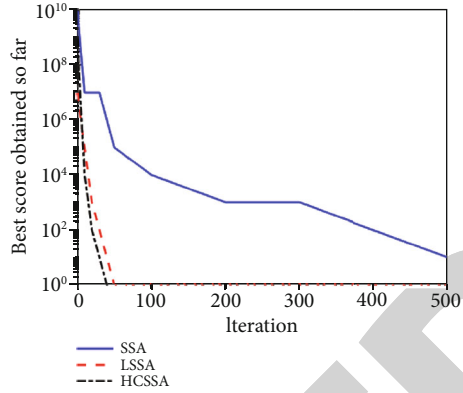
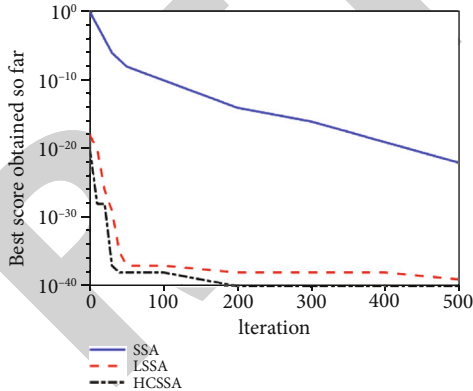
According to equation (20), it can be concluded that the hop size between the known node and the target node is

$$d = \left(10d'\right)^{\left(\text{RSS}(d)[\text{dBm}] - P_{\text{tr}} + P_{\text{loss}}(d') - x_{\xi}\right)/10\alpha}. \quad (21)$$

However, the RSSI values received by target nodes will be lost to a certain extent at a certain distance [44], resulting in deviations in the distance values, resulting in a cumulative error in the derived distance value. Therefore, we use the Gaussian fitting function to further correct the distance value. The collected RSSI values are processed through the Gaussian fitting function, the abnormal data are screened, and the processed RSSI values are substituted into equation (22) to obtain a more accurate internode distance. The optimized RSSI value is closer to the real hop size value. The Gaussian fitting function is as follows [45]:

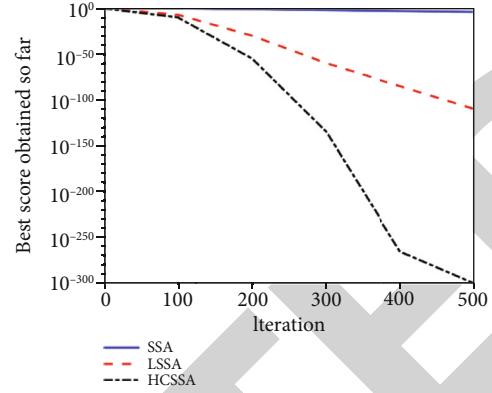
$$f(x_i) = x_0 + \frac{A}{\sigma\sqrt{\pi/2}} \times e^{-2((x_i - \mu)^2/\sigma^2)}, \quad (22)$$

where mean  $\mu = \sum_{i=1}^N \text{RSSI}_i / N$ , standard deviation  $\sigma = \sqrt{\sum_{i=1}^N (\text{RSSI}_i - \mu)^2 / (N - 1)}$ ,  $x_0$  and  $A$  are undetermined coefficients, which are determined by the relationship between the known node position and the signal value,  $x_i$

FIGURE 8: A roundabout way of  $F_5$ .FIGURE 9: A roundabout way of  $F_6$ .FIGURE 10: A roundabout way of  $F_7$ .

represents the  $i$ th signal distance value, and  $N$  is the total value of the received RSSI.

Most of the RSSI values in the Gaussian function are distributed between  $[\mu - \sigma, \mu + \sigma]$ , and the average value of this interval represents that the measured and actual values are close to each other. After being filtered by Gaussian filtering, the currently observed RSSI value output is

FIGURE 11: A roundabout way of  $F_8$ .

$$\text{RSSI}' = \frac{1}{n} \sum_{i=1}^n x_i(x_i \in [\mu - \sigma, \mu + \sigma]), \quad (23)$$

where  $n$  represents the number of RSSI values in  $[\mu - \sigma, \mu + \sigma]$ .

The ranging distance corrected by Gaussian fitting is the corrected distance of one-hop size:

$$d_N = \left(10d'\right)^{(\text{RSSI}' - P_{\text{tr}} + P_{\text{loss}}(d') - x_{\xi})/10\alpha}. \quad (24)$$

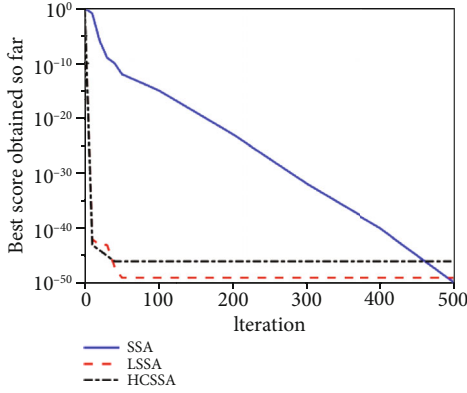
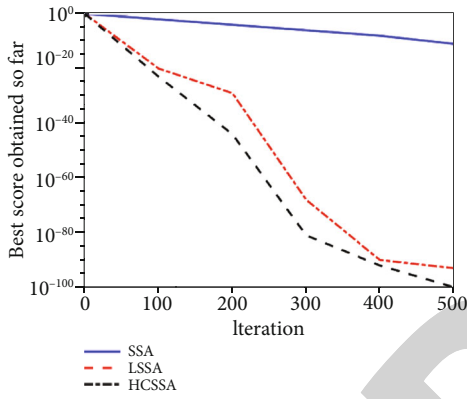
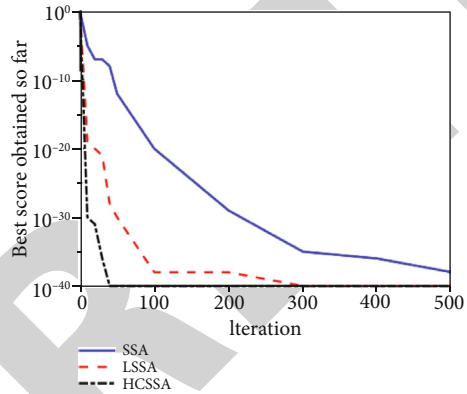
**4.2.2. Correction of Multihop Size.** In this article, when calculating the multihop size between a known node and a target node, the maximum distance similar link method is proposed based on the classical similar path search algorithm, which corrects the average hop size between the target node and the known node by finding the most similar pair of known node paths for the link from the target node to the noncoplanar known node. As the corrected average hop size value between the known node and the multihop target node, the optimal distance is obtained by using this average hop size multiplied by the optimized optimal hop size.

*Step 1.* Determine the maximum similarity link. After the exchange of the node information, each node keeps the information of each known node, as well as the identification of other nodes in the path to the minimum hop count experienced by each known node. The similarity link (SL) factor represents the path from the target node to a specific known node [46] and the degree of similarity between the paths from other known nodes to a specific known node. The calculation method is as follows:

$$\text{SL}(\kappa, \omega) = \frac{n(\kappa \cap \omega)}{\sqrt{n(\kappa) \times n(\omega)}}, \quad (25)$$

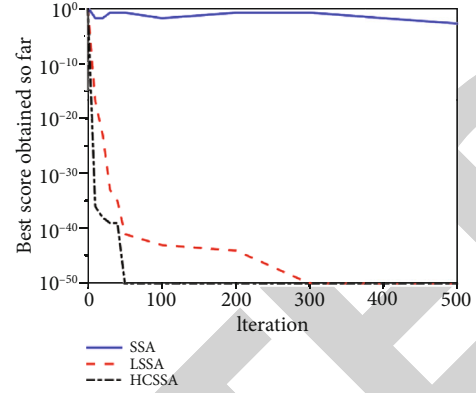
where  $\text{SL}(\kappa, \omega)$  represents the similarity between the path  $\kappa$  and path  $\omega$ ,  $\kappa$  represents target node to the specific noncoplanar known nodes by the minimum hop count between nodes on the link set of identification,  $\omega$  represents the residual known node in the network to the specific noncoplanar between known nodes, after the minimum hop count by a



FIGURE 12: A roundabout way of  $F_9$ .FIGURE 13: A roundabout way of  $F_{10}$ .FIGURE 14: A roundabout way of  $F_{11}$ .

collection of node id on a link, and  $n(\cdot)$  is the number of elements in set.

The similarity link factor SL is used to calculate the path from the target node to a specific noncoplanar known node and the similarity degree between the paths from other known nodes to a specific noncoplanar known node. The greater the value of SL, the higher the similarity degree. The path between the known nodes with the maximum value is determined as the possible path. When the calculated SL values with multiple paths are the same, compare

FIGURE 15: A roundabout way of  $F_{12}$ .

the Euclidean distance between each known node pair in the same SL value path. When the distance between two points of the node is larger, the calculated energy consumption of the node path is smaller, and the calculated average hop size is closer to the actual each hop size. Therefore, the path with the largest Euclidean distance of known node is selected as the result.

*Step 2.* Calculate the average hop size of similar links with maximum distance. The path obtained by Step 1 is the path between two known nodes, including specific known nodes. The Euclidean distance between nodes is calculated by using the coordinates of the two known nodes. The calculated distance is divided by the optimized minimum hop count between the two nodes, which is the average hop size used by the target node.

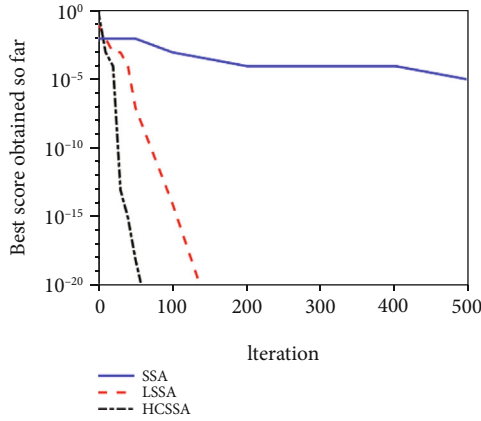
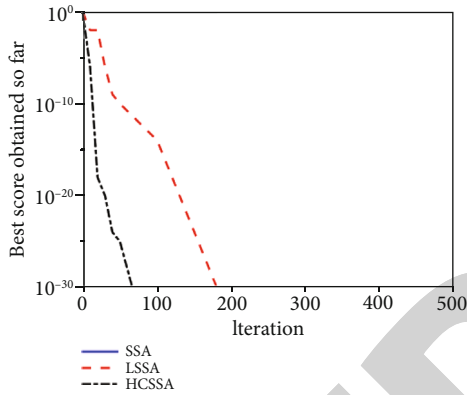
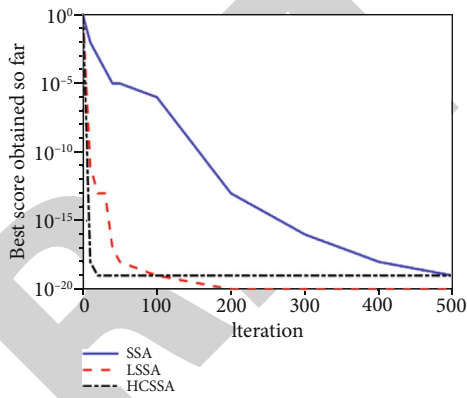
*Step 3.* Calculate the multihop size between the known node and the target node. To obtain the distance to the noncoplanar known node, each target node uses the calculated average hop size multiplied by the optimal hop count.

#### 4.3. Calculate Target Node Coordinates

*4.3.1. Determine Fitness Value.* The sine and cosine function search method effectively enhances the convergence of the sparrow algorithm, improves the convergence accuracy and the optimization effect, and improves the iterative efficiency. For this reason, this article redesigns the fitness function so that the fitness value after iteration can better correct the position deviation of the target node:

$$\text{fitness} = \frac{1}{n} \cdot \sum_{j=1}^n \left| \sqrt{(x_I - X'_j)^2 + (y_I - Y'_j)^2 + (z_I - Z'_j)^2} - D_{I,u} \right|, \quad (26)$$

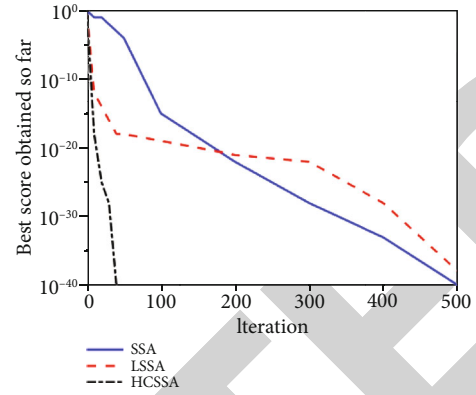
where  $(x_I, y_I, z_I)$ ,  $(X'_j, Y'_j, Z'_j)$  are the coordinates of the target node and known node, respectively.  $D_{I,u}$  is the distance from the target node  $u$  to the known node  $I$ .

FIGURE 16: A roundabout way of  $F_{13}$ .FIGURE 17: A roundabout way of  $F_{14}$ .FIGURE 18: A roundabout way of  $F_{15}$ .

**4.3.2. 3D-HCSSA Algorithm Flow.** The localization process of the 3DDV-hop algorithm based on 3D-HCSSA can be described as follows:

*Step 1.* The algorithm revises the hop counts by redefining the amendment factor to determine the optimal hop counts.

*Step 2.* Firstly, the Gaussian fitting function is used to reduce the error between the measured and actual values of the one-hop size between the known node and the target node; sec-

FIGURE 19: A roundabout way of  $F_{16}$ .

ondly, the average hop size between the known node and the target node of this path is corrected according to the maximum distance similar link method proposed in this article, and the distance between the known node and the target node is calculated after the correction.

*Step 3.* In the three-dimensional space,  $100\text{ m} \times 100\text{ m} \times 100\text{ m}$ -means clustering and sine and cosine search strategy are used to improve the sparrow search algorithm to optimize the localization of target nodes. Set the number of sparrow populations, and set the number of iterations and the localization of the population in initialization.

*Step 4.* Calculate the fitness values of all sparrow individuals through the fitness function, sort the fitness values of all sparrow individuals, and record the current optimal and worst sparrow positions.

*Step 5.* The entire iterative process iterates according to equations (3), (4), (5), and (12)–(15), updates the population position and calculates the new fitness value, and records the fitness value and position of the best individual after the update.

*Step 6.* The algorithm loops and calculates Step 5, and after iterating to the maximum, the global optimal position of the producer is obtained, that is, the optimal value of the coordinates of the target node and the algorithm.

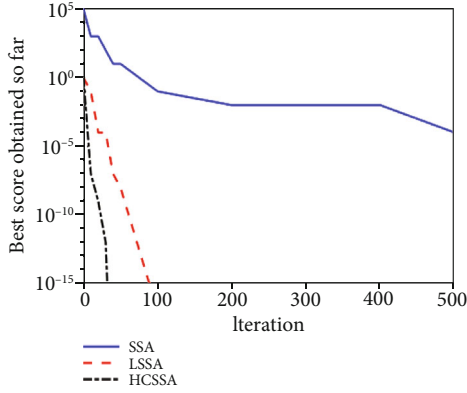
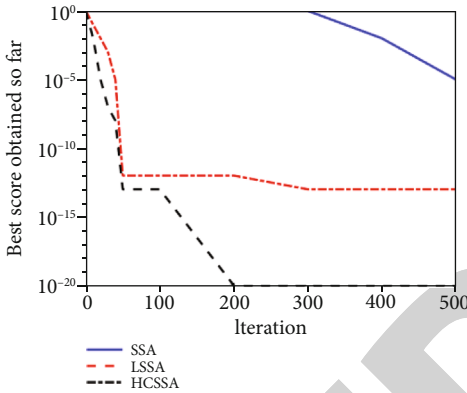
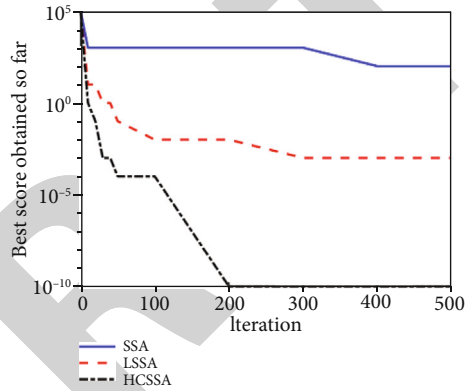
The flow chart of the 3D-HCSSA algorithm is shown in Figure 3.

Algorithm 1 is the pseudo-code of the spark search algorithm used to calculate the location of the target node.

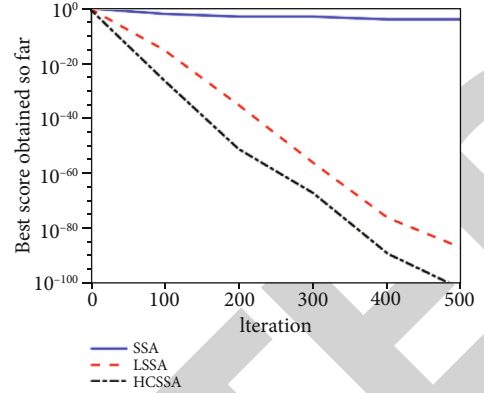
## 5. Simulation Results and Analysis

**5.1. Evaluation of the Performance.** This article compared HCSSA with SSA [21] and LSSA [47]. The parameters are set as shown in Table 1.

This section analyzes the performance of the improved sparrow search algorithm with 20 benchmark functions; as shown in Table 2, most of the benchmark functions come from the literatures [20, 42].

FIGURE 20: A roundabout way of  $F_{17}$ .FIGURE 21: A roundabout way of  $F_{18}$ .FIGURE 22: A roundabout way of  $F_{19}$ .

The algorithm in this article is compared with SSA and LSSA by 20 benchmark functions; Figures 4–23 show the details of the convergence curves of the SSA, the LSSA, and the HCSSA on the benchmark functions. From the figure, the iterative functions  $F_6$ ,  $F_{13}$ ,  $F_{14}$ ,  $F_{16}$ ,  $F_{17}$ ,  $F_{18}$ ,  $F_{19}$ , and  $F_{20}$  find the optimal solution before the number of iterations is reached in the iterative process. From this iterative process, the convergence speed of the HCSSA is better than the other two algorithms, and the algorithm is

FIGURE 23: A roundabout way of  $F_{20}$ .

less likely to fall into a local optimum. The convergence curves of each function are shown in Figures 4–23.

**5.2. Simulation Analysis.** In order to verify the performance of the proposed algorithm in localization, the 3DDV-hop localization algorithm, 3D-GAIDV-hop localization algorithm, and HCLSO-3D localization algorithm were analyzed separately. The relationship between the number of known nodes, the communication radius, and the total number of nodes and energy consumption is compared to analyze the positioning accuracy of the four algorithms.

**5.2.1. Experimental Parameter Setting.** To verify the performance of the algorithm 3D-HCSSA in localization in this article, simulation experiments are conducted using MATLAB. 100 simulation experiments were conducted in the same environment, and the average value is taken as the final result of simulation experiments.  $100\text{ m} \times 100\text{ m} \times 100\text{ m}$  is set as the simulation area, and 100 target nodes and 30 known nodes are taken. The specific experimental parameters are shown in Table 3. The random distribution of nodes in the 3D space is shown in Figure 24.

**5.2.2. The Localization Performance of the Model Is Evaluated by Means of the Average Localization Error Metric.**

$$\gamma_{\text{ALE}} = \frac{\sum_{I=1}^n \sqrt{(x_I - X'_I)^2 + (y_I - Y'_I)^2 + (z_I - Z'_I)^2}}{NR}, \quad (27)$$

where  $\gamma_{\text{ALE}}$  represents the average localization error,  $(x_I, y_I, z_I)$  represents the actual coordinate value of the target node  $I$ ,  $(X'_I, Y'_I, Z'_I)$  is the expected coordinate value of the node  $I$ ,  $N$  represents the total number of target nodes, and  $R$  represents the communication radius of the known node.

**5.2.3. Analysis of the Number of Known Nodes and the Average Localization Error.** From Figure 25, it can be seen that the average localization error of the algorithm in this article is smaller when the known nodes are the same. When the proportion of known nodes is 30%, the average localization error of the 3D-HCSSA algorithm is the smallest at 8.5%. At this time, the average localization errors of 3DDV-hop, 3D-GAIDV-

TABLE 3: Network environment and parameter setting.

Parameter	Value
The network area	100 m × 100 m × 100 m
Total number of nodes	100-300
Number of known nodes	10-30
Communication radius	25-45
Maximum iteration	300

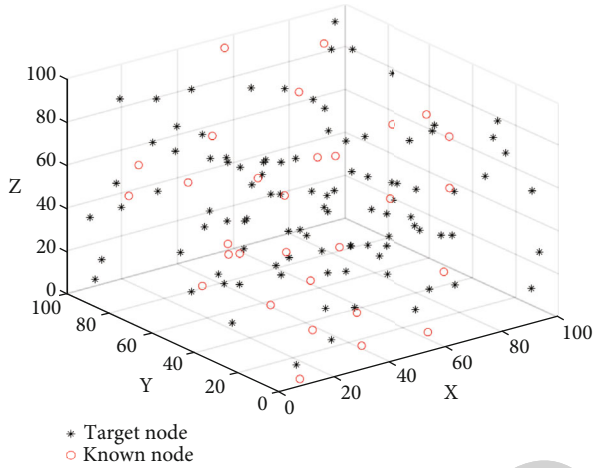


FIGURE 24: Random distribution of nodes in the three-dimensional space.

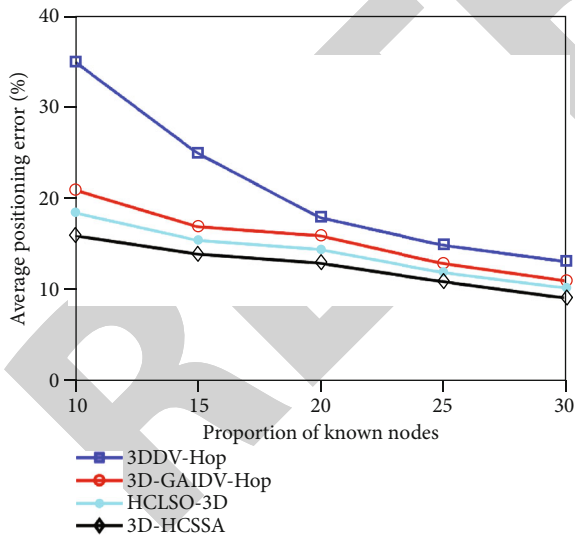


FIGURE 25: Compare and analyze the localization errors of different numbers of known nodes.

hop, and HCLSO-3D are 12.5%, 11.3%, and 9.8%, respectively, and the average localization errors of the 3D-HCSSA algorithm reduces compared with these three algorithms by 47.06%, 32.94%, and 15.29%, respectively. Therefore, when the number of known nodes is constant and the average positioning error curve is shown in the figure, the 3D-HCSSA algorithm has

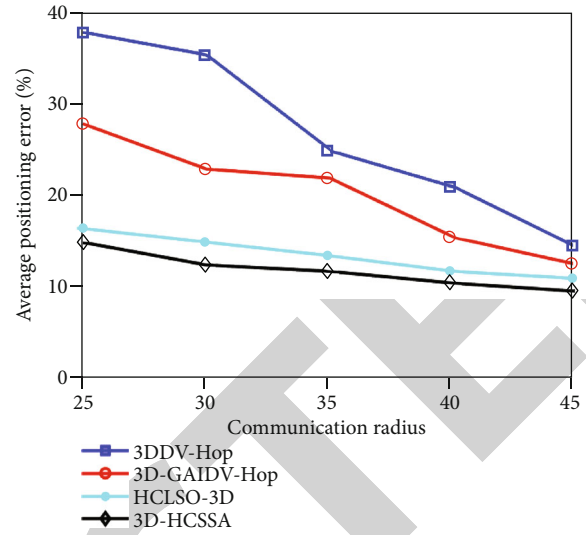


FIGURE 26: Compare the localization errors of different communication radii.

the advantage of high positioning accuracy compared with the other three algorithms.

**5.2.4. Analysis of Different Communication Radii and Average Localization Errors.** Figure 26 demonstrates the curve of average localization error that varies with communication radius. The proportion of known nodes is 10% in the network, and the communication radius is increased from 25 m to 45 m. By changing the communication radius, the localization performance of the four algorithms is compared and analyzed. The average localization error of the 3D-HCSSA algorithm is always the smallest. As the communication distance increases, the known node communicates directly with more nodes, so the average localization error gradually tends to be stable. The average localization error of the 3D-HCSSA algorithm is 9.6% minimum at the communication radius equal to 45 m. In this case, the average localization errors of 3DDV-hop, 3D-GAIDV-hop, and HCLSO-3D algorithms are 14.3%, 11.5%, and 11.2%, respectively. Compared with these three algorithms, the average localization errors of the 3D-HCSSA algorithm are reduced by 48.96%, 19.79%, and 16.67%, respectively. In summary, we can see by the change curve of communication radius from the figure that the average positioning error of the 3D-HCSSA algorithm is the smallest in different communication radius ranges, so the proposed algorithm in this article has the feature of high positioning accuracy.

**5.2.5. Total Number of Nodes and Average Localization Error Analysis.** Figure 27 demonstrates the curve of average localization error that varies with the total number of nodes. Sensor nodes are randomly deployed throughout the network with a communication radius of 30 m. The performance of the four algorithms demonstrates that the average localization error decreases gradually with the curve. The reason for this is that the network connectivity becomes better as the node density increases. Therefore, when the total number of nodes reaches a certain value, the average localization

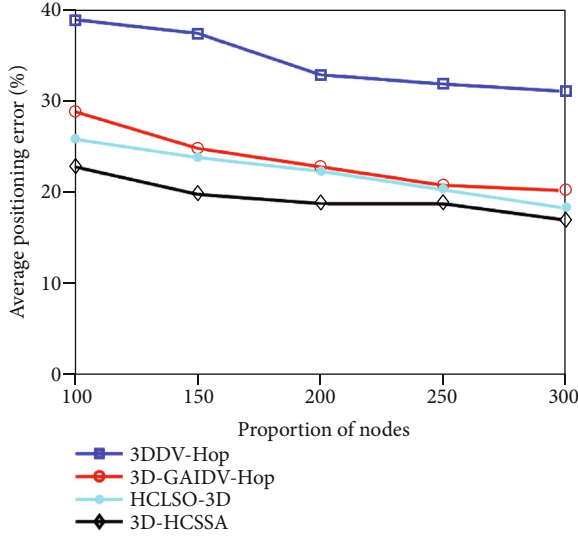


FIGURE 27: Compare and analyze the total number of nodes and the average localization error.

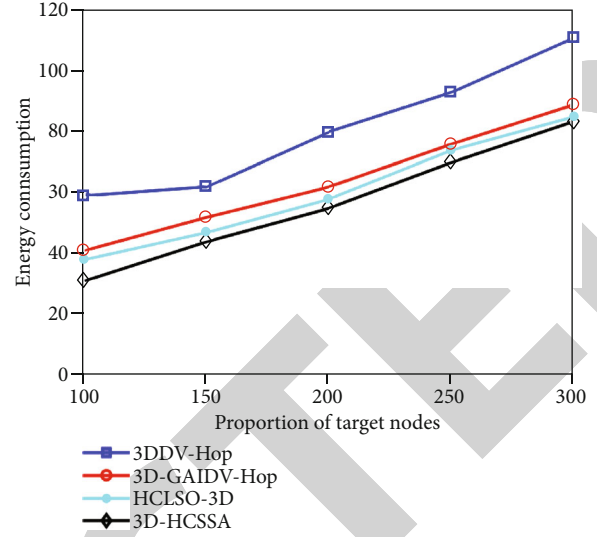


FIGURE 29: Compare and analyze the number of target nodes and energy consumption.

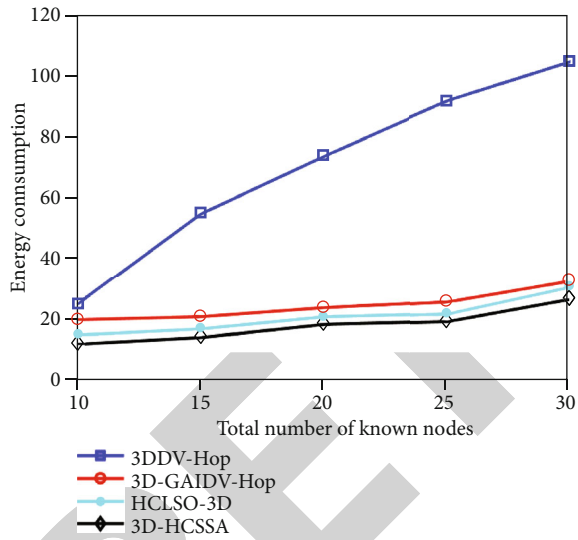


FIGURE 28: Compare and analyze the number of known nodes and energy consumption.

error of all four algorithms gradually stabilizes and does not change significantly. The average localization error of the 3D-HCSSA algorithm is always the smallest under the same conditions. When the total number of nodes reaches 300, the average localization error of the 3D-HCSSA algorithm is the smallest at 19.2%. In this case, the average localization errors of 3DDV-hop and 3D-GAIDV-hop and HCLSO-3D algorithms are 31.2%, 22.4%, and 19.9%, respectively. The 3D-HCSSA algorithm reduces the average localization error by 62.5%, 16.67%, and 3.64%, respectively, by comparison. Therefore, compared with the other three algorithms, the average positioning error of this algorithm is significantly reduced and the positioning accuracy is improved.

*5.2.6. Influence of the Number of Known Nodes on Energy Consumption.* Figure 28 demonstrates the curve of network energy consumption that varies with the number of known nodes. The energy consumption of the four algorithms increases gradually by randomly deploying sensor nodes throughout the network. The reason for this is that the increase in the number of known nodes leads to an increase in computation time. The energy consumption of the 3D-HCSSA algorithm is always the smallest throughout the process. When the number of known nodes is 30, the minimum energy consumption of 3D-HCSSA is 28. In this case, the energy consumption of 3DDV-hop, 3D-GAIDV-hop, and HCLSO-3D is 103, 35, and 33, respectively. Compared with the three algorithms, the energy consumption of 3D-HCSSA is reduced by 72.82%, 25%, and 20%, respectively. The known nodes consume large power in the network, which leads to the problem of high energy consumption of the whole network. It can be seen from the energy consumption curve in the figure that as the number of known nodes increases, the energy consumption is also increased, but the algorithm proposed in this paper has the advantage of low energy consumption compared with the other three algorithms.

*5.2.7. Influence of the Number of Target Nodes on Energy Consumption.* Figure 29 demonstrates the curve of network energy consumption that varies with the target number of nodes. The performance of the four algorithms are compared by randomly deploying sensor nodes within the entire network. The energy consumption of the four algorithms gradually increases as the total number of nodes increases, and the increase in the number of target nodes leads to an increase in computation time. The energy consumption of the 3D-HCSSA algorithm is always the smallest throughout the experiment. The energy consumption of the 3D-HCSSA algorithm is the smallest when the target node is 300 at 82. In this case, the energy consumption of 3DDV-hop, 3D-GAIDV-hop, and HCLSO-3D algorithms is 113, 90, and 87, respectively.

TABLE 4: Average running time of the four algorithms.

Algorithms	Average running time per second
3DDV-hop	32.3
3D-GAIDV-hop	49.2
HCLSO-3D	51.6
3D-HCSSA	53.4

Compared with the three algorithms, the energy consumption of the 3D-HCSSA algorithm is reduced by 37.8%, 9.76%, and 6.09%, respectively.

**5.2.8. Analysis of Calculation Cost.** The average running time of the algorithm is analyzed as an index of computational cost. Table 4 demonstrates the average running time of 3DDV-hop and 3D-GAIDV-hop and HCLSO-3D and 3D-HCSSA algorithms under the same experimental conditions. As can be seen from the experimental results, the average running time of the 3D-HCSSA localization algorithm is about 1.65 times that of the 3DDV-hop algorithm, about 1.08 times that of the 3D-GAIDV-hop algorithm, and about 1.03 times that of the HCLSO-3D algorithm. Because the 3D-HCSSA algorithm uses an intelligent algorithm to solve the target node coordinates, which results in the increase in the amount of calculation, the small increase in time consumption of the algorithm can be ignored, but the positioning accuracy is significantly improved.

**5.2.9. Time Complexity Analysis of the Localization Algorithm.** Since WSNs are usually limited by resources, in addition to positioning accuracy, the complexity of a localization algorithm is also one of the factors that must be considered. Suppose the number of nodes in the whole WSNs is  $n$  and the number of nodes is known to be  $m$ . The time complexity of computing the minimum counts of hop between nodes is  $o(n^3)$  in the 3DDV-hop algorithm, the time complexity of calculating the actual distance between nodes is  $o(n)$ , the time complexity of calculating the hop size from the target node to the known node is  $o(n \times m)$ , and the time complexity of calculating the localization of the target node through the maximum likelihood estimation method is  $o((n - m)^4)$ . Similarly, the complexity of 3D-GAIDV-hop and HCLSO-3D mentioned in this article increases  $o(n)$ , respectively, on the basis of the original 3DDV-hop algorithm. The time complexity of the proposed algorithm is also increased by  $o(n)$  on the basis of the 3DDV-hop algorithm. Therefore, the time complexity of the 3D-HCSSA algorithm does not increase significantly, but the positioning accuracy is better improved.

## 6. Conclusion

Aiming at the obvious error problem of node localization in the 3DDV-hop algorithm, a sparrow search localization algorithm 3D-HCSSA based on hop size correction and improvement is proposed. The algorithm redefines the amendment factor based on the original hop count to reduce the hop count error and proposes the maximum distance similar link method to correct the multihop size between

nodes and uses  $K$ -means clustering and sine-cosine search strategy to improve the traditional sparrow search algorithm. If it is insufficient, optimize the position of the target node and improve the positioning accuracy. The simulation results demonstrate that the average positioning errors of the 3D-HCSSA algorithm are reduced by 52.84%, 23.13%, and 11.87%, respectively, compared with the 3DDV-hop algorithm, the 3D-GAIDV-hop algorithm, and the HCLSO-3D algorithm. Therefore, the algorithm improves the node positioning accuracy and reduces the energy consumption of the algorithm. For the future research directions, we will focus on these aspects: firstly, to explore a better way to build an integrated network with seamless coverage within the network by combining 5G/6G technology with WSNs to solve the solution set coverage problem in the sparrow optimization search algorithm, reduce coverage voids, and improve positioning accuracy, and secondly, how to constrain the residual energy of nodes and enhance the application of the algorithm in various heterogeneous networks.

## Data Availability

The data used to support the findings of this study are available from the corresponding authors upon request.

## Conflicts of Interest

The authors declare no conflict of interest.

## Acknowledgments

This work was supported by the National Natural Science Foundation of China under Grant 71961028 and the Education Research Project of AFCEC, China, under Grant 2019-AFCEC-079.

## References

- [1] C. Yuan, W. Chen, and D. Li, "A hierarchical matrix decomposition-based signcryption without key-recovery in large-scale WSN," *Wireless Communications and Mobile Computing*, vol. 2018, Article ID 5929828, 10 pages, 2018.
- [2] B. Sheng, "On element selection in STAR-RIS for NOMA transmission," *Mobile Information Systems*, vol. 2022, Article ID 1335829, 8 pages, 2022.
- [3] T. F. Chen, L. J. Sun, Z. Q. Wang, Y. Wang, Z. Zhao, and P. Zhao, "An enhanced nonlinear iterative localization algorithm for DV\_hop with uniform calculation criterion," *Ad Hoc Networks*, vol. 111, article 102327, 2021.
- [4] X. Y. Liu and C. Liu, "Wireless sensor network dynamic mathematics modelling and node localization," *Wireless Communications and Mobile Computing*, vol. 2018, Article ID 1082398, 8 pages, 2018.
- [5] Y. F. Jia, K. X. Zhang, and L. Q. Zhao, "Improved DV-hop location algorithm based on mobile anchor node and modified hop count for wireless sensor network," *Journal of Electrical and Computer Engineering*, vol. 2020, Article ID 9275603, 9 pages, 2020.

- [6] J. Cheon, H. Hwang, D. Kim, and Y. Jung, "IEEE 802.15.4 ZigBee-based time-of-arrival estimation for wireless sensor networks," *Sensors*, vol. 16, no. 2, p. 203, 2016.
- [7] K. Rao, T. Kumar, and C. Venkatnaryana, "Selection of anchor nodes in time of arrival for localization in wireless sensor networks," *Proceedings of the International Conference on Soft Computing Systems*, vol. 397, pp. 45–57, 2016.
- [8] Y. Zhang, M. Wang, Z. Tan et al., "Design of wireless sensor network localization algorithm based on TDOA," in *2019 IEEE 3rd Information Technology, Networking, Electronic and Automation Control Conference (ITNEC)*, pp. 70–75, Chengdu, China, 2019.
- [9] W. Wang, P. Bai, Y. Zhou, X. L. Liang, and Y. B. Wang, "Optimal configuration analysis of AOA localization and optimal heading angles generation method for UAV swarms," *IEEE Access*, vol. 7, pp. 70117–70129, 2019.
- [10] Y. Shi, H. Liu, W. Zhang, Y. Wei, and J. Dong, "Research on three-dimensional localization algorithm for WSN based on RSSI," in *Advances in Intelligent Systems and Computing*, vol. 928, pp. 1048–1055, Springer Nature, Switzerland, 2020.
- [11] A. Stanoev, S. Filiposka, V. In, and L. Kocarev, "Cooperative method for wireless sensor network localization," *Ad Hoc Networks*, vol. 40, pp. 61–72, 2016.
- [12] Z. Liu, X. Feng, J. J. Zhang, T. Li, and Y. L. Wang, "An improved GPSR algorithm based on energy gradient and APIT grid," *Journal of Sensors*, vol. 2016, Article ID 2519714, 7 pages, 2016.
- [13] G. S. Li, S. S. Zhao, J. H. Wu, C. L. Li, and Y. Liu, "DV-hop localization algorithm based on minimum mean square error in Internet of things," *Procedia Computer Science*, vol. 147, pp. 458–462, 2019.
- [14] N. Dragoş and B. Nath, "DV based positioning in ad hoc networks," *Telecommunication Systems*, vol. 22, no. 1/4, pp. 267–280, 2003.
- [15] B. F. Gumaida and J. Luo, "Novel localization algorithm for wireless sensor network based on intelligent water drops," *Wireless Networks*, vol. 25, no. 2, pp. 597–609, 2019.
- [16] G. Venter and J. S. Sobieski, "Particle swarm optimization," *AIAA Journal*, vol. 41, no. 8, pp. 1583–1589, 2003.
- [17] L. M. Schmitt, "Theory of genetic algorithms," *Theoretical Computer Science*, vol. 259, no. 1-2, pp. 1–61, 2001.
- [18] M. Dorigo, M. Birattari, and T. Stutzle, "Ant colony optimization," *IEEE Computational Intelligence Magazine*, vol. 1, no. 4, pp. 28–39, 2006.
- [19] S. Mirjalili, S. M. Mirjalili, and A. Lewis, "Grey wolf optimizer," *Advances in Engineering Software*, vol. 69, pp. 46–61, 2014.
- [20] K. M. Passino, "Biomimicry of bacterial foraging for distributed optimization and control," *IEEE Control Systems Magazine*, vol. 22, no. 3, pp. 52–67, 2002.
- [21] J. K. Xue and B. Shen, "A novel swarm intelligence optimization approach: sparrow search algorithm," *Systems Science & Control Engineering*, vol. 8, no. 1, pp. 22–34, 2020.
- [22] J. Mohit, S. Vijander, and R. Asha, "A novel nature-inspired algorithm for optimization: squirrel search algorithm," *Swarm and Evolutionary Computation*, vol. 44, pp. 148–175, 2019.
- [23] S. Arora and S. Singh, "Butterfly optimization algorithm: a novel approach for global optimization," *Soft Computing*, vol. 23, no. 3, pp. 715–734, 2019.
- [24] V. Kanwar and A. Kumar, "DV-hop localization methods for displaced sensor nodes in wireless sensor network using PSO," *Wireless Networks*, vol. 27, no. 1, pp. 91–102, 2021.
- [25] S. P. Singh and S. C. Sharma, "Implementation of a PSO based improved localization algorithm for wireless sensor networks," *IETE Journal of Research*, vol. 65, no. 4, pp. 502–514, 2019.
- [26] S. P. Singh and S. C. Sharma, "A PSO based improved localization algorithm for wireless sensor networks," *Wireless Personal Communications*, vol. 98, no. 1, pp. 487–503, 2018.
- [27] H. Zhang, D. Y. Long, T. Qin, X. Wang, and J. Yang, "Improved DV-hop localization algorithm based on continuous hop," *Journal of Chinese Computer Systems*, vol. 42, no. 11, pp. 2388–2393, 2021.
- [28] W. S. Fang, Z. Wang, W. W. Wu, and Z. D. Hu, "PSO localization algorithm based on node density weighting and distance correction," *Transducer and Microsystem Technologies*, vol. 39, no. 7, pp. 127–133, 2020.
- [29] X. J. Cai, P. H. Wang, Z. H. Cui, W. Zhang, and J. Chen, "Weight convergence analysis of DV-hop localization algorithm with GA," *Soft Computing*, vol. 24, no. 23, pp. 18249–18258, 2020.
- [30] V. Kanwar and A. Kumar, "DV-hop-based range-free localization algorithm for wireless sensor network using runner-root optimization," *The Journal of Supercomputing*, vol. 77, no. 3, pp. 3044–3061, 2021.
- [31] T. K. Mohanta and D. K. Das, "Class topper optimization based improved localization algorithm in wireless sensor network," *Wireless Personal Communications*, vol. 119, no. 4, pp. 3319–3338, 2021.
- [32] S. S. Jacob, K. Muthumayil, M. Kavitha et al., "A modified search and rescue optimization based node localization technique in WSN," *Computers, Materials Continua*, vol. 70, no. 1, pp. 1229–1245, 2022.
- [33] P. Z. Gou, X. Z. Liu, M. Y. Sun, and B. He, "Three-dimensional localization algorithm based on hop correction and lion swarm optimization in WSNs," *Computer Engineering and Science*, vol. 43, no. 8, pp. 1405–1412, 2021.
- [34] A. Kaushik, D. K. Lobiyal, and S. Kumar, "Improved 3-dimensional DV-hop localization algorithm based on information of nearby nodes," *Wireless Networks*, vol. 27, no. 3, pp. 1801–1819, 2021.
- [35] V. Kanwar and A. Kumar, "Range free localization for three dimensional wireless sensor networks using multi objective particle swarm optimization," *Wireless Personal Communications*, vol. 117, no. 2, pp. 901–921, 2021.
- [36] J. Cheng, Y. L. Dong, J. X. Chen, and Z. H. Liu, "An improved three-dimensional DV-hop algorithm with continuous hop values," *Acta Electronica Sinica*, vol. 48, no. 11, pp. 2122–2130, 2020.
- [37] X. Cai, P. Wang, L. Du, Z. Cui, W. Zhang, and J. Chen, "Multi-objective three-dimensional DV-hop localization algorithm with NSGA-II," *IEEE Sensors Journal*, vol. 19, no. 21, pp. 10003–10015, 2019.
- [38] G. Sharma and A. Kumar, "Improved range-free localization for three-dimensional wireless sensor networks using genetic algorithm," *Computers and Electrical Engineering*, vol. 72, pp. 808–827, 2018.
- [39] S. Dong, X. G. Zhang, and W. G. Zhou, "A security localization algorithm based on DV-hop against Sybil attack in wireless sensor networks," *Journal of Electrical Engineering and Technology*, vol. 15, no. 2, pp. 919–926, 2020.

## *Retraction*

# **Retracted: Realization Path of the Social Development of Meteorological Services Based on Intelligent Data Analysis**

### **Wireless Communications and Mobile Computing**

Received 25 July 2023; Accepted 25 July 2023; Published 26 July 2023

Copyright © 2023 Wireless Communications and Mobile Computing. This is an open access article distributed under the Creative Commons Attribution License, which permits unrestricted use, distribution, and reproduction in any medium, provided the original work is properly cited.

This article has been retracted by Hindawi following an investigation undertaken by the publisher [1]. This investigation has uncovered evidence of one or more of the following indicators of systematic manipulation of the publication process:

- (1) Discrepancies in scope
- (2) Discrepancies in the description of the research reported
- (3) Discrepancies between the availability of data and the research described
- (4) Inappropriate citations
- (5) Incoherent, meaningless and/or irrelevant content included in the article
- (6) Peer-review manipulation

The presence of these indicators undermines our confidence in the integrity of the article's content and we cannot, therefore, vouch for its reliability. Please note that this notice is intended solely to alert readers that the content of this article is unreliable. We have not investigated whether authors were aware of or involved in the systematic manipulation of the publication process.

Wiley and Hindawi regrets that the usual quality checks did not identify these issues before publication and have since put additional measures in place to safeguard research integrity.

We wish to credit our own Research Integrity and Research Publishing teams and anonymous and named external researchers and research integrity experts for contributing to this investigation.

The corresponding author, as the representative of all authors, has been given the opportunity to register their agreement or disagreement to this retraction. We have kept a record of any response received.

### **References**

- [1] F. Guo, Y. Feng, and H. Xiao, "Realization Path of the Social Development of Meteorological Services Based on Intelligent Data Analysis," *Wireless Communications and Mobile Computing*, vol. 2022, Article ID 8904136, 8 pages, 2022.



## Research Article

# Realization Path of the Social Development of Meteorological Services Based on Intelligent Data Analysis

Fang Guo <sup>1</sup>, Yufang Feng,<sup>2</sup> and Han Xiao<sup>3</sup>

<sup>1</sup>Meteorological Bureau of Liaocheng, Shandong University, Liaocheng, 252000 Shandong, China

<sup>2</sup>Computer Science and Technology, Suzhou University, 215006 Shandong, China

<sup>3</sup>Computer Graphics, Shandong University of Technology, 255049 Shandong, China

Correspondence should be addressed to Fang Guo; 1417421428@st.usst.edu.cn

Received 19 January 2022; Revised 19 April 2022; Accepted 22 April 2022; Published 10 May 2022

Academic Editor: Shalli Rani

Copyright © 2022 Fang Guo et al. This is an open access article distributed under the Creative Commons Attribution License, which permits unrestricted use, distribution, and reproduction in any medium, provided the original work is properly cited.

In recent years, with the development of social economy, the working efficiency of meteorological system has been gradually improved. The socialization of meteorological service refers to the use of intelligent data analysis technology to achieve accurate forecast and real-time monitoring of weather forecast and provide personalized services for users based on this information. This paper studies the realization path of meteorological service socialization in order to bring convenience to people's life. This paper mainly uses a simulation experiment method, investigation method, and statistical method to conduct in-depth research on the social development of meteorological services. Experimental data show that more than 70 percent of people get weather information from their smartphones. The system designed in this paper can basically meet the requirements.

## 1. Introduction

In recent years, weather service has become a new hot topic. This paper will focus on data mining and social analysis and conduct intelligent integration and visual management of meteorological information resources based on intelligent multisource and social network platforms. The socialized development of weather service refers to the comprehensive management of weather forecast by using intelligent data analysis technology, including weather warning, automatic broadcast, information push, and other functions.

There are many theoretical achievements on the realization path of the socialized development of meteorological service based on intelligent data analysis. For example, in order to further improve the timeliness of weather warning, some scholars have made great efforts to improve the level of refined meteorological service [1, 2]. Some scholars use UNIT's speech recognition and natural interaction technologies to create intelligent interactive weather services [3, 4]. Some scholars believe that in the context of international service system reform, socialization of meteorological service is an important direction for future development and reform

[5, 6]. Therefore, this paper makes an in-depth study on the realization path of meteorological service socialization development by using an intelligent data analysis method.

This paper first studies the development of meteorological service and sharing and expounds the basic concepts and theories of meteorological service and sharing. Secondly, the intelligent forecasting method based on a neural network is analyzed, and the meteorological service system is designed by using this algorithm. Then, it expounds the selection of meteorological service socialization index. Then, the overall design of meteorological information service system is made. Finally, the feasibility of the system is verified by experiments.

## 2. The Realization Path of the Social Development of Meteorological Services Based on Intelligent Data Analysis

*2.1. Meteorological Services and Shared Development.* Meteorological service is a big concept. In the era of traditional planned economy, meteorological service is completely invested by the government and provided to users for free.

This unique investment model is obviously difficult to meet the needs of meteorological services in all aspects of society and economy. Our country's meteorological services (products) can be divided into three categories: one is nonprofit meteorological services (public products), including decision-making meteorological services and public meteorological services. The second is paid weather service. The third is commercial weather services [7, 8]. The status of various services is as follows:

Decision-making services refer to the meteorological services provided by major party and government departments at all levels to guide social development and national economic construction. It is a special weather service with Chinese characteristics, and the operating cost comes from national funds. From the perspective of service content, decision-making weather services are mainly for weather forecasting services for major disasters, transitional periods, and important social activities and provide accurate and timely meteorological scientific basis for decision-making [9, 10].

Although the weather telephone service started earlier, its progress has been slower. Based on the convenience of the masses, the promotion is rapid and social benefits are paramount. Many places popped up suddenly, and the general public responded well. They think this kind of service is practical, fast, and close to people's lives. The weather telephone service not only improves people's living standards but also serves as a good assistant and consultant for citizens. The service content has been continuously enriched and extended from a single air pollution weather forecast service, somatosensory, temperature, weekend commuting, etc. This largely meets the needs of society and the public [11, 12].

Newspaper weather service is also one of the most important forms of public weather service.

Since the founding of New China, the state has directly provided full funding to meteorological agencies, and meteorological stations at all levels have provided unique nonprofit meteorological services. After the Third Plenary Session of the Eleventh Central Committee of the Communist Party of China, with the change of the main direction of the party's work and the continuous deepening of reform and opening up, various economic fields and some users have many new special needs for meteorological services [13].

The concept of common development has four main connotations. The first is shared by all; that is to say, that common development is appreciated by everyone; everyone has something. The second is global sharing, that is, sharing development means sharing the achievements of the country's economic, political, cultural, social, and ecological civilization construction and fully guaranteeing the rights and legitimate interests of the people in all aspects. The third is to build and share together. Only by coconstruction can we share, and the process of coconstruction is also a process of sharing. The fourth is progressive division. Joint development must have a bottom-up, unbalanced to balanced process; even if it reaches a very high level, there will be differences. This definition emphasizes the universality and

content of joint development issues. The completeness of the development phase, the participation process, and the gradual advancement provide effective guidance for scientists and experts enable them to fully understand and understand the importance of joint development. However, if you want to implement coconstruction, you need to further deconstruct and refine the concept of coconstruction, so that every specific goal and goal can be achieved and enforced and promote the realization and evaluation of results [14].

The meaning of public service is often linked with the concept of public goods. Public goods are material goods, while public services emphasize an intangible service. To fully understand the concept of public services, we need to start with the analysis of the connotation of public products. From the introduction of public services to the present, public services have become an important issue affecting government functions, social development, and people's happiness. Equalization of public services means that the state can provide public products or services to different economic components, different social classes, or different interest groups without discrimination, including roughly similar financial investment, income and cost sharing. The balance of public utilities includes a large number of realizable, targeted, and planned value judgments. The pursuit of "balance" reflects the fair value orientation of public utilities [15].

## 2.2. Intelligent Prediction Method Based on Neural Network.

Artificial neural network is called neural network for short. This data model is extracted from a biological network containing many interconnected neurons to build a more complex network. One of the most important characteristics of neural networks is its topological structure, which is generally divided into direct neural networks and return neural networks. Feedforward neural network is the most common and simplest model in artificial neural network. According to different information processing methods, neurons can be divided into input layer neurons, hidden layer neurons, and output layer neurons. The signal from the input layer to the output layer flows in one direction.

Generally speaking, the learning methods of artificial neural networks (ANN) can be divided into two types: learning with tutors and learning without tutors. The artificial neural network model is a simplified mathematical model that simulates the function of the biological nervous system. Its properties are summarized as follows:

- (1) It has a very parallel structure and information processing capabilities
- (2) It has strong self-learning ability and information storage ability
- (3) It has strong fault tolerance
- (4) It has strong nonlinear approximation ability

In the BP neural network algorithm, if the actual output of the output layer matches the expected output, it becomes the actual output. That is, if the actual output of the output

layer does not match the expected output, you must enter another process of the algorithm.

Because BP neural network has self-organization, self-learning, and self-adaptive capabilities and better fault tolerance, it can be used for prediction, but BP neural network is easy to fall into its loopholes. The initial weights and thresholds are initialized randomly, so it is difficult to get the overall optimal initial value, which further reduces the accuracy of prediction. The PSO algorithm is used to optimize the weights and thresholds of the BP neural network, and an intelligent prediction model based on PSO-BPNN is established. The basic process is as follows:

- (1) Initialize the particle swarm randomly
- (2) Calculate the fitness value of each particle
- (3) Compare the fitness value of the current particle with the previous best fitness value, compare the two, and take the larger value as the best fitness value of the current particle
- (4) Choose the best of all particle fitness values as the overall optimal solution
- (5) Use formula (1) to calculate the forward speed of each particle, namely,

$$w_m(s+1) = \psi w_m(s) + d_1 q_1 (o_m - a_m(s)) + d_2 q_2 (o_h - a_m(s)) \quad (1)$$

- (6) Calculate the position of each particle after advancing, namely,

$$a_m(s+1) = a_m(s) + w_m(s+1) \quad (2)$$

- (7) Reduce the inertia weight  $W$  according to

$$W = W_{\max} - \frac{W_{\max} - W_{\min}}{m_{\text{termax}} m_{\text{ter}}} \quad (3)$$

- (8) Change the acceleration coefficient  $d_1$  and  $d_2$  according to

$$d_1 = d_{1 \max} \frac{W_{1 \max} - W_{1 \min}}{m_{\text{termax}} m_{\text{ter}}}, \quad (4)$$

TABLE 1: Proportion of channels through which the public obtains weather warning information.

	TV	Smart phone	Internet	Other
2016	21.1%	65%	9%	5.9%
2017	18.6%	67.9%	8.5%	5.1%
2018	17.5%	69%	9.5%	5%
2019	16.6%	72.4%	7.1%	3.9%
2020	15.3%	75.9%	6.4%	2.4%

$$d_2 = d_{2 \max} \frac{W_{2 \max} - W_{2 \min}}{m_{\text{termax}} m_{\text{ter}}} \quad (5)$$

- (9) Until the algorithm reaches the maximum number of iterations or until the convergence criterion is met, do not leave the PSO algorithm
- (10) Continue to train the neural network, compare the results of the two, if it is better than the training result of the PSO algorithm, generate a BP neural network; otherwise, generate a neural network for PSO training

### 2.3. Selection of Socialization Indicators for Meteorological Services

**2.3.1. Weather Warning Coverage.** The scope of meteorological warning information is mainly the range of meteorological warning information transmitted to the public and users through secondary warning communication means such as mobile phones, television, radio, and the Internet. The assessment of the coverage area of meteorological disaster warning information is a scientific benchmark for the development of effective tools, high-quality, and equal meteorological disaster prevention and control. Our country's meteorological disaster warning coverage rate should reach more than 90%, and the goal is to achieve full coverage and meet the different needs of the national public for meteorological information services, so as to achieve meteorological science and technology achievements, the people, and disaster reduction services for economic and social development. This indicator is measured by the percentage of the population covered by weather warning information, also known as the coverage rate of weather warning information per capita.

Table 1 shows the results of the national public weather service survey from 2016 to 2020 show that the three main methods for obtaining weather warning information from the public, television, telephone, laptop computer, and the Internet are still relatively weak.

As shown in Figure 1, we can see that smartphones are the most reliable channel for obtaining weather information. Therefore, this article divides the broadcast methods of weather warning information into four categories: TV, mobile phone, and Internet. The coverage of weather warning information includes four coverage factors: TV broadcast weather warning information coverage, mobile phone

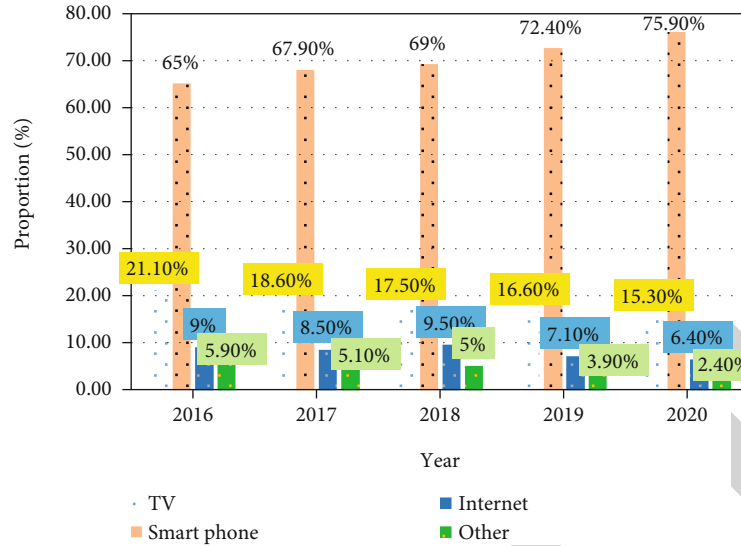


FIGURE 1: Proportion of channels through which the public obtains weather warning information.

coverage, network warning information coverage, and weather information coverage. Form other means.

**2.3.2. Benefits of Weather Disaster Risk Management and Mitigation.** The direct role of weather services is to seek strengths and avoid weaknesses. The benefits of meteorological disaster prevention and reduction are mainly reflected in two aspects. The first is to reduce the impact of meteorological disasters on GDP, and the second is to improve economic and social benefits. Since the benefits of weather disaster prevention and mitigation are different from the economic and social benefits of weather services, they are essentially the same. Therefore, this article uses the benefits of weather services to express the benefits of weather disaster prevention and mitigation. Meteorological service profit refers to the comparison between labor costs and the profit generated by meteorological services. The meteorological service income of branches is the sum of the income obtained by all commercial organizations of various departments of the economy from the application of meteorological service products or services. The cost of meteorological service is the sum of the financial investment of various levels of government to the meteorological department and the income-generating resources of departmental science and technology services.

**2.3.3. Public Satisfaction.** The highest measure of weather service is whether the public is satisfied or dissatisfied. Meteorological services must always follow the development direction, adhere to the people-oriented approach, serve life, and fully meet the growing service needs of the people. Satisfaction is a measure of satisfaction. In order to provide the public with a comprehensive and in-depth understanding of the objectives and overall evaluation of our country's meteorological services, overall satisfaction with public weather services also examined the four most important rating indicators considered by the public, without the global service

TABLE 2: Hardware environment configuration parameter information.

Name	Set
Internal storage	2G DDR
CPU	Pentium IV
Video card	GeForceMx 440
Indicator	19-inch pure screen
Hard drive	320G

impact assessment index survey. It includes timely availability, convenience, accuracy, and functionality.

**2.3.4. Meteorological Equipment.** Weather forecast and early warning services are based on meteorological observation, while meteorological observation services depend on the development of meteorological equipment. This shows that the development and progress of meteorological services cannot be separated from the support of advanced technical equipment. The level of meteorological equipment not only is a direct manifestation of the basic level of meteorological modernization but also affects the overall level of meteorological modernization. The evaluation indicators for the further development of meteorological equipment can be divided into two levels. The first layer is the complete index, including the device configuration layer and the device management and application layer.

**2.4. Overall Design of Meteorological Information Service System.** With the advent of Java technology, component technology quickly became popular. These components are transactional, extensible, and portable. The use of Java technology infrastructure allows repeated calls to business components. From the perspective of business function design and implementation, the framework can be used as a benchmark. It is perfectly able to abstract and analyze the context

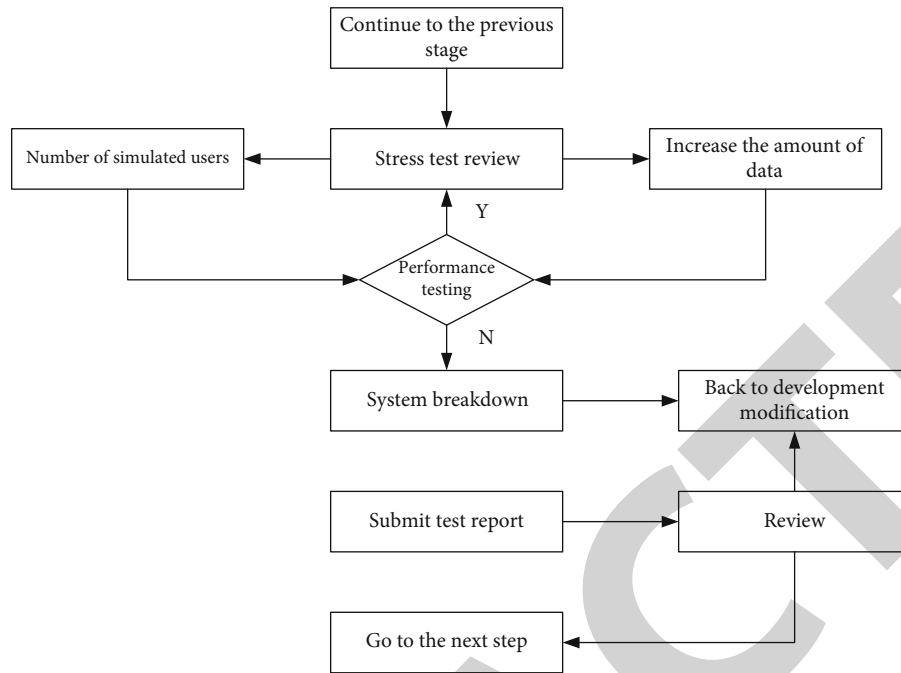


FIGURE 2: System performance test process.

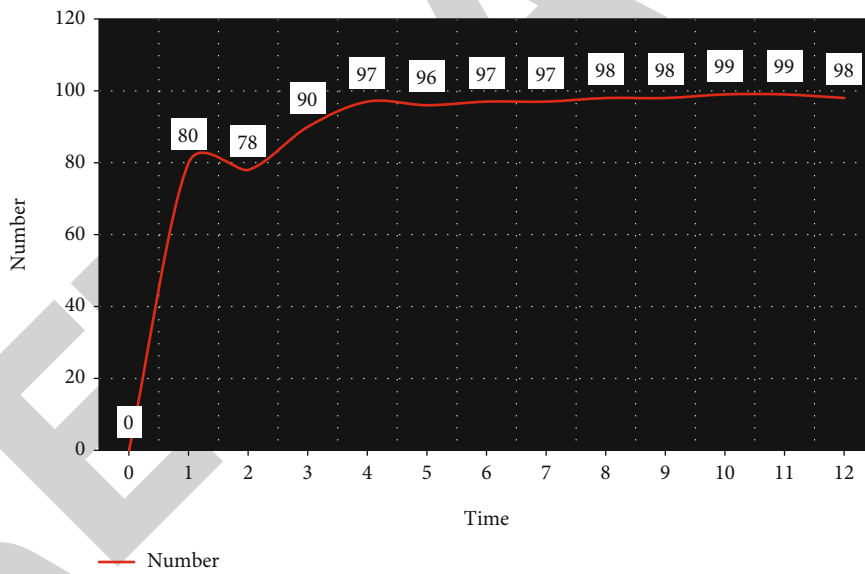


FIGURE 3: Changes in system throughput as load increases.

of industrial applications and industry requirements, so that the available components not only have the technical characteristics of transactional, scalability, and portability but also are closer to the real world, system-specific application industries, and meteorological service company specialty. Once such a business framework is in place, building top-level services will be faster, easier to manage and maintain.

The weather information service system weather website structure is as follows: application layer, middle layer, and data layer. And it is divided into several modules such as sys-

tem login interface, system homepage, platform data maintenance, information statistics, user operation authority, keyword management, platform, weather service information, and sending SMS. Based on the B/S model, design the functional structure of the weather information service system and construct the weather information service system. The functions of the basic structure of the meteorological information service system are as follows:

- (1) The database is used to store the data structure of weather service processing information

- (2) The data access layer provides interfaces or functions for efficient data access. When entering the database through this layer, other operations such as adding, selecting, deleting, and updating other databases are designed
- (3) System access layer, system login interface, system homepage, platform data maintenance, information statistics, user operation authority, platform keyword management, weather service information, and short message transmission module realize this design model based on B/S

System security design mainly includes three aspects: equipment and physical security, network and data security, and server security. Due to the phenomena of memory card damage, falling, power failure, and touch failure in the terminal, all devices are interchangeable, the power-on state is the same, and the operation is consistent. According to the security strategy of hierarchical protection, combined with the characteristics of management services, the security of information exchange between security domains, boundary protection, and the security of the local IT environment of the security domain should take into account each security domain and external networks. The platform domain and the intranet platform domain share the weather management system.

### 3. Meteorological Information Service System Test

**3.1. Test Environment.** In order to ensure the quality of the software development of the weather information service system, specific and standardized testing and analysis of the weather information service system designed and implemented by the weather service organization should be carried out. Software testing is aimed at reflecting the stable operation of the system and complete functions. The weather service system tests the use cases of the system weather service functions and summarizes and analyzes whether the system meets the system design requirements. In addition, in order to reflect the results of the system design, test and analyze the functional operating status of the meteorological information service, as well as the response and access parameters of the software.

**3.2. Test Objectives.** If the test object is considered to be an open box, it represents a white box test, and the weather information service system test uses the white box test procedure.

- (1) According to the use case test of the weather information service system software system, conduct the main function use case test, analyze the weather data query, add functions, and test the user verification module
- (2) As part of the designed network architecture, run software modules in various scenarios and examine the impact on them

TABLE 3: The CPU usage of the system obtained in the flat test changes over time.

Time	CPU
0	31
1	32
2	23
3	24
4	26
5	24
6	42
7	40
8	22
9	26
10	36
11	43
12	25
13	29
14	24
15	27
16	45
17	32
18	28
19	22
20	23
21	25
22	28
23	26
24	22

- (3) Interface testing is a relatively simple and intuitive testing method in the testing process, provided that the testing process is carefully checked according to the requirements of the interface. In the process of interface testing, we need to focus on testing interface typos, vague content, content titles, and other issues that do not conform to the harmony of the overall system

**3.3. Environment Configuration.** The required software environment and hardware environment generally include the system test. The weather information service system test environment refers to the server environment. The details are shown in Table 2.

**3.4. System Performance Test.** Through capacity test, strength test, and load test, the performance of meteorological information service system is reflected. The system performance test process is shown in Figure 2.

- (i) Capacity test: verify the maximum number of users of the system online at the same time to ensure the stability of the system.

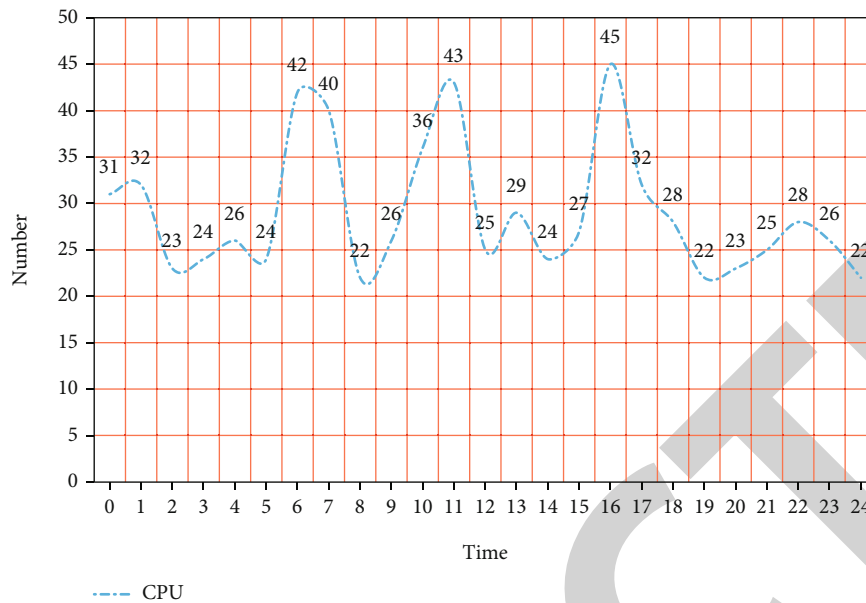


FIGURE 4: The CPU usage of the system obtained in the flat test changes over time.

- (ii) Strength test: strength test is a performance test. The specific situation of the test system occupying computer resources.
- (iii) Stress test: Since the program can be run and executed in a crowded environment, stress test is an analysis of performance test parameters. In observational indicators, test various system performance indicators, simulate various normal, peak and abnormal load conditions, and use automated testing tools for observational testing.

#### 4. Analysis of Test Results

**4.1. Changes in System Throughput as Load Increases.** The flow rate increases steadily and stabilizes at a certain point. Since all threads on the server are already occupied, they will be processed when they are idle.

As shown in Figure 3, we can see that although the throughput remains stable, the response time of the weather information service system has also increased. Thereafter, when the weather information service system reaches a saturation point, the throughput of the server remains stable. This is because the request cannot be processed in time and the response time increases.

**4.2. The CPU Usage of the System Obtained in the Flat Test Changes over Time.** As the load of the system increases or decreases, the execution queue also grows or shrinks. The execution queue also suffers from unstable load, peak waveforms appear from time to time, and the CPU usage rate is not smooth. The details are shown in Table 3:

As shown in Figure 4, we can see that the transaction response time in the system is similar to this fluctuating pattern. The execution queue curve is very similar to the graph of CPU usage, and a waveform appears every once in a while. Through the process of these performance tests, the

performance parameters obtained show that the meteorological information service system meets actual needs.

#### 5. Conclusion

The socialized demand of meteorological service can be obtained from data analysis. The goal of the socialized meteorological service system designed in this paper is to realize the real-time dynamic collection of weather information, temperature, and other parameters through the analysis of meteorological data and to make decisions and judgments and manage according to the obtained information. Users can collect, sort out and analyze the data of meteorological information on the platform. Data collation and analysis of collected meteorological information. Simulation experiments show that the system designed in this paper can meet the requirements of most people.

#### Data Availability

The data underlying the results presented in the study are available within the manuscript.

#### Conflicts of Interest

There is no potential conflict of interest in our paper, and all authors have seen the manuscript and approved to submit to your journal. We confirm that the content of the manuscript has not been published or submitted for publication elsewhere.

#### References

- [1] L. Ming, X. Yafen, and L. Jun, "Research on the socialization of grassroots meteorological services in agricultural supply-side structural reform," *Meteorological and Environmental Research*, vol. 10, no. 4, pp. 35–40, 2019.

## Research Article

# An Effective Path Planning of Intelligent Mobile Robot Using Improved Genetic Algorithm

Zhongzhe Chen <sup>1,2</sup>, Jianzhang Xiao,<sup>1,2</sup> and Guifeng Wang<sup>1,2</sup>

<sup>1</sup>College of Mechanical and Electrical Engineering, Jinhua Polytechnic, Jinhua, 321007 Zhejiang, China

<sup>2</sup>Key Laboratory of Crop Harvesting Equipment Technology of Zhejiang Province, Jinhua Polytechnic, Jinhua, 321007 Zhejiang, China

Correspondence should be addressed to Zhongzhe Chen; 20151030@jhc.edu.cn

Received 25 January 2022; Revised 22 March 2022; Accepted 4 April 2022; Published 9 May 2022

Academic Editor: Shalli Rani

Copyright © 2022 Zhongzhe Chen et al. This is an open access article distributed under the Creative Commons Attribution License, which permits unrestricted use, distribution, and reproduction in any medium, provided the original work is properly cited.

With the rapid development of the robotics industry, the problem of effective and fast path planning for intelligent mobile robots has always been one of the hot spots in the field of robotics research. Intelligent mobile robot path planning is divided into global path planning and local path planning, and its mathematical modeling and adaptive algorithms are different. Therefore, the research of robot path planning based on improved genetic algorithm is of great significance. This paper mainly studies the robot path planning problem based on improved genetic algorithm. Based on the research of the basic genetic algorithm, the improved genetic algorithm is applied to the mobile four-wheel robot to guide the four-wheel robot to complete path planning and other related tasks. Experiments show that the optimization probability and convergence speed of the genetic algorithm can be improved by improving the genetic algorithm. Studies have shown that evolutionary algebra and population size are inversely proportional to the optimal path length, so it is directly proportional to the search ability. However, as the evolutionary algebra and population size increase, the amount of calculation is also increasing, and the calculation time increases. Comprehensive considerations according to various factors, the best value of population size is 60, the best value of mutation probability is 0.09, the best value of crossover probability is 0.8, and the best value of evolutionary algebra is 150 generations.

## 1. Introduction

With the development of the times, it is more and more difficult for robots fixed in one place to do the same job to meet the requirements of robots in various industries [1, 2], and the development of navigation technology makes it possible for robots to handle more complex things. Vision-based navigation research will create conditions for mobile robots to move independently from human control and is one of the basic tasks for mobile robots to play a greater role [3, 4]. The problem of path planning is the core problem of navigation. The quality of the feasible path planned by the path planning system is directly related to whether the robot can bypass all obstacles and reach the target point safely and quickly. It is the key link of the navigation system [5–6]. Therefore, mobile robot technology

will usher in new development opportunities under the promotion of a large amount of government investment and enterprise demand [7, 8].

In the research of robot path planning based on improved genetic algorithm, many scholars have studied it and achieved good results. For example, the autonomous mobile robot designed by Qi et al. adopts two wheel differential speeds. In order to adjust the movement direction, a laptop is used as the control center, which can be controlled remotely or move autonomously [9]. There are four modular configuration schemes for free selection, which can meet different needs and adapt to different workplaces. The CASIA-1 mobile robot studied by Gao et al. has 32 infrared sensors, which are evenly installed around the fuselage at an angle of 22.5 degrees. One-half of them are used to detect obstacles at close range. One-half is used to detect long-



distance obstacles. The robot also has ultrasonic sensors, and the obstacle information obtained by two different types of sensors is fused [10].

This article uses the literature research method to retrieve literature, works, articles, etc. related to keywords such as “genetic algorithm,” “path planning,” and “intelligent mobile robots,” then uses a comparative experiment method to talk about the robots before and after improvements. The effective path ratio is compared.

Through more in-depth research and improvement of genetic algorithm and trying to combine it with other algorithms, we can achieve better results in path planning, which is of great practical significance to expand the application range of mobile intelligent robot.

## 2. Robot Path Planning Based on Improved Genetic Algorithm

**2.1. Principle of Robot Path Planning Based on Genetic Algorithm.** In this paper, the genetic algorithm uses the grid method to mark the geographical environment information and maps the environmental information to the grid. Black represents obstacles, and white represents obstacles. Combine the grid method with the array, the array  $a[x][y]$  represents the grid,  $a[0][0]$  represents the upper left square, and  $a[X][Y]$  represents the lower right square;  $X$  and  $Y$  are the maximum number of horizontal and vertical grids. Import the obstacle information into the array,  $a[x][y] = 0$  means that there is no obstacle at the square.

**2.1.1. Initialization.** Randomly generate a certain number of codes of a certain length as the initial population, which represents the path of the robot from the start point to the end point [11]. The robot path planning of the genetic algorithm is to perform genetic operations on these paths, and then generate the optimal path group, and output the most optimal path [12].

The robot plans the path according to the path code. If it encounters obstacles during walking, it will judge that the current path is invalid and gives up. If the robot can reach the end point, it is judged that the current solution is a feasible solution [13]. Of course, the randomly generated path code is not a feasible solution. Whether most randomly generated path codes are failed path codes, that is, the robot cannot complete the movement task from the starting point to the end point in the direction indicated by it.

However, in the same way, it is not to say that the failed solution generated at the beginning can not become a feasible solution after a series of genetic operations such as crossover, mutation, deletion, and insertion. Similarly, in terms of the fitness function value, the value of the infeasible path is greater than the value of the feasible path; that is, the infeasible solution is better than the feasible solution in the individual evaluation process, indicating that the infeasible solution is more effective than the feasible solution in a certain range. If the infeasible solution is further optimized to make it an excellent feasible solution, the optimal solution obtained in this way is also feasible. Therefore, in the individual evaluation process, different evaluation criteria can

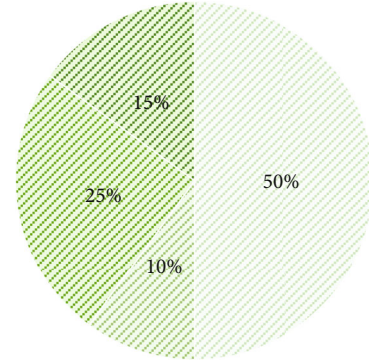


FIGURE 1: Roulette.

be used for feasible and infeasible paths to further improve the degree of superiority of the solution population [14, 15].

**2.1.2. Genetic Operator.** Genetic operators include individual evaluation, single-point crossover, multipoint crossover, deletion operators, and so on.

**2.1.3. Individual Evaluation.** The idea of roulette selection is applied to the process of constructing the fitness function of robot path planning. The idea of roulette selection is to use a pie chart to represent the roulette used for gambling, as shown in Figure 1.

Assuming that the robot path code is a certain block in a specified pie chart, the size of the block in the pie chart is proportional to the size of the fitness function value of the path code. The higher the fitness function value of the path code, the larger the area occupied in the pie. When imitating gambling, put a small ball on the roulette wheel to see where the ball stops, that is, select the path code corresponding to it. The probability that the path code is selected is proportional to its fitness function value.

A fitness function based on a penalty function can also be used, and the fitness function is often set as a penalty function in path planning. For example, let the penalty function be  $FitQ$ .

$$FitQ = \frac{Fitq2}{Fitq1},$$

$$Fitq2 = \begin{cases} 1 & R = 1, \\ 0 & R = 0, \end{cases} \quad (1)$$

$$Fitq1 = \sum_{i=2}^{N_p} Dis(Pt_i, Pt_{i-1}) + Dis(ST_p, Pt_i) + Dis(Pt_{NP}, ET_p) + M \times F_{est}.$$

$R$  is defined as the path safety factor. If the robot is already in the danger zone, the safety distance is greater than the linear distance between the robot and the obstacle, then  $R = 0$ ; if the robot is already in the safety zone, the safety distance is less than the linear distance between the robot and the obstacle, then  $R = 1$ .

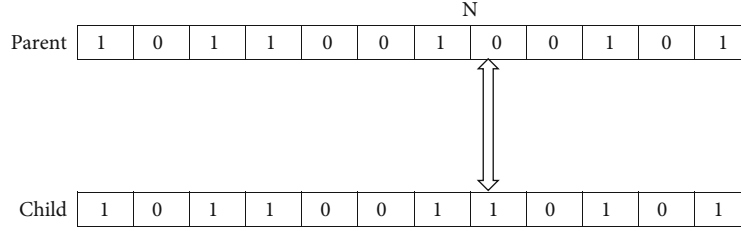


FIGURE 2: Single point mutation.

$N_p$  represents the number of grids in the path (excluding the start point and end point),  $Pt_i$  represents the  $i$ -th grid,  $ST_p$  and  $ET_p$  represent the start point and end point.  $Dis(X, Y)$  represents the straight-line distance between the starting point  $(X_a, Y_b)$  and the end point  $(X_A, Y_B)$ , expressed as follows:

$$Dis(X, Y) = \sqrt{(X_a - X_A)^2 + (Y_b - Y_B)^2}. \quad (2)$$

$M$  is the penalty coefficient, and  $F_{cst}$  is the penalty function.

$$F_{cst} = \sum_{i=1}^{N_{ob}} (W(i) + kWL'(i)). \quad (3)$$

Define  $W(i)$  as the number of paths that pass through the grid.  $K$  is a proportional coefficient, which can be a constant.

Definition  $L'(i)$  is the shortest distance between the path and the obstacle and the number of grids from the obstacle to the path as a vertical line.

The robot moves from grid  $a[X_a][Y_b]$  to  $a[X_A][Y_B]$  time  $T$ , the average speed of the robot  $V$ . This method is generally applicable to square grids.

$$T = \frac{\sqrt{(X_a - X_A)^2 + (Y_b - Y_B)^2}}{V}. \quad (4)$$

In some genetic algorithms, the fitness function value of the robot path planning is modeled according to the distance between the robot and the end point. The binary code of each path is compiled, and then, the result obtained is put into the path test base class to judge the distance between the robot and the end point and finally returns a function value.

**2.1.4. Single Point Mutation.** Randomly generate a numerical value, and the numerical value is in between, indicating the probability of mutation. When the probability of mutation is less than the set threshold probability, mutation of the code of the corresponding bit is performed. The core idea is shown in Figure 2.

The mutation operation is to reverse the code value at the selected position. In this article, the binary code 0 and 1 values of the selected position are converted; that is, the direction of the robot path in the original code is changed after the code conversion; for example, when the original

code, the two-digit code group 01 means that when the robot moves toward the south, the path code changes to 11, and the robot changes to the south and then turns to the west, and the direction of movement changes. The machine will reverse it to 0 by the mutation operation and if the binary code is 1 in the human path coding, and vice versa.

**2.1.5. Termination Conditions.** The termination of genetic algorithm is divided into two cases. In the first case, if  $t = T$ , the population has evolved to the maximum evolutionary algebra, and the individual with the current maximum fitness function value is output as the optimal solution, and the calculation is terminated; in the second case,  $t < T$  algorithm exits early, the selected individual has met the optimal standard, and the output is the optimal solution.

Constraints can also be introduced,  $f_{(n+1)}$  is the fitness of the best individual in the  $n + 1$ th generation, and  $\delta$  is an integer.

$$|f_{(n+1)} - f_{(n)}| < \delta. \quad (5)$$

When  $|f_{(n+1)} - f_{(n)}|$  is less than a set constant, the algorithm is judged to end and the algorithm exits.

## 2.2. Robot Path Planning Based on Improved Genetic Algorithm

**2.2.1. Robot Path Planning Principle Based on Improved Genetic Algorithm.** In this paper, the VC++ 6.0 program and the use of nwu-rr-i intelligent mobile robot simulation experiments and comparison of different parameter settings under the different effects of path planning, statistics, and analysis of data verify the correctness of the algorithm.

**2.2.2. Fitness Function.** The traditional grid size must meet the free movement of the robot in the grid, which stipulates that the minimum distance of the grid must be the length of the robot, which increases the size of the grid and reduces the diversity of the grid area, which is not conducive to smallness. In the experiment, the indication of obstacles and the description of specific environment information are added. This paper fully considers the flexibility and variability of grid division and the reality that the robot is not a particle and proposes a safe distance operator. The safe distance is determined by the volume of the robot. Set the ratio between the simulated map and the actual map to  $1 : \alpha$ , then the safe distance is set to the length/ $\alpha$  of the robot. The obstacle is expanded, and the distance of

expansion is set to the actual map scale safe distance. The ratio of the safe distance to the grid size is the number of black grids around the obstacle. If the safety distance is less than 1, it will be expanded by 1 grid count, set the grid within the safe distance of the map to black, which means the dangerous area; other points that are not black are the range of safe route selection. In the robot path planning system, the dangerous area should be directly set as an obstacle in advance to simplify the amount of information processed by the algorithm. The setting method of the safe distance operator fully considers the safety of the path and the convenience of the algorithm.

In the simulation, it is assumed that after the obstacles are marked, the robot can pass through a path in a single grid space. The grid size is divided according to pixels. The size of the path display area has been determined. The proportional relationship is calculated, and the pixel size of the grid height and width is input to determine the number of grids. The length of the character string encoded by the robot path is half of the number of grids, and the number of grids is variable.

The improved robot path planning scheme breaks through the constraint that the grid can only be a grid. Researchers can set the length and width of the grid according to their needs. When the grid is not square, if the path of the robot is a connection between two grid vertices, the connection between the two vertices is not completely drawn through the center of each grid, which increases the difficulty of the display, and in order to compare with the previous chapter the algorithm is unified, and the robot still stipulates that the robot will only move in the four directions of due east, due west, due south, and due north. When comparing algorithms, even if the robot will not advance diagonally, the robot will not have acute or obtuse corners, but since neither the algorithm before or after the improvement can achieve diagonal movement, the comparison evaluation factor convergence speed, optimization time, path smoothness, etc. Not affected, the results still have a certain degree of credibility.

*2.2.3. Other Genetic Operators.* In genetic algorithm, in order to improve the population quality, the algorithm directly copies the optimal individuals in the current population to the next generation. However, the new population can not meet the requirements of crossover and mutation operation, and the algorithm is easy to fall into premature state. Therefore, it is necessary to rejudge the differences within a certain evolutionary algebra, discard the populations that do not meet the differences in the short term, and create a new population. Multipoint crossover is used for crossover operation, and multipoint mutation is used for mutation operation. The positions of crossover points and mutation points are randomly determined, and multiple experiments are required to obtain empirical values.

*2.2.4. Delete Operator.* Introduce the idea of mathematical modeling in the deletion operator, encode the path as a binary string in the raster map, and each grid corresponds to an array coordinate. Combine the deletion operator and

the array  $a[x][y]$  to delete. For codes that enter the same array in the same path, the codes after  $a[x][y]$  are directly moved forward to shorten the code length. This method effectively reduces redundant and blocked paths and reduces the path length.

The algorithm refers to the concept of the parent node. The node that the robot walks through is regarded as the parent node and saved independently. When the robot finds that the parent node is repeatedly saved during the path planning process, the path is judged as an invalid path and discarded, using recursive calling. Thinking step by step back to the parent node that was repeatedly saved, and then branch from the parent node to other paths, until a feasible path is found, the invalid branch is deleted, and only one valid path is retained. When programming, the grid and array coordinates are related to each other, which greatly facilitates the participation of the delete operator.

The parent node appears in the definition of the tree and belongs to the knowledge of the data structure. The parent node is a component of the tree. Each node of the parent node has only one antecedent. The root node is the root node. The root node is the ancestor of all nodes in the tree except itself. The root node has no parent node. In this algorithm, the starting point of the robot is the root node, and the robot can only move from the starting point. It can also be seen in the virtual map introduced later that the starting point of the path can only be the starting point of the robot.

*2.2.5. Principles of Robot Step Length Setting.* Set the step size. The step length represents the number of times the robot moves from the start point to the end point, that is, the superimposed sum of the number of grids that the path of each generation of the robot passes through. Taking into account the specific environmental path planning of the NWU-RR-I intelligent mobile robot, set a parameter for the step length, which is expressed by iT Route Count and limited to 3000 steps. If there are too many steps, the population is judged to be an invalid population, discarded, and restarted. The code is as follows: TRACE ("Search path failed\n").

### *2.3. Robot Path Planning Based on Improved Genetic Algorithm*

- (1) Activate the start button
- (2) Calculate the safety distance, set the start and end points of the robot, and mark the obstacle area
- (3) Initialize the population and judge the difference of the population
- (4) Calculate the value of the population fitness function and judge whether it meets the optimal standard. If the population meets the optimal standard, the current solution is output, and the current solution is the optimal solution; if the population does not meet the optimal standard, a series of genetic operations are performed on the population, such as crossover, mutation, deletion, and step size judgment. Return to Step (4).

```

class CASRSystem;
interface IASRMotion;
protected:
  BOOL BuildSystem(); //library function initialization
  void DestroySystem();//Library function exit
private:
  CASRSystem* m_ pRobot; //Define library system pointer
  IASRMotion*
  m_ pMotion; //Define library interface pointer
  enum {SPEED VALUE = 500; //Set the robot's movement speed

```

CODE 1.

(5) Output the optimal path

### 3. Experimental Research on Robot Path Planning Based on Improved Genetic Algorithm

#### 3.1. Path Planning Simulation of Genetic Algorithm

##### 3.1.1. Simulation Scheme

(1) *VC++6.0 Is Selected as the Software Platform.* VC++6.0 is a visual integrated development environment IDE (integrated development environment) based on the Windows operating system. It supports C++ language, which is easy to use with databases such as SQL and is easy for man-machine interaction. The realization of the interface has a wide range of uses.

The hardware platform uses NWU-RR-I intelligent mobile robot. The NWU-RR-I intelligent mobile robot system library function NWU-RR-ISetupbuild.EXE is compatible with VC++6.0 and can be programmed to control the robot directly in VC. Click to install NWU-RR-ISetupbuild.EXE. You need to add "NWU-RR-ISystem.h" in front of each header file during programming, which means that VC is compatible with all the functions in the NWU-RR-I robot library. The specific syntax is as follows: #include "NWU-RR-ISystem.h".

Similarly, the control interface function should be added to the CmotionDemoDIg class, and each interface should be initialized. The code is as follows:

(2) *Establishment of Simulation Environment.* Divide the environment into a series of grids, and mark obstacles in the grid. Obstacles represent 1, and obstacles are represented as 0.

(3) *Genetic Algorithm.* According to the algorithm coding rules, the path is coded, the population is initialized, and a series of genetic operations are performed on it, and it is judged whether the population meets the termination condition. If the termination condition is met, the optimal path is output, and the result is displayed; if the termination condition is not met, the genetic operation is continued until the termination condition is met.

The NWU-RR-I intelligent mobile robot moves according to the instructions of the simulation results and completes the path planning task from the start point to the end point.

#### 3.1.2. Path Planning Realization of Genetic Algorithm

- (1) *Comparison of the Number of Obstacles in Different Situations.* In the same geographic environment, within the same area, the starting point and ending point do not change, and the number of obstacles in the main path area is set differently
- (2) *Implementation of Genetic Algorithm Path Planning for Different Starting Points and End Points.* In the same geographical environment, within the same area, the number of obstacles in the main path area is set the same, and the starting point and ending point are changed

3.2. *Simulation of Improved Genetic Algorithm and Comparison of Results.* The software platform selects VC++6.0 to make a human-computer interaction interface, and the operation idea of manual selection is added to the traditional robot path planning simulation. The differences are mainly in the following two aspects.

3.2.1. *Simulation Scheme.* The improved simulation program combined with the actual environment can select obstacles multiple times; select the starting point and end point of the robot multiple times; change the grid size multiple times; reproduce the path and so on. The simulation mode of traditional robot path planning is changed, and the correlation between the simulation environment and the actual environment is increased, which is convenient for simulation experiments in different environments. The adjustability of the number of grids facilitates the comparison of different amounts of information in the same environment. This scheme improves the reliability of robot path planning simulation and has high portability and certain reference value.

3.2.2. *Algorithm Improvement.* Improvements are mainly proposed from fitness function, deletion operator, termination conditions, etc., which increase the convergence speed of the algorithm and improve the safety of robot path planning.

TABLE 1: The relationship curve between effective path ratio and population size.

Mutation rate = 0.09	Population size	10	20	30	40	50	60	70	80	100	150	200	300
Crossover probability = 0.8	Before improvement	0	20	40	41	42	43	42	43	42	38	40	39
Evolutionary algebra = 150	After improvement	80	77	79	78	82	83	83.5	79	80	80.5	81.5	81

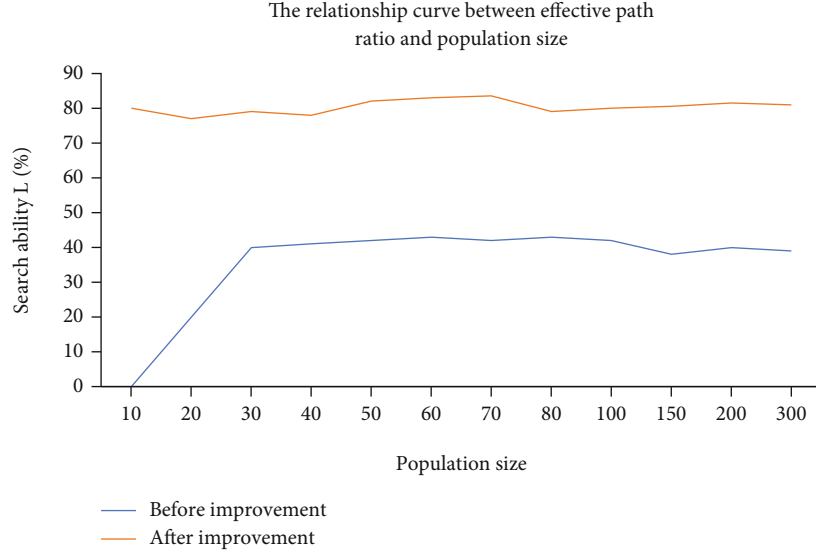


FIGURE 3: The relationship curve between effective path ratio and population size.

TABLE 2: The relationship curve between effective path ratio and evolutionary algebra.

Mutation rate = 0.09	Evolutionary algebra	10	20	30	40	50	60	80	100	150	200	500	1000
Crossover probability = 0.8	Before improvement	0	3	4	15	21	23	42	43	62	50	59	70
Population size = 60	After improvement	72	81	80	79	80	81	82	80	79	80	81	80

The population is a binary code generated by a random operator, and its code length changes with the number of grids, so the path of each run is different, but an average can be obtained through various average evolutionary algebras and average path smoothness. The reference value in the sense has a certain universality. In addition, the randomly generated path is not affected by the artificially determined population individuals on the algorithm, and the accuracy of the algorithm can be verified by only multiple measurements and averaging.

#### 4. Experimental Research and Analysis of Robot Path Planning Based on Improved Genetic Algorithm

*4.1. Relationship Curve between the Effective Path Ratio and the Population Size before and after the Algorithm Is Improved.* Because the path planning algorithm needs to execute a large number of loops, and the C language program is 300 times more efficient than the MATLAB program for loop execution, the algorithm is written in C language,

but MATLAB has good graphics processing functions, so MATLAB is used for simulation.

In order to improve computational efficiency, it is necessary to determine the optimal value of genetic parameters. The traditional genetic algorithm equates the search capability  $L$  of the mobile robot with the ratio of the effective path at the end of evolution, namely:

$$L = \frac{\text{number of effective paths}}{\text{population size}} \text{ (at the end of evolution).} \quad (6)$$

By analyzing Table 1 and Figure 3, the following conclusion can be drawn: In the algorithm of this paper, the genetic parameter that has the greatest impact on the effective path ratio is the mutation probability. 95.64% gradually decreased to 73.42%. It can be seen from the mutation probability graph that when the mutation probability is 0.09, the effective path ratio is 80.65%. From the other three graphs, it can be seen that no matter how the population size, evolutionary algebra, and crossover probability are selected, as long as the mutation probability is taken as 0.09, the effective path ratio is about 80%. The effective path

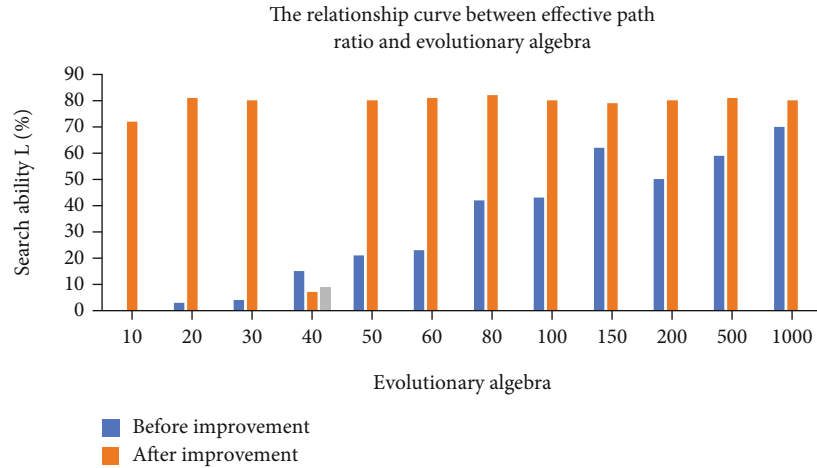


FIGURE 4: The relationship curve between effective path ratio and evolutionary algebra.

ratio of the improved algorithm has been maintained at a relatively high level, and it is obviously better than the previous algorithm in terms of numerical value and stability, so it proves that the improvement of the genetic algorithm in this paper is successful.

*4.2. Relationship Curve between the Effective Path Ratio before and after the Algorithm Improvement and the Evolution Algebra.* It can be seen from Table 2 and Figure 4 that the effective path ratio is inversely proportional to the mutation probability but has little to do with population size, evolutionary algebra, and crossover probability. The greater the mutation probability, the more irreparable paths are generated during the mutation process, so the mutation probability is inversely proportional to the effective path ratio, but the mutation probability will increase the diversity of the population, which can avoid the premature solution, so the search is only judged from the effective path ratio. The capacity is inappropriate. Because path planning seeks the shortest path without collision from the starting point to the target point, this paper also proposes a method to measure the search ability; that is, the shortest path length obtained at the end of evolution is used to measure the size of the search ability.

## 5. Conclusions

With the continuous progress of social science and technology, especially in the field of artificial intelligence and intelligent control, relevant theories continue to be in-depth research, and technological methods are changing with each passing day. With the improvement of social industrial manufacturing automation, robots will play an increasingly important role in industrial production, personal services, and other industries. In this paper, the genetic algorithm is improved by rejudging the difference and discarding precocious population in the process of genetic algorithm iteration. The improved genetic algorithm is used to plan the robot's path. It can be seen from the experimental results that the effective path ratio of the improved algorithm

remains at a high level, and it is obviously superior to the previous algorithm in terms of numerical value and stability, which proves that the improvement of the genetic algorithm in this paper is successful. In the future society, robot research will be more in-depth; robot path planning research will make great progress, to show us a higher level of robots.

## Data Availability

The data underlying the results presented in the study are available within the manuscript.

## Conflicts of Interest

The authors declare that they have no conflicts of interest.

## References

- [1] Y. Z. Wang, X. Y. Zheng, C. Lu, and S. P. Zhu, "Structural dynamic probabilistic evaluation using a surrogate model and genetic algorithm," *Proceedings of the Institution of Civil Engineers: Maritime Engineering*, vol. 173, no. 1, pp. 13–27, 2020.
- [2] R. Fitriana, P. Moengin, and U. Kusumaningrum, "Improvement route for distribution solutions MDVRP (multi depot vehicle routing problem) using genetic algorithm," *IOP Conference Series: Materials Science and Engineering*, vol. 528, no. 1, article 012042, 2019.
- [3] G. A. Rovithakis, M. Maniadakis, and M. Zervakis, "A hybrid neural network/genetic algorithm approach to optimizing feature extraction for signal classification," *IEEE Transactions on Systems, Man and Cybernetics, Part B (Cybernetics)*, vol. 34, no. 1, pp. 695–703, 2004.
- [4] J. Ma, Y. Liu, S. Zang, and L. Wang, "Robot path planning based on genetic algorithm fused with continuous Bezier optimization," *Computational Intelligence and Neuroscience*, vol. 2020, no. 1, Article ID 9813040, 2020.
- [5] T. Hwu, A. Y. Wang, N. Oros, and J. L. Krichmar, "Adaptive robot path planning using a spiking neuron algorithm with axonal delays," *IEEE Transactions on Cognitive & Developmental Systems*, vol. 10, no. 2, pp. 126–137, 2018.

- [6] D. Zhang, X. You, S. Liu, and H. Pan, "Dynamic multi-role adaptive collaborative ant colony optimization for robot path planning," *Access*, vol. 8, pp. 129958–129974, 2020.
- [7] M. Zhao, H. Lu, S. Yang, and F. Guo, "The experience-memory Q-learning algorithm for robot path planning in unknown environment," *Access*, vol. 8, pp. 47824–47844, 2020.
- [8] S. D. Han and J. Yu, "DDM: fast near-optimal multi-robot path planning using diversified-path and optimal sub-problem solution database heuristics," *IEEE Robotics and Automation Letters*, vol. 5, no. 2, pp. 1350–1357, 2020.
- [9] J. Qi, H. Yang, and H. Sun, "MOD-RRT\*: a sampling-based algorithm for robot path planning in dynamic environment," *IEEE Transactions on Industrial Electronics*, vol. 68, no. 8, pp. 7244–7251, 2021.
- [10] L. Gao, R. Liu, F. Wang et al., "An advanced quantum optimization algorithm for robot path planning," *Journal of Circuits, Systems and Computers*, vol. 29, no. 8, pp. 2050122–2050143, 2020.
- [11] S. Nafea, E. Kadum, and D. Hamza, "Path loss optimization in WIMAX network using genetic algorithm," *International Journal of Computers, Communications & Control*, vol. 20, no. 1, pp. 24–30, 2020.
- [12] E. Joeliando, D. Christian, and A. Samsi, "Swarm control of an unmanned quadrotor model with LQR weighting matrix optimization using genetic algorithm," *Journal of Mechatronics, Electrical Power, and Vehicular Technology*, vol. 11, no. 1, pp. 1–10, 2020.
- [13] S. Quraishi and A. J. Khan, "Genetic algorithm for shortest path optimization in network," *International Journal of Scientific and Research Publications*, vol. 9, no. 7, article 9188, 2019.
- [14] M. R. Islam, P. Protik, S. Das, and P. K. Boni, "Mobile robot path planning with obstacle avoidance using chemical reaction optimization," *Soft Computing*, vol. 25, no. 8, pp. 6283–6310, 2021.
- [15] E. Behmanesh and J. Pannek, "A comparison between memetic algorithm and genetic algorithm for an integrated logistics network with flexible delivery path," *Operations Research Forum*, vol. 2, no. 3, pp. 1–24, 2021.

## Research Article

# Research on Data Analysis of Digital Economic Management under the Background of Big Data

Jie Huang 

College of Business Administration, Zhejiang Institute of Economics and Trade, Hangzhou, 310000 Zhejiang, China

Correspondence should be addressed to Jie Huang; [rolatata@zjiet.edu.cn](mailto:rolatata@zjiet.edu.cn)

Received 18 January 2022; Revised 9 February 2022; Accepted 14 February 2022; Published 6 May 2022

Academic Editor: Shalli Rani

Copyright © 2022 Jie Huang. This is an open access article distributed under the Creative Commons Attribution License, which permits unrestricted use, distribution, and reproduction in any medium, provided the original work is properly cited.

In order to study the application of big data in the field of digital economy, data management improves the needs of business model to a certain extent and responds to the pace of rapid development of science and technology and the transformation of business model in special times, so as to promote economic development. Based on the information extracted from the software system log, this study introduces machine learning algorithms such as spatial convolution and fuzzy multicolumn convolution, deduces the interaction between visitors and software according to the system software access log, wavelet algorithm, and denoising algorithm, deduces the data value index of the secondary market, constructs the simulation software under Matlab, and compares it with the previous system. By improving the prediction sensitivity of interaction and the prediction coupling of data value, it is confirmed that the system improves the efficiency of data management, so as to achieve the purpose of digital economic management and promote economic development and progress.

## 1. Introduction

In recent years, with the development of computer science and technology, big data has become a new type of technological reform. In the process of scientific and technological innovation, it has subverted the conventional technical mode and broken the dilemma that traditional technology is difficult to develop sustainably.

When big data was used to describe network search in the early days, it needed to process or analyze a large number of data. It was a hot subject in academic and computer research at that time. In subsequent related data research, such as data warehouse, data security, data analysis, and data visualization, it has become the focus of various fields.

McKinsey, a world-renowned consulting firm, was the first to define “big data”: data has penetrated into every industry and business functional field and become an important production factor. People’s discussion and application of large quantities of data indicate the emergence of new production initiatives and the change of new consumption concepts.

The enterprise’s operation mode changes with the development of the times. How to face difficulties in special times

and the transformation of operation mode brings more vitality to the enterprise. Taking the retail industry in the epidemic situation in 2019 as an example, this paper describes the forced transformation of the retail industry, the use of big data technology to convert the previous offline sales to online sales, and profound changes have taken place through the operation mode and consumption mode, so as to seek a breakthrough for enterprise development [1]. Digital economy is the concept of economics. It is a process in which human beings integrate resources directly or indirectly through big data to make them play a role, so as to promote economic development. In this paper, the role of “block-chain + big data” is to promote the transformation of old and new economic models, as well as major reforms in economic operation and daily life style, so as to achieve the purpose of improving the level of national economic development [2].

Russia is a country with more land and fewer people and has land advantages. This paper analyzes the data of global agricultural development, puts forward the digital agricultural system, establishes the relationship between its elements and the external environment, and develops a



private method to implement major adjustments to agricultural planning and evaluate the economic efficiency and risks brought by the digital innovation and development of regional crop production [3].

The digital economy has attracted worldwide attention, and foreign countries have also applied the digital economy to various fields. This is because the traditional management is not perfect in data application, resulting in incomplete information collection in all aspects, which can only be managed manually, resulting in backward management of the overall system. After integrating the information through big data, the required data can be extracted. It can more accurately solve the needs of enterprises.

With the popularization and application of big data, digital economy has become the driving force of global economic development, promoting the transformation of human economic form and reducing social transaction costs. Starting from the international environment, this paper analyzes the development direction and benefits of some important international organizations in the field of digital economy, so as to analyze the current situation of China's digital economy development and make progress from all aspects. This paper demonstrates and puts forward some suggestions to promote the development of China's digital economy [4]. Sadyrin et al., national economic transformation, proposed the application of digital technology to enterprise economic activities. The application of big data technology in digital economy has involved many financial fields. This paper discusses how to effectively use big data in financial analysis and apply big data to various management decisions to effectively improve its efficiency [5].

The application of big data not only breaks the disadvantages of conventional models, leads enterprises to open up new business models, promotes economic development, but also improves decision-making efficiency [6]. This study deduces the data value index of the secondary market according to the information extracted from the software system log, deduces the interaction between the visitor and the software according to the system software access log, as well as the wavelet algorithm and denoising algorithm, and realizes the purpose of economic management with a new model.

## 2. Structure and Evaluation Logic of Digital Economy Market

The emergence of big data has been applied to physics, biology, environmental ecology, and other fields, as well as finance, communication, military, and other industries. However, it has been paid more attention because of the development of the Internet industry in recent years [7].

Many people do not know what digital mode is. It refers to the form of promoting the development of economic structure by using digital knowledge and information as the main body, high-tech information network as the carrier, and information and communication technology as the means to improve efficiency [8].

According to the white paper, in 2017, China's total digital economy was more than 28 trillion yuan, with a year-on-

year nominal growth of nearly 20% and a GDP ratio of more than 30%. It shows that this economic model has become the driving force to promote China's economic growth in recent years [9]. In the long run, when the proportion of digital economy GDP will exceed 50%, China will fully enter the era of digital economy [10].

If the digital sharing interactive system is regarded as an economic system, the natural person participants in the economic system, in addition to the data manager, only include two roles: visitors to the software platform software and traders in the big data asset secondary trading market. Visitors obtain relevant data information through software and trade in the secondary market through resource integration, so as to achieve benefits. The whole architecture is to collect, store, extract, manage, and analyze large-scale data, so as to obtain relevant information efficiently and quickly.

In Figure 1, visitors obtain information through the software system or exchange information through the software system, and the relevant information data are stored in the software background. The interaction volume and price can be fed back from the access log. After data analysis and processing, these data can provide reference value for the operation of enterprises and provide services for their circulation and transaction in the subsequent secondary market, so as to realize digital data management. Wavelet transform is the process of de quantization. Different units are transformed and compared.

The footprints left by visitors on the software platform form an access log. A large amount of data can be obtained according to the access log information. After processing, it is related data assets and resources that can be circulated in the secondary market. The main reference object of this research is access log, and even the whole research is carried out around access log.

*2.1. Deduce the Interaction between Visitors and Software according to the Access Log.* The access log mentioned above is the main core of the whole research. The access log left on the software system is the key of the whole architecture and the core of the management of digital economy. The correlation between access log and output can be deduced through the following formula.

The evaluation mode of interaction between visitors and software is deduced according to the access log, as shown in formula (1):

$$X_i(t) = \gamma_T \cdot T_i + \gamma_S \cdot S_i(t) + \gamma_P \cdot P_i(t) + \gamma_G \cdot G_i(t). \quad (1)$$

Among them,  $X_i(t)$  is the weighted result of data trigger amount of user  $I$  at time  $t$ ;  $S_i(t)$  is data submission amount of user  $I$  at time  $t$  (submit method);  $P_i(t)$  is the amount of data logs of user  $I$  at time  $t$  (post method);  $G_i(t)$  is the data usage of user  $I$  at time  $t$  (get method);  $T_i$  is the other data trigger amount of user  $I$  at time  $t$ ;  $\gamma_T$ ,  $\gamma_S$ ,  $\gamma_P$ , and  $\gamma_G$  are weighting factors of the above four evaluation factors.

In the actual economic treatment, the equation needs to be processed by linear integration after accumulation, as

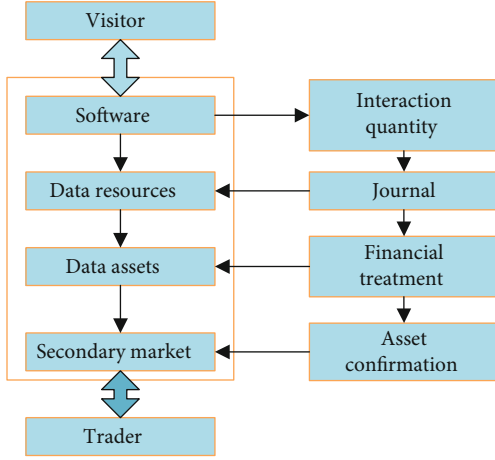


FIGURE 1: Structure of digital economy market.

shown in formula (2):

$$S_X = \int_m^n \sum_{i=1}^r X_i(t) dt. \quad (2)$$

Among them,  $S_X$  is the access log evaluation factor;  $m$ ,  $n$  is the time period threshold of integral function;  $r$  is the number of users investigated by the integral function. The meanings of other mathematical symbols are the same as those above.

According to the above principles, machine learning algorithms such as spatial convolution and fuzzy multicolumn convolution are introduced to push forward the time  $t$  axis for a certain period to form multiple interaction prediction values based on depth Iterative Regression from T1 to TN. the algorithm logic is shown in Figure 2.

As shown in Figure 2, the basis function of the spatial convolution algorithm is shown in formula (3); the node function of FNN fuzzy neural network selects the sixth-order polynomial depth Iterative Regression basis function, as shown in formula (4); the node function of multi column fuzzy neural network selects the logarithmic depth Iterative Regression basis function, as shown in formula (5).

$$y = \int_{-\infty}^{+\infty} g(x)q(t-x)dt. \quad (3)$$

Among them,  $g(x)$  is the convoluted array function;  $q(t-x)$  is the convolution kernel function;  $t$  is the convolution pointer;  $x$  is the convolution control variable;  $y$  is the convolution result.

$$y = \sum_{i=1}^n \sum_{j=0}^5 A_j x_i^j, \quad (4)$$

$$y = \sum_{i=1}^n (A \bullet \log_e x_i + B) \quad (5)$$

Among them,  $x_i$  is the input value of the  $i$ th node of the previous neural network;  $y$  is the output value of this node;  $n$

is the number of nodes of the previous neural network;  $A$  and  $B$  are variables to be regressed, which refer to the variables to be regressed of the  $j$ th-order polynomial.

In the figure, the user's access log in a certain period is analyzed, and the machine learning algorithms such as spatial convolution and fuzzy multicolumn convolution are introduced to predict the interaction between the visitor and the software. This study is mainly aimed at the impact of data management on the economy and deduces the interaction volume and price trend of a product through the data obtained from the access log.

*2.2. Deduce the Data Value Index of the Secondary Market according to the Interaction Volume Data.* The interaction volume data is the total information production of the network platform. The correlation between the interaction volume data and the data value index of the secondary market is subtle. If they are intuitive and lack a direct logical relationship, but after denoising, it is concluded that the data signal-to-noise ratio is very low, the data value index of the secondary market can be deduced according to the interaction volume.

In Figure 3, wavelet transforms the interactive data, refines the data through translation, and pulls back the curve deviated from the original axis, which can finally meet the analysis requirements by itself. After the difference noise reduction, the unavailable information is eliminated to obtain a credible correlation function. Due to the complexity of the information obtained, it is necessary to convert different units when comparing. Wavelet transform is a dimensionless process and a new transformation analysis method.

In the actual data processing, the lightweight data processed by wavelet transform can form the characteristic matrix through Fourier transform. At the same time, the original data needs to be Fourier transformed to form the original characteristic matrix, so as to provide sufficient data to be measured for the subsequent fuzzy neural network.

Daubechies (DBN) wavelet is adopted for wavelet transform, and its basis function is as follows: (6)–(8):

$$p(y) = \sum_{k=0}^{n-1} C_k^{n-1+k} y^k, \quad (6)$$

$$C_0(\omega) = \frac{1}{\sqrt{2}} \sum_{k=0}^{2n-1} h_k e^{-jk\omega} = \sqrt{\left(\cos^2 \frac{\omega}{2}\right) p\left(\sin^2 \frac{\omega}{2}\right)}, \quad (7)$$

$$\psi(y) = \int p(y)p(t-y)dt. \quad (8)$$

Among them,  $n$  and  $k$  are the pointer variables;  $y$  is the controlling dependent variable;  $\omega$  is the transformed periodic dependent variable;  $\psi(y)$  is the final function of wavelet transform;  $p(y)$  is the wavelet transform control function;  $C$  is the wavelet transform factor function;  $e$  is the natural constant.

In the process of denoising, unnecessary data are processed, and queue interference factors can better obtain

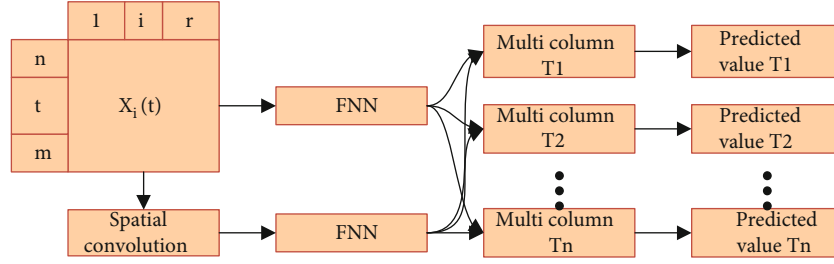


FIGURE 2: Logic diagram of data prediction algorithm.

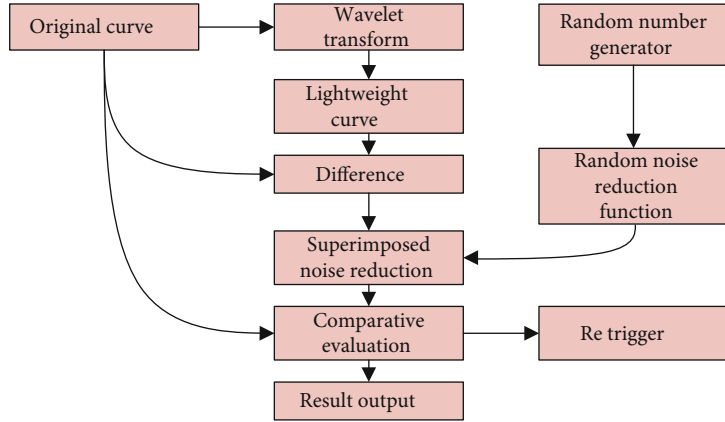


FIGURE 3: Logic of generation algorithm of transaction price estimation curve in secondary market.

high-quality data, so as to provide guarantee for subsequent analysis of data.

The generation algorithm of random noise reduction function is shown in formula (9):

$$\Delta F(x) = \rho_A \cdot \text{Rand} \cdot \sin(\rho_B \cdot \text{Rand} \cdot x + \rho_C \cdot \text{Rand}) + \rho_D \cdot \text{Rand}. \quad (9)$$

Among them, Rand is the random numbers with interval on  $[0,1]$ ;  $\rho_A$ ,  $\rho_B$ ,  $\rho_C$ , and  $\rho_D$  are the interval adjustment factors of random number;  $x$  is the independent variable;  $\Delta F(x)$  is the dependent variable.

The algorithm of noise reduction process is shown in formula (10):

$$F_S(t) = X_i(t) - \psi(y) + \Delta F(x). \quad (10)$$

Among them, the meaning of mathematical symbols is the same as that above.

In the formula, the dependent variables include different data structures such as  $t$ ,  $y$ , and  $X$ . However, according to the conversion method of the previous formula, all dependent variables can be normalized and isomorphic, which is limited by space. Its processing method is not discussed here. Through the comprehensive use of wavelet transform, random waveform superposition noise reduction, and cyclic learning, data analysis with high coupling degree can be realized under the condition of data relationship with low signal-to-noise ratio. Because the data prediction algorithm

designed in Section 2.1 has fully expanded the independent variable function, the coupled dependent variable function can realize the follow-up expansion, so as to realize the data prediction analysis based on curve estimation algorithm.

### 3. Algorithm Effectiveness Evaluation

The simulation software is constructed under Matlab, and the data prediction module of digital economic management information system is constructed based on the algorithm. The data prediction module of digital economic management information system supported by more mature nonlinear overall planning algorithm for complex systems in the technical market is selected with reference to the group, and the data performance of the two is compared.

**3.1. Prediction Sensitivity to Interaction.** Interaction refers to communication and interaction. It is built on a software system platform for sharing resources, information, or services or for mutual communication between the software system platform and users and between users and users, so as to obtain more ideas and meet some needs among users. The amount of interaction refers to all information data on the network platform.

Through the real-time interactive data of Guiyang big data asset exchange and the log data of five big data systems investigated, the software system access log records all data information of the software platform, extracts and analyzes the data information in the access log, and introduces machine learning algorithms such as spatial convolution

TABLE 1: Comparison of prediction sensitivity of data interaction volume of software platform (the data source is the real-time interactive data of Guiyang big data asset exchange).

Sensitivity	Submit data	Post data	Get data	Other data	Comprehensive
The system	96.32%	88.76%	92.41%	85.42%	90.74%
Previous system	90.21%	84.43%	85.38%	81.87%	85.47%
$T$	5.28	8.12	6.48	5.87	4.58
$P$	0.009	0.007	0.008	0.007	0.008

TABLE 2: Comparison of predicted coupling degree of software data asset value (the data source is the real-time interactive data of Guiyang big data asset exchange).

Coupling degree	Data inflection point	Opening value	Closing value	Peak value	Valley value	Comprehensive
The system	85.14%	78.65%	84.26%	92.45%	90.23%	86.15%
Previous system	78.23%	70.41%	77.56%	83.79%	80.96%	73.47%
$t$	4.75	5.12	6.29	5.08	4.17	5.24
$P$	0.008	0.007	0.009	0.008	0.006	0.007

and fuzzy multicolumn convolution to inverse the interaction between visitors and software. The reference group selects the data prediction module of the digital economic management information system supported by the more mature nonlinear overall planning algorithm for complex systems in the technical market and observes its prediction sensitivity to the interaction volume of the access log on the software.

In Table 1, bivariate  $t$ -test was conducted for two different systems, and it was found that  $T < 10.000$ ,  $P < 0.01$ , with credible statistical difference;  $T$  value is the value in the output result of bivariate  $t$  verification. When  $T < 10.000$ , it is considered that there is a statistical difference between the two columns of data, and the smaller the  $T$  value, the more significant the statistical difference is. When  $P < 0.01$ , it is considered that the statistical result has a significant statistical difference, and the smaller the  $P$  value, the more significant the statistical meaning is. It shows that the system is different from the previous system, and the system improves the sensitivity of interaction prediction.

In order to more intuitively reflect the prediction sensitivity of the upper system log data to the interaction volume, visualize the data in Table 2 to get Figure 4.

In Figure 4, sensitivity refers to the proportion of all true positive data in all positive data. Although the difference between this scheme and the previous system algorithms is not great, the prediction sensitivity of the overall interaction volume is relatively satisfactory. Among them, the prediction sensitivity of submit data reaches more than 96%. Today's Turing test standard, neural network has more than 95% sensitivity, that is, its machine learning ability has fully met the needs of data management. These data can provide reference value for enterprises in operation and provide services for circulation and trading in the subsequent secondary market.

**3.2. Prediction Coupling of Data Value.** The data source is the real-time interactive data of Guiyang big data asset

exchange and the log data of five big data systems investigated. The data cycle is from January 2019 to June 2021. In a three-and-a-half-year data cycle, analyze the data within a certain time limit and explore the prediction coupling degree of software system log to data value.

As shown in Table 2, bivariate  $t$ -test was conducted for different systems, and it was found that:  $T < 10.000$ ,  $P < 0.01$ , with believable statistical difference. It shows that the system significantly improves the prediction coupling degree of software data asset value on the basis of the previous system. The data obtained from the software system log not only has high sensitivity to the prediction of interaction volume, but also has a certain correlation to the coupling degree of software data asset value prediction, so as to improve the accuracy of software data asset value.

In order to more intuitively reflect the prediction coupling degree of the upper system log data to the value of software data assets, visualize the data in the table to get Figure 5.

In Figure 5, after the influencing factors in the data are removed through the wavelet exchange algorithm, the data more conducive to the research is obtained. Through the data, the software data asset value is predicted to obtain a higher coupling degree, which is conducive to the analysis of big data and improves the efficiency of data management.

## 4. Summary

Now China's scientific and technological level has entered a stage of rapid development. The changes of the times have led to the transformation of economic model [11]. In recent years, the traditional economic model has gradually declined, and the changes of market environment and business mode have promoted the reform of economic system. The cross-border integration of Internet information data on major data industries and the innovation of application technology data have promoted the development of digital industry and produced relevant big data background. It

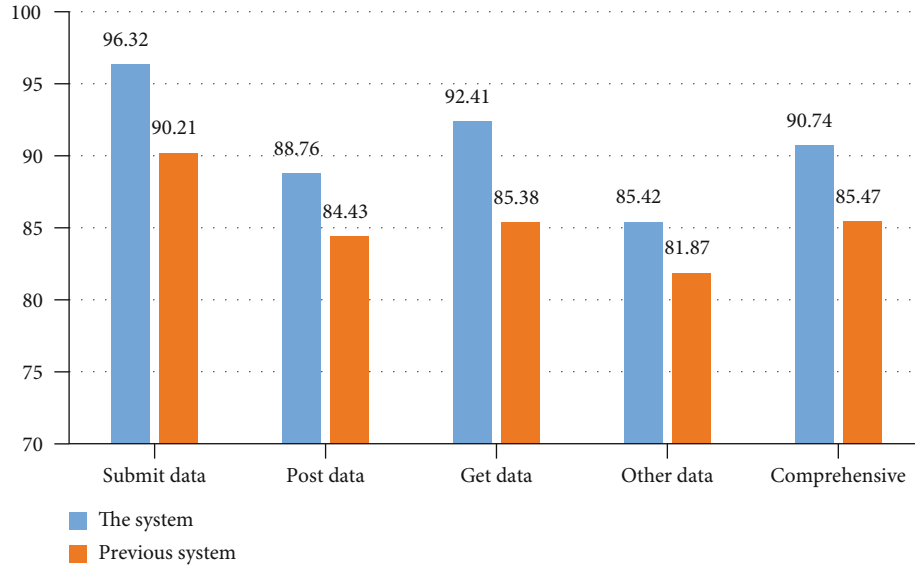


FIGURE 4: Visual diagram of prediction sensitivity of data interaction volume of software platform.

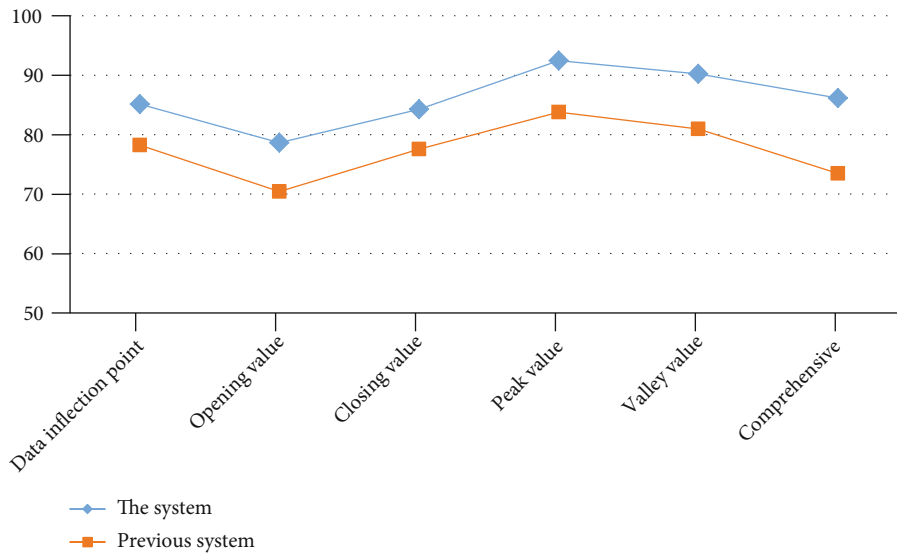


FIGURE 5: Visual diagram of prediction coupling degree of software data asset value.

can systematically manage scattered data, facilitate people’s real life, and improve management efficiency. Quan et al., starting from the demand relationship, demonstrate the data and digital infrastructure, introduce the characteristics of digital economy, and analyze the prospect of digital economy in the future from many aspects [12].

The application of big data information management is changing the traditional life mode and business philosophy, realizing the integration and docking of digital information technology in many aspects, and promoting the development of big data information management into a new stage [13]. In recent years, the management of big data has received unprecedented attention in various fields. Only by fully mining the value trend of big data management, predicting the feasibility of big data management, and formulat-

ing effective schemes for implementation can we really transform data management into the practice of digital economy [14].

The research extracts the prediction sensitivity of software interaction volume through the software access log. The extraction of data is helpful to analyze the economic management data [15], convert the data into resource information, provide reference value for the operation, circulation, and transaction services of enterprises in the subsequent secondary market, and convert the data information into knowledge reserve and intelligent production, so as to achieve the purpose of promoting economic development. At this stage, the research of logarithmic digital economic management data is still at the level of attempt. Therefore, we need to comprehensively improve the foundation of

digital management, deeply tap and release the potential of digital economy, wait for scientific and technological progress, and further develop the application of big data in economic management.

### Data Availability

The data underlying the results presented in the study are available within the manuscript.

### Conflicts of Interest

There is no potential conflict of interest in our paper.

### Authors' Contributions

The author has seen the manuscript and approved to submit to your journal.

### Acknowledgments

This work was supported by the Zhejiang Philosophy and Social Science Program (22NDJC336YBM).

### References

- [1] X. Lida and L. Wa, "Remapping digital operations iClick is promoting big data technologies among companies to facilitate high-quality economic growth," *China Report ASEAN*, vol. 6, no. 5, pp. 48–49, 2021.
- [2] Z. Zhiyuan and C. Baoli, "New path of digital economy development from the perspective of "blockchain + big data", " *Journal of Guiyang University (Social Science Edition)*, vol. 16, no. 2, pp. 48–54, 2021.
- [3] A. R. Sayfedinov and P. V. Sayfedinova, "Basic economic principles of the digital transformation in Russian agriculture," *IOP Conference Series: Earth and Environmental Science*, vol. 745, no. 1, article 012009, 2021.
- [4] Z. Tao, W. Zai Qun, and Z. Xiao Yu, "Research on the international development trend of big data and digital economy and its reference to China," *E3S Web of Conferences*, vol. 233, article 01171, 2021.
- [5] S. Igor, S. Olga, and L. Olga, "Prospects for using big data in financial analysis," *SHS Web of Conferences*, vol. 110, article 05004, 2021.
- [6] A. N. Raikov, A. N. Ermakov, and A. A. Merkulov, "Assessments of the economic sectors needs in digital technologies," *Lobachevskii Journal of Mathematics*, vol. 40, no. 11, pp. 1837–1847, 2019.
- [7] M. Kwet, "Digital colonialism: US empire and the new imperialism in the Global South," *Race & Class*, vol. 60, no. 4, pp. 3–26, 2019.
- [8] D. Helbing, "Societal, Economic, Ethical and Legal Challenges of the Digital Revolution: From Big Data to Deep Learning, Artificial Intelligence, and Manipulative Technologies," in *Towards Digital Enlightenment* Springer, Cham.
- [9] N. Kshetri, "The emerging role of big data in key development issues: opportunities, challenges, and concerns," *Big Data & Society*, vol. 1, no. 2, 2014.
- [10] S. Leonelli, "Why the current insistence on open access to scientific data? Big data, knowledge production, and the political economy of contemporary Biology," *Bulletin of Science, Technology & Society*, vol. 33, no. 1–2, pp. 6–11, 2013.
- [11] X. X. Quan, J. F. Yang, and Z. Luo, "Models in digital business and economic forecasting based on big data IoT data visualization technology," *Personal and Ubiquitous Computing*, 2021.
- [12] X. X. Quan, J. F. Yang, and Z. R. Luo, "Correction to: models in digital business and economic forecasting based on big data IoT data visualization technology," *Personal and Ubiquitous Computing*, 2021.
- [13] Y. S. Hu, "The impact of increasing returns on knowledge and big data: from Adam Smith and Allyn Young to the age of machine learning and digital platforms," *Prometheus*, vol. 36, no. 1, pp. 10–26, 2020.
- [14] "Sunke Problems and Thoughts on the value development of data elements," *ICT and Policy*, vol. 47, no. 6, pp. 63–67, 2021.
- [15] L. Mingxing, S. Berui, and L. Linjian, "Endogenous logic and path construction of data resource capitalization," *New Economy Guide*, no. 3, pp. 43–49, 2021.

## *Retraction*

# **Retracted: A Survey on Location Privacy Attacks and Prevention Deployed with IoT in Vehicular Networks**

### **Wireless Communications and Mobile Computing**

Received 12 December 2023; Accepted 12 December 2023; Published 13 December 2023

Copyright © 2023 Wireless Communications and Mobile Computing. This is an open access article distributed under the Creative Commons Attribution License, which permits unrestricted use, distribution, and reproduction in any medium, provided the original work is properly cited.

This article has been retracted by Hindawi, as publisher, following an investigation undertaken by the publisher [1]. This investigation has uncovered evidence of systematic manipulation of the publication and peer-review process. We cannot, therefore, vouch for the reliability or integrity of this article.

Please note that this notice is intended solely to alert readers that the peer-review process of this article has been compromised.

Wiley and Hindawi regret that the usual quality checks did not identify these issues before publication and have since put additional measures in place to safeguard research integrity.

We wish to credit our Research Integrity and Research Publishing teams and anonymous and named external researchers and research integrity experts for contributing to this investigation.

The corresponding author, as the representative of all authors, has been given the opportunity to register their agreement or disagreement to this retraction. We have kept a record of any response received.

### **References**

- [1] N. Ahmed, Z. Deng, I. Memon, F. Hassan, K. H. Mohammadani, and R. Iqbal, "A Survey on Location Privacy Attacks and Prevention Deployed with IoT in Vehicular Networks," *Wireless Communications and Mobile Computing*, vol. 2022, Article ID 6503299, 15 pages, 2022.

## Review Article

# A Survey on Location Privacy Attacks and Prevention Deployed with IoT in Vehicular Networks

Nadeem Ahmed <sup>1</sup>, Zhongliang Deng,<sup>1</sup> Imran Memon <sup>2</sup>, Fayaz Hassan <sup>1</sup>,  
Khalid H. Mohammadani <sup>1</sup> and Rizwan Iqbal <sup>3</sup>

<sup>1</sup>School of Electronic Engineering, Beijing University of Posts and Telecommunications, Beijing 100876, China

<sup>2</sup>Department of Computer Science, Bahria University, Karachi Campus, Karachi, Sindh, Pakistan

<sup>3</sup>Department of Computer Engineering, Bahria University, Karachi Campus, Karachi, Pakistan

Correspondence should be addressed to Nadeem Ahmed; nadeempitafi@yahoo.com

Received 16 December 2021; Accepted 2 April 2022; Published 26 April 2022

Academic Editor: Ali Kashif Bashir

Copyright © 2022 Nadeem Ahmed et al. This is an open access article distributed under the Creative Commons Attribution License, which permits unrestricted use, distribution, and reproduction in any medium, provided the original work is properly cited.

Vehicular ad hoc networks (VANETs) connect two or more vehicles wirelessly to enable data exchange in an Internet of Things (IoT) environment. In VANETs, location privacy is the most crucial piece of information, and its protection is the top priority. However, the location privacy threats have not been adequately addressed in positioning for IoT in VANETs. This paper provides an overview of location privacy attacks and their solutions to address the problems caused by attacks in any IoT environment. Secondly, we have analyzed specific solutions based on anonymity (pseudonym) and cryptographic solutions using a digital signature technique. This enables to improve user privacy and security of location-based services for IoT in VANET. Moreover, we have proposed a faster 5G solution for the VANETs as it rapidly disseminates the data in fast-moving vehicles.

## 1. Introduction

VANET helps to ensure traffic safety through improved traffic flow and significantly reduces car accidents within the IoT environment [1–3]. VANET provides many valuable tools and advantages for VANET clients and requires implementation operations. Due to the personal transport trend, the number of vehicles has increased in the last few years. This has resulted in high density and over speeding of vehicles causing a significant rise in road accidents [4, 5].

VANET technology is aimed at equipping vehicle technology to reduce these factors by transmitting informative messages to each other [6–8]. Significant traffic problems like road accidents and congestion require new and more efficient transport systems [3, 9]. The Intelligent Transport System (ITS) for the IoT environment tackles critical issues such as the safety of the public and road congestion. It combines information and communication technology into the

transport and vehicle infrastructure. VANET includes different communication modes: vehicle to vehicle (V2V), infrastructure to vehicle (I2V), and the hybrid mode. In V2V, the connectivity media used are short-delayed and have a higher transmitting rate. This network infrastructure is used in various broadcast warning situations (emergency, reduced speed, crash, and slowing down the vehicle's speed) [10]. In I2V, the vehicle network considers the application of roadside unit (RSU) infrastructure points that multiply services in communication through Internet portals. Hybrid mode is the amalgamation of V2V and I2V techniques [11, 12].

VANET is intended to raise public awareness by broadcasting and aggregating current information on current or imminent transportation-related occurrences. The nodes of VANET are mostly segregated into two types: the first is an on-board unit (OBU), a radio device is mounted in automobile, and the other is road-side unit (RSU), therefore to ensure the protection of all passengers of vehicles and riders. Although ad hoc often connects vehicles in the network



topology in VANETs, it can be inadequate and ineffective to extend existing communication methods intended for traditional mobile ad hoc networks directly to massive VANETs with quick-moving vehicles [13].

The entire communication in VANETs is open access, which makes VANETs more prone to attacks. The attacker can intercept, alter, insert, and delete vehicular ad hoc network messages [14–16].

The intruder can control the traffic messages used to direct the road vehicles. The attacker can alter these messages and spread false road information causing traffic congestion and road hazards.

Many researchers have addressed the security and privacy issues associated with VANET. There is already much literature on addressing privacy issues in various aspects of vehicular communication. To the best of our knowledge and based on searches in different well-known databases, we have found that just a few attacks on VANETs have been discussed to date. This research has covered almost all attacks that severely affect privacy and security. Table 1 shows the types of attacks, security service breached, and its countermeasures. The main contribution of this paper is that the security countermeasures are defined by different problem-solving methods. Table 2 shows the Abbreviations used in the paper.

Figure 1 shows the overall VANET structure. We can see all entities involved in the connectivity of VANET nodes. Below are the entities of the VANETs with some details of their working principles.

*1.1. Entities of VANET. Road-side units (RSUs).* The RSUs are installed in the VANET: RSUs are positioned along the road and serve as radios for DSRC communications. The main functions of RSUs are as follows: (i) to expand the communication range of VANETs by transferring messages to other OBUs and RSUs, (ii) enable running protection applications, such as reporting traffic conditions or accident warnings, and (iii) provide OBUs with Internet access [3, 17].

*On-board unit (OBU).* In the automobile, OBUs are installed, which are radio devices that will constantly be in moving conditions, although OBUs link the vehicles with RSUs. For an intrinsic part of VANET and effective communication, nodes require such functionalities to help them receive information, notify their neighbors, and make decisions by analyzing all their collected data.

*Trusted authority (TA).* This is accountable for the confidence and safety management of all VANETs, including the authenticity verification of vehicles and the removal of nodes for vehicles that convey false messages or malicious behavior [18]. The TA, therefore, requires high computing capabilities and adequate storage space [19].

*Radar.* Radar is used on different moveable objects, including vehicles, to detect the direction, speed, and distance.

*Computing platform.* A computing platform for the VANETs is required for the drivers to see the data received during driving, like the details of the VANET environment, i.e., position, distance of the vehicle, and the hazard informa-

tion, and it is a digital platform on which any software or app can be executed.

*Event data recorder.* The event data recorder is an intelligent part of the VANET; it can be said that it is the “black box” of the vehicle. Any unusual event in the vehicle is recorded so that the issue can be appropriately addressed, and the transport authorities will identify the reason.

*1.2. Communication Patterns with IoT Environment in VANETs. Dedicated short-range communications.* Its normal transmission range is between 300m and 1,000 meters. The DSRC system has a maximum speed of 200km/h and a 6 to 27 megabits per second (Mbps) data rate range. DSRC operates in the 5.9GHz frequency range. It is a short- to medium-range communication technology that can be used for public safety and private purposes. The IEEE standard for vehicular networks is IEEE 802.11p WAVE (Wireless Access in Vehicular Environments). Some of the applications for which DSRC is deployed in VANET include emergency vehicle warning systems, Cooperative Forward Collision Warning, transit or emergency vehicle signal priority, and an approaching emergency vehicle warning.

*Vehicle-to-vehicle (V2V) communication.* V2V communication is established between vehicles as an ad hoc network. Vehicles can transmit or share helpful information in V2V, such as traffic conditions, i.e., traffic jams and accidents [20–22].

*Vehicle to infrastructure (V2I).* V2I communication is used to disseminate information between the network infrastructure and vehicles [12]. In V2I, a vehicle can connect to RSUs to provide and communicate with the Internet.

Figure 2 shows the internal and external components of a smart car; the components are required to connect the vehicle smartly with VANETs to exchange the information between the drivers. Smart cars are enabled with features, which include Global Positioning System (GPS), omnidirectional antennas, sensors, alarms, camera, on-board processors, and event data recorder (EDR) [23].

This paper is categorized into six sections; a graphical paper organization is shown in Figure 3.

*1.3. Importance of Location Information.* From the privacy point of view, location information is the most crucial part for a vehicle and its driver. Since VANET gathers the location information, this information must remain confidential; otherwise, the attackers can quickly gain access to the driver and attack the driver’s privacy, and attackers can promptly attack the VANET to disturb the efficiency of the network. Different types of attacks target the other areas of a VANET. However, attacks on confidentiality are hazardous for the privacy of location information. In a secured VANET, the data must be exchanged securely for smooth operation, and messages should be transferred between the authorized parties. However, if the attackers’ targets against attacks like eavesdropping, then the data of VANET can be compromised, and the attacker can easily access the location information.

TABLE 1: Classification of attacks and goals achieved after implementation of different algorithms.

Reference	Type of attack	Security service	Goals and targets achieved by implementation of algorithms
[58]	Eavesdropping	Availability	Solving attack problems by asymmetric cryptography technique To improve the wireless security, enhance the efficiency
[80]	Multiple types	Availability	The framework can reduce the cost and gain outperformed results.
[81]	Jamming	Availability	Blowfish cryptosystem is used for encryption and decryption to make secure routes in MANET.
[51]	Malware	Availability	To protect location privacy and improve the quality of service in the network
[82]	Greedy behavior attack	Target availability	To improve the GSM security via CL-PKC while the handshaking procedure is being done
[70]	Blackhole	Availability	To improve the MANET security using fixed slot length, the attacker cannot continue the attack on the network.
[83]	Multiple	Availability	Present multiple challenges and solutions for preventing IoT overcloud.
[4]	Multiple	Confidentiality	Use encryption technique. Use VIPER technique for V2I communications.
[23]	Sybil attack and DoS	Confidentiality	Present multiple solutions to prevent an attack on smartphones.
[84]	Sybil attack	Confidentiality	Use a distributed and robust approach
[85]	Impersonation attack	Authentication	Make use of SPECS (secure and privacy enhancing communication schemes). Make use digital certificates.
[28]	Spoofing attack	Authentication	Present some open challenges in hybrid network of cloud and 5G.
[52]	Repudiation attack	Nonrepudiation	Make use of digital signatures. Use PKC-based pseudoidentities.
[71]	Sybil attack and DoS	Availability	By the use of signature-based authentication and bit commitment, the impact of DoS attack is reduced. A central authority for validation (VA) deployment validates the network's components in real time. The working principle of validation will be direct and indirect.
[72]	Sybil attack	Authentication availability	By cryptographic technique, nodes that want to establish a direct link authenticate VA indirect validation. VA can use temporary certificates. By using the validation technology, VA is a protected option for attacks.
[86]	Jamming	Availability	Change the transmission channel and use FHSS frequency hop technology to produce pseudorandom hopping numbers for the algorithm by using cryptographic algorithms. This strategy needs improvement to the existing OFDM standard.
[87]	Certificate and or key replication	Authentication and confidentiality	For certificate and key replication, cross-certification among the various VANET certification authorities CRL (revocation certificate) real-time validity test for digital certificates Use validated and certified disposable keys.
[88]	Greedy Malware Wormhole Tunneling Blackhole Spamming	Availability Nonrepudiation Authentication Confidentiality Integrity	The cryptographic technique does not provide practical solutions for these attacks, but specific recommended methods can minimize adverse effects such as digital software signatures.

## 2. Location Privacy Challenges in VANET

Attacks on privacy are linked to unauthorized access to sensitive vehicle information. There is a direct relationship between the driver and vehicle. If the intruders gain unauthorized access to some data, the driver's privacy will be compromised [24–26]. In most cases, the car owner is also its driver; if an attacker obtains the owner's identity, the vehicle's privacy may be risked; this form of privacy assault is known as identity disclosing. One of the most

well-known privacy threats is known as location tracking. In this attack, the vehicle's position or the path taken by the car at a specific point in time is considered personal data.

VANETs are dynamically complex ad hoc networks with limited network latency and multiple facilities. The communication modes are categorized as vehicle-to-vehicle (V2V), vehicle-to-infrastructure (V2I), and hybrid, as shown in Figure 4. Hybrid mode is a merger of the former two approaches, already discussed earlier.

TABLE 2: Abbreviations used in the paper.

Abbreviation	Definition
ABAKA	Anonymous Batch Authenticated and Key Agreement Scheme for Value-Added Services in Vehicular Ad Hoc Networks
CRL	Certificate revocation list
DDoS	Distributed denial of service
DoS	Denial of service
EDR	Event data recorder
GPS	Global Positioning System
I2V	Infrastructure to vehicle
IoT	Internet of Things
ITS	Intelligent Transport System
OBU	On-board unit
OTP	One-time password
PKC	Public key cryptography
PKI	Public key infrastructure
RSU	Road-side unit
SNR	Signal-to-noise ratio
TA	Trusted authority
V2V	Vehicle to vehicle
VANET	Vehicular ad hoc network
5G	5 <sup>th</sup> generation network

In VANETs, protection must ensure that communication messages exchanged are not intercepted or manipulated by assailants. Furthermore, the drivers' responsibility is to accurately notify the traffic situation under a time limit [4, 27]. The security threats occur due to the unique characteristics of VANETs. The exploitation of these security issues leads to other restrictions.

Here are a few of the security challenges:

### 2.1. Characteristics of VANETs

#### (i) Network topology and communication mode

- (a) *Unbounded and Scalable Networks.* For one or more towns and nations, VANETs can be implemented. It needs coordination and management of security requirements.
- (b) *Wireless Communication.* The connection of nodes and their data exchange is made through wireless channels. There is a need to establish communication.
- (c) *High Mobility and Rapidly Changing Network Topology.* Nodes travel at fast and unpredictable speeds that make it harder to determine their location and the network's topology.
- (d) In data security, the privacy of the node causes repeated disconnections, instability, and inability of the handshake. Its failure is a reasonably long-term situation (for example, a password)

and is inefficient to secure vehicle communication. Under these conditions, the delay in disseminating warnings should be acknowledged. Quick cryptographic algorithms or entity authentication and timely message delivery require good delay performance. For all this, prioritizing data packets and preventing congestion should prioritize traffic safety [28] and productivity data more quickly than others. Real-time and multimedia technologies are proposed compared to the efficiency and cross-layer across transport and network layers [29, 30]

- (ii) Automobiles and driver mode in IoT environment
  - (a) *Heavy Processing Power and Optimal Energy.* VANET nodes have no energy and computing resource problem. The vehicles are equipped with their battery and fast computational capabilities to perform complex cryptographic calculations.
  - (b) *Improved Physical Safety.* In VANETs, nodes are physically strengthened. It is tougher to compromise physically and can minimize the impact of infrastructure attacks.
  - (c) *Recognized Moments and Positions.* Utmost vehicles are packed with GPS because many applications depend on location and area. A leak-proof GPS is often used to protect the position of nodes against attackers in protected localization.
  - (d) *Most Members Are Trustworthy.* Most motorists are considered successful and helpful in locating a challenger.
  - (e) *Existing Law Enforcement Infrastructure.* They capture the adversary who attacked the device through law enforcement officers.
  - (f) *Interior Registration with Routine Inspection and Maintenance.* Automobiles are listed on the central registration authority and have a specific ID (licensing plate). Periodical updating of vehicles is for software and hardware upgrades. In the PKC (public key cryptography), maintenance is undertaken to update the certificate credentials and to acquire a renewed CRL (certificate revocation list). In short, the network of vehicles (VANETs) is an interface between drivers' actions, networks, and infrastructure cooperation. Proving a security solution must find a way to include both groups.
  - (g) In VANETs, safety must ensure that messages transferred are not manipulated or altered by the adversaries

2.2. *VANET Security Challenges.* VANETs have recently introduced a new safety concern, deemed a significant

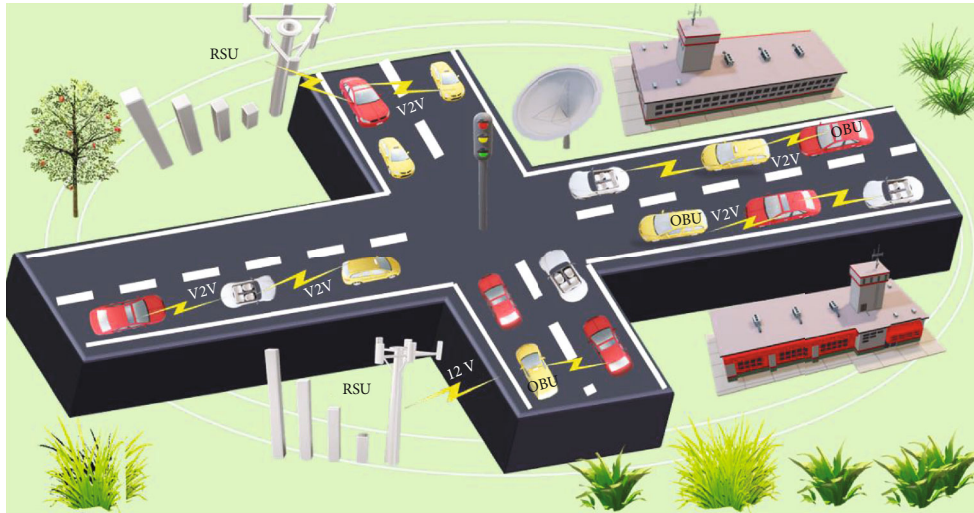


FIGURE 1: The illustrative architecture of VANET.

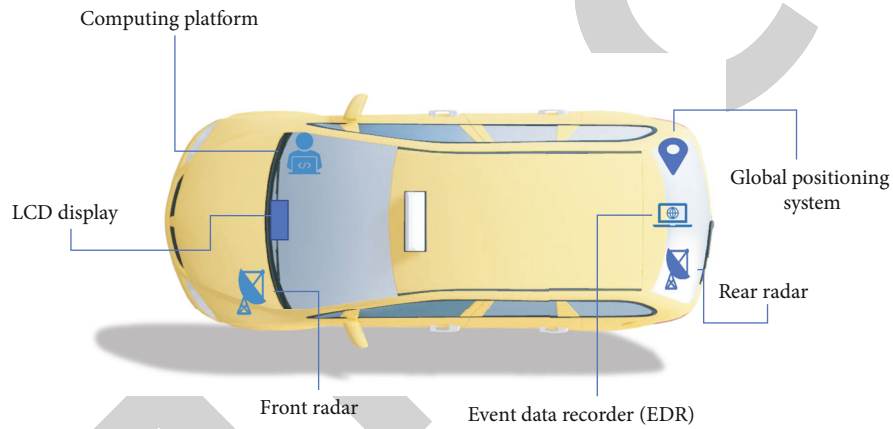


FIGURE 2: VANET enabled smart car [2].

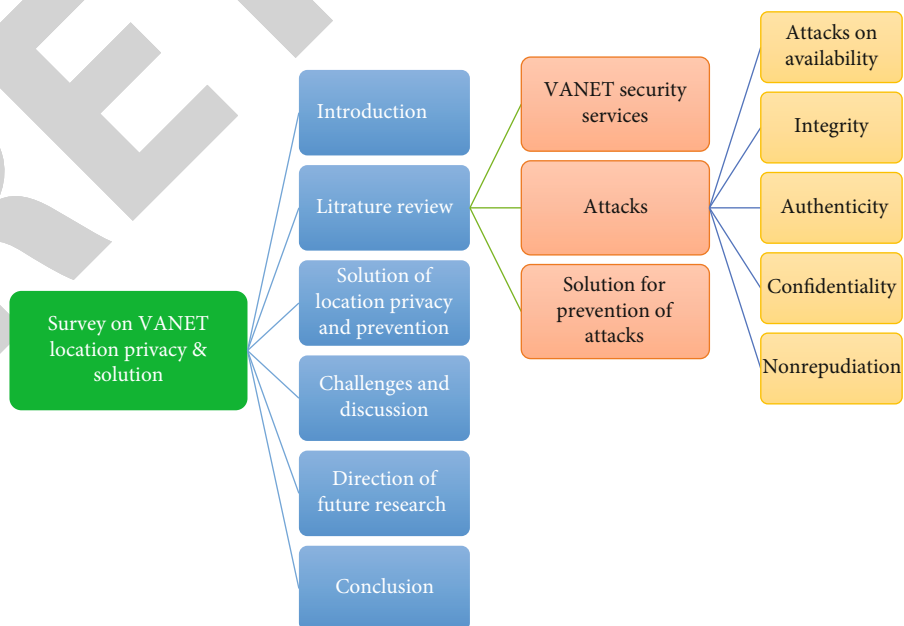


FIGURE 3: Organization of the survey paper.

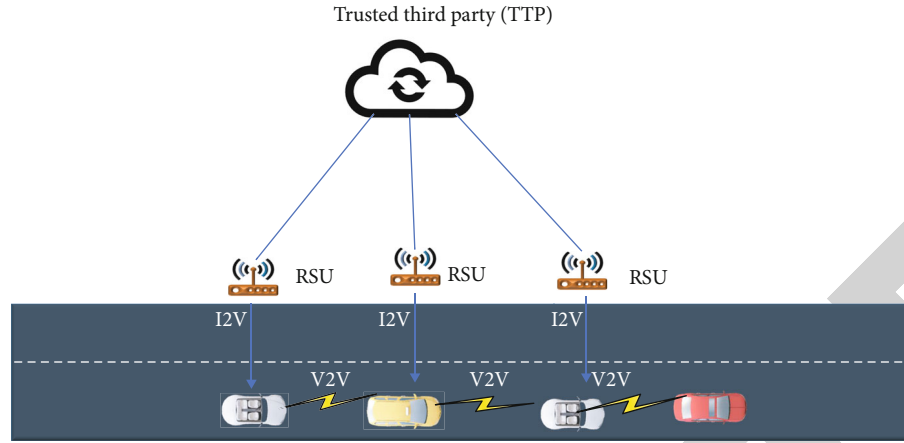


FIGURE 4: V2X connectivity through VANET architecture.

problem for researchers to tackle safety purposes, including a small number of major central points, mobility, inadequate wireless communication, and the issue of drivers. VANET protection ensures that the messages sent are not inserted or amended by the attackers. In addition, the motorist is accountable for providing detailed information on traffic conditions within a specific time frame. Due to their distinctive features, VANETs are more susceptible to attack. Several restrictions are created for securing VANET communications [23, 31].

(iii) Some more challenges are given below

(a) Volatility

VANET lacks the relatively long-lived context but contacting user devices to hot-spot demands a lifetime secret code. An attribute like this is unrealistic for secure intercommunication [32].

(b) Low tolerance for error

As VANETs deal with human life, there is an extremely low tolerance for error. If there is any delay in information dissemination due to attacks like DoS and DDoS [33–35], it can be harmful.

(c) High mobility and network scalability

Because of high mobility and network scalability, the network should work at its optimal level; if attackers target the VANETS, this can be disastrous for human life.

**2.3. Encryption of User Information.** Concern, the introduction of VANET privacy is one of the biggest challenges. Nonetheless, most drivers want to protect their data and do not want to share their confidential details [36, 37]. Personal information such as driver identification, driving behavior, the vehicle's history, and the present location is given. The critical problem is how do we build a program that respects users' privacy while concurrently defending

them against malicious nodes. To avoid circumstances in which each movement can be traced, the program must guarantee users' privacy. Therefore, the users' privacy in the correspondence exchanged must be guaranteed, thus maintaining the trustworthy VANET-based framework [38].

Besides, information can be received by any network node as it is transmitted through wireless broadcasts. The information is subject to confidentiality (vehicle location, time, original ID, speed, and time) and car sensor data internally [39, 40]. It is easier to monitor the online identity of malicious people such as terrorists and lawbreakers.

VANET privacy attacks specifically relate to the unlawful collection of confidential vehicle information. Given the relationship between a vehicle and its driver, it could affect the driver's privacy by obtaining some data on the conditions of a vehicle. Then, such attacks can lead to identity disclosure. The identity of the owner of a particular vehicle may jeopardize its privacy. Typically, the car owner is also the driver, making it easier to collect personal data. The location or route of a vehicle at a specific time is known as personal data. It enables the creation of the profile for this vehicle and its driver [40, 41] through the transmission of middle nodes.

The recipient message verifies that the message is complete and authentic through the corresponding public key. It is difficult for a node to imitate since it is just private. The message sent in a VANET should be encrypted with safety or warning messages, particularly. Those messages that act as inputs for the protection framework may also be signed. Now, the critical advantage is that digital signature requirements are minimal, i.e., nodes need to have the capability to obtain/generate and store pairs of cryptographic keys. To build and verify signatures, they need computational capacity. The key problem is imitation and DoS (denial of service) attacks. In [42–46], the proposed method uses pseudonymous certificates that can hide users' true identities. Even though there is no known relationship between anonymous certificates and the true identities of key holders, the messages that have a given a key, by logging that message, the privacy can be violated [3, 26], group signature, and ID-based signatures [47, 48] are the conditional privacy protocol. The significant advantage of using

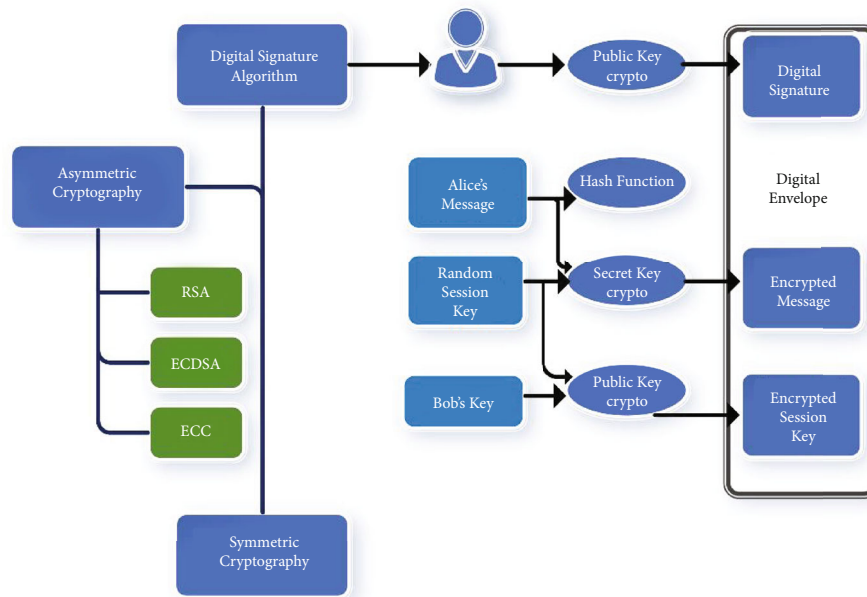


FIGURE 5: Digital signature algorithm.

a group signature is that they guarantee message unambiguity as group members can sign incognito on behalf of the group [39, 47].

The digital signature algorithm is shown in Figure 5. Digital signatures are the public-key primitives of message authentication; this technique binds the person or entity with digital information; the receiver and the third party verify this unique binding. In the digital data exchange, the digital signature algorithm authenticates the originality of data. This technique is very efficient for the security and privacy of a VANET. Digital signatures have various advantages, i.e., message authentication, data integrity, and nonrepudiation. If the attacker hacks the system and attacks the data to modify the data integrity, the digital signature verification at the receiving end fails. Hence, the receiver can safely deny the message, assuming that the data integrity has been breached [9, 29, 40].

In [49], SeGCom (Secure Group Communications) framework introduced a simplified approach while generating and disseminating emergency messages. V2V scenario issues with only using one encryption method. Several other researchers also proposed PKI and digital signatures for VANET protection [23].

In [50], a protocol was proposed to revoke malicious vehicle certification throughout misbehaving vehicles. The biggest challenge for VANET PKI-based schemes is the heavy load of certificate creation, storage, distribution, verification, and revocation. A steady communication architecture based on a PKI and a virtual cluster-controlled network was proposed to intelligently avoid collisions caused intentionally by malicious vehicles [32]. However, this approach comes up with an incredible overhead and a cluster head building bottlenecks. In [49, 51], an ID-based cryptosystem (for security-related applications) is proposed, which imposes strong rejection and minimizes the over-

heads linked to the certificate management prevailing in PKI systems. The mix zone approach in [42] has been used to maximize unrecognized vehicles. This approach is based on preloading in each vehicle group of unknown certificates. Elliptic curve cryptography is designed to reduce transmission and overhead delay. The elliptic curve logarithm problem (unsolved NP problem) is defined by ABAKA's (Anonymous Batch Authenticated and Key Agreement Scheme for Value-Added Services in Vehicular Ad Hoc Network) privacy. One of the researchers proposed a detection algorithm to deal with the invalid request problem because of the batch verification failure [52]. The researchers arranged hierarchical identity-based cryptography for location-based signature verification to provide location assurance and pseudonym-based privacy authentication. For a location-based signature generation and location assurance verification scheme, the ID-based validated vital agreement between a vehicle and an RSU, and a hierarchical ID-based signature has been used in [53]. The above system provides unconditional privacy and eliminates the need for a group manager. A signatory can generate a signature on behalf of an ad hoc group without using the ring members' public keys. This scheme has limited functionality in VANETs because it offers absolute privacy without non-repudiation [54].

**2.3.1. The High Mobility of Nodes.** In the VANET, the high mobility of the nodes causes enormous complexity. Classical node and message authentication techniques are challenging due to the high level of mobility. A handshake protocol cannot be proposed since some nodes communicate only once, and a lack of time restricts the validity of messages received from these nodes. Therefore, securing mobility issues is a significant concern. Although many researchers have tackled these issues, many problems still need to be

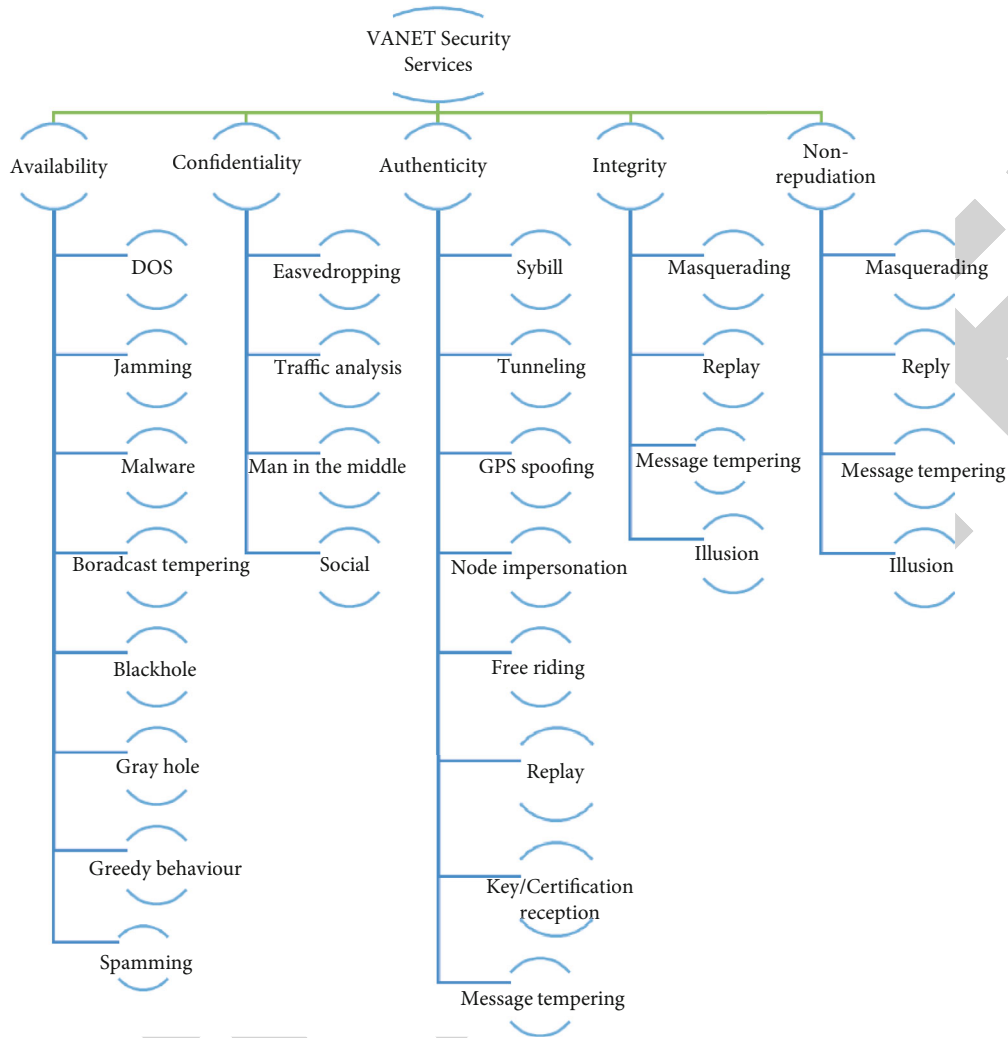


FIGURE 6: Attack type classified category wise.

addressed [10, 53]. This strategy does not enforce particular routes or speeds for drivers to follow [53].

Günay et al. [55] addressed several concerns of privacy, in which business organizations can use the data of their employees' cars when they are parked in the company's parking space. Police can also use the information of the driver from the beacon frames. Insurance companies can track their consumer data to evaluate their actions. Therefore, privacy violations occur when the user's confidential data is owned by third parties or by a separate node not entitled to the data [5, 56].

**2.3.2. The Relationship between Security and Privacy.** User hesitancy is one of the main barriers to VANET technology. Users have a negative perception, believing that a third party is monitoring them. If a hostile user changes, the message privacy can be compromised. Some potential attacks may encrypt or fake the data; hence, privacy can be breached in the VANETs.

**2.3.3. Security Threats and Hazards in VANET.** In this section, we address each security services' attacks and threats.

There are bundles of security and privacy attacks in VANETs affecting the overall performance of a VANET. The attacker attacks on different VANET security services, i.e., availability, confidentiality, authenticity, integrity, and nonrepudiation, as shown in Figure 6.

### 3. Location Privacy Attack Methods and Prevention for IoT in VANET

In location privacy, attackers target the VANET to disturb the network's performance through different types of attacks. To prevent these attacks, various researchers have proposed multiple approaches. Researchers in [19] have proposed enhanced privacy using an asymmetric cryptography scheme. Moreover, pseudonym-changing strategies [57–59] effectively prevent location attacks.

**3.1. Attack on Availability.** Data availability (vehicle information) is essential for VANETs to ensure that the network is operational and valuable information is always accessible; this is a necessity for VANETs to ensure the safety of users' lives [60, 61]. Table 3 shows the list of some well-known

TABLE 3: Basic types of attacks.

Types	Descriptions	Purpose
Counterfeit information	Adversaries modify or disburse the wrong data on the network.	To interrupt other motorists for particular illegal purposes and public order [89]
Denial of service	Adversaries insert irrelevant bulk messages to VANETs. Attackers interpose irrelevant bulk messages into the network.	To interrupt the communication process and use the computing resources of other nodes, making VANET unavailable [62]
Impersonate	Attackers claim to be valid nodes such as authenticated RSUs or cars.	To include fraudulent information across the network, not only to trick other vehicles but also to eliminate the innocent drivers whose IDs were taken out of the service [90]
Eavesdropping	Adversaries are located in vehicles or false RSUs.	It is for collecting vehicle data from overhead vehicle communications.
Message suspension	Adversaries hold messages to delay for some time	To avoid the registration and insurance authorities learning about collisions involving the attacker's vehicles. Moreover, prevent collision reports from being delivered to road-side access points [71, 91].
Hardware tampering	Adversaries exploit vehicle and RSU hardware.	It is disturbing the user for unlawful purposes [1, 92].

attacks, e.g., denial of service attack (DoS) and jamming attack.

- (a) *DoS (Denial of Service Attack)*. In this attack, an attacker attempts to make the network resources and facilities inaccessible to the user. It is either by active channel jamming or sleep deprivation. DoS attacks include a family of attacks to deliver network services, particularly for VANET applications. DoS attacks are listed due to their associated risks and consequences. They can occur via deceptive explicit or implicit network nodes. Control channel floods with large numbers of purposefully generated messages [25, 62]. Network nodes (RSU and OBU) cannot accommodate the massive amount of data obtained. Distributed denial of service (DDoS) is a changed variant of DoS attacks [63]. It is an attack disseminated by the primary attacker, the “attack operator” of other agents who may be victims inadvertent. In most cases, the DDoS attacks flood the unnecessary data in the network, to produce the congestion and delay in the network, and the results are invariably disastrous. DoS attacks include both blackhole attacks and jamming.
- (b) *Jamming*. Jamming is a type of denial-of-service attack that prevents other nodes from using the channel to communicate since they occupy the medium on which the communication between the nodes is established. A significant threat to wireless channel access reduces the receiver's signal-to-noise ratio (SNR). The jammer would simultaneously control the value of the jamming signal [64]. The most effective signal transmission model that best combines the receiver should also be selected if efficient jamming is accomplished in a VANET. Some researchers, including [17, 65], examined some strategies to minimize the impact of jamming on ad hoc mobile networks.

- (c) *Malware*. An intruder continues to send network spam messages to waste network bandwidth and increase latency. This attack is difficult to manage due to the lack of centrally controlled infrastructure and management. Intruder broadcasts unwanted messages to a user's group. These messages act like advertisements.
- (d) *Broadcast Tampering Attack*. The offender is trying to render and insert fake security warnings in the network in this type of attack. The proper security messages can be withheld from legitimate users, and network security can be seriously affected [17]. This kind of assault is usually probable for a legal node.
- (e) *Blackhole Attack*. A fraudulent node determines the short-lived route to receive and then routes and reroutes the data. The fraudulent node may decrypt or preserve the data packet. The forged route is built successfully relying on the malicious node sending the packet wherever it chooses.
- (f) *Gray Hole Attack*. This attack only involves deleting data packets from vulnerable applications due to packet loss [66, 67]. Gray hole is known as a variant of the blackhole attack.
- (g) *Greedy-Behavior Attack*. Greedy's attack is an intrusion of the function of the MAC layer in line with the OSI model architecture. The greedy node recognizes the channel access system and still wants to connect to the media. The fundamental purpose is to prevent using other nodes of support and services. A greedy action node often reduces its time to wait for quick access to the channel and penalizes other undefeated nodes [48, 68]. Transmission congestion and collision issues are caused by greedy behavior, which causes delays in the services of authorized consumers. Greedy behavior is



autonomous and is shielded from the top layers, so a mechanism designed for those layers cannot detect them.

- (h) *Spam*. The spam attacks are mainly used to increase latency and bandwidth usage and decrease the overall efficiency of the network and services.

**3.2. Authenticity and Identification Attacks.** Authenticity is a big security problem for VANETs. Before accessing the available resources, all existing network stations must authenticate. Any infringement or attack targeting the recognition or authentication process would adversely impact the entire network. Ensure legitimate nodes in a vehicle network from outside or inside attackers with a false identity. The benefit of verification of identity is that in the majority of the time, a vehicle joins the network or service. There are several types of attacks in this category [69, 70].

- (a) *Sybil Attack*. The Sybil attack is hazardous because the vehicle can act as if it has multiple identities simultaneously [71, 72]. One of the main ways that two entities can convince a third that they are independent is by performing activities that cannot be performed by a single entity alone. Many techniques such as computational testing resources, memory, and communication challenges have been recommended to protect the identity of a node. The Sybil attack is risky in VANETs because of the catastrophic consequences. The attacker can manipulate the behavior of other vehicles so that the receiving node can think that the message was sent by another vehicle. As a result, they believe that there is a traffic jam on the road, and the user changes the route to clear the road.
- (b) *Tunneling Attack*. The tunneling attack imitates the wormhole attack [26]. In a tunneling attack, attackers use the identical network to communicate privately (tunnel) in this attack, while in the wormhole, the attackers use a separate radio channel (assumed external) to exchange packets. This tunneling attack joins two remote parts of the vehicle network through a communication channel such as a tunnel [73]. Therefore, the victims of two remote network parts would link as their neighbors.
- (c) *Position Information Deception (GPS Spoofing)*. Secreted automobiles produce fake crash locations. GPS does not work.
- (d) *Node Impersonation Usurpation*. The intruder attempts to imitate an additional node. The intruder does malicious things to gain rights and then reveals that the better one is the doer.
- (e) *Free Riding*. Such attacks are highly dominant and generate an active malicious user by fake authentication when connected with cooperative message authentication. A malicious person can take advan-

tage of several other users' authentication contributions without providing their own identity to this threat. This attack could pose a serious threat to the authentication of a cooperative message [74].

- (f) *Replay or Reiteration Attack*. Malicious or unauthorized drivers try to use new frames that have been built into new connections to create legitimate RSU users [93].
- (g) *Key Certification/Replication*. This attack is identified as a replay attack that arises when legitimate information is transmitted false or allows an unwanted or malicious effect to be caused by delay. The VANET needs more time with a greater cache to test the messages received to overcome this attack.
- (h) *Message Tampering or Alteration*. The intruder drops packets from the network or alters the message's contents. In addition to alteration attacks, a new message is produced or repeated by displaying old messages or threats to falsify or introduce mass amounts of false vehicle emergency warnings. Broadcast tampers, where the attacker infuses fake security messages into the network to cause significant problems.

**3.3. Attacks on Confidentiality.** Confidentiality is an essential safety requirement for VANETs, ensuring authorized parties read the data. Failure to provide confidentiality between node communication within a vehicle network means that exchanged messages are susceptible to threats. The intruder can collect information regarding the vehicle, its route, and the user's privacy in such cases. Without a confidentiality system, the data collected would affect individual privacy. It is hard to detect such an intrusion since the user is inherently passive and does not personally know the database [5, 75, 76].

- (a) *Eavesdropping Attack*. Eavesdropping is a privacy attack; listening to media is a direct attack on networks like VANET. It is also submissive, and the victim does not know that the connection is compromised. Several valuable data can be easily accessible during this attack, such as the position information used to track vehicles.
- (b) *Traffic Analysis Attack*. An attack on traffic inside a VANET is a significant passive threat to privacy and anonymity. The attacker investigates the data obtained after listening to the network and retrieves as much information as possible.
- (c) *Man-in-the-Middle Attack (MiM)*. The communication between various vehicles is perceived by a malicious node. It tries to pretend that they are responding to each other. It transmits false knowledge between them.
- (d) *Social Attack*. A social attack frequently diverts the driver's focus. The attacker sends deceptive and immoral messages to the vehicles. The attackers

aim to make drivers respond to these immoral messages, thereby impacting the driving of cars and the efficiency of the VANET network [2].

**3.4. Data Integrity.** It guarantees that the messages' quality is not altered during the interaction process. The public key infrastructure can be assured in VANETs and cryptography revocation.

- (a) *Masquerading Attack.* The attacker's legitimate identity, known as a mask, attempts to build a black hole or generate false messages from an authentic node in this attack, for example, slowing down the speed of a vehicle or lane change. A malicious node claims to be a vehicle of emergency, for example, cheating other cars [26, 77].
- (b) *Replay Attack.* It is a traditional attack that involves recreating (broadcasting) a message that was already sent at the time of submission. Moreover, the intruder injects this again into the previously obtained network packets. This attack can be used to replay frames for beacons [9] so that the attacker can handle the location and the routing table of nodes. Unlike many other attacks, nonlegitimate users replay attacks [8, 78].
- (c) *Alteration of Message.* This attack is against credibility by changing, deleting, restoring, and changing existing information. It can happen by altering a particular part of the message to be sent [79]. Suppose the assailant fabricates the information indicating that the road is jammed and alters it to cheat users, thereby implying that congestion is not occurring and the road traffic is regular. In such an attack, the offender can also delete part of the message change or create new messages that help him reach his malicious objective.
- (d) *Illusion Attack.* The illusion attack is a direct application to fabricate messages that attack integrity and data trust. It involves voluntarily putting sensors that produce false data [1]. Such data will usually be moved around the network and require drivers' involvement. Authentication mechanisms cannot detect this attack since the attacker authenticates to the network.

**3.5. Attacks on Nonrepudiation.** Nonrepudiation in data security indicates that the sender and recipient are people pretending to have sent or received the message, respectively [54]. Otherwise, the failure to repudiate the data sources shows that the data has been sent, and nonrepudiation of arrival proves that the data have been obtained. In the scope of VANETs, the compromised data regarding the user's safety and anonymity, confidentiality sets, and hardware, device, and software adjustments (updates, changes, and additions) should always be provable [53].

- (a) Nonrepudiation and accountability attacks

*Traceability of lost events:* considering its significance, no critical information dealing with this attack was found in the

context of VANET. Besides, such nonrepudiation attacks allow an attacker to reject one or more actions. This type of attack focuses primarily on eradicating signs of behavior and uncertainty for the auditing group. Many attacks may be used for a preventive attack against nonrepudiation, for example, Sybil and key and certificate replication.

**3.6. Solution for Location Privacy Attacks in an IoT Environment.** We analyze various attacks and their solutions in Table 1.

## 4. Discussion

As we know, a flawless VANET can make highway traffic smoother, safer, and faster. However, the attackers can gain system access to disrupt the VANET-based drivers, thus reducing the overall performance of the VANET. Consequently, user privacy and security are the main targets of attackers. User privacy must not be compromised at any cost; otherwise, it becomes difficult to attract drivers to use VANET services. All VANET-based communication contains sensitive private information such as driver identity, personal identification number, driver number, travel time, and route details. Therefore, VANET communication information must be secured to ensure the safety of user information and vehicle information for smooth operation.

Moreover, the consequences of a security breach in VANETs are serious and threatening. In a highly demanding environment characterized by vehicles arriving and frequently departing simultaneously and a short connection time, implementing a solution to protect complete privacy is challenging. There is a great need to secure data transmission paths in VANETs, and some approaches have already been proposed to address related issues. Since the main challenges discussed here are privacy and security, the solutions to improve these problems are addressed accordingly. We have thoroughly analyzed various papers and approaches for privacy and security problems. We have found solutions to overcome privacy and DoS attacks by using signature-based authentication and bit commitment. The impact of DoS and Sybil attacks is reduced by using signature-based authentication.

For jamming attacks, many techniques are used by different researchers. Our findings show that the Blowfish cryptosystem is efficient as it is used for encryption and decryption to create safe routes in VANETs. It changes the transmission channel and uses FHSS frequency-hopping technology; it is possible to develop pseudorandom hopping numbers for the algorithm using cryptographic algorithms. On the other hand, this strategy needs to be improved, especially for the existing OFDM standard.

We found cross-certification between the different VANET certification authorities for confidentiality and authentication attacks. CRL (revocation certificate) real-time validity test is for digital certificates.

Certificate and or key replication affects the services like authentication and confidentiality; this technique protects the security in a well-organized manner. For attacks like greedy malware, wormhole, tunneling, blackhole, spamming,

availability, nonrepudiation, authentication, confidentiality, and integrity, we found that cryptographic technique does not provide practical solutions for these attacks. Still, specific recommended methods can minimize adverse effects, such as using digital software signatures. Existing protocols and values can be modified by using trusted hardware, which practically cannot even be approved. We also propose an OTP (one-time password) system that should maximize the security of drivers from attackers. A simplified approach is that a policy-based method is more suitable when mobile consumers prefer the service level of complete privacy. A cryptographic technique is a practical solution for users who care deeply about privacy and require a high level of confidentiality. They are less concerned about the overhead of data processing and communications.

In addition, anonymization and obfuscation techniques and spatial and temporal information would be best for a mobile user to disguise. The infrastructure is location-based services, benefits, applications, and privacy concerns. We have primarily addressed the privacy issue of LBS and analyzed several different approaches. We classify the existing mechanisms into a tree structure to evaluate the efficiency of additional security measures and study them in detail on their benefits and limitations. We have successfully analyzed various shortcomings and gaps in privacy technology. Location protection is an essential element of LBS. To benefit from the specified services, users use current locations as information. Without the necessary precautions, the lack of privacy protection in the services could hinder the regular use of this smart technology. We have highlighted the threats posed by LBS services that intentionally or unintentionally compromise the privacy of VANET users. We have outlined their basic ideas and recent developments by examining typical techniques. In the following section, we have provided a comparison and analysis. Finally, we have identified some interesting topics for future research that should be investigated in the context of privacy protection in the future. We also emphasized that the intersection of LBS and other popular technologies will lead to further scientific growth in this area to address user needs.

## 5. Direction of Future Research

As privacy is a core issue in VANETs, our detailed review has anticipated some potential future directions.

- (i) As in the VANETs, all entities and information are placed under the shelter of TA, RSU, and drivers, so the tracking system of vehicles should have a robust mechanism of digital signature and pseudonym identity to avoid privacy attacks. A more robust and more reliable digital signature system should be introduced
- (ii) There should be a dual authentication system to secure data transmission on the VANETs, as nowadays, on the Internet, all email systems and personal accounts are based on a dual authentication system.

In this way, the attackers cannot cheat the drivers and the network

- (iii) There is an efficient need for the VANET tracking app to double-check the security. Both ends of connectivity, i.e., TA and driver, may understand that there is no attacker or alternation in the messages
- (iv) There should be a faster communication method so that privacy may not be disturbed along with speedier data dissemination
- (v) VANETs should be switched to the 5G technology. VANET service providers and users can benefit from the high speed of 5G, as 5G is faster and information dissemination will be quicker

## 6. Conclusion

Security and privacy play a vital role in this fast-growing technological era. Modern cyber-physical technologies such as VANETs are particularly lucrative targets for fundamental information breaches. Breaching a mobile VANET node can lead to physical attacks, such as tracking delay of data dissemination, leading to severe problems. It is impossible to run a VANET in a compromised condition. We have analyzed the privacy and security-based attacks in VANETs. Various types of attacks were considered, which can halt the VANET efficiency. To resolve the problems, different beneficial techniques such as cryptography and pseudonyms were found adequate to protect the network and user's privacy from various attacks. Moreover, OTP-based system mechanism can make the network's confidentiality more secure. It is a real-time double verification for VANETs. Moreover, the incorporation of 5G is also a good option for new and innovative real-time applications via VANET. Furthermore, integration with other supporting technologies such as cloud computing and IoT will enhance the robustness of data dissemination.

## Data Availability

The data used to support the findings of this study are included within the article.

## Conflicts of Interest

The authors declare that there are no conflicts of interest regarding the publication of this paper.

## References

- [1] R. Hemalatha and J. A. Samath, "A survey: security challenges of VANET and their current solution," *Turkish Journal of Computer and Mathematics Education (TURCOMAT)*, vol. 12, no. 2, pp. 1239–1244, 2021.
- [2] M. A. Ferrag, L. Maglaras, and A. Ahmim, "Privacy-preserving schemes for ad hoc social networks: a survey," *IEEE Communication Surveys and Tutorials*, vol. 19, no. 4, pp. 3015–3045, 2017.

- [3] S. Khan, I. Sharma, M. Aslam, M. Z. Khan, and S. Khan, "Security challenges of location privacy in VANETs and state-of-the-art solutions: a survey," *Future Internet*, vol. 13, no. 4, pp. 96–122, 2021.
- [4] L. Sleem, H. N. Noura, and R. Couturier, "Towards a secure ITS: overview, challenges and solutions," *Journal of Information Security and Applications*, vol. 55, article 102637, 2020.
- [5] C. Hu, J. Zhang, and Q. Wen, "An identity-based personal location system with protected privacy in IoT," *2011 4th IEEE International Conference on Broadband Network and Multimedia Technology*, vol. 2011, no. 2011, pp. 192–195.
- [6] W. Han and Y. Xiao, "Privacy preservation for V2G networks in smart grid: a survey," *Computer Communications*, vol. 91–92, pp. 17–28, 2016.
- [7] G. Sun, Y. Zhang, D. Liao, H. Yu, X. Du, and M. Guizani, "Bus-trajectory-based street-centric routing for message delivery in urban vehicular ad hoc networks," *IEEE Transactions on Vehicular Technology*, vol. 67, no. 8, pp. 7550–7563, 2018.
- [8] J. Mahmood, Z. Duan, Y. Yang, Q. Wang, J. Nebhen, and M. N. M. Bhutta, "Security in vehicular ad hoc networks: challenges and countermeasures," *Security and Communication Networks*, vol. 2021, 20 pages, 2021.
- [9] M. A. Al-Shareeda, M. Anbar, S. Manickam, and A. A. Yassin, "VPPCS: VANET-based privacy-preserving communication scheme," *IEEE Access*, vol. 8, pp. 150914–150928, 2020.
- [10] A. Ullah, X. Yao, S. Shaheen, and H. Ning, "Advances in position based routing towards ITS enabled FoG-oriented VANET-a survey," *IEEE Transactions on Intelligent Transportation Systems*, vol. 21, no. 2, pp. 828–840, 2020.
- [11] O. S. Al-Heety, Z. Zakaria, M. Ismail, M. M. Shakir, S. Alani, and H. Alsariera, "A Comprehensive Survey : Benefits, Services, Recent Works, Challenges, Security, and Use Cases for SDN-VANET," *IEEE Access*, vol. 8, pp. 91028–91047, 2020.
- [12] E. Farsimadan, F. Palmieri, L. Moradi, D. Conte, and B. Paternoster, "Vehicle-to-everything (V2X) communication scenarios for vehicular ad-hoc networking (VANET): an overview," *Computational Science and Its Applications - ICCSA*, no. article 12956, pp. 15–30, 2021.
- [13] G. Sun, L. Song, H. Yu, V. Chang, X. Du, and M. Guizani, "V2V routing in a VANET based on the autoregressive integrated moving average model," *IEEE Transactions on Vehicular Technology*, vol. 68, no. 1, pp. 908–922, 2019.
- [14] R. Mishra, A. Singh, and R. Kumar, "VANET security: issues, challenges and solutions," *2016 International Conference on Electrical, Electronics, and Optimization Techniques (ICEEOT)*, vol. 2016, pp. 1050–1055, 2016.
- [15] A. Yang, J. Weng, N. Cheng, J. Ni, X. Lin, and X. Shen, "DeQoS attack: degrading quality of service in VANETs and its mitigation," *IEEE Transactions on Vehicular Technology*, vol. 68, no. 5, pp. 4834–4845, 2019.
- [16] J. Jiang, G. Han, H. Wang, and M. Guizani, "A survey on location privacy protection in wireless sensor networks," *Journal of Network and Computer Applications*, vol. 125, pp. 93–114, 2019.
- [17] S. R. Shetty and D. H. Manjaiah, "A comprehensive study of security attack on VANET," *Data Management, Analytics and Innovation*, vol. 71, pp. 407–428, 2022.
- [18] S. A. Soleymani, S. Goudarzi, M. H. Anisi, M. Zareei, A. H. Abdullah, and N. Kama, "A security and privacy scheme based on node and message authentication and trust in fog-enabled VANET," *Vehicular Communications*, vol. 29, article 100335, 2021.
- [19] P. Mundhe, S. Verma, and S. Venkatesan, "A comprehensive survey on authentication and privacy-preserving schemes in VANETs," *Computer Science Review*, vol. 41, article 100411, 2021.
- [20] I. Memon, "Distance and clustering-based energy-efficient pseudonyms changing strategy over road network," *International Journal of Communication Systems*, vol. 31, no. 11, article e3704, 2018.
- [21] M. M. Hamdi, Y. A. Yussen, and A. S. Mustafa, "Integrity and authentications for service security in vehicular ad hoc networks (VANETs): a review," *2021 3rd International Congress on Human-Computer Interaction, Optimization and Robotic Applications (HORA)*, vol. 2021, 2021.
- [22] F. Liu, Z. Chen, and B. Xia, "Data dissemination with network coding in two-way vehicle-to-vehicle networks," *IEEE Transactions on Vehicular Technology*, vol. 65, no. 4, pp. 2445–2456, 2016.
- [23] V. Primault, A. Boutet, S. Mokhtar, and Ben; Brunie, L., "The long road to computational location privacy: a survey," *IEEE Communication Surveys and Tutorials*, vol. 21, no. 3, pp. 2772–2793, 2019.
- [24] M. Wernke, P. Skvortsov, F. Dürr, and K. Rothermel, "A classification of location privacy attacks and approaches vol. 18, no. 1, pp. 163–175.
- [25] T. Pavithra and B. S. Nagabhushana, "A survey on security in VANETs," in *2020 Second International Conference on Inventive Research in Computing Applications (ICIRCA)*, vol. 2020, pp. 881–889, Coimbatore, India, 2020.
- [26] A. S. Mustafa, M. M. Hamdi, H. F. Mahdi, and M. S. Abood, "VANET: towards security issues review," in *2020 IEEE 5th International Symposium on Telecommunication Technologies (ISTT)*, pp. 151–156, Shah Alam, Malaysia, 2020.
- [27] P. Vijayakumar, M. S. Obaidat, M. Azees, S. H. Islam, and N. Kumar, "Efficient and secure anonymous authentication with location privacy for IoT-based WBANs," *IEEE Transactions on Industrial Informatics*, vol. 16, no. 4, pp. 2603–2611, 2020.
- [28] A. Sharma and A. Jaekel, "Machine learning approach for detecting location spoofing in VANET," in *2021 International Conference on Computer Communications and Networks (ICCCN)*, pp. 1–6, Athens, Greece, 2021.
- [29] A. A. O. Affia, R. Matulevičius, and A. Nolte, "Security risk management in cooperative intelligent transportation systems: a systematic literature review," in *OTM Confederated International Conferences "On the Move to Meaningful Internet Systems*, pp. 282–300, Cham, 2019.
- [30] M. R. Schurgot, D. A. Shinberg, and L. G. Greenwald, "Experiments with security and privacy in IoT networks," in *2015 IEEE 16th International Symposium on a World of Wireless, Mobile and Multimedia Networks (WoWMoM)*, pp. 1–6, Boston, MA, USA, 2015.
- [31] C. Huang, R. Lu, X. Lin, and X. Shen, "Secure automated valet parking: a privacy-preserving reservation scheme for autonomous vehicles," *IEEE Transactions on Vehicular Technology*, vol. 67, no. 11, pp. 11169–11180, 2018.
- [32] H. C. Pöhls, V. Angelakis, S. Suppan et al., "RERUM: building a reliable IoT upon privacy- and security- enabled smart objects," in *2014 IEEE wireless communications and networking conference workshops (WCNCW)*, pp. 122–127, Istanbul, Turkey, 2014.

- [33] R. K. Sahu and A. M. Malla, "Security attacks with an effective solution for DOS attacks in VANET," *International Journal of Computer Applications*, vol. 66, pp. 975–8887, 2013.
- [34] Y. Kim, I. Kim, and C. Y. Shim, "A taxonomy for DOS attacks in VANET," *2014 14th International Symposium on Communications and Information Technologies (ISCIT)*, vol. 2018, Article ID 1640167, pp. 26–27, 2014.
- [35] K. Verma, H. Hasbullah, A. Kumar et al., "Prevention of DoS attacks in VANET," *Wireless Personal Communications*, vol. 73, no. 1, pp. 95–126, 2013.
- [36] M. Grissa, B. Hamdaoui, and A. A. Yavuza, "Location privacy in cognitive radio networks: a survey," *IEEE Communication Surveys and Tutorials*, vol. 19, no. 3, pp. 1726–1760, 2017.
- [37] H. Li, L. Pei, D. Liao, S. Chen, M. Zhang, and D. Xu, "FADB: a fine-grained access control scheme for VANET data based on blockchain," *IEEE Access*, vol. 8, pp. 85190–85203, 2020.
- [38] S. Kudva, S. Badsha, S. Sengupta, I. Khalil, and A. Zomaya, "Towards secure and practical consensus for blockchain based VANET," *Information Sciences*, vol. 545, pp. 170–187, 2021.
- [39] H. Zhong, B. Huang, J. Cui, J. Li, and K. Sha, "Efficient conditional privacy-preserving authentication scheme using revocation messages for VANET," in *2018 27th International Conference on Computer Communication and Networks (ICCCN)*, pp. 1–8, Hangzhou, China, 2018.
- [40] G. Sun, V. Chang, M. Ramachandran et al., "Efficient location privacy algorithm for Internet of Things (IoT) services and applications," *Journal of Network and Computer Applications*, vol. 89, pp. 3–13, 2017.
- [41] J. Daubert, A. Wiesmaier, and P. Kikiras, "A view on privacy & trust in IoT," in *2015 IEEE International Conference on Communication Workshop (ICCW)*, pp. 2665–2670, London, UK, 2015.
- [42] Y. Xu, F. Li, and B. Cao, "Privacy-preserving authentication based on pseudonyms and secret sharing for VANET," *2019 Computing, Communications and IoT Applications (ComComAp)*, vol. 2019, pp. 157–162, 2019.
- [43] Q. A. Arain, D. Zhongliang, I. Memon et al., "Privacy preserving dynamic pseudonym-based multiple mix-zones authentication protocol over road networks," *Wireless Personal Communications*, vol. 95, no. 2, pp. 505–521, 2017.
- [44] U. Rajput, F. Abbas, H. Eun, R. Hussain, and H. Oh, "A two level privacy preserving pseudonymous authentication protocol for VANET," in *2015 IEEE 11th International Conference on Wireless and Mobile Computing, Networking and Communications (WiMob)*, pp. 643–650, Abu Dhabi, United Arab Emirates, 2015.
- [45] U. Rajput, F. Abbas, and H. Oh, "A hierarchical Privacy preserving pseudonymous authentication protocol for VANET," *IEEE Access*, vol. 4, pp. 7770–7784, 2016.
- [46] J. Qi and T. Gao, "A privacy-preserving authentication and pseudonym revocation scheme for VANETs," *IEEE Access*, vol. 8, pp. 177693–177707, 2020.
- [47] J. Zhang and Q. Zhang, "On the security of a lightweight conditional privacy-preserving authentication in VANETs," *IEEE Transactions on Information Forensics and Security*, vol. 14, p. 1, 2021.
- [48] J. Ni, X. Lin, and X. Shen, "Toward privacy-preserving valet parking in autonomous driving era," *IEEE Transactions on Vehicular Technology*, vol. 68, no. 3, pp. 2893–2905, 2019.
- [49] S. S. Kaushik, "Review of different approaches for privacy scheme in VANETS," *International Journal of Advances in Engineering & Technology*, vol. 5, pp. 356–363, 2013.
- [50] J. Serna, R. Morales, M. Medina, and J. Luna, "Trustworthy communications in vehicular ad hoc networks," *2014 IEEE World Forum on Internet of Things (WF-IoT)*, vol. 2014, pp. 247–252, 2014.
- [51] B. K. Pattanayak, O. Pattnaik, and S. Pani, "Dealing with Sybil attack in VANET," *Intelligent and Cloud Computing*, vol. 194, pp. 471–480, 2021.
- [52] W. Xiong, R. Wang, Y. Wang, F. Zhou, and X. Luo, "CPPA-D: efficient conditional privacy-preserving authentication scheme with double-insurance in VANETS," *IEEE Transactions on Vehicular Technology*, vol. 70, no. 4, pp. 3456–3468, 2021.
- [53] L. E. Funderburg and I. Y. Lee, "Efficient short group signatures for conditional privacy in vehicular ad hoc networks via ID caching and timed revocation," *IEEE Access*, vol. 9, pp. 118065–118076, 2021.
- [54] M. Obaidat, M. Khodjaeva, J. Holst, and M. Zid, "Ben Security and Privacy Challenges in Vehicular Ad Hoc Networks," in *Connected Vehicles in the Internet of Things*, Z. Mahmood, Ed., pp. 223–251, Springer, Cham, 2020.
- [55] F. B. Günay, E. Öztürk, T. Çavdar, Y. S. Hanay, and A. Khan, "Vehicular ad hoc network (VANET) localization techniques: a survey," *Archives of Computational Methods in Engineering*, vol. 28, no. 4, pp. 3001–3033, 2021.
- [56] K. Xue, Q. Yang, S. Li et al., "PPSO: a privacy-preserving service outsourcing scheme for real-time pricing demand response in smart grid," *IEEE Internet of Things Journal*, vol. 6, no. 2, pp. 2486–2496, 2019.
- [57] A. Boualouache, S. M. Senouci, and S. Moussaoui, "A survey on pseudonym changing strategies for vehicular ad-hoc networks," *IEEE Communication Surveys and Tutorials*, vol. 20, no. 1, pp. 770–790, 2018.
- [58] I. Saini, B. St Amour, and A. Jaekel, "Intelligent adversary placements for privacy evaluation in VANET," *Information*, vol. 11, p. 443, 2020.
- [59] L. Benarous, B. Kadri, and S. Boudjit, "Alloyed pseudonym change strategy for location privacy in VANETs," in *2020 IEEE 17th Annual Consumer Communications & Networking Conference (CCNC)*, pp. 1–6, Las Vegas, NV, USA, 2020.
- [60] A. Verma, R. Saha, G. Kumar, and T. H. Kim, "The security perspectives of vehicular networks: a taxonomical analysis of attacks and solutions," *Applied Sciences*, vol. 11, p. 4682, 2021.
- [61] S. Sharma, A. Kaul, S. Ahmed, and S. Sharma, "A detailed tutorial survey on VANETs: emerging architectures, applications, security issues, and solutions," *International Journal of Communication Systems*, vol. 34, no. 14, 2021.
- [62] M. Al-Mehdihara and N. Ruan, "MSOM: efficient mechanism for defense against DDoS attacks in VANET," *Wireless Communications and Mobile Computing*, vol. 2021, 17 pages, 2021.
- [63] F. G. Abdulkadhim, Z. Yi, C. Tang, A. N. Onaizah, and B. Ahmed, "Design and development of a hybrid (SDN + SOM) approach for enhancing security in VANET," *Applied Nanoscience*, vol. 1, pp. 1–12, 2021.
- [64] D. Xu, "Proactive eavesdropping of suspicious non-orthogonal multiple access networks," *IEEE Transactions on Vehicular Technology*, vol. 69, no. 11, pp. 13958–13963, 2020.
- [65] H. Bangui, M. Ge, B. Buhnova, and L. Hong Trang, "Towards faster big data analytics for anti-jamming applications in vehicular ad-hoc network," *Transactions on Emerging*

## Retraction

# Retracted: Real Time Facial Expression Recognition for Online Lecture

### Wireless Communications and Mobile Computing

Received 8 August 2023; Accepted 8 August 2023; Published 9 August 2023

Copyright © 2023 Wireless Communications and Mobile Computing. This is an open access article distributed under the Creative Commons Attribution License, which permits unrestricted use, distribution, and reproduction in any medium, provided the original work is properly cited.

This article has been retracted by Hindawi following an investigation undertaken by the publisher [1]. This investigation has uncovered evidence of one or more of the following indicators of systematic manipulation of the publication process:

- (1) Discrepancies in scope
- (2) Discrepancies in the description of the research reported
- (3) Discrepancies between the availability of data and the research described
- (4) Inappropriate citations
- (5) Incoherent, meaningless and/or irrelevant content included in the article
- (6) Peer-review manipulation

The presence of these indicators undermines our confidence in the integrity of the article's content and we cannot, therefore, vouch for its reliability. Please note that this notice is intended solely to alert readers that the content of this article is unreliable. We have not investigated whether authors were aware of or involved in the systematic manipulation of the publication process.

In addition, our investigation has also shown that one or more of the following human-subject reporting requirements has not been met in this article: ethical approval by an Institutional Review Board (IRB) committee or equivalent, patient/participant consent to participate, and/or agreement to publish patient/participant details (where relevant).

Wiley and Hindawi regrets that the usual quality checks did not identify these issues before publication and have since put additional measures in place to safeguard research integrity.

We wish to credit our own Research Integrity and Research Publishing teams and anonymous and named external

researchers and research integrity experts for contributing to this investigation.

The corresponding author, as the representative of all authors, has been given the opportunity to register their agreement or disagreement to this retraction. We have kept a record of any response received.

### References

- [1] H. Wu, "Real Time Facial Expression Recognition for Online Lecture," *Wireless Communications and Mobile Computing*, vol. 2022, Article ID 9684264, 11 pages, 2022.

## Research Article

# Real Time Facial Expression Recognition for Online Lecture

Haobang Wu 

University of Sydney Faculty of Engineering, Australia

Correspondence should be addressed to Haobang Wu; hawu3115@uni.sydney.edu.au

Received 25 January 2022; Revised 8 March 2022; Accepted 22 March 2022; Published 14 April 2022

Academic Editor: Vinayakumar Ravi

Copyright © 2022 Haobang Wu. This is an open access article distributed under the Creative Commons Attribution License, which permits unrestricted use, distribution, and reproduction in any medium, provided the original work is properly cited.

In order to better improve online teaching during the epidemic, teachers can adjust the teaching according to the students' understanding. During the epidemic period, online teaching has become a basic way for teachers to teach. One big problem with online teaching is that the lecturers find it hard to see the students' facial expressions. According to the study, the students' facial expressions are essential for the instructor to understand the students' understanding of the course material. There are some relevant studies on the recognition of human facial expressions. However, most of them did not consider some expressions such as "Enlightened," "Confused," or "Bored." This study helps teachers to improve the quality of teaching by designing a program to provide them with students' facial expressions. The study, implemented on students' computers, can capture their faces from a camera, identify some common and useful facial expressions, and send them to lecturers regularly during online lectures. The main research methods used in this paper are as follows: (1) Use the face recognition algorithm provided by OpenCV to capture faces. (2) Train a convolutional neural network model to recognize the expression "Happy," "Surprised," "Neutral," "Enlightened," "Confusion," and "Boredom." (3) Use the message protocol EMQX to transmit the expression information. This study can successfully capture faces, and about 80% accuracy can identify expressions and successfully transmit expression information. This study contains some expressions rarely studied by others and is innovative in the field of facial expression recognition. Datasets, deep learning models, and results are available for other research teams.

## 1. Introduction

Online teaching has become an essential method for the university to continue holding semesters for students, researchers, and professors during the pandemic. The online conference platforms are playing a significant role in delivering the online lecturer. These platforms can help restore the traditional lecture model by allowing the lecturers to show the course materials through screen sharing or to write notes on the virtual whiteboard. However, what online teaching can not restore is efficient interaction between the lecturers and their students. Although the online conference platforms can allow attendees to see and talk to each other through the webcams, it is not realistic for the lecture to interact with many students due to network bandwidth and video processing limitations. From the lecturers' perspective, students' videos are showed in windows which occupied a part of the lecturer's screen. There will be more windows showing on the screen if more students are attending the lecture. When the number of windows reaches the

capacity of a screen, the windows will shrink to smaller sizes if more students are coming in the lecture room. For courses with a large number of students, lecturers will have trouble seeing the faces of students through the small and packed windows on the screen, not to mention reading their facial expressions. According to research, the students' facial expressions are the most used nonverbal communication mode in a lecture and are related to their emotions, which can help the lecturer recognize their comprehension of the lecture. Suppose there is a tool that can provide students' facial expressions to the lecturers periodically during an online lecture. In that case, it can restore the reading facial expression scenarios, and the lecturer can get useful interaction feedbacks from their students and can adjust their ongoing lectures accordingly.

This study designed and constructed a program on identifying common facial expressions of students in class. The program can automatically capture students' facial expressions from the camera and identify some common and useful facial expressions, including Boring, Confused, Cheerful,

Happy, Surprised, and Neutral, and expression messages can be sent to the lecturer during online lectures.

## 2. Literature Review

Studies in computer vision show that machine learning algorithms are effective in human facial expression recognition. Among all the subfields of machine learning, deep learning is one of the most popular algorithms used by researchers.

In this paper, Shengjun designed a face recognition device with fill light performance [1]. Wu and others designed a privacy security scheme for face recognition based on Facenet and state secret algorithm [2]. Li et al. designed the face recognition system from the aspects of MTCNN and Facenet [3]. The paper written by Gory et al. summarizes the performance of different machine learning models in recognizing facial expressions. The research team applied and tested several machine learning algorithms, including AdaBoost, logistic regression, and two deep learning models: dense neural network (DNN) and convolutional neural network (CNN), which are used to identify the seven most common expressions in the paper. Gory et al. tested the performance of different machine learning models and proved that the CNN may be the most suitable [4].

Jiankui and others used the AdaBoost algorithm to study the application of face recognition technology in smart construction site [5]. Yanxiu and others studied the hotel management system and used facial recognition technology to build an intelligent hotel management system [6]. Zhenqian and Weizeng applied biometric technology to the design of online authentication module [7].

As one of the most remarkable developments in the computer vision field, the convolutional neural network (CNN) has a significant ability to recognize objects from an image [8]. The CNN is a type of deep learning model that contains convolutional layers and dense layers. For each convolutional layer, several convolutional kernels are used to detect a certain feature of the image. The different convolutional layers can detect different features of an image. With all the convolutional layers stacked together, the image's features will be collected and delivered to the following fully connected layers. The fully connected layers can learn the nonlinear combinations of the high-level features extracted by the convolution layers and do the classifications.

To investigate how the CNN model can be used to do the recognition, I read the paper of Dr. Hussain and Dr. Balushi. The authors propose using a deep CNN model to do a real-time face emotion classification and recognition. The paper's core approach is to build a CNN model based on a well-known model called VGG16. VGG16 is a CNN model with a structure containing five different convolutional layers, each with different numbers and sizes of kernels and three fully connected layers. The final accuracy of the trained model described in the paper is 0.88.

The convolutional neural network has an excellent performance on human facial expression recognition. Chenhao used a complex convolutional neural network to study and verify face recognition in mixed scenes [9]. Zhichao and others designed a driver fatigue dangerous driving detection

system based on face recognition [10]. Li et al. studied the multispectral face recognition system [11]. Kezheng et al. used two-dimensional linear discriminant analysis and collaborative representation for face recognition [12]. From privacy concerns to improving recognition accuracy, Zijian is concerned about the dynamic application of face recognition technology in business application Governance [13].

Liu et al. designed a CNN model with an accuracy of 65% [14]. Fathallah et al.'s CNN models can have an accuracy of 90% when testing on datasets CK+, RaFD, and MUG [15]. The data that can be potentially used for my thesis is not sufficient. Most of the available collected datasets from other researchers do not contain emotions like boredom, confusion, and enlightened. It is hard to build a large dataset in a short time. Therefore, a technique that can do expression recognition on a small dataset is needed. Heidari and Fouladi-Ghaleh introduced and applied such a technique: transfer learning in their paper. Transfer learning can help to utilize the knowledge of a pretrained model onto a new model so that only a portion of the parameters in the new model needs to be trained. Therefore, the new model can be trained with a smaller dataset and within a shorter time. The research team froze the trained parameters of the first four convolutional layers (these parameters are untrained) and only trained the last convolutional layer and the fully connected dense layers. According to the paper, the result accuracy is 95.62%, which is higher than some other common methods.

Although the goal of the paper is different from mine, the idea of using transfer learning with the help of pretrained models will be potentially helpful in the situation where data is not enough. The key to transfer learning is to choose a proper pretrained model. Caroppo et al. compared them by evaluating three widely used pretrained models of facial expression recognition (VGG16, AlexNet, and GoogLeNet) on four different benchmark datasets (FACES, Lifespan, CIFE, and FER2013) [16]. Full experiments and results provide the reader with good performance of transfer learning in different modalities and help me to make decisions in the paper.

## 3. Methods

Let us first recap the goal of the thesis: to design and build a program that can automatically capture students' faces from cameras; can recognize the most common and useful facial expressions, including boredom, confused, enlightened, happy, surprised, and neutral; and can send the expression information to the lecturer periodically during an online lecture.

There are three steps to accomplish the goal: (1) Capture students' faces with their cameras. (2) Design and build a deep learning model that can accurately recognize the target facial expressions. (3) Build an output pipeline that can return the information to the lecturer. Different methods are used for each step.

The purpose of the model is to recognize the facial expressions after training using a dataset with limited data. Inspired by the research of Caroppo et al. and the paper of



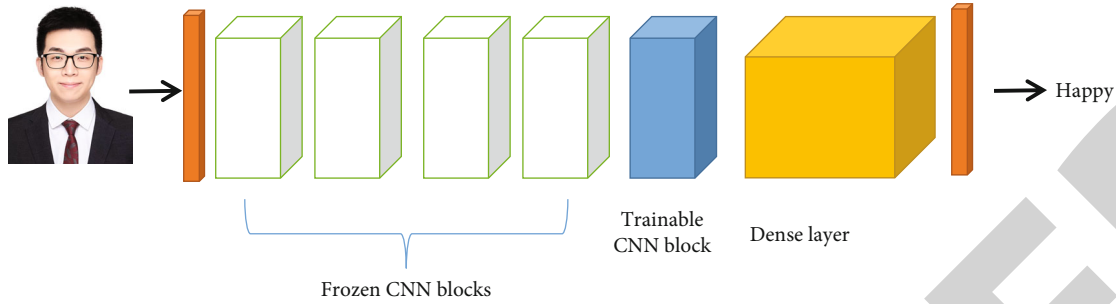


FIGURE 1: The complete model structure: including one input layer, 4 frozen CNN blocks, 1 trainable CNN block, dense layers, and one output layer.

Heidari and Fouladi-Ghaleh [17], I built a convolutional neural network by applying the transfer learning method. The pretrained model I chose is VGG16, provided by a python library called Keras. As I mentioned in Literature Review, VGG16 contains five convolutional blocks and three fully connected layers. My CNN model had the same structure but with some add-ons and modifications. The complete model structured is shown in Figure 1. The input layer is modified to accept an input image of size  $160 * 160 * 3$ . There are two convolutional layers and one 2D max-pooling layer for each convolutional block (Figure 2). The five convolutional blocks contain 64, 128, 256, 512, and 512 convolutional kernels of a size of  $3 * 3$  for each convolutional layer. Three fully connected layers with a number of 512 neural follow the convolutional blocks. Each layer is followed by a “RELU” activation function. Besides, two dropout layers of a rate of 50% are added after the second and the third fully connected layer. The final output layer contains six output neural followed by a “Softmax” activation function. The last layer’s output is a vector consisting of six values, and each value represents the prediction probability of each category. The prediction of the model is the expression with the highest prediction probabilities. I chose to freeze the first four convolution layers so that the parameters are not trained. The last convolutional block plus the following linear layers is trainable. Although the training data is not sufficient, the fact that fewer parameters are trainable can guarantee an acceptable result of the model performance. The two dropout layers are helping to fight against potential overfitting problems caused by a lack of data.

To build the dataset, I collected 1073 images: 200 images each for expression boredom, confusion, happy, surprised, and neutral and 73 images for expression enlightened. The images are collected from three sources. Most of the data are the self-collected. I asked volunteers to take selfies about the six required expressions. This part of data is the most validated because the labels of the pictures are provided directly by the person who makes the expressions. Plus, the volunteers are all students and the students are exactly the objects for the recognition task. Another big portion of the data comes from open sources, including the dataset provided by Sara Zhalehou and Bahcesehir University ECE Department, “Bahcesehir University Multimodal Face Database of Spontaneous Affective and Mental States” [18]. The data are collected during research experiments with the

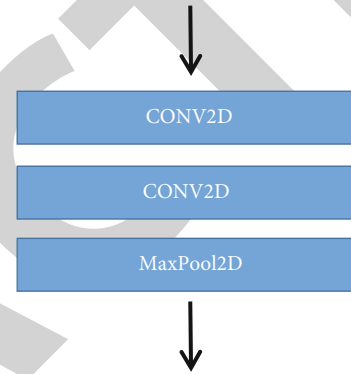


FIGURE 2: The structure of each convolutional block.

volunteered students and are labeled by the researchers. The data are carefully examined and organized before providing to the public. I used the pictures labeled with the six same facial expressions to expand my dataset. The final part of the data is collected from online sources like image web-pages and social media. I searched the pictures using the facial expression terms as the keywords and collected after manually selection by a selection team. The team consists of my supervisor, my classmates, and me. The pictures are chosen and labeled if all members agreed that they correspond to the facial expression keywords.

With the collected raw data, a preprocessing step is needed before the deep learning model train. The pictures are converted into greyscale and are resized into a resolution of  $160 * 160$  pixels. A greyscale face image can reduce the unexpected problems caused by different skin colors, and uniform image sizes are required for the model training. The label of the data is represented using one hot vector. In this case, the one hot vector is a vector with six values of 1 or 0. There is one value of “1” representing the corresponding category of the data, and the rest are “0.”

For model training, the dataset is divided into a training dataset and a validation dataset with a ratio of 4:1. The input of the CNN model is the  $160 * 160 * 3$  cropped face images from the training dataset. The output of the model is a list of prediction probabilities for the six expressions. The model is trained with a learning rate of 0.001 and is trained for 100 epochs. For each epoch, the loss is calculated with a cross-entropy loss function (Equation (1)),

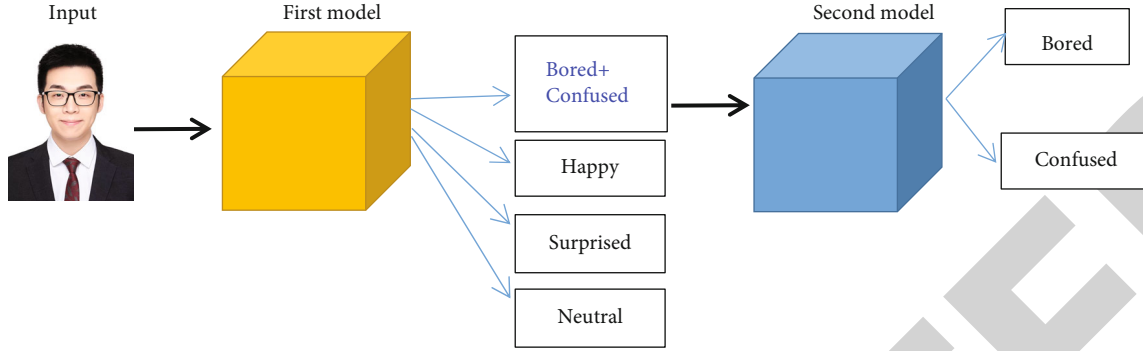


FIGURE 3: The structure of the third implementation.

and the model is optimized with stochastic gradient descent (Equation (2)). The accuracy of the output equals the portion of the number of correct predictions among all predictions.

$$\text{Cross entropy loss} = -\sum t_i * \log(p(x)), \quad (1)$$

$$W = W - \eta \Sigma \frac{\partial \text{Loss}}{\partial w_j}. \quad (2)$$

For testing the performance of the trained model, three-fold cross-validation testing is used. The model's performance is evaluated by watching the pattern of the training and validation loss/accuracy graph (against the number of epochs) and the accuracy of predictions for each expression. The whole coding for training the model is written using Python. The Python library Keras is used to create, train, and test the model.

The method of how to build the CNN model for training is clearly stated in the previous section. In my thesis work, the method is implemented in different ways to get different aspects of the results. The first implementation uses the CNN model to train with the data that contains all six facial expressions. Because the number of images about Enlightened is only 73, which is much less than the number of other expressions (200), I have to choose a dataset that contains 73 images for each expression for the training/testing procedure. The insufficient data may lead to a result that can be badly overfitting on training data. This is the trade-off I have to make due to the limited size of my dataset.

The second implementation uses a slightly different CNN model from the first one. Because the result from the first implementation implies that the model's performance in recognizing the expression "Enlightened" is very poor, I chose to evaluate the model without the "Enlightened." This time, the numbers of data for training and testing are larger: 200 images for each expression. With more training data involved and less output category, the result of the second implementation should have a better performance than the first one.

The third implementation is a combination of two CNN models. (Figure 3) After combining the two models, the implementation can output a classification for the five facial expressions. The method is innovative and sounds reason-

able, and you can expect a better result than the second implementation.

## 4. Results and Discussion

*4.1. Results and Discussion about First Implementation.* The first implementation is to use the CNN model to recognize all six facial expressions (Boredom, Confusion, Neutral, Enlightened, Happy, and Surprised). The CNN model is the modified model from pretrained VGG16 and has an output layer with six output neural. The dataset used for this implementation contains 438 images in total: 73 images for each emotion. The data is divided into a training/validation dataset with a ratio of 4:1. Before the training, the data is enlarged using the default data augmentation method provided by Keras. The model is trained with cross-entropy loss, SGD optimizer, and a learning rate of 0.001. The performance of the model is evaluated using three-fold cross-validation. There are three different sets of the training/validation dataset, and the performances of the model on all the sets are counted.

Figures 4 and 5 are the plots for the training/validation loss against the number of epochs and the training/validation accuracy against the number of epochs for the model performed on one of the sets. From the plot of loss vs. epochs, it is clear that the validation loss (orange curves) stopped decreasing after around 30 epochs and finally floated around a loss of 0.8 to 1.0 while the training loss (blue curves) kept decreasing and converged to zero in the end. A similar pattern was also showed in the plot of accuracy vs. epochs. The validation accuracy increased very slowly and floated around 72%. Table 1 shows the average accuracy of the cross-validation data. The specific accuracy on recognizing each of the six expressions is shown in the table. The model has accuracies around 80% for Happy, Surprised, and Neutral. Accuracies for Boredom and Confusion are lower and are around 70%. Accuracy for recognizing Enlightened faces is the worst and is only 56%. The total accuracy for the model is 72%. The confusion matrix of predictions and labels is shown in Figure 6.

The overall result of the first implementation is poor. The trained model is not an acceptable one for the design. The performance of the expression "Enlightened" is the worst because the training data about "Enlightened" is

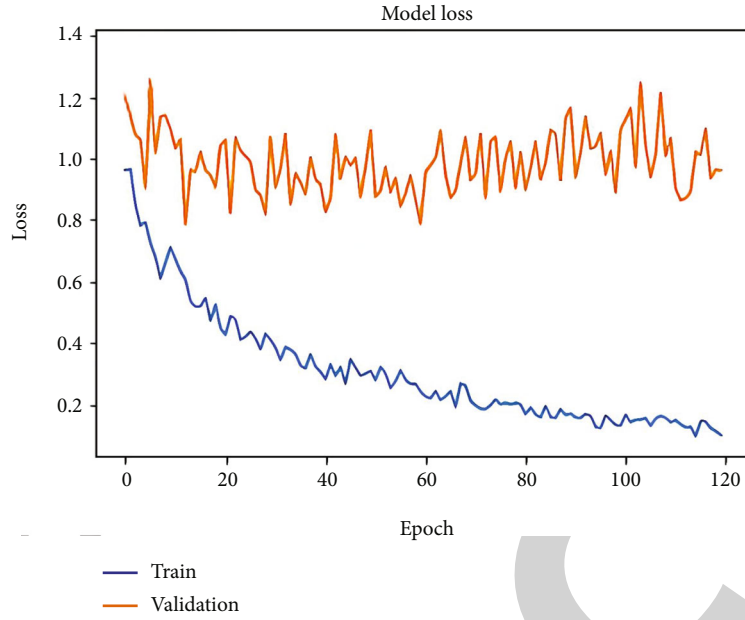


FIGURE 4: First implementation: loss.

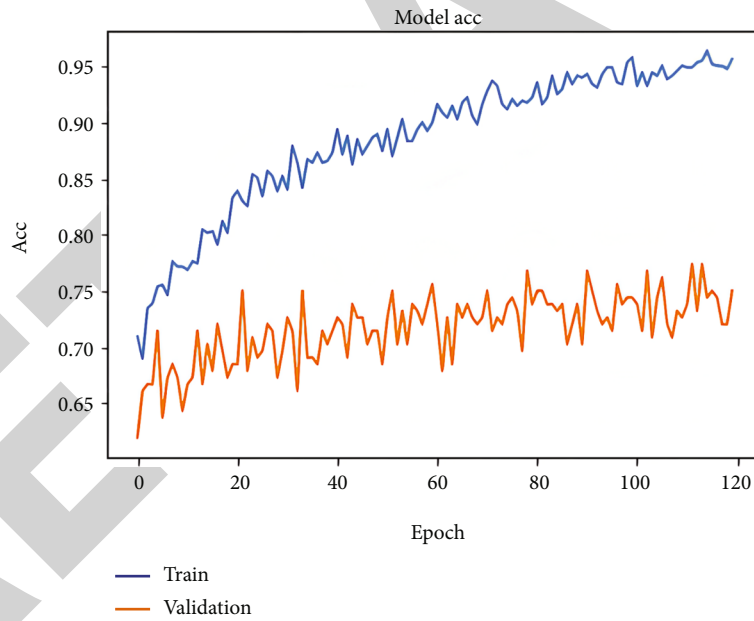


FIGURE 5: First implementation: accuracy.

TABLE 1: Experiment results for the first implementation.

	Total	Happy	Surprised	Neutral	Boredom	Confusion	Enlighten
Accuracy	0.72	0.86	0.81	0.78	0.67	0.69	0.56

collected and labeled only based on my own opinion. Since there is no convincing and valid dataset about this facial expression, I decided to exclude the expression “Enlightened” from my thesis goal and focus on classifying the other five facial expressions, which is my second implementation.

*4.2. Results and Discussion about Second Implementation.* Second implementation uses the CNN model to recognize the five facial expressions, excluding “Enlightened” (Boredom, Confusion, Neutral, Happy, and Surprised). The CNN model is similar to the one used in the first

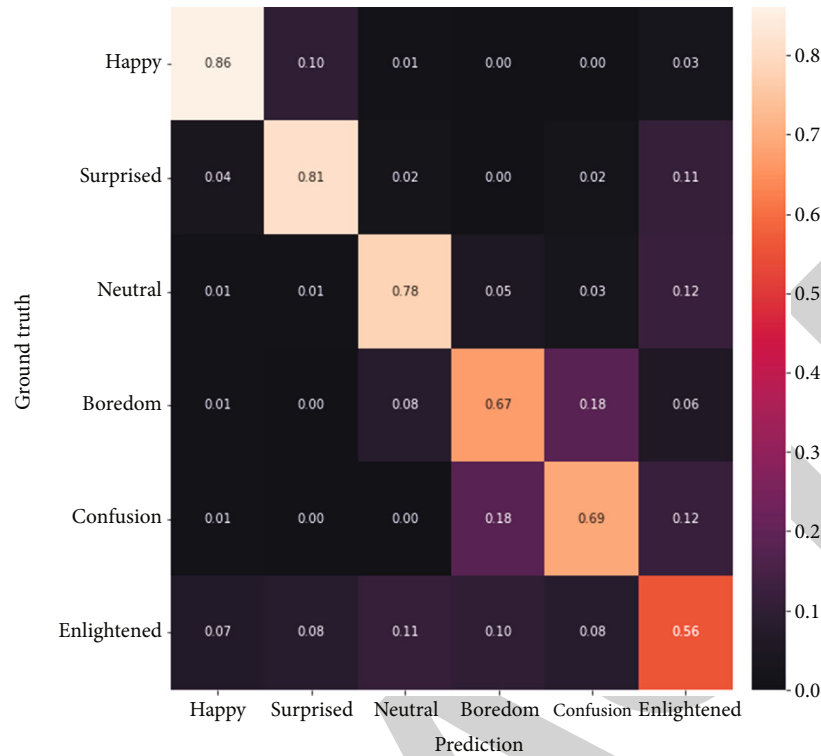


FIGURE 6: First implementation: confusion matrix.

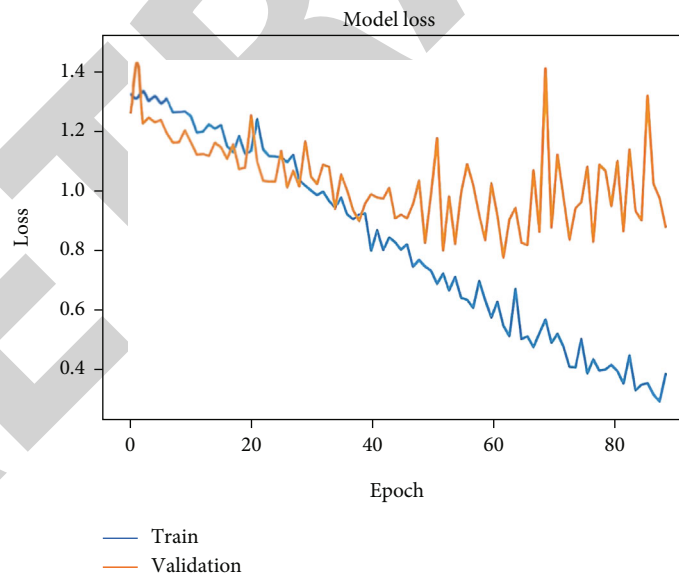


FIGURE 7: Second implementation: loss.

implementation. Again, it is a modified model from pre-trained VGG16 but has an output layer with five output neural this time. The dataset now used for this implementation contains 1000 images in total: 200 images for each emotion. The data is still divided into a training/validation dataset with a ratio of 4:1 and is enlarged with Keras data augmentation function. The model is trained with cross-entropy loss, SGD optimizer, and a learning rate of 0.001, and the

model's performance is evaluated using three-fold cross-validation.

Figures 7 and 8 are the plots for the training/validation loss against the number of epochs and the training/validation accuracy against the number of epochs for the model performed on one of the sets. From the loss vs. epochs plot, the validation loss stopped decreasing after around 50 epochs and finally floated around a loss of 1.0 while the

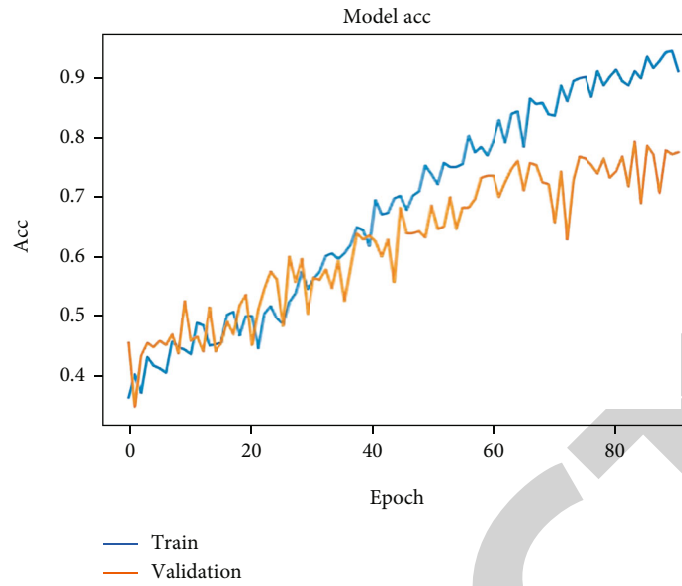


FIGURE 8: Second implementation: accuracy.

TABLE 2: Experiment results for the second implementation.

	Total	Happy	Surprised	Neutral	Boredom	Confusion
Accuracy	0.75	0.85	0.81	0.80	0.65	0.63

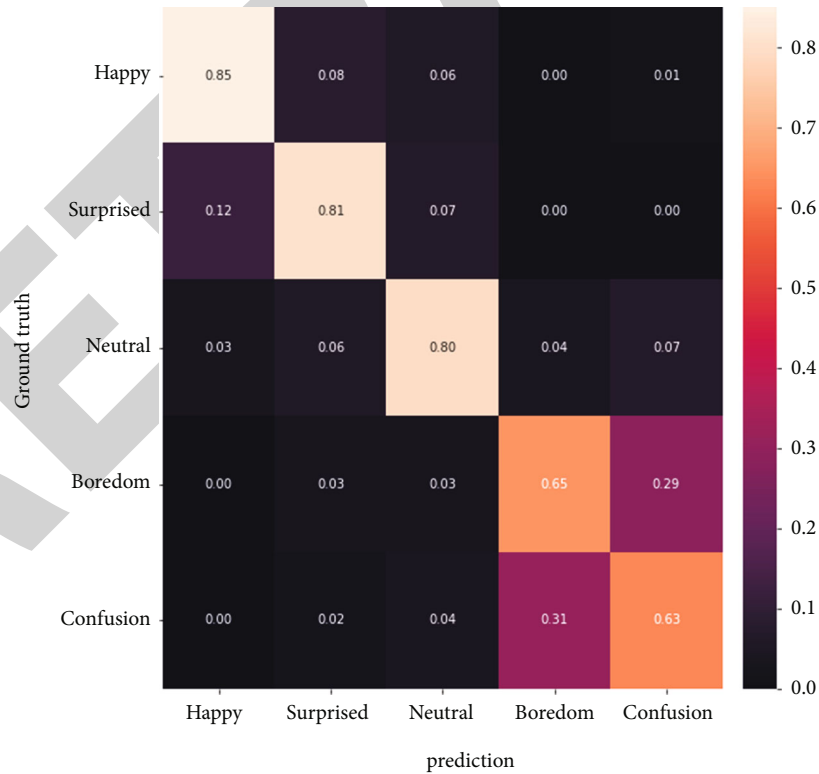


FIGURE 9: Second implementation: confusion matrix.

training loss kept decreasing. In the accuracy vs. epochs plot, the validation accuracy increased along with the training accuracy and finally floated around 75%. Table 2 shows the

model’s average accuracy in predicting the facial expressions of all three sets of data. The model has accuracies around 85% for Happy and 80% for Surprised and Neutral.

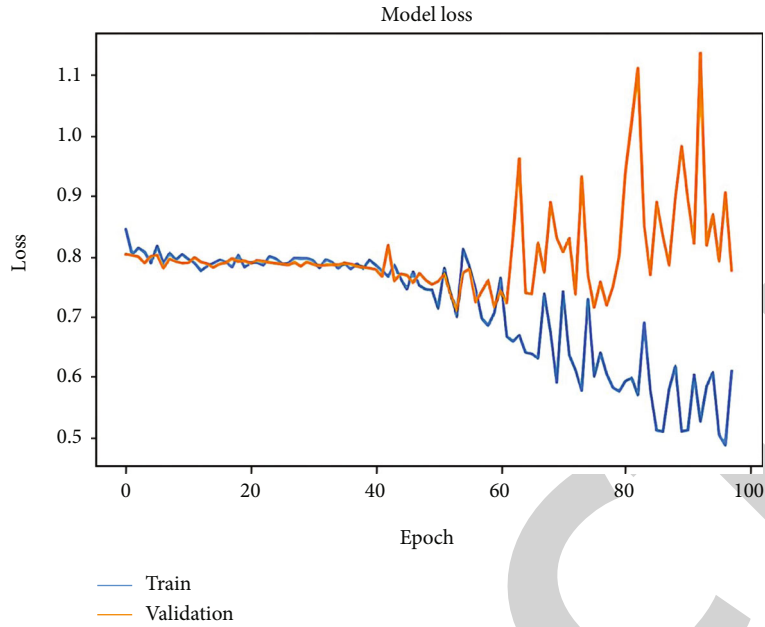


FIGURE 10: Third implementation, B+C model: loss.

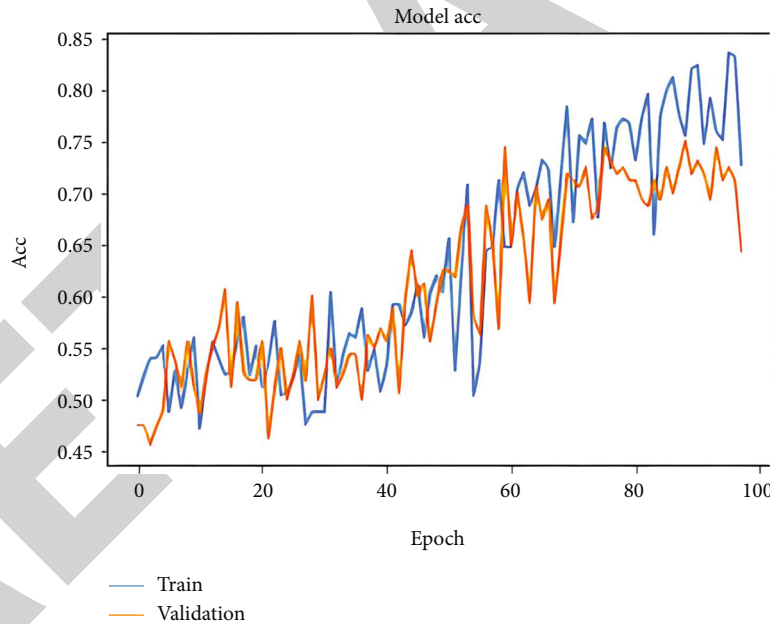


FIGURE 11: Third implementation, B+C model: accuracy.

Accuracies for Boredom and Confusion are still lower: they are below 70%, just like the first implementation. The model’s total accuracy is 75% because the worst accuracy of Enlightened is excluded and can no longer drag down the average. The confusion matrix of predictions and labels is shown in Figure 9.

From the graphs of the “loss/accuracy vs. epochs” (Figures 10 and 11), it is clear that the model is still overfitting on training data. The validation loss finally converged to around 0.9, and the validation accuracy finally converges to around 75%. The results from the two plots show the same

TABLE 3: Experiment results for B+C model.

	Total	Boredom	Confusion
Accuracy	0.75	0.76	0.74

problem as stated in the first implementation. The model that tends to fit on training data is not good at generalizing for unseen data. From the table of accuracy, the accuracies for “Happy,” “Surprised,” and “Neutral” are still around 80%, which is similar to the last result, whereas accuracy

TABLE 4: Experiment results for the combination model.

	Total	Happy	Surprised	Neutral	Boredom	Confusion
Accuracy	0.77	0.83	0.79	0.81	0.71	0.69

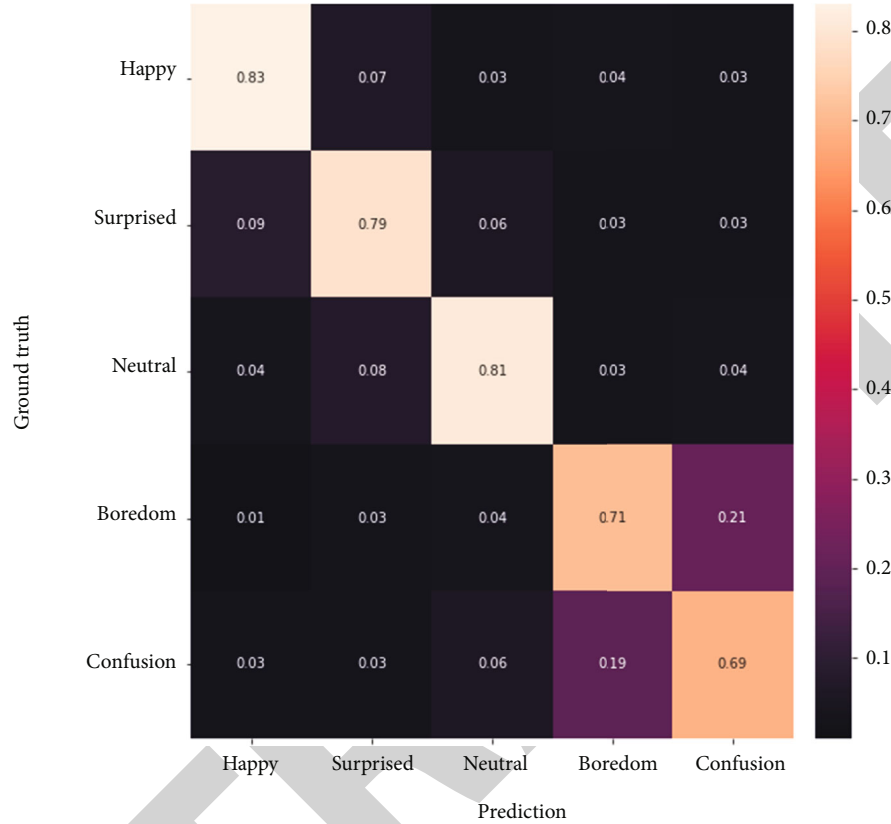


FIGURE 12: Combination implementation: confusion matrix.

for “Boredom” and “Confusion” decreased slightly compared to the first implementation. The model’s total accuracy is increased because the low accuracy category “Enlightened” is not involved this time.

It is out of my expectation that the model did not improve a lot after getting rid of “Enlightened” and training with more data. The performance on recognizing “Happy,” “Surprised,” and “Neutral” is acceptable when compared to the result of other related researches. However, the model had a poor performance on recognizing “Boredom” and “Confusion.” To find out why, I check every single prediction of the validation data for these two expressions. Surprisingly, I found out that the images of these two expressions are often classified to be the other one incorrectly.

**4.3. Results and Discussion about Third Implementation (Combination Model).** The third implementation combines two CNN models to recognize the five facial expressions (Boredom, Confusion, Neutral, Happy, and Surprised). Both two CNN models are similar to those used in the previous implementations but with different output layers. The first model regards “Boredom” and “Confusion” to be one category. Thus, it contains an output layer with four neurons.

The dataset contains 800 images in total: 200 images for each category are used to train the model. If the output of the first model is the “B+C” category for an image, the image will go through the second model to be further classified as either “Boredom” or “Confusion.” The second model is trained to classify these two expressions, so it has a binary output layer. The dataset to train this model contains 200 images for each expression. The datasets are still divided into training/validation dataset with a ratio of 4:1 and are enlarged using Keras default data augmentation method. The models are trained with cross-entropy loss, SGD optimizer, and a learning rate of 0.001. The results of the two models will be discussed separately, and the performance for the combination of the models will be evaluated as well.

From the result, we can conclude that the model still has an acceptable performance on recognizing “Happy,” “Surprised,” and “Neutral,” and this time, it can clearly classify expressions “Boredom” and “Confusion” with the other three expressions. If my second binary classification model can also have a good performance, the accuracy for recognizing these two will be higher than before.

The combination model contains the first model after training for 100 epochs and the second model after training

for 60 epochs. To evaluate the performance of the third implementation, I used the combination model to predict the validation dataset and check the accuracy. The data first went through the first model and then recognized as one of the four categories (Happy, Surprised, Neutral, or B+C). If the data is one of the first three expressions, it will be output and compared to the ground truth. If the data is B+C, it was further classified by the second model and was compared to the ground truth. The accuracy of the further B+C model is showed in Table 3. The accuracy of the combination model is showed in Table 4. The confusion matrix of predictions and labels is shown in Figure 12.

When compared to the result of the model in the second implementation (Table 2), the accuracy for Boredom increases from 65% to 71%, and the accuracy for Confusion increases from 63% to 69%. The total accuracy, therefore, increased from 75% to 77%. Although the third implementation indeed improved from the second one, it still did not reach what I have expected: an average accuracy of 80%.

## 5. Conclusion

The main goal of this study is to improve the interaction between lecturers and students during the online lectures. The program designed and constructed in this paper achieves this goal by informing the teacher of students' facial expressions. This study contains some expressions rarely studied by others and is innovative in the field of facial expression recognition. Datasets, deep learning models, and results are available for other research teams. The dataset insufficiency is a big limitation that prevents me from building more accurate programs that makes the final program not perfect. The dataset insufficiency is a big limitation that prevents me from building more accurate programs that makes the final program not perfect. This can be an experiment in a university to let students take pictures of the required facial expressions. The second step is to test message transmission performance between two computers. Tests can include delayed testing and message loss rate testing. The final step in the future is to better display the facial expression information on the teacher's screen. The idea of this study was to use emojis to represent each student in a small window, consistent with the received facial expression, which is a direct expression for the teacher to see more intuitively.

## Data Availability

The data underlying the results presented in the study are available within the manuscript.

## Conflicts of Interest

There is no potential conflict of interest in our paper, and all authors have seen the manuscript and approved to submit to your journal. We confirm that the content of the manuscript has not been published or submitted for publication elsewhere.

## References

- [1] W. Shengjun, "A face recognition device design with light-filling performance," *Electronic Technology*, vol. 51, no. 2, pp. 172-173, 2022.
- [2] J. Wu, P. Changgen, T. Weijie, and W. Zhenqiang, "Face Enc Auth: face recognition privacy and security scheme based on Face Net and national security algorithm," *Computer Engineering and Application*, vol. 18, no. 3, pp. 1-7, 2022.
- [3] L. Zhihua, Z. Jianyu, and W. Zhongcheng, "Design of the face recognition system based on MTCNN and Facenet," *Modern Electronic Technology*, vol. 45, no. 4, pp. 139-143, 2022.
- [4] S. Gory, M. Al-Khassaweneh, and P. Szczurek, "Machine learning approach for facial expression recognition," in *2020 IEEE International Conference on Electro Information Technology (EIT)*, pp. 32-39, Chicago, IL, USA, 2020.
- [5] L. Jiankui, C. Yang, H. Xiaoxing, and L. Hui, "Application of facial recognition technology of Adaboost algorithm in intelligent construction site," *Single-chip microcomputer and embedded system application*, vol. 21, no. 4, 2021.
- [6] Y. Yanxiu, Y. Rui, and Y. Feijie, "An intelligent hotel management system based on facial recognition," *Innovations*, vol. 8, no. 1, 2021.
- [7] J. Zhenqian and X. Weizeng, "Design of an online authentication module based on biometric identification technology," *Information system Engineering*, vol. 10, 2020.
- [8] Y. Zhang and Q. Ji, "Active and dynamic information fusion for facial expression understanding from image sequences," *IEEE Transactions on pattern analysis and machine intelligence*, vol. 27, no. 5, pp. 699-714, 2005.
- [9] Y. Chenhao, "Research and implementation of mixed scene face recognition based on complex convolutional neural network," *Electronic World*, vol. 2, 2022.
- [10] H. Zhichao, Z. Hongmei, E. Chan, and T. Yaosen, "Driver fatigue dangerous driving detection system based on facial recognition," *Electromechanical Engineering Technology*, vol. 50, no. 12, pp. 143-146, 2021.
- [11] C. Li, L. Zhihong, L. Yanping, R. Xiaoguang, and B. Changchun, "Review of multispectral facial recognition systems studies," *Technology Wind*, vol. 35, 2021.
- [12] L. Kezheng, X. Deng, and Z. Yulun, "Two-dimensional linear discriminative analysis and collaborative representation of facial recognition methods," *Small Microcomputer system*, vol. 42, no. 8, pp. 1688-1693, 2021.
- [13] Z. Zijian, "Face recognition technology business application governance dynamics: from privacy concerns to improved recognition accuracy concerns," *Competition Policy Research*, vol. 3, pp. 81-91, 2021.
- [14] K. Liu, M. Zhang, and Z. Pan, "Facial expression recognition with CNN ensemble," in *2016 International Conference on Cyberworlds (CW)*, pp. 163-166, Chongqing, China, 2016.
- [15] A. Fathallah, L. Abdi, and A. Douik, "Facial expression recognition via deep learning," in *2017 IEEE/ACS 14th International Conference on Computer Systems and Applications (AICCSA)*, pp. 745-750, Hammamet, Tunisia, 2017.
- [16] A. Caroppo, A. Leone, and P. Siciliano, "Comparison between deep learning models and traditional machine learning approaches for facial expression recognition in ageing adults," *Journal of Computer Science and Technology*, vol. 35, no. 5, pp. 1127-1146, 2020.



## Research Article

# Optimal Recognition of Volleyball Player's Arm Movement Track Based on Embedded Microprocessor

Ming Liu <sup>1</sup>, Jingtao Wu,<sup>2</sup> and Jiangan Tao<sup>3</sup>

<sup>1</sup>Department of Public Physical Art Education, Zhejiang University, Hangzhou, 310058 Zhejiang, China

<sup>2</sup>College of Physical Education, Leshan Normal University, Leshan, 614000 Sichuan, China

<sup>3</sup>College of Marxism & Mental Health Education Center, Yanshan University, Qinhuangdao 066004, China

Correspondence should be addressed to Ming Liu; michael616504@zju.edu.cn

Received 25 December 2021; Revised 26 January 2022; Accepted 23 February 2022; Published 13 April 2022

Academic Editor: Shalli Rani

Copyright © 2022 Ming Liu et al. This is an open access article distributed under the Creative Commons Attribution License, which permits unrestricted use, distribution, and reproduction in any medium, provided the original work is properly cited.

An embedded microprocessor is the core part of the integrated circuit system, and it represents one of the highest levels of a digital integrated circuit design. Therefore, the design of low-power embedded microprocessors has become an important research direction in the integrated circuit design. Volleyball has always been a very important sport in our country, and it is a sport that the masses of people like to see. The basic techniques of volleyball include ready posture and movement, serving, hot ball, passing, smashing, and netting. The research content of this article is a simulation study of volleyball players' arm trajectory optimization recognition. In response to the above problems, this paper proposes an optimized recognition method based on the volleyball player's arm motion trajectory. The simulation results show that the method has high recognition accuracy and provides a strong scientific basis for improving the volleyball players' spike skills. Without interference from the right arm, the controller input and position tracking error will not fluctuate in  $1 \leq T \leq 3$ , the controller input is stable, and the output error is zero. Based on the above simulation analysis, it can be seen that the control method does not require the robot kinematics and dynamics model to generate any regression matrix when designing the controller. The controller is suitable for the performance tracking of humanoid robot arms.

## 1. Introduction

The anthropomorphic double-arm robot has its unique advantages in industrial fields such as precision grinding, precision assembly, and heavy load handling. It is the direction of the intelligent development of the next generation of industrial robot arms. At the same time, volleyball, as the only collective sports event to win the Olympic championship in China's three major balls, occupies a very important position in the hearts of Chinese people. The Chinese women's volleyball team won the 2019 Women's Volleyball World Cup and successfully defended the title. This is the tenth World Championship won by the Chinese women's volleyball team, and it is also a special birthday gift they sent to the 70th birthday of the People's Republic of China. General Secretary Xi Jinping called to congratulate everyone and encouraged everyone to continue to maintain high fighting spirit, not be arrogant or impetuous, and achieve better

results. The spirit of women's volleyball encourages all walks of life to struggle forward. As the development of the world volleyball team enters the new century, volleyball has also developed rapidly. In recent years, international competitions have continued to increase. Various countries are also actively participating in preparations, whether in the overall team tactics or player physical fitness. Quickly, in addition, it has attracted a large number of commercial resources, and the commercial development of volleyball has also become colorful, so this has increased the healthy competition between sports teams in various countries, thereby greatly promotes the popularity of volleyball worldwide, and also makes volleyball more professional and commercial.

From the evolution of apes to humans, human use of various tools is becoming more flexible and even making complex arm movements, which is more challenging for the analysis of athlete arm trajectories. More and more arm movement makes human upper limbs, especially the

arms and fingers, not only developed but also very flexible, as if they were skillful [1, 2]. The flexibility of the joints tends to be perfect, the structural characteristics are very reasonable, the movement can be optimized and the most flexible, and the ability to adapt to the environment is extremely strong, which makes the human survival ability easier than other organisms [3, 4]. From ancient times to the present day, human beings have been learning and exploring the world from the rich world. Many of the inspirations for human technologies and inventions come from the colorful natural world [5, 6]. Therefore, the natural world is the source of human progress and development and an inexhaustible treasure trove of ideas and inventions [7, 8]. Learning from nature, imitating various movements of creatures to serve humanity has developed into a discipline, i.e., bionics [8, 9]. As the most important branch of research in bionics, the research of humanoid itself is also one of the most popular research fields at present [10, 11]. In recent years, there have been many studies at home and abroad where two single-arm robots coordinate and cooperate with each other to accomplish a certain task and have achieved many research results [12, 13]. However, it is difficult to deal with emergency accidents by a simple combination of two one-handed robots to complete complex and flexible actions like humans [14, 15]. Therefore, it is very meaningful to study and implement the dual-arm robot to flexibly and steadily perform various actions like humans in a complex environment [16, 17]. The traditional robot trajectory construction method relies on manual programming by the operator, and the efficiency is relatively low [18, 19]. In recent years, a method based on imitation-based automatic generation of robot trajectories has received increasing attention from researchers [5, 20]. This method has higher efficiency than traditional methods and has the advantages of strong adaptability for different execution tasks [21, 22]. It enables robots to learn new skills and knowledge by interacting with other individuals in the environment, such as humans or other robots, just like humans [8]. The automatic generation method of movement track based on imitation makes the robot more adaptable. By observing the movement of the teacher with marked points, the movement information of the teacher can be quickly and accurately obtained, and the computer passes the obtained data through. A certain algorithm is processed to generate a reasonable robot trajectory and store it and then controls the robot to repeat the same actions as the teacher, so that the robot learns useful actions and enables it to quickly adapt to new tasks and environments [23, 24].

Learning the spatiotemporal representation of motion information is essential for human action recognition. However, most existing features or descriptors cannot effectively capture motion information, especially for long-term motion. To solve this problem, Shi et al. proposed a long-term motion descriptor called a sequential depth trajectory descriptor (sDTD). Specifically, Shi et al. project dense trajectories into a two-dimensional plane and then uses CNN-RNN networks to learn effective representations of long-term motion. Unlike the popular two-stream ConvNets, the sDTD stream is introduced into a three-stream

framework in order to recognize actions from video sequences. Therefore, this three-stream framework can simultaneously capture the static spatial features, short-term motion and long-term motion in the video. Extensive experiments were performed on three challenging data sets: KTH, HMDB51, and UCF101. Experimental results show that Shi et al.'s method has the most advanced performance on the KTH and UCF101 datasets and is comparable to the latest method on the HMDB51 dataset [25]. Fahn et al. introduced a gesture recognition method for human-machine interface. This recognition method is based on a learning ranking model. Experimental results show that the AdaRank model is effective for improving recognition accuracy. Combining the learning ranking model with the hand movement trajectory has made a breakthrough in modeling a complex combination of 8 recognized gestures. The construction of the gesture recognition system can effectively detect the gestures of one hand or two hands in basic directions (such as moving up, moving down, moving left, and moving right). In order to make users more friendly to the proposed system, Fahn et al. can combine basic directions and expand into more gestures for applications. Experimental results show that Fahn et al.'s method has high performance and can run in real time. For practical applications, the accuracy of this method is also very high [26]. The energy expenditure of the human arm is important for seeking the optimal human arm trajectory. Zhou et al. proposed a new method to calculate the metabolic energy expenditure of the human arm movement, aimed at revealing the relationship between the energy expenditure and the arm movement trajectory and the contribution of acceleration and arm direction. Zhou et al. studied the horizontal motion of the human arm with the Qualisys motion capture system, and motion data were postprocessed by biomechanical models to obtain metabolic consumption, including results on arm motor kinematics, kinetics, and metabolic energy expenditure [27].

This study starts from the whole and observes the characteristics of shoulder dysfunction, such as morphology, muscle strength, mobility, proprioception, etc., using the shoulder joint as a ring, and putting it into the whole whip chain from the torso to the arm. For analysis, the simulation test system was applied to volleyball for the first time to test the strength, speed, power, etc. of spiking, and combined with EMG, infrared high-speed camera and other tests, a comprehensive analysis of the dynamic mechanism of shoulder dysfunction. The function of proprioception is to receive external stimuli and structural deformations produced by joint muscle movements and transmit this information to the center to adjust limb position and muscle activity, so as to protect and maintain joint stability and avoid sports injuries caused by excessive movements. This article observes the morphological characteristics of people with shoulder dysfunction; tests their activity, muscle strength, and proprioception; and observes the changes in proprioception after static strength exercise fatigue; through simulation tests, surface electromyography, and biomechanical tests, the analysis caused dysfunction dynamic mechanism. In this paper, the automatic generation method of robot trajectory based on

imitation is to record and process the motion data of the teacher and then map it into the corresponding trajectory of the robot and optimize it to make the robot reproduce the motion of the teacher.

## 2. Proposed Method

*2.1. Volleyball Player Movement Analysis.* In volleyball spiking, upper limb movements are all coordinated by shoulder straps, shoulder joints, elbow joints, radial ulnar joints, wrist joints, and finger joints. The movement of the shoulder strap always follows the movement of the shoulder joint to increase the amplitude of the upper arm movement. The swinging action of the swing arm is to lift the shoulder joint as the axis directly to the back of the shoulder and accelerate forward and upward. Therefore, during jumping and air strikes, the movement of the upper limb can be decomposed into a shoulder strap: shoulder blade bony rotation-rotation-down maneuver-forward extension and lowering; shoulder joint motion: upper arm flexes-inner rotation extension when shoulder joint abducts; and elbow joint motion: when swinging the upper arm, the triceps contract explosively to straighten the elbow joint. The flexor muscles of the wrist and fingers contract, and although the force generated by the action is not large, the effective transmission of momentum, the determination of the final position of the end ring, and the decisive influence on the final state. During the whiplash of the upper limbs, the muscles that complete the exercise usually first passively elongate and then contract to apply force. Muscles, a form of work that is forced to rapidly centrifugal contract and then turn into centripetal contraction, is called “stretch-shorten cycle.”

*2.2. Arm Trajectory Model.* The typical joint morphology is mainly on the kinematic joint surface (the articular surface is the contact surface of each related bone that constitutes the joint. Each joint includes at least two articular surfaces, generally one convex and one concave. The convex one is called the joint head, and the concave one is called the joint socket), when it is described in joint kinematics. The shape of the articular surface is mostly a curved surface or a slightly curved surface. This forms a concave-convex relationship at the joint. The concave-convex relationship of the joints allows them to adapt to each other, increase the surface area to dissipate the contact force, and help guide the movement between bones. Almost half of the humeral bone of the shoulder joint is a solid sphere. It forms the convex surface of the glenohumeral joint. In this concave-convex relationship, there are three basic forms of motion: rolling, sliding, and rotating. When the human arm is in motion, three types of motion will move on the convex and concave surfaces. The definitions for scrolling, sliding, and rotating are shown in Table 1.

Since rotation is more important for the humanoid dual-arm robot in the later period, the following introduction and examples are given here. The humanoid dual-arm robot is capable of having a stronger grip and a longer arm span than humans, which mimics the human arm structure to complete a similar movement to the human arm. One of the

main ways of bone rotation is through the rotation of its joint surface to counter the articular surface of another bone. Generally, it mainly occurs in the rotation of the forearm and the glenohumeral joint and the flexion and extension of the hip joint.

In the process of arm movement, the shoulder joint, elbow joint, and wrist joint complex mainly rely on the rotation method. In order to better evaluate the movement of the arm, this section uses the triangle rule to study the shoulder joint as an example, as shown in Figure 1. In the triangle, the value of the trigonometric function can be calculated through the relationship between the angle and the edge. The sides of the triangle can represent physical quantities such as distance, force, and speed. Here, we first define the representation of right-angle trigonometric functions in biomechanical relations, sine  $\sin(\alpha)$ , cosine  $\cos(\alpha)$ , tangent  $\tan(\alpha)$ , and cotangent  $\cot(\alpha)$ , where each trigonometric function represents a specific given angle value. If the vector representing two sides is known in a right triangle, the third side is the hypotenuse, which can be determined by the Pythagorean theorem. If, in addition to a right angle, a side and an angle are known in a right triangle, then the remaining sides of the triangle can be represented by one of four trigonometric functions. The angle can be obtained by knowing any two sides using an inverse trigonometric function. The angle of insertion of the deltoid muscle in the shoulder joint is 45 degrees from the bone. Based on the selected work coordinate reference system, the rectangular part muscle force  $M$  is synthesized by  $Mx$  parallel to the arm and perpendicular to the arm  $My$ .

When the elbow joint is subjected to external resistance, the muscle provides power for the arm to resist the resistance. It belongs to the internal force category of the elbow joint. This muscle strength can be decomposed into  $Mx$  parallel to the forearm (radial) and vertical  $My$  by the right triangle method. These forces affect the stability of the joint. When the muscle component  $My$  parallel to the forearm passes through the axis of rotation at the elbow joint, there is no torque, so there is no rotation. When the component force,  $My$  perpendicular to the forearm passes through the rotation axis, a torque is generated, and therefore, rotation occurs. This vertical component also produces a tangential force on the humeral radius joint. The direction is along the positive direction of the  $Y$  axis.

Arm movements include plate support, pull-up, push-ups, and back push-ups. Embedded processor is the core of the embedded system, which is the hardware unit of control and auxiliary system operation. As the core of the embedded system, the embedded processor undertakes the important tasks of control and system work, making the host equipment function intelligent, flexible design, and simple operation.

*2.3. Principle of Identification.* In the process of identifying the trajectory of the volleyball player's arm, we first obtain the joint points of the human arm movement, extract the key feature point trajectory of the arm movement trajectory, obtain the data of the arm trajectory feature point of each frame of image, and obtain the dynamic volleyball player

TABLE 1: Three kinds of motion definition in joint kinematics.

Exercise method	Definition	Performance of joints in motion
Scroll	Multiple points of one rotating joint surface are in contact with multiple points of another joint surface	Tyre movement on the road
Slide	A single point of one joint surface is in contact with multiple points of another joint surface	Tires slip on smooth ice
Spin	Rotation of a single point on one joint surface with a single point on another joint surface	The ball turns a little on the ground

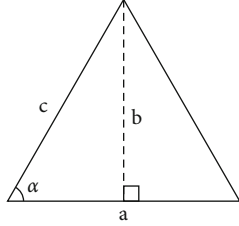


FIGURE 1: The triangle rule.

arm movement sequence diagram. We establish a volleyball player arm movement trajectory recognition model to complete the volleyball player arm movement trajectory recognition.  $a$  represents the distance between the wrist joint and the shoulder joint,  $b$  represents the distance between the wrist joint and the elbow joint, and  $c$  represents the distance between the elbow joint and the shoulder joint. Then, using Equation (1), we first obtain the coordinates of the human arm joint.

$$\alpha^\partial(\Gamma) = \frac{\varphi(\partial) \times X}{c \times M(\alpha) \cdot b} * (Z). \quad (1)$$

In the formula,  $M(\alpha)$  represents the distance between the joints of the left arm and the shoulder joints in the space.  $\varphi(\partial)$  represents the distance between the joints and the shoulder joints. Vector  $Z$  represents the change range of joint point of arm movement. Suppose that  $\eta(I_d, I_Y)$  represents any pixel in the single-pixel picture of the volleyball player's arm movement in a certain frame, and  $I_d$  and  $I_Y$  represent the horizontal axis and ordinate  $\partial_n(I_d, I_Y)$  of  $I$ , respectively, and represent the subsequent  $n$ -frame single-pixel athlete's arm movement picture, Equation (2) gets the data of the feature points of the arm's motion trajectory for each frame of the image:

$$\eta(\tau) = \frac{\eta(I_d, I_Y) \otimes \partial_n(I_d, I_Y)}{I_d \otimes I_Y} \times \alpha^\partial(\Gamma). \quad (2)$$

Assuming that  $I'(I'_x, I'_y)$  represents the corner point of the right arm end and then uses Equation (3) to obtain the data of the arm trajectory feature points of each frame image:

$$I'(I'_x, I'_y) = \frac{\partial_n(I_d, I_Y) \times \eta(I_d, I_Y)}{I_d \otimes \lambda(M)}. \quad (3)$$

In the formula,  $\lambda(M)$  represents the offset of the depth feature from the original position. Assuming that  $f_i(I, Y)$  represents the segmentation position feature of the hand region,  $B(\mu, \nu)$  represents the processed motion trajectory, and  $\theta$  represents the conversion data of the lower arm of the arm, and then, we use Equation (4) to obtain the dynamic volleyball player arm motion sequence diagram.

$$\omega_b^{a_n}(\ell, l) = \left[ x'_b \right] \otimes \frac{(E \otimes f_i(I, Y))}{B(\mu, \nu)} \times \theta. \quad (4)$$

In the formula,  $x'_b$  represents the characteristic parameter of the arm motion, and  $E$  represents the characteristic value of the connected area to mark the initial frame image. Based on the above, formula (5) is used to build a volleyball player arm movement trajectory recognition model.

$$\mu(\varphi) = \frac{[f_i(I, Y)] \oplus \alpha \partial(\Gamma) * (Z)}{\omega_b^{a_n}(\ell, l) \otimes \lambda(\xi)}. \quad (5)$$

In the formula,  $\lambda(\xi)$  represents the change range of joint trajectory. The above can explain the principle of volleyball player arm movement trajectory recognition, which can be used to identify the volleyball player arm movement trajectory.

In the process of recognizing the trajectory of the volleyball player's arm movement, the fusion of the background difference principle is first used to detect the athlete's movement trajectory, and the dynamic arm tracking is performed by the particle filter of the color histogram. Suppose that  $u_t$  represents the corresponding pixel of the background image,  $u_{t+1}$  represents the updated pixel of the volleyball player arm motion background image, and it represents the pixel of the current frame volleyball player arm motion image; then, we use formula (6) to collect the detected volleyball player's arm motion sequence images.

$$\mu_{t+2} = \begin{cases} \mu_t, I_t(x, y), \\ \alpha_{\mu_{t+1}} + (1-\alpha)I_t \otimes I_f. \end{cases} \quad (6)$$

In the formula,  $\alpha$  represents the update rate of the background model,  $I_f$  represents the mask value of the pixels of the current frame image. In the RGB recognition of the volleyball player's arm movement trajectory, the skin color of the arm is yellowish, and the brightness of the pixels of the

skin color is greater. The pixel corresponding to the skin color of the volleyball player's arm corresponds to the brightness  $\chi(p)$  representing the back projection image of each frame of arm movement, and then, the binary image of the arm movement trajectory is detected by using

$$v\_temp = \begin{cases} \chi(p) \otimes \eta(\beta), \\ v \times \partial(Y) \times r. \end{cases} \quad (7)$$

In the formula,  $\partial(Y)$  represents the different channels of the RGB image,  $\eta(\beta)$  represents the proportional coefficient of the skin color of the athlete's arm movement, and  $r$  represents the pixels of the skin area of the moving arm. Suppose that  $w_k^i(x_{0:k})$  is the weight representing the time of the  $i$ th particle  $k-1$ ,  $w_{k-1}^i$  is the likelihood probability observed by the volleyball player's arm motion trajectory system, and the weight of the particle is obtained by calculating the Barr coefficient of the color histogram.

In the formula,  $P(u)$  represents the color histogram of the arm motion area where each particle is located, and  $q(u)$  represents the sensitivity of the color space to light.

In summary, it can be explained that in the process of volleyball player arm movement trajectory recognition, the background difference principle is first used to detect the athlete's movement trajectory, and the color histogram particle filter is used for dynamic arm tracking, which provides a volleyball player arm movement trajectory recognition.

**2.4. The Processing Power of the Microprocessor.** We know that a program written in a high-level language needs to be compiled, assembled, and linked with a compiler, assembler, and linker, respectively, to generate object codes that can be directly executed by the microprocessor. The object code consists of a series of computer instructions. We define the performance of a microprocessor as

$$PER = \frac{1}{EXET}. \quad (8)$$

In the above formula, EXET represents a period of program execution time, and another commonly used performance indicator is MIPS, that is, how many millions of instructions are executed per second

$$MIPS = \frac{EIC}{ET(s) * 10^6}. \quad (9)$$

The total service delay can be expressed as follows:

$$T(TA) = \left\{ \frac{Task}{c} + wm, \frac{Task}{c_2} + wm, \frac{Task}{c_3} + wm, \dots, \frac{Task}{c_m} + wm \right\} + \phi. \quad (10)$$

The solution of the task distribution coefficient can be transformed into a vector solution, which is modeled as

the following optimization problem:

$$\sum_{i=1}^k TA(i) = Task, \quad (11)$$

$$I = \prod_{i=1} [Task_{min}, Task_{max}] = \prod_{i=1} [0, Task].$$

The total service response delay under the condition of no failure can be expressed as follows:

$$t = \max \left\{ \frac{D}{C} + Wl, \frac{D_c}{C_c} + Wl \right\}. \quad (12)$$

The communication delay between computing nodes in the CE-IIoT architecture can be expressed as follows:

$$W = \frac{D}{L} \times \frac{T(1+P)}{1-P}. \quad (13)$$

Then, the time delay for a successful transmission of a data packet is calculated as follows:

$$T = \frac{L}{R},$$

$$W_{vi,vj} = \frac{D}{r} \times \frac{1-l}{1+l}. \quad (14)$$

Similarly, the communication delay between the MEC device and the cloud server C can be calculated as follows:

$$W_c = \phi \frac{D}{r} \times \frac{1-P}{1+P}. \quad (15)$$

The overall structure of the obtained controller is shown in Figure 2. It searches according to the address output by the MMU and returns the corresponding result if it hits; otherwise, it sends a request to the outside to interface with the BIU.

### 3. Experiments

**3.1. Subjects and Data Sources.** In order to prove the effectiveness of the proposed volleyball player arm trajectory optimization recognition method based on chaos theory, this paper builds an experimental platform for volleyball player arm trajectory recognition through related experiments and MATLAB environment. The experimental data comes from the record of the 2017~2019 Chinese Women's Volleyball League. The game uses a French-made camera with an internal time scale of G · V16mm and shoots two different swings of the swinging arm at position 2 from the front side. The shooting frequency is 90 frames per second. The upper edge of the reference body is 2.4m above the ground, the height of the camera's main optical axis from the ground is 1.67m, and the take-off point of the athlete's spike is 20m. A total of 60 spiking moves of 5 main players were shot, and a better image frame of each spiking action was selected as experimental data.

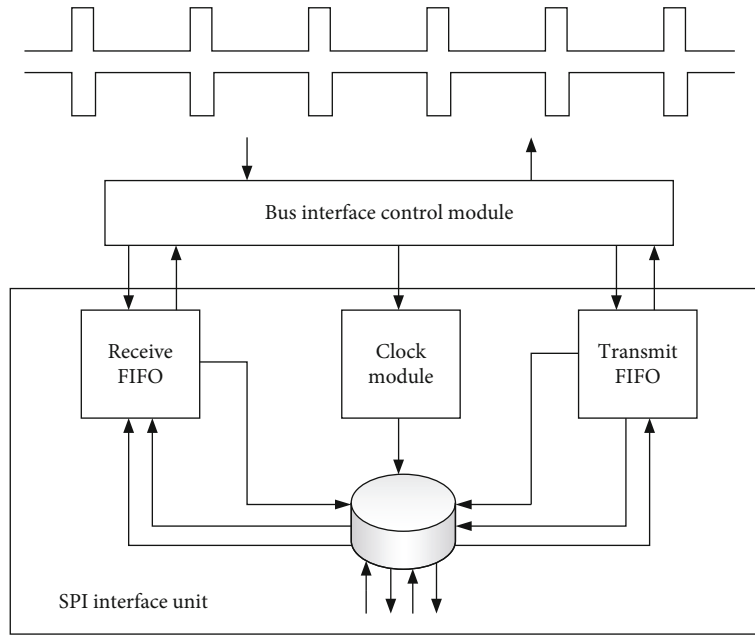


FIGURE 2: SPI overall structure diagram.

**3.2. Experimental Software System Platform.** In order to facilitate the user's operation, a software application platform with a simple graphical interface was written. The experimental platform mainly includes the following modules: data acquisition and processing module, trajectory generation module, 3D simulation module, and robot communication module, as shown in Figure 3.

This platform is modular, portable, and extensible, and at the same time, supports TCP/UDP network communication and the storage of related data and control instructions. The process flow for the robot control software to plan the robot's dynamic motion is shown in Figure 4.

The programming languages of the software platform are mainly MATLAB and C#. In order to take advantage of MATLAB's excellent numerical computing power, the processing of arm motion data, the generation of trajectories, and the three-dimensional simulation are carried out in MATLAB. The three-dimensional simulation interface establishes a three-dimensional model of the robot.

## 4. Discussion

**4.1. Centrifugal/Centripetal Ratio Analysis.** The relationship between the eccentric and centripetal ratio of the shoulder joint flexor and extensor is the relationship between the active muscle and the antagonist muscle. On the contrary, when the extensors of the shoulders perform centripetal movements, the flexors of the shoulders adjust the movement of the shoulder joints by eccentric movements. The ratio of shoulder joint antagonistic eccentric/active muscle centripetal contraction is shown in Table 2.

It is generally believed that isotonic eccentric contraction is when the tension on the tendon reaches a certain level and may damage the muscle. The Golgi tendon in the skeletal muscle tendon sends out a return impulse to the central ner-

vous system, which has an inhibitory effect on the motor nerve. Inhibition of muscle activity can prevent muscle strain. We analyze the number of technical actions assisted by running, the distance of each step, and the distance of approach, as shown in Table 3:

The purpose of the run-up is to increase the take-off height on the one hand, and on the other hand, to obtain a certain forward momentum after the take-off, and to choose a suitable hitting point.

Combining the data in Table 2, an analysis of the shoulder joint antagonistic muscle centrifugal/active muscle centripetal ratio can be obtained, as shown in Figure 5.

During the volleyball swing arm spiking process, the flexor, abductor, and external rotation muscle groups mainly increase the angle of the shoulder joint to generate potential energy, and the extensor, internal rotation, and horizontal adduction muscle groups during the arm swing stage contract to produce strength and accelerate the movement of the upper limbs, and the flexor, external rotation, and horizontal abduction muscle groups do eccentric contraction. On the one hand, they must resist the force generated by the concentric contraction of the internal rotation muscle group. On the other hand, they must also cushion the inertia of the upper limbs to prevent the shoulder joint from concentric contraction of the internal rotator from the extreme movement beyond the physiological range in a certain direction. By regularly performing constant-speed strength test on the shoulder joint, the balance of the antagonistic eccentric/eccentric force of the two shoulder joints and the centripetal force of the original motor muscle is compared to prevent the occurrence of sports injuries. The ratio of the external rotation centrifugal/internal rotation centripetal and horizontal adduction centrifugal/horizontal abduction centripetal right hand is smaller than the left hand. This discovery should attract enough attention, because the

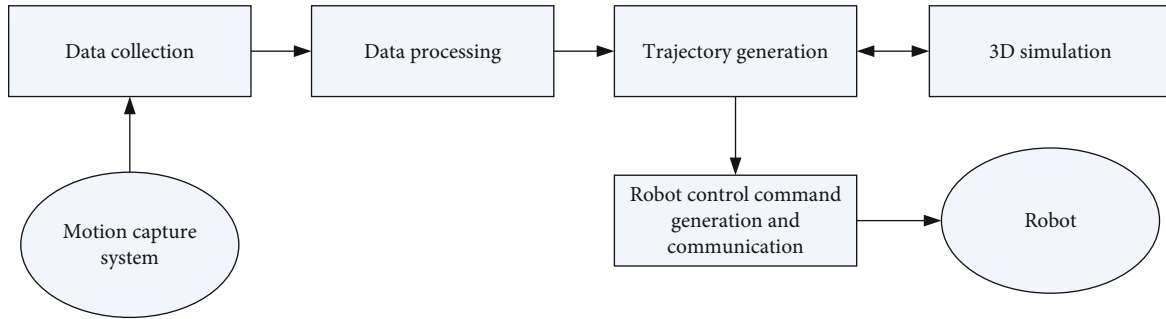


FIGURE 3: Software platform structure.

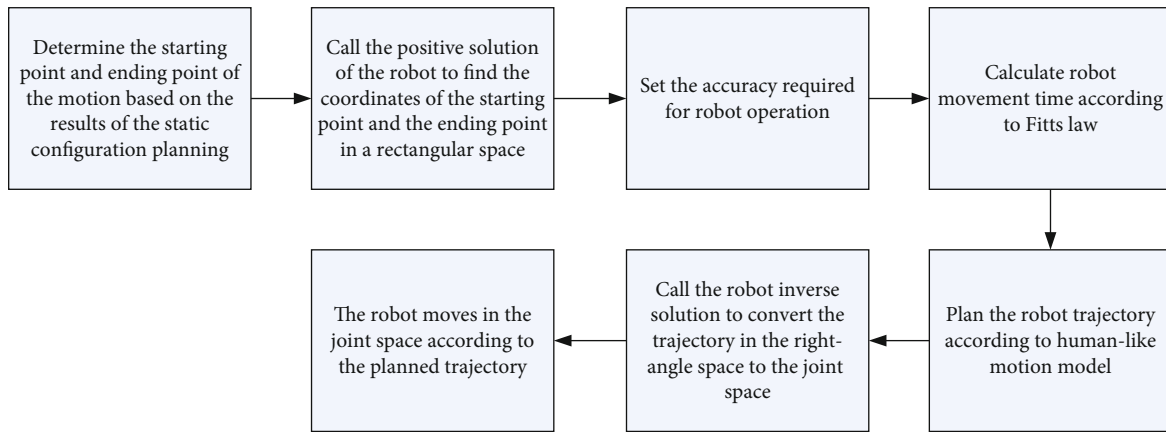


FIGURE 4: Robot control software to plan the processing flow of robot dynamic motion.

TABLE 2: Shoulder joint antagonist eccentric/active muscle centripetal contraction ratio.

Researcher	Object	Speed	Result
Yu He	Men’s volleyball	60°/s	Flexion/centrifugation
Noffal	Men’s baseball	60°/s	External spin centrifuge/internal spin centrifuge
Sirota	Men’s tennis	60°/s	External spin centrifuge/internal spin centrifuge
Mikesky	Man athlete	60°/s	External spin centrifuge/internal spin centrifuge

TABLE 3: Step distances of different technologies.

	Jump serve		Back smash		Front row smash	
	L jump 1	L jump 2	L after 1	L after 2	L front 1	L front 2
1	0.75	1.01	0.74	1.04	0.64	1.30
2	0.84	1.29	0.88	1.22	1.01	0.88
3	0.78	1.05	0.91	1.14	0.86	1.11
4	0.96	1.06	1.04	1.14	1.26	0.82
5	0.72	1.03	0.88	1.18	0.76	1.17

horizontal adduction muscles and external rotation muscles play an important buffering role in the completion of the pull arm and batting movements. During the deceleration of the batting action, the centrifugal contraction of the external rotation muscle generates greater tension to control the degree of centripetal contraction of the internal rotation muscle. After frequent practice of the above movements,

the overloaded work due to eccentric contraction increases the risk of muscle injury or worsening strain. Therefore, the external rotation centrifugal force and horizontal adduction centrifugal force should be strengthened to maintain the balance of shoulder joint muscle strength.

**4.2. Comparative Analysis of Volleyball Players’ Upper Limb Rapid Strength Kinematics Index.** The shoulder rotation angle refers to the angle formed by the line between the shoulders of the athlete and the horizontal plane and represents the rotation angle of the upper body. When the tested athletes completed the entire batting action in the air, the angle change of the shoulder rotation angle at the maximum of the arm and the moment of the shot can reflect the rotation amplitude.

By analyzing the data in Table 4, it can be seen that when the male athlete has the largest arm before and after the experiment, the shoulder rotation angle differs by about 5

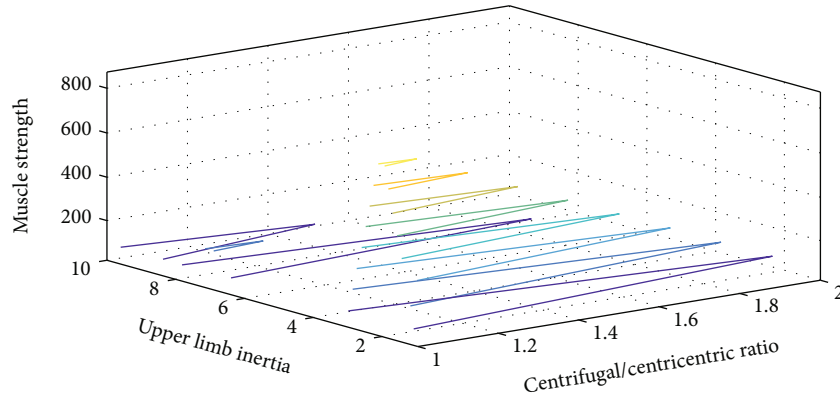


FIGURE 5: Analysis of the ratio of antagonistic eccentric/active muscle centripetal of the shoulder joint.

TABLE 4: The angle of shoulder rotation angle before and after the experiment.

		Before the experiment		After the experiment		<i>T</i> value	<i>P</i> value
Gender	Batting action	Average value	Standard deviation	Average value	Standard deviation		
Male	When the arm is maximum	42.13	2.16	47.27	2.33	0.288	<0.05
	Hitting moment	13.48	1.43	14.76	1.53	0.167	>0.05
	Angle change value	28.65	1.66	32.48	1.75	0.604	<0.05
Female	When the arm is maximum	37.62	1.87	40.12	2.06	0.316	<0.05
	Hitting moment	17.93	1.52	18.05	1.23	0.342	>0.05
	Angle change value	19.65	1.79	22.08	1.55	0.931	<0.05

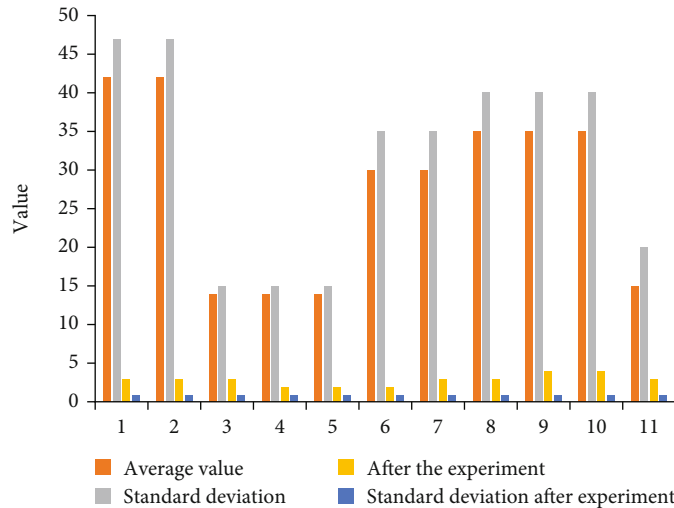


FIGURE 6: Comparative analysis of volleyball players' upper limb rapid strength kinematics index.

degrees,  $P < 0.05$ , showing a significant difference, which can be seen after the experiment. The body width has been significantly improved. Combining the data in Table 3, a comparative analysis of the volleyball players' upper limb fast strength kinematics indicators can be obtained, as shown in Figure 6.

The angle of the shoulder spin angle of the male athlete at the moment of hitting the ball did not change much,  $P > 0.05$ , and there was no significant difference, so the athlete did not change significantly after the experiment. The angle change value differs by about 5 degrees before and after the experiment,  $P < 0.05$ , showing a significant difference. It



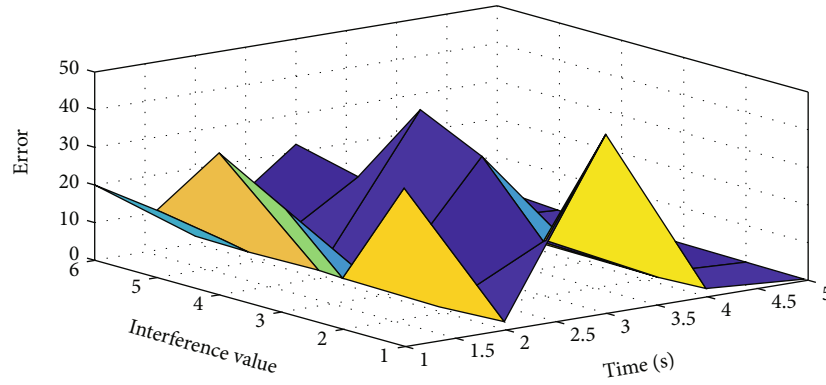


FIGURE 7: Actual and observed values of nonlinear disturbance observers with sliding mode adaptive inversion control.

TABLE 5: Take-off level analysis.

	Jump serve	Back smash	Front row smash
$V$ and	$3.02 \pm 0.49$	$3.58 \pm 0.17$	$3.42 \pm 0.21$
$V$ double 1 (m/s)	$2.08 \pm 0.28$	$2.06 \pm 0.22$	$1.68 \pm 0.35$
$V$ double 2 (m/s)	$2.53 \pm 0.24$	$2.82 \pm 0.23$	$2.72 \pm 0.33$
Horizontal speed damage rate	$0.29 \pm 0.07$	$0.38 \pm 0.07$	$0.48 \pm 0.09$
Horizontal speed conversion rate	$2.52 \pm 0.22$	$2.03 \pm 0.47$	$1.61 \pm 0.47$
Jump height (m)	$0.71 \pm 0.09$	$0.84 \pm 0.09$	$0.82 \pm 0.11$
Jump distance (m)	$1.72 \pm 0.29$	$2.16 \pm 0.17$	$1.55 \pm 0.29$

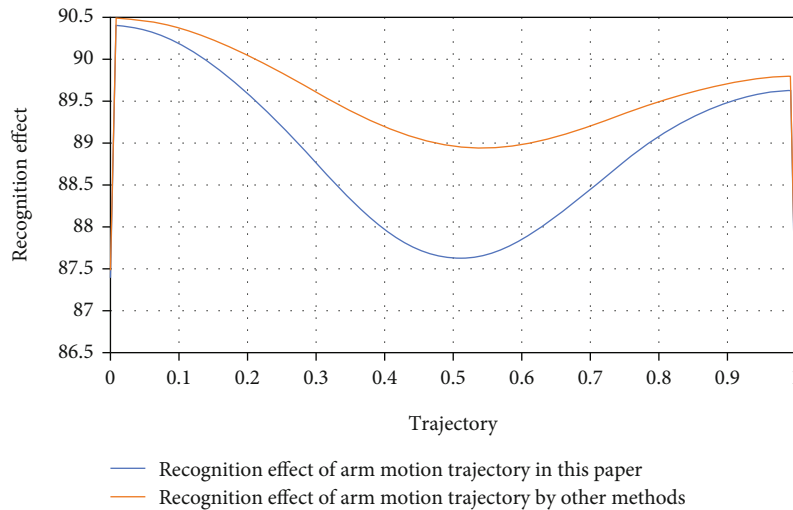


FIGURE 8: Comparison results of two different methods for recognizing the effect of athlete’s arm trajectory.

can be seen that the amplitude of the male athlete’s rotation after the experiment has increased greatly, which also shows that the athlete’s spiking strength has also been compared. A large increase, the difference between the angle change value before and after the experiment is about 3 degrees,  $P < 0.05$ , showing a significant difference. It can be seen that the amplitude of the athlete’s rotation after the experiment has

increased greatly, which also shows that the athlete’s spiking strength has also been greatly improved. The experimental results provide theoretical help for the optimal recognition of the volleyball player’s arm movement trajectory.

4.3. Analysis of Sliding Mode Adaptive Inversion Control Based on Nonlinear Disturbance Observation. Simulation of

sliding mode adaptive inversion control based on nonlinear disturbance observation is used. Nonlinear disturbance observation is used to estimate matching interference. The purpose of the sliding mode observation period is to reduce the total interference of the system. The simulation is based on a humanoid robot and DC motor driver. The actual and observed values of the nonlinear disturbance observer for sliding mode adaptive inversion control are shown in Figure 7.

As shown in the figure, the output error of the left arm's position tracking under disturbance. It can be clearly seen that the left arm's input and position tracking error have obvious fluctuations under the interference condition. In the case of no interference, there is no fluctuation between the controller input and position tracking error between 1 and 3, the controller input is smooth and stable, and the output error is zero. Based on the above simulation analysis, it can be seen that this control method does not require the robot kinematics and dynamic model to generate any regression matrix when designing the controller. In addition, it proves that using this controller ensures that all signals of the closed-loop system converge exponentially. The tracking error consistency is ultimately bounded. The controller is suitable for performance tracking of humanoid robot arms.

The conversion rate of the horizontal speed of the back-row smash and the jump-initiated jump is much lower than that of the front-row smash. Jump serve has certain characteristics of rushing jump. The analysis of take-off level speed conversion rate is shown in Table 5:

**4.4. Contrast Analysis on the Recognition Effect of Arm Motion Trajectory by Different Methods.** The method of this article and other methods are used to carry out the experiment of volleyball player's arm movement trajectory recognition. Two different methods are used to compare the effect of the athlete's arm movement trajectory recognition. The comparison results are shown in Figure 8.

It can be analyzed that the effect of using this method to identify the trajectory of the arm is significantly higher than the effect of using other methods to identify the trajectory of the arm of the volleyball player. This is mainly because when using this method for arm movement trajectory recognition, it is first combined with the background difference principle to detect the athlete's movement trajectory, using color histogram particle filtering for dynamic arm tracking, and fused with chaos theory to obtain sports space. We reconstruct the athlete's arm trajectory to ensure the effectiveness of the method in this paper to identify the arm's trajectory. In the method of this paper, when the recognition of the volleyball player's arm trajectory is optimized, the phase space of the player's arm trajectory is reconstructed using chaos theory. From the reconstructed phase space, the chaotic invariant representing the trajectory of the athlete's arm is extracted, and it has three-dimensional space characteristics. The arm movement trajectory is converted into a one-dimensional arm movement trajectory. On this basis, the optimized recognition of the volleyball player's arm movement trajectory is completed, thereby ensuring the comprehensive effective-

ness of the volleyball player's arm movement trajectory identification method.

## 5. Conclusions

In this paper, when the current method is used to identify the movement trajectory, the characteristics of the athlete's arm movement trajectory cannot be accurately extracted, and the volleyball player's arm movement trajectory cannot be accurately identified. A new method for volleyball player's arm trajectory optimization recognition based on chaos theory is proposed. The simulation results show that the proposed method has high recognition accuracy and provides a strong scientific basis for improving the volleyball player's spiking technique.

This article focuses on the research of the volleyball player's arm movement mechanism. The goal is to reproduce the human's coordinated movement of the human arm on the humanoid two-armed robot. Systematic and in-depth research has been carried out on aspects such as rotational motion evaluation, human trajectory capture and inverse kinematics, model matching between human trajectory and dual-arm robot, and coordinated control method of dual-arm.

There are still some deficiencies in this paper. Although this paper has made some research progress, it still needs to further optimize the algorithm in human motion capture, and the experimental design needs to increase the sample value. In terms of control algorithm, the control space of the dual-arm robot is still very large, and there are still many problems that need further research.

## Data Availability

No data were used to support this study.

## Conflicts of Interest

The authors declare that they have no conflicts of interest.

## Authors' Contributions

Ming Liu contributed to the writing and editing. Jingtao Wu contributed to the formal analysis. Jiangan Tao contributed to the methodology.

## References

- [1] E. I. Barakova, P. Bajracharya, M. Willemsen, T. Lourens, and B. Huskens, "Long-term LEGO therapy with humanoid robot for children with ASD," *Expert Systems*, vol. 32, no. 6, pp. 698–709, 2015.
- [2] W. He, W. Ge, Y. Li, Y. J. Liu, C. Yang, and C. Sun, "Model identification and control design for a humanoid robot," *IEEE Transactions on Systems Man & Cybernetics Systems*, vol. 47, no. 1, pp. 1–13, 2016.
- [3] M. Fakoor, A. Kosari, and M. Jafarzadeh, "Humanoid robot path planning with fuzzy Markov decision processes," *Social Science Electronic Publishing*, vol. 14, no. 5, pp. 300–310, 2016.

- [4] J. Zhao, X. Mao, H. Hu, L. Niu, and G. Chen, "Behavior-based SSVEP hierarchical architecture for telepresence control of humanoid robot to achieve full-body movement," *IEEE Transactions on Cognitive and Developmental Systems*, vol. 9, no. 2, pp. 197–209, 2017.
- [5] E. Tidoni, P. Gergondet, G. Fusco, A. Kheddar, and S. M. Aglioti, "The role of audio-visual feedback in a thought-based control of a humanoid robot: a BCI study in healthy and spinal cord injured people," *IEEE Transactions on Neural Systems & Rehabilitation Engineering*, vol. 25, no. 6, pp. 772–781, 2017.
- [6] J. Baltes, K. Y. Tu, S. Sadeghnejad, and J. Anderson, "Huro-Cup-competition for multi-event humanoid robot athletes," *Knowledge Engineering Review*, vol. 1, no. 1, pp. 1–14, 2016.
- [7] F. Guo, T. Mei, M. Luo et al., "Motion planning for humanoid robot dynamically stepping over consecutive large obstacles," *Industrial Robot*, vol. 43, no. 2, pp. 204–220, 2016.
- [8] J. Andreu-Perez, F. Cao, H. Hagra, and G. Z. Yang, "A self-adaptive online brain-machine interface of a humanoid robot through a general type-2 fuzzy inference system," *IEEE Transactions on Fuzzy Systems*, vol. 26, no. 1, pp. 101–116, 2018.
- [9] S. Guo, H. Xu, N. M. Thalmann, and J. Yao, "Customization and fabrication of the appearance for humanoid robot," *The Visual Computer*, vol. 33, no. 1, pp. 63–74, 2017.
- [10] F. Guo, T. Mei, M. Ceccarelli, Z. Zhao, T. Li, and J. Zhao, "A generic walking pattern generation method for humanoid robot walking on the slopes," *Industrial Robot*, vol. 43, no. 3, pp. 317–327, 2016.
- [11] T. Kishi, S. Shimomura, H. Futaki et al., "Development of a humorous humanoid robot capable of quick-and-wide arm motion," *IEEE Robotics and Automation Letters*, vol. 1, no. 2, pp. 1081–1088, 2016.
- [12] M. Rogó , H. Zeng, C. Xuan, D. S. Wiersma, and P. Wasylczyk, "Soft robotics: light-driven soft robot mimics caterpillar locomotion in natural scale (advanced optical materials 11/2016)," *Optical Materials*, vol. 4, no. 11, pp. 1902–1902, 2016.
- [13] C. Yang, T. Teng, B. Xu, Z. Li, J. Na, and C. Y. Su, "Global adaptive tracking control of robot manipulators using neural networks with finite-time learning convergence," *International Journal of Control Automation & Systems*, vol. 15, no. 4, pp. 1916–1924, 2017.
- [14] M. Geravand, P. Z. Korondi, C. Werner, K. Hauer, and A. Peer, "Human sit-to-stand transfer modeling towards intuitive and biologically-inspired robot assistance," *Autonomous Robots*, vol. 41, no. 3, pp. 575–592, 2017.
- [15] R. Caccavale and A. Finzi, "Flexible task execution and attentional regulations in human-robot interaction," *IEEE Transactions on Cognitive and Developmental Systems*, vol. 9, no. 1, pp. 68–79, 2017.
- [16] B. Fang, Q. Zhang, H. Wang, and X. Yuan, "Personality driven task allocation for emotional robot team," *International Journal of Machine Learning and Cybernetics*, vol. 9, no. 12, pp. 1955–1962, 2017.
- [17] C. Nomine-Criqui, A. Germain, A. Ayav, L. Bresler, and L. Brunaud, "Robot-assisted adrenalectomy: indications and drawbacks," *Updates in Surgery*, vol. 69, no. 2, pp. 127–133, 2017.
- [18] M. N. V. Oosterom, H. Simon, L. Mengus et al., "Revolutionizing (robot-assisted) laparoscopic gamma tracing using a drop-in gamma probe technology," *American Journal of Nuclear Medicine and Molecular Imaging*, vol. 6, no. 1, pp. 1–17, 2016.
- [19] E. Celik, R. Semrau, C. Baues, M. Trommer-Nestler, W. Baus, and S. Marnitz, "Robot-assisted extracranial stereotactic radiotherapy of adrenal metastases in oligometastatic non-small cell lung cancer," *Anticancer Research*, vol. 37, no. 9, pp. 5285–5291, 2017.
- [20] D. Ao, R. Song, and J. W. Gao, "Movement performance of human-robot cooperation control based on EMG-driven Hill-type and proportional models for an ankle power-assist exoskeleton robot," *IEEE Transactions on Neural Systems & Rehabilitation Engineering*, vol. 25, no. 8, pp. 1125–1134, 2017.
- [21] D. H. Lim, W. S. Kim, H. J. Kim, and C. S. Han, "Development of real-time gait phase detection system for a lower extremity exoskeleton robot," *International Journal of Precision Engineering & Manufacturing*, vol. 18, no. 5, pp. 681–687, 2017.
- [22] M. E. Giannaccini, C. Xiang, and A. Atyabi, "Novel design of a soft lightweight pneumatic continuum robot arm with decoupled variable stiffness and positioning," *Soft Robotics*, vol. 5, no. 1, pp. 54–70, 2018.
- [23] H. Mehdi and O. Boubaker, "PSO-Lyapunov motion/force control of robot arms with model uncertainties," *Robotica*, vol. 34, no. 3, pp. 634–651, 2016.
- [24] A. Izadbakhsh and S. Khorashadizadeh, "Robust task-space control of robot manipulators using differential equations for uncertainty estimation," *Robotica*, vol. 35, no. 9, pp. 1923–1938, 2017.
- [25] Y. Shi, Y. Tian, Y. Wang, and T. Huang, "Sequential deep trajectory descriptor for action recognition with three-stream CNN," *IEEE Transactions on Multimedia*, vol. 19, no. 7, pp. 1510–1520, 2017.
- [26] C. S. Fahn, C. Y. Kao, C. B. Yao, and M. L. Wu, "Exploiting AdaRank model and trajectory of hand motion for hand gesture recognition," *Sensor Letters*, vol. 14, no. 10, pp. 1061–1065, 2016.
- [27] L. Zhou, S. Bai, and Y. Li, "Energy optimal trajectories in human arm motion aiming for assistive robots," *Modeling, Identification and Control (MIC)*, vol. 38, no. 1, pp. 11–19, 2017.

## *Retraction*

# **Retracted: Research on the Coupling and Coordinated Development of Sports Tourism and Cultural Industry under the Background of Artificial Intelligence Era**

### **Wireless Communications and Mobile Computing**

Received 26 September 2023; Accepted 26 September 2023; Published 27 September 2023

Copyright © 2023 Wireless Communications and Mobile Computing. This is an open access article distributed under the Creative Commons Attribution License, which permits unrestricted use, distribution, and reproduction in any medium, provided the original work is properly cited.

This article has been retracted by Hindawi following an investigation undertaken by the publisher [1]. This investigation has uncovered evidence of one or more of the following indicators of systematic manipulation of the publication process:

- (1) Discrepancies in scope
- (2) Discrepancies in the description of the research reported
- (3) Discrepancies between the availability of data and the research described
- (4) Inappropriate citations
- (5) Incoherent, meaningless and/or irrelevant content included in the article
- (6) Peer-review manipulation

The presence of these indicators undermines our confidence in the integrity of the article's content and we cannot, therefore, vouch for its reliability. Please note that this notice is intended solely to alert readers that the content of this article is unreliable. We have not investigated whether authors were aware of or involved in the systematic manipulation of the publication process.

Wiley and Hindawi regrets that the usual quality checks did not identify these issues before publication and have since put additional measures in place to safeguard research integrity.

We wish to credit our own Research Integrity and Research Publishing teams and anonymous and named external researchers and research integrity experts for contributing to this investigation.


The corresponding author, as the representative of all authors, has been given the opportunity to register their agreement or disagreement to this retraction. We have kept a record of any response received.

### **References**

- [1] C. Hong, J. Shi, Y. Xing, and Z. Chang, "Research on the Coupling and Coordinated Development of Sports Tourism and Cultural Industry under the Background of Artificial Intelligence Era," *Wireless Communications and Mobile Computing*, vol. 2022, Article ID 3191655, 6 pages, 2022.

## Research Article

# Research on the Coupling and Coordinated Development of Sports Tourism and Cultural Industry under the Background of Artificial Intelligence Era

Chao Hong,<sup>1</sup> Jianmin Shi ,<sup>2</sup> Yan Xing,<sup>2</sup> and Zejun Chang<sup>3</sup>

<sup>1</sup>School of Department of PE, Dankook University, Yongin-si, Republic of Korea

<sup>2</sup>College of Physical Education, Hoseo University, Asan, Republic of Korea

<sup>3</sup>Beijing Union University, Beijing, China

Correspondence should be addressed to Jianmin Shi; [shijianmin@bucea.edu.cn](mailto:shijianmin@bucea.edu.cn)

Received 25 January 2022; Revised 9 February 2022; Accepted 8 March 2022; Published 11 April 2022

Academic Editor: Shalli Rani

Copyright © 2022 Chao Hong et al. This is an open access article distributed under the Creative Commons Attribution License, which permits unrestricted use, distribution, and reproduction in any medium, provided the original work is properly cited.

In the new era of rapid development of intelligent information, sports tourism and cultural industry have become a new goal to improve China's urban competitiveness and realize the development of urban industry. Based on the integration of sports tourism industry and cultural industry, this paper establishes the relevant information data interface mode. This paper constructs the information coupling system model of sports tourism industry and cultural industry under the background of artificial intelligence era and obtains the corresponding data results by using the invisible statistical logic computer independent judgment (IDIJA) method of artificial intelligence system under the condition of incomplete data. The application of the coordinated development system of coupling industry can realize the rapid development of sports tourism and cultural reconstruction mode and achieve the new effect of intelligent sports tourism cultural comprehensive experience. It can not only improve the people's quality of life but also provide feasible suggestions for improving the continuous development of the coupling and coordination of sports tourism and cultural industry.

## 1. Introduction

In recent years, with the rapid development of China's intelligent era, the integration of culture and sports tourism has become a new trend and model of the development of intelligent socioeconomic industry, as well as a new direction and new bright spot of comprehensive industrial economic development. Sports tourism is one of the important parts of sports industry and a special way of tourism in modern people's tourism. The mutual penetration of sports industry and tourism has formed a new economic market, which belongs to the category of economic service industry. The purpose is to obtain social and economic income by providing relevant services for sports tourism activities of sports tourism. Cultural industry is a production activity that takes culture as the core content and is aimed at meeting people's spiritual and cultural needs. Cultural industry is not only the inevitable product of the development of productive forces but also a special cultural form and economic form. It is

one of the emerging industries formed by the gradual improvement of social and economic market and the improvement of production mode. Under the background of artificial intelligence, the integration of sports tourism and cultural industry stems from the improvement of educational and cultural level and the increase of sports tourism demand. It is a comprehensive symbiotic industry with more spiritual and entertainment based on the sports tourism industry with single original function. The new trend of the integration and development of the two industries directly promotes the coupling and coordinated development of tourism industry and cultural industry.

Wang said in his new thinking research in the era of artificial intelligence that big data and artificial intelligence in the era of intelligence have been closely integrated and pushed to the development direction of "intelligence" and "personalization" from different angles. New changes in the era of artificial intelligence actively adapt to the new environment of intelligence and build a new direction of

collaborative growth of intelligence [1]. In the research on the integrated development of urban tourism and sports tourism, Chen believes that based on the internal motivation of the industrial integration and integrated development of tourism and sports tourism, he puts forward the urban integrated development strategy, including integrating the new cultural characteristics formed by resources, giving full play to the “Internet +” mode, and breaking the existing bottleneck of urban economic development, and provide new ideas for the integrated development of sports tourism [2]. Yulan and Keyin pointed out that the online business model of sports tourism should be activated from the aspects of market demand, reform and innovation, industrial integration, and so on; improve the management level of sports tourism; and improve the user experience effect of sports tourism consumers [3]. The integrated development of sports tourism and cultural industry has become the internal driving force for the development of China’s sports industry, and there are many aspects and factors in the actual integration process. In the research on the integrated development of sports tourism and cultural industry, Yao et al. pointed out that the new integrated development model with culture as the soul and sports tourism as the support carrier has become the inevitable trend of building the current economic development. The coupled and coordinated development of sports tourism and cultural industry presents a new situation of steady development year by year, so as to create a new consumption ecological system of “new consumption, new mode, and new business form” and drive a new driving force of social and economic growth [4]. Lei and Xiujuan analyzed the evaluation research on the coupled and coordinated development of sports tourism and cultural industry. It is said that the resource coupled and coordinated development of sports tourism and cultural industry is a practical problem to be solved in the process of academic and industrial economic development. Through the demonstration of the coupled and coordinated development, it is concluded that the degree of coupling and coordination between industries is still in the initial stage of coupling. However, it has a certain level of development and also puts forward targeted suggestions for improving the evaluation of the coupling and coordinated development of sports tourism and cultural industry [5].

Yi anf Yiyang said in the exploration of urban organic renewal path guided by cultural rejuvenation that with the urbanization process entering the stock era, realizing urban high-quality development and building high-quality life have become the main goal of urban organic renewal. Under the guidance of building a park city, the urban construction mode has changed from simple space construction to complex scene construction. Cultural rejuvenation has become an important part of the organic renewal of the old urban area, comprehensively driving the industrial upgrading and vitality improvement of the area [6]. Zhengzhen and Shuhan analyzed the innovation strategy of the deep integration of culture and science and technology in Chengdu. In their research, they believed that the deep integration of culture and science and technology can not only promote new business forms, stimulate new driving forces, and cultivate new engines of economic growth but also

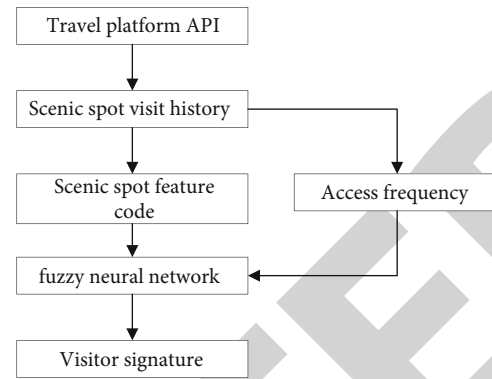


FIGURE 1: Logical architecture of tourist signature extraction algorithm.

help to realize the transformation, upgrading, and innovative development of the cultural industry; promote the deep integration of culture and science and technology; and help the cultural industry achieve high-quality development [7].

## 2. Evaluation System for the Coupling and Coordinated Development of Sports Tourism and Cultural Industry under the Background of Artificial Intelligence Era

*2.1. Logical Structure of Tourist Signature Code.* Under the background of artificial intelligence era, sports tourism has changed from passive guidance mode to tourists’ active experience mode. Various tourism platforms and humanized tourism methods have also become the mainstream development direction, and network tourism information data has gradually become an important information feature source. According to the big data of tourists on the tourism platform and relevant data such as tourists’ relevant signature information, the coupling analysis of artificial intelligence (IDIJA) data results is carried out for tourists. The data analysis results can be used to directly extract relevant tourists’ signature codes from the big data of the platform and judge the information of key customers of the tourism platform. The evaluation results of the intelligent characteristic information data can provide a reference basis for better in-depth positioning and research of sports tourism in practice. Under the background of artificial intelligence, the tourist feature code of sports tourists can eliminate irrelevant or redundant feature information and improve the accuracy of platform tourist information. The logical architecture of tourist feature code extraction algorithm is shown in Figure 1:

In Figure 1, the logical structure of tourist feature code shows that the historical data of tourists visiting the scenic spot can be obtained from the API database of the tourism platform, and the feature code of tourists entering and leaving the scenic spot can be obtained. The data information of tourist feature code can be obtained through fuzzy neural network algorithm. It can also calculate the tourist signature information directly by fuzzy neural network through the historical data and frequency of scenic spots on the tourism platform.

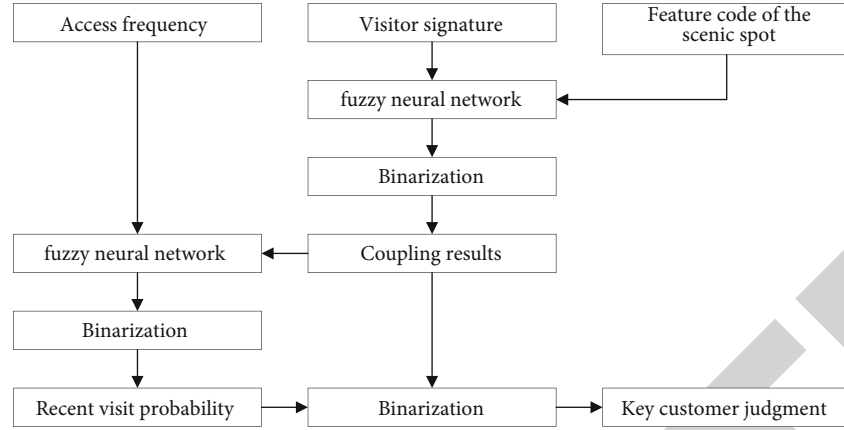


FIGURE 2: Logical architecture of key customer judgment algorithm.

## 2.2. Logic Architecture of Key Customer Judgment Algorithm.

In view of the travel platform system under the background of the intelligent era, the visit frequency and relevant characteristic codes of sports tourists in the scenic spot are analyzed by IDIJA data to judge the key customers of the scenic spot, as shown in Figure 2:

In Figure 2, the logical structure of key customer judgment algorithm shows that according to the feature code of the scenic spot and the feature code information data of tourists, the coupling degree result of information data is obtained after fuzzy neural network calculation and binarization, and the coupling degree result is binarized again to obtain the judgment information result of key customers on the tourism platform. The probability of recent visitors can also be obtained through fuzzy neural network calculation and binarization according to the results of visitors' visit frequency and platform data coupling. The judgment information results of key customers can be obtained by binarization of recent visitors' probability again.

**2.3. Statistical Methods.** Using fuzzy neural network to control the recent change law of time series data, or using the minimum number of nodes to realize fuzzy convolution of data, it is necessary to use the sixth-order polynomial depth iterative regression basis function expression, and the formula of the sixth-order polynomial depth iterative regression fuzzy neural network is as follows:

$$y = \sum_{i=1}^n \sum_{j=0}^5 A_j x_i^j. \quad (1)$$

Among them,  $A_j$  is the coefficient to be regressed of the  $j$ -order polynomial; that is, each node in the formula contains 6 coefficients to be regressed from  $A_0$  to  $A_5$ ;  $j$  is the polynomial order;  $n$  is the number of nodes of the upper neural network.

The binarization formula is shown in

$$y = \sum_{i=1}^n \frac{1}{A + B \cdot e^{x_i}}. \quad (2)$$

Among them,  $e$  is the natural constant. Other mathematical symbols have the same meaning as formula (1).

The statistical significance of the binarization function is to make the projection points of all results fully shift towards both ends in the  $[0,1]$  interval without changing the sequence order, so as to obtain the binarization and fully logical results. The neural network model can judge the convergence degree of neural network training.

## 3. Coupling Characteristics of Sports Tourism and Cultural Industry in the Intelligent Era

The core feature of the coupled development of sports tourism and cultural industry under the background of intelligent era is the mutual penetration, intersection, and reorganization of new industrial chain. The coupled new industry has more economic value and competitive advantage than the original single industry. According to the nature and function of industrial coupling resources, the new industry promotes the coordinated development of the mutual integration of culture and sports tourism and promotes the process of the integration of the new industry.

Figure 3 shows the coupling relationship of new industries. The cultural industry, sports industry, and tourism industries are closely related and traction each other in space, and the industrial elements play a driving role. The higher the mutual resource utilization rate of the coupled new industries, the more market value and economic benefits will be obtained.

## 4. Effect of Coordinated Development after Industrial Coupling

**4.1. Effective Communication Rate of Tourism Platform.** In the research on the coupling and coordinated development of sports tourism and cultural industry in the era of artificial intelligence, relying on the Internet system, intelligent technical means such as artificial intelligence and information big data are used to optimize the allocation and upgrading of resources for the coupled new industry, to open a new mode of deep integration of offline experience, online services, and resource values of various sports tourism industries. In order to analyze the evaluation of coordinated development after

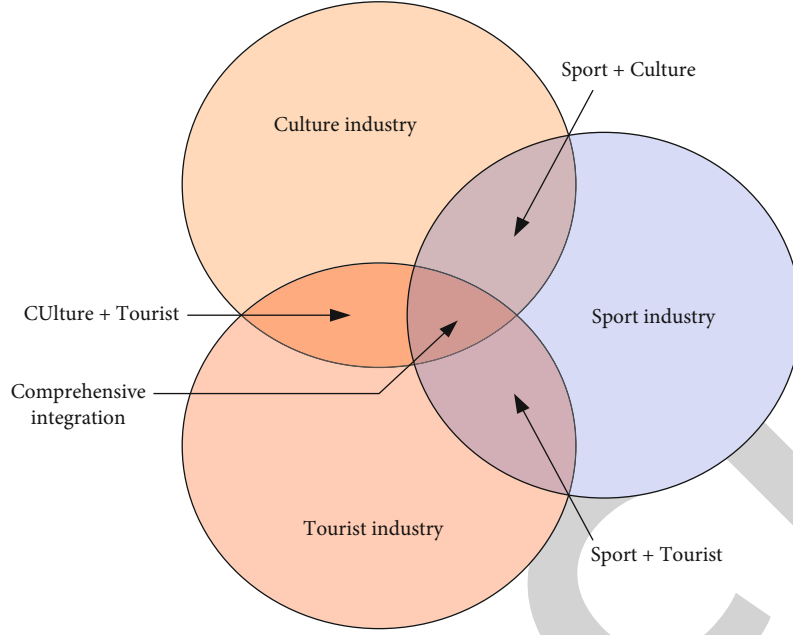


FIGURE 3: Coupling diagram of cultural industry and sports tourism.

industrial coupling, Beijing sports tourism industry and Hainan sports tourism industry are selected to compare the effective communication rate effect of tourism platforms before and after coupling in practical application under the same number of tourism platforms, as shown in Table 1:

In Table 1, it is obvious that there are obvious differences between the selected Beijing sports tourism industry and Hainan sports tourism industry before and after coupling. The effective communication rate of the new industry after coupling on the tourism platform is better than that before coupling, and the  $t$  value  $< 10.000$  and  $P$  value  $< 0.05$ . It is considered that there is statistical significance between the two, and the comparison results are statistically significant.

In the evaluation of the coupling and coordinated development of sports tourism and cultural industry, according to the coupling analysis of artificial intelligence (IDIJA) data results in the evaluation system, it can not only extract different tourist feature codes and key customer information results of the tourism platform from big data to accurately locate the platform tourists and judge the relevant characteristic behaviors, but also in the investigation and evaluation of the effective communication rate and customer satisfaction of the big data tourism platform, It is believed that the coupled new industry can accelerate the effective integration of sports tourism industry and cultural industry, and can effectively promote the coupled development of the industry.

TABLE 1: Comparison before and after cultural tourism industry coupling.

Group	$n$	Before coupling	After coupling
Beijing sports tourism industry	12	$48.5 \pm 4.5$	$67.2 \pm 2.3$
Hainan sports tourism industry	12	$50.3 \pm 4.1$	$63.8 \pm 2.4$
$t$ value		8.579	9.134
$P$ value		0.009	0.008

The method of arithmetic mean and standard deviation rate is adopted, as shown in the following formula:

$$\sigma = \frac{1}{n-1} \sqrt{\sum_{i=1}^n (x_i - \mu)^2}, \quad \mu = \frac{1}{n} \sum_{i=1}^n x_i. \quad (3)$$

Among them,  $\sigma$  is the calculation result of the standard deviation rate of input sequence  $x$ ;  $n$  is the number of elements of the input sequence  $x$ ;  $x_i$  is the  $i$  input value of the input sequence  $x$ ; and  $\mu$  is the arithmetic mean of the input sequence  $x$ .

Results of the bivariate  $t$ -check under SPSS are shown in the following formula:

$$t = \frac{\mu_1 - \mu_2}{\sqrt{\left(\frac{(n_1 - 1)\sigma_1^2 + (n_2 - 1)\sigma_2^2}{n_1 + n_2 - 2}\right) \left(\frac{1}{n_1} + \frac{1}{n_2}\right)}}. \quad (4)$$



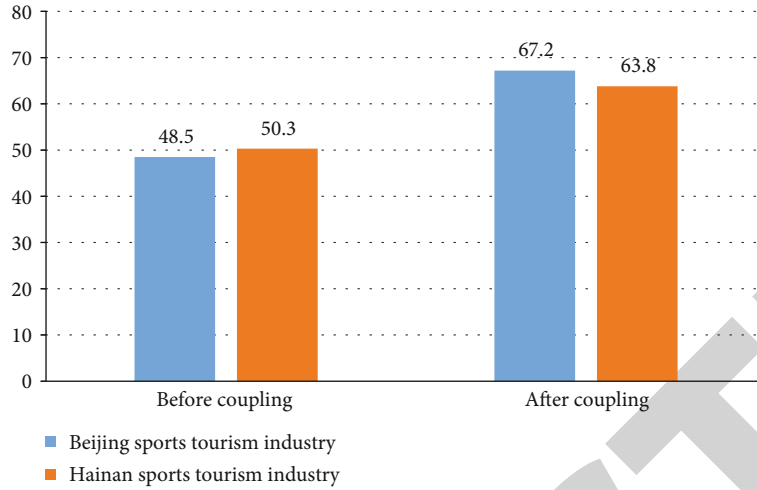


FIGURE 4: Visual comparison before and after cultural tourism industry coupling.

TABLE 2: Customer satisfaction questionnaire of travel platform.

Serial number	Travel platform customer satisfaction survey project	Options	
1	Service level of travel platform	Quite satisfied	Satisfied
2	Service timeliness of travel platform	Satisfied	Satisfied
3	Economy of customer travel expenses	Quite satisfied	Quite satisfied
4	Platform customer travel security	Quite satisfied	Satisfied
5	Consistency of online and offline tourism projects	Quite satisfied	Satisfied
6	Attitude of scenic spot service personnel	Quite satisfied	Quite satisfied
7	Accommodation of travel process problems	Quite satisfied	Quite satisfied
8	Integrity of travel platform project	Quite satisfied	Satisfied
9	Personalized travel service	Quite satisfied	Quite satisfied
10	Satisfaction of travel vehicles	Satisfied	Satisfied
11	Satisfaction of platform customer service handling problems	Quite satisfied	Quite satisfied
12	Return visit content and service attitude	Satisfied	Satisfied
13	Comprehensive satisfaction	Quite satisfied	Quite satisfied

Among them,  $\mu_1\mu_2$  is the arithmetic mean of the two compared series,  $n_1n_2$  is the number of elements of the two compared sequences,  $\sigma_1\sigma_2$  is the standard deviation rate of two compared series (see formula (4) for details); and  $t$  is the bivariate  $t$  verification result.

Visual comparison is made before and after the coupling of the Beijing sports tourism industry and Hainan sports tourism industry, as shown in Figure 4.

In Figure 4, in the visualization of sports tourism industry in Beijing and Hainan, the effect after coupling has an obvious growth trend than that before coupling, which shows that the coupling and coordination of sports tourism and cultural industry under the background of artificial intelligence era are an effective way for the development of industrial economy, improve the market value of sports tourism industry, and further meet the diversified needs of customers.

**4.2. Customer Satisfaction Survey.** In order to better understand the evaluation effect of the coupling and coordinated development of sports tourism and cultural industry under the background of artificial intelligence era, some customers

were selected from the travel platform integrated into the new industry for satisfaction survey, as shown in Table 2.

In Table 2, in the survey of customer satisfaction with the travel platform in the intelligent era, it can be seen that in the process of customers' experience of the coupled new sports tourism industry, the overall satisfaction with the service level, service attitude, problem handling, cost economy, and security of the online travel platform is better. It proves the feasibility of the evaluation of the coupling and coordinated development of sports tourism and cultural industry under the background of artificial intelligence and can improve the satisfaction of tourists.

## 5. Discussion

Due to the rapid development of the national economy, people's consumption level is growing, and diversified and personalized sports tourism projects are also emerging, showing an upward trend. Under the background of this intelligent era, the coupling of cultural industry and sports tourism is also an inevitable trend of industrial economic development.

## Research Article

# Course Certificate Integration Based on Wireless Communication ‘1 + X’ Intelligent Finance and Taxation

Jing Li 

*Shaanxi Institute of International Trade and Commerce, Xi'an, 712406 Shaanxi, China*

Correspondence should be addressed to Jing Li; [jili@csiic.edu.cn](mailto:jili@csiic.edu.cn)

Received 13 January 2022; Revised 2 March 2022; Accepted 12 March 2022; Published 8 April 2022

Academic Editor: Shalli Rani

Copyright © 2022 Jing Li. This is an open access article distributed under the Creative Commons Attribution License, which permits unrestricted use, distribution, and reproduction in any medium, provided the original work is properly cited.

Due to the ever-changing market environment and fierce competition, tax personnel are increasingly pursuing intelligence. Based on the background of smart finance and taxation, this article explains the issues related to the “1 + X” certificate and analyzes the development ideas and reform directions of the teaching plan and certificate integration teaching mode. This paper presents a study on the integration of academic certificates under the background of “1 + X” intelligent finance and taxation wireless communication. From 2018 to 2019, the development trend of smart finance and taxation has been rising. In 2018, the lowest was 11%, and the highest was 25%; in 2019, the lowest was 16%, and the highest was 37%. The lowest growth rate in 2019 was 5%, and the highest was 21%; the results show that although many relevant personnel understand smart finance and taxation, they have not planned how to use smart finance and taxation to improve their professional capabilities. The results show that smart fiscal and taxation is becoming more and more important in social development and has been widely used. However, traditional fiscal and taxation teaching can no longer meet the requirements of today’s society for fiscal and taxation personnel, so related fiscal and taxation teaching should be innovated.

## 1. Introduction

In order to effectively alleviate the structural employment pressure in China, national and local higher education institutions are currently pursuing new education development models, such as the “comprehensive teaching plan and accreditation” education curriculum development model. Under this model, professional students learn professional knowledge, strengthen their theoretical and practical abilities, and obtain professional qualification certificates. The intelligent financial support system is a specific application in the financial field, which integrates the traditional support system and the artificial intelligence expert system.

Wireless communication is a communication method that utilizes the characteristic that electromagnetic wave signals can propagate in free space to exchange information. In the field of information communication in recent years, wireless communication is the fastest growing and most widely used. In recent years, artificial intelligence technology has been introduced in financial fields such as accounting,

taxation, and auditing, and the structure of the financial team will inevitably undergo tremendous changes. Financial artificial intelligence will realize financial automation in the future. Therefore, it is necessary to study the career planning of accountants and improve the training of talents. In the context of the rapid development of artificial intelligence, accountant career planning and training have become more and more important, and the training of new intelligent accountants has become a top priority.

The rapid development of information technology and the development of the world economy have brought tremendous changes to the development environment of the finance and tax industries. The original theories and methods of merging finance, taxation, and certification are difficult to adapt to today’s financial environment that combines architectural features for software-controlled soft error recovery. The design utilizes classic fault-tolerant technologies, such as error detection and instruction restart, implemented at the microarchitecture level, and adds instructions for error recovery. When the instruction is submitted to the architectural state, an error is detected. If an

exception occurs at this time, the software can restore the correct machine state and restart execution. Software recovery allows a comprehensive inspection of the machine to determine the root cause of the error. The newly added instructions also help chip verification of hardware and software recovery mechanisms. The design uses a commercial low-standby power 90-nanometer body process, and the prototype operating frequency is up to 336 MHz. Finally, Farnsworth et al. presented the results of proton irradiation. The processor demonstrated the correct recovery of the program operation from more than 500 detected errors, and the results showed that there were no unrecoverable errors [1]. Hida et al. found that in the era of the Internet of Things, it is necessary to extend the battery life of edge devices to achieve sensory connection to the Internet. The goal of Hida et al. is to reduce the power consumption of microprocessors embedded in such devices by using a novel dynamically reconfigurable accelerator. Traditional microprocessors consume a lot of power in memory access, registers, and control of the processor itself, which reduces energy efficiency. The dynamic reconfigurable accelerator reduces this redundant power by performing parallel calculations on the reconfigurable switch and processing element array. Hida et al. proposed a novel dynamically reconfigurable accelerator, which is composed of a dynamically reconfigurable data path and a static array. Static arrays can process instructions in parallel without registers and improve energy efficiency. The dynamically reconfigurable data path includes registers and many dynamically reconfigured switches to resolve the operand dependency between mapped instructions [2]. Wu and Fan found that providing reliable broadband wireless communications in high-mobility environments such as high-speed railway systems is still one of the main challenges facing the development of next-generation wireless systems. Wu and Fan conducted a systematic review of high-mobility communications. Wu and Fan first summarized a list of key challenges and opportunities in high-mobility communication systems and then comprehensively reviewed the technologies that can meet these challenges and take advantage of unique opportunities. The review covers a wide range of communication operations, including accurate modeling of high-mobility channels, transceiver structures that can take advantage of the characteristics of high-mobility environments, signal processing that can reap the benefits, and mitigate interference and damage in high-mobility systems. There are also mobility management and network architectures designed for high-mobility systems [3]. Dhillon et al. found that with the help of ubiquitous wireless connections, declining communication costs, and the emergence of cloud platforms, the deployment of IoT devices and services is accelerating. Most major mobile network operators regard communication networks that support the Internet of Things as an important source of new revenue. Dhillon et al. discussed the needs of wide-area M2M wireless networks, especially short data communications to support a large number of IoT devices. Dhillon et al. first briefly outline the current and emerging technologies that support wide-area M2M and then use communication theory principles to discuss the basic challenges and potential solutions of

these networks, focusing on the trade-offs and strategies of random access and scheduled access. Finally, Dhillon et al. put forward suggestions on how the future 5G network should be designed to achieve efficient wide-area M2M communication [4]. Bennis et al. have discovered that ultrareliable and low-latency communications for 5G wireless networks and other networks are essential and are currently receiving great attention from academia and industry. At its core, URLLC requires a departure from a network design method based on expected utility. In this method, relying on average numbers is no longer an option, but a necessity. On the contrary, there is lack of a principled and extensible framework that takes into account the delay, reliability, data packet size, network architecture and topology, and decision-making under uncertainty. To achieve this vision, after providing definitions of latency and reliability, Bennis et al. carefully studied the various enablers of URLLC and their inherent trade-offs. Subsequently, Bennis et al. focused his attention on various technologies and methods related to URLLC requirements and their application through selected use cases [5]. Rattso and Stokke studied how different national taxation plans interact with geographic differences in productivity and consumption facilities to determine regional populations and used equilibrium models to analyze the current nominal income tax system. The analysis is based on estimated regional income differences, taking into account observable and unobservable personal characteristics and empirical value. Given the regional differences in income and housing prices, quality of life and productivity are calibrated to simulate equilibrium. In contrast to the undistorted equilibrium of one-time taxation, the nominal income tax prevents it from being placed in productive, high-income areas. The deadweight loss due to regional inefficiency is 0.18% of GDP. Rattso and Stokke researched actual income tax and equal actual tax as an alternative tax system. Both of these options will produce a geographical distribution of the population that is closer to the undistorted equilibrium, so the loss is lower [6]. Bsenberg et al. developed an economic growth model to study the impact of extensive capital taxes (profits, dividends, and capital gains) on the macroeconomic outcomes of small open economies and to identify the steady state and transitional effects of shocks on economic outcomes. The selected framework is suitable for structural estimation, and given the simplicity of the model, it can fit well the data of 79 countries from 1996 to 2011. A counterfactual analysis based on the estimation model shows that capital tax relief has a positive impact on output and capital stock. These effects are economically significant and adjusted within a 5-year time window, after which there is no further economic response. It is found that the economic aggregate has the strongest response to changes in the corporate profit tax rate, while the response to dividends and capital gains tax is relatively weak [7]. Moriconi et al. first study whether product market regulation affects the taxation of commodities in open trading economies, and second, Moriconi et al. study the strategic interaction of regulatory measures between trading partner countries. Moriconi et al. proposed a two-country general equilibrium model, in which a destination-based commodity

tax provides funding for public products, and product market supervision affects the number of companies and product diversity in the market. According to the data of 21 OECD countries from 1990 to 2008, Moriconi et al. provided empirical evidence that product market supervision is a strategic supplementary policy, and domestic supervision has a negative impact on domestic commodity taxation [8]. Through the experiments of scholars, it can be seen that wireless communication is very necessary for the study of certificate integration under the background of “1 + X” intelligent finance and taxation. However, there are still some shortcomings in the experiments of scholar, which leads to low reliability of the experiment. In general, finance and taxation are very important to the country and society, and it is also very important to make good use of the integration of academic certificates in the context of wireless communication and smart finance and taxation.

The innovations of this article are as follows: (1) Introduced the relevant theoretical knowledge of intelligent finance and taxation and used the data mining method based on wireless communication to investigate and analyze how to develop the integration of academic certificates under the background of “1 + X” intelligent finance and taxation. (2) Based on the data mining method and the fusion algorithm, carry out the experiment and analysis of the fusion of academic certificates under the background of “1 + X” intelligent finance and taxation. Through investigation and analysis, wireless communications can improve the professional ability of taxation personnel in the context of “1 + X” intelligent taxation.

## 2. Data Mining Method Based on Wireless Communication

*2.1. The Concept of Wireless Communication and Data Mining.* In recent years, China has made certain progress in the development and application of intelligent financial systems. UIDA and Kingdee have developed Haibolong, Brio, and other business intelligence software [9]. Data mining refers to the process of searching for information hidden in a large amount of data through algorithms. Data mining is usually related to computer science and achieves the above goals through many methods such as statistics, online analytical processing, intelligence retrieval, machine learning, expert systems, and pattern recognition. However, current smart financial software is limited to the use of charts and tables to describe current data. The data mining structure diagram is shown in Figure 1:

As shown in Figure 1, to find the required information from the data, the first step is to collect data and use various visualization libraries to observe the content of the data, that is, data visualization, and the last step of data preprocessing. It is possible to perform mining with a small amount of data. In fact, most data mining algorithms can be executed with a small amount of data to obtain results [10]. However, too little data can also be analyzed manually, and too little data often fails to reflect the general characteristics of the real world.

Communication technology is a technology for popularizing information. Modern society has been very dependent on communication technology. In the past few decades, communication technology has made amazing progress, and the design and manufacturing technology of wireless communication integrated circuits have achieved leapfrog development [11]. Modern communication technology has changed people’s way of life in all aspects. People are increasingly relying on wireless communication technology and supporting the application of these technologies.

Wireless communication refers to the long-distance transmission and communication between multiple nodes without spreading through conductors or cables. Wireless communication can be carried out wirelessly. The wireless communication method is implemented through a wireless communication system. First, the various information to be transmitted is converted into electrical signals by sending terminal equipment, which is called baseband signal, as shown in Figure 2:

As shown in Figure 2, wireless communication includes a variety of fixed, mobile and portable applications such as two-way radios, mobile phones, mobile information terminals, and wireless networks. Modern society has higher and higher requirements for real-time information, and the role of communication technology in society is becoming more and more important. With the rapid development of communication methods, people have higher and higher requirements for the reliability of communication [12].

The analysis of basic data is carried out in the management layer, and then the analysis results are sent to the decision-making layer, and then, the decision-making plan is sent to the management layer. After the management layer has a specific understanding, it is decomposed into various business requirements and delegated to the accounting layer for execution, as shown in Figure 3:

As shown in Figure 3, the functions to be realized by smart fiscal and taxation should be based on the abovementioned traditional functions, through the application of data mining technology, analysis, and mining of multilevel and multiangle information, including current, historical, fuzzy, clear, external, and internal, using mathematical methods such as neural networks, fuzzy mathematics, and mathematical statistics, analyzing the collected effective data, establishing a model, and realizing the auxiliary role of dynamic and intelligent decision-making [13].

### *2.2. The Main Decision Tree Algorithm Based on Data Mining*

#### (1) ID3 algorithm

To find the most suitable method for the sample, the function of the most balanced division must be realized, so it is necessary to realize the acquisition of information. The core of the ID3 algorithm is “information entropy.” The ID3 algorithm calculates the information gain of each attribute and regards high information gain as a high-quality attribute. Each time the attribute is segmented, the attribute with high information gain is selected as the segmentation

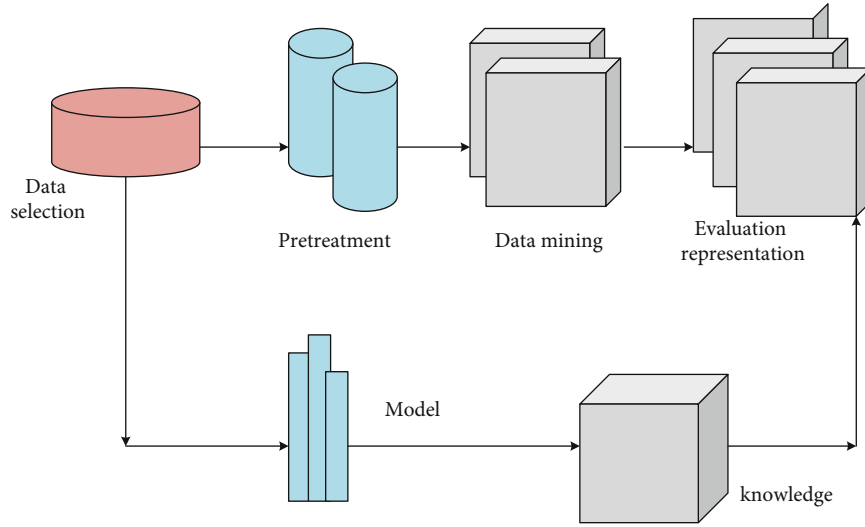


FIGURE 1: Mining process diagram.

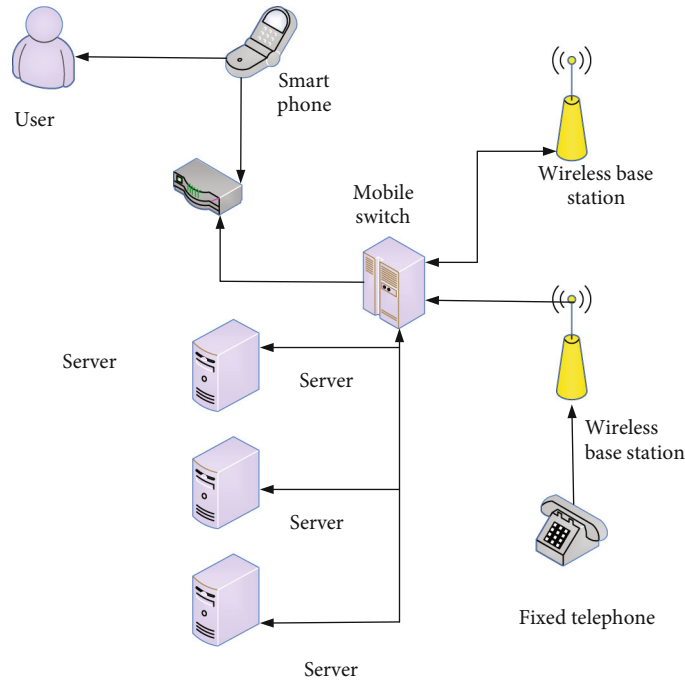


FIGURE 2: Wireless communication structure diagram.

criterion, and the process is repeated [14]. The derivation of its formula is as

$$I(a_1, a_2, \dots, a_M) = - \sum_{i=1}^m p_i \log_2 p_i \quad (1)$$

The ID3 algorithm uses information gain as an evaluation criterion when selecting the branch attributes of the root node and each internal node, so as to obtain the shortcomings of the information and select attributes with more numerical values. In some cases, this attribute may not provide too valuable information [15].

For a given subset  $a_j$ , its information expectation is

$$E(A) = - \sum_{i=1}^m P_{ij} \log_2 (P_{ij}). \quad (2)$$

Among them,  $\log_2(P_{ij})$  is the probability of  $E$  in sample  $a_j$ .

After determining the root node, the same method is used as above to calculate recursively. Before the end condition is met, the decision will finally be generated, as shown in Figure 4.

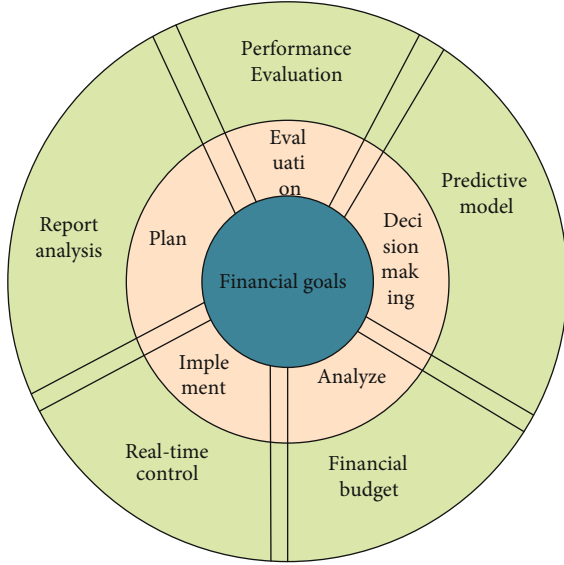


FIGURE 3: Financial support system diagram.

As shown in Figure 4, decision trees usually include decision points, key points, plan branches, and probability branches. Drawing multiple branches from the decision point, each branch represents an alternative, that is, a planned branch. Points are connected behind the branch of the plan, and various straight lines are drawn from the points to indicate different things [16].

## (2) Improvement of ID3 algorithm

Dividing  $A$  into class  $V$ , record  $\{A_1, A_2, \dots, A_V\}$  as the total number of instances, and the number of instances of class  $i$  is  $A_i$ , then the probability that an instance belongs to the  $i$ th class is  $P(A_i)$ , and

$$P(A_i) = \frac{|A_i|}{|A|}. \quad (3)$$

From the formula for calculating information entropy, then, the degree of decision tree to  $S$  is

$$H(A) = - \sum_{i=1}^V p(A_i) \log_2 p(A_i). \quad (4)$$

Supposing the attribute is  $A$ , its value is  $\{A_1, A_2, \dots, A_V\}$ , the number of instances of  $A_i$  belonging to the  $i$ th category is  $A_{ij}$ , and the probability of  $A_{ij}$  belonging to the category  $i$  is  $P(A_i/w = a_j)$ ; then, its calculation formula is

$$P\left(\frac{A_i}{w = a_j}\right) = \frac{|A_{ij}|}{|A_j|}. \quad (5)$$

Among them,  $A_{ij}$  represents the number of instances of the molecule set, and the resulting instance is represented

by  $P(A_i/w = a_j)$  [17]. The conditional entropy of the training set for attribute  $A$  is

$$H(B_j) = - \sum_{i=1}^V P\left(\frac{A_i}{B}\right) \log_2 P\left(\frac{A_i}{B}\right). \quad (6)$$

Then, the information entropy of node  $A$  is as

$$\text{Gain}(a, b) = h(b) - h\left(\frac{b}{a}\right). \quad (7)$$

Decision tree technology is a basic technology in the field of artificial intelligence, which can achieve better judgments for some relatively small and relatively simple models [18]. In the case of decision trees, there are often situations that are simple or do not require data preparation. In other technologies, the data must first be generalized, such as removing redundant attributes and blank attributes [19].

$Q$  is the label of a certain category,  $S_1$  is the probability that the sample belongs to  $S_n$ ,  $S_1$  is the number of samples on the category  $S_n$ , and the entropy that is divided into subsets according to the attribute  $Q$  is as

$$E(Q) = \sum \frac{S_1 + S_2 + \dots + S_n}{s} * I. \quad (8)$$

$B$  is an attribute, with  $A$  different values, and the information gain is shown in

$$\text{Gain}(A) = I(B_1, B_2, \dots, B_n) \quad (9)$$

## 2.3. Single-Antenna and Multiantenna Models Based on Wireless Communication

### (1) Single antenna model

In network management, multiuser downlink beamforming technology based on service quality constraints has been very popular in recent years, because this technology is very attractive for network management [20]. However, when there are a large number of users sharing the wireless channel, or when the service quality constraints are too strict, this problem will become infeasible and unsolvable. At this time, it is necessary to use access control. The single antenna model is shown in Figure 5.

As shown in Figure 5, the introduction of single-antenna model access control is a cross-layer method. That is, the joint optimization of multiuser downlink beamforming and access control ensures that as many users as possible can be served under the premise of satisfying service quality constraints. However, this core problem is often difficult to solve [21], and it can be compensated by convex approximation.

Now, the joint optimization problem of user access control and power control is modeled as a two-step optimization problem. The first-step optimization problem is

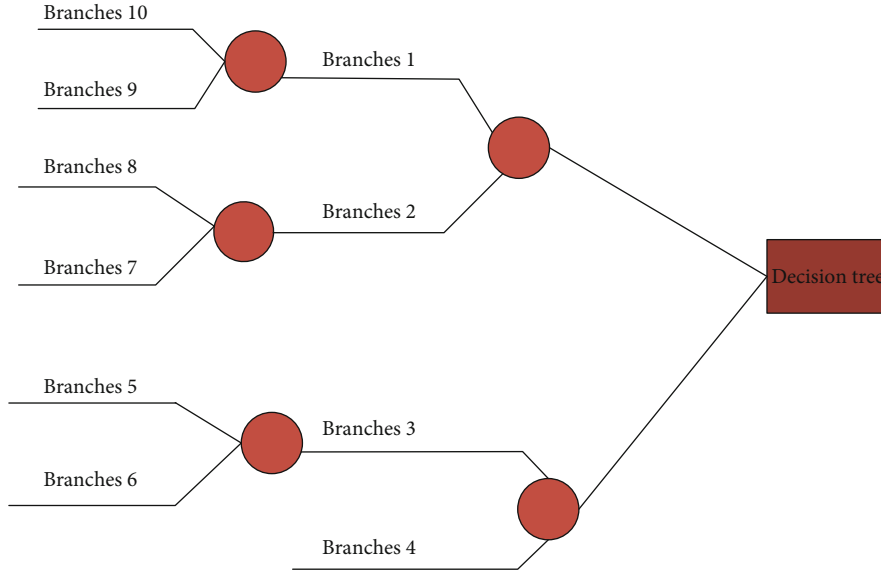


FIGURE 4: Decision tree structure diagram.

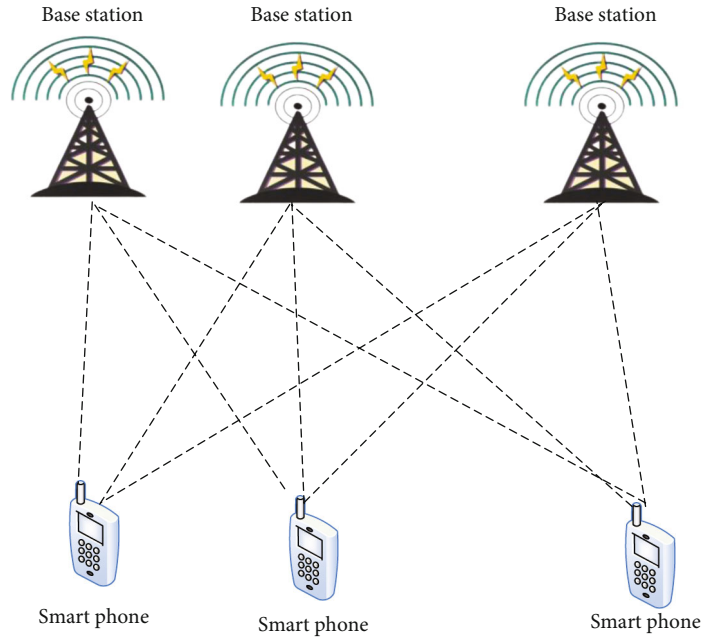


FIGURE 5: Example of a single-antenna model scheme.

expressed as follows. Among them,  $\mathcal{G}_{mm}$  indicates the set of accessible users, and  $p_{mm}$  indicates the cardinality of the set, as shown in

$$\text{SINR}_M = \frac{\mathcal{G}_{mm} p_{mm}}{\sigma_m^2}. \quad (10)$$

Using  $\gamma_m$  to represent the maximum allowed access set, and this set may not be unique. The second step is to minimize the total transmission energy in this set, as in

$$\text{SINR}_m > \gamma_m. \quad (11)$$

After a certain formula deformation, it can be proved that formula (10) and formula (11) can be integrated and equivalent to

$$\min \|y\|_0 + \alpha(p^{\max})^2 q = 0. \quad (12)$$

As a single-antenna model, formula (12) is very easy to solve. However, in the multiantenna model, the structure of the problem is not such a simple power control problem, so it cannot be converted into a simple single-antenna model [22].

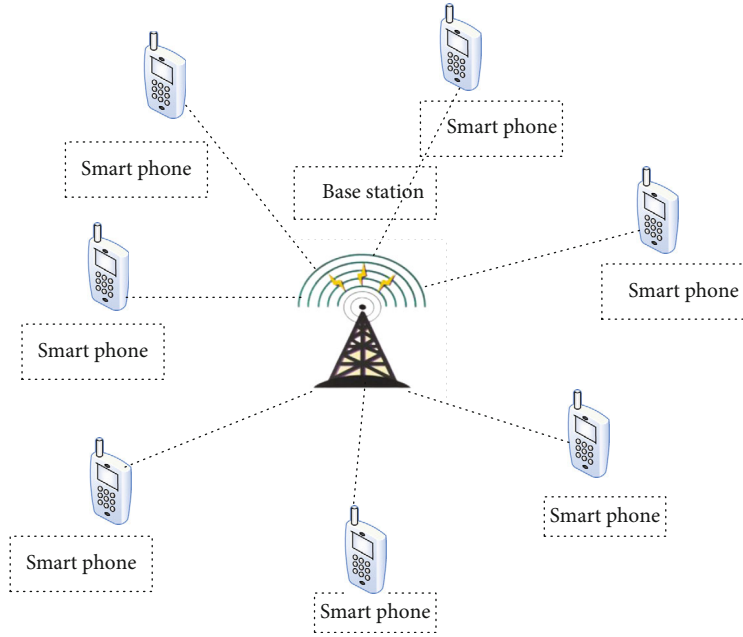


FIGURE 6: Example of a multiantenna model solution.

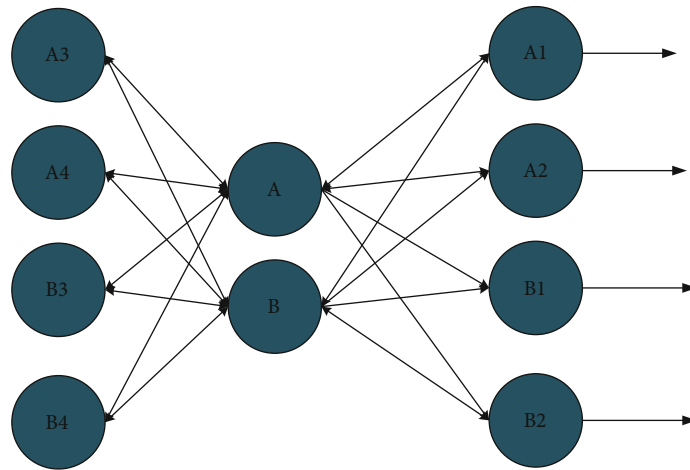


FIGURE 7: RBF neural network structure.

(2) Multiantenna model

This article will briefly introduce a user access control scheme in a multiantenna model. However, in the case of multiple antennas, compared to the single-antenna model, beamforming technology is additionally required to deal with, and the two research directions proposed in this paper are also realized by beamforming technology. Therefore, it is also necessary to give a brief introduction to beamforming technology [23], as shown in Figure 6.

As shown in Figure 6, consider a single-cell wireless communication network composed of a base station equipped with  $K$  antennas and  $M$  single-antenna users. Here, cooperative processing is implemented between base

stations, that is, each base station may serve any user [24–26]. Therefore, the transmit beamforming matrix is

$$Q = [Q_1, \dots, Q_M] = \text{SINR}_m. \tag{13}$$

The beamforming matrix  $U$  and auxiliary binary variables are

$$V_m = \min \sum_{m=1}^m \|U\|^2 + (S_M + 1)^2. \tag{14}$$



TABLE 1: A survey on the level of understanding of smart finance and taxation among 200 finance and economics students.

Learn degree	Quantity	Percentage	Effective percentage	Cumulative percentage
Learn	134	72.5%	72.5%	145%
Do not understand	66	27.5%	27.5%	55%
Total	200	100%	100%	200%

TABLE 2: 200 finance and economics students answered the crisis awareness survey form.

Crisis awareness	Quantity	Percentage	Effective percentage	Cumulative percentage
Yes	101	51.3%	51.3%	102.6%
No	99	48.7%	48.7%	97.4%
Total	200	100%	100%	200%

In particular,  $U$  and  $S$  will have restrictions, as

$$\delta \leq \min \frac{4\gamma^{-1}}{p \max \|h_n\|^2 + \sigma^2}. \quad (15)$$

**2.4. Quantum Genetic Algorithm Based on Deep Learning.** As a branch of machine learning, deep learning also uses learning algorithms to allow the computer itself to learn from a large amount of known data or extract the hidden laws and features. It is used to intelligently identify new unknown data or make reliable predictions about the possibility of unknown events [27, 28]. The radial basis function optimized by the quantum genetic algorithm is a neural network detection algorithm. The basic principle is to use the global optimization function of the quantum genetic algorithm to perform a rough search and then use the neural network to perform detailed detection, so as to overcome the problem of the network easily falling into the local optimum and achieve the purpose of ensuring the detection performance of the RBF network [29–31]. It can be seen that the algorithm consists of two main parts:

- (1) Radial basis function neural network (RBF neural network)

In the field of mathematical modeling, radial basis function network is an artificial neural network that uses radial basis function as activation function. The output of a radial basis function network is a linear combination of the input radial basis function and neuron parameters. Radial basis function networks have a variety of uses. The RBF neural network is a traditional 3-layer neural network, and its structure is shown in Figure 7:

As shown in Figure 7, radial basis function refers to a type of function whose value is only the distance from the origin. Any function that satisfies the above characteristics

is called radial basis function. The most commonly used radial basis function is

$$\psi_k = \exp\left(-\frac{\|x - c_h\|^2}{\sigma_h^2}\right), \quad (16)$$

where  $h = 1, 2, \dots, n$ ,  $h$  is the  $i$ -dimensional input vector,  $c_h$  is the center of the  $h$ th radial basis function,  $\sigma_h^2$  is the width of the radial basis function of the  $h$ th hidden layer neuron, and  $\|x - c_h\|$  is the Euclidean norm of the vector  $x - c_h$ . Then, the output form of the  $n$ th node of the network is as shown in

$$x_n = b_n + \sum_{h=1}^n w_{nh} \cdot \exp(\sigma^2 h). \quad (17)$$

The training process of the RBF network is divided into two parts. First, the center and width of the radial basis function of the hidden layer are obtained through the learning method. Then, the label information is used to perform the connection weight of the output layer. The trained RBF network can implement tasks such as approximation and classification based on the label data.

- (2) Quantum genetic algorithm (QGA)

The QGA algorithm is based on the genetic algorithm and uses the quantum computing theory to improve the coding and update of the algorithm, so that the traditional genetic algorithm has a stronger global search ability. Compared with traditional genetic algorithm, QGA uses a new way of individual coding, called the Q gene. The Q gene is derived from the concept of qubits in quantum computing. Q bit is the smallest unit of information storage in two-state quantum computing, as shown in

$$\psi = \alpha^2 y + \beta x^2. \quad (18)$$

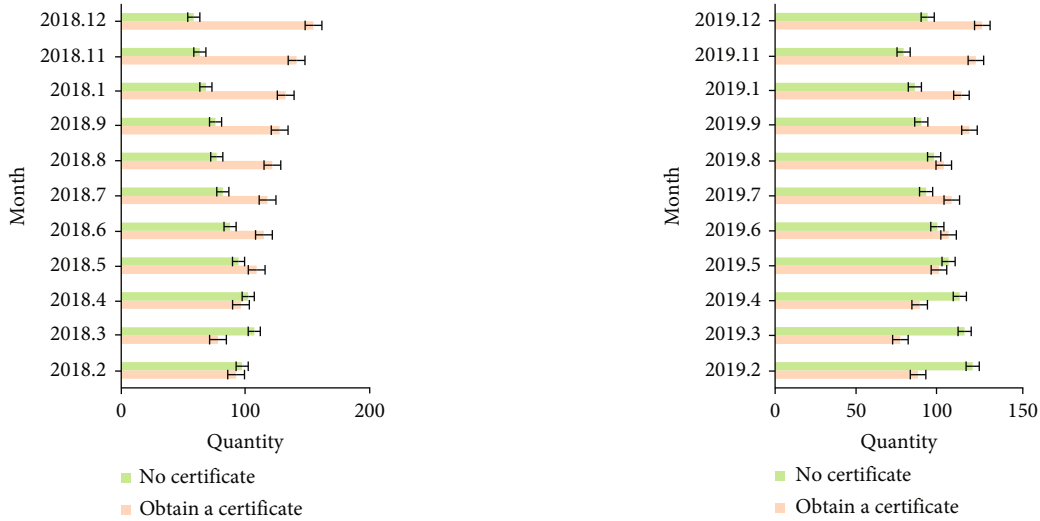
In the algorithm, assuming that the population size is  $\alpha$ , and each individual is composed of  $k$  Q genes, the population inherited to any  $t$ th band can be expressed as

$$q_J^T = \begin{bmatrix} \alpha_1^t, \alpha_2^t, \dots, \alpha_n^t \\ \beta_1^t, \beta_2^t, \dots, \beta_n^t \end{bmatrix}. \quad (19)$$

During the operation of the algorithm, operations such as crossover mutation are used to perform genetic updates, and quantum gates are used to control the update direction of  $\alpha$ , so that the individual state is close to the optimal

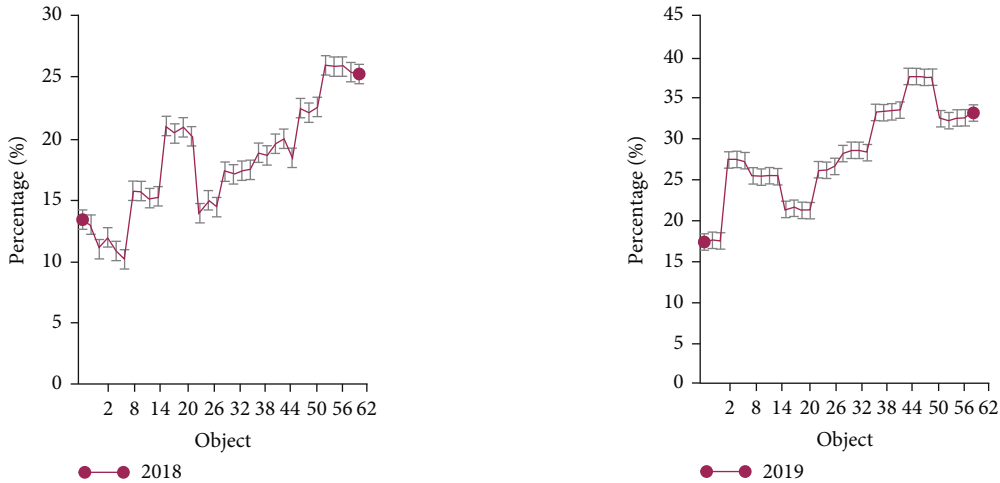
TABLE 3: Questionnaire on whether there are career planning for finance and taxation positions for 200 finance and economics students.

Career planning	Quantity	Percentage	Effective percentage	Cumulative percentage
Already planned	57	33.3%	33.3%	66.6%
Planning	38	20.5%	20.5%	41%
Do not want to plan	105	46.2%	46.2%	92.4%
Total	200	100%	100%	200%



(a) In 2018, whether financial students obtained the certificate of “1 + X” (b) In 2019, whether financial students obtained the certificate of “1 + X”

FIGURE 8: Comparison of whether financial students obtained certificates in 2018 and 2019.



(a) Trends in the development of smart finance and taxation in 2018 (b) Trends in the development of smart finance and taxation in 2019

FIGURE 9: Comparison of trends in the development of smart fiscal and taxation in 2018 and 2019.

solution. There are many methods, among which the most commonly used is the quantum revolving gate, which is

$$W(\theta) = \begin{bmatrix} \cos \theta, & -\sin \theta \\ \sin \theta, & -\cos \theta \end{bmatrix}. \quad (20)$$

In addition to these commonly used detection algorithms, there are still many improved algorithms with better performance. Most of the detection algorithms can only highlight one aspect of the detection performance and complexity, but it is difficult for both to be excellent at the same time. The following article will introduce detection

TABLE 4: Questionnaire on certificates obtained by 100 employment finance and taxation personnel.

Certificate type	Quantity	Percentage	Effective percentage
Nothing at all	45	48%	48%
Senior finance	26	27%	27%
Intermediate finance	12	10.5%	10.5%
Junior finance	11	10%	10%
CPA	6	5.5%	5.5%

algorithms that are constructed using deep neural network methods and have good performance and low complexity.

### 3. Experiments Based on the Questionnaire Survey Based on Fiscal Intelligence

It is difficult for traditional fiscal and taxation systems to extract necessary knowledge from it, so it is very difficult for fiscal and taxation personnel to learn new knowledge, so they have to process a large amount of data to obtain the required knowledge. For taxation personnel, due to the lack of necessary skills and tools, a lot of time and energy are often wasted. Intelligent fiscal and taxation is an effective method to solve this problem. It can effectively process a large amount of data and information and obtain relevant knowledge from it.

This article mainly uses questionnaire survey methods to study the theories of related career planning and analyzes the status quo, problems, and countermeasures of accountant career development. The rapid development of smart finance and taxation has brought huge challenges to the employment of accounting practitioners. Accountants should adapt to the pace of economic development, cultivate and use their unique management skills and knowledge flexibly, respond to the rapid development of artificial intelligence, and continuously improve themselves.

This article conducted a survey on the understanding of smart finance and taxation of 200 finance and economics students, as shown in Table 1.

Through the analysis of Table 1, it can be seen that there are 134 students who understand smart finance and taxation, accounting for 72.5%; it can be seen that most people still understand smart finance and taxation. According to the analysis of Table 1, there are 134 students who understand smart finance and taxation, accounting for 72.5%; 66 students who do not understand intelligent finance and taxation, accounting for 27.5%. The proportion is 43.5% higher; it can be seen that most people still understand smart finance and taxation.

This article investigates whether 200 finance and economics students have crisis awareness, as shown in Table 2.

Through the analysis of Table 2, it can be seen that there are 101 financial and economic students with job crisis awareness, accounting for 51.3%, and 99 students without job crisis awareness, accounting for 48.7%; it can be seen that most of the students still have a sense of job crisis.

This article conducted a survey on whether 200 finance and economics students have career plans for finance and taxation positions, as shown in Table 3.

Through the analysis of Table 3, it can be seen that there are 57 financial students who have planned their job and career plans; 38 are planning their job and career plans; 105 of them do not know how to plan their job and career plans.

Therefore, after analysis, it can be known that although most accounting personnel understand and have realized the impact of artificial intelligence on accounting positions. But there are still a large number of people who are aware of the impact, but do not know how to plan their careers. It shows that the awareness of career planning needs to be strengthened.

This article conducts a survey and comparison of whether financial students obtained certificates in 2018 and 2019, as shown in Figure 8.

As shown in Figure 8, the number of people who obtained the certificate in 2018 increased from 100 in January to 156 in December, and the number of people who obtained the certificate in 2019 increased from 106 in January to 147 in December. It can be seen that the number of people getting the certificate has been increasing. The basic accounting business of finance is mostly replaced by financial artificial intelligence robots, but the number of financial posts in the market has not changed much. This stage will have a serious impact on the work of accountants. The person in charge of accounting who is engaged in basic accounting work faces the risk of being replaced by artificial intelligence robots. With the emergence and gradual popularization of artificial intelligence technology, accounting personnel engaged in basic accounting, document classification, book binding, report processing, tax declaration, and tax adjustment are gradually replaced by artificial intelligence robots. At this time, the relevant personnel should strengthen their own abilities. Students majoring in finance and economics can work hard to obtain the "1 + X" certificate.

At present, the professional skills of accountants cannot meet the needs of financial management in the era of artificial intelligence. There are too many accountants in China, the education level is different, the financial management expertise is also different, and the overall personal qualities are also different. Some accountants have the qualifications of certified accountants, certified tax or internationally recognized accountants, and some accountants have intermediate and senior professional positions. Some accountants only have an accounting qualification certificate, and some corporate accountants have even been engaged in accounting for many years but have not yet obtained an accounting qualification certificate. This article investigates the development trend of smart finance and taxation in 2018 and 2019, as shown in Figure 9.

As shown in Figure 9, smart finance and taxation has developed rapidly. Among them, the "Smart Finance and Taxation" vocational skill certificate was formally established. This is mainly for accounting, financial management, and other majors in universities. The expert's reference

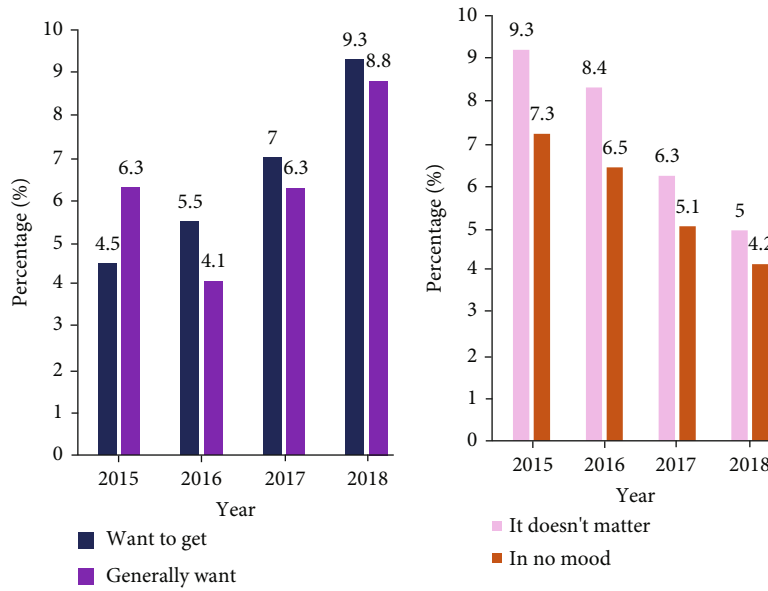


FIGURE 10: The degree of willingness of 200 finance and accounting students from 2015 to 2018 whether they want to obtain a “1 + X” certificate.

standards include three-level smart financing and tax professional skills, elementary, intermediate, and advanced levels. The level of professional competence requirements is different, and more detailed and higher-level requirements will be put forward for the recruitment of accounting talents in the future. From the current point of view, the accounting major of colleges and universities needs to actively introduce the “1 + X” certificate of smart finance and taxation to realize the comprehensive combination and positioning of the training target plan for accounting experts. This article conducted a survey on the certificates obtained by 100 taxpayers who have been employed, as shown in Table 4.

As shown in Table 4, the types of certificates obtained by 100 employed fiscal and taxation personnel include no certificate, primary qualification certificate, intermediate qualification certificate, advanced qualification certificate, and CPA. Among them, there are 45 people who have not obtained the qualification certificate, and the number of people who have obtained the primary qualification certificate is 26, the number of CPA is the least, only 6 people. It can be seen that there are not many people who have obtained certificates, and the ability of accounting personnel needs to be strengthened.

This article conducted a survey on the willingness of 200 accounting students from 2015 to 2018 to obtain a “1 + X” certificate, as shown in Figure 10:

As shown in Figure 10, the degree of willingness of accounting students to obtain the “1 + X” certificate is that they want to obtain it, generally want to obtain it, it does not matter to obtain it, and does not want to obtain it. It can be seen from Figure 10 that in 2015, the proportion of students who want to obtain the “1 + X” certificate is 4.5%, and the proportion of students who generally want to obtain the “1 + X” certificate is 6.3%. The proportion of students

who do not want to obtain the “1 + X” certificate is 7.3%, and the proportion of students who do not care to obtain the “1 + X” certificate is 9.3%. In 2016, the proportion of students who want to obtain the “1 + X” certificate is 5.5%, and the proportion of students who generally want to obtain the “1 + X” certificate is 4.1%. The proportion of students who do not want to obtain the “1 + X” certificate is 6.5%, and the proportion of students who do not care to obtain the “1 + X” certificate is 8.4%. It can be seen that the number of students who want to obtain a certificate is increasing year by year, and the proportion of students who do not want to obtain a certificate decreases with the increase of years. Therefore, more and more students agree with the certificate.

In order to obtain the “1 + X” smart finance and tax certificate, more schools have established the “certificate merger” curriculum reform model, which has realized the combination of accounting professional courses and smart finance and tax “1 + X” certificates. At the same time, especially with regard to students’ majors, it is necessary to clarify the evaluation content of the certificate and conduct more skill training. Therefore, in the context of the “1 + X” smart finance and tax certificate, it is very necessary to promote the development of the curriculum reform model of “consolidation of courses and certificates.”

#### 4. Discussion

This article analyzes how to study the integration of academic certificates under the background of “1 + X” intelligent finance and taxation wireless communication. The concepts related to microprocessor wireless communication and intelligent finance and taxation are expounded, the related theories wireless communication are studied, and

the method of research on the integration of academic certificates under the background of “1 + X” intelligent finance and taxation is explored. And through the questionnaire survey method case, the importance of smart finance and taxation to contemporary society was discussed, and finally, the integration of data mining into smart finance and taxation as an example to explore the relationship between the two was taken.

This article also makes reasonable use of data mining algorithms. With the increasing range of data mining algorithms and their importance gradually becoming more and more prominent, many scholars have begun to match the theory of data mining algorithms with real-life application scenarios and put forward feasible algorithms. Data mining algorithm is a kind of mathematical operation. According to the calculation, wireless communication is essential for the study of certificate fusion under the background of “1 + X” intelligent finance and taxation.

Through the questionnaire survey method, this article knows that the research on the integration of academic certificates under the background of smart finance and taxation can promote the contemporary social economy. Therefore, combining the characteristics of the era of intelligent fiscal and taxation background and finding a new integrated curriculum that enables people to improve their professional capabilities is an important factor in promoting the development of the fiscal and taxation industry.

## 5. Conclusions

This article mainly focuses on the related concepts of smart finance and taxation, wireless communication. The beginning part introduces the necessity of smart finance and taxation. In the context of artificial intelligence, accountants are faced with huge challenges, and the number of jobs has been drastically reduced. Companies are increasingly demanding the ability of accounting personnel, and the types of accounting personnel required by companies are also changing. Therefore, the application of smart fiscal and taxation is essential. Then, the method part is based on the data mining method and neural network model of wireless communication. The application of data mining method and neural network model in smart finance and taxation is studied, and it is found that data mining method can play an active role in the study of certificate fusion under the background of “1 + X” smart finance and taxation. The last part of the experiment conducted a related survey of finance and taxation students and personnel and found that there are still relatively few people with certificates, and the abilities of relevant personnel cannot keep up with the requirements of modern enterprises for financial personnel. Therefore, it can be concluded that if want to continue to develop in the financial position, it must improve business capabilities and obtain corresponding certificates.

## Data Availability

Data sharing is not applicable to this article as no new data were created or analyzed in this study.

## Conflicts of Interest

The author states that this article has no conflict of interest.

## Acknowledgments

This paper was supported by the research on the integration mode of Shaanxi Universities' courses and certificates under the background of “1 + X” intelligent Finance and Tax certificates in the 2020 general topic of Shaanxi Education Science “13th Five-Year Plan”, project number: SGH20Y1523.

## References

- [1] C. Farnsworth, L. T. Clark, A. R. Gogulamudi, V. Vashishtha, and A. Gujja, “A soft-error mitigated micro-processor with software controlled error reporting and recovery,” *IEEE Transactions on Nuclear Science*, vol. 63, no. 4, pp. 2241–2249, 2016.
- [2] I. Hida, S. Takamaeda-Yamazaki, M. Ikebe, M. Motomura, and T. Asai, “A high performance and energy efficient micro-processor with a novel restricted dynamically reconfigurable accelerator,” *Circuits & Systems*, vol. 8, no. 5, pp. 134–147, 2017.
- [3] J. Wu and P. Fan, “A survey on high mobility wireless communications: challenges,” *Opportunities and Solutions. IEEE Access*, vol. 4, no. 1, pp. 450–476, 2017.
- [4] H. S. Dhillon, H. Huang, and H. Viswanathan, “Wide-area wireless communication challenges for the internet of things,” *IEEE Communications Magazine*, vol. 55, no. 2, pp. 168–174, 2017.
- [5] M. Bennis, M. Debbah, and H. V. Poor, “Ultrareliable and low-latency wireless communication: tail, risk, and scale,” *Proceedings of the IEEE*, vol. 106, no. 10, pp. 1834–1853, 2018.
- [6] J. Rattso and H. E. Stokke, “National income taxation and the geographic distribution of population,” *International Tax and Public Finance*, vol. 24, no. 5, pp. 879–902, 2017.
- [7] S. Bsenberg, P. Egger, and B. Zoller-Rydzek, “Capital taxation, investment, growth, and welfare,” *International Tax and Public Finance*, vol. 25, no. 2, pp. 325–376, 2018.
- [8] S. Moriconi, P. M. Picard, and S. Zanaj, “Commodity taxation and regulatory competition,” *International Tax and Public Finance*, vol. 26, no. 4, pp. 919–965, 2019.
- [9] X. Chen, N. Wei, W. Xin, and Y. Sun, “Optimal quality-of-service scheduling for energy-harvesting powered wireless communications,” *IEEE Transactions on Wireless Communications*, vol. 15, no. 5, pp. 3269–3280, 2016.
- [10] A. S. Hamza, J. S. Deogun, and D. R. Alexander, “Wireless communication in data centers: a survey,” *IEEE Communications Surveys & Tutorials*, vol. 18, no. 3, pp. 1572–1595, 2016.
- [11] J. M. Romero-Jerez and F. J. Lopez-Martinez, “A new framework for the performance analysis of wireless communications under Hoyt (Nakagami-q) fading,” *IEEE Transactions on Information Theory*, vol. 63, no. 3, pp. 1693–1702, 2017.
- [12] A. Ghazal, Y. Yi, C. X. Wang et al., “A non-stationary IMT-advanced MIMO channel model for high-mobility wireless communication systems,” *IEEE Transactions on Wireless Communications*, vol. 16, no. 4, pp. 2057–2068, 2017.

- [13] S. H. Won, S. S. Jeong, S. Y. Cho, and H. N. Lim, "Method and apparatus for managing congestion in wireless communication system," U.S. Patent No. 9,961,586, 2018.
- [14] Y. Zhang, Y. Shen, W. Hua, J. Yong, and X. Jiang, "On secure wireless communications for IoT under eavesdropper collusion," *IEEE Transactions on Automation Science and Engineering*, vol. 13, no. 3, pp. 1281–1293, 2016.
- [15] N. N. Alotaibi and K. A. Hamdi, "Switched phased-array transmission architecture for secure millimeter-wave wireless communication," *IEEE Transactions on Communications*, vol. 64, no. 3, pp. 1303–1312, 2016.
- [16] H. Wei, H. J. Zhi, Y. Chao et al., "Multibeam antenna technologies for 5G wireless communications," *IEEE Transactions on Antennas & Propagation*, vol. 65, no. 12, pp. 6231–6249, 2017.
- [17] S. Bayat, Y. Li, L. Song, and Z. Han, "Matching theory: applications in wireless communications," *IEEE Signal Processing Magazine*, vol. 33, no. 6, pp. 103–122, 2016.
- [18] K. E. Kolodziej, J. G. McMichael, and B. T. Perry, "Multitap RF canceller for in-band full-duplex wireless communications," *IEEE Transactions on Wireless Communications*, vol. 15, no. 6, pp. 4321–4334, 2016.
- [19] M. Mozaffari, W. Saad, M. Bennis, and M. Debbah, "Wireless communication using unmanned aerial vehicles (UAVs): optimal transport theory for hover time optimization," *IEEE Transactions on Wireless Communications*, vol. 16, no. 12, pp. 8052–8066, 2017.
- [20] K. V. S. S. S. G. Sairam and N. Redd S R, "Bluetooth in wireless communication," *Communications Magazine IEEE*, vol. 97, no. 6, pp. 1–9, 2017.
- [21] M. S. Islim and H. Haas, "Augmenting the spectral efficiency of enhanced PAM-DMT-based optical wireless communications," *Optics Express*, vol. 24, no. 11, pp. 11932–11949, 2016.
- [22] Z. Zhang, K. Long, A. V. Vasilakos, and L. Hanzo, "Full-duplex wireless communications: challenges, solutions, and future research directions," *Proceedings of the IEEE*, vol. 104, no. 7, pp. 1369–1409, 2016.
- [23] "IEEE Transactions on green communications and networking," *IEEE Transactions on Green Communications & Networking*, vol. 1, no. 3, p. C2, 2017.
- [24] M. Olaf, "Automation and taxation," *Port strategy: Insight for Port Executives*, vol. 1017, no. 5, p. 47, 2017.
- [25] M. Naseri, M. A. Raji, M. R. Hantehzadeh, A. Farouk, A. Boochani, and S. Solaymani, "A scheme for secure quantum communication network with authentication using GHZ-like states and cluster states controlled teleportation," *Quantum Information Processing*, vol. 14, no. 11, pp. 4279–4295, 2015.
- [26] H. Abulkasim, A. Farouk, S. Hamad, A. Mashatan, and S. Ghose, "Secure dynamic multiparty quantum private comparison," *Scientific Reports*, vol. 9, no. 1, pp. 1–16, 2019.
- [27] M. Adil, M. K. Khan, M. Jamjoom, and A. M. H. A. D. B. O. R. Farouk, "AI-enabled administrative distance based opportunistic load balancing scheme for an agriculture internet of things network," *IEEE Micro*, 2022.
- [28] I. K. Osamh and G. M. Abdulsahib, "Energy efficient routing and reliable data transmission protocol in WSN," *International Journal of Advances in Soft Computing and its Application*, vol. 12, no. 3, pp. 45–53, 2020.
- [29] K. Urazaliev, "About taxation on electronic commerce," *International Finance and Accounting*, vol. 2019, no. 3, p. 25, 2019.
- [30] A. Farouk, J. Batle, M. Elhoseny et al., "Robust general N user authentication scheme in a centralized quantum communication network via generalized GHZ states," *Physics*, vol. 13, no. 2, pp. 1–18, 2018.
- [31] M. Rajalakshmi, V. Saravanan, V. Arunprasad, A C Khalaf, O I, and C. Karthik, "Machine learning for modeling and control of industrial clarifier process," *Intelligent Automation & Soft Computing*, vol. 32, no. 1, pp. 339–359, 2022.

## *Retraction*

# **Retracted: Sidelobe Reduction in NC-OFDM-Based CRNs Using Differential Evolution-Assisted Generalized Sidelobe Canceller**

### **Wireless Communications and Mobile Computing**

Received 12 December 2023; Accepted 12 December 2023; Published 13 December 2023

Copyright © 2023 Wireless Communications and Mobile Computing. This is an open access article distributed under the Creative Commons Attribution License, which permits unrestricted use, distribution, and reproduction in any medium, provided the original work is properly cited.

This article has been retracted by Hindawi, as publisher, following an investigation undertaken by the publisher [1]. This investigation has uncovered evidence of systematic manipulation of the publication and peer-review process. We cannot, therefore, vouch for the reliability or integrity of this article.

Please note that this notice is intended solely to alert readers that the peer-review process of this article has been compromised.

Wiley and Hindawi regret that the usual quality checks did not identify these issues before publication and have since put additional measures in place to safeguard research integrity.

We wish to credit our Research Integrity and Research Publishing teams and anonymous and named external researchers and research integrity experts for contributing to this investigation.

The corresponding author, as the representative of all authors, has been given the opportunity to register their agreement or disagreement to this retraction. We have kept a record of any response received.

### **References**

- [1] R. Ahmed, N. Gul, S. Ahmed, M. S. Khan, S. M. Kim, and J. Kim, "Sidelobe Reduction in NC-OFDM-Based CRNs Using Differential Evolution-Assisted Generalized Sidelobe Canceller," *Wireless Communications and Mobile Computing*, vol. 2022, Article ID 9449400, 11 pages, 2022.

## Research Article

# Sidelobe Reduction in NC-OFDM-Based CRNs Using Differential Evolution-Assisted Generalized Sidelobe Canceller

Rashid Ahmed <sup>1</sup>, Noor Gul <sup>1,2</sup>, Saeed Ahmed,<sup>2</sup> Muhammad Sajjad Khan <sup>3</sup>,  
Su Min Kim <sup>2</sup> and Junsu Kim <sup>2</sup>

<sup>1</sup>Department of Electronics, University of Peshawar, Peshawar 25000, Pakistan

<sup>2</sup>Department of Electronics Engineering, Tech University of Korea (TU Korea), Republic of Korea

<sup>3</sup>Department of Electrical Engineering, Faculty of Engineering and Technology, International Islamic University, Islamabad 44000, Pakistan

Correspondence should be addressed to Junsu Kim; [junsukim@kpu.ac.kr](mailto:junsukim@kpu.ac.kr)

Received 1 October 2021; Revised 24 January 2022; Accepted 14 March 2022; Published 4 April 2022

Academic Editor: Ali Kashif Bashir

Copyright © 2022 Rashid Ahmed et al. This is an open access article distributed under the Creative Commons Attribution License, which permits unrestricted use, distribution, and reproduction in any medium, provided the original work is properly cited.

Noncontiguous orthogonal frequency division multiplexing (NC-OFDM) is considered a suitable candidate for the cognitive radio network (CRN) to accomplish efficient data transmission. The NC-OFDM allows secondary users (SUs) to access the primary user (PU) spectrum while being detected idle. However, interference may occur in the adjacent frequency bands of the PU due to sidelobes of the SU transmission. The use of cancellation carriers (CCs) and generalized sidelobe canceller (GSC) is a widely adopted technique to tackle the sidelobes. To this end, this paper presents a differential evolution- (DE-) based GSC (DE-GSC) scheme to suppress unwanted sidelobes. At first, in the DE-GSC1 scheme, the adaptive weight vector is calculated using the DE algorithm while considering the complete samples of the sidelobes for optimization. The optimized weights are then added with the original weights to reduce the sidelobe issue. Next, in the DE-GSC2 scheme, selected elements for the adaptive weight vector near the main NC-OFDM signal are computed using the DE to reduce the search space. The performance of the proposed methods in terms of power spectral density (PSD) is compared with some of the recent techniques employing five different scenarios. Simulation results in the presence of single and multiple spectral hole scenarios validate that the proposed DE-GSC1 and DE-GSC2 methods result in enhanced suppression performance compared with the: original signal, simple CC, simple GSC, DE-based CC (DE-CC), and genetic algorithm- (GA-) based CC (GA-CC) schemes.

## 1. Introduction

The radio spectrum demand is rising with the increase in the number of wireless devices and services. The spectrum estimation surveys show that most spectrum bands are underutilized most of the time [1]. A progressively adaptable spectrum managing approach is required to solve the spectrum underutilization problems. Several ideas regarding adaptive spectrum management exist such as dynamic sharing of the spectrum. Therefore, the administrative bodies have started reconsidering the static spectrum access to shift towards dynamic spectrum access.

The cognitive radio network (CRN) allows secondary users (SUs) to opportunistically access spectrum resources using its detection, learning, and intelligence features [2]. The major problem in CRN occurs when a SU accesses a licensed band but fails to notice the existence of the primary user (PU), causing interference [3]. Hence, the responsibility of the interference management mostly depends on the SUs.

In the interweave mode of CRN, SUs are allowed to opportunistically access the spectrum based on noninterference to the PUs [3–6]. To detect the occupancy of the PU spectrum, commonly used detection schemes adopted by the SUs are the generalized likelihood ratio test detector



(GLRT), matched filter detector (MFD), feature detector, and energy detectors [7, 8]. Subsequent measures are required at the transmitter side to control the shape of the transmitted signal; therefore, both the SU and PU can have similar spectrum assets with low interference [6, 9].

Noncontiguous orthogonal frequency division multiplexing (NC-OFDM) is considered the best candidate for CRN [10, 11]. The NC-OFDM transmits signals on narrow-band channels reducing the effect of intercarrier interference (ICI) and intersymbol interference (ISI) [12]. It is a multicarrier system that splits the existing overall bandwidth into numerous narrow orthogonal channels/subcarriers. In parallel, NC-OFDM has some downsides due to the existence of the sidelobes that generate high out-of-band (OOB) radiations.

To handle the OOB radiations issue, different strategies are suggested in the time and frequency domains. The time-domain techniques include adaptive symbol transmission [13], filtering [14], and windowing [15, 16], while the frequency-domain incorporates cancellation carrier (CC) insertion [17] and generalized sidelobe canceller (GSC). To reduce the sidelobe issues in the PU regions, the CC scheme employs extra subcarriers, known as CCs at the edges of the OFDM symbol. These CCs do not contribute to the data transmission; however, they consume the extra bandwidth. Therefore, the CCs are considered detrimental. On the contrary, extra subcarriers are not used in the GSC; rather the given NC-OFDM signal is passed through the upper and lower branches of the GSC to suppress the OOB radiations. The GSC is the simplest version of linearly constrained minimum variance (LCMV), where the constrained optimization problem is converted into an unconditional problem.

Some of the schemes to reduce sidelobes power are the subcarrier weighting [18], advanced subcarrier weighting [19], efficient subcarrier weighting [20], insertion of modified CCs using heuristic techniques [9], peak to the average method of suppression constellation adjustment [21], and GSC [22]. The other methods in use are the additive signal method [23], extended active interference cancellation [24], efficient sidelobe suppression technique [25], minimization of sidelobe using modify GSC [26], a mongrel technique to reduce sidelobes [27], multiple generalized sidelobe technique for suppression of sidelobes [28], joint peak to average power ratio (PAPR) reduction technique [29], filter-based sidelobe reduction scheme [30], and hybrid PAPR method [31].

Conventionally, GSC adjusts the weights of the adaptive weight vector using the numerical solution to suppress high OOB radiations. On the other hand, the CC techniques reduce available bandwidth opportunity for the SUs with the insertion of extra CCs. Contrary to the above-mentioned schemes, we employed the differential evolution (DE) to optimize the adaptive weight vector of the GSC as an alternative to the numerical solution to attain improved sidelobe suppression. Major contributions of this paper are listed below:

- (i) The DE-based GSC (DE-GSC) scheme is suggested in the paper. We proposed two schemes: DE-GSC1

and DE-GSC2. Both the proposed schemes, DE-GSC1 and DE-GSC2, are modified versions of the simple GSC scheme, where the adaptive portion of the simple GSC is tuned using the DE to get maximum OOB suppression results

- (ii) To reduce the sidelobe weights using the DE-GSC1, a considerably large set of values in the adaptive weight vector are optimized through the DE algorithm. Similarly, the DE-GSC2 reduces sidelobe issues in the NC-OFDM by optimizing some of the adaptive weight vector values near the main NC-OFDM signal
- (iii) The effectiveness and reliability of the proposed schemes are compared with widely adopted existing schemes, like simple GSC, simple CCs, Brandes-based CCs (Brandes-CC), genetic algorithm- (GA-) based CCs (GA-CCs), and DE-based CCs (DE-CCs). Simulation results for the single and multiple white spaces in five different cases show improved sidelobe concealment performance by the proposed DE-GSC1 and DE-GSC2 as compared with the other schemes

The remaining paper is organized as follows. In Section 2, the system model is discussed. Section 3 gives a detailed description of the proposed scheme. Simulation results are discussed in Section 4. The paper is concluded in Section 5.

## 2. System Model and Background

*2.1. System Model.* Consider that  $K$  number of SUs is trying to access the PU spectrum in the interweaved mode. We assume that both the PU and the SUs are based on the NC-OFDM. Consider the spectrum band is divided into  $S$  subcarriers out of which  $S_d$  subcarriers are allocated to the  $d^{\text{th}}$  SU, such that  $S_d \leq S$ . These subcarriers are modulated with binary phase-shift keying (BPSK) or quadrature phase-shift keying (QPSK). The baseband NC-OFDM signal for the  $d^{\text{th}}$  SU in one symbol time-domain duration is

$$x_d(t) = \sum_{n=r}^{S_d-1} p_{n,d} e^{j2\pi f_n t} I(t), \quad (1)$$

where  $x_d(t)$  is the NC-OFDM signal of the  $d^{\text{th}}$  SU,  $p_{n,d}$  are the data modulated symbol of the  $d^{\text{th}}$  SU on the  $n^{\text{th}}$  subcarrier,  $r$  is any arbitrary subcarrier,  $f_n$  define the subcarrier frequencies, and  $I(t)$  is a rectangular function [32] that can be defined as

$$I(t) = \begin{cases} 1, & T_{\text{gu}} \leq t \leq T_s, \\ 0, & \text{otherwise,} \end{cases} \quad (2)$$

where  $T_{\text{gu}}$  and  $T_s$  are the guard interval length and symbol duration, respectively. The Fourier transform of (1) is given as

$$X_d(f) = \sum_{n=r}^{S_d-1} p_{n,s} \text{sinc}(\pi(f-f_n)T'), \quad (3)$$

where  $\text{sinc}(x) = \sin(\pi x)/\pi x$  is the sinc function with symbol duration  $T' = T_s + T_{\text{gu}}$ . The sidelobe power in the frequency domain decays as a function  $1/f^2 S_d$  in Figure 1 that results in extreme interference to the PU transmission.

**2.2. Generalized Sidelobe Canceler (GSC).** The input NC-OFDM signal passes through both the upper and the lower portions of the GSC in Figure 2. The upper portion comprises of quiescent weight vector  $\mathbf{w}_q$  constructed by several constraints, to maintain the desired segment of the signal, termed fixed beamformer (FBF), while the lower portion comprises a blocking matrix  $\mathbf{B}$  and an adaptive weight vector  $\mathbf{w}_a$ . The blocking matrix blocks desired segment of the signal and preserves the undesired segment of the signal as in Figure 1.

The adaptive weight vector  $\mathbf{w}_a$  then adjusts the weights of the undesired segments that result in the sidelobe reduction when the signals from the upper and the lower portions are subtracted.

To evaluate the expression for  $\mathbf{w}_a$ ,  $\mathbf{B}$ , and  $\mathbf{w}_q$ , the NC-OFDM in (3) and Figure 1 is first one sampled into equally spaced  $C$  values and collected in vector  $\mathbf{v} = [v_1 \ v_2 \ \dots \ v_C]^T$ , where each sample element represents NC-OFDM signal magnitude. This is made with an assumption that all NC-OFDM samples are uncorrelated, which are next passed through the GSC to get the output as

$$Y = \mathbf{w}^H \mathbf{v}, \quad (4)$$

where  $\mathbf{w} = [w_1 \ w_2 \ \dots \ w_C]^T$  is a vector with the size  $(C \times 1)$ , where  $H$  denotes Hermitian. The weight vector  $\mathbf{w}^H$  is determined using LCMV [33] that minimizes the output power using multiple linear constraints. The optimization problem of the LCMV is formulated as

$$\begin{aligned} \min_{\mathbf{w}} \quad & \mathbf{w}^H \mathbf{R}_v \mathbf{w} \\ \text{s.t.} \quad & \mathbf{w}^H \mathbf{J} = \mathbf{g}^H, \end{aligned} \quad (5)$$

where  $\mathbf{R}_v = E[\mathbf{v}\mathbf{v}^H] = \sigma^2 \mathbf{I}$  represents a correlation matrix, with  $C \times C$  dimension, and  $\mathbf{g} = [1 \ 1 \ \dots \ 1]^T$  is a gain vector with dimension  $N \times 1$  consisting of desired gain associated with each steering vector. Similarly,  $\mathbf{I}$  represents an identity matrix with  $C \times C$  dimension,  $\sigma^2$  denotes the variance, and  $\mathbf{J}$  shows the constraint matrix with the size  $C \times N$ .

After solving (5) using Lagrange's multipliers, we get

$$l = \mathbf{w}^H \mathbf{R}_v \mathbf{w} + (\mathbf{w}^H \mathbf{J} - \mathbf{g}^H) \lambda + \lambda^H (\mathbf{J}^H \mathbf{w} - \mathbf{g}), \quad (6)$$

$$\frac{\partial}{\partial \mathbf{w}^H} (\mathbf{w}^H \mathbf{R}_v \mathbf{w} + \mathbf{w}^H \mathbf{J} \lambda - \mathbf{g}^H \lambda + \lambda^H \mathbf{J}^H \mathbf{w} - \lambda^H \mathbf{g}) = 0, \quad (7)$$

$$\mathbf{w} = -\mathbf{R}_v^{-1} \mathbf{J} \lambda, \quad (8)$$

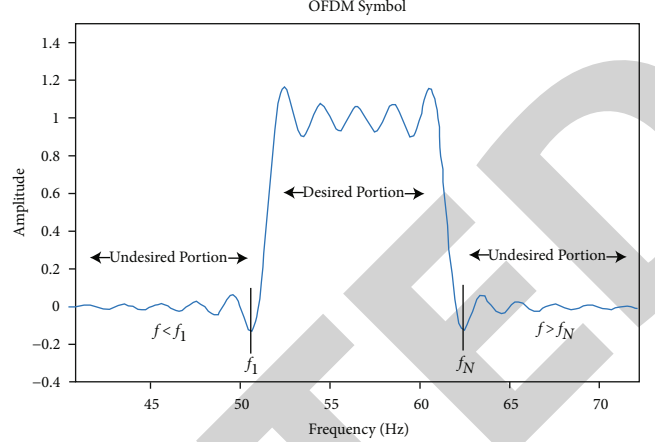


FIGURE 1: OFDM symbol with high sidelobes.

where  $\lambda$  is the Lagrange multiplier,  $(\partial/\partial \mathbf{w}^H)(\mathbf{w}) = 0$  and  $(\partial/\partial \mathbf{w}^H)(\mathbf{w}^H) = 1$ . Put (8) into the constraint equation  $\mathbf{w}^H \mathbf{J} = \mathbf{g}^H$ , we get

$$-\lambda^H \mathbf{J}^H \mathbf{R}_v^{-1} \mathbf{J} = \mathbf{g}^H. \quad (9)$$

For solving  $\lambda$ , substitute (9) into (8)

$$\mathbf{w}^H = \mathbf{g}^H (\mathbf{J}^H \mathbf{R}_v^{-1} \mathbf{J})^{-1} \mathbf{J}^H \mathbf{R}_v^{-1}. \quad (10)$$

The  $N$  steering vectors of  $\mathbf{J}$  matrix are specified as

$$\mathbf{J} = [\mathbf{s}_1 \ \mathbf{s}_2 \ \dots \ \mathbf{s}_N], \quad (11)$$

where  $N$  is the overall frequency in the desired portion of the signal, as in Figure 1. Similarly,  $\mathbf{s}_i = [s_{i1} \ s_{i2} \ \dots \ s_{iC}]^T$  is the  $i^{\text{th}}$  steering vector that consists of  $C$  samples in the  $i^{\text{th}}$  spectrum bearing  $C \times 1$  dimensions.

The employment of LCMV is to split a field with  $C \times C$  dimension into the constraint subfield well-defined by the columns of  $\mathbf{J}$  ( $C \times N$ ) the matrix and an orthogonal subfield denoted as  $\mathbf{B}$  having dimension  $C \times (C - N)$

$$\mathbf{J}^H \mathbf{B} = \mathbf{O}, \quad (12)$$

where  $\mathbf{O}$  represents a null matrix with dimension  $N \times (C - N)$  and  $\mathbf{B}$  symbolizes a blocking matrix that blocks the desired portion of the NC-OFDM signal.

The  $\mathbf{B}$  can be determined through singular value decomposition or QR factorization [34]. It is constructed, by first finding  $\mathbf{P}_o = \mathbf{I} - \mathbf{P}_c$  with  $\mathbf{P}_c$  and  $\mathbf{P}_o$  representing matrix projection onto the constraint and orthogonal subfields with  $C \times C$  dimension, formerly orthonormalizing  $\mathbf{P}_o$  and choosing the first  $(C - N)$  columns of the orthonormalized matrix to construct a blocking matrix  $\mathbf{B}$ , having the property [33].

$$\mathbf{B}^H \mathbf{B} = \mathbf{I}. \quad (13)$$

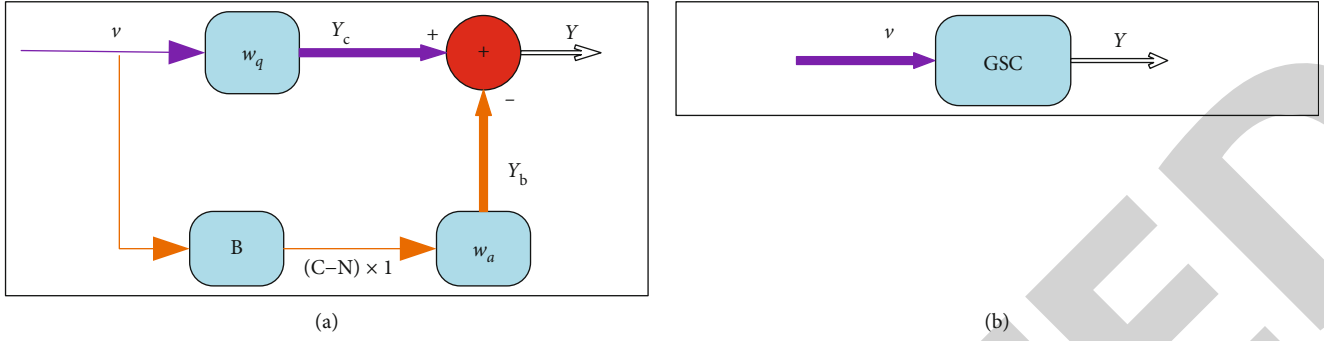


FIGURE 2: Generalized sidelobe canceller (GSC): (a) block diagram of GSC; (b) equivalent block diagram of GSC.

The quiescent weight vector  $\mathbf{w}_q^H$  of the GSC is determined as

$$\mathbf{w}_q^H = \mathbf{g}^H [\mathbf{J}^H \mathbf{J}]^{-1} \mathbf{J}^H. \quad (14)$$

Similarly, the optimal value of the adaptive weight vector is achieved as

$$\mathbf{w}_{a(\text{opt})}^H = \mathbf{w}_q^H \mathbf{R}_v \mathbf{B} (\mathbf{B}^H \mathbf{R}_v \mathbf{B})^{-1}. \quad (15)$$

Hence, the GSC outcomes in (4) yield

$$Y = (\mathbf{w}_q - \mathbf{B} \mathbf{w}_a)^H \mathbf{v}. \quad (16)$$

Similarly, the output power of GSC is as

$$P = (\mathbf{w}_q - \mathbf{B} \mathbf{w}_a)^H \mathbf{R}_v (\mathbf{w}_q - \mathbf{B} \mathbf{w}_a). \quad (17)$$

The block diagram of GSC with its components is shown in Figure 2.

### 3. Proposed Sidelobe Cancellation Method

In this section, we present DE-GSC1 and DE-GSC2 as the proposed schemes for sidelobe reduction. The proposed schemes are the modified versions of the conventional GSC that will result in the reduction of sidelobes. In this paper, the optimization portion of GSC, i.e., the adaptive weight vector, is carried out using the DE algorithm.

**3.1. Differential Evolution Based Weighting Method.** In the proposed DE-GSC1 scheme, all elements of the adaptive weight vector  $\mathbf{w}_a$  are optimized using DE. The elements of the adaptive weight vector are selected from both ends of the OFDM sidelobe. To optimize the performance of the proposed DE-GSC 1, the entire vector element from each sidelobe is considered for the reduction of OOB radiation, while in the DE-GSC2 some of the adaptive weight vector elements with high OOB radiation magnitudes near the main OFDM symbol in Figure 1 are determined using the DE algorithm. A total of eight sample elements from each sidelobe are collected for optimization in the DE-GSC2. These weights are the maximum and minimum weights from the sidelobes. The other elements of the adaptive

weight vector in the DE-GSC2 are determined using the sidelobe decaying formula. The main steps involved in the DE algorithm to solve the given problem are discussed as follows.

**3.1.1. Step 1: Initialize Population.** In the first step, the weight vectors to suppress the OOB radiations of the NC-OFDM symbol are initialized randomly with  $N_p$  population members (candidate solutions) consisting of  $D$  total dimensions.

$$\mathbf{u}_{i,j}^G = h + \text{randj}(h_j - l_j), \quad i = 1, 2, \dots, N_p, j = 1, 2, \dots, D. \quad (18)$$

The vector  $\mathbf{u}_{i,j}^G$  in (18) is the target vector,  $\text{randj}$  is a uniformly distributed random number between (0,1),  $h_j$  and  $l_j$  are the upper and lower bound limits of the  $j^{\text{th}}$  decision parameter, respectively. Here, the dimension  $D$  is identical to the total number of elements in the adaptive weight vector. The fitness of each of these target vectors is determined in the form of sidelobe suppression, and the vector with minimum OOB radiations is selected.

**3.1.2. Step 2: Mutation.** For each weight vector in the given population, three dissimilar random numbers  $b_1$ ,  $b_2$ , and  $b_3$  are generated such that they are different from the running index as well. Now, the initial population in (18) and the random numbers  $b_1$ ,  $b_2$ , and  $b_3$  are used to form a new population. The mutation results in the mutant or the donor vector as

$$\mathbf{m}_i^{G+1} = \mathbf{u}_{b_1}^G + F(\mathbf{u}_{b_2}^G - \mathbf{u}_{b_3}^G), \quad i = 1, 2, 3 \dots, N_p, b_1 \neq b_2 \neq b_3 \neq i. \quad (19)$$

Here,  $\mathbf{m}_i^{G+1}$  is the mutant or mutation vector. The scaling factor  $F$  is the tuning parameter and is problem-dependent. It is carefully selected keeping the value of the decision parameter between  $l_j$  and  $h_j$  to finalize optimum weight vector with minimum sidelobe power. The scaling factor  $F$  is selected as 0.2 in the proposed schemes for better sidelobe suppression results. The difference employed in the mutation process in (19) forms the given algorithm as DE.

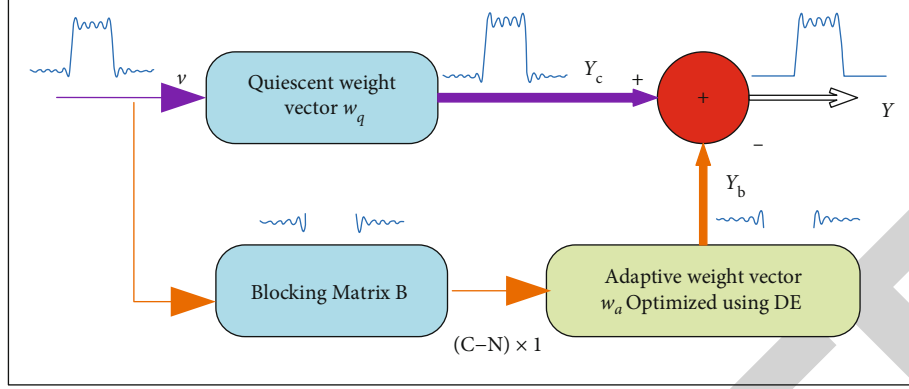


FIGURE 3: Proposed DE-GSC.

3.1.3. *Step 3: Crossover.* The crossover is performed between donor and target vectors. The resultant crossover is formed as follows:

$$\mathbf{z}_{i,j}^{G+1} = \begin{cases} \mathbf{m}_{i,j}^{G+1}, & \text{rand}(j) \leq \xi \text{ or } j = \text{randn}(i), \\ \mathbf{u}_{i,j}^G, & \text{rand}(j) > \xi \text{ or } j \neq \text{randn}(i), \end{cases} \quad (20)$$

where  $\text{rand}(j) \in [0, 1]$  is the uniformly distributed random number, while  $j$  is the element number of the candidate solution; i.e.,  $j \in 1, 2, \dots, D$  and  $-\text{randn}(i)$  is an integer, randomly selected from 1 to  $D$ . Similarly,  $\mathbf{z}_{i,j}^{G+1}$  is the trial vector, and  $\xi$  is the cross-over rate selected (0.9).

3.1.4. *Step 4: Selection.* In this step, a comparison is made between the trial vector  $\mathbf{z}_{i,j}^{G+1}$  and target vector  $\mathbf{u}_i^G$  in terms of its fitness. The weight vector with an improved fitness function that shows better sidelobe reduction is selected for the next generation as

$$\mathbf{u}_i^{G+1} = \begin{cases} \mathbf{z}_{i,j}^{G+1}, & f(\mathbf{z}_{i,j}^{G+1}) < f(\mathbf{u}_i^G) \\ \mathbf{u}_i^G, & f(\mathbf{z}_{i,j}^{G+1}) \geq f(\mathbf{u}_i^G) \end{cases}. \quad (21)$$

The vector  $\mathbf{u}_i^{G+1}$  is an offspring for the next generation. As the objective of the proposed work is to reduce sidelobe power, hence, it is considered a minimization problem. The sidelobe weights are optimized with DE after several iterations and subtracted from the original weight resulting in the sidelobes suppression as follows:

$$f = |\mathbf{u}_s - \mathbf{u}|. \quad (22)$$

In (22),  $\mathbf{u}_s$  is the sidelobe original weights and  $\mathbf{u}$  consists of the optimized weight vector using the DE algorithm. The block diagram of the DE-GSC is shown in Figure 3.

A pseudocode of the proposed algorithm that determines the adaptive weight vector of the GSC for reducing sidelobe power due to the SUs transmission is as follows:

```

(1) Start Differential Evolution
(2)  $t = 1$ 
(3) Initialize-population  $\mathbf{u}^t = \{\mathbf{u}_i^t, i = 1, 2, 3 \dots, N\}$ ;
(4) While conditions are not satisfied
(5) For  $i=1$  to  $N$  do
(6) Randomly select  $b_1, b_2, b_3 \in 1, 2, \dots, N$ ;
(7) Randomly select  $\delta_i \in 1, \dots, n$ ;
(8) For  $j = 1$  to  $n$ 
(9)  $m_{i,j}^{t+1} = \mathbf{u}_{b_1}^t + F(\mathbf{u}_{b_2}^t - \mathbf{u}_{b_3}^t)$ 
(10)  $b_1 \neq b_2 \neq b_3 \neq i$ 
(11) If  $\text{rand}(j) > \xi$  or  $j \neq \text{randn}(i)$ 
(12)  $\mathbf{z}_{i,j}^{t+1} = m_{i,j}^{t+1}$ 
(13) Else
(14)  $\mathbf{z}_{i,j}^{t+1} = \mathbf{u}_{i,j}^t$ 
(15) End if
(16) End For
(17) If  $f(\mathbf{z}_i^{t+1}) < f(\mathbf{u}_i^t)$ 
(18)  $\mathbf{u}_i^{t+1} = \mathbf{z}_i^{t+1}$ 
(19) Else
(20)  $\mathbf{u}_i^{t+1} = \mathbf{u}_i^t$ 
(21) End if
(22) End For
(23)  $t = t + 1$ 
(24) End While
(25) End Differential Evolution

```

PSEUDOCODE 1

## 4. Numerical Results and Discussions

The simulation results are drawn to compare the performance of the proposed and existing schemes in sidelobe concealments of the NC-OFDM symbol. This section discusses five different cases, i.e., one spectral hole, multiple spectral holes, SUs with equal bandwidth distribution, PUs with equal bandwidth distribution, and PUs and SUs with unequal bandwidth distribution as in Table 1. The DE algorithm performance is analyzed with a population size of 100 with a total of 800 iterations and random selection of the base vector. The scaling factor is tuned at 0.2 for local minimum. The crossover rate is binomial and fixed as 0.9. The total number of cancellation carriers in the CC technique

TABLE 1: Simulation parameters.

Parameter	Case 1	Case 2	Case 3	Case 4	Case 5
Hole availability	One	Four holes with equal SU and PU regions	Four holes with equal SUs regions	Four holes with equal PU regions	Four holes with unequal PUs and SUs regions
Population size	100	100	100	100	100
Iterations	800	800	800	800	800
Scaling factor	0.2	0.2	0.2	0.2	0.2
Subcarriers in each hole	16	16	16	35, 15, 40, 20	45, 20, 25, 30
Extra subcarriers in the CC technique	2	2	2	2	2

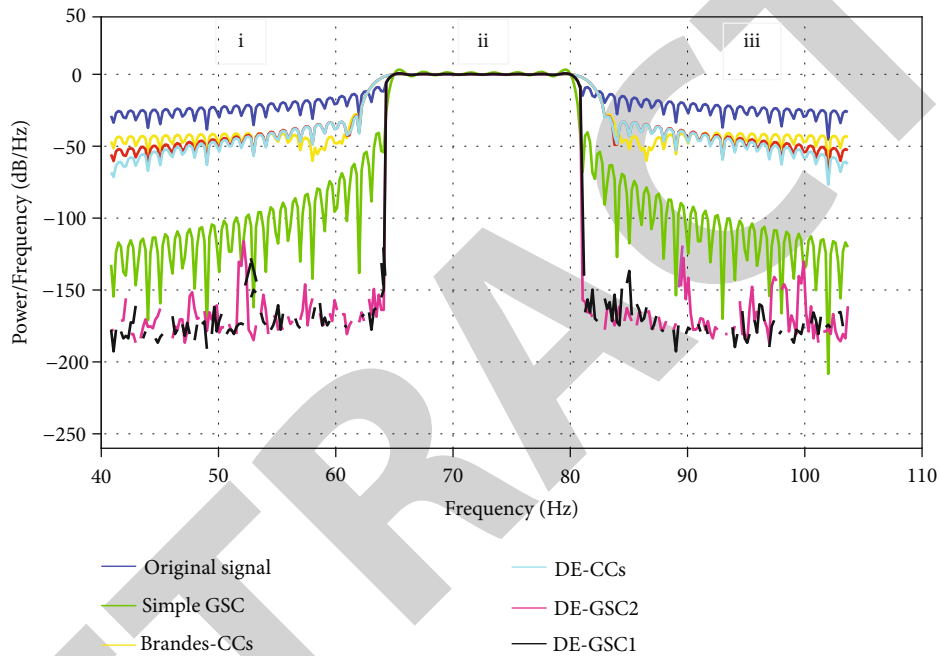


FIGURE 4: PSD of the original signal, simple GSC, DE-GSC2, DE-GSC1, Brandes-CCs, GA-CCs, and DE-CCs in case 1.

is 2. Simulation results of the proposed DE-GSC1 and DE-GSC2 along with simple GSC, Brandes-CCs, GA-CCs, and DE-CCs are shown in the form of normalized power spectral density (PSD) in Figures 4–8.

**4.1. Case 1: Single White Space and Two Equal PU Bands.** In the first case, three subbands are considered with single whitespace available for the SUs. In Figure 4, regions (i) and (iii) are available for the PU, whereas region (ii) is occupied by the SUs dynamically. A total of 16 subcarriers is considered in this case that is further modulated with the BPSK modulation. The PSD of the NC-OFDM signal on all its subcarriers is normalized to 1. The results are compared with some existing techniques such as (1) CCs on NC-OFDM signal for clampdown of sidelobes [17], (2) optimized CCs using DE algorithm with GA [9], and (3) sidelobe suppression using simple GSC in [22]. Figure 4 shows that the proposed DE-GSC1 and DE-GSC2 can effectively reduce

unwanted sidelobes in PU regions (i) and (iii) as compared with the original signal, simple GSC, Brandes-CC, DE-CC, and GA-CC techniques.

A comparison of the proposed and other schemes is further elaborated in Table 2, which reveals the sidelobes' power in the PU regions. The results in Figure 4 and Table 2 show that the original signal has a sidelobe power of -28 dB and -27 dB in regions (i) and (iii). It is clear from Table 2 that the GSC scheme reduces sidelobes' power in both regions to -131 dB and -132 dB. Similarly, the Brandes-CC results show a reduction in the sidelobes' power in regions (i) and (iii) to -48 dB each. Sidelobe power in the GA-CCs is lowered to -56 dB in region (i) and -55 dB in region (iii), while the DE-CCs further reduce that to -64 dB in region (i) and -66 dB in region (iii). The sidelobe power minimization ability is almost similar to the traditional Brandes-CCs, GA-CCs, and DE-CCs in regions (i) and (iii). A significant reduction in the sidelobes' power is

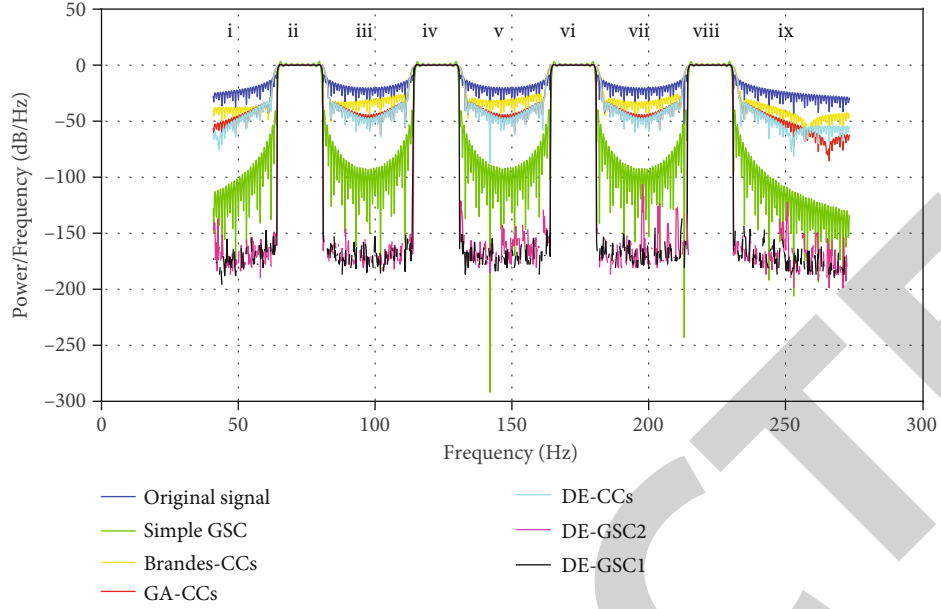


FIGURE 5: PSD of the original signal, simple GSC, DE-GSC2, DE-GSC1, Brandes-CCs, GA-CCs, and DE-CCs in case 2.

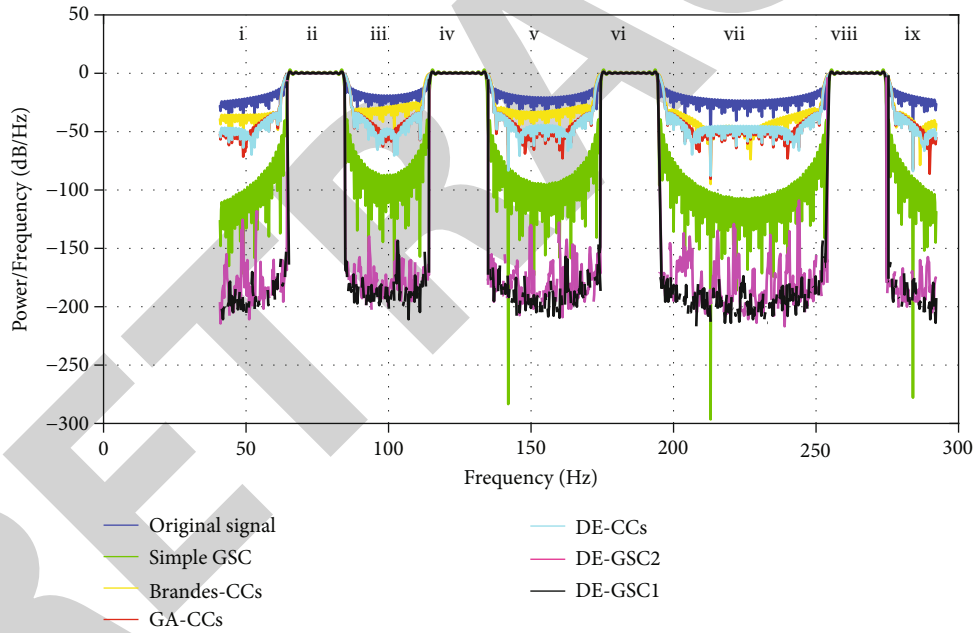


FIGURE 6: PSD of the original signal, simple GSC, DE-GSC2, DE-GSC1, Brandes-CCs, GA-CCs, and DE-CCs in case 3.

observable when the proposed DE-GSC1 and DE-GSC2 schemes are practiced in the given scenario. The results obtained by the proposed DE-GSC1 are -175 dB in region (i) and -173 dB in region (iii). Similarly, the proposed DE-GSC2 reduces sidelobes' power to -153 dB in region (i) and -155 dB in the region (iii). Hence, the proposed schemes can reduce sidelobes' powers significantly as compared with simple GSC, DE-CC, GA-CC, and Brandes-CC techniques.

**4.2. Case 2: Four Equal White Spaces and Five Equal PU Bands.** In this case, the spectrum is divided into multiple subbands with four white spaces for the SUs and five PU

bands. The available bandwidth is distributed between PUs and SUs, as follows: spaces (i), (iii), (v), (vii), and (ix) are available for the PU, whereas regions (ii), (iv), (vi), and (viii) are occupied by SUs. The total number of subcarriers used by the SUs in case 2 is 16 which are modulated using the BPSK modulation. Figure 5 shows that the DE-GSC1 and DE-GSC2 considerably reduce the sidelobe power in PU regions (i), (iii), (v), (vii), and (ix) as compared with the simple GSC, DE-CC, GA-CC, and Brandes-CC techniques.

Table 3 shows the numerical values of the resultant sidelobes power in five PU regions (i), (iii), (v), (vii), and (ix).

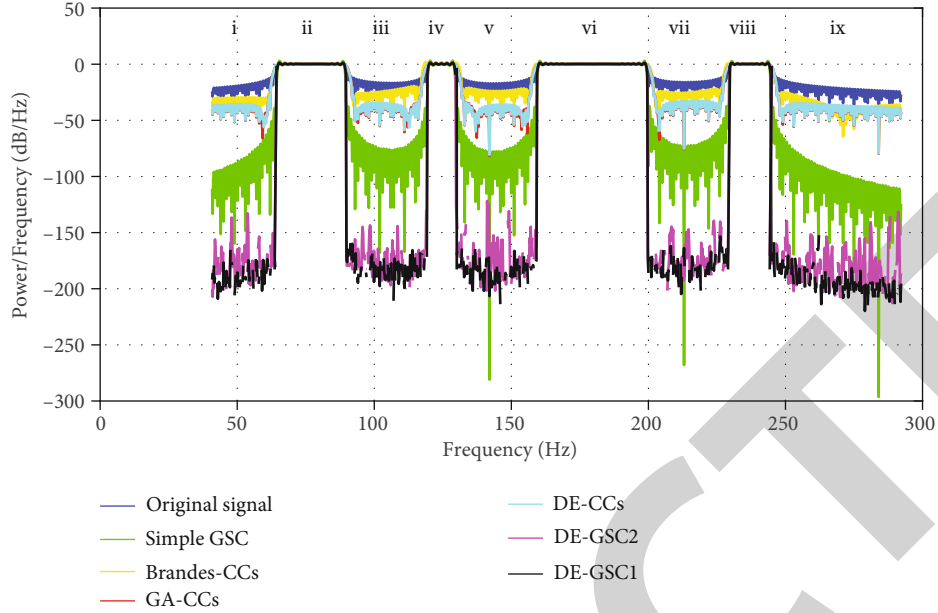


FIGURE 7: PSD of the original signal, simple GSC, DE-GSC2, DE-GSC1, Brandes-CCs, GA-CCs, and DE-CCs in case 4.

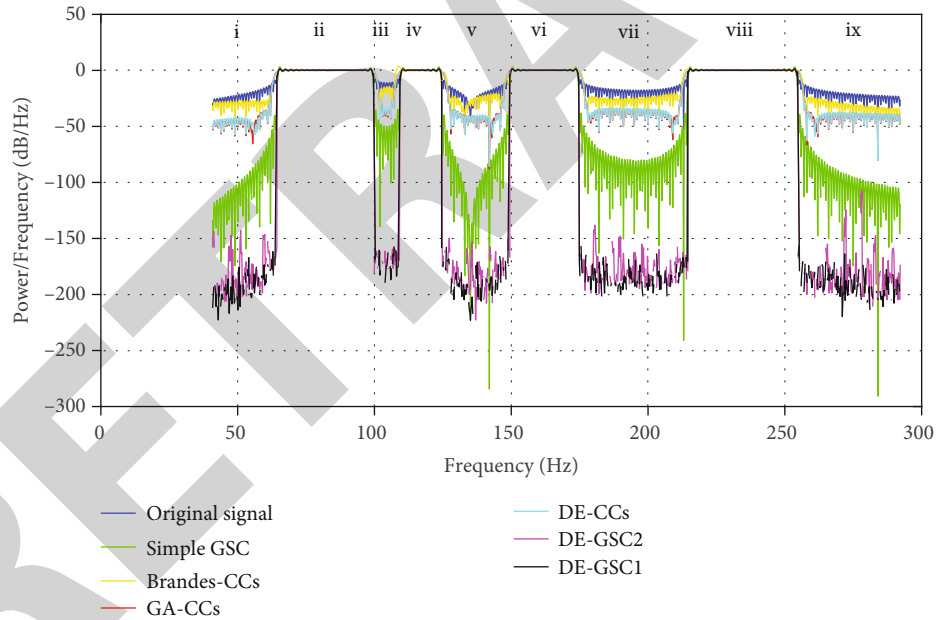


FIGURE 8: PSD of the original signal, simple GSC, DE-GSC2, DE-GSC1, Brandes-CCs, GA-CCs, and DE-CCs in case 5.

These results show that the original signal has an average sidelobe power of  $-24.8$  dB that is reduced by the Brandes-CCs to an average of  $-48.8$  dB. The average sidelobe results of the GA-CCs and DE-CCs are  $-64.8$  dB and  $-52.2$  dB, while the simple GSC average power is  $-134.6$  dB. Similarly, the proposed DE-GSC1 and DE-GSC2 schemes can reduce sidelobe power to an average of  $-165.4$  dB and  $-159.8$  dB in these regions.

**4.3. Case 3: Four Equal White Spaces and Five Unequal PU Bands.** In the third case, the spectrum is divided into mul-

multiple subbands. The bandgap of PUs in this case is unequal, i.e., regions (i), (iii), (v), (vii), and (ix), whereas SU regions (ii), (iv), (vi), and (viii) are of equal bandwidth. The total subcarriers utilized at the SUs, in this case, are 16. BPSK modulation is followed to modulate these subcarriers. In Figure 6 and Table 4, the comparison between the proposed and existing schemes is shown. The results obtained for the proposed DE-GSC1 and DE-GSC2 have the lowest sidelobe power among all the other schemes in the case of unequal spectrum regions (i), (iii), (v), (vii), and (ix).

TABLE 2: Sidelobe power in case 1.

Techniques	Sidelobe power in PU locations	
	i	iii
Original signal	-28 dB	-27 dB
Simple GSC	-132 dB	-131 dB
Brandes-CCs	-48 dB	-48 dB
GA-CCs	-56 dB	-55 dB
DE-CCs	-64 dB	-66 dB
DE-GSC1	-175 dB	-173 dB
DE-GSC2	-153 dB	-155 dB

TABLE 3: Sidelobe power in case 2.

Techniques	Sidelobe power in PU locations				
	i	iii	v	vii	ix
Original signal	-26 dB	-23 dB	-23 dB	-26 dB	-26 dB
Simple GSC	-130 dB	-135 dB	-136 dB	-136 dB	-136 dB
CC-Brandes	-48 dB	-49 dB	-49 dB	-49 dB	-49 dB
CC-GA	-56 dB	-54 dB	-51 dB	-50 dB	-50 dB
CC-DE	-64 dB	-65 dB	-65 dB	-65 dB	-65 dB
DE-GSC1	-170 dB	-168 dB	-164 dB	-162 dB	-163 dB
DE-GSC2	-155 dB	-165 dB	-162 dB	-155 dB	-162 dB

TABLE 4: Sidelobe power in case 3.

Techniques	Sidelobe power in PU locations				
	i	iii	v	vii	ix
Original signal	-32 dB	-29 dB	-28 dB	-27 dB	-28 dB
Simple GSC	-130 dB	-132 dB	-134 dB	-135 dB	-136 dB
Brandes-CCs	-40 dB	-42 dB	-43 dB	-44 dB	-45 dB
GA-CCs	-50 dB	-52 dB	-51 dB	-50 dB	-50 dB
DE-CCs	-51 dB	-53 dB	-52 dB	-53 dB	-54 dB
DE-GSC1	-180 dB	-175 dB	-178 dB	-179 dB	-177 dB
DE-GSC2	-160 dB	-158 dB	-161 dB	-160 dB	-157 dB

TABLE 5: Sidelobe power in case 4.

Techniques	Sidelobe power in PU locations				
	i	iii	v	vii	ix
Original signal	-26 dB	-25 dB	-24 dB	-25 dB	-26 dB
Simple GSC	-136 dB	-137 dB	-138 dB	-133 dB	-137 dB
Brandes-CCs	-48 dB	-48 dB	-47 dB	-46 dB	-48 dB
GA-CCs	-56 dB	-54 dB	-53 dB	-53 dB	-53 dB
DE-CCs	-64 dB	-65 dB	-62 dB	-64 dB	-66 dB
DE-GSC1	-178 dB	-177 dB	-176 dB	-175 dB	-176 dB
DE-GSC2	-165 dB	-163 dB	-165 dB	-166 dB	-164 dB

Table 4 shows numerical results of the sidelobe powers in case 3 for the proposed and other schemes. It is noticeable that the proposed DE-GSC1 while reducing sidelobe power

TABLE 6: Sidelobe power in case 5.

Techniques	Sidelobe power in PU locations				
	i	iii	v	vii	ix
Original signal	-24 dB	-26 dB	-23 dB	-26 dB	-26 dB
Simple GSC	-136 dB	-135 dB	-136 dB	-130 dB	-133 dB
Brandes-CCs	-48 dB	-47 dB	-45 dB	-47 dB	-49 dB
GA-CCs	-52 dB	-50 dB	-51 dB	-50 dB	-50 dB
DE-CCs	-66 dB	-65 dB	-67 dB	-66 dB	-64 dB
DE-GSC1	-179 dB	-178 dB	-176 dB	-172 dB	-173 dB
DE-GSC2	-160 dB	-161 dB	-162 dB	-159 dB	-162 dB

is the most suitable scheme under unequal band gaps occupied by the PU. It is clear from Table 4 that the original signal has an average sidelobe power of -28.8 dB that is reduced by the Brandes-CCs to an average of -42.8 dB. The DE-CC and GA-CC average suppression results are -52.6 dB and -50.6 dB, while the simple GSC average suppression results are -133.4 dB. The DE-GSC1 and DE-GSC2 average suppression results in the PU regions are -177.8 dB and -159.2 dB.

**4.4. Case 4: Four Unequal White Spaces and Five Equal PU Bands.** In this case, the SUs have unequal band gap distribution, while the PUs have an equal band gap distribution. Here, regions (ii), (iv), (vi), and (viii) are occupied by SU as illustrated in Figure 7, and regions (i), (iii), (v), (vii), and (ix) are occupied by PUs. The total subcarriers used at the SU's regions are 35, 15, 40, and 20, respectively. The results in Figure 7 show that the proposed DE-GSC1 and DE-GSC2 efficiently reduce sidelobes' powers in the PU equal regions, i.e., (i), (iii), (v), (vii), and (ix).

The original signal in Table 5 has the average sidelobe power of -25.2 dB that is reduced by the Brandes-CCs to an average of -47.4 dB. The GA-CCs and DE-CCs can suppress more and reduce sidelobe power to an average result of -53.8 dB and -64.2 dB. Similarly, the simple GSC suppression results are -136.2 dB, while the proposed DE-GSC1 and DE-GSC2 schemes have -164.6 dB and -176.4 dB on average.

**4.5. Case 5: Four Unequal White Spaces and Five Unequal PU Bands.** A multiple subband with unequal SUs and PUs bandgap allocation is discussed in case 5. Unequal bandgap regions (ii), (iv), (vi), and (viii) are allotted to the SUs. However, regions (i), (iii), (v), (vii), and (ix) are occupied by the PUs. The total numbers of subcarriers at the SUs are 45, 20, 25, and 30, respectively.

Figure 8 shows that the proposed DE-GSC1 and DE-GSC2 have better sidelobe reduction as compared with the simple GSC, Brandes-CCs, GA-CCs, and DE-CCs. The numerical results of the sidelobe power are shown in Table 6. It is clear from the results that the original signal average sidelobe power is -25 dB which is reduced by the Brandes-CCs to an average of -47.2 dB. The GA-CC and DE-CC average suppression results are -50.6 dB and -65.6 dB. The simple GSC results in better performance than the CC techniques while achieving an average of -134 dB. Both the proposed DE-GSC1 and DE-GSC2 dominate the schemes with better average suppression results of -175.6 dB and -160.8 dB.



Hence, it can be concluded from the above comparison that both the proposed DE-GSC1 and DE-GSC2 schemes performed better than the simple GSC, GA-CCs, DE-CCs, and Brandes-CCs in various scenarios and produce high accuracy to reduce sidelobe power in the PU locations.

## 5. Conclusion

The use of the NC-OFDM scheme in the free spectral hole has a sidelobe issue that results in interference in the legitimate PU regions. In this paper, a sufficiently large number of sidelobe sample points are taken into consideration for optimization using the DE algorithm in the DE-GSC1. The DE algorithm determines a suitable adaptive weight vector for the GSC that results in efficient reduction of the sidelobes issues in the PU region. However, the DE-GSC2 takes the initial sample points in the sidelobe region near the main NC-OFDM signal and determines the remaining points utilizing the sidelobes decay function. The different cases discussed in the paper show superiority of the proposed schemes to efficiently access the available spectrum holes without hindering the PU transmission. The results confirmed a significant reduction in the sidelobe interference by following the proposed scheme as compared with the existing techniques.

As the GSC has been examined widely in radar and communication systems where the desired signal needs to be measured either in time or at the amplitude level, it is suggested that a dual function radar and communication system can be designed by controlling the main lobe for radar and sidelobes for the communication systems employing the DE-based GSC approach, presented in this paper.

In a future work, we intend to reconfigure the adaptive vector of the GSC while utilizing machine learning techniques aiming to improve interference suppression. Furthermore, time and computational complexity analysis will be carried out to compare with existing interference minimization schemes such as optimization-based CCs and GSC.

## Data Availability

The data used to support the findings of this study are included in the article.

## Disclosure

This work was funded and supported in part by the National Research Foundation of Korea (NRF) grant funded by the Korean Government (MSIT) (Nos. 2016R1C1B1014069 and 2021R1A2C1013150).

## Conflicts of Interest

The authors declare no conflict of interest.

## References

- [1] P. Kolodzy, "Spectrum policy task force: findings and recommendations," *Federal Communications Commission*, vol. 2, no. 35, pp. 1–14, 2003.
- [2] N. Gul, I. M. Qureshi, S. Akbar, M. Kamran, and I. Rasool, "One-to-many relationship based Kullback Leibler divergence against malicious users in cooperative spectrum sensing," *Wireless Communications and Mobile Computing*, vol. 2018, 14 pages, 2018.
- [3] A. Patel, M. Z. Khan, S. N. Marchant, U. B. Desai, and L. Hanzo, "The achievable rate of interweave cognitive radio in the face of sensing errors," *IEEE Access*, vol. 5, pp. 8579–8605, 2017.
- [4] T. Renk, C. Kloeck, and F. K. Jondral, "A cognitive approach to the detection of spectrum holes in wireless networks," in *4th IEEE Consumer Communications and Networking Conference*, pp. 1118–1120, Las Vegas, NV, USA, 2007.
- [5] X. Hong, C. X. Wang, H. H. Chen, and Y. Zhang, "Secondary spectrum access networks," *IEEE Vehicular Technology Magazine*, vol. 4, no. 2, pp. 36–43, 2009.
- [6] N. Gul, I. M. Qureshi, A. Naveed, A. Elahi, and I. Rasool, "Secured soft combination schemes against malicious-users in cooperative spectrum sensing," *Wireless Personal Communications*, vol. 108, no. 1, pp. 389–408, 2019.
- [7] N. Gul, I. M. Qureshi, A. Omar, A. Elahi, and S. Khan, "History based forward and feedback mechanism in cooperative spectrum sensing including malicious users in cognitive radio network," *PLoS One*, vol. 12, no. 8, pp. 1–21, 2017.
- [8] N. Gul, I. M. Qureshi, A. Elahi, and I. Rasool, "Defense against malicious users in cooperative spectrum sensing using genetic algorithm," *International Journal of Antennas and Propagation*, vol. 2018, 11 pages, 2018.
- [9] A. Elahi, I. M. Qureshi, F. Zaman, and F. Munir, "Reduction of out of band radiation in non-contiguous OFDM based cognitive radio system using heuristic techniques," *Journal of Information Science and Engineering*, vol. 32, pp. 349–364, 2016.
- [10] R. W. Chang, "Synthesis of band-limited orthogonal signals for multichannel data transmission," *Bell System Technical Journal*, vol. 45, no. 10, pp. 1538–1966, 1966.
- [11] G. M. Abdalla, "Orthogonal frequency division multiplexing theory and challenges," *Khartoum University Engineering Journal*, vol. 1, no. 2, pp. 1–8, 2011.
- [12] B. Farhang-Boroujeng and R. Kempter, "Multicarrier communication techniques for spectrum sensing and communication in cognitive radios," *IEEE Communication Magazine*, vol. 46, no. 4, pp. 80–85, 2008.
- [13] H. A. Mahmoud and H. Arslan, "Sidelobe suppression in OFDM-based spectrum sharing systems using adaptive symbol transition," *IEEE Communications Letters Magazine*, vol. 12, no. 2, pp. 133–135, 2008.
- [14] D. Nogu et, M. Gautier, and V. Berg, "Advances in opportunistic radio technologies for TVWS," *EURASIP Journal on Wireless Communications and Networking (JWCN)*, vol. 2011, no. 1, pp. 1–12, 2011.
- [15] T. Weiss, J. Hillenbrand, A. Krohn, and F. K. Jondral, "Mutual interference in OFDM-based spectrum pooling systems," in *2004 IEEE 59th vehicular technology conference. VTC 2004-Spring*, pp. 118–1877, Milan, Italy, 2005.
- [16] A. Sahin and H. Arslan, "Edge windowing for OFDM based systems," *IEEE Communications Letters*, vol. 15, no. 11, pp. 1208–1211, 2011.
- [17] S. Brandes, I. Cosovic, and M. Schenell, "Reduction of out-of-band radiation in OFDM systems by insertion of cancellation carriers," *IEEE Communications Letters*, vol. 10, no. 6, pp. 420–422, 2006.

## Research Article

# Intelligent Optimization Control Strategy for Secondary Pollution of Flue Gas in Municipal Solid Waste Incineration

Yongsheng Ju 

Department of Mechanical and Electrical Engineering, Shandong Vocational College of Science & Technology, Weifang, Shandong 261053, China

Correspondence should be addressed to Yongsheng Ju; [juyongsheng@sdvcst.edu.cn](mailto:juyongsheng@sdvcst.edu.cn)

Received 20 January 2022; Revised 15 March 2022; Accepted 16 March 2022; Published 4 April 2022

Academic Editor: Shalli Rani

Copyright © 2022 Yongsheng Ju. This is an open access article distributed under the Creative Commons Attribution License, which permits unrestricted use, distribution, and reproduction in any medium, provided the original work is properly cited.

Aiming at the problem of serious secondary pollution caused by improper control strategy in the waste incineration process, this paper proposes an intelligent optimization control strategy for secondary pollution of flue gas in municipal solid waste incineration. Firstly, the control difficulties of waste incineration and cybernetic characteristics of combustion process in incinerators are analyzed, and the basic algorithm based on human simulated intelligent control is proposed accordingly. Then, genetic algorithm is used to improve particle swarm algorithm and search ability in wide space, which can avoid the premature phenomenon of local optimum. Finally, improved particle swarm algorithm is utilized to optimize the parameters in human simulated intelligent control algorithm to realize intelligent optimization control in the waste incineration process. Based on MATLAB simulation platform, experimental results show that when delay parameters and time constant change significantly, there are large disturbances, and the process response of proposed strategy is fast and stable, which is superior to other comparison strategies.

## 1. Introduction

With the rapid development of domestic economy and acceleration of urbanization process, the municipal waste disposal problem has become more and more prominent. At present, the main waste disposal methods include landfill, composting, and incineration for power generation (Figure 1). Among them, landfill disposal not only causes serious environmental pollution but also occupies lot of land and wastes lot of resources. Composting treatment is difficult to deal with the current complicated types of domestic waste and high cost [1, 2]. Waste incineration power generation treatment has received great attention from government agencies and scientific researchers because of its advantages of resource utilization, reduction, and harmlessness [3].

However, due to the inadequate level of waste classification and treatment at present, the calorific value of waste is generally low, and dioxins cannot be effectively decomposed. Its direct pollution reaches a range of 5 km, which makes waste incineration environmental protection projects often turn into pollution-intensive emission projects [4]. Dioxins belong to

chlorinated ring triaromatic compounds, which are very stable, difficult to decompose, and first-class carcinogens with toxic strength. Once the human body is contaminated by dioxins, it cannot be degraded or discharged in the body. It can cause major damage to the immune and reproductive functions of human body, causing large-scale deformities, cancer, and other diseases. Thus, the ecological pollution hazards of dioxin in developed countries have received considerable attention [5].

In view of the seriousness and universality for waste incineration flue gas pollution, many scientific researchers have explored the waste incineration pollution control from multiple angles. In particular, it is aimed at avoiding the dioxin secondary pollution problem caused by improper control of combustion flue gas temperature. However, there are still some shortcomings in terms of control strategies [6, 7], among which the commonly used forms of waste incinerators are shown in Figure 2. However, the flue gas treatment link, that is, the treatment and control strategy of devices in dashed box in Figure 2 on the harmful gas, needs to be improved.

In order to improve the intelligent control during incineration of domestic waste, it is necessary to develop a set of



FIGURE 1: Municipal solid waste incineration.

simulators. For now, the simulators of large thermal power plants have been widely promoted and applied in major power stations and universities. However, there are few simulators for waste incineration power plants [8]. This is mainly because the domestically operated incinerators and other key equipment still rely on foreign imports. Many of the corresponding supporting control systems have problems with the transfer and use of patented technologies [9, 10]. Therefore, it is of great significance to study the simulation and its control system of waste incineration power plants. Besides, it is necessary to conduct an in-depth study on the secondary pollution control caused by waste incineration from the perspective of control engineering.

Aiming at the secondary pollution problem caused by improper control in the waste incineration process, this paper proposes an intelligent optimization control strategy for secondary pollution of flue gas in municipal solid waste incineration. The main innovations are summarized as follows:

- (1) Because the traditional control strategy cannot match the characteristics of incineration rate control theory, a human simulated intelligent control algorithm is proposed to achieve the optimal control of flue gas temperature in the waste incineration
- (2) In order to solve the problems of low search accuracy, premature convergence, and low later iteration efficiency of particle swarm algorithm, the proposed strategy adopts genetic algorithm to improve particle swarm algorithm. The genetic crossover operator is used to increase the diversity of particles and improve search ability in a wide range of spaces

## 2. Materials and Methods

The waste incineration technology originated from abroad and has been quite perfect after more than 100 years of development. It already has some advanced technologies and methods, such as expert system real-time control, fuzzy control, neural network control, and simulation intelligent control [11, 12]. Among them, the conventional Proportional Integral Derivative (PID) controller has been able to meet the requirements of on-site operation, but the control

optimization problem for secondary pollution is less involved [13, 14]. Reference [15] studied the difficult control and disposal problem of residues for fly ash purification from domestic waste incineration, such as vitrified materials, and tested factors affecting the alteration rate. Reference [16] developed a new melting system on the basis of discussing operating conditions of ash slag melting furnace for municipal solid waste incinerator to solve the problem in the ash treatment of municipal solid waste incinerator. However, the dependence on external control factors such as temperature was relatively large. Reference [17] proposed a heat treatment method for solid domestic waste (SDW) to meet the conditions of SDW incineration and flue gas purification. However, the types of domestic garbage were complicated, and their universality was not good. Reference [18] proposed a method for the treatment of domestic garbage on the island, which uses diesel engine flue gas to dry garbage and shells to purify the gas generated by garbage incineration. This method can effectively reduce the energy consumption and pollution degree of waste incineration but did not consider the secondary pollution problem in the flue gas.

At the same time, there are many systematic discussions on waste incineration. Reference [19] focused on the production mechanism and preventive measures of major secondary pollutants such as dioxins, heavy metal elements, and oxidizing oxides produced by incineration of domestic waste. However, the specific implementation methods were not studied and only remain at the theoretical level. Reference [20] combined the characteristics of domestic waste, people's environmental awareness, willingness to pay, and its influencing factors and proposed a differentiated treatment plan for urban and rural domestic waste. Reference [21] analyzed the changes in operating parameters of domestic waste incinerator after cofiring of medical waste and the impact of the system on operating conditions, equipment life, and production costs by comparing operating data before and after the domestic waste incineration power plant. But it lacked the optimization research of corresponding control strategy. Reference [22] deeply studied the generation, treatment, and impact range of municipal solid waste and did not conduct a feasibility analysis of the waste treatment method.

In addition, in order to better grasp the combustion of garbage in incinerator, some scholars use numerical simulation to simulate the movement and combustion of garbage in incinerator to improve theoretical support for control system optimization [23, 24]. But overall, the treatment effect on secondary pollution caused by municipal solid waste incineration is not good. The control strategy needs to be improved.

## 3. Combustion Stability Control and HSIC Control Algorithm

*3.1. Control Difficulties of the Incineration Process.* The control difficulty in the incineration process is mainly reflected in the uncertainty for calorific value of waste. The calorific value of waste as a raw material for incineration process will vary depending on specific conditions of the city, as well as with changes in the climate, residents, and waste collection

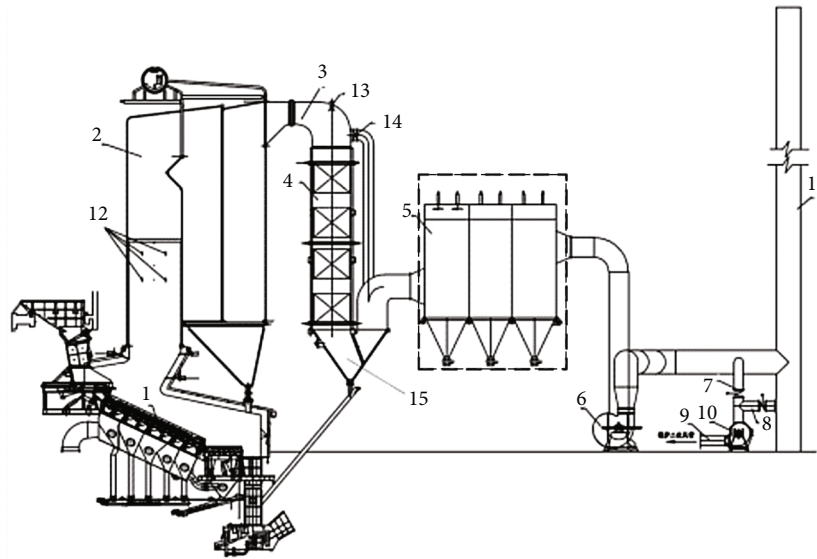


FIGURE 2: Principle and structure of typical incinerators.

conditions. Thus, the calorific value of municipal solid waste is extremely unstable. At the same time, the waste incinerator will also experience changes in the thermal characteristics of incinerator due to long-term equipment operation, overhaul, and transformation, such as difficulty in ignition, incomplete combustion, slagging in the furnace, corrosion, and increased secondary pollution. The effect of waste incineration, the control of pollutant generation, and economics of treatment are difficult to reach expectations [25].

The traditional control strategy is difficult to accurately grasp the characteristics of incinerator object, because the combustion process in incinerator is a very complex physical and chemical process. The incinerator itself is a strongly coupled multi-input, multioutput, nonlinear system, and it is difficult to establish an accurate mathematical model and implement paradigm quantitative control. Because its safe operation is closely related to the stability of combustion process, once the combustion stability declines, it will lead to increased incomplete combustion, reduced combustion efficiency, increased emissions of incineration pollutants, secondary pollution, and increased high-temperature corrosion. Therefore, it has a serious impact on the safety and economy of incinerator. The abovementioned are the control difficulties in the incineration process.

### 3.2. Cybernetic Characteristics of the Incineration Process.

The reason why the incineration process is difficult to accurately control is that the selected control strategy does not match the cybernetic characteristics of waste incinerator combustion process. Starting from the analysis of control difficulties, it is not difficult to summarize the cybernetic characteristics of combustion process:

- (1) The composition of waste is complex and changeable, and there are many factors that affect combustion. The calorific value of waste as a combustion raw material has great uncertainty. For uncertain

processes, it is difficult to implement effective control using mathematical modeling methods

- (2) The incinerator is a complex object with a high degree of nonlinearity. Although there are many existing nonlinear control methods, they are not suitable for application in incinerator control engineering due to the excessive complexity of the control methods
- (3) The problem of semistructured and unstructured in combustion process control of incinerator is prominent. It is difficult to describe the semistructured and unstructured processes using quantitative mathematical methods. Since traditional control belongs to the category of quantitative control, traditional control cannot do anything about the unknown, time-varying, and randomness of semistructured and unstructured process parameters, as well as the unknown and time-varying process delays
- (4) In the complex combustion process, each combustion element restricts each other and is highly coupled. It is impossible for traditional control to decouple and implement control
- (5) The external environment of incineration process is harsh, and industrial interference is serious. Traditional control does not have the ability to resist strong industrial interference

In short, the cybernetic characteristics of combustion process are mainly manifested as follows: the uncertainty for calorific value of waste; the randomness, unknown, and time-varying nature of other parameters process; the correlation and nonlinearity between process variables; the thermal inertia and process; the unknown and time-varying nature of time lag; and the unknown, diversity, and randomness of external interference. For the abovementioned cybernetic characteristics, it is impossible to use traditional control strategies to match its cybernetic characteristics. Therefore,

the control strategy and control algorithm that match its process characteristics must be adopted.

**3.3. HSIC Control Algorithm.** The control process model of Human Simulated Intelligent Controller (HSIC) is shown in Figure 3. In the figure,  $r(t)$  and  $y(t)$  are the input and output of control process, respectively.  $e(t)$  and  $G(t)$  are error and controller output, respectively.

$\hat{e}$  is the error rate of change, and the error phase plane is shown in Figure 4, which reflects the law of error change. When  $e \cdot \hat{e} > 0$  or  $e = 0$  and  $\hat{e} \neq 0$ , the absolute value function  $\text{Abs}(e)$  shows an increasing trend; when  $e \cdot \hat{e} < 0$  or  $\hat{e} = 0$ ,  $\text{Abs}(e)$  shows a decreasing trend and eventually tends to zero.

The above results show that when  $e = 0$  and  $\hat{e} \neq 0$  or  $e \cdot \hat{e} > 0$ , the control should select the ‘‘proportional’’ mode; when  $\hat{e} = 0$  or  $e \cdot \hat{e} < 0$ , the control should select the ‘‘hold’’ mode.

Summarizing the above two basic control modes, the basic control algorithm is as follows:

$$G = \begin{cases} K_p \cdot e + \kappa \cdot K_p \cdot \sum_{i=1}^{n-1} e_{\max}^i, & e \cdot \hat{e} > 0 \cup e = 0, \hat{e} \neq 0, \\ \kappa \cdot K_p \cdot \sum_{i=1}^{n-1} e_{\max}^i, & e \cdot \hat{e} < 0 \cup \hat{e} = 0, e \neq 0, \end{cases} \quad (1)$$

where  $e_{\max}^i$  and  $\hat{e}$ , respectively, represent the  $i$  peak value of the maximum error and error rate of change;  $G$  is the controller output;  $\kappa$  is the suppression coefficient;  $K_p$  is the proportional coefficient.

The HSIC algorithm is characterized in that different control modes are adopted for different positions of error characteristic in the error phase plane. The simplest case is to realize the control of controlled process with open and closed loop alternate control [26, 27]. For complex processes, the operator’s control skills, skills and wisdom, expert knowledge, and practical experience can be incorporated into the control algorithm. With the help of production rules in artificial intelligence, an HSIC control algorithm that matches the characteristics of process cybernetics is constructed [28]. In the error phase plane, if vertical coordinate  $\hat{e}$  is divided into  $\hat{E}_1$  and  $\hat{E}_2$  according to the characteristic threshold for the error rate of change,  $\hat{E}_2 \geq \hat{E}_1$ . Divide the abscissa  $e$  into  $E_1, E_2, E_3, E_2 \geq E_1$ , and  $E_3 \geq E_2$  according to the error characteristic threshold. Then, the error phase plane can be divided into multiple different control areas, so as to obtain HSIC control algorithm that is more suitable for the error characteristic mode of each area, which is expressed as follows:

$$\begin{cases} g = \text{sgn}(e) \cdot G, |e| \geq E_1, \\ g = K_{P1} \cdot e + K_{D1} \cdot \hat{e}, |e| < E_1 \cap |e| \geq E_2, \\ g = K_{P2} \cdot e + K_{D2} \cdot \hat{e}, |e| < E_2 \cap |\hat{e}| \geq \hat{E}_1, \\ g = K_{P3} \cdot e + K_{D3} \cdot \hat{e}, |e| < E_2 \cap |\hat{e}| < \hat{E}_1 \cap |e| > E_3 \cap |\hat{e}| > \hat{E}_2, \\ g = g_{n-1}, |e| \leq E_3 \cap |\hat{e}| < \hat{E}_2, \end{cases} \quad (2)$$

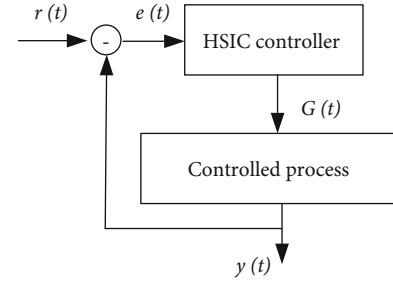


FIGURE 3: HSIC control process model.

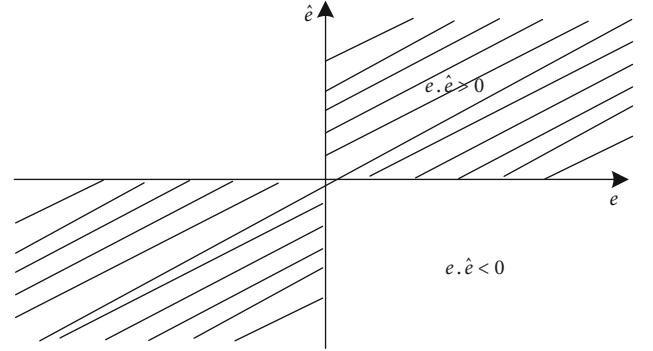


FIGURE 4: Error phase plane.

where  $E_1, E_2, E_3, \hat{E}_1$ , and  $\hat{E}_2$  are the different characteristic thresholds of process error and its rate of change, respectively. The control parameters to be set are  $K_{P1}, K_{D1}, K_{P2}, K_{D2}, K_{P3}$ , and  $K_{D3}$ , where  $g_{n-1}$  is the output value of the previous control cycle of controller.

## 4. Intelligent Control Strategy Based on Improved PSO Algorithm

**4.1. Standard Particle Swarm Optimization Algorithm.** The particle swarm optimization algorithm is an optimization algorithm based on iterative mode. It is a group of  $m$  particles flying at a certain speed in the  $D$  dimensional search space. When each particle searches, it considers the best historical point it has searched and the historical best point of other particles in the group and changes its position on this basis. The  $j$  particle of the particle swarm is composed of 3  $H$  dimensional vectors:

Current position

$$x_j = (x_{j1}, x_{j2}, \dots, x_{jH}). \quad (3)$$

Best location in history

$$l_j = (l_{j1}, l_{j2}, \dots, l_{jH}). \quad (4)$$

Speed

$$v_j = (v_{j1}, v_{j2}, \dots, v_{jH}), \quad (5)$$

where  $j = 1, 2, \dots, m$ . Currently, location is regarded as a coordinate describing a point in space. In each iteration of

Parameter meaning:

Initialize the particle swarm, including randomly generating  $m$  particles in space  $R^n$ ; setting: search space dimension  $n$ , particle swarm size  $m$ , learning factors  $c_1$  and  $c_2$ , inertia weight coefficients  $\omega_{\max}^0$  and  $\omega_{\min}^0$  and the maximum number of iterations  $t_{\max}$ . The current number of iterations is 1, the coding method forms a population matrix and a particle velocity change matrix;

Begin

1. For  $t=0, t=t+1$  Do
  2. Update the inertia weight coefficient and calculate the fitness of each particle;
  3. Genetic manipulation produces next-generation particles;
  4. Update the individual extreme value of particle;
  5. Update the global extremum of the population;
  6. Generate new populations.
  7. End
  8. If the set conditions are met, the search will stop and results will be output
- End

ALGORITHM 1: Pseudocode of IPSO algorithm.

algorithm, the current position  $x_j$  is evaluated as the problem solution. If the current position  $l_j$  is better than the historical optimal position, then the current position replaces the vector  $l_j$ . In addition, the best position found so far in the entire particle swarm is recorded as the vector  $l_b = (l_{b1}, l_{b2}, \dots, l_{bH})$ .

For each particle, the change of its first dimension ( $1 \leq h \leq H$ ) is as follows:

$$\begin{cases} v_{jh} = \omega \cdot v_{jh} + c_1 \cdot \text{rand}() \cdot (l_{jh} - x_{jh}) + c_2 \cdot \text{rand}() \cdot (l_{bh} - x_{jh}), \\ x_{jh} = x_{jh} + v_{jh}, \end{cases}$$

$$\omega = \omega_{\max} - \frac{t}{t_{\max}} (\omega_{\max} - \omega_{\min}), \quad (6)$$

where  $\omega$  is the inertia weight,  $\omega_{\max}$  and  $\omega_{\min}$  are the maximum and minimum inertia weights,  $t_{\max}$  is the maximum number of iterations to run,  $c_1$  and  $c_2$  are the learning factors, and  $\text{rand}()$  is a random function with a value in the range of  $[0,1]$ . The particle speed is limited to a range  $[V_{\max}, V_{\min}]$ , that is, after the speed update formula is executed, we get the following:

$$\begin{cases} \text{if } v_{jh} < V_{\min} \text{ then } v_{jh} = V_{\min}, \\ \text{if } v_{jh} > V_{\max} \text{ then } v_{jh} = V_{\max}. \end{cases} \quad (7)$$

**4.2. Control Parameter Optimization.** There are only  $\kappa, K_p, K_D$ , and other control parameters in the above HSIC algorithm. Parameter optimization is relatively simple, and manual tuning can generally be used in engineering based on control experience [29]. However, for multimodal control algorithms, due to the numerous control parameters, it is difficult to tune the optimal control parameters using manual methods. Therefore, it is necessary to study the method of optimization and setting of control parameters [30].

It is due to the fast convergence speed of particle swarm algorithm and the strong generality of algorithm. However, there are also shortcomings such as low search accuracy, premature convergence, and low later iteration efficiency

[31]. To this end, based on genetic ideas, an Improved Particle Swarm Optimization (IPSO) is proposed. The basic idea is as follows: based on genetic algorithm (GA), it is easy to perform cross-mutation operations and improve the search ability in a wide space, so that the global optimal solution can be efficiently searched. In the iterative process, IPSO can increase diversity of particles with the help of genetic crossover operations, thereby speeding up the convergence speed of particles and avoiding the premature phenomenon of local optimum. Moreover, the global and local search capabilities are determined by the inertia weight  $\omega$ . In order to improve the convergence performance of original algorithm, the inertia weight is realized by a nonlinear decreasing method, and the inertia weight is selected as follows:

$$\omega_i = (\omega_{\max}^0 - \omega_{\min}^0) \cdot \left( \frac{t_i}{t_{\max}} \right)^2 + (\omega_{\max}^0 - \omega_{\min}^0) \cdot \left( \frac{2t_i}{t_{\max}} \right) + \omega_{\max}^0, \quad (8)$$

where  $t_i$  is the current iteration algebra, respectively; since the inertia weight is changing,  $\omega_{\max}^0$  and  $\omega_{\min}^0$ , respectively, represent the maximum and minimum values of the initial inertia weight. It can be seen that in the iteration, the inertia weight coefficient appears to be nonlinearly decreasing. Thus, a balanced global and local search capability can be obtained.

In summary, the pseudocode of IPSO algorithm is shown in Algorithm 1.

## 5. Results

In the experiment, proposed control strategy is researched based on MATLAB simulation platform. The parameter settings of IPSO are as follows:  $\omega_{\max}^0$  and  $\omega_{\min}^0$  are 1.4 and 0.5, respectively, the learning factor  $c_1 = c_2 = 1.1$ , the maximum number of particle swarms is 100, and the maximum number of iterations is 800.

**5.1. Parameter Tuning.** Compare the two control strategies to determine the optimal strategy parameter settings. The control parameters  $K_p, K_I$ , and  $K_D$  of control strategy 1

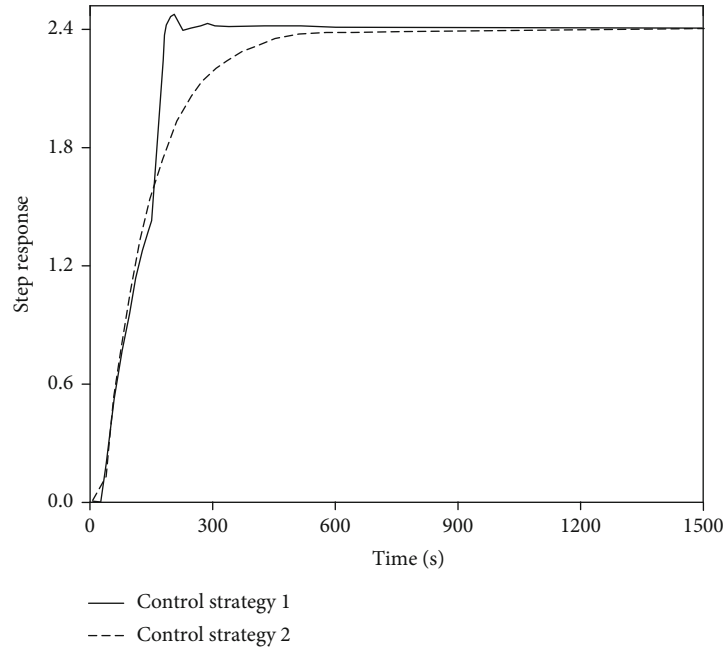


FIGURE 5: Comparison of process response curve.

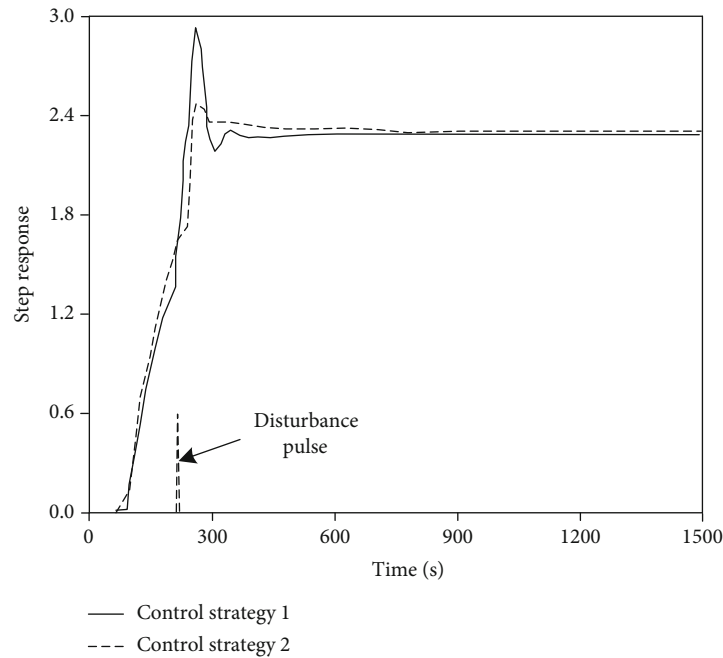


FIGURE 6: Comparison of response under pulse interfering.

are 0.398, 0.002, and 3.240, respectively; the control parameters  $K_{P1}$ ,  $K_{D1}$ ,  $K_{P2}$ ,  $K_{D2}$ ,  $K_{P3}$ , and  $K_{D3}$  of control strategy 2 are 6.340, 8.854, -6.707, 0.148, 26.486, and 3.053, respectively.

The simulation process control uses unit step input. Under the control of the two algorithms, the step response is shown in Figure 5.

It can be seen from Figure 5 that the two control strategies can make the intelligent optimization system of flue gas in municipal solid waste incineration reach a stable state. Among them, control strategy 1 has overshoot and oscilla-

tion, which is not desirable. On the contrary, control strategy 2 does not have overshoot and oscillation, has better control quality, and is obviously more suitable for the application of the treatment process of secondary pollution in the flue gas.

To investigate the influence of external disturbances on the process, we can start from analyzing the anti-interference performance of control strategy. Assuming that the two control strategies both impose a disturbance pulse at  $t = 150$  s, with an amplitude of 0.5 and a width of 10 s, the response curve of process is shown in Figure 6.

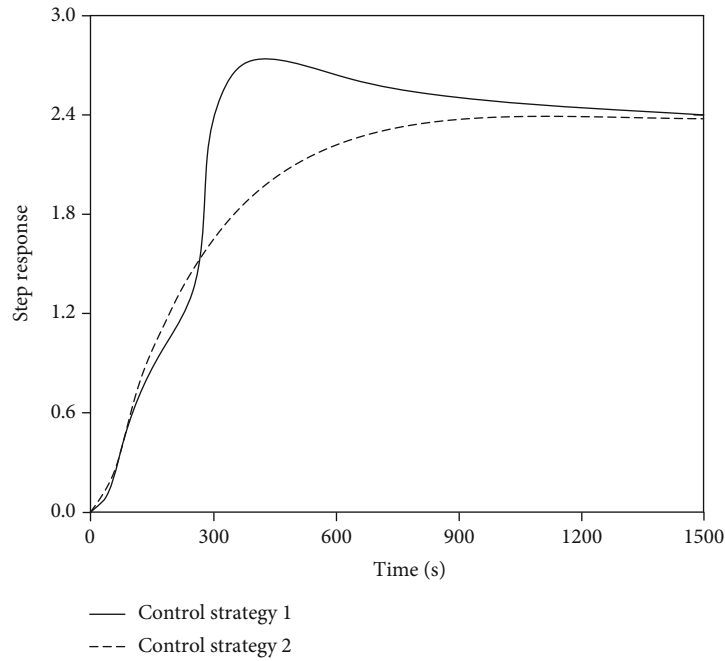


FIGURE 7: Comparison of process response at  $\tau = 160$  s.

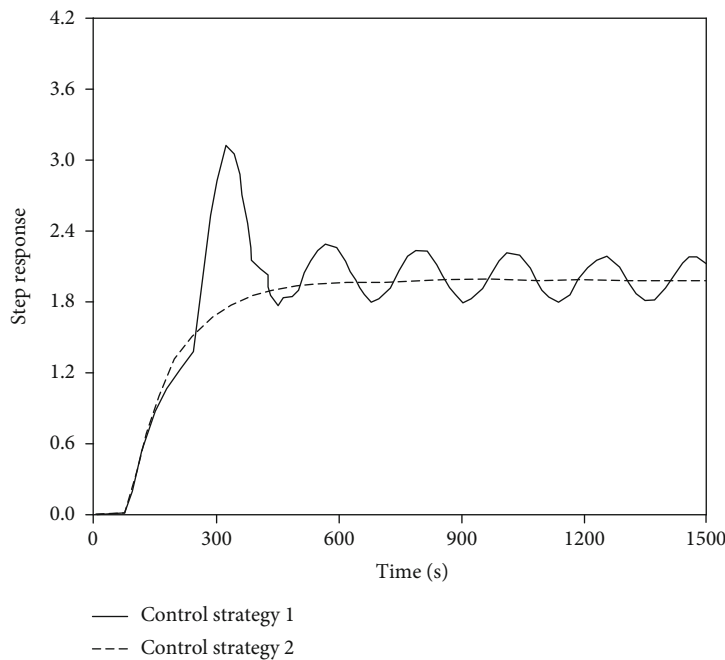


FIGURE 8: Comparison of process response at  $\tau = 160$  s.

As can be seen from Figure 6, the simulation response curves of these two control strategies have overshoot. However, the overshoot and oscillation amplitude of control strategy 1 is large, and the oscillation frequency is relatively high. Obviously, the anti-interference performance of control strategy 2 is better. Considering the influence of process internal parameter disturbance on the process, the robustness analysis of control strategy can be carried out. If it is robust, then control strategy 2 is preferable.

When the time constant changes from  $T = 75$  s to  $T = 160$  s, the step response curve of process is shown in Figure 7.

It can be seen from Figure 7 that the control strategy 1 obviously has a large overshoot, and the adjustment time to reach a steady state is long. Control strategy 2 does not produce overshoot, the process response is very stable, and the control effect on process is obvious. Thus, control strategy 2 exhibits strong robust performance.



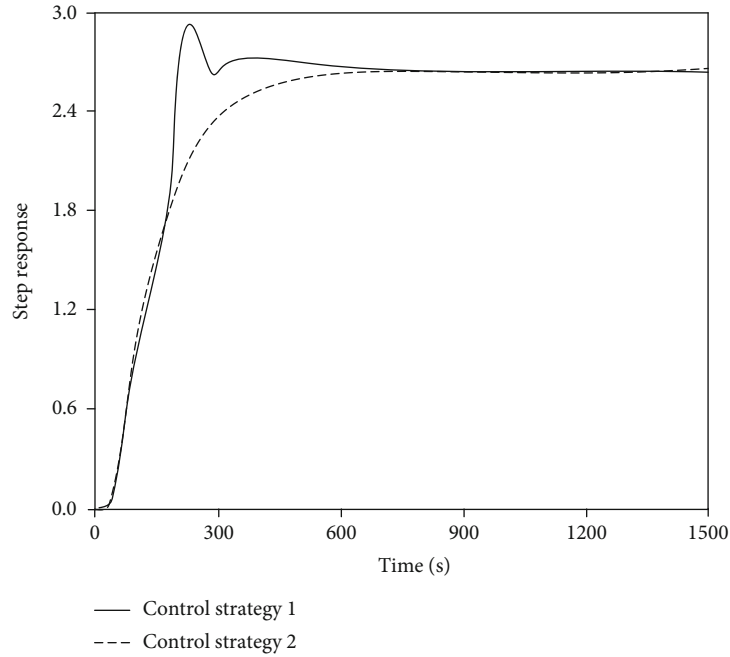


FIGURE 9: Comparison of response adding an inertia node.

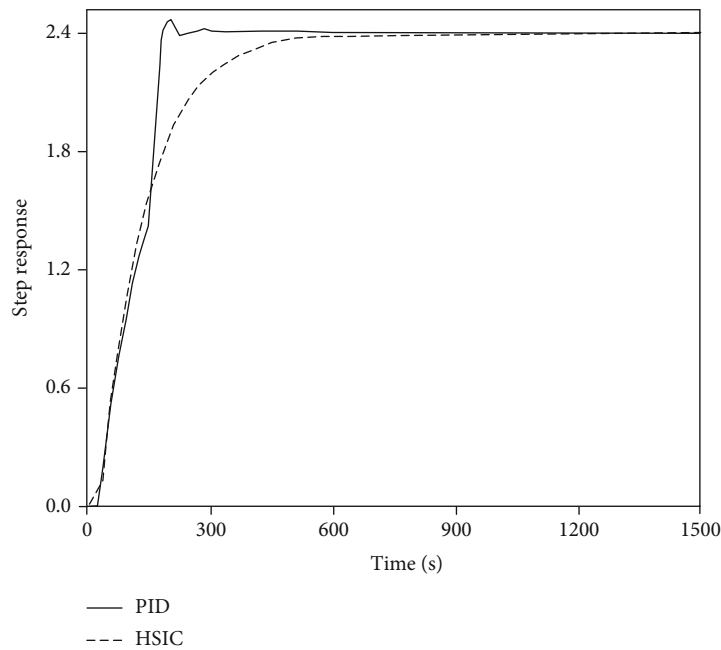


FIGURE 10: Comparison results of step response curves.

The time delay parameter changes from  $\tau = 20$  to  $\tau = 60$ , and the process response curve is shown in Figure 8.

It can be seen from Figure 8 that the control strategy 1 produces a large overshoot and a strong oscillation. The oscillation frequency is high, and the process cannot reach the desired steady state at all. Therefore, it must not be used for process control in this case. Control strategy 2 has no overshoot, the process response is very stable, and the control effect on the process is obvious. Even when the delay parameter is increased by 3 times, the control strategy 2 still

shows very strong robust performance and excellent control quality. In control engineering, this is very valuable.

When an inertia link is added to the original process model, when the process model becomes  $G_1(s) = 7.8125 e^{-20s} / (74s + 1)(5s + 1)$ , the process response curve is shown in Figure 9.

It can be seen from Figure 9 that the control strategy 2 has better control quality than the control strategy 1, the process response is stable, the response rise time is fast, the adjustment time is short, and the stable state can be reached

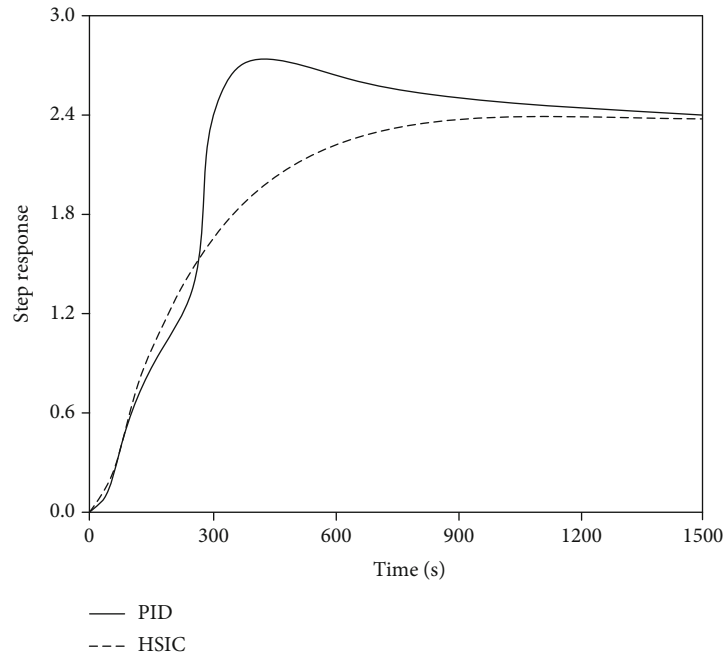


FIGURE 11: Comparison results of response with time constant change.

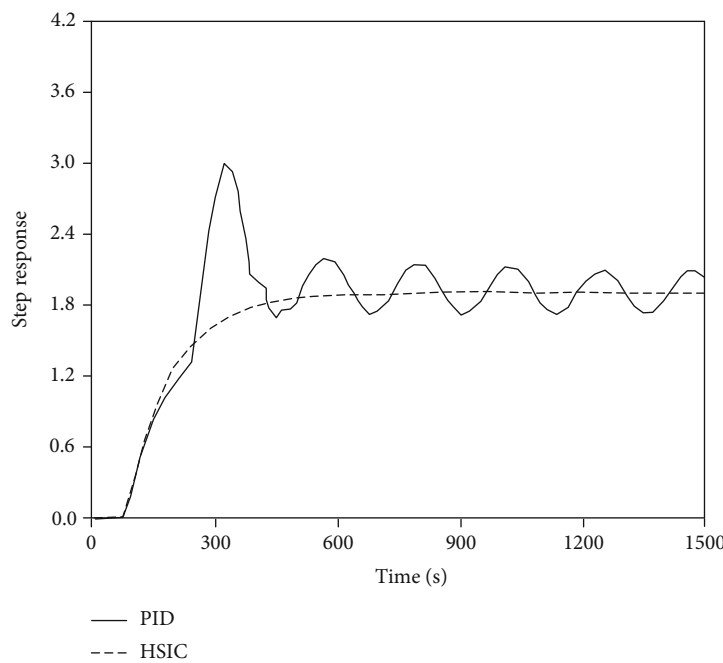


FIGURE 12: Comparison results of process response at  $\tau = 50$  s.

relatively quickly. Control strategy 1 produces severe overshoot and oscillation, which is undesirable.

*5.2. Comparison with PID Control Algorithm.* In order to demonstrate the performance of proposed HSIC control algorithm, it is compared and analyzed with PID control algorithm. It can be determined that the three parameters of PID control algorithm are  $K_P = 0.398$ ,  $K_I = 0.002$ , and  $K_D = 3.240$ ; the six parameters of HSIC control algorithm

are  $K_{P1} = 6.340$ ,  $K_{D1} = 8.854$ ,  $K_{P2} = -6.707$ ,  $K_{D2} = 0.148$ ,  $K_{P3} = 26.486$ , and  $K_{D3} = 3.053$ . In the process, the step response of these two algorithms is shown in Figure 10 under the action of a step excitation with an input amplitude of 3.

It can be seen from Figure 10 that PID control algorithm has overshoot and oscillation. However, the proposed HSIC algorithm does not have oscillation and overshoot. Obviously, HSIC is better than PID control.

Considering the perturbation of internal parameters process, if the time constant changes from  $T = 75$  s to  $T = 160$  s and the input amplitude is 3 step response in the process, the process step response curves of these two algorithms are shown in Figure 11.

It can be clearly seen from Figure 11 that PID control algorithm takes a long time to reach a steady state and has a large overshoot. The HSIC control algorithm process response is very stable without overshooting, showing strong robust performance.

When the time delay parameter changes from  $\tau = 20$  to  $\tau = 60$ , the process step response curves of these two algorithms are shown in Figure 12 under the action of a step excitation with an input amplitude of 3 in the process.

It can be seen from Figure 12 that the process step response curve of PID control algorithm produces a large overshoot and a strong oscillation with a high oscillation frequency. It is impossible to control to a stable desired state. The HSIC control process responds very smoothly, and there is no overshoot. The response curve shows that even when the time delay parameter is increased by 3 times, HSIC control still shows strong robustness and excellent control quality.

## 6. Conclusion

Waste incineration is an ideal method for harmlessness, reduction, and recycling of municipal solid waste, but the temperature control of incineration process is extremely critical. Existing strategies have poor control effects and are prone to secondary pollution of flue gas. Therefore, this paper proposes an intelligent optimization control strategy for secondary pollution of flue gas in municipal solid waste incineration. HSIC algorithm is proposed by combining the control difficulties and cybernetic characteristics of waste incineration. Moreover, IPSO is used to optimize the parameter settings in HSIC algorithm to achieve optimal temperature control during the incineration process and reduce the secondary pollution of flue gas. Experimental demonstration based on MATLAB simulation platform shows that the control performance of proposed strategy is the best when  $K_{P1}$ ,  $K_{D1}$ ,  $K_{P2}$ ,  $K_{D2}$ ,  $K_{P3}$ , and  $K_{D3}$  of HSIC algorithm are set to 6.340, 8.854, -6.707, 0.148, 26.486, and 3.053, respectively. Besides, when the delay parameters and time constant change greatly and there is a large disturbance, the process response is fast and stable, which is better than PID control strategy. Thus, it is feasible, reasonable, and usable to use the optimized HSIC algorithm for temperature control in the incineration process.

Domestic awareness and systems regarding waste sorting and disposal are not perfect, and there are many types of waste, which will result in low-quality waste that can be used for incineration. In the next study, a control strategy will be designed for different types of waste to achieve intelligent temperature control, so as to achieve high-quality incineration of waste and ensure that it will not cause secondary pollution.

## Data Availability

The data included in this paper are available without any restriction.

## Conflicts of Interest

The author declares that there is no conflict of interest regarding the publication of this paper.

## References

- [1] M. Held, O. Flardh, and J. Martensson, "Optimal speed control of a heavy-duty vehicle in urban driving," *IEEE Transactions on Intelligent Transportation Systems*, vol. 20, no. 4, pp. 1562–1573, 2019.
- [2] J. L. Li, T. S. Zhang, X. Liang, J. H. Zhang, H. L. Shu, and Z. Zhang, "Influencing factors of organic carbon accumulation in black shale of marine sedimentary environment: a case study in the northern part of Yunnan-Guizhou area, China," *Fresenius Environmental Bulletin*, vol. 29, no. 4, pp. 30–38, 2020.
- [3] K. K. Obrou, E. J. Vl, T. Moravcová, K. V. Blah, and P. Fojtík, "Numerical modeling of batch formation in waste incineration plants," *Polish Journal of Chemical Technology*, vol. 17, no. 1, pp. 1–6, 2015.
- [4] A. Hakki, K. Ali, H. Ibrahim et al., "Evaluation of phenology, growth, yield and technological characteristics of some winter green lentil (*Lens culinaris* Medik.) genotypes grown under Mediterranean environment," *Fresenius environmental bulletin*, vol. 28, no. 7, pp. 34–44, 2019.
- [5] T. Ertugrul and I. Hasan, "Antibiotic resistance genes of *Escherichia coli* in coastal marine environment of eastern Black Sea, Turkey," *Fresenius Environmental Bulletin*, vol. 28, no. 2A, p. 56, 2019.
- [6] D. Wan, Q. Li, Y. Liu, S. H. Xiao, and H. J. Wang, "Simultaneous reduction of perchlorate and nitrate in a combined heterotrophic-sulfur-autotrophic system: secondary pollution control, pH balance and microbial community analysis," *Water Research*, vol. 165, no. 11, pp. 115004–115011, 2019.
- [7] Y. Liu, S. Xie, Y. Li, and Y. S. Liu, "Novel mercury control technology for solid waste incineration:(STS) as mercury capturing agent," *Environmental Science & Technology*, vol. 41, no. 5, pp. 1735–1739, 2007.
- [8] Q. Li, J. Wu, and H. Wei, "Reduction of elemental mercury in coal-fired boiler flue gas with computational intelligence approach," *Energy*, vol. 160, no. OCT.1, pp. 753–762, 2018.
- [9] W. H. Gui, W. C. Yue, and Y. F. Xie, "A review of intelligent optimal manufacturing for aluminum reduction production," *Zidonghua Xuebao/Acta Automatica Sinica*, vol. 44, no. 11, pp. 1957–1970, 2018.
- [10] Q. Guo, H. Cai, Y. Wang, and W. Chen, "Distributed secondary voltage control of islanded microgrids with event-triggered scheme," *Journal of Power Electronics*, vol. 17, no. 6, pp. 1650–1657, 2017.
- [11] J. Kim and J. Y. Lee, "Mitigation of inhibition effect of acid gases in flue gas using trona buffer for autotrophic growth of *Nannochloris* sp.," *Biochemical Engineering Journal*, vol. 117, no. 7, pp. 15–22, 2017.
- [12] S. Stucki, M. Schaub, G. Doka et al., "Integral assessment of a new process for waste incineration with optimized material recovery," *Journal of Agricultural and Resource Economics*, vol. 27, no. 2, pp. 433–449, 2003.
- [13] H. R. Marzban and H. Pirmoradian, "A direct approach for the solution of nonlinear optimal control problems with multiple delays subject to mixed state-control constraints," *Applied mathematical modelling*, vol. 53, no. 5, pp. 189–213, 2018.

- [14] T. Nkaya and M. Akansel, "Coordinated scheduling of the transfer lots in an assembly-type supply chain: a genetic algorithm approach," *Journal of Intelligent Manufacturing*, vol. 28, no. 4, pp. 1–11, 2017.
- [15] P. Frugier, N. Godon, and E. Vernaz, "Influence of composition variations on the initial alteration rate of vitrified domestic waste incineration fly-ash," *Waste Management*, vol. 22, no. 2, pp. 137–142, 2020.
- [16] T. Washizu, T. Nagasaka, and M. Hino, "Viscosity of liquid Fe-Cu-Si alloy formed in new melting process for domestic waste incineration residue," *Materials Transactions*, vol. 42, no. 3, pp. 471–477, 2001.
- [17] A. N. Tugov, V. F. Moskvichev, G. A. Ryabov, V. I. Ugnachev, A. N. Smirnov, and Y. V. Petrov, "Experience gained from making the incineration of solid domestic wastes a factory standard at thermal power stations in Russia," *Thermal Engineering*, vol. 53, no. 7, pp. 552–558, 2006.
- [18] H. Guo, B. Bi, R. Dong, Z. B. Ding, X. Z. Zhao, and X. Y. Lian, "Study on drying of island domestic waste and dechlorination of flue gas by shells," *IOP Conference Series: Earth and Environmental Science*, vol. 252, no. 4, pp. 024–035, 2019.
- [19] J. Li, "The Key to Avoiding Secondary Pollutants in the Incineration of Domestic Waste Lies in Prevention," *Procedia Environmental Sciences*, vol. 16, no. 1, pp. 669–673, 2012.
- [20] Z. Han, D. Zeng, G. Shi, L. Shen, W. Xu, and Y. Xie, "Characteristics and management of domestic waste in a rural area of the Tibetan Plateau," *Journal of the Air & Waste Management Association*, vol. 65, no. 11, pp. 1365–1375, 2015.
- [21] W. L. Wang, "Advantage and disadvantage of waste incinerator burning domestic waste with medical waste:taking Shanghai Yuqiao domestic waste incineration plant as an example," *Environmental Sanitation Engineering*, vol. 21, no. 2, pp. 18–20, 2013.
- [22] K. Hideaki, "Disposal and movement of domestic waste in Nagano Prefecture," *Annals of the Association of Economic Geographers*, vol. 48, no. 1, pp. 71–89, 2002.
- [23] K. Lu, J. Hu, J. Huang, D. Tian, and Z. Chao, "Optimisation model for network progression coordinated control under the signal design mode of split phasing," *IET Intelligent Transport Systems*, vol. 11, no. 8, pp. 459–466, 2017.
- [24] I. Nielsen, Q. V. Dang, G. Bocewicz, and Z. Banaszak, "A methodology for implementation of mobile robot in adaptive manufacturing environments," *Journal of intelligent manufacturing*, vol. 28, no. 5, pp. 1171–1188, 2017.
- [25] S. Wang, J. Yu, X. Qiu, M. Pawelczyk, A. Shaid, and L. Wang, "Active sound radiation control with secondary sources at the edge of the opening," *Applied Acoustics*, vol. 117, no. 4, pp. 173–179, 2017.
- [26] Z. Zhang and L. Jia, "Optimal feedback control of pedestrian counter flow in bidirectional corridors with multiple inflows," *Applied Mathematical Modelling*, vol. 90, no. 2, pp. 474–487, 2021.
- [27] J. Liu, X. Luo, S. Yao, Q. G. Li, and W. S. Wang, "Influence of flue gas recirculation on the performance of incinerator-waste heat boiler and NO<sub>x</sub> emission in a 500 t/d waste-to-energy plant," *Waste Management*, vol. 105, no. 4, pp. 450–456, 2020.
- [28] S. Y. Kang, H. U. Shin, S. M. Park, and L. Kyo-Beum, "Optimal voltage vector selection method for torque ripple reduction in the direct torque control of five-phase induction motors," *Journal of Power Electronics*, vol. 17, no. 5, pp. 1203–1210, 2017.
- [29] L. M. Abaecherli, E. Capón-García, A. Szijarto, and K. Hungerbühler, "Optimized energy use through systematic short-term management of industrial waste incineration," *Computers & Chemical Engineering*, vol. 104, pp. 241–258, 2017.
- [30] G. Fraysse, D. Venditti, and S. Durecu, "An innovative injection device to enhance NO<sub>x</sub> abatement by SNCR in waste combustion flue-gases," *High temperature materials and processes*, vol. 27, no. 5, pp. 383–390, 2008.
- [31] S. A. Mansouri, D. Gallear, and M. H. Askariazad, "Decision support for build-to-order supply chain management through multiobjective optimization," *International Journal of Production Economics*, vol. 135, no. 1, pp. 24–36, 2012.

## Research Article

# Microgrid Data Security Sharing Method Based on Blockchain under Internet of Things Architecture

Jian Shang <sup>1,2</sup>, Runmin Guan,<sup>2</sup> and Yuhao Tong<sup>2</sup>

<sup>1</sup>Hohai University, College of Computer and Information, Jiangsu, Nanjing 211100, China

<sup>2</sup>Jiayuan Technology Co. Ltd., Division of Research and Innovation, Jiangsu, Nanjing 211100, China

Correspondence should be addressed to Jian Shang; shangjian@jiyuantech.com

Received 18 January 2022; Revised 2 March 2022; Accepted 7 March 2022; Published 4 April 2022

Academic Editor: Shalli Rani

Copyright © 2022 Jian Shang et al. This is an open access article distributed under the Creative Commons Attribution License, which permits unrestricted use, distribution, and reproduction in any medium, provided the original work is properly cited.

The efficient and secure data sharing mechanism can support the microgrid to achieve more accurate business control, while the current data processing methods have the problems of large computing overhead and low data sharing security. Aiming at the current problems, this paper proposes a microgrid data sharing method based on blockchain technology based on the processing mode of cloud-edge-terminal architecture. Firstly, the elliptic curve encryption algorithm is used on the edge side to encrypt the data collected by the terminal equipment reliably, so as to improve the security and efficiency of microgrid key management. Then, in the cloud, the Reputation-Evaluation Practical Byzantine Fault Tolerant mechanism (REPBFT) based on smart contract and reputation evaluation can effectively manage the data sharing of edge computing devices, avoid the waste of network computing resources, and further improve the efficiency of microgrid data sharing. The simulation results show that when the number of edge devices reaches 25, the calculation and communication overhead of the proposed method are 63.46 ms and 2.66 KB, respectively, and when the processing data reaches 1024 KB, the security of the microgrid system is still 95%, which can realize safe and reliable data sharing and interaction, and can stably support the optimal operation of the microgrid.

## 1. Introduction

Microgrid aims to promote the consumption of renewable energy and realize multisource power supply for load [1, 2]. Since most distributed generators are closer to the load side, their power supply flexibility and efficiency will be greatly improved, making the power grid operation more efficient and rich [3].

In order to maximize the advantages of renewable energy, the energy interaction between microgrids has developed into a popular method [4]. However, the effectiveness of energy interaction between microgrids largely depends on the authenticity of power generation and consumption information, as well as the efficiency and security of energy transactions [5]. Therefore, it is of great significance to study the efficient and secure data processing between microgrids.

The traditional microgrid adopts centralized operation mode and symmetric encryption algorithm to realize data management and credibility operation, but the data has the

risk of being copied and leaked by third-party institutions [6]. In addition, the symmetric encryption algorithm will consume a lot of computing memory in the process of key operation, which is difficult to achieve efficient and reliable data sharing.

The development of blockchain provides a new idea for efficient and reliable interaction of microgrid data [7, 8]. The blockchain generates data into blocks according to the sequence of data time scales and adopts cryptography to ensure that the data cannot be tampered with, so as to realize the security management of massive data [9]. However, it should be pointed out that although the traditional blockchain data processing method can improve the security of data storage to a certain extent, there are few corresponding studies on the efficiency of micro grid data sharing [10], which cannot meet the requirements of safe and efficient data sharing among micro grid groups.

Aiming at the current problems, this paper proposes a microgrid data sharing method based on blockchain based

on the cloud edge collaborative processing mode. The main innovations of the article are as follows:

In order to meet the efficient and fast requirements of microgrid data sharing, this paper uses the elliptic curve encryption algorithm (ECC) to ensure the friendly interaction between microgrid terminal equipment and edge computing devices and improve the security of microgrid data while alleviating the pressure of key management and reducing the system computing overhead.

The collaborative strategy of cloud side interaction is adopted to realize the interoperability and convenience of data sharing between edge computing devices based on cloud smart contract, and Reputation-Evaluation Practical Byzantine Fault Tolerant mechanism (REPBFT) is introduced to complete data information evaluation, which can improve the data processing efficiency of microgrid and ensure the security and credibility of data sharing.

## 2. Related Research

Microgrid generally consists of distributed power sources such as wind power and photovoltaic, energy storage system, and micropower supply system composed of multicategory loads [11]. Microgrid data has the characteristics of multi-source heterogeneity and large quantity. The attribute characteristics of different business data are different, including structured data such as state, electrical, simulation and operation, and semistructured data related to the physical information model [12].

For system controllability, the more reliable the collected data is, the more stable the system operation is [13]. Microgrid system realizes the friendly interaction between source network load and storage through interactive sharing of multidimensional and multi service data and data analysis and fusion based on big data and artificial intelligence algorithms [14]. Therefore, safe and reliable microgrid data sharing is particularly important for users' high-quality power supply and the safe and stable operation of the power grid.

At present, most of the power grid data management adopts the traditional power grid centralized management. Reference [15] proposed a cloud based energy management system to realize microgrid data interaction to realize the optimal operation of low-cost system, but the system may be attacked and lead to data leakage, and the measures only stay at the theoretical level. Reference [16] proposed a privacy protection multiauthority attribute-based smart grid data sharing scheme. The essence of the scheme is centralized computing and processing mode, which has the problem of low encryption efficiency. Therefore, it can be seen that the centralized data sharing interaction mode has been difficult to support the optimal operation of microgrid.

As a popular technology in recent years, blockchain realizes the secure and trusted storage and processing of user data sets by combining database consistency mechanism and cryptography. Reference [17] constructs an encrypted data storage and sharing architecture based on threshold proxy reencryption and blockchain consensus algorithm to meet a wide range of data access requirements. Reference [18] integrates fair data delivery into the phased data deliv-

ery protocol in the blockchain consensus process, avoiding third-party data processing and realizing safe data sharing. At the same time, the immutable recording characteristics of blockchain guarantee transactions also provide a new idea for the safe processing of microgrid data [19, 20]. Reference [21] uses blockchain to build a secure and transparent power grid operation allocation model to resist malicious attacks against microgrid; reference [22] realizes continuous monitoring and analysis of materials by integrating audit mechanism and blockchain into the material management and control system of electric power company; reference [23] realizes data analysis of energy management system based on blockchain and reinforcement learning, which can detect improper energy use behavior and improve energy output efficiency; reference [24] reduces the total cost of energy consumption by implementing independent monitoring of intelligent devices and power consumption billing through smart contracts. However, the above reference only analyzes the application security of blockchain in the power grid business scenario, not from the perspective of data sharing security and efficiency trade-off. There is also the problem of uneven distribution of network computing resources, which is difficult to support the stable and reliable operation of microgrid.

To solve this problem, this paper introduces edge computing technology and REPBFT mechanism into the microgrid data security sharing method to support accurate state analysis and fast action execution of the microgrid system.

## 3. Proposed Method

*3.1. Overall Architecture of Microgrid Data Security Sharing.* The overall architecture of microgrid data security sharing adopts the data communication mode of cloud side cooperation, as shown in Figure 1. In other words, the edge layer realizes the effective collection of microgrid status data through terminal device registration and data encryption processing. At the same time, the edge layer data information is aggregated and uploaded to the cloud, which shares and accesses data based on smart contracts [25, 26].

*3.1.1. Terminal Equipment Layer: Edge Layer.* The edge computing device gathers real-time power data collected by terminal equipment such as smart meter, photovoltaic inverter, energy storage converter and wind power inverter. Through the method of "registration before encryption", secure and reliable data transmission between terminal equipment layer and edge layer equipment is realized, the credibility of information interaction between microgrid equipment is guaranteed, and the storage and sharing of multi-dimensional heterogeneous power data are realized.

*3.1.2. Edge Layer: Cloud Layer.* For the problem of "data island" in the microgrid cloud control center, the cloud-edge-terminal architecture mode and the data sharing and access control model based on smart contract are adopted to realize the stable data sharing between different edge computing devices.

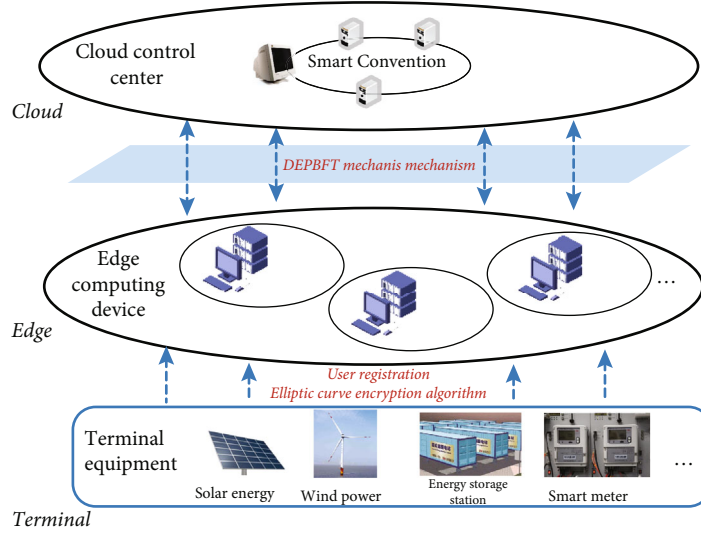


FIGURE 1: Microgrid data security sharing architecture.

**3.2. Terminal Equipment Layer: Edge Layer Equipment Data Acquisition and Encryption.** In order to ensure the trusted data interaction between microgrid devices, a trusted terminal device registration mechanism needs to be designed between edge computing devices and terminal devices. The asymmetric encryption algorithm is introduced into the data transmission at both ends to ensure the reliable and safe data collection.

The terminal equipment registration process is as follows:

- (1) The terminal device sends the public key and private information of the terminal device, such as physical address and identity information, to the edge computing device
- (2) After receiving the terminal device information and checking it, the edge computing device encrypts the public key of the terminal device with the private key of the edge computing device to form a digital signature sign and returns the sign to the terminal device
- (3) The terminal device uses its own public key and sign to create an account. Other terminal devices can verify the authenticity of the sign with the public key of the edge computing device, so as to ensure the authenticity of the account

After the terminal equipment completes registration and accesses the edge computing device, it enters the data acquisition stage. At the same time, for security reasons, this paper adds an encryption module for security authentication to the intelligent terminal equipment and edge computing device, realizes the security authentication mechanism through hardware encryption, and encrypts and decrypts the data, as shown in Figure 2.

In the traditional symmetric encryption algorithm, every time a pair of terminal devices use the encryption algorithm, they need to use the unique secret key that other terminals do not know, so that the sending and receiving ends have

a large number of keys, resulting in large key management overhead. The asymmetric encryption algorithm represented by elliptic curve encryption algorithm (ECC) uses different secret keys for encryption and decryption. One of the keys is encrypted [27], and the other is used for decryption. Each terminal device only needs to process a pair of keys, so as to reduce the corresponding key management burden and reduce the system computing overhead. The flow chart of asymmetric encryption algorithm is shown in Figure 3.

In this paper, the ECC encryption algorithm is used to realize data trusted processing. The encryption process is as follows:

- (1) Determine the finite field  $F_p$ , which has and has only  $p$  elements
- (2) Terminal equipment a selects elliptic curve  $E_p(a, b)$  in the finite field and takes a point on the elliptic curve as the base point  $D$
- (3) The terminal device a randomly selects a prime number between  $1 \sim p-1$  as the private key  $k$  and generates the public key  $K = kD$  according to the addition rule
- (4) Terminal equipment a transmits  $E_p(a, b)$  and points  $K$  and  $D$  to terminal equipment B
- (5) After receiving the information, terminal equipment B encodes the plaintext to be transmitted to a point  $H$  on  $E_p(a, b)$  and generates a random integer  $e$  ( $0 < e < 1$ )
- (6) Terminal equipment B calculation points  $C_1 = H + eK$ ,  $C_2 = eD$
- (7) Terminal equipment B transmits  $C_1$  and  $C_2$  to terminal equipment A
- (8) After receiving the information, terminal device A calculates  $C_1 \sim kC_2$ , determines point  $H$ , and then decodes point  $H$  to obtain plaintext

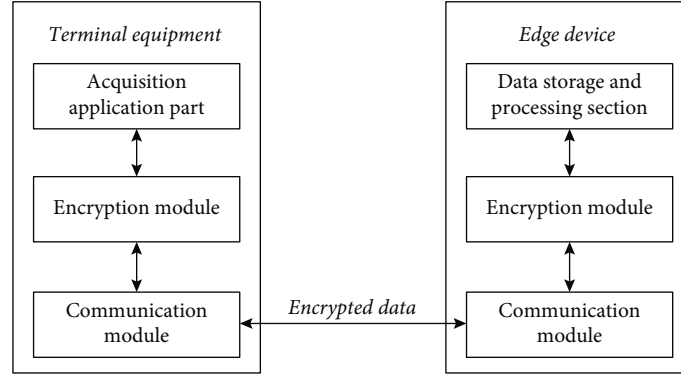


FIGURE 2: Encrypted communication mode between terminal equipment and edge computing device.

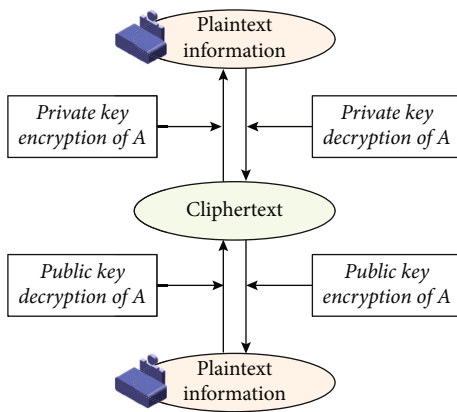


FIGURE 3: Asymmetric encryption algorithm flow.

In this process, the attacker can only obtain  $E_p(a, b)$ ,  $K$ ,  $D$ ,  $C_1$ , and  $C_2$ . It is very difficult to obtain  $k$  through  $K$  and  $D$  or  $e$  through  $C_2$  and  $D$ . It is difficult to steal the plaintext transmitted between terminal devices.

Figure 4 shows the encryption and decryption flow of the elliptic curve algorithm.

**3.3. Data Security Sharing.** It can be seen from the above analysis that the data of each downstream terminal device is stored in the microgrid edge computing device. Further, based on blockchain, this paper realizes the secure data sharing of microgrid in the mode of cloud-edge-terminal architecture.

Based on the cloud-edge-terminal architecture, the proposed data security sharing scheme links the adjacent edge computing devices into a private chain to realize the data sharing of terminal devices. The method includes the following entities: edge computing devices, terminal devices, private chains, and smart contracts for cloud control centers. As shown in Figure 5, the data security sharing scheme is divided into two modules according to functions. The left is the data sharing model, and the right is the blockchain. The data sharing model supports the storage of the blockchain, and the blockchain supports the security protection of the data sharing model. The microgrid user transmits

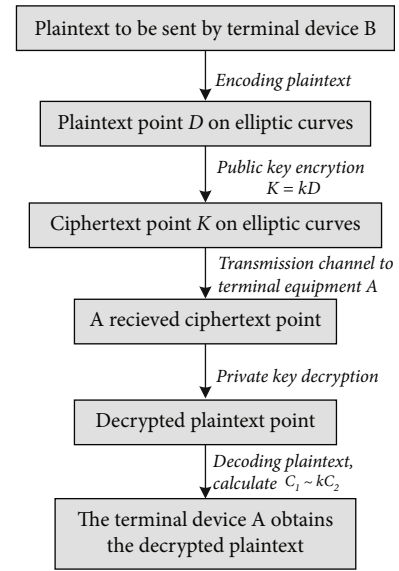


FIGURE 4: ECC encryption process.

the storage request to the edge computing device through the terminal device, and the process is recorded in the blockchain.

In this paper, offchain storage is used, only the user name, user address, and recorded information are stored in the block, the collected original microgrid data is stored in the storage node of the edge computing device, and the ECC algorithm described above is used to encrypt the data.

The steps of data sharing are as follows:

- (1) Register edge computing devices and terminal devices, and the system does not allow unregistered edge computing devices and terminal devices to join data sharing
- (2) The registered terminal device initiates a data storage request to the edge computing device and uploads its own data to the edge computing device through the encryption mechanism proposed above
- (3) The edge computing device 1 publishes the data to the smart contract through the private chain on



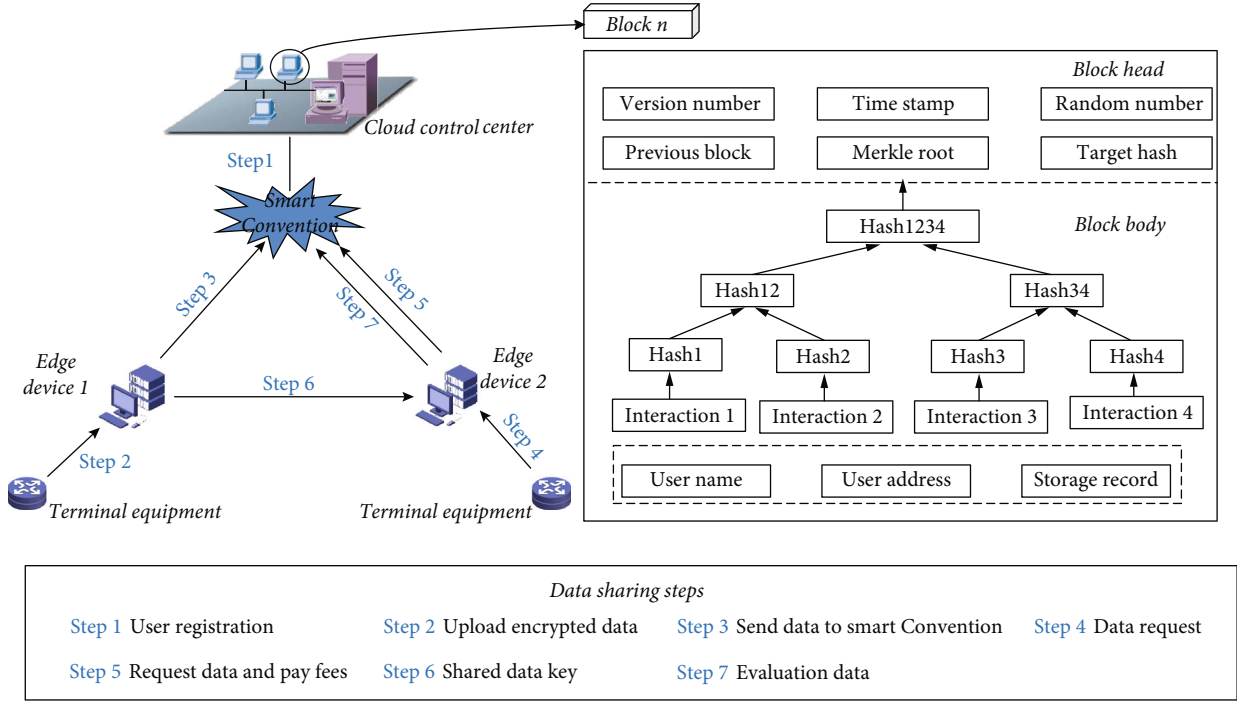


FIGURE 5: Model diagram of data sharing system.

behalf of the terminal device, so that the terminal device can request and retrieve the data information

- (4) If the terminal equipment downstream of the edge computing device 2 requires shared data, it is necessary to initiate a request for shared data
- (5) The edge computing device 2 requests the key of encrypted data from the smart contract on behalf of the terminal device
- (6) The edge computing device 1 sends the key of the encrypted data to the edge computing device 2, so that the edge computing device 2 obtains the permission to access the data, and encrypts and transmits the data to its downstream terminal device
- (7) The terminal equipment will evaluate the shared data, and the system will also check the evaluation to prevent abnormal evaluation

**3.3.1. Consensus Mechanism for Block Generation.** This paper uses the consensus mechanism based on REPBFT to evaluate the trusted data sharing process between edge computing devices. The credit evaluation algorithm in REPBFT is mainly composed of reward mechanism and punishment mechanism. The credit value is mainly used as a reference for preferentially responding to the request of the edge computing device. The rewards include the following: actively initiating change messages, reporting and sending false information, and contributing idle computing power; Penalties include the following: sending false messages and falsely accusing other edge computing devices, as shown under the credit evaluation algorithm.

Among them,  $w_1$ ,  $w_2$ , and  $w_3$  are the parameters of reward mechanism, and  $v$  is the parameters of punishment mechanism. The calculation formula is as follows:

$$w_1(T, L, O) = \alpha \frac{O_i}{e^{L_{ij} T^2}}, \quad (1)$$

$$w_2(T, L, O) = \alpha \frac{O_i}{e^{L_{ij} F^2}}, \quad (2)$$

$$w_3(L, O_i, N_i) = \alpha \frac{N_i}{e^{L_{ij} O_i}}, \quad (3)$$

$$v(F, L, O_i) = -\beta \frac{O_i}{e^{L_{ij} F^2}}, \quad (4)$$

where  $\alpha$  is the system reward coefficient,  $\beta$  is the system penalty coefficient,  $T$  is the real message level, and  $F$  is the level of false information. When  $V_i$  sends the data information  $M_{V_i}$  to the system,  $V_i$  can first obtain the reward for actively providing idle computing power last time, that is, the current credit value plus  $w_3(L, O_i, N_i)$ , and then  $N$  starts counting again from 0. If no device reports  $V_i$ , the credit value of  $V_i$  can be added with  $w_1(T, L, O)$ . In addition, when a device reports  $V_i$  data information, the cloud control center judges the report. If the report is true, the credit value of the device initiating the report can increase  $w_2(T, L, O)$ , and the  $V_i$  sending false information will be punished.

**3.3.2. Data Sharing Method.** On the basis of trusted data processing between edge computing devices, cloud control center is further introduced to realize trusted data sharing. When the terminal device requests data, it will notify the proxy edge computing device, and the proxy edge

Input  $M_{V_i}$  is the data information transmitted by the edge computing device  $i$ ;  $M_{ij}$  is the edge computing device  $V_i$  reporting data information to  $V_j$ ;  $L_{ij}$  is the distance between edge computing device  $V_i$  and  $V_j$ ;  $O$  is the data density of cloud control center;  $N_i$  is the number of times the edge computing device provides idle computing power;

Output  $Re_{V_i} \boxtimes Re_{V_j}$

- 1) if  $M_{ij}$  does not exist
- 2) for  $V_i$  perform  $Re_{V_i} \leftarrow Re_{V_i} + w_1(T_{M_{V_i}}, L_{ij}, O_i) + w_3(L_{ij}, O_i, N_i)$
- 3) end for
- 4) else
- 5) if  $M_{V_i}$  is ture
- 6) for  $V_i$  perform  $Re_{V_i} \leftarrow Re_{V_i} + w_1(T_{M_{V_i}}, L_{ij}, O_i) + w_3(L_{ij}, O_i, N_i)$
- 7) end for
- 8) end if
- 9) end if

ALGORITHM 1: Reputation Evaluation Algorithm ().

computing device will initiate a data request to the cloud control center.

- (1) requestKey() generates a transaction  $Y$  according to the parameters input by the terminal device, where  $EA_{Rdevice}$  is the private chain address when the terminal device requests data;  $EA_{REdge}$  is the address when the edge computing device requests data;  $EA_{SEdge}$  is the address when the edge computing device returns data;  $ID_{data}$  is the data identification of the purchase.  $t$  is the time when the edge computing device initiates the purchase request, and  $S$  is the unique identification of a transaction

$$Y = (ID_Y, EA_{Rdevice}, EA_{REdge}, EA_{SEdge}, ID_{data}, t), \quad (5)$$

$$ID_Y = (EA_{Rdevice}, EA_{buyer}, EA_{seller}, ID_{data}, t). \quad (6)$$

- (2) The edge computing device 1 digitally signs the transaction  $Sign(Y, v_{REdge})$  using its elliptic curve private key and sends the public key  $v_{REdge}$ , signature message  $Sign$  and requests plaintext  $Y$  of the edge computing device to the cloud control center
- (3) The edge computing device 2 verifies the signature  $(Y, Sign, v_{REdge})$  of the edge computing device 1 with the transaction  $Y$ , the signature message  $Sign$ , and the public key  $v_{REdge}$  to confirm that there is no problem with the identity of the edge computing device 1
- (4) The edge computing device 2 encrypts the key cv of the encrypted data  $W_{cv}(\text{data})$  with the public key  $v_{REdge}$  of the edge computing device 1 by the elliptic curve encryption algorithm, and the ciphertext obtained by the elliptic curve encryption algorithm is  $CT(v_{REdge}, cv)$

- (5) The edge computing device 2 transmits the ciphertext  $CT$  to the edge computing device 1 through the cloud control center

In order to ensure the credibility of the data provided by the edge computing device, the terminal equipment needs to evaluate the data after obtaining the data, which will affect the credit value of the edge computing device.

$\sigma$  is defined as the number of evaluations,  $\sigma_{bad}$  is the number of poor evaluations,  $\sigma = \sigma_{good} + \sigma_{bad}$ , and  $Z_{PEdge}$  is the credit value of the edge computing device 1.

The calculation formula is as follows:

$$Z_{PEdge} = \begin{cases} Z_{PEdge} & 0 \leq \sigma_{bad} \leq \frac{1}{5}\sigma, \\ Z_{PEdge} - \lambda \cdot \frac{\sigma_{bad}}{\sigma} & \frac{1}{5}\sigma \leq \sigma_{bad} \leq \frac{4}{5}\sigma, \\ Z_{PEdge} - \gamma \frac{\sigma_{bad}}{\sigma} & \frac{4}{5}\sigma \leq \sigma_{bad} < \sigma, \end{cases} \quad (7)$$

where  $\lambda$  and  $\gamma$  are regulatory factors,  $\lambda > 1$ ,  $\gamma > 1$ .

According to formula (7), when the number of negative comments is less than  $\sigma/5$ , the credit value of the edge computing device will not decrease. When the number of bad comments is in the interval  $[\sigma/5, 4\sigma/5]$ , it indicates that the data quality provided by the edge computing device needs to be improved, and the credit value will be reduced. When the number of negative comments is in the range  $[4\sigma/5, \sigma]$ , it indicates that the data provided by the edge computing device has a large problem, and the credit value will be greatly reduced.

In order to prevent the abnormal evaluation of the terminal equipment from affecting the credit value of the edge computing device, an evaluation check mechanism is used to restrict the evaluation behavior of the terminal equipment.

(1) *Determination of Untrusted terminal Equipment.* It is assumed that in a cycle time, an edge computing device receives  $\sigma$  evaluations from  $i$  terminal devices, the total

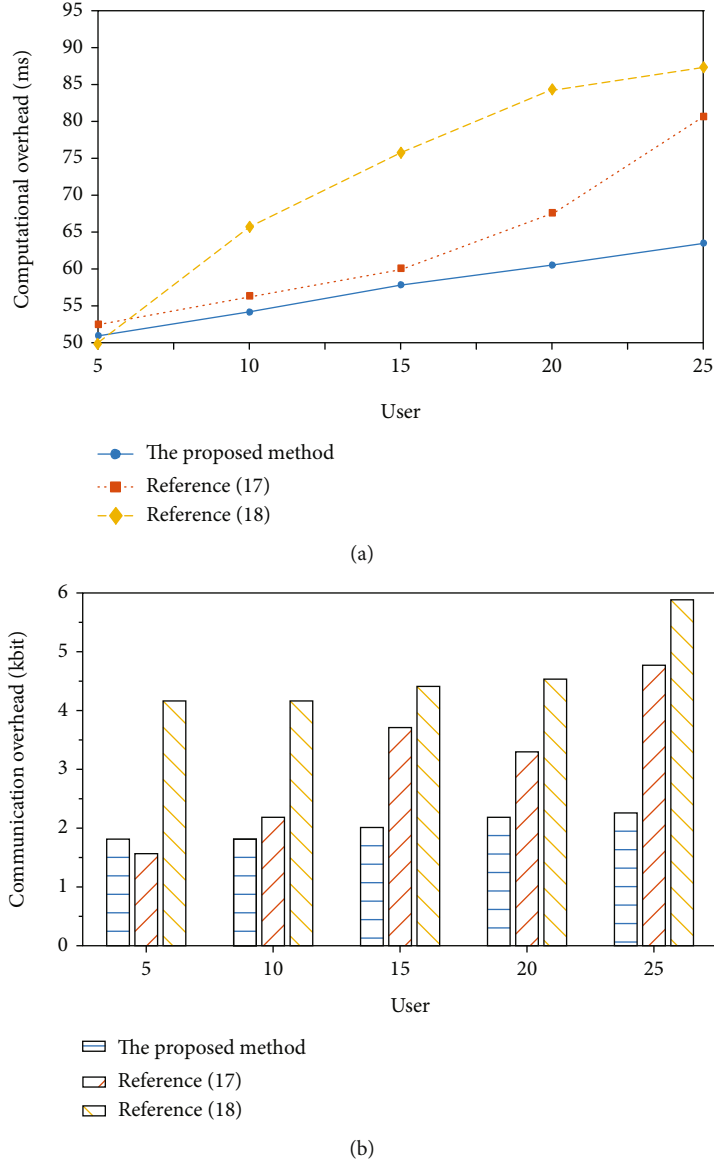


FIGURE 6: Algorithm performance under different methods.

number of terminal devices  $i = i_{\text{good}} + i_{\text{bad}}$ , and the total number of terminal devices  $\sigma = \sigma_{\text{good}} + \sigma_{\text{bad}}$ .

$\max(\sigma_{\text{good}}, \sigma_{\text{bad}})$  is used to represent the evaluation results of most terminal equipment. If the vast majority of terminal devices are high praise  $\sigma_{\text{good}} = \max(\sigma_{\text{good}}, \sigma_{\text{bad}})$ , the  $i_{\text{good}}$  terminal devices with high praise are honest terminal devices, while the  $i_{\text{bad}}$  terminal devices with poor evaluation are untrusted terminal devices. On the contrary, the same is true.

(2) *Judgment of Abnormal Terminal Equipment.* Count the determination times of untrusted terminal equipment in a certain period. If the number of times the terminal equipment is determined to be untrusted exceeds the threshold, it is determined that the terminal equipment is an abnormal terminal equipment.

## 4. Experiment and Analysis

The experimental environment uses 30 hosts to build the proposed microgrid data sharing system, of which 5 are used as edge computing devices, the hardware is set as 32 GB memory and Intel i5 processor, the remaining 25 are used as terminal devices, and the hardware is set as 16 GB memory and Intel I3 processor. The data storage nodes in the blockchain are interconnected by distributed architecture between hosts.

In the experiment, relying on the Ubuntu 20.04 operating system realizes software operation. Remix IDE (2020.6.4 last version) is used as the development tool of private chain smart contract, the program is written in Solidity language, and the private chain adopts MetaMask software.

4.1. *Algorithm Overhead Analysis.* In order to better support the edge computing device to realize data trusted

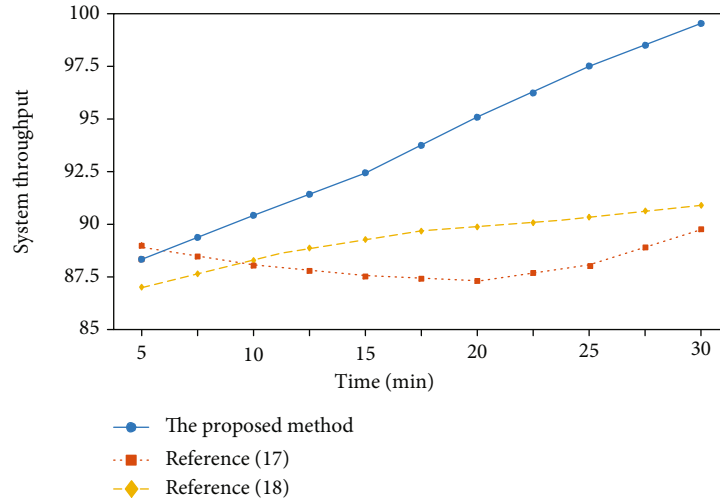


FIGURE 7: System throughput under different methods.

transmission, this paper uses different encryption methods for comparative analysis. This paper realizes the simulation experiment analysis based on charm library. Charm library is a function library that can be used for prototype development of the cryptosystem. This paper selects secp384r1 elliptic curve from charm library to test the system performance. At the same time, reference [17] and reference [18] are used as comparison methods to prove the optimality of algorithm overhead performance. In the same operating environment, the least algorithm overhead proves that it can better support the microgrid and realize the optimal data interaction.

Figure 6 shows the calculation and communication overhead under three methods.

As shown in Figure 6, the calculation and communication overhead under the three data processing methods increase linearly with the increase of the number of terminal equipment access. When  $n = 25$ , the data analysis performance of the proposed method is the best. The calculation and communication overhead of microgrid data encryption are 63.46 ms and 2.36 KB, respectively. The network performance under the comparison method is poor. The calculation and communication overhead in reference [18] are 87.32 ms and 5.87 KB, respectively. At the same time, the calculation overhead curve in reference [17] changes in the form of quasiexponential. There is a risk of system downtime when the number of users is large. This is because the introduction of ECC algorithm not only reduces the calculation consumption of key management but also effectively releases the corresponding algorithm efficiency and improves the communication performance to a certain extent. In contrast, although the comparison method releases the processing pressure of the third party to a certain extent, it still has some limitations in computing power and communication memory.

The essence of network throughput is the total amount of data passing through the network in unit time, which can evaluate the operation of the network. Therefore, this paper further carries out optimization analysis based on

the network throughput index in literature [17] and literature [18], as shown in Figure 7.

As can be seen from Figure 7, with the increase of time, both the proposed method and the microgrid under reference [18] obtain higher system throughput, while the system throughput in reference [17] decreases first and then increases and remains relatively stable in the range (87, 90). The system throughput reaches the minimum value at 20 min. However, the throughput of reference [18] and the method in this paper change with time and have good network sensitivity. In contrast, the change of system throughput in this paper is faster than that in reference [18], which can realize the linear change of higher proportion coefficient in the simulation run cycle. Therefore, it can be proved that the incentive mechanism added in the proposed method is effective. The reward mechanism will reward the profit of the edge computing devices that contribute resources, and the punishment mechanism will punish the abnormal nodes, which ensures that the edge computing devices can actively participate in the consensus process, reduces the probability of abnormal nodes participating in the consistency, and effectively improves the throughput of the system. The consensus mechanism in the comparison method does not involve the analysis and discussion of the corresponding reward and punishment coefficient. Therefore, in this experiment, it is realized that the performance of the comparison method is far worse than that of the proposed method.

**4.2. Safety Analysis.** The proposed data sharing method adopts a series of means such as ECC algorithm, REPBFT mechanism, and smart contract to improve the credibility and security of data. Therefore, the proportion of abnormal data sharing behaviors such as resisting external attacks is taken as the security analysis standard, and the specific index is the ratio of the number of successful prevention of abnormal data sharing to the number of all abnormal data sharing.

In this paper, reference [22] and reference [23] are used as comparative methods for optimal comparative analysis of

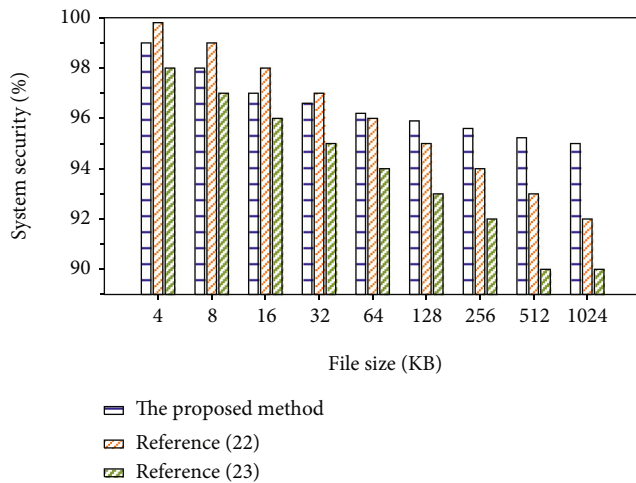


FIGURE 8: Comparison of safety performance of different methods.

security. All data processing methods are implemented in the same experimental environment. The security comparison of different methods is shown in Figure 8.

The larger the file, the more data to be shared, and better data sharing and interaction can be achieved.

As can be seen from Figure 8, compared with other comparison methods, the proposed method has the highest security performance and can resist the most external network threats. When the file size reaches 1024 KB, its security is 95%, much higher than 80%. In reference [23], when the file size is 512 KB, the security has been reduced to about 90%.

The reason is that ECC algorithm and REPBFT mechanism are introduced into the data sharing method to realize efficient and reliable data encryption and friendly interaction between devices, so as to avoid invalid data occupying limited resources. At the same time, relying on the cloud-edge-terminal architecture model, the data sharing and access control model based on smart contract realizes the friendly interaction and stable sharing of data between different edge computing devices. However, there is a lack of analysis and discussion on the status of network nodes in the comparative reference, which leads to the waste of network resources to a certain extent and reduces the data flow efficiency of microgrid.

## 5. Conclusion

In order to realize the secure and trusted sharing of microgrid data, this paper proposes a data sharing method based on cloud-edge-terminal architecture mode and blockchain. After the terminal device registration step, the trusted data encryption between the terminal device and the edge computing device is realized by using the elliptic encryption algorithm. The REPBFT mechanism is introduced into the cloud-edge-terminal architecture to realize the effective utilization of microgrid network computing resources, reduce the system computing overhead, and improve the security of data sharing. Experimental results show that the proposed method can meet the security and efficiency requirements of microgrid data sharing.

With the continuous promotion of energy Internet strategy, power grid data also presents an explosive growth form. This paper still lacks in-depth consideration on the refinement of computing capacity of data sharing model. In the next research, we need to consider the mode capacity of shared storage and the scalability of blockchain to meet the rapidly growing demand for power data processing.

## Data Availability

Data sharing not applicable to this article as no datasets were generated or analyzed during the current study.

## Conflicts of Interest

The authors declare that they have no conflicts of interest.

## References

- [1] J. Li and W. Qi, "Toward optimal operation of internet data center microgrid," *IEEE Transactions on Smart Grid*, vol. 9, no. 2, pp. 971–979, 2018.
- [2] K. Moharm, "State of the art in big data applications in microgrid: A review," *Advanced Engineering Informatics*, vol. 42, no. 1, pp. 100913–100945, 2019.
- [3] J. Arkhangelski, A. T. Mahamadou, and G. Lefebvre, "Day-ahead optimal power flow for efficient energy management of urban microgrid," *IEEE Transactions on Industry Applications*, vol. 57, no. 2, pp. 1285–1293, 2021.
- [4] O. Ciftci, M. Mehrtash, and A. K. Marvasti, "Data-driven non-parametric chance-constrained optimization for microgrid energy management," *IEEE Transactions on Industrial Informatics*, vol. 16, no. 4, pp. 2447–2457, 2020.
- [5] H. M. Huang, F. Liu, X. M. Zha et al., "Robust bad data detection method for microgrid using improved ELM and DBSCAN algorithm," *Journal of Energy Engineering*, vol. 144, no. 3, p. 04018026, 2018.
- [6] S. Pouralafi-kheljan, M. Ugur, E. Bozulu, B. C. Çalıřkan, O. Keysan, and M. Gol, "Centralized microgrid control system in compliance with IEEE 2030.7 standard based on an advanced field unit," *Energies*, vol. 14, no. 21, pp. 1–31, 2021.
- [7] B. Liu, M. Wang, J. Men, and D. Yang, "Microgrid trading game model based on blockchain technology and optimized particle swarm algorithm," *Access*, vol. 8, no. 1, pp. 225602–225612, 2020.
- [8] W. T. Zhao, J. Lv, X. L. Yao et al., "Consortium Blockchain-based microgrid market transaction research," *Energies*, vol. 12, no. 20, pp. 3812–3822, 2019.
- [9] B. Kirpes, E. Mengelkamp, G. Schaal, and C. Weinhardt, "Design of a microgrid local energy market on a blockchain-based information system," *IT - Information Technology*, vol. 61, no. 2-3, pp. 87–99, 2019.
- [10] J. Kim, Y. Chang, and D. H. Choi, "Intelligent micro energy grid in 5G era: platforms, business cases, testbeds, and next generation applications," *Electronics*, vol. 8, no. 4, pp. 422–468, 2019.
- [11] H. Qiu, W. Gu, X. Xu et al., "A historical-correlation-driven robust optimization approach for microgrid dispatch," *IEEE Transactions on Smart Grid*, vol. 12, no. 2, pp. 1135–1148, 2021.

- [12] D. S. De and R. Prasad, "Digitalization of global cities and the smart grid," *Wireless Personal Communications*, vol. 113, no. 3, pp. 1385–1395, 2020.
- [13] A. Hussain, A. O. Rousis, I. Konstantelos, G. Strbac, J. Jeon, and H. M. Kim, "Impact of uncertainties on resilient operation of microgrids: a data-driven approach," *IEEE Access*, vol. 7, no. 1, pp. 14924–14937, 2019.
- [14] L. Cheng, Y. Jia, and X. Zhao, "DRO-MPC-based data-driven approach to real-time economic dispatch for islanded microgrids," *IET Generation Transmission & Distribution*, vol. 14, no. 24, pp. 5704–5711, 2020.
- [15] E. Anthi, A. Javed, O. Rana, and G. Theodorakopoulos, "Secure data sharing and analysis cloud-based energy management systems," in *Proceedings of cloud infrastructures, services, and IoT Systems for Smart Cities*, pp. 228–242, Springer, Cham, 2018.
- [16] L. Zhang, J. Ren, Y. Mu, and B. Wang, "Privacy-preserving multi-authority attribute-based data sharing framework for smart grid," *IEEE Access*, vol. 8, no. 1, pp. 23294–23307, 2020.
- [17] Y. W. Chen, B. W. Hu, H. J. Yu, Z. Duan, and J. Huang, "A threshold proxy re-encryption scheme for secure IoT data sharing based on blockchain," *Electronics*, vol. 10, no. 19, pp. 1–18, 2022.
- [18] L. Wang, J. Y. Liu, and W. Y. Liu, "Staged data delivery protocol: a blockchain-based two-stage protocol for non-repudiation data delivery," *Concurrency and Computation-Practice & Experience*, vol. 33, no. 13, pp. 1–20, 2021.
- [19] L. Wang, J. Wu, R. Yuan et al., "Dynamic adaptive cross-chain trading mode for multi-microgrid joint operation," *Sensors*, vol. 20, no. 21, pp. 6020–6096, 2020.
- [20] Z. L. Zhao, J. T. Guo, X. Luo et al., "Energy transaction for multi-microgrids and internal microgrid based on blockchain," *IEEE Access*, vol. 8, no. 1, pp. 144362–144372, 2020.
- [21] W. Xu, J. Li, M. Dehghani, and M. GhasemiGarpachi, "Blockchain-based secure energy policy and management of renewable-based smart microgrids," *Sustainable Cities and Society*, vol. 72, no. 6, p. 103010, 2021.
- [22] A. Marín-López, S. Chica-Manjarrez, D. Arroyo, F. Almenares-Mendoza, and D. Díaz-Sánchez, "Security information sharing in smart grids: persisting security audits to the blockchain," *Electronics*, vol. 9, no. 11, pp. 1816–1865, 2020.
- [23] G. Vasukidevi and T. Sethukarasi, "BBSSE: blockchain-based safe storage, secure sharing and energy scheme for smart grid network," *Wireless Personal Communications*, vol. 4, no. 1, pp. 1–22, 2021.
- [24] M. Afzal, Q. Huang, W. Amin, K. Umer, A. Raza, and M. Naeem, "Blockchain enabled distributed demand side management in community energy system with smart homes," *IEEE Access*, vol. 8, no. 1, pp. 37428–37439, 2020.
- [25] S. S. Karthik and A. Kavithamani, "Fog computing-based deep learning model for optimization of microgrid-connected WSN with load balancing," *Wireless Networks*, vol. 27, no. 4, pp. 2719–2727, 2021.
- [26] Q. L. Duan, N. V. Quynh, H. M. Abdullah et al., "Optimal scheduling and management of a smart city within the safe framework," *IEEE Access*, vol. 8, no. 1, pp. 161847–161861, 2020.
- [27] K. Aldriwish, "A double-blockchain architecture for secure storage and transaction on the Internet of Things networks," *International Journal of Computer Science and Network Security*, vol. 21, no. 6, pp. 119–126, 2021.

## *Retraction*

# **Retracted: Federated Deep Learning Approaches for the Privacy and Security of IoT Systems**

### **Wireless Communications and Mobile Computing**

Received 31 October 2023; Accepted 31 October 2023; Published 1 November 2023

Copyright © 2023 Wireless Communications and Mobile Computing. This is an open access article distributed under the Creative Commons Attribution License, which permits unrestricted use, distribution, and reproduction in any medium, provided the original work is properly cited.

This article has been retracted by Hindawi following an investigation undertaken by the publisher [1]. This investigation has uncovered evidence of one or more of the following indicators of systematic manipulation of the publication process:

- (1) Discrepancies in scope
- (2) Discrepancies in the description of the research reported
- (3) Discrepancies between the availability of data and the research described
- (4) Inappropriate citations
- (5) Incoherent, meaningless and/or irrelevant content included in the article
- (6) Peer-review manipulation

The presence of these indicators undermines our confidence in the integrity of the article's content and we cannot, therefore, vouch for its reliability. Please note that this notice is intended solely to alert readers that the content of this article is unreliable. We have not investigated whether authors were aware of or involved in the systematic manipulation of the publication process.

Wiley and Hindawi regrets that the usual quality checks did not identify these issues before publication and have since put additional measures in place to safeguard research integrity.

We wish to credit our own Research Integrity and Research Publishing teams and anonymous and named external researchers and research integrity experts for contributing to this investigation.

The corresponding author, as the representative of all authors, has been given the opportunity to register their agreement or disagreement to this retraction. We have kept a record of any response received.

### **References**

- [1] M. B. Alazzam, F. Alassery, and A. Almulihi, "Federated Deep Learning Approaches for the Privacy and Security of IoT Systems," *Wireless Communications and Mobile Computing*, vol. 2022, Article ID 1522179, 7 pages, 2022.

## Research Article

# Federated Deep Learning Approaches for the Privacy and Security of IoT Systems

Malik Bader Alazzam <sup>1</sup>, Fawaz Alassery <sup>2</sup>, and Ahmed Almulihi <sup>3</sup>

<sup>1</sup>Faculty of Computer Science and Informatics, Amman Arab University, Jordan

<sup>2</sup>Department of Computer Engineering, College of Computers and Information Technology, Taif University, P.O. Box 11099, Taif 21944, Saudi Arabia

<sup>3</sup>Department of Computer Science, College of Computers and Information Technology, Taif University, P.O. Box 11099, Taif 21944, Saudi Arabia

Correspondence should be addressed to Malik Bader Alazzam; [m.alazzam@aau.edu.jo](mailto:m.alazzam@aau.edu.jo)

Received 27 October 2021; Revised 6 November 2021; Accepted 18 March 2022; Published 1 April 2022

Academic Editor: Shalli Rani

Copyright © 2022 Malik Bader Alazzam et al. This is an open access article distributed under the Creative Commons Attribution License, which permits unrestricted use, distribution, and reproduction in any medium, provided the original work is properly cited.

Using federated learning, which is a distributed machine learning approach, a machine learning model can train on a distributed data set without having to transfer any data between computers. Instead of using a centralised server for training, the model uses data stored locally on the device itself. After that, the server uses this model to create a jointly trained model. Federated learning asserts that privacy is preserved because no data is sent. Botnet attacks are detected using on-device decentralised traffic statistics and a deep autoencoder. This proposed federated learning approach addresses privacy and security concerns about data privacy and security rather than allowing data to be transferred or relocated off the network edge. In order to get the intended results of a previously centralised machine learning technique while also increasing data security, computation will be shifted to the edge layer. Up to 98% accuracy is achieved in anomaly detection with our proposed model using features like MAC IP and source/destination/IP for training. Our solution outperforms a standard centrally managed system in terms of attack detection accuracy, according to our comparative performance analysis.

## 1. Introduction

While [1] is credited with coining the term “federated learning,” the first description of its implementation can be found in [2]. Multiple devices work together to train a shared model in federated learning. Multiple clients’ parametric improvements are combined over numerous training rounds to achieve this. Several customers compete in each round to improve a globally available model using data that they have access to only locally. Figures 1 and 2 show the steps in such a round.

Because the models are assumed to be smaller in size than the data set, federated learning reduces data transfer while also addressing privacy concerns associated with sending personal information to a server [3]. Another advantage is that all computation can be performed on the clients’ devices. Maintaining server farms, calculating new models,

and dealing with large amounts of data are all made easier as a result.

While federated learning’s round-based nature means models are smaller than the amount of data that can be exchanged, it is possible that a significant amount of bandwidth will be needed. Federated learning’s communication costs should be reduced, especially for mobile users with limited data access. As a result, a number of communication cost-cutting techniques have been developed.

In some cases, Figure 3 federated learning outperforms existing models. Mobile device implementations for next word prediction and emoticon prediction [4] were demonstrated by Google researchers. These use cases show how effective federated learning can be in a variety of situations.

In Minneapolis, when one of these coupons is delivered to the home of a high school student, her father calls the



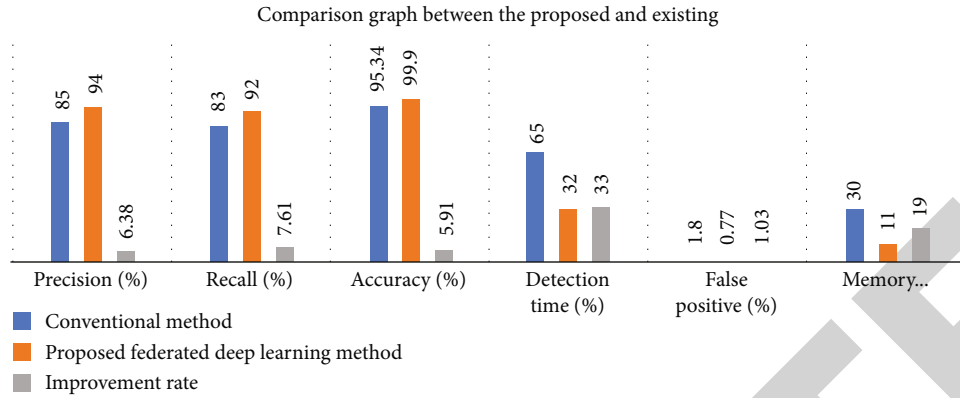


FIGURE 1: Comparison graph between the existing and proposed methods.

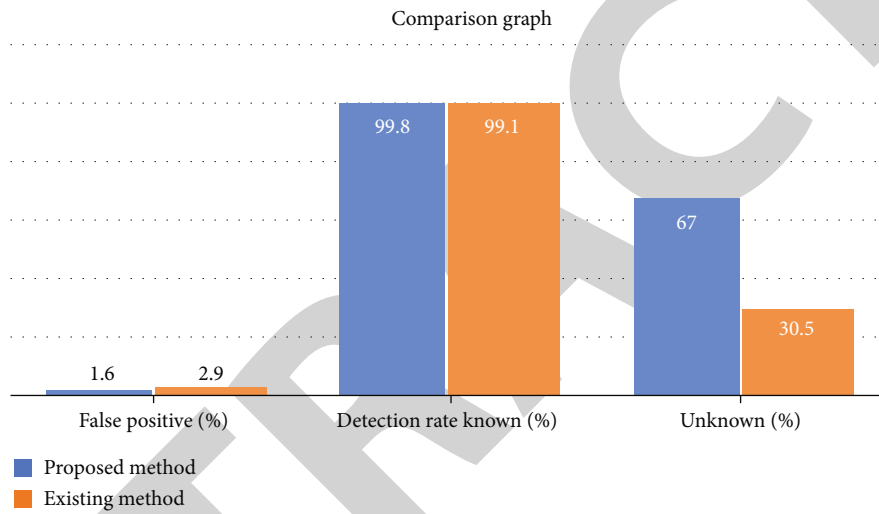


FIGURE 2: Comparison graph.

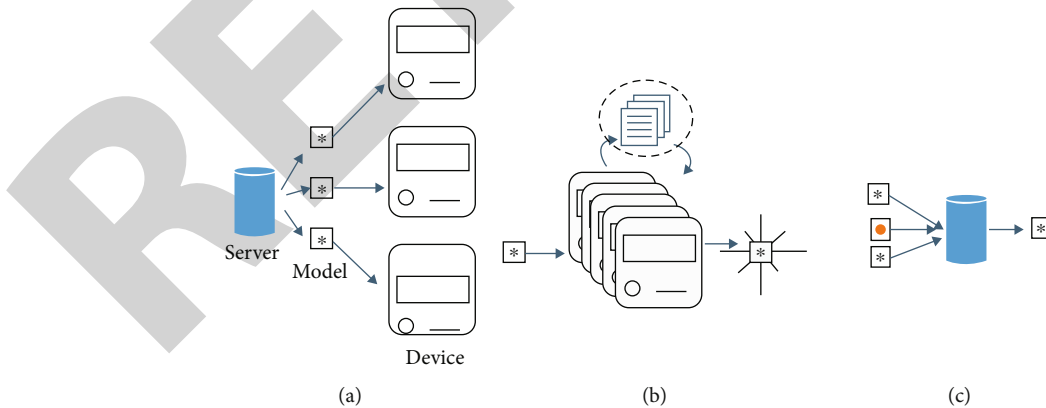


FIGURE 3: Working diagram of federated learning.

store manager and inquiries about the coupon’s contents. It was only after this incident that Target’s management began paying attention to customer complaints [5]. These stories can help us see how critical it is to safeguard personal information stored digitally.

## 2. Related Work

A federated learning approach to developing WID models is proposed by [6]. As shown in Figure 4, edge devices can first train their local models using local data. Local models are

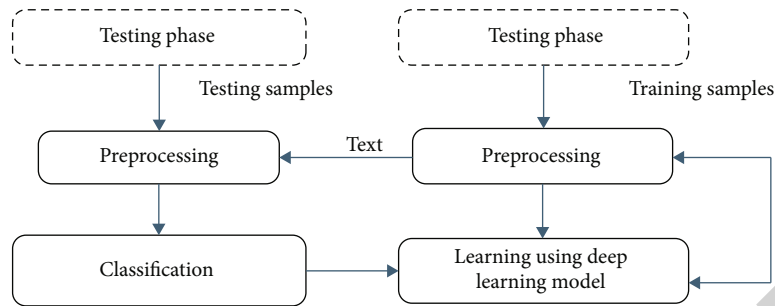


FIGURE 4: Deep learning-based classification process.

then averaged to create a global model. Edge devices do not have to share raw training data this way. These devices train a local model and send only model parameters to the server instead of raw training data.

**2.1. Privacy and Security.** Due to the fact that privacy and security are often used in the same context, it is critical to know the difference. Transferring data securely does not guarantee privacy, and keeping it private does not guarantee security from intruders. A malicious adversary is one whose primary objective is to obtain victim-specific personal data [7]. This particular victim is either a preselected candidate or was selected at random. This section also gives some background on privacy preservation from a legislative standpoint.

Privacy can be loosely defined as “the control to determine to whom personal information is revealed.” As such, for a system to be privacy-preserving would, in theory, mean that it:

- (i) Reveals no personal information to anyone other than those with consent
- (ii) Reveals no nonconsensual personal information

In practice, however, what is regarded as personal information is only that which can be appointed specifically to the person. Security, on the other hand, can be defined as “the state of being free from danger or threat.” In the current context, these are primarily unintended distribution of sensitive data (or data leakage). Whatever is done with the leaked data is in this context irrelevant but could be as malicious [8–11]. There is a notion in encryption and cybersecurity that it is impossible to have an entirely secure system. This stems from the fact that security systems must have a key or password of sorts. The space in which to define such a key is finite by design. A password for instance commonly has a maximum amount of characters and a finite set of characters to pick from. Therefore, a program can be written that checks all combinations of keys. This will crack the system given enough computational resources. This is called a brute force attack. In practice, keys of lengths higher than a certain length are commonly regarded as being unbreakable because the number of combinations to check would take far too much time and resources [12]. The costs of trying this would far exceed any value an adversary gets from breaking the security.

There is however a balancing act. Because performing the encryption and decryption also has an associated computational cost, which makes it a challenge to minimize security costs while maximizing the security of the system. Another notion of security is security by obscurity, meaning that you can minimize security risks by not disclosing the details of your protective measures [13]. This has been widely criticized and shall be cast aside as a viable security measure for the remainder of the thesis. Any adversary is considered to have complete knowledge of how the system works which includes complete knowledge of the implemented security measures.

### 3. Background

For security researchers and industry professionals, DL has recently become a hot topic. DNNs, also known as deep learning (DL), are a subset of AI that are inspired by how the brain works. Architectures based on deep learning (DL) can understand the meaning of large amounts of data and automatically update derived meaning without domain expert knowledge.

An important part of feature engineering is feature extraction, and doing so requires some familiarity with the subject matter [14]. The classifier’s performance is dependent on feature extraction. The 1950s saw the introduction of the NN ML technique. It has the ability to automatically extract and classify features without the involvement of a human. To some extent, the classical NN performs admirably. However, using advanced NN, also known as deep learning, it is possible to completely avoid the phase of feature engineering (DL) [15–17]. Figure 5 shows the training and testing processes involved in traditional ML algorithms and DL architectures. Because of this, the DL was able to outperform other long-standing AI applications in a variety of fields.

Figure 4 depicts DL architecture classifications. The terms neural networks (NNs), machine learning (ML), and deep learning (DL) are all intertwined in AI discourse. All of these fields are frequently misunderstood. DL is a branch of machine learning that developed from neural networks (NNs). By processing data and generating patterns, this simulates the workings of the human brain. When it comes to DL, the most important part is the NNs, and the term “many NNs” usually means just that many NNs [18]. Vanishing and exploding gradients and, most importantly, the lack of

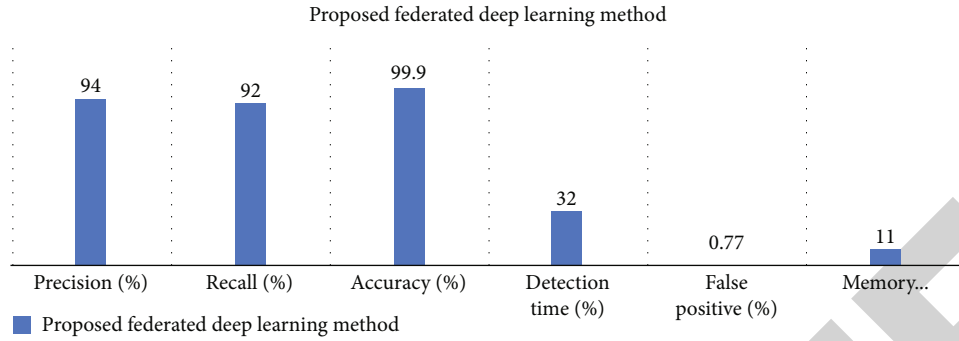


FIGURE 5: Parameter analysis graph for the proposed method.

high-performance computing systems arise when NNs are deep.

As computing systems have improved, new kinds of DL architectures have been introduced, and improvements have been made in optimizers, activation functions, loss functions, and the disappearing and exploding gradient issues. DL is now being used to solve a variety of cyber security problems, and it outperforms that classical ML in every case depicts two types of DL architecture: generative and discriminative [19]. Deep Boltzmann machine (DBM), deep autoencoder (DAE), deep belief network (DBN), and recurrent structures are used to generate new ideas. Recurrent structures and convolutional neural networks are used to discriminate between these new ideas and the old ones (CNN).

#### 4. Proposed Architecture

Our process architecture is depicted in Figure 5. Botnet assaults are detected with the use of a decentralised FL-based deep anomaly detection engine. As depicted in the diagram, IoT security gateways are responsible for operating and monitoring traffic to and from IoT devices. FL and anomaly detection are two examples of forensics-based IoT security gateways. This is due to the fact that port mirroring keeps track of network traffic. The network traffic entering and departing the IoT security gateway is monitored since botnets might masquerade as regular traffic. Infected Internet of Things devices frequently transmit signals to unexpected locations [20]. Once connected to their FL server, which would host device models, the IoT security gateways will be able to communicate with one another. The security gateway will communicate with the FL server in order to determine the deep autoencoder model to use.

Based on data from the global FL server, which is connected to the same network as the proposed IoT device, the FL model is only applicable to computer learning. As discussed previously, the security gateway hardware can be customised to work with a wide range of devices and hardware. We claim that a security gateway can use port mirroring to record all network traffic and process it afterwards. We can exchange information with our virtual worker by taking a snapshot of it. These gateways can even host multiple virtual employees simultaneously. The truth is that each security gateway can host an unlimited number of virtual workers.

It is up to employees to obtain the company a specific gadget. Although a gateway can handle several virtual employees, only one is required per gateway. In this thesis, we will regard security gateways and virtual employees as one-to-one interactions.

*4.1. Deep Autoencoder.* Figure 5 shows a special deep learning algorithm that uses two symmetrical deep belief networks with four or five shallow layers. Half of the network encodes and decodes. Autoencoders are a subset of neural networks. PCA and PCA are closely related, but PCA is much more flexible. Unlike PCA, which can only perform linear transformations, autoencoders can encode data in nonlinear ways [21]. Using autoencoders can maximize data utilization by reducing reconstruction error. Each layer has the same number of neurons using autoencoders (input and output).

- (i) This is done in the first step of the deep autoencoder, which uses PyTorch linear layers for all steps of the ML process, encoding and decoding continuously as each layer is added and subtracted. Data from the first layer represents the source IP, destination IP, and UDP/TCP socket details and is encoded to 75% of its original size before being sent to the second layer for decompression
- (ii) The input from the previous layer will be passed on to the next sequential layer for encoding. Half of the input size will be encoded in the next encoding layer, reducing the size by 50%. The input is reduced by 33% in size in the third layer, which continues the encoding process. The input will be encoded down to 25% of the previous step again in the final encoding layer. The compression level is the lowest at this point
- (iii) The effects of the encoding stage will be undone during the decoding stage. It decodes the input and then adds on to the size of it for the next layer, using the same encoding and decoding values and the same decompression aids as input features. Using the decoder's opposing direction helps to produce a decompressed data set that is not 1-to-1 identical to the input, as well as expanding and

zeroing out some data points to help produce the threshold

- (iv) The output layer will recreate the encoding and decoding process. After encoding and decoding the network traffic's behaviours, a threshold is generated and used for testing by comparing the input and output

**4.2. Dataset.** Massive amounts of data are now available due to the proliferation of data collectors like smartphones [22]. In terms of building machine learning models, these data are priceless! New approaches, tailored for decentralised settings, are needed to make use of all this data. More data helps machine learning models because it allows them to be trained on a broader set of features rather than having to remember the details of each individual training example. Overfitting occurs when a neural network memorises training samples rather than looking for correlations in the general characteristics of an input. Machine learning models frequently overfit data. When data is gathered for training purposes from a variety of dispersed and possibly infrequently used devices, three common characteristics emerge.

**4.3. Massively Distributed.** Because data is stored across a large number of clients, the amount of data available to each client may be significantly smaller than the average amount of data available to each client.

**4.4. Non-IID.** When compared to other clients, the data provided for a particular client may be taken from dramatically different distributions. This means that the data that is readily available in the local area does not accurately reflect the broader data dispersion.

**4.5. Example.** The photographs stored on a cat enthusiast's mobile phone may be radically different from those kept on a vehicle enthusiast's mobile phone.

**4.6. Unbalanced.** The amount of data that is available for a single customer can vary significantly from one client to the next.

The centralised model is the most widely used machine learning technique for decentralised data since it is the most conventional. Because it is explained, it is possible to see how this model differs from that of collaborative techniques in practise.

**4.7. Matrix.** The following metrics are used to determine overall performance of the IDS model:

*Detection accuracy:* how many samples were correct out of the total sample population.

$$\text{Accuracy} = \frac{(\text{TP} + \text{TN})}{(\sum \text{P} + \sum \text{N})}. \quad (1)$$

*Recall:* fraction of relevant instances over the total amount of relevant instances.

TABLE 1: Parameters.

Parameters	Conventional methods	Proposed federated deep learning method	Improvement rate
Precision (%)	85	94	6.38
Recall (%)	83	92	7.61
Accuracy (%)	95.34	99.9	5.91
Detection time (s)	65	32	33
False positive (%)	1.8	0.77	1.03
Memory utilization (mb)	30	11	19

$$\text{Recall} = \frac{\text{TP}}{(\text{TP} + \text{FN})}. \quad (2)$$

*F1 score:* weighted average of the precision and recall.

$$\text{F1} = \frac{2 \times (\text{Precision} \times \text{Recall})}{\text{Precision} + \text{Recall}}. \quad (3)$$

*False positive rate:* the rate at which alerts are generated for normal samples.

$$\text{FPR} = \frac{(\text{FP})}{(\text{FP} + \text{TN})} = 1 - \text{precision}. \quad (4)$$

*False negative rate:* the rate at which attacks are missed.

$$\text{FNR} = \frac{(\text{FN})}{(\text{FN} + \text{TP})} = 1 - \text{Recall}. \quad (5)$$

## 5. Results and Discussion

Existing traditional procedures are contrasted with the federated deep learning method that is being proposed. The results are encouraging. The data set is being utilized to determine the effectiveness of the proposed method, which is being evaluated. First, the new approach is compared to the old one in terms of detection performance, and the results are compared. The results of the tests, which were carried out, are presented in Tables 1 and 2 as well as Figure 1. Table 3 has been demonstrated that the proposed method has a greater detection rate than current methods. The proposed detection approach is evaluated on the basis of criteria such as precision value, recall value, accuracy, detection time, false positives, and memory utilization, among others. Based on Table 1, it is clear that the new method outperforms the current one.

Figure 5 shows the TN, TP, FP, and FN rates for studies with input dimensions ranging from 15 to 115. These matrices represent the non-FL baseline and the proposed FL techniques lowest and highest tested input features.

Figure 1 displays false positives that resulted in results up to 43954 on the non-FL figure, contrast this with which shows the same parameters but using a multiworker

TABLE 2: Matrix comparison table between the existing and proposed method.

Metric	Proposed method	Existing method
False positive (%)	1.6	2.9
Detection rate known (%)	99.8	99.1
Unknown (%)	67	30.5

TABLE 3: Parameter analysis table for the proposed federated deep learning method.

Parameters	Proposed federated deep learning method
Precision (%)	94
Recall (%)	92
Accuracy (%)	99.9
Detection time (s)	32
False positive (%)	0.77
Memory utilization (mb)	11

technique. This is a positive reflection on the model, which maintains performance even when the number of workers increases. This applies to all input dimensions, including those with larger dimensions than the default. In Table 2, the non-FL model, for example, produced 31 false positives; however, the multiworker model, in Figure 1, produced 36 false positives, proving that the model's performance can be maintained across several workers.

## 6. Conclusion

Then, we demonstrate how to make use of these federated learning datasets in a simulated learning environment. If we compare federated deep learning to server-trained deep learning in the context of wireless intrusion detection, the results are similar. In contrast to the conventional deep learning approach, the suggested model does not transmit data to a central server, thereby safeguarding the privacy of the user. Because of this, they rush to repair and patch equipment, leaving new and existing networks exposed. For proactive threat detection, we demonstrated a viable proof-of-concept model. FL is a reliable performer in enterprise networks. This technique secures Internet of Things devices and allows for the creation of complicated machine learning models. On edge networks, gateways provide self-updating attack detection thanks to their self-learning capabilities. In the simulation, it is demonstrated that accuracy and scores are maintained when there are sufficient features to train a model. IoT devices connected to a corporate network can be protected through the use of a large variety of security gateways and devices.

## Data Availability

The data underlying the results presented in the study are available within the manuscript.

## Disclosure

The study was performed as a part of the Employment of Institutions.

## Conflicts of Interest

The authors declare that they have no conflicts of interest regarding the publication of this paper.

## Acknowledgments

We deeply acknowledge Taif University for supporting this study through Taif University Researchers Supporting Project Number (TURSP-2020/344), Taif University, Taif, Saudi Arabia.

## References

- [1] S. Badotra, D. Nagpal, S. N. Panda, S. Tanwar, and S. Bajaj, "IoT-enabled healthcare network with SDN," in *In 2020 8th International Conference on Reliability, Infocom Technologies and Optimization (Trends and Future Directions) (ICRITO)*, pp. 38–42, Noida, India, 2020.
- [2] I. Udrea, I. Gheorghe Viorel, A. Cartal Laurentiu et al., "IoT solution for monitoring indoor climate parameters in open space offices," in *E3S Web of Conferences*, Romania, 2020.
- [3] T. Alladi, V. Chamola, B. Sikdar, and K. R. Choo, "Consumer IoT: security vulnerability case studies and solutions," *IEEE Consumer Electronics Magazine*, vol. 9, no. 2, pp. 17–25, 2020.
- [4] S. Almutairi, S. Mahfoudh, S. Almutairi, and J. S. Alowibdi, "Hybrid botnet detection based on host and network analysis," *Journal of Computer Networks and Communications*, vol. 2020, Article ID 9024726, 2020.
- [5] H. Haddad Pajouh, R. Khayami, A. Dehghantanha, K.-K. R. Choo, and R. M. Parizi, "AI4SAFE-IoT: an AI-powered secure architecture for edge layer of Internet of Things," *Neural Computing and Applications*, vol. 32, no. 20, pp. 16119–16133, 2020.
- [6] H. U. Rahman, M. A. Habib, S. Sarwar, N. Mahmood, M. Ahmad, and H. Ahmad, "Fundamental issues of future Internet of Things," in *In: 2020 International Conference on Engineering and Emerging Technologies (ICEET)*, pp. 1–6, Lahore, Pakistan, 2020.
- [7] H. Haddad Pajouh, A. Azmoodeh, A. Dehghantanha, and R. M. Parizi, "MVFC: a multi-view fuzzy consensus clustering model for malware threat attribution," *IEEE Access*, vol. 8, pp. 139188–139198, 2020.
- [8] A. A. Hamad and L. M. Thivagar, "Conforming dynamics in the metric spaces," *Journal Of Information Science And Engineering*, vol. 36, no. 2, pp. 229–279, 2020.
- [9] N. A. Noori and A. A. Mohammad, "Dynamical approach in studying GJR-GARCH (Q, P) models with application," *Tikrit Journal of Pure Science*, vol. 26, no. 2, pp. 145–156, 2021.
- [10] W. A. Saeed and A. J. Salim, "Convergence solution for some harmonic stochastic differential equations with application," *Tikrit Journal of Pure Science*, vol. 25, no. 5, pp. 119–123, 2020.
- [11] R. N. Salih and M. A. Al-jawaherry, "Finding minimum and maximum values of variables in mathematical equations by applying firefly and PSO algorithm," *Tikrit Journal of Pure Science*, vol. 25, no. 5, pp. 99–109, 2020.

## Research Article

# Deep Learning-Based Anomaly Traffic Detection Method in Cloud Computing Environment

Junjie Cen<sup>1</sup> and Yongbo Li<sup>2</sup>

<sup>1</sup>College of Computer Science and Technology, Henan Institute of Technology, Xinxiang, Henan 453002, China

<sup>2</sup>College of Computer and Information Engineering, Henan Normal University, Xinxiang, Henan 453002, China

Correspondence should be addressed to Junjie Cen; [cen@hait.edu.cn](mailto:cen@hait.edu.cn)

Received 25 January 2022; Revised 3 March 2022; Accepted 7 March 2022; Published 31 March 2022

Academic Editor: Shalli Rani

Copyright © 2022 Junjie Cen and Yongbo Li. This is an open access article distributed under the Creative Commons Attribution License, which permits unrestricted use, distribution, and reproduction in any medium, provided the original work is properly cited.

To address the problem of poor detection performance of existing intrusion detection methods in the environment of high-dimensional massive data with uneven class distribution, a deep learning-based anomaly traffic detection method in cloud computing environment is proposed. First, the fuzzy *C*-means (FCM) algorithm is introduced and is combined with the general regression neural network (GRNN) to cluster the samples to be classified in the original space by FCM. Then, the GRNN model is trained and the center point is updated using the sample closest to the FCM clustering center until a stable cluster center is obtained. The parameters in FCM-GRNN are optimized using the global optimization feature of the modified fruit fly optimization algorithm (MFOA), and the optimal spread value is found using the three-dimensional search method through an iterative search. Finally, experiments are conducted based on the KDD CUP99 dataset, and the results demonstrate that the detection rate (DR) and false alarm rate (FAR) of the proposed FCM-MFOA-GRNN method are 91% and 1.176%, respectively, which are better than those of the comparison methods. Therefore, the proposed method has good anomaly traffic detection ability.

## 1. Introduction

Nowadays, network traffic anomaly detection has become an important part of cyberspace security, and the explosive growth of traffic data has led to increasing requirements for efficiency and robustness when various methods are applied to learn data [1]. For example, the update of communication protocols and hardware upgrades have a great impact on the stability of the whole network environment [2, 3]. On the other hand, the scenarios of network attacks and the corresponding means of attack have become much more complex, and the currently used traffic anomaly detection techniques are likely to be no longer applicable at some point in the future. The development of traffic anomaly detection should always be one step ahead of the attackers, especially when the current techniques are already relatively mature and well known to the attackers. It is necessary to open up new research directions [4–7]. In recent years, research on deep learning models has mainly focused on the fields of speech, image, and natural language and has

received more and more attention because of the outstanding achievements [8–11].

Cloud computing can provide users with various resources in the form of services through the network. “Everything can be a kind of service and can be provided to users in the form of lease” is the basic concept of cloud computing [12–14]. However, the rapid development and the universal application of cloud computing brings some new problems which cannot be underestimated. The first and foremost problem is the security of cloud computing, which is increasingly widely concerned by the industry [15–17]. Cloud computing has many features, such as self-service on demand, Internet access, fast elastic architecture, virtualized resource pools, measurability, and multiuser. Although these features provide a more convenient and faster computing mode to users, they also pose new challenges to the security of cloud computing platforms.

To address the problem of poor detection performance of existing intrusion detection methods in the environment of high-dimensional massive data with uneven class

distribution, a deep learning-based anomaly traffic detection method in cloud computing environment is proposed. The contributions are as follows:

- (1) The fuzzy  $C$ -means (FCM) algorithm is introduced and combined with the general regression neural network (GRNN). The samples to be classified in the original space are clustered by the FCM algorithm, and the sample closest to the FCM clustering center is used to train the GRNN model and update the center until a stable clustering center is obtained, which improves the stability of the anomaly traffic detection system
- (2) The parameters of the FCM-GRNN method are optimized by using the global search feature of the modified fruit fly optimization algorithm (MFOA). And the optimal spread value is found by an iterative search using the three-dimensional search method with the keen olfactory and visual functions of fruit flies, so that the proposed algorithm can converge faster

## 2. Related Works

In recent years, scholars have conducted in-depth research on abnormal traffic detection methods. The results show that for all abnormal traffic detection data sets, deep learning methods are better than traditional methods. Literature [18] proposed a sliding window abnormal traffic detection method based on the mixed dimension of time and space. The detection algorithm adopts the combination of machine learning and neural network. A sliding window anomaly detection method based on network traffic was studied in the Literature [19]. The method combined the sliding window and deep learning architecture to analyze network traffic, and features in each window were extracted, vectored and then put into a deep neural network for training. Literature [20] proposed a network intrusion detection method based on a lenet5 model, which improved the detection accuracy. Blanco et al. used the genetic algorithm (GA) to optimize a CNN classifier to find better input feature combination [21]. Literature [22] converts variable length data sequence into fixed length data through LSTM and uses an automatic encoder to process fixed length data under unsupervised conditions, so as to reduce the dimension of input data and extract reliable features at the same time. On the basis of cross validation, the threshold is set to classify the abnormal parts in the input traffic data series. In Literature [23], a deep autoencoder-based intrusion detection method was investigated with layer-by-layer greedy training to avoid overfitting. A self-learning framework based on stacked self-encoders for feature learning and dimensionality reduction was proposed in Literature [24]. It applied the support vector machine (SVM) approach for classification, which shows good performance in two-class and multiclass classification. In Literature [25], an unsupervised deep autoencoder model was used for training so as to learn normal network behaviors and generate optimal parameters. Then, the estimation

algorithm of the ADE model was introduced in a supervised deep neural network model to efficiently tune its parameters and classify the network traffic. Literature [26] proposed a supervised LSTM-based intrusion detection algorithm that can detect DoS attacks and probe attacks that have unique time series features. Zhang et al. proposed a parallel cross convolution neural network (PCCN) based on deep learning [27]. By fusing the traffic features learned from the two branches of CNN, a better feature extraction effect is obtained. Literature [28] combines CNN and LSTM to learn the temporal and spatial characteristics of network traffic. The above methods are difficult to effectively mine data features and have poor detection performance in the face of high-dimensional data, resulting in low detection rate as well as high false alarm rate.

## 3. Application Scenarios of the Proposed Method

In the design process of the anomaly traffic detection and analysis model, the principle of modular design is followed. The modular design of the anomaly traffic detection and analysis is conducive to simplifying the complex problems, which is easy to find the problem in the design and can facilitate the update and maintenance of the system at a later stage. The specific functions of each module are shown as follows. As shown in Figure 1, the whole model can be divided into four major modules: SDN controller module, traffic collection module, traffic analysis module and traffic cleaning module.

SDN controller can realize the centralized control of the whole network. The floodlight controller is used to divert the traffic from each OpenFlow switch to the traffic collection module to collect network traffic. As illustrated in Figure 1, the traffic in switch A, switch B, and switch C will be controlled by the SDN controller and converged to the traffic collection module through the secure channel. The traffic analysis module is the core of the entire anomaly traffic detection model. It uses the FCM-MFOA-GRNN algorithm to cluster and analyze the collected traffic to separate the normal traffic from the attack traffic with different attack behaviors. The traffic cleaning module consists of many physical devices that can clean different attack traffic, such as IDS, UTM, WAF, and other physical devices.

## 4. The Proposed Method

*4.1. Algorithm Flow Chart.* Although the FCM algorithm can cluster the data and perform mining analysis, many intrusion ways cannot be accurately classified because there are many kinds of data characterizing intrusion categories in intrusion detection systems and the differences between these data are subtle. Therefore, combined with the characteristics of GRNN, this paper proposes an improved FCM-MFOA-GRNN algorithm based on the FCM algorithm. The flow chart of FCM-MFOA-GRNN algorithm is shown in Figure 2. It can be seen that the core module of the algorithm includes five parts, which are the FCM clustering algorithm, initial selection of network training data, MFOA-GRNN network training, MFOA-GRNN network prediction, and network training data selection in order.

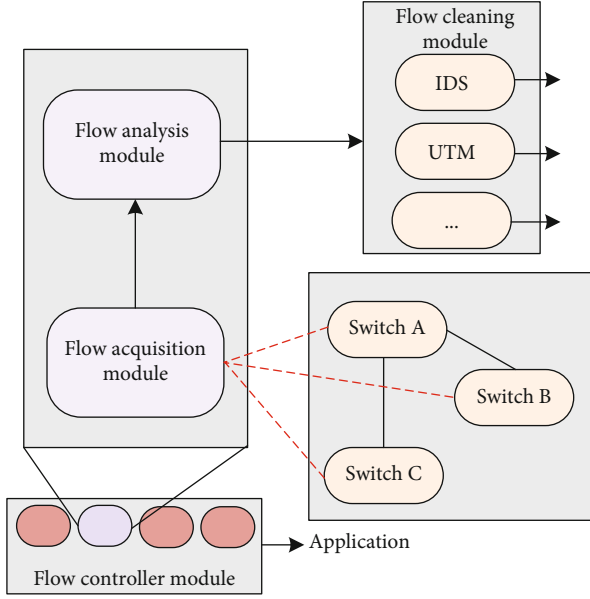


FIGURE 1: Anomaly traffic detection model based on FCM-MFOA-GRNN.

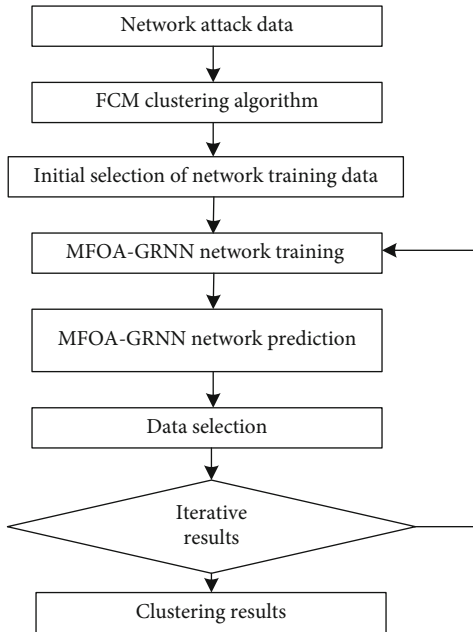


FIGURE 2: Flow chart of the FCM-MFOA-GRNN algorithm.

## 4.2. MFOA-GRNN Network

**4.2.1. Network Structure of GRNN.** Figure 3 shows the structure diagram of the GRNN network. The input of the network is  $X = [x_1, x_2, \dots, x_n]^T$ , the output is  $Y = [y_1, y_2, \dots, y_n]^T$ .

- (1) The number of neurons in the input layer is equal to the vector dimension of the learning sample and is the same as the number of neurons in the mode layer. The neuron transfer function in the mode layer is

$$P_i = e^{[-(X-X_i)^T(X-X_i)/2\sigma^2]}, \quad (1)$$

where  $X$  is the network input variable and  $X_i$  is the learning sample corresponding to the  $i$ th neuron.

The input of neurons is

$$D_i^2 = (X - X_i)^T(X - X_i). \quad (2)$$

- (2) There are two types of summation applied in the summation layer; the first one is

$$\sum_{i=1}^n e^{[-D_i^2/2\sigma^2]}. \quad (3)$$

It performs arithmetic summation on the outputs of all neurons in the mode layer, and the transfer function can be written as

$$S_D = \sum_{i=1}^n P_i. \quad (4)$$

Another calculation formula is

$$\sum_{i=1}^n Y_i e^{[-D_i^2/2\sigma^2]}. \quad (5)$$

It performs a weighted summation of all neurons in the mode layer, and the connection weight between the  $i$ th neuron in the mode layer and the  $j$ th neuron in the summation layer is the  $j$ th element of the  $i$ th output sample  $Y_i$ . Thus, the transfer function can be formulated as

$$S_{N_j} = \sum_{i=1}^n Y_{ij} P_i. \quad (6)$$

- (3) The output of the neuron corresponds to the  $j$ th element of the estimation result, and the output can be written as

$$y_i = \frac{S_{N_j}}{S_D}. \quad (7)$$

**4.2.2. Network Flow of MFOA-Optimized GRNN.** The performance of GRNN can be directly affected by the value of  $\sigma$ . This paper proposes a new MFOA-optimized GRNN, which is named as MFOA-GRNN, for the purpose of optimizing the spread value. FOA is prone to local extremes and cannot search for the global optimum, which is mainly caused by its fitness function. Hence, the fitness function must be modified to get rid of the local extremes. On the other hand, if the distance  $\text{Dist}(i)$  is positive, its reciprocal



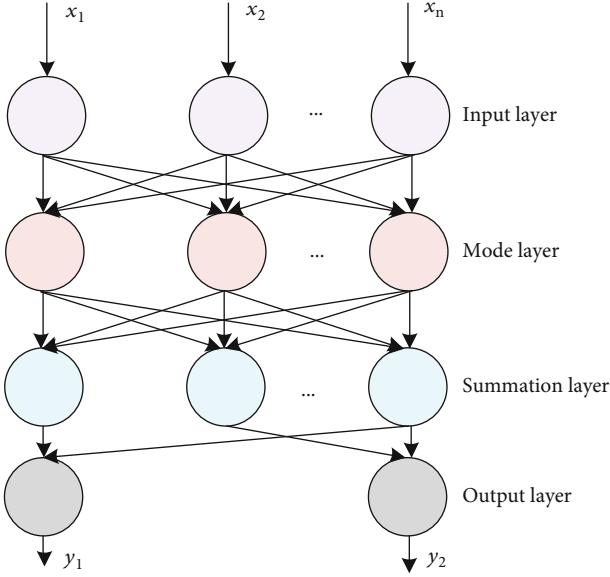


FIGURE 3: Structure of GRNN.

must be positive, which is the lack of negative values of fitness function as pointed out by many scholars. By adding  $S_i$  to an escape parameter, not only can the local minima be got rid of but also the fitness function can get negative values.

In addition, the flight area of fruit flies in real life is three-dimensional space, which is different from the two-dimensional search space of the original fruit fly algorithm. Using the three-dimensional space search method, the optimal spread value can be found iteratively by using the sharp olfactory and visual abilities of fruit flies. At this point, the mean squared error (MSE) is the smallest and  $\sigma$  is the optimal concentration value for taste. The foraging diagram of fruit flies in the three-dimensional space is illustrated in Figure 4.

The specific implementation steps are as follows.

*Step 1.* Randomly generate the initial position ( $X_{Init}, Y_{Init}, Z_{Init}$ ), the number of individuals, and the maximum number of iterations of the fruit fly group.

*Step 2.* Define random flight direction and distance:

$$\begin{aligned} x_i &= X_{Init} + \text{random value}, \\ y_i &= Y_{Init} + \text{random value}, \\ z_i &= Z_{Init} + \text{random value}. \end{aligned} \quad (8)$$

*Step 3.* Calculate the distance  $\text{Dist}(i)$  between each point and the initial point.

$$\text{Dist}(i) = \sqrt{(x_i^2 + y_i^2 + z_i^2)}, \quad (9)$$

$$S_i = \frac{1}{\text{Dist}(i)} + \Delta, \quad (10)$$

where  $S_i$  is the distribution parameter of GRNN.

*Step 4.* The mean square error is used as the determination function of taste concentration:

$$\text{Smell}(i) = \text{MSE}(i) = \frac{1}{n} \sum (y_{\text{pre}} - y). \quad (11)$$

*Step 5.* Find the individual with the optimal  $\text{Smell}(i)$  in the population, i.e., the minimal value of MSE.

*Step 6.* Retain the optimal taste concentration value  $S_i$  and the corresponding coordinate; the population will fly towards that position using visual advantage.

*Step 7.* Repeat steps 2 to 5 to repeatedly find the best solution. If true, proceed to step 6.

*Step 8.* Determine whether the maximum number of iterations is reached, and take the optimal spread value retained into the GRNN model to obtain the final prediction result.

*4.3. Intrusion Detection Model Based on the FCM-MFOA-GRNN Algorithm.* The intrusion detection model based on FCM-MFOA-GRNN algorithm consists of the FCM clustering algorithm, initial selection of network training data, MFOA-GRNN network training, MFOA-GRNN network prediction, and network training data selection.

- (1) The role of the FCM clustering algorithm is that when a large number of network attack data streams drained from the software-defined network enter into the system, these data streams are preprocessed first and then divided into  $n$  classes using the FCM algorithm, in which the clustering center  $c_i$  and affiliation matrix  $U$  of each class can be obtained
- (2) The selection of the initial data of network training is based on the selection of those samples closest to each type of center from the results of FCM clustering as the initial data of network training:
- (3) Randomly generate the initial position ( $X_{Init}, Y_{Init}, Z_{Init}$ ), number of individuals, and maximum number of iterations of the Drosophila population and generate the random direction and distance of flight

*Step 1.* First find the sample mean  $\text{mean}_i$  of each class in the  $n$  classes divided from the FCM clustering separately.

*Step 2.* Then, for all samples  $X$  in each class, calculate their distances to the sample mean  $\text{mean}_i$  separately to form a distance matrix  $d_i$ .

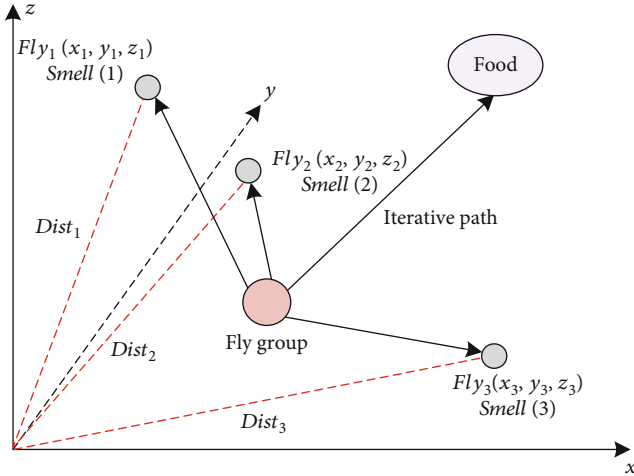


FIGURE 4: Schematic diagram of the iterative search for food of the fruit fly group.

*Step 3.* Find  $m$  number of samples with the shortest distance in the matrix  $d_i$ , and compose them into a group. Assume that their corresponding outputs are  $i$ . As  $n$  classes are divided finally, a total of  $n \times m$  groups of training data can be obtained after this step. At this point, the network intrusion feature vector is the input, and the intrusion class is its output.

Calculate the distance  $\text{Dist}(i)$  between each point and the initial point and the taste concentration determination value  $S_j$ . Let  $S_j$  be the distribution parameters of GRNN.

- (4) MFOA-GRNN network training. The role of this section is to take the selected training data to train the FOA-GRNN network. This is done in MATLAB by using the GRNN network training function `newgrnn()`
- (5) Based on all input sample data  $X$ , the network output sequence  $Y$  corresponding to them can be predicted

**4.4. Evaluation Metrics.** The algorithm performance is demonstrated by metrics such as the detection rate (DR) and false alarm rate (FAR). DR refers to the percentage of the number of abnormal data correctly detected in the actual number of abnormal data, which reflects the probability that an attack will be detected. FAR refers to the percentage of the number of abnormal data incorrectly detected in the number of all detected abnormal data, which reflects the probability of a normal behavior being treated as an attack. These two metrics are calculated as

$$\text{DR} = \frac{\text{TP}}{\text{TP} + \text{FN}}, \quad (12)$$

$$\text{FAR} = \frac{\text{FP}}{\text{TN} + \text{FP}}, \quad (13)$$

where TP is the abnormal data detected as abnormal, FN

is the abnormal data detected as normal, TN is the normal data detected as normal, and FP is the normal data detected as abnormal.

## 5. Experiment and Analysis

**5.1. Hardware.** The experimental platform is based on Windows 8, configured with Intel(R) Core(TM) i7 CPU M370 @ 2.7GHz, 16G memory, 500G hard disk. The simulation is conducted on MATLAB R2016b and neural network toolbox. Hadoop is used to build a cloud computing platform. Hadoop is an open-source distributed data processing framework and contains the functions needed for cloud computing, mainly including distributed file system HDFS, distributed computing model MapReduce, unstructured file storage system HBase, relational database transfer tool Sqoop, and distributed cluster negotiation service software Zookeeper.

**5.2. Dataset and Preprocessing.** In this paper, the algorithm is trained using the KDD CUP99 dataset with 500,000 training subsets and 500,000 test subsets, using the training subsets as the data for the training section of the algorithm. In the 500,000 training subsets, there are 97,278 pieces of Normal, 391,458 pieces of DoS, 52 pieces of U2R, 1,126 pieces of R2L, and 4,107 pieces of Probe. The KDD CUP99 dataset is processed network traffic data with 41 features for each connection, including 9 basic TCP features, 13 content features of TCP connections, 9 time-based network traffic statistics features, and 10 host-based network traffic statistics features.

These features are character-based and numeric, where numeric features contain discrete numbers and continuous numbers. And the data range of each feature varies greatly, which would make the features with low order of magnitude lose information if the raw data is used directly. In order to improve the accuracy of the machine learning algorithm, the dataset is standardized and normalized, which is processed as follows.

- (1) Numerical processing: convert character-based features to numerical features
- (2) Standardization: first, the mean value of each attribute and mean absolute error can be calculated as

$$\bar{x}_k = \frac{1}{n} \sum_{i=1}^n x_{ik}, \quad (14)$$

$$S_k = \sqrt{\frac{1}{n} \sum_{i=1}^n (x_{ik} - \bar{x}_k)^2}, \quad (15)$$

where  $\bar{x}_k$  denotes the mean value of the  $k$ th attribute,  $S_k$  denotes the mean absolute error of the  $k$ th attribute, and  $x_{ik}$  denotes the  $k$ th attribute of the  $i$ th record.

Next, each data record is standardized, which can be calculated as

$$Z_{ik} = \frac{x_{ik} - \bar{x}_k}{S_k}, \quad (16)$$

where  $Z_{ik}$  represents the value of the  $k$ th attribute in the  $i$ th data record after normalization.

- (3) Normalization: normalize each value after standardization to the interval [0,1].

$$X' = \frac{X - \min}{\max - \min}, \quad (17)$$

where max and min are the maximum and minimum values of the sample data, respectively.

**5.3. Iterative Optimization Trajectory of the Proposed Method.** Let the initial position of Drosophila population be  $[0, 0.5, 0]$ , the population size be 8, and the number of iterations be 150. Select 200 groups as training samples and 10 groups as prediction samples. The models proposed in this paper are used for prediction at the same time, and the results are shown in Figure 5. It can be seen that the fruit fly group in the proposed model does not follow a certain directional path to find the optimal solution sequentially, but there are only 6 position points in the trajectory route.

**5.4. Intrusion Detection Results Based on the FCM-MFOA-GRNN Algorithm.** In order to reflect a real network environment as much as possible, a number of data are selected from the KDD CUP99 dataset to create 5 groups of datasets, each of which contains 3800 normal data and 100 attack data. And these 5 groups of datasets need to be as even as possible in selecting attack categories. Table 1 shows the results of three simulation experiments on each dataset using the FCM-MFOA-GRNN algorithm, respectively, and the experimental results are taken as the average of the three results. Among them, two parameters are important metrics that can indicate the performance of the algorithm, i.e., DR and FAR. As shown in Table 1, DR and FAR of the proposed method are 91% and 1.176%, respectively.

In order to demonstrate the performance of the proposed method, it is compared with the methods proposed in Literature [27] and Literature [28] under the same experimental conditions, and the comparison results are shown in Table 2. From the experimental results, it can be noted that DR of the method proposed in Literature [27] is only 89.24% and FAR is 2.075%. DR of the method of Literature [28] is 90.1% and FAR is 1.237%. DR and FAR of the proposed method are 91% and 1.176%, respectively, which are better than those of the comparison methods. This is because the proposed method combines the FCM algorithm with GRNN, so as to cluster the samples to be classified in the original space by the FCM algorithm and then use the sample closest to the FCM clustering center to train the GRNN model and update the center point until a stable clustering center is obtained. Therefore, it can better distinguish the

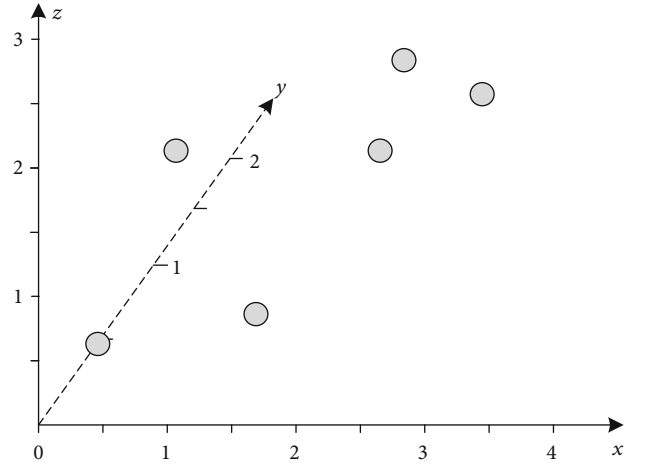


FIGURE 5: Iterative optimization trajectory of fruit flies in the proposed method.

TABLE 1: Intrusion detection results based on the FCM-MFOA-GRNN method.

	Normal	Attack	DR	FAR
Date set 1	3742	91	91%	1.175%
Date set 2	3758	93	93%	1.297%
Date set 3	3756	90	90%	1.138%
Date set 4	3697	89	89%	1.109%
Date set 5	3762	92	92%	1.161%
Average value	3743	91	91%	1.176%

TABLE 2: Performance comparison of different methods in intrusion detection.

Method	DR	FAR
Literature [27]	89.24%	2.075%
Literature [28]	90.1%	1.237%
Proposed method	91.0%	1.176%

small differences of attributes in complex spatial data and improve the accuracy of detection. In contrast, the comparison methods do not effectively mine the features of high-dimensional data, and therefore, the detection performance is poor.

In order to compare the running time of the proposed method with the methods of Literature [27] and Literature [28], different amount of data are selected from the KDD CUP99 dataset for testing. The running time of each algorithm was compared, and the results are shown in Figure 6. The minimum number of data selected is 200, and the maximum number is 20000. It can be easily seen from Figure 6 that the method of Literature [27] takes the most average detection time during the whole experiment, and the proposed method takes the shortest time. This is because the parameters of the FCM-GRNN model are optimized by using the global search feature of MFOA, and the three-dimensional search method is used to find the optimal

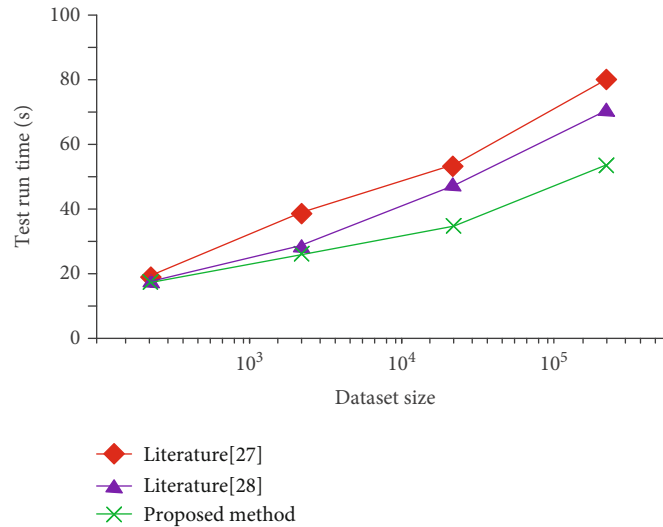


FIGURE 6: Comparison of running time when different sizes of datasets are detected by different methods.

spread value iteratively by using the sharp olfactory and visual advantages of fruit flies, making the algorithm converge faster and the time consumption be shortened. Therefore, the FCM-MFOA-GRNN method is feasible and efficient for processing large data volumes in cloud computing environments.

## 6. Conclusion

Aiming at the poor detection performance of existing intrusion detection methods in the environment of high-dimensional massive data and uneven class distribution, an anomaly traffic detection method based on deep learning in cloud computing environment is proposed. By introducing the combination of the FCM algorithm and GRNN, the stability of anomaly traffic detection system is improved. Meanwhile, MFOA is used to optimize the parameters of the FCM-GRNN method to speed up the convergence. Experimental results show that the proposed method has good detection ability.

The experiment only considers one intrusion detection dataset, so more datasets can be involved to train the detection model in the future. Moreover, anomaly detection is only one aspect. How to take mitigation measures to reduce the damage caused by network attack is also a direction of great research value.

## Data Availability

The data used to support the findings of this study are included within the article.

## Conflicts of Interest

The authors declare that there is no conflict of interest regarding the publication of this paper.

## References

- [1] Z. H. A. N. G. Yong-dong, C. H. E. N. Si-yang, P. E. N. G. Yu-he, and Y. A. N. G. Jian, "A survey of deep learning based network intrusion detection," *Journal of Guangzhou University Natural Science Edition*, vol. 18, no. 3, pp. 17–26, 2019.
- [2] J. Huang, W. Zhang, W. Huang, W. Huang, L. Wang, and Y. Luo, "High-resolution fiber optic seismic sensor array for intrusion detection of subway tunnel," in *2018 Asia Communications and Photonics Conference (ACP)*, pp. 1–3, Hangzhou, China, October 2018.
- [3] C. Deng and H. Qiao, "Network security intrusion detection system based on incremental improved convolutional neural network model," in *International Conference on Communication and Electronics Systems.*, pp. 1–5, Coimbatore, India, 2016.
- [4] M. H. Bhuyan, D. K. Bhattacharyya, and J. K. Kalita, "Network anomaly detection: methods, systems and tools," *IEEE Communication Surveys and Tutorials*, vol. 16, no. 1, pp. 303–336, 2014.
- [5] N. El Moussaid and A. Toumanari, "Overview of intrusion detection using data-mining and the features selection," in *International Conference on Multimedia Computing and Systems*, pp. 1269–1273, Marrakech, Morocco, 2014.
- [6] A. Milenkoski, M. Vieira, S. Kounev, A. Avritzer, and B. D. Payne, "Evaluating computer intrusion detection systems," *ACM Computing Surveys*, vol. 48, no. 1, pp. 1–41, 2015.
- [7] A. Khraisat, I. Gondal, P. Vamplew, and J. Kamruzzaman, "Survey of intrusion detection systems: techniques, datasets and challenges," *Cybersecurity*, vol. 2, no. 1, pp. 1–22, 2019.
- [8] R. Domingues, M. Filippone, P. Michiardi, and J. Zouaoui, "A comparative evaluation of outlier detection algorithms: experiments and analyses," *Pattern Recognition*, vol. 74, no. 4, pp. 406–421, 2018.
- [9] Y. Mehmood, M. A. Shibli, U. Habiba, and R. Masood, "Intrusion detection system in cloud computing: challenges and opportunities," in *2nd National Conference on Information Assurance*, pp. 59–66, Rawalpindi, Pakistan, 2013.

- [10] A. Drewek Ossowicka, M. Pietrołaj, and J. Rumiński, "A survey of neural networks usage for intrusion detection systems," *Journal of Ambient Intelligence and Humanized Computing*, vol. 12, no. 1, pp. 497–514, 2021.
- [11] M. Ring, S. Wunderlich, D. Scheuring, D. Landes, and A. Hotho, "A survey of network-based intrusion detection data sets," *Computers & Security*, vol. 86, no. 6, pp. 147–167, 2019.
- [12] A. Bakshi and Sunanda, *A comparative analysis of different intrusion detection techniques in cloud computing*, Springer, Singapore, 2019.
- [13] S. G. Kene and D. P. Theng, "A review on intrusion detection techniques for cloud computing and security challenges," in *2nd international conference on electronics and communication systems*, pp. 227–232, Coimbatore, India, 2015.
- [14] N. Keegan, S. Y. Ji, A. Chaudhary, C. Concolato, B. Yu, and D. H. Jeong, "A survey of cloud-based network intrusion detection analysis," *Human-centric Computing and Information Sciences*, vol. 6, no. 1, pp. 1–16, 2016.
- [15] A. Aburomman and M. B. I. Reaz, "A survey of intrusion detection systems based on ensemble and hybrid classifiers," *Computers & Security*, vol. 65, no. 4, pp. 135–152, 2017.
- [16] A. Nisioti, A. Mylonas, P. D. Yoo, and V. Katos, "From intrusion detection to attacker attribution: a comprehensive survey of unsupervised methods," *IEEE Communication Surveys and Tutorials*, vol. 20, no. 4, pp. 3369–3388, 2018.
- [17] L. N. Tidjon, M. Frappier, and A. Mammar, "Intrusion detection systems: a cross-domain overview," *IEEE Communication Surveys and Tutorials*, vol. 21, no. 4, pp. 3639–3681, 2019.
- [18] C. Liu, J. Wang, J. Xu, J. Wang, C. Liu, and Y. Wang, "Abnormal data flow detection in the Internet of things," in *4th International Conference on Electronics and Communication Engineering*, Xi'an, China, 2021.
- [19] M. Alauthman, N. Aslam, M. Al-Kasassbeh, S. Khan, A. Al-Qerem, and K. K. R. Choo, "An efficient reinforcement learning-based Botnet detection approach," *Journal of Network and Computer Applications*, vol. 150, no. 11, article 102479, 2020.
- [20] W.-H. Lin, H.-C. Lin, P. Wang, B.-H. Wu, and J.-Y. Tsai, "Using convolutional neural networks to network intrusion detection for cyber threats," *international conference on applied system invention*, 2018, pp. 1107–1110, Chiba, Japan, 2018.
- [21] R. Blanco, P. Malagón, J. J. Cilla, and J. M. Moya, "Multiclass network attack classifier using CNN tuned with genetic algorithms," in *28th international symposium on power and timing modeling, optimization and simulation*, pp. 177–182, Platja d'Aro, Spain, 2018.
- [22] A. H. Mirza and S. Cosan, "Computer network intrusion detection using sequential LSTM neural networks autoencoders," *26th signal processing and communications applications conference*, 2018, pp. 1–4, Izmir, Turkey, 2018.
- [23] F. Farahnakian and J. Heikkonen, "A deep auto-encoder based approach for intrusion detection system," in *20th international conference on advanced communication technology*, pp. 178–183, Chuncheon, Korea (South), 2018.
- [24] M. Al-Qatf, Y. Lasheng, M. Al-Habib, and K. Al-Sabahi, "Deep learning approach combining sparse autoencoder with SVM for network intrusion detection," *IEEE Access*, vol. 6, no. 5, pp. 52843–52856, 2018.
- [25] A. L. H. Muna, N. Moustafa, and E. Sitnikova, "Identification of malicious activities in industrial Internet of things based on deep learning models," *Journal of Information Security and Applications*, vol. 41, no. 12, pp. 1–11, 2018.
- [26] R. C. Staudemeyer and C. W. Omlin, "Evaluating performance of long short-term memory recurrent neural networks on intrusion detection data," in *Proceedings of the South African Institute for Computer Scientists and Information Technologists Conference*, pp. 218–224, New York, NY, United States, 2013.
- [27] Y. Zhang, X. Chen, D. Guo, M. Song, Y. Teng, and X. Wang, "PCCN: parallel cross convolutional neural network for abnormal network traffic flows detection in multi-class imbalanced network traffic flows," *IEEE Access*, vol. 7, no. 9, pp. 119904–119916, 2019.
- [28] A. Pektaş and T. Acarman, "A deep learning method to detect network intrusion through flow-based features," *International Journal of Network Management*, vol. 29, no. 3, pp. 2019–2026, 2019.

## Research Article

# Behavior Dissection of NGWN Live Audio and Video Streaming Users with Enhanced and Efficient Modelling

Asia Ali <sup>1</sup>, Ihsan Ullah <sup>1</sup>, Atiq Ahmed <sup>1</sup>, Waheed Noor <sup>1</sup>, Ahasham Sajid <sup>2</sup>,  
and Inam Ullah Khan <sup>3,4</sup>

<sup>1</sup>Department of Computer Science & IT, University of Balochistan, Quetta, Pakistan

<sup>2</sup>Department of Computer Science, FICT, BUIITEMS, Quetta, Pakistan

<sup>3</sup>Department of Computer Science, Institute of IT & Computer Science, Afghanistan

<sup>4</sup>Department of Electronic Engineering, SEAS, Isra University, Islamabad Campus, Pakistan

Correspondence should be addressed to Inam Ullah Khan; [inamullahkhan05@gmail.com](mailto:inamullahkhan05@gmail.com)

Received 18 December 2021; Accepted 4 March 2022; Published 30 March 2022

Academic Editor: Shalli Rani

Copyright © 2022 Asia Ali et al. This is an open access article distributed under the Creative Commons Attribution License, which permits unrestricted use, distribution, and reproduction in any medium, provided the original work is properly cited.

Peer-to-peer (P2P) live video streaming is an application-level approach providing ease of deployment with low cost as compared to the IP multicast and client/server (C/S) architecture. These systems solely rely on end-hosts to disseminate the content; therefore, their performance largely banks on end-hosts, called peers. Since peers themselves are controlled by users, users' activities become activities of peers. In such a network, the highly dynamic behavior of users impacts the network performance. Therefore, for performance improvement, a thorough understanding of user behavior is crucial. To explore and understand user behavior, numerous studies have been carried out. However, user behavior is complex, having several elements with dependency relationships, which make it difficult for a single measurement study to represent it comprehensively. Therefore, this work takes a two-step approach. Firstly, it collects existing measurement studies and analyzes, compares, and contrasts them to extract user behavior metrics and their relationships from them. Secondly, in light of the observations gained, this research analyzes traces of user behavior collected from an operational system. Such an outcome is useful, on one hand, for user behavior modelling towards performance improvement in NGWN, and on the other hand, it provides insights for further measurements and analysis.

## 1. Introduction

Live video streaming is one of the Internet services that emerged and became popular late. It is a bandwidth-intensive service also requiring stringent playback deadlines. Enabling such a service has been a challenge which has led to the emergence of three major architectures. The first one, called client/server (C/S) architecture, is a centralized model which involves servers in order to provide video streams to clients over unicast links. Consequently, all the burden of broadcasting concentrates in centralized servers. Scalability and cost are thus the prominent issues in these systems as a surge in users' population involves an increase in the resource consumption of the servers. Content delivery networks (CDNs) are an improved form of the C/S model in which a distributed network shares the load of content dis-

semination [1]. This architecture involves the deployment of multiple servers at appropriate locations over the globe in order to allow the nearest server serve the user. However, these systems face challenges of high deployment cost and scalability against an increasing number of users.

Concerning the network perspective, IP multicast presents an effective solution to the bandwidth issues by involving routers to duplicate one stream over several network links. Nevertheless, due to the unavailability of IP multicast globally, it cannot be utilized at the Internet scale. Nonetheless, telecom operators use this approach in their Internet television (IPTV) systems inside their own networks.

By contrast, at application level, a P2P system is made of peers which unlike dedicated servers have intermittent presence. Moreover, the scalability of these systems relies on the contribution of peers. Therefore, organization of peers for

stream delivery becomes a crucial aspect of these systems [2]. Several strategies have been proposed that suggest various stream delivery mechanisms. These can be broadly classified into push-based, pull-based, and hybrid strategies.

The push-based approach defines a tree structure for stream delivery [3], in which peers are into the parent-child relationship. A parent peer pushes the content to child peers without requiring an explicit request. The single-tree system is its simplest form in which an individual tree is formed for each stream. Every parent peer pushes the stream to all its child peers soon after it receives the stream. These systems are a good choice in terms of efficiency and communication overhead; however, they are not robust in event of peer departure which occurs frequently in P2P systems. Furthermore, leaf nodes are deprived of using their active transmission capacity that results in poor resource utilization.

In view of limitations of single-tree systems, the multi-tree strategy [4, 5] works on the principle of dividing a single stream into multiple substreams through using applicable data-encoding method such as multiple description coding (MDC) [6]. The goal is to deliver each substream over a different tree from which a consumer peer can select the number of trees according to its bandwidth capacity. To ensure fair distribution of load and to decrease the impact of peer's departure, peers' placement into trees is managed in such a way that a peer becomes an intermediate node in a tree where it can relay the stream to others and a leaf in another tree. Hence, in case of a peer's exit from the network, the one substream is affected.

Pull-based strategy works on the mesh structure for stream delivery. In this approach, a peer can create and maintain simultaneous connections with multiple other peers [7]. This is a random structure in which the flow of stream is realized by the stream availability. The availability of content is notified through periodic advertisements by each peer to its neighbor peers. A provider peer only delivers the content on explicit requests for certain blocks. Pull-based systems provide robustness against the intermittent presence of peers but they are less efficient than push-based systems in terms of timely delivery of the stream.

A hybrid push-pull system [8] is aimed at mitigating the downsides of push- and pull-based systems. It combines the resiliency of pull-based systems and efficiency of push-based systems. In hybrid approach, each peer may operate in both push and pull modes. This approach attempts to deliver most of the content through push operation while pull operations are utilized in the start after arrival of a peer and afterwards, to retrieve the blocks missed during push function. An open issue within these systems is the selection of an upstream peer to receive contents through push operation.

P2P-based live video streaming involves low-cost installation and provides high scalability [9]; however, designing a P2P IPTV framework is not trivial. Existing works attempt to tackle these issues through the design of robust topologies and efficient stream distribution strategies. A major issue in these systems is their dependence on users in addition to heterogeneity of end-systems and their interconnection. A peer in these systems reflects the behavior of its user which

is highly dynamic; thus, affecting the performance such as a sudden exit of a peer from the network stops the relying peers from receiving the stream creating buffer underflows.

Numerous works are dedicated to study and understand user behavior, but due to the complex nature of the subject, any of the studies alone cannot capture all its aspects. Hence, such different works need a thorough analysis to bring their findings at one place for comparison and a concrete view. This research attempts to compile all such studies performed over IPTV systems in wired, wireless, and mobile networks and perform their thorough analysis to identify important metrics involved in the user behavior and also highlight factors that impact them. Furthermore, we analyze traces of user behavior, especially under those conditions which have been mostly ignored in the existing literature. Results of this work can be utilized in modelling user behavior in IPTV systems. Furthermore, these models can be adapted for the next-generation wireless networks (NGWNs), ant colony optimization [10], smart cities [11], and IoT's applications [12, 13].

The highlights of this work are as follows:

- (i) Collection of measurement studies aimed at user behavior in live streaming systems
- (ii) Analysis of observed variables found in different studies
- (iii) Synthesis of influential relationships among different variables
- (iv) Analysis of individual user behavior from a dataset of user activities in an operational system

This article is organized as follows. Section 2 presents the related work. Section 3 gives an overview of the measurements by elaborating various elements focused by each of them. This section also discusses the metrics of user behavior found in analyzed works and presents the dependency relationships among these metrics and other elements. Section 4 presents an analysis of user behavior traces collected from an operational system. Section 5 provides conclusion and perspectives.

## 2. Related Work

Existing works on P2P IPTV user behavior can be divided into two broad categories. The first one focuses on the understanding of user behavior through analysis of behavior logs. The second one is dedicated to user behavior models intended for integration into systems for their performance improvement. First, we discuss analysis-based works.

Reference [14] analyzes the influential factors of peer's stability and bandwidth contribution such as initial streaming quality leads to stable user sessions. Reference [15] analyzes arrival and departure behavior of users from IPTV traces and concludes that if a video delivery structure accommodates the departures, the consumption of system resources can be reduced. Reference [16] compares user behavior in mobile and land-line connectivity-based IPTV

TABLE 1: Summary of works.

Ref.	Focus	Limitation
Analysis-based works		
[14]	Influential factors of peer's stability and bandwidth	Global phenomenon
[15]	Arrivals and departures of users	Ignore other factors such as streaming quality
[16]	Stability in mobile and fixed nodes	Global behavior and missing factors
[18]	Impact of device type and connection type	Global behavior and missing factors
[19]	Difference in mobile and nonmobile cases	Global behavior and missing factors
[20]	Impact of download speed on user engagement	Ignore other factors
Model-based works		
[21]	Contextual model based on machine learning	Long learning time
[22]	Prediction of next channel	Ignores other metrics
[23]	Prediction of next channel	Ignores other metrics
[24]	Prediction of next channel	Ignores other metrics
[25]	Prediction of neighbor's QoS	Ignores other metrics
[27]	Priority: age, bandwidth, utilization	Considers only age for stability

services. They remark that users' sessions and popularity of content have different features in the two types of connectivity. Furthermore, they also note a difference in behavior between WiFi and 3G users

Since these mentioned works and other several contributions attempt to analyze one or a few aspects of user behavior, [17] synthesizes user behavior measurements performed over both live and video-on-demand users to present the consensual and contradictory findings. However, further measurements have been carried out after this work which may contain new observations. A few of such works are as follows.

Reference [18] analyzes logs from a commercial mobile IPTV service. They model browsing sessions and viewing sessions with different distributions. Furthermore, they notice the impact of the device type and network connection on user's playback patterns. Similarly, [19] analyzes users' sessions, activities, and arrival rates. They also compare the mobile and nonmobile and provide distribution models for sessions and activities. Reference [20] analyzes logs to know the causal impact of download speed on user engagement. They discern that lower speeds have a negative impact on user engagement in viewing longer videos

Concerning model-based works, [21] proposes a Bayesian network model that estimates user departure time from the past behavior in the current scenario from several metrics and parameters. They present a topology management framework aimed at stabilizing the topology. Reference [22] proposes a personalized channel recommendation system for live TV channels. This system learns from user behaviors when watching live channels using deep learning and predicts the next channel of a user. The main goal of this approach is to minimize channel switching by providing the channels of users' interest. To reduce the bootstrapping delay, [23] proposes to integrate agents to model user behavior. Aggregated knowledge of agents is distributed in the system through sharing among the agents. Agents predict the channels and then assign those to the users in order to minimize the switching delay. Similarly, [24] compares dif-

ferent classifiers to predict the next channel in an IPTV system. Reference [25] proposes to predict the QoS of neighbor peers through neural collaborative filtering. The predicted QoS can be used to choose a neighbor peer. Reference [26] uses reinforcement learning in a cloud-assisted P2P streaming system. The goal of using machine learning is to restrict the cloud rental cost according to a desired QoS level. To construct a P2P IPTV overlay, [27] uses fuzzy logic. They define a metric "priority" to choose a parent peer which is a combination of the peer's age, upload bandwidth, and utilization. Fuzzy logic is used to determine the overall priority of a peer for parent selection.

As shown in Table 1, the existing works consider only one or a few metrics while ignoring others. This work complements these works in such a way that instead of proposing a model or analyzing traces in isolation, we focus on almost all measurements and provide a global state of all observations made in different works. Based on these observations, we also present our own analysis of user behavior traces. In the next section, we collect these measurement metrics and thoroughly present their impact on IPTV streaming.

### 3. User Behavior Measurements

In view of the crucial role played by user behavior, numerous research efforts have been dedicated to measurement studies over the past decade. These works are mainly based on the analysis of traces collected from operational systems. Collected traces represent user activities over long time periods. Three different methods have been used for the trace collection.

*3.1. Log-Based Method.* It is the preferred one. In this approach, traces come from system logs which are automatically created by the system itself. Such traces can only be provided by the system operators.



**3.2. Crawlers Method.** A crawler in its initial step sends a request to the peer membership server for getting the list of online peers. Then, it repeatedly starts sending partnership request to every peer available in the list. After receiving the partners' list, it repeats the process for newly known peers. In this way, a few activities such as users' population and presence can be monitored.

**3.3. Passive Method.** It monitors the communication pattern of the local node with other peers to extract network-level information.

These two latter methods provide less concrete information as compared to the log-based method. Existing studies vary in terms of the collection method as well as measured metrics. It is perhaps due to the particular interest in a specific metric or due to unavailability of the required information.

**3.4. Measurement Parameters.** The commonly measured user behavior metrics within these studies are given below.

**3.4.1. Sojourn Time (ST).** Sojourn time or session duration represents the time duration for which a user holds a particular channel. In other words, it is the time period between arrival and departure from a channel. A longer sojourn time means a stable user.

**3.4.2. Streaming Quality (SQ).** Streaming quality is a generic term that includes several performance parameters. A few notable parameters are start-up time, rendering quality, buffering ratio, rate of buffering events, and average bitrate [28–33]. Since each work considers one or more of these metrics as streaming quality, we aggregate all of them under streaming quality in our work.

(1) *Start-Up Time.* The delay between a user request for a stream and the time the video is played is called start-up time.

(2) *Rendering Quality.* Frames per second determine the quality of the stream which may reduce due to congestion in the network.

(3) *Buffering Ratio.* It is the ratio of the whole session to the buffering time [28, 31].

(4) *Rate of Buffering Events.* Buffering events distract users from the content and it is annoying. A larger number of buffering events means low streaming quality [28, 31].

(5) *Average Bitrate.* The average amount of bits transmitted in a unit time during a session is called bitrate. The bitrate usually varies in an IPTV session due to the bursty traffic of the Internet [28, 31].

**3.4.3. Joining & Leaving (J/L).** The process of request by a user for a channel and the system's response to allow the user completes the joining. Similarly, leaving demonstrates the exit from the same which may be the result of quitting the system or switching from current channel to another channel.

**3.4.4. Channel Switching (CS).** It is the behavior event in which a user selects a new channel while viewing one. The time period between a user request for a new channel and the time the channel is played is called channel switching.

**3.4.5. Channel Popularity (CP).** Channel popularity is measured through the number of join requests for a channel as well as from the number of online users, also called the instantaneous popularity.

We collect measurements that analyze one or more of the abovementioned metrics and depict their summary in Table 2. It is evident that each measurement focuses on one or a few metrics. Furthermore, there are other variables identified by these studies which have influential relationships with these metrics. Such variables too are not present in a single study as a whole which further necessitates the analysis of these studies themselves for an abstract view. Next, we discuss the analysis of these metrics from the observations presented in different works.

**3.5. Analysis of Metrics.** Here, we present a synthesis of each user behavior metric which has been analyzed in different studies. Taking one metric at a time, we extract the observations regarding it, from different studies to provide an abstract view of all works. We commence our synthesis with the sojourn time.

**3.5.1. Sojourn Time.** Commonly, sojourn time is analyzed for its lengths during different sessions. General observations about the lengths [14, 41, 59] and fitting of statistical distributions [39, 45, 60] are the major aspects analyzed for sojourn time. According to their observations, majority of works report short sessions in larger numbers as compared to long sessions. A common reason for such a behavior can be channel surfing which leads to very short sessions as a user needs to select a channel for viewing. We tabulated the sojourn time distributions in Table 3.

Weibull distribution dominates this list which has been observed by a number of studies. Among other distributions, the generalized Pareto distribution is shown to fit best with dropped tail for long sessions while lognormal distribution for short sessions. Similarly, in the surfing mode, Burr distribution is a best fit for sojourn time and gamma distribution fits well with short sessions. Given these observations, the selection of a consensual model is not straight forward. It is due to the reason that some external factors such as network connectivity type, device type, and content type play a role in having an impact on length of a session. To address that we separate works that analyze sojourn time in the context of the device type and connection type and show them in Table 4. It is again evident that distributions vary according to the device type (mobile/nonmobile) and connection type (WiFi, fixed, and cellular). Therefore, in view of these observations, a consensus on one model is not reachable.

**3.5.2. Channel Popularity.** Authors in [16] define channel popularity in two ways. One is the ability to attract users that can be determined from the users' requests for a particular channel. The other is to hold users in session, which can

TABLE 2: Analysis of user behavior metrics in different studies.

Source	System	Provider	Observation period	Data	Observed metrics				
					ST	SQ	CS	CP	J/L
[34]		Spotify	2010–2011		C	C			
[35]			Dec. 2013–Jul. 2015				C		
[36]		P2P	06 months		C				
[37]		Unknown	2010	Log	C	C			
[38]			03-Jun.-12–30-Oct.-12		C				
[18]	P2P	PPTV	Apr 1 <sup>st</sup> –14 <sup>th</sup> , 2013		C				
[15]		Unknown	Aug. 2008–Apr. 2009		C		C		
[39]			Feb. to Nov. 2008	Crawler	C			C	
[40]		PPLive	Nov. 2006 (for 28 hrs)		C				
[41]			2006–2007	Crawler/passive	C			C	C
[42]		SopCast				C		C	
[43]			Unknown	Unknown	C				
[44]	CDN	Unknown	2-week period		C	C			
[45]	P2P	PPLive, PP-stream, sop- cast, TVants	Jun. 2006	Passive	C				
[46]			Dec. 2008–Jan. 2009		C	C		C	
[47]		SopCast	Feb.–Mar. 2013	Crawler	C				
[48]	P2P	Unknown	Oct. 2011 to Apr. 2012		C				
[14]		UUSee	May to Jun. 2008		C				
[49]		Telco managed	May 2007–Jun. 2008		C			C	C
[28]	IPTV	Unknown	2010	Log		C			
[31]		Akamai				C			
[50]		Akamai				C			
[29]	CDN	Unknown				C	C		
[51]								C	
[52]	P2P	PPLive	Unknown					C	
[53]				Unknown				C	
[54]	Hybrid CDN- P2P	Unknown				C			
[55]		SopCast				C			
[56]	P2P	Major League Baseball broadcaster	In 2009 (3 hours)	Crawler		C			
[19]		PPLive	Unknown	Log	C	C		C	C
[57]		PPStream	Unknown	Crawler				C	C
[58]	IPTV	Unknown	6-month period				C		

ST: sojourn time; SQ: stream quality; CS: channel switching; CP: channel popularity; J/L: joining/leaving.

be perceived from the total sojourn times of users. They observe that analyzing channel popularity on both these parameters lead to similar results. They find Pareto distribution as the best fit for popularity. Concerning other measurements, most of them consider the frequency of users' requests. We show the observed models of different measurements in Table 5. It can be seen that most of the models observe Zipf distribution; however, most often, it fits well with the head but not with the tail in the same manner. Consequently, in [49], the head is modeled with Zipf distribution and the tail is shown to fit well with exponential distribution.

**3.5.3. Peers Joining and Leaving Process.** Peers independently join and leave the system which turns the P2P network highly dynamic. This joint effect is called churn and it has

a crucial impact on the performance of the system. Analyses of joining and leaving by different measurement studies [41, 60] reveal high joining and leaving rates at the start and end of a program, respectively. Furthermore, they observe stability midway through a session; however, commercial breaks lead to channel switching. Concerning the arrival process, exponential distribution [60], piecewise-stationary Poisson process [65], and nonhomogenous Poisson nature [34] have been reported. Although the arrival process is not extensively studied as sojourn time and popularity, mostly, Poisson distribution is used for its modeling.

**3.5.4. Channel Switching.** Users may hold a session in two modes, namely, browsing and viewing. Browsing is the surfing behavior while in viewing mode, a user watches the content. Surfing leads to frequent switches among the channels.

TABLE 3: Sojourn time distributions.

Source	System	Sojourn time distributions
[61]	HTTP	Weibull distribution
[34]	Spotify	Weibull, log-normal
[59]	CNLive	Weibull ( $\alpha = 3.1323, \beta = 4.5861$ ), gen. Pareto ( $\kappa = 0.33795, \sigma = 605.74, \mu = 601.0$ ), log-normal ( $\sigma = 1.6394, \mu = 3.3172, \gamma = 6.1731$ )
[46]	SopCast	Weibull ( $\alpha = 2.032, \beta = 0.233$ ), log-normal ( $\mu = 0.823, \sigma = 1.459$ )
[62]	IPTV	Burr distribution ( $\alpha = 2.4, \beta = 5.06, \kappa = 0.81$ ), gamma distribution ( $\alpha = 0.453, \beta = 1192.1$ )
[16]	CNLive	Gen. Pareto ( $\kappa = 1.0259, \sigma = 4.0102, \mu = 1$ ), log-normal ( $\sigma = 1.3450, \mu = 1.8370$ )
[63]	IPTV	Pareto, Weibull
[45]	PPLive, PPStream, SopCast, TVAnts	Weibull ( $\lambda = 12.3, \kappa = 0.2$ ), Weibull ( $\lambda = 322.1, \kappa = 0.4$ ), Weibull ( $\lambda = 993.8, \kappa = 0.4$ ), Weibull ( $\lambda = 1572.8, \kappa = 0.6$ )
[45]	PPLive, PPStream, SopCast, TVAnts	Weibull ( $\lambda = 12.3, \kappa = 0.2$ ), Weibull ( $\lambda = 993.8, \kappa = 0.4$ ), Weibull ( $\lambda = 322.1, \kappa = 0.4$ ), Weibull ( $\lambda = 1572.8, \kappa = 0.6$ )
[60]	IPTV	Lognormal ( $\sigma = 1.6394, \mu = 6.351$ )
[34]	Spotify	Weibull, log-normal distribution

TABLE 4: Sojourn time distributions based on the type of connection (TC) and type of device (TD).

Source	System	TC	TD	Sojourn time distributions
[16]	CNLive			(log-normal with $\sigma = 1.2997, \mu = 2.0738$ for WiFi users), (log-normal with $\sigma = 1.3429, \mu = 1.5808$ for 3G users)
[18]	PPLive	WiFi/3G	Mobile/nonmobile, nonmobile	Pareto distribution
[19]	IPTV			Exponential distribution
[50]	CDN	Wired		Quasi-experimental designs

TABLE 5: Channel popularity distributions.

Source	Studied system	Observed distributions
[16]	CNLive	Pareto distribution type I
[49]	Telco managed	Zipf-like head, exponential tail
[49]	Telco managed	Zipf with $\alpha = 0.5$
[38]	China Telecom	Geometric
[64]	Twitch	Zipf
[60]	Telco managed	Zipf like

Surfing mode poses challenges in about all kinds of live streaming architectures as it involves the initialization of a new session for stream delivery and a starting delay is added. It has been observed that users use button preference and channel preference during channel switching. The former is concerned on the choice of the button such as up/down to switch frequently, and channel preference means how often a user watches a particular channel. Work [66] observes Zipf-like distribution for channel preference but does not find any pattern for button-preference [66]. Understandably, the channel switching probability is higher in the channel surfing mode [52].

Nonetheless, concerning button preferences, [49, 60] observe 56–60% linear switches where majority of switches

that are 69–72% happen to be upward while 28–31% are noted to be downward. Furthermore, [66] analyzes channel switching behavior through using a semi-Markov process and observes Poisson distribution for different channel switches. Reference [67] analyzes commercial IPTV real traces and analyzes how users select channels. They observe that usually, users switch 4 channels on average before they select a channel.

To conclude discussion on the analyses of user behavior metrics, a plethora of measurement works have been carried out. However, observations of these measurements are in isolation and seem to depend upon the system. Therefore, generalizing these observations is not trivial. Consequently, as a next step, we attempt to combine the relationships among different metrics and other factors observed in different measurements.

*3.6. Metric Relationships.* The analysis has given earlier the metrics which provide insight information utilizing models with changing conditions. Therefore, it is critical to analyze the impact of one metric on another and external impacting factors that influence these metrics. Studies on the user behavior also analyze such relationships usually for a subset of variables. Therefore, in this section, we focus on these relationships to put important variables of user behavior in perspective. One again, we begin with sojourn time and discuss its dependence on other variables.

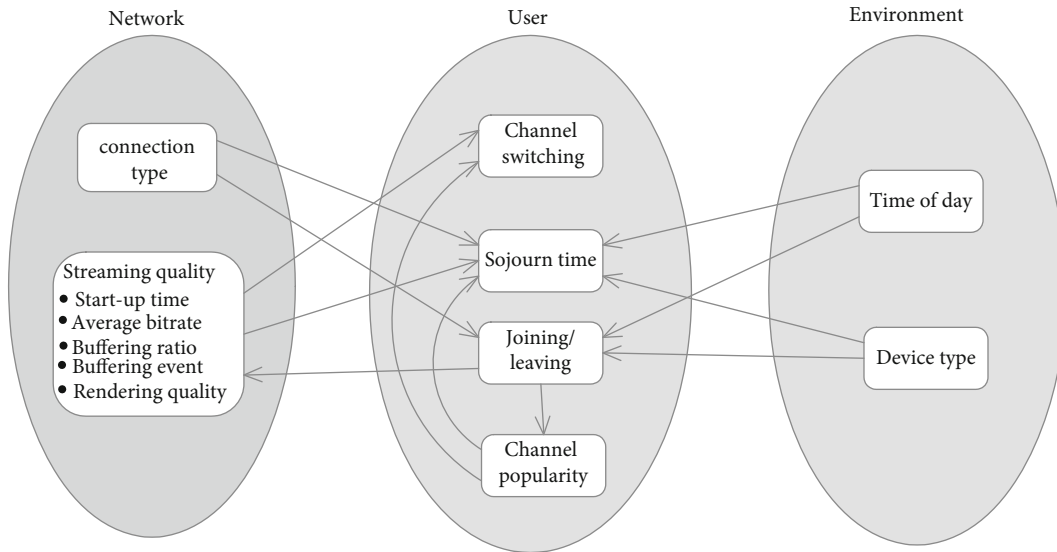


FIGURE 1: Causal graph of user behavior metrics and external elements.

**3.6.1. Sojourn Time.** Sojourn time is the core of user behavior, and it has been observed that it is impacted by a number of factors and metrics. These include the quality of streaming, channel popularity, time of the day, peers joining and leaving, device type, and connection type [16, 18, 50, 59]. Authors in [14] observe a strong correlation of it with the initial quality of streaming. It means that a user receiving a good quality stream in the start of a session tends to watch it for longer time. Similarly, user's sojourn time is longer while watching popular channels as compared to unpopular ones. Moreover, the time of the day influences sojourn time as observed in [14]. Such an observation indicates how users watch for longer or shorter durations over different times of a day due to their availability for short or long periods.

Authors in [68] observe that flash crowd degrades the streaming quality leading into an increase in early exit of users which indicates an impact of the arrival rate on session duration. Reference [34] remarks shorter sojourn times for mobile users than desktop users. Similarly, 3G users have shorter sojourn times than WiFi users. Furthermore, mobile TV users have shorter sojourn times than IPTV users [16]. All these observations show impact of the device type and connection type on sojourn time.

**3.6.2. Joining and Leaving Process.** Our extraction of findings from different studies reveals impact of several factors on joining and leaving rates of users. These include channel popularity, time of day, streaming quality, device type, and connection type. Works [16, 18, 31] have consensus on varying joining/leaving rates over different kinds of channels. High joining rates of users are observed in popular channels while the opposite has been noted in unpopular contents [15]. Similarly, it has been revealed that streaming quality influences the joining/leaving rates of peers where users find it hard to view channels of low streaming quality [19, 28, 31, 61]. Work [19] observes that due to poor connectivity, a noteworthy number of mobile users quits the

sessions as well as the proximity in order to reconnect, therefore indicating an impact of the connection and device types on arrival and departure.

**3.6.3. Channel Popularity.** Time of the day and joining and leaving of users influence the channel popularity. Studies [49, 60] observe diurnal patterns suggesting a peak of population around noon time and another higher peak at the beginning of the night. This clearly shows the influence of time-of-the-day on popularity. Concerning the arrival and departure rates, it is obvious that joining and leaving rates influence popularity as affirmed in [40, 49].

**3.6.4. Channel Switching.** According to user behavior measurements [51, 58, 66, 69], start-up delays, advertisements, and channel popularity have influence on channel switching. Start-up delay is part of the streaming quality which has an impact on channel switching. Similarly, advertisements are part of the content which has its own popularity so we keep advertisements and channel popularity together.

To get an abstract view of the observations discussed above, we place the involved variables into three groups and term them as user, network, and the environment. Here, sojourn time, popularity, joining/leaving, and channel switching make the user group where all these variables represent user behavior metrics. Streaming quality and connection type are put in the network group since they determine the network performance. Finally, we place the impacting factors from outside the user behavior and network in the environment which are time-of-the-day and device type. We demonstrate these groups in Figure 1 in the form of a causal graph. Here, the directed edge shows the impact of an element on the other. This graph gives a global view of all the observations made in different measurement studies and can be used as the baseline for further measurements and models.

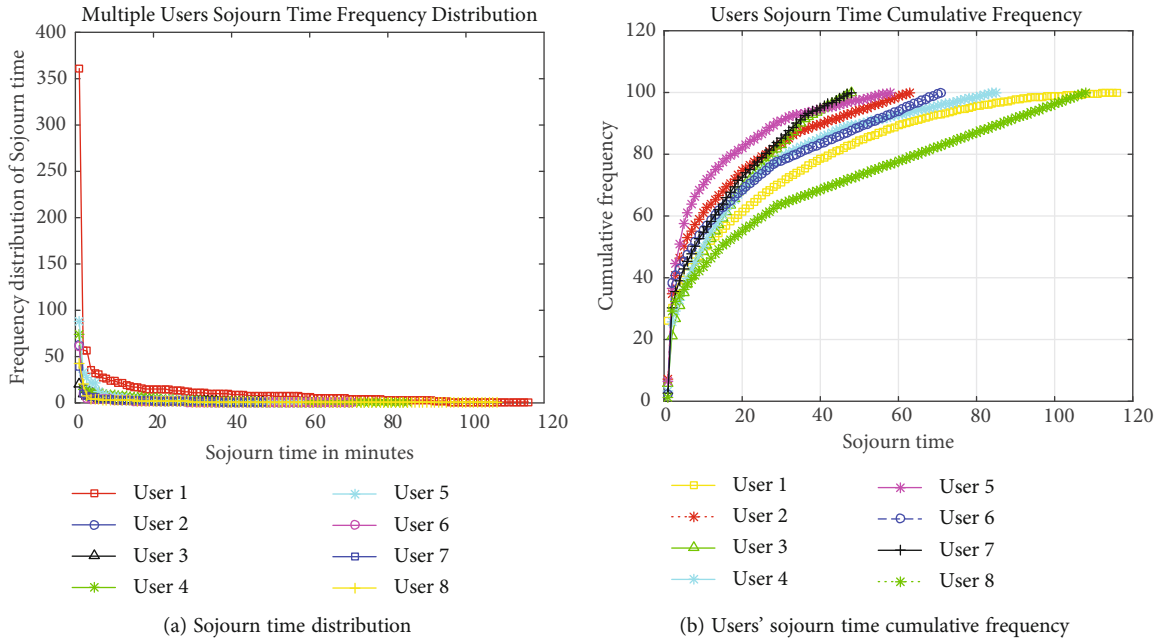
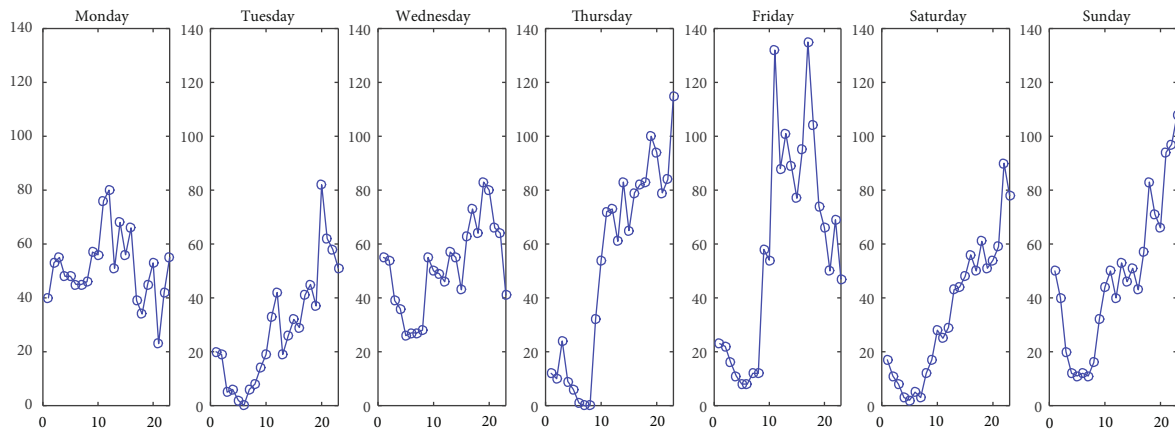


FIGURE 2: Sojourn time analysis of individual behaviors.

FIGURE 3: Population over days of a week: time in hours on the  $x$ -axis, population on the  $y$ -axis.

## 4. Analysis Results

This section presents an analysis of P2P traces collected from a deployed system. These traces are explained in detail in [48]. We analyze these data in light of the observations synthesized above and focus on those issues which have been ignored earlier. Now, we present our analyzed metrics one by one.

**4.1. Sojourn Time.** The existing studies on user behavior analyze user behavior from mixed traces of all the users of the system, and we are interested in individual behavior in certain cases for crucial decisions such as topology management in P2P systems; therefore, we focus on sojourn time of individual users. To do so, we separate data of an individual user from the traces based on their MAC addresses. As there are numerous users in the trace file,

we choose 8 users from it starting from one with more observations than others. We depict a plot of sojourn time frequency distribution in Figure 2(a). One can notice different frequencies for different users; however, to have a fair comparison, we also compute the percentage frequencies to eliminate the difference appearing due to different numbers of total sessions.

We show the percentage cumulative frequency distributions in Figure 2(b). It clearly demonstrates the different nature of sessions for different users, for example, the number of longer sessions is high for user 1 and user 8. By contrast, user 7 has all its sessions within a 50-minute limit. Similarly, user 5 has produced the highest percentage of short sessions which shows a user who is switching a lot of channels.

Sojourn time is a key metric in a P2P IPTV system and it has been extensively studied. However, these results add a

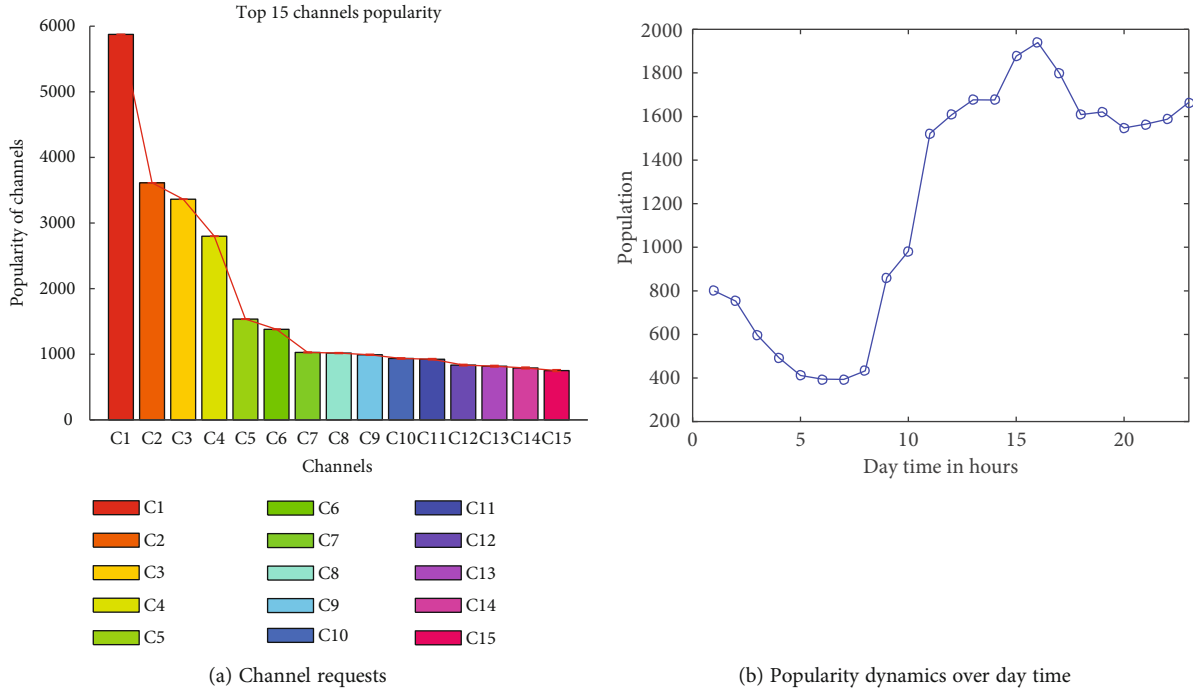


FIGURE 4: Popularity analysis.

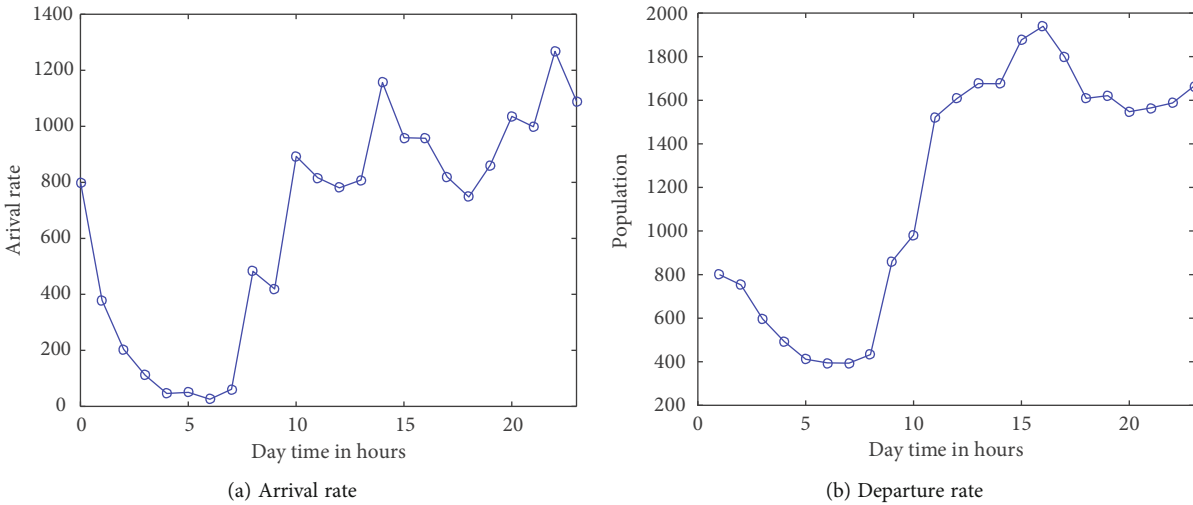


FIGURE 5: Joining and leaving rates.

new perspective to this area as they clearly show distinguished individual behavior.

**4.2. Channel Popularity.** We analyze the popularity from the number of online users and user’s requests for a channel. As shown in Figure 3, the number of online users over a typical week period during each hour of the day reveals that the number of users vary over different days of the week. Interestingly, the number of users increases as the weekend approaches while remaining low in the early week. To analyze the impact of the time of the day, we depict the population over day time in Figure 4(b). It is evident from this figure that the population varies during a day, remaining

low early while reaching peak in the afternoon when users come back home and turn their sets on.

To analyze the number of requests for different channels, we choose the top 15 channels and show the number of requests they get in Figure 4(a). Here, ch1 is the most popular channel with 6000 user requests. The curve is similar to Zipf distribution which is a consensually used model for channel popularity with little variations from system to system. We also observed that the user stays longer on popular channels as compared to unpopular channels.

**4.3. Joining and Leaving.** Joining and leaving of the users create a combined effect called churn which is a hot area of P2P

networking research. We analyzed joining and leaving during day time and depicted the results in Figures 5(a) and 5(b), respectively. It can be noticed from the figures that joining and leaving are time dependent just like the population, and interestingly, both of these increase and decrease simultaneously, along with the population. Therefore, an important insight from this observation can be drawn for the design of these systems to accommodate churn at peak hours.

To sum up the discussion on analysis of dataset, we observed that individual behavior is different than the global behavior and analysis of popularity and joining/leaving is consistent with other measurements. However, certain other key points need to be investigated which could not be accomplished from the current dataset due to its size. These key points are the behavior analysis of a single user from channel to channel and program to program.

## 5. Conclusion

User behavior in P2P IPTV is crucial for the performance of the system, and therefore, numerous efforts are aimed at its understanding. Each such study is restricted to a few variables due to the research interest, availability of data, and nature of the system. Therefore, one or a few studies cannot provide a comprehensive view of the user behavior. Keeping in view the impact of user behavior on the performance of the system, generalization of the user behavior in light of the existing studies can be helpful in P2P IPTV systems as well in other similar systems. Therefore, our work has two main parts. Firstly, we collect and synthesize existing measurements to get a comprehensive view of all works. We found that measurements show consensus in large to model users' requesting frequencies for popular content. Similarly, analyses of sojourn time remains consistent about the ratio of short sessions and long sessions. Concerning the observed distributions, they are shown to be varying among different studies in terms of models and/or parameters. Nonetheless, the behavior of individual users is not considered perhaps due to privacy and technical issues such as identification and tracking of individual user in the dataset. Furthermore, this work synthesizes the relationships among different elements of user behavior. It demonstrates the dependency insights from different measurements in a casual graph. This graph provides a consistent view of independent studies and it can be used for further investigation. Secondly, this work performs an analysis of individual user behavior from logs. It is noticeable from the results that individual users behave differently, and therefore, applying a global behavior to an individual user may not be reliable. Instead of considering a generalized behavior, clustering of users for similar behavior may produce better results.

## 6. Future Work

In future work, we intend to collect and analyze a larger dataset and see the possibility of clusters of users based on their behavior. This can further be extended towards individualized models for fine tuning the NGWN systems

according to the expected behavior of users. Machine learning could be an appropriate choice to build such models. These models could also be applicable to other areas to construct user-oriented networks.

## Data Availability

All the data are available in the paper.

## Conflicts of Interest

The authors declare that they have no conflicts interest.

## References

- [1] V. Stocker, G. Smaragdakis, W. Lehr, and S. Bauer, "The growing complexity of content delivery networks: challenges and implications for the Internet ecosystem," *Telecommunications Policy*, vol. 41, no. 10, pp. 1003–1016, 2017.
- [2] E. C. Miguel, C. M. Silva, F. C. Coelho, Í. F. S. Cunha, and S. V. A. Campos, "Construction and maintenance of p2p overlays for live streaming," *Multimedia Tools and Applications*, vol. 80, no. 13, pp. 20255–20282, 2021.
- [3] J. Zhang, L. Liu, L. Ramaswamy, and P. Calton, "PeerCast: churn-resilient end system multicast on heterogeneous overlay networks," *Journal of Network and Computer Applications*, vol. 31, no. 4, pp. 821–850, 2008.
- [4] Y. Liu, Y. Guo, and C. Liang, "A survey on peer-to-peer video streaming systems," *Peer-to-peer Networking and Applications*, vol. 1, no. 1, pp. 18–28, 2008.
- [5] D. Wu, C. Liang, Y. Liu, and K. Ross, "View-upload decoupling: a redesign of multi-channel p2p video systems," in *INFOCOM 2009, IEEE*, vol. 2009, pp. 2726–2730, IEEE.
- [6] V. K. Goyal, "Multiple description coding: compression meets the network," *IEEE Signal Processing Magazine*, vol. 18, no. 5, pp. 74–93, 2001.
- [7] X. Hei, Y. Liu, and K. W. Ross, "Iptv over p2p streaming networks: the mesh-pull approach," *IEEE Communications Magazine*, vol. 46, no. 2, pp. 86–92, 2008.
- [8] H. Ayatollahi, M. Khansari, and H. R. Rabiee, "A push-pull network coding protocol for live peer-to-peer streaming," *Computer Networks*, vol. 130, pp. 145–155, 2018.
- [9] D. Kim, E. Kim, and C. Lee, "Efficient peer-to-peer overlay networks for mobile iptv services," *IEEE Transactions on Consumer Electronics*, vol. 56, no. 4, pp. 2303–2309, 2010.
- [10] I. U. Khan, I. M. Qureshi, M. A. Aziz, T. A. Cheema, and S. B. H. Shah, "Smart iot control-based nature inspired energy efficient routing protocol for flying ad hoc network (fanet)," *IEEE Access*, vol. 8, pp. 56371–56378, 2020.
- [11] M. Faheem, M. Umar, R. A. Butt, B. Raza, M. A. Ngadi, and V. C. Gungor, "Software defined communication framework for smart grid to meet energy demands in smart cities," in *2019 7th International Istanbul Smart Grids and Cities Congress and Fair (ICSG)*, pp. 51–55, IEEE, 2019.
- [12] M. Faheem, G. Fizza, M. W. Ashraf, R. A. Butt, M. A. Ngadi, and V. C. Gungor, "Big data acquired by Internet of things-enabled industrial multichannel wireless sensors networks for active monitoring and control in the smart grid industry 4.0," *Data in Brief*, vol. 35, p. 106854, 2021.
- [13] M. Faheem, R. A. Butt, R. Ali, B. Raza, M. A. Ngadi, and V. C. Gungor, "Cbi4.0: a cross-layer approach for big data gathering

- for active monitoring and maintenance in the manufacturing industry 4.0,” *Journal of Industrial Information Integration*, vol. 24, article 100236, 2021.
- [14] Z. Liu, C. Wu, B. Li, and S. Zhao, “Distilling superior peers in large-scale p2p streaming systems,” in *INFOCOM 2009, IEEE*, vol. 2009, pp. 82–90, IEEE.
- [15] K. Park, D. Chang, J. Kim, W. Yoon, and T. Kwon, “An analysis of user dynamics in p2p live streaming services,” in *Communications (ICC), 2010 IEEE International Conference*, pp. 1–6, Cape Town, South Africa, 2010.
- [16] Y. Li, Y. Zhang, and R. Yuan, “Measurement and analysis of a large scale commercial mobile Internet tv system,” in *Proceedings of the 2011 ACM SIGCOMM conference on Internet measurement conference*, pp. 209–224, Berlin, Germany, 2011.
- [17] I. Ullah, G. Doyen, G. Bonnet, and D. Gaiti, “A survey and synthesis of user behavior measurements in p2p streaming systems,” *Communications Surveys & Tutorials, IEEE*, vol. 14, no. 3, pp. 734–749, 2011.
- [18] Z. Li, G. Xie, M. A. Kaafar, and K. Salamatian, “User behavior characterization of a large-scale mobile live streaming system,” in *Proceedings of the 24th International Conference on World Wide Web*, pp. 307–313, Florence, Italy, 2015.
- [19] Z. Li, M. Kaafar, K. Salamatian, and G. Xie, “Characterizing and modeling user behavior in a large-scale mobile live streaming system,” *IEEE Transactions on Circuits and Systems for Video Technology*, vol. 27, no. 12, pp. 2675–2686, 2017.
- [20] Q. Li, “Understanding the causal impact of the video delivery throughput on user engagement,” *Multimedia Tools and Applications*, vol. 78, no. 11, pp. 15589–15604, 2019.
- [21] I. Ullah, G. Doyen, G. Bonnet, and D. Gaiti, “An autonomous topology management framework for qos enabled p2p video streaming systems,” in *2012 8th international conference on network and service management (cnsm) and 2012 workshop on systems virtualization management (svm)*, pp. 126–134, Las Vegas, NV, USA, 2012.
- [22] C. Yang, S. Ren, Y. Liu, H. Cao, Q. Yuan, and G. Han, “Personalized channel recommendation deep learning from a switch sequence,” *IEEE Access*, vol. 6, pp. 50824–50838, 2018.
- [23] A. Ghaderzadeh, M. Kargahi, and M. Reshadi, “Redepoly: reducing delays in multi-channel p2p live streaming systems using distributed intelligence,” *Telecommunication Systems*, vol. 67, no. 2, pp. 231–246, 2018.
- [24] I. Basicovic, D. Kukolj, S. Ocovaj, G. Cmiljanovic, and N. Fimic, “A fast channel change technique based on channel prediction,” *IEEE Transactions on Consumer Electronics*, vol. 64, no. 4, pp. 418–423, 2018.
- [25] W. Ma, Q. Zhang, M. Chunxiao, and M. Zhang, “QoS prediction for neighbor selection via deep transfer collaborative filtering in video streaming P2P networks,” *International Journal of Digital Multimedia Broadcasting*, vol. 2019, Article ID 1326831, 10 pages, 2019.
- [26] M. Sina, M. Dehghan, and A. M. Rahmani, “CaR-PLive: Cloud-assisted reinforcement learning based p2p live video streaming: a hybrid approach,” *Multimedia Tools and Applications*, vol. 78, no. 23, pp. 34095–34127, 2019.
- [27] K. Pal, M. C. Govil, and M. Ahmed, “FLHyO: fuzzy logic based hybrid overlay for p2p live video streaming,” *Multimedia Tools and Applications*, vol. 78, no. 23, pp. 33679–33702, 2019.
- [28] F. Dobrian, V. Sekar, A. Awan et al., “Understanding the impact of video quality on user engagement,” *ACM SIGCOMM Computer Communication Review*, vol. 41, no. 4, pp. 362–373, 2011.
- [29] B. Athula, V. Sekar, A. Akella, S. Seshan, I. Stoica, and H. Zhang, “A quest for an Internet video quality-of-experience metric,” *Proceedings of the 11th ACM workshop on hot topics in networks*, 2012, pp. 97–102, Seattle, WA, USA, 2012.
- [30] X. Liu, F. Dobrian, H. Milner et al., “A case for a coordinated Internet video control plane,” in *Proceedings of the ACM SIGCOMM 2012 conference on Applications, technologies, architectures, and protocols for computer communication*, pp. 359–370, Helsinki, Finland, 2012.
- [31] B. Athula, V. Sekar, A. Akella, S. Seshan, I. Stoica, and H. Zhang, “Developing a predictive model of quality of experience for Internet video,” *SIGCOMM Computer Communication Review*, vol. 43, no. 4, pp. 339–350, 2013.
- [32] F. Dobrian, A. Awan, D. Joseph et al., “Understanding the impact of video quality on user engagement,” *Communications of the ACM*, vol. 56, no. 3, pp. 91–99, 2013.
- [33] M. F. M. Hossain, M. Sarkar, and S. H. Ahmed, “Quality of experience for video streaming: a contemporary survey,” in *2017 13th International Wireless Communications and Mobile Computing Conference (IWCMC)*, pp. 80–84, Valencia, Spain, 2017.
- [34] B. Zhang, G. Kreitz, M. Isaksson et al., “Understanding user behavior in spotify,” in *2013 Proceedings IEEE INFOCOM*, pp. 220–224, Turin, Italy, 2013.
- [35] M. Ghanem, O. Fourmaux, F. Tarissan, and T. Miyoshi, “P2ptv multi-channel peers analysis,” in *2016 18th Asia-Pacific Network Operations and Management Symposium (APNOMS)*, pp. 1–6, Kanazawa, Japan, 2016.
- [36] B. Athula, V. Sekar, A. Akella, and S. Seshan, “Understanding Internet video viewing behavior in the wild,” *Sigmetrics Performance Evaluation Review*, vol. 41, no. 1, pp. 379–380, 2013.
- [37] P. Wang, H. Huang, and C. Xie, “A pre-buffer mechanism in multi-channel p2p live streaming,” in *2013 IEEE Eighth International Conference on Networking, Architecture and Storage*, pp. 292–296, Xi’an, China, 2013.
- [38] N. Liu, S.-H. Huajie Cui, G. Chan, Z. Chen, and Y. Zhuang, “Dissecting user behaviors for a simultaneous live and vod iptv system,” *ACM Transactions on Multimedia Computing, Communications, and Applications (TOMM)*, vol. 10, no. 3, p. 23, 2014.
- [39] S. Spoto, R. Gaeta, M. Grangetto, and M. Sereno, “Analysis of p2p live through active and passive measurements,” in *2009 IEEE International Symposium on Parallel & Distributed Processing*, pp. 1–7, Rome, Italy, 2009.
- [40] F. Wang, J. Liu, and Y. Xiong, “Stable peers: existence, importance, and application in peer-to-peer live video streaming,” in *IEEE INFOCOM 2008 - The 27th Conference on Computer Communications*, pp. 1364–1372, Phoenix, AZ, USA, 2008.
- [41] X. Hei, C. Liang, J. Liang, Y. Liu, and K. W. Ross, “A measurement study of a large-scale p2p iptv system,” *IEEE Transactions on Multimedia*, vol. 9, no. 8, pp. 1672–1687, 2007.
- [42] I. Mnie-Filali, S. Rouibia, D. Lopez-Pacheco, and G. Urvoy-Keller, “On the impact of the initial peer list in p2p live streaming applications: the case of sopcast,” *Universal Journal of Communications and Network*, vol. 1, no. 4, pp. 142–150, 2013.
- [43] A. Ahmed, Z. Shafiq, and A. Khakpour, “Qoe analysis of a large-scale live video streaming event,” in *Proceedings of the*



- 2016 ACM SIGMETRICS International Conference on Measurement and Modeling of Computer Science, pp. 395–396, Antibes Juan-Les-Pins, France, 2016.
- [44] J. Jiang, V. Sekar, I. Stoica, and H. Zhang, “Shedding light on the structure of Internet video quality problems in the wild,” in *Proceedings of the ninth ACM conference on Emerging networking experiments and technologies*, pp. 357–368, California, USA, 2013.
- [45] S. Thomas, O. Fourmaux, A. Botta et al., “Traffic analysis of peer-to-peer iptv communities,” *Computer Networks*, vol. 53, no. 4, pp. 470–484, 2009.
- [46] A. Borges, P. Gomes, J. Nacif, R. Mantini, J. M. Almeida, and S. Campos, “Characterizing sopcast client behavior,” *Computer Communications*, vol. 35, no. 8, pp. 1004–1016, 2012.
- [47] A. B. Vieira, A. P. C. da Silva, F. Henrique, G. Goncalves, and P. de Carvalho Gomes, “Sopcast p2p live streaming: live session traces and analysis,” in *Proceedings of the 4th ACM multimedia systems conference*, pp. 125–130, Oslo, Norway, 2013.
- [48] Y. Elkhatib, M. Mu, and N. Race, “Dataset on usage of a live & vod p2p iptv service,” in *14-th IEEE International Conference on Peer-to-Peer Computing*, pp. 1–5, London, UK, 2014.
- [49] T. Qiu, Z. Ge, S. Lee, J. Wang, Q. Zhao, and J. Xu, “Modeling channel popularity dynamics in a large iptv system,” *ACM SIGMETRICS Performance Evaluation Review*, vol. 37, no. 1, pp. 275–286, 2009.
- [50] S. Krishnan and S. Ramesh, “Video stream quality impacts viewer behavior: inferring causality using quasi-experimental designs,” *Networking, IEEE/ACM Transactions*, vol. 21, no. 6, pp. 2001–2014, 2013.
- [51] D. A. G. Manzato and N. L. S. da Fonseca, “Providing fast channel switching in p2p iptv systems,” *IEEE Journal on Selected Areas in Communications*, vol. 31, no. 9, pp. 326–337, 2013.
- [52] D. A. Manzato and N. L. da Fonseca, “A channel switching scheme for iptv systems,” in *2010 IEEE Global Telecommunications Conference GLOBECOM 2010*, pp. 1–6, Miami, FL, USA, 2010.
- [53] A. Alireza, B. E. Wolfinger, J. Lai, and C. Vinti, “Modeling the behavior of iptv users with application to call blocking probability analysis,” *PIK-Praxis der Informationsverarbeitung und Kommunikation*, vol. 35, no. 2, pp. 75–81, 2012.
- [54] M. Meskovic, H. Bajric, and M. Kos, “Content delivery architectures for live video streaming: hybrid cdn-p2p as the best option,” *The Fifth International Conference on Communication Theory, Reliability, and Quality of Service, CTRQ 2012*, pp. 175–180, ACM, 2012.
- [55] F. H. Ferreira, A. P. C. da Silva, and A. B. Vieira, “Characterizing peers communities and dynamics in a p2p live streaming system,” *Peer-to-Peer Networking and Applications*, vol. 9, no. 1, pp. 1–15, 2016.
- [56] N.-F. Huang, M.-H. Wang, T.-C. Wang, and S.-S. Peng, “Measuring qoe/qos of large scale p2p iptv service,” in *2011 13th Asia-Pacific Network Operations and Management Symposium*, pp. 1–8, Taipei, Taiwan, 2011.
- [57] K. Shami, D. Magoni, H. Chang, W. Wang, and S. Jamin, “Impacts of peer characteristics on p2ptv networks scalability,” in *IEEE INFOCOM 2009*, pp. 2736–2740, Rio de Janeiro, Brazil, 2009.
- [58] F. M. V. Ramos, J. Crowcroft, R. J. Gibbens, P. Rodriguez, and I. H. White, “Reducing channel change delay in iptv by predictive pre-joining of tv channels,” *Signal Processing: Image Communication*, vol. 26, no. 7, pp. 400–412, 2011.
- [59] Y. Li, Y. Zhang, and R. Yuan, “Characterizing user access behaviors in mobile tv system,” in *2012 IEEE International Conference on Communications (ICC)*, pp. 2093–2097, Ottawa, ON, Canada, 2012.
- [60] M. Cha, P. Rodriguez, J. Crowcroft, S. Moon, and X. Amatriain, “Watching television over an ip network,” in *Proceedings of the 8th ACM SIGCOMM conference on Internet measurement*, pp. 71–84, Vouliagmeni, Greece, 2008.
- [61] T. Ilias, A. H. Zahran, and C. J. Sreenan, “Mobile network traffic: a user behaviour model,” in *2014 7th IFIP Wireless and Mobile Networking Conference (WMNC)*, pp. 1–8, Vilamoura, Portugal, 2014.
- [62] A. Alireza, B. E. Wolfinger, J. Lai, and C. Vinti, “Elaboration and formal description of iptv user models and their application to iptv system analysis,” *MMBnet*, vol. 2011, 2011.
- [63] G. Vijay, R. Jana, R. Knag, K. K. Ramakrishnan, D. F. Swayne, and V. A. Vaishampayan, “Characterizing interactive behavior in a large-scale operational iptv environment,” in *2010 Proceedings IEEE INFOCOM*, pp. 1–5, San Diego, CA, USA, 2010.
- [64] K. Pires and G. Simon, “Youtube live and twitch: a tour of user-generated live streaming systems,” in *Proceedings of the 6th ACM Multimedia Systems Conference*, pp. 225–230, Portland, OR, USA, 2015.
- [65] E. Veloso, V. Almeida, W. Meira et al., “A hierarchical characterization of a live streaming media workload,” *IEEE/ACM Transactions on Networking*, vol. 14, no. 1, pp. 133–146, 2006.
- [66] C. Y. Lee, C. K. Hong, and K. Y. Lee, “Reducing channel zapping time in IPTV based on user’s channel selection behaviors,” *IEEE Transactions on Broadcasting*, vol. 56, no. 3, pp. 321–330, 2010.
- [67] M. Cha, K. Gummadi, and P. Rodriguez, “Channel selection problem in live iptv systems,” *Proc. of ACM SIGCOMM Poster*, vol. 1, 2008.
- [68] B. Li, G. Y. Keung, S. Xie, F. Liu, Y. Sun, and H. Yin, “An empirical study of flash crowd dynamics in a p2p-based live video streaming system,” in *IEEE GLOBECOM 2008 - 2008 IEEE Global Telecommunications Conference*, pp. 1–5, New Orleans, LA, USA, 2008.
- [69] H. Joo, H. Song, D.-B. Lee, and I. Lee, “An effective iptv channel control algorithm considering channel zapping time and network utilization,” *IEEE Transactions on Broadcasting*, vol. 54, no. 2, pp. 208–216, 2008.

## Research Article

# Impact of Wireless Sensor Data Mining with Hybrid Deep Learning for Human Activity Recognition

Rajit Nair <sup>1</sup>, Mahmoud Ragab <sup>2,3</sup>, Osama A. Mujallid,<sup>4</sup> Khadijah Ahmad Mohammad <sup>5</sup>,  
Romany F. Mansour <sup>6</sup> and G. K. Viju <sup>7</sup>

<sup>1</sup>School of Computing Science and Engineering, Vellore Institute of Technology, Bhopal, Madhya Pradesh, India

<sup>2</sup>Information Technology Department, Faculty of Computing and Information Technology, King Abdulaziz University, Jeddah 21589, Saudi Arabia

<sup>3</sup>Centre of Artificial Intelligence for Precision Medicines, King Abdulaziz University, Jeddah 21589, Saudi Arabia

<sup>4</sup>Public Administration Department, Faculty of Economic and Administration, King Abdul-Aziz University, Jeddah 21589, Saudi Arabia

<sup>5</sup>Department of Pharmaceutical Chemistry, Faculty of Pharmacy, King Abdulaziz University, Alsulaymanyah, Jeddah 21589, Saudi Arabia

<sup>6</sup>Professor and Dean, Post Graduate Studies, University of Garden City, Khartoum, Sudan

<sup>7</sup>Department of Mathematics, Faculty of Science, New Valley University, El-Kharga, 72511, Egypt

Correspondence should be addressed to G. K. Viju; [prof.gkviju@ugc.edu.sd](mailto:prof.gkviju@ugc.edu.sd)

Received 4 February 2022; Revised 20 February 2022; Accepted 4 March 2022; Published 27 March 2022

Academic Editor: Shalli Rani

Copyright © 2022 Rajit Nair et al. This is an open access article distributed under the Creative Commons Attribution License, which permits unrestricted use, distribution, and reproduction in any medium, provided the original work is properly cited.

Human activity recognition is a time series classification problem that is difficult to solve (HAR). Traditional signal processing approaches and domain expertise are necessary to appropriately create features from raw data and fit a machine learning model for predicting a person's movement. This work aims to demonstrate how a hybrid deep learning model may be used to recognize human behavior. Deep learning methodologies such as convolutional neural networks and recurrent neural networks will extract the features and achieve the classification goal. The suggested model has used wireless sensor data mining datasets to predict human activity. The model's performance has been assessed using the confusion matrix, accuracy, training loss, and testing loss. Thus, the model has achieved greater than 96% accuracy, superior to other state-of-the-art algorithms in this field.

## 1. Introduction

Human activity recognition (HAR) is concerned with recognizing people's daily routines using sensor-based time-series information [1]. Sensors, the Internet of Things (IoT), cloud computing, and edge computing have all advanced in the last decade. Because sensors are affordable and can be easily incorporated or implanted in both portable and nonportable devices, HAR research has shifted to sensor technologies [2]. Using IoT wearable devices with sensors, it is possible to swiftly capture a variety of body movements for human activity detection [3]. Due to the rapid growth of low-cost smartphones and smartwatches, wearable inertial

measurement units (IMUs), which consist of accelerometers and gyroscopes that can easily identify and pinpoint human movements, have become widely available in recent years. The fact that HAR based on wearable sensors can be used to identify and document numerous daily acts including eating, drinking, brushing your teeth, and detecting sleep disorders demonstrates the importance of HAR.

Actions in HAR are divided into two categories: primary and sophisticated [4]. Brushing your teeth or dribbling a ball is examples of complicated human activities that need two separate actions: the simple human activity itself and the transitional action. In machine learning, the HAR challenge is one of multivariate time series categorization as well as

supervised learning [5]. Traditional algorithms like SVM and Random Forest have been combined with newer deep learning approaches like ANN, CNN, and RNN for previous activity recognition research [6]. With conventional algorithms, feature engineering and feature extraction require a lot of manual labor and take a long time. When it comes to categorizing human actions, however, deep learning approaches are better suited because they can learn features automatically from data [7].

Deep learning models that can accurately classify 18 daily routine complex and specific human activities from the WISDM dataset into three categories: (a) ambulation-oriented activities such as jogging and other ambulatory activities; (b) nonambulation-oriented activities such as driving and other motorized activities. Writing, typing, and other general hand-oriented activities are included in this category [8]. Aside from that, data gathered from low-level time series sensors, such as the accelerometers and gyroscopes found in smartwatches and smartphones, can be utilised to study hand-oriented behaviours like eating chips and spaghetti [9].

It is possible to extract local features using a one-dimensional convolutional neural network (CNN) [10]. An alternative approach that takes advantage of neural networks with built-in memory and the ability to retrieve previously stored information is GRU. With the help of CNN and GRU, humans can perform complex activities with great precision. This hybrid model was compared to baseline models like InceptionTime and DeepConvLSTM, which were built using AutoML based on the McFly open-source python module [11].

In this paper, hybrid deep learning model is implemented by combining convolutional neural network and recurrent neural network for analysing the human activities. Mainly six types of body activities are recognized by using the proposed model.

The work is presented in 6 sections. The first section contains the introduction of the work. Section 2 provides a literature assessment of human activity recognition algorithms and methodologies. Methodology and framework for recognizing human activities are laid out in Section 3. Section 4 compares the performance metrics of the various models. To compare and contrast different models, Section 5 presents the findings and conclusions drawn from those other models' outputs and future directions. The last section covers the references.

## 2. Literature Survey

In the past, methods based on machine learning were used to detect human activities. Decision trees are favored over more sophisticated models because of their ease of interpretation and low processing costs [12]. SVMs and  $K$ -nearest neighbor (KNN) are two of the most common HAR classifiers that use sensor data [13]. Particle swarm optimization by Tharwat et al. [14] produced an improved  $k$ -NN classifier that outperformed  $K$ -nearest neighbor classifiers when applied to accelerometer data.  $K$ -next neighbor, an instance-based learning (IBL) technique, is computationally

demanding since it compares an incoming instance with every training example. Consequently, it is able to rapidly react to new information and discard outdated data. For six different indoor activities, implemented SVMs that did not require a lot of processing power or memory to identify them accurately.

Classifiers, such as the bagging and boosting ensemble meta-algorithm, can be combined to increase the final classification quality. Ensemble algorithms, on the other hand, require a larger number of base-level algorithms to be trained and evaluated. Diverse studies have documented deep learning algorithms' current state-of-the-art performance. For the opportunity dataset, Ordonez and Roggen [15] implemented DeepConvLSTM with a convolutional and recurrent layer combination to achieve 95.8%, whereas Hammerla et al. [16] used bidirectional LSTM with two parallel recurrent layers that reach into the "future" and the "past." Wearable sensors are required in order to collect both datasets, which necessitates the use of multiple sensors, making the technology more intrusive. Human action signals were employed in a categorization model established by Sikder et al. [17]. The frequency and power parameters of the collected signals were used. Using the fast Fourier transform (FFT) of each input channel, Ronao and Cho trained a four-layer CNN using raw sensor data [18]. In contrast, Ignatov [19] used a shallow CNN using raw sensor data input, 40 statistical characteristics, and a 95.2 percent success rate in order to achieve a 95.2 percent accuracy rate. The real-time solution would require more time and computing power since noise filters were applied to the accelerometer and gyroscope signal before sampling the dataset in fixed-width sliding windows with 50% overlap (128 readings/window).

The WISDM (wireless sensor data mining) lab developed two datasets: WISDM and Actitracker. All six physical activities (upstairs, downstairs, walking, jogging, sitting, and standing), four of which are the same and two that are unique, are captured by triaxial accelerometers in both datasets (upstairs and downstairs for the WISDM dataset and stairs and lying down, respectively, for the Actitracker dataset) [20]. The outcomes of these implementations are uneven because there is no preselection of datasets for training and testing.

All previous attempts on the WISDM dataset have produced solutions that are dependent on the user, with the exception of. Using the leave-one-out testing technique, Kolosnjaji and Eckert [21] used hand-crafted features and random forest or dropout classifiers on top of them to achieve 83.46 percent and 85.36 percent  $f1$  scores using a cross-validation procedure seven times with five participants excluded from the testing dataset and the remainder included in the training dataset. Manzi et al. [22] make use of depth camera data to identify human activity. This technique uses a machine-learning system to distinguish human activity. The action is represented using a different number of clusters obtained independently from the activity instances, in contrast to earlier methodologies. CAD-60 and TST datasets were used to train a multiclass SVM, then used to generate these models. The SOM optimization was used to prepare the SVM on both datasets. Depending on

the input sequence and activity, these numbers can fluctuate, resulting in dynamically created clusters.

Milenkoski et al. [23] trained an LSTM network to identify raw accelerometer data windows, and their accuracy was only 88.6 percent based on an 80/20 split. Pienaar and Malakian [24] used a random 80/20 split to train an LSTM and an RNN and achieved a 93.8 percent accuracy rate. With the help of Microsoft Kinect data and Minkowski distances between joint data,

Another group of researchers developed a pose descriptor for differential quantities encoders and efficiently captured the information of a human joint's posture in a frame sequence using differential quantities encoders [25]. When joining the descriptor, they used the  $k$ -nearest neighbor method, although their results were nonparametric and had low latency recognition.

Siirtola and Rönning [26] sampled the custom dataset at a frequency of 40 Hz, whereas the WISDM and Actitracker datasets were sampled at a frequency of 20 Hz. According to the authors, 98% and 99% of the walking activity's power were confined below 10 Hz and 15 Hz. The fundamental could only be expressed in terms of 5 percent of the total signal strength at higher frequencies. It was shown that when a mobile device was carried at a hip region, the major frequencies were lower than 18 Hz. To save power and storage space, lower sample rates can be used. The ideal window size has been the subject of much research; however, most implementations employ window sizes between 1 and 10 seconds. In contrast to most other implementations, which use fixed window sizes ranging from 1.28 s to 2.56 s to 3.2 s to 10.7 s. In comparison, Ignatov et al. tested their implementation over a range of window sizes from 1 to 10.6 s. Most other implementations use variable window sizes ranging from 1.2 to 10 seconds.

### 3. Proposed Work

In this section, the proposed work will be explained in which wireless sensor data mining (WISDM) dataset will be used to perform the human activity recognition. The features will be extracted first using CNN and then classifier will be done using LSTM model [27]. Figure 1 displays the flowchart of the proposed work, let us discuss the proposed work in detail.

**3.1. Dataset.** In this work, wireless sensor data mining (WISDM) is the dataset cited in this work for the detection of human activities [28]. Among the samples in the collection are 1,098,207 examples of diverse physical activities from all around the world (sampled at 20 Hz). This dataset can also be found on the Wisdom website at <https://www.cis.fordham.edu/wisdm/dataset.php>. There are mainly six activities such as walking, jogging, upstairs and downstairs, as well as sitting and standing, are all included in the data collection.

**3.2. Data Preprocessing.** In this section, data preprocessing approaches will be discussed. First, feature extraction is per-

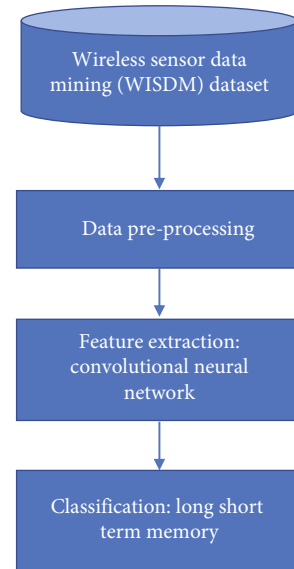


FIGURE 1: Flowchart of the proposed work.

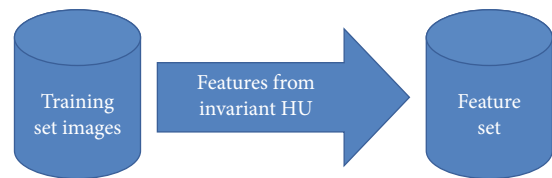


FIGURE 2: Machine learning.

formed then classification will be done by using deep learning model.

**3.2.1. Feature Extraction.** An example will help us comprehend the feature [29]. As soon as a photo is taken, the next step is to identify it; however, in order to do so, the user must keep vast numbers of photos that take up a lot of storage space and measure each photo in terms of pixels per inch. We must therefore do features extraction in order to store this image. The image's dimensions will be reduced as a result of a feature extraction. As far as computer vision is concerned, a "feature" is an important notion. An important element or piece of information is referred to as a "feature." The edges or the artefacts may be such details.

Zernike and Fourier descriptors are two examples of extraction algorithms [30]. To put it another way, descriptors are numbers assigned to describe a particular kind of thing. There are a few of them, such as

- (i) The number of form pixels in an area
- (ii) The number of pixels that fall within the shape's boundaries
- (iii) Extend the shape to fit on a smaller rectangle by elongating a rectangle. Afterward, compute your height and width
- (iv) Rectangularity refers to how much of an object's surface area is contained within a rectangular shape

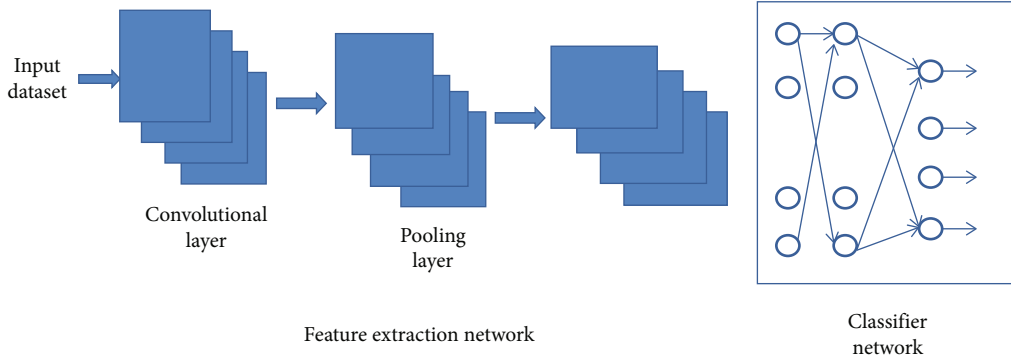


FIGURE 3: Architecture of convolutional neural network.

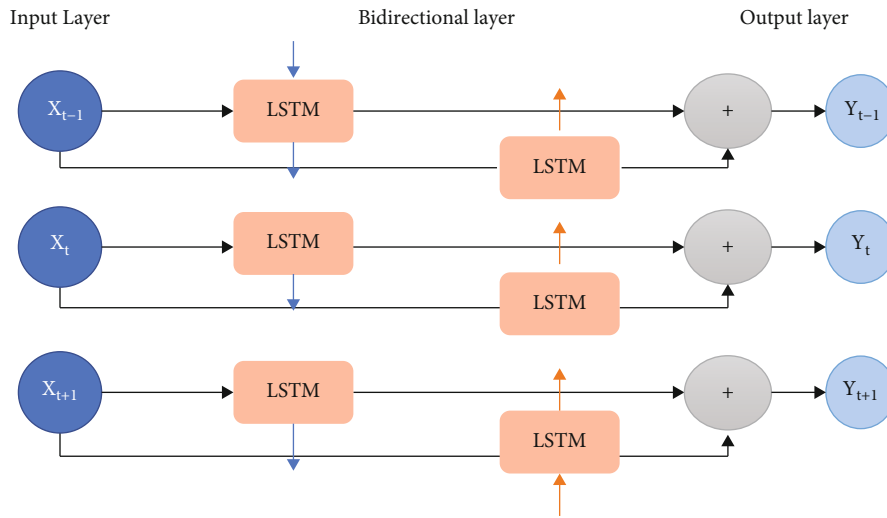


FIGURE 4: Architecture of recurrent neural network.

This refers to the shape’s general orientation.

Recognition of human activity is accomplished in two stages:

(1) Collecting the training set and convolutional neural network feature extraction. Figure 2 shows the feature extraction approach.

(i) *Training Dataset.* Changes to the dataset are recorded in preparation for the training phase. Data is comprised of five distinct gestures, with a total of one hundred and fifty different possible outcomes. As a result, the system is better able to deal with a wide range of gestures consistently. Thus, it aids comprehension of the operation under diverse conditions

(ii) *Feature Extraction.* All images in training are retrieved and saved using the HU moment set approach, and the results are saved in a file for each training image. Descriptor values and classification levels for each image are stored in a matrix in the file

(iii) *Normalization.* The features that are measured and processed are represented as a matrix in each row,

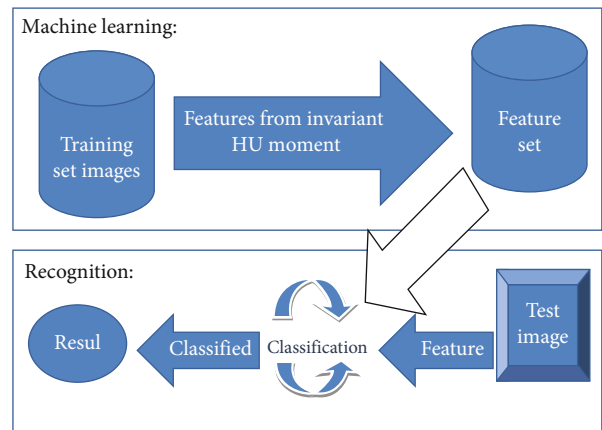


FIGURE 5: Recognition of the images.

which represents an image. There is a distinct feature (attribute) for each matrix attribute. As a result, the data in each column should be uniform and unrelated to the others. The maximum amount of data that can be kept in each column is used to save

TABLE 1: Confusion matrix.

		Downstairs	Jogging	Sitting	Standing	Upstairs	Walking
True label	Downstairs	0.88	0.0093	0.0061	0	0.068	0.0043
	Jogging	0.0066	0.97	0.0001	0	0.016	0.0013
	Sitting	0.0048	0.013	0.94	0.027	0.0031	0.001
	Standing	0.021	0.0073	0.0071	0.94	0.014	0.0073
	Upstairs	0.060	0.026	0.0049	0.0024	0.89	0.0026
	Walking	0.0032	0.00079	0	0.0001	0.009	0.98
		Predicted label					

a file that will be classified later. The largest value of a particular characteristic (feature) is selected and used to divide the entire matrix (feature). The values that arise from this normalization are between 0 and 1. This greatly enhances the classification process. This will also reduce the likelihood of bias in classifications where each attribute is given equal weight

- (iv) *Convolutional Neural Network*. A convolutional neural network is a type of neural network designed to analyze multidimensional data, such as picture and time-series data (CNN). Feature extraction and weight computation are included in the training process. Using a convolution operator, these networks are referred recognized as convolutional networks. The fundamental advantage of CNNs is the ability to automatically extract features [2]. Figure 3 shows how the input data is first sent to a feature extraction network, and then the derived features are sent to a classifier network as illustrated. Convolutional and pooling layer pairs make up the feature extraction network. The input data is convoluted using a layer of digital filters called a convolutional layer. The threshold is set by the pooling layer, which serves as a dimensionality reduction layer. Several factors must be modified during backpropagation in order to reduce the number of connections in the neural network architecture

3.2.2. *Classification*. Classification involves basic steps shown in

- (i) Implementation of the deep learning model using recurrent neural network

Long-term short-term memory improvement is the result of improved recurrent neural networks (RNNs). When the gradient disappears or explodes, LSTM memory blocks instead of RNN units can fix the problem. Unlike RNNs, it adds a cell state to store long-term states, which is its main difference. An LSTM network can maintain track of and link data from the past with data collected in the current time. For the LSTM, there are three gates: an input gate, a “forget” gate, and an output gate. The input gate relates to the current input, while the “forget” gate refers to the previous input. The internal construction of the LSTM is

shown in Figure 4. This LSTM network layer has a total of 512 network units in its configuration. First, we employ two blocks of tightly linked layers, each of which has a size of 1024 network units and is activated by rectified linear units (ReLU). Following the activation of the ReLU, we employ dropout regularisation with a value of 0.8. During the training phase, dropout regularisation is used to prevent the complicated coadaptations of the fully linked layers by disregarding randomly picked neurons. During the training process, this prevents overfitting from occurring. Last but not least, a third fully connected layer with a softmax activation function to obtain predictions for the next action. Because we want to choose the activities that are most likely to occur in a certain sequence.

Figure 4 displays the architecture of recurrent neural network in which  $X$  represents the inputs. These inputs are the extracted features, and  $Y$  represents the output class of the input features.

- (ii) Recognition

The following are the steps involved in this procedure:

- (a) Hu moments are used first to determine the properties of the test image, followed by a second step  
 (b) When compared to selecting training apps, these characteristics are advantageous

Figure 5 shows the process of recognition of images through machine learning approach. In order to feed the network with such temporal dependencies, a sliding time window is used to extract separate data segments. The window width and the step size can be both adjusted and optimised for better accuracy. Each time step is associated with an activity label, so for each segment, the most frequently appearing label is chosen. Here, the time segment or window width is chosen to be 200, and time step is chosen to be 100.

## 4. Results

The hybrid deep learning model has been applied on the wireless sensor data mining datasets to perform the human activity recognition. The classifier achieves the accuracy of 95%, though it might presumably be slightly improved by decreasing the step size of sliding window. The following graphs show the train/test error/accuracy for each epoch

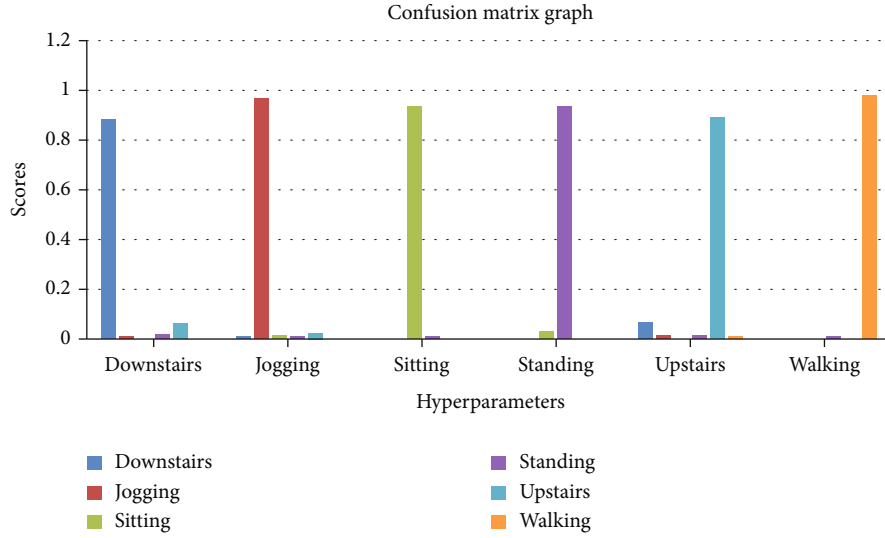


FIGURE 6: Graph of confusion matrix.

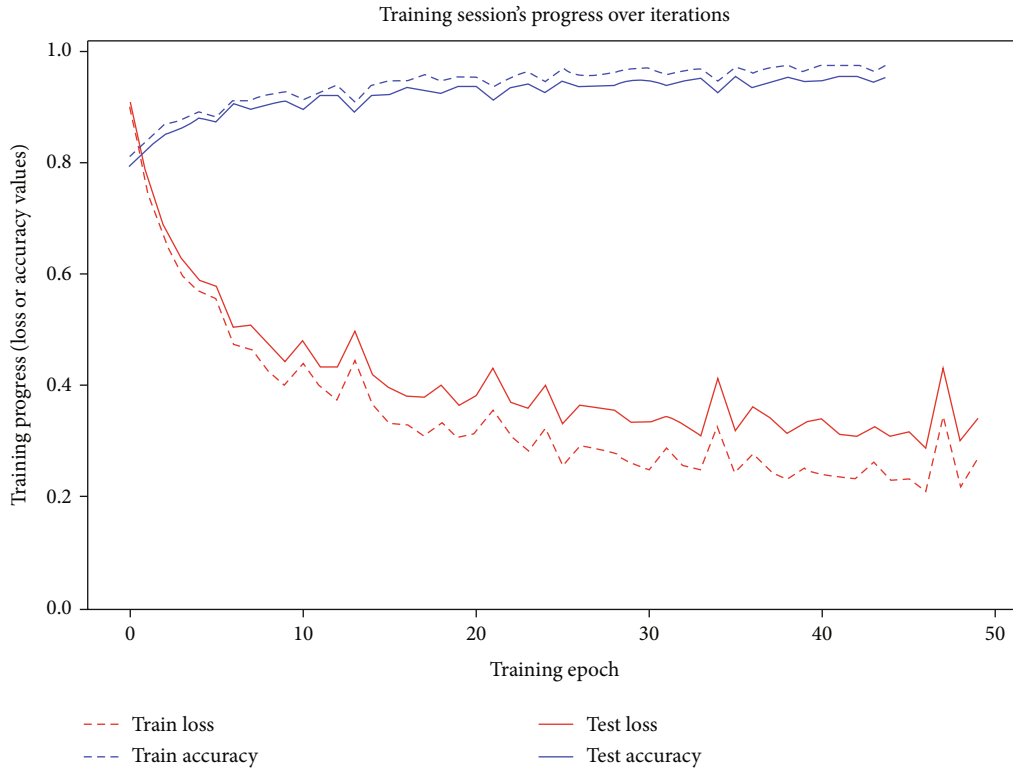


FIGURE 7: Graph representation of accuracy and loss.

and the final confusion matrix (normalised so that each row sums to one). The proposed work is implemented using Python programming language. The performance metrics used for the evaluation of the model are confusion matrix, accuracy, and the loss. The number of epochs used for the training of the model is 5000. The model hyperparameters are taken on the basis of human activities such as downstairs, jogging, sitting, standing, upstairs, and walking. The confusion matrix is also formed using these hyperparameters.

Table 1 has shown the confusion matrix generated by the hybrid deep learning model. Another parameter used for the evaluation of the model is accuracy and the error.

Figure 6 has represented the graph of confusion matrix. The graph is based on the hyperparameters.

Figure 7 has shown the graph based on generated train and test accuracy, train and test loss with respect to training epoch. The proposed work has achieved accuracy greater than 96%.

## 5. Conclusion

Because of the positive effects on our health and well-being, the ability to recognize our activities is increasingly in demand. It is now an essential instrument in the fight against obesity and the care of the elderly. The capacity to recognize human activity is based on using sensors to understand the body's gestures and motions and derive human activity or action. The activity recognizing systems can automate or simplify many ordinary human operations. Depending on the circumstances, human activity recognition systems may or may not be supervised. In this work, the human activity has been recognized using hybrid deep learning model, i.e., combination of convolutional neural network and the recurrent neural network. The parameters used for the evaluation of the model are confusion matrix, accuracy, and the errors. The results of the proposed model have shown that it has outperformed the existing models. In the future, the work can be improved by using Capsule Network in which we can take multiple convolutional neural networks for performing the activity recognition with different number of dropout layers, max pooling layers, and activation function.

## Data Availability

The dataset has been collected from the website <https://www.cis.fordham.edu/wisdm/dataset.php>, that is, mainly available for the research purpose.

## Conflicts of Interest

No potential conflict of interest was reported by the authors.

## Acknowledgments

The Deanship of Scientific Research (DSR) at King Abdulaziz University, Jeddah, Saudi Arabia has funded this project, under grant no. (RG-26-166-42). The authors, therefore, acknowledge with thanks DSR for technical and financial support.

## References

- [1] R. Nair, D. K. Singh, S. Yadav, and S. Bakshi, "Hand gesture recognition system for physically challenged people using IoT," in *2020 6th International Conference on Advanced Computing and Communication Systems (ICACCS)*, pp. 671–675, Coimbatore, India, 2020.
- [2] F. Demrozi, G. Pravadelli, A. Bihorac, and P. Rashidi, "Human activity recognition using inertial, physiological and environmental sensors: a comprehensive survey," *IEEE Access*, vol. 8, 2020.
- [3] R. Nair, P. Sharma, A. Bhagat, and V. K. Dwivedi, "A survey on IoT (internet of things) emerging technologies and its application," *International Journal of End-User Computing and Development*, vol. 7, no. 2, pp. 1–20, 2018.
- [4] L. Minh Dang, K. Min, H. Wang, M. Jalil Piran, C. Hee Lee, and H. Moon, "Sensor-based and vision-based human activity recognition: a comprehensive survey," *Pattern Recognition*, vol. 108, 2020.
- [5] R. Krishnamoorthi, S. Joshi, H. Z. Almarzouki et al., "A novel diabetes healthcare disease prediction framework using machine learning techniques," *Journal of Healthcare Engineering*, vol. 2022, Article ID 1684017, 10 pages, 2022.
- [6] C. Yang, W. Jiang, and Z. Guo, "Time series data classification based on dual path CNN-RNN cascade network," *IEEE Access*, vol. 7, pp. 155304–155312, 2019.
- [7] H. Z. Almarzouki, H. Alsulami, A. Rizwan, M. S. Basingab, H. Bukhari, and M. Shabaz, "An internet of medical things-based model for real-time monitoring and averting stroke sensors," *Journal of Healthcare Engineering*, vol. 2021, Article ID 1233166, 9 pages, 2021.
- [8] D. Mukherjee, R. Mondal, P. K. Singh, R. Sarkar, and D. Bhattacharjee, "EnsemConvNet: a deep learning approach for human activity recognition using smartphone sensors for healthcare applications," *Multimedia Tools and Applications*, vol. 79, pp. 41–42, 2020.
- [9] A. Taneja, S. Rani, A. Alhudhaif, D. Koundal, and E. S. Gündüz, "An optimized scheme for energy efficient wireless communication via intelligent reflecting surfaces," *Expert Systems with Applications*, vol. 190, p. 116106, 2022.
- [10] S. Sakib, A. Ahmed, J. K. Jawad, and H. Ahmed, *An overview of convolutional neural network: its architecture and applications*, Research Gate, 2018.
- [11] H. H. Rashidi, N. Tran, S. Albahra, and L. T. Dang, "Machine learning in health care and laboratory medicine: general overview of supervised learning and auto-ML," *International Journal of Laboratory Hematology*, vol. 43, no. S1, 2021.
- [12] J. Morales and D. Akopian, "Physical activity recognition by smartphones, a survey," *Biocybernetics and Biomedical Engineering*, vol. 37, no. 3, 2017.
- [13] S. Mohsen, A. Elkaseer, and S. G. Scholz, "Human activity recognition using K-nearest neighbor machine learning algorithm," *Proceedings of the International Conference on Sustainable Design and Manufacturing: KES-SDM 2021: Sustainable Design and Manufacturing*, Smart Innovation, Systems and Technologies, Springer, Singapore, 2022.
- [14] A. Tharwat, H. Mahdi, M. Elhoseny, and A. E. Hassanien, "Recognizing human activity in mobile crowdsensing environment using optimized k-NN algorithm," *Expert Systems with Applications*, vol. 107, pp. 32–44, 2018.
- [15] F. J. Ordóñez and D. Roggen, "Deep convolutional and LSTM recurrent neural networks for multimodal wearable activity recognition," *Sensors (Switzerland)*, vol. 16, no. 1, 2016.
- [16] N. Y. Hammerla, S. Halloran, and T. Plötz, "Deep, convolutional, and recurrent models for human activity recognition using wearables," 2016, <https://arxiv.org/abs/1604.08880>.
- [17] N. Sikder, M. S. Chowdhury, A. S. M. Arif, and A. al Nahid, "Human activity recognition using multichannel convolutional neural network," in *2019 5th International conference on advances in electrical engineering (ICAEE)*, pp. 560–565, Dhaka, Bangladesh, 2019.
- [18] C. A. Ronao and S. B. Cho, "Human activity recognition with smartphone sensors using deep learning neural networks," *Expert Systems with Applications*, vol. 59, pp. 235–244, 2016.
- [19] A. Ignatov, "Real-time human activity recognition from accelerometer data using convolutional neural networks," *Applied Soft Computing Journal*, vol. 62, pp. 915–922, 2018.
- [20] M. A. Alsheikh, A. Selim, D. Niyato, L. Doyle, S. Lin, and H. P. Tan, "Deep activity recognition models with triaxial



- accelerometers,” in *Workshops at the Thirtieth AAAI Conference on Artificial Intelligence*, Phoenix, AZ, USA, 2016.
- [21] B. Kolosnjaji and C. Eckert, “Neural network-based user-independent physical activity recognition for mobile devices,” in *International Conference on Intelligent Data Engineering and Automated Learning*, Lecture Notes in Computer Science, Springer, Cham, 2015.
- [22] A. Manzi, P. Dario, and F. Cavallo, “A human activity recognition system based on dynamic clustering of skeleton data,” *Sensors (Switzerland)*, vol. 17, no. 5, 2017.
- [23] M. Milenkoski, K. Trivodaliev, S. Kalajdziski, M. Jovanov, and B. R. Stojkoska, “Real time human activity recognition on smartphones using LSTM networks,” in *2018 41st International Convention on Information and Communication Technology, Electronics and Microelectronics (MIPRO)*, pp. 1126–1131, Opatija, Croatia, 2018.
- [24] S. W. Pienaar and R. Malekian, “Human activity recognition using LSTM-RNN deep neural network architecture,” in *2019 IEEE 2nd wireless africa conference (WAC)*, pp. 1–5, Pretoria, South Africa, 2019.
- [25] S. Agahian, F. Negin, and C. Köse, “An efficient human action recognition framework with pose-based spatiotemporal features,” *Engineering Science and Technology, an International Journal*, vol. 23, no. 1, 2020.
- [26] P. Siirtola and J. Röning, “Revisiting” recognizing human activities user-independently on smartphones based on accelerometer data”-what has happened since 2012?,” *International Journal of Interactive Multimedia and Artificial Intelligence*, vol. 5, no. 3, 2018.
- [27] S. Aggarwal, S. Gupta, A. Alhudhaif, D. Koundal, R. Gupta, and K. Polat, “Automated COVID-19 detection in chest X-ray images using fine-tuned deep learning architectures,” *Expert Systems*, vol. 39, no. 3, article e12749, 2022.
- [28] J. R. Kwapisz, G. M. Weiss, and S. A. Moore, “Activity recognition using cell phone accelerometers,” *ACM SigKDD Explorations Newsletter*, vol. 12, no. 2, 2011.
- [29] R. Nair and A. Bhagat, “Feature selection method to improve the accuracy of classification algorithm,” *International Journal of Innovative Technology and Exploring Engineering*, vol. 8, no. 6, pp. 124–127, 2019.
- [30] K. Bhalla, D. Koundal, S. Bhatia, M. K. I. Rahmani, and M. Tahir, “Fusion of infrared and visible images using fuzzy based siamese convolutional network,” *Computers, Materials and Continua*, vol. 70, no. 3, 2022.

## Research Article

# The Auxiliary Function of Intelligent Mobile Robot in the Standard Training of Children's Sports Movement

Kai Liu <sup>1</sup> and Cheng Guo<sup>1,2</sup>

<sup>1</sup>Graduate School, Capital University of Physical Education and Sports, Beijing 100191, China

<sup>2</sup>Sports Science Institute of Hebei Province Research Center, Shijiazhuang, 050011 Hebei, China

Correspondence should be addressed to Kai Liu; [kineticenergy@hotmail.com](mailto:kineticenergy@hotmail.com)

Received 4 January 2022; Revised 4 February 2022; Accepted 28 February 2022; Published 23 March 2022

Academic Editor: Shalli Rani

Copyright © 2022 Kai Liu and Cheng Guo. This is an open access article distributed under the Creative Commons Attribution License, which permits unrestricted use, distribution, and reproduction in any medium, provided the original work is properly cited.

Mobile robots belong to mechanical devices. Mobile robots are commanded by humans and restricted by the principles established by artificial intelligence technology, mainly to assist humans in dangerous tasks. Intelligent mobile robot is a system that integrates perception, analysis, and decision-making, and it integrates a number of high-end technologies. It is currently the most active field of technological development. Infant sport is essentially a process of cultivating and caring for the physical fitness of children. This article aims to explore the auxiliary role of intelligent mobile robots in the standard training of children's sports movements. The physique of the early childhood stage is closely related to the entire life stage. Once there is a deviation in the early childhood training stage, there will be very serious consequences. Therefore, the mobile intelligent robot is combined with children's physical training, and it is expected that it will give correct guidance to improve children's physical fitness. This article briefly designs the mobile robot, uses two independent wheels and a robotic arm with degrees of freedom, and analyzes the forward and inverse kinematics of the chassis and the robotic arm, which provides a theoretical basis for the design of the control algorithm. This article will focus on the training of children's sports, explore the current deficiencies in children's sports, and analyze the reasons and the role that intelligent mobile robots can provide in sports training. The experimental results in this paper show that the balance ability of children standing on one foot with eyes open is mainly distributed in the second, third, and fourth levels. Among them, the second level has the largest number of people, accounting for 52%, the third level accounts for 27%, the fourth level accounts for 22%, and the other levels are less distributed. When the intelligent mobile robot assists children's movement, the child's balance ability is generally distributed in the fourth and fifth levels. Among them, the fourth level has the largest number of people, accounting for 52%, followed by the fifth level, accounting for 26%, and the third level accounting for 14%. This shows that the intelligent mobile robot is effective in guiding the movement of young children.

## 1. Introduction

The robot integrates a number of high-end technologies and has a very high work efficiency. It can replace humans in work and save labor costs. Intelligent mobile robot technology covers structural design, visual calibration, SLAM (real-time positioning and map construction), path planning, multisensor information fusion, and other technologies. Intelligent mobile robots have become a hot spot in the field of robotics research. There are many tasks in dangerous environments that humans cannot complete, but robots do not have this

concern. Intelligent robots can complete various tasks organized and planned in various environments, which also enables intelligent robots to have vigorous vitality in various fields. For example, it can help with housework, complete diagnostic work in a hospital, complete explosion-proof work in a hazardous environment, and so on. With the continuous improvement of residents' living standards, it is the common wish of parents to promote the healthy development of children. Children are an important stage of individual intellectual development and movement development, and movement training is closely related to physical fitness. However,

compared with movement training, parents pay more attention to intellectual development and standardized movement training. This has also led to a lack of scientific coaches for children's sports activities in the market. Due to the lack of scientific quantitative standards, the scope of physical fitness research mainly focuses on three aspects: body shape, physiological function, and physical fitness. There have been few studies on psychological conditions so far, so the current physical fitness testing is only limited to the physical aspect. However, the movement training of young children is closely related to their physical fitness, and scientific methods must be formulated to enhance their physical fitness. This article combines the intelligent mobile robot with the standard training of children's sports movement and hopes that it can play a role in the training of children and enhance the physical fitness of children.

The current training of young children is concentrated in the field of intellectual development, and there is a lack of necessary research on the physical function and physique of young children, which leads to a lack of scientific and reasonable training for young children. Combining intelligent mobile robots with standard training for children's sports movements can provide scientific guidance for children's sports training, enhance their physique, promote their healthy growth, improve their quality of life, formulate correct training patterns for children, and exercise properly.

China has been practicing the "people-oriented" policy, and society is paying increasingly attention to people. As a disadvantaged group, young children have become the focus of attention. Due to the lack of children's sports training mechanisms in the market, a large number of experts and scholars have carried out research in this field. Tang et al. proposed a new classification-based virtual machine placement (CBVMP) algorithm for MCC, which aims to improve the efficiency of virtual machine (VM) allocation in large cloud data centers and the unbalanced utilization of underlying physical resources. In recent years, cloud computing services based on mobile terminals such as smart phones have developed rapidly. Cloud computing has the advantages of massive storage capacity and high-speed computing capabilities, which can meet the needs of different types of users. In this context, mobile cloud computing (MCC) is booming. Through simulation experiments based on the CloudSim cloud platform, the experimental results show that the new algorithm can improve the efficiency of VM placement and the utilization of underlying physical resources [1]. Li et al. proposed a hybrid intelligent algorithm for wheeled mobile robots (WMR) to achieve trajectory tracking and path tracking navigation tasks. A new control scheme combining kinematics and TSK fuzzy control was developed to track the required position, linear velocity, and angular velocity, so that WMR is affected by system uncertainty and interference. The TSK fuzzy controller he proposed deals with general dynamic models and has good antidisturbance capabilities. For the path following problem, the improved D\*lite algorithm determines the appropriate path between the initial position and the destination. The derived path is transformed into a tracking trajectory through a time function. The asymptotic stability of

the whole system is proved by Lyapunov theory. Finally, real-time experiments using the proposed hybrid intelligent algorithm on the figure-eight reference trajectory and long-distance movement proved the feasibility of actual WMR maneuvering [2]. Dayal aims to explore the possibility of a two-wheeled mobile robot (TWMR) generating an obstacle-free real-time optimal path in a cluttered environment, driven by two DC motors. During the exploration process, a new motion planning strategy called DAYANI arc contour intelligent technology was proposed, which is used for the navigation of a two-wheeled self-balancing robot in a global environment with obstacles. The developed new path planning algorithm considers five weight functions from the arc profile to evaluate the best next feasible moving point based on five independent navigation parameters. Through a series of calculations of path length and time, the authenticity of the proposed navigation algorithm is proved. Simulation and experimental verification found that the average error percentage is about 6%. This data proves that the two-wheel mobile robot can analyze the optimal path [3]. Karakaya et al. proposed a wheeled mobile robot navigation toolbox for Matlab. The toolbox includes algorithms for 3D map design, static and dynamic path planning, point stabilization, positioning, gap detection, and collision avoidance. The toolbox can be used as a test platform for developing custom mobile robot navigation algorithms. The toolbox allows users to insert/remove obstacles, upload/save custom maps, and configure simulation parameters in the robot workspace, such as robot size, virtual sensor position, Kalman filter, parameters for positioning, speed controller, and collision avoidance settings. It can simulate data from a virtual laser imaging detection and ranging (LIDAR) sensor to provide a map of the surrounding environment of the mobile robot. The differential drive forward kinematics equation and the positioning scheme based on the extended Kalman filter (EKF) are used to determine the position of the robot in each simulation step. The lidar data and navigation process are visualized using the developed virtual reality interface [4]. Karamipour et al. introduced the dynamic equations of reconfigurable nonholonomic mobile robots for space exploration and rescue operations. The dimensions of mobile robots generally remain the same, while they are programmed to determine new paths around obstacles. The purpose of developing this robot is to upgrade the mechanical structure so that its structure can be adapted to pass obstacles without path deviation. In addition, through the above reconfiguration, less motor power is required, thereby optimizing energy consumption. To this end, the longitudinal and lateral adjustment of the robot is defined. In view of the movement limitations of traditional wheels, the robot structure adopts omnidirectional wheels, and its characteristics are considered when deriving the motion equation. Therefore, the robot can move in the direction of the wheel axis. To evaluate the designed mechanism, the system was simulated in ADAMS, and the results were compared with the derived equations of motion. The research results proved that the system is practical [5]. Sunjin proposed an object tracking algorithm that can be applied to mobile robot systems based on Android. The

advantage of the Android system is that it can be low-cost, portable, and versatile. To achieve this, the author implemented a particle filter-based algorithm to track objects in the input image from the smartphone camera in real time on the Android system. The proposed algorithm transmits the motion signal in the form of a data packet to the mobile robot by Bluetooth communication, so that the mobile robot can track the moving object. In addition, when a moving obstacle is detected and the object is completely occluded, an ultrasonic sensor will be used to suspend robot's motion, so as not to reduce robot's tracking accuracy. In the experimental results, the author proposed an optimal algorithm for his system by comparing the performance of other tracking algorithms [6]. Satoshi proposed a new mechanism that uses a single actuator to control the manipulation of a wheeled robot. The design uses the elements of snake board and two-wheeled skateboard propulsion. Two passive wheels, i.e., casters that can control the direction, are installed on the front and back of the robot's body. The rotor rotates above the body and uses its reaction torque to induce the body to advance. Three degrees of freedom of movement, namely, the direction of each of the rotors and the two casters, are mechanically coupled to a single actuator through a torque limiter. The stopper is used to limit the angle of the caster direction, and the torque limiter allows the rotor to continue to rotate without being restricted by stopper's range of motion. Experiments show that the rotation of the sinusoidal rotor can push the robot forward, and adding an increased or reduced offset to the rotation of the sinusoidal rotor can bend the motion of the robot [7]. Although these theories have discussed intelligent mobile robots and infant sports training to a certain extent, the combination between the two is not enough, resulting in insufficient practicability.

At present, children's movement training lacks corresponding scientific standards. Combining intelligent mobile robots with children's training can standardize children's sports movement training. In addition, the robot uses a general-purpose single-chip microcomputer to realize wheeled movement. The robot motor drive and closed-loop speed regulation technology can enable the intelligent mobile robot to effectively avoid obstacles, and the intelligent mobile robot integrates motion control and other technologies to make the robot cool and enjoy the benign control ability.

## **2. The Auxiliary Function Method of Intelligent Mobile Robot in the Standard Training of Children's Sports Movement**

*2.1. Overview of Smart Mobile Robots.* With the continuous development of industrial technology, the demand in the production field is increasing. The opposite is the increasing degree of population aging and the decline in the number of labor forces [8]. To solve the labor problem, it is possible to put robots in industrial production. Robots have the advantages of flexible operation, improved production efficiency, labor cost savings, and improved product quality, and have

been widely used. Although the current robotics industry is very advanced, easy to operate, and has a high level of production, the robotics industry has gone through a certain stage of development to achieve such an achievement [9, 10]. The first stage of the robot was in the middle of the last century. At that time, the robot was relatively simple and only repeated an action according to the code design. The second stage of the robot can complete different actions according to the teaching program and start to officially put it in the factory. In the third stage of the rapid development of robots, robots have certain feedback and perception capabilities. With the continuous development of industrialization, robots cover a number of high-end technologies and possess certain logical decision-making capabilities [11]. At present, it belongs to the stage of intelligence, manufacturing, upgrades, industrial automation, and robots replacing humans. To make robots more environmentally adaptable and independent, robots are required to have logical thinking and decision-making capabilities. As a representative of the robotics field, intelligent mobile robots have also become a current research hotspot. It can not only replace human work in harsh natural environments but also has different functions according to changes in human needs [12]. For example, in a medical service robot, it can observe patient's physical status in real time and provide treatment advice, and it can also deliver water, food, medicine, newspapers, and magazines to people, which greatly improves hospital's service level. Figure 1 shows the basic model of an intelligent mobile robot.

With the continuous development of industrial technology, the demand in the production field is increasing. The opposite is the increasing degree of population aging and the decline in the number of labor forces [8]. To solve the labor problem, it is possible to put robots in industrial production. Robots have the advantages of flexible operation, improved production efficiency, labor cost savings, and improved product quality and have been widely used. Although the current robotics industry is very advanced, easy to operate, and has a high level of production, the robotics industry has gone through a certain stage of development to achieve such an achievement [9, 10]. The first stage of the robot was in the middle of the last century. At that time, the robot was relatively simple and only repeated an action according to the code design. The second stage of the robot can complete different actions according to the teaching program and start to officially put it in the factory. In the third stage of the rapid development of robots, robots have certain feedback and perception capabilities. With the continuous development of industrialization, robots cover a number of high-end technologies and possess certain logical decision-making capabilities [11]. At present, it belongs to the stage of intelligence, manufacturing, upgrades, industrial automation, and robots replacing humans. To make robots more environmentally adaptable and independent, robots are required to have logical thinking and decision-making capabilities. As a representative of the robotics field, intelligent mobile robots have also become a current research hotspot. It can not only replace human work in harsh natural environments but also have different

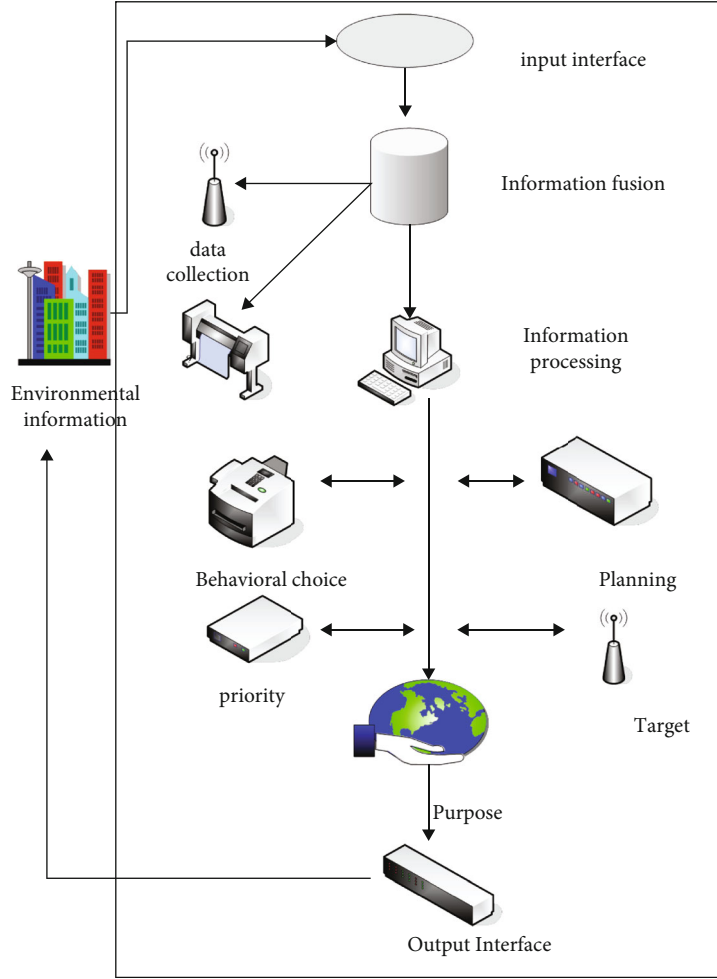


FIGURE 1: The basic model of an intelligent mobile robot.

functions according to changes in human needs [12]. For example, in a medical service robot, it can observe patient's physical status in real time and provide treatment advice, and it can also deliver water, food, medicine, newspapers, and magazines to people, which greatly improves hospital's service level. Figure 1 shows the basic model of an intelligent mobile robot (Figure 2).

China's research on robots started late, but the country has given a lot of support to high-end technologies in this century, so generally speaking, certain achievements have been made in robot research and development [13–18], taking the multifunctional outdoor mobile intelligent robot as an example. This series of robots covers multiple technologies such as path planning and information fusion, laying a foundation for the development of robots. In 2016, Xiaomi released a self-developed sweeping robot, which covers the SLAM algorithm inside. It can construct a room map based on the collected data and then complete the cleaning work according to the cleaning path. The robot has an automatic charging function. Compared with the previously developed robot, the degree of intelligence has been qualitatively improved [19]. Figure 3 shows the model of the multifunctional intelligent mobile robot system.

**2.2. Robot Dynamics.** In essence, the research on robots still needs to explore its power support. Understanding the internal motion correlation of the robot can provide theoretical support for the exploration of control algorithms [20]. The most fundamental problem of motion planning is to allocate robot's speed reasonably based on the current position, direction, and speed of the robot, so that it can quickly achieve the desired position, direction, and speed. The goals that the control algorithm expects to achieve include time optimization and path optimization. Figure 4 is a schematic diagram of the motion model of the intelligent mobile robot.

$$\varphi = (\partial \gamma i)^{\mathfrak{R}}. \quad (1)$$

Among them,  $\varphi$  represents the position and posture of the intelligent robot;  $\partial$  and  $\gamma$  represent the seat position.

$$\dot{\varphi} = (\dot{\partial} \dot{\gamma} i)^{\mathfrak{R}}, \quad (2)$$

where  $\dot{\varphi}$  represents the speed of the intelligent robot.

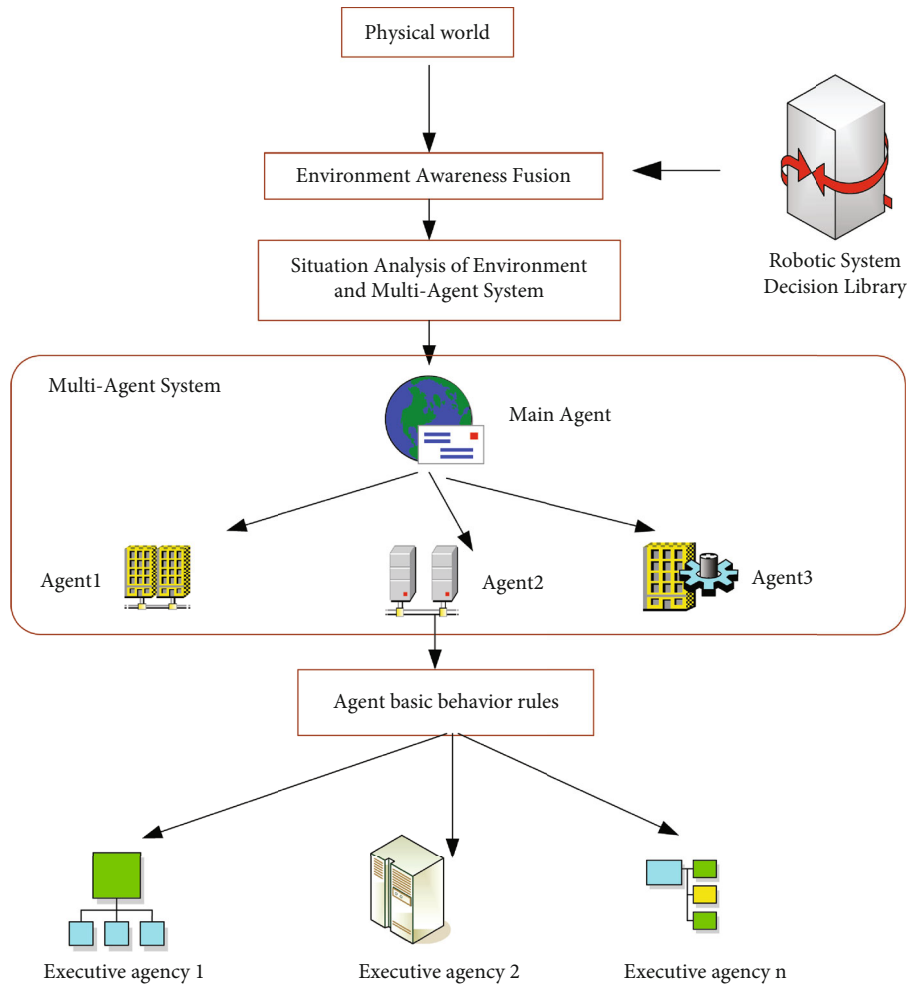


FIGURE 2: Mobile robot system model.

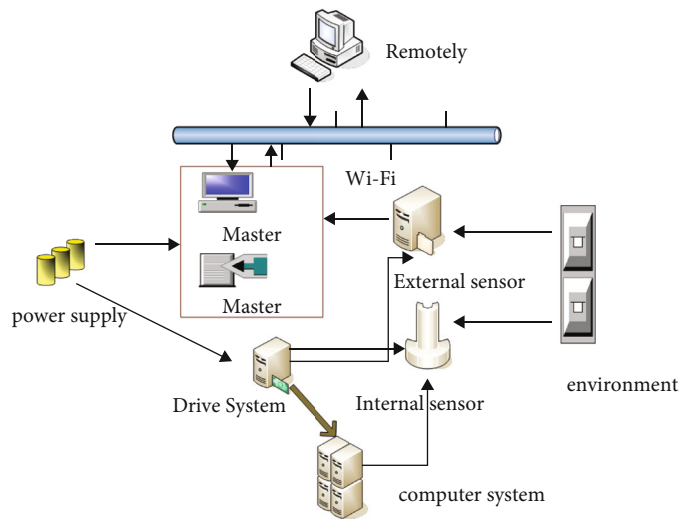


FIGURE 3: Multifunctional intelligent mobile robot system model.

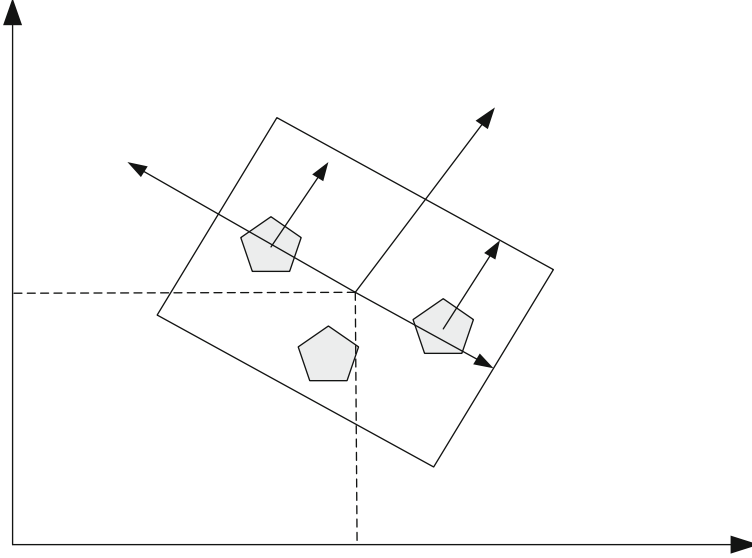


FIGURE 4: Intelligent mobile robot motion model.

$$W(\iota) = \begin{pmatrix} \cos \iota & \sin \iota & 0 \\ -\sin \iota & \cos \iota & 0 \\ 0 & 0 & 0 \end{pmatrix}. \quad (3)$$

Among them,  $W(\iota)$  represents the orthogonal rotation angle of the intelligent robot.

$$(-2 \ 0 \ \mathfrak{F})W(\iota)\phi + F\mathfrak{N} = 0. \quad (4)$$

Formula (4) indicates that the speed of the robot in the left direction is zero.

$$(-2 \ 0 \ \mathfrak{F})W(\iota)\phi + F\mathfrak{N}_t = 0. \quad (5)$$

Formula (5) indicates that the speed of the robot in the right direction is zero.

$$\begin{pmatrix} \dot{a} \\ \dot{b} \\ \dot{i} \end{pmatrix} = \frac{3}{4} \begin{pmatrix} \cos \iota & \cos \iota \\ \sin \iota & \sin \iota \\ -\frac{1}{\iota} & \frac{1}{\iota} \end{pmatrix}. \quad (6)$$

Among them, formula (6) is a summary of formula (4) and formula (5).

$$\begin{cases} \iota = \iota_0 + \frac{1}{\iota} \int_0^1 s(\partial_1 - \partial_2) du, \\ a = a_0 + \frac{s}{3} \int_0^1 \cos \iota (\partial_1 + \partial_2) du, \\ b = b_0 + \frac{s}{3} \int_0^1 \sin \iota (\partial_1 + \partial_2) du. \end{cases} \quad (7)$$

Among them,  $\iota_0$ ,  $a_0$ , and  $b_0$  indicate the position of the robot at different times.

$$\begin{cases} q = \sqrt{\dot{a}^2 + \dot{b}^2}, \\ e_1 = \frac{2q + \alpha \iota}{3s}, \\ e_2 = \frac{2q - \alpha \iota}{3s}. \end{cases} \quad (8)$$

Formula (9) represents the reverse motion speed of the robot.

Current inverse motion solving methods include algebraic methods and neural network algorithms [21]. In general, the algebraic method is the simplest; the algebraic method is simple to operate and has strong versatility, but requires a lot of iterative operations, is low in efficiency, and cannot get a convergent solution in the singular position, and its specific function expressions are as follows:

$$R = \begin{pmatrix} b_1 b_{23} & b_1 d_{23} & -d_1 \\ d_1 b_{23} & d_1 d_{23} & b_1 \\ 0 & 0 & 0 \end{pmatrix}, \quad (9)$$

$$R_i = \begin{pmatrix} b_4 b_5 b_6 + d_4 d_6 & -b_4 b_5 b_6 + d_4 d_6 \\ -d_5 b_6 & d_5 b_6 \\ b_4 b_5 b_6 - d_4 d_6 & -b_4 b_5 b_6 - d_4 d_6 \end{pmatrix}. \quad (10)$$

$R$  represents the position of each joint of the robot.  $b_i = \cos \partial$ ,  $d_i = \sin \partial$ , and the motion equation of the robot proportion is  $W = R * R_i * b_i * d_i$ .

$$b_{23} = \cos (\partial_1 - \partial_2) = b_2 b_3 + d_2 d_3, \quad (11)$$

$$d_{23} = \sin(\partial_1 - \partial_2) = d_2 b_3 + b_2 d_3. \quad (12)$$

According to formula (11) and formula (12), we make the robot's wrist as:

$$w = \begin{pmatrix} e_{11} & e_{12} & e_{13} \\ e_{21} & e_{22} & e_{23} \\ e_{31} & e_{32} & e_{33} \\ 0 & 0 & 0 \end{pmatrix}. \quad (13)$$

From this, the coordinate position of the wrist can be calculated:

$$a = b_1 b_{23} f - b_1 b_{23} s + b_1 (fb + f), \quad (14)$$

$$g = d_1 b_{23} f - d_1 d_{23} s + b_1 (fb + f), \quad (15)$$

$$j = d_{23} f - b_{23} s + b_1 (fb + f). \quad (16)$$

According to the coordinate axis of the wrist, the coordinate position of the chest of the robot can be obtained:

$$y_1 = x_1 x_{23} (x_1 x_2 x_3 + d_4 d_5) - x_1 d_3 x_3 d_6, \quad (17)$$

$$y_2 = x_1 x_{23} (x_1 x_2 x_3 + d_4 d_5) + x_1 d_3 x_3 d_6, \quad (18)$$

$$y_3 = x_{23} (x_1 x_2 x_3 + d_4 d_5). \quad (19)$$

Among them,  $y_1$ ,  $y_2$ , and  $y_3$  represent the 3 typical characteristic points of the chest.

Without considering that the robot encounters obstacles, the optimal solution is as follows:

$$S = \frac{\sum_{H=1}^4 j |\alpha_h(g+2) - \alpha_h(g)|}{\sum_{H=1}^4 j}, \quad (20)$$

where  $j$  represents the length of the joint.

**2.3. Children's Sports Training.** With the improvement of living standards, people pay increasingly attention to physical health, so sports training is very popular [22]. There are many sports activities on the market today, and each sports item has a focus. Therefore, there is no unanimous view on "children's sports training" [23, 24]. However, one thing is not controversial; infant sports is the cultivation of children's physical health. It is fundamentally different from the competitive sports mentioned in our daily lives, and it is also different from children's regular outdoor activities. Based on its particularity, the state incorporates children's sports into the health field in the form of games [25]. In terms of academic concepts, children's sports include basic movements, sports games, and basic gymnastics. Although sports activities have not been fully defined academically, from the content of previous researchers, they include basic movements and gymnastics [26]. Basic movements for children include walking, running, jumping, throwing, balancing, drilling, and climbing; basic gymnastics includes changing formations and queues. This experiment is also

carried out around the basic movements, Figure 5 is a schematic diagram of children's sports training:

Basic movements have a developmental process [27]. The so-called development refers to the change of things from small to large, from simple to complex, and from low-level to high-level. The development of basic work for children is related to age, and the development process is continuous and uninterrupted. The development of children's basic movements is a prerequisite for their normal life and learning [28, 29].

Children are in a stage of continuous learning. In this process, they need to be instructed in their physical training. The so-called guidance is pointing and leading. Guidance in the adult world refers to the advice of elders to younger generations. In the world of young children, guidance refers to support, pointing, and helping behavior in daily life [30]. Figure 6 shows the exploration route of this article on the basic movements of children.

### 3. The Auxiliary Function Experiment of Intelligent Mobile Robot in the Standard Training of Children's Sports Movement

**3.1. Experimental Subjects.** For the special experimental objects of the infant group, the choice of experimental actions needs to be scientific and rigorous, and it is operability under the premise of ensuring the norms of the actions. Table 1 is the related information about the subjects of this experiment.

According to the data in Table 1, two classes in two schools were investigated in this experiment. In the first school, there are 9 boys and 5 girls in class A, a total of 14 people; class B has 7 boys and 11 girls, a total of 18 people; the two classes have a total of 32 students. In the second school, there are 7 boys and 9 girls in class A, a total of 16 people; class B has 12 boys and 7 girls, a total of 19 people; the two classes have a total of 35 students.

**3.2. Physical Activity Guidance.** The basic sports training of young children is essential, and it will have an important impact on the subsequent growth of children. Although there is a certain understanding of this theory, there is still a lack of guidance in real life.

According to the data in Table 2, among the 75 items of actual action guidance, 40 items do not pay attention to the basic work instruction of young children, accounting for 53%. There is no corresponding guidance when performing these exercises, or even no exercise. Only 47% pay more attention to action guidance. These data show that the current exercise guidance for young children is very irregular.

According to the data in Table 3, out of the 45 unguided actions surveyed, 15 lacked emphasis on sports rules, accounting for 33.3%; 18 sports did not provide safety tips for young children, accounting for 40%; there are 5 items that do not provide guidance on children's communication principles, accounting for 11.1%; other aspects that do not provide guidance account for 15.6%.





FIGURE 5: Sports training for young children.

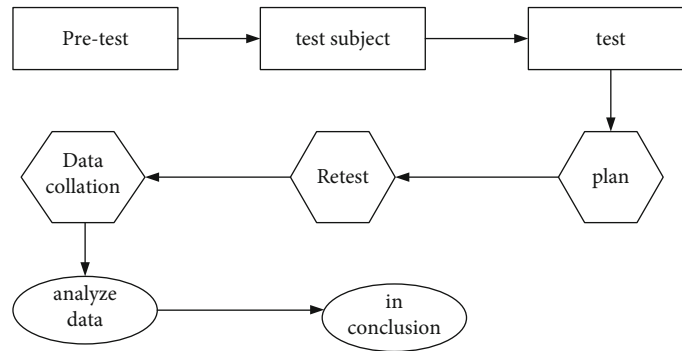


FIGURE 6: The exploration route of children's basic movements.

TABLE 1: Experimental subject information.

Category	Classes	Number of people	Number of experiments		Total number of people
			Male	Female	
1	a	18	9	5	14
	b	24	7	11	18
2	a	20	7	9	16
	b	26	12	7	19

TABLE 2: Distribution of movement instruction content.

Category	Number	Proportion
Ignore the action	40	53
Movement instruction	35	47
Total	75	100

TABLE 3: Specific cases of lack of guidance.

Category	Number	Proportion (%)
Rules	15	33.3
Safety	18	40
Principles of interaction	5	11.1
Other	7	15.6
Total	45	100

3.3. Intelligent Mobile Robot Parameters. The robot parameters used in this experiment are shown in Table 4.

#### 4. The Auxiliary Role of Intelligent Mobile Robots in the Standard Training of Children's Sports Movements

4.1. Balanced Items. In infants, the balance ability is generally poor, and young children are a relatively active group, often an imbalance in daily activities, causing different degrees of injury to the knee or other parts. Strengthening balance training is conducive to coordinating children's sense of space.

According to the data in Figure 7, the experimental results are divided into 7 levels in the experiment. This experiment process divides the experiment objects into an experiment group and a control group. In the experimental group, the balance level of children before the experiment was generally in the third and fourth levels. Among them, the third level accounted for 32%, the fourth level accounted for 27%, the second level accounted for 15%, and the fifth level accounted for 14%, but there are fewer people in other levels. After the experiment, the fifth level accounted for the largest proportion, which was as high as 42%; it was followed by the fourth level, accounting for 28%. The sixth level accounted for 13%, the third level accounted for 12%, and the number of other levels was relatively small. According to these data, it can be found that after the professional coaching training of intelligent mobile robots, the balance ability of children improves very quickly.

TABLE 4: Intelligent mobile robot parameters table.

Category	Parameters	Category	Parameters
Lengths	40 cm	Drive wheel width	7 cm
Width	60 cm	Linear speed	80 cm/s
Wheelbase front and rear	45 cm	Angular speed	260 cm/s
Drive wheel length	18 cm	Weight	50 kg

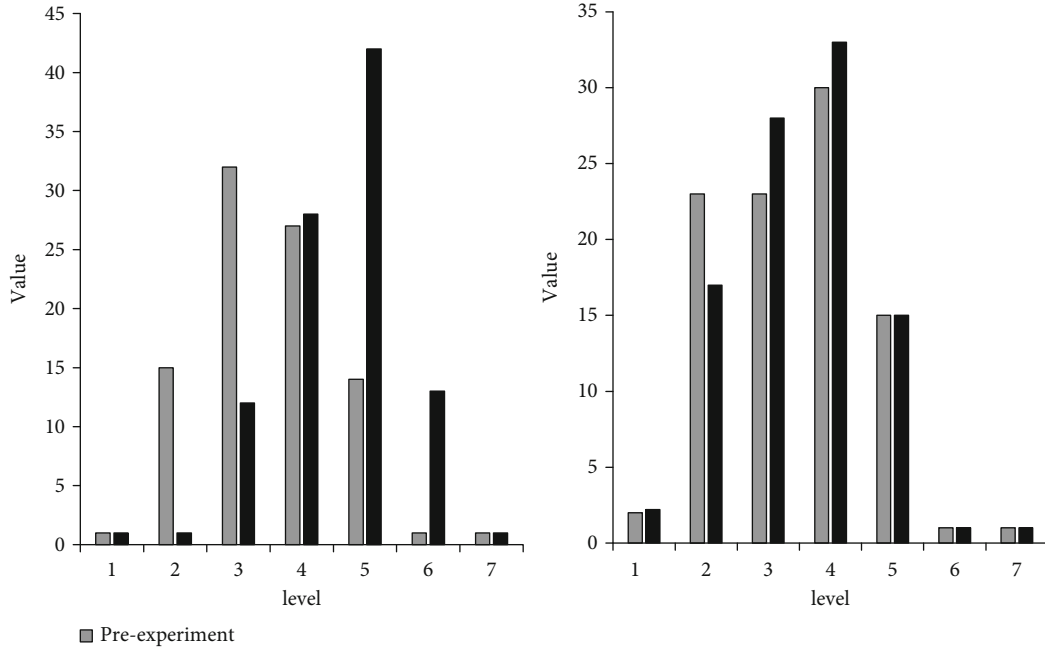


FIGURE 7: Standing on one foot with eyes open.

In the control group, the balance ability of the children before the experiment was generally concentrated in the third and fourth levels, which was consistent with the data of the experimental group. After the experiment, the balance ability of the children in the control group is still concentrated in the third and fourth levels, which shows that the balance training of the children has not achieved the effect.

According to the data in Figure 8, we also divided the balance of children into 7 levels and set up an experimental group and a control group. In the information of the experimental group, we can see that before the experiment, the balance ability of children standing on one foot with eyes open is mainly distributed in the second, third, and fourth levels. Among them, the second level has the largest number of people, accounting for 52%, the third level accounts for 27%, the fourth level accounts for 22%, and the other levels are less distributed. After the intelligent mobile robot coached the children’s movement, it was found that the children’s balance level has been significantly improved. After training, the balance ability of young children is generally distributed in the fourth and fifth levels. Among them, the fourth level has the largest number of people, accounting for 52%, and the fifth level is closely followed, accounting for 26%, the third level accounts for 14%, and the distribu-

tion of other levels is relatively small. From the perspective of the balance level distribution before and after the experiment, the intelligent mobile robot is still very effective in guiding the movement of children.

The basic information of the control group before training was consistent with that of the experimental group, and the balance ability of the children was also concentrated in the second, third, and fourth levels. Among them, the second level has the largest number of people, accounting for 50%, the third level accounts for 25%, the fourth level accounts for 20%, and the other levels are less distributed. The infants in the control group were given general action instructions. After training, infants’ balance ability distribution levels were still concentrated in the fourth and fifth levels. Among them, the fourth level accounted for the largest proportion, as high as 47%, the fifth level accounted for 26%, and the third level accounted for 14%. Although the balance level of infants has improved compared with before training, there is still a certain gap compared with the data of the experimental group, which also shows that the intelligent mobile robot is effective in guiding children’s movement.

Children stand upright on one foot with eyes open and closed, which can adjust children’s visual influencing factors. It enables children to carry out movement training under the

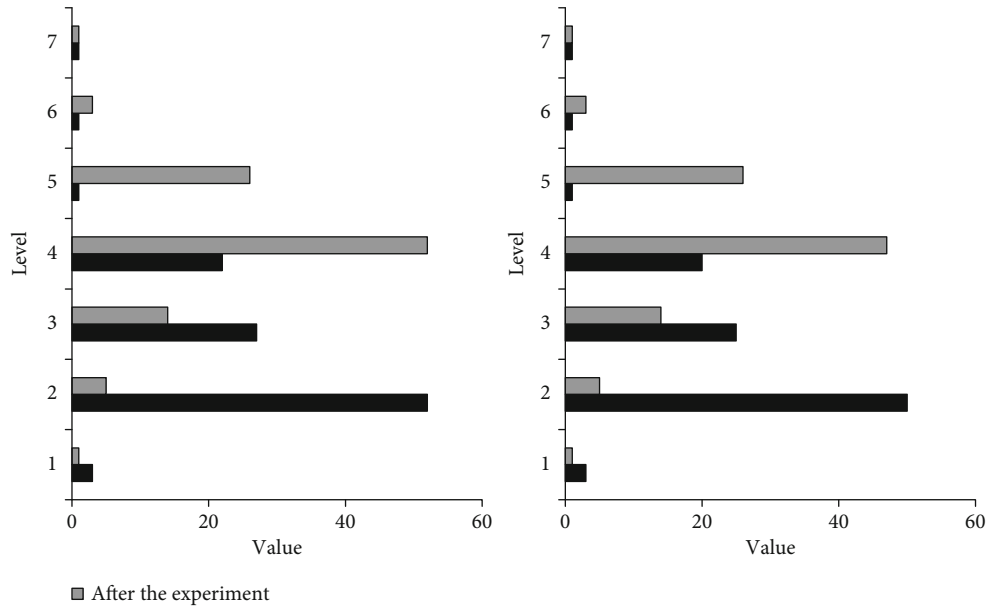


FIGURE 8: Standing on one foot with eyes open.

influence of visual factors and removal of visual interference, so that children can complete movement training more freely and promote the development of their own balance.

**4.2. Differences in Balance Ability.** According to the data in Figure 9, we divided the experimental results into 7 levels and set up the experimental group and the control group during the training of stepping with closed eyes for children. The experimental group uses intelligent mobile robots for guided action training, while the control group uses routine guided action training. Before the experiment, the balance ability of the children in the experimental group was concentrated in the third and fourth levels. Among them, the fourth level accounted for the largest proportion, as high as 33%, the third level followed by 27%, the second level accounted for 18%, the fifth level accounted for 11%, and the other levels had fewer people. After the intelligent mobile robot provides action guidance, the balance ability of young children is concentrated in the fourth and fifth levels. Among them, the fifth level accounted for the highest proportion, reaching 42%, the fourth level accounted for 28%, and the other levels were less distributed. From this data, it can be seen that the level of children's stepping with closed eyes has been qualitatively improved.

In the control group, the balance level before training was similar to that of the experimental group, and the balance ability of young children was concentrated in the third and fourth levels. Among them, the fourth level accounted for the most, up to 30%, the third level followed by 25%, the second and fifth levels accounted for 18%, and the other levels had fewer people. After regular training, the balance ability of young children is concentrated in the fourth level, accounting for as much as 52%. It can also be seen from the amplitude of the curve in Figure 9 that the level of children after routine training has not improved to a large level, and there is a certain gap compared with the results of the exper-

imental group. These data also illustrate the effect of intelligent mobile robots in training.

The upward and forward movement is to adjust and control the dynamic training intensity of young children in different motion planes such as the coronal plane and the sagittal plane by changing the direction of movement. It can increase the movement form and exercise intensity of the limbs in the dynamic movement training of young children.

**4.3. Vestibular Step Level.** According to the data in Figure 10, it can be seen that the experimental process is the same as the previous experiment. Before the vestibular step training, children's vestibular step levels are mainly distributed in the fourth and fifth levels. Among them, the fifth level accounted for the largest proportion, as high as 35%, the fourth level accounted for 13%, and the third level accounted for 11%; the distribution of other levels is relatively small. When the intelligent mobile robot provides action guidance, the children's vestibular step level has been greatly improved. From the data in Figure 10, it can be seen that the number of people in the first four levels has decreased significantly compared with that before the experiment. The proportion of the fifth level has reached 68%, and the number of people in the sixth and seventh levels has also increased compared with that before the experiment.

The data of the control group before the experiment was consistent with that of the experimental group, and children's vestibular step levels were mainly distributed in the fourth and fifth levels. Among them, the fifth level accounted for the largest proportion, up to 50%, the fourth level accounted for 13%, the third level accounted for 11%, and the other levels were less distributed. According to the experiment of the control group, it can be seen that children's vestibular step level did not change significantly before and after the experiment, which shows that the

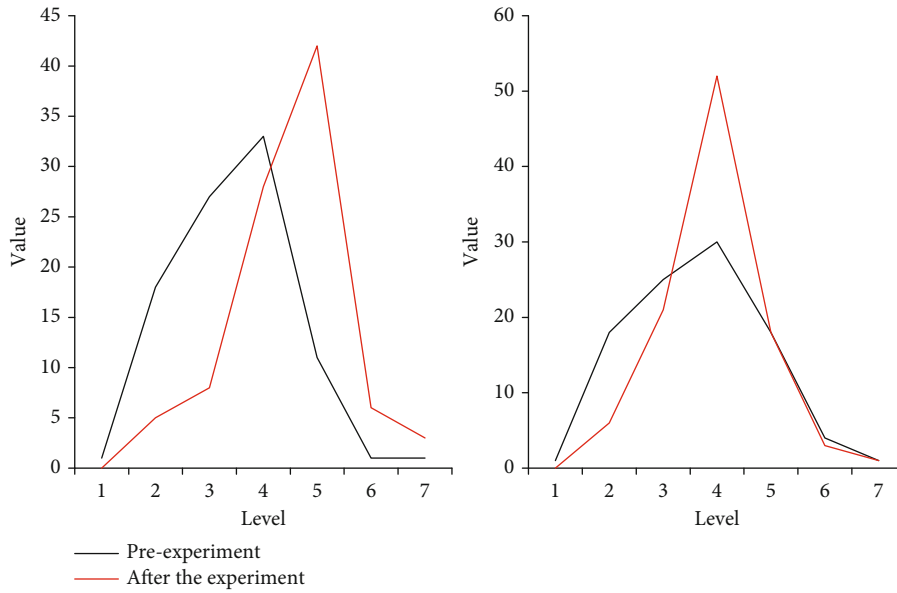


FIGURE 9: Stepping in place with closed eyes.

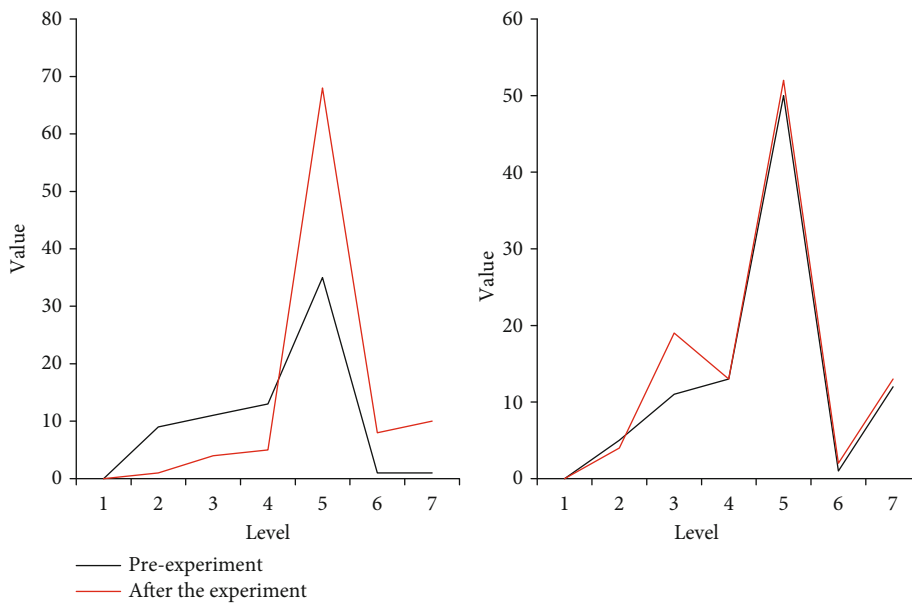


FIGURE 10: Analysis of vestibular step hierarchy.

conventional training has no effect. These data also illustrate the effect of intelligent mobile robots in the vestibular step training program.

### 5. Conclusions

Technical development will not only bring progress to the production field but also have a significant impact on daily life. The continuous development of robot technology and the continuous improvement of capabilities have enabled the continuous expansion of the scope of use of robots, and they can replace humans in completing many dangerous

and complex tasks. Because young children are in the learning stage, motion training requires professional guidance, but the current market lacks such professional guidance, so people have turned their attention to robotics. This article is based on this background and aims to explore the auxiliary role of intelligent mobile robots in the standard training of children’s sports movements. In this article, the following work has been mainly completed: (1) by analyzing the physical structure of the wheeled mobile robot, the motion model of the mobile robot is obtained. (2) A brief overview of children’s easy sports guidance was given, and the conclusion was drawn that intelligent mobile robots can effectively assist

children in sports movement training. (3) Children's movement training programs should be in line with their age, and safety education must always be given during training.

### Data Availability

The data underlying the results presented in the study are available within the manuscript.

### Conflicts of Interest

The authors declare that they have no conflicts of interest.

### Authors' Contributions

Kai Liu and Cheng Guo contributed equally to this work as co-first authors.

### References

- [1] Y. Tang, Y. Hu, and L. Zhang, "A classification-based virtual machine placement algorithm in mobile cloud computing," *Ksii Transactions on Internet & Information Systems*, vol. 10, no. 5, pp. 1998–2014, 2016.
- [2] I. H. Li, Y. H. Chien, W. Y. Wang, and Y. F. Kao, "Hybrid intelligent algorithm for indoor path planning and trajectory-tracking control of wheeled mobile robot," *International Journal of Fuzzy Systems*, vol. 18, no. 4, pp. 595–608, 2016.
- [3] R. Dayal, "Development and analysis of DAYANI arc contour intelligent technique for navigation of two-wheeled mobile robot," *Industrial Robot: An International Journal*, vol. 45, no. 5, pp. 688–702, 2018.
- [4] S. Karakaya, G. Kucukyildiz, and H. Ocak, "A new mobile robot toolbox for Matlab," *Journal of Intelligent and Robotic Systems*, vol. 87, no. 1, pp. 125–140, 2017.
- [5] E. Karamipour, S. F. Dehkordi, and M. H. Korayem, "Reconfigurable mobile robot with adjustable width and length: conceptual design, motion equations and simulation," *Journal of Intelligent and Robotic Systems*, vol. 99, no. 3-4, pp. 797–814, 2020.
- [6] Y. Sunjin, "Android based robot vision tracking system for mobile robot," *Journal of Korean Institute of Intelligent Systems*, vol. 27, no. 4, pp. 283–288, 2017.
- [7] I. Satoshi, "mechanism and control of a one-actuator mobile robot incorporating a torque limiter," *Journal of Intelligent and Robotic Systems*, vol. 97, no. 2, pp. 431–448, 2020.
- [8] J. Keogh and P. W. Winwood, "The epidemiology of injuries across the weight-training sports," *Sports Medicine*, vol. 47, no. 3, pp. 479–501, 2017.
- [9] M. H. Davenport, T. S. Nagpal, M. F. Mottola et al., "Prenatal exercise (including but not limited to pelvic floor muscle training) and urinary incontinence during and following pregnancy: a systematic review and meta-analysis," *British Journal of Sports Medicine*, vol. 52, no. 21, pp. 1397–1404, 2018.
- [10] L. An, B. Li, D. Ming, and W. Wang, "Multislice spiral CT image analysis and meta-analysis of inspiratory muscle training on respiratory muscle function," *Journal of Healthcare Engineering*, vol. 2021, 2021.
- [11] C. F. Finch, L. Fortington, A. Muhammed et al., "152 Exercise training to prevent sports injuries: results from a clustered randomised controlled trial," *Injury Prevention*, vol. 22, Suppl 2, pp. A56.1–A5A56, 2016.
- [12] J. Darren, "Agility in team sports: testing, training and factors affecting performance," *Sports Medicine*, vol. 46, no. 3, pp. 421–442, 2016.
- [13] E. Khooshab, I. Jahanbin, S. Ghadakpour, and S. Keshavarzi, "Managing parenting stress through life skills training: a supportive intervention for mothers with visually impaired children," *International Journal of Community Based Nursing & Midwifery*, vol. 4, no. 3, pp. 265–273, 2016.
- [14] L. Garnweidner-Holme, H. S. Haugland, I. Joa et al., "Facilitators and barriers to healthy food selection at children's sports arenas in Norway: a qualitative study among club managers and parents," *Public Health Nutrition*, vol. 24, no. 6, pp. 1–7, 2020.
- [15] D. Francesca, B. Daniela, and R. Rosa, "Transmitting sport values: the importance of parental involvement in children's sport activity," *Europe's Journal of Psychology*, vol. 13, no. 1, pp. 75–92, 2017.
- [16] J. L. Donkers, L. J. Martin, K. F. Paradis, and S. Anderson, "The social environment in children's sport: cohesion, social acceptance, commitment, and enjoyment," *International Journal of Sport Psychology*, vol. 46, no. 4, pp. 275–294, 2016.
- [17] T. Buszard, M. Reid, R. Masters, and D. Farrow, "Scaling the equipment and play area in children's sport to improve motor skill acquisition: a systematic review," *Sports Medicine*, vol. 46, no. 6, pp. 829–843, 2016.
- [18] K. L. Quarrie, J. Brooks, N. Burger, P. A. Hume, and S. Jackson, "Facts and values: on the acceptability of risks in children's sport using the example of rugby - a narrative review," *British Journal of Sports Medicine*, vol. 51, no. 15, pp. 1134–1139, 2017.
- [19] M. Pan, Y. Liu, J. Cao, L. Yu, C. Li, and C.-H. Chen, "Visual recognition based on deep learning for navigation mark classification," *IEEE Access*, vol. 8, pp. 32767–32775, 2020.
- [20] J. Jin, Y. G. Kim, S. G. Wee, D. H. Lee, and N. Gans, "A stable switched-system approach to collision-free wheeled mobile robot navigation," *Journal of Intelligent and Robotic Systems*, vol. 86, no. 3-4, pp. 599–616, 2017.
- [21] R. Alazrai, M. Momani, H. A. Khudair, and M. I. Daoud, "EEG-based tonic cold pain recognition system using wavelet transform," *Neural Computing and Applications*, vol. 31, no. 7, pp. 3187–3200, 2019.
- [22] S. Sridhar and A. Eskandarian, "Cooperative perception in autonomous ground vehicles using a mobile-robot testbed," *IET Intelligent Transport Systems*, vol. 13, no. 10, pp. 1545–1556, 2019.
- [23] M. Gheisarnejad and M. H. Khooban, "Supervised control strategy in trajectory tracking for a wheeled mobile robot," *IET Collaborative Intelligent Manufacturing*, vol. 1, no. 1, pp. 3–9, 2019.
- [24] Y. Bian, J. Peng, and C. Han, "Finite-time control for nonholonomic mobile robot by brain emotional learning-based intelligent controller," *International journal of innovative computing, information and control*, vol. 14, no. 2, pp. 683–695, 2018.
- [25] M. Rezaie, M. Malekmakan, A. Shirehjini, and S. Shirmohammadi, "The effect of room complexity on physical object selection performance in 3-D mobile user interfaces," *IEEE Transactions on Human-Machine Systems*, vol. 50, no. 4, pp. 349–357, 2020.

- [26] J. Leaman and H. M. La, "A comprehensive review of smart wheelchairs: past, present and future," *IEEE Transactions on Human-Machine Systems*, vol. 47, no. 4, pp. 486–499, 2017.
- [27] X. Zhou and S. Wen, "Analysis of body behavior characteristics after sports training based on convolution neural network," *Computational Intelligence and Neuroscience*, vol. 2021, 2021.
- [28] T. Zhang, S. Fan, J. Hu et al., "A feature fusion method with guided training for classification tasks," *Computational Intelligence and Neuroscience*, vol. 2021, 11 pages, 2021.
- [29] K. Lee and H. Choo, "Predicting user attitudes toward smartphone ads using support vector machine," *International journal of mobile communications: IJMC*, vol. 14, no. 3, pp. 226–243, 2016.
- [30] A. Soroka and L. Rigali, "Industry 4.0 and Smart City in mobile machine's control systems," *IFAC-PapersOnLine*, vol. 52, no. 27, pp. 473–476, 2019.

## Research Article

# Application of Hybrid Teaching Mode in College Students' English Reading Using Intelligent Wireless Communication Multimedia

Jiayun Yan 

*School of Foreign Language, North China Institute of Aerospace Engineering, Langfang, 065000 Hebei, China*

Correspondence should be addressed to Jiayun Yan; 2111805063@e.gzhu.edu.cn

Received 31 December 2021; Revised 16 February 2022; Accepted 26 February 2022; Published 23 March 2022

Academic Editor: Shalli Rani

Copyright © 2022 Jiayun Yan. This is an open access article distributed under the Creative Commons Attribution License, which permits unrestricted use, distribution, and reproduction in any medium, provided the original work is properly cited.

The development of multimedia technology and the rise of mixed teaching modes have introduced new forms of teaching organization to the field of education, the traditional teaching methods have been improved, and the advantages of the traditional teaching methods have been brought into play. At the same time, the development of online courses has also provided a new basis for teaching and improved the current teaching environment. The current rapid development of intelligent technology and wireless communication networks provides opportunities for the innovation of multimedia technology and also provides technical support for offline and online teaching in a hybrid teaching mode. What this article needs to discuss is the application of hybrid teaching mode in the English reading teaching of college students under the background of intelligent wireless communication network multimedia technology and explore whether the combination of hybrid teaching mode and intelligent technology can improve the teaching level of college students' English reading, etc. This paper shows through experimental research that under the teaching organization form of the mixed teaching mode under the background of intelligent wireless communication multimedia, college students' interest in the course of English reading has increased significantly, and their English reading scores will increase by at least 93%, which can improve students' autonomous learning ability for college English reading courses.

## 1. Introduction

The development of intelligent technology and wireless communication network has made multimedia technology unprecedented development, and it has been widely used in various fields. Especially the application in the field of education has promoted the informatization of education and has also promoted the birth of online courses, providing an opportunity for the innovation of traditional classroom teaching models. The combination of online teaching and traditional teaching has given birth to a hybrid teaching model. The hybrid teaching model combines online teaching and traditional teaching together, which greatly promotes the quality and level of teaching. Moreover, the rise of the mixed teaching model is highly respected by people from all walks of life in the education field. It is hoped that this teaching mode will change the teaching mode of the

teacher-led college English reading course, improve the students' main position in the English reading class, and stimulate the students' initiative in the college English reading course.

The hybrid teaching mode combined with the application of intelligent technology and multimedia technology in the teaching field can improve teachers' teaching methods, update teachers' teaching concepts, enable college students to gradually realize the goals of resource sharing, timely communication, and personalized learning in English teaching, make students' English learning develop towards individualization and independent learning, and improve students' enthusiasm for English learning. Combining wireless communication network and multimedia technology, improve the teaching organization method of the mixed teaching mode and have a positive impact on improving the reading ability of students through the mixed teaching

mode. And on this basis, stimulate students' interest in learning English reading, improve students' self-learning ability in English reading and change students' learning concept of English reading; the blended teaching model breaks through the limitations of learning time and learning space; among them, the online course platform in the hybrid teaching mode realizes the whole process of evaluating students' English reading learning, so that teachers can intelligently manage the students' English reading learning, promote the reform of English reading teaching, and realize a student-centered teaching model.

In order to promote the organizational innovation of college English teaching, change teachers' teaching concepts, enhance students' dominant position in the classroom, and stimulate students' autonomous learning and innovation capabilities, and many scholars are interested in improving the teaching methods of English reading and how to improve students. A lot of research has been carried out on the enthusiasm and initiative of English reading and learning. Among them, Zhang studied the application of the flipped classroom in college English learning based on the mastery of learning theory and cooperative learning theory, using computer network language teaching auxiliary technology, and experiments show that the computer network flipped classroom teaching is beneficial to improve the teaching and learning of college English [1]. Sun proposed that the blended teaching mode has the advantages of combining traditional teaching methods with online teaching, explored cloud-based college English teaching based on the blended teaching mode, and found that this teaching mode enables students to participate more in classroom activities and gradually realizes autonomous learning [2]. Ma proposed that there is a certain relationship between English reading and schema theory. Teachers should make full use of schema theory to improve teaching strategies and focus on cultivating students' schemata, thereby improving students' English reading ability and information processing ability [3]. Ge and Zhang analyzed the application of EAP mode in college English teaching in China and believed that EAP can simulate the actual situation of English academic communication and stimulate students' initiative and creativity in professional English learning [4]. Yeon explored the direct and indirect contributions of college students' English acceptance and productive vocabulary knowledge to second language reading and explored the impact of vocabulary knowledge on English reading, revealing the relationship between second language receptive vocabulary and productive vocabulary knowledge and second language reading ability [5]. Jung explored the feasibility of extensive courses at the university level and explored an effective teaching model to motivate students. The research results show that cooperative English reading courses can help improve students' English reading ability and stimulate students' English reading motivation [6]. However, none of these studies mentioned that teachers should change the dominant position of teachers in the English teaching classroom and give full play to the main role of students in the teaching of English reading; in addition, it did not discuss how to update teachers' teaching concepts and students'

learning ideas and failed to fundamentally change the defects in traditional teaching. There is no detailed elaboration on how to improve students' autonomous learning ability in English reading, ignoring the shortcomings of traditional teaching.

The research of this article has the following innovations: (1) this article combines wireless communication network on the basis of analyzing the influence of multimedia technology on college students' English reading teaching. Making the online course platform intelligent, which can intelligently record students' learning, intelligently assess students' English reading ability and intelligently test the improvement of students' English reading ability online, (2) this article combines multimedia technology and intelligent technology and applies it to examples of college students' English reading resources and mixed teaching mode and further analysis and improvement in actual teaching practice, in order to improve the positive influence of the mixed teaching mode in college students' English reading teaching; (3) realizing the sharing of English reading resources through intelligent wireless communication network and multimedia, so that students can take classes in multimedia classrooms, adopt a hybrid teaching mode, and use multimedia equipment to learn and teach independently in the classroom, and (4) students can use multimedia equipment to search for materials and discuss on the Internet in real time in the classroom, give full play to their main role, let teachers play the role of guidance, and allow traditional teaching methods to maximize their strengths and avoid weaknesses.

## **2. The Teaching Method of College Students' English Reading Supported by Modern Technology**

### *2.1. Intelligent Wireless Communication and Multimedia Technology*

*2.1.1. Smart Wireless Communication.* Wireless communication network refers to a network that can realize the interconnection of various communication devices without wiring. It breaks the limitations of time, space, and objects, enables humans to communicate with people anytime and anywhere, and greatly improves the quality and level of human life, work, and learning [7]. In the field of education, the openness of intelligent wireless communication networks, and the rich resources stored in science and technology such as big data, enable students to obtain them through wireless networks, allowing students to share learning resources. The wireless network is shown in Figure 1.

The intelligent wireless communication network is to optimize the network infrastructure on the basis of the wireless communication network and effectively add storage and voice technology to the wireless network terminal. Based on the wireless communication network, our teaching equipment needs to be intelligent. That is, the multimedia technology we use for teaching needs to be intelligent. The realization of the intelligent wireless communication network requires corresponding programs to be set between



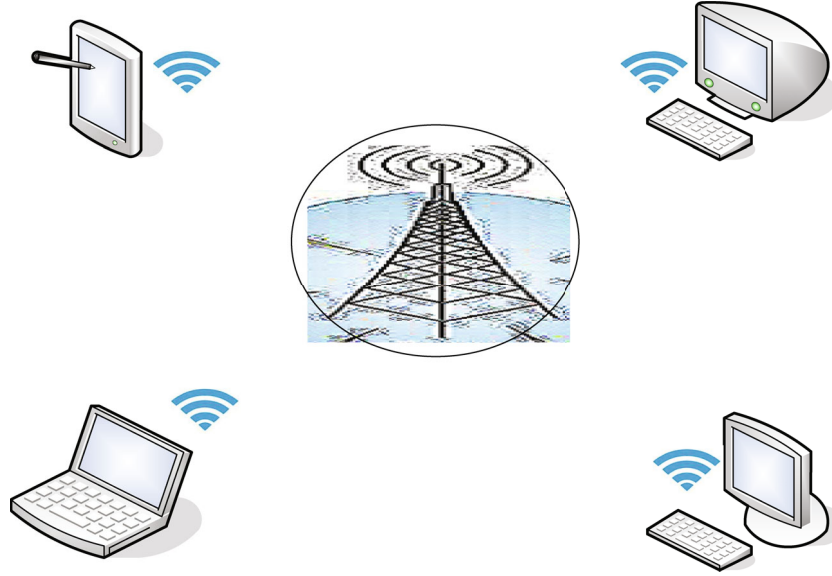


FIGURE 1: Wireless network.

the devices to realize remote control. For example, we need to use network equipment before the college English reading class. If the equipment fails, the technician can repair it remotely. The control principle is as follows:

A remote control system is set up between two devices. One is the server, and the other is the control. The principle of this system is as follows:

$$A \xrightarrow{\exp \left\{ \prod_s^t \pi^2 \right\} * \varphi} B. \quad (1)$$

Among them,  $t$  is the network speed of the wireless communication network,  $s$  is the recording time of the remote control repair,  $A$  is the server,  $B$  is the client, and  $\varphi$  is a correlation coefficient matrix:

$$\varphi = \left\{ \begin{array}{ccc} (A_1, B_1) & \cdots & (A_1, B_N) \\ (A_2, B_1) & \cdots & (A_2, B_N) \end{array} \right\}. \quad (2)$$

Through remote control and wireless communication network, the equipment can be repaired through remote control, saving a lot of time, avoiding problems with multimedia equipment, and ensuring the progress and efficiency of the classroom [8]. With the development of wireless communication technology and the popularization of mobile phones and computers, the mobile computers we use daily have basically realized wireless communication, and the emergence of video conversation and live broadcast functions that can realize long-distance communication also represents the continuous deepening of the intelligent trend of wireless network communication technology [9]. The intelligent wireless network is shown in Figure 2.

The smart device and wireless network shown in Figure 2 constitute a smart wireless network. The so-called smart wireless communication network means that smart devices can connect and communicate through the wireless

network. Just like the 5G network, we are currently developing, it is becoming smarter and smarter.

**2.1.2. Intelligent Multimedia Technology.** Multimedia technology has been in the field of teaching for many years. Early multimedia devices need to be wired through the network to be able to use. However, with the development of wireless networks, such as the development of 5G networks, multimedia devices can be used through wireless networking, and there is no need to worry about short-term network physical lines, which also brings convenience to teaching. Multimedia is composed of media. These information media include the following: text, sound, graphics, images, animation, and video. Intelligent multimedia is centered on the central control host, and the wireless touch screen is the control terminal, using big data, sensors, and other technologies to intelligitize the media, such as the application of our intelligent video in multimedia technology. Multimedia technology has the characteristics of multidimensionality, integration, interactivity, and digitization.

The characteristic of multimedia multidimensionality means that multimedia technology can extend data information spatially and transform, classify, and integrate the information in multimedia memory [10]. The principle of its internal drive information conversion is as follows:

$$A = \frac{x f_i^2}{\sum_t^x G_i^2 - G * f_i}, \quad (3)$$

$$A = \frac{2f^2}{\sum_x G_i^2} * f_i * \omega = B. \quad (4)$$

Among them,  $x$  is the amount of information that needs to be transformed,  $t$  is the length of time required for intelligent calculation of the transformation,  $f$  is the weight of the internal information transformation of the multimedia

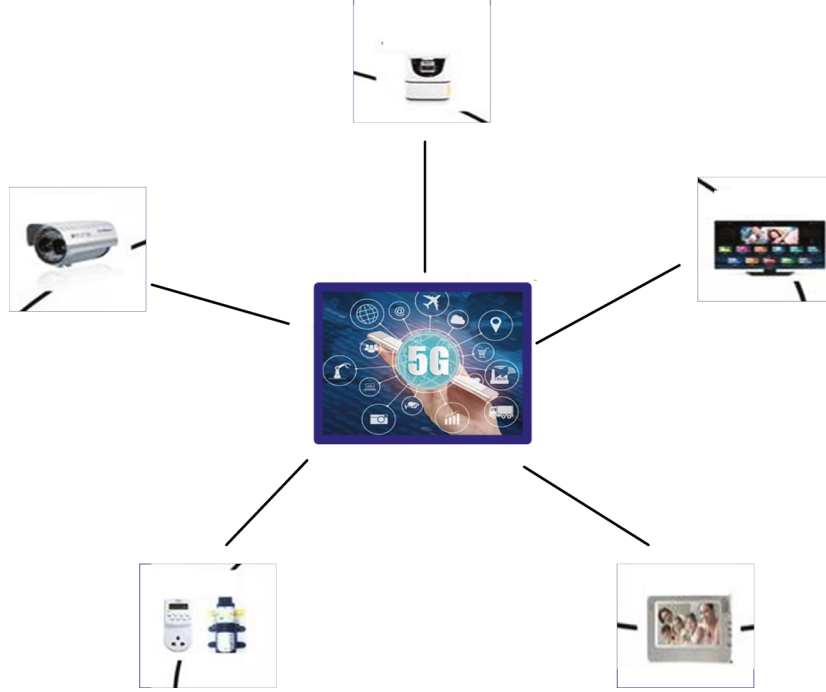


FIGURE 2: Smart wireless network.

technology,  $G$  is the number of information streams in the multimedia memory,  $i$  is the smart label in each information stream, and  $\varpi$  is a parallel matrix that can only be generated to ensure the balance of the amount of information during data information conversion:

$$\varpi = \begin{bmatrix} t & A & i \\ G & f & x \\ g & B & s \end{bmatrix}. \quad (5)$$

This matrix is a homogeneous coordinate. The homogeneous coordinate is convenient for the conversion operation of image information. When the image is converted into ratio, rotation, symmetry, and crosscutting, the multimedia technology will intelligently select the matrix part:

$$T_1 = \begin{bmatrix} t & A \\ G & f \end{bmatrix}. \quad (6)$$

If the image information is translated, the multimedia technology will intelligently select the following parts:

$$T_2 = [gB]. \quad (7)$$

If it is to project the data information, the multimedia technology will intelligently convert according to the command instructions, and the selected matrix form is as follows:

$$T_3 = \begin{bmatrix} i \\ x \end{bmatrix}. \quad (8)$$

If it wants to make a total ratio transformation of data information, multimedia technology will intelligently select the following matrix parts:

$$T_4 = [s]. \quad (9)$$

The characteristic of multimedia integration refers to the ability to obtain, store, organize, and synthesize information in a multichannel unified manner [11]. Multichannel acquisition means that the information needs to be obtained uniformly through multiple roads through the wireless network. If there are multiple channels, the principle of multichannel unification of information is

$$W_1 = \sum_{s_1}^{t_1} \frac{x_1}{D_1} * \sigma, \quad (10)$$

$$W_2 = \sum_{s_2}^{t_2} \frac{x_2}{D_2} * f * \sigma, \quad (11)$$

$$W_n = \sum_{s_n}^{t_n} \frac{x_n}{D_n} * f^{(n-1)} * \sigma. \quad (12)$$

The principles of information organization and synthesis are as follows:

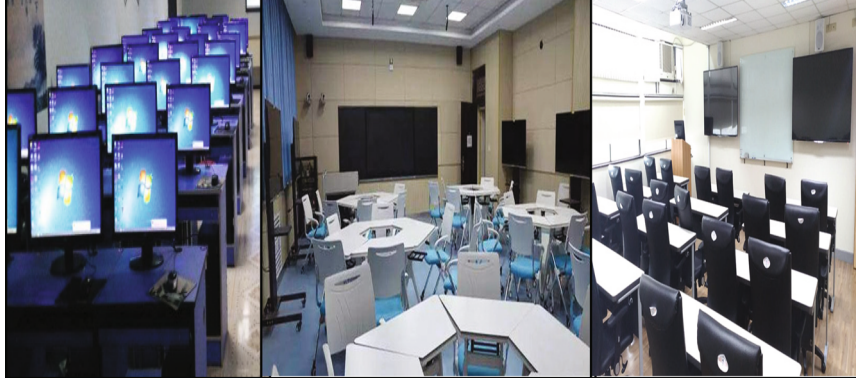


FIGURE 3: Smart multimedia classroom.

$$W_1 + W_2 + \dots + W_n = \frac{1}{n} * \sigma * \left( \sum_{s_1}^{t_1} \frac{x_1}{D_1} + \sum_{s_2}^{t_2} \frac{x_2}{D_2} * f + \dots + \sum_{s_n}^{t_n} \frac{x_n}{D_n} * f^{(n-1)} \right). \quad (13)$$

Among them,  $t$  represents the time for the information to be unified from multiple channels,  $s$  is the network speed of the wireless communication network,  $f$  is the threshold of the multimedia system generated during information integration,  $\sigma$  is a matrix, and its form is as follows:

$$\sigma = \begin{Bmatrix} W_1 & \dots & W_n \\ t_1 & \dots & t_n \\ s_1 & \dots & s_n \end{Bmatrix}. \quad (14)$$

The interactive feature of multimedia refers to that multimedia technology allows people to independently select the information they need and control the use of multimedia equipment [12]. The principle is as follows:

$$P_{\text{demand}} \longrightarrow \prod_s^t * \sum_i^f * \omega \longrightarrow M. \quad (15)$$

Among them,  $P$  is the command issued by the person,  $\omega$  is the matrix mentioned above, and  $M$  is the information generated by the multimedia receiving the command instruction, so that people can actively select and control the information.

The characteristic of multimedia digitization refers to the existence of media in digital form. Digitization refers to that in a multimedia computer system, and various media information is stored in a computer in digital form and processed. The principle is as follows:

$$R_{(\text{digital})} = E * \left[ \sum_s^t f * W_n * i \right]. \quad (16)$$

The use of multimedia technology in the teaching field can help teachers change the teaching style. The use of intelligent multimedia can use big data, cloud computing, and other technologies to simplify the difficult-to-understand

teaching materials, and convert the materials into the forms we need to make students understandable. It can make teachers' teaching resources more vivid and interesting, can also make students feel the happiness brought by different teaching methods, and stimulate students' interest in learning [13]. The intelligent multimedia classroom is shown in Figure 3.

As shown in Figure 3, a smart multimedia classroom uses smart wireless communication networks and multimedia technologies. The smart multimedia classroom implements five functions: centralized control and hierarchical management, educational resource management cloud platform, classroom interaction, real-time attendance and feedback, and big data platform analysis [14], enabling students in the classroom to use multimedia equipment to find the learning resources they need on the Internet in real time.

*2.2. College English Reading Teaching with Blended Teaching Mode.* The blended teaching mode is a mode that combines the advantages of online teaching and traditional teaching. Through the organic combination of the two forms of teaching organization, learners' learning can be guided from shallow to deep to deep learning [15]. The current mixed teaching mode is shown in Figure 4.

The blended teaching model described in Figure 4 combines traditional teaching methods with online courses. Traditional teaching methods are used in class, and online teaching methods are used after class. In college English reading teaching, a hybrid teaching mode combining online and offline can be realized, but it is impossible to conduct both online and offline at the same time. Because our current teaching equipment is still unable to realize online learning in the classroom, we can only carry out independent online learning after class, but there is no guarantee that every student will independently participate in the course learning on the online platform after class [16]. Although the current mixed teaching model reflects the student's dominant position to a greater extent, the teacher's dominant position is still stronger. Although the resources are wired in the classroom, due to the lack of multimedia equipment, only the teacher uses the multimedia equipment to display. The students just sit in the classroom and stare at the teacher and teach according to the multimedia display screen. The students only read and learn based on the online English

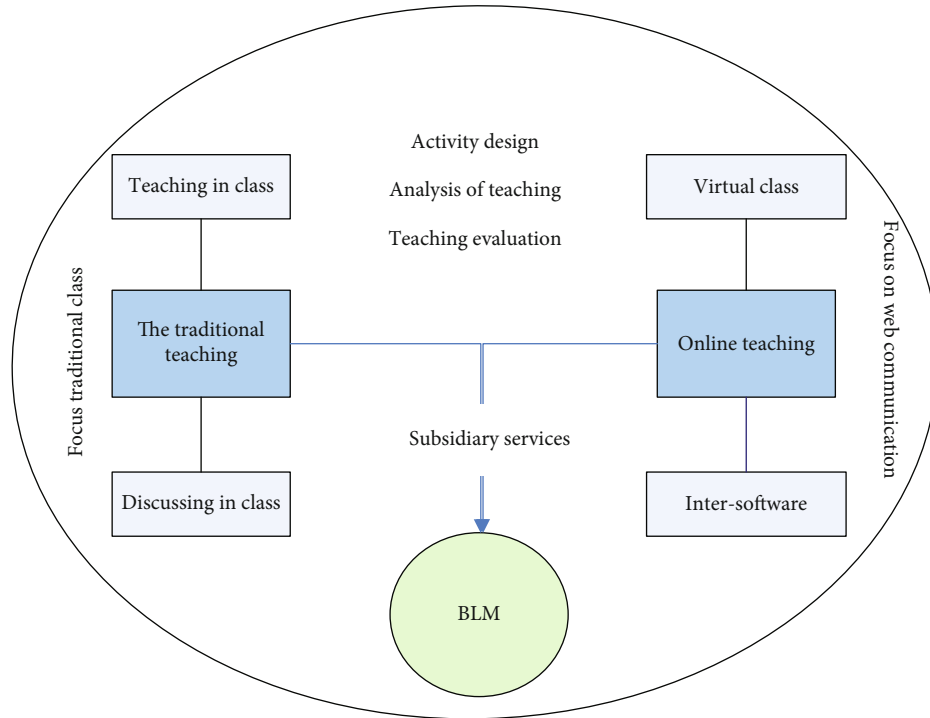


FIGURE 4: Mixed teaching mode.

reading resources provided by the classroom. It is difficult to get the students' own ideas from it.

In addition, if online teaching is conducted, the learning atmosphere is also insufficient, which will directly affect students' learning enthusiasm. Although online teaching can communicate with teachers online, it cannot guarantee constant interaction between teachers and students, which will lead to insignificant learning effects. Therefore, we need to make the online and offline classrooms of the hybrid teaching mode proceed on time at the same time to ensure that students interact with the classroom at all times, but also allow students to communicate more in offline classrooms. In fact, the so-called mixed teaching model is mostly students sitting in offline classrooms, but watching a teacher's live broadcast or recording on the computer. When there is a problem, there is an on-site teaching assistant to tutor the students. Although this method is similar to the blended teaching model, it is actually a dual-teacher teaching.

At present, teachers always believe that traditional teaching methods should be used in college English reading courses, but the main obstacle to students' English reading is not the difficulty of words, and the difficulty of reading materials is not just English words and grammar [17]. In order to overcome the shortcomings of the traditional English teaching model, we can use a blended teaching model to innovate in English reading teaching. Before the class, the teacher can provide a video about reading the text. Then students submit their confused questions or content to the class for discussion with the teacher. The extracurricular reading content can be uploaded to the online classroom in the form of text or video, through online discussion and solution of typical problems, and the discussion can be completed in the classroom [18]. Teachers post videos and addi-

tional learning resources, such as listening materials or readings of new words and phrases, to public online platforms, which can be used by all students to realize resource sharing. In this way, students not only keep their English reading learning on the surface but also enable students to achieve deep learning in their college English reading learning. The process of the mixed teaching mode is shown in Figure 5.

As shown in Figure 5, the blended teaching model is that teachers allow students to study, discuss, and communicate online before and after class and then use traditional teaching methods in the classroom. Online and offline courses cannot be paralleled at the same time.

*2.3. Hybrid Teaching Mode Based on Intelligent Wireless Communication Multimedia.* Online teaching needs to use the multimedia technology we mentioned above; so, the intelligent multimedia classroom provides equipment support for the hybrid teaching mode. In the smart multimedia classroom, students can equip a multimedia device in the classroom to collect information about the content of the classroom teacher's explanation online. Then, the students integrate and understand by themselves, and then the teacher can let the students share the information they collect with the classmates, so that the dominance of the students in the classroom can be realized, and the students can also participate in the entire classroom independently. The process of mixed teaching mode under intelligent multimedia is shown in Figure 6.

As shown in Figure 6, in the hybrid teaching mode of the intelligent multimedia classroom, teachers only need to run out the topic of this English reading course before class. Then, students can use the multimedia equipment in the

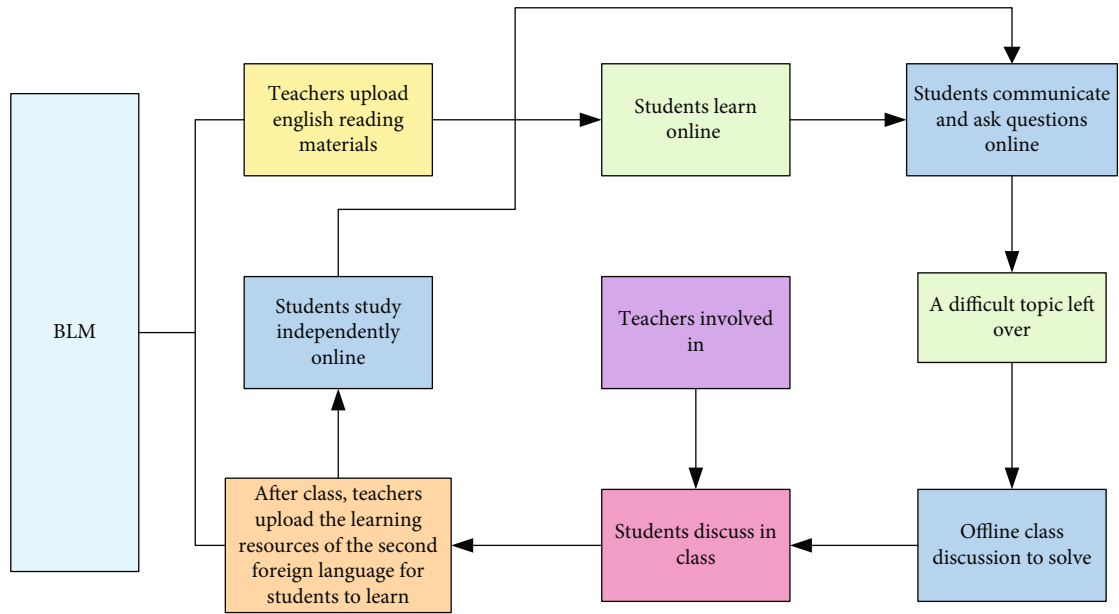


FIGURE 5: Mixed teaching mode process.

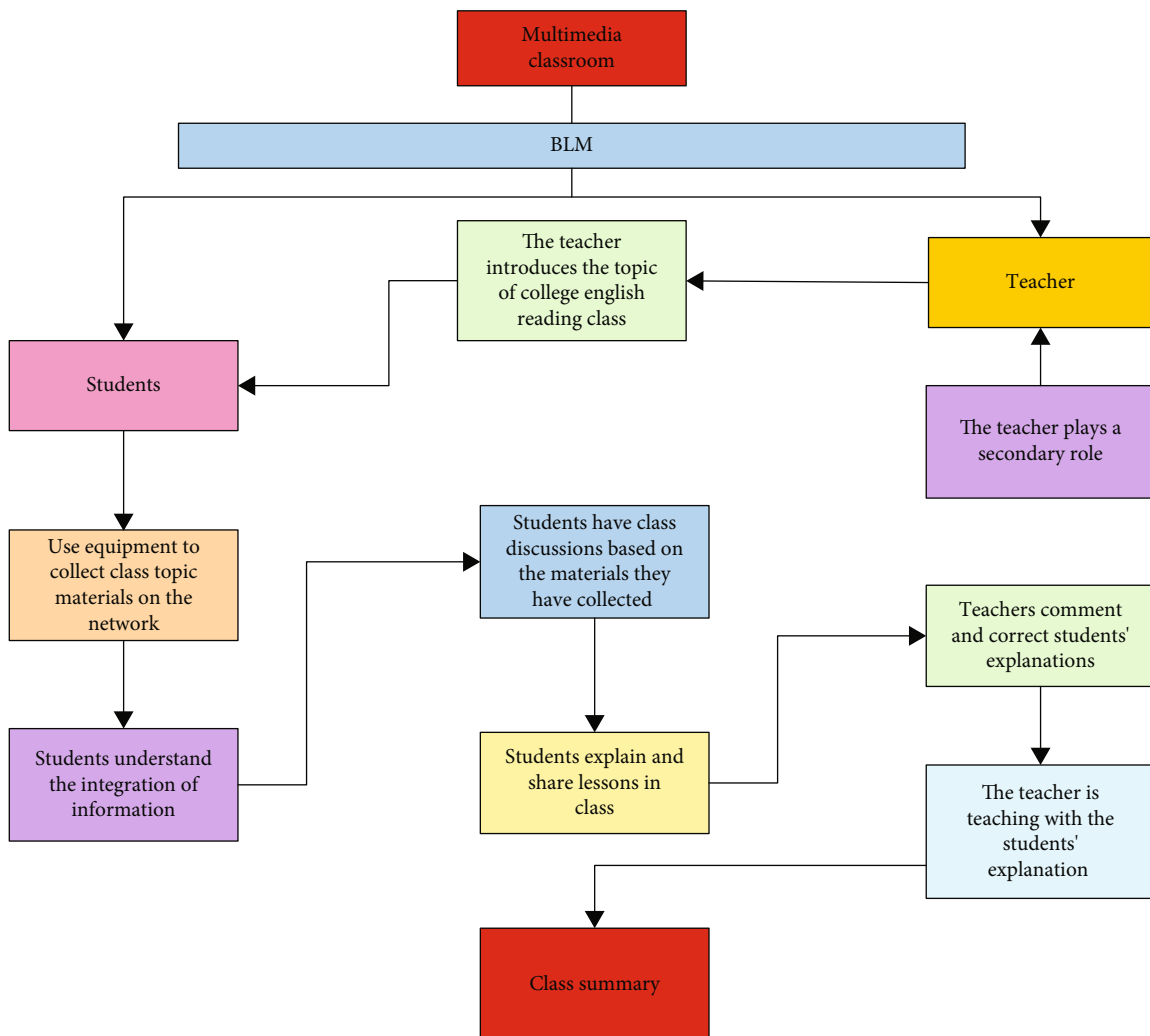


FIGURE 6: The process of mixed teaching mode under intelligent multimedia.

classroom to search for relevant materials through the wireless network according to the theme. Because college students are individuals who already have independent consciousness, their own understanding of the curriculum is also different. After the students find and discuss the materials in the classroom, they will explain the content by themselves on the podium. The teacher only needs to listen carefully to the students' explanation and then comment on the students' performance and correct the inappropriate places that the students have said. In this way, students can play their main role in the classroom and exercise their innovative consciousness and independent learning ability [19]. Then, the teacher can further deepen the class based on the students' understanding and the teaching content prepared by himself and finally make the same summary. This teaching mode can promote students' learning from shallow to deep and realize students' deep learning of English reading courses.

In addition, the blended teaching model not only realizes the blending of online and offline courses of college English reading courses but it can also realize the blending of teaching resources and the blending of evaluation methods [20]. The hybrid teaching mode can integrate various learning resources. As shown in Figure 6, students can freely use multimedia and wireless networks to find learning resources for English reading courses, enhance the interoperability of resources on the same platform and different platforms, and improve the utilization rate of English reading learning resources. The evaluation method of blended teaching is different from that of traditional teaching. Blended teaching can evaluate the results of students' learning, as well as the process of students' learning, so that it will be more fair and just [21–23].

With the development of wireless networks, many online courses for college English reading are also appearing one after another. It can learn only with electronic devices. Therefore, teachers use multimedia classrooms in the classroom, and after class, they can also arrange some content for students to learn online and ask questions and exchange learning experiences on the online platform. In addition, in order to ensure students' extracurricular learning of English reading courses, the students' academic performance recorded on the online background can also be included in the final assessment, and the students' assessment results can be evaluated in an all-round way. For example, our MOOC platform will record students' study time in the background, launch intelligent online tests to consolidate students' knowledge points, and make intelligent assessments of students' learning situation every time they study. Based on multiple forms of objective, fair, comprehensive, and systematic mixed assessments, the online platform can feed back the learning results to students in a timely manner, so that students can understand their deficiencies in English reading and learning, and they can also clarify their own advantages in this course. Therefore, they can improve their own shortcomings in a targeted manner and clarify their strengths in the English reading course. Combining the two, learners can choose a learning method that is more suitable for them, so as to enhance their motivation and confi-

dence in learning, and improve their enthusiasm and initiative in learning.

Therefore, modern education must make full use of wireless networks and multimedia equipment, broaden students' horizons, change the traditional teaching mode, and let students have a sense of participation in the classroom, so as to stimulate their enthusiasm for learning English reading courses. Especially for college English reading courses, the teachers' teaching concepts and the leading role in the classroom are changed, and the students' main role in the classroom is fully stimulated, so that students have a sense of classroom participation, so as to stimulate their enthusiasm for English reading and learning. In this way, the education quality and level of college English reading courses can be comprehensively improved.

### 3. Experiment and Analysis of Intelligent Multimedia and Hybrid Teaching Mode on College Students' English Reading Teaching

*3.1. Experimental Design.* In this experiment, three classes with the same number of students and majors will be selected in a college. These three classes are the first, second, and third classes of English translation for juniors, and these three classes are all taught by the same teacher, with a total of 20 students in each class. In this experiment, the teacher explained the reading article First Inaugural Address by John F. Kennedy in the Advanced English textbook. Teachers will use different teaching methods to teach, one class uses a combination of intelligent multimedia and hybrid teaching methods, the second class uses a mixed teaching method, and the third class uses a traditional teaching method.

This experiment will compare three classes of students' mastery of the knowledge points of this English reading article and changes in students' learning abilities, students' participation in class, and the participation of each class in group cooperative learning. Of course, in order to better compare the changes in the teaching situation of these three classes before and after the implementation of different teaching modes, before the experiment, we learned about the teaching situation of the three classes, as shown in Table 1.

From Table 1, the teaching levels of the three classes are relatively close, the teaching effectiveness of the teachers is not very high, the outstanding rate of the students in the class is relatively low, and the students' classroom participation and enthusiasm for learning are relatively low.

#### 3.2. Experiment and Analysis

*3.2.1. The Mastery of the Knowledge Points of the Students in the Three Classes.* Dividing the three classes into four groups with five people in each group, after the teaching is over, the students will be tested uniformly and then compare the average scores of the five students in each group to compare the three classes' mastery of the knowledge points of this text. Then, the average score of each group in the three classes is shown in Table 2.

TABLE 1: Teaching situation.

Class	Proportion of excellent grades	Proportion of students with good grades	Student participation in class	Students' learning enthusiasm	Teacher's teaching effectiveness
First	25%	86.6%	40%	45.75%	47.45%
Second	30%	85.7%	35%	42.3%	46.43%
Third	25%	86.6%	45%	43.45%	48.12%

TABLE 2: Average results of the group.

Class	Study groups	The average scores
First	1	87.6
	2	88.4
	3	82.4
	4	79.8
Second	1	82.5
	2	77.6
	3	76.5
	4	68.9
Third	1	77.5
	2	72.6
	3	71.4
	4	66.5

It can be seen from Table 2 that the average score of each group in a class is higher than that of his two classes. Among them, the average scores of three groups reached excellent, while only one group of the second class reached excellent, and the average scores of the third group were basically at a good stage. Therefore, it can be seen that the teaching method of a class using intelligent multimedia combined with a hybrid teaching mode can enable students to master the knowledge points of this article. The test results are stronger and better than the other two classes. However, the test scores of the students in the third class using the traditional teaching method are obviously inferior to those of the students in the first and second classes. It can be seen that the knowledge points are not very solid, and the ideal teaching effect has not been achieved.

*3.2.2. Comparison of the Influence of Different Teaching Modes.* In the classroom, we observed the students' participation in the classroom learning of this text and deeply understood the sense of classroom participation of the students in the three classes. The results are shown in Figure 7.

Judging from Figure 7, the overall sense of class participation in class one is relatively good, reaching 93%, while class two is slightly inferior. The proportion of class participation in class reaches 79.42%, only 67.7% of the students in the third class participated in the class. From the perspective of the group situation, the group of class one is the most active to participate in class discussion, the group of class two is slightly inferior, and the group of class three is not very active in participating in class discussion.

In addition, we also conducted in-depth exchanges with students in three classes. The students in class one said that

the use of a hybrid teaching model in intelligent multimedia teachers gave us more sense of participation. They can collect a lot of information about this article from the Internet, discuss it, and share it on stage, making the study of this article more in-depth. The students who adopt the blended teaching model said that they will study online before class, but the effect of online learning is not very good. Because in the offline class, teachers still lecture on the podium. They just take the stage to teach what they learn online step by step, and there is not much discussion among students. The students in class 3 said that they only need to listen to the teacher's lecture on stage, copy notes, and review the notes when they have time after class. They do not feel that they are in class at all, and they just passively receive knowledge. The comparison of all aspects of the three classes and the comparison before and after the implementation of the intelligent multimedia classroom combined with the hybrid teaching mode in the first class are shown in Figure 8.

The comparison before and after the implementation of the mixed teaching mode in the second class and the comparison of the autonomous learning ability of the students in the three classes are shown in Figure 9.

It can be seen from Figure 8(a) that the teaching situation of class one is better than the other two classes. Although the proportion of students in class three with good grades is higher than that in class two, class two is in excellent grade. The proportion of students in the school has increased significantly compared with the original, and it is also 25% higher than the excellent rate of the third class. Looking at the comparison of a class before and after the implementation of the new teaching model in Figure 8(b), it can be clearly seen that after the implementation of the new teaching model, all aspects have improved, especially in the excellent rate, which has increased by 45%, classroom teaching efficiency has also increased by about 50%, and students' sense of participation is stronger than before. Looking at the comparison of the changes before and after the implementation of the mixed teaching model in the second class from Figure 9(a), it can be found that the excellent rate of the second class students has increased. However, the ratio of the good stage has dropped, but the overall teaching effect has risen, and all other aspects have risen. From Figure 9(b), the learning ability of the students in the first class is greatly improved, and the learning ability of the students in the second class is slightly inferior to that of the first class, but the learning ability of the students in the third class is not significantly improved.

*3.3. Experiment Summary.* A series of experiments show that the combination of intelligent multimedia and hybrid

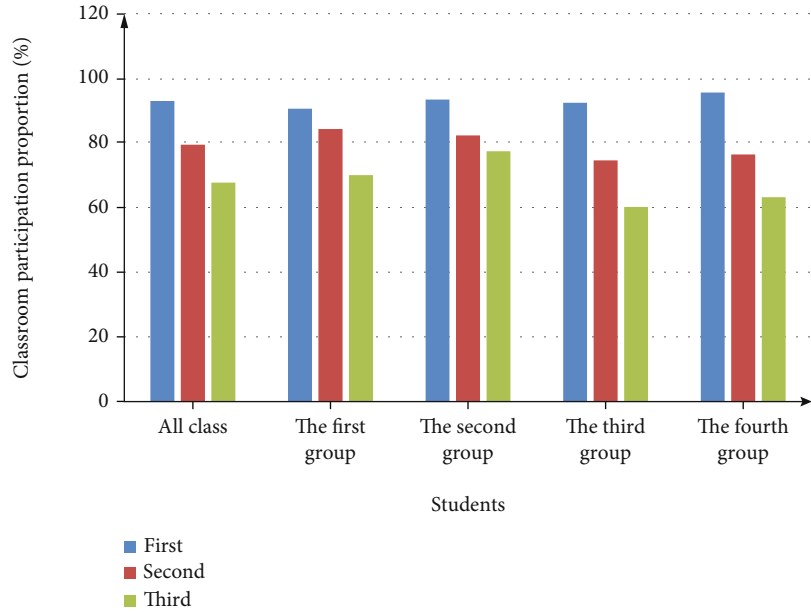
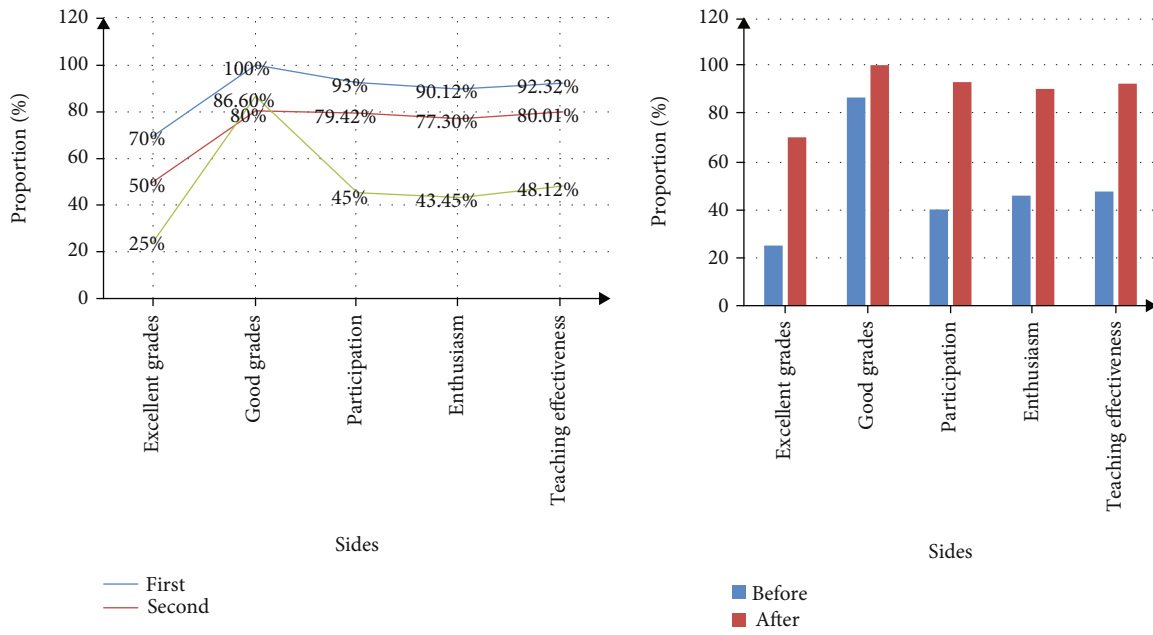


FIGURE 7: Student participation in class.



(a) Comparison of all aspects of the three classes

(b) Before and after comparison of each class in the first class

FIGURE 8: Comparison of all aspects.

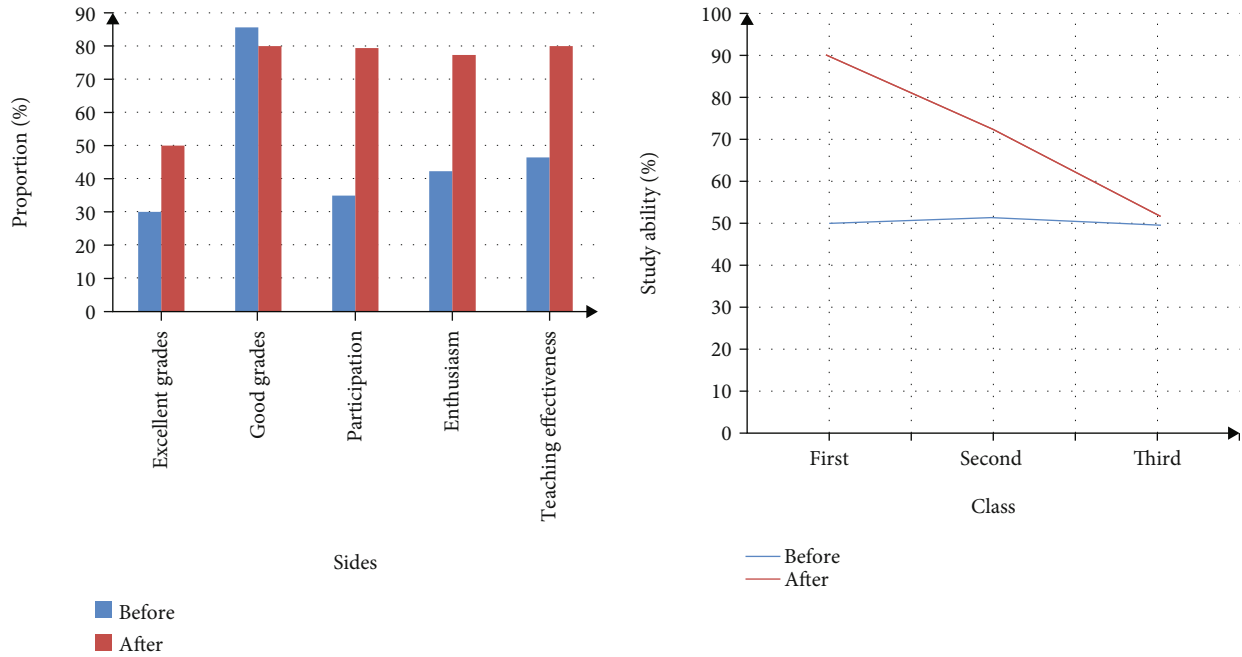
teaching mode has great effects on students' teaching and can improve the teaching efficiency and teaching level of college students' English reading courses. From the perspective of the performance, teaching effectiveness, and improvement of students' learning ability in the three classes in the experiment, the improvement of the class that implements the intelligent multimedia combined with hybrid teaching mode is the most obvious. Therefore, it can be found that the combination of intelligent multimedia and hybrid teaching mode is beneficial to improve college students' interest in college English reading courses and promote students' par-

ticipation and sense of participation in English reading classes. It can also improve students' teaching ability and self-learning enthusiasm and let students learn how to use wireless networks to improve college English reading courses.

#### 4. Discussion

This article first discusses the intelligent wireless network and multimedia technology, fully discusses the application of wireless network and multimedia in the field of education, and then proposes to combine the two to propose an





(a) Comparison before and after the second class (b) Changes before and after the learning ability of students in each class

FIGURE 9: Before and after comparison of all aspects.

intelligent multimedia classroom. Compared with traditional classrooms, intelligent multimedia classrooms have more modern equipments. These equipments can search for learning resources in the classroom through wireless networks, so as to fully provide students with learning resources on various network platforms. After that, this article discusses the promotion and implementation of the mixed room teaching model in the education field, which improves the enthusiasm of students and the teaching level of teachers. This article describes the mixed teaching mode, which provides a theoretical basis for the following teaching methods that combine intelligent multimedia and mixed teaching mode.

The proposal of implementing a hybrid teaching model in intelligent multimedia classrooms proposed in this paper can give full play to students' subjective initiative in college English reading courses and at the same time can fully stimulate students' interest in English reading courses. Students can give full play to the main role of students in the classroom, allowing them to integrate their own resources in the classroom and then teach themselves at the podium. Teachers can comment and correct the content of the students' lectures and play an auxiliary role. Under this new teaching model, students can find various college English reading materials on the Internet in the classroom and discuss and share them in the classroom, allowing teachers to comment and correct in time, effectively improve teaching effectiveness, and introduce students to deep learning in college English courses.

The experiments in this article show that this new teaching model not only combines the advantages of modern science and technology but also fully combines the advantages of traditional teaching methods. This new teaching model

has more advantages than the traditional blended teaching model. In addition to online learning outside of class, students can also perform in-depth learning in the classroom, which can fully stimulate students' enthusiasm for learning and improve students' performance and independent learning ability. In addition, teachers' teaching concepts can be changed. Teachers and teachers fully consider the main role of students in the classroom, so that teachers are more inclined to adopt mixed teaching methods with the help of multimedia classrooms.

### 5. Conclusions

This article discusses the application of the hybrid teaching mode in the English reading teaching of college students under the background of intelligent wireless communication multimedia. First, the intelligent wireless communication network and multimedia technology are combined. Next, intelligent multimedia is proposed, which allows college English reading courses to implement a hybrid teaching mode in intelligent multimedia classrooms. Experiments show that this new teaching model is more suitable for college English reading courses, can fully stimulate students' interest and enthusiasm for college English reading courses, improve the teaching efficiency and teaching level of college English reading courses, and change teachers' traditional teaching concepts and the traditional teaching methods of teachers. Therefore, the implementation of the hybrid teaching mode under the background of intelligent multimedia has great practical significance for the teaching of college English reading courses. However, what this article is studying is a blended teaching model in college English reading courses. It is hoped that the teaching of more subjects can

be involved in future research, and the teaching level and quality of the entire education sector can be improved.

## Data Availability

Data sharing is not applicable to this article as no new data were created or analyzed in this study.

## Conflicts of Interest

The author states that this article has no conflict of interest.

## References

- [1] Y. Zhang, "An empirical study on computer network flipped classroom teaching model in college english learning," *CeCa*, vol. 42, no. 5, pp. 2227–2231, 2017.
- [2] Q. Sun, "The application of "Yunban class" for college English based on blended teaching mode," *Sino-US English Teaching*, vol. 16, no. 11, 2019.
- [3] Y. Ma, "The application of schema theory in the teaching of English reading in senior high schools," *Region - Educational Research and Reviews*, vol. 3, no. 3, pp. 17–20, 2021.
- [4] X. Ge and X. Zhang, "Research on the application of eap mode in Chinese college english teaching," *Boletin Tecnico/Technical Bulletin*, vol. 55, no. 11, pp. 157–163, 2017.
- [5] H. Yeon, "Roles of receptive and productive vocabulary knowledge in L2 writing through the mediation of L2 reading ability," *ENGLISH TEACHING*, vol. 72, no. 1, pp. 3–24, 2017.
- [6] S. Jung, "Extensive reading through collaborative approach," *The Journal of Mirae English Language and Literature*, vol. 22, no. 2, pp. 295–320, 2017.
- [7] L. Zhang, "The application of online and offline hybrid teaching mode in college physics classroom," *Creative Education Studies*, vol. 9, no. 2, pp. 451–455, 2021.
- [8] M. A. Hoque, J. Rios-Torres, R. Arvin, A. Khatkhat, and S. Ahmed, "The extent of reliability for vehicle-to-vehicle communication in safety critical applications: an experimental study," *Journal of Intelligent Transportation Systems*, vol. 24, no. 3, pp. 264–278, 2020.
- [9] O. A. Saraereh, L. Al-Tarawneh, and A. Ali, "Design and analysis of a novel antenna for THz wireless communication," *Intelligent Automation and Soft Computing*, vol. 31, no. 1, pp. 607–619, 2022.
- [10] C. Yuen, G. C. Alexandropoulos, X. Yuan, M. D. Renzo, and M. Debbah, "IEEE TCCN special section editorial: intelligent surfaces for smart wireless communications," *IEEE Transactions on Cognitive Communications and Networking*, vol. 7, no. 2, pp. 336–339, 2021.
- [11] Y. Qi-Yue, "intelligent radio for next generation wireless communications: an overview," *Wireless Communications, IEEE*, vol. 26, no. 4, pp. 94–101, 2019.
- [12] Y. Yuejue, S. Xinze, L. Bingyue, and X. Wang, "Construct a teaching system combining image linguistics and multimedia technology," *Wireless Communications and Mobile Computing*, vol. 2021, Article ID 6699010, 11 pages, 2021.
- [13] D. Xin, "Application value of multimedia artificial intelligence technology in English teaching practice," *Mobile Information Systems*, vol. 2021, Article ID 3754897, 11 pages, 2021.
- [14] Y. Niu, "Penetration of multimedia technology in piano teaching and performance based on complex network," *Mathematical Problems in Engineering*, vol. 2021, Article ID 8872227, 12 pages, 2021.
- [15] K. Dong, "Multimedia pop music teaching model integrating semifinished teaching strategies," *Advances in Multimedia*, vol. 2022, Article ID 6200077, 13 pages, 2022.
- [16] Y. Lu and W. Lizhi, "Construction of multimedia assisted legal classroom teaching model based on data mining algorithm," *Scientific Programming*, vol. 2021, Article ID 9948800, 11 pages, 2021.
- [17] P. K. Sahoo, Y. K. Prajapati, and R. Tripathi, "PPM- and GMSK-based hybrid modulation technique for optical wireless communication cellular backhaul channel," *IET Communications*, vol. 12, no. 17, pp. 2158–2163, 2018.
- [18] T. Ernest, A. S. Madhukumar, R. P. Sirigina, and A. K. Krishna, "Hybrid-duplex communications for multi-UAV networks: an outage probability analysis," *IEEE Communications Letters*, vol. 23, no. 10, pp. 1831–1835, 2019.
- [19] S. H. Won, S. S. Jeong, and S. Y. Cho, "Method and apparatus for managing congestion in wireless communication system," *Dental Traumatology*, vol. 17, no. 2, pp. 93–95, 2018.
- [20] N. Dey and V. Santhi, "Studies in Computational Intelligence," in *Intelligent Techniques in Signal Processing for Multimedia Security Volume 660 || StegNmark: A Joint Stego-Watermark Approach for Early Tamper Detection*, pp. 427–452, 2017.
- [21] I. Butun, P. Österberg, and H. Song, "Security of the Internet of Things: vulnerabilities, attacks, and countermeasures," in *IEEE Communications Surveys & Tutorials*, vol. 22, no. 1, pp. 616–644, 2020.
- [22] O. I. Khalaf and G. M. Abdulsahib, "Frequency estimation by the method of minimum mean squared error and P-value distributed in the wireless sensor network," *Journal of Information Science and Engineering*, vol. 35, no. 5, pp. 1099–1112, 2019.
- [23] X. Li, H. Jianmin, B. Hou, and P. Zhang, "Exploring the innovation modes and evolution of the cloud-based service using the activity theory on the basis of big data," *Cluster Computing*, vol. 21, no. 1, pp. 907–922, 2018.

## Research Article

# A Federated Deep Learning Empowered Resource Management Method to Optimize 5G and 6G Quality of Services (QoS)

Hemaid Alsulami <sup>1</sup>, Suhail H. Serbaya,<sup>1</sup> Emad H. Abualsauod <sup>2</sup>, Asem Majed Othman,<sup>3</sup> Ali Rizwan <sup>1</sup> and Asadullah Jalali <sup>4</sup>

<sup>1</sup>Department of Industrial Engineering, Faculty of Engineering, King Abdulaziz University, Jeddah 21589, Saudi Arabia

<sup>2</sup>Department of Industrial Engineering, College of Engineering, Taibah University, 41411, Madina Almonawara, Saudi Arabia

<sup>3</sup>Department of Industrial and Systems Engineering, College of Engineering, University of Jeddah, Jeddah 21959, Saudi Arabia

<sup>4</sup>American University of Afghanistan, Kabul, Afghanistan

Correspondence should be addressed to Asadullah Jalali; [ajalali@auaf.edu.af](mailto:ajalali@auaf.edu.af)

Received 11 January 2022; Accepted 9 February 2022; Published 23 March 2022

Academic Editor: Shalli Rani

Copyright © 2022 Hemaid Alsulami et al. This is an open access article distributed under the Creative Commons Attribution License, which permits unrestricted use, distribution, and reproduction in any medium, provided the original work is properly cited.

The quality of service (QoS) in 5G/6G communication enormously depends upon the mobility and agility of the network architecture. An increase in the possible uses of 5G vehicular network simultaneously expands the scope of the network's quality of service (QoS). To this end, a safety-critical real-time system has become one of the most demanding criteria for the vehicular network. Although different mathematical and computation methods have traditionally been used to optimize the allocation of resources, but the nonconvexity of optimization issues creates unique type of challenges. In recent years, machine learning (ML) has emerged as a valuable tool for dealing with computational complexity that involves large amounts of data in heterogeneous vehicular networks. By using optimization and cutting-edge machine learning techniques, this article gives readers an insight about how 5G vehicular network resources can be allocated to reinforce network communication. Furthermore, a new federated deep reinforcement learning- (FDRL-) based vehicle communication method is presented as a new insight. Finally, a UAV-aided vehicular communication system based on FDRL-based UAVs is proposed as a novel resource management technique to optimize 5G and 6G quality of services.

## 1. Introduction

Nowadays, it is imperative to develop a robust 5G new radio (NR) system [1] because of exponential increase in cellular mobile devices and automobiles. On one hand, people's lives are improved in a variety of ways due to wide range of applications, but on the other hand, the required quality of services (QoS) also need to be ensured. In this regard, optimization of resources like computing power, sum-rate maximization, and delay minimization has been the focus of optimization problem formulations [2, 3]. Meanwhile, simple convex optimization also suffices as one of the basic scenarios to fulfil these aims. It is observed that wireless resource management issues tend to be nonconvex and polynomial, thus creating unique type of challenges. Due to complexity of mathematical calculations, it is difficult to find

algorithms that are effective or powerful enough to reach suboptimal locations. Although the vehicular network increases the range of new services and mobility options, still producing a massive volume of data that is difficult to comprehend. To address these problems, new and more powerful methods of calculation are required. In addition, the DRL algorithm may be used without sharing the vehicle's dataset via federated deep reinforcement learning, besides eliminating the delay issues. As a flying BS in vehicle networks, drones are utilized to ensure that all vehicles are continually connected. An FL technique, specifically a UAV-aided vehicular network proposed FDRL approach, to improve connection and minimize latency is also being studied. Proposals have also been made for an FDRL-based vehicle communication system. As a flying BS in-vehicle network, drones are utilized to ensure that all vehicles are

continually connected. All vehicle-to-vehicle, infrastructure (V2I), and other interconnections like 5G heterogeneous vehicle networks are included in this concept (V2X) as shown in Figure 1.

Vehicle-to-vehicle (V2V) communication (SRC) channels are known as DSRCs (dedicated short-range communication). It is possible to expand the variety of services available to VUEs by using macro-BSs and RSUs in conjunction with a cellular vehicular network. In space, satellite communications and air-to-air communications commonly take place in which exchange of data and information is carried out. For UAVs to communicate with each other, they must fly lower in the sky. Communicating with planes and with the ground is the primary function of these unmanned aerial vehicles (UAVs). For heterogeneous 5G and 6G vehicle networks, the requirements for quality of service (QoS) have increased. For ultrareliable and low-latency connectivity, 5G NR supports a wide variety of new QoS criteria. Data sent and received by machines is referred to as massive machine-type communications (mMTC) and mobile broadband (MBB). Similarly, in case of dependability, the URLLC service requires an end-to-end (E2E) latency of one millisecond (ms) and can support up to one million devices per square metre (km<sup>2</sup>).

## 2. Historical Background

A machine learning technique known as “deep reinforcement learning” (DRL) is used to train computers to learn, in which reinforcement learning (RL) and deep learning (DL) are part of it (DL).

*2.1. Reinforcement Learning.* Sequential decision-making can be addressed by limiting the reward when dealing with an unfamiliar environment. Because it does not require many datasets to train, the method is well-suited for use in 5G and 6G vehicle networks, which have more dynamic environments [4, 33]. In this regard, an agent is a person or organisation that performs a task for compensation. Consequently, the agent’s activities take place in the physical world. Whenever an agent interacts with the environment, it is presented with a representation of the environment’s current state. In this way, a list of activities is selected by an agent. After completing the task, the agent is given a prize. Q-learning is a popular algorithm in the field of reinforcement learning. Kisacanin has highlighted the way to calculate the reward value, which is  $Q$ , while the learner’s rate is one, and the discount factor is also one [5]. The letter “ $r$ ” denotes the award.

*2.2. Extensive Education and Training.* Deep learning (DL) is based on artificial neural networks (ANNs), which are also known as “deep networks” (ANN); a completely linked deep network is shown in Figure 2.

Neuron cells in the deeper layers of a densely coupled network are known as LSTM cells in this paradigm. Deep Q-learning makes use of DL networks (e.g., RNN models) to estimate the  $Q$  value. Inputs to a DL network can include, for example, the states’  $S$  and  $Q$  values of all potential

actions. Fully connected neural networks (FCNNs) are artificial neural networks whose architecture connects all nodes (neurons) in one layer. CNNs are trained to find and extract the best characteristics from photos. Their primary asset and the classifier strength of a CNN’s last layers connect them all. As CNNs integrate FC layers, these two topologies are not competitors. Unconnected convolutional layers are substantially more specialised and efficient. Fully linked layers have connections to all preceding layers, and each connection has its own weight. It is just feed forward neural networks. Fully connected layers are the network’s final layers. The final pooling or convolutional layer output is flattened and fed into the fully connected layer.

## 3. QoS Requirements in 5G and 6G Mobile Networks

*3.1. Service Excellence Requirements.* A 5G vehicle network large mMTC (machine-to-machine communications) is one of the three categories that 5G is planned to include, along with ultrareliable, low-latency connectivity (URLLC). The V2X application scenario is defined in the new 5G V2X service standard. Some of the more advanced uses include vehicle platooning and remote driving. The 5G network is built on top of the 4G network. In information-centric networks, the notion of a packet data unit (PDU) session was born.

Each PDU session has many Qualities of Service (QoS) flows. The granularity of a PDU session’s QoS distinction is described here. In most situations, QoS metrics are specified by a set of parameters like PER (percent) and GMB (kps). PER stands for the percentage of packets that fail to arrive at their destination. Vehicle platooning services must meet E2E latency norms of 10 ms and be 99.99% reliable. Advanced driving services necessitate larger bandwidth and reduced E2E latency, whereas ordinary driving services necessitate higher dependability and a bit rate of up to one gigabit per second. Figure 3 shows the model that is an operation on edge computing, and fog computing is also playing a very important role in the process of calculation of fog in the cars.

The physical infrastructure is identical to that used by the MVNOs (mobile network providers) (MNO). Queue length distributions are modelled using the extreme value theory (EVT). A method known as the maximal likelihood estimate (MLE) is employed to ascertain this information. To reduce signalling overheads, a distributed FL is utilized. Transmissions at an optimal power level remove the backlog to improve vehicle-to-vehicle communication system that lowers signalling costs while maintaining high reliability and low latency [6]. The distribution of resources in area of information (AoI) is discussed. If the volume of data grows too large, it might create an issue of information piracy. This research examines the trade-off between growing network knowledge and lowering AoI over a particular threshold. To predict the future of AoI, a Gaussian process regression (GPR) is applied. It is observed that unsupervised learning performs well in the dynamic vehicular network,

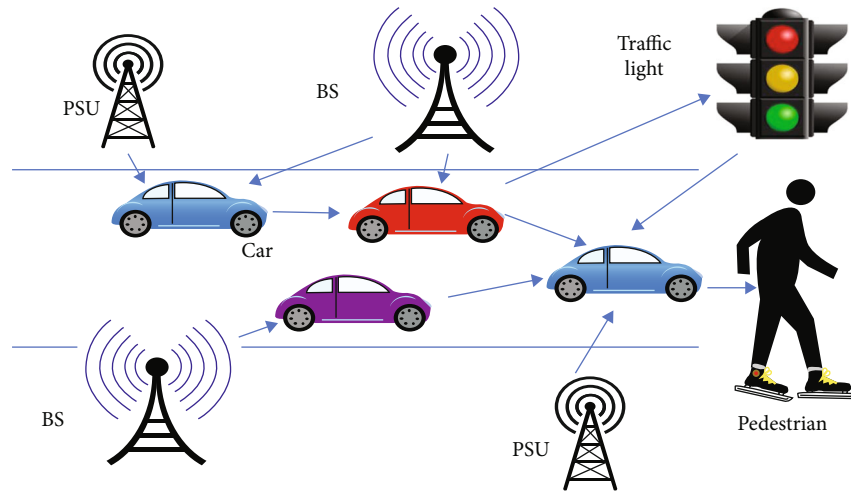


FIGURE 1: A 5G heterogeneous vehicular network.

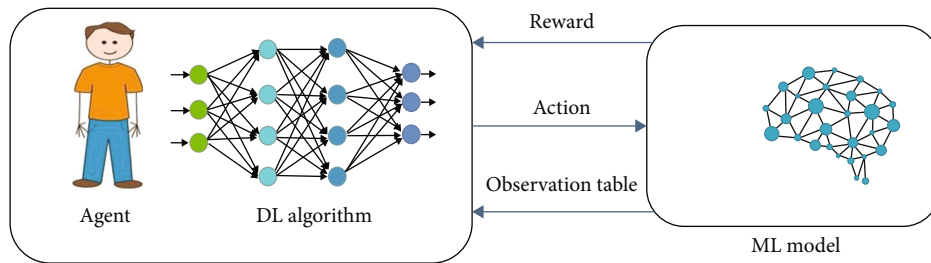


FIGURE 2: A completely linked deep network.

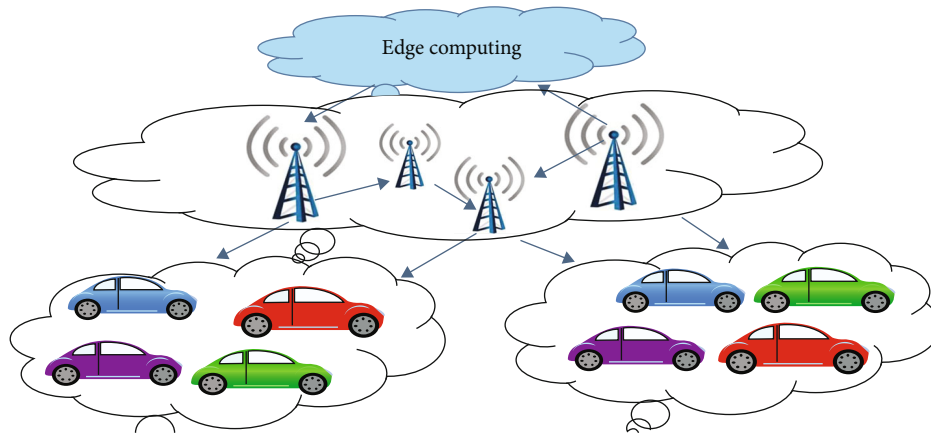


FIGURE 3: A computer model for calculating fog in a car.

which is a good thing, but the training data for ML models is challenging to collect especially in dynamic situations.

A DRL approach represents optimal resource allocation, which is used to provide safe and secure vehicle communication. These challenges are interwoven with vehicle network spectrum and computation power allocation challenges. Then, the optimum solution is found using a combination of single-agent and multiagent RL. Low-latency communication might be problematic due to high latency and security

and privacy problems. Using a fog computing network helps lower the latency of cloud computing networks for cars.

Fog computing is a subset of fog networking. There are fog servers that can execute calculations and store resources in place of cloud servers. It provides service to a wide range of different and scattered devices. Fading computer networks are seen in Figure 4. The other option is to connect RSUs and BSs to fog computing servers through wired transmission. Fog servers are more convenient for end users than

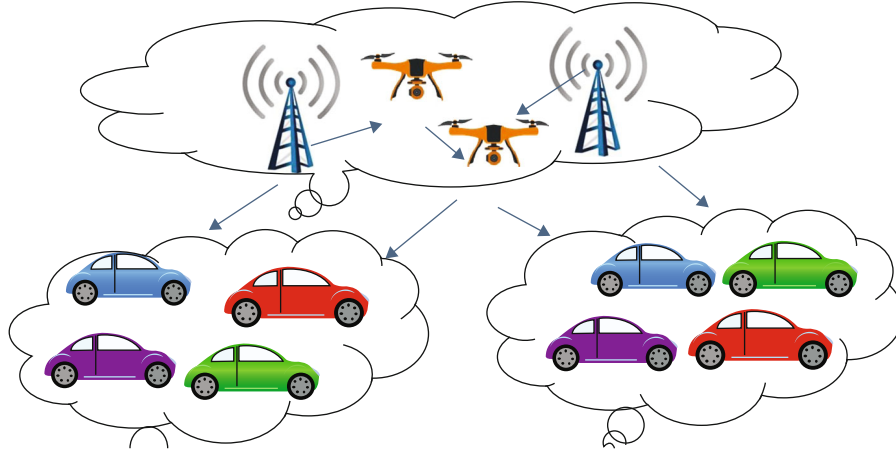


FIGURE 4: UAV-assisted vehicular communication model.

cloud servers (e.g., VUEs). When compared to cloud computing, this speeds up the transmission of data. This strategy reduces the time it takes to respond to end VUEs, especially during busy periods [7].

**3.2. Theories and Applications of Optimization.** A combined optimization examines user association, radio resource allocation, and power consumption. It describes a cloud and fog network cross-computing layer as a technique of assigning computing resources to clouds and fog. It controls traffic signal and traffic management on a global scale. Contract-based incentives and matching-based computation work assignments [8] will also be implemented. Fog computing vehicle networks may be established without orthogonal multiple access, or NOMA, according to the proposed design [9, 10]. There is also the possibility of using RL to address the issue of user mobility. Two methods used to optimize the subchannel and power allocation: CRO and RCCRO (real-coded chemical-reaction optimization). Researchers integrate user association with resource allocation [11]. The joint optimization problem is solved using a mixed-integer nonlinear algorithm. The Perron-Frobenius theory helps minimize transmission delays. The mentioned study also incorporates resource allocation and distributed computation offloading to allow vehicle networks [12]. Joint optimization is a nonconvex and NP-hard issue that might be solved by outsourcing computing tasks to dispersed computers and allocating resources accordingly (CCORAO). As a result, both the communication time and the utility of the system are improved [13]. The DNN method, on the other hand, is limited to short-term predictions of traffic flow. Having additional information about traffic patterns helps the network system to improve distribution of resources. The LSTM algorithm has been used to develop a time-series traffic flow prediction technique [14]. The LSTM may be used to depict both short-term and long-term traffic flow projections. As a result, gathering of data with a purpose to train the ML model is a huge undertaking. Because missing of data makes it impossible for the machine learning system to accurately anticipate traffic flow. As a result,

resources are being preallocated incorrectly. For both autos and network infrastructure, radio resources are ineffective.

For traffic flow prediction with lacking data, an LSTM approach is proposed in this study. The missing data is dealt with using multiscale temporal smoothing. It uses an LSTM-DNN algorithm [15], which predicts traffic flow and parking conditions. The data on traffic has been used to allocate resources for vehicular fog communication throughout the short- and long-term future (VFC). To allocate spectrum across automobiles, RSUs analyse the forecasted data and utilize it as a guide. Data transmission and computation times are reduced by this suggestion. As stated in the study, the RL-based radio resource allocation algorithm proposed in the study takes the network's future state into consideration as specified in the study [16]. This choice is also influenced by future network circumstances. The agent's compensation is maximized based on predicted outcomes. In terms of throughput, the results are better than the vehicle network. Packet loss has also been reduced to a minimum. As previously stated, learning methods can be used for both supervised and unsupervised learning. Various ways can be used to reduce latency. Obtaining training data in a diverse vehicular network is quite tough. Because of this, DRL is being used to deal with this problem. An algorithm called DRL has been developed to address this issue.

The optional QoS level measurement equals the number of mapped 5QIs. This statistic indicates the proportion of unconstrained DL data volume for UEs in the cell, i.e., when all data can be transported in one slot and no UE throughput sample can be determined. To calculate the UE data volume, multiply the number of primary carriers by the number of supplementary carriers. The measurement can be subdivided by QoS level. Wireless transmission bandwidth and predicted vehicle power contribution are explored in depth in the work [17]. Markov decision process (MDP) models demonstrate the incorporation of processing and storage capacity in a comparable situation [18]. Perception-reaction time refers to the length of time it takes for a driver to react in a safe manner. This research examines the integration of fog resource virtualization (FRV) with

information-centric networking (ICN). Deep neural networks are employed in combination with an actor-critic (A3C) (DNN) to maximize the utilization of computing resources.

Similarly, fog node is helpful for mobile customers, it supports different operations in varied scenarios [19]. In the current world, a car's mobility is a significant feature. Choosing the optimal fog node for clients is an important consideration. This study offers an effective allocation of resources to cars so that they can better serve their customers. Once the problem is solved, the nondominated sorting genetic algorithm is applied. MDP was first proposed as a tool for making resource decisions [20]. In order to better understand fog computing, researchers are looking at SDV-F (software-defined vehicular-based fog computing). Consequently, a method known as DRL is used to shorten the amount of time it takes for fog servers to accomplish operations. BSs employ a wide range of mission-oriented strategies. Each BS has its own edge computing server. The vehicle network may benefit from edge computing since it is both long-term and cost-effective. To maximize fog layer processing capacity, this is done. Consequently, according to the article, a method known as DRL is used to shorten the amount of time it takes for fog servers to accomplish operations. BSs employ a wide range of mission-oriented strategies. Each BS has its own edge computing server. The vehicle network may benefit from edge computing since it is both long-term and cost-effective.

**3.3. Resource Allocation.** An adaptive and online resource allocation has been created to improve the user experience [21]. Communication loss can be reduced in a vehicular edge computing network. An examination of radio and computer resources has been initiated by the discovery of unknown network statuses. A mobility-aware greedy algorithm has also been studied [22].

These methods are effective in reducing latency and maximizing energy efficiency. Nonconvex and NP-hard optimization problems, on the other hand, are extremely challenging to solve [23]. Then, it is a real challenge to decipher them. This challenge was solved using a machine learning method. In this way, the complexity of a nonlocal computer system is minimized. If the QoS criterion in a vehicle network is not met, a distributed user association algorithm is being evaluated. By allocating radio resources intelligently, the network load may be balanced while latency is decreased. Furthermore, two game theories [24] were used to test the load balancing scheme's effectiveness. Within the limits of maximum allowable delays, the idea of reducing the processing time of vehicles is examined. An SDN-based task offloading system for FiWi (fiber-wireless interconnect) approaches is then developed. As a result, network performance is improved while latency is kept to a minimum. The radio resource management challenge for the 5G vehicle network is developed with an age of information (AoI) awareness [25]. An LSTM and a DRL are used to conduct online decentralised testing at the VUE pairings. It gives RSUs the ability to allocate bandwidth and make decisions about packet scheduling. Even though just a portion of the network's state can be viewed, this method nonetheless manages to maximize the efficient use of available resources

without requiring any prior knowledge of the network's dynamics. The DNN model incorporates a convolutional neural network (CNN) [26]. A rough approximation of the offloading scheduling strategy and value function is made using this technique. A DRL was then added.

DRLOSOM's goal is to reduce energy consumption while also maximizing the number of retransmitted activities and costs. Researchers are examining the ADMM, or alternate-direction method of multipliers. The algorithm is dispersed. Content caching and computation are made possible by information-centric heterogeneous network infrastructure. Users with diverse virtual services can share communication, processing, and caching resources on the intended network system. Also, in the work of [27], mobility-based approach VEC servers are used to do conscious task offloading.

Entry points are being investigated. But, when a server is overloaded, a second server can be assigned the overloading duty. In this manner, the processing and computing delays are decreased, while the vehicle's performance is improved. However, due to difficulties in obtaining the training data set, the DRL technique has been adopted.

Figure 5 shows the comparison of centralised and federated learning, in which a server-side machine learning method is employed in a distributed model. Data from VUEs is first processed and analysed by servers. It is found that machine learning methods are used at every level in distributed federated systems. VUEs also use server and ML techniques, where the only information sent to the server is information specific to the VUEs' local ML algorithms. As a result, privacy may be assured. A distributed machine learning model reduces latency and improves accuracy. On the other hand, FL is a distributed machine learning approach in which a shared model is trained by several vehicles. Instead of transmitting all the raw data to the central server, the vehicles just communicate the updated parameters of the common model to the central server using their own local data. This approach was used to reduce congestion in the transportation sector, where UAVs are being deployed [28]. In order to acquire information about their surroundings, imaginary automobiles are equipped with cameras and GPS systems. RSUs [29] receive the sensing data from the vehicles and relay it to the servers. The vehicle network can survive jamming attempts due to a hill-climbing UAV relay device. In this way, the utility of vehicle communication is increased by lowering the bit error rate. Moreover, energy-conscious dynamic power optimization for each vehicle's energy usage has been developed [30], in which the optimal dynamic power is found by examining vehicle collaboration and noncooperation while maintaining the privacy of the vehicle's information based on FL techniques [31, 32].

## 4. Methodology

Despite a lack of resources, the usage of multiaccess edge computing and software-based network services is developed to increase the diversity of traffic patterns using this strategy. 5G and 6G mobile network QoS standards are diverse and need further research to ensure that they can be met.

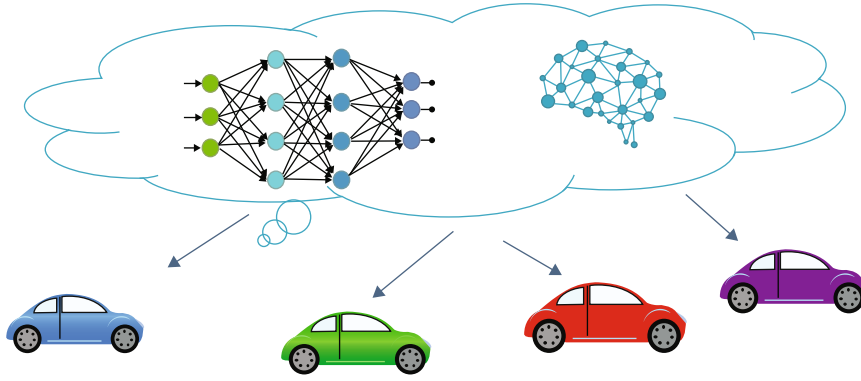


FIGURE 5: Improved federated deep reinforcement learning model.

1. The main server, at the start of the decision period  $t = 0$ , set the global DRL model  $Q_f$  to a random value of  $f = 0$
2. Vehicles owned and operated by the local community, local DRL models  $Q$  and  $N$  should be initialised to a value of  $n = 0$  for all of the models
3. Obtain a copy of  $f_0$  from the central server and set  $n$  to a value between 0 and 1
4. Initiate  $D$ 's replay memory, in each decision period  $t = 0$  to  $T$ , perform the following: the FLZ function calculation, vehicles owned and operated by the public:  
 $t > 0$  do while
5. for each car  $n$  in parallel, perform the following:  
 Get  $f_t$  from the controller.  
 In this case, let  $t \geq f_t$
6. On the present service requests  $Q_{nt}$ , train the DRL agent locally using  $n_{nt}$
7. upload the weights that have been trained to the central server
8. Receive all weight updates, not just the most recent ones execute federated averaging for this step.  
 Broadcast weights  $f_{t+1}$  averages
9. Until then, we are out of time

ALGORITHM 1: Improved FDRL method.

*4.1. Challenges, Unanswered Questions, and Future Directions.* SDN (switch function virtualization) and network function virtualization (NFV) are two terms used interchangeably. In 5G NR, there is a large-scale and diverse vehicle ad hoc network. Because of these features, ML algorithms cannot be used successfully. Network slicing and software-defined networking (SDN) have lately been proposed as solutions for the 5G automobile network. All kinds of various QoS services and heterogeneous networks are not an issue for this programme. With technologies such as SDN and NFV, it is possible to meet the QoS requirements of 5G NR, which depicts a multiaccess edge computing solution that addresses the demand for processing capacity, resource allocation, and storage capacity. A wide range of quality of service (QoS) demands may be met by the 5G vehicle network [31]. The 6G vehicle network features ultralow latency and high data transfer speeds, as well.

*4.1.1. Unmanned Aerial Vehicle Assistive Vehicle Cargo Network.* In today's more complex automotive environment and computing requirements, mathematical optimization methods have been around for a long time are not up to the task. For machine learning models, obtaining training data is a huge challenge because the vehicular network is always evolving. In the absence of data, a DRL approach

and training are required. The use of a DRL algorithm in the local training models of the end vehicles of 5G and 6G automotive networks is regarded as a potential option for reducing latency and enhancing privacy needs.

*4.1.2. Caching and FL Communication Technique.* End-user automobiles benefit from reduced computation and processing time due to MEC servers that use relevant FL techniques. BSs and RSUs have been discussed. MEC servers and eventually automobiles use DRL algorithms that have been trained to perform a specific task. Communication, processing, and caching strategies of the FL model must be thoroughly examined to increase network efficiency while preserving the heterogeneous QoS standards of the FL model.

The third aspect is the ability to share information with others. Cars, RSUs, BSs, drones, edge servers, and so on are all part of the vehicular network. Using the FL methodology, an effective resource allocation method for these heterogeneous devices must be investigated for 5G and 6G vehicle networks. One of the most important characteristics of the vehicle network is its high mobility. The activities of unmanned aerial vehicles (UAVs) have a significant impact on their effectiveness. By using the FDRL protocol, it can be possible to circumvent the problem of UAV servers



TABLE 1: Optimality performance of Fdrl model.

# of clusters	Bound 1		Bound 2	
	$\delta = p$	$\delta = p/2$	$\delta = p$	$\delta = p/2$
11	2.01	2.77	2.01	2.97
12	2.02	2.83	2.02	2.35
13	2.02	2.85	2.02	2.54
14	2.04	2.94	2.04	2.42
15	2.03	2.86	2.03	2.65
16	2.04	2.87	2.04	2.78
17	2.03	2.86	2.03	2.69
18	2.03	2.88	2.03	2.85
19	2.03	2.76	2.03	2.67
20	2.05	2.86	2.05	2.63
21	2.04	2.76	2.04	2.69
22	2.03	2.87	2.03	2.74

requiring different kind of data from other vehicles having limited resources. Self-learning and reporting back to central servers, such as MEC servers that are placed on UAVs, is possible while utilizing this technology. By allocating radio frequencies, the UAVs, as flying BSs, are obligated to give VUEs the bandwidth they need. As a result, the employment of unmanned aerial vehicles (UAVs) is essential. A method that concentrates on the core area may cause latency. With an FDRL strategy, VUEs will always have access to enough spectrum resources. To construct an accurate prediction model, UAVs can collaborate with each other and use data from previous spectrum allocations.

Table 1 indicates that FDRL algorithm performs better than theoretically possible lower constraints on optimality. Two distinct limits can be employed, in which it is assumed that each UFB can support a set of MTC devices with a total utilization of at most 1, while the minimum bandwidth required for allocation of the MTC devices is defined as the inverse of its period; i.e.,  $p$  and the inverse of its jitter  $p/2$ , respectively, to ensure that the MTC devices are allocated in an equitable manner. There are two effective bounds for implicit deadlines and synchronous device situations. These theoretical limitations represent lower bounds on the optimality of the associated situations; therefore, it is important to keep this in mind. The results of simulations are shown for a range of cluster sizes, from 11 to 22. The proposed model represents the iterative convex optimization technique with low complexity, and maximum energy efficiency algorithm shows the strategy which may maximum energy efficiency [26]. The energy efficiency is defined as the ratio of total sum rate to overall utilized power of all D2D connections.

Table 2 shows the correlation between the objective function value and the bit rate requirement. An increase in D2D link bit rate simultaneously increases the objective function values from 14.1227 to 33.2101. For federated deep reinforcement learning model, data ratios vary from 48.25 to 51.68, and admission gain increases 11.25 to 36.35 that shows the good performance. Unmanned aerial vehicle capacity UAV trajectory planning must be appropriately

TABLE 2: Performance in terms of bit rate requirement, admission gain, and objective function of the proposed FDRL model.

Bit rate	Admission gain	Data ratio (%)	Federated deep reinforcement learning objective function
4	11.25	50.63	14.1227
4.25	15.87	49.25	16.6546
5	16.58	49.47	18.1553
5.25	36.25	48.25	20.6424
6	28.25	51.23	21.5115
6.25	11.69	52.05	24.0631
7	25.35	51.68	25.4336
7.25	22.87	49.98	28.0442
8	13.68	50.61	30.5231
8.25	12.28	49.36	31.3984
9	14.68	50.27	33.2101

established due to the battery's limited computing, storage, processing, and energy capabilities. The mobility and energy of UAVs must be shared in order to maximize resources for all VUEs in air-to-air communication (i.e., UAV-to-UAV communication). Because of privacy issues, a decentralised learning technique like FDRL may be used to learn about local energy consumption and estimate future demand. Using this method, UAVs may choose their own path.

*4.1.3. Assistive UAV-Based Vehicular Network.* MEC servers use macro-BSs, RSUs, and UAVs to reduce the amount of time it takes to do computation and processing tasks. There are five specific conditions that must be met when using a distributed FDRL for vehicular communication. For a variety of technological reasons, edge devices (e.g., VUEs) cannot send data to the cloud. Another aspect is that the training model must be fast enough, since the global model and its local models must often swap parameters (e.g., in VUEs). Because of this, it is imperative that all the models can communicate with each other in a timely manner. Data from edge devices must be labelled fast and accurate on the same machines. Similarly, to train their local data models efficiently, edge devices must have enough processing power and storage capacity to handle the workload.

## 5. Conclusions

The research is aimed at examining the most advanced techniques in traditional optimization theory, machine learning, and specifically DRL-based resource management. A wide variety of quality of service (QoS) criteria are examined in the cloud, fog, and edge layers. An FL technique, specifically a UAV-aided vehicular network proposed FDRL approach, is examined to improve connection and minimize latency. Proposals have also been made for an FDRL-based vehicle communication system. It also explains 5G's existing difficulties and possible future paths in vehicle networks. The initial step is to examine a multiaccess edge computing method to generate ideas for more study. This study provides new opportunities for future researchers to work on

FDRL-based UAV-assisted 5G and 6G vehicular communication issues. Consequently, 5G and 6G vehicle networks can meet a wide range of quality of service (QoS) standards. Open study areas include an FDRL technique-based vehicular network, an FDRL technique-based unmanned aerial vehicle (UAV), and an FDRL technique-based drone. By using FDRL-based UAVs, any possible delay or reduction can be handled with the help of UAV-based vehicular communication using the FDRL technique. Furthermore, ML algorithms can manage all the communication challenges that were previously difficult to handle. As future work, for 6G networks, integrated aerial-terrestrial communication can be expanded for channel modeling and routing. In order to improve deployment tactics and UAV payloads, additional information is needed on the signal transmission between the user on the ground and the flying base station. There presently exist a multitude of channel models that handle wireless propagation in an urban context. No channel models consider UAV-to-vehicle connectivity which is crucial for UAV-enabled ITS. Moreover, the variants accessible include restricted frequency range, fixed base nonmobile end-users, or stations. A model that corrects these flaws can lead to a better grasp of the fading effects between buildings and properly plan drone deployment. Also, mobile BSs and mobile vehicles can help determine the ideal drone load-out. Lastly, the link multihop infrastructure loss may be calculated more precisely. In this way, DRL and FDTL techniques are helpful to meet a wide range of quality of service (QoS) standards involving 5G and 6G vehicle networks.

## Data Availability

Data will be available on request.

## Conflicts of Interest

The authors declare that they have no conflicts of interest.

## References

- [1] J. Navarro-Ortiz, P. Romero-Diaz, S. Sendra et al., "A survey on 5G usage scenarios and traffic models," *IEEE Communication Surveys and Tutorials*, vol. 22, no. 2, pp. 905–929, 2020.
- [2] S. A. A. Balamurugan, J. F. Lilian, and S. Sasikala, "The future of India creeping up in building a smart city: intelligent traffic analysis platform," in *in the 2018 Second International Conference on Inventive Communication and Computational Technologies (ICICCT)*, pp. 518–523, Coimbatore, India, 2018.
- [3] T. Huang, W. Yang, J. Wu, J. Ma, X. Zhang, and D. Zhang, "A survey on green 6G network: architecture and technologies," *IEEE Access*, vol. 7, no. 7, pp. 175758–175768, 2019.
- [4] M. Peters, W. Ketter, M. Saar-Tsechansky, and J. Collins, "A reinforcement learning approach to autonomous decision-making in smart electricity markets," *Machine Learning*, vol. 92, no. 1, pp. 5–39, 2013.
- [5] B. Kisanin, "Deep learning for autonomous vehicles," in *in 2017 IEEE 47th International Symposium on Multiple-Valued (ISMVL)*, p. 142, Novi Sad, Serbia, 2017.
- [6] M. K. Abdel-Aziz, S. Samarakoon, M. Bennis, and W. Saad, "Ultra-reliable and low-latency vehicular communication: an active learning approach," *IEEE Communications Letters*, vol. 24, no. 2, pp. 367–370, 2020.
- [7] Y. Qiu, H. Zhang, K. Long, H. Sun, X. Li, and V. C. M. Leung, "Improving handover of 5G networks by network function virtualization and fog computing," in *in 2017 IEEE/CIC International Conference on Communications in China (ICCC)*, pp. 1–5, Qingdao, China, 2017.
- [8] Z. Zhou, P. Liu, J. Feng, Y. Zhang, S. Mumtaz, and J. Rodriguez, "Computation resource allocation and task assignment optimization in vehicular fog computing: a contract-matching approach," *IEEE Transactions on Vehicular LAR Technology*, no. 4, pp. 3113–3125, 2019.
- [9] J. Li, C. Natalino, D. P. Van, L. Wosinska, and J. Chen, "Resource management in fog-enhanced radio access networks to support real-time vehicular services," in *in 2017 IEEE 1st International Conference on Fog and Edge Computing (ICFEC)*, pp. 68–74, Madrid, Spain, 2017.
- [10] Y. Liu, H. Zhang, K. Long, H. Zhou, and V. C. M. Leung, "Fog computing vehicular network resource management based on chemical reaction optimization," *IEEE Transactions on Vehicular Technology*, vol. 70, no. 2, pp. 1770–1781, 2021.
- [11] A. Masaracchia, M. Nguyen, and A. Kortun, "User mobility into NOMA assisted communication: analysis and a reinforcement learning with neural network based approach," *EAI Endorsed Transactions on Industrial Networks and Intelligent Systems*, vol. 7, no. 25, 2021.
- [12] J. Zhao, Q. Li, Y. Gong, and K. Zhang, "Computation offloading and resource allocation for cloud assisted mobile edge computing in vehicular networks," *IEEE Transactions on Vehicular Technology*, vol. 68, no. 8, pp. 7944–7956, 2019.
- [13] A. Yu, H. Yang, W. Bai, L. He, H. Xiao, and J. Zhang, "Leveraging deep learning to achieve efficient resource allocation with traffic evaluation in datacenter optical networks," in *in Optical Fiber Communications Conference and Exposition (OFC)*, pp. 1–3, San Diego, CA, USA, 2018.
- [14] B. Yang, S. Sun, J. Li, X. Lin, and Y. Tian, "Traffic flow prediction using LSTM with feature enhancement," *Neurocomputing*, vol. 332, pp. 320–327, 2019.
- [15] S. S. Lee and S. Lee, "Resource allocation for vehicular fog computing using reinforcement learning combined with heuristic information," *IEEE Internet of Things Journal*, vol. 7, no. 10, pp. 10450–10464, 2020.
- [16] Y. Zhou, F. Tang, Y. Kawamoto, and N. Kato, "Reinforcement learning-based radio resource control in 5G vehicular network," *IEEE Wireless Communications Letters*, vol. 9, no. 5, pp. 611–614, 2020.
- [17] J. Zhao, M. Kong, Q. Li, and X. Sun, "Contract-based computing resource management via deep reinforcement learning in vehicular fog computing," *IEEE Access*, vol. 8, pp. 3319–3329, 2020.
- [18] X. Chen, S. Leng, K. Zhang, and K. Xiong, "A machine-learning based time constrained resource allocation scheme for vehicular fog computing," *China Communications*, vol. 16, no. 11, pp. 29–41, 2019.
- [19] T. Mekki, R. Jmal, L. Chaari, I. Jabri, and A. Rachedi, "Vehicular fog resource allocation scheme: a multi-objective optimization-based approach," in *in 2020 IEEE 17th Annual Consumer Communications Networking Conference (CCNC)*, pp. 1–6, Las Vegas, NV, USA, 2020.
- [20] M. Ibrar, A. Akbar, R. Jan et al., *ArtNet: Ai-based resource allocation and task offloading in a reconfigurable internet of*

- vehicular networks*, IEEE Transactions on Network Science and Engineering, 2020.
- [21] X. Sun, J. Zhao, X. Ma, and Q. Li, "Enhancing the user experience in vehicular edge computing networks: an adaptive resource allocation approach," *IEEE Access*, vol. 7, pp. 161074–161087, 2019.
  - [22] R. Kashyap, "Applications of Wireless Sensor Networks in Healthcare," in *Advances in Wireless Technologies and Telecommunication*, pp. 8–40, 2020.
  - [23] A. Kovalenko, R. F. Hussain, O. Semiari, and M. A. Salehi, "Robust resource allocation using edge computing for vehicle to infrastructure (V2I) networks," in *2019 IEEE 3rd International Conference on Fog and Edge Computing (ICFEC)*, 2019, pp. 1–6, Larnaca, Cyprus, 2019.
  - [24] J. Zhang, H. Guo, J. Liu, and Y. Zhang, "Task offloading in vehicular edge computing networks: a load-balancing solution," *IEEE Transactions on Vehicular Technology*, vol. 69, no. 2, pp. 2092–2104, 2020.
  - [25] M. Khayyat, I. A. Elgendy, A. Muthanna, A. S. Alshahrani, S. Alharbi, and A. Koucheryavy, "Advanced deep learning-based computational offloading for multilevel vehicular edge-cloud computing networks," *IEEE Access*, vol. 8, pp. 137052–137062, 2020.
  - [26] W. Zhan, C. Luo, J. Wang et al., "Deep-reinforcement-learning-based offloading scheduling for vehicular edge computing," *IEEE Internet of Things Journal*, vol. 7, no. 6, pp. 5449–5465, 2020.
  - [27] R. Kashyap, *Miracles of Healthcare with Internet of Things, Smart Devices, Applications, and Protocols for the IoT*, 2019.
  - [28] M. T. Nguyen, L. H. Truong, and T. T. H. Le, "Video surveillance processing algorithms utilizing artificial intelligent (AI) for unmanned autonomous vehicles (UAVs)," *MethodsX*, vol. 8, p. 101472, 2021.
  - [29] H. T. Do, H. T. Hua, H. T. Nguyen et al., "Formation control algorithms for multiple-UAVs: a comprehensive survey," *EAI Endorsed Transactions on Industrial Networks and Intelligent Systems*, vol. 8, no. 27, 2021.
  - [30] L. Xiao, X. Lu, D. Xu, Y. Tang, L. Wang, and W. Zhuang, "UAV relay in VANETs against smart jamming with reinforcement learning," *IEEE Transactions on Vehicular Technology*, vol. 67, no. 5, pp. 4087–4097, 2018.
  - [31] Q. Pham, F. Fang, V. N. Ha et al., "A survey of multi-access edge computing in 5G and beyond: fundamentals, technology integration, and state-of-the-art," *IEEE Access*, vol. 8, pp. 116974–117017, 2020.
  - [32] M. Mahmoud, M. Oyediji, and Y. Xia, "Path planning in autonomous aerial vehicles," pp. 331–362.
  - [33] M. Hausknecht and P. Stone, *Deep Recurrent Q-Learning for Partially Observable MDPs*, 2015 AAAI Fall Symposium Series, 2015.

## Review Article

# Rating of Modern Color Image Cryptography: A Next-Generation Computing Perspective

Muhammad Samiullah,<sup>1</sup> Waqar Aslam ,<sup>1</sup> Muhammad Asghar Khan ,<sup>2</sup>  
Haya Mesfer Alshahrani,<sup>3</sup> Hany Mahgoub,<sup>4</sup> Ako Muhammad Abdullah ,<sup>5</sup> M. Ikram Ullah,<sup>6</sup>  
and Chien-Ming Chen <sup>7</sup>

<sup>1</sup>Department of Computer Science & IT, The Islamia University of Bahawalpur, Pakistan

<sup>2</sup>Hamdard University, Islamabad, Pakistan

<sup>3</sup>Department of Information Systems, College of Computer and Information Sciences, Princess Nourah Bint Abdulrahman University, P.O. Box 84428, Riyadh 11671, Saudi Arabia

<sup>4</sup>Department of Computer Science, College of Science & Art at Mahayil, King Khalid University, Saudi Arabia

<sup>5</sup>Computer Science Department, College of Basic Education, University of Sulaimani, Iraq

<sup>6</sup>Department of Information Sciences, University of Education, Lahore, Pakistan

<sup>7</sup>Shandong University of Science and Technology, Qingdao, China

Correspondence should be addressed to Chien-Ming Chen; [chienmingchen@ieee.org](mailto:chienmingchen@ieee.org)

Received 27 December 2021; Revised 17 February 2022; Accepted 2 March 2022; Published 22 March 2022

Academic Editor: Shalli Rani

Copyright © 2022 Muhammad Samiullah et al. This is an open access article distributed under the Creative Commons Attribution License, which permits unrestricted use, distribution, and reproduction in any medium, provided the original work is properly cited.

Issues such as inefficient encryption architectures, nonstandard formats of image datasets, weak randomness of chaos-based Pseudorandom Number Generators (PRNGs), omitted S-boxes, and unconvincing security metrics leading to increased computational time and inadequate security level of chaos and Deoxyribonucleic Acid- (DNA-) based image encryption schemes need careful examination towards the development of more stable encryption schemes in terms of efficiency and reasonable security. A new taxonomy of image encryption based on chaotic systems, hyperchaotic systems, and DNA is propounded to assess the impact of these issues on the performance and security metrics. The primary emphasis of this research is to study various recent encryption architectures centered on a variety of confusion and diffusion methods. It is aimed at assessing the performance and security of various ciphers using a cipher rating criterion that categorizes ciphers into different classes. The parameters that are included in the rating criteria are information entropy, chi-squared goodness of fit test for histogram uniformity analysis, encryption efficiency, key space, differential attacks (Number of Pixels Change Rate and Universal Average Changing Intensity), key sensitivity analysis, encryption time, randomness tests such as NIST-R (a statistical suite for validating the randomness designed by the National Institute of Standards and Technology), correlation coefficient analysis, contrast analysis, energy analysis, homogeneity analysis, Mean Absolute Error, peak signal-to-noise ratio, and robustness to noise and occlusion attacks.

## 1. Introduction

Digital images are the most attractive and valuable type of data in social networks owing to the sufficient supply of information. The information about people, Electronic Patient Records (EPRs), things, places, and lifetime events can be documented in the form of images and are frequently used in the world of the internet for communicating sensi-

tive and confidential data. Over the past few years, governments and organizations have taken serious concern for the confidentiality and integrity of data at rest or in transit. In this respect, cryptography as a solution is playing an eminent role. Modern chaos and DNA-based cryptography must guarantee security with low computational needs; otherwise, the proposed cryptosystems would be discarded by the potential users. Chaotic systems are nonlinear

dynamical systems having sensitive dependence on initial conditions. The properties of chaotic systems such as sensitive dependence on initial conditions, randomness in the generated sequence, and complex behaviors have been attracting the researchers to implement it in encrypting and decrypting the images, and its efficient implementation with efficient encryption architectures produces excellent results as compared to existing cryptographic algorithms such as Data Encryption Standard (DES), 3DES, and Advanced Encryption Standard (AES). To improve the security and encryption efficiency, numerous gray and color image cryptosystems have emerged recently with excellent results. The work presented by [1] uses 2D alteration models to encrypt images, audios, and videos. This scheme provides high security features with low correlation, ideal entropy value, and faster encryption speed for gray-level image encryption. An image encryption scheme by [2] uses Piecewise Linear Chaotic Map (PWLCM) and Hyperchaotic Lorenz System (HLS) for DNA encoding, permutation, and diffusion. The test results of this scheme have shown a reasonable level of security with faster encryption speeds for gray-level and small-sized color images. Another image encryption/decryption algorithm proposed by [3] uses two rounds of permutation-diffusion by using two chaotic systems, dynamic DNA coding and sequencing operations. This scheme can resist statistical, plaintext, brute force, and differential attacks, but the encryption efficiency is degraded for larger dimensions and sizes of color images. Novel chaos and bit-level permutation proposed by [4] has good security and faster encryption speed advantage. But the special formats and size of the color images are not mentioned in the experimental results.

In this study, a systematic review with new taxonomy of image encryption based on chaotic systems, hyperchaotic systems, and DNA computing is propounded to assess the impact of the mentioned issues on the performance and security metrics. Moreover, some criteria are also selected to judge and quantify the worthiness of any cryptosystem. Issues such as inefficient encryption architectures, nonstandard formats of image datasets, weak randomness of chaos-based PRNGs, omitted S-boxes, and unconvincing security metrics leading to increased computational time and inadequate security level of chaos and DNA-based image encryption schemes need careful examination towards the development of a more stable encryption scheme in terms of efficiency and reasonable security. Additionally, there is a need to quantify and classify the encryption schemes into different classes by using some criteria. To this end, our specific contribution investigates the encryption architectures along with the findings of various symmetric image ciphers; a taxonomy of image encryption and cipher rating criteria to judge and quantify the worthiness of any cryptosystem is propounded.

The rest of the paper is structured as follows. Section 2 deals with definitions depicted in the taxonomy. Related work comprising encryption architectures of various image encryption schemes is given in Section 3. The encryption efficiency of some recently published cryptosystems is presented in Section 4. A review of chaotic and biometric-

based substitution box is given in Section 5. And some proposed criteria to judge the cryptosystems are given in Section 6. Conclusion with future directions is given in Section 7.

## 2. Definitions and Taxonomies

In this section, definitions related to modern cryptography are presented. An extended taxonomy of modern cryptography is shown in Figure 1. Modern cryptography is comprised of asymmetric, symmetric, quantum cryptography, and hash functions, while symmetric cryptography is further decomposed into block and stream cipher. Block cipher is further divided into chaotic, hyperchaotic, and cosine/sine transform-based cryptography. And stream cipher can be subdivided into synchronous, asynchronous, and one-time pad.

*2.1. Asymmetric Cryptography.* In asymmetric cryptography, two different keys are created for encryption and decryption, i.e., at the sender's side, the sender encrypts the plaintext with a key called public key and sends it to the communication network. The receiver on the other side decrypts the encrypted text with another key called secret key which is only known to the receiver (see Figure 2). Examples of asymmetric cryptography include Diffie-Hellman and RSA.

*2.2. Symmetric Cryptography.* In symmetric cryptography, a single key (same key) is used to encrypt and decrypt the data (see Figure 3). In order to safeguard the symmetric key, the asymmetric cipher can be used to share it among sender and receiver. Symmetric cryptography is further divided into block ciphers and stream ciphers. Block ciphers encrypt and decrypt the plaintext by taking a block of data, e.g., 32-bit and 64-bit, while stream ciphers process a single bit or byte at a time. Stream ciphers are further subdivided into synchronous ciphers, self-synchronizing (asynchronous), and one-time pad (OTP). In synchronous ciphers, an independent keystream is produced from the plaintext and ciphertext. Any character modification in the ciphertext does not influence the decryption process for the rest of the ciphertext, but insertion or deletion of character from the ciphertext will result in the failure of synchronization as well as the decryption process. In contrast, asynchronous ciphers generate their keystream from a particular number, say  $p$ , of former ciphertext digits and the key. Therefore, this scheme can handle the insertion or deletion of ciphertext character problems as was present in synchronous cipher. One-time pad is also called one-time encryption.

*2.3. Chaotic Cryptography.* It is the efficient implementation of mathematical chaos theory in the form of chaotic maps or systems to encrypt and decrypt the data (text, image, audio, and video) to transmit or preserve it in a secure way. The control parameters and initial conditions of chaotic maps are used as secret keys that are shared between transmitter and receiver. The secret key can then be again encrypted by using stream ciphers such as RSA for secure communication. The initial conditions can be generated by some mechanism from the input data. Many chaotic systems with varying dimensions until now have been implemented for the encryption of gray and color images. Chaotic systems

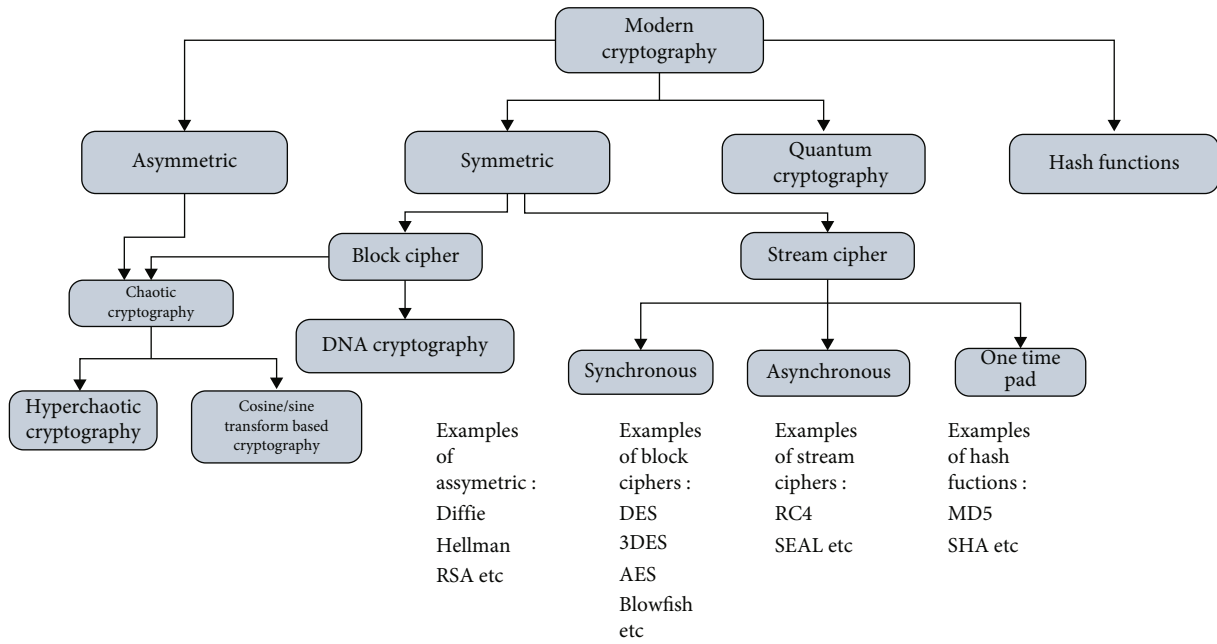


FIGURE 1: A taxonomy of modern cryptography.

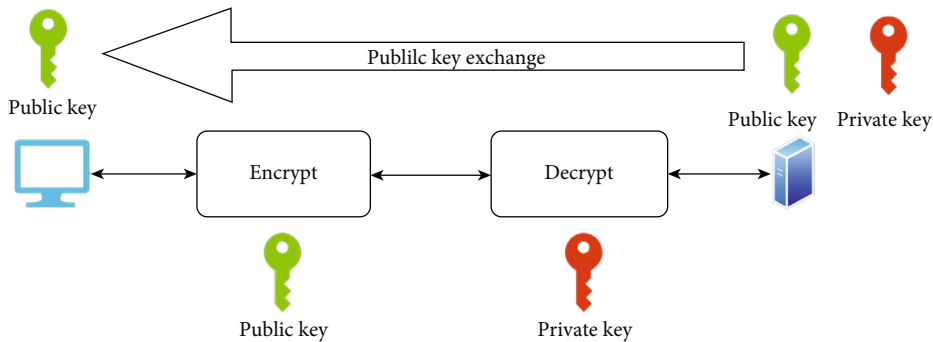


FIGURE 2: Asymmetric cryptography.

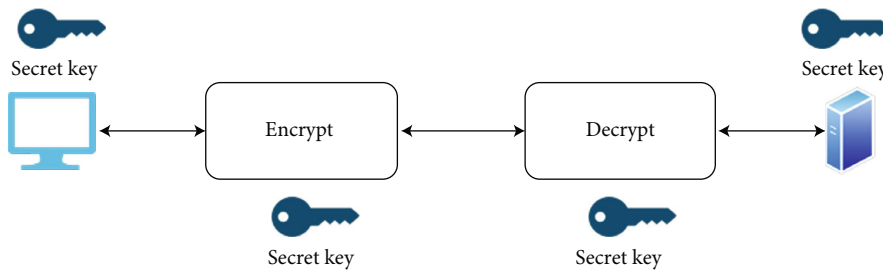


FIGURE 3: Symmetric cryptography.

can be subdivided into continuous and discrete time chaotic systems. For example, Chua’s circuit (continuous time chaotic physical system) is the simplest electronic circuit that reveals chaotic behavior. Other continuous time chaotic systems are Duffing equation, folded-towel hyperchaotic map, Hadley chaotic circulation, Rossler attractor, etc. While the discrete time chaotic maps include logistic map, Arnold’s cat map, Baker’s map, Bagdonov map, and Henon map. The chaotic maps generate a random sequence that can further

be improved to make it PRNGs. The intrinsic random sequence generated by the chaotic map is used for confusion or diffusion of the input image. Various cryptographic algorithms have been developed since 1989 to ensure the security of data at rest or in transit. Till 1995, cryptography used one-time pad with a chaotic system, though it is not suitable for encryption of image, audio, and video data. Later, the ergodicity property of chaotic maps is the focus of researchers towards designing cryptographic algorithms.

However, cryptosystems were not considered better due to being less efficient and less secure [5].

**2.4. Hyperchaotic Cryptography.** The tasks of cryptography are done through hyperchaotic systems. Hyperchaotic systems show complex dynamical behavior and high sensitive dependence on initial conditions with more than one positive Lyapunov exponents ( $\lambda$ ) as compared to chaotic systems. Sensitive dependence is quantified by calculating Lyapunov exponents. The sequence generated by hyperchaotic systems has better randomness as compared to chaotic systems and can be used for image scrambling and diffusion [6]. Some hyperchaotic systems' sequences can be used as PRNGs. Therefore, give better encryption results [7], a hyperchaotic map with higher dimensions has better ergodicity, more complex dynamic behavior, better randomness, and more than one positive Lyapunov exponents than low-dimensional hyperchaotic systems [8].

**2.5. DNA Cryptography.** Deoxyribonucleic Acid (DNA) shown in Figure 4 is biological DNA which is located in the cell's nucleus and carries genetic information about all the organisms. DNA is basically a double helix (double-stranded) structure formed by base pairs attached to the sugar-phosphate backbone. Replication is an important property of DNA. The 4 chemical bases, i.e., adenine (A), guanine (G), cytosine (C), and thymine (T), on a single strand form a specific sequence called a genetic code. These bases are connected to the bases of the opposite DNA strand, i.e., A with T and C with G called base pairs. The group of base, sugar, and phosphate is called a nucleotide. DNA can be used in cryptography for storing, encrypting, key generation, and transmitting the image data by using digital DNA datasets available on NCBI. Using biological DNA for storing, processing, and encrypting information demands higher technical laboratory requirements. To this end, cryptography based on biological DNA is still in its infancy and needs further theoretical discussions and experiments. For the sake of simplicity, digital DNAs are being used for encrypting and decrypting the data and information by mimicking the biological DNA operations such as Conservative Site-Specific Recombination (CSSR), DNA pairing, DNA annealing, and DNA replication (Figure 5). DNA-based cryptography is done by using the DNA mapping rules and DNA operations [9–16].

**2.6. Sine and Cosine Chaotic Maps.** Cosine or sine chaotic maps are considered more complex chaotic maps due to the simplicity in structure and high chaotic behavior with an infinite chaotic range thus leading to large key space and unpredictability. Sine- and cosine-based chaotic maps may be used as general frameworks for the existing chaotic maps. For example, a one-dimensional discrete cosine polynomial chaotic map (Equation (1)) is used for image encryption in two phases, i.e., row phase and column phase. Row and column phases do permutation-substitution based on pseudorandom sequence generated by 1D-DCP. The authors replaced the sequential permutation-substitution architecture with parallel permutation-substitution architec-

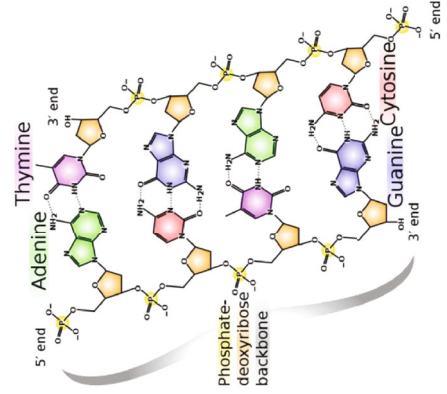


FIGURE 4: Biological DNA.

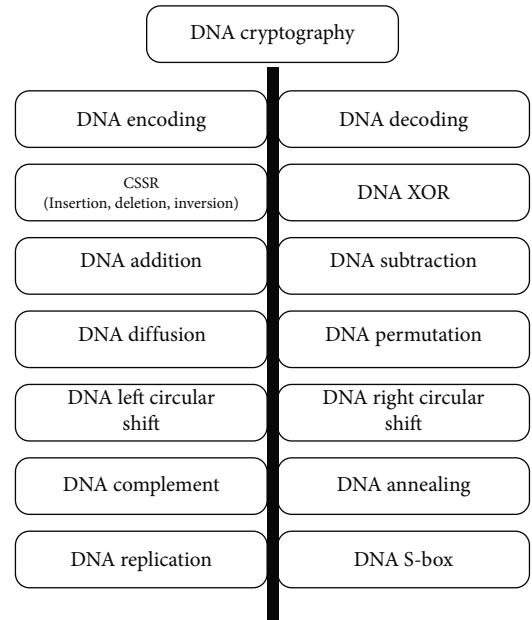


FIGURE 5: Various DNA operations in DNA-based cryptography.

ture and reduced the processing time while encrypting an image and showed better security metrics results [17]:

$$\{f : [-1; 1] \implies [-1; 1] x_{n+1} = f(x_n) = \mu(x_n^3 + x_n)\}. \quad (1)$$

The DCP scheme is shown in Figure 6. According to this figure, the sequence generated by 1D-DCP is used for the permutation and substitution of row and column pixel values simultaneously in  $T$  number of rounds. Similarly, the one-dimensional sine transform-based chaotic map (1D-STBCM) proposed by [18] gives a larger chaotic range and more complex behavior and gives excellent performance. 1D-STBCM (Equation (2)) [18] can be used as a general framework for any two existing chaotic maps:

$$x_{i+1} = \text{sinsin}(\pi(f(a, x_i) + g(b, x_i))), \quad (2)$$

where  $f(a, x_i)$  and  $g(b, x_i)$  are two existing chaotic maps also called seed maps which may or may not be the same.  $a$  and  $b$

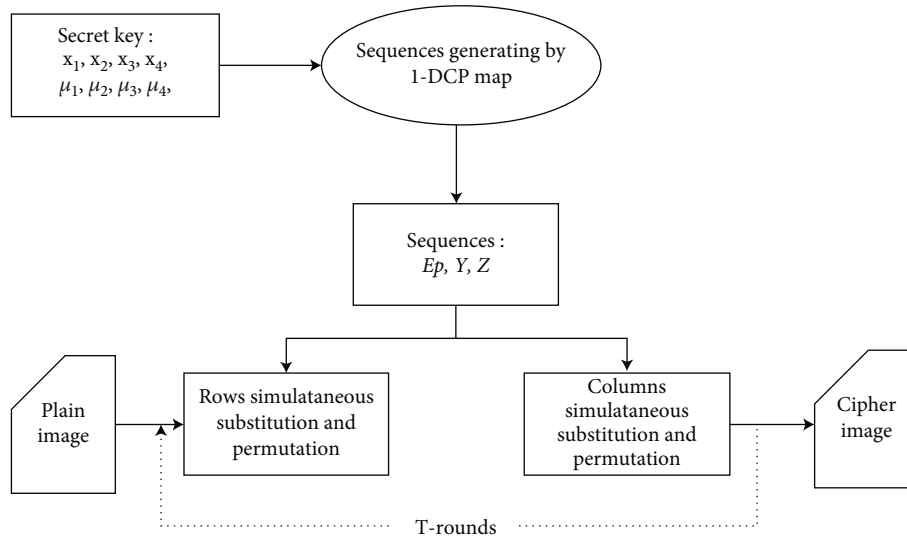


FIGURE 6: Flowchart of the DCP image encryption scheme [17].

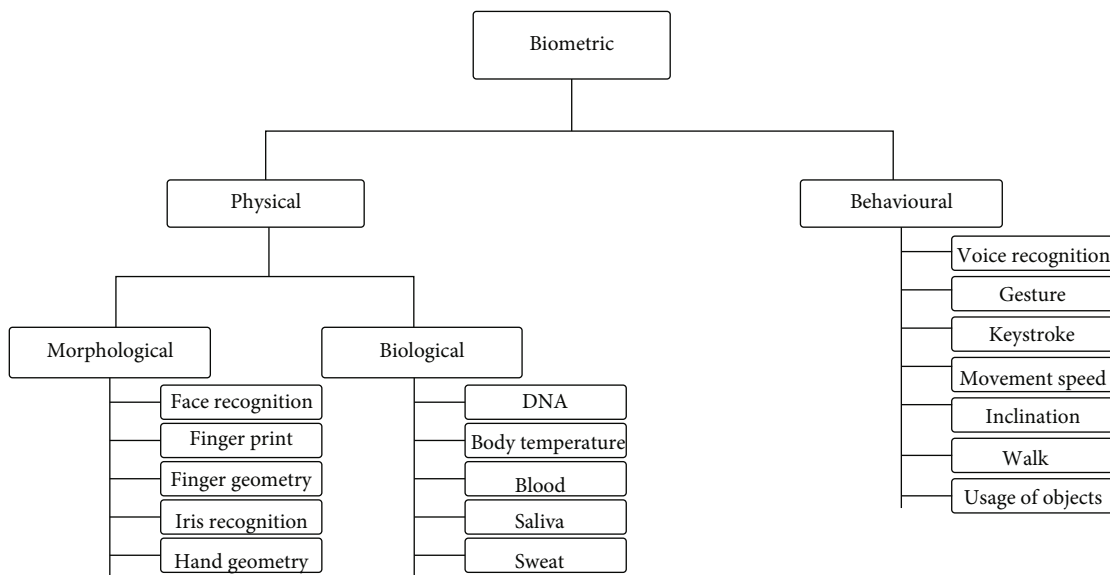


FIGURE 7: Biometric subdivisions [52].

are the control parameters, and  $x_i$  signifies the input in each iteration. The input  $x_i$  along with control parameters  $a$  and  $b$  is supplied to two seed maps, i.e.,  $f(a, x_i)$ , and  $g(b, x_i)$  in each iteration, and then, the sine-based transformation is executed. Last but not least, a large number of chaotic maps with different chaotic behaviors can be generated by extending Equation (2) to three or more seed maps. Therefore, the extended system may have a higher degree of randomness and unpredictable output sequences.

The author in [19] proposed a 3D sine map to permute an image and obtained high security, fast speed, and resistivity against some common attacks. A second-order nonlinear differential equation with cosine transform is employed to generate chaotic S-box which was found to be much better in Strict Avalanche Criterion (SAC) and

nonlinearity and can be used for encrypting the input image by using some substitution processes such as the Rijndael substitution process [20].

**2.7. Quantum Cryptography.** Peter Shor’s 1994 algorithm for factoring large prime numbers is one of the main motives to divert the attention of security experts to make use of quantum computing towards quantum cryptography. Quantum cryptography is dependent on quantum computing which is still in its infancy stage and cannot be considered true quantum architectures. True quantum computing will further transform the current cryptography into new amazing dimensions. Quantum cryptography is based on the principles of quantum mechanics (quantum superposition, quantum annealing, and quantum entanglement) to encrypt



TABLE 1: Different forms of permutation-substitution.

Ref	Encryption architecture	Findings
[19]	<i>3D permutation method</i> : in this architecture, 3D orthogonal Latin squares and matching matrices generated from 3D sine map are combined to permute the plain image; then, each component of the permuted matrix is subdivided into subblocks of the same size. The corresponding blocks of each component are linked and shifted (cyclic shift) according to the sorted position matrix generated by the 3D sine map chaotic sequence. In addition, singular value decomposition (SVD) is also applied on the 3 <sup>rd</sup> chaotic sequence to produce three more matrices, namely, $u1, s1, v1$ . Finally, the cyclic shifted matrix is modulated with $u1$ to produce the encrypted version of plain image.	It saves encryption time as Latin squares are composed of integers only. It has resistivity against various attacks, fast speed, and high security.
[20]	<i>Chaotic S-box-based substitution</i> : in this architecture, 2 <sup>nd</sup> order nonlinear differential is employed to generate chaotic S-box which was found to be much better in Strict Avalanche Criterion (SAC) and nonlinearity. The input image is rotated clockwise by 90°, a random column is added to the left of the rotated image, and values are substituted with S-box by using the Rijndael substitution process.	The rotation and addition of random columns increased the immunity against plaintext attacks (PTAs). The encrypted image passed most of the NIST randomness tests.
[25]	<i>Key substitution architecture (KSA)</i> : it includes one round of key scheming and novel substitution method. The key scheming phase is based on a logistic chaotic map whose initial conditions are calculated from the weighted summation method. And the substitution is composed of random grouping, chaotic S-box construction, and random substitution.	Yielded satisfactory encryption performance, better security, and computational efficiency as compared to traditional substitution-permutation architectures. But encryption time increases for large-sized color images.
[26]	<i>Cross-plane permutation and nonsequential diffusion process</i> : in cross-plane, a single operation shuffles randomly all the RGB pixel positions. And in nonsequential diffusion process, the pixels are permuted according to the chaotic sequence generated by using 2D-Logistic Tent Modular Map (LTMM). Nonsequential diffusion process takes two rounds for good diffusion.	The encryption speed is rapid as it employs simple implementations of encryption structures and chaotic map. It can mitigate the data losses and noises, i.e., robust against noise attacks and resists differential, chosen-plaintext attacks, and statistical attacks and is extremely sensitive to its secret key. It can serve real-time applications in an efficient way.
[27]	<i>Cyclic shift-based scrambling and diffusion based on household decomposition method</i> : in this architecture, the number of left shifts for the rows and columns is determined by the chaotic sequence; then, the cyclic shift algorithm is performed on rows and columns. After this, diffusion is employed by using household orthogonal decomposition. In the end, XOR operation is performed between the chaotic sequence and the output of diffusion based on household orthogonal decomposition.	The encryption speed is not mentioned in the paper. It has better entropy, NPCR, UACI, and correlation coefficients and is robust to occlusion attacks up to 25% and salt & pepper noise attacks up to 0.01.
[28]	<i>Lorenz-based diffusion and Rossler-based confusion</i> : Lorenz chaotic map is used to scramble the input image. In scrambling, RGB pixel positions are rearranged by using the histogram equalized Lorenz chaotic sequence. And pixel substitution based on Rossler system is achieved through XOR operation.	The encryption time is not mentioned in the paper. It has better entropy, NPCR, UACI, and correlation coefficient results and is robust to classical attacks to some extent. The encrypted image also passed the NIST SP 800-22 randomness tests; therefore, it can be used as PRNG.
[29]	<i>Latin square-based confusion and diffusion</i> : in diffusion phase, pixel permutation is achieved in two steps: <i>step 1</i> : shuffle the pixel rowwise to a new coordinate $(x, LSQ(x, y))$ , where LSQ is a Latin square. An intermediate permuted image is produced in this step; <i>step 2</i> : similarly, shuffle the pixels of the intermediate permuted image columnwise to new coordinate $(LSQ(x, LSQ(x, y)), LSQ(x, y))$ , while in the confusion phase, the pixel values are modified according to this equation $(c(n) = k(n) \oplus \{[p(n) + k(n)] \bmod 256\} \oplus c(n - 1))$ , where $k(n), p(n), c(n), c(n - 1)$ are the current key value, current pixel, cipher pixel, and previous cipher pixel.	Although the cryptosystem demands less computational complexity, the cryptosystem can be broken by chosen-plaintext attack (CPA) combined with chosen-ciphertext attack (CCA) [29]. Moreover, the cryptosystem used the same key in each round of encryption.
[30]	<i>Logistic map-based permutation</i> : in this cryptosystem, the architecture for permuting the input color image is based on 1D logistic map. A chaotic sequence is first generated by using initial values, sequence is sorted, and finally, the input image is scrambled using the sorted sequence.	The cryptosystem gave high probability of resisting brute force attacks and better encryption effect and is able to recover images that were 25% covered with some other pixels.

TABLE 1: Continued.

Ref	Encryption architecture	Findings
[31]	<i>Random permutation-substitution based on modular function:</i> in this lightweight encryption architecture, a set of random permutation-substitutions through modular function at bit level followed by image rotations is performed. The encryption structure is scalable, i.e., any number of key sizes with any number of rounds may be used.	The smaller overhead with minimum number of rounds and simple structure reduces encryption time and energy consumption without reducing security level.
[32]	<i>12 × 12 S-box-based substitution with linear permutation:</i> 12 × 12 S-box is constructed through chain ring method $R_{12}$ ; then, it is extended to 24-bit extended lookup table. The 24-bit lookup table is decomposed into three cells of 8 bit each called L, M, R. Red, green, and blue components of input image are substituted with L, M, and R. Then, linear permutation is applied to produce permuted matrices. In the end, XOR is applied between permuted matrices and L, M, and R to get the encrypted image.	The ciphered image passed the NIST randomness tests. Less computational complexity and near to 8 bit/pixel entropy and resistance to some common attacks are the encouraging features of this encryption architecture.
[33]	<i>Lifting scheme-based permutation and substitution:</i> pseudorandom chaotic sequence (S) of about half the size of the input image is generated and is circularly shifted called as A and substituted with S-box called as B. Then, input image after splitting, repeat predicting and updating steps of lifting scheme by making use of B for the purpose of permutation and substitution. The prediction and update repeat four times.	The proposed cryptosystem is faster and secure for three loops but becomes a little slow with a little bit more security level when it is run for more than three loops. It is also scalable for workstations and supercomputers and can run on resource-constrained devices with a minimum number of loops and rounds. It can lie in the category of lightweight ciphers as it takes less number of cycles per byte (NCPB) = 276.8842.
[34]	<i>Kronecker product-based confusion-diffusion:</i> input image is mapped to finite fields called P; then, scrambling and diffusion of P based on Kronecker product over finite field is done to produce R. Then, DNA operations based on Chen's hyperchaotic system are applied on R to produce an encrypted image.	Permutation-substitution over finite fields using Kronecker product makes the cryptosystem capable of resisting known-plaintext attacks and chosen-plaintext attacks. The cryptosystem also has a good randomness, uniform histograms, and better entropy, NPCR, and UACI values.
[35]	<i>Fusion of two maps and transformation:</i> a new chaotic map is produced by the fusion of two maps. The chaotic sequence of new map is exploited in the mathematical transformation function to convert the plain image into cipher image.	The obtained results in terms of NPCR, UACI, PSNR, entropy, histogram variances, correlation, and attacks are comparable to most of the recent studies.
[36]	<i>Image scrambling by using a mix of random, rotation, and zigzag permutation:</i> in this approach, plain image is splitted into nonoverlapping subblocks. These subblocks are permuted by zigzag, rotation, and random fashion. Finally, XOR operation is performed between a key and scrambled image to get the encrypted image. Here, key is generated by using logistic map.	The simulation on 170 images of JPG type each having dimensions $512 \times 512$ reveals the efficiency of the proposed approach in terms of security and time complexity. The time complexity of the proposed approach comes out to be $O(M \times N)$ .

and decrypt the messages with guaranteed security. The cryptographic tasks require a quantum computer. The quantum computer with its immense power can break the RSA's 2048-bit asymmetric algorithm in a few seconds on a mature quantum architecture; otherwise, it will take billions of years on classical computing architecture [21]. Quantum computing uses qubits to encode the information. Unlike a classical bit, the qubit is the basic building block in quantum computing (see Figure 7). The quantum superposition principle is used to set a qubit to form a quantum state. Several combinations of 0's and 1's can be processed on quantum architectures at the same time at a very less computational time. A qubit can exist in a state of  $|0\rangle$ ,  $|1\rangle$  and in a combined state of 0 and 1 called a superposition state and is denoted by  $|\psi\rangle = a|0\rangle + b|1\rangle$ . The qubit's superposition state can be entangled with another quantum bit to make a new valid state. The qubits in quantum architecture are probabilistic

as compared to classical bits which are deterministic [22]. The branches of quantum cryptography including Quantum Secret Sharing (QSS), Quantum Key Distribution (QKD), Quantum Secure Direct Communication (QSDC), Quantum Signature (QS), Quantum Private Query (QPQ), Quantum Anonymous Voting (QAV), Quantum Sealed bid Auction (QSA), Quantum Public Key (QPK) cryptosystem, Quantum Key Agreement (QKA), and Quantum Identity Authentication (QIA) needs further development, review, and experiments to mature the field of quantum cryptography [23].

### 3. Related Work

In this section, the encryption architectures along with their findings of various image encryption schemes are presented. Various improvements in permutation-substitution

TABLE 2: Comparison of some recently published cryptosystems with the prime focus of NCPB.

Ref	Image	Size (kB)	ET	Entropy	NPCR, UACI	Corr (Avg)	KS	NCPB
[38]	256 × 256	111	0.021 s	7.9971	99.56, 33.28	<0.01	$2^{231}$	314.0836
	512 × 512	284	0.093 s	—	—	—		543.6427
	1024 × 1024	768	0.387 s	—	—	—		1147.879
[39]	256 × 256	111	0.0759	7.9971	99.55, 33.27	-0.0026	$2^{277}$	1135.188
	512 × 512	284	0.3156 s	7.9971	99.59, 33.28	0.0082		1844.878
	1024 × 1024	768	1.3153 s	—	—	—		3899.292
[17]	256 × 256	111	0.0111 s	7.9992	99.64, 33.43	0.0004	$2^{392}$	166.0156
	512 × 512	284	0.036 s	7.9993	99.66, 33.45	—		210.4423
	1024 × 1024	768	0.1342 s	7.9989	—	—		397.8446
[40]	256 × 256	111	0.3422 s	7.9996	99.62, 33.45	0.0057	$2^{180}$	5118.067
	512 × 512	284	0.9232 s	—	—	—		5396.677
	1024 × 1024	768	1.9133 s	—	—	—		5672.102
[33]	256 × 256	111	—	—	—	—	$2^{512}$	—
	512 × 512	—	49.18 Mbps	7.997	99.60, 33.46	<0.001		276.8842
	1024 × 1024	1238	—	—	—	—		—
[41]	256 × 256	111	0.0491 s	7.9942	99.50, 33.32	—	$2^{1773}$	734.3574
	512 × 512	284	0.0921 s	7.9951	99.45, 33.34	<0.0063		538.3817
	1024 × 1024	1238	2.3541 s	7.9841	—	—		6978.882
[42]	256 × 256	111	—	7.9977	99.60, 33.35	0.0102	$2^{256}$	—
	512 × 512	263	0.9872	7.9990	99.59, 33.42	-0.0165		6231.583
	1024 × 1024	1238	—	—	—	—		—
[38]	256 × 256	268	0.079 s	7.9971	99.56, 33.28	<0.01	$2^{231}$	488.755
	512 × 512	768	0.096 s	—	—	—		210.978
	1024 × 1024	1238	1.212 s	—	—	—		2832.189
[43]	256 × 256	268	—	—	—	—	$2^{256}$	—
	512 × 512	—	44.93 Mbps	7.9991	99.60, 33.46	<0.0005		302.6931
	1024 × 1024	1238	—	—	—	—		—
[44]	256 × 256	268	—	—	—	—	$2^{170}$	—
	512 × 512	—	31.97 Mbps	7.997	99.59, 33.46	<0.0003		425.3988
	1024 × 1024	1238	—	—	—	—		—
[45]	256 × 256	—	0.097 s	7.9992	—	—	$2^{200}$	147.3328
	512 × 512	768	0.276 s	7.9993	99.62, 33.68	<-0.0003		583.6487
	1024 × 1024	1238	0.664 s	7.9993	—	—		890.4231
[46]	256 × 256	260	8.2 s	7.9992	99.64, 33.4	0.00106	$(2 \times 10^{47} \times 256^{65536 \times 3})$	52358.77
	512 × 512	768	16.43 s	7.9998	—	—		35516.1
	1024 × 1024	1238	38 s	—	—	—		37547.96

architecture and permutation only architecture have been done after the classical chaos-based architectures [24]. Encryption architecture is a way or a method of doing substitutions, permutations, and transformations in the encryption algorithms by exploiting an encryption key.

The key can be generated from a chaotic or hyperchaotic system. While encrypting an image whether color or gray, a good encryption algorithm strictly follows the principles of confusion and diffusion. Encryption architectures include substitution-permutation network (SPN), Feistel Network

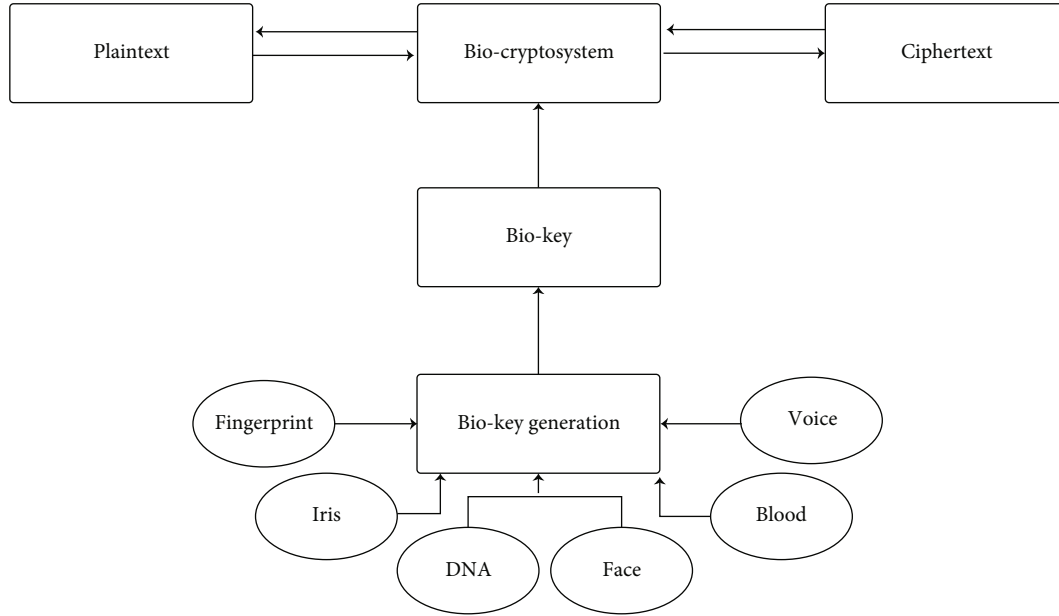


FIGURE 8: A depiction of biocryptography.

(FN), Generalized Feistel Structure (GFS), and its different variants. Different forms of improved permutation-substitution techniques proposed by various researchers are listed in Table 1.

#### 4. Encryption Efficiency of Cryptosystems

Another most important criterion of analyzing the cryptographic algorithms is encryption efficiency, especially for evaluating the cryptosystems for real-time internet applications. Based on the encryption time (ET), the encryption efficiency [37] in terms of encryption throughput ( $ET_h$ ) and number of cycles per byte (NCPB) is calculated by

$$ET_h = \frac{PI_{size}}{ET}, \quad (3)$$

$$NCPB = \frac{CPU_{speed}}{ET_h}, \quad (4)$$

where  $PI_{size}$ , ET, and  $CPU_{speed}$  are the plain image size in bytes, encryption time in seconds, and processor speed in Hertz, respectively, while NCPB is the number of cycles per byte. For example, 1-DCPIE proposed by [17] takes 36.1 ms to encrypt a  $512 \times 512$  grayscale image of size 263 kB. Its encryption efficiency in terms of NCPB according to the abovementioned formulas will be 228 cycles per byte.

In this section, some recently published cryptosystems with minimum encryption time and encryption efficiency in terms of minimum number of cycles per byte (NCPB) are focused, and NCPB is computed. NCPB is computed on a 1.7 GHz processor with 2 GB RAM. The basic purpose is to identify the cryptosystems for real-time internet applications. The identified cryptosystems having better NCPB

may be selected as lightweight ciphers, and improvements in these cryptosystems can be done.

The effort to attain a desired state or value of any cryptanalysis metric may affect the other cryptanalysis metrics such as encryption speed and robustness against noise attacks. Too much trade-off among security metrics may be caused by inefficient encryption architectures having multiple rounds and extensive formatting operations and using multiple chaotic systems, extensive DNA encoding, decoding, inefficient looping structures, inefficient source codes, etc.

A good cipher maintains a balance among these metrics by keeping an eye on the encryption architecture, type and size of input data, etc.; for example, the author in [9] proposed a hybrid model of DNA computing for encrypting the grayscale images of different sizes. The experimental results indicate that the proposed cryptosystem gives a good encryption effect, resists against known attacks, and is sufficiently fast for practical applications. In this regard, we have implemented this algorithm for color images of different sizes. The experimental results for color images of larger sizes greater than or equal to  $512 \times 512$  degrade the performance of the algorithm in terms of encryption time by keeping the security level maximum. Therefore, it is not suitable in terms of speed for practical real-time applications that deal with color images of larger size. Many researchers while developing cryptosystems achieve a sufficient level of security by making encryption architectures too much complicated which results in increased encryption and decryption time and makes them inapplicable for real-time communications especially in IoT. Therefore, the scrutinizing of the cryptosystems based on minimum encryption time (ET) by considering other cryptanalysis metrics such as entropy, NPCR, UACI, encryption efficiency (EE), correlation (Corr), key space (KS), and robustness is done and listed in Table 2.

TABLE 3: Selected criteria to rate various cryptosystems.

Analysis metrics	Class	Condition	Weight
ET (s)	VH	>50 and <100	VH = 1, H = 2, M = 3, L = 4, VL = 5
	H	>20 up to 50	
	M	$\geq 10$ and $\leq 20$	
	L	$\geq 1$ and $\leq 9$	
	VL	<1	
EE (NCPB)	H	<1000	H = 4, M = 3, L = 2, VL = 1
	M	$\geq 1000$ and $\leq 10000$	
	L	>ten thousand and <25000	
	VL	>25000	
NIST-R	P	$\geq 50\%$	P = 1, F = 0
	F	<50%	
Entropy	H	$\geq 99\%$ and $\leq 100\%$	H = 3, M = 2, L = 1
	M	$\geq 98\%$ and <99%	
	L	>95% and <98%	
Corr	S	Close to 1	S = 0, W = 1
	W	Close to 0	
HistU	U	U = 1 (if chi-squared statistic lies in the accepted region)	
	NU	NU = 0 (if chi-squared statistic does not lie in the accepted region)	
NPCR	H	$\geq 99\%$ and <100%	H = 3, M = 2, L = 1
	M	$\geq 98\%$ and <99%	
	L	>95% and <98%	
UACI	H	$\geq 33\%$	H = 3, M = 2, L = 1
	M	$\geq 30\%$ and <33%	
	L	>28% and <30%	
MAE	H	$\geq 80$	H = 4, M = 3, L = 2, VL = 1
	M	$\geq 70$	
	L	$\geq 65$	
	VL	$\geq 60$ and <65	
KS	H	$\geq 2^{300}$	H = 4, M = 3, L = 2, VL = 1
	M	$\geq 2^{200}$	
	L	$\geq 2^{100}$	
	VL	$\geq 2^{80}$ < $2^{100}$	
KS <sub>n</sub> /avalanche	H	$\geq 0.5$	H = 3, M = 2, L = 1
	M	$\geq 0.45$	
	L	>0.38 and <0.45	
RbN (up to 10%)	H	PSNR > 30	H = 4, M = 3, L = 2, VL = 1
	M	PSNR > 20	
	L	PSNR > 10 and $\leq 20$	
	VL	PSNR $\geq 8$ and $\leq 10$	
RbO (up to 50%)	H	PSNR > 30	H = 4, M = 3, L = 2, VL = 1
	M	PSNR > 20	
	L	PSNR > 10 and $\leq 20$	
	VL	PSNR $\geq 8$ and $\leq 10$	
PSNR (E-D)	H	Infinity	H = 4, M = 3, L = 2, VL = 1
	M	$\geq 80$	
	L	$\geq 70$	
	VL	$\geq 50$ and <70	

TABLE 4: A quantified comparison of some recently published gray-level image cryptosystems based on Table 3.

Ref	ET (5)	EE (4)	NIST-R (5)	Entropy (3)	Corr (1)	HistU (1)	NPCR (3)	UACI (3)	MAE (4)	KS (4)	Avalanche (3)	RbN (4)	RbO (4)	PSNR (E-D) (4)	Scores
[9]	VL (5)	H (4)	P (5)	H (3)	W (1)	U (1)	H (3)	H (3)	H (4)	H (4)	M (2)	L (2)	M (3)	H (4)	45/48
[34]	L (4)	H (4)	P (5)	H (3)	W (1)	U (1)	H (3)	H (3)	M (3)	H (4)	M (2)	L (2)	M (3)	H (4)	42/48
[65]	—	—	—	H (3)	W (1)	U (1)	H (3)	H (3)	—	H (4)	M (2)	L (2)	L (2)	H (4)	25/30
[66]	—	—	—	H (3)	W (1)	U (1)	H (3)	M (2)	—	M (3)	M (2)	VL (1)	VL (1)	H (4)	21/30
[67]	L (4)	M (3)	—	H (3)	W (1)	U (1)	H (3)	H (3)	—	H (4)	H (3)	L (2)	L (2)	H (4)	32/39
[65]	—	—	—	H (3)	W (1)	U (1)	H (3)	H (3)	—	H (4)	M (2)	L (2)	L (2)	H (4)	24/30
[68]	VL (5)	M (3)	—	H (3)	H (3)	U (1)	H (3)	H (3)	M (3)	H (4)	M (2)	L (2)	M (3)	H (4)	39/43
[69]	L (4)	L (2)	P (5)	H (3)	H (3)	U (1)	H (3)	H (3)	M (3)	H (4)	M (2)	L (2)	ND	H (4)	39/44
[27]	—	—	—	H (3)	W (1)	U (1)	H (3)	H (3)	—	M (3)	M (2)	L (2)	M (3)	H (4)	25/30
[70]	L (4)	M (3)	P (5)	H (3)	W (1)	U (1)	H (3)	H (3)	—	H (4)	M (2)	L (2)	L (2)	H (4)	37/44
[2]	L (4)	L (2)	P (5)	H (3)	W (1)	U (1)	H (3)	H (3)	—	H (4)	H (3)	—	—	H (4)	29/36
[30]	VL (5)	H (4)	—	H (3)	W (1)	U (1)	H (3)	H (3)	—	H (4)	M (2)	H (4)	—	H (4)	34/37
[71]	VL (5)	VL (1)	P (5)	H (3)	W (1)	U (1)	H (3)	H (3)	—	H (4)	H (3)	—	—	H (4)	33/36
[72]	—	—	—	H (3)	W (1)	U (1)	H (3)	H (3)	M (3)	M (3)	H (3)	L (2)	L (2)	H (4)	28/34
[73]	VL (5)	H (4)	—	—	W (1)	U (1)	H (3)	H (3)	—	M (3)	H (3)	—	—	H (4)	27/40
[74]	VL (5)	H (4)	P (5)	H (3)	W (1)	U (1)	H (3)	H (3)	—	H (4)	H (3)	—	—	H (4)	36/40
[75]	VL (5)	H (4)	—	H (3)	W (1)	U (1)	H (3)	H (3)	—	M (3)	H (3)	L (2)	—	H (4)	32/35
[76]	L (4)	L (2)	—	H (3)	W (1)	U (1)	H (3)	H (3)	—	H (4)	M (2)	M (3)	L (2)	H (4)	32/39
[77]	L (4)	M (3)	—	H (3)	W (1)	U (1)	H (3)	H (3)	—	H (4)	M (2)	L (2)	L (2)	H (4)	32/39
[78]	L (4)	L (2)	—	H (3)	W (1)	U (1)	H (3)	H (3)	—	M (3)	M (2)	—	—	H (4)	28/31
[79]	M (3)	L (2)	—	H (3)	W (1)	U (1)	H (3)	H (3)	—	M (3)	M (2)	—	—	H (4)	25/31
[80]	M (3)	L (2)	—	H (3)	W (1)	U (1)	H (3)	H (3)	M (3)	H (4)	M (2)	L (2)	L (2)	M (3)	32/43

TABLE 5: A quantified comparison of some recently published color cryptosystems based on Table 3.

Ref	ET (5)	EE (4)	NIST-R (5)	Entropy (3)	Corr (1)	HistU (1)	NPCR (3)	UACI (3)	MAE (4)	KS (4)	Avalanche (3)	RbN (4)	RbO (4)	PSNR (E-D) (4)	Scores
[81]	—	—	—	H (3)	W (1)	U (1)	H (3)	H (3)	M (3)	H (4)	M (2)	VL (1)	VL (1)	H (4)	27/34
[82]	H (2)	L (2)	P (5)	H (3)	W (1)	U (1)	H (3)	H (3)	M (3)	H (4)	M (2)	L (2)	L (2)	H (4)	37/48
[3]	L (4)	L (2)	—	H (3)	H (3)	U (1)	H (3)	H (3)	—	H (4)	M (2)	L (2)	L (2)	H (4)	34/43
[72]	—	—	—	H (3)	H (3)	U (1)	H (3)	H (3)	M (3)	H (4)	M (2)	L (2)	L (2)	H (4)	31/34
[83]	VL (5)	M (3)	—	H (3)	H (3)	U (1)	H (3)	H (3)	L (2)	H (4)	M (2)	L (2)	M (3)	H (4)	38/43
[84]	L (4)	M (3)	—	H (3)	H (3)	U (1)	H (3)	H (3)	ND	H (4)	H (3)	L (2)	L (2)	H (4)	35/39
[68]	VL (5)	M (3)	—	H (3)	H (3)	U (1)	H (3)	H (3)	M (3)	H (4)	M (2)	L (2)	M (3)	H (4)	39/43
[69]	L (4)	L (2)	P (5)	H (3)	H (3)	U (1)	H (3)	H (3)	M (3)	H (4)	M (2)	L (2)	ND	H (4)	39/44

TABLE 6: Proposed CRT of some recently published image cryptosystems.

Ref	Scaling factors	Key space sensitivity	Key Histogram	Visual analysis (PSNR (plain-decrypte))	Correlation analysis	Contrast analysis	Energy analysis	Homogeneity analysis	NPCR	UACI	Brute force attack	Information entropy	NIST-randomness	CPA MAE	Robustness against noise	Robustness against occlusion	Encryption time	Decryption time	Encryption efficiency
[85]	Rating (1-5)	4	4	5	5	3	3	4	4	4	5	5	4	5	5	3	1	1	1
	Marking factor	2	2	2	2	1	2	2	2	2	2	2	3	3	2	2	3	3	3
	Total marks	10	10	10	10	5	10	10	10	10	10	10	15	15	10	10	15	15	15
	Obtained marks	8	8	10	10	3	6	8	8	8	10	10	12	15	10	6	3	3	3
	Sum											157							
71.363636 (working class)																			
[86]	Rating (1-5)	4	4	5	5	2	3	4	5	5	5	5	5	4	4	3	4	4	4
	Marking factor	2	2	2	2	1	2	2	2	2	2	2	3	3	2	2	3	3	3
	Total marks	10	10	10	10	5	10	10	10	10	10	10	15	15	10	10	15	15	15
	Obtained marks	8	8	10	10	2	6	8	10	10	10	10	15	12	8	6	12	12	12
	Sum											187							
85 (upper middle class)																			
[87]	Rating (1-5)	4	4	5	5	2	3	4	5	5	5	5	5	4	4	3	4	4	3
	Marking factor	2	2	2	2	1	2	2	2	2	2	2	3	3	2	2	3	3	3
	Total marks	10	10	10	10	5	10	10	10	10	10	10	15	15	10	10	15	15	15
	Obtained marks	8	8	10	10	2	6	8	10	10	10	10	15	12	8	6	12	12	9
	Sum											184							
83.636364 (upper middle class)																			
[88]	Rating (1-5)	3	4	5	5	2	4	4	5	5	5	5	5	4	4	3	4	4	4
	Marking factor	2	2	2	2	1	2	2	2	2	2	2	3	3	2	2	3	3	3
	Total marks	10	10	10	10	5	10	10	10	10	10	10	15	15	10	10	15	15	15
	Obtained marks	6	8	10	10	2	8	8	10	10	10	10	15	12	8	6	12	12	12
	Sum											185							
84.090909 (upper middle class)																			
[89]	Rating (1-5)	4	5	5	5	4	4	4	5	5	5	5	5	5	4	3	4	4	3
		2	2	2	2	1	2	2	2	2	2	2	3	3	2	2	3	3	3



TABLE 6: Continued.

Ref	Scaling factors	Key space	Key sensitivity	Histogram	Visual analysis (PSNR (plain-decrypted))	Correlation analysis	Contrast analysis	Energy analysis	Homogeneity analysis	NPCR	UACI	Brute force attack	Information entropy	NIST-randomness	CPA	MAE	Robustness against noise	Robustness against occlusion	Encryption time	Decryption time	Encryption efficiency	
	Marking factor																					
	Total marks	10	10	10	10	10	5	10	10	10	10	10	10	15	15	10	10	10	15	15	15	
	Obtained marks	8	10	10	10	10	4	8	8	10	10	10	10	15	15	8	8	6	12	12	9	
	Sum																					193
	Percentage count																					87.727273 (upper middle class)
	Rating (1-5)	4	5	5	5	5	3	3	3	5	5	5	5	5	4	4	3	3	5	5	3	
	Marking factor	2	2	2	2	2	1	2	2	2	2	2	2	3	3	2	2	2	3	3	3	
[68]	Total marks	10	10	10	10	10	5	10	10	10	10	10	10	15	15	10	10	10	15	15	15	
	Obtained marks	8	10	10	10	10	3	6	6	10	10	10	10	15	12	8	6	6	15	15	9	
	Sum																					189
	Percentage count																					85.909091 (upper middle class)
	Rating (1-5)	5	5	5	5	5	3	3	3	5	5	5	5	5	5	4	3	3	4	4	4	
	Marking factor	2	2	2	2	2	1	2	2	2	2	2	2	3	3	2	2	2	3	3	3	
	Total marks	10	10	10	10	10	5	10	10	10	10	10	10	15	15	10	10	10	15	15	15	
[9]	Obtained marks	10	10	10	10	10	3	6	6	10	10	10	10	15	15	8	6	6	12	12	12	
	Sum																					191
	Percentage count																					86.818182 (upper middle class)
	Rating (1-5)	5	5	5	5	5	3	3	3	5	5	5	5	5	5	4	3	3	4	4	3	
	Marking factor	2	2	2	2	2	1	2	2	2	2	2	2	3	3	2	2	2	3	3	3	
	Total marks	10	10	10	10	10	5	10	10	10	10	10	10	15	15	10	10	10	15	15	15	
[80]	Obtained marks	10	10	10	10	10	3	6	6	10	10	10	10	15	15	8	6	6	12	12	9	
	Sum																					188
	Percentage count																					85.454545 (upper middle class)
	Rating (1-5)	3	4	5	5	5	3	3	3	5	5	5	5	5	5	4	3	3	3	3	4	
[90]	Marking factor	2	2	2	2	2	1	2	2	2	2	2	2	3	3	2	2	2	3	3	3	
	Total marks	10	10	10	10	10	5	10	10	10	10	10	10	15	15	10	10	10	15	15	15	
	Obtained marks	10	10	10	10	10	3	6	6	10	10	10	10	15	15	8	6	6	12	12	15	
	Sum																					188
	Percentage count																					85.454545 (upper middle class)



## 5. Novel S-Boxes

No doubt, S-box as a nonlinear lookup table plays a pivotal role in obscuring the relationship between the key and ciphertext. Although it has been adopted in some chaos-based ciphers, it is very rarely adopted in DNA-based image ciphers [47]. Numerous researchers have seriously neglected the importance of S-boxes in their chaos and DNA-based image encryption algorithms [26, 39, 48–51]. Uniqueness of the values and no correlation between the values in S-box are the indicators of a good S-box. The methods such as heuristic, Pseudorandom Number Generators (PRNGs), finite field inverse, and finite field exponent have been used for generating S-boxes to further enhance the security level of image cryptographic algorithms [52]. Chaos theory has also been implemented in designing S-box. For example,  $8 \times 8$  S-box based on chaotic maps is used in an image cryptographic algorithm [53]. The design of dynamic S-box by using the Zhangtang chaotic system is proposed in [54]. A 3D controlled chaotic plasma-based algorithm is presented in [55] to generate S-box. Artificial Bee Colony (ABC) and 6D hyperchaotic system are utilized in the generation of S-box [56]. An optimal S-box based on the firefly algorithm and discrete chaos is created in [57]. Multiple chaotic systems can be exploited in designing optimal S-boxes. The author in [58] used two chaotic systems, i.e., Chen's and Henon maps for creating chaotic S-box with improved randomness. The chaotic system called Logistic Sine System (LSS) having a wider chaotic range and better chaotic properties is employed in creating a single S-box of size  $16 \times 16$  [59].

Biometric subdivisions are shown in Figure 8. The biometric subdivisions such as face, fingerprint, iris, and DNA can be utilized to generate initial conditions for hyperchaotic systems and to generate cryptographic keys that will aid in constructing the novel S-boxes in the cryptographic algorithms. To this end, fingerprint-based S-box with minimum execution time is generated in [52] by using ridge ending features of the fingerprints. The iris dataset is used by [60], to create the initial conditions for logistic map and sine map for creating crypto S-box. The crypto S-box contains unique values.

Similarly, biological DNA can be converted into digital DNA, and digital DNA can be used in designing S-boxes. A  $16 \times 16$  S-box generated from the two DNA sequences (DS1 and DS2) taken from GenBank is proposed in [61]. The DS1 is converted into  $16 \times 16$  S-box where each cell consists of four nucleotide bases equivalent to 1 byte. The DS2 is used to compute (row, col) pair. The DS1 DNA values are picked sequentially and placed in the third empty S-box according to the (row, col) pair computed from DS1. The S-box is generated by splitting the numbers (0-255) into four sets, and each set is independently coded into a DNA strand. In this way, four DNA strand sets are obtained. Perform the reverse Watson Crick on all the DNA strand sets. Another DNA strand is taken from GenBank, and XOR operation between DNA strand sets and GenBank DNA strand is performed. And finally, central dogma is applied to get the entries of DNA-based S-box [62]. Another

approach to construct an S-box with nonrepeating values is composed of DNA coding, DNA addition and subtraction, XOR and arithmetic operations, and finally, the search procedure to eliminate the duplicate values [63]. In order to increase the level of confusion in cryptographic algorithms, the concept of multiple DNA or RNA-based S-boxes has also been proposed by the researchers. For example, [64] accomplished this task in three steps: (1) user string is converted into DNA string by using DNA mapping/coding rules, (2) DNA string is transformed into mRNA by simulating the biological replication and transcription processes, (3) mRNA size is reduced by splitting, addition, subtraction, and XOR operations, and (4) the reduced mRNA is used to construct S-box with 256 different hexadecimal values.

Cryptography based on physical and behavioral biometrics can be called as biocryptography. Biometric parameters (iris, DNA, fingerprint, etc.) can be exploited to generate a secret key while designing cryptographic algorithms. Biometric-based secret keys can lessen the demand for key storage and generation. Another concept of biohashing can be used to make secret keys in which biometric parameters are combined with hash algorithms such as MD5 and SHA-512.

## 6. Proposed Criteria to Evaluate Cryptosystems

Comparing cryptosystems' performance and cryptanalysis parameters without noting image size and format is not rational. To the best of our knowledge, criteria to quantify the cryptosystems are not proposed. In this section, some criteria to quantify some recently published color image cryptosystems are proposed which are indicated in Table 3. Based on these criteria, we allocate weights to various cryptanalysis parameters, and overall scores of a cipher in the sense of security and robustness can be computed. The criteria include encryption time (ET), encryption efficiency (EE) in terms of NCPB, National Institute of Science and Technology-Randomness Test (NIST-R), entropy, correlation (Corr), histogram uniformity (HistU), Number of Pixels Change Rate (NPCR), Universal Average Changing Intensity (UACI), Mean Absolute Error (MAE), key space (KS), key sensitivity (KSn), robustness against noise (RbN), robustness against occlusion (RbO), and peak signal-to-noise ratio between encrypted and decrypted images (PSNR (E-D)). The proposed judgement criteria given in Table 3 can be used for gray-level and color images and can be extended by including other metrics as well. The scores of some recently published ciphers based on the chosen criteria of Table 3 are given in Tables 4 and 5.

Similarly, Cipher Rating Taxonomy (CRT) to rate various ciphers is designed as a next proposal that can facilitate security researchers to assess the trustworthiness of their ciphers in double figures. The ratings of cryptanalysis parameters given in Table 3 can be extended, i.e., from 1 to 5 or 1 to 3. For example, to rate the entropy, we can rate it as  $\geq 7.9999$  (rating 5),  $\geq 7.999$  (rating 4),  $\geq 7.99$  (rating 3),  $\geq 7.9$  (rating 2), and  $< 7.9$  (rating 1). We have also introduced a critical marking factor or weight, which represents the significance of the cryptanalysis parameter, and it ranges from

1 (least significant) to 3 (most significant). Other than cryptanalysis parameters, other vulnerabilities such as Insecure Data Storage, Broken Cryptography, Insecure Data Transport, Cryptographic Flaw, and Privacy Concerns (secret key sharing, key management, etc.) can be added in the proposed CRT to assess the cryptosystems. Furthermore, CRT is an effort to further classify the past, present, and future ciphers and security systems in different classes and to bolster the transparent examination system. The proposed CRT shown in Table 6 presents the ratings and classifications of some recently published ciphers. We have divided the ciphers into 5 classes, namely, lower class, working class, lower middle class, upper middle class, and upper class. The criteria to classify the ciphers are the following: percentage count (pc) of a cipher is  $\geq 90$  (upper class),  $pc \geq 80$  (upper middle class),  $pc \geq 75$  (lower middle class),  $pc \geq 70$  (working class), and below 70 (lower class). Like so, lightweight ciphers can also be categorized by using the similar rating or modified rating method. The potential benefit of proposing CRT is that we can judge the cipher in a single shot, i.e., to (i) which class it belongs, (ii) which test metrics it has passed and which test metrics it has not passed, and (iii) which test metrics it has not performed. For example, a stakeholder needs a security algorithm for some application scenarios and demands moderate-level security with higher encryption speed to encrypt the bulk of image data. So, in this case, he/she can consult the CRT chart to match his/her demands.

## 7. Conclusions and Future Directions

We have covered the various aspects of chaotic and DNA-based cryptography. Assessment of various recently published cryptosystems based on encryption architectures, encryption efficiency, average encryption time, and number of cycles per byte is also done. Moreover, Cipher Rating Taxonomy (CRT) to rate various ciphers is also proposed that can facilitate security researchers to classify and assess the trustworthiness of their ciphers. For example, a stakeholder needs a security algorithm for some application scenarios and demands moderate-level security with higher encryption speed to encrypt the bulk of image data. So, in this case, the organization can consult the CRT chart to match its demands by considering its resources. The inclusion of hyperchaos-based confusion and diffusion in the cryptographic algorithms produces excellent security results but needs optimization to create an optimal trade-off between security and encryption efficiency and to make it lightweight. Moreover, hyperchaos coupled with genetic codes may advance the security of cryptographic practical applications besides the stoppage of side channel attacks.

No doubt, modern cryptography has transformed human existence and will continue to do so in communications, e-commerce, smart phones, digital signatures, and digital rights management (DRM) in the most advanced forms. Moreover, the proposed criteria may be extended, refined, and modified according to the classes of performance and cryptanalysis metrics under study.

## Data Availability

All data generated or analyzed during this study are included in this article.

## Conflicts of Interest

The authors declare no conflict of interest.

## Acknowledgments

The authors extend their appreciation to the Deanship of Scientific Research at King Khalid University for funding this work under grant number (RGP 2/46/43) and Princess Nourah Bint Abdulrahman University Researchers Supporting Project number (PNURSP2022R237), Princess Nourah Bint Abdulrahman University, Riyadh, Saudi Arabia.

## References

- [1] I. Yasser, M. A. Mohamed, A. S. Samra, and F. Khalifa, "A chaotic-based encryption / decryption framework for secure multimedia communications," *Entropy*, vol. 22, no. 11, pp. 1–23, 2020.
- [2] Z. Li, C. Peng, W. Tan, and L. Li, "A novel chaos-based image encryption scheme by using randomly dna encode and plaintext related permutation," *Applied Sciences (Switzerland)*, vol. 10, no. 21, p. 7469, 2020.
- [3] S. Zhou, P. He, and N. Kasabov, "A dynamic DNA color image encryption method based on SHA-512," *Entropy*, vol. 22, no. 10, pp. 1–23, 2020.
- [4] Z. Li, C. Peng, W. Tan, and L. Li, "A novel chaos-based color image encryption scheme using bit-level permutation," *Symmetry*, vol. 12, no. 9, p. 1497, 2020.
- [5] J. Gayathri and S. Subashini, "A survey on security and efficiency issues in chaotic image encryption," *International Journal of Information and Computer Security*, vol. 8, no. 4, pp. 347–381, 2016.
- [6] F. Yang, J. Mou, Y. Cao, and R. Chu, "An image encryption algorithm based on BP neural network and hyperchaotic system," *China Communications*, vol. 17, no. 5, pp. 21–28, 2020.
- [7] H. M. Ghadirli, A. Nodehi, and R. Enayatifar, "An overview of encryption algorithms in color images," *Signal Processing*, vol. 164, pp. 163–185, 2019.
- [8] S. Sun, Y. Guo, and R. Wu, "A novel image encryption scheme based on 7D hyperchaotic system and row-column simultaneous swapping," *IEEE Access*, vol. 7, pp. 28539–28547, 2019.
- [9] E. Z. Zefreh, "An image encryption scheme based on a hybrid model of DNA computing, chaotic systems and hash functions," *Multimedia Tools and Applications*, vol. 79, no. 33–34, pp. 24993–25022, 2020.
- [10] S. Kalsi, H. Kaur, and V. Chang, "DNA cryptography and deep learning using genetic algorithm with NW algorithm for key generation," *Journal of Medical Systems*, vol. 42, no. 1, 2018.
- [11] X. Aqeel-ur-Rehman, M. Liao, A. Hahsmi, and R. Haider, "An efficient mixed inter-intra pixels substitution at 2bits-level for image encryption technique using DNA and chaos," *Optik*, vol. 153, pp. 117–134, 2018.
- [12] X. Wu, J. Kurths, and H. Kan, "A robust and lossless DNA encryption scheme for color images," *Multimedia Tools and Applications*, vol. 77, no. 10, pp. 12349–12376, 2018.

- [13] X. Zhang, F. Han, and Y. Niu, "Chaotic image encryption algorithm based on bit permutation and dynamic DNA encoding," *Computational Intelligence and Neuroscience*, vol. 2017, 11 pages, 2017.
- [14] B. Wang, Y. Xie, S. Zhou, X. Zheng, and C. Zhou, "Correcting errors in image encryption based on DNA coding," *Molecules (Basel, Switzerland)*, vol. 23, no. 8, 2018.
- [15] G. Bachira and N. Khan, "A new hybrid image encryption algorithm based on 2D-CA, FSM-DNA rule generator, and FSBI," *IEEE Access*, vol. 7, pp. 81333–81350, 2019.
- [16] L. Sharp, *DNA Sequencing and Sorting: Identifying Genetic Variations*, COMAP, Bedford, USA, 2015.
- [17] M. Z. Talhaoui, X. Wang, and M. A. Midoun, "A new one-dimensional cosine polynomial chaotic map and its use in image encryption," *The Visual Computer*, pp. 1–11, 2021.
- [18] Z. Hua, B. Zhou, and Y. Zhou, "Sine-transform-based chaotic system with FPGA implementation," *IEEE Transactions on Industrial Electronics*, vol. 65, no. 3, pp. 2557–2566, 2018.
- [19] J. Zhou, N.-R. Zhou, and L.-H. Gong, "Fast color image encryption scheme based on 3D orthogonal Latin squares and matching matrix," *Optics & Laser Technology*, vol. 131, article 106437, 2020.
- [20] A. Javeed, T. Shah, and A. Attaullah, "Lightweight secure image encryption scheme based on chaotic differential equation," *Chinese Journal of Physics*, vol. 66, pp. 645–659, 2020.
- [21] C. R. Logan, O. Mailloux, C. D. Lewis II, and M. R. Grimaila, "Post-quantum cryptography what advancements in quantum computing mean for IT professionals logan," *Cybersecurity And Privacy*, vol. 18, no. 5, pp. 42–47, 2016.
- [22] A. Nanda, D. Puthal, S. P. Mohanty, and U. Choppali, "A computing perspective of quantum cryptography [energy and security]," *IEEE Consumer Electronics Magazine*, vol. 7, no. 6, pp. 57–59, 2018.
- [23] H. Zhang, Z. Ji, H. Wang, and W. Wu, "Survey on quantum information security," *China Communications*, vol. 16, no. 10, pp. 1–36, 2019.
- [24] J. Fridrich, "Symmetric ciphers based on two-dimensional chaotic maps," *International Journal of Bifurcation and Chaos*, vol. 8, no. 6, pp. 1259–1284, 1998.
- [25] Y. Song, Z. Zhu, W. Zhang, H. Yu, and Y. Zhao, "Efficient and secure image encryption algorithm using a novel key-substitution architecture," *IEEE Access*, vol. 7, pp. 84386–84400, 2019.
- [26] Z. Hua, Z. Zhu, S. Yi, Z. Zhang, and H. Huang, "Cross-plane colour image encryption using a two-dimensional logistic tent modular map," *Information Sciences*, vol. 546, pp. 1063–1083, 2021.
- [27] X. Wang, W. Xue, and J. An, "Image encryption algorithm based on tent-dynamics coupled map lattices and diffusion of household," *Chaos, Solitons and Fractals: the interdisciplinary journal of Nonlinear Science, and Nonequilibrium and Complex Phenomena*, vol. 141, pp. 110309–110317, 2020.
- [28] D. S. Malik and T. Shah, "Color multiple image encryption scheme based on 3D-chaotic maps," *Mathematics and Computers in Simulation*, vol. 178, pp. 646–666, 2020.
- [29] G. Hu, D. Xiao, Y. Wang, and X. Li, "Cryptanalysis of a chaotic image cipher using Latin square-based confusion and diffusion," *Nonlinear Dynamics*, vol. 88, no. 2, pp. 1305–1316, 2017.
- [30] A. Hadj Brahim, A. Ali Pacha, and N. Hadj Said, "Image encryption based on compressive sensing and chaos systems," *Optics and Laser Technology*, vol. 132, article 106489, 2020.
- [31] S. Medileh, A. Laouid, E. M. B. Nagoudi et al., "A flexible encryption technique for the internet of things environment," *Ad Hoc Networks*, vol. 106, p. 102240, 2020.
- [32] T. ul Haq and T. Shah, "12×12 S-box design and its application to RGB image encryption," *Optik*, vol. 217, article 164922, 2020.
- [33] Y. Zhang, "The fast image encryption algorithm based on lifting scheme and chaos," *Information Sciences*, vol. 520, pp. 177–194, 2020.
- [34] X. Zhu, H. Liu, Y. Liang, and J. Wu, "Image encryption based on Kronecker product over finite fields and DNA operation," *Optik*, vol. 224, pp. 1–27, 2020.
- [35] Y. Abanda, A. Tiedeu, and G. Kom, "Image encryption with fusion of two maps," *Security and Communication Networks*, vol. 2021, 16 pages, 2021.
- [36] S. T. Kamal, K. M. Hosny, T. M. Elgindy, M. M. Darwish, and M. M. Fouda, "A new image encryption algorithm for grey and color medical images," *IEEE Access*, vol. 9, pp. 37855–37865, 2021.
- [37] G. Zhang, W. Ding, and L. Li, "Image encryption algorithm based on tent delay-sine cascade with logistic map," *Symmetry*, vol. 12, no. 3, p. 355, 2020.
- [38] J. Tang, Z. Yu, and L. Liu, "A delay coupling method to reduce the dynamical degradation of digital chaotic maps and its application for image encryption," *Multimedia Tools and Applications*, vol. 78, no. 17, pp. 24765–24788, 2019.
- [39] L. Liu and S. Miao, "A new simple one-dimensional chaotic map and its application for image encryption," *Multimedia Tools and Applications*, vol. 77, no. 16, pp. 21445–21462, 2018.
- [40] H. S. Ye, N. R. Zhou, and L. H. Gong, "Multi-image compression-encryption scheme based on quaternion discrete fractional Hartley transform and improved pixel adaptive diffusion," *Signal Processing*, vol. 175, p. 107652, 2020.
- [41] Y. Liu, Z. Jiang, X. Xu, F. Zhang, and J. Xu, "Optical image encryption algorithm based on hyper-chaos and public-key cryptography," *Optics and Laser Technology*, vol. 127, article 106171, 2020.
- [42] A. A. Abbasi, M. Mazinani, and R. Hosseini, "Chaotic evolutionary-based image encryption using RNA codons and amino acid truth table," *Optics and Laser Technology*, vol. 132, article 106465, 2020.
- [43] S. Mohammad Seyedzadeh and S. Mirzakuchaki, "A fast color image encryption algorithm based on coupled two-dimensional piecewise chaotic map," *Signal Processing*, vol. 92, no. 5, pp. 1202–1215, 2012.
- [44] S. Cai, L. Huang, X. Chen, and X. Xiong, "A symmetric plaintext-related color image encryption system based on bit permutation," *Entropy*, vol. 20, no. 4, pp. 1–20, 2018.
- [45] M. Asgari-Chenaghlu, M. R. Feizi-Derakhshi, N. Nikzad-Khasmakhi et al., "Cy: chaotic yolo for user intended image encryption and sharing in social media," *Information Sciences*, vol. 542, pp. 212–227, 2021.
- [46] K. C. Jithin and S. Sankar, "Colour image encryption algorithm combining Arnold map, DNA sequence operation, and a Mandelbrot set," *Journal of Information Security and Applications*, vol. 50, article 102428, 2020.
- [47] E. Tanyildizi and F. Ozkaynak, "A new chaotic S-box generation method using parameter optimization of one dimensional chaotic maps," *IEEE Access*, vol. 7, pp. 117829–117838, 2019.
- [48] M. H. Annaby, M. A. Rushdi, and E. A. Nehary, "Color image encryption using random transforms, phase retrieval, chaotic

- maps, and diffusion,” *Optics and Lasers in Engineering*, vol. 103, pp. 9–23, 2018.
- [49] A. Adeel, J. Ahmad, H. Larijani, and A. Hussain, “A novel real-time, lightweight chaotic-encryption scheme for next-generation audio-visual hearing aids,” *Cognitive Computation*, vol. 12, no. 3, pp. 589–601, 2019.
- [50] X. Zhang and X. Wang, “Digital image encryption algorithm based on elliptic curve public cryptosystem,” *IEEE Access*, vol. 6, pp. 70025–70034, 2018.
- [51] R. Ge, G. Yang, J. Wu, L. Luo, and S. Member, “A novel chaos-based symmetric image encryption using bit-pair level process,” vol. 7, pp. 99470–99480, 2019.
- [52] O. Sengel, M. A. Aydin, and A. Sertbas, “An efficient generation and security analysis of substitution box using fingerprint patterns,” *IEEE Access*, vol. 8, pp. 160158–160176, 2020.
- [53] G. Chen, “A novel heuristic method for obtaining  $S$ -boxes,” *Chaos, Solitons Fractals*, vol. 36, no. 4, pp. 1028–1036, 2008.
- [54] Ü. Şavuşoğlu, A. Zengin, I. Pehlivan, and S. Kaçar, “A novel approach for strong S-box generation algorithm design based on chaotic scaled Zhongtang system,” *Nonlinear Dynamics*, vol. 87, no. 2, pp. 1081–1094, 2017.
- [55] N. M. G. Al-saidi, “A new S-box generation algorithm based on multistability behavior of a plasma perturbation model,” *IEEE Access*, vol. 7, pp. 124914–124924, 2019.
- [56] Y. Tian and Z. Lu, “S-box: six-dimensional compound hyperchaotic map and artificial bee colony algorithm,” *Journal of Systems Engineering and Electronics*, vol. 27, no. 1, pp. 232–241, 2016.
- [57] H. A. Ahmed, M. F. Zolkipli, and M. Ahmad, “A novel efficient substitution-box design based on firefly algorithm and discrete chaotic map,” *Neural Computing and Applications*, vol. 11, pp. 1–18, 2019.
- [58] F. Özkaynak, “Construction of robust substitution boxes based on chaotic systems,” *Neural Computing and Applications*, vol. 31, no. 8, pp. 3317–3326, 2019.
- [59] Q. Lu, C. Zhu, and X. Deng, “An efficient image encryption scheme based on the LSS chaotic map and single S-box,” *IEEE Access*, vol. 8, pp. 25664–25678, 2020.
- [60] F. Özkaynak, “From biometric data to cryptographic primitives: a new method for generation of substitution boxes,” in *Proceedings of the 2017 International Conference on Biomedical Engineering and Bioinformatics*, pp. 27–33, Bangkok, Thailand, 2017.
- [61] A. H. Al-wattar, R. Mahmud, Z. A. Zukarnain, and N. I. Udzir, “A new DNA-based S-box,” *International Journal of Engineering & Technology*, vol. 15, no. 4, pp. 1–10, 2015.
- [62] A. H. S. Al-Wattar, R. Mahmud, Z. A. Zukarnain, and N. I. Udzir, “Generating a new S-box inspired by biological DNA,” *International Journal of Computer Science and Application*, vol. 4, no. 1, pp. 32–42, 2015.
- [63] F. A. Kadhim, G. H. A. Majeed, and R. S. Ali, “Proposal new S-box depending on DNA computing and mathematical operations,” in *Al-Sadiq International Conference on Multidisciplinary in IT and Communication Techniques Science and Applications, AIC-MITCSA 2016*, pp. 142–147, 2016.
- [64] A. K. Farhan, R. S. Ali, H. R. Yassein, N. M. G. Al-Saidi, and G. H. Abdul-Majeed, “A new approach to generate multi S-boxes based on RNA computing,” *International Journal of Innovative Computing, Information and Control*, vol. 16, no. 1, pp. 331–348, 2020.
- [65] T. Wang and M. H. Wang, “Hyperchaotic image encryption algorithm based on bit-level permutation and DNA encoding,” *Optics and Laser Technology*, vol. 132, article 106355, 2020.
- [66] A. A. Abd El-Latif, B. Abd-El-Atty, and M. Talha, “Robust encryption of quantum medical images,” *IEEE Access*, vol. 6, pp. 1073–1081, 2018.
- [67] Y. Luo, X. Ouyang, J. Liu, and L. Cao, “An image encryption method based on elliptic curve Elgamal encryption and chaotic systems,” *IEEE Access*, vol. 7, pp. 38507–38522, 2019.
- [68] B. Arpacı, E. Kurt, and K. Çelik, “A new algorithm for the colored image encryption via the modified Chua's circuit,” *Engineering Science and Technology, an International Journal*, vol. 23, no. 3, pp. 595–604, 2020.
- [69] R. Anandkumar and R. Kalpana, “Designing a fast image encryption scheme using fractal function and 3D Henon map,” *Journal of Information Security and Applications*, vol. 49, p. 102390, 2019.
- [70] A. Sahasrabuddhe and D. S. Laiphrakpam, “Multiple images encryption based on 3D scrambling and hyper-chaotic system,” *Information Sciences*, pp. 1–31, 2021.
- [71] A. Banik, Z. Shamsi, and D. S. Laiphrakpam, “An encryption scheme for securing multiple medical images,” *Journal of Information Security and Applications*, vol. 49, article 102398, 2019.
- [72] X. Wang and S. Gao, “Application of matrix semi-tensor product in chaotic image encryption,” *Journal of the Franklin Institute*, vol. 356, no. 18, pp. 11638–11667, 2019.
- [73] C. L. Li, Z. Y. Li, W. Feng, Y. N. Tong, J. R. Du, and D. Q. Wei, “Dynamical behavior and image encryption application of a memristor-based circuit system,” *AEU - International Journal of Electronics and Communications*, vol. 110, article 152861, 2019.
- [74] W. Gao, J. Sun, W. Qiao, and X. Zhang, “Digital image encryption scheme based on generalized Mandelbrot-Julia set,” *Optik*, vol. 185, pp. 917–929, 2019.
- [75] H. Liu, A. Kadir, and J. Liu, “Color pathological image encryption algorithm using arithmetic over Galois field and coupled hyper chaotic system,” *Optics and Lasers in Engineering*, vol. 122, pp. 123–133, 2019.
- [76] H. Wu, J. Wang, Z. Zhang, X. Chen, and Z. Zhu, “A multi-image encryption with super-lager-capacity based on spherical diffraction and filtering diffusion,” *Applied Sciences*, vol. 10, no. 16, p. 5691, 2020.
- [77] L. Ding and Q. Ding, “A novel image encryption scheme based on 2D fractional chaotic map, DWT and 4D hyper-chaos,” *Electronics (Switzerland)*, vol. 9, no. 8, p. 1280, 2020.
- [78] W. Hou, S. Li, J. He, and Y. Ma, “A novel image-encryption scheme based on a non-linear cross-coupled hyperchaotic system with the dynamic correlation of plaintext pixels,” *Entropy*, vol. 22, no. 7, pp. 1–21, 2020.
- [79] J. A. P. Artilles, D. P. B. Chaves, and C. Pimentel, “Image encryption using block cipher and chaotic sequences,” *Signal Processing: Image Communication*, vol. 79, pp. 24–31, 2019.
- [80] Y. Luo, S. Tang, J. Liu, L. Cao, and S. Qiu, “Image encryption scheme by combining the hyper-chaotic system with quantum coding,” *Optics and Lasers in Engineering*, vol. 124, article 105836, 2020.
- [81] A. Alghafis, F. Firdousi, M. Khan, S. I. Batool, and M. Amin, “An efficient image encryption scheme based on chaotic and deoxyribonucleic acid sequencing,” *Mathematics and Computers in Simulation*, vol. 177, pp. 441–466, 2020.

- [82] M. Samiullah, W. Aslam, H. Nazir et al., "An image encryption scheme based on DNA computing and multiple chaotic systems," *IEEE Access*, vol. 8, pp. 25650–25663, 2020.
- [83] W. Xingyuan, Z. Junjian, and C. Guanghui, "An image encryption algorithm based on ZigZag transform and LL compound chaotic system," *Optics and Laser Technology*, vol. 119, 2019.
- [84] L. L. Huang, S. M. Wang, and J. H. Xiang, "A tweak-cube color image encryption scheme jointly manipulated by chaos and hyper-chaos," *Applied Sciences (Switzerland)*, vol. 9, no. 22, p. 4854, 2019.
- [85] Y. Khedmati, R. Parvaz, and Y. Behroo, "2D hybrid chaos map for image security transform based on framelet and cellular automata," *Information Sciences*, vol. 512, pp. 855–879, 2020.
- [86] M. Gafsi, M. A. Hajjaji, J. Malek, and A. Mtibaa, "Efficient encryption system for numerical image safe transmission," *Journal of Electrical and Computer Engineering*, vol. 2020, Article ID 8937676, 12 pages, 2020.
- [87] I. Yasser, F. Khalifa, M. A. Mohamed, and A. S. Samrah, "A new image encryption scheme based on hybrid chaotic maps," *Complexity*, vol. 2020, 23 pages, 2020.
- [88] M. Gafsi, N. Abbassi, M. A. Hajjaji, J. Malek, and A. Mtibaa, "Improved chaos-based cryptosystem for medical image encryption and decryption," *Scientific Programming*, vol. 2020, 22 pages, 2020.
- [89] S. M. Ismail, L. A. Said, A. G. Radwan, A. H. Madian, and M. F. Abu-ElYazeed, "A novel image encryption system merging fractional-order edge detection and generalized chaotic maps," *Signal Processing*, vol. 167, p. 107280, 2020.
- [90] K. K. Butt, G. Li, F. Masood, and S. Khan, "A digital image confidentiality scheme based on pseudo-quantum chaos and Lucas sequence," *Entropy*, vol. 22, no. 11, pp. 1–20, 2020.

## Retraction

# Retracted: Curriculum Design of College Students' English Critical Ability in the Internet Age

### Wireless Communications and Mobile Computing

Received 25 July 2023; Accepted 25 July 2023; Published 26 July 2023

Copyright © 2023 Wireless Communications and Mobile Computing. This is an open access article distributed under the Creative Commons Attribution License, which permits unrestricted use, distribution, and reproduction in any medium, provided the original work is properly cited.

This article has been retracted by Hindawi following an investigation undertaken by the publisher [1]. This investigation has uncovered evidence of one or more of the following indicators of systematic manipulation of the publication process:

- (1) Discrepancies in scope
- (2) Discrepancies in the description of the research reported
- (3) Discrepancies between the availability of data and the research described
- (4) Inappropriate citations
- (5) Incoherent, meaningless and/or irrelevant content included in the article
- (6) Peer-review manipulation

The presence of these indicators undermines our confidence in the integrity of the article's content and we cannot, therefore, vouch for its reliability. Please note that this notice is intended solely to alert readers that the content of this article is unreliable. We have not investigated whether authors were aware of or involved in the systematic manipulation of the publication process.

In addition, our investigation has also shown that one or more of the following human-subject reporting requirements has not been met in this article: ethical approval by an Institutional Review Board (IRB) committee or equivalent, patient/participant consent to participate, and/or agreement to publish patient/participant details (where relevant).

Wiley and Hindawi regrets that the usual quality checks did not identify these issues before publication and have since put additional measures in place to safeguard research integrity.

We wish to credit our own Research Integrity and Research Publishing teams and anonymous and named external

researchers and research integrity experts for contributing to this investigation.

The corresponding author, as the representative of all authors, has been given the opportunity to register their agreement or disagreement to this retraction. We have kept a record of any response received.

### References

- [1] J. Shen, Y. Chen, and J. Lin, "Curriculum Design of College Students' English Critical Ability in the Internet Age," *Wireless Communications and Mobile Computing*, vol. 2022, Article ID 5609450, 7 pages, 2022.



## Research Article

# Curriculum Design of College Students' English Critical Ability in the Internet Age

Jie Shen,<sup>1</sup> Yukun Chen,<sup>2</sup> and Jiaxin Lin <sup>1</sup>

<sup>1</sup>School of Foreign Languages, Guangdong University of Finance and Economics, Guangzhou 510655, China

<sup>2</sup>School of Humanities, Nanyang Technological University, Singapore, Singapore 639798

Correspondence should be addressed to Jiaxin Lin; [jasonlin@gdufe.edu.cn](mailto:jasonlin@gdufe.edu.cn)

Received 25 January 2022; Revised 15 February 2022; Accepted 24 February 2022; Published 18 March 2022

Academic Editor: Shalli Rani

Copyright © 2022 Jie Shen et al. This is an open access article distributed under the Creative Commons Attribution License, which permits unrestricted use, distribution, and reproduction in any medium, provided the original work is properly cited.

“Speculation” is considered to be one of the important qualities that modern students should possess, and it is also the goal of modern education. With the advent of the Internet age, teaching models have been continuously combined with technology. From mixed teaching to flipped classroom, teaching with different methods of information transmission can achieve the best results. This paper is aimed at studying the curriculum design of college students' English critical thinking ability in the Internet era. On the basis of analyzing the significance of cultivating college students' critical thinking ability and the curriculum design of critical thinking ability, the flipped classroom mode is used for teaching practice through the experimental method and questionnaire survey method. The personality tendency and the cultivation of students' critical thinking ability in the flipped classroom were analyzed statistically. Finally, it was concluded that the students' critical thinking skills have been improved to a certain extent through the various links set in the flipped classroom teaching.

## 1. Introduction

In the global economy, the competition for talents is fierce, and exercising the practical ability of applying English can better improve the international competitiveness of our talents. Due to the long-term test-oriented education, college students lack the ability to think critically and creatively in English, and the content is monotonous. Therefore, how to effectively cultivate college students' English critical thinking ability is extremely important [1, 2].

More and more experts and scholars are interested in the research of speculative ability. Quattrucci introduced a new method of teaching advanced laboratories at the undergraduate level. The purpose of this method is to allow students to participate more in laboratory experience and apply speculative skills to solve problems [3]; Matos et al. stated that speculative skill education has always been a growing concern in the context of Portuguese higher education. The field is designed to meet the demands of the labor market and the most demanding and complex social challenges. However,

there is a lack of systematic literature review studies to describe teachers' use of different speculative education practices [4]; Ulger proposes that problem-based learning methods are implemented. A one-semester treatment method for higher education visual arts students was proposed. One examines its influence on the creative thinking and critical thinking tendency of these students. The problematic learning method has a significant influence on creative thinking, but has little influence on critical thinking tendency [5]; Colln-Appling and Giuliano said that the ability to succeed in speculative skills has a significant impact on the decision-making process. Critical ability is a concept that is difficult to embed in nursing courses, and it needs continuous practice to improve professional ability and improve professional future ability [6]. The research on the problem of English critical thinking at home and abroad is still in its infancy. In the teaching of English as a subject, articles on how to cultivate students' critical thinking ability, improve the effectiveness of English teaching, and promote students' long-term development are still relatively few.

Therefore, this paper intends to study this topic in depth, hoping to give scientific guidance to the future teaching practice.

Compared with foreign researchers, this paper mainly analyzes and practices the significance of cultivating college students' critical thinking ability and the course design of critical thinking ability. The flipped classroom model is used for teaching practice, and the students' thinking personality tendency and the cultivation of students' critical thinking ability in flipped classroom are carried out. Through statistical analysis, it is concluded that students' critical thinking skills have been improved to a certain extent through the various links set up in the flipped classroom teaching.

## 2. Curriculum Design of College Students' English Critical Ability in the Internet Age

### 2.1. The Significance of Cultivating College Students' Thinking Ability

*2.1.1. Help Stimulate Students' Interest in Learning.* English teachers cultivate students' thinking skills in the classroom, so that all students can fully integrate into the classroom and actively participate in classroom activities, so that students have a strong interest in English courses. The most taboo in English teaching is that teachers blindly explain and preach. In order to make the classroom full of vitality and make students feel happy, English teachers need to constantly inspire and motivate students in the classroom, stimulate students' interest in learning, use speculative teaching methods to activate the original boring English, analyze the meaning of things, and look at things dialectically [7, 8].

*2.1.2. Help Students Consolidate Their Internalized English Subject Knowledge.* English teachers cultivate students' thinking skills in English classes, help students consolidate their knowledge of ideological and political issues, and actively establish a knowledge system. On the basis of thinking and analysis, he constantly processes and processes the knowledge he has learned and constantly internalizes him to form his own independent and stable cognitive structure and way of thinking. Teachers do not need unnecessary guidance. The teaching content in students' hearts has been internalized and externalized into action, and students' thinking ability has also been improved [9, 10].

*2.1.3. Help Students Develop the Spirit of Questioning and Innovation.* Teachers should guide and cultivate students' logical thinking ability in English class, let our students participate personally, and make our students truly become the main body in the classroom based on students' practice. This is conducive to the performance and display of the students' personality and give play to their strengths. Teachers must first focus on stimulating and guiding students to think independently and provide some incentives for their students' logical thinking and put forward their own views, and cultivating students' logical thinking ability is conducive to promoting the democratic equality between students and

teachers, promoting students' sense of innovation, and enhancing students' challenge spirit [11, 12].

### 2.2. Curriculum Design for Cultivating Thinking Ability

#### 2.2.1. Preclass Learning Task Design

*(1) Task List for Self-Study before Class.* The preview before the flipped classroom is a task assigned by the teacher, such as completing exercises related to the content of the video resource. However, students may not be able to complete the exercise correctly after watching the microclass video. This is okay, because the purpose of this exercise is to tell the teacher that the student has a problem, just like giving the student a pulse. The homework completed by the students must be handed over to the teacher before the class, which can be achieved with the help of an information technology platform. As an expert in a certain field, teachers may have forgotten the difficulties that beginners face when they are exposed to new knowledge, so the task before flipping the classroom is to help teachers understand the problems of students.

*(2) Students Study Independently before Class, and Teachers Collect Feedback on Questions.* After students receive the preclass self-study materials and self-study homework list, follow the instructions in the preclass self-study homework list to watch the instructional video and complete the homework on the self-study homework list. Teachers can track and guide students' autonomous learning through the network platform and understand the problems students face when participating in classroom learning. The teacher collects the tasks completed by the students and the related exercises of the self-study task list, summarizes the problems faced by the students and the suggestions made by the students, and prepares for the next step of classroom teaching.

*2.2.2. Organization of Teaching Activities in Class.* In this paper, the teaching activities in the flipped classroom are designed as the following links, and the process is shown in Figure 1.

*(1) Warm-Up before Class.* The warm-up activities before class enable students to prepare themselves and learn some new knowledge well and to participate in the following learning activities wholeheartedly, attracting the interest and attention of the majority of students. Teachers can fully attract the interest and attention of teachers and students by quoting content and methods that are closely related to the content of the course teaching, mobilize their interest and curiosity, and promote the initiative and enthusiasm of teachers and students to participate in classroom activities. At the same time, in the warm-up and exploration part of the preclass content in this flipped classroom, teachers can guide students to carefully review all self-study content before class through oral questions and form a feedback for students through reflection and feedback to prepare for occasional problems.

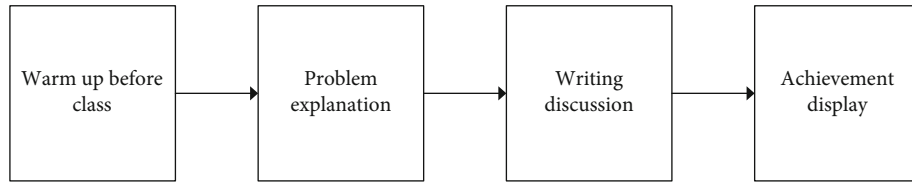


FIGURE 1: Flipped classroom activity flow chart.

TABLE 1: Pretest analysis of the status quo of students' speculative personality tendency.

	Minimum	Maximum	Average per question	Standard deviation
Analytical	18.00	29.00	4.924	3.132
Curiosity	22.00	33.00	5.044	3.856
Toughness	14.00	26.00	4.237	3.275
Confidence	22.00	30.00	4.058	2.702
Truth-seeking	12.00	34.00	3.069	6.301
Maturity	13.00	30.00	3.034	4.237
Openness	14.00	26.00	3.316	4.297
Sense of justice	14.00	29.00	3.797	4.567

TABLE 2: Posttest analysis of the status quo of students' speculative personality tendency.

	Minimum	Maximum	Average per question	Standard deviation
Analytical	14.00	29.00	4.991	4.283
Curiosity	19.00	35.00	5.052	4.723
Toughness	12.00	26.00	4.247	3.338
Confidence	15.00	34.00	4.133	5.078
Truth-seeking	14.00	28.00	3.205	3.666
Maturity	17.00	35.00	3.170	4.708
Openness	14.00	35.00	3.401	4.286
Sense of justice	14.00	28.00	3.942	3.281

(2) *Problem Explanation.* When a student starts self-study before class, due to the differences in the knowledge structure and the level of their cognitive abilities between different students, the different knowledge of the students may also be different, which leads to some cognitive errors and imbalances between them. In the flipped education classroom of this article, students can be the main participants in classroom teaching and activities. The teacher will use our students in the whole process of self-observation and the difficult points collected in the classroom study as cases to illustrate. These cases are encountered by all students in the process of self-study. The students are quite aware of the content and have strong personal emotions. Through discussion with teachers, students can gradually form new knowledge in the constant unbalance of understanding and realize the understanding and internalization of knowledge.

(3) *Collaborative Discussion.* Once students solve the existing problems, they can deepen their knowledge through communication and mutual assistance between students, thus forming their own cognitive structure and knowledge system. According to the traditional teaching model, students complete their homework independently after class and cannot communicate with peers and get help in a timely manner when encountering difficulties. At this point, they will realize that they cannot complete the task entirely on their own, so their confidence in learning will be affected. The teaching activities in the flipped classroom of this article will create a bond of help and mutual assistance for students and enhance students' confidence in completing learning tasks through peer communication and collaboration.

(4) *Display of Results.* After cooperation and mutual assistance, teachers guide students to share and evaluate the results of their study or group. Students summarize the results of individuals and groups, select group representatives to show their learning results, and can also ask questions worthy of in-depth discussion. Through in-depth discussion of the problems, the in-depth understanding and absorption of knowledge can be further promoted. At the same time, through the exchange of results between groups to further promote exchanges between students and through mutual evaluation between groups to enhance the recognition of group results, students can experience the satisfaction and sense of completion of learning in shared sharing.

### 3. Experiment

3.1. *Survey Method.* This article selects a class of non-English majors in a university as the research object, a total of 50 people, including 9 boys and 41 girls. This class serves as both the experimental group and the control group. The selected experimental mode is the single-factor single-group pretest and posttest experimental mode. This article conducts experiments in a real environment to explore whether the flipped classroom model can cultivate students' thinking ability. Before the experiment, this article will use the questionnaire survey method to grasp the students' attitudes towards college English courses and the understanding of the flipped classroom teaching mode, which will be used as the basis for observing the changes in students' thinking ability after the flipped classroom teaching is implemented. After the experiment, a questionnaire was designed for different links in the teaching practice to analyze the changes in students' thinking ability before and after the teaching experiment.

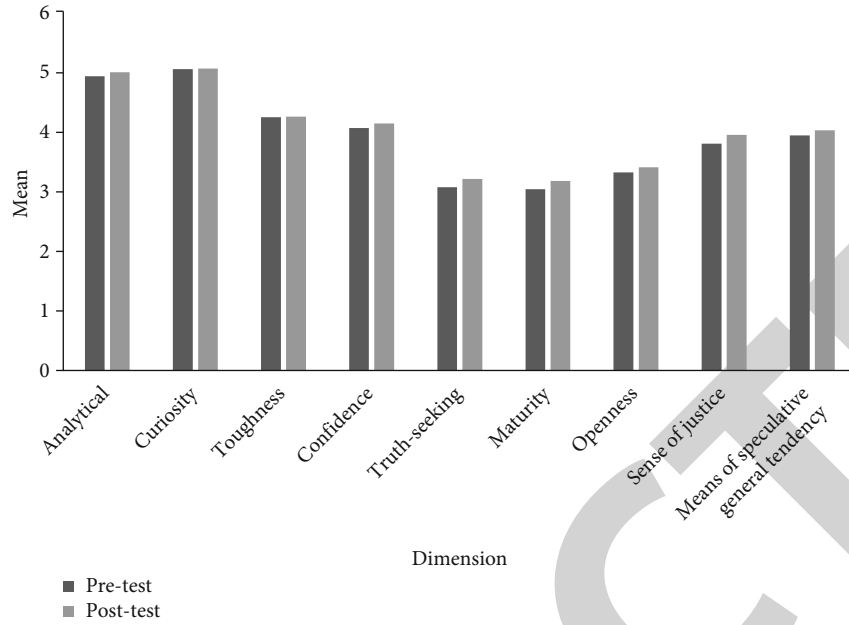


FIGURE 2: Changes in the dimensions of speculative personality tendency and total speculative ability.

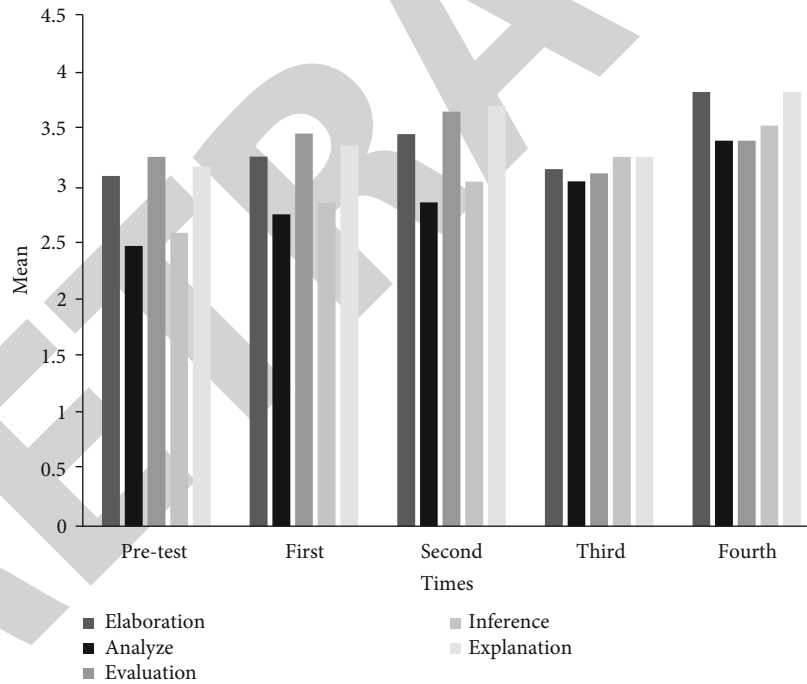


FIGURE 3: Analysis of the overall level of students' thinking ability.

3.2. *Questionnaire Reliability Test.* In order to test the reliability and stability of the questionnaire, the variance of the questionnaire results was first calculated, and then the reliability of the returned questionnaire was tested by the method of “half-half reliability”. Using formula (1) to calculate the reliability coefficient, the correlation coefficient of the questionnaire is  $r = 0.883$ . According to the theories and methods of modern scientific research, when the reli-

ability of a test reaches 0.80 or more, it can be regarded as a test with higher reliability. The test results confirm that the questionnaire is reliable.

$$S^2 = \frac{(M - X_1)^2 + (M - X_2)^2 + (M - X_3)^2 + \dots + (M - X_n)^2}{n}, \tag{1}$$

TABLE 3: Analysis of the overall level of students' thinking ability.

	Elaboration	Analyze	Evaluation	Inference	Explanation	Total value of thinking ability
Pretest	3.082	2.466	3.249	2.582	3.166	14.55
First	3.253	2.744	3.455	2.846	3.349	15.65
Second	3.449	2.849	3.649	3.033	3.699	16.68
Third	3.142	3.034	3.106	3.249	3.249	15.78
Fourth	3.820	3.392	3.392	3.525	3.820	17.95
Overall	3.349	2.897	3.370	3.047	3.457	16.12

$$r = 1 - S^2 \frac{(1 - r_1)}{S_n^2}, \quad (2)$$

$$r = \frac{2r_{\text{ban}}}{1 + r_{\text{ban}}}. \quad (3)$$

## 4. Discussion

*4.1. Analysis of the Status Quo of College Students' Speculative Personality Tendency.* Table 1 shows that the total value of students' speculative personality tendencies is  $3.935 < 4$ , so students have negative speculative personality tendencies. However, the analysis, curiosity, tenacity, and self-confidence of these eight dimensions have an average value of  $>4$  for each question, which means that these four dimensions have a positive thinking personality tendency. Among them, the subjects' curiosity score was 5.044, which was higher than the other several dimensions. Analytical is second, with an average value of 4.925. It can also be seen from this data that students' truth-seeking and cognitive maturity are relatively low, with the average values being 3.069 and 3.034, respectively.

It can be seen from Table 2 that the total value of students' speculative personality tendencies is  $4.018 > 4$ , so students have positive speculative personality tendencies. And the average value of each question of analytical, curiosity, tenacity, and self-confidence in these eight dimensions is  $>4$ , which means that these four dimensions also have a positive thinking personality tendency. Among them, the average score of subjects' curiosity was 5.052, which was higher than the other several dimensions. Analytical is second, with an average value of 4.99. It can also be seen from these data that students' truth-seeking and cognitive maturity are relatively low, with the average values being 3.205 and 3.170, respectively.

As can be seen from Figure 2, it can be seen from the comparison of the pre- and posttest that the posttest values of the eight dimensions are all larger than the pretest values, and compared with the pretest values, the posttest mean of the total speculative tendency is also improved. Among these eight dimensions, students have the highest mean values of curiosity and self-confidence, while the mean values of students' authenticity and maturity are relatively low. The other dimensions are not much different.

*4.2. The Overall Situation and Trend Changes of College Students' Thinking Ability.* In order to test whether the flipped classroom can cultivate students' thinking ability,

TABLE 4: Average statistics of self-regulation and affective traits.

Times mean	Self-regulation pretest	Self-regulation posttest	Pretest of emotional traits	Emotional traits posttest
First test	2.852	3.274	2.592	3.232
Second test	3.027	3.899	2.677	3.601
Third test	3.299	3.943	2.916	3.619
Fourth test	3.370	4.000	3.250	3.681

this article presents the average of the total scores of the thinking ability and the scores of various subskills in the four English tests.

According to the scoring standard, the full score of speculative skills is 25 points, and the maximum score of each subskill is 5 points. In order to observe the changes of each speculative subskill and the total value of speculative skills in the 4 tests, Figure 3 can be used to judge.

From Table 3 and Figure 3, it can be seen that in the first two tests, students' thinking skills increased from  $\bar{15.65}$  to  $\bar{16.68}$  and the average score of interpretation and evaluation skills was the highest, but the average score of students' analytical skills was the lowest. In the third test, some subskills of students showed a downward trend, especially in evaluation and interpretation. However, in the fourth test, the average value of the students' speculative subskills increased from 15.78 to 17.95.

*4.3. The Changing Trend of College Students' Self-Regulation and Emotional Traits.* In this article, in addition to the analysis of the overall situation of speculative skills and various subskills, the trend of self-regulation and students' emotional characteristics is also studied, and it is hoped that through their changes, we can judge whether process-flipping classroom teaching can improve students' performance. Table 4 uses data to study the changes in the self-regulation and emotional characteristics of students' writing.

In order to observe the changes of self-regulation and emotional characteristics in the four English tests more intuitively, Figure 4 can be used to judge.

Table 4 and Figure 4 show that in the first test, the students' self-regulation and emotional traits were 2.852 and 2.592 in the pretest, and the posttest averages were 3.274

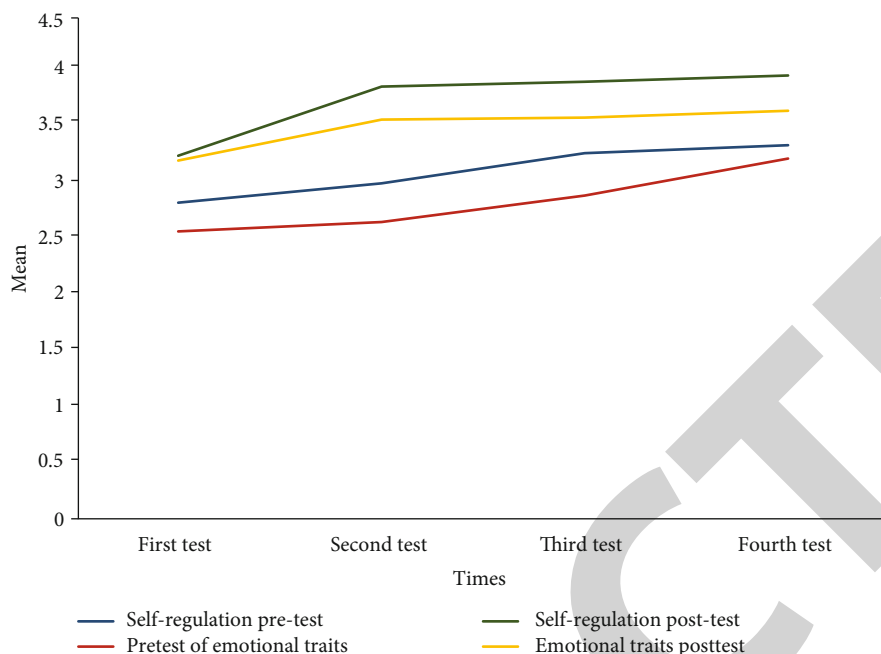


FIGURE 4: Average statistics of self-regulation and affective traits.

TABLE 5: The limitations of the existing works.

Serial number	Limitation
1	The number of the students being tested in the research is relatively small
2	The development of students' critical thinking ability is only carried out in college English classrooms as a different classroom activity, and this classroom activity only takes up a small part of each class

and 3.232; in the second test, the pretest averages of students' self-regulation and emotional traits were 3.027 and 2.677, and the posttest averages were 3.899 and 3.601; in the third test, the pretest averages of students' self-regulation and emotional traits were 3.299 and 2.916, and the posttest averages were 3.943 and 3.619; in the fourth test, the pretest averages of students' self-regulation and emotional traits were 3.370 and 3.250, and the posttest averages were 4.000 and 3.681. The four sets of data clearly show that the average of self-regulation and emotional traits has improved in the four tests and the average of the posttest is greater than the average of the pretest.

## 5. Conclusions

Today, the Internet has completely penetrated into our daily lives. The "Internet+" teaching strategy covers the shortcomings of traditional teaching, enriches teaching methods, expands teaching content, optimizes teaching evaluation, and more effectively carries out student education. Aiming at the difficulties and doubts of traditional classrooms, flipped classrooms are used to fully build students' learning, analysis, and evaluation abilities; guide students to learn and explore independently; and cultivate high-level thinking skills.

## 6. Limitation and Suggestions for the Further Research

**6.1. Limitation.** In this paper, there are still some limitations in the research on the subject of English critical thinking ability course design for college students in the Internet era. The specific performance is shown in Table 5.

**6.2. Suggestions.** The above limitations should be avoided in future research, and it should also be noted that despite such limited time, students' critical thinking is still greatly improved. Therefore, if the training time is prolonged, the students' critical thinking deficit will be greatly improved.

### Data Availability

The data underlying the results presented in the study are available within the manuscript.

### Disclosure

We confirm that the content of the manuscript has not been published or submitted for publication elsewhere.

## *Retraction*

# **Retracted: Supply Chain Management System for Automobile Manufacturing Enterprises Based on SAP**

### **Wireless Communications and Mobile Computing**

Received 25 July 2023; Accepted 25 July 2023; Published 26 July 2023

Copyright © 2023 Wireless Communications and Mobile Computing. This is an open access article distributed under the Creative Commons Attribution License, which permits unrestricted use, distribution, and reproduction in any medium, provided the original work is properly cited.

This article has been retracted by Hindawi following an investigation undertaken by the publisher [1]. This investigation has uncovered evidence of one or more of the following indicators of systematic manipulation of the publication process:

- (1) Discrepancies in scope
- (2) Discrepancies in the description of the research reported
- (3) Discrepancies between the availability of data and the research described
- (4) Inappropriate citations
- (5) Incoherent, meaningless and/or irrelevant content included in the article
- (6) Peer-review manipulation

The presence of these indicators undermines our confidence in the integrity of the article's content and we cannot, therefore, vouch for its reliability. Please note that this notice is intended solely to alert readers that the content of this article is unreliable. We have not investigated whether authors were aware of or involved in the systematic manipulation of the publication process.

Wiley and Hindawi regrets that the usual quality checks did not identify these issues before publication and have since put additional measures in place to safeguard research integrity.

We wish to credit our own Research Integrity and Research Publishing teams and anonymous and named external researchers and research integrity experts for contributing to this investigation.




The corresponding author, as the representative of all authors, has been given the opportunity to register their agreement or disagreement to this retraction. We have kept a record of any response received.

### **References**

- [1] P. Lin, M. Shu, B. Hsu, C. Hu, and J. Huang, "Supply Chain Management System for Automobile Manufacturing Enterprises Based on SAP," *Wireless Communications and Mobile Computing*, vol. 2022, Article ID 5901633, 10 pages, 2022.

## Research Article

# Supply Chain Management System for Automobile Manufacturing Enterprises Based on SAP

Pao-Ching Lin,<sup>1</sup> Ming-Hung Shu ,<sup>2,3</sup> Bi-Min Hsu,<sup>4</sup> Chien-Ming Hu ,<sup>2</sup>  
and Jui-Chan Huang <sup>5</sup>

<sup>1</sup>Chizhou University, Anhui 247000, China

<sup>2</sup>Department of Industrial Engineering and Management, National Kaohsiung University of Science and Technology, Kaohsiung City 80778, Taiwan

<sup>3</sup>Department of Healthcare Administration and Medical Informatics, Kaohsiung Medical University, Kaohsiung City 80708, Taiwan

<sup>4</sup>Department of Industrial Engineering and Management, Cheng Shiu University, Kaohsiung City 83347, Taiwan

<sup>5</sup>Yango University, Fuzhou, 350015 Fujian, China

Correspondence should be addressed to Chien-Ming Hu; [i108143101@nkust.edu.tw](mailto:i108143101@nkust.edu.tw)

Received 7 January 2022; Revised 22 February 2022; Accepted 7 March 2022; Published 18 March 2022

Academic Editor: Shalli Rani

Copyright © 2022 Pao-Ching Lin et al. This is an open access article distributed under the Creative Commons Attribution License, which permits unrestricted use, distribution, and reproduction in any medium, provided the original work is properly cited.

The heavy-duty truck industry has always been regarded as an “economic vane,” and as the carrier of production materials, its degree of cold and heat can better reflect the quality of the macroeconomic environment. The SAP system is currently the ERP software with the largest functions and the most sales and has been widely used by large domestic and foreign manufacturing enterprises. Because of its specific development for enterprises, it is also the most expensive ERP software in the world. This research integrates the existing information resources, takes SAP (system applications and products in data processing) system as the enterprise’s information platform, unifies the information platform into SAP system by integrating the existing information resources (financial system, logistics system, cost control system, production control system, etc.), avoids the information island phenomenon as far as possible, and finally realizes the integrated and unified enterprise information management, which is convenient for the rapid traceability of historical data, providing the best decision analysis method for managers. It is possible to eliminate all non-value-added operations in the value chain, find out the point of cost reduction and efficiency increase, comprehensively optimize the production value chain, improve production efficiency, and finally achieve the purpose of this book. The project implementation of automobile company adopts independent minicomputer system (HP server), with SAPR/3 system as the core and C/S (customer/service) architecture, so as to gradually expand the system function in the future. From the comparison before and after the launch of the SAP project, the above two indicators have increased by 1.5 times, the order fulfillment rate has increased from 30% to 45%, and the timely delivery rate has increased from 60% to 90%. Effective cost control can reduce costs, produce products with larger output and better quality at the same cost, and enable enterprises to maintain an advantage in the competition; effective cost control can also enable enterprises to develop a variety of configurations at the same cost. Products meet the individual needs of customers. The design of this article makes the company’s supply, production planning, logistics, and demand synchronized and integrated.

## 1. Introduction

Based on the solution, implementation model and elements of the SAP system activity-based costing method, as well as the implementation method of each element in the module, formulate the implementation standard and standard determination method of each element in the module and find

and analyze new solutions and existing cost accounting methods. The average interest rate of automobile manufacturing industry is reduced. In order to make the enterprise have enough competitiveness and healthy long-term development, it is more important to improve the inventory management level and reduce the enterprise cost. Many production-oriented enterprises are faced with the



common problems, such as production shortage and waiting for materials, excessive inventory reserve, low inventory turnover rate, and serious sluggish phenomenon. Inventory proportion is high, there are many kinds, and the management is difficult, so the research on inventory management of automobile manufacturing enterprises has extensive reference significance [1]. Financial general ledger (manually processed business accounting vouchers, which can be queried through subject details), detailed data (supply chain module picking details, income details, etc.), and cost drivers are calculated through statistical indicators under the activity-based costing method and other data.

This study selects the successful case of SAP management system implemented by a medium-sized car manufacturer, an automobile company, to analyze its successful experience, hoping to inspire and help similar enterprises. Relatively speaking, the level of manufacturing industry in developed countries and regions is higher than that in developing countries. According to the actual situation of automobile manufacturing plants, the existing logistics distribution system is integrated, and a set of more suitable overall solution for automobile production control and logistics distribution system is formulated, which lays a good foundation for improving the level of workshop control and logistics management [2]. This research puts forward the safeguard measures for automobiles to implement the standard activity-based costing method from four aspects: enterprise organization, activity-based costing system, personnel management and training, and implementation process.

With the substantial improvement of production technology and management level, the automobile market and consumption environment have been greatly improved, heralding the arrival of China's automobile consumption era. Croxton et al. provided the strategy and operation description of each of the eight supply chain processes determined. Although he provides a series of opportunities for researchers to further develop the field, the research process lacks data [3]. The main purpose of Samaranayake is to document the research related to the development of the conceptual framework of the supply chain. The framework he proposed is based on a unified structured technology, which combines the bill of materials, warehouse list, project network, and operation routes in the manufacturing and distribution network into one structure. He described the framework and illustrated digital examples in the manufacturing and distribution environment. Each network in the supply chain in his research provides integrated methods for planning and executing many components and can provide visibility, flexibility, and maintainability but is not certain to further improve the supply chain environment [4]. Wu believes that as the traditional supply chain becomes more and more intelligent, there is an unprecedented opportunity. He researches and explores the status quo and remaining issues of intelligent supply chain management. In addition, five key research topics were formulated and studied. According to the review questions defined in the research, he reviews, classifies, and analyzes the research in the above-mentioned subject areas. Although the topic of convergence of atoms and numbers in his

research has attracted more and more attention [5], Gold mentioned that the endorsement of the point of view may dissolve the firm pursuit of profit and other economic performance goals in order to recall the real problem. Although he discussed how far the acknowledged theoretical point of view has taken root in the European institutionalized corporate social relations tradition, it cannot be regarded as a rediscovery of the true European manufacturing business [6]. With the increasing awareness of environmental protection in countries around the world, the auto industry is bound to face new rectifications and challenges. For auto companies, how to effectively control costs during their operations is an important issue that cannot be ignored.

How to scientifically select suppliers as strategic partners of enterprises, strengthen information sharing and information exchange capabilities between enterprises and suppliers, and achieve seamless connection of supply chain systems has gradually become a new demand for enterprise procurement management. This study mainly discusses the design and implementation of supply chain management system for automobile manufacturing enterprises based on SAP. This research integrates the existing information resources, takes SAP system as the enterprise's information platform, unifies the information platform into SAP system by integrating the existing information resources (financial system, logistics system, cost control system, production control system, etc.), avoids the information island phenomenon as far as possible, and finally realizes the integrated and unified enterprise information management, which is convenient for the rapid traceability of historical data, providing the best decision analysis method for managers. The project implementation of automobile company adopts independent minicomputer system (HP server), with SAPR/3 system as the core and C/S (customer/service) architecture, so as to gradually expand the system function in the future. According to the idea of ERP (Enterprise Resource Planning) management system and combined with the actual situation of the enterprise, the functions of the system include warehouse area management, material basic information management, inventory operation management, inventory operation management, and statistical query management. The process of material information input can transfer material master data information with SAP system through blockchain technology. This study is helpful to provide guidance for the long-term development of enterprises. From the perspective of sustainable supply chain partnership, the determination principles of sustainable supply chain partners and the main factors affecting partner selection can be analyzed, and the evaluation index system of sustainable supply chain partner selection is established accordingly.

## 2. Supply Chain Management of Automobile Manufacturing Enterprises

2.1. SAP. SAP (system applications and products in data processing, data processing systems, applications, and products) is the leader among ERP software vendors. SAPR/3 system (SAP's flagship product) is a standard enterprise ERP application system product. Its main function modules

include SD (sales and distribution), MM (material management), PP (production planning), PM (factory maintenance), HR (human resources), and FICO (finance and cost) [7]. The types of production operations supported by SAP ERP are make-to-order, batch production (mass production), contract production, discrete-type production (discrete type), make-to-stock (production by inventory), and so on. Its due industries include automotive, electronics, steel, chemical, and electrical manufacturing. The various functional modules of SAPR/3 have good solutions in many aspects of enterprise management. The SAPR/3 module is structured and can meet the unique needs of enterprise data processing. It is a comprehensive and standard ERP software product [8]. The SAP system is shown in Figure 1. In the B/S mode, the user requests access to many servers distributed on the network through the browser, the browser's request is processed by the server, and the processing result and corresponding information are returned to the browser; other data processing and requests are all done by web server.

In the manufacturing resource system, whether in space or time, the force driving the movement of manufacturing resources should be consistent with the gradient direction of manufacturing resource potential [9]. Therefore, the potential energy of manufacturing resources can be expressed as

$$dM = f(dv, dp, dH). \quad (1)$$

Among them,  $dM$  is the potential energy of manufacturing resources, and  $dH$  is the change of manufacturing resource potential [10]. According to system resource optimization configuration requirements, let

$$p(T) = \sum_{i=1}^n p_i M_i, \quad (2)$$

$$F_1 = e^{-rt} [a_1 F_s + a_2 F_E + a_3 F_0].$$

Among them,  $F_1$  is the value of manufacturing asset  $F$ , which is [11, 12]

$$F = \lambda_1 + \sum_{m=t}^M a_m \frac{Y}{Y_m}. \quad (3)$$

The optimal combination model of production unit resources is established [13].

$$H(X) = e^{\lambda} \prod_{n=1}^N X_n^{a_n}, \quad (4)$$

$$\frac{F}{F_i} = \varphi_i + \sum_{n=1}^N A_n \frac{X}{X_i}.$$

**2.2. Supply Chain.** Sustainable supply chain management has developed into a unique research field at an exponential rate, but its progress in sustainability has been quite slow, and it has guided companies to integrate sustainability into their operations and supply chains [14]. The theoretical basis for coherence is still missing [15]. According to the funding gaps

occurring at different stages in the supply chain process, different forms of financing models can be obtained [16, 17].

$$F_i(X) = e^{\lambda} \prod_{n=1}^N X_n^{a_n}. \quad (5)$$

$F$  is the number of products [18].

$$P = \lambda_i + \sum_{n=1}^N B_n F. \quad (6)$$

Among them,

$$\begin{aligned} F_t &= F_{i,t+1} - F_{i,t}, \\ X_i &= X_{i+1}. \end{aligned} \quad (7)$$

Determine parameter  $a$  by regression identification or DEA method, and set the macroscopic effect function of the  $q$ -level system [19]:

$$H_q(X, t) = \int_0^T e^{-rt} [A_1 P_E + a A_2 P_E + A_3 P_0] F dt + X t. \quad (8)$$

Among them,  $r$  is the bank interest rate, which mainly considers the time value of resource allocation [20]. Then,

$$A = \left[ \frac{F_i}{e^{\lambda_i t} \prod_{n=1}^N P/P_i \alpha} \right]^F. \quad (9)$$

Defined by the resource structure [21]

$$\frac{Y}{Y_i} = \frac{Y_1}{Y_m} + \frac{H}{H_m}. \quad (10)$$

$Y$  is the resource allocation structure [22].

$$Q_E = \frac{1}{\sum_{n=1}^N a_n} \left( \frac{X}{X_m} \sum_{n=1}^N A + \sum_{n=1}^N \frac{S_i}{S} + A \sum_{n=1}^N \frac{P}{P_i} + K \right). \quad (11)$$

Suppose  $K$  is the unit at  $i$  time, then [23, 24]

$$\Delta R = W_t + \Delta N_t + D_t = W_t + \frac{R_1}{R} \Delta R + D_t. \quad (12)$$

### 3. Experiment of Supply Chain Management System for Automobile Manufacturing Enterprises

**3.1. System Design Scheme.** Integrate the existing information resources, and use the SAP system as the enterprise information platform. By integrating the existing information resources (financial system, logistics system, cost control system, etc.), try to avoid the phenomenon of information islands, and finally realize integrated and unified enterprise information management, which facilitates

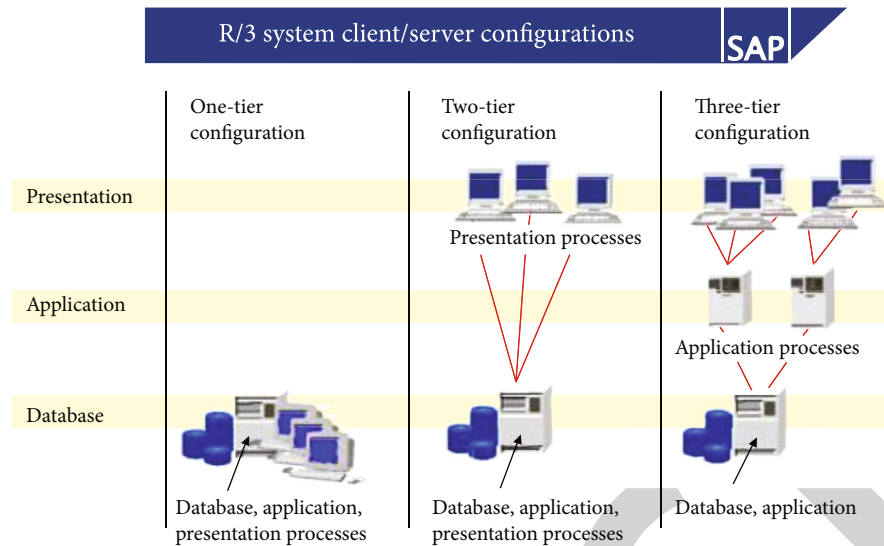


FIGURE 1: SAP system (<http://alturl.com/x8bn6>).

the rapid system for automobiles and determines to implement the five modules of FI, CO, PP, MM, and SD first.

The following departments are mainly involved in the implementation process:

- (1) Financial system: finance department: manage the finance and cost control of the automobile company
- (2) Production system

① Production department: responsible for coordinating the sales plan of the sales company, formulating the production plan of the stamping branch, welding branch, painting branch, and assembly branch of the automobile company, and making statistics on the implementation of the production plan

② Purchasing and supply department: responsible for the procurement business and managing the suppliers of a certain automobile company

③ Logistics department: responsible for the management of warehouse operations and logistics distribution of each branch

④ Manufacturing plant (final assembly branch, painting branch, welding branch, stamping branch, online library within each production plant, and work-in-process library between each production plant)

- (3) Procurement system

① Purchasing and supply department: supplier management and development, procurement contract maintenance, and procurement business

② Logistics department: responsible for managing warehouse operations and logistics distribution of each branch

- (4) Sales system: the sales company of the automobile company is a sales department dedicated to final consumers. However, in this project, the sales company does not implement sales and distribution ser-

vices for the time being. The main function of the sales system is to sell the products of the manufacturing company to the catalog company and to distribute the catalog. The whole vehicle purchased by the company is sold to the sales company

- (5) Other departments

① Technical department: master data management, including material master data, BOM, work center, and process route

② Operation management office: information system, performance appraisal, and comprehensive management

- ③ Quality department: supplier quality management

**3.2. System Architecture Design.** The project implementation of the automobile company adopts an independent minicomputer system (HP server and SAPR/3 system as the core), adopts C/S (customer/service) architecture, and gradually expands system functions in the future (B/S structure). Some of the notable advantages of the company are simple optimization and faster and more convenient system upgrades; no matter how many clients need to be upgraded, you only need to upload the required plugins online; the information is fully shared and transparent, not only the inventory information between the various departments of the enterprise sharing, and suppliers can also see all shipping information, avoiding a lot of disputes caused by missing information; network requirements are reduced, saving internal hardware requirements of the enterprise, you can directly query the required data on the browser, and you do not need to store a lot of data yourself. From a comprehensive analysis point of view, the use of the B/S structure is more able to meet the needs of enterprise operation and management. Here, the B/S structure needs to be enabled, and the network topology structure is required to realize the connection of the software and hardware structure of the entire system. The network topology of the system is shown in Figure 2.

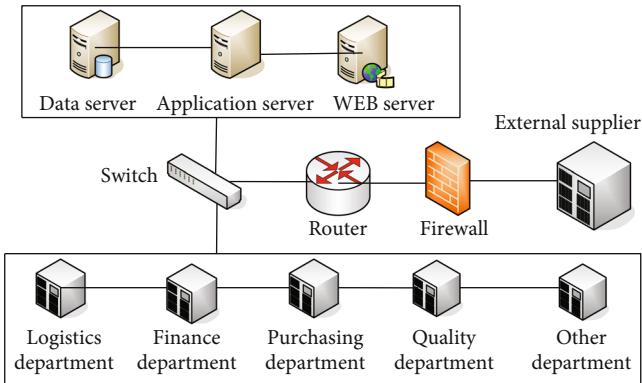


FIGURE 2: The network topology of the system.

**Purchasing and supply department:** supplier management and development, procurement contract maintenance, procurement business.

**Logistics department:** responsible for managing warehouse operations and logistics distribution of each branch.

**Technology department:** master data management, including material master data, BOM, work center, and process route. **Operation management office:** information system, performance appraisal, and comprehensive management. **Quality department:** supplier quality management.

According to the idea of ERP management system, combined with the actual situation of the enterprise, the system includes the following functions:

- (1) Warehouse area management: classification and coding management of the warehouse area
- (2) Material basic information management: material ABC classification attribute management; provide material classification management. There are various measurement units of materials, and the conversion between measurement units can be realized; the maximum and minimum inventory is set to realize the alarm of missing parts and overflow of materials; alarm: automatic generation of demand order function
- (3) Inventory business operation management: inventory management multilevel operation authority to ensure data security; inventory material status query, understand the current available material quantity, and the status of broken scrap, occupancy, and order; automatically generate operation vouchers and query them as inventory operation records; basis: query previous inventory operation records
- (4) Inventory job management: inventory plan preparation and direct printing of inventory table; support cycle inventory method and freeze inventory method
- (5) Statistical query management: provide multiple combinations of query, inventory status, supplier delivery status, customer sales quantity query, etc.

3.3. *System Function Module Design.* According to the company's existing SAP system, the E-supply system, and the

customer's KMS Kanban pull system that are not fully used, a simple and easy-to-operate inventory management system is designed on the basis of these three systems. It can realize basic functions such as management of enterprise internal inventory, customer receipt and reconciliation management, and supplier delivery reconciliation management, which brings opportunities for the small-scale A company to be quickly put into use. The functions of each module of the information system are introduced as follows:

(1) System management module

- (i) Modify personal information
- (ii) Allocate system usage authority of each functional department. **Planner functions:** can operate each module, maintain the main basic data, assign management authority, inventory management, inventory query statistics; **information officer:** inventory document entry, order and transfer of goods, plan outbound warehousing document entry, inventory query

(2) Basic data maintenance module

- (i) Material information input: including material name, material number, project name, part number, supplier name, unit packaging quantity, safety stock quantity, and other information input, delete, modify, query, and exchange material master with SAP system data information
- (ii) Location information input: location number, location category, material name, and material classification
- (iii) Customer information query: customer information and shipping orders are directly obtained by the KMS Kanban pull system
- (iv) Supplier information query: supplier information is obtained from the E-supply system
- (v) Beginning inventory entry: the initial part inventory quantity, set the maximum inventory and minimum inventory

(3) Inventory counting module

- (i) Preparation of inventory plan: material name, material category, and inventory specification
- (ii) Inventory list entry: part number, part name, part category, and location number
- (iii) Inventory confirmation: initial quantity, reexamination quantity, draw quantity, and confirmation
- (iv) Inventory query: part name, part number, inventory quantity, and location number

(4) Inventory business module

- (i) Finished product delivery: printing of finished product delivery note, printing of stocking list, delivery confirmation
  - (ii) Finished and semifinished product warehousing: finished product warehousing and semifinished product warehousing, finished product material number, quantity
  - (iii) Order entry: part number, part name, date, and quantity
  - (iv) Disposal of scrap list: part number and location
  - (v) Planned outbound and outbound order: material number, material name, applicant, and date
- (5) Inventory query statistics module
- (i) Inventory status query: query which location the part is in, which supplier it belongs to, and the inventory quantity
  - (ii) Inventory operation query: what operations have been performed on the part, as well as the operator and date of operation
  - (iii) Material classification query: the category of the material, whether it is a raw material
  - (iv) Inventory warning: if the quantity of materials is less than the minimum inventory and greater than the maximum inventory, the shortage alarm and overflow alarm are required
  - (v) Inventory balance query: query the remaining inventory quantity of each material, and adjust it in time
  - (vi) Statistical query: summary of monthly material storage and material consumption

*3.4. Strategies Implemented by SAP.* Implementation strategies include overall implementation and step-by-step implementation. The overall implementation means that all processes and system solutions are designed, implemented, and delivered at the same time. Step-by-step implementation refers to the process, and system plan is divided into several components; each part is designed, implemented, and delivered in batches according to the order of completion. The overall implementation requires more resources in a certain period of time, but the overall implementation time is shorter. Step-by-step implementation is mainly used for projects with limited resources. It requires less investment in a certain period of time, but it will prolong the implementation cycle of the project. Based on years of project experience, the implementation team believes that the overall implementation efficiency is better than stepwise implementation.

- (1) Using a step-by-step implementation strategy, the system schemes completed in the previous batch are likely to be readjusted during the design and

implementation of the latter batch of schemes. Moreover, every time the system function is expanded, the whole system scheme must be reintegrated test to ensure the integration of the system, and the users must also gather for retraining. These repetitive tasks will consume time. The overall implementation strategy is adopted, all processes are defined in the same time period, all system solutions are designed, implemented, and tested in the same time period, and all user training and permission definitions are also completed in the same time period, thereby avoiding step-by-step implementation causes rework problems

- (2) Using a step-by-step implementation strategy, the project implementation team will face the dual work pressure of support and implementation within the same time period. It will not only provide support for the system that has been put into use but also carry out the design and development of new functions. On the contrary, the overall implementation strategy clearly defines the main tasks and key submissions of each stage. The project team members only need to focus on the most important tasks in this stage within the same time period, and the quality of work can be fully guaranteed
- (3) Adopting a step-by-step implementation strategy will take up more time for project team members and will affect the normal operation of the enterprise for a longer time. With the overall implementation strategy, with the exception of some support personnel, most members of the project team can be released to invest in other work or projects after the completion of the system support handover. Based on the above considerations, the automobile company adopts an overall implementation strategy, which is conducive to shortening the project time, saving project costs, and improving implementation efficiency

## 4. Results and Discussion

*4.1. SAP System Usage Analysis.* The importance of ERP training SAP is a set of highly information-based management software. If you want to fully apply SAP software, you must understand a lot of knowledge, IT knowledge and business management knowledge. Therefore, if you want SAP to serve the enterprise, to enhance the enterprise, it is necessary to carry out technical training vigorously, and the implementation of ERP must not be an optional tool. Therefore, it is necessary to train the company on the principles of ERP, train the principles and functions of ERP, why do you want to go to ERP, let the company have a full understanding, and also train the management so that leaders should pay enough attention to the role of ERP in the company and support the implementation of ERP and be able to lead the team to implement ERP effectively. Only when the leaders of the enterprise pay attention to it, the grassroots employees can pay attention to it. Therefore, ERP training

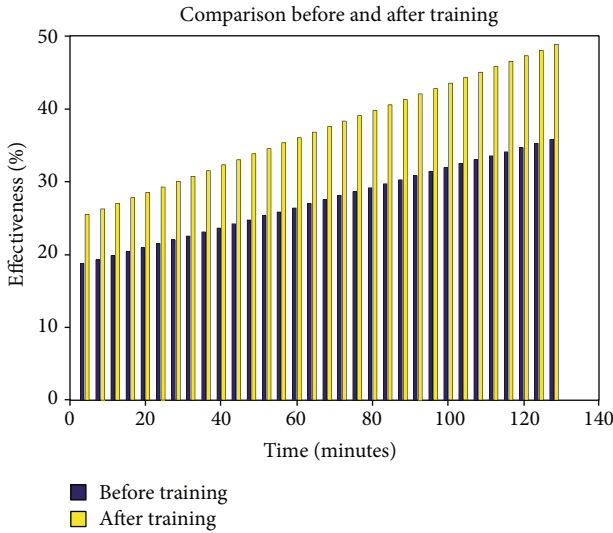


FIGURE 3: Comparison of employee work efficiency before and after training.

is very important in enterprises. Not only need to carry out theoretical training, but also to carry out operation and application training for grassroots employees, which can improve the efficiency of daily work. The comparison of the work efficiency of employees before and after training is shown in Figure 3.

During the project implementation process, the implementing party assisted the automobile company base to introduce advanced management concepts and refined the ideas through process design. After implementing the SAP ERP system, automobile manufacturing company A has realized the whole process of automation of the company’s business process from sales order to order delivery, and the whole process can be carried out under the supervision and control of management personnel. This complete and lean management model has significantly improved the order fulfillment rate and timely delivery rate of automobile manufacturing company A. From the comparison before and after the launch of the SAP project, the above two indicators have increased by 1.5 times, the order fulfillment rate has increased from 30% to 45%, and the timely delivery rate has increased from 60% to 90%. The order situation of the automobile manufacturing company is shown in Figure 4.

Faced with the challenges of mixed-line production requiring timely and accurate distribution and reducing inventory, the SAP system realizes efficient coordination and information sharing of production, inventory, and procurement and flexibly supports JIT (Just-In-Time) Kanban, VMI supplier management inventory, etc. A variety of business models improve the efficiency of business processing and achieve the purpose of full logistics collaboration. Based on the status quo of basic management and information construction of an automobile company, the goal of this project is to establish a new core operating system for the base through the implementation of the SAP system and to lay a solid foundation for the development of the base business in City A. Due to the successful launch and smooth opera-

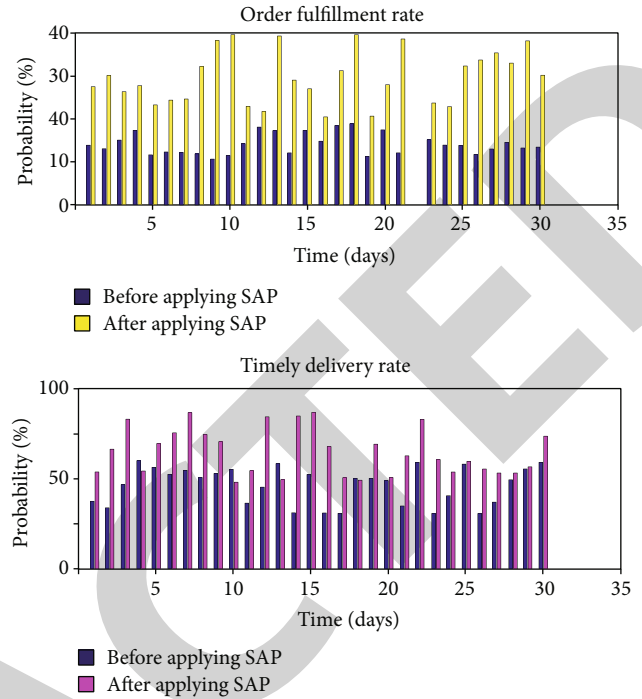


FIGURE 4: Order status of automobile manufacturing companies.

TABLE 1: Specific economic benefits.

Contrast content	Before implementation	After implementation
Sales revenue	RMB 8.2 billion	RMB 12 billion
Gross margin	24%	42%
Delivery achievement rate	60%	90%
Turnover of finished products	15 days	8 days
Finished product inventory accuracy rate	76%	98%
Days of accounts receivable	56 days	38 days
Bad debt rate	5%	2%
Proportion of expenses	10%	5%

tion of the SAP ERP system, the overall informatization level of car manufacturing company A has been greatly improved, which has improved the communication efficiency between departments, headquarters, and branches and indirectly increased the overall operating costs of the group. After the SAP ERP system went live, the total turnover of automobile manufacturing company A increased from RMB 8.2 billion to RMB 12 billion in two years. The specific economic benefits are shown in Table 1.

In the process of implementing the SAP ERP system in car manufacturing company A, the manpower of key departments was organized, and the master data of each module was cleaned and converted, which ensured that the SAP project of car manufacturing company A can be successfully launched. SAP inventory is shown in Figure 5.

4.2. *Company’s Economic Benefits.* With the continuous increase in the business scope of car manufacturing

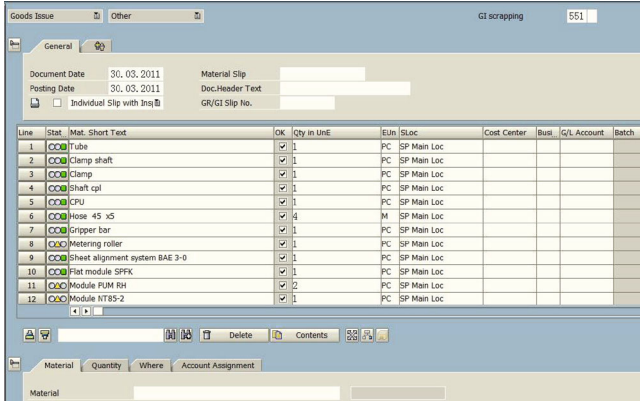


FIGURE 5: SAP inventory (<http://alturl.com/or6i4>).

TABLE 2: Specific economic benefits.

Compare content	Before implementation	After implementation
Average number of projects per month	30	10
Monthly sluggish material scrap	1.5 million	200,000
Daily production plan achievement rate	59%	89%
Weekly production plan achievement rate	56%	85%

company A and the continuous increase in product types, in the two years since the SAP ERP system was launched and then operated smoothly, the number of engineering changes proposed by the company each month has been greatly reduced, thus making group A overall quantity and amount of sluggish materials significantly reduced. The specific economic benefits are shown in Table 2.

In addition, the monthly production plan achievement rate increased from 50% to 82%. The on-time warehousing rate of production orders has increased from 60% to 88%. The one-time pass-through rate of products increased from 78% to 92%. The FQC pass rate has been increased from 90% to 95%. The product quality customer complaint rate dropped from 6% to 1%. The product quality is shown in Figure 6.

In the process of implementing the SAP ERP system, automobile manufacturing company A has configured an alarm function for the company's safety stock, the quantity and total amount of stock sluggish materials in the MM module. This time, through the implementation of the SAP system by car manufacturing company A, these information flows were integrated and unified, and the operation was carried out under a SAP platform. According to this platform, the overall operating efficiency of car manufacturing company A will be greatly improved, and corporate management costs will be reduced accordingly. The economic benefits of material management are shown in Table 3.

After implementing SAP system inventory improvement measures, company A's inventory management has been effectively improved, and the effect is significant. After implementing the SAP ERP system, automobile manufactur-

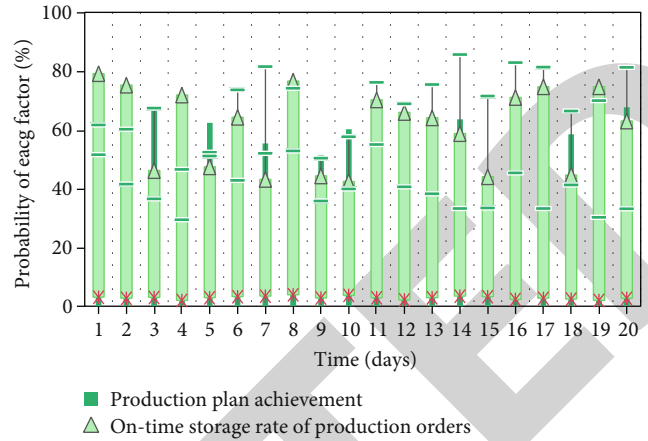


FIGURE 6: Product quality.

TABLE 3: Economic benefits of material management.

Contrast content	Before implementation	After implementation
Procurement delivery time achievement rate	40%	98%
Qualified rate of supplier incoming materials	86%	96%
PPAP submission achievement rate	Unable to count	95%
PPAP incoming material qualification rate	Unable to count	90%
Inventory accuracy	80%	95%
Finished product inventory turnover accuracy rate	86%	92%
Number of days around semifinished product	15 days	8 days

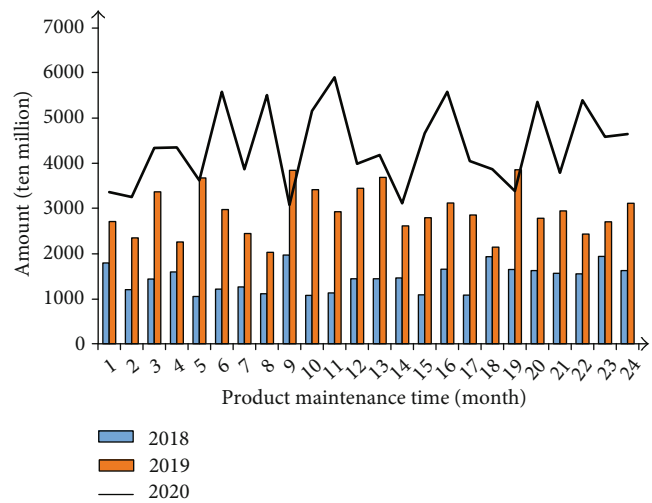


FIGURE 7: 2018-2020 financial situation of company A.

ing company A uses the powerful data analysis and data intelligent processing functions of the SAP ERP system to present the financial, cost, and profit management analysis of automobile manufacturing company A in a good form.

As a result, automobile manufacturing company A has made great progress in scientific, digital, and intelligent management of the enterprise. The financial situation of company A in 2018-2020 is shown in Figure 7.

## 5. Conclusion

This study mainly discusses the design and implementation of supply chain management system for automobile manufacturing enterprises based on SAP. This research integrates the existing information resources, takes SAP system as the enterprise's information platform, unifies the information platform into SAP system by integrating the existing information resources (financial system, logistics system, cost control system, production control system, etc.), avoids the information island phenomenon as far as possible, and finally realizes the integrated and unified enterprise information management, which is convenient for the rapid traceability of historical data, providing the best decision analysis method for managers. The project implementation of automobile company adopts independent minicomputer system (HP server), with SAPR/3 system as the core and C/S (customer/service) architecture, so as to gradually expand the system function in the future. The functions of the system include warehouse area management. The process of material information input can transfer material master data information with SAP system through blockchain technology. This study is helpful to provide guidance for the long-term development of enterprises. The establishment of the supply chain of this paper is centered on the vehicle manufacturer. Under this model, the position of parts manufacturers, dealers, and other members and how the thinking of enterprise informatization construction should be coordinated with the vehicle manufacturers also need to be further studied.

## Data Availability

No data were used to support this study.

## Disclosure

We confirm that the content of the manuscript has not been published or submitted for publication elsewhere.

## Conflicts of Interest

There are no potential competing interests in our paper.

## Authors' Contributions

All authors have seen the manuscript and approved to submit to your journal.







## References

- [1] W. U. Jianlong and R. Shang, "Research on configuration optimization of escalator assembly profiles based on SAP system," *International Journal of Plant Engineering and Management*, vol. 23, no. 4, pp. 57–64, 2018.
- [2] T. N. Varma and D. A. Khan, "SAP system as vendor fraud detector," *Journal of Supply Chain Management Systems*, vol. 6, no. 2, pp. 1–13, 2017.
- [3] K. L. Croxton, S. J. Garcia-Dastugue, D. M. Lambert, and D. S. Rogers, "The supply chain management processes," *International Journal of Logistics Management*, vol. 12, no. 2, pp. 13–36, 2001.
- [4] P. Samaranayake, "A conceptual framework for supply chain management: a structural integration," *Supply Chain Management*, vol. 10, no. 1, pp. 47–59, 2005.
- [5] L. Wu, X. Yue, A. Jin, and D. C. Yen, "Smart supply chain management: a review and implications for future research," *International Journal of Logistics Management*, vol. 27, no. 2, pp. 395–417, 2016.
- [6] S. Gold and M. C. Schleper, "A pathway towards true sustainability: a recognition foundation of sustainable supply chain management," *European Management Journal*, vol. 35, no. 4, pp. 425–429, 2017.
- [7] J. Sayos, C. Wu, M. Morra et al., "Pillars article: the X-linked lymphoproliferative disease gene product SAP regulates signals induced through the co-receptor SLAM. Nature. 1998.395: 462-469," *Journal of Immunology*, vol. 199, no. 5, p. 1534, 2017.
- [8] M. Papert and A. Pflaum, "Development of an ecosystem model for the realization of Internet of things (IoT) services in supply chain management," *Electronic Markets*, vol. 27, no. 3, pp. 1–15, 2018.
- [9] S. K. Jauhar, M. Pant, and R. Dutt, "Performance measurement of an Indian higher education institute: a sustainable educational supply chain management perspective," *International Journal of System Assurance Engineering and Management*, vol. 9, no. 1, pp. 180–193, 2018.
- [10] D. J. Fiorino and M. Bhan, "Supply chain management as private sector regulation: what does it mean for business strategy and public policy?," *Business Strategy & the Environment*, vol. 25, no. 5, pp. 310–322, 2016.
- [11] A. Garai, P. Mandal, and T. K. Roy, "Intuitionistic fuzzy T-sets based optimization technique for production-distribution planning in supply chain management," *Opsearch*, vol. 53, no. 4, pp. 950–975, 2016.
- [12] Y. Dou, Q. Zhu, and J. Sarkis, "Green multi-tier supply chain management: an enabler investigation," *Journal of Purchasing and Supply Management*, vol. 24, no. 2, pp. 95–107, 2018.
- [13] K. Nishitani, K. Kokubu, and T. Kajiwar, "Does low-carbon supply chain management reduce greenhouse gas emissions more effectively than existing environmental initiatives? An empirical analysis of Japanese manufacturing firms," *Journal of Management Control*, vol. 27, no. 1, pp. 33–60, 2016.
- [14] C. Liu and T. Ma, "Traceability and management method of supply chain information based on wireless sensor network," *Wireless Communications and Mobile Computing*, vol. 2021, Article ID 8612814, 15 pages, 2021.
- [15] Z. Gao, X. Lei, C. Lin, X. Zhao, Y. Lu, and W. Shi, "CoC: a unified distributed ledger based supply chain management system," *Journal of Computer Science and Technology*, vol. 33, no. 2, pp. 237–248, 2018.
- [16] D. Krause, D. Luzzini, and B. Lawson, "Building the case for a single key informant in supply chain management survey research," *Journal of Supply Chain Management*, vol. 54, no. 1, pp. 42–50, 2017.



## Research Article

# Optimization of Electric Automation Control Model Based on Artificial Intelligence Algorithm

Run Ma <sup>1</sup>, Shahab Wahhab Kareem <sup>2,3</sup>, Ashima Kalra <sup>4</sup>, Rumi Iqbal Doewes <sup>5</sup>,  
Pankaj Kumar <sup>6</sup> and Shahajan Miah <sup>7</sup>

<sup>1</sup>School of Automation, Chongqing Industry Polytechnic College, Chongqing 401120, China

<sup>2</sup>Department of Technical Information System, Erbil Technical Engineering College, Erbil Polytechnic University, Erbil, Iraq

<sup>3</sup>Department of Information Technology, College of Engineering and Computer Science, Lebanese French University, Erbil, Iraq

<sup>4</sup>ECE Department, Chandigarh Engineering College, Landran, Mohali, India

<sup>5</sup>Faculty of Sport, Universitas Sebelas Maret, Jl. Ir. Sutami, 36A, Kentingan, Surakarta, Indonesia

<sup>6</sup>Department of Computer Science & Engineering, Lloyd Institute of Engineering & Technology, Greater Noida, 201306 Uttar Pradesh, India

<sup>7</sup>Department of EEE, Bangladesh University of Business and Technology (BUBT), Dhaka, Bangladesh

Correspondence should be addressed to Run Ma; [runma969@126.com](mailto:runma969@126.com) and Shahajan Miah; [miahbubt@bubt.edu.bd](mailto:miahbubt@bubt.edu.bd)

Received 25 December 2021; Revised 8 February 2022; Accepted 14 February 2022; Published 18 March 2022

Academic Editor: Shalli Rani

Copyright © 2022 Run Ma et al. This is an open access article distributed under the Creative Commons Attribution License, which permits unrestricted use, distribution, and reproduction in any medium, provided the original work is properly cited.

To effectively solve the problems faced by modern electrical engineering, the design of an electrical automation control system based on artificial intelligence technology is realized. A model of electrical automation control system based on an artificial intelligence algorithm is presented. The control parameters are optimized by using the artificial intelligence algorithm control strategy. The research results show that when there is 20% load interference and 2.1 Hz frequency interference, the maximum failure rate of the turbine under system control is 0.02, indicating that the system has high anti-interference. Therefore, in the automatic control of electrification, the application of the artificial intelligence algorithm can greatly improve the control response time of the automatic control of electrification, save cost, and achieve efficient production.

## 1. Introduction

With artificial intelligence iterative growth and maturity as a component of modern information technology, it has been widely explored and popularized in a range of industries, notably in the field of electrical automation control, assisting in the evolution of electrical automation. AI technology naturally integrates the information and intelligent content of electronics, telecommunications, computers, and other fields and disciplines. In a multitude of areas, it can be utilized to simulate human awareness or thinking. Because AI technology has computer advantages, such as the ability to perform precise control operations, reduce reliance on human interaction, and efficiently prevent avoidable mistakes caused by human factors, its use in related sectors may significantly increase the level of intelligence in these industries [1, 2].

Social development makes economic production increasingly dependent on scientific and technological progress, be it agriculture, industry, or tertiary industry, which has been widely used in electrical automation control technology; in electrical automation control technology, artificial intelligence technology has become the core part of electrical automation technology research and application [3]. Artificial intelligence technology integrates many technologies, including computer technology, sensor technology, and GPS technology. Industrial production uses intelligent technology, which greatly reduces the work intensity of employees, greatly improves the production efficiency of enterprises, and effectively reduces the production cost, which makes enterprises more competitive in the market [4]. In particular, the use of artificial intelligence technology in dangerous areas can greatly reduce the damage to operators. In industrial and agricultural

production, the introduction of artificial intelligence technology can reduce the unit cost and labor cost of production and improve the operation accuracy in the process of industrial and agricultural production; on the basis of minimizing manual operations, the safety of production activities is effectively improved, and production efficiency and enterprise benefits are improved [5]. Machine learning has expanded the capabilities and scope of electrical engineering optimization, resulting in major advances not just in terms of cost but also in terms of safety and real-time operation control [6]. Nguyen et al. robust adaptive strategy based on pseudofuzzy logic and sliding mode control (PFSMC) is proposed. Due to the robustness of the sliding-mode control technology, reduced sensitivity to uncertainty, and enhanced resistance to pseudofuzzy mechanism interference, the proposed control algorithm can not only guarantee the stability of the system but also improve the steady-state tracking error. To verify the design efficiency of PFSMC, simulations and laboratory tests of the proposed protocol and conventional PID schemes were performed and compared below. In a computer environment, test cases with and without certainty are implemented using two controllers to visualize comparative responses. Then, both control methods are integrated into a real hardware platform to obtain practical results [7]. With the continuous growth of power demand in China, the requirements of electrical control system are constantly improving; the traditional electrical control system cannot keep up with the pace of social development [8]. The electrical automation control system using artificial intelligence technology can effectively improve the level of control and finally achieve modernization and intelligence.

Electrical automation control is highly significant in the electrical industry; if electrical control automation is achieved, production efficiency can be effectively enhanced, lowering production costs including human resource expenses. Fuzzy control, expert systems, neural networks, and other artificial intelligence technologies are being employed in electrical automation control. Artificial intelligence in the growth of automation not only can promote the overall progress in the field of electrical automation control but also can promote the growth of automatic control of progress, so in the field of electrical industrial applications, innovation requires the support of artificial intelligence, using artificial intelligence technology to improve the consciousness of mechanical ability and strengthening the electrical automatic control [9, 10]. The manual technology in electrical automation control is analyzed. An efficient and precise control mode is an important basis of electrical automation control. Automation control mainly studies the application of computer data processing, the classification and identification processing of data digitalization, the structural optimization of system composition, the control of electrical automation, and all small branches [11]. On the basis of automation control technology, by combining with an artificial intelligence algorithm, the work efficiency of electrical automation control will be greatly improved to some extent, save the time consumed in the traditional electrical control, reduce the energy and human resources consumed in the operation of equipment, greatly improve

the control of machine time, and control the accuracy of electrical automation control. Shi et al. proposed a clone selection optimization system based on the joint learning framework. The heuristic clone selection strategy in local model optimization was used to optimize the effects of joint training. First, the process improves the adaptability and robustness of the federated learning solution and improves the modeling performance and training efficiency. In addition, this study tries to improve the privacy security defense capability of federal learning programs through differential privacy preprocessing. Simulation results show that the clone selection optimization system based on joint learning has significant optimization capability for the basic performance, stability, and privacy of the model [12].

A single controller's automated running of a large electrical power distribution network can enhance efficiency and reliability while cutting maintenance costs. For the control to be most successful, the controller must have a general overview of the whole network to reason about the cause of the readings of the multiple sensing devices positioned across the network. Conventional power system control methods rely on a network of local devices that make choices based on the instantaneous reading of a single sensor. These single-parameter results may occasionally be incorrect due to sensor malfunctions [13, 14]. Based on this, a model of electrical automation control system based on the artificial intelligence algorithm is proposed. It is applied in the experiment; after testing in different working conditions, when there is 20% load interference and 2.1 Hz frequency interference, the control effect of the system is better than the traditional PID control system; under the control of the system, the output frequency fluctuation of the turbine system is small and has fast convergence to the optimal frequency, and under the control of the system in this paper, the maximum failure rate of the turbine is 0.02, which has high robustness; it is predicted that the electrified industry in the future will inevitably rely heavily on artificial intelligence algorithms. In the automatic control of electrification, the application of the artificial intelligence algorithm can greatly improve the control reaction time of the automatic control of electrification, save cost, and achieve efficient production.

## 2. Research Methods

### 2.1. Electrical Automation Control System Based on Artificial Intelligence Algorithm

*2.1.1. Hardware Design.* The electrical automation control system based on the artificial intelligence algorithm is around the turbine regulation, as the goal, through a single neural network-based PID intelligent controller module; based on the adaptive ant colony genetic artificial intelligence algorithm, the optimal control of PID intelligent controller is realized.

*2.1.2. System Structure.* The core components of the system include water turbine, pressure water inlet, and large motors, among which the PID intelligent controller module based on a single neural network is included, which belongs to the

feedback control system. The structure diagram of the electrical automation control system based on the artificial intelligence algorithm is shown in Figure 1. In Figure 1,  $a$  represents a given rotational speed signal,  $b$  represents the output control signal, and  $c$  represents the load disturbance signal; for a parallel operating unit, its output power variation does not interfere with the frequency of the power system; based on this kind of situation, the function of the turbine regulating feedback system is 0; in this case, the PID intelligent controller module based on a single neural network can enable the follow-up system function. Figure 1 illustrates that the turbine governor has experienced the development process from the mechanical hydraulic governor to the process of analog circuit to the microcomputer electrohydraulic governor. Prior to the appearance of the microcomputer governor, the main mission of the governor (mainly machine governor and analog circuit governor) was to adjust the water guide mechanism/paddle mechanism (injection needle/converter mechanism) according to the unit frequency deviation of the rating, and the turbine governor is mainly a speed regulator.

**2.1.3. PID Intelligent Controller Module Based on Single Neural Network.** The core of the intelligent PID controller is a single neuron, which can complete self-learning and has good adaptability, and the structure is simple and can quickly adapt to the nearby environment, the field adjustment parameters are few and easy to adjust, which can ensure that the control system belongs to the optimal state in practical application, and its control effect is better than the ordinary PID controller. Based on using a single neuron, the adaptive PID controller can play a better role. For the converter input, it can make the turbine controlled process, and PID control settings can be optimized, such as setting  $S(r)$ ; the output can be transformed into the number of relevant states required in neuron-based learning control; in the state coefficient  $Y_1, Y_2, Y_3$  of the output of the converter,  $Y_1(r)$  is equal to  $\varphi(r)$ ,  $Y_2(r)$  operates on  $\varphi(r) - \varphi(r-1)$ ,  $Y_3(r)$  operates on  $\varphi(r) - 2\varphi(r-1) + \varphi(r-2)$ ,  $S$  describes the performance index,  $R$  describes the neuron proportional coefficient, and neurons using association retrieval can derive control signals  $H_p, H_i, H_d$ ; then, the control strategy of the artificial intelligence algorithm is used to realize the optimal adjustment control of three kinds of control signals, that is, the three kinds of control parameters.

## 2.2. Control Strategy Based on Artificial Intelligence Algorithm

**2.2.1. Node and Path Generation.** Set  $H_p, H_i, H_d$  as the three variables to be set in the PID, the controller suppose there are five significant digits for each of the three variables. Set the 5 digits of  $H_p, H_i, H_d$  according to the value condition in the PID controller 1 placed before the decimal point and 4 places after the decimal point, for example, 1.0025. Then, the ant path graph is optimized according to the ant colony algorithm with this parameter. For these three parameter values, they are abstractly described in the  $xOy$  plane; the method is to draw 15 equally spaced and equally

long line segments  $A_1, A_2, \dots, A_{15}$  perpendicular to the  $x$ -axis; among them,  $A_1 \sim A_{15}, A_6 \sim A_{10}, A_{11} \sim A_{15}$  describes the first to fifth digits of  $H_p, H_i, H_d$  in turn. Divide each line segment equally; that is, obtain 10 nodes from each line segment and describe the digit values represented by the line segment in turn. So far, there are  $15 \times 10$  nodes in the  $xOy$  plane, and set 1 node as  $a(x_j, y_{j,i})$ , where  $x_j$  describes the  $x$ -coordinate of line segment  $A_j$ ;  $y_{j,i}$  describes the ordinate of node  $i$  on  $A_j$ , and the value corresponds to the ordinate value  $y_{j,i}$  of the node. Suppose an ant starts at the origin  $O$ , and after crawling to a random point in segment  $A_j$ , implement a loop, and its crawling path can be described as  $B = \{O, a(x_1, y_{1,i}), a(x_2, y_{2,i}), \dots, a(x_j, y_{j,i})\}$ , where  $a(x_j, y_{j,i})$  node is in line segment  $A_j$ ; then, the value described by this path is shown in

$$\begin{cases} H_p = y_{1,i} \times 10^0 + y_{2,i} \times 10^{-1} + y_{3,i} \times 10^{-2} + y_{4,i} \times 10^{-3} + y_{5,i} \times 10^{-4}, \\ H_i = y_{6,i} \times 10^0 + y_{7,i} \times 10^{-1} + y_{8,i} \times 10^{-2} + y_{9,i} \times 10^{-3} + y_{10,i} \times 10^{-4}, \\ H_d = y_{11,i} \times 10^0 + y_{12,i} \times 10^{-1} + y_{13,i} \times 10^{-2} + y_{14,i} \times 10^{-3} + y_{15,i} \times 10^{-4}. \end{cases} \quad (1)$$

**2.2.2. Algorithmic Control Process.** The control process based on the artificial intelligence algorithm is as follows:

- (1) According to the parameter tuning method, namely, Z-N method, the calculated PID parameter is  $H_{p,s-M}, H_{i,s-M}, H_{d,s-M}$
- (2) The number of ant colonies is  $n$ , and each ant  $h$  has 15 ordinate values and crawling path attributes that are used to store the 15 nodes passed by ants
- (3) Hybrid algorithm parameter initialization: put the ant at the starting point
- (4) Set the value of variable  $j$  to 1; if the parameter  $p < p_0$ , then calculate the probability  $Q_{ji}^h(t)$  of ants transferring each node in line segment  $A_j$  by formula (2). On the contrary, formula (3) is used to select the subsequent nodes through the wheel selection method, and the value of this node is introduced in the table, as shown in

$$\delta(t) = \begin{cases} 0.95\delta(t-1), & 0.95(t-1) \geq \delta_{\min}, \\ \delta_{\min}, & \text{else,} \end{cases} \quad (2)$$

where  $\delta(t)$  describes local pheromone parameters, as shown in

$$Q_{ji}^h(t) = \begin{cases} \frac{[\psi_{ji}(t)]^1 \cdot [\vartheta_{ji}(t)]^2}{\sum_{h \in \text{allowed}_h} [\psi_{ji}(t)]^1 \cdot [\vartheta_{ji}(t)]^2}, & i \in \text{allowed}_h, \\ 0, & \text{else,} \end{cases} \quad (3)$$

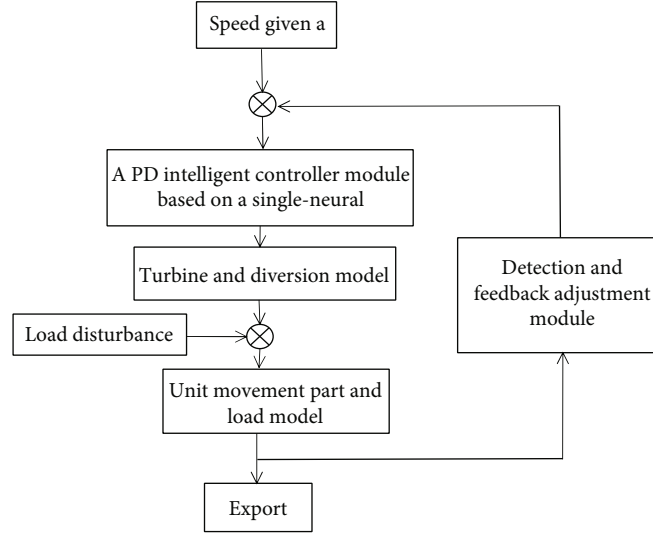


FIGURE 1: Structure of electrical control system based on artificial intelligence algorithm.

where allowed<sub>*h*</sub> describes the nodes that ant *h* can select next,  $[\vartheta_{ji}(t)]^2$  describe the importance of visibility factors, and  $[\psi_{ji}(t)]^{-1}$  describes the importance of pheromone locus intensity

- (5) When each ant finishes a node, equation (4) is adopted to refresh the local pheromone, and the local information volatility coefficient is adaptively transformed, as shown in

$$\psi_{ji} \leftarrow (1 - \delta) \cdot \psi_{ji} + \delta \cdot \Delta\psi_{ji}. \quad (4)$$

Type  $\Delta\psi_{ji} = P_1/S_{PID1}, S_{PID1}$  describe the node path passed; the value of local pheromone parameter  $\delta$  is adaptive.  $\Delta\psi_{ji}$  describe the track pheromone intensity per unit length.

- (6) Set  $j = j + 1$ , if the value of *j* is not greater than 15, jump to Step (3); otherwise, jump to Step (7)
- (7) Following the path that the ant *h* has climbed (array  $G_h$ ), calculate the PID parameter  $H_p^h, H_i^h, H_d^h$  corresponding to this path. Implement computer simulation to obtain the performance index  $s_z^h$  of the system, steady-state adjustment error  $d^h$ , and overshoot  $e^h$ . Calculate the corresponding objective function of ant *h*, record the best path and the best performance index in this cycle, and lead  $H_p^h, H_i^h, H_d^h$  into  $H_p^*, H_i^*, H_d^*$
- (8) Assuming  $h \leftarrow h + 15$ , all pheromones are refreshed according to equation (5), and the volatile coefficient of all information is adaptively adjusted. As shown in

$$\psi_{ji} \leftarrow (1 - \partial) \cdot \psi_{ji} + \partial \cdot \Delta\psi_{ji}, \quad (5)$$

where  $\partial$  describes the volatilization coefficient of all pheromones

- (9) Use the single point crossing strategy to cross (cross when crossing constraint variable  $\theta < 0.000001$ ) and generate new individuals
- (10) Using the basic mutation (mutation occurs when crossing the constraint variable  $\theta < 0.01$ ) scheme, calculate each parameter value again; if the performance index obtained is close to the objective function *F*, so if the mutation is not removed, the pheromone is updated, and conversely, the mutation is removed
- (11) If all ants do not converge to the same path, put all ants at the starting point again and jump to the step; otherwise, the loop stops and outputs the optimal path and the corresponding optimal PID parameters  $H_p^*, H_i^*, H_d^*$

**2.3. Functions of the Electrical Automation Control System.** The function of the electrical automation control system is control; the premise of the control function is to analyze the data to provide a control basis.

- (1) *Information Collection.* The electrical system is required to have relevant data terminal collection and software equipment; the main function of information collection is to provide a basic guarantee for the realization of the control function [15]. Terminal equipment and software are used to collect equipment, operation, and environment in the power system; it mainly includes operation time, equipment quantity, ambient temperature, fault condition,

and alarm system and signals using the data collected by the software and equipment with real-time information on the power system to provide operational information for the staff, so that the staff can effectively deal with the emergency

- (2) *Information Transmission.* Information is two-way transmission, that is, terminal equipment and software collect information to the processing center for transmission, and the processing center is the transmission of control processing instructions to the execution terminal [16, 17]. Therefore, the process of information transmission is particularly important, and information transmission is also the main condition to realize the control and supervision of the control system. Transmission equipment of the power system mainly includes video cable, signal cable, coaxial cable, and optical cable; the corresponding transmission mode can be selected according to transmission distance and type, to ensure the quality and speed of information transmission and to avoid information loss, not timely transmission, coding disorder, and information confusion [18]. The controller is required to include a control module, power module, communication module, and editing module, to ensure the coordination of the system
- (3) *Information Analysis.* Information analysis refers to the main process of control and monitoring of the control system; the control system should process and analyze the information collected by terminal equipment and software; after the collected information is sent to the database, the control system and software are displayed, and the system cannot be handled independently by the staff to use the system to help achieve the corresponding work [19]. In addition, the system should collect data to achieve storage, including the environment, equipment, and other real-time data, which can be printed through graphs, reports, etc., to facilitate staff analysis
- (4) *Diagnostic Control.* Diagnostic control belongs to the main function of the electrical automation control system; after information collection and analysis, the control system should be able to diagnose autonomously, based on the analysis results, including computer, controller, and field terminal equipment diagnosis, so that the system can run stably [20]. In addition, the analysis and diagnosis results to achieve control include power system fault detection and operation detection, so that the power system can operate stably

### 3. Result Analyses

The electrical automation system is more complex, including many disciplines and fields. For example, in terms of electrical automation equipment operation, the operators are required to have good comprehensive quality and perfect professional knowledge. In addition, the complexity of elec-

TABLE 1: Parameters of the turbine system in the experiment.

Parameter	Working condition of A	Working condition of B
Turbine transfer coefficient 1	-0.31	-0.27
Turbine transfer coefficient	0.75	1.28
Turbine transfer coefficient	1.47	0.93
Turbine transfer coefficient	0	0
Turbine transfer coefficient	0.78	1.07
Turbine transfer coefficient	0.48	0.36
Generator self-adjusting coefficient	0.21	0.21

trical automation focuses on operational effectiveness, which can reduce the shutdown or other accidents caused by operation errors or improper operation. Therefore, AI technology plays an important role in facing this real problem. Take the computer theory as the basis, write a program, which can realize the computer-based intelligent control. Intelligent operation of electrical equipment can replace the problem of insufficient human brain labor force, not only improving work efficiency but also reducing cost input. In addition, the use of artificial intelligence technology can improve the scientific operation of electrical automation equipment and realize the optimization of the real environment of equipment operation. The system is used in a hydropower station to realize the optimal PID control of the turbine in the hydropower station. A single machine sets the isolated load, setting two types of working conditions: working condition A is the design head rated power work; working condition B is the design head, working with partial load. Unit parameters are the following: runner model is HL220-LJ-410; single unit capacity is 102.7 MW; the hydrodynamic inertia time constant is 1.11 s, and the unit inertia time constant is 6.66 s. The parameters of the traditional PID control system are set as  $H_p = 4.04$ ,  $H_i = 1.23$ ,  $H_d = 2.67$ . The parameters of the turbine system in the experiment are shown in Table 1.

In working condition A, under the control of the system and the traditional PID control system, the response curve of the turbine system subjected to 20% load interference and 2.1 Hz frequency interference is shown in Figure 2. In working condition B, under the control of the system and the traditional PID control system, the response curve of the turbine system subjected to 20% load interference and 2.1 Hz frequency interference is shown in Figure 2. Analysis of the control results in Figures 2 and 3 shows that the control effect of the system in this paper is better than that of the traditional PID control system. Under the control of the system in this paper, the output frequency of the hydraulic turbine system fluctuates less and converges quickly to the

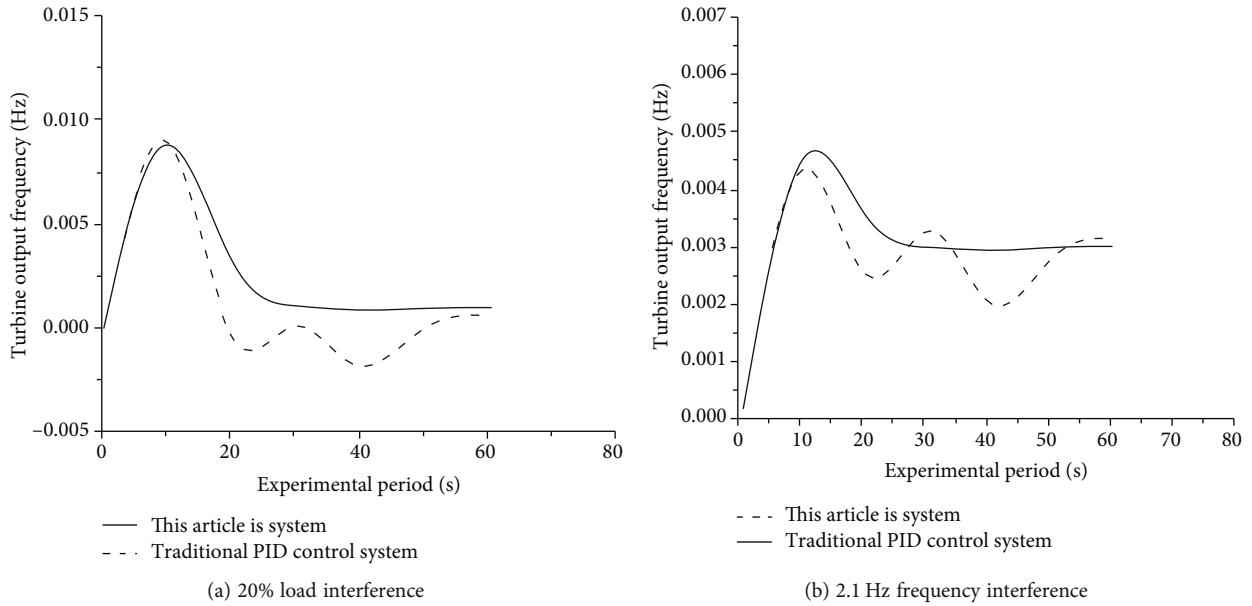


FIGURE 2: Comparison of control effects under working condition A.

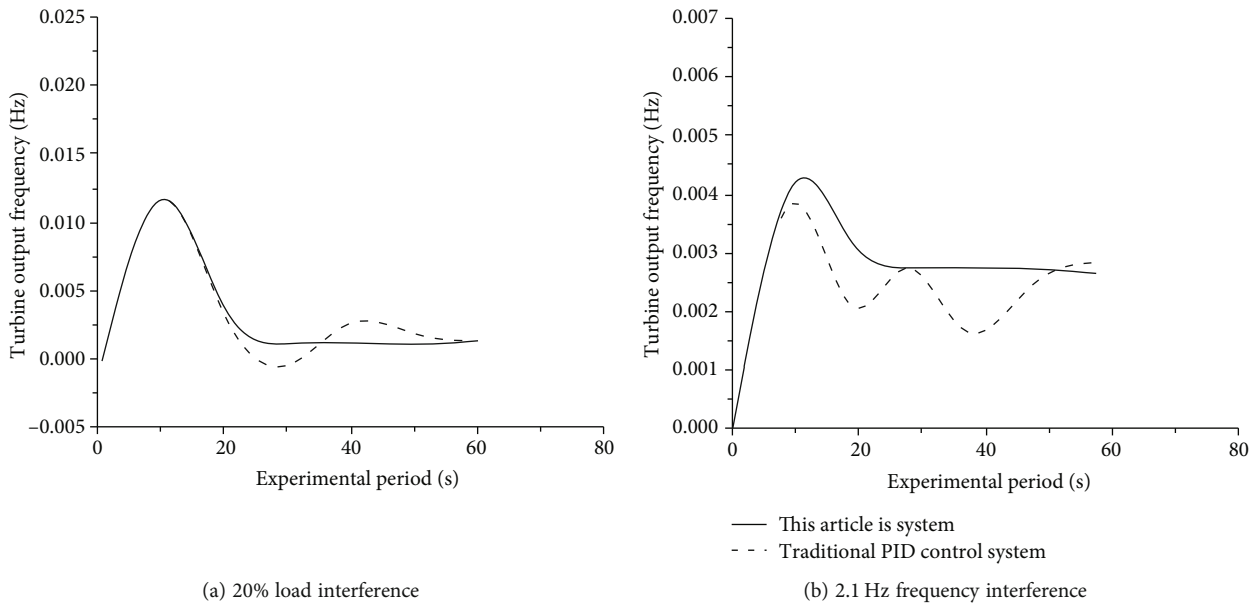


FIGURE 3: Comparison of control effects under working condition B.

optimal frequency. The output frequency of the hydraulic turbine is stable at about 20 s and remains at 0.000~0.005 between; under traditional PID control, the output frequency of the hydraulic turbine system fluctuates greatly, especially in 20 s-40 s, the output frequency of the hydraulic turbine fluctuates up and down, and it can converge to the optimal frequency when the experiment takes about 50 s. It can be seen that the control effect of the system in this paper is the best.

When 20% load interference and 2.1 Hz frequency interference are tested, the failure rate of the turbine is shown in Figure 4 after the system control is adopted. In Figure 4, the

maximum failure rate of the turbine under system control is 0.02 for both 20% load interference and 2.1 Hz frequency interference, indicating that the system in this paper has high anti-interference performance.

Set the input of the turbine system as a unit step signal. Set the number of ants to 30 and the number of iterations to 100. The range of PID control parameters is  $H_p = H_i = H_d = [0.00001, 20]$ ; it is compared with the PLC electrical automation control system and electrical control system of conveyor controllable variable speed device. Figure 5 is the PID step response diagram of the turbine system under the control of three kinds of systems.

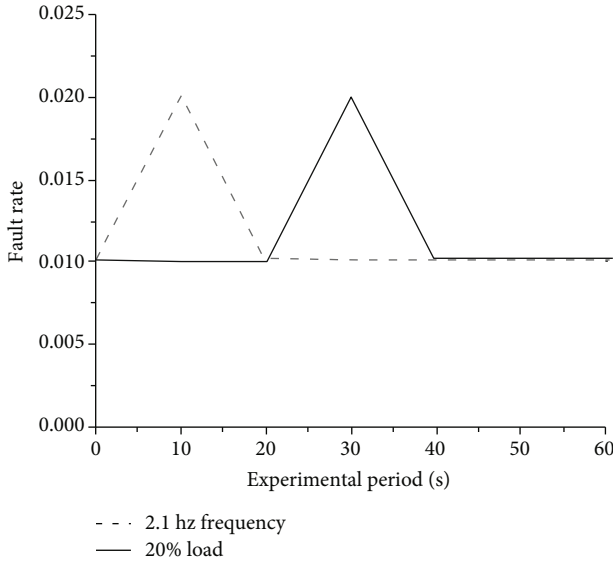


FIGURE 4: Failure rate of hydraulic turbine controlled by the system in this paper.

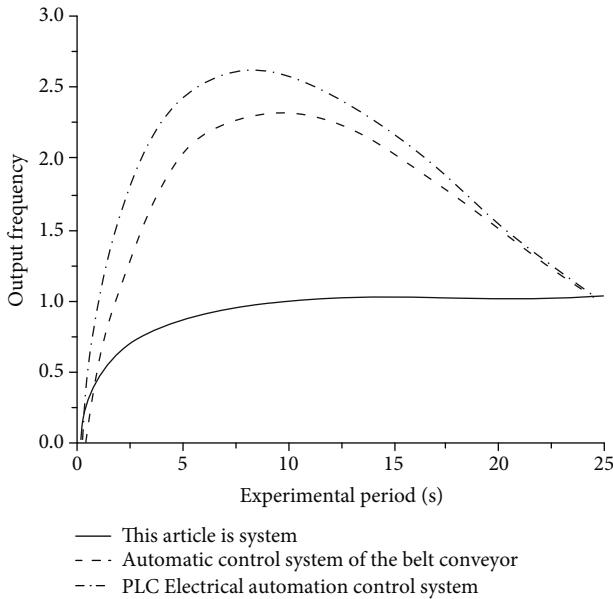


FIGURE 5: Unit step PID response of hydraulic turbine system.

Table 2 shows PID tuning parameters and system unit step performance indicators. Based on the data in Figure 5 and Table 2, it can be seen that the three PID parameters of the system control have the best effect. Compared with the other two systems, the adjustment time of the turbine system is only 10.26, while that of the other two systems is 37.36 and 16.59 which is much higher than the system. The steady state adjustment error and the number of overshoots are only 0.1677 and lower than the other two systems. Therefore, the system control performance is the best.

TABLE 2: Unit step performance index of hydraulic turbine system.

Indicators	System	PLC system	Belt conveyor controllable speed change device system
$H_p$	8.0031	4.59	10.1
$H_i$	0.0072	1.7	1.9945
$H_d$	0.6489	0.9	1.6879
Adjust the time	10.26	37.36	16.59
Steady-state adjustment error	0.1677	8.2575	4.4408
The number of overshoot	0.1677	35.9715	18.1964

#### 4. Discussion

The function of the electrical automation control system is control, and the premise of the control function is to analyze the data to provide the control basis. (1) Information collection: the electrical system is required to have corresponding data terminal collection and software equipment, and the main function of information collection is to provide the basic guarantee for the realization of the control function. The terminal equipment and software are used to collect the operation and environment of the equipment in the power system, mainly including the operation time, equipment quantity, environmental temperature, fault situation, and alarm system and signal. Use the data collected by the software and equipment to provide operation information to the real-time information in the power system, so that the staff can effectively handle emergencies. (2) Information transmission: information is two-way transmission; that is, the terminal equipment and software collect information to the processing center for transmission; the processing center is to control the processing instructions to the execution terminal transmission. Therefore, the information transmission process is particularly important, and the information transmission is also the main condition for the control and supervision of the control system. Power system transmission equipment mainly includes video cable, signal cable, coaxial cable, and optical cable, to choose the corresponding transmission mode by transmission distance and model type, to ensure the quality and speed of information transmission, and to avoid information loss, untimely transmission, coding confusion, and information confusion. The controller is required to include the control module, power supply module, communication module, and editing module, to ensure the working coordination of the system. The control results of Figures 2 and 3 show that the control effect of the system is better than the traditional PID control system, and the output frequency of the turbine system fluctuates less and quickly converges to the optimal frequency. Under the traditional PID control, the output frequency of the turbine system can converge to the optimal frequency at about 50 s. Therefore, the system controls the best.

## 5. Conclusions

Under the background of the rapid development of modern science and technology, our life has been changed; artificial intelligence technology has promoted the development of modern civilization; as a new high technology, it has high use value in real life. Design an electric automation control model optimization based on the artificial intelligence algorithm, and apply it in the experiment, after testing in different working conditions; when there is 20% load interference and 2.1 Hz frequency interference, the control effect of the system is better than the traditional PID control system; under the control of the system, the output frequency of the turbine system fluctuates less, converges quickly to the optimal frequency, and has high robustness; it is predicted that the future electrification industry will inevitably rely on the artificial intelligence algorithm. In the automatic control of electrification, the application of the artificial intelligence algorithm can greatly improve the control reaction time of the automatic control of electrification, save cost, and achieve efficient production. Therefore, the application of artificial intelligence algorithms is very broad. The application of AI technology to electrical automation control systems is crucial to the development of various fields. At present, the electrical automation control system has been widely used in intelligent buildings and has achieved certain application results. When creating the electrical automation control system, people must fully consider the actual requirements, use appropriate methods to calculate the automatic control system parameters, and actively use artificial intelligence technology to improve the effect of electrical automation control. The design and development of the electrical automation control system must analyze the working environment interfering with the operation of equipment and the operation of equipment and pay great attention to the interference of external environment during design. In addition, to ensure that the system can complete a stable power transmission, based on the system research and development and design cycle, the system research and development personnel must accurately grasp the working principle of the system.

## Data Availability

The data can be made available from the corresponding author upon request.

## Conflicts of Interest

The authors declare that there is no conflict of interest regarding the publication of this paper.

## References

- [1] G. Rastogi and R. Sushil, "Cloud computing implementation: key issues and solutions," in *2015, 2nd International Conference on Computing for Sustainable Global Development (INDIACom)*, pp. 320–324, New Delhi, India, 2015.
- [2] S. Saxena, S. Vyas, B. S. Kumar, and S. Gupta, "Survey on online electronic paymentss security," in *2019 Amity International Conference on Artificial Intelligence (AICAI)*, pp. 751–756, Dubai, United Arab Emirates, 2019.
- [3] Q. Shao, C. Xu, and Y. Zhu, "Multi-helicopter search and rescue route planning based on strategy optimization algorithm," *International Journal of Pattern Recognition and Artificial Intelligence*, vol. 33, no. 1, 2019.
- [4] R. Nimri, T. Battelino, L. M. Laffel, R. H. Slover, and M. Phillip, "Insulin dose optimization using an automated artificial intelligence-based decision support system in youths with type 1 diabetes," *Nature Medicine*, vol. 26, no. 9, pp. 1380–1384, 2020.
- [5] B. Sultan, I. Shafi, and J. Ahmad, "Swarm intelligence-based uplink power control in cognitive Internet of things (CIoT) for underlay environment," *International Journal of Applied Metaheuristic Computing*, vol. 12, no. 3, pp. 180–194, 2021.
- [6] V. Bhatia, S. Kaur, K. Sharma, P. Rattan, V. Jagota, and M. A. Kemal, "Design and simulation of capacitive MEMS switch for Ka band application," *Wireless Communications and Mobile Computing*, vol. 2021, Article ID 2021513, 8 pages, 2021.
- [7] H. Nguyen, T. P. Nguyen, and H. Ngo, "Improving the tracking performance under nonlinear time-varying constraints in motion control applications: from theoretical servo model to experimental validation," *Mathematical Problems in Engineering*, vol. 2021, Article ID 9950098, 15 pages, 2021.
- [8] J. Bholra and S. Soni, "A study on research issues and challenges in WSN," in *2016, International Conference on Wireless Communications, Signal Processing and Networking (WiSP-Net)*, pp. 1667–1671, Chennai, India, 2016.
- [9] Q. Li and S. Li, "Optimization of artificial cnn based on swarm intelligence algorithm," *Journal of Intelligent Fuzzy Systems*, vol. 40, no. 4, pp. 6163–6173, 2021.
- [10] X. Ren, C. Li, X. Ma et al., "Design of multi-information fusion-based intelligent electrical fire detection system for green buildings," *Sustainability*, vol. 13, no. 6, p. 3405, 2021.
- [11] S. Gupta, S. Vyas, and K. P. Sharma, "A survey on security for IoT via machine learning," in *2020, International Conference on Computer Science, Engineering and Applications (ICCSEA)*, pp. 1–5, Gunupur, India, 2020.
- [12] M. Shi, Y. Zhang, H. Wang, J. Hu, and X. Wu, "A clonal selection optimization system for multiparty secure computing," *Complexity*, vol. 2021, Article ID 7638394, 14 pages, 2021.
- [13] G. Rastogi, S. Narayan, G. Krishan, and R. Sushil, "Deployment of the cloud using open-source virtualization: study of Vm migration methods and benefits," in *Big Data Analytics*, pp. 553–563, Springer, Singapore, 2018.
- [14] S. F. Suhel, V. K. Shukla, S. Vyas, and V. P. Mishra, "Conversation with automation in banking through chatbot using artificial machine intelligence language," in *2020, 8th International Conference on Reliability, Infocom Technologies and Optimization (Trends and Future Directions)(ICRITO)*, pp. 611–618, Noida, India, 2020.
- [15] W. Li, X. Meng, Y. Huang, and J. Yang, "Efficient particle swarm optimization with multidimensional mean learning," *International Journal of Pattern Recognition and Artificial Intelligence*, vol. 35, no. 3, 2021.
- [16] M. N. Kumar, V. Jagota, and M. Shabaz, "Retrospection of the optimization model for designing the power train of a formula student race car," *Scientific Programming*, vol. 2021, Article ID 9465702, 9 pages, 2021.
- [17] F. Wu, X. Liu, and Y. Wang, "Research on software design of intelligent sensor robot system based on multidata fusion,"



*Journal of Sensors*, vol. 2021, Article ID 8463944, 10 pages, 2021.

- [18] J. Bhola, M. Shabaz, G. Dhiman, S. Vimal, P. Subbulakshmi, and S. K. Soni, "Performance evaluation of multilayer clustering network using distributed energy efficient clustering with enhanced threshold protocol," *Wireless Personal Communications*, pp. 1–15, 2021.
- [19] Q. Zhou, H. Q. Li, and J. Wang, "Deep model-based reinforcement learning via estimated uncertainty and conservative policy optimization," *Proceedings of the AAAI Conference on Artificial Intelligence*, vol. 34, no. 4, pp. 6941–6948, 2020.
- [20] W. J. Romero-Rodriguez, R. Baltazar, J. M. Carpio Valadez et al., "A novel model for optimization of intelligent multi-user visual comfort system based on soft-computing algorithms," *Journal of Ambient Intelligence and Smart Environments*, vol. 13, no. 2, pp. 95–116, 2021.

## Retraction

# Retracted: Application Research of Time Delay System Control in Mobile Sensor Networks Based on Deep Reinforcement Learning

### Wireless Communications and Mobile Computing

Received 25 July 2023; Accepted 25 July 2023; Published 26 July 2023

Copyright © 2023 Wireless Communications and Mobile Computing. This is an open access article distributed under the Creative Commons Attribution License, which permits unrestricted use, distribution, and reproduction in any medium, provided the original work is properly cited.

This article has been retracted by Hindawi following an investigation undertaken by the publisher [1]. This investigation has uncovered evidence of one or more of the following indicators of systematic manipulation of the publication process:

- (1) Discrepancies in scope
- (2) Discrepancies in the description of the research reported
- (3) Discrepancies between the availability of data and the research described
- (4) Inappropriate citations
- (5) Incoherent, meaningless and/or irrelevant content included in the article
- (6) Peer-review manipulation

The presence of these indicators undermines our confidence in the integrity of the article's content and we cannot, therefore, vouch for its reliability. Please note that this notice is intended solely to alert readers that the content of this article is unreliable. We have not investigated whether authors were aware of or involved in the systematic manipulation of the publication process.

Wiley and Hindawi regrets that the usual quality checks did not identify these issues before publication and have since put additional measures in place to safeguard research integrity.

We wish to credit our own Research Integrity and Research Publishing teams and anonymous and named external researchers and research integrity experts for contributing to this investigation.

The corresponding author, as the representative of all authors, has been given the opportunity to register their

agreement or disagreement to this retraction. We have kept a record of any response received.

### References

- [1] W. Zhu, T. Garg, S. Raza, S. Lalar, D. D. Barak, and A. W. Rahmani, "Application Research of Time Delay System Control in Mobile Sensor Networks Based on Deep Reinforcement Learning," *Wireless Communications and Mobile Computing*, vol. 2022, Article ID 7844719, 7 pages, 2022.

## Research Article

# Application Research of Time Delay System Control in Mobile Sensor Networks Based on Deep Reinforcement Learning

Wenwu Zhu <sup>1</sup>, Tanya Garg <sup>2</sup>, Saleem Raza <sup>3</sup>, Sachin Lalar <sup>4</sup>, Dheer Dhvaj Barak <sup>5</sup>,  
and Abdul Wahab Rahmani <sup>6</sup>

<sup>1</sup>Department of Electrical Engineering, Anhui Technical College of Mechanical and Electrical Engineering, Anhui, Wuhu 241002, China

<sup>2</sup>Thapar Institute of Engineering and Technology, Patiala, Punjab, India

<sup>3</sup>Quaid-e-Awam University of Engineering, Science and Technology, Larkana, Pakistan

<sup>4</sup>Department of Computer Science and Applications, Kurukshetra University, Kurukshetra, India

<sup>5</sup>Department of Computer Science and Engineering, Vaish College of Engineering, Rohtak, Haryana, India

<sup>6</sup>Isteqlal Institute of Higher Education, Kabul, Afghanistan

Correspondence should be addressed to Wenwu Zhu; [wenzuzhu66@163.com](mailto:wenzuzhu66@163.com) and Abdul Wahab Rahmani; [ab.wahab.professor@isteqlal.edu.af](mailto:ab.wahab.professor@isteqlal.edu.af)

Received 18 January 2022; Revised 10 February 2022; Accepted 28 February 2022; Published 18 March 2022

Academic Editor: Shalli Rani

Copyright © 2022 Wenwu Zhu et al. This is an open access article distributed under the Creative Commons Attribution License, which permits unrestricted use, distribution, and reproduction in any medium, provided the original work is properly cited.

One of the main problems of networked control systems is that signal transmission delay is inevitable due to long distance transmission. This will affect the performance of the system, such as stability range, adjustment time, and rise time, and in serious cases, the system cannot maintain a stable state. In this regard, a definite method is adopted to realize the compensation of network control system. To improve the control ability of mobile sensor network time delay system, the control model of mobile sensor network time delay system based on reinforcement learning is proposed, and the control objective function of mobile sensor network time delay system is constructed by using high-order approximate differential equation, combined with maximum likelihood estimation method for parameter estimation of mobile sensor network time delay, the convergence of reinforcement learning methods for mobile sensor network control and adaptive scheduling, and sensor network time delay system control model of multidimensional measure information registration in strengthening tracking learning optimization mode to realize the adaptive control of mobile sensor network time delay system. The simulation results show that the proposed method has good adaptability, high accuracy of estimation of delay parameters, and strong robustness of the control process.

## 1. Introduction

Recent advances in wireless telecommunications and electronics have opened the way for the development of low-cost, low-power, and multifunctional sensor nodes that are small in size and wirelessly connect. Merely a little distance, the tiny sensor nodes, sensor components, data processing components, and connection components are supplied, allowing you to apply the sensor idea. Network sensor networks are an essential component of today's environment step up from standard sensors [1, 2]. Wireless sensor network (WSN) is a new mode of information acquisition and

processing which integrates sensor, embedded, wireless communication, distributed information processing, and other technologies. It is widely used in military, national security, environmental science, traffic management, disaster prediction, medical and health care, manufacturing, urban information construction, and other fields. In the Ministry of Industry and Information Technology released in November 2011, the Internet of Things "twelfth five-year" plan, the emphasis is put forward: in the field of wireless sensor networks, the need for sensor nodes and operating system, close range wireless communication protocol, sensor network networking technologies such as research,

developed low power consumption, high performance, and applicable range of the wireless sensor network systems and products. It shows that both at the national level and in the field of industrial application, wireless sensor network is believed to have a large application market and development potential in the future. Under the current wave of the industrial Internet, many traditional industrial production modes have carried out the corresponding technological innovation and upgrading, such as the optimization of the production process on the industrial site and the optimal allocation and coordination of social production resources. All above application scenarios require the wireless sensor networks to transmit real-time production data, supply, and demand information or equipment status back to the control center, to provide important reference data for production optimization and resource scheduling [3].

The wireless sensor network (WSN) is an infrastructure-free wireless network that analyzes system, physical, and environmental parameters through the ad hoc distribution of such a large number of wireless sensors. WSN controls and monitors the environment in a specified region by utilizing sensor nodes in combination with an embedded CPU. They are linked to the base station, which serves as the processing unit again for WSN system [4, 5]. With the development of mobile sensor network communication technology, mobile sensor network transmission is adopted to carry out large-scale data transmission and realize mobile sensor network data balanced scheduling and adaptive allocation; to improve the fidelity and transmission efficiency of data transmission, mobile sensor network time delay control is needed in the design of mobile sensor network. Combined with the design of mobile sensor network time delay control algorithm, the optimization design of mobile sensor is carried out; this paper studies the time-delay system control model of mobile sensor network and combines the channel equalization control method to improve the data and information transmission quality of mobile sensor network. The research on time-delay system control method of mobile sensor network has attracted great attention. However, the main shortcoming of the wireless sensor network of mobile sink node is that it increases the time delay of the network, and the data detected by the sensor node must be stored temporarily in the cache of the node and can only be forwarded to the mobile node when the mobile node moves nearby. This results in excessive delay, which in some cases cannot be tolerated. For example, in the case of pollution monitoring in cities, when there is an emergency sudden leakage of data, it must be transmitted to the base station for processing before causing serious consequences. Wireless sensor network has been widely used in industrial production, intelligent transportation, environmental monitoring, and other fields. The main challenges are focused on real-time, energy management, deployment and positioning, routing, data fusion and compression, etc. The purpose is to solve the problem of maximizing the utility of wireless sensor network under the limited energy.

In recent years, to solve the problem of unbalanced energy consumption of traditional wireless sensor network nodes, the network connectivity and coverage cannot be

guaranteed. Some researchers propose to introduce moving sink nodes to solve the problem, i.e., moving sink wireless sensor networks (MWSNs). Lin and Yan established a mathematical model of the operation process of ZigBee standard wireless network of the remote monitoring system based on Markov chain device. This model is used to evaluate the operation process of MAC CSMA/CA algorithm of IEEE802.15.4 ZigBee standard [6]. A new integral inequality is developed by using Wirtinger integral inequality and Leibniz-Newton formula [7]. The ZigBee protocol was designed to transport data in high-frequency RF situations such as those seen in commercial and industrial applications. The new version expands on the present ZigBee standard by unifying market-specific application profiles, allowing any device, independent of market designation or purpose, to be wirelessly joined in the same network. Furthermore, a ZigBee certification procedure ensures that devices from different manufacturers may communicate with one another [8]. Guo et al. adopt the method of delay partition, by constructing an augmented Lyapunov-Krasovskiy functional with three and four integrals and using some standard integral inequality techniques, obtained the asymptotic stability criterion of the relevant neural network. By converting the sampling period into a bounded time-varying delay, the error dynamics of the generalized neural network considered is derived using a dynamical system with sampling [9]. These and other sensor network applications necessitate the use of mobile intermittently connected methods. Many algorithms and algorithms for typical wireless ad hoc networks have been suggested, but they are not well adapted to the particular characteristics and application needs of sensing devices [10, 11]. Khujamatov et al. established a mathematical model of the operation process of ZigBee standard wireless network of a remote monitoring system based on Markov chain device. This model is used to evaluate the operation process of MAC CSMA/CA algorithm of IEEE802.15.4 ZigBee standard. The characteristic of this mathematical model is that it considers the load level of network elements and the potential malformation of transmission packets under the influence of interference. The developed mathematical model is used to analyze the main characteristics of the network operation process, such as the dependence of the successful transmission probability of packets on the system load (number of nodes and minimum length of competing windows) and the dependence of the bandwidth of channel noise on the system load (minimum length of competing window) [12]. Reinforcement learning is a subfield of machine learning. It all comes down to taking the appropriate actions to maximize your profit in a particular situation. A number of applications and computers utilize it to find the best possible action or course in a given event. Reinforcement learning differs from supervised learning in that the answer key is included in supervised learning, allowing the model to be trained with the correct answer, whereas reinforcement learning does not include an answer and instead relies on the reinforcement agent to decide what to do to complete the task. In the absence of a training dataset, it is compelled to learn from its own experience [13, 14]. Reinforcement learning is used

to solve node scheduling and routing problems in wireless sensor networks. Finally, simulation experiments are carried out to demonstrate the superiority of the proposed method in improving the control ability of mobile sensor network time delay system.

Sensor network has a large application market and development potential. This method can effectively control the mobile sensor network time delay system, and the output time delay is smaller, the stability is better, and the bit error rate is lower.

## 2. Transmission Delay Control and Parameter Analysis of Mobile Sensor Network

*2.1. Composition of Routing Transmission Delay.* There are two types of data operations in MWSNs: (A) The observer issues query instructions, and the query instructions go through the base station, mobile chat, cluster head, and finally to the sensor that detects the data; after receiving instructions, the sensor will implement data sampling. After the sampling, the data will be transmitted hop by hop to the sensor cluster head for storage, waiting for moving chat to collect data, and finally, the data will be returned to the base station to query the data, which is a passive network, as shown in Figure 1(a). There is no query instruction for data operation. The monitoring data will be sent out only when the monitoring data of a node exceeds its own monitoring threshold or is sampled according to a preset period (that is, it is based on events and time driven, respectively). Through the cluster head storage, moving sinks down to the base station, i.e., an active network, as shown in Figure 1(b).

In wireless sensor network measurement and control system, due to its own characteristics, when transmitting information, time delay with the packet loss phenomenon is inevitable, so in the greenhouse wireless sensor network measurement and control system also has this problem the topic. We assume that  $\tau_1$  for the underlying through gathering the information collected by the sensor node and then transmitted to the monitoring center through the base station by gathering node generated by the time delay,  $\tau_2$  after optimization algorithm to the control center, and control information via the base station transmitted to a base station will converge node; it generated when the control node transmission delay. Here, it is assumed that the monitoring center and control node are event driven; the sensor node is clock driven. Assume that the total extension of the closed loop is less than the sampling period  $T$ , and ignore the noise interference in the measurement and control system. When the packet loss occurs in the system, we make it resend. Therefore, for the system, the packet loss can be treated as a special delay.

Based on the active data operation mode, the transmission process of the sensor node sending data packets to the destination base station is divided into the following stages:

- (A)  $n_i$  Sensor nodes form a static cluster. Data collected by nodes in the cluster reaches the cluster head after multiple hops, and the delay is  $\tau_{s0}$

- (B) The sensor node or cluster head waits for the moving node  $M_k$  to enter its transmission range [3]. When  $M_k$  enters transmission range, the transmitter node (or cluster header) sends data to. The time delay is  $\tau_{s0}$ , referred to as waiting time delay  $M_k$
- (C) The data carried by  $M_k$  gradually approached to the target base station through several relays of moving sinks, and the time delay was measured as  $\tau_{mm}$
- (D) Mobile budget node transmits data to the base station nearest to itself. The time delay is  $\tau_{mun}$
- (E) Data is transmitted between base stations and finally arrives at the destination base station. The time delay is  $\tau_{bb}$
- (F) Thus, the time delay of a packet from being produced to being transmitted to the user can be calculated as  $D^{\text{total}}$

$$D^{\text{total}} = \tau_{sc} + \tau_{sm} + \tau_{nm} + \tau_{mb} + \tau_{bb}b, \quad (1)$$

where  $\tau_{sc}$  and  $\tau_{sm}$  delay is the main components affecting network delay, compared with  $\tau_{sc}$ , and  $\tau_{mn}$ ,  $\tau_{mb}$ , and  $\tau_{bb}$  stages have a very mature transmission technology (ad hoc mobile communication technology, etc.); they are predictable and do not vary much. In addition, in some application models, the mobile sink node is a user; that is,  $D^{\text{total}} \approx \tau_{sc} + \tau_{sm}$ . Therefore, this time delay study mainly analyzes these two parts.

*2.2. Reinforcement Learning Model for Sensor Network Delay System Control.* Reinforcement learning method is used to carry out convergence control and adaptive scheduling of mobile sensor network.  $M$  sink nodes are set to collect the transmission information of the mobile sensor network. The distribution amplitude of the network output bit sequence flow is AC, and the coherent distribution sources transmitted by the mobile sensor network are  $P$  interference signals; the discrete signal controlled by the mobile sensor network delay system is  $x$ . Let the code feature sequence of the original input mobile sensor network be  $x = [x(0) \cdots x(n-1)]$ , where  $X(n)$  is the bit stream transmitted by the finite length discrete mobile sensor network,  $0 < k < n-1$ . The channel model of mobile sensor network delay system control obtained by vectorization processing method is as follows:

$$X(k) = \sum_{n=0}^{N-1} x(n) \exp\left(-j \frac{2\pi}{N} nk\right), \quad (2)$$

where  $0 < k < n-1$  represents the length of data transmitted by the mobile sensor network, signal  $X(n)$  is processed by the discrete orthogonal wavelet transform, and  $X = \text{DEF}(x)$  represents the bandwidth controlled by the mobile sensor network delay system. In the discrete distribution sequence  $x$ , the enhanced tracking learning method is used to carry out channel equalization control of mobile

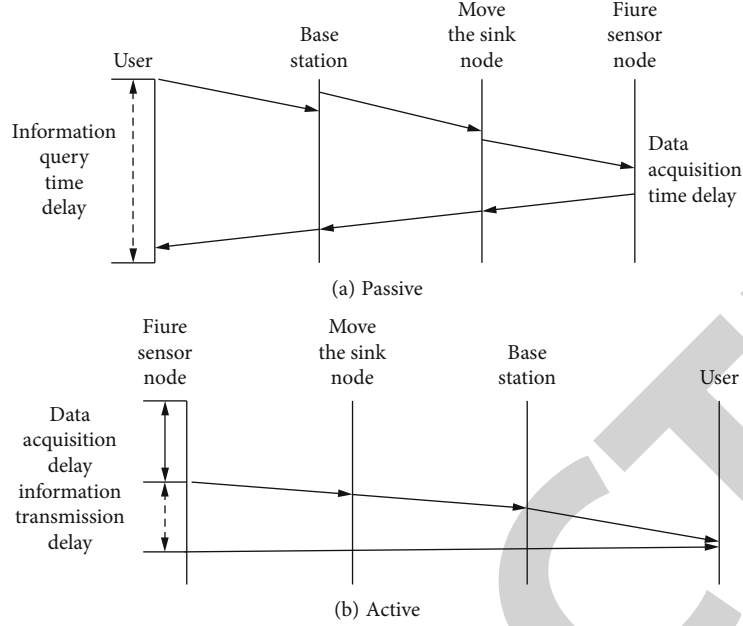


FIGURE 1: Schematic diagram of terminal-to-break network.

sensor network transmission [12]. By analyzing the computational complexity of each iteration, the characteristic quantity of statistical information of mobile sensor network time-delay system control is obtained as follows:

$$X = [X(0), \dots, X(N-1)]. \quad (3)$$

In the transmission channel of mobile sensor network, the relation point between vectorization and Kronecker product satisfies  $j=0, 1, \dots, M$ ; the energy function controlled by the time delay system of mobile sensor network is  $E_j = \sum_k |C_i(k)|^2$ ; for integer  $N_0$  and  $N_1$  transmission channels, the pass band of mobile sensor network transmission delay system control is  $C^{(j)}$ , and reinforcement learning method is used to carry out mobile sensor network channel equalization control. Each block signal corresponds to the characteristic number of Baud interval sampling at 1-dimensional distance. The scattering point function of time delay control at each distance is as follows:

$$\begin{aligned} C^{(0)} &\leftarrow \text{DFT}\{x\}, \\ \{C^{(j)}, W^{(j)}\} &\leftarrow \text{AFB}(C^{(j-1)}, N^{(j)}, N_1^{(j)}), \\ w^{(j)} &\leftarrow \text{DEF}^{-1}\{W^{(j)}\}, \\ c^{(j)} &\leftarrow \text{DEF}^{-1}\{C^{(j)}\}, \end{aligned} \quad (4)$$

where  $N$  represents the length of data transmitted by the mobile sensor network and  $J$  is the frequency of characteristic sampling. Based on the above analysis, a reinforcement learning model of sensor network time-delay system control is built, and the mathematical modeling of system control is

carried out in combination with the time delay estimation method.

Applications are being developed in a range of scientific fields. Extensive seismic testing, habitat monitoring, and intelligent transportation systems are just a few of the exciting ongoing endeavors [15, 16]. Home and building automations, as well as military applications, are important application fields. The performance gain of mobility on the network is verified by simulation. To simplify the simulation, the data collection method uses mobile sink nodes to collect data directly from each sensor node. After sensing and collecting data, the sensor node will cache the data in memory and wait for the mobile sink node to collect. The physical layer adopts ZigBee wireless network technology, and the MAC layer and routing layer protocols of sensor nodes, respectively, use S-MAC protocol [17] and TTOD protocol [18]. ZigBee is a set of greater communication systems great for small projects that require wireless connectivity. It is used to create connectivity using small, minimal digital radios, such as for home automation, medical device data gathering, or other reduced, reduced demands. As a result, ZigBee is a reduced, reduced wireless ad hoc network that works near to each other. The ZigBee standard outlines a technology that is intended to be simpler and less expensive than existing wireless personal area networks (WPANs) such as Bluetooth or wider wireless networking such as Wi-Fi. Examples of applications include wireless switches, home energy monitors, traffic management systems, and other consumer and industrial equipment that require short-range low-rate wireless data transfer [19, 20]. 1000 static sensor nodes are uniformly deployed in a 10000 m  $\times$  10000 m area, and the moving chat moves in the moving model's random direction. The packet generation rate of the sensor node is 1 packet/cycle, and the simulation runs for 1 cycle. Default parameters are used for other parameters [21].

Performance indexes such as average data transmission delay, data transmission success rate, and packet sharing rate are mainly investigated [22]. The average data transmission delay is defined as the time experienced by data from generation to successful receipt of the moved chat nodes, which is mainly the waiting time. To compare the relationship among speed  $v$ , number  $m$ , transmission radius  $r$ , and packet size  $L$  of moving sinks, as shown in Figure 2, the more  $m$  move sinks, the smaller the time delay. The simulation results are in good agreement with the above analysis. The results also show that the appropriate moving sink velocity should be selected. When the velocity  $v$  of moving sink is too low, the sensor node needs to wait a long time to get the data transmission service of moving sink. And if the speed  $v$  of moving chat is too fast, although the probability of meeting the chat node and sensor node is increased, it leads to long sinks which cannot be transmitted within a service period (in real network, the packet can only be transmitted in fragments).

### 3. Experimental Test Analyses

The delay compensation is realized by designing the predictive controller, and the stability condition of the system and the expression of the controller are obtained by choosing the Lyapunov function reasonably. Considering the case of packet loss, the delay compensation is still compensated by predictive controller, and the packet loss problem can be established as a random Bernoulli sequence, so the model established for the network control system becomes a stochastic control system model. After that, the stability of the established stochastic system is studied, and the controller is solved.

To test the method in the implementation of mobile sensor network time delay system control performance, the analysis of time delay, mobile sensor network time delay system control node distribution in homogeneous array area of 200 m by 200 m, mobile sensor network with element transfer rate of 20 k Baud, time delay control system of carrier frequency for 24 kHz, the output signal-to-noise ratio of -15 dB, initial coverage radius for the sensor network is taken of 10 m, and the node energy  $E_0 = 200$ . Firstly, packet loss is established as a random Bernoulli sequence with values of 0 and 1, and the stability of the stochastic system is given. By adopting predictive control scheme to deal with delay, the influence of delay and packet loss on NCS is improved effectively. Then, the delay compensator designed at the actuator end is used to select the latest control data to compensate the delay from the controller to the actuator. According to the above simulation environment and parameter settings, the mobile sensor network time delay system is controlled, and the distribution of the output transmission code sequence of the mobile sensor network is obtained, as shown in Figure 2.

Taking the data in Figure 2 as the research object, the mobile sensor network time delay system is controlled, and the optimized control output is shown in Figure 3.

Analysis diagram 3, using the method can effectively control the mobile sensor network time delay system, the

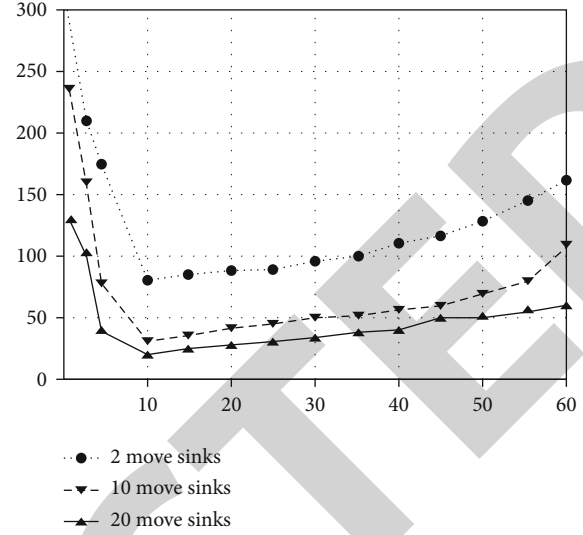


FIGURE 2: Output code sequence of mobile sensor network.

output of the time delay is small, stable, improve the transmission stability of the mobile sensor network, test the output error, by contrast, the results are shown in Table 1, as shown in the analysis, the method to control after the mobile sensor network time delay system reduces the output bit error rate of the network [23].

Mobile sensor network time delay control is combined with the design of mobile sensor network time delay control algorithm and mobile sensor optimization design [24]. The extraction of mobile sensor network, transmission delay information of the average mutual information, combined with squares estimation method and maximum likelihood estimation method, control the time delay and parameter estimation, in strengthening tracking learning optimization mode adaptive control to realise the mobile sensor network time delay system, is based on the reinforcement learning system control model of mobile sensor network time delay. It improves the transmission balance of mobile sensor network and reduce the delay [25]. The results show that the proposed method can effectively control the time delay system of mobile sensor network, and the output time delay is smaller, the stability is better, and the bit error rate is lower.

### 4. Analysis

In recent decades, more and more experts and scholars have paid attention to the research and application of time-delay systems. The phenomenon of time delay often affects the parameter performance of the system and sometimes even makes the system collapse. Therefore, the theoretical study of time delay system has important theoretical significance and practical value. For a system with time delay, the first thing to consider is its stability. Under the premise of stability, the maximum time delay allowed by the system is often the focus of research. Many experts and scholars put forward a series of innovative ideas and formed a relatively perfect theoretical system. For the study of time-delay systems, many theoretical achievements have been made, such as

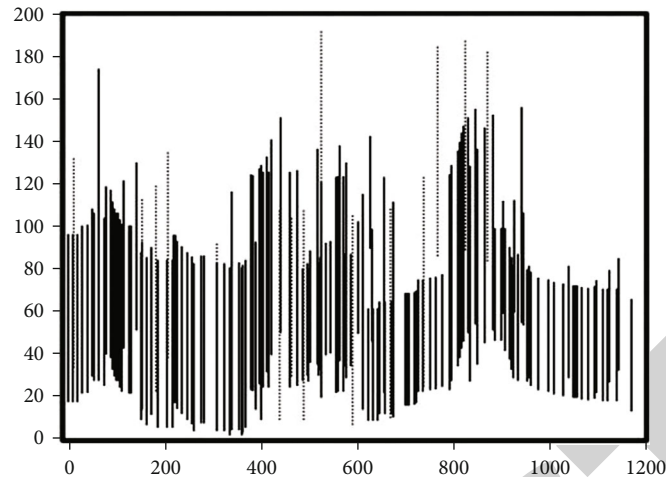


FIGURE 3: Optimized control output of mobile sensor network delay system.

TABLE 1: Comparison of output bit error rates.

Signal to noise ratio/dB	Methods/dB	The literature/dB [12]	The literature/dB [9]
-10	0.063	0.143	0.254
-8	0.041	0.121	0.143
-6	0.023	0.112	0.146
-4	0	0.103	0.122
0	0	0.072	0.110

time-delay of variable time-delay system research, guaranteed performance control of variable delay systems, and other related robust stability.

## 5. Conclusions

The method in this paper reduces the output bit error rate of the network after controlling the delay system of the mobile sensor network. The bit error rate is reduced to about 0. A new adaptive recursive channel estimation algorithm, in which the last channel estimation, is used to initialize the iteration process of the current channel estimation; thus, the channel estimation and tracking are performed. In addition, the channel estimation is recursively updated, and the matrix inversion method is applied to reduce the complexity of calculation [19]. According to the analysis and simulation of the new algorithm, compared with the RLS algorithm, the proposed algorithm can estimate and track the channel changes more accurately in the fast fading environment without affecting the performance of the system error, which shows that the proposed algorithm is robust to the high Doppler shift. Mobile sensor network time delay control is combined with the design of mobile sensor network time delay control algorithm and mobile sensor optimization design. Time delay control of mobile sensor network time delay system based on reinforcement learning control mathematical modelling Wen-wen Yang, the extraction of mobile sensor network, transmission delay information of the average mutual information, combined with squares estimation

method and maximum likelihood estimation method, time delay control of mobile sensor network time delay system based on reinforcement learning control mathematical modelling Wen-wen Yang, and the parameter estimation. The adaptive control of mobile transmitter network delay system is realized in the enhanced tracking learning optimization mode, which improves the transmission balance of mobile sensor network and reduces the delay. This method can effectively control the time delay system of mobile sensor network, and the output time delay is smaller, the stability is better, and the bit error rate is lower.

## Data Availability

All the data pertaining to this article is in the article itself.

## Conflicts of Interest

The authors declare that there is no conflict of interest regarding the publication of this paper.

## References

- [1] Y. Zhan, S. Guo, P. Li, and J. Zhang, "A deep reinforcement learning based offloading game in edge computing," *IEEE Transactions on Computers*, vol. 69, no. 6, pp. 883–893, 2020.
- [2] S. Saxena, S. Vyas, B. S. Kumar, and S. Gupta, "Survey on online electronic paymentss security," in *2019 Amity International Conference on Artificial Intelligence (AICAI)*, p. 756, Dubai, United Arab Emirates, 2019.
- [3] W. Hong and Y. Peng, "Delay control system of intelligent traffic scheduling based on deep learning and fuzzy control," *Journal of Intelligent and Fuzzy Systems*, vol. 38, no. 6, pp. 7329–7339, 2020.
- [4] P. Lin, Q. Song, J. Song, A. Jamalipour, and F. R. Yu, "Cooperative caching and transmission in CoMP-integrated cellular networks using reinforcement learning," *IEEE Transactions on Vehicular Technology*, vol. 69, no. 5, pp. 5508–5520, 2020.
- [5] M. Sehgal and D. Bhargava, "Knowledge mining: an approach using comparison of data cleansing tools," *Journal of*



## Research Article

# Virtual Reality Primary School Mathematics Teaching System Based on GIS Data Fusion

Yi Xie , Yaoqi Hong, and Yanni Fang

*School of Primary Education, Yuzhang Normal University, Nanchang, 330103 Jiangxi, China*

Correspondence should be addressed to Yi Xie; [xieyi1013@yuznu.edu.cn](mailto:xieyi1013@yuznu.edu.cn)

Received 3 January 2022; Revised 10 February 2022; Accepted 19 February 2022; Published 16 March 2022

Academic Editor: Shalli Rani

Copyright © 2022 Yi Xie et al. This is an open access article distributed under the Creative Commons Attribution License, which permits unrestricted use, distribution, and reproduction in any medium, provided the original work is properly cited.

Virtual reality technology is becoming more and more well-known by more and more people. Informatization of education is vigorously promoted in the modernization of the country. As a new type of digital information processing platform, virtual reality technology has a huge advantage in elementary school mathematics teaching. It is based on three-dimensional spatial data for modeling, analysis, and display. In addition, as a data synthesis and processing technology, data fusion is actually the integration and application of many traditional disciplines and new technologies. Geographic information system (GIS) is a specific and very important spatial information system. This article mainly uses the method of case analysis, giving examples of virtual experimental teaching system, intelligent auxiliary teaching system, and virtual classroom teaching system to analyze the related technologies and then apply the investigation method and experimental method to test the system proposed in this article and organize students' opinions systematic attitude. Experimental data and survey results show that 78 students believe that the virtual mathematics education system is most suitable for simulating operation experience and understanding principles. And more than 50% of students believe that the virtual experimental education system has significantly increased their interest in learning. For this reason, the research on the virtual reality elementary school mathematics teaching system based on GIS data fusion is of great significance.

## 1. Introduction

The application of virtual reality in the education field can solve some teaching problems. Using virtual reality technology, dynamic interactive multilevel spatial analysis can be realized. The system can process the original image data according to the user's intention and generate a two-dimensional array for automatic identification. Teachers can use the GIS system to obtain the required information resources and provide real-time data support and services during the teaching process.

Mathematics teaching is a process of continuous development, which needs to be updated and improved with the times. Teachers must be able to fully understand the concepts and principles involved in the construction of virtual reality systems. Students should also be able to correctly understand virtual reality technology and improve their ability to analyze learning content and solve problems. When constructing a virtual reality teaching system, teachers

should rely on teaching materials and teaching videos to ensure the sharing of information resources and facilitate compatibility between different versions.

In recent years, as the country attaches importance to education, more and more experts and scholars have begun to pay attention to the application of virtual reality technology in teaching. With the continuous advancement of science and technology and the rapid economic growth, my country's talent training model is also undergoing rapid changes. There are many theoretical results on the GIS data fusion and virtual reality primary school mathematics teaching system. For example, Wang et al. used the world's leading geographic information system (GIS) technology to establish a student information database, as well as a management and analysis system, in response to the general problem that the current university student information management methods cannot meet the local first-line teaching needs. Min said that the investigation of classroom teaching behavior is one of the important research topics.

When using the Flemish system to conduct quantitative research on high-quality courses, it is found that teachers of high-quality courses generally use self-examination for teaching [1, 2]. Liu analyzes the value of the deep integration of Changyan's multimedia interactive education system and rural elementary school mathematics teaching based on the function of Changyan's multimedia interactive education system and proposes effective strategies for rural elementary school mathematics teaching [3]. Demitriadou et al. said that elementary school students often find it difficult to understand the difference between two-dimensional and three-dimensional geometric shapes. Using virtual reality and augmented reality to visualize the possibility of 3D objects, we studied the potential of using virtual reality and augmented reality technology to teach 3D geometry courses to elementary school students [4]. Goehle provides a "virtual reality" course on common computing topics, including a description of how to implement the course in virtual reality and augmented reality hardware systems [5]. The purpose of Shin's research is to analyze the characteristics of virtual applications, which can be used to teach students who have difficulty learning mathematics [6]. Clay BS reported on classroom observations of high school mathematics teaching, focusing on the use of digital technology. The object of consideration is teachers who participate in the extracurricular course "Mathematical Structure" [7]. On the basis of these predecessors' related research, this article intends to study GIS data fusion and then analyze and design the virtual reality elementary school mathematics teaching system.

The research innovations of this article mainly include the following aspects: the first is the novelty of the research perspective. This article studies the elementary school mathematics teaching system and starts with virtual reality technology and GIS technology. The second is the innovation of research methods. This article analyzes the primary school mathematics system by studying the virtual experimental teaching system, the intelligent auxiliary teaching system, and the virtual classroom teaching system. The third is that the research conclusions are innovative. This article not only draws the benefits of virtual reality in teaching but also finds related problems.

## 2. Virtual Reality Primary School Mathematics Teaching System Based on GIS Data Fusion

*2.1. Virtual Experimental Teaching System.* Virtual experiment is a link that cannot be ignored in the teaching process of distance education. For disciplines with strong practicality, experiment is a necessary link to acquire knowledge, improve skills, and participate in practice. Therefore, it is of great significance to study the teaching effect and application of the virtual experimental system, optimize the experimental teaching in distance education, perfect the teaching theory of distance education, and give full play to the advantages of distance education. Experimental distance learning is an important part of overall distance learning, but there are differences between experimental distance learning and theoretical distance learning [8, 9].

The so-called virtual reality technology is a comprehensive technology that makes full use of powerful computer software and hardware resources and various advanced sensors. The virtual experience seems to be a simulation experience in the broadest sense, but from the perspective of the real fidelity of the experience and the universality of the application, as well as the real-time experience and experience effects of the experimenter, the traditional computer simulation experience is absolutely unparalleled [10, 11].

The role of virtual reality technology in virtual experience is as follows.

Make up for the lack of distance learning conditions. In distance education, due to testing facilities, testing facilities, and teaching aids, some educational experiments to be set up cannot be carried out. The use of the virtual reality system can overcome these shortcomings: students can have various experiences without the same experience as the real experience, enriching perceptual knowledge and deepening the understanding of course content. Avoid all kinds of dangers caused by real experience or operation. In the past, when the experiment was dangerous, TV video was often used as a substitute for the experiment. Students cannot directly participate in experiments and gain perceptual knowledge. Using virtual reality technology for virtual experience can avoid this problem. Students can enter and observe the inside of these objects [12–15].

The virtual experimental education system is a networked computer education system that uses virtual reality technology to simulate real-life experience and provide a virtual laboratory for education. As an important supplement to the existing laboratory functions, the virtual experimental education system can support classic experimental education. Therefore, in recent years, schools of all levels and types have paid attention to the development of experimental virtual education systems. With the continuous development and maturity of the virtual experimental education system, the virtual experimental education system has emerged from the ivory towers of some colleges and universities and has been popularized in various education and training institutions [16–18].

The development of the virtual experimental education system has roughly gone through three stages: virtual demonstration experience, interactive virtual experience, and distributed virtual experience. Although the implementation methods and technical support of the three are different, the basic ideas are the same. Both use different system mathematical models, physical models, virtual reality models, and mathematical effects models to study relatively complex or abstract real systems.

*2.2. Data Fusion and GIS Technology.* Data fusion refers to the analysis and integration of information obtained in actual teaching through different methods and technical means to achieve the expected purpose, improve work efficiency, and enhance learning benefits. Data fusion is based on a large number of mathematical operations, combining reality with virtual reality, and analyzing these real worlds to obtain the required information [19, 20]. When building a virtual reality system, data needs to be analyzed. First,

build a three-dimensional space model. Through the processing function of GIS software, the model is transformed into a two-dimensional rectangular coordinate system and four-dimensional coordinate information is expressed. Then, the relationship between all elements in the three-dimensional scene is determined according to the attributes of the generated graphic objects and the features contained in the corresponding database. In the virtual reality system, establish the corresponding data dictionary. Finally, the three-dimensional space is divided into different regions by dividing it. It is very necessary to use GIS data fusion software to establish a virtual reality database. When constructing this database, the relevant parameters of various places need to be managed uniformly. At the same time, it is also necessary to formulate operating standards that comply with local usage habits and have scalability requirements based on actual conditions. First, various graphics and words are processed and sorted, and then different types and different types of information are combined to form a complete, independent, and perfect, easy to call, easy to maintain, and easy to query and retrieve [21, 22].

People are aware of the convenience brought by data fusion technology to decision makers, enabling people to obtain more accurate and effective data. As far as my country's current research on data fusion is concerned, it is specifically focused on two aspects: web document data fusion and data fusion of related data. Data fusion is mostly aimed at similar information, and modeling and fusion of heterogeneous information cannot provide a more complete solution [23, 24].

**2.2.1. The Functional Model of Data Fusion.** From the perspective of the functional model of information fusion, the functional model has the following functions: sensor registration monitoring area, each time the registered objects are collected for measurement and evaluation, and various measurement parameters (parameter d'object and state) transmission. The function of data calibration is to unify the time and space reference points of each sensor. Related processing is used to process new reports collected from a specific sensor and report data from other sensors. State estimation includes merging a new data set with the original data each time and estimating the parameters of the monitored object according to the observation value of the sensor [25, 26].

**2.2.2. The Process of Data Fusion.** According to the process shown in Figure 1, the fusion operation is carried out step by step. In the fusion process, it is necessary to verify predicate conflicts and attribute value conflicts. When the resolution method is adopted in the realization process, the conflict of the predicate is resolved by syntactic fusion. When attribute values conflict, verify the accuracy of the resource. If there is no identity, continue to perform the fusion operation, otherwise, end this execution.

**2.2.3. Technical Methods of Data Fusion.** Assuming that the action function of the BP neural network is a sigmoid non-

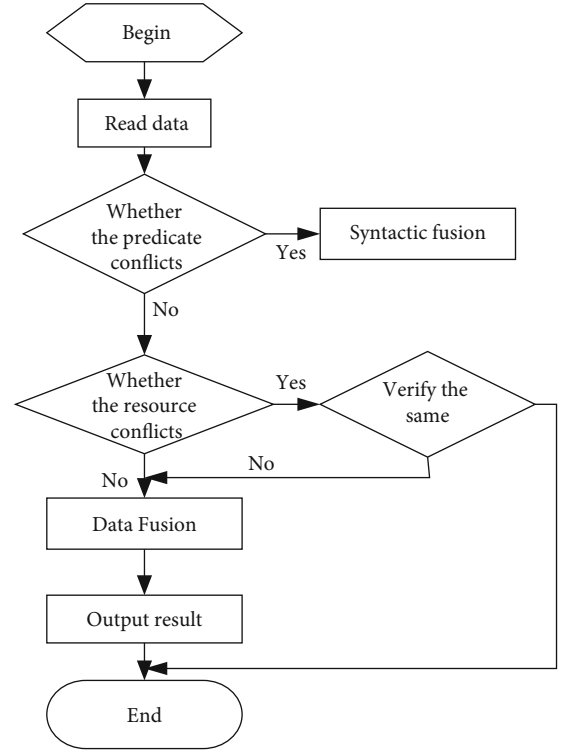


FIGURE 1: Data fusion process.

linear function, the output  $n_k^l$  of the hidden layer node  $l$ :

$$n_k^l = g \left( \sum_{i=1}^x \omega_{ik} n_i^l - \alpha_k \right), k = 1, 2, \Lambda, q. \quad (1)$$

Among them,  $\omega_{ik}$  is the connection weight from the input layer to the hidden layer, and  $\alpha_k$  is the threshold of the hidden layer. The output  $d_k^l$  of the corresponding output layer node  $s$  is

$$d_k^l = g \left( \sum_{k=1}^q w_{ks} n_k^l - \kappa_s \right), s = 1, 2, \Lambda, p. \quad (2)$$

Among them,  $w_{ks}$  is the connection weight from the hidden layer to the output layer, and  $\kappa_s$  is the threshold of the output layer. According to the actual output  $d_k^l$  and the desired output mode, calculate the generalized error  $d_k^l$  of each unit of the output layer:

$$e_k^l = \left( \kappa_s^l - d_k^l \right), s = 1, 2, \Lambda, q. \quad (3)$$

The goal of network learning is to minimize the error function  $F_1$ , which is defined as follows:

$$F_1 = \sum_{s=1}^p \frac{(z_s^l)^2}{2}. \quad (4)$$

Use the method of gradient descent to find the adjustment amount of,  $w_{ks}$ ,  $\kappa_s$ ,  $\hat{w}_{ik}$ , and  $\alpha_k$ .

GIS is based on geographic information system, which records and expresses spatial information through graphics and text. GIS is a type of geographic information system, which uses graphics, text, and other technologies to represent complex data as an organic combination of graphics and sound. Its purpose is to satisfy user needs by analyzing and processing spatial information. In the digital society, GPS can be used to realize the automatic map conversion function. Use the 3D reconstruction method to build the model. The use of coordinate transformation principles to construct virtual reality mathematical models, etc. is all application models based on GIS software. It is a set of dynamic graphics systems developed based on geographic information systems, which has high practical value and a wide range of applications. GIS is the use of graphics, images, text, and other technologies to collect all kinds of information in geographic space and then use the computer as the basis after sorting it out. It has powerful data storage functions and analysis capabilities. Through GIS technology, graphics, text, and other information can be effectively processed to form geospatial data with certain laws and characteristics. It contains a large number of rich and diverse related to human production and life and can be widely used in various fields.

**2.3. Intelligent Auxiliary Teaching System Based on Data Mining.** According to the learner's personalized information feature vectors  $r$ ,  $r_1$  (student number), it can be known that the feature vectors of different learners constitute their personalized information feature matrix. Web usage mining is one of the key technologies for the overall analysis of learning resources. The similarity matrix  $\lambda_{a \times 30}$  between a certain learner and learners with similar characteristics is as follows:

$$RS_{a \times 30} = \begin{Bmatrix} r_{1.1} & r_{1.2} & \Lambda & r_{1.30} \\ r_{2.1} & r_{2.2} & \Lambda & r_{2.30} \\ \Lambda & \Lambda & \Lambda & \Lambda \\ r_{a.1} & r_{a.2} & \Lambda & r_{a.30} \end{Bmatrix}, \quad (5)$$

$$\lambda_{a \times 30} = R \times RS_a = \begin{Bmatrix} \lambda_{1.1} & \lambda_{1.2} & \Lambda & \lambda_{1.30} \\ \lambda_{2.1} & \lambda_{2.2} & \Lambda & \lambda_{2.30} \\ \Lambda & \Lambda & \Lambda & \Lambda \\ \lambda_{a.1} & \lambda_{a.2} & \Lambda & \lambda_{a.30} \end{Bmatrix}. \quad (6)$$

Using the Euclidean distance formula in the fuzzy concept, we get

$$D_2(m, n) = \left( \sum_{i=1}^a |m_i - n_i| \right)^{1/2}. \quad (7)$$

Among them,  $m = (m_1, m_2, \Lambda, m_i)$ ,  $n = (n_1, n_2, \Lambda, n_i) \in R$

. Then the Euclidean distance of feature encoding:

$$D(m, n) = \sum_{l=1}^a |\lambda_m(l_i) - \lambda_n(m_i)|. \quad (8)$$

When  $D(m, n)$  is small, it means that the characteristics of the learner and another learner are very similar. The calculation method using the characteristic prc is as follows:

$$\text{prc} = \{ \langle q, \text{weight}(q, \text{prc}) \rangle | q \in q, \text{weight}(q, \text{prc}) | \geq \lambda \}. \quad (9)$$

Among them,

$$\text{weight}(q, \text{prc}) = \left[ \frac{1}{c} \right] * \sum_{r \in P} W(q, r). \quad (10)$$

Assuming that the current session of the user can be expressed as  $P = \{p_1, p_2, \Lambda, p_a\}$ , and the overall usage characteristic  $D$  can be expressed as  $D = \{W_{1d}, W_{2d}, \Lambda, W_{ad}\}$ .

$$\text{Match}(p, d) = \frac{[\sum_l (W_l^d * p_l)]}{\left\{ \left[ \sum (p_l)^2 * \sum_l (W_l^d)^2 \right]^{1/2} \right\}}. \quad (11)$$

The recommendation coefficient of using web structure crawler technology to judge whether a website is recommended to learners can be expressed as

$$\text{Recommend}(q, p) = [\text{weight}(q, d) * \text{match}(p, d)]^{1/2}. \quad (12)$$

With the rapid development of the Internet and computer technology, various WEB-based auxiliary education systems are increasingly used in colleges and universities at all levels. The auxiliary education system can be used for online learning, online testing, online tutoring, teaching aids, tutoring materials, and communication and interaction between teachers and students, and between students.

The system is mainly composed of two parts, an offline processing module and an online processing module, as shown in Figure 2.

The online processing module of the personalization system will recommend the hyperlink that the user will visit based on the user's profile and the page currently being browsed. The user can follow the recommendation or click on other hyperlinks. The system interface transmits the user's current access operation to the web log usage pattern mining module, which can obtain the current user access operation to obtain the results of web log usage pattern mining and recommend resources for users.

**2.4. Design of Intelligent Teaching System Development Architecture.** In the EGL language development environment EDT, various development wizards are provided to automatically generate different components of the EGL language. From the creation of the EGL project to the development and debugging of the EGL project, it runs through the entire development cycle of the EGL project. In the project creation cycle, EDT provides a wealth of project templates

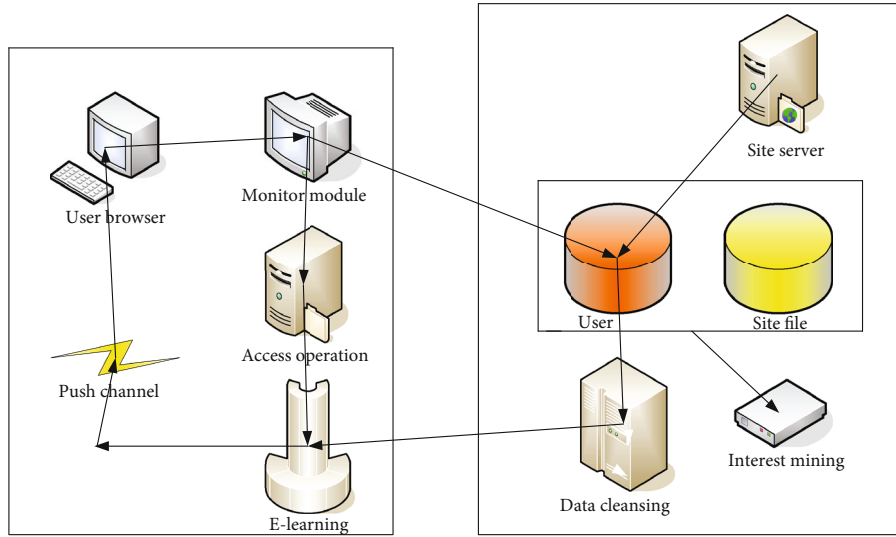


FIGURE 2: Personalized model architecture.

for the EGL language to provide developers with services for different purposes. If needed, users can customize template types to provide new template support for new projects in the form of plug-ins.

Intelligent teaching system is an important development direction for computer-assisted teaching. It means that developers use artificial intelligence technology to make computers play the role of educators in personalized teaching and implement personalized teaching models for learners. Different learning strategies are adopted for learners with different learning characteristics and different learning abilities, and the learners' future learning directions are adaptively taught to achieve the purpose of truly individualized teaching. The logical structure of the intelligent teaching system is generally divided into a three-module structure and a four-module structure. However, with the development of science and technology and the emergence of new technologies, the logical structure of the intelligent teaching system has also undergone corresponding changes. This intelligent teaching system is mainly provided by application servers, database servers, and Web servers, etc., and teachers, administrators, and students can access the system through the Internet. Generally speaking, the basic logical structure of the intelligent teaching system is roughly composed of three basic modules: student module, teacher module, and knowledge base.

The intelligent teaching system is mainly composed of three parts: web server, application server, and database server. The system can be accessed through the Internet. However, these three parts are divided below, as shown in Figure 3.

The intelligent education system is an adaptive education system supported by artificial intelligence: replace the role of the teacher with a computer, implement personalized teaching, transfer knowledge to learners with different characteristics and needs, and let learners guide them. With the help of the Internet, students and teachers can learn and teach through the Internet's intelligent e-learning and e-consulting systems. On the intelligent teaching system plat-

form, teachers can guide students according to their learning situation, update the knowledge base according to various information of students, and formulate test questions that are more suitable for students to learn independently. Through the personalized on-demand function of the system, the intelligent teaching system can provide learners with educational resources that are more in line with the needs of learners and help learners improve their learning efficiency.

A complete computer adaptive test needs to involve many links of work, including parameter estimation (mainly refers to the estimation of the testee's ability and project parameter), question bank construction, question selection, and determination of test termination conditions. The computer adaptive testing process can be roughly divided into two stages: the first stage is the preliminary estimation stage, which is mainly used to roughly estimate the level of the subject at the beginning of the test. The second stage is the precise estimation stage, which is mainly based on the initial value of the ability estimation in the first stage, using the maximum likelihood method or other estimation methods to estimate the ability value of the subjects in the process of answering questions.

**2.4.1. Item Response Theory.** The parameter estimation in item response theory is a very important process, and it is also a very difficult process. Based on the partial independence hypothesis of item response theory, the results of each subject do not affect each other when answering different items, and the results of different subjects answering the same item are also independent of each other.

When only one subject participates in the test consisting of  $A$  items,  $k=1$ , and the item response vector can be expressed as

$$K(V_1, V_2, \Lambda, V_A | \alpha, X, Y, Z) = \prod_{i=1}^A Q_i^{V_i} P_i^{1-V_i}. \quad (13)$$

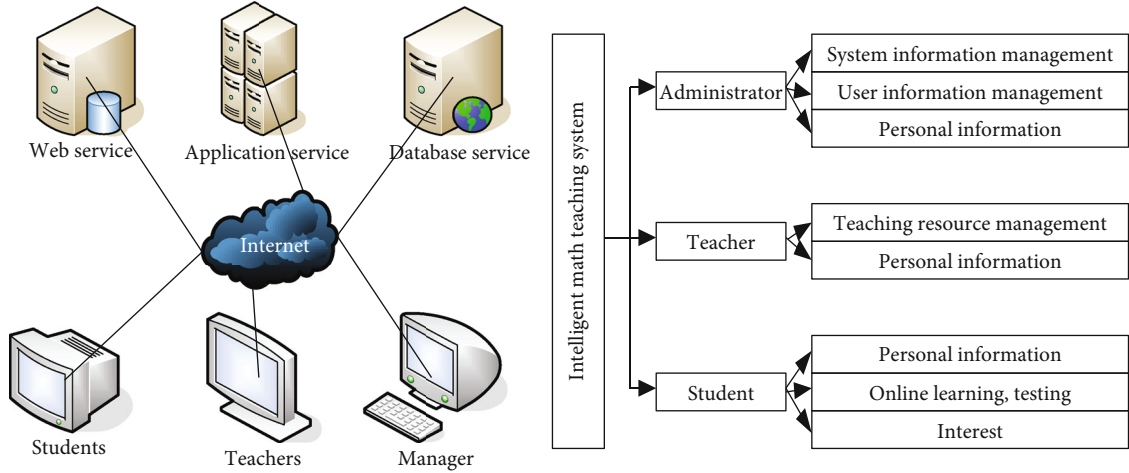


FIGURE 3: The functional design and system topology of the intelligent teaching system.

TABLE 1: Comparison of pretest results between experimental class and control class.

	Number of students	Sample standard deviation	Pretest		
			Passing rate	Excellent rate	Average score
Experimental group	41	12.1	50%	9%	56
Control group	39	58.9	53%	6%	61
<i>Z</i>			0.5328		
<i>P</i>			0.061		

TABLE 2: Comparison of posttest results between experimental class and control class.

	Number of students	Sample standard deviation	Posttest		
			Passing rate	Excellent rate	Average score
Experimental group	41	15.6	74%	30%	76
Control group	39	10.7	69%	21%	64
<i>Z</i>			2.512		
<i>P</i>			0.007		

TABLE 3: Comparison of the interest in mathematics learning between the experimental class and the control class.

	Very interested	Interested	General	No interest
Experimental group	38%	31%	20%	11%
Control group	16%	20%	30%	24%
Total	54%	51%	50%	45%

When  $A$  subjects participate in a test consisting of  $n$  items, the above formula (13) is transformed into

$$K(V|\alpha, X, Y, Z) = \prod_{k=1}^A \prod_{i=1}^a Q_{ik}^{V_{ik}} P_{ik}^{1-V_{ik}}. \quad (14)$$

Among them,  $Q_{ik}$  is the probability that subject  $k$  answers item  $i$  correctly, and  $P_{ik}$  is the probability that sub-

ject  $k$  answers item  $i$  incorrectly.  $\alpha$  is the ability value of the subjects, and  $X$ ,  $Y$ , and  $Z$  are the degree of discrimination, difficulty, and guessing degree of each item.

Through observation, it is known that formula (14) is a continuous multiplication formula, and it is very inconvenient to calculate the derivative. For the same parameter value, both achieve the maximum value at the same time. This style is transformed into the following continuous addition style:

$$\ln K(V|\alpha, X, Y, Z) = \sum_{k=1}^A \sum_{i=1}^a [\lambda_{ik} \ln Q_{ik} + (1 - \lambda_{ik}) \ln P_{ik}]. \quad (15)$$

Differentiate  $\alpha$ ,  $X$ ,  $Y$ , and  $Z$  to get the equations as

$$\frac{\eta \ln K}{\eta \alpha_k} = 0, \quad (16)$$

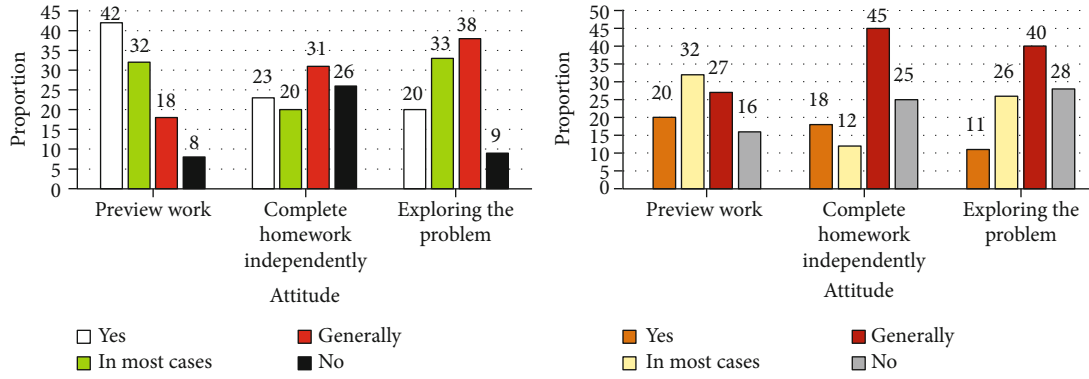


FIGURE 4: Statistics of learning attitude of experimental class and control class.

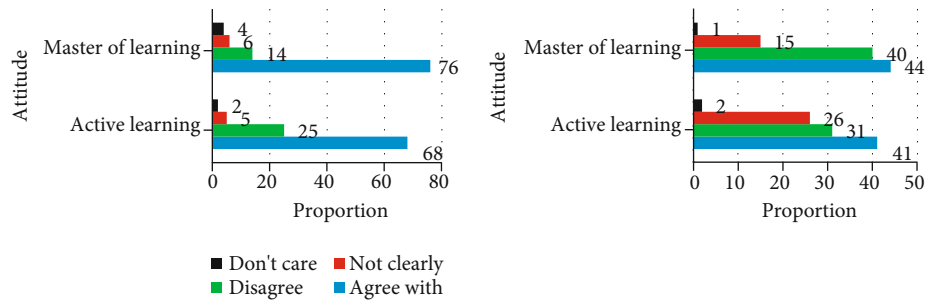


FIGURE 5: Evaluation of students' subjective consciousness in experimental class and control class.

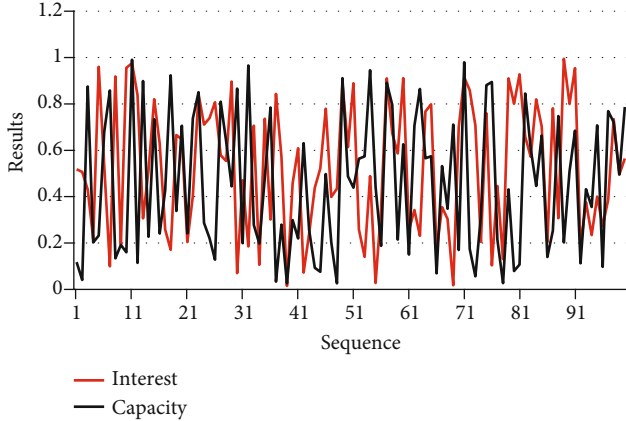


FIGURE 6: Students' interest performance and ability training in virtual experimental teaching system.

$$\frac{\eta \ln K}{\eta X_i} = 0, \quad (17)$$

$$\frac{\eta \ln K}{\eta Y_i} = 0, \quad (18)$$

$$\frac{\eta \ln K}{\eta Z_i} = 0. \quad (19)$$

There are four formulas on the surface. In fact, since there are  $A$  subjects and  $a$  items, each item has three parameters. Then, the parameter estimation process is transformed into the problem of solving nonlinear equations (sets).

2.4.2. *Conditional Maximum Likelihood Estimation.* Let  $g(m) = 0$  be the nonlinear equation to be solved,  $m_0$  is an approximate root of this equation,  $m$  is the exact root of the equation, and  $em$  is the error of the root, then  $m = m_0 + em$ ,  $g(m) = 0$  can be transformed into

$$g(m_0 + em) = 0. \quad (20)$$

The conditional maximum likelihood method has many limitations, which are mainly reflected in that when the subject answers all the items in a test correctly or incorrectly, this method cannot be used to estimate the ability of the subject.

2.5. *The Key Technology of Virtual Classroom Teaching System.* Virtual reality technology is the synthesis and integration of various scientific technologies such as computer graphics technology, multimedia technology, sensors, human-computer interaction technology, and simulation technology. Virtual reality technology can be divided into two categories: hardware and software. Hardware technology is mainly embodied in the development and application of sensing and display equipment. Software technology is mainly embodied in the development and application of virtual reality systems.

GIS-based virtual reality teaching is based on computers and uses multimedia equipment to achieve interactive functions in a three-dimensional dynamic environment. The system collects and transmits information such as graphics, images, and voice in real time. After obtaining the original

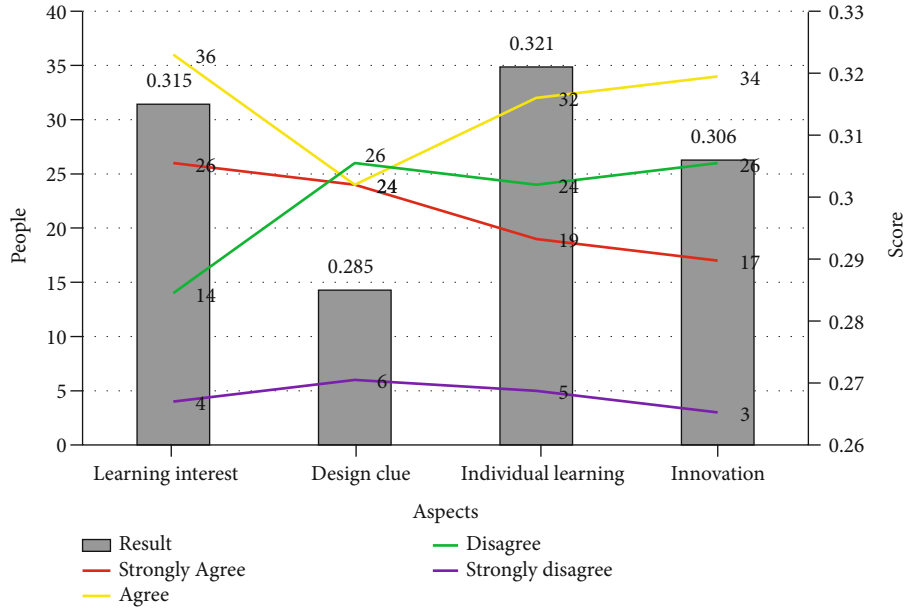


FIGURE 7: Students' attitudes towards virtual teaching.

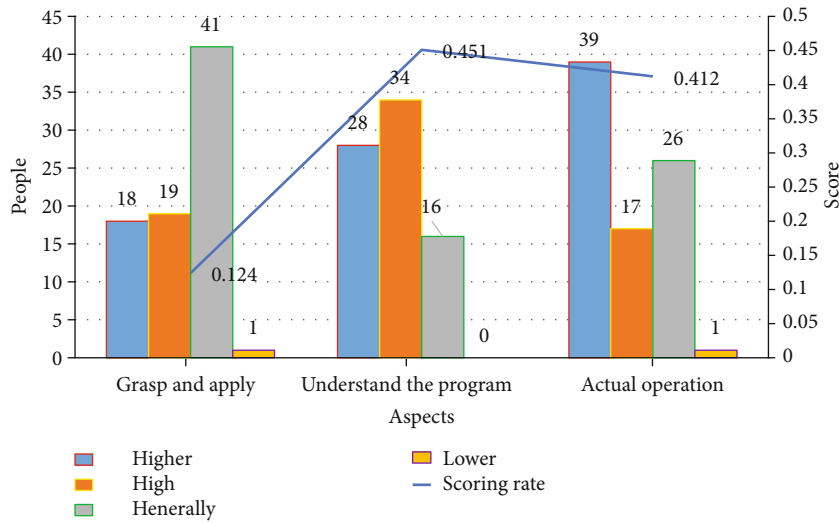


FIGURE 8: The transfer ability of knowledge learning in real experiment and virtual experiment environment.

data, the coordinates of the spatial point and the corresponding parameters (such as terrain undulation) are generated for the user to select the learning content according to the needs. Then store these data in the database for later analysis and processing. Finally, the calculation result is returned and displayed on the man-machine interface for the user to refer to, so as to achieve the interactivity of the teaching effect.

The virtual reality system is divided into three levels. The first level is a simple virtual reality system that is a desktop virtual reality system. The system uses the mouse, keyboard, and projection screen as interactive tools. The second level is the more mature virtual reality system (hereinafter referred to as the second level virtual reality system). This level is also the virtual reality system developed by major commercial companies. It is divided into two categories. The first cate-

gory is based on augmented reality. The second category is mainly AR glasses. When students are in class, they only need to wear VR glasses on their heads, and they can wander in the ocean of knowledge. The third level is an interactive full-experience virtual reality system, which can realize a full-scale, multiuser interaction, and excellent virtual reality experience. However, due to the technology and financial resources required by the system, the current education field is far from reach.

Compressing and encoding multimedia data are an essential step in the virtual classroom teaching system. Spatial data format refers to the use of GIS software to process each virtual object, convert this information into a digital form, and display and store it on the computer. After the coordinate system is determined, it is the work that needs to be done in the process of establishing the three-



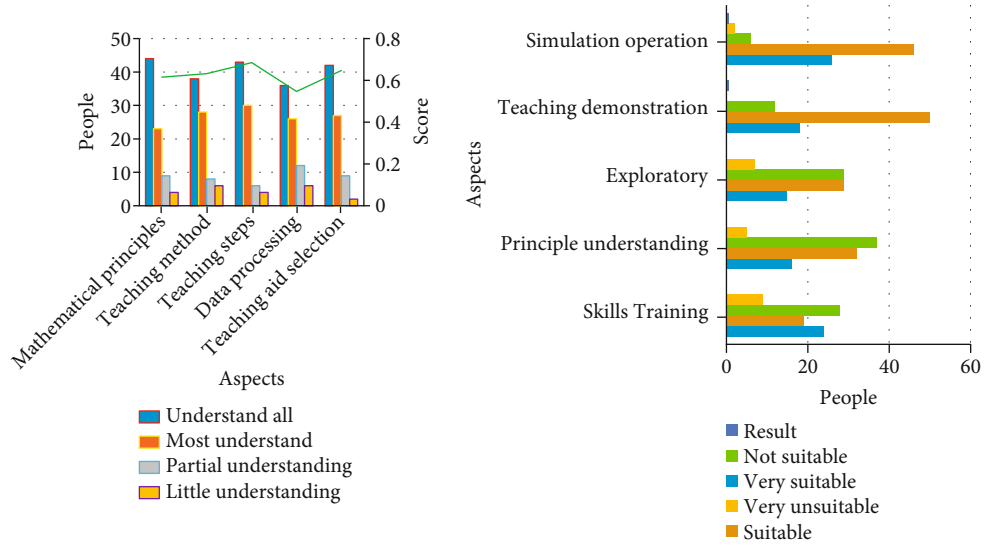


FIGURE 9: Students' evaluation and understanding of the applicable field of virtual experimental teaching system.

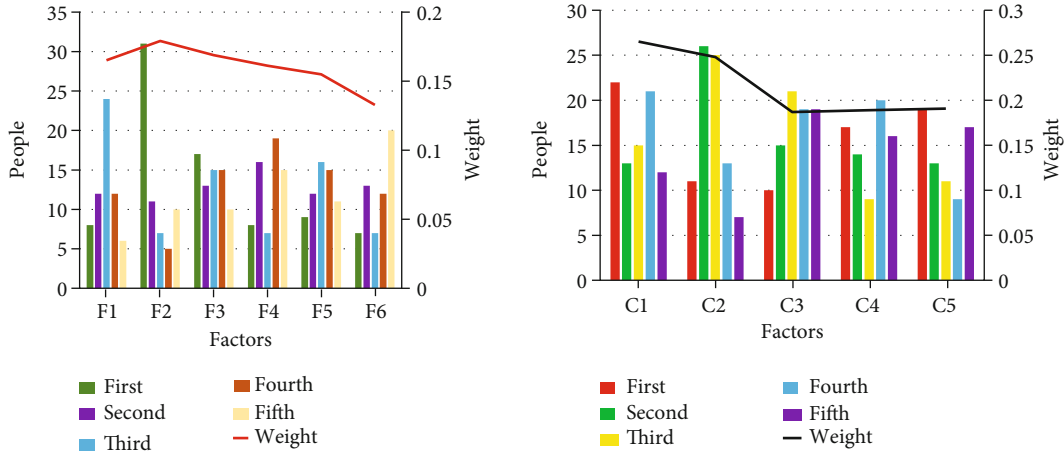


FIGURE 10: The advantages and disadvantages of virtual teaching and the reasons for experimental results.

TABLE 4: Results of closed-book test of experimental class and control class.

	Number	Average	Standard deviation	Standard error mean
Experimental class (pre)	41	92.56	3.1657	0.4506
Control class (pre)	39	89.92	3.6568	0.5125
Experimental class (post)	41	94.25	2.5132	0.6258
Control class (post)	39	90.21	2.5109	0.6425

dimensional coordinates. First, select a suitable location and set the coordinate origin according to the actual site conditions. Then set the attributes of the three-dimensional coordinates according to certain rules. Finally, it is converted into a two-dimensional spatial data format file for easy use and management, which is convenient for users to learn and train in a virtual environment. The format of spatial data means that various types of graphics can be converted, that is, a three-dimensional rectangular coordinate system can be established for any object, and at the same time, a certain accuracy must be ensured.

In virtual reality teaching, it is mainly about the processing of graphics information, but for students, they prefer the data itself. Therefore, we convert these digitized images into a two-dimensional space that can be visually displayed through certain means. This method can effectively solve the problem of the mismatch between traditional two-dimensional floor plans and real life. At the same time, it can also improve teaching efficiency and accuracy. In terms of information processing, it is mainly through the acquisition of raw data, including graphics and text. The first thing to do is to extract the required information. Make a

preliminary analysis. Then, based on this preprocessing, the results are obtained and the space coordinates and virtual world model are established. Finally, use the GIS software to generate a three-dimensional solid map or attribute vector to form a new surface profile curve to display its shape characteristics and boundary conditions and to calculate the positional relationship of each point in the plane and on the plane, so as to realize the description and expression of the three-dimensional geometric form, visualization, and other functions. Through the application of virtual reality technology, we can realize three-dimensional information processing, which mainly refers to the use of GIS software, graphical language, and professional knowledge to complete the editing, storage, and display of original two-dimensional spatial data.

In the process of virtual reality teaching, teachers can acquire the knowledge they need more conveniently and quickly by processing three-dimensional information on students. The first is data collection. Use GIS software to build a three-dimensional geometric model. Then according to the requirements of different users for graphics, text, and other image elements, select the appropriate equipment for parameter settings. The second is to analyze the relationship and interaction between the research object and the background data. Finally, there are errors in the process of comparing and verifying the modeling and operation results and the size of the error range, and corresponding treatments are made to facilitate the completion of teaching tasks and provide students with a good learning environment.

### 3. Virtual Teaching Function Test

*3.1. Virtual Teaching Function Test.* In order to test whether the virtual teaching system developed in this paper can meet the requirements of various functions, tests are carried out, including virtual teaching function test and virtual practical training teaching function. This article takes elementary school mathematics as an example to elaborate on the testing process of its virtual teaching and virtual training.

System testing is a process of comprehensively testing all modules and aspects of the system. After the development of the mathematics teaching system based on .NET is completed, and we will also conduct reasonable tests on it. The test of this system mainly includes function, performance, safety, and other tests.

*3.2. Development Environment Construction.* Download the integrated package of Eclipse and EGL tools suitable for the computer environment in EDT Project Home, download and unzip it before use. Open Eclipse and open the Eclipse installation plug-in interface through Help->InstallNew Software. And write the installation URL corresponding to EDT0.8 in the input box behind "WorkWith" on the page. Click the "Next" button on the page to enter the Web2.0 client application setting page with service, where the user can create a basic package name and select widget items.

*3.3. Use the System to Realize the Flipped Classroom.* When developing the EDT Web front-end program, the elemen-

tary school mathematics personalized intelligent teaching system needs to perform proper operations on the deployment of EDT. After operating the EDT deployment, the system will deploy the automatically generated service in the target Web program. The target code of RUIHandler and the target code of RUIHandler. At the same time, other operations such as the configuration file that should be bound to the service target code in the current EGL project will be configured in the target web program, so that users can directly deploy the target project in the application server.

Before class, the teacher puts the content to be learned into the system, and the students log in to the system to conduct self-study of theoretical knowledge before class, complete each task point in the preview, and give feedback on the students' preview situation during the formal class, for the next step, the teaching determines the important and difficult points.

#### 3.4. Online Feedback and Evaluation of Learning Content

*3.4.1. Prediction.* Before conducting the experimental class, conduct a comprehensive analysis of the control group and the experimental group, compare with the students' knowledge level and learning attitude, and strive to ensure that there is no significant difference between the experimental class and the control class.

*3.4.2. Posttest.* During the experiment, students in the experimental group are encouraged to use the virtual experimental teaching system to complete the specified experimental tasks outside of the normal course. All learning resources of the virtual experimental teaching system can be used to control the classroom, and students only need to complete the normal course. At the end of the semester, the control group and the experimental group were tested.

### 4. Result Analysis

*4.1. Test Data Statistics before and after the Experiment in the Experimental Class and the Control Class.* Before the test, this article investigated and analyzed the conditions of the experimental class and the control class, including the number of students, grades, outstanding, and passing rates. And use the global double  $Z$  test to evaluate the difference between the two groups. It can be seen from Table 1 that before the experiment between the experimental class and the control class, the value of the significance probability  $P$  of the two classes is greater than 0.05, indicating the difference in the skills and knowledge of the students before the experimental class and the control class.

As shown in Table 2, after one semester of virtual experiment courses in the laboratory and the control class, the average score, pass rate, and excellent rate of the experimental class are higher than those of the control class, with significant differences. Facts have proved that the implementation of virtual experimental education in elementary school distance learning mathematics has a very good effect on improving students' academic performance on a large scale.

*4.2. Comparison of Interest, Habits, and Attitudes of the Experimental Class and the Control Class.* The data in Table 3 shows that 69% of the students in the experimental class are very interested and interested in primary school mathematics, while only 36% of the students in the control class are interested in mathematics learning. The interest of the experimental class students who are not interested in mathematics learning at the stage is also much lower than that of the control class.

As shown in Figure 4, the experimental teaching of the virtual experimental education system has stimulated students' interest in the otherwise boring and difficult basic mathematical knowledge. 74% of the students in the experimental class would read the textbook carefully before starting the experiment, while only 52% of the students in the control class would preview. Nearly 43% of the students in the experimental class think that they can conduct experiments independently through self-study, while only 30% of the students in the control class think that they can conduct experiments independently. If there are any learning problems in the course, 53% of the students in the experimental class said they would use the virtual experimental teaching system for exploratory learning, while only 37% of the students in the control group said.

All this shows that the use of the virtual experimental education system can help stimulate students' enthusiasm and initiative, generate interest in the curriculum, improve the awareness of actively using the virtual experimental education system, and learn to learn autonomously.

Figure 5 shows that there is a significant difference between the experimental class and the control class in the two assessments of subject knowledge, indicating that virtual experimental education has played the role of students' subjects and has also significantly increased students' significant subject knowledge, which shows that virtual experimental education has played a role in disciplines and has significantly improved students' knowledge of important disciplines, encouraging students to explore and innovate.

#### *4.3. Survey on Interest Performance and Ability Development.*

From Figure 6, we can see that in virtual experimental education, students show a higher level of interest, attention, independent thinking, and active participation. It can be seen that virtual experiments are novel compared to traditional experimental methods, which can attract students' interest and attention and increase students' learning initiative and enthusiasm.

In terms of professional training, the effect of virtual experimental education on abstract thinking and students' thinking analysis ability is relatively ideal, but it is not ideal to promote students' overall applicability in the virtual environment.

When students use the virtual experimental education system, the statistics in Figure 7 show that more than 50% of the students believe that the virtual experimental education system has significantly increased their experimental interest and improved design ideas and capabilities, from independent enhancement and heuristic experience to stronger and innovative thinking.

*4.4. Survey on the Degree of Understanding of Mathematics Knowledge.* It can be seen from Figure 8 that the formation of virtual mathematics teaching experience is conducive to understanding the principles and laws, and students can apply the knowledge they have learned well in the virtual experience in actual operations. The knowledge that students have cannot be used well in the virtual experience, because the virtual experience cannot reflect the mathematical principles and rules very well. And the knowledge organization process of the student staff and the understanding of the content of the experimental course are not sufficient.

It can be seen from Figure 9 that more than 60% of students have reached the intermediate to advanced level in their understanding of teaching methods, teaching principles, tool selection, teaching methods, and data processing through the use of virtual mathematics classes. The highest score is the element of the teaching stage, indicating that students have mastered the teaching stage in the virtual environment and can complete their own learning as needed.

It can be seen from Figure 9 that students think that the virtual mathematics education system is most suitable for simulating operation experience and understanding principles. The main reason is that the virtual teaching system is based on the real world and can simulate various teaching aids during the experiment. The virtual system allows students to conveniently and intuitively use the equipment and observe the results obtained. The research field is unknown.

#### *4.5. Advantages of Virtual Teaching and Reasons for Experimental Results.*

There are six main reasons that affect the effect of virtual teaching. This article lists them as F1 ~ F6. The specific ones are no collaborative experiment environment is provided, the system cannot well reflect the authenticity of the operation experiment process, and the experiment content is not systematically complete. The stability of the system and the simulation effect are poor, there is no space for exploring knowledge, and the guidance of teachers and the communication help of students are lacking. The advantages of the virtual experimental teaching system mainly have five factors, represented by C1 ~ C5. Specifically, it includes being able to not be restricted by time, space, and space, being able to try to operate equipment that is not available in the laboratory, not damaging the experimental equipment, the experimental environment is relatively safe, and being familiar with the structure, function, and purpose of the experimental instrument.

It can be seen from Figure 10 that the main reasons for using virtual experience are lack of space for knowledge, lack of teacher guidance, lack of communication support for students, and system stability and simulation effects. Facts have proved that in order to improve the efficiency of the virtual experimental education system, students must have a space for rapid positioning and communication, while ensuring the stability of the virtual experimental education system itself and the authenticity of the simulation. It needs improvement to give learners a good learning effect.

The students saw the advantages of the virtual experiment system as an auxiliary tool for distance learning: time

and place are free. Experiments can be carried out easily anytime and anywhere. Expensive equipment is not available in the laboratory. And the simulated virtual experiment teaching system is also helpful to familiarize yourself with the structure of the experimental instrument. It is especially important for remote students to complete the experiment homework conveniently anytime and anywhere. It also pays great attention to the connection between virtual experience and actual operation.

**4.6. Effect Analysis.** It can be found from Table 4 that due to the analysis results of the SPSS software, the mean, standard deviation, and standard error of the mean are different for the two classes. Through interviews with students in the experimental class after class, most students believe that virtual reality systems are better than other methods of elementary school mathematics teaching.

Through the experiment of virtual reality system to assist in understanding mathematics teaching, it can be concluded that virtual reality system plays a significant role in primary school mathematics teaching and is conducive to the mastery of students' knowledge, improvement of grades, and enhancement of spatial ability.

## 5. Conclusion

With the continuous development of education informatization, the interaction between teachers and students becomes more and more frequent in the teaching process. Under the background of the rapid popularization of multimedia technology, virtual reality technology, and the rapid rise of new technology applications such as computers and network communications, the realization of teacher-student interaction has become an urgent problem to be solved. Elementary school mathematics is the beginning of logic, and the mastery of elementary school mathematics is conducive to the construction of thinking ability. Virtual reality takes real natural scenes as the research object. By creating a virtual environment, students can be immersed in it. It can provide teachers with a real and vivid environment and learning space. By simulating concrete things, it is easier for students to understand abstract concepts or mathematical models. The design of the virtual reality elementary school mathematics teaching system based on GIS data fusion has gained a lot in its research methods and impact value. The research and development of this system have brought scientific and technological civilization and convenience to human teaching.

## Data Availability

No data were used to support this study.

## Conflicts of Interest

The authors declare that there is no conflict of interest with any financial organizations regarding the material reported in this manuscript.

## References

- [1] W. Yuhong, L. Ying, Y. Zhanliang, and D. U. Jiusheng, "GIS-based integrated spatial management and analysis system for college student information," *Laboratory Research and Exploration*, vol. 36, no. 3, pp. 105–110, 2017.
- [2] M. I. N. Yi-xuan, "Primary school mathematics classroom teaching research based on Flanders system," *Forest District Teaching*, no. 2, pp. 85–87, 2019.
- [3] L. Bin, "Research on effective teaching strategies of the deep integration of Changyan interactive multimedia teaching system and rural elementary school mathematics classroom teaching," *Urban Family Education Monthly*, no. 11, pp. 66–67, 2017.
- [4] E. Demitriadou, K. E. Stavroulia, and A. Lanitis, "Comparative evaluation of virtual and augmented reality for teaching mathematics in primary education," *Education and Information Technologies*, vol. 25, no. 1, pp. 381–401, 2020.
- [5] G. Goehle, "Teaching with virtual reality: crafting a lesson and student response," *The International Journal for Technology in Mathematics Education*, vol. 25, no. 1, pp. 35–45, 2018.
- [6] M. Shin, "An analysis of mobile virtual manipulatives apps for the teaching of elementary school mathematics," *Journal of Korea Multimedia Society*, vol. 20, no. 6, pp. 935–949, 2017.
- [7] B. S. Clay, N. Fotou, and J. Monaghan, "The use of software in academic stream high school mathematics teaching," *International Journal for Technology in Mathematics Education*, vol. 24, no. 1, pp. 37–45, 2017.
- [8] M. Soliman, Z. Lavicza, T. Prodromou, M. Al-Kandari, and T. Houghton, "Enhancing Kuwaiti teachers' technology-assisted mathematics teaching practices," *International Journal for Technology in Mathematics Education*, vol. 26, no. 2, pp. 73–80, 2019.
- [9] M. A. Linhua, Y. Shi, S. Cai, and Y. Cui, "GIS-based database construction and spatial analysis of Ganfu Plain Irrigated District," *Paiguan Jixie Gongcheng Xuebao/Journal of Drainage and Irrigation Machinery Engineering*, vol. 36, no. 11, pp. 1157–1162, 2018.
- [10] F. S. Mukhametzhanova, "Developing creativity of schoolchildren through the course "developmental mathematics"," *Eurasia Journal of Mathematics Science & Technology Education*, vol. 13, no. 6, pp. 1799–1815, 2017.
- [11] D. Polly, C. Wang, R. Lambert et al., "Supporting kindergarten teachers' mathematics instruction and student achievement through a curriculum-based professional development program," *Early Childhood Education Journal*, vol. 45, no. 1, pp. 121–131, 2017.
- [12] M. M. Marjanović, "A survey of the system N of natural numbers assigned to primary teachers," *Acta Medica Iranica*, vol. 54, no. 4, pp. 347–351, 2017.
- [13] J. Valle-Lisboa, L. Cabana, R. Eisinger et al., "Cognitive abilities that mediate SES's effect on elementary mathematics learning: the Uruguayan tablet-based intervention," *Prospects*, vol. 46, no. 1, pp. 1–15, 2017.
- [14] N. O. García, M. F. D. Velásquez, C. A. T. Romero, J. H. O. Monedero, and O. I. Khalaf, "Remote academic platforms in times of a pandemic," *International Journal of Emerging Technologies in Learning*, vol. 16, no. 21, pp. 121–131, 2021.
- [15] Y. Tang, Q. Fan, and P. Liu, "Computer-aided teaching system based on data mining," *Wireless Communications and Mobile Computing*, vol. 2021, Article ID 3373535, 12 pages, 2021.

- [16] A. Jimenez, M. C. Monroe, N. Zamora, and J. Benayas, "Trends in environmental education for biodiversity conservation in Costa Rica," *Environment Development & Sustainability*, vol. 19, no. 1, pp. 221–238, 2017.
- [17] M. Li, L. Xie, A. Zhang, and F. Ren, "Reinforcement emotion-cognition system: a teaching words task," *Computational Intelligence and Neuroscience*, vol. 2019, Article ID 8904389, 13 pages, 2019.
- [18] S. Kim, H. Ko, J. Y. Hong, and H. Choi, "A study on experience contents of Baekje Muryeong royal tomb using virtual reality," *Journal of Ambient Intelligence and Humanized Computing*, no. 4, 2019.
- [19] A. Milman, J. M. Marston, S. E. Godsey, J. Bolson, H. P. Jones, and C. S. Weiler, "Scholarly motivations to conduct interdisciplinary climate change research," *Journal of Environmental Studies and Sciences*, vol. 7, no. 2, pp. 239–250, 2017.
- [20] M. N. Varga, R. Merrison-Hort, P. Watson, R. Borisyuk, and D. Livingstone, "Tadpole VR: virtual reality visualization of a simulated tadpole spinal cord," *Virtual Reality*, vol. 25, no. 1, pp. 1–17, 2021.
- [21] P. Rau, *Can Virtual Reality Help Children Learn Mathematics Better? The Application of VR Headset in Children's Discipline Education*, vol. 10912, Springer, Cham, 2018.
- [22] X. Liang and V. R. Young, "Annuity and asset allocation under exponential utility," *Insurance Mathematics and Economics*, vol. 79, pp. 167–183, 2018.
- [23] T. Kumar and B. Arun, "Materialized view selection using HBMO," *International Journal of System Assurance Engineering & Management*, vol. 8, Supplement 1, pp. 1–14, 2017.
- [24] D. Avola, L. Cinque, G. L. Foresti, M. R. Marini, and D. Pannone, "VRheab: a fully immersive motor rehabilitation system based on recurrent neural network," *Multimedia Tools & Applications*, vol. 77, no. 19, pp. 24955–24982, 2018.
- [25] L. Zeng and X. Dong, "Design of pulse wave feature vigilance detection system based on computer software technology," *Mobile Information Systems*, vol. 2021, Article ID 3596095, 8 pages, 2021.
- [26] B. Ma, S. Nie, M. Ji, J. Song, and W. Wang, "Research and analysis of sports training real-time monitoring system based on mobile artificial intelligence terminal," *Wireless Communications and Mobile Computing*, vol. 2020, Article ID 8879616, 10 pages, 2020.

## Research Article

# Histogram Shifting-Based Quick Response Steganography Method for Secure Communication

Geno Peter <sup>1</sup>, Anli Sherine <sup>2</sup>, Yuvaraja Teekaraman <sup>3</sup>, Ramya Kuppusamy <sup>4</sup>,  
and Arun Radhakrishnan <sup>5</sup>

<sup>1</sup>CRISD, School of Engineering and Technology, University of Technology Sarawak, Malaysia

<sup>2</sup>School of Computing and Creative Media, University of Technology Sarawak, Malaysia

<sup>3</sup>Mobility, Logistics, and Automotive Technology Research Centre, Faculty of Engineering, Vrije Universiteit Brussel, Brussels 1050, Belgium

<sup>4</sup>Department of Electrical and Electronics Engineering, Sri Sairam College of Engineering, 562 106, Bangalore City, India

<sup>5</sup>Faculty of Electrical & Computer Engineering, Jimma Institute of Technology, Jimma University, Ethiopia

Correspondence should be addressed to Arun Radhakrishnan; [arun.radhakrishnan@ju.edu.et](mailto:arun.radhakrishnan@ju.edu.et)

Received 23 October 2021; Accepted 22 December 2021; Published 12 March 2022

Academic Editor: Shalli Rani

Copyright © 2022 Geno Peter et al. This is an open access article distributed under the Creative Commons Attribution License, which permits unrestricted use, distribution, and reproduction in any medium, provided the original work is properly cited.

Steganography is a tool which allows the data for transmission by concealing secret information in a tremendously growing network. In this paper, a novel technique quick response method (QRM) is proposed for the purpose of encryption and decryption. Existing system uses side match vector quantization (SMVQ) technique which has some challenges such as security issues and performance issues. To handle the security and performance issues, the proposed system uses two methods, namely, quick response method and shifting method. In the proposed system, encoding part calculates the performance for capacity, PSNR (peak signal-to-noise ratio), MSE (mean square error), and SSIM (structural similarity index method), and the decoding part calculates the performance of MSE (mean square error) and PSNR (peak signal-to-noise ratio). The shifting method is used to increase the data hiding capacity. In this system, the encryption part embeds the secret image using steganography and the decryption part extracts the original image. By analyzing and comparing the proposed system with the existing system, it is proved that the system proposed was much better than the existing systems.

## 1. Introduction

For the security purpose, data hiding process is used to embed the data into digital media. It delivers large volume for secret information hiding which results into stego image imperceptible to human vision. Data hiding such as image and text that permits the cover image to be improved after the embedded message is mined from the marked image. Data hiding is broadly used to hide the secret information into a cover information like a video file, an audio file, and an image [1]. For efficient storage and transmission, embed data into an image and link with compression. Medical images are transferred from one hospital to another hospital for review by physicians across the globe. Such medical image data has to be stored

in the database for future reference of patients. Normally, these medical images are compressed and stored before being transmitted over the Internet. Similarly, the patient data is also embedded within the medical images. The hidden and the host image data can be recovered from the embedded image without any data loss [2]. In RDH (reversible data hiding), the data to be covered up is embedded in the cover image. Data hiding technique and image compression technique can be integrated as one single module [3]. Reversible data hiding can embed the message data in a host image without any loss of the host image. If watermarked image is used for image authentication, with the improved histogram-based reversible data hiding scheme which is based on prediction and sorting, the original image can be reverted before the embedding

process. This histogram-based embedding increases the capacity of the embedding process [4]. The steganography method is aimed at secretly hiding the data in a multimedia medium between two sides to conceal the occurrence of the message. It is based on two important factors such as embedding payload and efficiency. It gives the result that creates it suitable to transfer data without being censored and the data interrupted. Data security is broadly based on encryption and for few cases based on an extra layer of security [5]. A high embedding performance is offered by transform domain JPEG image steganography method [6]. Histogram shifting technique in integer wavelet transform area converts information into higher frequency wavelet coefficients subbands. The histogram modification approach is useful to avoid overflow and underflow. It reallocates a fraction of the larger frequency wavelet subband histogram and consequently inserts data with the help of generated histogram zero-point.

The proposed method performance with data embedding payload is compared with the performance of existing methods in integer cosine transform domain, spatial domain, and integer wavelet transform domain. The maximum embedding payload in the same visual quality is computer by PSNR or has a higher PSNR in the same payload. At the time of shifting operation performed high-frequency integer wavelet subbands, the overflow (e.g., for an 8-bit image, the value of pixel grayscale exceeds 255) and/or underflow (e.g., for an 8-bit image, the pixel grayscale value below 0) could take place, hence preventing the lossless need consecutively to overcome overflow and/or underflow [7]. Image decompression is based on side match vector quantization (SMVQ). At the sender side, vector quantization is applied to composite blocks, to manage visual deformation and error flow. Image is segmented into nonoverlapping blocks. The leftmost and upmost blocks are compressed using vector quantization. Remaining blocks are compressed by side match vector quantization (SMVQ). At the receiver side, reconstruction of image takes place. Extraction phase consists of exactly reverse process, i.e., decompression side match vector quantization (DSMVQ) [8].

## 2. Related Work

A high-capacity modified steganography technique using wavelet transform was reported by Ali et al. In this technique, the original cover image was preadjusted such that the reconstructed pixels from the embedded coefficients would not exceed its threshold value. The drawback of the proposed method is the computational overhead. This technique obtained the PSNR value of 40.98%. Acharya et al. have proposed a method to hide multiple secret images and keys in color cover image using integer wavelet transform (IWT) using image steganography technique. The average PSNR value obtained is 44.7%. Sathish et al. suggested a high-capacity and optimized image steganography technique based on ant colony optimization algorithm. This technique achieved the PSNR value of 40.83. Ahmed et al. used nonlinear properties of quantum walks to design a novel technique for constructing S-boxes and applied those

S-boxes to design a new steganography technique. The proposed method obtained the PSNR value which is 44.26%. Nadish et al. embedded the data in the edge pixel of carrier image using an improved image steganography. The PSNR value for this technique obtained is 45.33%. The organization of the paper is categorized as follows. Section 1 explains the introductory part of data hiding and steganography. Section 2 illustrates the related work based on the steganography. Section 3 describes the proposed quick response technique-based steganography. Section 4 elaborates the results and discussion. Finally, Section 5 gives the conclusion of the paper.

## 3. Proposed Quick Response-Based Steganography

The proposed quick response technique is developed such that the capacity for encoding process is increased. With the help of ZXing (open source library) and MATLAB, it can be retrieved. The algorithms are applied to process the QR codes which include some geometric properties like area, centroid, bounding box for finding and varying the color of "finder patterns," and its conditions for each code with several colors in MATLAB thus maximizing into three dimensions. To create three-dimensional quick response code encoding process, three processed codes are added for three separate messages. The reverse operation was performed for decoding process such that encoded code was initially delayed by splitting the red, green, and blue channels and subsequently thresholded to go again the originally encoded quick response codes. The improved patterns include the most important in covert applications. Histogram shifting method prevents overflow and underflow issues which enhances the visual quality of image and data hiding capacity. Quick response code technique is used to encrypt the cover image and later decrypt the original information with high quality.

Initially, the image data is partitioned into two main blocks. In the processing step, the histogram is created for every block. The quantity of data which can be embedded within image blocks is more by comparing the embedding within a single image. The proposed block schematic for encoding and decoding process is shown in Figures 1 and 2.

*3.1. Image Acquisition.* The input image was color which may be in the file format of (jpg, png, bmp, and tiff) and compressed or uncompressed formats. Then, the image is transformed into a color space. The different color spaces are RGB, HSV, YIQ, LAB, and YCbCr. Image enhancement is to increase the quality of images using spatial, frequency, and watermark transform domain.

*3.2. Filter Image.* The filtering takes both spatial and intensity domain information in calculating the edge-preserving smoothing output for an input image. It replaces the intensity of each pixel with intensity values from nearby pixels.

*3.3. Histogram Shifting.* Monotonic mapping between a test and reference image of histograms is computed by histogram shifting. Test and reference images can be any of the

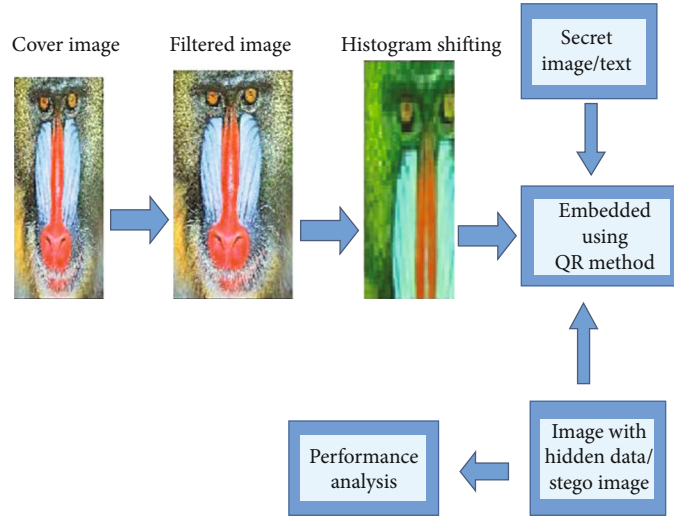


FIGURE 1: Block diagram proposed quick response encoding process.

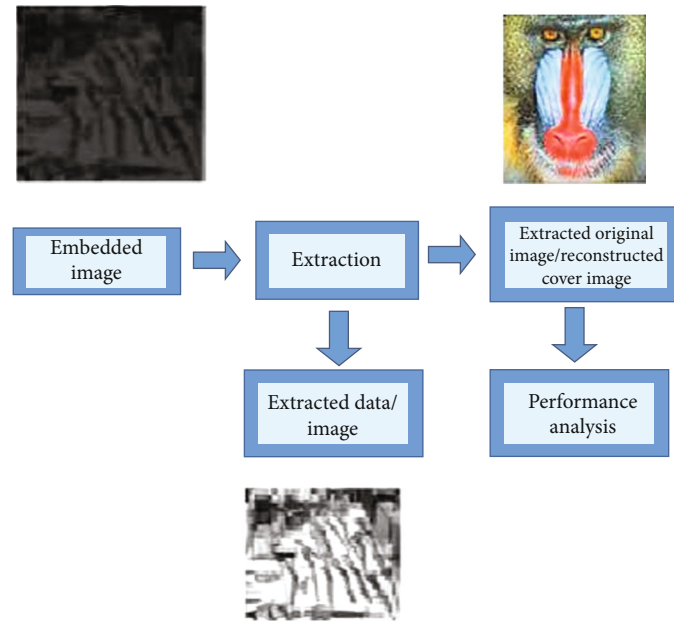


FIGURE 2: Block diagram proposed quick response decoding process.

permissible data types and need not be equal in size. This shifting technique increases the contrast based on similarity between test and reference image.

**3.4. QR Method.** QR code is two-dimensional barcode which is categorized in matrix barcode that can store large alphanumeric information. Barcode consists of black modules arranged in white background. Data can be restored even if the symbol is partially dirty or damaged.  $EF$  of a given image  $D$  in the form of a matrix is defined as

$$D = E \times F, \quad (1)$$

where  $E$  is an orthonormal matrix and  $F$  is an upper triangular matrix.  $D$  and  $E$  are denoted as  $D = [d_1, d_2, d_3, \dots, d_n]$  and  $E = [e_1, e_2, \dots, e_n]$ , respectively.

Embedding algorithm:

- (i) Read a test image
- (ii) Make QR decomposition with a watermark image
- (iii) Apply discrete wavelet transform (DWT) on both test and QR decomposition images
- (iv) Insert the QR decomposition image into test image
- (v) Reconstruction of test image to apply inverse of DWT
- (vi) Finally, we get embedded image

Extraction algorithm:

- (i) Read the embedded image and test image



- (ii) Apply DWT on both test and embedded images
- (iii) Subtract embedded image with the test image and get the QR decomposition image
- (iv) By using QR decomposition reader extract watermark image from the QR decomposition image

Cover: the data or image which is masked inside the secret message. Embedding and extraction processes: in this process, the secret data was enveloped inside the cover and the hidden data can be recovered. Encryption: this is an embedding process where the secret data is coded [9]. Stego information: the information obtained at the end of the embedding process is known as stego information. Decoding process: the extraction phase can be followed by a suitable decoding phase depending upon whether encryption was used or not during embedding [10]. Steganography: steganography based on text, audio, video, or image is used as the cover medium. Digital image stenographic concepts are very famous mediums applied worldwide for data transfer in addition to data hiding [11]. Steganography mapping for a digital image using embedding and extraction process is given by

$$\begin{aligned} M_1 &= \{C_1 \times K_1 \times T_1\} \longrightarrow C_1', \\ X_1 &: \{C_1' \times (K_1)\} \longrightarrow C_1, \end{aligned} \quad (2)$$

where  $M_1$  is the embedding function,  $X_1$  the extraction function,  $C_1$  the cover image,  $C_1'$  the stego image,  $K_1$  the set of keys, and  $T_1$  the set of secret messages.

**3.5. Peak Signal-to-Noise Ratio and Mean Square Error Computation.** The PSNR calculates the peak signal-to-noise ratio, among the two different images expressed in terms of decibels. This relation is frequently used as an excellence measurement between the original and a compressed image. For better quality measurement, the value of PSNR should be high; thus, it produces a high-quality image even if it is a compressed or reconstructed image [12]. The mean square error (MSE) and the peak signal-to-noise ratio (PSNR) are the two most important terms for the accurate image quality determination. When the value of MSE is lower, the error obtained is also reduced [13].

PSNR can be calculated using equations (3) and (4).

$$\text{MSE} = \sum_{M_1, N_1} \frac{[I_1(m_1, n_1) - I_2(m_2, n_2)]^2}{M_1 \times N_1}, \quad (3)$$

where  $M_1$  is the number of rows and  $N_1$  is the number of columns in the input image. After that, the block calculates the PSNR using the given equation:

$$\text{PSNR} = 10 \log_{10} \left( \frac{r^2}{\text{MSE}} \right), \quad (4)$$

where  $r$  can be varied based on the input image data type.

**3.6. Structural Similarity Index Method.** The structural similarity index method (SSIM) is a method for determining the stego image quality. SSIM is used for computing the similarity of two images. This measures the image quality based on an uncompressed or distortion-free image. SSIM is simulated to develop on the latest techniques such as peak signal-to-noise ratio (PSNR) and mean squared error (MSE) [14]. SSIM is measured from the host image and the dense image. It is calculated based on the important metrics, namely, contrast and luminance [15].

The SSIM index is measured based on various images. The measure between two images  $a$  and  $b$  of common size  $B \times B$  is

$$\text{SSIM}(a, b) = \frac{(2\mu_1 a \mu_1 b + C_2)(2\sigma_1 ab + C_1)}{(\mu_1 a^2 + \mu_1 b^2 + C_1)(\sigma_1 a^2 + \sigma_1 b^2 + C_1)}, \quad (5)$$

where  $\mu_1 a$  is the average of  $a_i$ ,  $\mu_1 b$  is the average of  $b_i$ ,  $\sigma_1 a^2$  is the average of  $a_i^2$ ,  $\sigma_1 b^2$  is the average of  $b_i^2$ , and  $\sigma_1 ab$  is the covariance of  $a$  and  $b$ .

$C_1 = (N_1 L)^2$ ,  $C_2 = (N_2 L)^2 C_1$ ,  $C_2$  provides a weak denominator to stabilize.  $L$  is the pixel dynamic range value,  $N_1 = 0.01$  and  $N_2 = 0.03$  by default. The symmetry condition for SSIM index is  $\text{SSIM}(a, b) = \text{SSIM}(b, a)$  using this formula:

$$(a, b) = \frac{2\mu_a \mu_b + C_1}{\mu_a^2 + \mu_b^2 + C_1} \text{lu} \quad (6)$$

$$\text{co}(a, b) = \frac{2\sigma_a \sigma_b + C_2}{\sigma_a^2 + \sigma_b^2 + C_2} \text{co}(a, b) = \frac{2\sigma_a \sigma_b + C_2}{\sigma_a^2 + \sigma_b^2 + C_2},$$

$$\text{st}(a, b) = \frac{\sigma_{ab} + C_3}{\sigma_a \sigma_b + C_3} \text{st}(a, b) = \frac{\sigma_{ab} + C_3}{\sigma_a \sigma_b + C_3}. \quad (7)$$

With, in addition to the above definition,

$$C_3 = \frac{C_2}{2} C_3 = \frac{C_2}{2}. \quad (8)$$

SSIM is the a weighted combination of those comparative measures

$$\begin{aligned} \text{SSIM}(a, b) &= \left[ d(a, b)^\alpha \cdot c(a, b)^\beta \cdot s(a, b)^\gamma \right] \text{SSIM}(a, b) \\ &= \left[ d(a, b)^\alpha \cdot c(a, b)^\beta \cdot s(a, b)^\gamma \right], \end{aligned}$$

Setting the weights  $\alpha, \beta, \gamma$  to 1. (9)

Generally, SSIM expression is based on three measurements between the test images of  $a$  and  $b$ : luminance (lu), contrast (co), and structure (st). The entity comparison approach evaluates the image quality [16].

## 4. Results and Discussion

The proposed technique was evaluated for the security efficiency on both the gray level and color images. The

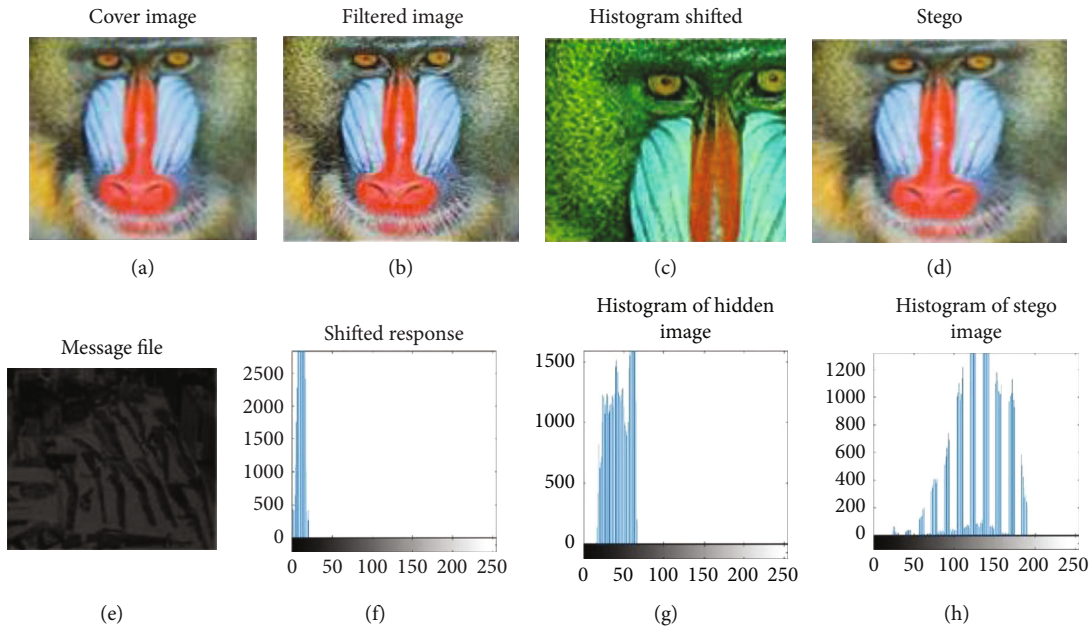


FIGURE 3: (a) Cover image; (b) filtered image; (c) histogram shifted image; (d) stego; (e) message file; (f) shifted response; (g) histogram of hidden image; (h) histogram of stego image.



FIGURE 4: Cover image segmentation.

following subsections describe the encoding and decoding process and their performance analysis of the proposed system [17]. The encoding process of the proposed system consists of the following subprocesses: (i) input image, (ii) filtered image, (iii) histogram shifting, (iv) embedding, and (v) stego image. The decoding process of the proposed technique consists of the following subprocesses: (i) embedded image and (ii) extraction.

**4.1. Encoding Process.** The following section describes the encoding process of the proposed system. Initially, the cover image is taken as an input image [18]. Then, the input image is filtered using trilateral filter and the filtered image is given to the histogram shifting to increase the data hiding capacity of the proposed system. The resultant image is embedded with secret. Image/text using embedding technique is called the quick response method. The stego image is obtained from the embedded image, and the evaluation of the performance provides better results than the other existing systems.

Input image is given by the user. Figure 3(a) shows the user given over image. The filtered image is obtained from the given input image using trilateral filter as shown in Figure 3(b). Histogram shifting is a technique which is done on each block of the image. Figure 3(c) shows the histogram shifted image and its histogram [19]. Embedding is the process of inserting text/image behind the original image. This process is carried out using the quick response method. This

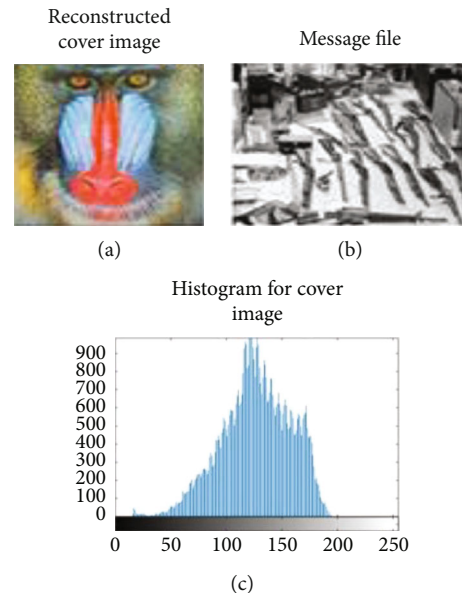


FIGURE 5: (a) Reconstructed cover image; (b) message file; (c) histogram for cover image.

method improves the data hiding capacity of the proposed system. Figure 3(d) shows the message file and histogram of hided image. At first, cover image segmentation is done

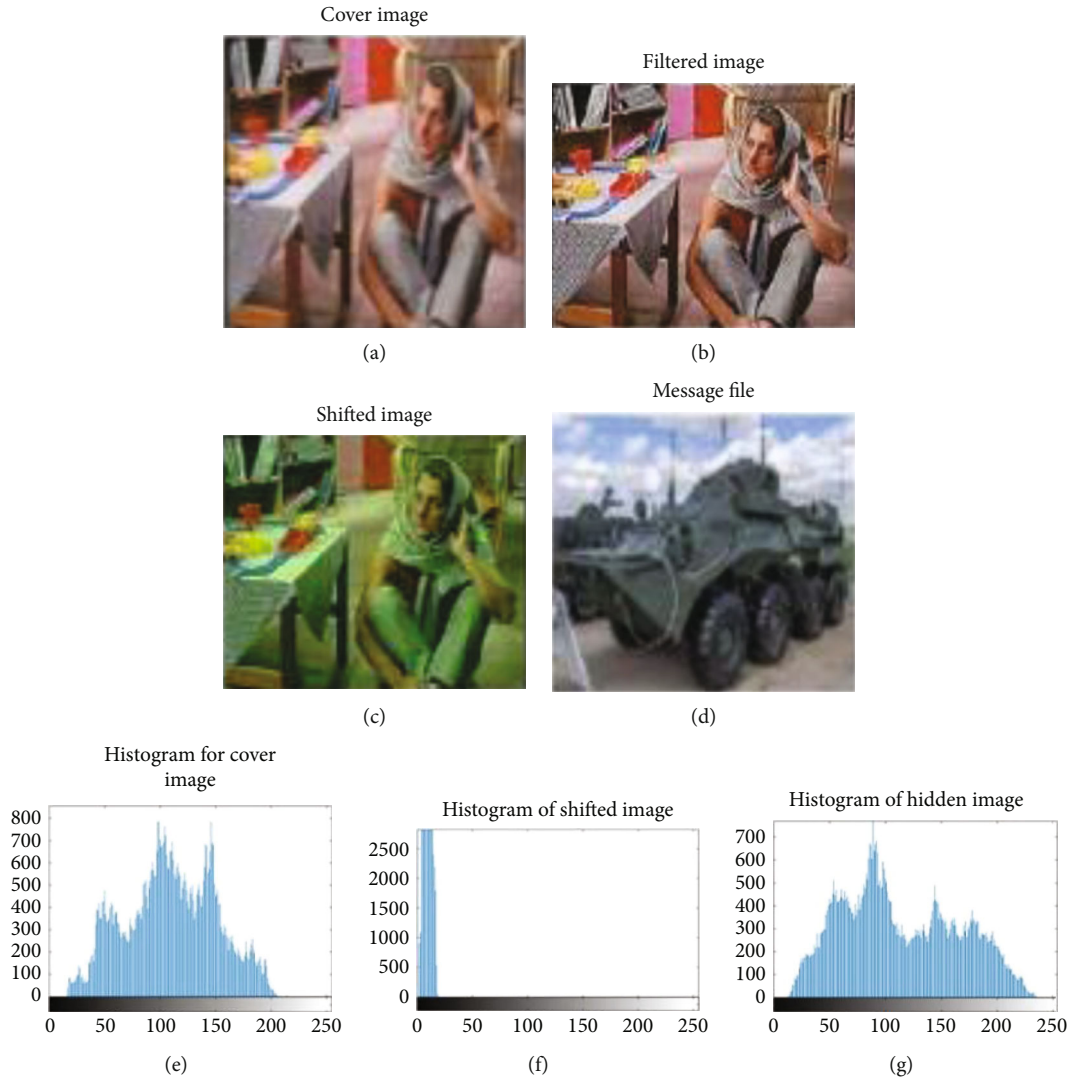


FIGURE 6: (a) Cover image; (b) histogram for cover image; (c) filtered image; (d) histogram of shifted image; (e) shifted image; (f) message file; (g) histogram of hidden image.

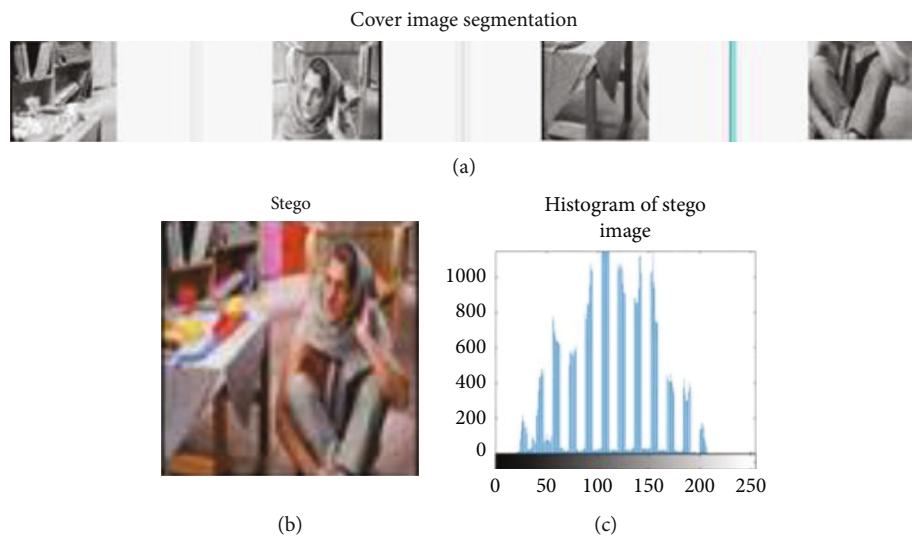


FIGURE 7: (a) Cover image segmentation; (b) stego; (c) histogram of stego image.

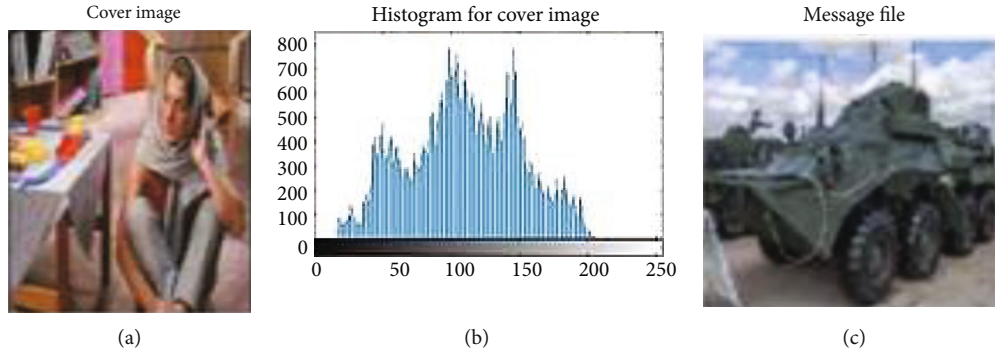


FIGURE 8: (a) Cover image; (b) histogram for cover image; (c) message file.

TABLE 1: Performance analysis of the proposed QR-based steganography.

Test images	Secret image	Capacity	SSIM	Encoding		Decoding	
				MSE	PSNR	MSE	PSNR
Barbara	Data	71061	0.9291	4.6266	52.5359	0.23	78.80
	Image		0.9340	5.0853	52.0185	0.234	78.80
Helen	Data	71076	0.9872	4.6688	52.4915	0.25	81.79
	Image		0.9961	5.1484	51.9526	0.207	81.90
Lenna	Data	70965	0.9645	4.6285	52.5335	0.26	78.87
	Image		0.9760	5.0780	52.0264	0.269	78.81
Lighthouse	Data	70919	0.9907	4.6542	52.5029	0.21	78.74
	Image		0.9834	5.0899	52.0136	0.251	78.63
Mandrill	Data	71169	0.9623	4.5675	52.6072	0.19	78.56
	Image		0.9669	5.0186	52.0901	0.180	78.51
Owl	Data	71281	0.9825	4.8155	52.3153	0.18	79.45
	Image		0.9522	5.2936	51.8026	0.148	78.51
Penguin	Data	70850	0.9591	4.4858	52.7078	0.18	77.02
	Image		0.9695	4.9354	52.1810	0.189	76.99
Pepper	Data	70868	0.9926	3.0433	55.02	0.24	76.58
	Image		0.9909	3.3089	54.4968	0.234	76.56
Taj Mahal	Data	71064	0.9810	4.8616	52.2632	0.18	77.46
	Image		0.8349	5.300	51.7961	0.154	77.41

on the embedded image and it is the process of dividing the images using discrete wavelet transform. Figure 4 shows the representation of cover image segmentation.

Steganography is a process of communicating secretly where the text/image is hidden in another image. It increases the data hiding capacity of the proposed system. The figure shows the stego image and its histogram.

**4.2. Decoding Process.** The following section explains the decoding process of the proposed system. Initially, the reconstructed cover image is taken as an input image. The hidden text/image is extracted from the reconstructed cover image or embedded image using inverse quick response method [20]. Finally, the performance evaluation is done on the reconstructed cover image and it provides better results than the other existing systems. Figures 5(a)–5(c)

show the reconstructed cover image, the hidden text/image extracted from the reconstructed cover image, and its histogram.

**4.3. For Color Image.** Similarly, the encoding and decoding process of the proposed system was carried out for the color images. Figures 6(a) and 6(b) show the cover image and its histogram. Figure 6(c) shows the filtered image which is done with the help of trilateral filter for color images. The histogram shifted image and its shifted histogram are shown in Figures 6(d) and 6(e). The filtered color image is given as an input for histogram shifting technique [21]. The histogram shifted image is embedded with message file using quick response method as shown in Figures 6(d) and 6(e). Figures 6(f) and 6(g) show the message file and its histogram.

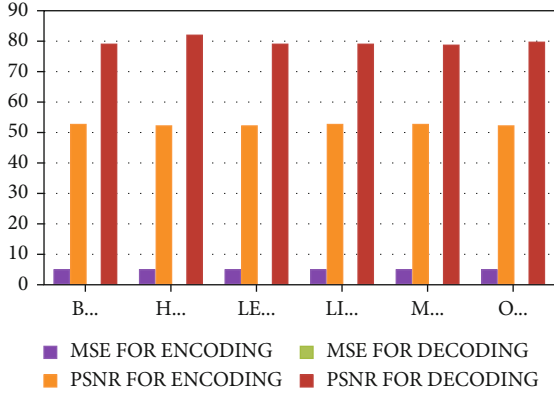


FIGURE 9: MSE and PSNR graph for encoding and decoding.

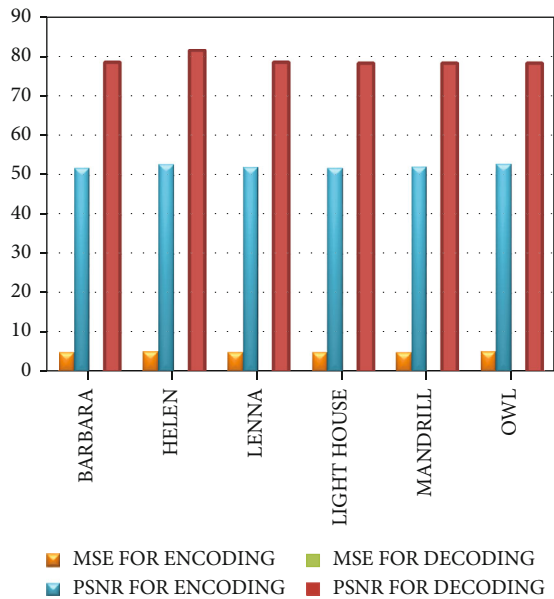


FIGURE 10: MSE and PSNR graph for secret image.

The cover image segmentation for color image is carried out using discrete wavelet transforms as shown in Figure 7(a) [22]. The stego image is obtained from the resultant embedded image. Figures 7(b) and 7(c) show the stego image and its histogram. Finally, the hidden data/image is extracted from the cover image. Figures 8(a)–8(c) show the cover image, message file, and histogram for the cover image.

Table 1 shows the performance analysis of both encoding and decoding process of the proposed system using quick response-based steganography technique. The table illustrates the simulation results including the following parameters: test images, secret image, capacity, and encoding and decoding parameters (Mishra, 2016). The encoding parameters are SSIM, MSE, and PSNR. The decoding parameters are MSE and PSNR. QR-based steganography technique with various message sizes on various grayscale images is determined. Moreover, the mean square error and average PSNR values are explained.

Mean square error and PSNR values for secret data are clearly illustrated for the test images such as Barbara, Helen,

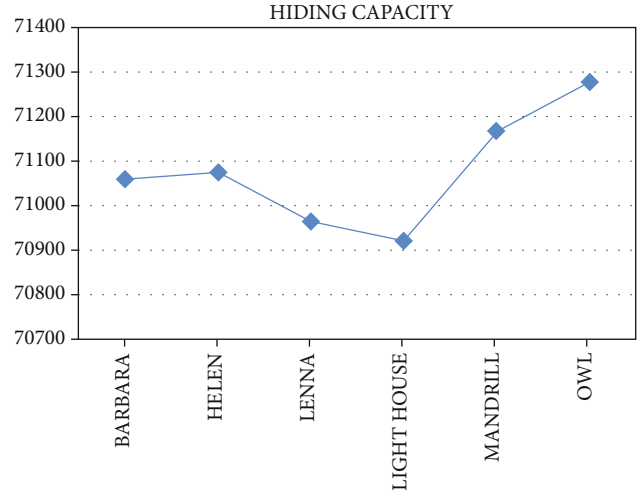


FIGURE 11: Hiding capacity for test images.

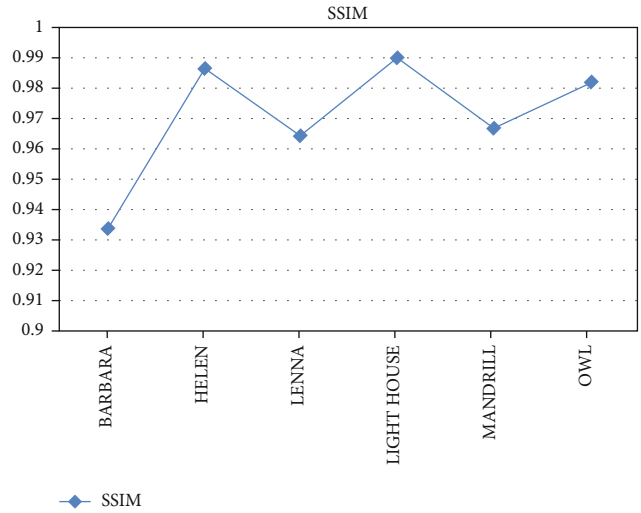


FIGURE 12: SSIM graph for test images.

Lenna, Lighthouse, Mandrill, and Owl as shown in Figure 9. The MSE for encoding process, MSE for decoding process, PSNR value for encoding process, and PSNR value for decoding process are described in this graph.

The result of simulation shows the mean square error and PSNR values for secret images are clearly illustrated for the test images such as Barbara, Helen, Lenna, Light-house, Mandrill, and Owl as shown in Figure 10. The MSE for encoding process, MSE for decoding process, PSNR value for encoding process, and PSNR value for decoding process are described in this graph. Figure 10 depicts the graphical representation of obtained hiding capacity values for the test images. The test image Owl has higher capacity compared to other test images. From the graph, the test image light images have the lower hiding capacity value. The results of steganography capacity denote the most significant view of any stenographic method.

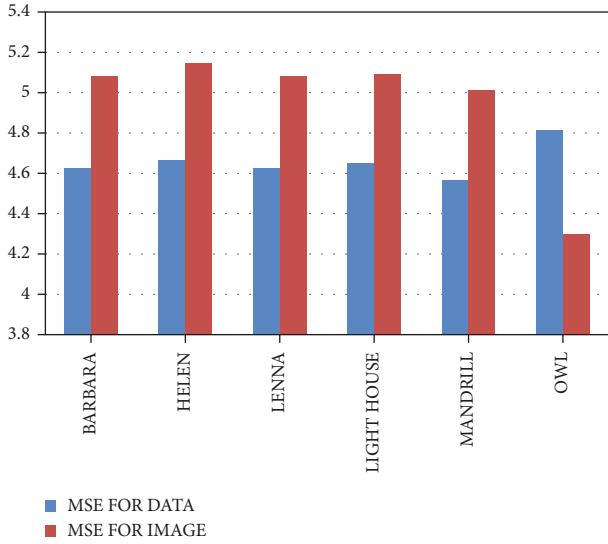


FIGURE 13: Graphical representation of MSE difference between the secret image and data.

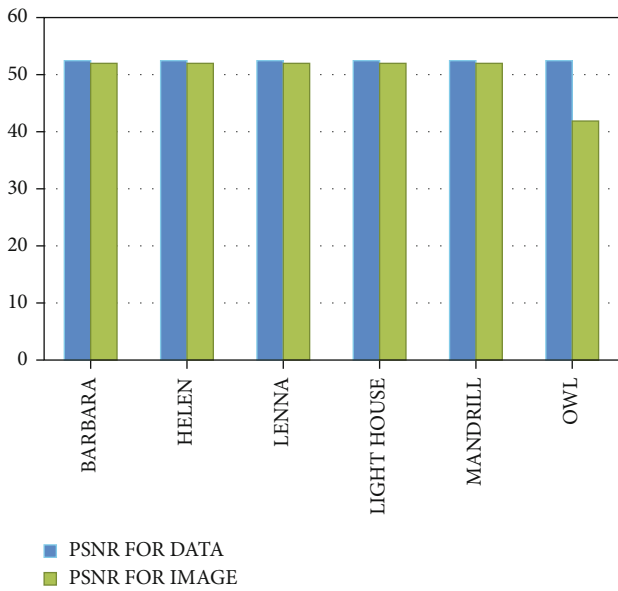


FIGURE 14: Graphical representation of PSNR difference between the image and data.

Figure 11 depicts the graphical representation of obtained hiding capacity values for the test images. The test image Owl has higher capacity compared to other test images. From the graph, the test image light images have the lower hiding capacity value. The results of steganography capacity denote the most significant view of any steganographic method. The capacity of all cover images to embed the secret image increases, and the QR method increases the security of the secret information.

The SSIM graphical representation for the test images is shown in Figure 12. By using the proposed technique, the obtained value for SSIM using different test images is clearly mentioned to evaluate the proposed method performance.

TABLE 2: Comparative study of various algorithm-obtained PSNR for steganography.

Author and year	Algorithm	Cover image	PSNR (dB)
Shabir et al., 2010	Pixel repetition method	Barbara	45.13
		Mandrill	45.16
		Lenna	45.14
		Pepper	45.21
Iyad et al., 2016	Reversible data hiding	Barbara	48.70
		Mandrill	48.71
		Lenna	48.70
		Pepper	48.71
Mehdi et al., 2017	Parity-bit pixel value difference and improved rightmost digit replacement	Barbara	36.90
		Mandrill	38.55
		Lenna	39.09
		Pepper	39.11
Ahmed et al., 2019	Quantum substitution boxes	Barbara	44.18
		Mandrill	44.19
		Lenna	44.13
		Pepper	44.11
Inas et al., 2020	Dual tree complex wavelet transform	Barbara	51.42
		Mandrill	51.02
		Lenna	51.37
		Pepper	51.19
Proposed	Quick response	<b>Barbara</b>	<b>52.53</b>
		<b>Mandrill</b>	<b>52.60</b>
		<b>Lenna</b>	<b>52.53</b>
		<b>Pepper</b>	<b>52.61</b>

Figure 13 shows the graph for MSE difference between the secret image and data.

Figure 14 shows the graph for PSNR difference between the digital image and data. From the graph, the PSNR value obtained for secret data is higher for all test images compared to the PSNR value for secret images. Secret messages should be protected not only in the cyber domain but also in the complex physical domain [23]. The results of Table 2 show that the proposed QR-based steganography method yields better results than all the existing techniques in almost all stenographic images. From this table, by using the proposed method, the PSNR value obtained for the test images Barbara, Mandrill, Lenna, and Pepper is 52.53 dB, 52.60 dB, 52.53 dB, and 52.61 dB, respectively. Steganography conceals the existence of a secret message while cryptography alters the message format itself [24].

Figure 15 clearly shows the comprehensive results of different algorithms as well as the proposed quick response algorithm. The proposed algorithm was considered to be the threshold value to calculate the PSNR percentage for all the existing algorithms.

From Figure 16, it is proved that the PSNR is much improved in the proposed quick response algorithm by

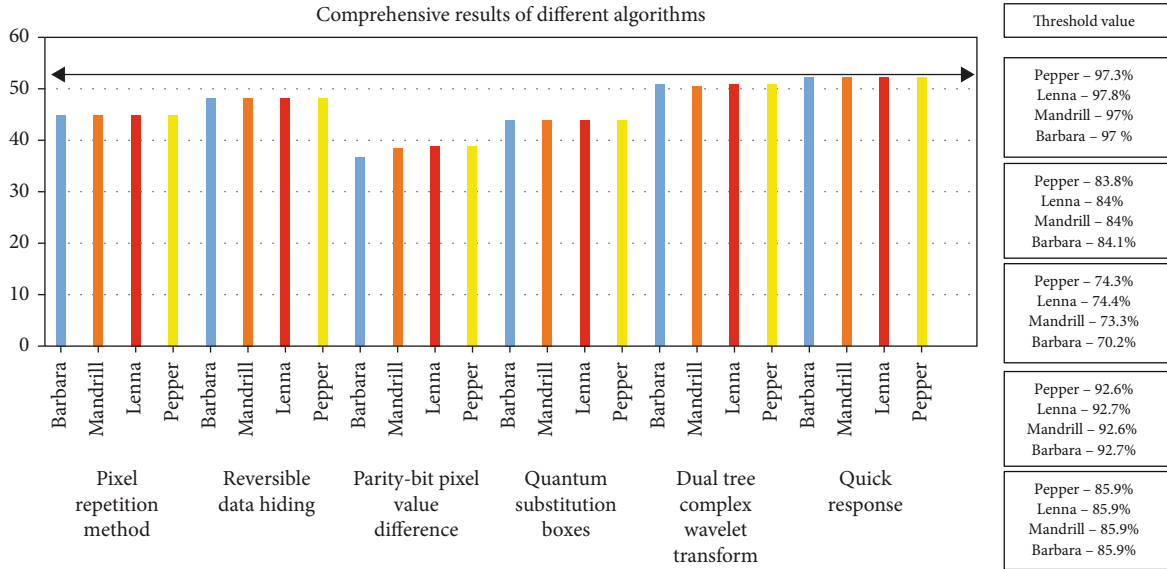


FIGURE 15: Comprehensive results of different algorithms.

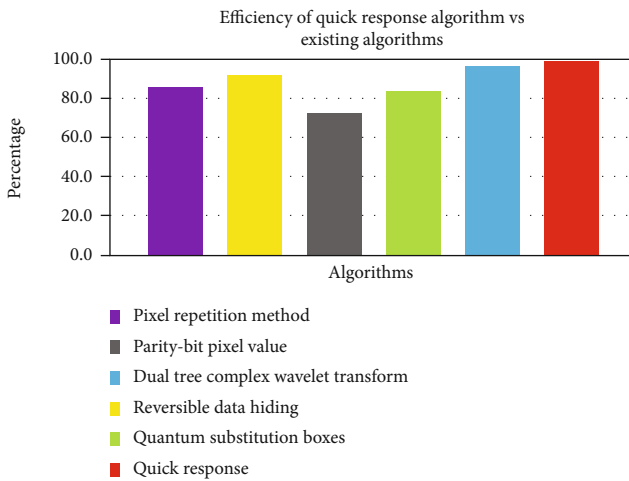


FIGURE 16: Efficiency of quick response algorithm vs. existing algorithms.

2.5% compared to the best existing algorithm. The higher the PSNR, the better the quality of the compressed or reconstructed image.

### 5. Conclusion

The data hiding and stenographic capacity is the most significant aspect of the proposed system. A novel data hiding technique is proposed to improve the security of the proposed system. The histogram shifting method ensures the improvement in data hiding capacity, and the quick response method is helpful in extracting the hidden data or image from the original cover image. Several images were taken as test images, and the experiment was carried out on these test images. The resultant images proved that the proposed technique enhances the data hiding capacity by

embedding the secret data/image in the cover image using the shifting method. The performance analysis of both encoding and decoding process provides better result than any other techniques used for data hiding.

### Data Availability

The data used to support the findings of this study are available from the corresponding author upon request.

### Conflicts of Interest

The authors declare that they have no conflicts of interest.

### References

- [1] O. F. AbdelWahab, A. I. Hussein, H. F. A. Hamed, H. M. Kelash, A. A. M. Khalaf, and H. M. Ali, "Hiding data in images using steganography techniques with compression algorithms," *Telkomnika*, vol. 17, no. 3, pp. 1168–1175, 2019.
- [2] U. D. Acharya and P. R. Kamath, "A secure and high capacity image steganography technique," *International Journal*, vol. 4, no. 1, pp. 83–89, 2013.
- [3] N. Ayub and A. Selwal, "An improved image steganography technique using edge based data hiding in DCT domain," *Journal of Interdisciplinary Mathematics*, vol. 23, no. 2, pp. 357–366, 2020.
- [4] S. Bhavani and B. Raviteja, "Secure data transmission through RDH," *International Journal of Signal Processing, Image Processing and Pattern Recognition*, vol. 7, no. 6, pp. 261–272, 2014.
- [5] Y. Zandi Mehran, M. Nafari, A. Nafari, and N. Zandi Mehran, "Histogram shifting as a data hiding technique: an overview of recent developments," *Communications in Computer and Information Science*, vol. 166, pp. 770–786, 2011.
- [6] A. E. L.-L. AA, B. Abd-El-Atty, and S. E. Venegas-Andraca, "A novel image steganography technique based on quantum

- substitution boxes,” *Optics and Laser Technology*, vol. 116, pp. 92–102, 2019.
- [7] L. Buzo and R. M. Gray, “An algorithm for vector quantizer design,” *IEEE Transactions on Communications*, vol. 28, no. 1, pp. 84–95, 1980.
- [8] A. Al-Ataby and F. Al-Naima, “A modified high capacity image steganography technique based on wavelet transform,” *International Arab Journal of Information Technology*, vol. 7, pp. 358–364, 2010.
- [9] C. Chang and W. C. Wu, “Fast planar-oriented ripple search algorithm for hyperspace VQ codebook,” *IEEE Transactions on Image Processing*, vol. 16, no. 6, pp. 1538–1547, 2007.
- [10] C. C. Chang, G. M. Chen, and M. H. Lin, “Information hiding based on search-order coding for VQ indices,” *Pattern Recognition Letters*, vol. 25, no. 11, pp. 1253–1261, 2004.
- [11] W. C. Du and W. J. Hsu, “Adaptive data hiding based on VQ compressed images,” *IEE Proceedings-Vision, Image and Signal Processing*, vol. 150, no. 4, pp. 233–238, 2003.
- [12] L. S. T. Chen and C. J. C. Lin, “Steganography scheme based on side match vector quantization,” *Optical Engineering*, vol. 49, no. 3, article 037008, 2010.
- [13] C. C. Chen and C. C. Chang, “High capacity SMVQ-based hiding scheme using adaptive index,” *Signal Processing*, vol. 90, no. 7, pp. 2141–2149, 2010.
- [14] C. De Vleeschouwer, J. F. Delaigle, and B. Macq, “Invisibility and application functionalities in perceptual watermarking an overview,” *Proceedings of the IEEE*, vol. 90, no. 1, pp. 64–77, 2002.
- [15] M. Hussain, A. W. Abdul Wahab, A. T. S. Ho, N. Javed, and K. H. Jung, “A data hiding scheme using parity-bit pixel value differencing and improved rightmost digit replacement,” *Signal Processing: Image Communication*, vol. 50, pp. 44–57, 2017.
- [16] C. C. Lin, S. C. Chen, and N. L. Hsueh, “Adaptive embedding techniques for VQ-compressed images,” *Information Sciences*, vol. 179, no. 1-2, pp. 140–149, 2009.
- [17] M. Mishra and B. K. Mishra, “Secret communication through information camouflaging in the mimesis and the crypsis way,” in *2016 International Conference on Electrical, Electronics, and Optimization Techniques (ICEEOT)*, pp. 3045–3050, Chennai, India, 2016.
- [18] A. Priya, “High capacity and optimized image steganography technique based on ant colony optimization algorithm,” *International Journal of Emerging Technology and Innovative Engineering*, vol. 4, no. 6, pp. 1989–1993, 2018.
- [19] S. Parah, J. Sheikh, J. Akhoun, and N. Loan, “Electronic health record hiding in images for smart city applications: a computationally efficient and reversible information hiding technique for secure communication,” *Future Generation Computer Systems*, vol. 108, 2018.
- [20] M. M. Rani and L. Shanti, “An integrated method of data hiding and compression of medical images,” *International Journal of Advanced Information Technology*, vol. 6, no. 1, pp. 43–51, 2016.
- [21] R. Shamir and L. Adleman, “A method for obtaining digital signatures and public-key cryptosystems,” *The Computer*, vol. 21, no. 2, pp. 120–126, 1978.
- [22] W. J. Wang, C. T. Huang, and S. J. Wang, “VQ applications in steganographic data hiding upon multimedia images,” *IEEE Systems Journal*, vol. 5, no. 4, pp. 528–537, 2011.
- [23] Z. Luo, W. Xie, B. Wang, Y. Tang, and Q. Xing, “EasyStego: robust steganography based on quick-response barcodes for crossing domains,” *Symmetry*, vol. 11, no. 2, p. 222, 2019.
- [24] M. S. Taha, M. S. Rahim, S. A. Lafta, M. M. Hashim, and H. M. Alzuabidi, “Combination of steganography and cryptography: a short survey,” *IOP Conference Series: Materials Science and Engineering*, vol. 518, no. 5, article 052003, 2019.



## Retraction

# Retracted: Construction of Innovation and Entrepreneurship Education Ecosystem in Higher Vocational Colleges from the Perspective of System Theory

### Wireless Communications and Mobile Computing

Received 25 July 2023; Accepted 25 July 2023; Published 26 July 2023

Copyright © 2023 Wireless Communications and Mobile Computing. This is an open access article distributed under the Creative Commons Attribution License, which permits unrestricted use, distribution, and reproduction in any medium, provided the original work is properly cited.

This article has been retracted by Hindawi following an investigation undertaken by the publisher [1]. This investigation has uncovered evidence of one or more of the following indicators of systematic manipulation of the publication process:

- (1) Discrepancies in scope
- (2) Discrepancies in the description of the research reported
- (3) Discrepancies between the availability of data and the research described
- (4) Inappropriate citations
- (5) Incoherent, meaningless and/or irrelevant content included in the article
- (6) Peer-review manipulation

The presence of these indicators undermines our confidence in the integrity of the article's content and we cannot, therefore, vouch for its reliability. Please note that this notice is intended solely to alert readers that the content of this article is unreliable. We have not investigated whether authors were aware of or involved in the systematic manipulation of the publication process.

In addition, our investigation has also shown that one or more of the following human-subject reporting requirements has not been met in this article: ethical approval by an Institutional Review Board (IRB) committee or equivalent, patient/participant consent to participate, and/or agreement to publish patient/participant details (where relevant).

Wiley and Hindawi regrets that the usual quality checks did not identify these issues before publication and have since put additional measures in place to safeguard research integrity.

We wish to credit our own Research Integrity and Research Publishing teams and anonymous and named external researchers and research integrity experts for contributing to this investigation.

The corresponding author, as the representative of all authors, has been given the opportunity to register their agreement or disagreement to this retraction. We have kept a record of any response received.

### References

- [1] C. Zheng, L. Sun, and H. Guo, "Construction of Innovation and Entrepreneurship Education Ecosystem in Higher Vocational Colleges from the Perspective of System Theory," *Wireless Communications and Mobile Computing*, vol. 2022, Article ID 5805056, 8 pages, 2022.

## Research Article

# Construction of Innovation and Entrepreneurship Education Ecosystem in Higher Vocational Colleges from the Perspective of System Theory

Chuanjuan Zheng , Liandong Sun, and Huifang Guo 

Zhejiang Tongji Vocational College of Science and Technology, Hangzhou, China

Correspondence should be addressed to Huifang Guo; [z20120191101@zjtongji.edu.cn](mailto:z20120191101@zjtongji.edu.cn)

Received 25 January 2022; Revised 14 February 2022; Accepted 16 February 2022; Published 11 March 2022

Academic Editor: Shalli Rani

Copyright © 2022 Chuanjuan Zheng et al. This is an open access article distributed under the Creative Commons Attribution License, which permits unrestricted use, distribution, and reproduction in any medium, provided the original work is properly cited.

Innovation and entrepreneurship (IAE) education in higher vocational education is mainly to cultivate college students' innovative spirit and ability, and it is an important way to promote economic development. However, the current academic research on the construction of IAE education ecosystem in higher vocational school (HVS) is relatively weak. In order to improve the IAE education ecosystem of HVS and strengthen the innovation of HVS education system, this study systematically discusses and analyzes the system from the four aspects of system boundary, state, power, and movement and further innovates and constructs the IAE education ecosystem of HVS on the basis of university education system, subject cooperation, and mechanism management. The results prove the feasibility of HVS IAE education ecosystem from the perspective of system theory, enhance the cultivation of HVS talents' IAE ability, and are of great significance to promote the comprehensive reform of higher vocational school education system.

## 1. Introduction

Innovation and entrepreneurship (IAE) education in higher vocational education is mainly to cultivate college students' innovative spirit and ability, serve the construction of an innovative country, and is an important way to promote economic development [1]. The report of the 19th National Congress of the Communist Party of China clearly puts forward, actively encourages IAE to drive employment, and helps fresh college students achieve employment and entrepreneurship [2]. Compared with general education, higher vocational education is more closely connected with industry and market and has the natural advantage of developing IAE education. Many domestic scholars began to pay attention to IAE education. Bo et al. explored the deep integration path of professional education and IAE education, hoping to realize the coordinated development of vocational education and IAE Education [3]. Dongmei took Jilin Engineering Vocational College as an example to explore the IAE education system of higher vocational school (HVS) through three

aspects: full coverage, hierarchy, and modularization [4]. IAE education of HVS is a systematic project promoted as a whole, which requires mutual cooperation and cooperation among participants, and more attention should be paid to the coupling relationship between top-level design and implementation.

With the proposal of China's education reform, the theories of integrity and systematicness in the field of ecology have been applied in pedagogy, gradually forming the theory of educational ecology and putting forward the IAE education ecosystem. The construction of the IAE education ecosystem of HVS is of great significance to IAE Education [5], but the current academic research on the construction of the IAE education ecosystem of HVS is relatively weak. As a result, the so-called educational reform is still in the exploratory stage. Shunbo and Wei explored the path of building IAE ecosystem from five system aspects based on type characteristics [6]. Yang took Sichuan Vocational College of cultural industry as an example, analyzed the necessity of building IAE education ecosystem, and summarized the

specific measures of IAE education ecosystem construction of HVS [7].

With the reform of education system by social development, the construction of IAE education ecosystem of HVS is an inevitable requirement to serve the national development strategy and an inevitable trend to enhance the adaptability of vocational and technical education. This paper discusses the reform of education ecosystem.

## 2. Practical Problems and Available Resources for IAE Education in HVS

*2.1. Practical Problems.* The construction of IAE education ecological embodiment in colleges and universities is a complex main project involving many problems. As a result of efforts in recent years, the existing IAE education ecosystem of HVS in China has taken shape, but its future development still faces bottlenecks [8]. Sha analyzed the significance and existing problems of enterprise school cooperation in IAE talent training through the exploration of talent training path and believed that we should pay more attention to IAE Education [9]. Jianzhong believes that the current HVS's IAE education thinking concept is backward, the teachers are not enough, and the system is not perfect, which needs to be further improved [10]. Guofeng also believes that the current IAE education system has immature concept, imperfect management mechanism, chaotic internal structure, and insufficient fund investment [11]. Yang and Wu further improved and optimized the IAE education system from the aspects of responsibility implementation, curriculum system, teaching staff, cultural atmosphere, and establishment of practice platform and policy guarantee, so as to improve students' high-quality employment and realize the high-quality development of the school [12].

In the past, the teaching methods of the normal education system in colleges and universities were jointly participated by the student department, schools, and school enterprise cooperation units in the teaching process. School support was adopted for entrepreneurship with college students. Students raised their own funds, school enterprise job fairs, and individuals took the initiative to apply online. Most students preferred employment, and the number of students who started their own businesses was relatively small.

*2.2. Available Resources.* The education ecosystem is a system composed of horizontal subject coordination and vertical mechanism coordination, which needs the support of the government and society through policy and resource drainage. At this time, students still do not have more resources and experience for the society. The education is more to provide guidance. Colleges and universities and teachers and students expand the output of achievements through teaching and practical training and realize the development pattern of two-way promotion. According to the viewpoint of system theory, the system is analyzed from four aspects: boundary, state, power, and motion.

*2.2.1. Openness of System Boundary: Support and Output.* From the perspective of the external sources of the IAE edu-

cation ecosystem of HVS, the government has issued relevant policies to guide IAE education in colleges and universities and provided financial support for IAE education in colleges and universities through financial allocation. The society provides technical support and platform support for IAE education in colleges and universities through school enterprise cooperation. From the internal perspective of the IAE education ecosystem of HVS, colleges and universities have received various external support and realized the output of innovative talents, innovative technologies, and innovative projects. Border openness is a necessary prerequisite for the internal and external exchange and resource exchange of IAE ecosystem in manuscript colleges and also determines the characteristics of system state, system power, and system movement.

*2.2.2. Non Equilibrium of System State: Dissipation and Disorder.* Because of the expanding boundary openness of the IAE education ecosystem of HVS, it presents a nonequilibrium state. From the perspective of dissipative structure of resource allocation, the support for IAE education of HVS is different in different regions. This "disorderly" nonequilibrium state can promote the transfer of IAE education resources in higher vocational colleges and form the power of complementary advantages and disadvantages. From the perspective of the dissipative structure of subject cooperation, due to the different value choices and professional levels of different subjects, the division of labor of IAE education in HVS is also different. This "disorderly" unbalanced state promotes institutionalized cooperative governance and efficient cooperation.

*2.2.3. Nonlinearity of System Dynamics: Interleaving and Catalysis.* The complexity of IAE education of HVS makes the interaction mode of factors at all levels no longer a simple linear relationship, but a spiral trajectory. When the IAE education strategy of HVS was just put forward, there was a simple linear relationship between the government, universities, and teachers and students. After promoting the cooperation between schools and enterprises and the integration of industry and education, it became a complex nonlinear relationship of multipoint cooperation among the government, universities, society, teachers, and students. In the future, with the increasing depth and breadth of participation of various subjects of HVS IAE education, the nonlinear role of this system will also be strengthened, and the effectiveness of HVS IAE education ecosystem will be brought into full play.

*2.2.4. Fluctuation of System Motion: Jump and Qualitative Change.* The nonlinear relationship of IAE education ecosystem of HVS makes the results of system movement show huge fluctuation. At the level of external fluctuation, the adjustment of top-level design and the change of educational environment will lead to the deviation of the internal structure of the ecosystem, and the nonlinear relationship is more significant, which promotes the IAE education of HVS to reform and adjust in depth and develop with higher quality. At the level of internal fluctuation, the change of cooperation

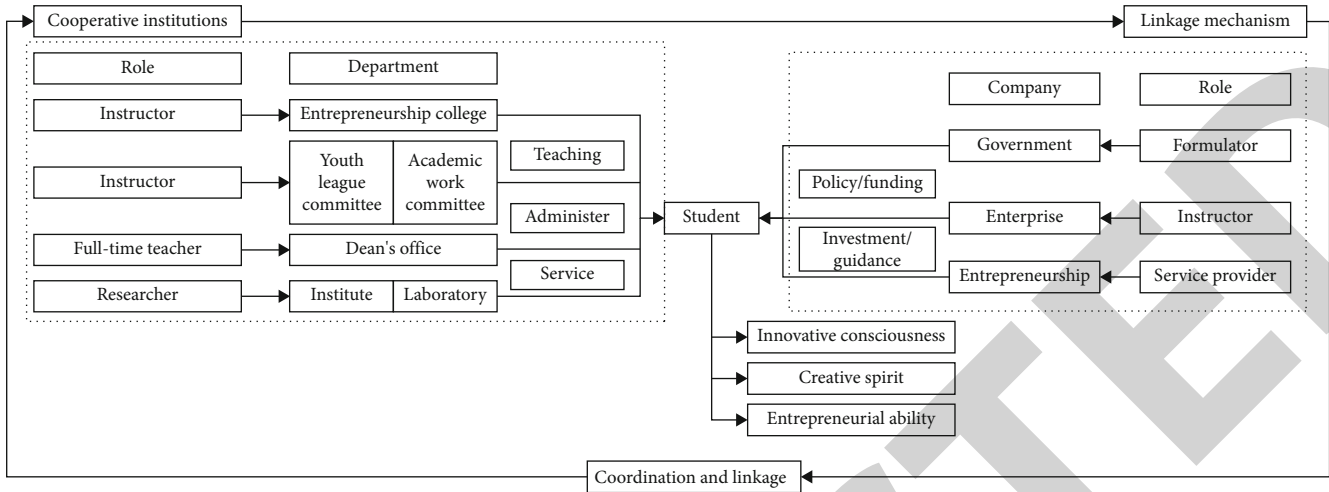


FIGURE 1: Main subsystem of innovation and entrepreneurship education.

mechanism and the change of teachers' and students' needs will make the internal structure of the system develop out of order, expand the nonlinear auxiliary relationship, promote the in-depth adjustment of IAE education mode and mechanism of HVS, and pay more attention to the cultivation of college students' enthusiasm, creativity, and ability.

The openness of the boundary, the nonequilibrium of the state, the nonlinearity of the dynamic, and the fluctuation of the movement are the characteristics of the IAE education ecosystem of HVS. Firstly, the openness of the system boundary is the symbol of the effectiveness of IAE education in HVS, which determines the existence and sustainable development of the system. Secondly, the greater the diversity of IAE education in HVS, the greater the intensity of reform; the key to promoting the IAE education reform of HVS is the imbalance of the system state. Thirdly, the richer the participants of the IAE education system of HVS, the more perfect its coordination system and the more scientific its mechanism; the formation source of IAE education synergy of HVS is the nonlinearity of system dynamics. Finally, the internal cause of the high-quality development of IAE education of HVS is the fluctuation of system movement. The reform and adjustment of internal and external linkage has greatly promoted the improvement of IAE education quality of HVS.

### 3. Innovation in the IAE Education Ecosystem of HVS

The education ecosystem is a complex system, developed from a simple system, and is a development process of orderly growth. In this process, the coordination among subjects plays a key role, which requires multidimensional coordination among subjects such as government, schools, and enterprises. This requires not only teacher sharing, project docking, resource coconstruction, and other methods but also public opinion guidance, policy support, financial investment, interest balance and so on. The structure of the IAE education subject subsystem is shown in Figure 1.

In Figure 1, the government, as the initiator, advocate, and policy maker of IAE education, defines the implementation path and objectives of IAE education through top-level design; as the main body of direct connection and implementation, the colleges and universities include entrepreneurship college, youth league committee, academic work committee, academic affairs office, research institute, laboratory, and other departments, which, respectively, undertake the roles of IAE education, teaching, guidance, and scientific research. It is necessary to specify the IAE education development plan according to the university's conditions and Cather's theory and practice courses of IAE education, so as to create an atmosphere for the development environment of IAE in colleges and universities; as the carrier and platform of IAE education, enterprises provide practice opportunities and internships for college students, provide guidance for entrepreneurship projects, and provide favorable external conditions for IAE education. The entrepreneurship park provides IAE with entrepreneurship venues, policy consultation, entrepreneurship guidance, and information services and plays a leading role in IAE education. In the process of participating in various entrepreneurial projects, college students' innovation awareness and entrepreneurial spirit have been improved, and their entrepreneurial experience has become richer and richer. Finally, their achievements have been transformed into real enterprises, providing more students with jobs and entrepreneurial opportunities.

The education system is a typical open system with certain complexity. In order to improve the IAE education system, we need to combine the overall planning of education, the optimization of policy supply and the enhancement of resource symbiosis, establish a guarantee system of external subject coordination and internal department linkage to ensure policy implementation resources, determine the training level and content, and adjust and supplement the talent training plan, through the combination of all aspects of the system to achieve the training goal. The IAE education talent training system is shown in Figure 2.

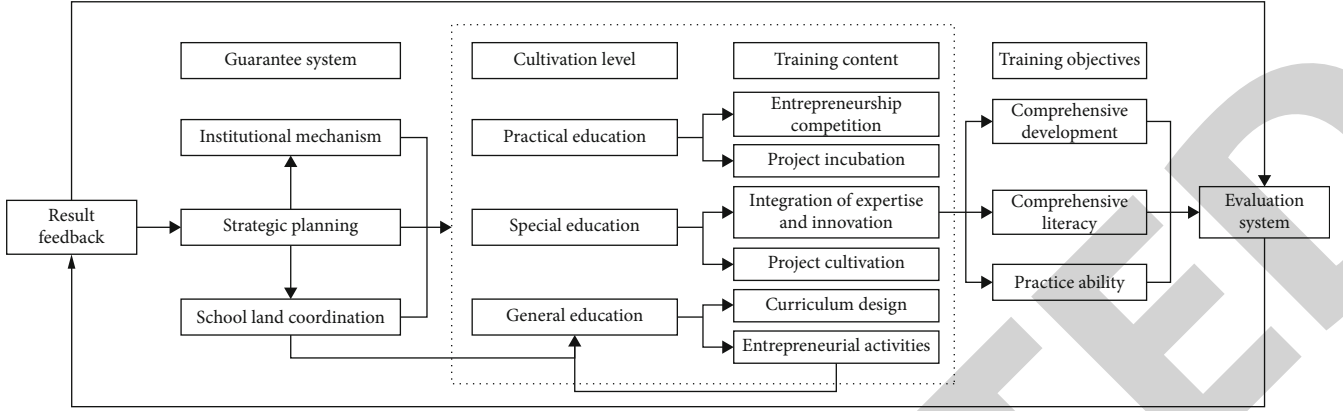


FIGURE 2: The whole system promotes the government, colleges and universities, enterprises, society, and academic circles to form school local coordination, encourages the government and enterprises to participate in the education platform of colleges and universities, carry out strategic planning and establish effective institutional mechanisms to form a security system, so as to carry out general education, characteristic education, and practical education, determine the training level and refine various training contents, so as to achieve the training goal of promoting vocational ability, comprehensive quality, and all-round development of higher vocational students and feedback the results through the evaluation system.

#### 4. Teaching Experiment and Test Results

**4.1. Basic Information of Students and Teaching Grouping.** In order to increase higher vocational students' all-round cognition of IAE ecological education system, 2000 graduates of a HVS in 2020 and 2021 were randomly investigated in groups. The graduates in 2020 were a group of normal higher vocational education, with an average of 18.5-20 years old, 1245 boys and 755 girls. The higher vocational students in 2021 are another group receiving IAE education system, with an average age of 18-20.6 years, 1087 boys and 913 girls.

**4.2. Teaching Methods and Teaching System.** The graduates in 2020 adopt the teaching methods of the normal education system of colleges and universities. In the teaching process, the student department, schools, and school enterprise cooperation units jointly participate in the school support for entrepreneurship with college students. Students raise funds by themselves, and school enterprise job fairs and personal active online recruitment. Most students give priority to employment, and the number of students who start their own businesses is relatively small.

In 2021, the graduates adopted the teaching method of HVS IAE ecological education system. During the teaching process, they reformed the previous education system, sought various educational preferential policies to provide financial support for students, and greatly improved the students' active learning habits in the way of combining teaching theory with practice. The school will provide guidance and support in many aspects to graduates with innovative and entrepreneurial ideas and encourage students to participate in independent entrepreneurship.

**4.3. Observation Contents and Statistical Methods.** For the two groups of students in 2020 and 2021, observe the mass entrepreneurship and innovation education under the reform education, investigate and count the cognition of

the education system, the entrepreneurial scale and entrepreneurial success rate of the two groups of students, and evaluate the results of systematic application.

Among them, in the application of the teaching system, the arithmetic mean and standard deviation rate method in statistics and the bivariate  $t$ -test method need to be used for statistical analysis in the calculation of students' entrepreneurial results. The arithmetic mean and standard deviation rate are shown in formula (1)

$$\sigma = \frac{1}{n-1} \sqrt{\sum_{i=1}^n (x_i - \mu)^2}, \mu = \frac{1}{n} \sum_{i=1}^n x_i, \quad (1)$$

where  $\sigma$  is calculation result of standard deviation rate of input sequence  $x$ ,  $n$  is the number of elements of the input sequence  $x$ ;  $\mu$  is the arithmetic mean of the input sequence  $x$ .

The bivariate  $t$  verification method is shown in formula (2)

$$t = \frac{\mu_1 - \mu_2}{\sqrt{(n_1 - 1)\sigma_1^2 + (n_2 - 1)\sigma_2^2/n_1 + n_2 - 2 \cdot ((1/n_1) + (1/n_2))}}, \quad (2)$$

where  $\bar{x}$  is the arithmetic mean of the sample series of IAE education system;  $\mu$  is the average value of the sample series of IAE education system, and  $t$  is the result of bivariate  $t$ -test.

#### 5. Discussion on Teaching Experiment Results and Achievements

**5.1. Investigation on Students' Basic Cognition.** Through the relevant investigation on the IAE education ecosystem of HVS students, it is found that a small number of students have very limited understanding of the IAE education system and need the promotion and publicity of the school. After accepting the IAE education ecosystem, most students

TABLE 1: Questionnaire on entrepreneurial cognition of higher vocational students.

Grouping/year	Number of graduates	Entrepreneurship priority	Work priority	Public recruitment	Other
2020	2000	485 (24.2)	530 (26.5)	495 (24.75)	490(24.5)
2021	2000	735 (36.75)	610 (30.5)	427 (21.35)	228(11.4)
<i>t</i> value		8.429	9.034	9.127	8.926
<i>P</i> value		0.007	0.009	0.008	0.007

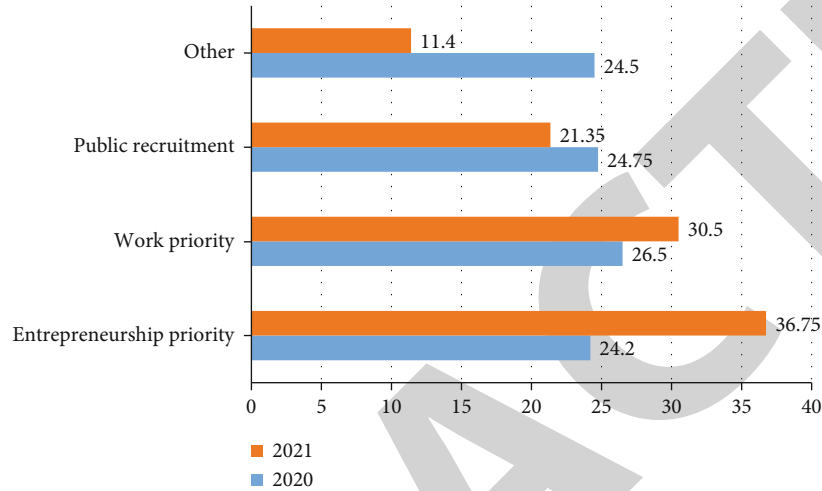


FIGURE 3: Visualization of students' IAE cognitive survey results.

take the initiative to strengthen the learning of education methods and teaching contents. Various optimization policies are also being applied and well utilized. With the innovative application of the IAE education system, higher vocational students preparing to start a business are very confident in the prospect of entrepreneurship. The investigation on students' entrepreneurial cognition of a HVS in 2020 and 2021 is as shown in Table 1.

Table 1 shows that in the survey on entrepreneurship awareness of HVS students in the same number and different years, the number of graduates in 2020 gives priority to employment, followed by the industries of public recruitment and independent entrepreneurship. In 2021, after the students who accepted the IAE education system of colleges and universities made effective use of educational reform and innovation and preferential government subsidies, the number of students who chose to give priority to entrepreneurship increased significantly, followed by the students who chose to give priority to work and participate in public recruitment.

By visualizing the cognitive survey results of the same number of students in the HVS in 2020 and 2021 in terms of IAE, Figure 3 is obtained.

In Figure 3, it is obvious that the proportion of entrepreneurial students who accept the application of IAE education system in 2021 is significantly higher than that in 2020, indicating that the application of IAE education system can be recognized by most students and improve the number of entrepreneurs of higher vocational students, which is worthy of being popularized and applied in HVS.

TABLE 2: Statistics of student entrepreneurship scale and success rate.

Year/yuan	20000	40000	60000	100000
2020	21.4 ± 4.3	16.4 ± 3.5	11.2 ± 5.1	6.3 ± 5.1
2021	35.2 ± 2.7	32.6 ± 2.9	22.5 ± 4.7	12.4 ± 4.3
<i>t</i> value	9.561	8.687	9.104	9.002
<i>P</i> value	0.007	0.009	0.008	0.009

20000 element.

**5.2. Student Entrepreneurship Scale and Success Rate.** The HVS college students choose to start a business after graduation every year, accounting for about 5% of the number of graduates in the same year, but the success rate of students' entrepreneurship only accounts for about 3% of the 5%. The above data show that the success rate of students' entrepreneurship is very low and in an obvious form of success weakness. Although students' independent entrepreneurship accounts for a large proportion, few can succeed in independent entrepreneurship without the support of policies of colleges and universities and social parties, according to the investigation and statistics on the entrepreneurial scale and entrepreneurial success power of fresh graduates of a higher vocational college in 2020 and those who received IAE education ecosystem in 2021, see Table 2.

Table 2 shows the success rate of HVS graduates in 2020 and 2021 with different entrepreneurship funds such as 20000 yuan, 40000 yuan, 60000 yuan, and 100000 yuan, and the IAE education ecosystem in 2021, the success ratio

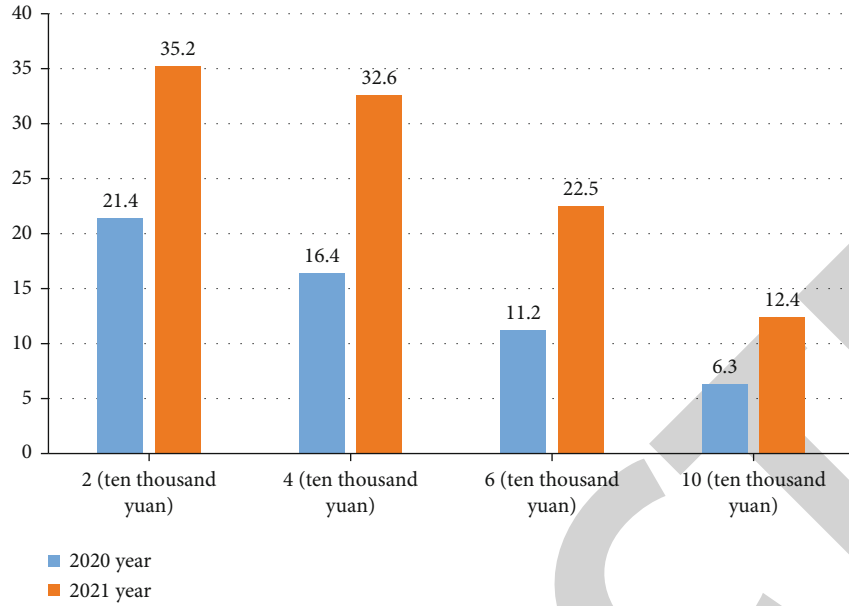


FIGURE 4: Visualization of statistical results of entrepreneurship scale and success rate of higher vocational students.

TABLE 3: Index weight of IAE education ecosystem in higher vocational colleges.

Serial number	Educational ecology system index	PCA weight	AHP weight	Entropy weight
1	Education system	0.038	0.054	0.152
2	Mechanism management system	0.046	0.061	0.067
3	Subject cooperation system	0.063	0.076	0.075
4	School teaching philosophy	0.065	0.068	0.059
5	School teaching methods	0.071	0.059	0.049
6	Teaching content system	0.040	0.054	0.162
7	Teaching platform system	0.072	0.061	0.042
8	Teaching practice system	0.057	0.054	0.034
9	Organization and coordination model	0.061	0.056	0.047
10	Education fund support	0.050	0.052	0.054
11	Education policy support	0.027	0.037	0.123
12	Educational environment support	0.048	0.053	0.050
13	School enterprise cooperation support	0.062	0.058	0.065
14	Achievement transformation system	0.068	0.064	0.037

of entrepreneurial students in different entrepreneurial scales was significantly higher than that in 2021, and the survey results were  $t < 10.000$  and  $P < 0.01$ , through the visual chart of the survey and statistics results of different entrepreneurial scale and entrepreneurial success rate of higher vocational graduates in 2020 and 2021, as shown in Figure 4.

Figure 4 shows that the graduates of higher vocational education in 2021 have received various preferential policies of IAE education system, various entrepreneurship models, and relevant support of entrepreneurship funds. The entrepreneurship scale and success rate have increased significantly, which improves the students' entrepreneurial enthusiasm and success rate, and can promote the sustainable development of HVS and socioeconomic market.

5.3. Discussion on Teaching Test Results. After the establishment of HVS IAE education ecological index system, it is also necessary to evaluate the index weight reasonably. Weight is an important index system for the comprehensive evaluation of the system. The key of index weight is how to reasonably allocate weight for quantitative evaluation. The accuracy and objectivity of the weight of each evaluation index directly affect the scientificity of the evaluation. Therefore, when allocating the weight of the system index, the statistical law and authoritative value between the system index data should be considered. The index weight of the system is shown in Table 3.

Table 3 shows that the weight indicators of the system are quantitatively evaluated by objective weighting method

(PCA), subjective weighting method (AHP), and entropy weight method. The PCA weight is a statistical method to investigate the correlation between variables. This method uses the principle of data information concentration and has the characteristics of objective weight. The AHP weight is a hierarchical model that builds the decision-making problem according to the order of overall goal, subgoals, and evaluation criteria. It is the weight of each index to the overall goal and has the characteristics of subjective weight. The entropy weight method determines the objective weight according to the variability of the index. Generally, the smaller the information entropy of an index, the greater the variability of the index value, the more information it provides, and the greater the role and weight it plays. Considering the advantages and disadvantages of the three methods, AHP, PCA, and entropy method are optimized. According to the subjective weight, objective weight, and entropy weight obtained from each index of HVS IAE education ecosystem, the geometric mean is recalculated and normalized, and the final weight results affecting each index of HVS IAE education ecosystem can be obtained.

In the application of the above index data, the result formula of the normalization algorithm is shown in (3) as follows:

$$y_i = \frac{x_i - \min(x)}{\max(x) - \min(x)}, \quad (3)$$

where  $y_i$  is the output item corresponding to the  $i$  input item;  $\min(x)$  is the minimum value in the input sequence  $x$ ; and  $\max(x)$  is the maximum value in the input sequence  $x$ .

In the research on the construction of HVS IAE education ecosystem from the perspective of system theory, after analyzing the current practical problems and available resources, optimize and innovate the HVS IAE education ecosystem, such as IAE education subject subsystem and IAE education talent training system, and conduct teaching experimental research and analysis according to the specific situation of higher vocational students and teaching method system. The results show that the students' cognitive effect of IAE education in the basic cognitive survey is better, and the entrepreneurial scale and success rate are also significantly improved [13].

In the ecological education system, optimize the subjective weight and objective weight and come to the conclusion that effective education methods and scientific courses are an important part of the IAE education ecosystem of HVS. The combination of teaching theory and practice platform will form a new innovation and entrepreneurship education system supported by various policies and promote the development of the education level of HVS, effectively stimulate and cultivate students' entrepreneurial spirit and innovation potential.

## 6. Summary

With the continuous development and progress of various forms of education, HVS's education system also needs to strengthen innovation and integrate with other special edu-

cation to form an education ecosystem in the new era [14]. Constructing HVS IAE curriculum education ecology from the perspective of system theory can stimulate the innovative consciousness of college students, make use of the relevant characteristics of HVS and students, and combine the ability of college IAE education ecology theory and practice to effectively form HVS diversified ecological education system. Based on the university education system, subject cooperation, and mechanism management, this study draws lessons from the system theory as the integration of education system theory and practice to build the HVS IAE education ecosystem system. The IAE education system is gradually improved through the basic characteristics and structural levels of ecological education. According to the needs of colleges and students, the subjective weight and objective weight indicators are combined and optimized in the education ecosystem to obtain the comprehensive weight index results of the IAE education ecosystem. The results prove the feasibility of HVS IAE education ecosystem from the perspective of system theory, enhance the cultivation of HVS talents' IAE ability, and are of great significance to promote the comprehensive reform of higher vocational school education system. In the future practice, the IAE curriculum education ecology of HVS still has great prospects to be further developed.

## Data Availability

The data underlying the results presented in the study are available within the manuscript.

## Disclosure

We confirm that the content of the manuscript has not been published or submitted for publication elsewhere.

## Conflicts of Interest

There is no potential conflict of interest in our paper, and all authors have seen the manuscript and approved to submit to your journal.

## References

- [1] L. Miaobing, "Research on the construction of innovation and entrepreneurship curriculum system in higher vocational college under the vision of education ecology [J]," *Journal of Guangdong Transportation Vocational and Technical College*, vol. 20, no. 4, pp. 65–68, 2021.
- [2] L. Xiaoyan, "Research on innovation and entrepreneurship education system in higher vocational colleges [J]," *Writer World*, vol. 7, pp. 186–187, 2021.
- [3] B. Wang, Z. Qijing, and F. Xueliang, "Path of the deep integration of higher vocational innovation and entrepreneurship education and professional education [J]," *Journal of Ningbo Vocational and Technical College*, vol. 25, no. 6, pp. 15–18, 2021.
- [4] J. Dongmei, "Exploration of innovation and entrepreneurship education in higher vocational colleges [J]," *Educational Observation*, vol. 10, no. 34, pp. 36–38, 2021.



## Research Article

# Enhanced Security Against Volumetric DDoS Attacks Using Adversarial Machine Learning

Jugal Shroff <sup>1</sup>, Rahee Walambe <sup>1,2</sup>, Sunil Kumar Singh <sup>3</sup> and Ketan Kotecha <sup>1,2</sup>

<sup>1</sup>Symbiosis Institute of Technology (SIT), Symbiosis International (Deemed University), India

<sup>2</sup>Symbiosis Centre for Applied Artificial Intelligence, Symbiosis Institute of Technology (SIT), Symbiosis International (Deemed University), India

<sup>3</sup>School of Computer Science and Engineering, VIT-AP University, India

Correspondence should be addressed to Rahee Walambe; rahee.walambe@sitpune.edu.in and Ketan Kotecha; drketankotecha@gmail.com

Received 7 November 2021; Accepted 24 February 2022; Published 11 March 2022

Academic Editor: Shalli Rani

Copyright © 2022 Jugal Shroff et al. This is an open access article distributed under the Creative Commons Attribution License, which permits unrestricted use, distribution, and reproduction in any medium, provided the original work is properly cited.

With the increasing number of Internet users, cybersecurity is becoming more and more critical. Denial of service (DoS) and distributed denial of service (DDoS) attacks are two of the most common types of attacks that can severely affect a website or a server and make them unavailable to other users. The number of DDoS attacks increased by 55% between the period January 2020 and March 2021. Some approaches for detecting the DoS and DDoS attacks employing different machine learning and deep learning techniques are reported in the literature. Recently, it is also observed that the attackers have started leveraging state-of-the-art AI tools such as generative models for generating synthetic attacks which fool the standard detectors. No concrete approach is reported for developing and training the models which are not only robust in the detection of standard DDoS attacks but which can also detect adversarial attacks which are created synthetically by the attackers with harmful intentions. To that end, in this work, we employ a generative adversarial network (GAN) to develop such a robust detector. The proposed framework can generate and classify the synthetic benign (normal) and malignant (DDoS) instances which are very similar to the corresponding real instances as evaluated by similarity scores. The GAN-based model also demonstrates how effectively the malicious actors can generate adversarial DDoS network traffic instances which look like normal instances using feature modification which are very difficult for the classifier to detect. An approach on how to make the classifiers robust enough to detect such kinds of deliberate adversarial attacks via modifying some specific attack features manually is also proposed. This work provides the first step towards developing a generic and robust detector for DDoS attacks originating from various sources.

## 1. Introduction

According to [1], cybercrimes have increased by over 600% during the COVID-19 pandemic. Organizations have a huge amount of sensitive public data which needs to be protected. A cyber-attack can severely damage their reputation and consumer trust, leading to loss of customers and sales, thus resulting in financial losses. Further implications of this could result in harassment and cyberbullying of the individuals whose data is hacked or stolen. Additionally, there are legal consequences such as heavy fines imposed by the government that an orga-

nization might face after suffering a cyber-attack. Therefore, with the increasing number of Internet users, cybersecurity is becoming more and more critical. Cyber-attacks can be divided into two categories:

- (1) Passive attacks: these cause damage to data confidentiality. In this kind of attack, an intruder monitors the system for information that can later be used for malicious purposes. The information remains unchanged, and the system has no impact. Some of the examples include an attacker trying to scan a

device or a server to find vulnerabilities such as open ports or an attacker trying to monitor a website's traffic [2, 3]

- (2) Active attacks: active attacks cause damage to the integrity and availability of the system. In this kind of attack, an attacker uses the information gained during the passive attack to exploit a device or a server. Unlike passive attacks, the information can be changed, and system service may be harmed during an active attack. Some of the examples of active attacks are DoS/DDoS attacks [4], MITM attacks [5], and Trojan attacks [6]

Among all the attacks, DoS and DDoS attacks are two of the most common types of cyber-attacks [7]. Between the period of January 2020 and March 2021, DDoS attacks increased by 55% with the technology sector being the most impacted ones [8].

A denial of service (DoS) attack is the type of attack in which an attacker tries to make a website or a computer server unavailable to other users by flooding the website or the server with heavy traffic. The attacker sends much more traffic than the server or the website can accommodate. A distributed denial of service (DDoS) attack is a DoS attack originating from multiple sources on the same target. DDoS attacks can be divided into 3 types [9]:

- (1) Volume-based attacks: in this type of attack, heavy traffic is sent to the server to consume all its network bandwidth
- (2) Protocol attacks: in this type of attack, the aim is to exploit server resources such as firewalls and load balancers
- (3) Application layer attacks: these types of attacks are considered as the most serious types of attacks and exploit the weaknesses present in the application layer

Figure 1 shows the frequency of different DDoS attacks from January 2020 through March 2021 [8].

From Figure 1, it can be observed that volumetric DDoS attacks have higher chances of occurring than other types of attacks. Therefore, security systems must be able to detect such volumetric DDoS attacks and raise an alarm at the right time to prevent any damage.

*1.1. Detecting DDoS Attacks with Standard Approaches.* One of the ways to mitigate a DDoS attack is to limit the number of requests a server or a device from a particular IP address can send. However, with this approach, even legitimate requests can be blocked in some cases such as a user trying to refresh a page multiple times. Another way includes filtering out network traffic based on certain features, but identifying those features is not an easy task. With the recent advancements in AI, many researchers have tried to apply various machine learning and deep learning algorithms to detect DDoS attacks. In [10], multiple linear regression [11] is employed to detect DDoS attacks using CIC-IDS

2017 dataset [12]. The authors shortlisted some important features using the information gain technique [13]. First, the top 16 features are used to train the model and predict the classes. The reported prediction accuracy is 73.79% for the Friday afternoon dataset. Further, 10 statistically insignificant attributes are eliminated, reducing the accuracy to 71.7% on the same dataset. Later on, the authors experimented with the ensemble model [14] and obtained an accuracy of 97.86%. The authors in [15] have used machine learning (ML) methods, namely, linear regression,  $K$ -nearest-neighbors (KNN), Naive Bayes (NB), decision tree (DT), random forest (RF), artificial neural network (ANN), and support vector machine (SVM), to detect DDoS attacks where the ANN outperforms the rest of the methods. Elsayed et al. proposed another method to detect DDoS attacks in [16] in which they have used a recurrent neural network (RNN) [17] along with an autoencoder [18] on the CICDDoS-2019 dataset [19]. They were able to outperform the previous models with an accuracy of 99%. In [20], a bidirectional RNN [21] along with long-short-term memory (LSTM) [22] and gated recurrent unit (GRU) [23] (to eliminate the vanishing gradient problem of RNN) to detect DDoS attacks is implemented. UNB ISCX Intrusion Detection Evaluation 2012 dataset [24] is used to demonstrate the approach, and maximum accuracy of 97.996% and 98.410% using two different datasets is reported.

*1.2. Detecting DDoS Attacks Using Adversarial Machine Learning (AML) Paradigm.* Various AI algorithms to detect DDoS attacks are proposed in [10, 15, 16, 20]. However, ML- and deep learning- (DL-) based classification models may perform poorly when there are changes in the input feature space [25]. This problem of generalization can be used by some malicious actors to trick the classifiers into making a wrong decision. This falls under the adversarial machine learning (AML) paradigm. AML techniques attempt to fool the AI detectors by supplying deceptive input with a primary reason to cause the malfunction in the machine learning model. Most ML models are designed to work on a specific dataset where the train and test data come from the same independent and identical distribution (IID). However, in the real-world scenario, if the data that is supplied to this model does not satisfy this statistical assumption and comes from a different IID, the results may get compromised [26, 27]. Adversarial attacks can be classified into two categories:

- (1) Poisoning attacks: these types of attacks occur during the AI model training phase. In this type of attack, either the training dataset is poisoned with the malicious input data or the model training algorithm is modified by the attacker, thus changing the way the algorithm learns to classify input data
- (2) Evasion attacks: they are the most prevalent type of attack, wherein the data is modified to be classified as legitimate and evade detection after deployment

To mitigate this problem, GANS [28] can be used to generate synthetic benign and DDoS instances and validate if the security systems are robust enough to identify those

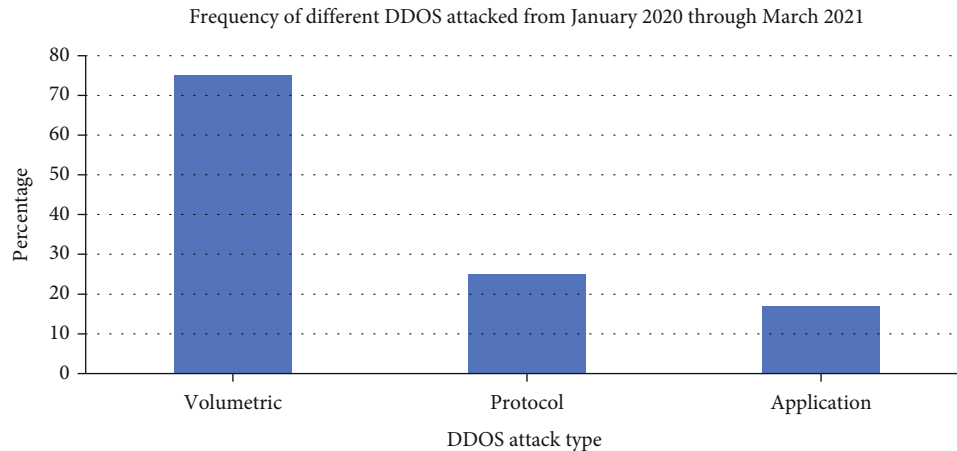


FIGURE 1: Frequency of different DDoS attacks from January 2020 through March 2021.

generated instances with high accuracy. In [29], the authors have introduced a “DoS-WGAN” model, which is used to generate DoS traffic that looks similar to normal traffic and can bypass a classifier trained using CNN [30], thus reducing the detection rate of the classifier. A “Wasserstein GAN with Gradient Penalty” (WGAN-GP) model [31] is used and implemented for the KDD CUP’99 dataset [32]. Although they were able to reduce the classifier’s accuracy to approximately 46.27% from 97.34%, the dataset used is very old. It has several significant issues, such as the huge number of replicated records [33]. Charlier et al. [34] introduced a “SynGAN” framework that can generate synthetic network attacks of high quality using publicly available datasets like NSL-KDD [35] and CICIDS2017 [12]. A root mean square (RMS) error of 0.10 is reported on adversarial generated attacks, showing a close similarity between the artificially generated attacks and real attacks. An area under curve (AUC) score of 75% is also reported, proving that the evaluator cannot differentiate between the real data and the generated synthetic data. In [36], it is shown that even after defensive systems are developed which employ incremental learning, they can still be vulnerable to new attacks if the attack profile is changed. Another challenge while detecting DoS and DDoS attacks is to be able to differentiate between the flash crowds and the actual attacks. An unexpected increase in the number of visitors visiting a website due to some event is known as flash crowds. Gursun et al. [37] first described how to differentiate between DDoS attacks and Flash crowds by statistically characterizing certain traffic features. Later on, in the same paper, the authors proved that even DDoS attack instances could be made to look like flash crowds using AI techniques.

Although [29, 34, 36, 37] have described and proved that an AI model can be trained to generate new synthetic instances and fool the security systems, they have not provided any concrete solution on how a classifier can be trained to detect such kind of generated synthetic adversarial instances. An attacker can use these generated synthetic instances to generate evasion attacks on the security systems to make the classifier misclassify those samples. Having undetected DDoS traffic can turn out to be very costly, and

a robust classifier capable of detecting DDoS traffic instances even when there are some changes in the nonattack features of DDoS instances is essential. For this purpose, the GAN framework can generate new DDoS instances and check if the classifier is robust enough to detect such generated synthetic instances. [38] have implemented a GAN-based framework wherein they have used the discriminator model to detect DDoS attacks. Although the discriminator model in GANs can help make the system less sensitive to adversarial attacks, traditional GANs are known to suffer from problems like vanishing gradients and mode collapse. To that end, in this work, a framework consisting of a special type of GAN for the generation and detection of DDoS attacks is proposed.

The contribution of this work is:

- (1) Development of a deep neural network- (DNN-) based classifier that can differentiate between DDoS instances and benign instances from the dataset
- (2) Development of two separate GAN-based models to generate synthetic traffic instances
  - (a) First generator that is capable of generating the benign instances which look very similar to benign instances from the dataset
  - (b) Second generator that is capable of generating the DDoS instances, which look very similar to DDoS instances from the dataset

These synthetic traffic instances (benign and DDoS from a and b, respectively) are used to test the classifier and check if they can predict those generated instances correctly.

- (3) Modifying the values present in the DDoS-specific features in the generated benign instances to convert them into DDoS instances. We test if the classifier can predict such adversarial instances as DDoS instances even though they look very similar to

benign ones. This is carried out to check if the trained classifier can detect evasion/adversarial attacks after deployment

- (4) Development and demonstration of an approach to train the classifier to differentiate between benign and DDoS instances when both of them look very similar

The rest of the paper is divided as follows: Section 2 gives a brief background of the GAN framework implemented in this work. Section 3 describes the methodology proposed in this research for developing a GAN-based framework for generating and detecting attacks. The performance of the classifier at different stages is also discussed briefly in this section. Section 4 describes the experimentation and results, followed by their analysis. Finally, Section 5 concludes the paper and presents some future work ideas.

## 2. Materials and Methods

The work proposed in this research primarily employs the generative adversarial network- (GAN-) based framework. In this section, firstly, the basic GAN architecture is discussed. This is followed by the specific approach WGAN employed here.

*2.1. Generative Adversarial Networks (GANs) [28].* A GAN model consists of 2 submodels: generator (G) and discriminator (D). The role of the generator is to generate new examples and make the discriminator classify them as the real ones. The role of the discriminator is to classify which examples are generated ones and which are real. This process works as a zero-sum game [39].

The accuracy of the generator is defined by how well it can fool the discriminator by making the discriminator classify its generated examples as real ones. The accuracy of the discriminator is measured by how well it can differentiate between the examples generated by the generator and the real examples. Essentially, both G and D networks strive to train better, and the model achieves convergence where further improvement in outcomes is not possible.

The methodology for training the GAN model (refer to Figure 2) is as follows:

- (1) Initially, a random noise vector is given to the generator submodel
- (2) The generator tries to produce some examples from the noise vector given to it
- (3) The generated example is then passed on to the discriminator to classify it as real or generated
- (4) Based on the output of the discriminator, the generator is trained to make it generate even better examples that can fool the discriminator
- (5) Similarly, based on the discriminator's ability to classify the generated examples as real ones or fake ones,

the discriminator is trained to classify the examples more correctly

Mathematically, the loss function of a GAN model can be defined as [28]:

$$\min_G \max_D V(D, G) = E_{x \sim P_{\text{data}}(x)} [\log D(x)] + E_{z \sim p_z(z)} [\log (1 - D(G(z)))], \quad (1)$$

where  $p_z(z)$  is the input noise variable; the goal of the generator is to generate new adversarial samples  $G(z)$  that come from the same distribution of  $x$ . The discriminator model "D" returns the probability  $D(x)$  that the given sample "x" is not generated by  $G$  and is actually from a real dataset. The goal of  $G$  is to maximize the probability of  $D$  predicting the generated data as a real one, whereas for  $D$ , the goal is to minimize this probability.

The GAN model that is mentioned in Section 3.1 faces the problem of vanishing gradients and mode collapse. To avoid this problem, a special type of loss function known as "Wasserstein Loss" is used by [40].

*2.2. Wasserstein Generative Adversarial Networks (WGANs) [40, 41].* A WGAN is a type of GAN that uses Wasserstein Loss as the loss function. In WGANs, the role of the discriminator is to identify the probability of the given sample being real or fake. But in the case of WGANs, instead of having a discriminator, a critic is present whose job is to identify how real or fake the given sample is instead of just predicting the probability of the given sample being real or fake. That is, the critic predicts the realness of the given sample.

The WGAN function is given by [31]:

$$\min_G \max_{D \in D} E_{x \sim P_r} [D(x)] - E_{\tilde{x} \sim P_g} [D(\tilde{x})], \quad (2)$$

where  $P_r$  is original data distribution,  $P_g$  is the generative model distribution,  $D(x)$  is the predictions made by the critic on original data distribution, and  $D(\tilde{x})$  is the predictions made by the critic on generated data samples. The goal of the generator is to minimize the distance between  $D(x)$  and  $D(\tilde{x})$ , whereas the goal of the critic is to maximize the distance between  $D(x)$  and  $D(\tilde{x})$ .

*2.3. Wasserstein Generative Adversarial Networks with Gradient Penalty (WGAN-GP) [31].* To further optimize WGAN, a gradient norm penalty method was introduced by [31] to generate samples of even high quality. The WGAN-GP function is given as [31]:

$$L = E_{\tilde{x} \sim P_g} [D(\tilde{x})] - E_{x \sim P_r} [D(x)] + \lambda E_{\tilde{x} \sim P_\alpha} [(\|\nabla_{\tilde{x}} D(\tilde{x})\|_2 - 1)^2]. \quad (3)$$

Wasserstein loss augmented with a gradient norm penalty for random samples  $\tilde{x} \sim P_\alpha$  to achieve Lipschitz continuity. The 2<sup>nd</sup> part of the equation is the applied gradient norm penalty function as discussed in this section. In this work, the WGAN-GP model is employed.

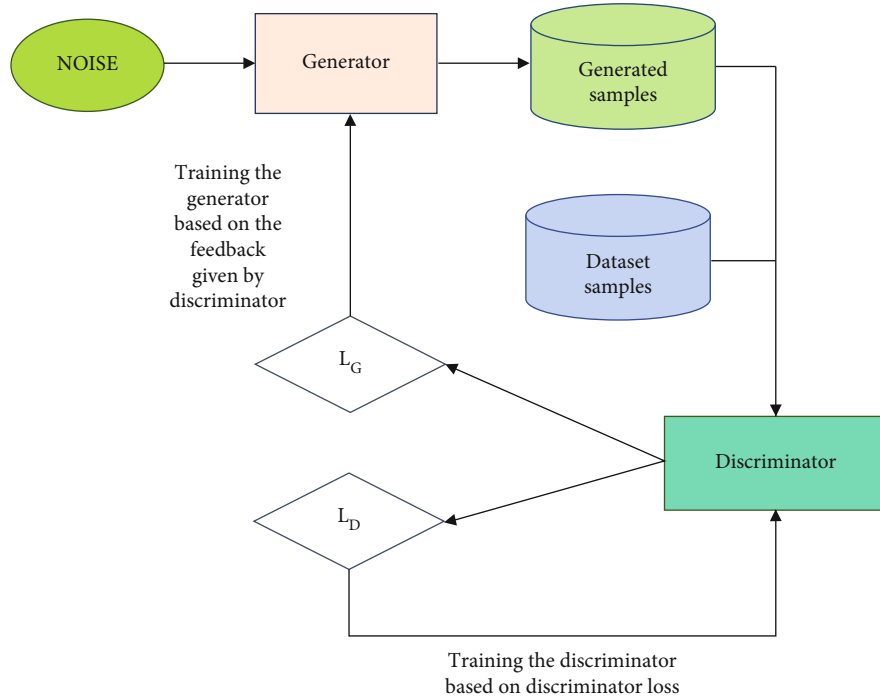


FIGURE 2: GAN training process.

TABLE 1: Abbreviations used in this and further sections.

b	Benign/nonmalicious samples from the dataset
m	DDoS/malicious samples from the dataset
bg	Generated benign instances which look like b
mg	Generated DDoS instances which look like m
bgm	Generated DDoS instances which look like b
clf-1	Classifier trained only on b and m
clf-2	Classifier trained on b, m, bg and bgm

### 3. Methodology

The proposed methodology based on the GAN-based model is described in this section. The performance of the classifier at various stages is also briefly mentioned. Detailed results are mentioned in Section 4.

For the simplicity purpose and to improve readability, the abbreviations shown in Table 1 are used throughout this work.

**3.1. Datasets.** Two different datasets are employed for experiments and validation.

- (i) CIC-DDoS2019 [19] dataset which contains the most common types of DDoS attacks. From this dataset, 533052 samples of UDP-based DDoS attacks were considered for the study. UDP-based DDoS attack is a type of volumetric DDoS attack. 3134 samples of benign traffic data are also considered. Since the data in this dataset was not balanced, we augmented the benign class data from another dataset, namely, CIC-IDS2017 [12]

- (ii) CIC-IDS2017 [12] dataset contains benign traffic data and some other types of attack data. 529918 samples of benign data instances from this dataset are combined with the 3134 samples from the CIC-DDoS2019 [19] dataset

After collecting data from both datasets, the two-class data were merged based on common features. The features which were not common to both datasets were not considered. Finally, the combined dataset has a total of 533052 instances of UDP-based DDoS attack data, a total of 533052 instances of benign traffic data, and 79 features.

**3.2. Preprocessing.** The first step of data preprocessing is to change the target label. Label “0” for benign data and “1” for UDP-based DDoS attack data is used. Followed by this, some of the features were omitted, either because they were unnecessary or because the data distributions in those features were highly uneven. Further, all the infinite values were replaced with the maximum value of that feature. Finally, to scale all the data evenly, a min-max scaler was used. After carrying out all the preprocessing steps, our final dataset has 533052 instances of UDP-based DDoS attack data, 533052 instances of benign traffic data, and 54 features. Figure 3 describes the preprocessing steps.

**3.3. Model Architecture.** The proposed framework consists of one classifier and two generator models. The primary goal of the classifier is to classify the given input data as a benign one or a DDoS attack. The classifier is a DNN-based model with 5 layers consisting of 128, 64, 32, 16, and 1 neuron[s], respectively. Rectified linear unit (ReLU) activation [42] is employed in the first four layers, followed by a sigmoid

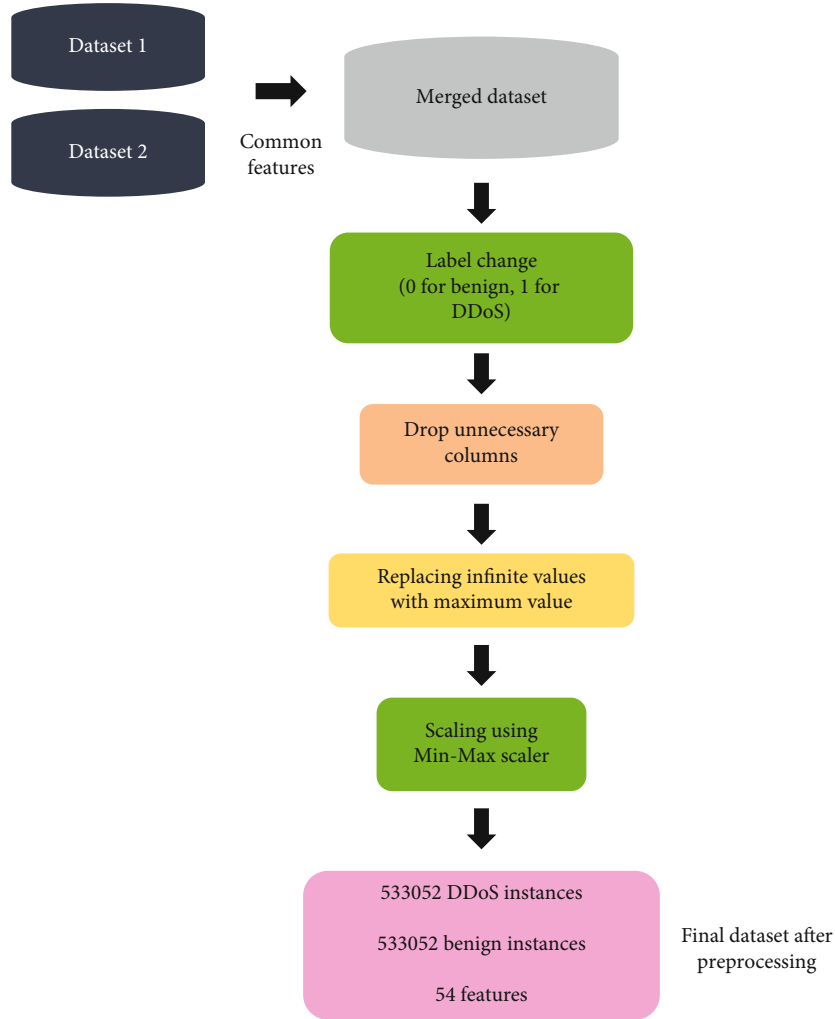


FIGURE 3: Preprocessing steps.

TABLE 2: List of DDoS specific attack features (functional features).

FlowDuration	Duration of flow in a millisecond
FwdPacketLengthMax	Max packet size sent in a forward direction
AvgFwdSegmentSize	Average segment size sent in a forward direction
TotalLengthofFwdPackets	The total length of packets sent in the forward direction
BwdPacketLengthStd	Standard packet size sent in the backward direction
AveragePacketSize	The average size of the packet while in transmission
AvgBwdSegmentSize	Average segment size sent backward direction
PacketLengthStd	The standard deviation of packet length
FlowLATStd	The standard deviation of interarrival time between two flows
ACKFlagCount	Packet counts with ACK
BwdPacketLengthMean	Mean of number of packets sent in the backward direction

activation [43] at the last layer. Since the classifier is trying to find the probability of an instance being benign or malicious independently, the sigmoid activation function is implemented instead of the standard Softmax function [43] in the last layer. The binary cross-entropy loss function with ADAM optimizer is employed. Our trained classifier will

be able to detect the following two types of attacks after deployment:

- (1) Automated adversarial DDoS attacks generated using the methodology similar to the ones suggested by [29, 34, 36, 37]

TABLE 3: Cosine similarities of bg, mg, and bgm with that of dataset instances.

Instances [sample 1, sample 2]	Mean cosine similarity (20 samples of sample 1 with the whole sample 2 dataset)
[bg, b]	85.40
[mg, m]	95.37
[bgm, b]	77.74

- (2) Instances that look very similar to the benign ones where some DDoS specific attack features were manually manipulated to make classifier misclassify them as benign instances

Along with detecting these two types of attacks, our classifier will also be able to differentiate the benign instances from the malignant DDoS instances, thus reducing the number of false positives after deployment.

The two generators are WGAN-GP models. The role of the first generator is to generate bg instances, and the role of the second generator is to generate mg instances. A WGAN-GP model consists of 2 submodels: a generator and a critic. The generator is responsible for generating the required instances. The role of the critic is to give feedback to the generator on these generated instances. Based on the feedback given by the critic, the generator learns to generate instances of even higher quality. The generator in model 1 will generate benign instances, and the generator in model 2 will generate the malignant DDoS instances.

The generators in both the models consist of 5 layers with 128, 64, 64, 32, and 54 neurons. ReLU activation function is used in all the layers except the last layer, where the LeakyReLU [44] activation function with the alpha value of -0.01 is employed. A negative alpha value is used in the last layer since a network packet can never have negative value data inside it and should preferably have a nonzero positive value.

The critics in both the models have five layers with 128, 64, 64, 32, and 1 neuron(s). For layers 1, 2, and 3, the ReLU activation function is employed. No activation function is used for the last two layers to allow the critic to use negative values in its output to demonstrate its predicted realness to the given input [45].

### 3.4. Model Training

- (1) First, both b and m datasets are split into training and testing sets. The training sets are denoted as b\_train and m\_train and testing sets as b\_test and m\_test. The classifier is trained using b\_train and m\_train. After training, the classifier is tested on b\_test and m\_test. The classifier can predict the instances with high accuracy
- (2) Next, two generators are trained: the first generator is trained to generate bg instances that look very similar to b, and the second generator is trained to generate mg instances that look very similar to m. After generating mg instances, the values present in

DDoS-specific attack features are modified with the values of the DDoS instances from the dataset (m). This is done to validate the attack

The DDoS specific attack features are shown in Table 2.

- (3) The trained classifier is retested on bg and mg and found to be able to correctly predict those instances. From this, we conclude that our trained classifier can detect adversarial attacks generated using AI models when there are no manual changes made in any of the feature values in the generated synthetic instances
- (4) Further, we test if the classifier will be able to detect the attack when there are some manual changes made in the attack features of the generated benign instances. For this, bg instances are considered, and the values present in DDoS-specific attack features are modified with the values of DDoS instances (m) from the dataset. This way, the generated benign instances get converted to DDoS instances, and they look very similar to b. These new instances are “bgm” as described in Table 1

The cosine similarities of bg, mg, and bgm with that of the original dataset are mentioned in Table 3.

- (5) The classifier is tested on bgm. The classifier is predicting them as “benign” even though they are DDoS instances. From this, it can be concluded that the classifier trained only using the dataset cannot correctly predict the instances based on DDoS-specific attack features. As mentioned in Table 1, at this stage, the classifier is termed as “clf-1”
- (6) Next, the bg and bgm instances are split into training and testing sets. To make the classifier robust enough, further training of the classifier is carried out on bg\_train and bgm\_train. This way, the classifier learns to differentiate between DDoS and benign instances giving more weightage to the attack features
- (7) The classifier is tested on bg\_test, bgm\_test, b, and m. The classifier is correctly able to predict all the instances. At this stage, the classifier is termed as “clf-2”

Figure 4 shows the workflow of the implementation.

The detailed results and comparison between the working of clf-1 and clf-2 are mentioned in Section 4.

## 4. Results and Discussion

Since most of the bg, mg, and bgm instances were used up in training the classifier, new bg and mg instances are generated to check the performance of both the classifiers “clf-1” and “clf-2” on newly generated data. New bgm instances are also generated using the same approach previously employed to generate bgm instances. These newly generated

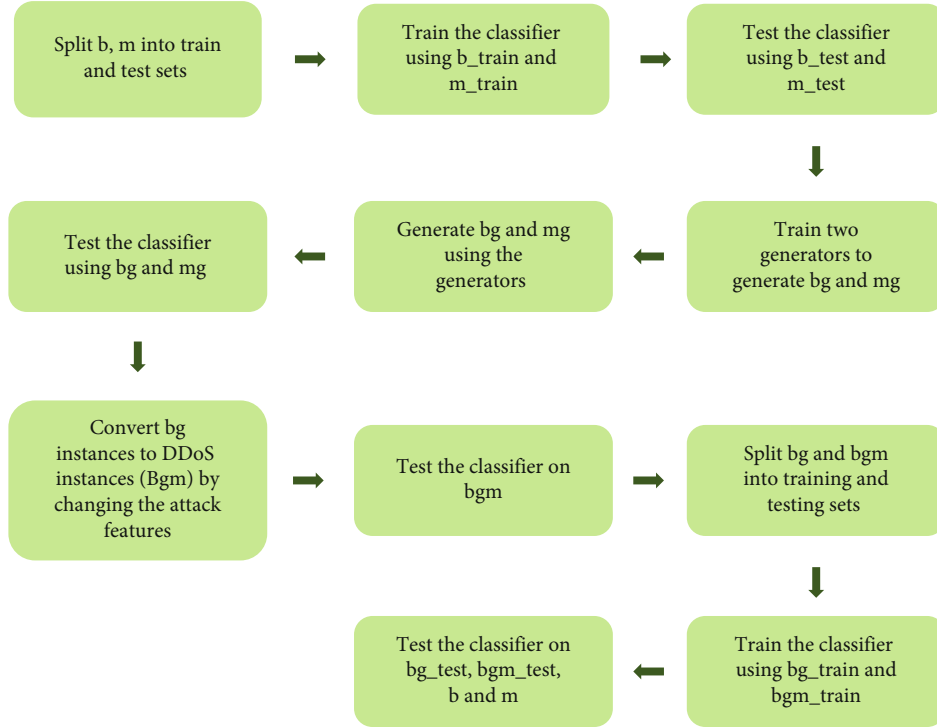


FIGURE 4: Workflow of the implementation.

TABLE 4: Cosine similarity table for newly generated samples used for testing the classifier.

Instances [sample 1, sample 2]	Mean cosine similarity (20 samples of sample 1 with the whole sample 2 dataset)
[bg_new, b]	85.34
[mg_new, m]	95.63
[bgm_new, b]	78.07
[bgm_new, bg_new]	78.62

TABLE 5: Confusion matrix for clf-1 on [bg\_new, mg\_new].

	Predicted benign	Predicted DDoS
Actual benign	533052	0
Actual DDoS	0	533052

TABLE 6: Confusion matrix for clf-1 on [bg\_new, bgm\_new].

	Predicted benign	Predicted DDoS
Actual benign	533052	0
Actual DDoS	533052	0

TABLE 7: Confusion matrix for clf-2 on [bg\_new, mg\_new].

	Predicted benign	Predicted DDoS
Actual benign	532880	172
Actual DDoS	0	533052

instances are termed as “bg\_new,” “mg\_new,” and “bgm\_new.” The cosine similarities of newly generated instances are mentioned in Table 4.

From Tables 3 and 4, it can be concluded that both the generators can generate instances that look very similar to benign and DDoS instances from the dataset. The predictions made by the classifiers are mentioned below:

4.1. B, M. B is the combination of bg\_new and b, and M is the combination of mg\_new, bgm\_new and m.

As can be observed from Table 5, the classifier trained only using the dataset can correctly classify the generated benign and DDoS instances when they look like benign and DDoS instances from the dataset. Therefore, this classifier, which is trained only using the dataset, will be able to classify both generated adversarial attack instances and benign instances correctly, similar to the discriminator model trained by [38] as long as there are no manual changes made in the input features of the generated instances. But from Table 6, it is concluded that such a classifier will not be able to predict the attack if the values of DDoS-specific attack features are changed in benign instances to make them malicious. From Tables 7–10, we conclude that the classifier trained using the approach suggested in this work is correctly able to differentiate between DDoS attack instances and benign instances using the attack features and will be able to detect DDoS attacks with high accuracy even if someone tries to make them look as benign as possible by manually changing some features.



TABLE 8: Confusion matrix for clf-2 on [bg\_new, bgm\_new].

	Predicted benign	Predicted DDoS
Actual benign	532880	172
Actual DDoS	27	533025

TABLE 9: Confusion matrix for clf-1 on [B, M].

	Predicted benign	Predicted DDoS
Actual benign	1066097	7
Actual DDoS	533053	1066103

TABLE 10: Confusion matrix for clf-2 on [B, M].

	Predicted benign	Predicted DDoS
Actual benign	1065164	940
Actual DDoS	28	1599128

## 5. Conclusion and Future Work

With the recent advancements in AI, many attackers have started using AI to generate adversarial attacks and bypass the security systems. Therefore, it is necessary to build the security systems that are robust enough so that they can correctly identify different types of adversarial attacks, thus helping in preventing them and minimizing the damage.

In this work, we first described how one can generate synthetic instances using GANs. We have used a special type of GAN framework called “WGAN-GP” for generating both benign and DDoS instances. These generated instances can be used to test if the classifiers are robust enough to detect automated attacks generated using AI techniques. Later on, we proved how a classifier, which is correctly able to detect the automated attacks generated using GANs, can be made to misclassify the samples by using other techniques described in adversarial AI paradigm. Lastly, we suggested an approach on how a classifier can be trained to detect evasion attacks by changing the DDoS attack features in the generated benign instances manually. This approach can also be used to test the classifier after deployment.

Recently many new AI techniques and frameworks are being introduced. Therefore, it is important to understand how one can leverage these new techniques in the cybersecurity domain. This work only focuses on volumetric DDoS attacks, since they are one of the most common types of attacks. However we believe that this approach can be used to detect other types of attacks. Similar approach can also be used in malware detection as well.

## Data Availability

All the datasets used for training the models are publicly available and their links are provided in the reference section. The preprocessed and the generated datasets can be accessed via the link provided below: [https://drive.google.com/drive/folders/1lu-cf0RLj0R7AioLmGeMh8b1\\_nCRZS1?usp=sharing](https://drive.google.com/drive/folders/1lu-cf0RLj0R7AioLmGeMh8b1_nCRZS1?usp=sharing).

[https://drive.google.com/drive/folders/1lu-cf0RLj0R7AioLmGeMh8b1\\_nCRZS1?usp=sharing](https://drive.google.com/drive/folders/1lu-cf0RLj0R7AioLmGeMh8b1_nCRZS1?usp=sharing).

## Conflicts of Interest

The authors declare that there is no conflict of interest regarding the publication of this paper.

## Acknowledgments

This work was supported by Symbiosis Centre for Applied Artificial Intelligence (SCAAI) and Symbiosis International University (SIU) under its research support fund.

## References

- [1] PURPLESEC, “Cyber-security-statisticsPURPLESECSeptember 2021, <https://purplesec.us/resources/cyber-security-statistics/>.
- [2] A. Bhattacharya, “Active-and-passive-attacks,” Encryption Consulting, 2021, September 2021, <https://www.encryptionconsulting.com/active-and-passive-attacks/>.
- [3] N. Hassan, “What-active-attack-vs-passive-attack-using-encryption,” Venafi, 2020, September 2021, <https://www.venafi.com/blog/what-active-attack-vs-passive-attack-using-encryption>.
- [4] Paloalto networks, “What-is-a-denial-of-service-attack-dos-Palo Alto NetworksSeptember 2021, <https://www.paloaltonetworks.com/cyberpedia/what-is-a-denial-of-service-attack-dos>.
- [5] Imperva, “Man-in-the-middle-attack-mitm/ImpervaSeptember 2021, <https://www.imperva.com/learn/application-security/man-in-the-middle-attack-mitm/>.
- [6] Kaspersky, “TrojansKasperskySeptember 2021, <https://www.kaspersky.co.in/resource-center/threats/trojans>.
- [7] J. Melnick, “Top-10-most-common-types-of-cyber-attacks,” Netwrix Blog, 2018, September 2021, <https://blog.netwrix.com/2018/05/15/top-10-most-common-types-of-cyber-attacks/>.
- [8] D. Warburton, “Ddos-attack-trends-for-2020,” F5 Labs, 2021, September 2021, <http://www.f5.com/labs/articles/threat-intelligence/ddos-attack-trends-for-2020>.
- [9] S. M. Poremba, “Types-of-ddos-attacks,” eSecurity Planet, 2017, September 2021, <https://www.esecurityplanet.com/networks/types-of-ddos-attacks/>.
- [10] S. Sambangi and L. Gondi, “A machine learning approach for DDoS (distributed denial of service) attack detection using multiple linear regression,” *Proceedings*, vol. 63, no. 1, p. 51, 2020.
- [11] J. Brownlee, “Linear-regression-for-machine-learning/,” Machine Learning Mastery, 2020, September 2021, <https://machinelearningmastery.com/linear-regression-for-machine-learning/>.
- [12] “Ids-2017.htmlUniversity of New Brunswick - Canadian Institute for CybersecuritySeptember 2021, <https://www.unb.ca/cic/datasets/ids-2017.html>.
- [13] J. Brownlee, “Information-gain-and-mutual-information/,” Machine Learning Mastery, 2020, September 2021, <https://machinelearningmastery.com/information-gain-and-mutual-information/>.

- [14] J. Brownlee, "Ensemble-methods-for-deep-learning-neural-networks/," Machine Learning Mastery, 2019, September 2021, <https://machinelearningmastery.com/ensemble-methods-for-deep-learning-neural-networks/>.
- [15] K. S. Sahoo, A. Iqbal, P. Maiti, and B. Sahoo, "A machine learning approach for predicting DDoS traffic in software defined networks," in *2018 International Conference on Information Technology (ICIT)*, pp. 199–203, Bhubaneswar, India, December 2018.
- [16] M. S. Elsayed, N. -A. Le-Khac, S. Dev, and A. D. Jurcut, "DDoSNet: a deep-learning model for detecting network attacks," in *2020 IEEE 21st International Symposium on "A World of Wireless, Mobile and Multimedia Networks" (WoW-MoM)*, pp. 391–396, Cork, Ireland, 2020.
- [17] A. Sherstinsky, "Fundamentals of recurrent neural network (RNN) and long short-term memory (LSTM) network," *Physica D: Nonlinear Phenomena*, vol. 404, article 132306, 2020.
- [18] J. Jordan, "Autoencoders/," 2018, September 2021, <https://www.jeremyjordan.me/autoencoders/>.
- [19] "Ddos-2019.html University of New Brunswick - Canadian Institute for Cybersecurity September 2021, <https://www.unb.ca/cic/datasets/ddos-2019.html>.
- [20] X. Yuan, C. Li, and X. Li, "DeepDefense: identifying DDoS attack via deep learning," in *2017 IEEE International Conference on Smart Computing (SMARTCOMP)*, pp. 1–8, Hong Kong, China, May 2017.
- [21] M. Schuster and K. K. Paliwal, "Bidirectional recurrent neural networks," *IEEE Transactions on Signal Processing*, vol. 45, no. 11, pp. 2673–2681, 1997.
- [22] S. Hochreiter and J. Schmidhuber, "Long short-term memory," *Neural Computation*, vol. 9, no. 8, pp. 1735–1780, 1997.
- [23] J. Chung, C. Gulcehre, K. H. Cho, and Y. Bengio, "Empirical evaluation of gated recurrent neural networks on sequence modeling," 2014, <https://arxiv.org/abs/1412.3555>.
- [24] "ids.html University of New Brunswick - Canadian Institute for Cybersecurity September 2021, <https://www.unb.ca/cic/datasets/ids.html>.
- [25] C. Yinka-Banjo and O. A. Ugot, "A review of generative adversarial networks and its application in cybersecurity," *Artificial Intelligence Review*, vol. 53, no. 3, pp. 1721–1736, 2019.
- [26] A. Kurakin, G. Brain, I. Goodfellow, and S. Bengio, "Adversarial machine learning at scale," <https://arxiv.org/pdf/1611.01236.pdf>.
- [27] I. Goodfellow, P. McDaniel, and N. Papernot, "Making machine learning robust against adversarial inputs," *Communications of the ACM*, vol. 61, no. 7, pp. 56–66, 2018.
- [28] I. Goodfellow, J. Pouget-Abadie, M. Mirza et al., "Generative adversarial nets," 2014, <https://arxiv.org/pdf/1406.2661.pdf>.
- [29] Q. Yan, M. Wang, W. Huang, X. Luo, and F. R. Yu, "Automatically synthesizing DoS attack traces using generative adversarial networks," *International Journal of Machine Learning and Cybernetics*, vol. 10, no. 12, pp. 3387–3396, 2019.
- [30] J. Brownlee, "Convolutional-layers-for-deep-learning-neural-networks/," Machine Learning Mastery, 2020, September 2021, <https://machinelearningmastery.com/convolutional-layers-for-deep-learning-neural-networks/>.
- [31] I. Gulrajani, F. Ahmed, M. Arjovsky, V. Dumoulin, and A. Courville, "Improved training of Wasserstein GANs," <https://arxiv.org/pdf/1704.00028.pdf>.
- [32] "kddcup99.html," UCI, 1999, September 2021, <http://kdd.ics.uci.edu/databases/kddcup99/kddcup99.html>.
- [33] S. Choudhary and N. Kesswani, "Analysis of KDD-Cup'99, NSL-KDD and UNSW-NB15 datasets using deep learning in IoT," *Procedia Computer Science*, vol. 167, pp. 1561–1573, 2020.
- [34] J. Charlier, A. Singh, G. Ormazabal, R. State, and H. Schulzrinne, "SynGAN: towards generating synthetic network attacks using GANs," September 2021, <https://arxiv.org/pdf/1908.09899.pdf>.
- [35] "nsl.html University of New Brunswick - Canadian Institute for Cybersecurity September 2021, <https://www.unb.ca/cic/datasets/nsl.html>.
- [36] R. Chauhan and S. Shah Heydari, "Polymorphic adversarial DDoS attack on IDS using GAN," in *2020 International Symposium on Networks, Computers and Communications (ISNCC)*, Montreal, QC, Canada, October 2020.
- [37] G. Gursun, M. Sensoy, and M. Kandemir, "On context-aware DDoS attacks using deep generative networks," in *2018 27th International Conference on Computer Communication and Networks (ICCCN)*, Hangzhou, China, 2018.
- [38] M. P. Novaes, L. F. Carvalho, J. Lloret, and M. L. Proença Jr., "Adversarial deep learning approach detection and defense against DDoS attacks in SDN environments," *Future Generation Computer Systems*, vol. 125, pp. 156–167, 2021.
- [39] "Zero-sum\_game Wikipedia September 2021, [https://en.wikipedia.org/wiki/Zero-sum\\_game](https://en.wikipedia.org/wiki/Zero-sum_game).
- [40] M. Arjovsky, S. Chintala, and L. Bottou, "Wasserstein GAN," <https://arxiv.org/pdf/1701.07875.pdf>.
- [41] J. Brownlee, "How-to-implement-wasserstein-loss-for-generative-adversarial-networks/," Machine Learning Mastery, 2019, September 2021, <https://machinelearningmastery.com/how-to-implement-wasserstein-loss-for-generative-adversarial-networks/>.
- [42] J. Brownlee, "Rectified-linear-activation-function-for-deep-learning-neural-networks/," Machine Learning Mastery, 2020, September 2021, <https://machinelearningmastery.com/rectified-linear-activation-function-for-deep-learning-neural-networks/>.
- [43] "Activations/Keras.io September 2021, <https://keras.io/api/layers/activations/>.
- [44] "Leaky-relu paperswithcode September 2021, <https://paperswithcode.com/method/leaky-relu>.
- [45] "Improved\_wgan.py GitHub September 2021, [https://github.com/keras-team/keras-contrib/blob/master/examples/improved\\_wgan.py](https://github.com/keras-team/keras-contrib/blob/master/examples/improved_wgan.py).

## Research Article

# Action of College Chinese Education and Information Fusion Teaching Based on the Background of Big Data

Qiujuan Qi<sup>1</sup> and Xiaoli Wang<sup>2</sup> 

<sup>1</sup>College of Humanities and Education, Xijing University, Xi'an, 710123 Shaanxi, China

<sup>2</sup>Modern Educational Technology Center, Mudanjiang Medical University, Mudanjiang, 157011 Heilongjiang, China

Correspondence should be addressed to Xiaoli Wang; wangxiaoli@mdjmu.edu.cn

Received 11 January 2022; Revised 26 January 2022; Accepted 14 February 2022; Published 10 March 2022

Academic Editor: Shalli Rani

Copyright © 2022 Qiujuan Qi and Xiaoli Wang. This is an open access article distributed under the Creative Commons Attribution License, which permits unrestricted use, distribution, and reproduction in any medium, provided the original work is properly cited.

In order to meet the needs of the development of the times and the cultivation of innovative talents, various countries have carried out a series of educational reforms. It seeks more diversified talent training methods through innovative education and teaching methods. With the development of science and technology and the diversification of information, the integration of multilevel, distributed, and massive information has become the development direction of various disciplines. Therefore, this research is based on the background of big data, exploring the way of university Chinese education and information fusion teaching under the education reform and helping students establish a systematic subject knowledge system. This article chooses two parallel classes of similar level as the experimental group and the control group. It analyzes the results of the four aspects of the students' ancient and modern language and writing analysis, college students' Chinese reading comprehension, college students' Chinese writing application, and college students' language expression and communication through test papers. The experimental results of this article show that the  $P$  values of these four aspects are all less than 0.05, indicating that the learning effect of the experimental group is higher than that of the control group.

## 1. Introduction

**1.1. Background.** With the rapid economic development, social technology has entered the public's field of vision, and artificial intelligence, robots, and big data are no longer just imagined [1, 2]. They are gradually changing people's living standards, improving people's work efficiency, and leading the advancement of mankind. However, these have not been vigorously promoted in education, especially in the classroom teaching of college Chinese; some teachers still have the original teaching mode. If things go on like this, students who are curious about social information and knowledge will gradually lose their interest in learning because of this traditional teaching model. Therefore, based on the background of the big data era, Chinese teaching should be combined with information fusion to realize the high efficiency of Chinese teaching. However, there are not many related studies on the application of information fusion technology in the education industry

through the search of relevant materials. Therefore, it provides a reference for future related research in school education and social training industry.

**1.2. Significance.** With the application of new technologies such as big data, cloud computing, and artificial intelligence, the education industry has ushered in unprecedented challenges and opportunities. The traditional education industry is gradually moving towards informatization, and various teaching applications have emerged. However, how to combine subject teaching and information fusion based on the background of various teaching applications, so as to obtain more efficient teaching, still faces many problems. This shows that the research in this article has practical significance.

**1.3. Related Work.** With the development and popularization of social informatization, information fusion can exert an influence that cannot be underestimated in all walks of

life. In order to optimize the fault diagnosis of the Rocket Hydraulic Drive Servo System (HDSS), Liu et al. proposed an information fusion diagnosis method based on D-S evidence theory and BP neural network. Their research shows that the multisensor information fusion fault diagnosis method improves the reliability of HDSS [3]. The information fusion method of INS/GPS navigation system based on filtering technology is the current research hotspot. In order to improve the accuracy of navigation information, Liu et al. proposed a navigation technology based on adaptive Kalman filter with attenuation factor to suppress noise. The algorithm continuously updates the measurement noise variance and processes the noise variance of the system by collecting estimated and measured values, which can suppress white noise. According to the test results, the accuracy of their proposed algorithm is 20% higher than that of the traditional adaptive Kalman filter [4]. In the classification of hyperspectral image (HSI), it can use the combination of spectral information and spatial information to improve the classification performance. In order to better characterize the variability of spatial features at different scales, Hong et al. proposed a new framework called multiscale spatial information fusion (MSIF). MSIF consists of three parts: multiscale spatial information extraction, local one-dimensional embedding (L1-DE), and information fusion. First, they use spatial filters of different scales to extract multiscale spatial information. Then, they used L1-DE to map the spectral information and spatial information of different scales into one-dimensional space. Finally, they use the obtained one-dimensional coordinates to mark the unlabeled spatial neighbors of the labeled sample [5]. Shibo et al. proposed a dangerous cargo container monitoring system based on multisensor. In order to improve the accuracy of monitoring, multiple sensors will be used inside the dangerous goods container. Shibo et al. proposed a multisensor information fusion solution for dangerous cargo container monitoring. They elaborated on information preprocessing, homogeneous sensor fusion algorithm, and information fusion based on BP neural network. The application of multisensor in the field of container monitoring has certain novelty [6]. At the same time, the realization of diversified courses and information management in the education industry has become a concern of scholars. In his research, Shim revealed the shortcomings of Chinese classics as a liberal art through its transformation process and present state and proposed ways to improve it. He suggested that the curricula of Chinese studies should be developed in the direction of providing the overall foundation of Oriental studies, rather than carefully reading the original works. Textbooks should also take into account the specific conditions of students for detailed analysis and choose texts based on a diverse society. In addition, it is necessary to set up courses that consider the differences of students' abilities [7]. Taking Russia as an example, Albekov et al. study the factors that promote the effectiveness of university education. They determined the management point of view to maximize the effectiveness of university education. Their research shows that the most important factor in the effectiveness of university education is the number of universities

and the number of faculty and staff. The viewpoint of maximizing the efficiency of university education is related to human capital management [8]. In summary, it cannot be seen that in recent years, information fusion has not only been studied in the aviation field but has also very good application prospects in the civil field. With the advancement of social science and technology, information fusion technology has become a new trend in research in various countries. But there are not many practical studies on education. Therefore, in order to further promote the development of education, the practical research of subject education and information fusion teaching brooks no delay.

*1.4. Innovation.* Driven by the needs of military technology, automation, and intelligence, information fusion has received extensive attention from academia and industry, and many new theories and methods have been made in recent years [9–11]. However, in recent years, most of the research on college Chinese education has remained at the theoretical level. Therefore, this article adopts action research, starting from practice, and tries to explore the teaching mode of combining college Chinese education and information fusion. It seeks to improve the teaching efficiency of Chinese, so that students have better growth.

## 2. College Chinese Education and Related Theories of Information Fusion

*2.1. Big Data Background.* With the advent of the era of big data, all walks of life in society are affected by big data. The traditional teaching mode of colleges and universities has also been greatly impacted by big data. Based on the arrival of new teaching reforms based on big data platforms, we can reform traditional courses [12, 13]. Colleges and universities from various countries have built big data platforms, such as China's Youmu course. The platform categorizes and organizes the massive information of a large number of users by building different data models and abstracts different user images. This can not only push the most suitable high-quality teaching resources for individuals but also optimize and organize teaching resources to promote more humane and better quality teaching resources, which can also set a warning line for the user's image. It conducts specific observations on specific students and provides real-time guidance. This reduces the emergence of problematic students and promotes the healthy development of students in the process of growth. For example, under a big data platform such as Youmu class in a Chinese college, the teaching and research group of the school conducted a preliminary teaching reform attempt on the university Chinese course. It also compares the differences with the traditional teaching mode through the five links of preview, lecture, homework, extra-curricular tutoring, and testing [14].

*2.1.1. Preliminary Study of College Chinese.* In the course of learning the course, preview is a very important step. Each student can understand the difficulty of the knowledge points through the preview and then improve their learning efficiency. Teachers can also fully understand the level of

knowledge that students have now mastered in order to achieve the goal of high teaching effect. Therefore, a good preparation before class is the most important task before class. However, in the traditional teaching mode, teachers determine the focus and difficulty of teaching based on teaching experience and syllabus. In fact, this is not necessarily suitable, and it is easy to cause a huge gap between the classes taught by teachers with rich teaching experience and teachers who lack teaching experience [15]. However, under the big data platform, teachers can search for relevant teaching chapters in the Youmu course database in a more targeted way during the preview. They can also view the preview tasks and scores of different majors and different classes on the university language platform in recent years and then determine the focus and difficulty of the preview after sorting.

*2.1.2. The Teaching of University Language.* In traditional teaching, teachers mainly teach, and there is not much interaction between teachers and students [16]. Under the big data platform, the main focus is to improve the core quality of students, which is different from traditional teaching. Learning materials and learning tasks can be pushed to students online via mobile phones or classroom network devices [17–20]. The interaction between teachers and students in the classroom can clearly and intuitively introduce and teach the key points and difficulties to be taught in the classroom. It uses online resources to push knowledge points in the form of cartoons, etc., which can more stimulate students' enthusiasm and initiative in learning in the classroom.

*2.1.3. Homework in College Chinese.* Under the traditional teaching mode, the homework of college Chinese usually can only be small composition or essay practice, which is relatively simple and boring [21]. On the big data platform, teachers can arrange multiple choice questions, true or false questions, and interesting essay questions, which are richer and more interesting. And when the teacher finishes talking about a knowledge point, students can practice in class in time and train targeted on the platform based on past data. This enhances the core competence of students in college Chinese. On the big data platform, teachers can flexibly choose review questions and question types. This allows the left homework to cover the chapter knowledge points taught in the classroom. It can answer questions online and automatically mark papers; they can see the wrong questions of the students and find the places where the students' knowledge is not firmly grasped. This in turn can push the test questions in a targeted manner, so that students can consolidate the knowledge they have learned.

*2.1.4. Extracurricular Tutoring of College Chinese.* On the big data platform, teachers and students do not need to specifically arrange a time to meet; they can push the relevant learning materials of extracurricular tutoring online. Teachers online supervise students to study in a timely manner, complete the learning content, and expand the knowledge of the students. And through the continuous accumulation of relevant extracurricular tutoring materials

on the platform by teachers, it is more conducive to the construction of the university Chinese big data platform.

*2.2. Information Fusion Technology.* Information fusion technology is a technology that processes various information to meet the various needs of users. It is also called data fusion technology [10, 22, 23]. Multifeature attributes or the presence of multiple sensors perceives data. The actual work of information fusion technology is to obtain a description of the perceived object by eliminating the contradiction between various information. Therefore, it is also called multisource information fusion or multisensor information fusion [11, 24]. The process of multisensor information fusion is shown in Figure 1.

Redundant information is information repeated between sensors, while complementary information is external information sensed by sensors, which are independent of each other. Redundant information and complementary information are obtained by the multisource system through the data information of the sensor group [25–27]. The relationship between redundant information and complementary information is shown in Figure 2.

The sensor data has information redundancy in both time and space, that is, the continuity and consistency in time and the correlation of attributes in space. Based on this redundant information, there are temporal redundant information fusion methods and spatial redundant information fusion methods.

*2.2.1. Data-Level Information Fusion Algorithm Based on Time Dimension.* The data-level information fusion algorithm based on time dimension is mainly aimed at single sensor data, using redundant information in time for single-attribute time information fusion. It extracts redundant information in the time domain and frequency domain from the sensor data sequence in the window and establishes a mathematical model of attribute changes. According to the measurement data of the sensor, the optimal estimation function of the attribute change is given, and the fusion result is obtained [28, 29].

Frequency domain feature extraction is a data sequence composed of  $N$  data collected in time window  $[t_i, t_{i+1}]$ , and this data sequence usually contains important features of the measured attribute. It uses the frequency, amplitude, phase, and other parameters of each harmonic component in the signal obtained by frequency domain analysis to realize the description of the measured attribute characteristics.

For the data sequence  $\{x|n=0, 1, 2, \dots, N-1\}$  in the window, its discrete Fourier transform is

$$X(k) = \sum_{n=0}^{N-1} e^{-i(2\pi/N)nk} x(n), \quad k = 0, 1, 2, \dots, N-1. \quad (1)$$

The power spectrum estimation is defined as

$$S(\hat{\omega}) = \frac{1}{N} \left| \sum_{n=0}^{N-1} x_n e^{-j\omega n} \right|^2. \quad (2)$$

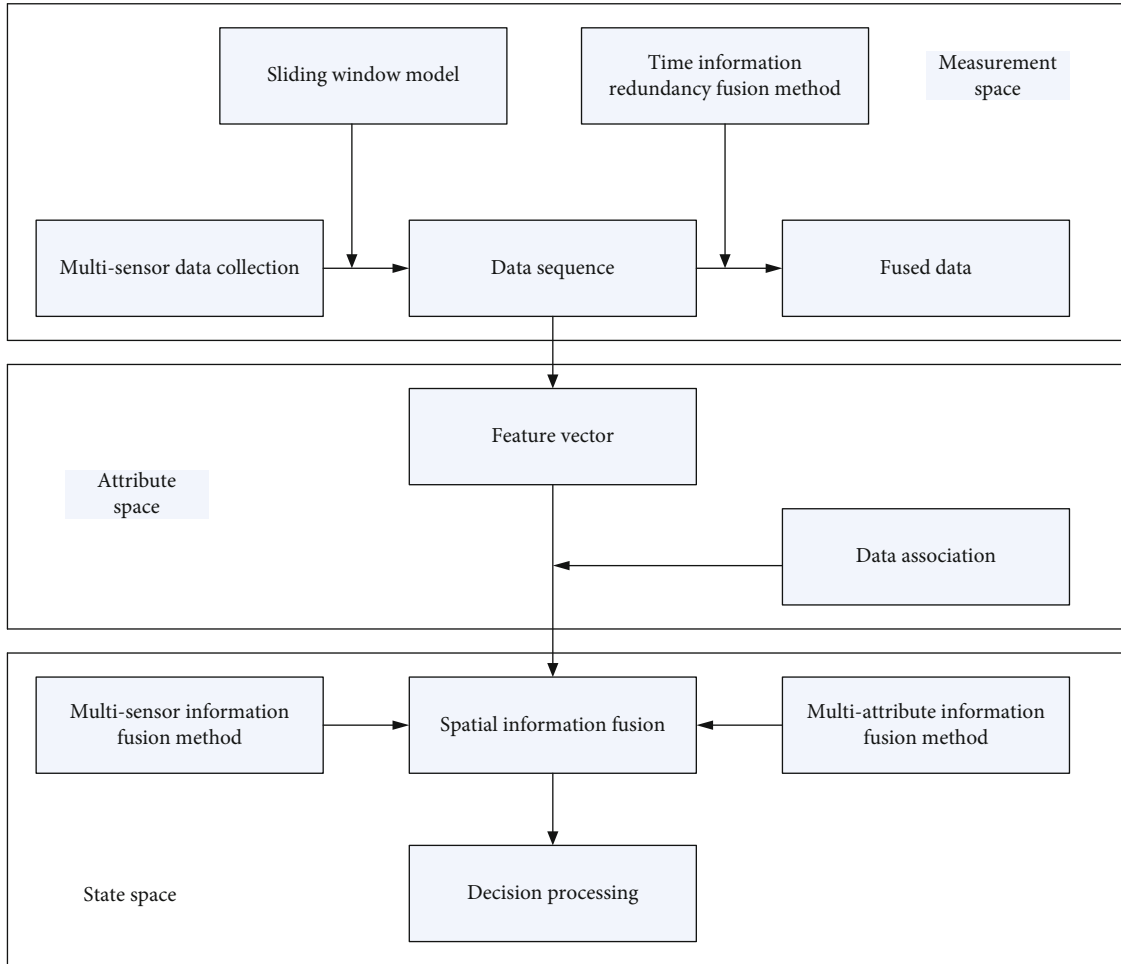


FIGURE 1: Multisensor information fusion process.

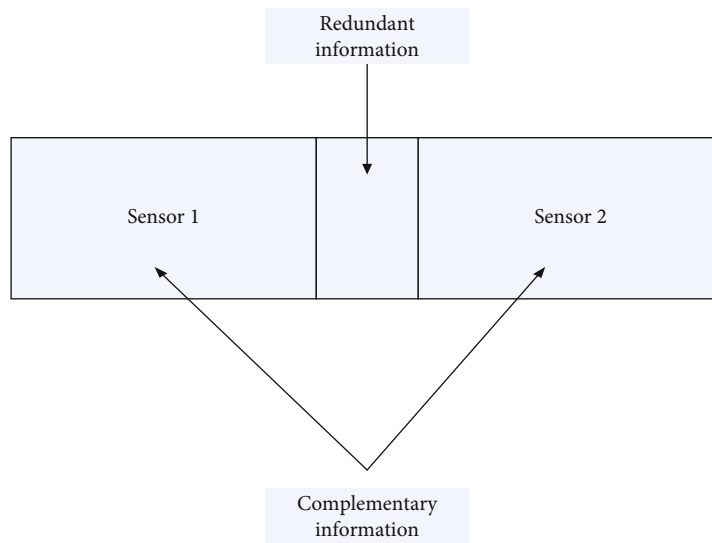


FIGURE 2: The relationship between redundant information and complementary information.

It can also be expressed as

$$S(\hat{\omega}) = \frac{1}{N} |X(\omega)|^2. \quad (3)$$

The signal is conserved in the process of transforming the signal from the time domain to the frequency domain, namely,

$$\sum_{n=0}^{N-1} |x_n|^2 = \sum_{k=0}^{N-1} |S(k)|^2. \quad (4)$$

Therefore,  $S_k(k=0, 1, 2 \dots N-1)$  can be regarded as an energy division of the original signal in the frequency domain space. In order to reduce the interference of noise to the frequency domain selection, this paper defines the power spectrum probability  $P_k$ .

$$P_k = \frac{S_k}{\sum_{k=1}^N S_k}. \quad (5)$$

The frequency domain whose power spectrum probability is less than a given threshold  $P_0$  is regarded as the noise corresponding spectrum, and its main frequency part is reserved. Therefore, the dominant frequency distribution  $\vec{f} = (f_0, f_2, \dots, f_i, \dots, f_{n-1})$  of the monitoring data signal is obtained, and this is used as the frequency domain distribution of  $f_i(x)$ , as shown in the following formula:

$$f_i(x) = \sum_{j=0}^{n-1} \left( a_{ij} \cos 2\pi f_j x + b_{ij} \sin 2\pi f_j x \right), \quad t_i \leq x \leq t_{i+1}. \quad (6)$$

where  $\vec{f}$  represents the main frequency distribution and  $a_{ij}$  and  $b_{ij}$  indicate amplitude.

From the above analysis, it can be seen that the vector composed of frequency domain distribution and frequency domain amplitude is used as the characteristic vector of the signal.

Extraction of the amplitude spectrum feature determines the amplitude in each frequency domain, and then, an estimate of  $f_i(x)$  can be obtained. This is shown in formula (7) to formula (10). Among them, it is assumed that the mean and variance of the known environmental noise are  $E(\sigma)$  and  $\sigma^2$ , respectively. Given the monitoring data  $F_i(t) = f_i(t) + \sigma_i(t)$ , assuming that the unbiased estimate of  $f_i(x)$  is  $f_i'(x)$ , then

$$F_i(t) = f_i'(t) + \sigma_i'(t) = f_i(t) + \sigma_i(t), \quad (7)$$

where  $\sigma_i'(t)$  is an estimate of  $\sigma_i(t)$ .

The difference between  $F_i(x)$  and  $f_i(x)$  is expected to be  $E(\sigma)$ , namely,

$$\sum_{j=0}^{N-1} [F_i(t_j) - f_i(t_j)] = E(\sigma). \quad (8)$$

The variance of the difference between  $F_i(x)$  and  $f_i(x)$  is  $\sigma^2$ :

$$\sum_{j=0}^{N-1} [F_i(t_j) - f_i(t_j)]^2 = \delta^2. \quad (9)$$

For amplitude constraints,

$$\sqrt{\alpha_{ij}^2 + \beta_{ij}^2} - \delta \leq \sqrt{a_{ij}^2 + b_{ij}^2} \leq \sqrt{\alpha_{ij}^2 + \beta_{ij}^2} + \delta. \quad (10)$$

From the above, the amplitudes  $\vec{a}$  and  $\vec{b}$  of at each frequency can be obtained, that is, the characteristic vector of the amplitude spectrum.

**2.2.2. Feature-Level Information Fusion Algorithm Based on Spatial Dimension.** Feature-level data fusion belongs to the middle-level fusion. It first extracts a set of characteristic information from the raw data collected by each sensor. It then uses the feature-level information fusion method to fuse each group of feature information. The feature-level fusion process is the mapping process from an  $n$ -dimensional measurement space to an  $m$ -dimensional attribute space [30, 31], as shown in Figure 3.

Feature-level attribute association fusion mainly includes three steps: feature vector selection, multisensor data association, and association fusion between attributes based on simple relationships [32].

The first point is the selection of feature vectors. The feature-level data fusion object is the feature vector. The requirement for the feature vector is that it can fully reflect the characteristics of the signal. And it has an objective compression rate and at the same time guarantees the loss of as little original information as possible. The eigenvector of the window signal expressed in the form of a complex number is shown in the following formula:

$$\vec{F}_f = \{\dots, 0, \dots, (a_{i0} + i \cdot b_{i0}), \dots, 0, \dots, (a_{im} + i \cdot b_{im}), \dots, 0, \dots\}, \quad 0 \leq m \leq n_f, \quad (11)$$

$$\vec{F}_g = \{\dots, 0, \dots, (\alpha_{i0} + i \cdot \beta_{i0}), \dots, 0, \dots, (\alpha_{ij} + i \cdot \beta_{ij}), \dots, 0, \dots\}, \quad 0 \leq j \leq n_g,$$

$$\vec{F}_h = \{\dots, 0, \dots, (\lambda_{i0} + i \cdot \gamma_{i0}), \dots, 0, \dots, (\lambda_{ik} + i \cdot \gamma_{ik}), \dots, 0, \dots\}, \quad 0 \leq k \leq n_h, \quad (12)$$

where  $(a_{im}, b_{im})$  represents the cosine and sine components at frequency  $f_m$  corresponding to the change in the frequency domain of the signal.

$a_{im} + i \cdot b_{im}$  is the plural form of  $(a_{im}, b_{im})$ .

The second point is multisensor data association. How to judge whether the data from different sensors represent the

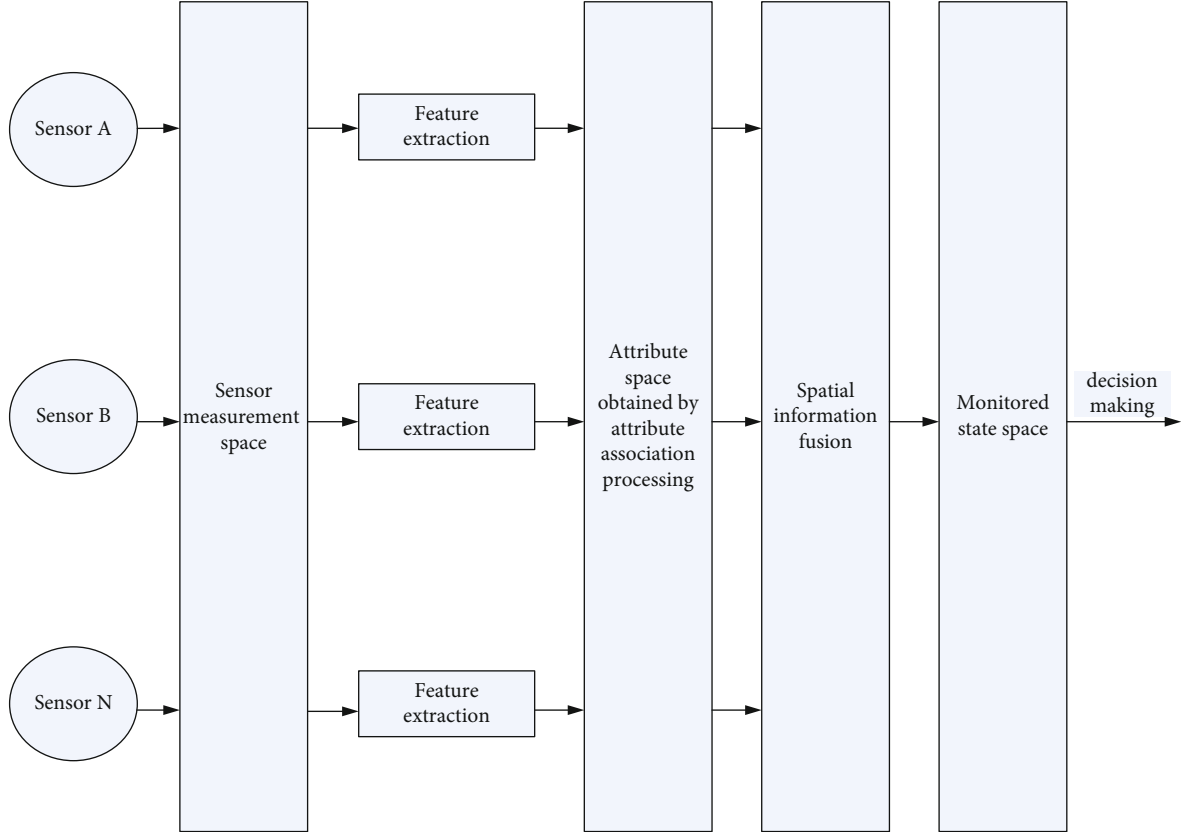


FIGURE 3: Feature-level information fusion process.

same target is the problem of data association. Therefore, the cosine value of the angle between feature vectors  $\vec{F}_1$  and  $\vec{F}_2$  can be used as a measure of the mutual support  $S_f$  of different sensors, namely,

$$S_f = \frac{\vec{F}_1 \cdot \vec{F}_2}{|\vec{F}_1| \times |\vec{F}_2|}. \quad (13)$$

When the cosine value reaches a certain threshold and can maintain long-term strong correlation, this means that the two sensors have a strong correlation and are used to measure the same attribute. This method can be used for the fusion of multiattribute information.

The third point is the fusion between attributes based on simple relationships. The main use of spatial information fusion is to use the interrelationships between attributes to merge information between attributes. Fusion based on simple relationships can be performed through linear relationships.

- (1) Linear relationship extraction. There is a simple linear relationship between sensor monitoring data, as shown in the following formula:

$$z = ax + by + c, \quad (14)$$

where  $x, y, z$  indicate measurement data of different attributes and  $a, b, c$  represent the coefficients corresponding to different attributes

The specific relationship of the three sensor data can be expressed as

$$f_i(x) = a \cdot g_i(x) + b \cdot h_i(x) + c. \quad (15)$$

After decomposition, the frequency amplitude of  $f_i(x)$  is the linear sum of the amplitudes of  $g_i(x)$  and  $h_i(x)$  at different frequency components. It is expressed in vector form as

$$\begin{aligned} \vec{a} &= a \cdot \vec{\alpha} + b \cdot \vec{\beta}, \\ \vec{b} &= a \cdot \vec{\beta} + b \cdot \vec{\gamma}. \end{aligned} \quad (16)$$

Then, the same linear relationship exists between the feature vectors:

$$\vec{F}_f = a \vec{F}_g + b \vec{F}_h. \quad (17)$$

When determining the relationship between different attributes, only the eigenvectors of the corresponding attributes need to be extracted to form the eigenvector matrix. If there is a linear correlation between the row vectors in the matrix, it means that there is a linear relationship



between the corresponding attributes. The state of another property can be estimated from the linear correlation and the state of the known property.

- (2) Linear relationship fusion. From the eigenvector matrix, different measurement data with linear relationship can be determined, and these data come from different sensors. There may be multiple sensors measuring the same attribute, or the attribute measured by a certain sensor is a linear combination of the measured attributes of several other sensors. As shown in Figure 4, the sensor information can be fused by the weighted fusion algorithm

Under the combined effect of monitoring attributexand noise (including the influence of sensors), the result is data  $x_1$  and  $x_2$ , if the noise satisfies a Gaussian distribution with a mean value of zero and a variance of  $\delta_1^2$  and  $\delta_2^2$ , respectively. As shown in Figure 5, the two distributions have a common area, indicating that the measurement data  $x_1$  and  $x_2$  have a supporting relationship.

$$\begin{cases} \alpha_1 = \frac{S_1}{(S_1 + S_2)}, \\ \alpha_2 = \frac{S_2}{(S_1 + S_2)}, \end{cases} \quad (18)$$

where  $\alpha_1$  and  $\alpha_2$  are expressed as the weight of the fusion of the two monitoring data. The obtained fusion estimation result is

$$x' = \alpha_1 x_1 + \alpha_2 x_2. \quad (19)$$

Similarly, for  $n$  sensors, the support and fusion weight of each monitoring data are

$$\begin{aligned} S_i &= \sum_{j \neq i}^n P_j(x_i), \\ \alpha_i &= \frac{S_i}{\sum_{j=1}^n S_j}. \end{aligned} \quad (20)$$

Then, the fusion estimation expression of  $n$  monitoring data is

$$x' = \sum_{i=1}^n \alpha_i x_i. \quad (21)$$

- (3) Multiattribute information fusion. Multiattribute fusion is based on the redundant information that exists between the measured attributes. It uses the method of information fusion to remove the uncertainty of measurement attributes. Multiattribute

information can be fused by means of multisensor information fusion

The measurement accuracy of  $n$  sensors is independent of each other, so the accuracy  $x'$  of attribute  $x$  can be expressed as

$$\delta_x^2 = \sum_{i=1}^n \alpha_i^2 \delta_i^2. \quad (22)$$

In the same way, the  $y$  measurement accuracy  $y'$  of the attribute is

$$\delta_y^2 = \sum_{j=1}^m \beta_j^2 \delta_j^2. \quad (23)$$

The equivalent sensor is a linear combination of attributes  $x$  and  $y$  after fusion, and its measurement accuracy is expressed as

$$\delta_z^2 = a^2 \delta_x^2 + b^2 \delta_y^2. \quad (24)$$

The multisensor information fusion method fully mines the associated information between attributes and uses this relationship for information fusion. It provides mutual support between attributes, reduces the uncertainty of information, and improves the accuracy of fusion.

**2.3. Effective Teaching Theory.** The evaluation index of the effectiveness of teaching refers to whether the student has a certain development in the learning process [33]. The effectiveness of the deep integration of information fusion technology and subject teaching refers to classroom teaching activities supported by information fusion technology. This enables students to benefit from their studies, improve their comprehensive abilities, and gain development. From the perspective of students, study time is the foundation, and students can obtain certain learning results through a period of study. It is not only the improvement of learning ability but also the improvement of learning efficiency. Similarly, the learning experience is also a key point that cannot be ignored. Students get a positive learning experience, and their learning efficiency will also increase, thereby promoting the improvement of learning effects. Therefore, in addition to learning time and learning results, learning experience is one of the goals of effective learning. From the perspective of teachers, most teachers teach based on their personal teaching experience or teaching process, and there is no teaching model that can be copied or referenced. Therefore, to model the teaching experience, teachers compile their own experience into a teaching model and think about the rationality of the model. In the teaching process, teachers think about which technologies should be used in each link of the model. This not only provides teachers with thinking points in teaching but also is a way to implement the combination of information fusion technology and subject teaching.

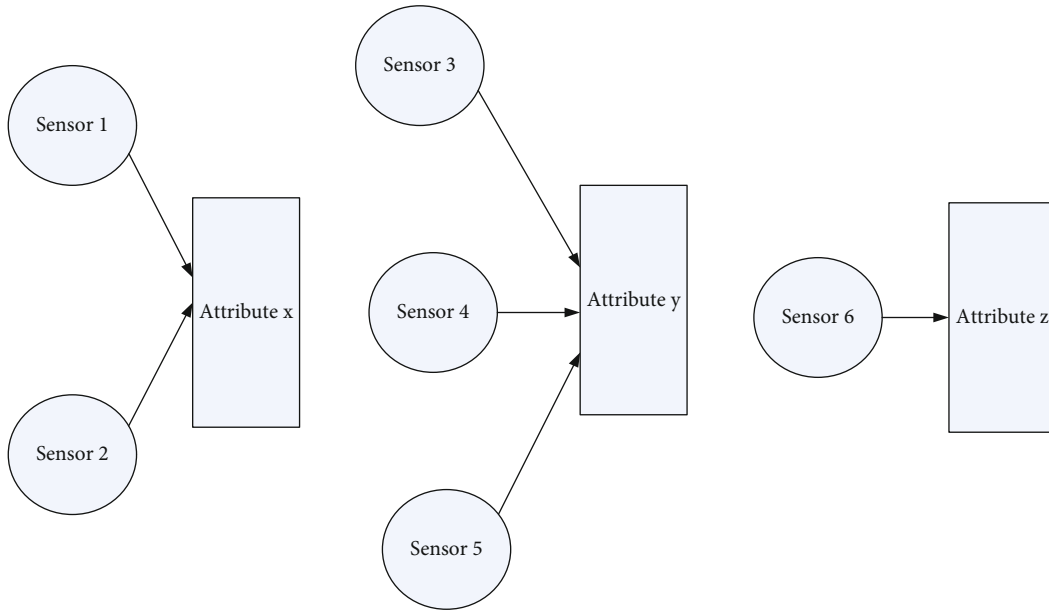


FIGURE 4: Multisensor system.

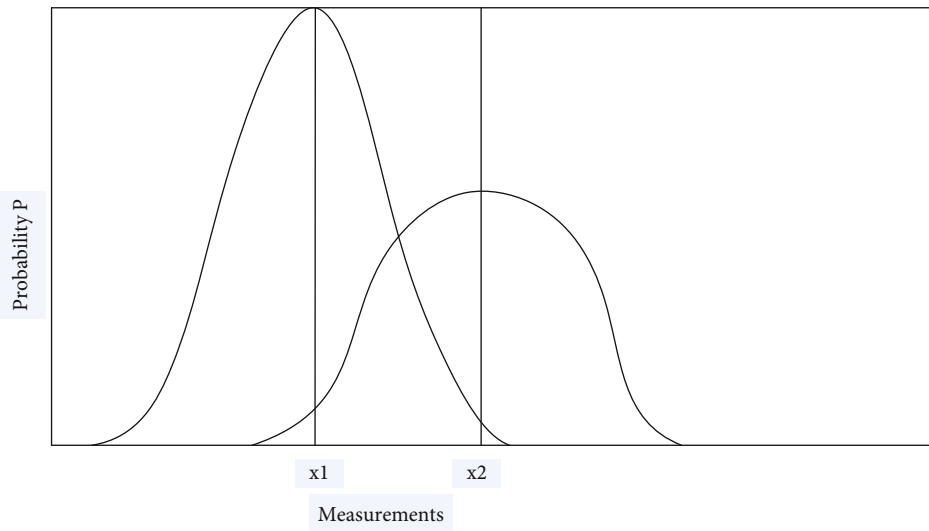


FIGURE 5: Probability distribution of measured values  $x_1$  and  $x_2$ .

### 3. Teaching Action Practice Based on Information Fusion in the Context of Big Data

In this experiment, two parallel classes with equivalent levels under natural teaching conditions were selected as the teaching objects. It adopts the traditional teaching mode and the teaching mode of university Chinese education and information fusion technology based on the background of big data. It teaches the same content through the overall teaching model and is completed by the same teacher. According to the teaching effect and the interview with teachers, the application effect of this teaching model is analyzed. The teaching mode of practical research in this article is shown in Figure 6.

This paper tests the four aspects of college students' mastery of ancient and modern language analysis, college students' Chinese reading comprehension, college students' Chinese writing application, and college students' language expression and communication effects. This article analyzes the learning effects of these four aspects under the two teaching modes through test paper testing. The test papers were distributed in the experimental group and the control group, and 70 copies were distributed in these four areas, and 70 copies were recovered. The experimental result data were all performed on the computer with SPSS statistical analysis software for independent sample  $T$  test.

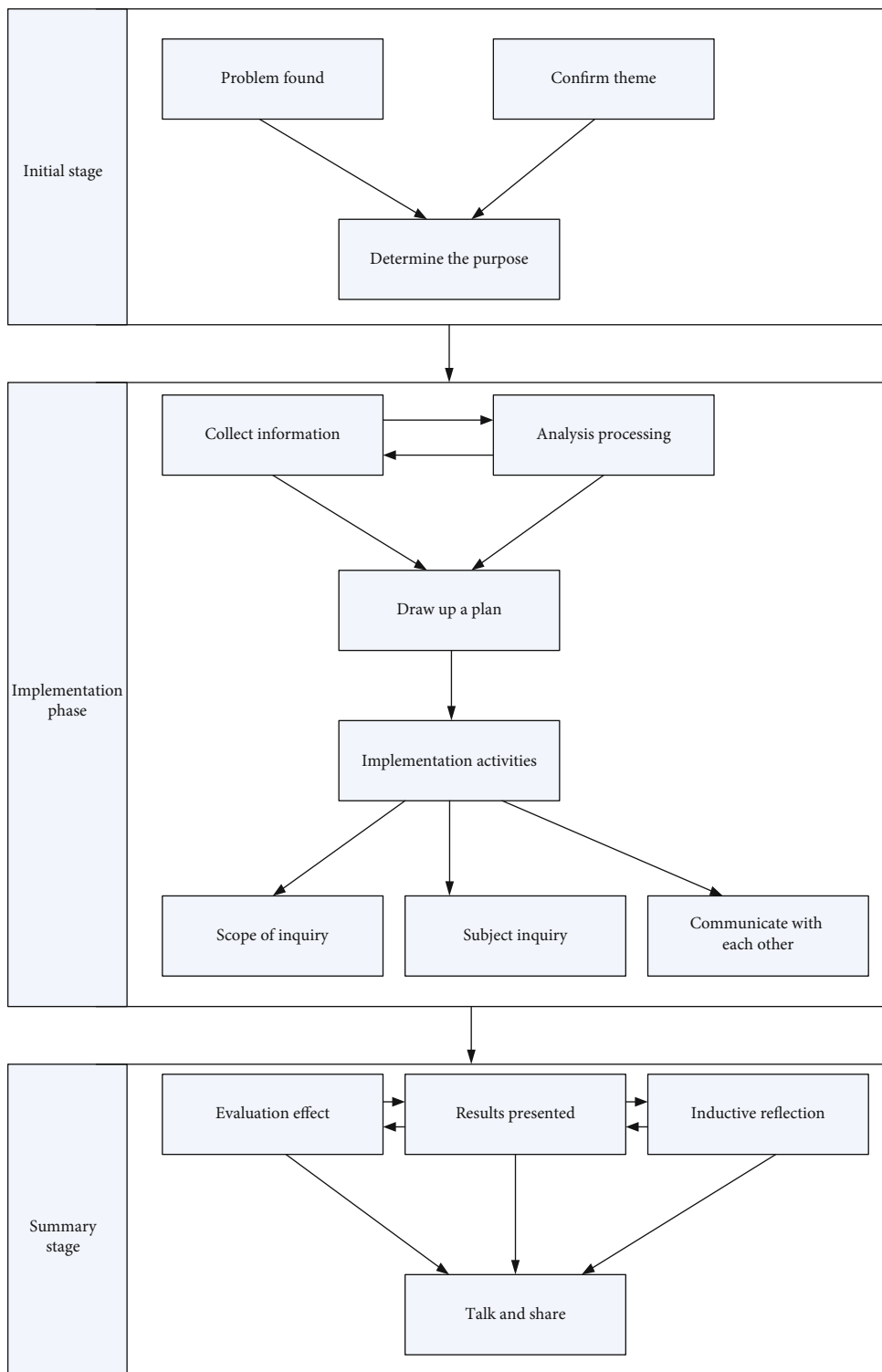


FIGURE 6: The teaching mode of college Chinese education and information fusion technology based on the background of big data.

### 3.1. The Effect of Students' Chinese Learning

- (1) The effect of college students on the analysis and mastery of ancient and modern languages

The students' mastery of the analysis of contemporary ancient languages and characters is obtained through the test paper, and the content of the test paper is mainly based on the words and words in the course they have learned. It is to analyze the students' understanding of words and the effect of using them under the two teaching modes through test paper tests. The analysis result is shown in Figure 7.

It can be seen from Figure 7 that the average teaching effect of the experimental group is 19.4222. The control group was significantly lower, with an average value of only 11.4000. Through further independent sample  $T$  test, the  $P$  value is 0.043 less than 0.05, which is significant. This shows that the performance results of the two teaching modes are significantly different. From this point of view, the learning effect of the experimental group was significantly higher than that of the control group. The sample  $T$  test of the pretest and posttest ancient and modern language analysis mastery of the experimental group is shown in Table 1.

- (2) The effect of college students' Chinese reading comprehension

Similarly, it learns about students' reading comprehension through examination paper tests. It chooses to take the extra-curricular reading that is similar to the school teaching content as the test content. The main analysis is shown in Figure 8.

As shown in Figure 8, it is obvious that the mean value of 31.3000 in the control group is lower than the mean value of 41.4222 in the experimental group through the comparison of the mean values of teaching effects. It can be explained that the average performance of the experimental group is higher than that of the control group. Through further independent sample  $T$  test on the teaching effect values of the two groups, the  $P$  value is 0.002, which is significant. Therefore, from the perspective of learning effects, the experimental group is higher than the control group. The sample  $T$  test of the pretest and posttest reading comprehension of the experimental group is shown in Table 2.

- (3) The effect of college students' Chinese writing application

Through the test of writing training, the effect of improving students' writing ability under the two teaching modes is tested. The data analysis is shown in Figure 9.

It can be found from Figure 9 that the standard deviation of the experimental group is smaller than that of the control group, indicating that the performance fluctuation range of the experimental group is smaller than that of the control group. Through further testing of the teaching effect values of the two groups, the  $P$  value is 0.016 less than 0.05, and the conclusion is significant. It can be seen from the effect of Chinese writing application that the learning effect of the experimental group is higher than that of the control

group. The sample  $T$  test of the pretest and posttest writing application in the experimental group is shown in Table 3.

- (4) The effect of college students' language expression and communication

It tests students' language expression ability by setting specific communication situations for the experimental group and the control group. The experimental results are shown in Figure 10.

Through independent sample  $T$  test,  $P$  value 0.029 is less than 0.05, and the conclusion is significant. This shows that the results of the two groups are significantly different. It is not difficult to see from Figure 10 that the mean value of the experimental group is higher than that of the control group, and the standard deviation is also smaller than that of the control group. This shows that the average performance of the experimental group is not only higher than that of the control group, but also the performance fluctuation range is small and relatively stable. The sample  $T$  test of the pretest and posttest language expression and communication of the experimental group is shown in Table 4.

3.2. *The Effect of Teacher Teaching.* After the teaching practice is over, this article discusses the teacher's feelings and views on the teaching model through interviews with teachers, and there are three main points.

First, teachers believe that the greatest advantage of this teaching model is that the initiative in the classroom is in the hands of students, and students are more willing to express themselves. This not only exercises students' language skills but also gives them room for independent thinking. In the teaching process, students are very motivated. Students are willing to participate in the classroom and express their ideas more directly. This not only allows them to have a healthy learning environment in their studies but also allows teachers to understand the situation of students, which is more conducive to teachers' targeted teaching.

Second, this teaching model brings a positive learning atmosphere, and students are more willing to communicate. Students with better grades can actively communicate their study habits and their own understanding of knowledge, while students with lower levels can encourage them to show more by expressing their opinions. Students learn from each other and promote each other. In this teaching mode, a very good growth environment has been created.

Thirdly, the teachers provided some suggestions worth considering for the teaching model. Teachers believe that the combination of university Chinese education and information fusion technology will not only help students' enthusiasm for learning but also make students more willing to communicate in such a good atmosphere. This will improve the ability of information integration and reflect on their own shortcomings, so as to promote the healthy growth of students in ideological and political.

## 4. Discussion

This paper conducts a practical research on college Chinese education and information fusion teaching action based on

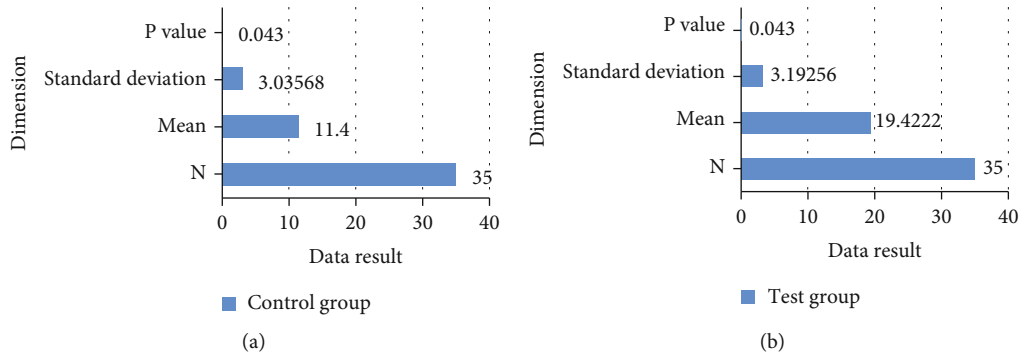


FIGURE 7: Independent sample  $T$  test of college students' mastery of ancient and modern language and character analysis: (a) independent sample  $T$  test of the control group; (b) independent sample  $T$  test of the experimental group.

TABLE 1: Pretest and posttest of the experimental group  $T$  test.

	Dimension	Category	Mean	Standard deviation	$t$	$P$ value	Conclusion
The mastery of ancient and modern language analysis	Word sound	Pretest	3.5300	1.27436	-6.767	0.001	Significant
		Posttest	6.2056	1.16523			
	Font	Pretest	6.0000	1.24623	-2.045	0.003	Significant
		Posttest	7.0000	1.06572			
	Word meaning	Pretest	4.0722	0.10369	-4.540	0.001	Significant
		Posttest	5.0400	0.08965			

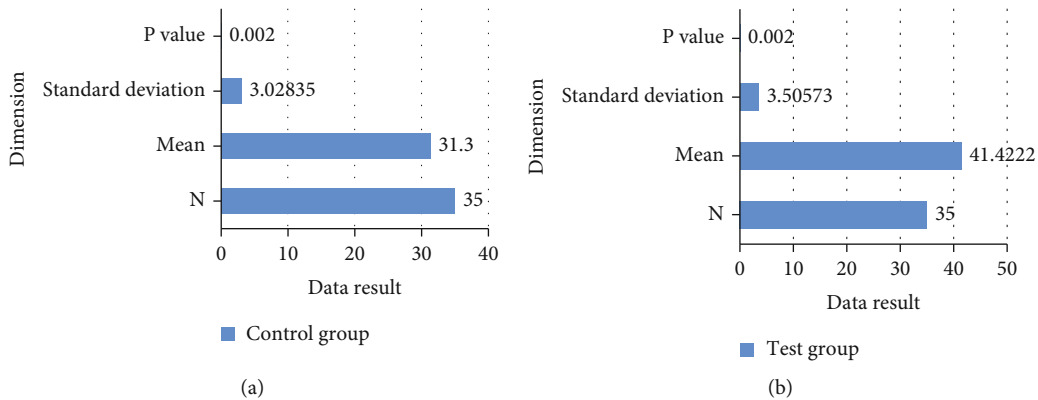


FIGURE 8: Independent sample  $T$  test of the effect of college students' Chinese reading comprehension: (a) independent sample  $T$  test of the control group; (b) independent sample  $T$  test of the experimental group.

TABLE 2: Sample  $T$  test of reading comprehension in the pretest and posttest of the experimental group.

	Dimension	Category	Mean	Standard deviation	$t$	$P$ value	Conclusion
	Read the article aloud	Pretest	4.0400	1.17072	-1.762	0.007	Significant
		Posttest	5.0556	0.78652			
	Overall perception	Pretest	4.3400	1.28068	-2.277	0.002	Significant
		Posttest	5.4400	1.10207			
Reading comprehension	Integrate information	Pretest	4.0600	1.18208	-4.087	0.001	Significant
		Posttest	5.6400	1.10480			
	Appreciation and evaluation	Pretest	4.3556	1.47511	-4.512	0.001	Significant
		Posttest	6.1222	1.00872			
	Form an explanation	Pretest	5.1222	0.61682	-2.285	0.002	Significant
		Posttest	6.0422	1.26808			

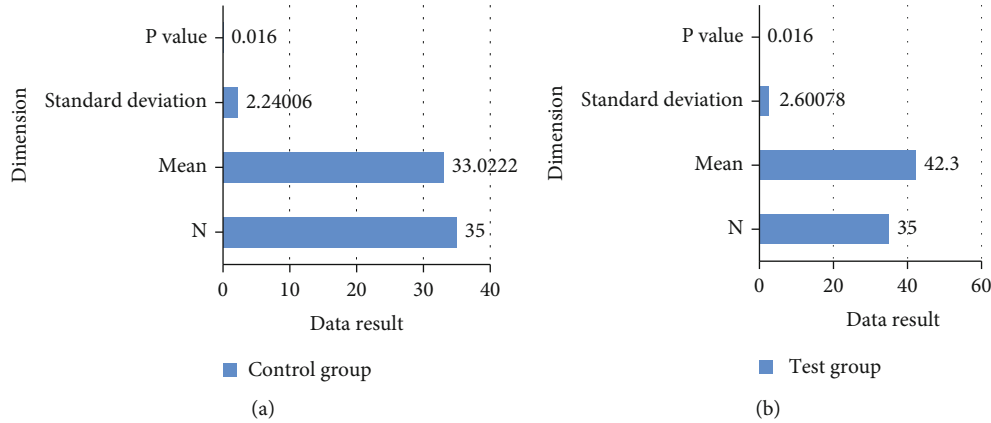


FIGURE 9: Independent sample *T* test of the application effect of college students' Chinese writing: (a) independent sample *T* test of the control group; (b) independent sample *T* test of the experimental group.

TABLE 3: Sample *T* test of the writing application of the pretest and posttest in the experimental group.

	Dimension	Category	Mean	Standard deviation	<i>t</i>	<i>P</i> value	Conclusion
Writing application	Examining questions accurately	Pretest	4.2722	1.02015	-3.236	0.001	Significant
		Posttest	5.3722	0.83104			
	Appropriate selection	Pretest	4.5400	0.63341	-5.800	0.001	Significant
		Posttest	6.2400	1.10764			
	Language expression	Pretest	4.8556	1.58032	-1.716	0.007	Significant
		Posttest	6.0556	1.44438			
	Rigorous structure	Pretest	5.0722	1.50065	-1.561	0.011	Significant
		Posttest	6.3222	1.42430			
Writing norms	Pretest	5.2722	1.44632	-2.180	0.002	Significant	
	Posttest	6.5722	1.08142				

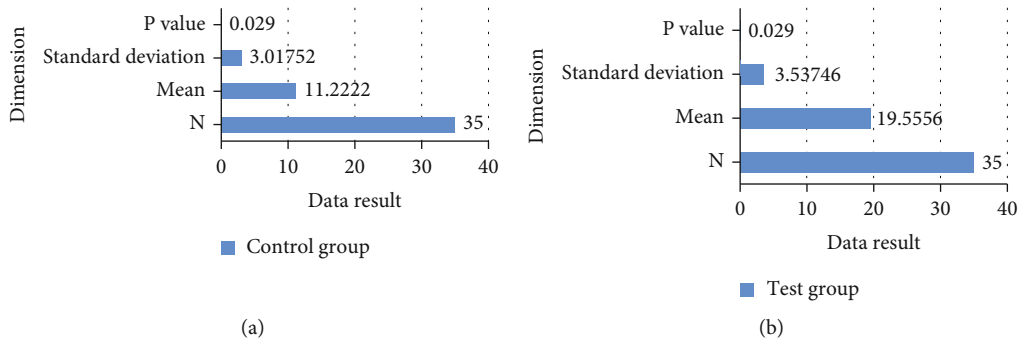


FIGURE 10: Independent sample *T* test of the effect of college students' language expression and communication: (a) independent sample *T* test of the control group; (b) independent sample *T* test of the experimental group.

TABLE 4: Sample *T* test of language expression and communication in the pretest and posttest of the experimental group.

	Dimension	Category	Mean	Standard deviation	<i>t</i>	<i>P</i> value	Conclusion
Verbal communication	Concise	Pretest	3.0722	1.74158	-5.560	0.001	Significant
		Posttest	4.7222	0.83878			
	Coherent	Pretest	6.1056	1.21306	-2.042	0.004	Significant
		Posttest	7.1000	1.22538			
	Decent	Pretest	4.8000	1.22410	-1.701	0.008	Significant
		Posttest	5.6400	0.87806			

the background of big data through test paper testing. From the data analysis results, the four aspects of the data show that the results are relatively good. With the support of information fusion technology in the analysis of ancient and modern languages and characters, students have a better understanding of language and characters. This can communicate smoothly with people at work, with smooth sentences and clear expression. This will be a very good help for students after entering the society. In terms of language reading comprehension, this is undoubtedly the idea to help students understand the article. Through abstract thinking and reasoning judgment, the realization of the mastery of the subject of the article will be very helpful to cultivate students' thinking activities. In the writing application part, in addition to cultivating students' ability in language understanding, students also need to cultivate clear thinking and rigorous structure. Therefore, after passing the writing training, students gradually master the logic and skills of writing. In terms of expression and communication, the use of language is not only in writing but also in daily life. Through the setting of the language situation in the classroom, it not only exercises the students' language expression ability but also makes them feel the importance of proper, concise, and accurate language in daily life, so as to reflect on their own shortcomings, point out, and improve themselves in a targeted manner.

## 5. Conclusion

This article is based on the action research of college Chinese education and information fusion teaching under the background of big data. Through examination papers, it conducted action research on the effects of ancient and modern language analysis, college students' Chinese reading comprehension, college students' Chinese writing application, and college students' language expression and communication. In this paper, an independent sample  $T$  test was performed on the experimental results of the experimental group before and after the test. From the performance of students, the results of the experimental group's performance before the test need to be strengthened. In terms of parsing ancient and modern languages, students will not actively communicate, and the learning method is mainly based on classroom explanations. Most students do not have a good understanding and use of words, and in terms of reading comprehension, students cannot successfully complete the course content and analyze the corresponding themes. In terms of writing application, some students are not proficient in the application of similar sentence patterns or writing techniques and description methods. The expression communication part is better for simple daily communication, but the expression of subjective issues needs to be strengthened. After the action research, students will express their opinions more enthusiastically and engage in communication with their classmates. Through communication with each other, they learned how to learn more efficiently. Students understand their own shortcomings, understand that they have many areas for improvement, and are more willing to explore with classmates to find solutions. This

shows that college Chinese education and information fusion teaching make the content of Chinese teaching more vivid and diversified. From the perspective of students' learning effects, this teaching model has a certain effect.

This research has achieved some results. However, due to the limited research time and ability of the researchers, this article still has many shortcomings. The premise of this teaching mode is that teachers have the ability to make topics and information literacy, so that they can deal with various problems in the teaching process. At the same time, students also need to have the corresponding abilities, such as concisely and clearly explain their own problems and directly address the doubts in the relevant teaching content. This prevents teachers from affecting the teaching process in order to solve the problem of students with different levels of information. Therefore, before conducting college Chinese education and information fusion teaching, it is necessary to conduct curriculum training on exploration and exchange of relevant topics for teachers and students. There are many teaching courses and limited time. Teachers need to spend more time to guide students to build knowledge through communication and learning. In the future teaching, what still needs to be explored and considered is how to make the language ability of college students in all grades more systematic. It needs to ensure that the ability goals of different grades form a complete system that is not single but is leveled by difficulty.

## Data Availability

The data that support the findings of this study are available from the corresponding author upon reasonable request.

## Conflicts of Interest

The authors declared no potential conflicts of interest with respect to the research, authorship, and/or publication of this article.

## Acknowledgments

This work was supported by Heilongjiang Province Higher Education Teaching Reform Project: Research on image report information extraction and association method based on deep learning.

## References

- [1] L. Qiao, Y. Li, D. Chen, S. Serikawa, M. Guizani, and Z. Lv, "A survey on 5G/6G, AI, and robotics," *Computers & Electrical Engineering*, vol. 95, article 107372, 2021.
- [2] Q. Wang and P. Lu, "Research on application of artificial intelligence in computer network technology," *International Journal of Pattern Recognition and Artificial Intelligence*, vol. 33, no. 5, article 1959015, 2019.
- [3] B. J. Liu, Q. W. Yang, X. Wu, S. D. Fang, and F. Guo, "Application of multi-sensor information fusion in the fault diagnosis of hydraulic system," *International Journal of Plant Engineering & Management*, vol. 22, no. 1, pp. 12–20, 2017.

- [4] Y. Liu, X. Fan, L. Chen et al., "An innovative information fusion method with adaptive Kalman filter for integrated INS/GPS navigation of autonomous vehicles," *Mechanical Systems and Signal Processing*, vol. 100, pp. 605–616, 2018.
- [5] L. Hong, Y. Song, and C. Chen, "Hyperspectral image classification based on multiscale spatial information fusion," *IEEE Transactions on Geoscience & Remote Sensing*, vol. 55, no. 9, pp. 5302–5312, 2017.
- [6] X. Shibo, S. Zhang, and W. Cao, "Study on the multi-sensors monitoring and information fusion technology of dangerous cargo container," *AIP Conference Proceedings*, vol. 1890, article 040077, 2017.
- [7] H.-n. Shim, "Suggestion for university general classical Chinese education - focused on Chung-Ang University's case," *The Society for Korean Language & Literary Research*, vol. 45, no. 1, pp. 347–368, 2017.
- [8] A. Albekov, T. Romanova, N. Vovchenko, and T. Epifanova, "Study of factors which facilitate increase of effectiveness of university education," *International Journal of Educational Management*, vol. 31, no. 1, pp. 12–20, 2017.
- [9] L. Peng, L. Bo, Z. Wen, Z. Li, and K. Li, "Predicting drug–target interactions with multi-information fusion," *IEEE Journal of Biomedical & Health Informatics*, vol. 21, no. 2, pp. 561–572, 2017.
- [10] B. S. Chandra, C. S. Sastry, and S. Jana, "Robust heartbeat detection from multimodal data via CNN-based generalizable information fusion," *IEEE Transactions on Biomedical Engineering*, vol. 66, no. 3, pp. 710–717, 2019.
- [11] F. Xiao, "Multi-sensor data fusion based on the belief divergence measure of evidences and the belief entropy," *Information Fusion*, vol. 46, pp. 23–32, 2019.
- [12] J. Aikat, T. M. Carsey, K. Fecho et al., "Scientific training in the era of big data: a new pedagogy for graduate education," *Big Data*, vol. 5, no. 1, pp. 12–18, 2017.
- [13] R. Tam, K. L. Beck, M. M. Manore, J. Gifford, V. M. Flood, and H. O'Connor, "Effectiveness of education interventions designed to improve nutrition knowledge in athletes: a systematic review," *Sports Medicine*, vol. 49, no. 3, pp. 1769–1786, 2019.
- [14] R. Cox, "Improvements in college teaching in the United Kingdom comparative approaches to higher education: curriculum, teaching and innovations in an age of financial difficulties: reports of the Hiroshima/OECD meetings of experts: part 2: curriculum and teach," *American Economic Review*, vol. 107, no. 10, pp. 79–87, 2017.
- [15] B. Burns, B. Mason, and K. Armington, "Role of education and training programs in the commercialization and diffusion of solar energy technologies," *Journal of Food Science*, vol. 44, no. 5, pp. 1280–1284, 2018.
- [16] U. D. Oviedo, "Discussion forums: tool to increase learning in higher education," *Internet & Higher Education*, vol. 12, no. 1, pp. 7–13, 2019.
- [17] J. W. Gray, "Bi-polar: college education and loans to small businesses headed by black females," *The Review of Black Political Economy*, vol. 39, no. 3, pp. 361–371, 2012.
- [18] X. Li, H. Liu, W. Wang, Y. Zheng, H. Lv, and Z. Lv, "Big data analysis of the internet of things in the digital twins of smart city based on deep learning," *Future Generation Computer Systems*, vol. 128, pp. 167–177, 2021.
- [19] Z. Lv, R. Lou, J. Li, A. K. Singh, and H. Song, "Big data analytics for 6G-enabled massive Internet of Things," *IEEE Internet of Things Journal*, vol. 8, no. 7, pp. 5350–5359, 2021.
- [20] M. Lee, L. Mesicek, and K. Bae, "AI advisor platform for disaster response based on big data," *Concurrency and Computation-Practice & Experience*, no. article e6215, 2021.
- [21] M. Scaperlanda, A. Mary, and Martha, "Putting first things first in a college education," *University of St. Thomas Law Journal*, vol. 15, no. 2, pp. 5–5, 2019.
- [22] S. V. B. Prasath, "Image denoising by anisotropic diffusion with inter-scale information fusion," *Pattern Recognition and Image Analysis*, vol. 27, no. 4, pp. 748–753, 2017.
- [23] Z. Lv and H. Song, "Trust mechanism of feedback trust weight in multimedia network," *ACM Transactions on Multimedia Computing, Communications, and Applications*, vol. 17, no. 4, 2021.
- [24] Z. Yu, L. Chang, and B. Qian, "A belief-rule-based model for information fusion with insufficient multi-sensor data and domain knowledge using evolutionary algorithms with operator recommendations," *Soft Computing*, vol. 23, no. 13, pp. 5129–5142, 2019.
- [25] C. Chahine, C. Vachier-Lagorre, Y. Chenoune, R. el Berbari, Z. el Fawal, and E. Petit, "Information fusion for unsupervised image segmentation using stochastic watershed and Hessian matrix," *IET Image Processing*, vol. 12, no. 4, pp. 525–531, 2018.
- [26] M. Adil, H. Song, J. Ali et al., "EnhancedAODV: a robust three phase priority-based traffic load balancing scheme for Internet of Things," *IEEE Internet of Things Journal*, 2021.
- [27] I. K. Osamh and G. M. Abdulsahib, "Energy efficient routing and reliable data transmission protocol in WSN," *International Journal of Advances in Soft Computing and its Application*, vol. 12, no. 3, pp. 45–53, 2020.
- [28] S. Li, H. Ma, T. Saha, and G. Wu, "Bayesian information fusion for probabilistic health index of power transformer," *Iet Generation Transmission & Distribution*, vol. 12, no. 2, pp. 279–287, 2018.
- [29] Z. Qi, Y. Yang, J. Ping et al., "A multi-fidelity information fusion metamodeling assisted laser beam welding process parameter optimization approach," *Advances in Engineering Software*, vol. 110, pp. 85–97, 2017.
- [30] H. C. Huang, "An evolutionary optimal fuzzy system with information fusion of heterogeneous distributed computing and polar-space dynamic model for online motion control of Swedish redundant robots," *IEEE Transactions on Industrial Electronics*, vol. 64, no. 2, pp. 1743–1750, 2017.
- [31] F. Groen, G. Pavlin, A. Winterboer, and V. Evers, "A hybrid approach to decision making and information fusion: combining humans and artificial agents," *Robotics and Autonomous Systems*, vol. 90, pp. 71–85, 2017.
- [32] F. Lei, X. Liu, Z. Li, Q. Dai, and S. Wang, "Multihop neighbor information fusion graph convolutional network for text classification," *Mathematical Problems in Engineering*, vol. 2021, Article ID 6665588, 9 pages, 2021.
- [33] H. Bardesi, A. Al-Mashaikhi, A. Basahel, and M. Yamin, "COVID-19 compliant and cost effective teaching model for King Abdulaziz University," *International Journal of Information Technology*, vol. 13, no. 4, pp. 1343–1356, 2021.



## Research Article

# Optimal Design of Intelligent Control System in the Communication Room Based on Artificial Intelligence

**Benkun Yao** <sup>1</sup>, **Rajnish Kler** <sup>2</sup>, **Sarfraz Fayaz Khan** <sup>3</sup>, **Gourav Bansal** <sup>4</sup>,  
**Ihtiram Raza Khan** <sup>5</sup> and **Bhupesh Kumar Singh** <sup>6</sup>

<sup>1</sup>Hangzhou Polytechnic Department, Institute of Urban Construction, Zhejiang Hangzhou 311402, China

<sup>2</sup>Motilal Nehru College (Evening), University of Delhi, Delhi, India

<sup>3</sup>SAT, Algonquin College, Ottawa, ON, Canada

<sup>4</sup>EPAM Systems Inc., USA

<sup>5</sup>Computer Science Department, Jamia Hamdard, Delhi, India

<sup>6</sup>Arba Minch Institute of Technology, Arba Minch University, Ethiopia

Correspondence should be addressed to Benkun Yao; [benkunyao863@163.com](mailto:benkunyao863@163.com) and Bhupesh Kumar Singh; [dr.bhupeshkumarsingh@amu.edu.et](mailto:dr.bhupeshkumarsingh@amu.edu.et)

Received 4 January 2022; Revised 10 February 2022; Accepted 14 February 2022; Published 8 March 2022

Academic Editor: Shalli Rani

Copyright © 2022 Benkun Yao et al. This is an open access article distributed under the Creative Commons Attribution License, which permits unrestricted use, distribution, and reproduction in any medium, provided the original work is properly cited.

With the current data-driven era, there is the potential to employ controllers that can store a large amount of data, which is not achievable with traditional controllers. Our goal is to propose an intelligent controller system for computer room management based on artificial intelligence that maintains data integrity, saves memory, minimizes computation, and simplifies program design. To upgrade the computer room management system's intelligence that is not high, the management mode that is not flexible, and the distributed large-scale management of the whole school that is difficult to realize, the original system is improved to the distributed computer room management system based on artificial intelligence. By starting from the actual situation of higher vocational college computer room, combined with the characteristics of the school computer room, we designed framework model based on distributed artificial intelligence machine room management system, the system by means of network communication technology and database access technology, put forward the B/S combined with C/S structure to realize the computer room management system model, and used radio frequency identification technology to develop radio frequency card. The results show that the optimization results of the traditional computer automatic control system in the computer room vary greatly and fluctuate between 0.6 and 0.8, while the control results of the automatic control system in this paper keep stable at 0.8, which can reach the ideal state in a short time. Through the outcome, it can be said that the proposed control method can be used of higher level of automation, flexibility, and robustness which will work effectively. Therefore, the improved system integrates software, hardware, communication, and distributed system technology into one, which greatly improves the control effect of computer automatic control process, and control result of computer automatic control process is more stable and has a certain practical application value.

## 1. Introduction

Using smart sensor technique to develop intelligent software apartments has also recognized as a dominant position in university renovation. In such an era of rapid advancement of machine learning and artificial intelligence, how to fully utilize technology, cloud platform, advanced analytics computing, and other resources to build a new intelligent control

and management platform, to achieve intelligent management of university network room teaching administration, has become the main production trend of university intelligent control and management system. At present, the construction of intelligent control and network technology-based computer room management system in colleges and universities is in the exploration stage. With the constant evolution, maturity, and perfection of Internet of Things,

information mechanism, schools will have different requirements for the application of the Internet of Things in various industries and fields. Strengthen the construction of intelligent control and management system of the college rooms, grant entire play to the function of science and technology in physical environment perception of the Internet of Things, and provide more personalized services for teachers and students in the teaching process and daily life. At present, there are many problems in management of computer rooms in many colleges and universities, such as heavy management workload, difficult arrangement of computer rooms, inconvenience of after-class computer and charge management, and many financial loopholes. Facing the high number and high investment of the school computer room, a set of functional integrity and practical, simple maintenance, high-security charge management system for improving the management efficiency of the computer room, reducing the intensity of work, and timely processing of the fault occurring in the computer room has important significance. How to use computer resources effectively and improve the utilization rate of computer room has put forward higher requirements on the management level of computer room. In this case, higher vocational colleges urgently need to develop a distributed IC card-based computer room management system for unified management, to achieve the modern management of computer room, and improve the management level of computer room [1].

Artificial intelligence, or AI for short, was first proposed in 1956 by John McCarthy and other scientists at the Dartmouth Institute in America. As a main division of computer science, artificial intelligence has become a broad interdisciplinary and frontier science after more than 60 years of rapid development. Artificial intelligence is considered as one of the three high-tech mechanisms in the 21st century. Artificial intelligence (AI) is a basic theory, methods and technology that combines computer software and hardware to refresh definite thinking processes and behaviors of human beings by studying the laws of human intelligence activities and building artificial systems with definite intelligent bearings. AI technology is a rapidly developing research field. The research on AI has not only become a hotspot of distributed artificial intelligence research but also a hotspot of computer technology research. At the same time, it has attracted wide attention from the scientific, educational, and industrial circles and has been applied increasingly widely in recent years. The reason for this is that AI-based systems have excellent advantages in problem-solving. AI technology provides a new distributed computing model and problem-solving approach, which can effectively relieve the constraints of sequential and centralized control on the system and seek the solution of problems in a concurrent and non-centralized way. It provides a new computational and problem-solving solution and will be a model for the next generation of complex distributed engineering systems. The traditional distributed computer room management system is usually a client/server structure. Compared with the client/server, AI does not need continuous network connection and can reduce the occurrence of network blocking. AI can move a piece of application code to the location of

the data, execute it at a high speed locally, and eventually remit the execution outcome to user, thus eliminating the transmission of a large amount of data on the network [2, 3]. AI refers to machine or software intelligence. When it comes to AI in control engineering, it is not necessarily about mimicking human intelligence. While seeing other people may teach you a lot about how to assist robots in solving difficulties, the vast bulk of intelligent control research focuses on real-world problems rather than people or animals. AI incorporates a variety of strategies, including search and mathematical optimization, reasoning, and probability-based procedures. Conventional control techniques and approaches are frequently less computationally demanding to implement than other AI applications and may be accomplished using low-capability microcontrollers. The successful deployment of emerging Industry 4.0 will contribute to the creation of more capable control systems and applications. AI advancements that will have an impact on control engineering include data mining techniques, multi-agent systems, and distributed self-organizing systems [4–6]. Radanliev et al. proposed a novel numerical technique for incorporating concepts from cognitive propulsion system, edge computing, artificial intelligence, and machine learning into automated intrusion detection. At the edge of the Internet of Things network, the engine uses machine learning technology to initiate process changes, providing actual intelligence with stability and operability for inferential network risk analysis. This will improve risk analysis capabilities and encourage the development of a systematic and comprehensive understanding of the challenges and threats that arise when deploying edge computing servers, as well as local IoT networks as machine learning and artificial intelligence technologies migrate to the Internet's periphery [7]. Artificial intelligence (AI) has found applications in society over the last decade. As AI applications become more challenging and use incidents expand, they highlight the significance of trying to address performance and power significant challenges in their implementation. Kurshan et al. [8] give a brief overview of what 3D integration offers in the design of machine learning chips, discuss emerging opportunities in the next generation of memristive architectures, and inspect challenges. Because of our limited knowledge of the activity and structures of the human mind, machine learning layout, which relies on the brain for inspiration and virtual world, faces serious challenges. However, a large sum is being invested in the development of memristive chips. We believe that three-dimensional integration not only provides tangible advantage for fee and versatile neuromorphic chip design, but it may also provide architecture flexibility when it comes of fusion, further enabling design in future works. For monitoring, the multivalent system can help in monitoring the condition of system and providing effective asset management by diagnostics and protection against faults. Both areas are built upon the multi-agent system properties, such as proactive, reactive, and social properties, as well as other fundamental properties. Moreover, they require highly developed communication protocols and specified architectures for the purpose of applications [9].

A major concern for the networked sensing and actuation of a large-scale system is the complexity, due to the number of components and their interaction patterns and communication delays. This complexity is raised when a control system is required to become intelligent by implementing a completely new variety of knowledge processing functions [10]. To sum up, this paper proposes a computer room management application process depending on artificial intelligence. Database design is the cornerstone of successful development of the system, so how to set up database tables, in which fields each table has to ensure data consistency, save memory, and reduce the amount of computation, which simplifies the program design is essential. According to the database design specification, to prevent abnormal data insertion, deletion, and update, the database design reaches three normal forms (3NF). The main data table of the system is user table, user on machine record table, user-type table, and rate table. The user table mainly includes the primary information of the user and the login information of the user. The user login record table mainly includes the login record registration; this table is convenient for the user to inquire their own login record. The user-type table includes user types such as super administrator, system administrator, general administrator, teacher, and student. The rate table mainly designs the system billing parameters. According to the rate, the way of billing, and the composition of measurement units, the database design also considers the needs of teaching, development, and conservation of the computer room. The intelligent managed process of communication computer room obtained by this study has a good system interface and easy to use, which is convenient for students to learn on the computer, reduces the management workload of computer room administrators, improves the utilization rate of equipment and work efficiency, realizes the modernization of computer room management, and has a certain practical application value.

## 2. Research Methods

### 2.1. System Pattern of Computer Room Supervised System Based on AI

*2.1.1. Workflow of the System.* The working flow of college students' computer room is as follows: for the students who have class arrangements, the computer room supervised process will allocate the computer room according to the class arrangement and assign a machine to the students who swipe the card; for free students on the machine at their own expense, the machine room management system must first check the situation of the machine room, to see if there is no idle machine that can be used; if not, then give a "no idle machine" prompt information; if there is idle machine, then arrange students on the machine, the following process and the normal students on the machine the same. Its working flow diagram is shown in Figure 1.

Figure 1 is the client-server paradigm, also known as client-server architecture, which is a distributed application framework that splits tasks between servers and clients that

are either in the same system or communicate over a computer network or the Internet. It can be seen from Figure 1 that in the client/server mode, the client and the server must always maintain the connection during the calculation process. A high number of median results need to be transmitted during the calculation system, which wastes bandwidth, etc., making it difficult to adapt to the high delay and unstable network environment. The main research is to introduce AI technology into the computer room management system and rebuild our existing computer room management system model. In this new model, AI is not only the basic component unit of the process but also the independent function entity of the process. This new design can constructively decrease the network link time, reduce the occupancy of network bandwidth, greatly improve the robustness and reliability of the system, give full play to the role of the network for distributed computer room management, realize nonconnection interaction, support weak clients, and enhance the performance of remote interaction. The flowchart of the system is shown in Figures 2 and 3. In Figure 2, a flowchart depicts the individual phases of a process in a logical sequence. It is a general tool that may be used for a wide range of applications and can be used to describe a number of processes like service processes and project plans. Similarly, for Figure 3, the flowchart of credit card exchange has been shown. The dotted line indicates whether the subserver requests the server according to the IC card information. If it is a self-charging server (no request can be made to the server when there is IC card information), if there is no free machine, the subserver can first complete the prompt to the user that the machine is unavailable [11, 12].

As can be seen from the figures, the processing between the card reader and the subserver does not have to wait, and the communication between the subserver and the master server can be completed.

### 2.2. System Platform Mode

*2.2.1. Common System Platform Patterns.* In recent years, with the rapid development of computer technology and network technology, the management of the computer room in colleges and universities has been transferred from manual management to intelligent automatic management. A client/server program works on the client side and connects with a remote server for information, whereas a web application runs entirely within a web browser. On a regular basis, the client server sends queries to the remote server to gain information. User interaction with the server is always accomplished via a client-side user interface or application. To connect with a web service, a web browser is used. A client server application might be platform-specific or cross-platform, depending on the programming language used. A web application is platform neutral since all it needs is a web browser. The cross-platform language makes an application look native to the platform or operating system of the client [13, 14]. In this process, the choice of the platform mode of the computer room management system is the main problem that the system designers meet. The platform

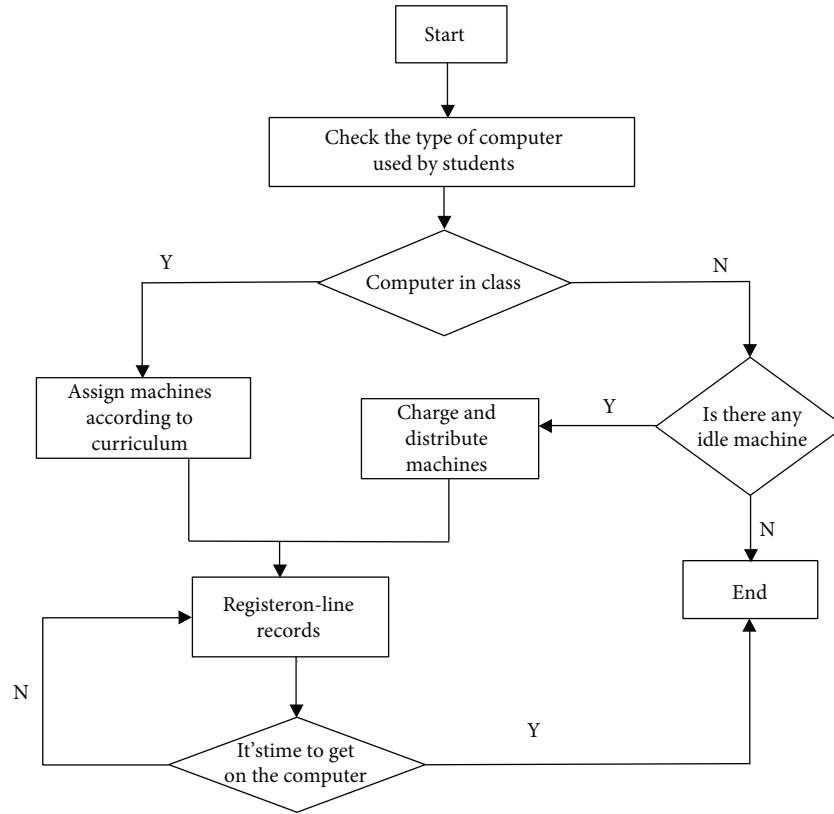


FIGURE 1: Flow diagram of the machine room.

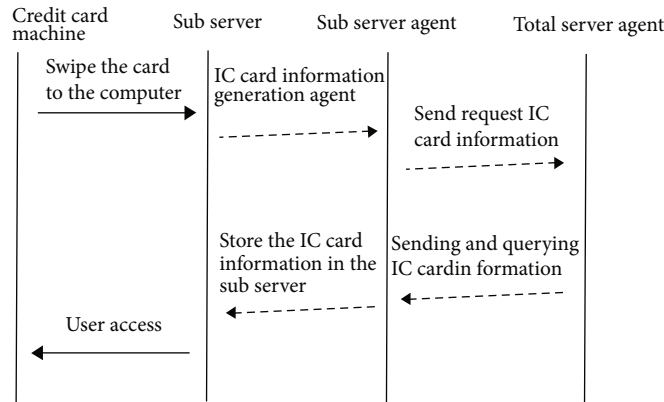


FIGURE 2: Flowchart of card swiping.

mode of computer room management system can be divided into four types: host terminal mode, file server mode, client/server mode (C/S for short), and web browser/server mode (B/S for short). The host terminal mode has been phased out due to limited hardware choices and unguaranteed hardware investment. The file server mode is only suitable for small-scale local area networks; for many users, a large amount of data will produce network bottlenecks, especially in the Internet which cannot meet the user requirements. Therefore, the platform mode of modern computer room management system should mainly consider C/S mode and B/S mode [15].

The broad classification of C/S- and B/S-type mode has been done in detail along with pros and cons. A client-server network's key advantage is the centralized control it gives. All of the required information is gathered in one spot. A client-server network's data is successfully secured due to its centralized architecture. It can be enforced using access controls, enabling only those who have been granted permission to do so. Client-server networks are extremely scalable. As needed, the user can increase the amount of resources such as clients and servers. As a consequence, the capacity of the server may be raised without creating substantial downtime [16, 17].

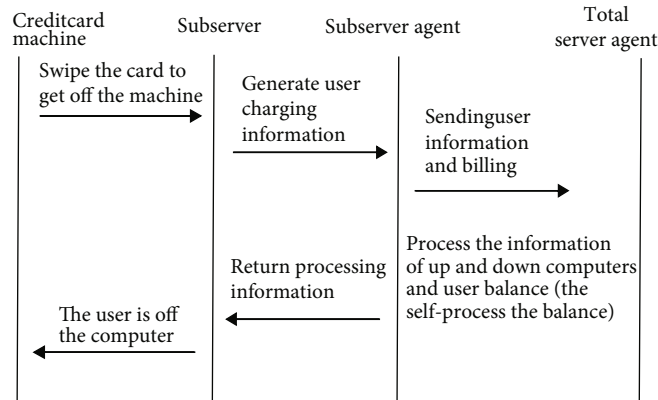


FIGURE 3: Flowchart of credit card discharge.

- (1) *C/S* structure: the client/server architecture, known as the client/server (*C/S* for short) architecture, is well known as the architecture. *C/S* architecture application is accompanied by the network database (such as Oracle, Informix, and Sybase) and desktop graphics interactive window application and development technology development and gradually formed. It separates the user interaction interface and business application processing of a complex network application from database access and processing. The dialogue between the server and the client is carried out through a message passing mechanism. The client sends the request to the server, and the server sends the request back to the client after the corresponding processing through the passing mechanism. A large number of operations to the database through the way of remote database access to the backstage database server to complete this mode to a certain extent to improve the speed of user interaction and response, reduce the requirements of the client to the CPU processing capacity, application development is simple and has more powerful foreground development tool. *C/S* business logic: the architecture is a two-tier system: the first layer combines the presentation on the client system and the second layer combines the database server over the network as shown in Figure 4

Generally, application software with *C/S* architecture is left at the client side, which makes the client side application still fast when dealing with complex applications, which is not consistent with the development trend of thin clients. In the remote database access database mode (obbc.sql), the client and the backstage database server data exchange frequently, and the amount of data is large, when a large number of users access easy to cause network bottlenecks. The traditional *C/S* mode has many shortcomings: such as low efficiency: inconvenient installation and operation, difficult to upgrade, and low safety performance [18]. Moreover, if all clients request data from the server at the same time, the service may become overburdened. As a result, the network may get overcrowded. If the server fails for whatever reason, none of the clients' requests will be fulfilled. As a

result, the expenses of implementing and maintaining a client-server strategy are rather high [19, 20].

- (2) The *B/S* structure: browser/server structure, namely, browser/server (referred to as *B/S*) structure, is a change or improvement of *C/S* structure with the rise of Internet technology. Its client is a standard browser (such as Internet Explorer and Netscape Navigator); the server side of the standard WEB server collaborative application server responds to the browser's request. The *B/S* mode is a three-tier structure system. The first-tier client is the user's interface to the entire system. Customers' applications are streamlined with general purpose browser software such as Netscape Navigator and Microsoft's Internet Explorer. The browser converts HTML code into an illustrated web page. The web page also has a certain interactive function, allowing users to input information on the application form provided by the web page to submit to the background and put forward processing requests. This background is the second layer of the web server. The second layer web server starts the process in response to the request and dynamically generates a string of HTML code that embeds the result of the processing and returns it to the client's browser. If the request submitted by the client includes access to data, the web server also needs to work with the database server to complete the processing. Tier 3 database server is similar to *C/S* mode, responsible for coordinating SQL requests from different web servers and managing the database

2.3. *System Platform Mode Used by the System.* There are many differences between *C/S* and *B/S*. First of all, *C/S* is built on the basis of local area network; *B/S* is built on the basis of wide area network. Second, the hardware environment is different: *C/S* is generally built on a dedicated network environment in a small-range LAN between the special server to provide connection and data exchange services. *B/S* is built on the WAN, which does not have to be a special network hardware environment, such as telephone Internet, there is a stronger than *C/S* to adapt to the range,

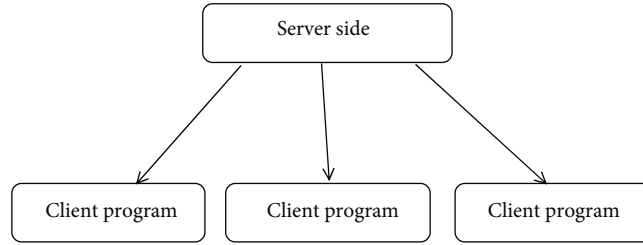


FIGURE 4: Architecture for C/S business logic.

generally as long as there is an operating system and browser on line. Although the two-layer C/S or B/S structure has many advantages, it has disadvantages in the following aspects:

- (1) Low efficiency in a distributed environment: in the general three-tier C/S or B/S structure access to the database process, because the client id direct with the application server and the application server and the database server hit, this will undoubtedly reduce the data access rate
- (2) For some special information form, through the database server makes the management very inconvenient. In the traditional three-tier C/S or B/S structure, data cannot be exchanged between the application servers. As for descriptive information, it must be exchanged through the database server. This not only causes the pressure of the database server but also is not easy to realize, thus affecting the application of the traditional two-tier C/S or B/S structure. We overcome this shortcoming by dividing the traditional application server layer into two parallel sublayers that can interact, thus making the three-tier C/S or B/S architecture more dynamic [21]. In the improved architecture, the two parallel sublayers not only have the functionality of their original application server layer, but they can interact with each other through some mechanism. The interaction principle between them is based on the principle of independence and mutual trust, that is, each sublayer is independent of the influence of another layer, and each sublayer has the integrity of the other side [22, 23]

AI technology is a good way to deal with in the past, the traditional C/S pattern cannot solve the problem, and its advantage lies in the following: 1 AI mode from the traditional C/S mode, the framework of the service request will be issued to the client code dynamically moved to execute on the server, the AI is not through the network transmission among the link and interact directly with the service source. This significantly reduces network bandwidth requirements and minimizes conflicts between multiple applications [24]. Of course, there are times when the code is moved to the client side for execution so that the interaction occurs locally on the client, which can achieve the same effect. Compared with the C/S mode, it is less dependent on

the network, does not need to keep the network always connected, allows discontinuous connection, and improves the utilization rate of the network [25].

### 3. Result Analyses

*3.1. Performance Test of Automatic Control System in the Computer Room.* To test in this paper, the performance of the automatic control system, computer rooms and the current classical room computer automatic control system optimization method on the same platform to carry on the simulation test, when the automatic control system by the outside factors under the condition of strong interference, the method and the traditional method of computer automatic control system of control results are shown in Figure 5. The dotted line in Figure 5 is the result line for the method proposed in the paper. It can be clearly seen that the output results have been stable which greatly improves the control effect of computer automatic control process. Through the outcome, it can be said that the proposed control method can be used of higher level of automation, flexibility, and robustness which will work effectively. This will address a major issue for the networked sensing and will solve the problems related to the communication delays. Under the condition of strong interference by outside factors, the traditional room change is very big, computer automatic control system optimization results in the output ups and downs unstable between 0.6 and 0.8, to achieve the ideal state of computer automatic control system control, long time-consuming, and results in this paper, the automatic control system control is steady in 0.8. It can reach the ideal state in a short time and improve the control effect of the computer automatic control system, and the control results of the computer automatic control system are more stable, with obvious advantages. The comparison results show that the optimization method of the automatic control system designed in this paper can solve the problems of large errors and low control efficiency in the optimization process of the automatic control system in the computer room.

*3.2. Implementation of AI-Based Computer Room Management System.* The client of this system includes the control client, the card swiping client, and the computer client, who are responsible for the server management, card swiping management, and the student computer control, and the client only carries on the data exchange with the subserver, without any contact with the central server. Take

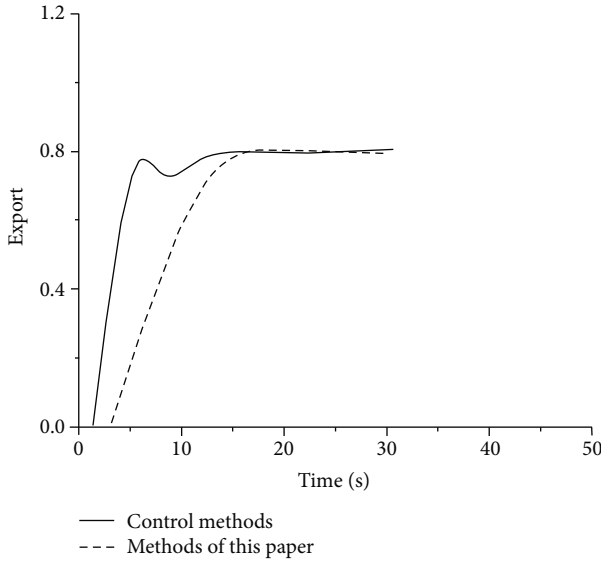


FIGURE 5: Output results of the automatic control system interference.

the swipe client as an example to describe the implementation of the client. The card swiping client is responsible for the student swiping card on and off the machine and communicates with the subserver to decide whether the student swiping card can get on the machine, including swiping card management and message processing, which are, respectively, composed of IC card identification, message sending thread, message sending thread, message queue, and so on. The structure of the operation process is shown in Figure 6.

The computer room management application system is designed by combining the foreground database with the background database. Database design is the cornerstone of the successful development of the system, so how to set up database tables, in which fields each table has to ensure data consistency, save memory, and reduce the amount of computation, which simplifies the program design is essential. According to the database design specification, to prevent abnormal data insertion, deletion, and update, the database design reaches three normal forms (3NF). The main data table of the system is user table, user on machine record table, user-type table, and rate table. The user table mainly includes the basic information of the user and the login information of the user. The user login record table mainly includes the login record registration; this table is convenient for the user to inquire their own login record. The user-type table includes user types such as super administrator, system administrator, general administrator, teacher, and student.

**4. Discussions**

The proposal is to create an artificial intelligence-based intelligent controller system for computer room management that protects data integrity, saves memory, reduces computation, and simplifies program design. As a result, the

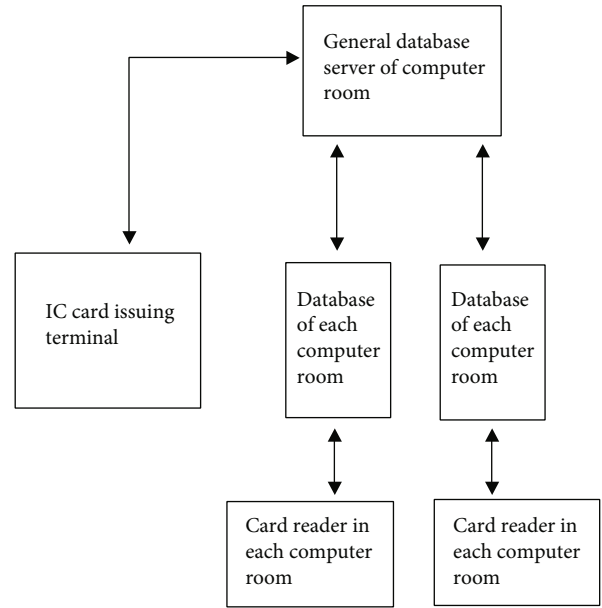


FIGURE 6: The overall design of database of the computer room management application system.

improved system combines software, hardware, communication, and distributed system technology into one, greatly improving the control effect of computer automatic control processes, as well as the control result of computer automatic control processes, which is more stable and has a practical application value. It is apparent that the output results have remained consistent, significantly improving the control impact of the computer automatic control process. As a result of the findings, it can be concluded that the suggested control approach may be utilized to achieve a better degree of automation, flexibility, and resilience, all of which will be beneficial.

**5. Conclusions**

Based on the analysis of the defects of the existing computer room management system and the characteristics of AI technology, a framework model of distributed computer room management system based on artificial intelligence is designed in combination with the characteristics of interaction, autonomy, and initiative of AI technology. The existing management system of the computer room in our school has been improved. A management system model based on B/S and C/S is proposed, and a radio frequency card is developed by using radio frequency identification technology. Run on the system in the management of basic normal, in computer room management for the school to save a large amount of manpower and material resources, improve the control effect of computer automatic control system, equipment utilization, and efficiency, and solve the existing current computer automatic control system optimization process, the control problem of low efficiency, and great error in computer room management, modernization has certain actual application value.

## Data Availability

The data used to support the findings of this study are available from the corresponding author upon request.

## Conflicts of Interest

The authors declare that there is no conflict of interest regarding the publication of this paper.

## References

- [1] K. Xu, Z. Wang, Z. Zhou, and W. Qi, "Design of industrial Internet of things system based on machine learning and artificial intelligence technology," *Journal of Intelligent and Fuzzy Systems*, vol. 40, no. 2, pp. 2601–2611, 2021.
- [2] V. Bellini, M. Guzzon, B. Bigliardi, M. Mordonini, S. Filippelli, and E. Bignami, "Artificial intelligence: a new tool in operating room management. Role of machine learning models in operating room optimization," *Journal of Medical Systems*, vol. 44, no. 1, pp. 20–20, 2019.
- [3] H. Woo and K. Kong, "Mechanical design optimization of a series elastic actuator considering the control performance," *Industrial Robot*, vol. 46, no. 2, pp. 311–323, 2019.
- [4] M. Demkah and D. Bhargava, "Gamification in education: a cognitive psychology approach to cooperative and fun learning," in *International Conference on Artificial Intelligence*, Dubai, United Arab Emirates, February 2009.
- [5] V. Jagota and R. K. Sharma, "Wear volume prediction of AISI H13 die steel using response surface methodology and artificial neural network," *Journal of Mechanical Engineering and Sciences*, vol. 14, no. 2, pp. 6789–6800, 2020.
- [6] M. K. Loganathan, S. S. Neog, and S. Rai, "Process safety and performance improvement in oil refineries through active redundancy and risk assessment method-a case study," in *International conference on industrial engineering and engineering management (IEEM)*, Bangkok, Thailand, December 2018.
- [7] P. Radanliev, D. De Roure, K. Page et al., "Design of a dynamic and self-adapting system, supported with artificial intelligence, machine learning, and real-time intelligence for predictive cyber risk analytics in extreme environments – cyber risk in the colonisation of Mars," *Safety in Extreme Environments*, vol. 2, no. 3, pp. 219–230, 2020.
- [8] E. Kurshan, H. Li, M. Seok, and Y. Xie, "A case for 3d integrated system design for neuromorphic computing and AI applications," *International Journal of Semantic Computing*, vol. 14, no. 4, pp. 457–475, 2020.
- [9] K. Fu, "Learning control systems and intelligent control systems: an intersection of artificial intelligence and automatic control," *IEEE Transactions on Automatic Control*, vol. 16, no. 1, pp. 70–72, 1971.
- [10] J. S. Heo and K. Y. Lee, "A multi-agent system-based intelligent control system for a power plant," in *IEEE Power Engineering Society General Meeting*, San Francisco, CA, USA, June 2005.
- [11] K. Sasakura, T. Aoki, and T. Watanabe, "Study on the prediction models of temperature and energy by using dcim and machine learning to support optimal management of the data centers," *ASHRAE Transactions*, vol. 125, no. 1, pp. 488–495, 2019.
- [12] A. Kumar, V. Jagota, R. Q. Shawl et al., "Wire EDM process parameter optimization for D2 steel," *Materials Today: Proceedings*, vol. 37, no. 2, pp. 2478–2482, 2021.
- [13] G. Rastogi and R. Sushil, "Cloud computing implementation: key issues and solutions," in *2nd International Conference on Computing for Sustainable Global Development*, New Delhi, India, March 2015.
- [14] S. F. Suhel, V. K. Shukla, S. Vyas, and V. P. Mishra, "Conversation to automation in banking through Chatbot using artificial machine intelligence language," in *8th International Conference on Reliability, Infocom Technologies and Optimization*, Noida, India, June 2020.
- [15] A. Sarda and A. Lenzi, "Suspension optimization for a compressor assembled on a refrigerator," *The Journal of the Acoustical Society of America*, vol. 145, no. 3, pp. 1881–1881, 2019.
- [16] A. Sharma and R. Kumar, "Service-level agreement—energy cooperative quickest ambulance routing for critical healthcare services," *Arabian Journal for Science and Engineering*, vol. 44, no. 4, pp. 3831–3848, 2019.
- [17] M. Poongodi, M. Hamdi, A. Sharma, M. Ma, and P. K. Singh, "DDoS detection mechanism using trust-based evaluation system in VANET," *IEEE Access*, vol. 7, pp. 183532–183544, 2019.
- [18] P. Swpu, "Recent progress and new developments of applications of artificial intelligence (ai), knowledge-based systems (kbs), and machine learning (ml) in the petroleum industry," *Petroleum*, vol. 6, no. 4, pp. 319–320, 2021.
- [19] V. Bhatia, S. Kaur, K. Sharma, P. Rattan, V. Jagota, and M. A. Kemal, "Design and simulation of capacitive MEMS switch for Ka band application," *Wireless Communications and Mobile Computing*, vol. 2021, 8 pages, 2021.
- [20] J. Bholra, S. Soni, and G. K. Cheema, "Recent trends for security applications in wireless sensor networks—a technical review," in *6th International Conference on Computing for Sustainable Global Development*, New Delhi, India, March 2019.
- [21] T. K. Lohani, M. T. Ayana, A. K. Mohammed, M. Shabaz, G. Dhiman, and V. Jagota, "A comprehensive approach of hydrological issues related to ground water using GIS in the Hindu holy city of Gaya," *World Journal of Engineering*, 2021.
- [22] R. Sucher and E. Sucher, "Artificial intelligence is poised to revolutionize human liver allocation and decrease medical costs associated with liver transplantation," *HepatoBiliary Surgery and Nutrition*, vol. 9, no. 5, pp. 679–681, 2020.
- [23] J. Bholra, M. Shabaz, G. Dhiman, S. Vimal, P. Subbulakshmi, and S. K. Soni, "Performance evaluation of multilayer clustering network using distributed energy efficient clustering with enhanced threshold protocol," *Wireless Personal Communication*, pp. 1–15, 2021.
- [24] J. W. Xiang, "Numerical simulation driving generative adversarial networks in association with the artificial intelligence diagnostic principle to detect mechanical faults," *Scientia Sinica Technologica*, vol. 51, no. 3, pp. 341–355, 2021.
- [25] M. N. Kumar, V. Jagota, and M. Shabaz, "Retrospection of the optimization model for designing the power train of a formula student race car," *Scientific Programming*, vol. 2021, Article ID 9465702, 9 pages, 2021.



## Research Article

# Architecture of Network-on-Chip (NoC) for Secure Data Routing Using 4-H Function of Improved TACIT Security Algorithm

N. Ashok Kumar <sup>1</sup>, G. Shyni <sup>2</sup>, Geno Peter <sup>3</sup>, Albert Alexander Stonier <sup>4</sup>  
and Vivekananda Ganji <sup>5</sup>

<sup>1</sup>Department of Electronics and Communication Engineering, Sree Vidyanikethan Engineering College, India

<sup>2</sup>Department of Electronics and Communication Engineering, Good Shepherd College of Engineering and Technology, India

<sup>3</sup>CRISD, School of Engineering and Technology, University of Technology Sarawak, Malaysia

<sup>4</sup>Department of Electrical and Electronics Engineering, Kongu Engineering College, India

<sup>5</sup>Department of Electrical and Computer Engineering, Debre Tabor University, Ethiopia

Correspondence should be addressed to Vivekananda Ganji; [drvivek@bhu.edu.et](mailto:drvivek@bhu.edu.et)

Received 12 January 2022; Revised 1 February 2022; Accepted 16 February 2022; Published 9 March 2022

Academic Editor: Vinayakumar Ravi

Copyright © 2022 N. Ashok Kumar et al. This is an open access article distributed under the Creative Commons Attribution License, which permits unrestricted use, distribution, and reproduction in any medium, provided the original work is properly cited.

In the technical world, NoC (network-on-chip) is a noticeable communication subsystem based on integrated circuits. It is mainly used in improving the performance of system-on-chip (SoC) by bridging the intellectual properties in the SoCs. But there is a need of protected architecture which is dealing with routing and processing data in the multicore system-on-chip (SoC). The recent issue with the above is there is still a drawback in enabling a better network routing system for accessing physical networks. The methodology of NoC mainly depends on the routing scheme, switching techniques, and structuring topologies. In this paper, we propose a new technique in implementing the chip in order to maintain the data privacy of NoC routers. There are many works with different algorithms that were evolved in enabling the secureness of NoCs, but due to the key size and block size, it is still not able to reach the expected effectiveness. Our proposed work is intended in designing a NoC architecture by means of embedding advanced TACIT security algorithm in Virtex-5 FPGA. Here, we used a hash function which is under a 4 hash function (4-H) scheme. The main advantage of this key generation scheme is it is applicable for block size and key size up to 'n' bit. Thus, this TACIT security algorithm enables 'n' bit using the software VHDL programming language in Xilinx ISE 14.2 and Modelsim 10.1 b which are applicable for 1024 bit and 'N' bits of block size on Virtex-5 FPGA systems. This design system can be enhanced by improving the factors like timing parameters, supporting memory, higher frequencies, and utilized summaries.

## 1. Introduction

Various technical methodologies are being evolved in sharing the information either in wired or wireless networks. But the main motto or requirement to be attained in the system is that the privacy of the information should be maintained while passing over the various communication channels. But losing of information is in higher state even in the technically globalized industry [1, 2]. If we compare and discuss about any encryption algorithm, the important thing should be noticed as well as maintained is its processing speed with data privacy. Because when there is an

increase in the sensitive of the information, the level of data privacy and speed are getting varied. In this concept, cryptography plays a vital role in achieving the data privacy [3, 4]. It is an art of expressing mathematical notation for encryption and decryption of data. When high sensitive data are stored or communicated, there is a possibility of privacy breach when those data are being passed through the unsecured networks. Cryptography is an art of data securing, and cryptanalysis is the concept of analyzing and damaging the secured communication systems [5]. Various kinds of cryptography techniques and algorithms used in the industry are DES, 3DES, AES, Kasumi Encryption Core, Blowfish,

RC4, and X-MODDES. Here, we compared the TACIT encryption algorithms based on the parameters like block size and key size. Next, the TACIT encryption algorithm was progressed on hardware description languages and it was analyzed with well commonly known encryption algorithms in the industry like AES as well as RSA.

*1.1. Cryptography Overview.* In cryptography [6, 7] the two factors involved are plain text and cipher text, in which the actual message or data to be viewed is known as plain text. Those texts which are encoded by means of key value are known as cipher text. This information is shared normally through the communication channels which are technically known as encryption. The reverse process of encryption which is being used in order to view the original text from encoding with key matching concept is known as decryption. The combination of these two processes is well known as cryptography which is involved in sharing the common or various keys in both ends. In technical factor, the sharing of the same key is called symmetric and by means of various keys is asymmetric key, respectively. Figure 1 is the pictorial representation of how the original text ( $X$ ) which is getting encrypted with the ( $k$ ) key value and communicated as cipher text with an expression  $Y = E [K, X]$ . The reverse process as mentioned above is shown by decryption algorithm with the expression  $X = E [K, Y]$  and same key ( $K$ ).

$$Y = [E, X]X = [E, Y]. \quad (1)$$

The important factor in the encryption algorithm is its secret key and key length. During the output, the key values vary by means of encryption algorithm.

According to the key values and exact substitutions, the algorithm produce varied outputs as per the key dependents. On discussing about the multiprocessor system-on-chip (MPSoC) and network-on-chip (NoC), the main drawback is maintaining the security channel. Network-on-chip is a well-known approach for designing any kind of subsystem that deals with the IP on system-on-chip. On the NoC communication architecture, the software and application layer are considered the crucial phases. If we get into a NoC template, it has a chip region and it is composed of chaining of chips. Those are physically isolated with the aid of regions through which they can communicate with each other. The switches in the architecture are composed of slots, which has computing and other resources. A resource can either be a memory, microprocessor, I/O, or FPGA resources. As the application layer is implemented by OSI layer, the resource connectivity among the network by means of switches and network interfaces. The networking services for the resources were gained by the network interfaces. The other layers implemented by network interfaces were presentation, session, and transport layers. Here, there is chain of connectivity between the switches and it is also connected to the network interfaces. The packet communication from source to destination is delivered by using the switches. The interconnection of network, data link, and physical layer is done by linking switches and metal wires. Figure 2 explains the NoC design which is structured by layer accord-

ingly for transmitting the data. We can say a resource can be represented as fixed type or floating point. According to the presentation layer, it must be a same type for converting some process. The session layer will establish the connection between the variable resources. The transport layer undertook checking of packet loss during the transmission. The network layer is implemented by the switches, which took the responsibility of handling the network topology and handled the addressing scheme among them. The passing of data between the points are done by the data link layer and physical layer holds the electrical properties.

## 2. Related Works

Various research works are done in NoC architectures [5, 8] in which several gains were yielded over conventional bus architecture. Common NoC architecture is a topology-based structure especially 3D-mesh topology, which is proposed with stacked mesh in [9]. In paper [8], wormhole switching is proposed and it is suitable for dealing with high speed and low power, in which NoC structure has routing as final protocol but most of routing technique failed to design mainly on the basis of power awareness. According to the work on [10], the routing is created based on the programmable routing tables especially for dealing with the faulty links in the NoCs. In paper [11], during the communication, in order to reduce the power consumption, a three-step routing algorithm is evolved. Here, they discussed about some of the open problems in the task routing. The work on [12] is composed of dead-lock free routing and adaptive routing in minimizing the routing latency. From paper [13], they discussed about the complex dynamic routing protocol in order to shun the conflicts of data buffering raised in the networks. The deflection routing protocol is proposed in [14] which is mainly proposed for dealing with output connection problems. In addition to these, various algorithms were developed in order to improve the NoC architecture performance on various factors such as dead-lock, low power, high speed, buffer connection, and low latency. But the abovementioned algorithms failed to address the security breach among the routing packets. In architecture, during communication, if the data is not secured, it is vulnerable to various attacks. Paper [15] shows the works of proposing the TACIT algorithm for the purpose of secure data communications. It uses hash function for key selection and distributing keys. The TACIT algorithm is the well-known bit-reverse process that can be easily predictable by the attackers. In this paper, our proposed work enhanced the TACIT algorithm by using 4-H key distribution (4-types of hash function) to implement secure routing system. It is too hard for the invader to destroy advanced TACIT algorithm, because of the design used in four types of hash function while generating the keys.

## 3. Research Gap

The achievement of effectiveness in internetworks mainly depends on the freedom while implementing the

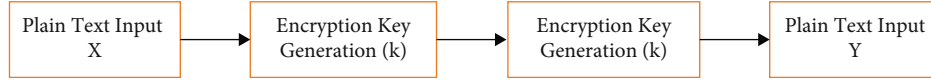


FIGURE 1: Symmetric encryption and decryption process.

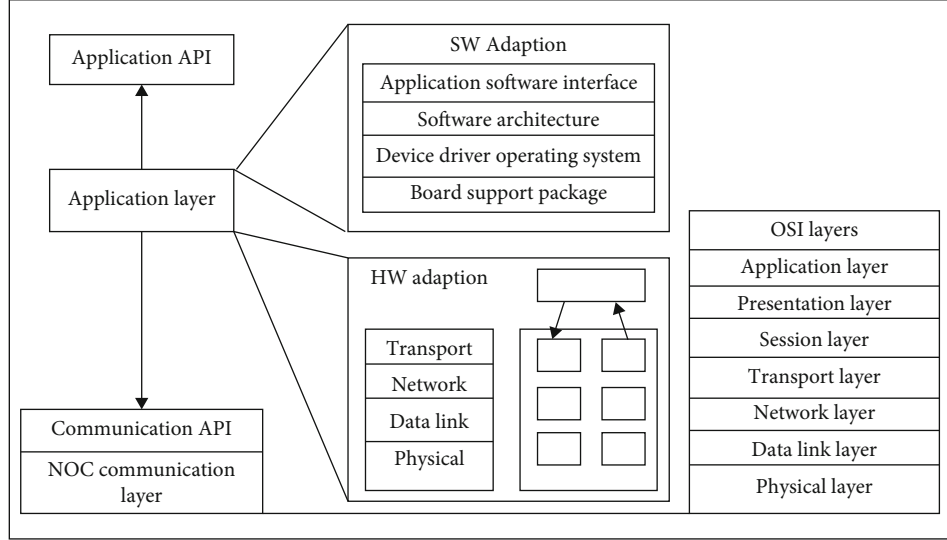


FIGURE 2: NoC architecture.

forwarding packets as well as routing. But traditional routing techniques have its own policies which restrict the routed traffic through specific paths for some administrative issues. These policies based routing intended the users to add policies which enable the packets selectively to pass through various paths. In a structured network, it is mainly required for a design to enable a route for secured data transmission till the destination. That is the reason for requirement in enabling secured policy based routing method. This paper analyses various methods in attaining security for networks. The methods discussed are DES, Triple DES, AES, Blowfish, RC4, Modes, and X-Modes but these have the limitation on block size and key size, in which the maximum size is 256 bits which is supported by AES algorithm. Finally, we proposed a new security algorithm known as TACIT. This TACIT is applicable for encryption and decryption on any network. The appreciable work of this proposed scheme is that it is designed to face ‘ $n$ ’ bits block size and ‘ $n$ ’ bits key size on any network. The implementation of hardware chip in the TACIT network security is proposed for future work with motto of achieving excellent result and even the key size is considered to be greater than the block size. The proposed algorithm is examined under various text files by implementing it on C, C++, C#, and Java programming languages. The TACIT can be used for encryption as well as decryption. It protects the theft of secret data in routers of network-on-chip by generating HASH key-based function. In case of proper right by the owner, the data protection unit does not create as problem to the unit. The main aim of the encryption and decryption algorithm is to provide the best secured database.

## 4. Proposed Key Generation Scheme

4.1. Procedure for Hash Function. We create streams  $A$  and  $B$ . Then, we exchange it. The above hash function has four cases are as follows:

Case 1:  $(A = B = i_g)$  and take ‘ $i$ ’ :  $x = H_1$  and  $y = H_1$ , where  $i_g = i > (j, k, l)$

Case 2:  $(A = B = j_g)$  and take ‘ $j$ ’ :  $x = H_2$  and  $y = H_2$ , where  $j_g = j > (i, k, l)$

Case 3:  $(A = B = k_g)$  and take ‘ $k$ ’ :  $x = H_3$  and  $y = H_3$ , where  $k_g = k > (i, j, l)$

Case 4:  $(A = B = l_g)$  and take ‘ $l$ ’ :  $x = H_4$  and  $y = H_4$ , where  $l_g = l > (i, j, k)$

Consider string  $A$  randomly at one end of transmitting such as source end and string  $B$  at receiving end. Here, both the strings were familiar among them and the hash table calculates the values between  $x$  and  $y$ . The value of random from the sender end is the range 0 to 9 with a code sequences in signifying the hash functions. It has four exist cases in order to break the key such as (i)  $i_g = i > (j, k, l)$ , (ii)  $j_g = j > (i, k, l)$ , (iii)  $k_g = k > (i, j, l)$ , and (iv)  $l_g = l > (i, j, k)$ . Table 1 shows the possible hash functions according to the proposed algorithms. In this,  $i_g$  represents the lower case alphabetic characters in the random sequence. If  $X$  and  $Y$  exchange between each other, value of ‘ $i$ ’ is the first value which is under generated sequence. The value of  $x$  and  $y$  is generated by the value of ‘ $i$ ’ to get the least prime numbers. This prime number is generated at both the ends by means of trial solution method. Thus, the biggest prime

TABLE 1: Hash table using the 4-H key.

$j$	Hash function			
	$H_1$ $i_g = i > (j, k, l)$	$H_2$ $j_g = j > (i, k, l)$	$H_3$ $k_g = k > (i, j, l)$	$H_4$ $l_g = l > (i, j, k)$
0	$i^l - i.j$	$j^k + j.k$	$k^l + k.l$	$l^i + l.i$
1	$i^k + (i+k)$	$j^l + (j+l)$	$k^i + (i+l)$	$l^j + (k+l)$
2	$i^l - (k+l)$	$j^i - (i+j)$	$k^l - (k+j)$	$l^k - (l+i)$
3	$j^k + (l.i)$	$i^l + (k.j)$	$k^j + (l.i)$	$l^i + (l.i)$
4	$j^l + (j.i)$	$i^k + (k.l)$	$k^j + (l.j)$	$l^i + (j.k)$
5	$j^i - i$	$i^l - j$	$k^l - l$	$l^k - k$
6	$k^i - i$	$l^i - j$	$i^k - k$	$j^l - l$
7	$k^l + (j+i-k)$	$l^i + (i+j-l)$	$j^l + (l-j-i)$	$i^k + (k-i-j)$
8	$k^l + (j+i+l-k)$	$l^k + (l+k+i-j)$	$i^j + (i+j+l-k)$	$j^i + (i+k+j-l)$
9	$i.j.l + (i.k)$	$j.k.l + (j.l)$	$i.j.k + (j.l)$	$k.l.j + (l.i)$

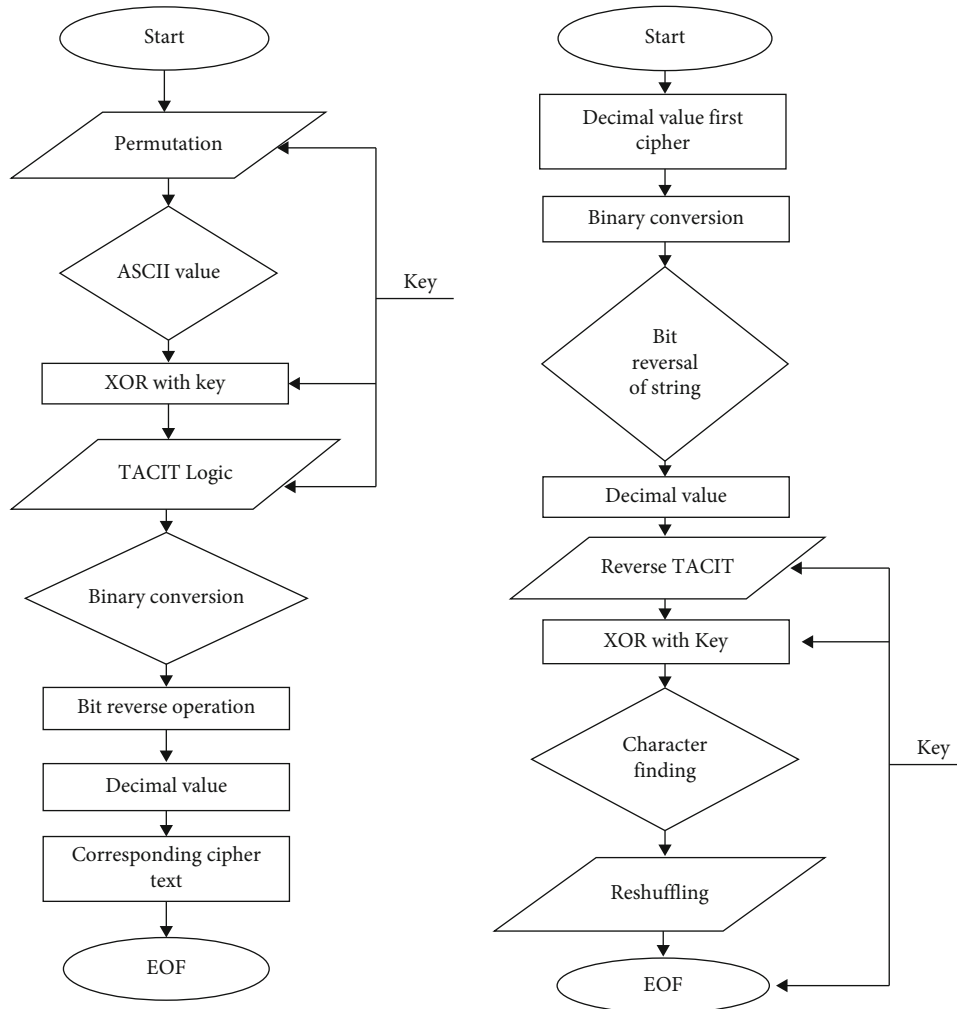


FIGURE 3: Encryption and decryption algorithm.

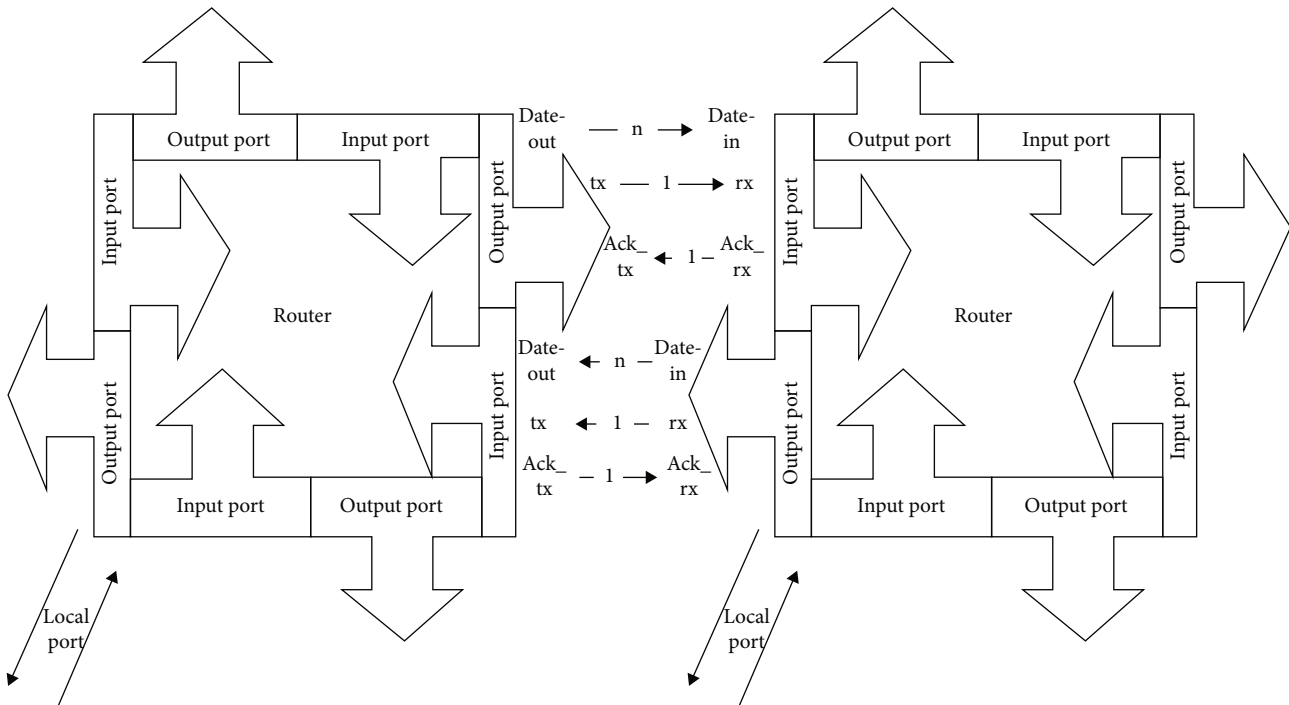


FIGURE 4: Router architecture of NOC.

number is between  $x$  and  $y$  with the average actual key. That generated key is proposed for processing the data encryption as well as decryption.

4.2. Key Generation

- (1) Let  $X = (4mph\#\%DH@897^{\wedge}jk\$)$  and  $Y = (7ln85JZ41@!60\&gt;)$
- (2) For  $X \{m = 4, n = 3, u = 2, v = 6\}$
- (3)  $X$  satisfies  $V_g$ . Therefore,  $P$  should use hash table H4. Here  $n = 4$
- (4) Therefore,  $P = V^m + (n.u) = >(6)^4 + (3 * 2)$ 
  - (i)  $1296 + 6 = 1302$
- (5) For  $Y \{m = 4, n = 6, u = 2, v = 3\}$
- (6)  $Y$  satisfies  $n_g$ . Therefore,  $Q$  should use Hash table H2. Here  $n = 7$
- (7) Therefore  $Q = V^m + (m + n - v) = >(3)^4 + (4 + 6 - 3)$ 
  - (i)  $81 + 7 = 88$ . Key:
- (8) Least prime number between 88 and 1302 = 89. Largest prime number between 88 and 1302 = 1301. Key = (Least Prime + Largest Prime)/2
  - (i)  $(1301 + 89)/2$ . Key = 695

4.3. TACIT Encryption Algorithm

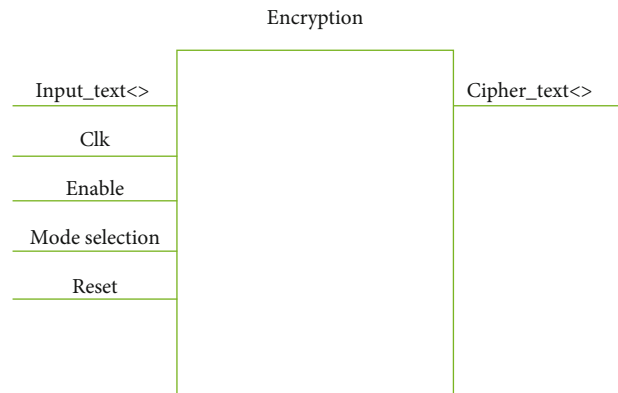


FIGURE 5: RTL view of developed encryption chip.

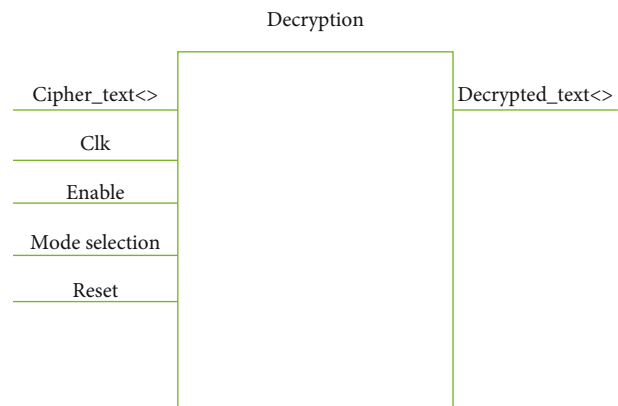


FIGURE 6: RTL view of developed decryption chip.

TABLE 2

Pins	Functional description
Reset	Used to reset sender and synchronized with clock of std_logic (1 bit)
Clk	Default input for sequential logic, rising edge of clock pulse of std_logic (1 bit)
input_text ( $N - 1 : 0$ )	Input text of the encryption end it can be of 'N' bit. It is of std_logic_vector type
Decryption_text ( $N - 1 : 0$ )	Decrypted text at receiving end, it is also of 'n' bit and of std_logic_vector type
Mode_Selection	1 bit input (std_logic) to select in a particular mode if mode_selection = '1' it is in encryption mode and mode_selection = '0', it is in decryption mode
Enable	1 bit input (std_logic) enable and disable the encryption logic. If enable = '1' encryption algorithms else decryption logic
Cipher_text ( $N - 1 : 0$ )	Cipher text is the text which is encrypted with key at the transmitting end. It can be any garbage value and it is of std_logic_vector type

*Step 1.* initially the text file is viewed and process for permutation approach in order to get the shuffle position for the characters using the key value.

*Step 2.* the text file characters were analyzed, and ASCII values are generated accordingly by means of character.

*Step 3.* the corresponding text specified the  $n$ -bit key value as XORed.

*Step 4.* TACIT logic is applied for nxorkk in order to perform some specified operations.

*Step 5.* the obtained resultant value is converted from Step 4 into binary one.

*Step 6.* reverse operation is applied on the resultant values from Step 5 on the binary string.

*Step 7.* the corresponding decimal value is to be analyzed.

*Step 8.* the decimal value according to the unicode character is formulated and that is the cipher text.

*Step 9.* perform all Steps from 1 to 7 for the remaining characters still the reaching the end of file (EoF).

The value for the first character and the key is generated using 4-H key function using ASCII table. This function is applied for doing the XOR operations. According to the TACIT logic (nk XOR kk), the value obtained is converted into binary forms by means of the preceding steps. In this stage, a modification is implemented in the TACIT logic that is the bit reverse operation which is processed after carrying out the bit XOR operations. As per [15], bit reverse operation is performed which the attacker can easily predict. To avoid this, the process is continuously performed based on the decimal value gained from the previous step. Those results involved the cipher text characters still its enciphered [16]. Visual cryptography technique allows visual information to be encrypted in such a way that the decrypted information appears as a visual image. Visual cryptography

allows digital images to be separated into few shares called transparent shares. For security reasons, it ensures that hackers cannot find any clues about the secret image from a single cover image. Transforming a secret message to add some protection using cryptography technique is called as encryption algorithm [6]. The encryption algorithm is unique to the master user who in turn protects the data from attackers. Encryption technique is of two types symmetric and asymmetric encryption. In symmetric encryption, the secret data can be encrypted and decrypted using a single key, without which it is impossible to decrypt the secret data. In asymmetric encryption, the secret data can be encrypted and decrypted using two different keys; it is difficult to decrypt the secret data without those keys. For the decryption process, the first character's decimal value is in ciphered packets. Then, according to the advanced TACIT algorithm logic, it is inversed as shown in Figure 3. For character determination, these processes were reshuffled and this implementation further carried out for all packets still gets deciphered.

#### 4.4. TACIT Decryption Algorithm

*Step 1.* the cipher text is the encoded text by means of encryption algorithm. The cipher text gives the approximate decimal value of the first character.

*Step 2.* reverse the corresponding binary values and examined

*Step 3.* according to the TACIT logic, inverse operation is processed.

*Step 4.* implementing XOR logical operation to the next key value or  $n$ -bit key value

*Step 5.* represent the corresponding character accordingly.

*Step 6.* by the help of key value reshuffle

*Step 7.* Steps from 1 to 6 is repeated still achieving EoF

TABLE 3: Device utilization summary of encryption and decryption.

Device part Block size	Encryption		Decryption	
	'1024' bit block size	'N' bit block size	'1024' bit block size	'N' bit block size
Number of slices	82 out of 1408, 6%	108 out of 1408, 8%	89 out of 1408, 6%	105 out of 1408, 8%
Number of slice flip-flops	134 out of 2816, 5%	184 out of 2816, 7%	147 out of 2816, 5%	187 out of 2816, 7%
Number of 4 input LUT's	48 out of 2816, 2%	72 out of 2816, 3%	144 out of 2816, 5%	168 out of 2816, 6%
Number of bonded IOB's	132 out of 140, 94%	132 out of 140, 94%	138 out of 140, 98%	138 out of 140, 98%
Number of GCLKs	1 out of 16, 6%	1 out of 16, 6%	1 out of 16, 6%	1 out of 16, 6%

TABLE 4: Timing parameters of encryption and decryption.

Device part Block size	Encryption		Decryption	
	'1024' bit block size	'N' bit block size	'1024' bit block size	'N' bit block size
Minimum period	1.56 ns	2.03 ns	1.442 ns	2.01 ns
Maximum frequency	786 MHz	793 MHz	754 MHz	768 MHz
Minimum input arrival time before clock	2.828 ns	2.915 ns	2.477 ns	2.545 ns
Maximum output required time after clock	5.807 ns	5.914 ns	5.112 ns	5.205 ns
Total memory usage	89943 kB	94248 kB	81175 kB	90298 kB

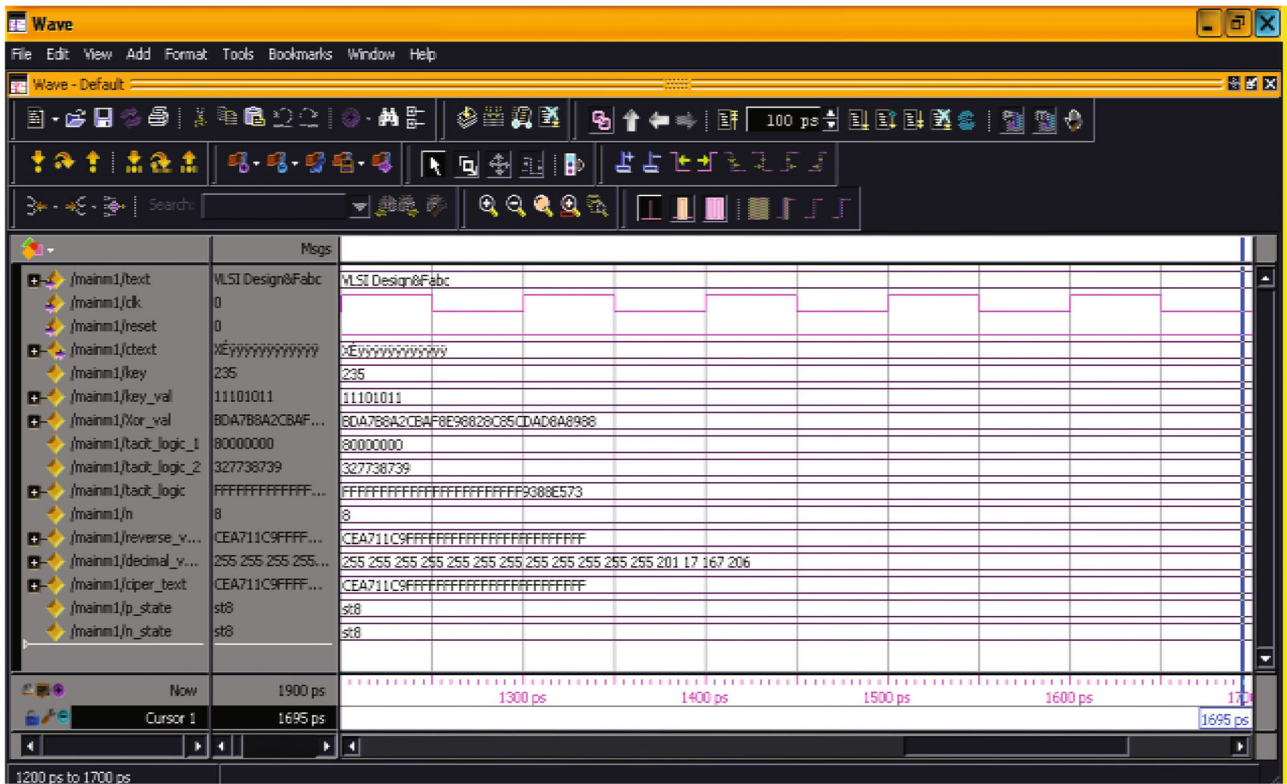


FIGURE 7: Modelsim simulation for data encryption.

4.5. *Implementing Advanced TACIT in NoC Architecture.* The developed network-on-chip (NoC) is successful for implementing in conventional bus architecture in an effective manner. The performance of NoC is improved by implementing some set of protocols. These protocols are mainly based on the working of topologies and routing and switching methodologies. This work is carried out by routing techniques [17] which are known to be deadlock free

mechanism. The proposed advanced TACIT algorithm-based router architecture of NoC is shown in below Figure 4.

## 5. Result and Discussion

The proposed work is modeled and developed in VHDL as a finite state machine. As shown in Figures 5 and 6, the

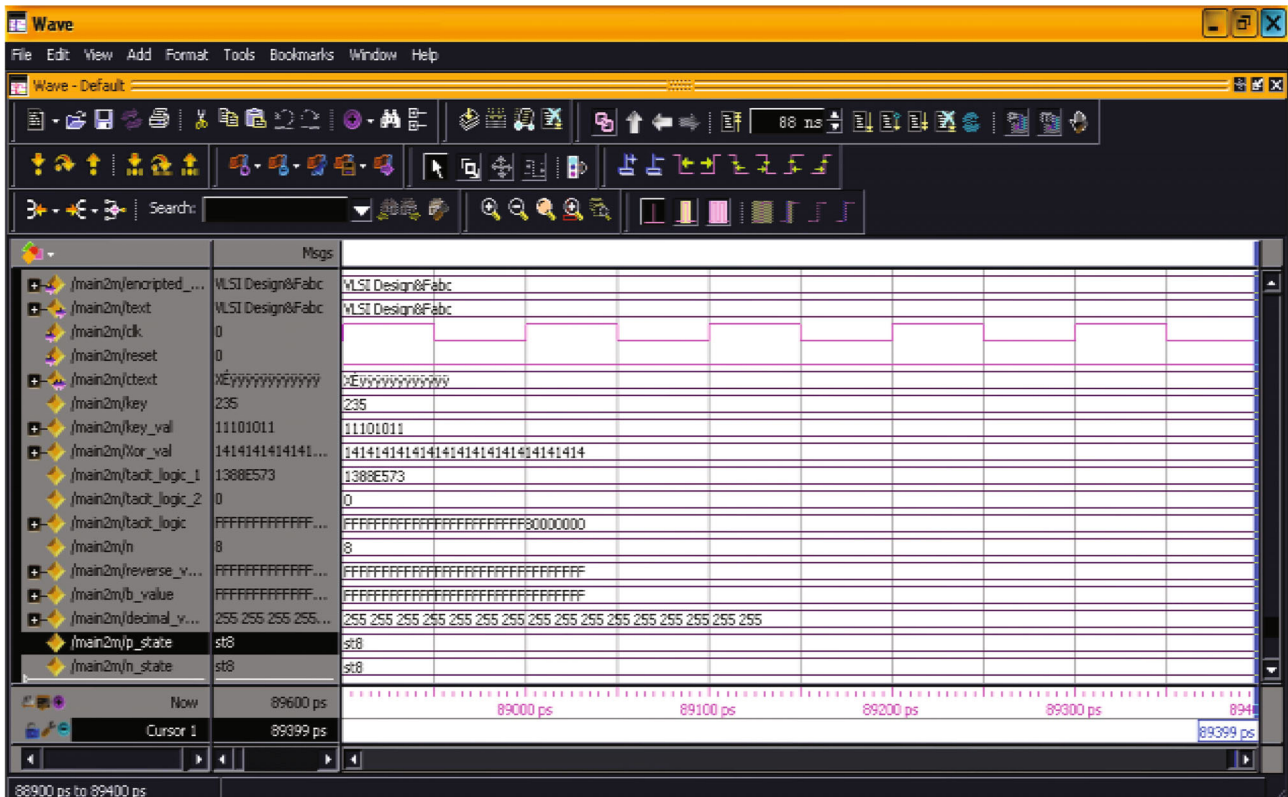


FIGURE 8: Modelsim simulation for data decryption.

register transfer level (RTL) is a developed view and Table 1 has the description of the chip.

Step input 1: reset = '1', the clk is for managing and run. At 50% duty cycle, every result was checked and rising edge is implied by clock pulse.

Step input 2: reset = '0', Select the input text and same clk is use for management.

Here, the Model\_selection has two modes such as to select encryption and decryption mode. By which particular logic is done by enabling input. Table 2 has description of the pins and by means of Mode\_selection is intended to perform the chip's functions [18]. There are two at Mode\_selection 1 data encryption logic and at 0 decryption logic [8]. Thus, integrated chip differentiates the encryption and decryption logic in the system. In which, by enabling '1,' the encryption logic began, and at 0, the decryption logic will be enabled by disabling the encryption logic. We force the mode selection and enable with input\_text <n bit>.

**5.1. Device Utilization and Timing Analysis.** The chip implementations and hardware device utilization is analyzed by the device utilization report. The implementation design has the device hardware which is based on no. of flip flops, no. of bounded IOBs, no. of gated clocks (GCLKs), no. of slices, and no. of input LUTs. The important details like minimum period value, minimum input arrival time before clock, information of delay, maximum frequency value, and maximum output required time after clock were resulted at timing details [19]. But the design is still incomplete, and by means total memory utilization value, it will

attain complete state. xc5vlx20t-2-ff323: it is the target device created with Virtex-5 FPGA. The simulated values of the design are tabulated in Tables 1, 3, and 4.

The achieved result is compared with existing work, and by means of ref. [5], the future work of chip development of TACIT cryptographic logic is proposed. On proposed work, the chip is designed and developed as per the logic. According to [2], the design is developed and created for 128 bit of block size. In the proposed work, it is designed to carry out for 1024 bit and  $N$  bits of block size with encryption maximum support frequency at 793 MHz.

The simulation output for data encryption and decryption using Modelsim is as shown in Figures 7 and 8 above. It is clearly evident that the proposed method has achieved its target with maximum security features.

## 6. Conclusion

In this paper, we proposed an advanced TACIT algorithm-based secured routing architecture for NoC (network-on-chip). In this mechanism, the key generation is based on the hash function (4-H key) scheme which is of four various types. According to this method, the intruder will not be able to break the key easily. This proposed scheme is simulated for the 'n' bit block size and key value. And the results are successfully implied on Virtex-5 FPGA for 1024 bit and 'N' bit of block size. Thus proving the efficiency of the proposed scheme compared to the other traditional approach in the industry. The flawless performance earns the remark for its achievement on being applicable for key size and block size



of 'n' bits. Based on the results the used memory and throughputs were tabulated and future work can be carried out for various NoC architectures.

## Data Availability

The data is available upon request to the corresponding author.

## Conflicts of Interest

The authors declare that they have no conflicts of interest.

## References

- [1] N. Ashok Kumar, P. Nagarajan, and P. Venkataramana, "Design challenges for 3 dimensional network-on-chip (NoC)," in *International Conference on Sustainable Communication Networks and Application*, vol. 39, pp. 773–782, Springer, 2020.
- [2] N. Ashokkumar and A. Kavitha, "A novel 3D NoC scheme for high throughput unicast and multicast routing protocols," *Technical Gazette*, vol. 23, no. 1, pp. 215–219, 2016.
- [3] A. Kumara, P. Kuchhal, and S. Singhal, "Secured network on chip (NoC) architecture and routing with modified TACIT cryptographic technique," *Procedia Computer Science*, vol. 48, pp. 158–165, 2015.
- [4] A. Ambashanke and P. N. Kumar, "Modified TACIT algorithm based on 4H-key distribution for secure routing in NoC architecture," *IEICE Electronics Express*, vol. 11, no. 13, 2014.
- [5] L. Benini and D. Bertozzi, "Network-on-chip architectures and design methods," *IEE Proceedings-Computers and Digital Techniques*, vol. 152, no. 2, pp. 261–272, 2005.
- [6] P. P. Pande, C. Grecu, M. Jones, A. Ivanov, and R. Saleh, "Performance evaluation and design trade-offs for network-on-chip interconnect architectures," *IEEE Transactions on Computers*, vol. 54, no. 8, pp. 1025–1040, 2005.
- [7] P. Guerrier and A. Greiner, "A generic architecture for on-chip packet-switched interconnections," in *DATE '00: Proceedings of the conference on Design, automation and test in Europe*, pp. 250–256, Paris, France, 2000.
- [8] P. Gope, A. Singh, A. Sharma, and N. Pahwa, "An efficient cryptographic approach for secure policy based routing (TACIT encryption technique)," in *2011 3rd International Conference on Electronics Computer Technology*, vol. 5, pp. 359–366, Kanyakumari, India, 2011.
- [9] X. Zhang and K. K. Parhi, "High-speed VLSI architectures for the AES algorithm," *IEEE Transactions on Very Large Scale Integration (VLSI) Systems*, vol. 12, no. 9, pp. 957–967, 2004.
- [10] B. S. Ferro and P. P. Pande, "Networks-on-chip in a three-dimensional environment: a performance evaluation," *IEEE Transactions on Computers*, vol. 58, no. 1, pp. 32–45, 2008.
- [11] Y. U. Ogras and R. Marculescu, "Analytical router modeling for networks-on-chip performance analysis," in *2007 Design, Automation & Test in Europe Conference & Exhibition*, pp. 1096–1101, Nice, France, 2007.
- [12] A. Shahabi, N. Honarmand, H. Sohofi, and Z. Navabi, "Degradable mesh-based on-chip networks using programmable routing tables," *IEICE Electronics Express*, vol. 4, no. 10, pp. 332–339, 2007.
- [13] S. Saeidi, A. Khademzadeh, and A. Mehran, "SMAP: an intelligent mapping tool for network on chip," in *2007 International Symposium on Signals, Circuits and Systems*, vol. 1, pp. 1–4, Iasi, Romania, 2007.
- [14] M. Palesi, R. Holsmark, S. Kumar, and V. Catania, "Application specific routing algorithms for networks on chip," *IEEE Transactions on Parallel and Distributed Systems*, vol. 20, no. 3, pp. 316–330, 2009.
- [15] H. Moussa, A. Baghdadi, and M. Jezequel, "Binary de Bruijn interconnection for a flexible LDPC/turbo decoder," in *2008 IEEE International Symposium on Circuits and Systems*, pp. 97–100, Seattle, WA, USA, 2008.
- [16] S. A. Alexander, T. Manigandan, M. D. Kumar, and R. V. Vardhan, "A comparison of simulation tools for power electronics," in *Proceedings of International Simulation Conference*, Institute for Applied Physics, Italian National Research Council, 2012.
- [17] P. Geno Peter and M. Rajaram, "An enhanced Z-source inverter topology-based permanent magnet brushless DC motor drive speed control," *International Journal of Electronics*, vol. 102, no. 8, pp. 1289–1305, 2015.
- [18] Y. S. Jeong and S. E. Lee, "Deadlock-free XY-YX router for on-chip interconnection network," *IEICE Electron Express*, vol. 10, no. 20, pp. 1–5, 2013.
- [19] G. Peter, J. Livin, and A. Sherine, "Hybrid optimization algorithm based optimal resource allocation for cooperative cognitive radio network," *Array*, vol. 12, article 100093, 2021.

## Research Article

# Animation Education Innovation of Big Data in the New Media Environment

Lu Zhang and Zhuoran Zhang 

*School of Fine Art and Design, Heze University, Heze, 274000 Shandong, China*

Correspondence should be addressed to Zhuoran Zhang; [zhangzhuoran@hezeu.edu.cn](mailto:zhangzhuoran@hezeu.edu.cn)

Received 13 January 2022; Revised 15 February 2022; Accepted 22 February 2022; Published 8 March 2022

Academic Editor: Shalli Rani

Copyright © 2022 Lu Zhang and Zhuoran Zhang. This is an open access article distributed under the Creative Commons Attribution License, which permits unrestricted use, distribution, and reproduction in any medium, provided the original work is properly cited.

Animation education is an essential part of art education. Animation education in China started late, and its development was intermittent. After entering the 21st century, animation education has developed at an unreasonably high speed and has formed layers of animation education bubbles. There are many problems and drawbacks behind the rapid development of animation education, but it has been slowly improved and some results have been achieved. In today's multimedia age, the digital revolution has brought a brand new environment and space for contemporary animation, and a large cross-field animation industry is gradually taking shape. China's animation industry should actively respond to the overall innovation of the global animation industry and build a new animation industry development model that adapts to the era of big data. And it builds an animation education system that adapts to the big data environment and continuously supplies talents for the animation industry. This article will study the innovation of animation education based on big data. This article introduces innovative methods of animation education based on big data and designs an animation education platform based on big data. It also conducted a questionnaire survey of learners using the platform based on the Technology Acceptance Model (TAM) and concluded: among the four-dimensional options of TAM, the average proportion of people who choose to agree is 49.5%, and the proportion of people who choose to disagree is 1.81%. This proves that most learners think that the animation learning platform in this article is useful and satisfied with the platform, and only a very small number of people have a poor experience of using the platform.

## 1. Introduction

Animation education in China began in the 1950s. In nearly half a century, there was only one university in China with dozens of students, and its development was slow. The real development of Chinese animation education began in 2004, and the development of animation education has shown an extremely rapid momentum from the beginning. In just a few years, it has blossomed all over the country, with animation schools, animation majors, and animation education institutions constantly appearing. However, the animation education of universities is still relatively weak for cultivating students' innovative ability. Therefore, how to cultivate college students' creative thinking in animation has become a central topic of college animation education. Affected by the new media revolution, the traditional anima-

tion industry has begun to change. It covers many fields, for example, clothing, toys, video games, advertising, and other industries. These industries include animation, derivatives, and industries that use animation to convey information.

Animation art education is an education implemented through animation art work, and its comprehensive knowledge contains more information than any single art form. In addition to the following the general laws of art education, animation art has its own laws. That is the unity of science and art, thought and technology, production, and market. Different from ordinary art work, animation is a market-oriented commercial industry, and its derivative products include comics, movies, TV, music, and even theme parks and website resources. As animation education continues to be hot today, animation educators must clearly understand the current situation of animation education,

and creators must have sufficient artistic accomplishment. Therefore, the focus of modern animation education should still be on technical education and art education. In today's Internet age, the use of big data technology to assist animation education is of great significance to the improvement of the effect of animation education.

The animation industry is a fast-growing industry, and the development of the industry has driven the development of animation education. Therefore so far, many scholars have also conducted research on animation education. Jian et al. showed that the lecturer's gestures can help capture, maintain, and guide students' attention in the classroom and enhance learning and retention capabilities. He proposed that the system allows users to effectively create accurate and effective stimuli for complex gesture research without the need for computer animation expertise or artist talent [1]. Shreesh and Tyagi use field experiments to evaluate the effectiveness of animation in education and try to eliminate the influence of external factors such as psychological factors and students' socioeconomic background. The research results show that animation can be used as an effective communication tool in pedagogy. If used properly, it can improve students' academic performance in elementary education, but this conclusion lacks data support [2]. Pinto et al. have created three storyboards and verified by 22 experts. The results show that the matching rate for care is above 80%. Storyboards enable people to understand the changes in scenes and dialogue more clearly and in more detail. Animation is an innovative educational technology that supports the teaching and learning of parents and families [3]. Suki and Suki aim to use the unified theory of acceptance and use of technical models as the guiding principle to examine the determinants of students' behavioral intentions in animation and storytelling. The research results show that university management and business school scholars should recognize that animation and storytelling are an effective educational method. And it actively integrates this strategy into the curriculum to cultivate business school students who are more creative in story communication. The lack of this research is the lack of detailed design [4]. The purpose of Farrokhnia et al. is to give an overview of the research in the field of stop motion animation (SMA) and to synthesize the research results. The results of the study show that if the appropriate scaffold is provided, SMA can facilitate deep learning. In addition, the scientific concepts proposed as SMA should be self-contained, dynamic, and not too difficult to express. The disadvantage of this research is that the research is not deep enough [5]. Earnest and Amador assign prospective teachers ( $N = 33$ ) to one of two widely used courses to generate lesson plans and corresponding animations. And it analyzes the homework data called "curriculum planning" to reveal how future teachers will use the curriculum to formulate the curriculum. He discussed the impact on theory, curriculum, and teaching, but the dimensions of analysis are somewhat less [6]. Yim focuses on discussing the social value of animation in the context of community culture and art education and exploring the policy direction of community animation art education. The analysis results show that the community's

understanding of the value of animation art education is low, and the educational needs are uncertain. However, it can be confirmed that the community can carry out animation art education for the elderly and young people. It would be better if the study can propose specific animation education measures [7].

The innovations of this article are (1) combining big data with animation education expounding the innovative methods of animation education based on big data. This is an innovation in method. (2) An animation education platform was designed based on big data, and the platform's functions, overall framework, and key technologies were all designed in detail. And after investigation, it is found that learners feel better about using this platform. This is an experimental innovation.

## 2. Innovative Research Methods of Animation Education Based on Big Data

### 2.1. Big Data

*2.1.1. Definition and Characteristics of Big Data.* From a technical point of view, big data is a large-scale, diverse, extremely fast-growing, and potentially valuable complex data spawned by the integration of the information technology, revolution, and human social activities; from a social point of view, big data is a new type of driving force that enhances interactivity, relevance, and personalization, creates social value, and changes human behavior [8]. In terms of data categories alone, big data refers to information that cannot be collected, stored, managed, and processed by traditional means. The scale of the data set exceeds the processing capacity of traditional methods, and more powerful methods are usually needed to process.

*2.1.2. Big Data Analysis Algorithm.* The related algorithms of big data analysis are essentially an application of collective intelligence. It collects answers from a large number of personnel information recorded in the information database to help obtain statistical conclusions. And these conclusions cannot be obtained with a small amount of data. Collaborative filtering algorithm is a recommendation algorithm that uses collective wisdom. It is an algorithm that generates corresponding recommendations to target users based on the rating data of similar neighbors. It can help people dig out related information from a large amount of information to generate the recommended content.

The implementation steps of the collaborative filtering algorithm are to collect user preference data, find similar users or similar items, and finally calculate the recommendation.

First, we use the Sqoop-based big data collection module to distribute mobile phone user preferences from various systems such as the education system and convert these historical records into a simple triple:

$$\langle \text{UserID}, \text{ItemID}, \text{Preference} \rangle . \quad (1)$$

Then, several similarity measures are used to calculate

the similarity between users, such as Euclidean distance and cosine similarity [9]. Euclidean distance represents the true distance between two points in a multidimensional space, and its calculation formula is as follows:

$$d(x, y) = \sqrt{\sum (x_i - y_i)^2}. \quad (2)$$

The similarity expressed by Euclidean distance is

$$\text{sim}(x, y) = \frac{1}{1 + \sqrt{\sum (x_i - y_i)^2}}. \quad (3)$$

The cosine similarity represents the cosine value of the angle formed by the vector values of two triples in the vector space. The formula is as follows:

$$\cos \omega = \frac{\sum x_i y_i}{\sqrt{\sum x_i^2} \sqrt{\sum y_i^2}}. \quad (4)$$

In the formula,  $x$  and  $y$  represent triples.

According to the similarity measurement value calculated by the abovementioned similarity calculation method, two types of methods can be used to obtain adjacent users or items [10]. That is, neighbors are based on the similarity threshold and a fixed number of neighbors, as shown in Figure 1.

### 2.1.3. Big Data Storage Method

(1) *Data Access Mode of the Storage System.* The basic form of recency-friendly data access mode is

$$(a_1, a_2, \dots, a_k, \dots, a_2, a_1)^n. \quad (5)$$

In the formula,  $k$  represents the number of data blocks, and  $n$  represents the number of cyclic visits. This data access mode has good data locality, that is, the currently accessed data has a high probability of being accessed again in the near future.

The basic form of Loop data access mode is

$$(a_1, a_2, \dots, a_k)^n. \quad (6)$$

The basic form of Frequency-friendly data access mode is

$$[(a_1, a_2, \dots, a_k)^m]P(b_1, b_2, \dots, b_i)^n. \quad (7)$$

In the formula,  $k$  represents the number of data blocks that have been accessed, and  $m$  represents the number of cycles to access  $k$  data blocks.  $m$  represents the number of data blocks that are accessed only once in a round of access.  $P$  represents the probability of accessing data blocks.  $n$  represents the number of cycles of the entire access process.

(2) *Cache Scheduling Strategy.* CRF (combined recency and frequency) is an attribute value associated with each data block. It represents the probability that the data block will be accessed in the near future. CRF is calculated by the following formula:

$$\text{CRF}_{t_0}(b) = \sum_{i=1}^k F(t_0 - t_b). \quad (8)$$

CRF integrates the contribution value of each access to a data block [11]. Let  $F(t)$  denote the contribution value brought by a data block access, and the contribution value gradually decreases with the passage of time, then

$$F(t) = \left( \frac{1}{\text{attenuation}} \right)^{w \times t}. \quad (9)$$

$W$  is the weight adjustment parameter. Update the size of the CRF in two cases. In one case, when the data block is accessed or submitted, the latest CRF can be updated according to the original CRF size. The calculation formula is

$$\text{CRF} = \text{CRF}_l \times (F - t_l). \quad (10)$$

In the formula,  $\text{CRF}_l$  represents the size of the last updated CRF, and  $t_l$  represents the time of the last update.

The second case is when a replacement operation occurs, the CRF values of all data blocks will be updated at this time. Because all data blocks must be sorted according to the latest CRF, the new CRF calculation formula is

$$\text{CRF} = \text{CRF}_l \times (t - t_l) \cdot F. \quad (11)$$

## 2.2. Educational Methods Based on Big Data

2.2.1. *Construction of the Evaluation Model of University Online Education Based on Big Data.* The application of big data technology in college network education is still in the stage of practical exploration. In order to better and objectively evaluate the achievements of college and universities, online education, and reflect the existing problems. This thesis is in the process of constructing a dynamic evaluation model of college online education based on big data, and it tries the combination of big data technology and traditional analysis methods and strives to increase the massive data advantage of big data on the basis of traditional methods [12]. The basic design of the evaluation model for college network education is shown in Figure 2.

Data processing is required before evaluation to eliminate the incomparability caused by directions and units. Generally speaking, there are two main forms for determining evaluation indicators, namely, subjective empowerment and objective empowerment. Subjective weighting is less likely to differ from actual common sense in the interpretation of the results, but it may affect the accuracy of the evaluation results; objective weighting has a rigorous

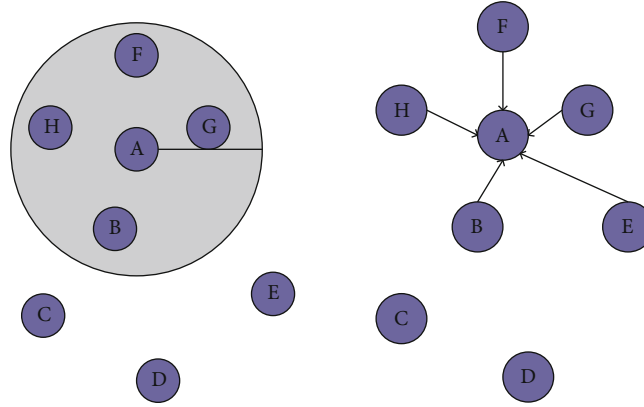


FIGURE 1: Diagram of the neighbor selection method.

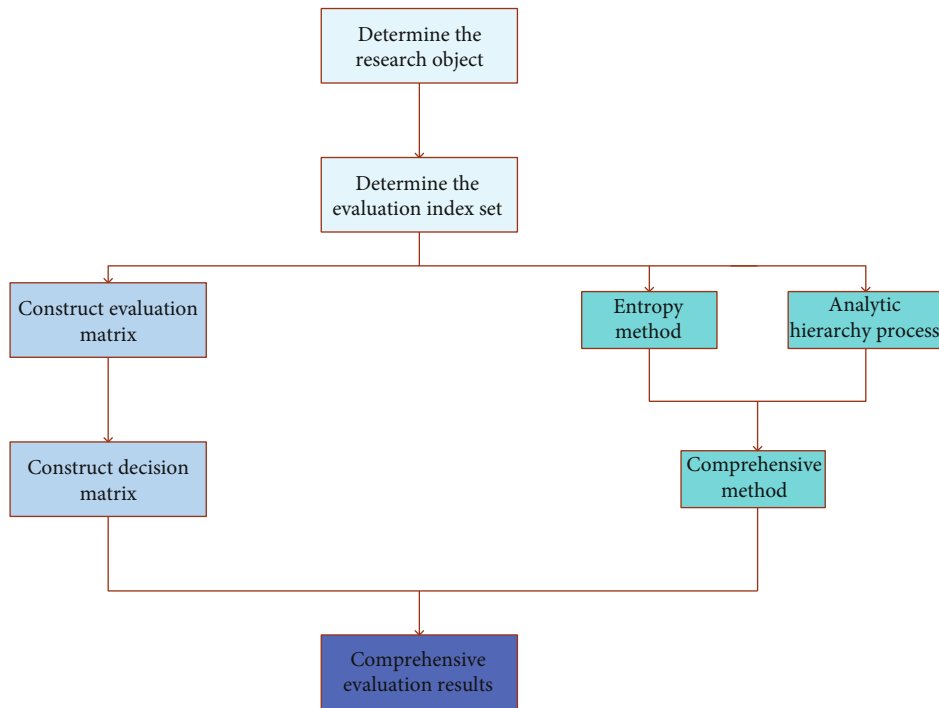


FIGURE 2: Basic design of evaluation model.

mathematical theoretical interpretation, but it may make the weight distribution unrealistic. Combining the advantages and disadvantages of the two methods, this chapter uses the analytic hierarchy process as the subjective weighting method, and the entropy method as the objective analysis method. The two weighting methods are integrated to get the reasonable weight value.

(1) *Analytic Hierarchy Process.* In the construction of the judgment matrix, relevant leaders, experts, scholars, and grassroots executives in the construction of campus network culture in China are invited to score relevant indicators and construct a corresponding judgment matrix. The weight value of each indicator is calculated from the judgment matrix of each person, and the average value of the weight value of each indicator is taken as the final weight of the cor-

responding indicator [13]. The subjective weight vector obtained by the analytic hierarchy process is

$$L = (l_1, l_2, \dots, l_n). \tag{12}$$

(2) *Entropy Method.* According to the characteristics of entropy, we can judge the randomness and disorder degree of an event by calculating the entropy value, or use the entropy value to judge the degree of dispersion of an indicator, the greater the degree of dispersion of the index, and the greater the impact of the index on the comprehensive evaluation. As an objective weighting method, the entropy method determines the weight based on the amount of information reflected by the confusion degree of each indicator. The entropy method calculates the proportion  $p$  of the index value of the  $j$ -th item under the  $i$ -th index. The

formula is

$$p = \frac{r_{ij}}{\sum_{i=1}^m r_{ij}}. \quad (13)$$

(3) *Comprehensive Approach*. The index weight vector obtained by the combination of analytic hierarchy process and entropy method:

$$W = (w_1, w_2, \dots, w_n). \quad (14)$$

According to the weighted calculation index value, the final evaluation result can be obtained.

### 2.2.2. Knowledge Level Diagnosis Method Based on Big Data

(1) *Project Reflection Theory IRT Mathematical Model*. IRT is a mathematical model used to analyze test scores or survey data. The goal of these models is to determine whether the underlying psychological characteristics can be reflected through the test questions, and the interactive relationship between the test questions and the testee. IRT uses a nonlinear probability model, and the most commonly used model is the logistic model. The model is divided into three-parameter model, two-parameter model, and single-parameter model. The three-parameter model is as follows:

$$P_i(\theta) = c_i + \frac{1 - c_i}{1 + e^{-1.7a_i(\theta - b_i)}}. \quad (15)$$

In the formula,  $P_i(\theta)$  represents the probability of a student with the ability level  $\theta$  of answering the question correctly.  $a_i$ ,  $b_i$ , and  $c_i$ , respectively, represent the degree of discrimination, difficulty, and guessing coefficient, and  $e$  is an irrational number, the base of natural logarithm [14].

The guess coefficient of some question types is quite small, that is, the value of  $c_i$  can be regarded as 0. At this time, the two-parameter model can be used, that is, there are

$$P_i(\theta) = c_i + \frac{1}{1 + e^{-1.7a_i(\theta - b_i)}}. \quad (16)$$

There are also some tests. Not only all project guesses may be 0, but the discrimination is very close to each other. That is to say,  $a$  is equal, and it can be set to  $a_i$  at this time, so a single parameter model is obtained, that is, there are

$$P_i(\theta) = c_i + \frac{1}{1 + e^{-1.7(\theta - b_i)}}. \quad (17)$$

2.2.3. *Intelligent Learning Path Recommendation Algorithm Based on Ant Colony Algorithm*. The structure of the smart learning engine includes a storage layer and a control layer. The storage layer is responsible for providing the databases needed for engine operation, including learner information database, group feature database, knowledge model and resource database, teacher guidance strategy database, and learning process database; the control layer is the operation

execution center of the engine. With the support of the storage layer, the control layer provides personalized services such as learning path recommendation, learning resource recommendation, adaptive presentation of learning resources, knowledge level diagnosis, and teacher guidance. Among them, the learning path recommendation is to use the smart learning path recommendation algorithm [15]. Support the smart learning of students and the smart guidance of teachers, dynamically track the learning process, and evaluate the learning effect. It dynamically adjusts its own rules and data according to the service effect to realize the continuous evolution of the engine. Its structure is shown in Figure 3.

(1) *Construction of Learning Object Network Graph*. After the learner selects the knowledge points to be learned, it is necessary to determine the population according to the mastery of all learners for the target knowledge points. Let  $L = \{l_1, l_2, \dots, l_n\}$  denote the set of knowledge levels of all learners who have completed the learning task (the population size is  $n$ ).  $l_i$  represents the knowledge level of the  $i$ -th learner. Let  $d(0 < d < 1)$  represent the degree of difference in knowledge level, then the population can be defined as

$$L_0 = L_1 + L_2, \quad (18)$$

$$L_1 = \{l_i \mid |l_o - l_i| \leq d\}, l_i \in L. \quad (19)$$

(2) *Evaluation of Learning Path*. The overall evaluation method of this chapter is that if the learner takes an evaluation after learning and his knowledge level improves, then the evaluation is adopted, otherwise, it is not adopted [16]. The reason for the decline in level is that the learning object may not be very effective, but the possibility of error and misleading is extremely low, so it can be ignored. After the learning of the learning object, the main reason for the decline in level is the learner's personal reasons. The global path evaluation is specifically expressed as suppose that user  $k$  completes the learning task, and  $A$  represents the learning path, then the evaluation update formula for each road section on path  $J$  is

$$\sigma_{ij}(t+1) = \begin{cases} \sigma_{ij}(t) * (1 - \rho) + \Delta\sigma_A^k(m_i \rightarrow m_j) \in A, \\ \sigma_{ij}(t) * (1 - \rho) (m_i \rightarrow m_j) \notin A. \end{cases} \quad (20)$$

Among them,  $\Delta\sigma_A^k$  is the evaluation of user  $k$  on the learning path.

2.3. *Animation Education Based on Big Data*. As early as the 1940s and 1950s, China began to open an animation department and carried out the earliest exploration of animation. Although there are no specific works left, the talents cultivated played an essential role after the founding of New China [17]. From the 1950s to the 1980s, Chinese animation creation entered a prosperous stage. It has created many excellent animated film and television works with strong oriental colors and Chinese characteristics, such as Snow Child,

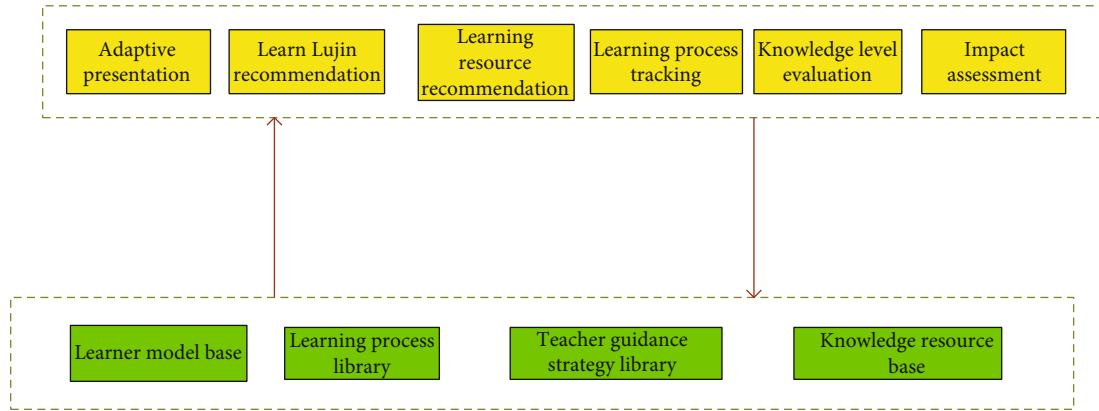


FIGURE 3: Basic structure of smart learning engine.

Magic Pen Ma Liang, Nezha Naohai, and Calabash Baby. As shown in Figure 4, it can be called a classic in the heart of a generation.

**2.3.1. Conventional Animation Course Setting.** In the animation production process, traditional animation courses are roughly divided into production preparation phase, midproduction phase, and postproduction phase. It mainly offers courses in ethics and law, college English, sketching, color, script writing, animation segmentation design, animation, motion law, and various software courses required for various animations. This includes two-dimensional animation production software courses and three-dimensional animation production software courses. And the curriculum setting is based on this production process [18]. The details are shown in Figure 5.

At present, the animation major is based on the basic process of the early stage of the animation production stage, the middle stage of the production stage, and the later stage of the production stage. This cannot meet the needs of all abilities that students need when creating short films, let alone the professional needs of a certain professional skill.

### 2.3.2. The Problem of Animation Education in Chinese Universities

**(1) Lack of Animation Talent.** According to statistics from the Animation Art Committee of the Chinese Artists Association, the national animation industry's demand for professional talent is about 150,000. However, at present, there are only 10,000 people in the domestic animation industry. The lack of talent can be said to be an important reason for the insufficient development of China's animation industry, which has caused deep anxiety to people. The lack of talent is not only a lack of numbers but also a lack of high-quality talent. That is to say, there are very few people who meet the high-quality requirements of domestic animation practitioners, and those who have the organic combination of art and technology [19].

**(2) Backward Teaching Methods.** As far as the teaching methods of animation in domestic colleges and universities

are concerned, whether it is an art course or a technical course, it basically still stays in the traditional mode of teachers talking and students listening. Moreover, with the continuous expansion of enrollment and the shortage of teachers, a teacher often has to face dozens or even hundreds of students to give lectures. This kind of large-class and indoctrinating teaching can improve efficiency relatively, but it is difficult to create an atmosphere that stimulates imagination and inspiration. There is a lack of communication and collision between teachers and students and between students and students. This one-way indoctrination method not only affects the cultivation of students' creative thinking and unique personality but is also incompatible with the laws of art education. As far as the status quo of art majors in Chinese colleges and universities is concerned, it is almost impossible to achieve "one-on-one" or small class teaching [20]. However, if the course content permits, the interaction between teachers and students, students and students can be realized in groups by grouping.

**(3) Insufficient Teachers.** In animation-related education, there are very few animation teachers with professional titles. If teachers have rich practical experience but lack theoretical ability, it is difficult to cultivate high-quality animation talents. Some schools will blindly recruit students when there is no animation professional teacher at all. If they have students, they will hire relevant teachers outside to teach completely, keeping the quality of teaching aside. Teachers are the core of education. To train professional students, a high-level teacher team must be established. This is the key to a good school animation education [21].

**2.3.3. Animation Education Suggestions Based on Big Data.** The rapid development of new media technologies represented by mobile phones, the Internet, and digital television has provided new channels for the dissemination of animation. Therefore, colleges and universities should seize the opportunity to use new media as the engine of artistic innovation, develop new forms of animation art, and meet people's new needs. The innovation of science and technology is changing with each passing day. Theoretical research not only needs to respond in time to the latest industrial



FIGURE 4: Excellent Chinese animation works.

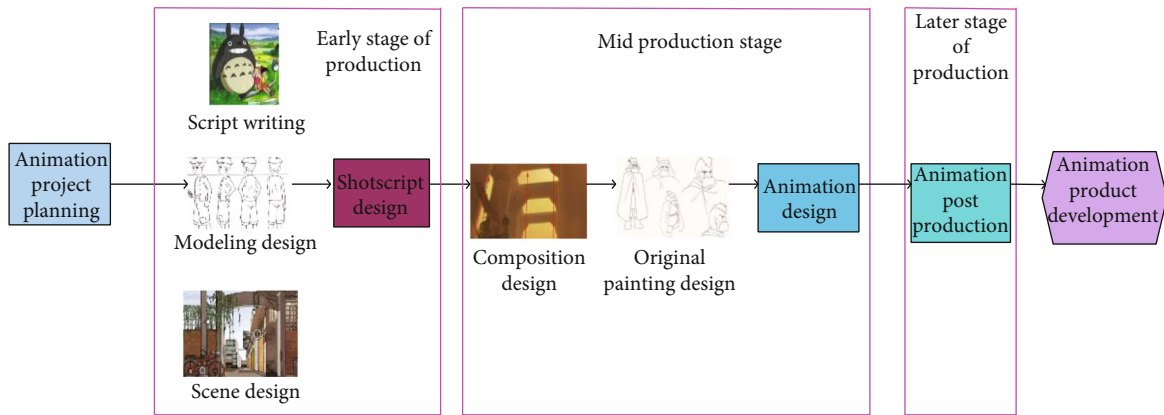


FIGURE 5: Traditional animation production process.

changes, technological innovations, artistic expressions, and media methods but also needs to be prepared for new things that may be about to emerge. For example, the merger of the three networks is in progress, if the design expectations can be realized, it will undoubtedly be another revolutionary leap for the new media. It will inevitably have a new impact on the current animation form, spawning new art forms, communication and aesthetic methods, and theoretical construction should be correctly guided for this [22].

With the advent of the digital age, the Chinese advertising market is bound to usher in a revolution in animation technology. Colleges and universities need to seize this opportunity to improve the current curriculum settings, accurately set up courses, and cultivate talents based on the pyramid distribution map of the demand for animation talent. Introduce real projects as much as possible, use real projects to create a working atmosphere for the enterprise, and realize the seamless connection between the school and the enterprise. Only in this way can we cultivate technical animation talents that are more suitable for the digital age. The talent structure diagram is shown in Figure 6.

### 3. Animation Learning Platform Based on Big Data

#### 3.1. Learning System Design

3.1.1. *The Overall Framework of the System.* This research integrates the five aspects of individual characteristics, interaction, technology, motivation and emotion, and learning

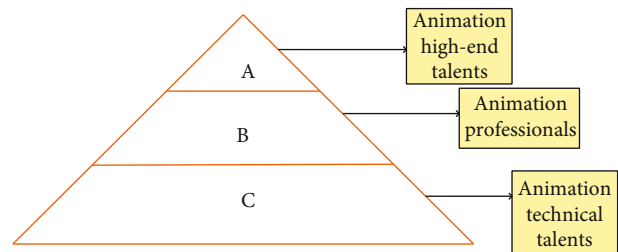


FIGURE 6: Animation talent demand distribution.

content in all aspects of learning system development. The development of an adaptive learning system for online animation education is to realize a customized learning plan based on the learner’s individual characteristic data. And it pushes personalized learning content and services, to achieve a multiplier learning effect. The overall framework of the system is shown in Figure 7.

The animation learning system records, stores, mines, and analyzes learners’ online learning data, such as individual characteristic data, learning interaction data, and motivational emotion data, and generates personalized learning monitoring and evaluation reports. Finally, according to the characteristics of the learners, the matching learning content is pushed.

#### 3.1.2. Function Design of Learning System

(1) *Learner Section.* The learner section is the most critical part of the learning system design. The quality of the learner



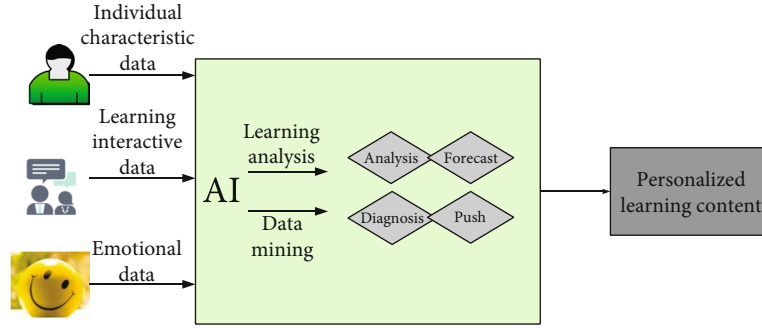


FIGURE 7: Platform framework.

module design will directly affect the learner's experience and satisfaction with the learning system. Therefore, to provide learners with a richer learning experience facing learner users, the learning system is mainly designed from three aspects: personal center, academic analysis, and personal settings. "Personal Center" mainly includes four aspects of my study, my wrong question book, my Q&A, and my exam; the analysis of academic situation is mainly based on big data, learning, analysis, and other technologies. Obtain, store, mine, and analyze the learning data of learners throughout the process, and provide learners with real-time learning, quality testing, and personalized guidance and services. The personal setting module mainly includes three contents: basic information setting, avatar setting, and password setting.

(2) *Teacher Section.* Teachers are supporters, guides, and facilitators of student learning. Aimed at teacher users, the research has carried out functional design from three aspects: curriculum management, examination management, and academic situation analysis. The course management module mainly includes six aspects: course list, chapter management, knowledge point management, learning object management, question management, question bank management, etc.; the examination management module is mainly composed of two parts: the "examination center" and the "marking center." It can help learners carry out targeted training on high-frequency knowledge points and weak knowledge points, enhance learning effects, and improve learning efficiency; learning situation analysis can help teachers grasp the learning process of learners, understand the learning situation of students' knowledge, and then improve teaching strategies.

### 3.1.3. Key Technologies of the Platform

(1) *Technical Support for the Overall System Architecture.* The system is mainly composed of five parts: database access layer, cache service layer, service layer, web layer, and session layer. The database access layer is mainly used to provide data persistence; the cache service layer is mainly responsible for providing a unified distributed cache service and improving the response speed of the entire system; the service layer is used to process the business logic of the system and is responsible for the transaction management of

the entire system; the web layer is mainly composed of web resource files; the session layer stores the session information after the user logs in in a cookie store, so that each web server node in the web cluster can recognize the session normally.

(2) *Learning Style Calculation.* The learning system uses data mining technology to mine the learning data of learners in the online learning process. If the learning style of a learner  $A$  is  $S(A)$ , let  $N$  denote the number of behavior patterns in each group of learning styles, then

$$S(A) = \frac{(\sum_{i=1}^n P_{iA})}{N}. \quad (21)$$

(3) *Personalized Recommendation Based on Collaborative Filtering.* This system uses collaborative filtering to make personalized recommendations to learners. This algorithm has been introduced in the method.

## 3.2. The Survey Design of the Experience of Using the Learning System

3.2.1. *Survey Object.* The subjects of this questionnaire are animation-related students from four universities in a provincial capital city. These students have all studied in the animation learning system designed in this article for more than one month, and the total number of students surveyed is 200. The questionnaire was sent to the students via QQ or WeChat, so that they could fill it out carefully.

3.2.2. *Questionnaire Design.* This survey mainly starts from the perspective of learners, through the questionnaire survey, we can understand the overall evaluation of the animation learners on the online education system, to provide a basis for subsequent revision and improvement of the system. The questionnaire is adapted from the Technology Acceptance Model (TAM), which is mainly used to study the survey respondents' the acceptance and use tendency of emerging technologies. It mainly includes four research dimensions: perceived ease of use (PEU), perceived usefulness (PU), user attitude (AT), and behavior intention (BI). Perceived ease of use refers to the degree of ease the user feels when operating a new technology; perceived usefulness is the degree to which the emerging technology used by the user helps improve daily life and academic performance;

user attitude is the subjective feeling that users have after using the new technology; behavioral willingness is the urgency of users to actually use new technology.

The questionnaire mainly contains two parts: one is a survey of basic information of students, which separately counts the gender and educational level of students; the other part is a survey of learners' use feelings adapted from the TAM model.

**3.2.3. User Experience Problem Design.** The problems in this part are designed based on the TAM model. The TAM model is divided into four dimensions. Then, there are 8 questions in this part of the questionnaire, with 2 questions in each dimension. The specific questions are designed as follows:

**Perceived ease of use (PEU):** (1) when using the system, you will not encounter situations where you do not know how to operate. (2) When using this system, I can easily enter the page, and I want to enter or get the learning resources I want.

**Perceived usefulness (PU):** (1) the learning content or resources recommended by the system are what I need. (2) The system can help me understand my own learning situation and help me to check for omissions.

**User attitude (AT):** (1) using this system for learning will make me feel satisfied and comfortable. (2) Overall, I like the design of the system.

**Behavioral willingness (BI):** (1) I am willing to continue to use this system for animation learning in the future. (2) I am willing to recommend this system to my friends. The options for these eight questions are all agreed, generally agreed, somewhat agreed, and disagree with these four options. We replace these four options with serial numbers 3, 2, 1, and 0, respectively.

### 3.3. Experimental Results and Analysis

**3.3.1. Experimental Reliability Analysis.** Import the data from the questionnaire of the mobile phone into the spss, and analyze the reliability of the questionnaire using the Kelbach coefficient, and the results are shown in Table 1. It is generally believed that when the Kelbach coefficient is greater than 0.9, the reliability of the questionnaire is very high; when the Kelbach coefficient is between 0.7 and 0.9, it indicates that the reliability is relatively ideal; when the Kelbach coefficient is between 0.6 and 0.7, it indicates that the reliability is acceptable; when the Kelbach coefficient is less than 0.6, it indicates that the reliability is very poor.

It can be seen from the table that the Kelbach coefficient of each dimension is greater than 0.8, and the comprehensive Kelbach coefficient of each dimension is 0.913. Therefore, the reliability of the questionnaire is relatively high and suitable for surveys.

**3.3.2. Statistics on the Basic Situation of Students.** As mentioned above, the first part of the questionnaire is the basic information survey of students. This part separately counts the gender and educational level of the students. The results are shown in Table 2.

TABLE 1: Questionnaire reliability.

Dimension	Number of topics	Kelbach coefficient
PEU	2	0.857
PU	2	0.891
AT	2	0.821
BI	2	0.836
Comprehensive evaluation	8	0.913

TABLE 2: Basic information of students.

Type	Option	Proportion
Gender	Male	47.31%
	Female	52.69%
	Specialty	18.73%
Educational level	Undergraduate	69.14%
	Graduate student	12.12%

According to Table 2, we can know the basic situation of students' gender and educational level. In the gender dimension, the proportion of men is 47.31% and the proportion of women is 52.69%. It can be seen that there are slightly more women than men in animation majors in these universities. In terms of academic level, undergraduates accounted for the largest proportion, accounting for 69.14%; graduate students, including masters and doctoral graduates, accounted for 12.12%.

#### 3.3.3. Analysis of the Experience of Using the TAM-Based Learning Platform

**(1) Perceived Ease of Use.** First of all, this experiment counts the results of the questionnaire survey of two questions in the perceptual ease of use (PEU) dimension, and the results are shown in Figure 8.

It can be seen from Figure 8 that in terms of perceived ease of use, whether it is question 1 or question 2, the number of people who choose to agree very much is the largest. Those who chose this option accounted for 48.7% and 47.1% of the two questions, respectively. Regarding these two questions, the proportions of those who chose little agree were 12.1% and 13.7, respectively, and the proportions that chose not to agree were 3.7% and 2.3%, respectively. This proves that there are still some learners who are not satisfied with the perceived ease of use of the learning platform.

**(2) Perceived Usefulness (PU).** The statistics in this part are the results of a survey of learners' satisfaction with the perceived usefulness of the learning platform. The results are shown in Figure 9.

It can be seen from the figure that in terms of perceived usefulness, whether it is question 1 or question 2, the

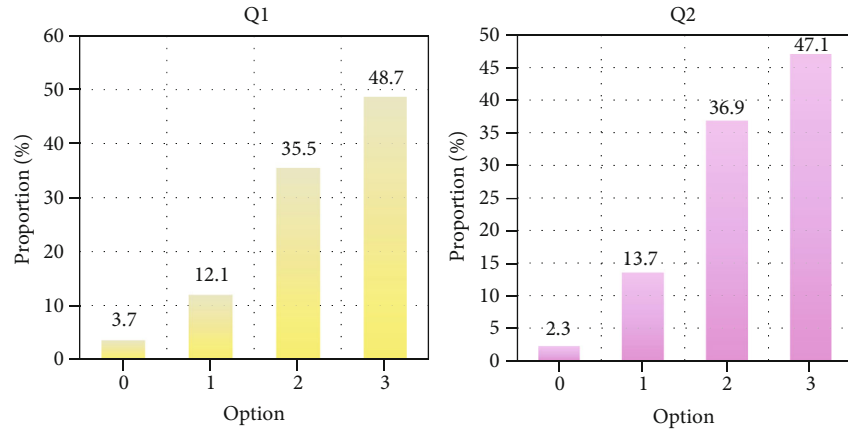


FIGURE 8: Perceived ease of use survey results.

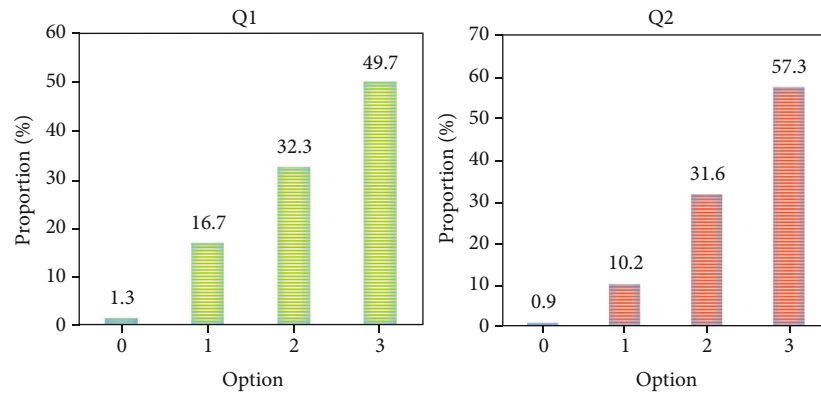


FIGURE 9: Perceived usefulness survey results.

number of people who choose to agree with each other is also the largest. Especially for question 2, the proportion of people who chose to agree very much was 57.3%. It is proved that the system can help most learners understand their own learning situation. Only 1.3% and 0.9% of the people who chose to disagree with these two questions proved that only a very small number of people believed that the system was not helpful for their own learning.

(3) *User Attitude and Behavior Willingness.* In this experiment, the survey results of the two dimensions of user attitudes and behavior intentions were analyzed together, and the results are shown in Figure 10.

It can be seen from Figure 10 that whether it is the dimension of user attitude or behavior willingness, the number of choices increases with the increase of option satisfaction. It proves that from an overall point of view, learners have relatively high user attitudes and behavioral willingness toward learn platforms. Among them, in the dimension of behavioral willingness, the people who strongly agree with the choice of question 1 are the most, accounting for 54.1%. It proves that many students are willing to continue

to use this system for animation learning in the future, which is a very good phenomenon. Among the four questions in these two dimensions, question 2 on user attitudes has the largest number of people who choose to disagree, accounting for 2.7%. It shows that 2.7% of learners do not like the design of the system.

(4) *Comprehensive Analysis of Usage Experience.* In this experiment, the evaluation of the above four dimensions is comprehensively summarized, and the proportion of the number of people who choose each option for the two questions in each dimension is averaged, and Table 3 is obtained.

From Table 3, we can know the average number of people who choose each option in each dimension, and we can also know the average number of people who choose each option in the four dimensions. Among the four dimensions, the average proportion of people who choose to agree is 49.5%, and the proportion of people who choose to disagree is 1.81%. It can be seen that most learners are generally satisfied with the experience of using the system, and only a small number of people are dissatisfied. It proves that the animation learning platform designed in this article is quite helpful for learners.

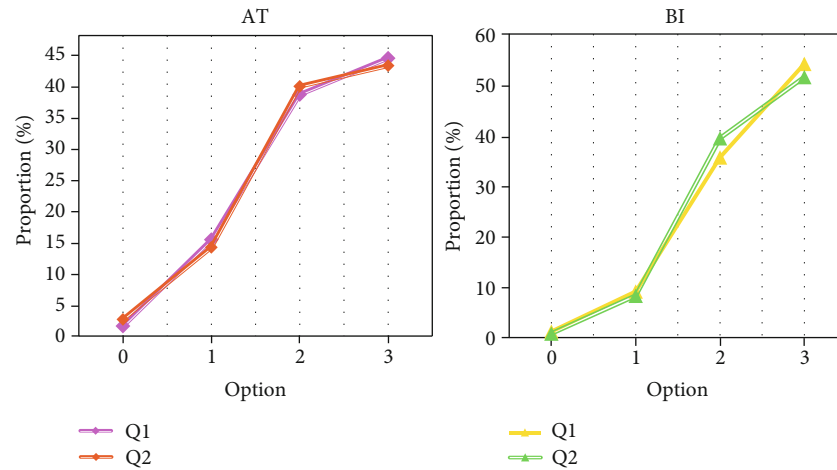


FIGURE 10: Survey results of user attitudes and behavior intentions.

TABLE 3: Comprehensive analysis table.

	Disagree	A little agree	General agreement	Quite agree
PEU	3%	12.9%	36.2%	47.9%
PU	1.1%	13.45%	31.95%	53.5%
AT	2.15%	14.8%	39.25%	43.8%
BI	1%	8.7%	37.5%	52.8%
Comprehensive	1.81%	12.46%	36.23%	49.5%

#### 4. Discussion

With the innovation and development of information and communication technology, human society has begun to enter the era of big data. It is possible to identify and record more types of data on a larger scale. Through the analysis and processing of the sent data, it is possible to dig deeper into the inherent information and core values. The education field is regarded as an important application field of big data. The close integration of big data application and education field is the actual demand and future trend of my country's education development. Animation education is a product of the development of the animation industry to a certain extent. Animation education supports the development of the animation industry and provides talents for the animation industry. Combining big data technology with animation education technology is believed to help cultivate more outstanding talents in the field of animation education.

#### 5. Conclusion

Big data is a product of the Internet era and is of great significance to many fields. And animation education is an important part of the development of the animation industry, and it transports talents to the animation industry. This article studies the animation education innovation based on big data. This article introduces the background, research significance, and related methods of big data and animation education. And the combined two expound the innovative

method of animation education based on big data. Finally, an animation education platform was designed based on big data, and a questionnaire was made using the Technology Acceptance Model (TAM). It investigates the use of the learning platform of this article by learners of animation majors in four universities in a certain area. Finally, I found that among the four dimensions of TAM's options, the people who strongly agree with them are the most. This proves that most learners have a good use of the learning platform, and the learning platform is very helpful to most learners. The next job is to investigate learners' suggestions for improvement of the animation learning platform and further improve the functions and design of the platform and then promote the animation learning platform to more animation learners.

#### Data Availability

Data sharing not applicable to this article as no datasets were generated or analyzed during the current study.

#### Conflicts of Interest

The authors declare that they have no conflicts of interest.

#### References

- [1] C. Jian, V. Popescu, N. Adamo-Villani, S. W. Cook, K. A. Duggan, and H. S. Friedman, "Animation stimuli system for research on instructor gestures in education," *IEEE Computer Graphics & Applications*, vol. 37, no. 4, pp. 72–83, 2017.
- [2] M. Shreesha and S. K. Tyagi, "Effectiveness of animation as a tool for communication in primary education: an experimental study in India," *International Journal of Educational Management*, vol. 32, no. 7, pp. 1202–1214, 2018.
- [3] T. Pinto, D. Castro, M. Bringuente, H. C. Sant'Anna, T. V. Souza, and C. C. Primo, "Educational animation about home care with premature newborn infants," *Revista Brasileira de Enfermagem*, vol. 71, Supplement 4, pp. 1604–1610, 2018.
- [4] N. M. Suki and N. M. Suki, "Determining students' behavioural intention to use animation and storytelling applying

- the UTAUT model: the moderating roles of gender and experience level,” *The International Journal of Management Education*, vol. 15, no. 3, pp. 528–538, 2017.
- [5] M. Farrokhnia, R. Meulenbroeks, and W. Joolingen, “Student-generated stop-motion animation in science classes: a systematic literature review,” *Journal of Science Education and Technology*, vol. 29, no. 6, pp. 797–812, 2020.
- [6] D. Earnest and J. M. Amador, “Lesson planimation: prospective elementary teachers’ interactions with mathematics curricula,” *Journal of Mathematics Teacher Education*, vol. 22, no. 1, pp. 37–68, 2019.
- [7] H. Yim, “Promoting the comic arts education in the context of community engagement,” *The Korean Journal of Animation*, vol. 13, no. 3, pp. 116–140, 2017.
- [8] Kim Jeeyoun, Choi Yoomi, Yoomi et al., “A study on the educational effect of smoking prevention education animation for preschoolers by 1 week delayed recall,” *The Korean Journal of Animation*, vol. 13, no. 2, pp. 62–74, 2017.
- [9] Y. H. Kim, H. Lee, M. J. Jung, and H. Jung, “The effects of flash animation facilitated oral self care education on the incidence of oral mucositis and performance of self-care in pediatric cancer patients undergoing chemotherapy,” *Journal of the Korean Society of Maternal & Child Health*, vol. 21, no. 2, pp. 130–138, 2017.
- [10] K. Upasana, V. Elizabeth, B. Sivakumar, and N. Prince, “Red cell indexes made easy using an interactive animation: do students and their scores concur?,” *Advances in Physiology Education*, vol. 42, no. 1, pp. 50–55, 2018.
- [11] Y. Mi, “Haptic VR contents of art education for children : focused on "Hephys" VR,” *The Korean Journal of Animation*, vol. 13, no. 3, pp. 62–79, 2017.
- [12] C. S. Ripoll, R. Oparka, A. Campbell, and C. Erolin, “The cell cycle: development of an eLearning animation,” *Journal of Audiovisual Media in Medicine*, vol. 40, no. 1, pp. 13–20, 2017.
- [13] L. Xu, C. Jiang, J. Wang, J. Yuan, and Y. Ren, “Information security in big data: privacy and data mining,” *IEEE Access*, vol. 2, no. 2, pp. 1149–1176, 2017.
- [14] S. Rajendran, O. I. Khalaf, Y. Alotaibi, and S. Alghamdi, “MapReduce-based big data classification model using feature subset selection and hyperparameter tuned deep belief network,” *Scientific Reports*, vol. 11, article 24138, 2021.
- [15] L. Kuang, F. Hao, L. T. Yang, M. Lin, C. Luo, and G. Min, “A tensor-based approach for big data representation and dimensionality reduction,” *IEEE Transactions on Emerging Topics in Computing*, vol. 2, no. 3, pp. 280–291, 2014.
- [16] Z. Yaoxue, “A survey on emerging computing paradigms for big data,” *Chinese Journal of Electronics*, vol. 26, no. 1, pp. 1–12, 2017.
- [17] A. Kusiak, “Smart manufacturing must embrace big data,” *Nature*, vol. 544, no. 7648, pp. 23–25, 2017.
- [18] R. Sahal, S. H. Alsamhi, K. N. Brown, D. O’Shea, and B. Alouffi, “Blockchain-based digital twins collaboration for smart pandemic alerting: decentralized COVID-19 pandemic alerting use case,” *Computational Intelligence and Neuroscience*, vol. 2022, Article ID 7786441, 2022.
- [19] O. I. Khalaf and G. M. Abdulsahib, “Optimized dynamic storage of data (ODSD) in IoT based on blockchain for wireless sensor networks,” *Peer-to-Peer Networking and Applications*, vol. 14, no. 5, pp. 2858–2873, 2021.
- [20] H. Xing, A. Qian, R. C. Qiu et al., “A big data architecture design for smart grids based on random matrix theory,” *IEEE Transactions on Smart Grid*, vol. 8, no. 2, pp. 674–686, 2017.
- [21] Y. Wang, L. A. Kung, and T. A. Byrd, “Big data analytics: understanding its capabilities and potential benefits for healthcare organizations,” *Technological Forecasting & Social Change*, vol. 126, pp. 3–13, 2018.
- [22] J. Liu, Q. Chen, and X. Tian, “3D virtual animation instant network communication system design,” *Wireless Communications and Mobile Computing*, vol. 2021, Article ID 9999113, 2021.

## Research Article

# Power Grid Low Carbon Collaborative Planning Method Using Improved Cat Swarm Optimization Algorithm in Edge Cloud Computing Environment

Xiang Li <sup>1</sup>, Chong Guo <sup>2</sup>, Chengjun Li <sup>1</sup>, Tianyuan Xu <sup>1</sup>, and Songyu Wu <sup>1</sup>

<sup>1</sup>Electric Power Research Institute, State Grid Liaoning Electric Power Co. Ltd., Shenyang, Liaoning 110006, China

<sup>2</sup>School of Information Science and Engineering, Shenyang Ligong University, Shenyang, Liaoning 110159, China

Correspondence should be addressed to Chong Guo; guochong5189@sylu.edu.cn

Received 5 January 2022; Revised 26 January 2022; Accepted 15 February 2022; Published 7 March 2022

Academic Editor: Shalli Rani

Copyright © 2022 Xiang Li et al. This is an open access article distributed under the Creative Commons Attribution License, which permits unrestricted use, distribution, and reproduction in any medium, provided the original work is properly cited.

The current power grid planning mostly realizes the calculation and analysis based on the factors of operation reliability or operation economy, but low-carbon green operation has become the main melody of power system development. Aiming to support the green and reliable operation of the power grid, this paper proposes a power grid low-carbon collaborative planning method based on improved cat swarm optimization algorithm. First, the carbon emission characteristics of the whole cycle of power grid construction are analyzed on the edge side, and a power grid planning model including environmental, economic, and reliability is constructed; on the cloud side, the cat swarm optimization algorithm is improved based on quantum mechanics and chaotic algorithm to achieve efficient solution to the power grid low-carbon planning model, which can support the stable and sustainable operation. Finally, the simulation experiment is realized based on IEEE 39 bus system. In this experiment, the construction cost and carbon emission of the proposed collaborative planning method are 23 million yuan and 2.28 t/MWh, respectively, which can reduce carbon emission while optimizing the construction cost and maintaining the low-carbon and stable operation.

## 1. Introduction

Traditional power grid planning is to formulate the planning scheme of the area where the power system is located on the basis of meeting the constraints of power balance, taking the load demand as the goal, taking safety, reliability, economy, and rationality as the basic conditions, and taking the location and capacity of power supply and power grid structure as the main contents [1, 2]. Reasonable power grid planning scheme plays a vital role in power grid construction and system operation.

In recent years, in order to improve global warming and maintain stable energy storage, green and sustainable energy supply strategy has become an important research object in power-related industries [3–5]. Power industry has significant carbon locking effect, which requires that the economy of the system and the benefits of carbon emission reduction should be included in power grid planning.

At the same time, vigorously developing renewable energy is an important demand for low-carbon transformation of social energy system. Large scale clean energy grid connection is an important feature of new energy power system. The proportion of renewable energy in the energy consumption structure in 2050 is expected to exceed 60%. Furthermore, as the main carbon emission source in the power industry, the low-carbon development planning of the power generation side has attracted extensive attention of scholars at home and abroad [6, 7].

In the traditional planning method, the goal of power grid planning is to achieve stable and reliable power supply. In addition to considering the reliability and economy, the new power system planning under the carbon trading environment should also include the carbon level into the evaluation system [8]. The essence of the evaluation decision-making of the model is the tripartite game of economic indicators, reliability indicators, and environmental indicators

[9]. How to combine carbon level assessment with power system planning decision-making [10], the establishment of low-carbon assessment system is the primary problem to ensure the optimal planning of new power system.

In view of the existing problems, in order to realize the low-carbon and efficient steady-state operation of power system, this paper proposes a collaborative planning method to realize the low-carbon sustainable development of power grid based on the efficient computing mode of cloud edge collaboration, which can effectively control the carbon emission content of power grid and ensure the green sustainable state of power grid. The main contributions of this paper are as follows:

- (1) Fully analyze the carbon emission characteristics of power transmission and transformation equipment in the power grid in the whole life cycle on the edge side, then establish the carbon emission evaluation model of equipment in the whole life cycle, model the network loss based on DC power flow, and embed it into the power grid planning model to provide reliable and comprehensive low-carbon power grid model support for cloud side planning solution
- (2) On the cloud side, the parameter update of cat swarm optimization (CSO) algorithm is improved based on quantum mechanics and chaos algorithm to solve the problem of local optimization of traditional algorithm. In the later stage of algorithm iteration, it can save population resources, improve the search ability of local optimization and the accuracy of global search, and then improve the efficiency of planning problem solving

The main contents of the rest of the paper are arranged as follows. The second section introduces the corresponding research on power grid low-carbon planning; the third section combs the overall framework of the paper; the fourth section realizes the simulation verification based on the improved standard example; the fifth section is the conclusion of this paper.

## 2. Related Work

Reasonable and effective planning methods for power grid to realize low-carbon economy will help to understand the actual low-carbon development level of power grid, feedback the implementation effect of low-carbon measures, and find the potential of power grid construction and improvement [11, 12]. And the research on power grid planning method and evaluation under the low-carbon development goal has very important practical significance for guiding the planning, construction, operation, and management of low-carbon power system.

The traditional linear programming model is essentially a nonlinear multiobjective optimization problem. At present, the existing power grid planning research only analyzes and discusses the reliability index or economic index, including the operation safety, power supply reliability,

investment scale, and economic return after the power grid is put into operation.

At present, China's carbon dioxide emissions from electricity account for 38.73% of China's total carbon emissions from fossil energy [13]. Therefore, on the premise of adapting to the national economic development, it is an urgent problem to realize the adjustment of power energy structure and strategic planning and the road of sustainable development of power under the low-carbon mode [14].

Therefore, it is particularly important to introduce environmental indicators into the construction of planning model [15, 16]. In the power grid planning, the key issue for the energy system is to promote the clean energy transformation of the energy strategy of building a "national network" by introducing the analysis of carbon emission characteristics.

In fact, the contribution of power grid links to the realization of low-carbon power cannot be ignored [17, 18]. A reasonable power grid structure can not only reduce the power grid operation energy consumption but also reduce the comprehensive carbon emission intensity at the power generation side.

The research on low-carbon power grid planning is mainly divided into the following three aspects [19, 20]: (1) establish a low-carbon benefit evaluation model to compare and analyze the low-carbon benefits of different power grid planning schemes; (2) introduce low-carbon power technology, analyze its influence mechanism on the change of optimization planning scheme; (3) internalize the carbon emission cost, embed the objective function of the traditional model, or increase the carbon emission constraints to establish a low-carbon power grid planning model.

At present, there is still a relative lack of research on low-carbon grid planning, taking into account the new energy grid connection for power grid reliability or construction economy analysis. Reference [21] proposed a multiobjective transmission network planning model based on flexibility and economy to realize the dual optimization of minimum construction cost and optimal renewable energy treatment; reference [22] takes the adaptability index of supply-demand balance as the objective function of unit planning stage and the adaptability index of operation state and network structure as the objective function of network planning stage to realize the dual planning of network source; a mixed integer linear stochastic model is proposed in reference [23], which is used for the optimal expansion planning of distribution network and green energy devices to support the reliable and stable state; reference [24] is oriented to the analysis of effective deployment of green energy in urban microgrid with reliable power supply and optimal operation as the objective function.

However, the above literature lacks the characteristic analysis of carbon emission in the planning model. Considering only from the perspective of power grid reliability or operation economy, the planning model is not complete, which is difficult to meet the development needs of green sustainability of current power grid.

Aiming to these problems, this paper analyzes the carbon emission characteristics of the whole cycle based on

the efficient treatment mode of cloud edge cooperation and constructs a power grid planning model including environmental, economic, and reliability; the improved CSO algorithm is introduced into the cloud to maintain the green and sustainable system.

### 3. Methodology Framework

**3.1. Overall Framework.** The processing and analysis mode of the integration of cloud computing and edge computing has strong data decision-making and analysis ability and can realize more accurate and fast model solving and calculation. Therefore, a power grid low-carbon planning method based on cloud side collaborative architecture to support the low-carbon sustainable operation of power grid is proposed. As shown in Figure 1, the low-carbon planning scheme under the cloud side collaborative architecture proposed in this paper includes two modules:

- (1) *Cloud Network Source Collaborative Planning Analysis.* With the help of cloud server cluster, the traditional CSO algorithm based on quantum mechanics and chaos algorithm is improved to form the hierarchical multi-objective model and power supply collaborative planning, solve the problem of local optimization in the traditional algorithm, and realize the low-carbon sustainability planning analysis of the current power grid
- (2) *Operation Characteristics and Model Analysis of Edge Network Source.* Aiming to better achieving the goal of power sustainability and green, taking into account the carbon emission characteristics of the whole life cycle of power grid planning, this paper establishes a green energy operation simulation model at the edge of the collaborative planning architecture to support the cloud to achieve efficient and accurate power grid low-carbon planning analysis

**3.2. Low Carbon Factor Analysis and Modeling of Power Grid at the Edge.** Aiming to better achieving the goal of sustainability and green, taking into account the carbon emission characteristics of the whole life cycle, this paper establishes a green energy operation simulation model at the edge of the collaborative planning architecture.

Taking wind power as an example, based on the historical output data, this paper simulates and generates the hourly sequential output sequence in line with the random output characteristics of new energy.

The wind speed model is

$$ds_{it} = -v_i(s_{it} - \bar{s}_i)dt + \sqrt{o(s_{it})}d\kappa_{it}, \quad (1)$$

$$o(s_{it}) = \frac{2v}{f(s)} \int_1^s (\bar{s} - x)f(x)dx, \quad (2)$$

where  $s_{it}$  is the simulated wind speed at time  $t$  of wind farm  $i$ ;  $v_i$  is the exponential attenuation coefficient of auto-correlation function of wind speed corresponding to wind

farm  $i$ ;  $\bar{s}_i$  is the average wind speed of wind farm  $i$ ;  $f(s)$  is the Weibull function of wind speed;  $d\kappa_{it}$  is a random number sequence with normal distribution.

The wind speed can be accumulated hourly according to  $ds_t$ :

$$s_{it} = s_{it-1} + ds_t. \quad (3)$$

The output of the wind farm is

$$P_{it} = m_{it}(1 - \xi_i)u_i(s_{it}j_{id}j_{is}), \quad (4)$$

where  $P_{it}$  is the output of wind farm  $i$  at time  $t$ ;  $m_{it}$  is the number of units available at time  $t$  of wind farm  $i$ ;  $\xi_i$  is the wake effect coefficient of wind farm;  $u_i$  is the output characteristic curve of wind turbine;  $j_{id}$  and  $j_{is}$  are the correction coefficients of daily and seasonal characteristics of wind speed, respectively.

**3.2.1. Life Cycle Carbon Emission Characteristics of Power Grid Planning.** The construction, operation, maintenance, and scrapping of a large number of power transmission and transformation equipment in the power grid will consume a lot of energy and produce carbon emissions. In this paper, the whole life cycle evaluation method is used to analyze each link of the power grid, which can more comprehensively and scientifically analyze the low-carbon planning and investment decision-making of the power grid.

The life cycle analysis of transmission equipment is shown in Figure 2.

Based on the analysis of the whole life cycle of transmission equipment, the carbon emission assessment model of the whole life cycle of transmission equipment can be established.

The whole life cycle carbon emission of transmission equipment can be decomposed into

$$\varepsilon_{ALL} = \varepsilon_C + \varepsilon_O + \varepsilon_M + \varepsilon_F + \varepsilon_D, \quad (5)$$

where  $\varepsilon_{ALL}$  is the carbon emission in the whole life cycle;  $\varepsilon_C$  is the carbon emission during construction;  $\varepsilon_O$  is the carbon emission in operation;  $\varepsilon_M$  is the carbon emission in maintenance;  $\varepsilon_F$  is the fault carbon emission;  $\varepsilon_D$  is the carbon emission from decommissioning.

Based on the above analysis, the investment cost model of new lines can be established by introducing carbon emission cost:

$$C = \sum_n^{N_{line}} (c_n^{line} + \sigma_n \varepsilon_n^{line}), \quad (6)$$

where  $N_{line}$  is the investment payback period of the line;  $c_n^{line}$  is the equivalent annual value of the line investment;  $\sigma_n$  is the carbon emission price in the  $n$  year;  $\varepsilon_n^{line}$  is the annual equivalent carbon emission of the line in year  $n$ . The line operation carbon emission caused by network loss is considered separately.  $\varepsilon_n^{line}$  and  $c_n^{line}$  can be calculated by the



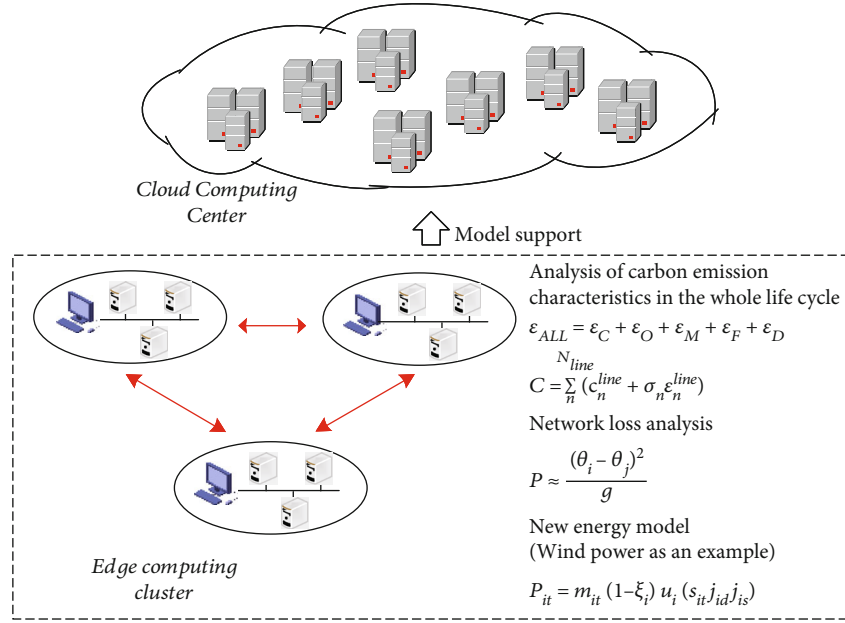


FIGURE 1: Overall architecture of the proposed method.

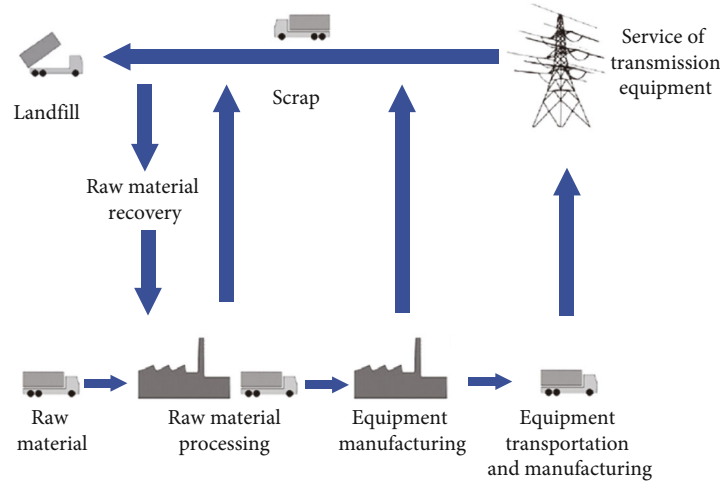


FIGURE 2: Life cycle of transmission equipment.

following formula:

$$\varepsilon_n^{\text{line}} = \frac{(\varepsilon_{\text{ALL}} - \varepsilon_O)}{N_{\text{line}}}, \quad (7)$$

$$c_n^{\text{line}} = \frac{(1 + \alpha)^{N_{\text{line}} - n} \alpha}{(1 + \alpha)^{N_{\text{line}}} - 1} C', \quad (8)$$

where  $C'$  is the investment amount of the line;  $\alpha$  is the capital discount rate.

**3.2.2. Reduce Power Grid Loss.** Power grid loss will increase additional carbon emissions on the power generation side. Reducing loss is the most direct low-carbon measure in power grid links. In this paper, the network loss is modeled

based on DC power flow and embedded into the power grid planning model to realize the collaborative optimization of network loss management and power grid planning [25].

Under the normal operation of high-voltage transmission network, the node voltage amplitude is close to 1.0 pu. Therefore, combined with the traditional AC power flow equation, the expression of active power loss  $P$  is

$$P \approx \frac{(\theta_i - \theta_j)^2}{g}, \quad (9)$$

where  $\theta_i - \theta_j$  is the voltage phase angle difference;  $g$  is the conductivity of the line.

Equation (7) shows that the line network loss can be approximately expressed as the product of line conductance

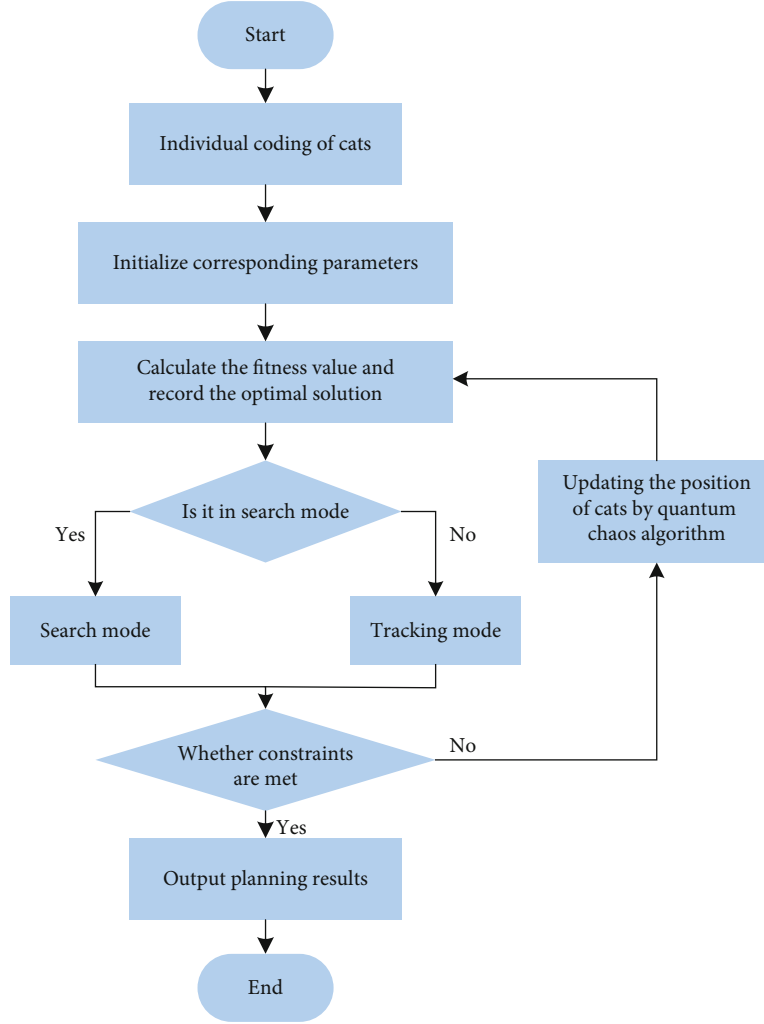


FIGURE 3: Power grid planning flow chart based on improved cat swarm algorithm.

and the square of node voltage phase angle difference, that is, the active power mainly depends on the node voltage phase angle difference.

**3.3. Cloud Side Network Source Collaborative Planning Model Optimization.** In this paper, the economy, reliability, and environmental benefits are comprehensively considered in order to build a hierarchical multiobjective collaborative planning model; based on the server cluster, the improved CSO algorithm is adopted to realize efficient multiobjective optimization and ensure the green sustainability of power grid planning and analysis.

**3.3.1. Network Source Collaborative Planning Model.** The low-carbon power grid planning model proposed in this paper is a bilevel planning model. The planning objectives and contents of each layer model are as follows.

- (1) The upper model is mainly the construction cost model. The planning economy considers the construction cost and the operation cost after putting into operation, mainly including power grid investment cost. The upper model is as follows:

$$C_1 = C_{NCG} + C_{NL} + C_{LS} + C_{NC} + C_{NE}, \quad (10)$$

where  $C_{NCG}$  is the construction cost of power grid peak shaving power plant;  $C_{NL}$  is the construction cost of power grid line;  $C_{LS}$  is the cost of grid loss;  $C_{NC}$  is carbon emission cost;  $C_{NE}$  is the power purchase cost.

The  $C_{NCG}$  calculation model of construction cost of power grid peak shaving power plant is

$$C_{NCG} = \sum_{i=1}^I \mu_{NCG,i} x_i = \sum_{i=1}^I B_{NCG,i} \cdot \frac{r(r+1)^{NI}}{(r+1)^{NI}} \cdot x_i, \quad (11)$$

where  $x_i$  is a 0-1 decision variable, indicating the operation status for peak shaving generator unit, where 0 represents shutdown and 1 represents operation;  $\mu_{NCG,i}$  refers to the annual value such as the investment cost of the generating unit  $i$ ;  $I$  refers to the number of generator units to be added;  $B_{NCG,i}$  refers to the initial investment cost of the generating unit  $i$ ;  $r$  refers to the annual discount rate of the investment;  $NI$  refers to the planned service life.

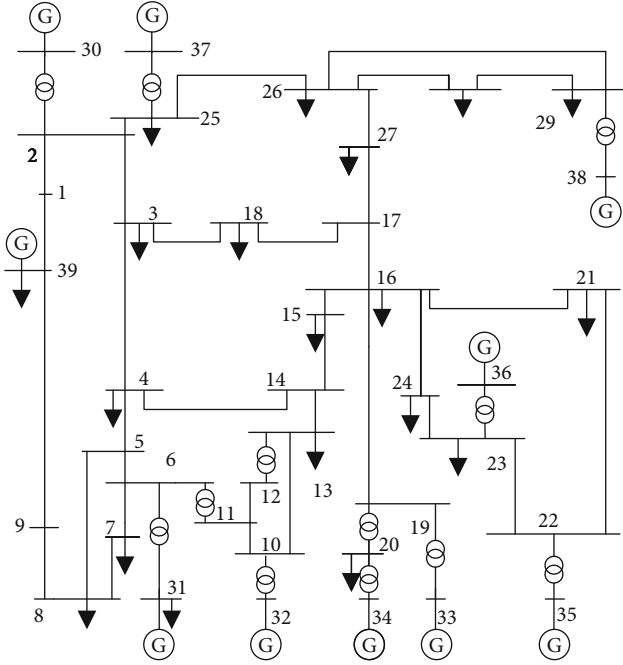


FIGURE 4: IEEE-39 bus power system.

TABLE 1: Characteristic parameters.

Generation type	Investment cost (¥/kW)	Operation cost (¥/MWh)	Fuel cost (¥/MWh)	Carbon emissions (t/MWh)
Wind power	8750	55	0	0
Solar energy	7850	75	0	0
Hydropower	25920	15	0	0
Nuclear power	17450	10	4	0
Gas	2990	35	100	0.75

The  $C_{NL}$  calculation model of power grid line construction cost is

$$\begin{aligned}
 C_{NL} &= \sum_{j=1}^J \mu_{NWT,j} y_j + \sum_{k=1}^K \mu_{NPV,k} z_k \\
 &= \sum_{j=1}^J B_{NWT,j} \cdot \frac{r(r+1)^{NJ}}{(r+1)^{NJ} - 1} \cdot y_j \\
 &\quad + \sum_{k=1}^K B_{NPV,k} \cdot \frac{r(r+1)^{NK}}{(r+1)^{NK} - 1} \cdot z_k,
 \end{aligned} \tag{12}$$

where  $y_j$  and  $z_k$  are 0-1 decision variables, indicating the operation status of grid connected lines of wind farm and photovoltaic power station;  $J$  and  $K$  refer to the number of grid connected lines of the wind farm and the number of parallel lines of the photovoltaic power station to be added;  $\mu_{NWT,j}$  and  $\mu_{NPV,k}$  are the equivalent annual values of the investment cost of the corresponding grid connected lines,

respectively;  $B_{NWT,j}$  and  $B_{NPV,k}$  are the corresponding initial investment costs, respectively;  $NJ$  and  $NK$  are the planned service life of corresponding lines, respectively.

The calculation model of power grid loss cost  $C_{LS}$  is

$$C_{LS} = \tau \sum_{d=1}^D \sum_{t=1}^T I_{d,t}^2 R_d t, \tag{13}$$

where  $\tau$  represents the unit network loss electricity price, 10000 yuan/(kW·h);  $D$  is the total number of transmission lines used by the system;  $I_{d,t}$  is the current on line  $d$  in the corresponding period  $t$ ;  $R_d$  is the resistance of the corresponding line;  $T$  refers to the total number of time periods.

$C_{NC}$  calculation model of carbon emission cost

$$C_{NC} = \omega \sum_{i=1}^I \sum_{t=1}^T e_{NCG,i} P_{NCG,i} \Delta t, \tag{14}$$

where  $\omega$  represents the market carbon emission price;  $e_{NCG,i}$  is the carbon emission intensity per unit power of unit  $i$ ;  $P_{NCG,i}$  is the corresponding active output of the unit  $i$ .

The power purchase cost  $C_{NE}$  can be set to a constant.

(2) The lower level model is mainly the new energy power generation cost model. The cost mainly includes the generation maintenance cost and power abandonment loss of new energy generator units. The loss caused by grid connection and power abandonment is taken as the reference objective function of power grid planning

$$C_2 = C_{NG} + C_{NQ}. \tag{15}$$

The  $C_{NG}$  calculation model of new energy power generation maintenance cost is

$$C_{NG} = \sum_{t=1}^T \left[ c_{NG} \sum_{h=1}^H P_{h,t} \right] \Delta t, \tag{16}$$

where  $c_{NG}$  is the unit power generation maintenance cost, respectively;  $P_{h,t}$  is the actual active output of the new energy power generator set  $h$  for period  $t$ ;  $T$  is the total number of time periods in the whole year.

The  $C_{NQ}$  calculation model of power loss cost is

$$C_{NQ} = \sum_{t=1}^T \left[ c_{NQ} \sum_{h=1}^H (P_{h,t} - P_{h0,t}) \right] \Delta t, \tag{17}$$

where  $c_{NQ}$  is the unit loss cost;  $P_{h0,t}$  is the planned active output of unit  $h$  for period  $t$ ;  $T$  is the total number of time periods in the whole year.

(3) For the above two-layer model, the following constraints are proposed in this paper

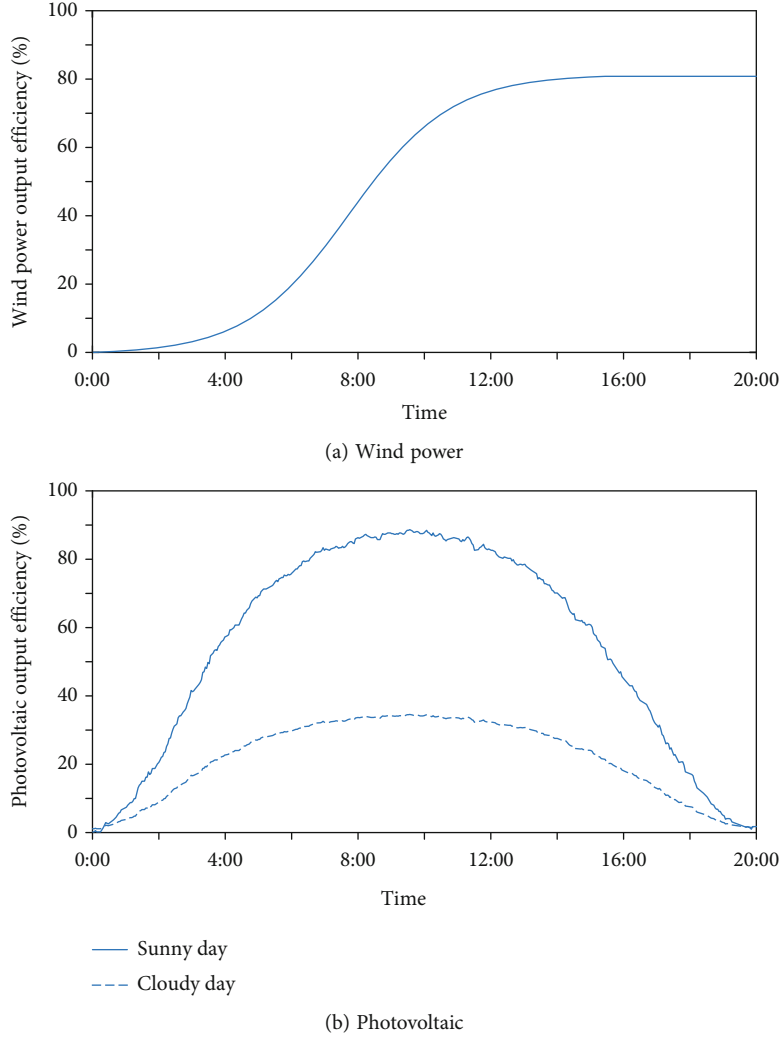


FIGURE 5: Output curve of new energy unit.

TABLE 2: Optimal planning schemes under different methods.

Method	New line ( $i \rightarrow j$ )	New green energy node and its unit capacity (MW)
The proposed method	21 $\rightarrow$ 27, 22 $\rightarrow$ 19, 17 $\rightarrow$ 26, 14 $\rightarrow$ 3, 5 $\rightarrow$ 8, 4 $\rightarrow$ 8, 2 $\rightarrow$ 8	22 (30), 21 (55), 17 (25), 14 (35), 5 (25), 4 (25)
Reference [21]	24 $\rightarrow$ 15, 24 $\rightarrow$ 14, 23 $\rightarrow$ 19, 14 $\rightarrow$ 2	24 (35), 23 (15), 18 (35), 14 (40), 5 (20)
Reference [22]	21 $\rightarrow$ 27, 16 $\rightarrow$ 3, 14 $\rightarrow$ 2, 11 $\rightarrow$ 3	21 (35), 16 (45), 14 (25), 11 (20)
Reference [24]	26 $\rightarrow$ 18, 17 $\rightarrow$ 4, 14 $\rightarrow$ 19	26 (20), 17 (35), 14 (25)

The power balance constraint formula is

$$P_t = A_t \theta_t, \quad (18)$$

where  $P_t$  refers to the injected power vector of the node in period  $t$ ;  $A_t$  refers to the admittance matrix of nodes in period  $t$ ;  $\theta_t$  refers to the phase angle vector of node voltage in period  $t$ .

The branch power flow constraint formula is

$$|P_{d,t}| \leq P_{d,\max}, \quad (19)$$

where  $P_{d,t}$  refers to the active power flow of branch  $d$  in period  $t$ ;  $P_{d,\max}$  is the upper limit value of branch  $d$  in period  $t$ .

The output constraint of generator set is

$$P_{NCG,\min} \leq P_{NCG,i} \leq P_{NCG,\max}, \quad (20)$$

where  $P_{NCG,i}$  refers to the corresponding active output of the unit  $i$ ;  $P_{NCG,\min}$  refers to the lower limit of active output corresponding to the unit  $i$ ;  $P_{NCG,\max}$  is the upper limit of active output corresponding to the unit  $i$ .

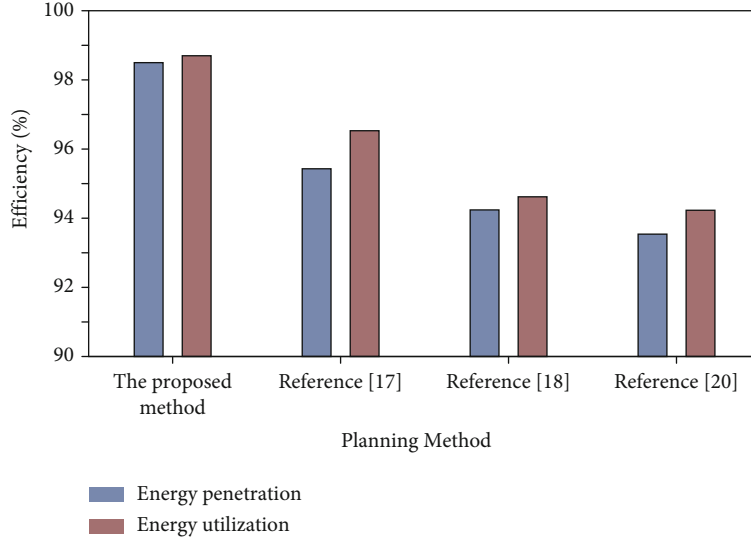


FIGURE 6: Grid connection of new energy under different methods.

TABLE 3: Analysis of economic and environmental indicators of different planning methods.

Method	Carbon emissions (t/MWh)	Total construction cost (100 million ¥)
The proposed method	2.28	0.23
Reference [21]	3.12	0.73
Reference [22]	4.85	1.23
Reference [24]	5.81	0.43

#### (4) Multiobjective programming model

The hierarchical multiobjective planning model is as follows:

$$\begin{cases} \min C_1 = C_{NCG} + C_{NL} + C_{LS} + C_{NC} + C_{NE}, \\ \min C_2 = C_{NG} + C_{NQ}. \end{cases} \quad (21)$$

Further, rewrite as

$$L - \min_{s \in S} [F_\nu C_\nu(s)]_{s=1}^L, \quad (22)$$

where  $C_\nu(s)$  ( $\nu = 1, \dots, L$ ) is the objective function;  $F_\nu$  ( $\nu = 1, \dots, L$ ) is used to mark that the objective function is at the  $\nu$  priority level; meanwhile,  $F_\nu \geq F_{\nu+1}$  ( $\nu = 1, \dots, L$ ) indicates that level  $\nu$  takes precedence over level  $\nu + 1$ ;  $s \in S$  represents a set of constraints;  $L - \min_{s \in S}$  represents the minimization condition, that is, the minimization analysis and calculation are carried out in the order of  $F_1, F_2, \dots, F_L$ .

The characteristic of hierarchical multiobjective optimization model is that each goal in the model does not have the same priority in the whole model and has targeted priority levels, and only one goal is considered in each level.

**3.3.2. Construction of Mathematical Model Based on Improved Cat Swarm Optimization Algorithm.** The essence of power grid multiobjective optimization algorithm is to obtain the equilibrium solution of double-layer function at the same time. The optimization of the model can be realized by means of intelligent algorithms such as genetic algorithm and CSO algorithm [26–28]. The CSO algorithm can be updated by cats in different modes according to the corresponding speed and position formulas. Through the continuous updating of the global optimal value and local optimal value, the optimal solution of the problem to be solved is finally obtained [29].

The speed and position update formula of the cat in the iterative process is

$$V_{j,k}^{i+1} = V_{j,k}^i + \alpha \times \beta \times (G_{\text{best}}^i - V_{j,k}^i), \quad (23)$$

$$G_{j,k}^{i+1} = G_{j,k}^i + V_{j,k}^{i+1}, \quad (24)$$

where  $V_{j,k}^{i+1}$  represents the updated velocity component of the  $j$ -th cat in the  $k$  dimensional space;  $\alpha$  is a constant;  $G_{\text{best}}^i$  represents the global optimal solution after the  $i$ -th iteration;  $\beta$  is the random number between  $[0, 1]$ ;  $G_{j,k}^{i+1}$  represents the updated position component of the  $j$ -th cat in the  $k$  dimensional space;  $i$  is the number of iterations.

However, it should be noted that when solving the problem based on CSO algorithm, the cats in tracking mode can be randomly distributed at any position in the search space, which has the problem of local optimization.

Aiming at solving this problem, the quantum mechanical model is combined with the CSO algorithm to optimize the individual position in the cat population by using the characteristics of quantum. In the quantization process, the cat in the tracking mode takes the individual optimal position and the global optimal position as the goal and updates the cat's position by constantly moving in the delta potential well.

Quantum mechanics is an important branch of physics in the field of micro matter. It is not only an important part of the four mechanics of physics but also widely used in other disciplines [30]. The quantum in the algorithm has the characteristics that individuals in other algorithms do not have: noncloning, superposition, entanglement, and collapse. Due to the randomness of the speed and position of cats in the delta potential well, cats in the tracking mode can be randomly distributed at any position in the search space in the iterative process of cat group optimization, which improves the ability to get rid of local optimal points. The update expression of individual position in quantum space is

$$G_{j,k}^{i+1} = D_{j,k}^i + dc^i \left| M_k^i - G_{j,k}^i \right| \ln(y_1^{-1}), \quad (25)$$

$$D_{j,k}^{i+1} = y_2 H_{j,k}^i + (1 - y_2) W_k^i, \quad (26)$$

$$q^i = q_1 - (q_1 - q_2) \frac{i}{i_m}, \quad (27)$$

$$b = \begin{cases} -1 & y_3 \leq 0.5, \\ 1 & y_3 > 0.5, \end{cases} \quad (28)$$

$$(O_1^i, O_2^i, \dots, O_k^i) = \frac{1}{n} \left( \sum_{j=1}^n H_{j,1}^i, \sum_{j=1}^n H_{j,2}^i, \dots, \sum_{j=1}^n H_{j,k}^i \right), \quad (29)$$

where  $G_{j,k}^{i+1}$  represents the updated position component of the  $j$ -th cat in  $k$  dimensional space;  $i$  is the number of iterations;  $q^i$  is the expansion compression factor of the  $i$ -th iteration;  $O_k^i$  is the optimal location center of the population in the  $k$  dimensional space of the  $i$ -th iteration;  $y_1$ ,  $y_2$ , and  $y_3$  are random numbers of  $[0, 1]$ ;  $H_{j,k}^i$  is the historical optimal position component of individual  $j$  in  $i$ -th iteration  $k$  dimensional space;  $q_1$  and  $q_2$  are the initial and end values of expansion compression factors, respectively. In this paper,  $q_1 = 1.25$  and  $q_2 = 0.62$ ;  $n$  is the population number;  $i_m$  is the maximum number of traces.

Aiming to ensuring the optimal performance of full cycle optimization, through the research and analysis of chaos, it is used to improve the update steps of the algorithm based on this. Therefore, on the basis of quantum optimization cat swarm algorithm, by introducing tent mapping and using its randomness and ergodicity, CSO algorithm can avoid premature. The individual position update expression for each cat is

$$g_{j,k}^{i+1} = \begin{cases} 2g_{j,k}^i & 0 \leq g_{j,k}^i \leq 0.5, \\ 2(1 - g_{j,k}^i) & 0.5 \leq g_{j,k}^i \leq 1, \end{cases} \quad (30)$$

where  $g_{j,k}^i \in [0, 1]$ , and the mutual mapping transformation of chaotic vector  $Og_{j,k}^i \in [a, b]$  can be realized based on the following formula.

$$g_{j,k}^i = \frac{Og_{j,k}^i - 1}{b - a} == \frac{a + g_{j,k}^i(b - a) - 1}{b - a}. \quad (31)$$

Although the combination of quantum mechanics and chaotic mapping theory and algorithm can balance the global and local search ability. However, the fixed mixing rate will weaken its balance effect in the early or late stage of the algorithm, so that the local and global search ability cannot achieve satisfactory results.

According to equation (30), this paper improves the value method of the mixing rate. The value of the mixing rate gradually decreases with the increase of the number of iterations, so that the number of individuals in the search mode can gradually increase with the increase of the number of iterations.

$$\eta^i = \eta_{\max}(\alpha)^{1+i/i_m - \cos(i/i_m)}, \quad (32)$$

where  $\eta_{\max}$  is the maximum value of mixing rate;  $\alpha$  is a fixed constant;  $i$  is the number of iterations;  $i_m$  is the maximum number of traces.

In the search mode of quantum chaotic cat swarm algorithm, the individuals with different fitness values have the same amount of variation, which makes the algorithm cannot make full use of the individuals with optimal fitness values in the search of local optimal values, thus, reducing the accuracy of local optimal solutions. As the number of individuals in the mutation pattern changes, the more the algorithm can adapt to the global variation, and the better the algorithm can adapt to the change of the number of individuals in the mutation pattern. The formula for copying an individual is

$$\zeta_j = \left[ 1 - \left| \frac{\text{fitness}_j}{\sum_{j=1} \text{fitness}_j} \right| \right] \times \zeta_{\text{sum}}, \quad (33)$$

where  $\zeta_j$  is the number of replicates of cat  $j$ ;  $\zeta_{\text{sum}}$  is the total number of replicates in the memory pool;  $\text{fitness}_j$  is the fitness value of cat  $j$ .

Figure 3 is the flow chart of low-carbon power grid collaborative planning method using quantum chaotic cat swarm algorithm proposed in this paper.

## 4. Experiment and Analysis

The simulation experiments all run in the same environment. The CPU processor is Intel (R) core (TM) i5-5200u and the fuselage memory is 12.0 GB. The simulation experiment and verification analysis are completed by MATLAB software.

**4.1. Experimental Background and Parameters.** IEEE 39 node is used as an example to realize the optimization experimental analysis. The simulation experimental system diagram is shown in Figure 4. There are 39 independent nodes in the system, of which 17 nodes have the installation conditions of renewable energy power supply. The IEEE 39 node standard example includes 39 terminal nodes (10

generator nodes, 21 load nodes, and 12 transformer nodes) and 46 power lines, of which 17 nodes have the installation conditions of renewable energy power supply.

The purpose of model optimization is to ensure the coordination and consistency between power supply and power grid planning and finally realize the low-carbon sustainable operation of power grid.

The unit operation characteristic parameters of various power generation modes are shown in Table 1. There is no difference in the parameters of the same type of unit set by each generator. The maximum capacity of reallocated to be connected to each node is 85 MW, and the allowable fluctuation range of node voltage is  $\pm 5\%$ . Where the transmission price is 0.43 yuan/kWh and the carbon trading price is 50 yuan/ton.

For more intuitive expression, the fan output curve and photovoltaic power generation output curve are given, as shown in Figure 5.

**4.2. Comparison of Different Optimization Objectives in Low Carbon Environment.** Aiming to comprehensively evaluate the clean and low-carbon characteristics, this paper further introduces two evaluation indexes such as green energy penetration  $\gamma$  and utilization efficiency  $\eta$  [31, 32]. Penetration efficiency  $\gamma$  refers to the proportion of the total power generation of green energy in the total power consumption of system load in the planning period, which represents the comprehensive utilization capacity of the system for renewable energy; utilization efficiency  $\eta$  refers to the ratio of the actual power generation of green energy to the maximum available power supply under natural conditions.

In this paper, reference [21], reference [22], and reference [24] are used as comparative methods to verify the optimality of the proposed method.

Table 2 shows the optimal planning schemes for IEEE 39 bus system under different analysis methods and describes the planned lines and deployment of new energy units accordingly.

Figure 6 shows the grid connection of new energy under different planning methods.

It can be seen from Table 2 and Figure 6 that the grid planning algorithm proposed can achieve efficient calculation and analysis of new energy grid connection. After planning, the green energy penetration  $\gamma$  and utilization efficiency  $\eta$  are 98.56% and 98.72%, respectively; the planning effect of the comparison method is obviously poor. The green energy permeability and utilization efficiency after planning in reference [24] are 93.54% and 94.23%, which are 5.02% and 4.49% lower than the results of the proposed algorithm.

The reason is that the algorithm proposed adopts the way of cloud edge cooperation to model and analyze the whole cycle of power grid construction carbon emission on the edge side, which makes the solution model more reliable and complete; in the cloud, CSO algorithm is improved based on quantum chaos algorithm to improve the processing and analysis efficiency of the planning model.

Furthermore, this paper also makes a quantitative analysis on the carbon emissions and construction costs of the results of different planning methods. Table 3 shows the comparison of the two indicators.

As shown in Table 3, the proposed planning method can achieve better carbon emission at lower construction cost, and the construction cost and carbon emission are 23 million yuan and 2.28 t/MWh, respectively; Compared with reference [21], the construction cost and carbon emission are optimized by about 50 million yuan and 0.84 t/MWh, respectively.

## 5. Conclusion

In order to support the power grid to realize low-carbon and stable operation, a power grid low-carbon planning method using improved CSO algorithm is proposed. Relying on the cloud side collaborative computing mode, this method integrates the carbon emission characteristics into the grid planning model on the edge side and effectively solves the low-carbon scale of power grid based on the improved CSO algorithm based on quantum chaos algorithm in the cloud, so as to avoid the model solution falling into a suboptimal solution. The simulation results show that the proposed collaborative planning method can achieve a more reliable and green power grid operation state under the condition of low construction cost.

The exploration and construction of carbon trading market have gradually become the focus of power market. The future research direction is to further consider the elements of low-carbon power market in the traditional planning model, and then establish a relatively complete new power system planning model.

## Data Availability

The data included in this paper are available without any restriction.

## Conflicts of Interest

The authors declare that there is no conflict of interest regarding the publication of this paper.

## Acknowledgments

This work was supported by Science and Technology Project of State Grid Corporation of China (Contract no: SGLNDKOOKJJS2100068).

## References


- [1] A. B. Birchfield, T. Xu, and T. J. Overbye, "Power flow convergence and reactive power planning in the creation of large synthetic grids," *IEEE Transactions on Power Systems*, vol. 33, no. 6, pp. 6667–6674, 2018.
- [2] Y. Luo, Y. Zhang, M. Tang et al., "A novel receiving end grid planning method with mutually exclusive constraints in alternating current/direct current lines," *Sustainability*, vol. 13, no. 13, article 7141, 2021.
- [3] J. Nieto-Martin, T. Kipouros, M. Savill, J. Woodruff, and J. Butans, "Technoeconomic distribution network planning using smart grid techniques with evolutionary self-healing network states," *Complexity*, vol. 2018, no. 1, Article ID 1543179, 18 pages, 2018.

- [4] Y. Yang, J. Qiu, J. Ma, and C. Zhang, "Integrated grid, coal-fired power generation retirement and GESS planning towards a low-carbon economy – science direct," *International Journal of Electrical Power & Energy Systems*, vol. 124, no. 1, pp. 1–12, 2021.
- [5] A. Bilich, E. Spiller, and J. Fine, "Proactively planning and operating energy storage for decarbonization: recommendations for policymakers," *Energy Policy*, vol. 132, no. 12, pp. 876–880, 2019.
- [6] L. Olmos Camacho, M. L. Rivier Abbad, and J. I. Pérez Arriaga, "Transmission expansion benefits: the key to redesigning the regulation of electricity transmission in a regional context," *Economics of Energy & Environmental Policy*, vol. 7, no. 1, pp. 47–62, 2018.
- [7] B. Ee and Z. Li, "Renewable energy based self-healing scheme in smart grid," *Energy Reports*, vol. 6, no. 1, pp. 166–172, 2020.
- [8] S. Karimi-Arpanahi, M. Jooshaki, M. Moein-Aghtaie, M. Fotuhi-Firuzabad, and M. Lehtonen, "Considering forecasting errors in flexibility-oriented distribution network expansion planning using the spherical simplex unscented transformation," *IET Generation, Transmission and Distribution*, vol. 14, no. 24, pp. 5970–5983, 2020.
- [9] S. Maximov, G. Harrison, and D. Friedrich, "Long term impact of grid level energy storage on renewable energy penetration and emissions in the Chilean electric system," *Energies*, vol. 12, no. 6, article 1070, 2019.
- [10] Z. K. Pecanak, M. Stadler, and K. Fahy, "Efficient multi-year economic energy planning in microgrids," *Applied Energy*, vol. 255, no. 1, pp. 113771–113779, 2019.
- [11] Z. G. Lu, J. T. Qi, B. Wen, and X. Li, "A dynamic model for generation expansion planning based on conditional value-at-risk theory under low-carbon economy," *Electric Power Systems Research*, vol. 141, no. 1, pp. 363–371, 2016.
- [12] A. A. Majd, E. Farjah, and M. Rastegar, "Composite generation and transmission expansion planning toward high renewable energy penetration in Iran power grid," *IET Renewable Power Generation*, vol. 14, no. 9, pp. 1520–1528, 2020.
- [13] Z. X. Yu, M. S. Li, Y. P. Xu, S. Aslam, and Y. K. Li, "Techno-economic planning and operation of the microgrid considering real-time pricing demand response program," *Energies*, vol. 14, no. 15, pp. 1–28, 2021.
- [14] X. H. Yang, Z. X. Chen, X. Huang, R. Li, S. Xu, and C. Yang, "Robust capacity optimization methods for integrated energy systems considering demand response and thermal comfort," *Energy*, vol. 221, no. 1, article 119727, 2021.
- [15] A. Jain, P. Das, S. Yamujala, R. Bhakar, and J. Mathur, "Resource potential and variability assessment of solar and wind energy in India," *Energy*, vol. 211, no. 1, article 118993, 2020.
- [16] A. Thomas and P. Racherla, "Constructing statutory energy goal compliant wind and solar PV infrastructure pathways," *Renewable Energy*, vol. 161, no. 1, pp. 1–19, 2020.
- [17] M. Kristiansen, M. Korpås, and H. G. Svendsen, "A generic framework for power system flexibility analysis using cooperative game theory," *Applied Energy*, vol. 212, no. 1, pp. 223–232, 2018.
- [18] K. Imran, "Importance of GHG emissions assessment in the electricity grid expansion towards a low-carbon future: a time-varying carbon intensity approach," *Journal of Cleaner Production*, vol. 196, no. 1, pp. 1587–1599, 2018.
- [19] H. Aimie, R. Thomas, and W. Ian, "Consumer engagement in low-carbon home energy in the United Kingdom: implications for future energy system decentralization," *Energy Research & Social Science*, vol. 44, no. 1, pp. 362–370, 2018.
- [20] X. Chen, J. Lv, M. B. McElroy, X. Han, C. P. Nielsen, and J. Wen, "Power system capacity expansion under higher penetration of renewables considering flexibility constraints and low carbon policies," *IEEE Transactions on Power Systems*, vol. 33, no. 6, pp. 6240–6253, 2018.
- [21] Z. Chen, Y. Hu, N. Tai, X. Tang, and G. You, "Transmission grid expansion planning of a high proportion renewable energy power system based on flexibility and economy," *Electronics*, vol. 9, no. 6, p. 966, 2020.
- [22] M. Tang, J. Wang, and X. Wang, "Adaptable source-grid planning for high penetration of renewable energy integrated system," *Energies*, vol. 13, no. 13, pp. 3304–3326, 2020.
- [23] M. Jooshaki, H. Farzin, A. Abbaspour, M. Fotuhi-Firuzabad, and M. Lehtonen, "A model for stochastic planning of distribution network and autonomous DG units," *IEEE Transactions on Industrial Informatics*, vol. 16, no. 6, pp. 3685–3696, 2020.
- [24] C. N. Kang and S. H. Cho, "Thermal and electrical energy mix optimization (EMO) method for real large-scaled residential town plan," *Journal of Electrical Engineering and Technology*, vol. 13, no. 1, pp. 513–520, 2018.
- [25] D. Li, S. Yang, W. Huang, J. He, Z. Yuan, and J. Yu, "Optimal planning method for power system line impedance based on a comprehensive stability margin," *IEEE Access*, vol. 9, no. 1, pp. 56264–56276, 2021.
- [26] X. J. Ran, X. B. Zhou, M. Lei, W. Tepsan, and W. Deng, "A novel K-means clustering algorithm with a noise algorithm for capturing urban hotspots," *Applied Sciences*, vol. 11, no. 23, pp. 11202–11221, 2021.
- [27] Z. H. Zhang, F. Min, G. S. Chen, S. P. Shen, Z. C. Wen, and X. B. Zhou, "Tri-partition state alphabet-based sequential pattern for multivariate time series," *Cognitive Computation*, vol. 2021, no. 1, pp. 1–19, 2021.
- [28] W. Deng, X. X. Zhang, Y. Q. Zhou et al., "An enhanced fast non-dominated solution sorting genetic algorithm for multi-objective problems," *Information Sciences*, vol. 585, no. 1, pp. 441–453, 2022.
- [29] A. A. Abou El-Ela, R. A. El-Sehiemy, E. S. Ali, and A. M. Kinawy, "Minimisation of voltage fluctuation resulted from renewable energy sources uncertainty in distribution systems," *IET Generation Transmission & Distribution*, vol. 13, no. 12, pp. 2339–2351, 2019.
- [30] M. W. Li, J. Geng, W. C. Hong, and Y. Zhang, "Hybridizing chaotic and quantum mechanisms and fruit fly optimization algorithm with least squares support vector regression model in electric load forecasting," *Energies*, vol. 11, no. 9, pp. 1–22, 2018.
- [31] G. Kim, H. Shin, and H. Jin, "Probabilistic estimation of wind generating resources based on the spatio-temporal penetration scenarios for power grid expansions," *IEEE Access*, vol. 9, no. 1, pp. 15252–15258, 2021.
- [32] K. Parker and P. Barooah, "A probabilistic method for reserve sizing in power grids with high renewable penetration," *IEEE Transactions on Power Systems*, vol. 36, no. 3, pp. 2473–2480, 2021.



## Research Article

# KL-Detection: An Approach to Detect Network Outages Based on Key Links

Ye Kuang , Dandan Li, and Xiaohong Huang 

*School of Computer Science (National Pilot Software Engineering School), Beijing University of Posts and Telecommunications, Beijing 100876, China*

Correspondence should be addressed to Xiaohong Huang; [huangxh@bupt.edu.cn](mailto:huangxh@bupt.edu.cn)

Received 18 January 2022; Revised 23 January 2022; Accepted 18 February 2022; Published 7 March 2022

Academic Editor: Shalli Rani

Copyright © 2022 Ye Kuang et al. This is an open access article distributed under the Creative Commons Attribution License, which permits unrestricted use, distribution, and reproduction in any medium, provided the original work is properly cited.

Monitoring the states of network links is essential to detect network outages and improve Internet reliability. Currently, existing work detects network outages by monitoring all the links, which requires thousands of probes and large-scale measurements, resulting in high resource occupancy and cost. To solve this problem, this paper proposes the KL-Detection approach, which detects network outages via key links instead of all links. Firstly, we recognize the key links based on flow density, degree centrality, and probe-distance centrality. Next, based on the recognized key links, we give the critical value of their Round-Trip Time (RTT). Then, we detect the network outages by observing whether the RTT of the key link exceeds the critical value. Finally, we leverage two historical events to evaluate our approach, and the results demonstrate that our approach can detect the network outages effectively by only monitoring less than 0.06% of the links in detection area.

## 1. Introduction

The unprecedented growth of the Internet has resulted in an explosive increase in network security issues, such as network outages. Network outages inevitably degrade network connectivity and influence network performance [1–4]. For example, the network outage caused by censorship in 2011 blocked the Internet access of Libya [5]. Hence, the detection of network outages has become vital.

Over the years, several detection approaches have been proposed to detect network outages. These approaches are based on active probing, which deploy a large number of probes to monitor the changes in link performance (e.g., delay and connectivity). Specifically, Fontugne et al. detected the network outages by analyzing the Round-Trip Time (RTT) of all links in detection areas [6]. Quan et al. detected the network outages by deploying the probes to observe the connectivity of all links in edge networks [5]. Padmanabhan et al. detected the network outages by using ThunderPing [7] to measure the connectivity of all residential links in detection areas [7].

The above work detected the network outages by monitoring the performance of all links in detection area. How-

ever, they lead to high resource occupancy and cost in practice. The reasons lie in the following: (1) monitoring the network performance of all links needs to perform a bulk of measurement tasks. These tasks will inject extra traffic into the network, which may occupy the link bandwidth, reduce the network transmission speed, and increase the network burden [8, 9]. (2) Monitoring all links in detection area needs to deploy more probes, and managing the probes is costly for network operators (e.g., periodic maintenance and electricity costs). Thus, how to reduce the resource occupancy and cost by reducing the number of monitoring links without compromising the validity of outage detection is a challenge.

Previous work of traffic monitoring provided initial inroads to address this challenge [10, 11]. Their research results showed that a few key links that deliver larger traffic flows can well represent the traffic load information of all links in the detection area. However, focusing on these key links recognized by traffic load information is inadequate to detect network outages.

This is because detecting the network outages also needs to focus on the changes in link performance, e.g., RTT [4,

12]. In fact, due to the presence of noise and the interaction between the RTT of links, the fluctuation of RTT of each link is different. Only the link whose RTT fluctuation can notably and accurately reflect the deviations between the state of network outages and normal state can be regarded as the key link. Based on the above analysis, recognizing the key links for network outage detection should consider two aspects, one is the traffic load information, another is the factors affecting the RTT of link.

To achieve it, we use the number of flows going through the links to describe the traffic load information and use connected relation as well as the position of the link to describe the factors affecting the RTT of link. The reasons are as follows: (1) the number of flows going through the links describes the ability of links delivering traffic flows [13]. The links delivering larger flows can approximatively represent the traffic load information of all links in the detection area [12]. (2) The RTT of links will be affected by neighbor correlation [4]. The RTT of the links with poorer connected relations will not be significantly influenced by the neighbor correlation because these links have fewer adjacencies [4]. This causes that the RTT of these links may not fluctuate obviously in the case of a network outage. Hence, monitoring the links with poor connected relation may fail to detect the network outages. (3) With the distance between the probes and the nodes of links increases, the noise of measurements inflates [14]. Generally, the link is closer to the probe, and the RTT of the link we obtain is more accurate. Hence, monitoring the links close to the probes can accurately obtain the fluctuation of its RTT, which can detect network outages effectively.

After recognizing the key links, we monitor their RTT and detect the network outages finally. Our contributions are summarized as follows:

- (i) For all we know, this is the first work that leverages the key links to detect network outages. Our approach can reduce the number of monitoring links notably without compromising the validity of outage detection
- (ii) This paper proposes a key link recognition algorithm based on three metrics, i.e., flow density, degree centrality, and probe-distance centrality of links. Specifically, flow density describes the number of flows going through the links in unit time, degree centrality describes the connected relation, and probe-distance centrality describes the position of the link
- (iii) This paper proposes a detection algorithm based on interquartile range, which detects the network outages by observing whether the RTT of any key link exceeds its critical value for a period of time. The experimental results demonstrate that our approach can detect network outages via key links rather than all links

The rest of this article is organized as follows. The following section provides a brief overview of network outage detection. Our approach and its architecture used for detect-

ing the network outages have been explained in Section 3. The performance of the detection approach is discussed in Section 4. Finally, we draw the conclusions in Section 5.

## 2. Related Work

Several approaches have been proposed to detect network outages based on active probing. These approaches can be roughly divided into three categories according to different performance indexes they are based on, i.e., the approaches based on RTT, the approaches based on the number of probe responses, and the approaches based on the number of links change, respectively.

RTT-based outage detection approaches, such as [1, 4, 6, 15], have been proposed by utilizing different statistical models to characterize the RTT of all links to detect the network outages. Fontugne et al. [1] first obtained the differential RTT of all links. Then, they leveraged normal distribution to model the measurements and detected the network outages by applying the Wilson score. However, [6] rarely investigated the performance of the last-mile network, and the last-mile network is the centerpiece of broadband connectivity. Hence, Fontugne et al. [1] improved the previous work [6] and captured the RTT of all links in last-mile networks. Then, they used the Welch method to analyze the measurements and detected the network outages.

Since several studies [16–18] reported that normal distribution failed to characterize several distinct modes of the RTT distribution of links, Fontugne et al. [15] leveraged the log-normal distribution to model the RTT of all links and identified all the modes of RTT distribution. Then, they detected the network outages by observing the transitions between the different modes. However, [15] cannot precisely distinguish whether RTT changes are caused by network outage events or “normal” RTT fluctuations. In response to this fact, B. Hou et al. [4] collected the RTT measurements of all links and utilized the change-point detection algorithm twice to detect network outages. Their approach can effectively reduce the false positive rate.

Other outage detection approaches detected network outages by probing all links in the detection area and analyzing the number of probe responses [5, 7, 19, 20]. Heidemann et al. [20] and Dainotti et al. [19] used pings to probe all links in detection areas and detected the network outages by observing the apparent decrease in the number of probe responses. However, these approaches [19, 20] achieved low accuracy of detection. In order to improve this, Quan et al. [5] proposed a detection system named Trinocular. Specifically, they probed all links in detection area to capture the number of probe responses. Then, they used Bayesian inference to analyze these measurements and detected the network outages. However, [5] did not study the effect of weather on last-mile Internet performance, and the performance of last-mile networks affects the network connectivity of a large number of users. Hence, Padmanabhan et al. [7] used ThunderPing [21] to probe all residential links in the detection area and obtained the number of probe responses.

Then, they applied statistics to analyze the measurements and detected the network outages.

Recently, a novel approach [14] has been proposed to detect network outages by monitoring the paths of all links in the detection area and analyzing the number of link changes. The authors used traceroute to obtain the stable state of all links and leveraged the notion of empathy to aggregate the paths that changed similarly over time. Then, they detected the network outages by analyzing the number of link changes.

Note that the existing work detected the network outages by monitoring different performance metrics of all links in the detection area. Although they can detect network outages, they will lead to high resource occupancy and cost in practice. In detail, (1) active probing injects a mass of traffic into the network. Monitoring all the links may occupy the link bandwidth, reduce the network transmission speed, and increase the network burden [8, 9]. (2) Active probing is subject to its scalability. Monitoring all links prompts researchers to deploy more probes, and the deployment and operation of probes (e.g., periodic maintenance, fault analysis, and electricity costs) increase the costs in practice.

To address these challenges, we propose an approach to detect network outages by monitoring the RTT of key links. We first recognize the key links in the detection area in terms of three aspects. Then, we give the critical value of RTT for each key link. Finally, we detect the network outages by observing whether the RTT of the key link exceeds the critical value.

### 3. Network Outage Detection Approach

In this section, we propose an approach to detect network outages based on key links. The approach is called KL-Detection, which mainly consists of four parts: *data preprocessing*, *key link recognition*, *critical value calculation*, and *detection algorithm*. The architecture is depicted in Figure 1. Next, we describe each part in turn.

**3.1. Data Processing.** In order to monitor the network state and detect the network outages of the detection area, we need to obtain the performance measurements of the links in the detection area, i.e., the RTT of links. Hence, this paper obtains the performance measurements from two public datasets, i.e., RIPE Atlas Dataset [22] and Maxmind GeoIP City Dataset [23]. Specifically, we collect the traceroutes from RIPE Atlas and map each hop (node) in traceroutes to the geographic location using GeoIP City Dataset. For a certain detection area  $D$ , we obtain their corresponding traceroutes, denoted as dataset  $A$ . For each traceroute in dataset  $A$ , we extract the links formed by every adjacent node and focus on the RTT of each link.

**3.2. Key Link Recognition.** In this section, we propose a key link recognition algorithm to recognize the key links in the detection area. Previous work of traffic monitoring provided initial inroads to recognize the key links [10, 11]. These work defined the key link as the link delivering the larger traffic flows in the detection area. However, based on a basic obser-

vation, we find that monitoring the links that deliver larger traffic flows is inadequate to detect the network outages (see Section 4). This is because detecting the network outages also needs to monitor the link performance, e.g., RTT [4, 12].

In fact, the RTT of the link is affected by multiple aspects, including the neighbor correlation [4] and the presence of noise [2]. Specifically, the RTT of the links with poorer connected relation (fewer adjacencies) is less affected by the RTT of other links [4]. This causes that the RTT of the links with poor connected relation may not fluctuate obviously in the case of a network outage [24]. Hence, monitoring their RTT may fail to detect the network outages even though they deliver larger traffic flows. Moreover, the accuracy of the RTT is influenced by the distance between probes and the nodes of links. Generally, the links are closer to the probes, and the RTT of the link can be measured more accurately [14]. Hence, we may fail to detect the network outages by monitoring the RTT of the links far from the probes, even though these links deliver larger traffic flows.

In response to this fact, we recognize the key links by considering the traffic load information and the factors affecting the RTT of the link, consisting of three metrics, i.e., flow density, degree centrality, and probe-distance centrality. The flow density describes the number of flows going through the links in unit time. The degree centrality describes the connected relation. The probe-distance centrality describes the distance (hop) between the node of the link and probes. Next, we give the definitions of these three metrics and describe the process of key link recognition.

**3.2.1. The Flow Density.** The flow density represents the number of flows going through the links in unit time. We conduct the measurement in the detection area with short time intervals and over long timescales (days to weeks). The flow density of links at different time intervals is represented by a matrix  $M \in R^{t \times l}$  which is given as

$$M = \begin{pmatrix} f_{11} & \cdots & f_{1l} \\ \vdots & & \vdots \\ f_{i1} & \cdots & f_{ij} & \cdots & f_{il} \\ \vdots & & \vdots & & \vdots \\ f_{t1} & \cdots & f_{tl} \end{pmatrix}, \quad (1)$$

where  $f_{ij}$  denotes the flow density of  $j$ -th link during the time interval  $i$ ,  $t$  denotes the number of consecutive time intervals (the number of rows),  $l$  denotes the number of total links in the network (the number of columns), and  $t \gg l$ .

Next, we perform the singular value decomposition (SVD) [25] on  $M$  and illustrate how SVD can recognize a small set of links that can well represent the flow density of all links in the detection area. The decomposition of matrix  $M$  is given as

$$M = U \sum V^T, \quad (2)$$

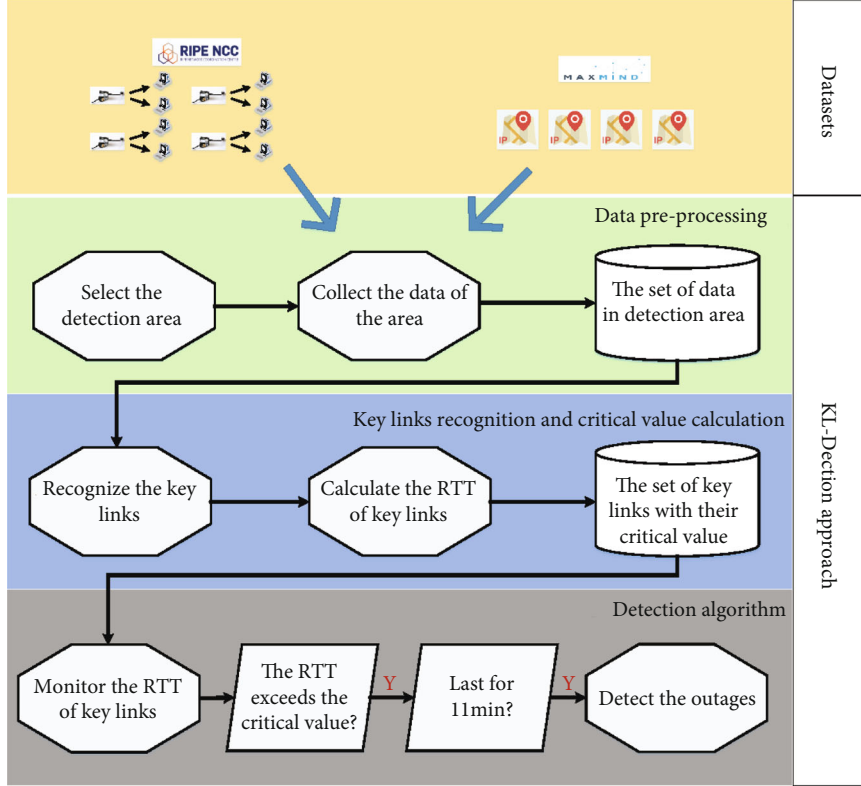


FIGURE 1: The architecture of KL-Dection.

where  $U \in R^{t \times l}$  and  $U^T U = I$ ,  $V \in R^{l \times l}$  and  $V^T V = I$ , and  $\Sigma$  is a  $t \times l$  diagonal matrix, whose diagonal entry  $\delta_i (\delta_i \geq 0)$  is known as the singular value and represents the importance of the link in the matrix  $M$ . The columns of  $U$  are denoted as  $\{u_i | i \in \{1, \dots, t\}\}$ , and the columns of  $V$  are denoted as  $\{v_j | j \in \{1, \dots, l\}\}$ . Hence, the matrix  $M$  can be calculated as

$$M = \delta_1 u_1 v_1^T + \delta_2 u_2 v_2^T + \dots + \delta_l u_l v_l^T, \quad (3)$$

Suppose there are  $q$  positive singular values among all singular values  $\delta_i$ ; this means that we can find  $q$  columns in  $M$  to represent itself according to the crucial property of SVD [25]. Moreover, existing work [10] demonstrated that the singular value of flow density matrix  $M$  is sparsely distributed, and there are only  $r$  large singular values among  $q$  positive singular values ( $r \ll q$ ). The  $r$  is called the effective rank of the matrix  $M$ , which means that the flow density of all links can be approximately represented by the flow density of  $r$  basic links in the detection area.

According to the analysis above, we first obtain the flow density matrix  $M$  of the detection area; then, we perform the SVD on matrix  $M$ ; finally, we extract  $r$  basic links based on the singular values. For convenience, the set of these  $r$  basic links is denoted as  $B$ .

**3.2.2. The Degree Centrality.** The degree centrality of the node represents the number of adjacencies of the node. In view of this definition, we extend it to describe the degree centrality of the link. According to the bucket effect, the cen-

trality of the link is constrained by the minimum of the centrality of its two nodes. Hence, we define the degree centrality of the link as the minimum of the degree centrality of its two nodes. Noting that the network is in a stable state during a period of time, we consider that the centrality of the link will not change over time. For convenience, the link formed by two adjacent nodes  $v_i$  and  $v_j$  is denoted as  $l_{i,j}$ . The degree centrality of the link  $l_{i,j}$  (i.e.,  $d_{i,j}$ ) is calculated as follows:

$$d_{i,j} = \min \{d(v_i), d(v_j)\}, \quad (4)$$

$$d(v_i) = \{N_u | u \in V, (u, v_i) \in E\}, \quad (5)$$

where  $d(v_i)$  is the degree centrality of the node  $v_i$ ,  $V$  represents the set of nodes,  $E$  represents the set of links, and  $N_u$  represents the number of nodes that  $v_i$  connected with. Note that the larger value of  $d_{i,j}$  represents that the link  $l_{i,j}$  has richer connected relation, and its RTT can reflect the network state notably.

**3.2.3. The Probe-Distance Density.** In order to describe the distance between the probes and the node of the link, we propose a metric called probe-distance centrality. Since the distance is obtained by calculating the number of hops between two nodes, we calculate the probe-distance centrality of the link  $l_{i,j}$  based on the following steps: (1) we extract the two nodes of  $l_{i,j}$ , and for each node, we calculate the average hops between it and all the probes in detection area;

(2) similar to the definition of the degree centrality of link, we select the minimum average hops as the probe-distance centrality of the link  $l_{i,j}$ .

The probe-distance centrality of the link  $l_{i,j}$  (i.e.,  $p_{i,j}$ ) is formulated as

$$p_{i,j} = \min \{p(v_i), p(v_j)\}, \quad (6)$$

$$p(v_i) = \frac{\sum_{k=1}^K \sigma_{(v_i,k)}}{K}, \quad (7)$$

where  $p(v_i)$  represents the average hops between node  $v_i$  and all probes in the detection area,  $K$  represents the number of probes in the detection area, and  $\sigma_{(v_i,k)}$  represents the number of hops between the node  $v_i$  and the  $k$ -th probe. Note that the lower value of  $p_{i,j}$  indicates that the link is closer to all the probes, and its RTT can reflect the network state accurately.

**3.2.4. Key Link.** Based on the definitions of these three metrics, we define key link as follows. For each link  $l_{i,j}$  in  $D$ , the set of key links  $K$  is defined as

$$K = \{l_{i,j} | P(l_{i,j} \in C, l_{i,j} \in E | l_{i,j} \in B) = 1\}, \quad (8)$$

where  $C$  represents the set of links with  $d_{i,j} \geq \Delta_1$  and  $E$  represents the set of links with  $p_{i,j} \leq \Delta_2$ .  $\Delta_1$  and  $\Delta_2$  are the critical value of the degree centrality and probe-distance centrality, respectively. As can be seen from Equation (8), if a link  $l_{i,j}$  is a basic link ( $l_{i,j} \in B$ ) and it meets the conditions of  $d_{i,j} \geq \Delta_1$  and  $p_{i,j} \leq \Delta_2$ , it can be regarded as the key link.

Note that the process of key link recognition is not limited by network topology and detection area. For convenience, we take Colorado as an example to illustrate how to obtain  $B$ ,  $C$ , and  $E$  in turn.

First, we extract the traceroutes from July 31 to August 30, 2020, in Colorado. Then, based on the traceroutes, we obtain the flow density matrix in this area, a  $11424 \times 556$  matrix, consisting of the flow density of 556 links during 11424 time intervals. Finally, we get 556 singular values and sort them in a descending order manner. We note that the 30-th singular value is already close to zero. Therefore, we only present the first 30 singular values of the matrix in Figure 2(a).

From Figure 2(a), we can observe that the singular value decreases rapidly from the first element to the 17-th element, and after the 17-th element, the singular value decreases slowly and eventually stabilizes. We note that the singular value becomes very small and is almost closed to zero after the 17-th element. Considering the fact is that the larger singular value, the more important the link is; hence, we conclude that the effective rank of the matrix is 17, which means that only 17 basic links are enough to represent the traffic load information of Colorado. Next, we use the QR factorization with column pivoting [25] to obtain these 17 basic links, which constitute the set  $B$ .

Then, based on Equation (4) and Equation (5), we give the distribution of the degree centrality of the links in Colorado. Figure 2(b) reveals that the percentage increases rapidly when the degree centrality is below 4; then, the percentage increases slowly between the degree centrality is 5 and 8; finally, the percentage stabilizes when the degree centrality is above 9. From Figure 2(b), we note that only about 10% of the links have a higher degree centrality ( $\geq 8$ ). As mentioned before, during the network outages, the RTT of links with high degree centrality may fluctuate substantially due to the influence of neighbor correlation, which can reflect the network state notably. Monitoring the RTT of these links can help the network managers to detect network outages. Therefore, we define the set of links with  $d_{i,j} \geq 8$  as  $C$ .

In addition, we also give the distribution of probe-distance centrality for all links according to Equation (6) and Equation (7). In Figure 2(c), the value of probe-distance centrality is divided into six bins. We note that a large share of links has the probe-distance centrality above 7 (first two bins). On the contrary, the links with lower probe-distance centrality ( $\leq 7$ ) only account for 26.52%, which indicates that they are closer to the probes in Colorado. As mentioned before, the RTT of the links with lower probe-distance centrality can reflect the network state accurately. Monitoring the RTT of these links can help the network managers to detect network outages. As a result, we define the set of links with  $p_{i,j} \leq 7$  as  $E$ .

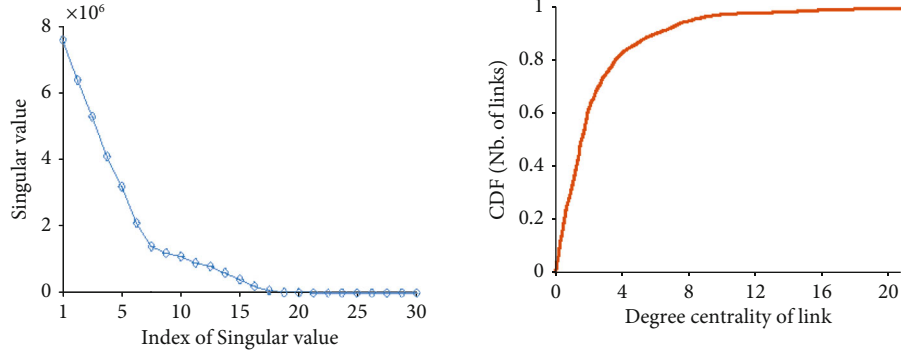
In conclusion, for each link  $l_{i,j}$  in Colorado, if it satisfies the conditions,

$$K = \{l_{i,j} | P(p_{i,j} \leq 7, d_{i,j} \geq 8 | l_{i,j} \in B) = 1\}, \quad (9)$$

it can be regarded as the key link. The process of the key link recognition is summarized in Algorithm 1. Specifically, we first select the detection area  $D$  and obtain the flow density matrix  $M$  of  $D$ . Then, we apply SVD on  $M$  and acquire  $r$  basic links. The set of these basic links are denoted as  $B$ . For all the links in  $B$ , we extract the links belonging to sets  $C$  and  $E$ . The results are the set of key links  $K$ .

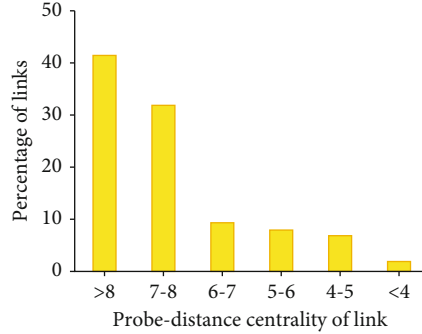
**3.3. Critical Value Calculation.** RTT is demonstrated as a key metric to gain insights into the performance of links [4, 7]. Moreover, the critical value of RTT can distinguish whether network outages occur [24]. Hence, we propose a critical value calculation algorithm based on interquartile and give the critical value of RTT for the recognized key links. Specifically, we first extract the raw RTT of each key link over a period of time and sort them in an ascending order manner. Then, for each key link  $l_{i,j}$ , we define  $R_{uq}(l_{i,j})$  as its upper quartile (the value located at 75% of the data range),  $R_{lq}(l_{i,j})$  as its lower quartile (the value located at 25% of the data range), and  $R_d(l_{i,j})$  as the difference between the upper and lower quartiles. The critical value  $R_{cv}(l_{i,j})$  is calculated as follows:

$$R_{cv}(l_{i,j}) = R_{uq}(l_{i,j}) + kR_d(l_{i,j}), \quad (10)$$



(a) The first 30 singular value of the flow density matrix

(b) The distribution of degree centrality



(c) The distribution of probe-distance centrality

FIGURE 2: The distribution of three metrics.

**Input:**  $D, r, \Delta_1, \Delta_2$ ;

**Output:**  $K$ ;

1: Calculate the matrix  $M$  in  $D$  and apply SVD over it,

2: Acquire  $r$  basic links, and denote them as the set  $B$ ,

3: According to  $\Delta_1, \Delta_2$ , extract the links that satisfy the conditions in  $B$ , and denote them as  $K$ ,

4: **return** The set of key links  $K$ .

ALGORITHM 1: The recognition of key links.

where  $k$  is the regular factor. Finally, according to [26], we set  $k$  as 1.5 and obtain the critical value of RTT for each key link.

**3.4. KL-Detection Algorithm.** Note that network outages are different from network congestion since they will persistently influence the state of the network [27–29]. Therefore, we add a constraint of duration to the definition of network outages. Existing work [5, 7] defined network outages as no response or missing a set of pings from any vantage point in 11 minutes. As a reference, in this paper, we define the network outage as the phenomenon that the RTT of any key link exceeds its critical value and lasts for more than 11 minutes.

Next, we summarize the process of the KL-Detection approach and give its pseudocode in Algorithm 2. Firstly, we select the detection area  $D$  and obtain their corresponding traceroutes, denoted as dataset  $A$ . Then, we recognize the key links from  $A$  using Algorithm 1. Next, we calculate the critical value  $R_{cv}(l_{i,j})$  of each key link  $l_{i,j}$ , respectively.

Finally, we detect the network outages by observing whether the RTT of any key link exceeds the critical value for more than 11 minutes. It is worth noting that the KL-Detection algorithm can be used in any network topology and detection area.

## 4. Results and Discussion

Although our approach is applicable for the network outage detection in any detection area, due to space limitations, we take California as the detection area for presentation. We first present the visualization results of key links in this area. Then, we leverage one outage event in California to demonstrate the validity of the definition of key link. Next, we leverage another outage event to demonstrate the validity of the KL-Detection approach. All outage events we considered occurred in the Internet. Finally, we compare the existing approach [14] and our approach in terms of the number of monitoring links in three detection areas.

**Input:**  $D, r, \Delta_1, \Delta_2$ ;  
**Output:** Network outage;  
 1: Extract the traceroutes in  $D$ , and denote them as dataset  $A$ ,  
 2: Recognize the key links from dataset  $A$  using Algorithm 1,  
 3: Obtain  $R_{cv}(l_{a,b})$  for each key link  $l_{a,b}$ ,  
 4: Monitor the RTT of  $l_{a,b}$  in parallel,  
 5: **if** The RTT of any  $l_{a,b}$  exceeds its corresponding critical value  $R_{cv}(l_{a,b})$  and lasts for more than 11 minutes **then**  
 6:     **return** Network outage,  
 7: **end if**

ALGORITHM 2: KL-Detection algorithm.

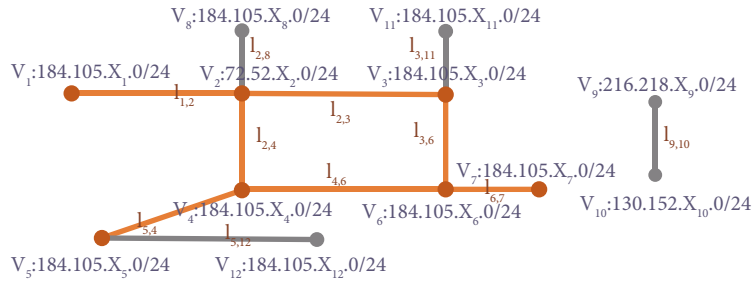


FIGURE 3: A part of visualization results of links. The topology of links is consistent with the practical environment. The orange lines represent the key links, which are used to detect two outage events. The gray lines represent the links, which are used to detect the outage event occurred on October 21, 2016.

TABLE 1: The critical value of RTT.

Key link	$l_{1,2}$	$l_{2,3}$	$l_{2,4}$	$l_{5,4}$	$l_{4,6}$	$l_{3,6}$	$l_{6,7}$
Critical value (ms)	26.0	81.9	25.4	19.3	27.6	21.5	18.0

4.1. *The Visualization Results of Key Links.* We first collect the traceroutes going through California from July 31 to November 30, 2020, in RIPE, corresponding to 2.7T data. Based on the data, we analyze 11936 links and leverage Algorithm 1 to recognize seven key links. The visualization results of these seven key links are shown in Figure 3. To protect the privacy of address information, we describe the nodes of key links in the form of prefixes.

Based on the key links, we extract their raw RTT from the 2.7T data and obtain their corresponding critical value. The critical value (ms) is shown in Table 1.

From Table 1, we can infer that the network outage is happening if the RTT of any key link exceeds its critical value and lasts for 11 minutes.

4.2. *The Validity of the Definition of Key Link.* After obtaining the critical value, we consider an outage event that occurred on October 21, 2016 [30], in California to evaluate the validity of the definition of key link. In this case study, we extract the RTT from 2016-10-21 11:00 UTC to 17:30 UTC for analysis.

The RTT of each key link during 2016-10-21 11:00 UTC to 17:30 UTC is shown in Figure 4. In each figure, the  $x$ -axis is the time (in hours), the  $y$ -axis is the RTT (ms), and the dotted line is the critical value of the RTT. We take Figure 4(a) as an example to illustrate. In Figure 4(a), the RTT is below the critical value before 11:53; then it

increases rapidly and exceeds the critical value during 11:53 to 12:45; afterward, the RTT is gradually back to normal during 12:45 to 17:10; next, the RTT increases again and exceeds the critical value during 17:10 to 17:30. From Figure 4(a), we can observe that the outage occurred from 11:53 to 12:45 and 17:10 to 17:30, respectively, which is in good agreement with the time reported in [31].

As can be seen from Figure 4, we can detect the network outages effectively by monitoring the RTT of any key link. It is worth noting that the time consumption of our approach is low because it monitors the state of all key links in parallel.

Next, in order to evaluate the validity of the definition of key link, we randomly select four links (except the key links), which represent different types of links in California. We present the three metrics of these four links in Table 2.

As can be seen from Table 2, only one metric of the first three links does not satisfy Equation (8), and the last link only satisfies the condition of flow density. Then, we leverage these four links to detect the outage event mentioned above, and the RTT of these four links is given in Figure 5. It can be seen from Figure 5 that the RTT of these four links has different fluctuations, but they do not exceed the critical value. Hence, we conclude that no network outage occurs, which is inconsistent with the ground truth. The results demonstrate that focusing on the links recognized by any one or two metrics alone is inadequate to detect network outages. Moreover, based on the comparison of the results between Figures 4 and 5, we can conclude that the definition of the key links proposed in this paper is effective in network outage detection.

4.3. *The Validity of KL-Detection Approach.* In order to evaluate the validity of KL-Detection approach, we consider an

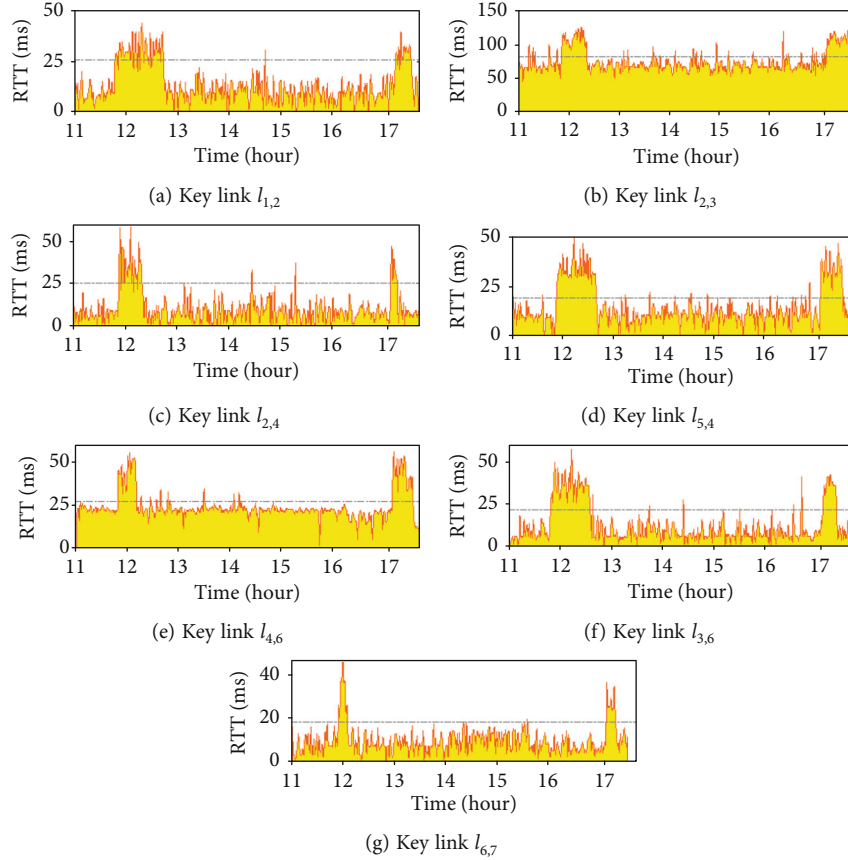


FIGURE 4: RTT of the key links.

TABLE 2: The three metrics of links.

Link	$l_{i,j} \subset B$	$l_{i,j} \subset C$	$l_{i,j} \subset E$
Link $l_{2,8}$	✓	☒	✓
Link $l_{9,10}$	✓	✓	☒
Link $l_{3,11}$	☒	✓	✓
Link $l_{5,12}$	✓	☒	☒

outage event that occurred on May 24, 2019, in California [32]. Since the outage event lasted from 21:47 to 23:58, we extract the RTT from 2019-05-24 20:00 UTC to 24:00 UTC for analysis.

From Figure 6, we can observe that the key links  $l_{2,3}$ ,  $l_{5,4}$ ,  $l_{3,6}$ , and  $l_{6,7}$  can detect the outage effectively. In detail, we can detect the outage from Figure 6(d) because the RTT exceeds the critical value and lasts from 23:30 to 23:50. Similarly, we can also detect the outage from Figure 6(g) because the RTT exceeds the critical value and lasts from 21:47 to 23:58. However, the duration of the outage event inferred from these two key links are different. This phenomenon can be explained by the fact that because part or parts of the power grid remain operational, the links in some areas of California still maintain the normal network state. This phenomenon is verified in electric disturbance events' annual summaries [32].

In addition, we found that the RTT of key links  $l_{1,2}$ ,  $l_{2,4}$ , and  $l_{4,6}$  is stable over time. This phenomenon can be explained by the fact that the outage event occurred far away from the location of these key links, and it did not affect the performance of these key links. The results of Figure 6 demonstrate that our approach can detect the outage event effectively by observing whether the RTT of any key link exceeds the critical value for more than 11 minutes.

**4.4. Performance Comparison.** In this section, we aim to compare the KL-Dection approach with the existing approaches in terms of the number of monitoring links when both approaches can detect the network outages successfully. Consider that the latest approach [14] detected the network outage by collecting the traceroute and monitoring the performance of all links in the detection area, which is similar to the dataset and detection mode adopted in this paper. As a consequence, we compare our approach with the latest approach [14] in terms of the number of monitoring links in three detection areas. Specifically, our approach and the existing work can successfully detect the outage event that occurred in these three detection areas [30], and the results of the comparison are shown in Table 3.

As can be seen from Table 3, the number of monitoring links our approach needed is notably smaller than the existing work [14]. This is especially true when the number of links in the detection area is large. Specifically, in California, our approach only needs to monitor less than 0.06% of the links



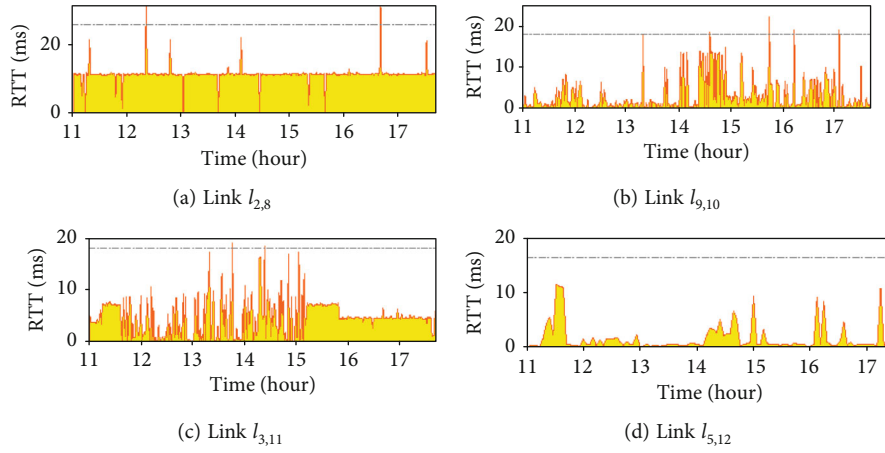


FIGURE 5: RTT of the links.

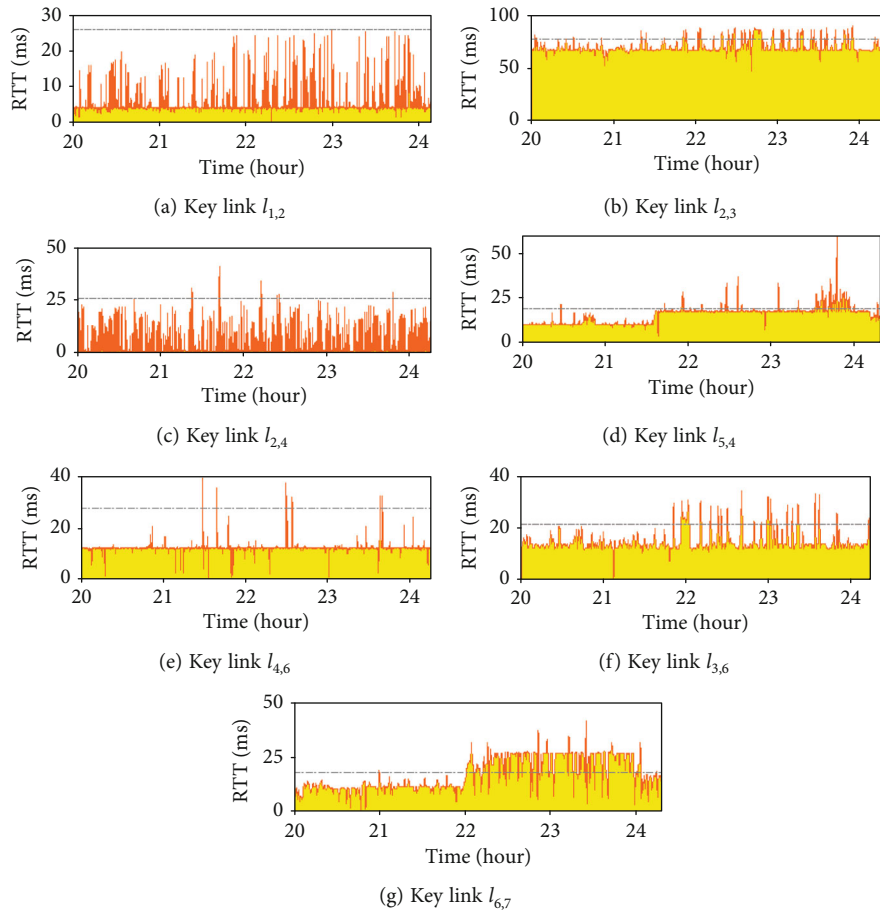


FIGURE 6: RTT of the key links.

TABLE 3: Existing approach [14] and KL-Detection approach all can detect the outage event that occurred on October 21, 2016 [30]. Under this case, we give the results of the comparison of the number of monitoring links in three detection areas.

Detection area	KL-Detection (ours)	Existing approach [14]
Colorado	5	5234
District of Columbia	6	7420
California	7	11936

for network outage detection, and the runtime of our approach is 2 seconds.

Monitoring a large number of links will prompt the researchers to deploy more probes and take continuous measurements, which may occupy the link bandwidth, reduce the network transmission speed, and increase the network burden [9]. Besides this, the operation of probes increases the costs (e.g., periodic maintenance, fault analysis, and electricity costs). Thus, the KL-Detection approach can obviously reduce resource occupancy and cost without compromising the validity of outage detection. We believe that our approach can provide better scalability and is more acceptable in practice than existing work.

## 5. Discussion

The results presented in this paper have several implications for the networking community. Because our approach is lightweight and effective, the network managers can leverage our approach to understand the network performance of their customers with less cost. Similarly, in the scenario of the Internet of Things, managers can also effectively understand the performance of the network by monitoring the connectivity of links that connect the key devices.

However, several limitations should be considered when leveraging our approach. First, the key links are recognized from vantage points, but the vantage points may not be representative of the detection area, especially when the number of Atlas probes is low. Hence, the results are prone to the bias of Atlas deployment. Second, in the scenario of the data center, the result of our approach is not satisfactory. This is because compared with edge network, the network topology of the data center is small, and a majority of links in data center have high flow density, degree centrality, and probe-distance centrality. Hence, our approach does not work well in this scenario. The solutions to these limitations are left as a future work.

## 6. Conclusion

In this paper, we propose KL-Detection approach, which detects network outages via key links instead of all links. Specifically, we recognize the key links in terms of three metrics, including flow density, degree centrality, and probe-distance centrality of links. Then, based on recognized key links, we give a critical value calculation algorithm on RTT that distinguishes whether network outages occur. Finally, we leverage two historical events to demonstrate that our approach can detect the network outages effectively.

## Data Availability

The data included in this paper are available without any restriction.

## Conflicts of Interest

The authors declare that there is no conflict of interest regarding the publication of this paper.

## Acknowledgments

This work is supported by the National Key Research and Development Program of China under Grant No. 2020YFE0200500.

## References

- [1] R. Fontugne, A. Shah, and K. Cho, "Persistent last-mile congestion: not so uncommon," in *Proceedings of the Internet Measurement Conference (IMC)*, pp. 420–427, New York, 2020.
- [2] J. Kučera, R. B. Basat, M. Kuka, G. Antichi, M. Yu, and M. Mitzenmacher, "Detecting routing loops in the data plane," in *Proceedings of the 2020 ACM CoNEXT Conference*, pp. 466–473, Barcelona, 2020.
- [3] G. Kumar, N. Dukkipati, K. Jang et al., "Swift: delay is simple and effective for congestion control in the datacenter," in *Proceedings of the ACM Special Interest Group on Data Communication (SIGCOMM)*, pp. 514–528, New York, 2020.
- [4] B. Hou, C. Hou, T. Zhou, Z. Cai, and F. Liu, "Detection and characterization of network anomalies in large-scale RTT time series," *IEEE Transactions on Network and Service Management*, vol. 18, no. 1, pp. 793–806, 2021.
- [5] L. Quan, J. Heidemann, and Y. Pradkin, "Trinocular: understanding internet reliability through adaptive probing," in *Proceedings of the ACM Special Interest Group on Data Communication (SIGCOMM)*, pp. 255–266, Hong Kong, 2013.
- [6] R. Fontugne, C. Pelsser, E. Aben, and R. Bush, "Pinpointing delay and forwarding anomalies using large-scale traceroute measurements," in *Proceedings of the Internet Measurement Conference (IMC)*, pp. 15–28, London, 2017.
- [7] R. Padmanabhan, A. Schulman, D. Levin, and N. Spring, "Residential links under the weather," in *Proceedings of the ACM Special Interest Group on Data Communication (SIGCOMM)*, pp. 145–158, Beijing, 2019.
- [8] N. Gaur, A. Chakraborty, and B. S. Manoj, "Delay optimized small-world networks," *IEEE Communications Letters*, vol. 18, no. 11, pp. 1939–1942, 2014.
- [9] M. Hasib and J. A. Schormans, "Limitations of passive & active measurement methods in packet networks," in *London Communications Symposium (LCS)*, London, UK, 2003.
- [10] J. Badshah, M. Alhaisoni, N. Shah, and M. Kamran, "Cache servers placement based on important switches for SDN-based ICN," *Electronics*, vol. 9, no. 1, pp. 39–65, 2020.
- [11] T. Yingying Cheng and X. Jia, "Compressive traffic monitoring in hybrid SDN," *IEEE Journal on Selected Areas in Communications*, vol. 36, no. 12, pp. 2731–2743, 2018.
- [12] D. Perdices, D. Muelas, I. Prieto, L. de Pedro, and L. de Vergara, "On the modeling of multi-point RTT passive measurements for network delay monitoring," *IEEE Transactions on*

- Network and Service Management*, vol. 16, no. 3, pp. 1157–1169, 2019.
- [13] M. S. Kang, S. B. Lee, and V. D. Gligor, “The crossfire attack,” in *2013 IEEE Symposium on Security and Privacy*, pp. 127–141, Berkeley, CA, 2013.
- [14] M. Di Bartolomeo, V. Di Donato, M. Pizzonia, C. Squarcella, and M. Rimondini, “Extracting routing events from traceroutes: a matter of empathy,” *IEEE/ACM Transactions on Networking*, vol. 27, no. 3, pp. 1000–1012, 2019.
- [15] R. Fontugne, J. Mazel, and K. Fukuda, “An empirical mixture model for large-scale RTT measurements,” in *2015 IEEE Conference on Computer Communications (INFOCOM)*, pp. 2470–2478, Hong Kong, China, 2015.
- [16] B.-Y. Choi, S. Moon, Z.-L. Zhang, K. Papagiannaki, and C. Diot, “Analysis of point-to-point packet delay in an operational network,” *Computer Networks*, vol. 51, no. 13, pp. 3812–3827, 2007.
- [17] S. Shakkottai, N. Brownlee, A. Broido, and K. Claffy, “The RTT distribution of TCP flows on the internet and its impact on TCP based flow control,” Technical report, Cooperative Association for Internet Data Analysis (CAIDA), 2004.
- [18] G. Maier, A. Feldmann, V. Paxson, and M. Allman, “On dominant characteristics of residential broadband internet traffic,” in *Proceedings of the Internet Measurement Conference (IMC)*, pp. 90–102, Chicago, 2009.
- [19] A. Dainotti, C. Squarcella, E. Aben et al., “Analysis of country-wide internet outages caused by censorship,” *IEEE/ACM Transactions on Networking*, vol. 22, no. 6, pp. 1964–1977, 2014.
- [20] J. Heidemann, L. Quan, and Y. Pradkin, “A preliminary analysis of network outages during hurricane sandy,” Tech. Rep, ISI-TR-685b, University of Southern California, Information Sciences Institute, 2012.
- [21] A. Schulman and N. Spring, “Pingin’ in the rain,” in *Proceedings of the Internet Measurement Conference (IMC)*, pp. 19–28, New York, 2011.
- [22] A. Milolidakis, R. Fontugne, and X. Dimitropoulos, “Detecting network disruptions at colocation facilities,” in *2019 IEEE Conference on Computer Communications (INFOCOM)*, pp. 2161–2169, Paris, France, 2019.
- [23] G. Aceto and A. Pescapé, “Internet censorship detection: a survey,” *Computer Networks*, vol. 83, pp. 381–421, 2015.
- [24] J. H. Wang and C. An, “A study on geographic properties of internet routing,” *Computer Networks*, vol. 133, pp. 183–194, 2018.
- [25] G. H. Golub and C. F. Van Loan, *Matrix Computations*, vol. 3, The Johns Hopkins Univ. Press, Baltimore, MD, USA, 2012.
- [26] K. L. Spafford, J. S. Meredith, and J. S. Vetter, “Quartile and outlier detection on heterogeneous clusters using distributed radix sort,” in *2011 IEEE International Conference on Cluster Computing*, pp. 412–419, Austin, TX, USA, 2011.
- [27] R. Zhao, Z. Li, Z. Xue, T. Ohtsuki, and G. Gui, “A novel approach based on lightweight deep neural network for network intrusion detection,” in *2021 IEEE Wireless Communications and Networking Conference (WCNC)*, pp. 1–6, Nanjing, China, 2021.
- [28] P. Thorat, N. K. Dubey, K. Khetan, and R. Challa, “SDN-based predictive alarm manager for security attacks detection at the IoT gateways,” in *2021 IEEE 18th Annual Consumer Communications & Networking Conference (CCNC)*, pp. 1–2, Las Vegas, NV, USA, 2021.
- [29] N. Leslie, “An unsupervised learning approach for in-vehicle network intrusion detection,” in *2021 55th Annual Conference on Information Sciences and Systems (CISS)*, pp. 1–4, Baltimore, MD, USA, 2021.
- [30] G. C. M. Moura, J. Heidemann, M. Müller, R. O. de Schmidt, and M. Davids, “When the dike breaks: dissecting DNS defenses during DDoS,” in *Proceedings of the Internet Measurement Conference (IMC)*, pp. 8–21, Boston, MA, USA, 2018.
- [31] S. Mansfield-Devine, “DoS goes mainstream: how headline-grabbing attacks could make this threat an organisation’s biggest nightmare,” *Network Security*, vol. 2016, no. 11, pp. 7–13, 2016.
- [32] “Electric disturbance events (oe-417) annual summaries,” <https://www.oe.http://netl.doe.gov/OE417annualsummary.aspx>.

## Research Article

# The Role of Wireless Sensors in the Quality Monitoring of Students' Physical Fitness Tests under the Background of National Fitness

Ruixia Xu 

Ministry of Physical Education, Henan University of Animal Husbandry and Economy, Zhengzhou, 450000 Henan, China

Correspondence should be addressed to Ruixia Xu; 81162@hnuhae.edu.cn

Received 7 January 2022; Revised 8 February 2022; Accepted 19 February 2022; Published 7 March 2022

Academic Editor: Shalli Rani

Copyright © 2022 Ruixia Xu. This is an open access article distributed under the Creative Commons Attribution License, which permits unrestricted use, distribution, and reproduction in any medium, provided the original work is properly cited.

With the continuous development of Chinese economy and the continuous improvement of national living standards, the country's emphasis on students' physique has also increased. This has greatly breakthrough the conditions for health testing of students' physique in our country. With the assistance of wireless sensors, students' physical health quality monitoring has accurate data statistics and research. Hop positioning algorithm, compressed sensing matching tracking algorithm, and RSSI technology have been analyzed from the perspectives of students' ideas, life, and learning, and school sports support. It is found that nearly 50% of students in a college are not very health-conscious, while only 26% have a good knowledge of health. In the 50 m running test, the average score for boys is  $807 + 124$  s, and the average for girls is  $914 \pm 108$  s. The data is accurate to 0.01% with the help of wireless sensor technology. At the same time, combined with the testing data of sports events, we found that the physical fitness of students is generally low. This has a lot to do with the living habits of the students and the physical exercises in the school.

## 1. Introduction

Student physical health evaluation is an important part of school physical education work and an important part of the school education evaluation system. In today's high-tech development, physical fitness monitoring should also keep pace with the times.

The establishment of a monitoring network and the development and utilization of high-tech systems such as data collection systems have greatly reduced the monitoring workload. The use of wireless sensors has also made a great breakthrough in the quality monitoring of students' physical fitness tests.

For the role of sensors, experts at home and abroad have done a lot of research. Musa et al. has developed a strategy that optimizes the typical deployment of sensors in the field and distributes the energy consumption of wireless sensor networks (WSN). This strategy focuses more on collecting information from the sensor, rather than the precise positioning of the sensor. Therefore, it is

measured based on the distribution or density of sensors in the area rather than their geographic location. Using this strategy, the lifetime of the network can be maximized under the constraint of maintaining connectivity [1]. Kaleem and Rehmani stated in the article that UAVs or microdrones equipped with sensors are becoming increasingly popular in various commercial, industrial, and public safety applications. However, uncontrolled deployment of drones poses challenges to highly security-sensitive areas such as the presidential palace, nuclear power plants, and commercial districts, as they may be used illegally. It discusses existing routing schemes for detection, tracking, and positioning and puts forward the limitations of these schemes as further research challenges [2]. Flores et al.'s study discusses the role of parents in monitoring student academic performance in the new learning system. To achieve this goal, the researchers used a descriptive correlation design [3]. Vituk et al. studied the formation process of the spelling ability of future teachers in the new Ukrainian school. He introduced that higher education

institutions use students' spelling skills as an integral part of language and communication skills. In the context of the current professional training requirements for experts in the new Ukrainian school, as a way to diagnose and control the spelling and punctuation literacy of higher education students, it can objectively evaluate the spelling skills of students, and improving educational activities is the main science of the research results [4]. Sugilar believes that the return rate of students can be used as one of the indicators of the service quality of educational institutions and student loyalty. Students who register for one semester will reregister in the next semester. He pointed out that there are many related variables that affect students' reentry. These variables mainly include monitoring the service quality, management of distance education, student characteristics, student academic performance, and the availability of student learning support services. He used a post hoc method to sample 3539 students and used the statistical technique of binary logistic regression to determine the factors related to the reentry of students at Terbuka University in Indonesia. The results show that students' reentry is affected by the adjustment factors of service quality management level: (1) personal characteristics of students, (2) success level of the previous semester, and (3) learning participation support services [5]. Hsu et al. study the important role of college students' physical activities and cultivate the concept of independent health management. At present, what kind of learning attitude do Taiwanese college students face in physical education? What motivations of students affect their attitudes towards physical education? What is the relevance? The above are the goals of this research. The research method adopts the questionnaire survey method, and the survey data adopts descriptive statistical analysis, independent sample test, one-way analysis of variance, LSD postcomparison method, and canonical correlation analysis method. Relevant practices have been adjusted in combination with data analysis. With scientific, reasonable, and efficient measures, the rate of student repetition has increased [6]. Прошева et al. explored the basic background, carrying capacity and effectiveness monitoring of problem solving based on the knowledge gained from the university preparatory training. The integrity of professional activities is related to the holistic, comprehensive, and systematic use of professional training processes. During the education process, the ability of students in the subject of "Descriptive Geometry and Engineering Graphics" was monitored. Monitoring is carried out through core lines such as problem discovery, goal setting, work planning and evaluation, and curriculum control. According to the results of the research, additional courses are organized for those students who have difficulties in the study of certain topics in the course [7].

School education should establish the guiding ideology of health, first, earnestly strengthen the spirit of "physical work," promote students to actively participate in physical exercise, develop the habit of regular physical exercise, and improve self-care ability and physical health. This has important practical significance and long-term social significance.

## 2. Past Students' Own Initiative and School Support

*2.1. Students' Own Health Awareness.* Consciousness governs behavior and correct consciousness, guides practice to give full play to subjective initiative, and promotes the development of things. Students' consciousness will directly affect their own behavior. If students think that health is not that important, then there will be no exercise behavior, and physical health cannot be guaranteed. Therefore, students must establish correct health awareness. A health awareness questionnaire was conducted for students from a certain university, as shown in Table 1.

In the health awareness questionnaire, it will be found that students still attach great importance to their own health, but their awareness of health-related knowledge is low, and the two are extremely incompatible. Schools should strengthen health and hygiene publicity and improve students' health awareness.

*2.2. The School's Support for Student Health.* School is a necessary place for students to study and live. Physical activity is an effective way for students to exercise. To improve the health of students, we need to ensure that students have a well-equipped environment (sports equipment) and software [8]. For the real situation of school facilities support, we have made corresponding investigations, as shown in Figure 1.

According to the distribution of school physical education teachers and the use of physical equipment statistics, it can be seen that the school's support for students' healthy exercise was still relatively lacking, which has a lot to do with the fact that students' health did not receive the attention of society at that time.

As of July 2002, since the Ministry of Education promulgated and implemented the "Students' Physical Health Standards," the Ministry of Education has paid increasing attention to the health of students. With the development of time and the advancement of science and technology, scientific and efficient testing techniques have been available for students' physical health. In the context of the knowledge-based electronic health and medical communication service, intelligent system National Fitness, wireless sensors have played a large role in the quality monitoring of students' physical fitness tests [9].

## 3. Wireless Sensor Technology Supports Students' Physical Fitness Test

*3.1. The Composition and Structure of the Sensor.* The component part of the wireless sensor is connected to the shell and is powered by a battery or a vibrator during operation, forming a wireless sensor network node system structure. After a large number of neurons are scattered, they are randomly distributed in or near the control area, and each node forms a network through self-regulation. The sensor node monitors the monitored object, and after the initial configuration of the monitoring data, it uses multiple relays for transmission according to its own protocol. In

TABLE 1: Questionnaire of students' own health awareness ( $m = 200$ ).

Investigate subject	Student's own health awareness survey form (m200)		
	Options	Result statistics	Percentage of total
Do you care about your health?	Very concerned	59	29.5
	Care	70	35
	Does not care	63	31.5
	It does not matter	11	5.5
Do you know health knowledge?	Learn	55	27.5
	Do not know much	89	44.5
	Do not understand	65	32.5
Think it is necessary to participate in physical exercise	Very necessary	55	27.5
	Is necessary	87	43.5
	Unnecessary	59	29.5
Are you satisfied with your current health?	Very satisfied	46	23
	Satisfy	69	34.5
	Generally	60	30
	Dissatisfied	30	15

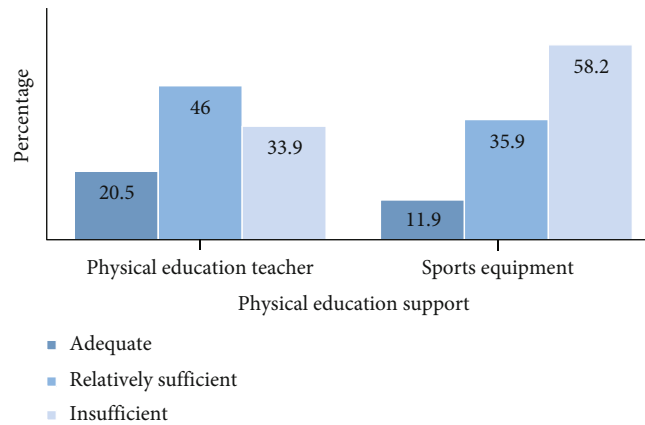


FIGURE 1: The school's support for students' healthy exercise.

the transmission system, the monitoring data is effectively processed by multiple nodes, and then through the pipeline, the control node is transmitted through satellite, Internet, and mobile communication network. End users efficiently configure and manage sensor networks through management nodes, release monitoring functions, and collect monitoring data [10], as shown in Figure 2.

Wireless sensors are widely used. The most commonly used technologies are 802.11, 802.15, Bluetooth, Wifi, Zigbee, etc., Each has its own technical advantages, but there are still disadvantages such as high energy consumption, poor interference from the power distribution wall, large volume, and the need to have multiple memory source. To this end, TI has introduced a low-power RF system suitable for simple RF networks and small SimpliciTI network protocols [11].

### 3.2. The Network Protocol of the Sensor

- (1) The SimpliciTI network protocol includes six main functional modules, namely, battery-only network,

encryption, range extender, frequency agility, access point, and network management module [12], as shown in Figure 3

The main function of the SimpliciTI network application layer is to provide network layer management, including some PINGS for external nodes to access and many interfaces for developers, as shown in Table 2.

This is a data-based communication protocol whose goal is to resolve protocol defects through a negotiation process between nodes. Before sending data, each node negotiates to determine whether other nodes need data; nodes use "metadata" (that is, to describe the characteristics of data collected by neurons to determine whether the obtained data contains duplicate information [13]). The working process of the agreement is shown in Figure 4.

LEACH protocol is the most representative routing protocol among hierarchical routing protocols [14]. The cluster head nodes are randomly selected in a circular manner, and the energy load of the entire network is evenly distributed to

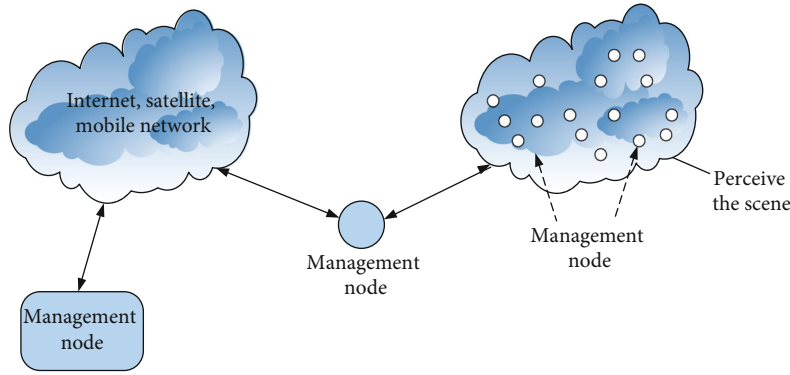


FIGURE 2: A sensor network system usually includes sensor nodes, sink nodes, and management nodes.

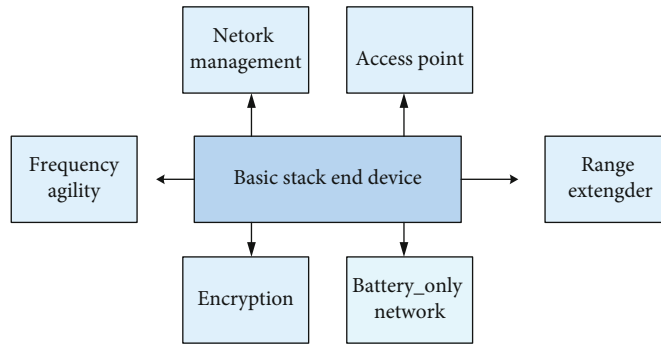


FIGURE 3: SimplicTI network protocol includes six major functional modules.

TABLE 2: Detailed application and description of the interface.

Application layer	Interface	Instruction
Ping	0 × 01	Similar to the application in the TCP/IP network, return the received data
Link	0 × 02	Establish the first connection between two node devices
Join	0 × 03	Used to obtain node access information
Security	0 × 04	Used for information encryption and key exchange
Freq	0 × 05	Complete the frequency calibration and frequency offset management of the communication module
Mgmt	0 × 06	Used in the network application layer, such as antenna interruption

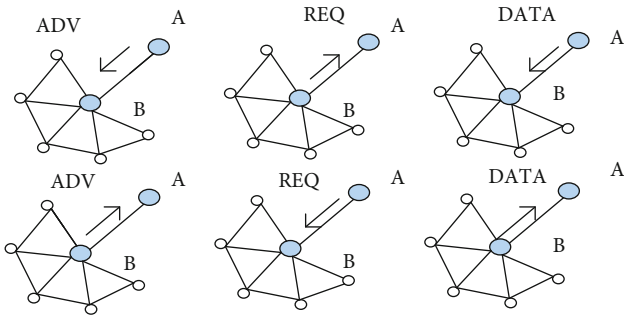


FIGURE 4: Data-centric adaptive communication routing protocol work.

each sensor node, to achieve the purpose of reducing network energy consumption and improving the overall survival time of the network. Simulation shows that LEACH

clustering protocol can extend the network life cycle by 15% compared with general planar multihop routing protocols and static hierarchical algorithms. To balance the energy consumption in the network nodes, the family head glands are randomly selected in a circular pattern. Collecting data from the cluster nodes in the middle of the combination and pass them through the channel. The network operation needs a “cycle” like a unit, and each circuit is composed of a startup phase and a stable phase. In the initial stage of each cycle, a node is randomly selected as the cluster head node, and the surrounding nodes are announced as the surrounding cluster head nodes. The measurement determines which group to join and informs the cluster head node. In the stable phase, the nerve ending collects data and sends the data to the cluster head unit. After running for a period of time in the stable phase, the network will resume the next phase of the working cycle [15]. The election method of the family

head node is each node generates a random number between 0 and 1. If the number is less than  $F(n)$ , the node is the cluster head. The calculation formula of  $F(n)$  is as follows:

$$F(n) = \begin{cases} \frac{b}{1 - b[c \bmod (1/b)]}, & n \in t, \\ 0, & \text{otherwise.} \end{cases} \quad (1)$$

Among them,  $b$  is the percentage of the number of cluster heads to the total number of nodes in the network,  $c$  is the current number of election rounds, and  $t$  is the set of nodes that are not cluster heads in the latest  $1/b$  round [16].

(2) The artificial neuron model has three basic elements

- (a) One group connection
- (b) Summation unit
- (c) A nonlinear excitation function

Expressed by mathematical formula as

$$w_k = \sum_{i=1}^b u_{kj} y_i, v_k = net_k = w_k - \theta_k, x_k = \varphi(v_k). \quad (2)$$

Among them,  $u_{kb}$  is the weight of neuron  $k$ ,  $w_k$  is the current combination result,  $\theta_k$  is the threshold,  $\varphi(\bullet)$  is the activation function, and  $x_k$  is the output of neuron  $k$ . If the input dimension is increased by one dimension,  $y_0 = -1$  or  $(+1)$ , and the weight is  $w_{k0} = \theta_k$ , the threshold  $\theta_k$  can be included [17]. Different types of neural networks use different activation functions  $\varphi(\bullet)$ , among which the most common is the threshold function (hardlim), linear function, (pirelin), and (sigmoid) functions [18]. The difference in transfer function also leads to differences in the structure and function of various neural networks, as shown in Figure 5.

MLCM is a maximum lifetime model. Wireless sensor network is an energy-restricted network. The energy consumption of a node will not exceed the remaining energy of the node. When the data forwarding rate of the node is  $g$  and node  $f$ , the life cycle of node  $v_i$  is

$$T(f) = \frac{H_n}{b_r(m) + b_t(n, m) + e_{\text{other}}} = \frac{H_n}{e_{nm} \cdot \sum_{v_n, v_m \in v, v_m \subseteq x} f_{v_n v_m}^{v_n s_d} + \rho \sum_{v_m, v_n \in v, v_m \subseteq x} f_{v_m v_n}^{v_n s_d} + e_{\text{other}}}. \quad (3)$$

Due to the lack of control over the wireless network application environment, network system operation, and wireless communication, it is unreliable. When building the network test platform, we encountered the following problems, including how accurately detects the power grid and the quantitative data evaluation of the network in this case, that is, how to conduct network testing; how to establish network monitoring; real-time simulation reflects

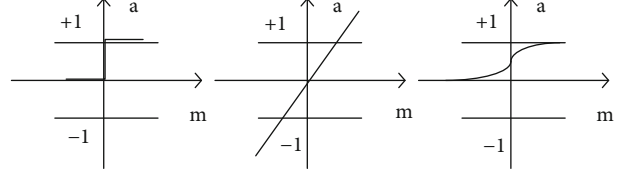


FIGURE 5: Differences in structure and function of neural networks.

the characteristics of large-scale network real-time application environment, that is, how to build test sites [19].

In the working state of wireless sensor network nodes, according to the node's influence on the data flow, the nodes can be divided into source nodes and intermediate nodes. The source node senses and generates data and can also receive data and forward the data containing itself to the next neighbor node; the intermediate node does not generate data and only forwards the received data to the next neighbor node [20]. The data flow of the two nodes is

$$\sum_{v_m, v_n \in v, v_m \subseteq x} f_{v_m v_n}^{v_n s_d} + \lambda_n g_n = \sum_{v_n, v_m \in v, v_m \subseteq x} f_{v_n v_m}^{v_n s_d}. \quad (4)$$

Among them

$$\lambda_n = \begin{cases} 1, & V_n \neq S_d, \\ -1, & V_n = S_d. \end{cases} \quad (5)$$

The network node life cycle model is

$$T_n(f) = \frac{E_n}{e_{nm} \left( \sum_{v_n, v_m \in v, v_m \subseteq x} f_{v_n v_m}^{v_n s_d} + \lambda_n g_n \right) + \rho \sum_{v_n, v_m \in v, v_m \subseteq x} f_{v_n v_m}^{v_n s_d} + e_{\text{other}}}. \quad (6)$$

The life cycle 1 of the network at a certain data forwarding rate is the smallest life cycle of all nodes:

$$T_{\text{sys}}(f) = \min_{n \in S} T_n(f). \quad (7)$$

The structure of the fault injection node used in the FIPES fault injection node modular structure experiment includes a data communication module, a clock module, a storage module, a power supply module, a charging module, and an indication module [21]. The hardware modular structure of the fault injection node of the system is shown in Figure 6.

When the node data is sent to the main control chip for communication and interaction through the serial communication module, the main control chip receives the time at this time. The read time is added in front of the data from the communication interface, and then the integrated data is written into the storage device. When it needs to receive the fault command sent by the host computer, the host computer sends a fault command to the main control chip. After the main control chip receives the command, it will call back the command and then send it to the node [22].

The research data of all above wireless sensors take the quality monitoring of the student's physical fitness



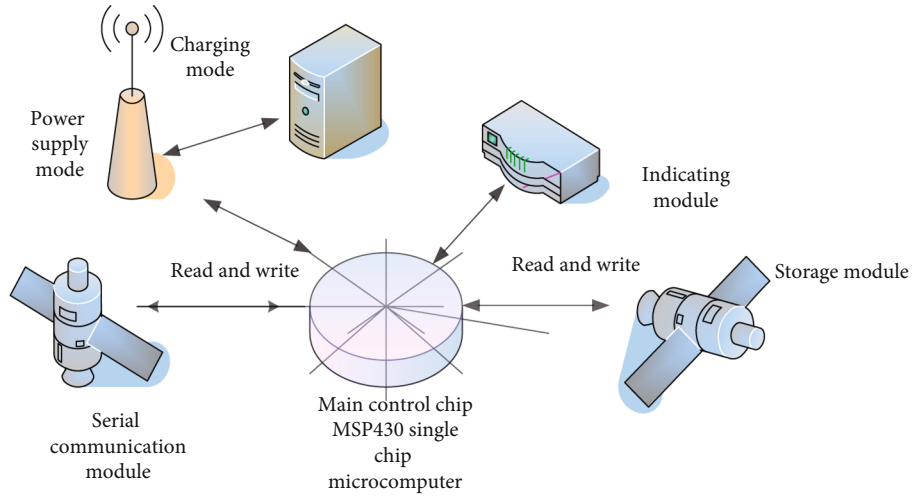


FIGURE 6: FIPES fault injection node modular structure work.

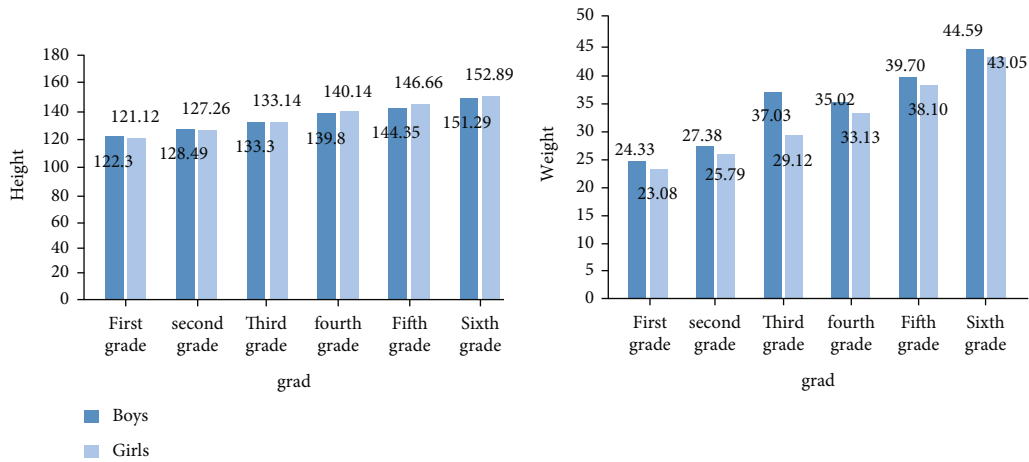


FIGURE 7: Comparison of height and weight of men and women in grades one to six.

test as the starting point to build a scientific and efficient physical fitness monitoring for the students, which requires the use of wireless sensor technology. It will not only promote the further development of my country’s physical education but also provide some new research ideas and methods for school sports science research. Applying all research methods to specific physical fitness tests of students, the quality monitoring of wireless sensors newly implemented by major universities also has good feedback. In the physical examination of students, the use of wireless sensor technology makes the monitored data more accurate, while reducing a lot of time and labor costs.

#### 4. Using Wireless Sensor Technology to Monitor Students’ Physical Test

The wireless sensor system is used in conjunction with the student health monitoring standards issued by the Ministry of Education to test the height, weight, vital capacity, seat bending, 50 meters, and other items of students of different

ages. Aiming at students of different ages is to ensure the authenticity of the test and try to avoid most accidents to prove the experimental research.

4.1. Height and Weight of Primary School Students. Parents should not neglect physical exercise, but only focus on cultivating children’s knowledge. Parents only pay attention to their children’s cultural achievements and neglect physical exercise. This is the norm for parents. However, we cannot just let it go. We should give parents a healthy awareness of physical exercise, establish the idea of “the body is the capital of the revolution,” and the family and school work together to give children a strong physique. The new “National Standards for Physical Fitness and Health of Students” have made major changes to the standards of students’ physical fitness, adding the BMI index (body length and square kilograms), and students must not only exercise regularly but also pay attention to diet [23]. Investigating and studying the average height and weight of men and women from grade one to grade six in a certain elementary school, as shown in Figure 7.

The research results show that the height gap between boys and girls is still a bit large, and boys are generally higher than girls. Moreover, the height growth trend of all students is flat, but the weight growth is indeed rapid. It can be seen that students are very lack of physical exercise.

The data signal monitored by the wireless sensor reconstructs the recently appeared subspace matching tracking algorithm and compressed sensing matching tracking algorithm. The reconstruction quality of these algorithms is comparable to straightforward procedures, and the reconstruction complexity is low. However, these algorithms are based on sparsity  $A$  [24]. However, in practical applications, the sparsity of  $A$ 's symptoms is usually unknown, and the tracking algorithm is automatically matched. When  $A$  is unknown, a positive reconstruction effect can be obtained. The concept of sparsity  $A$  sets the following basic conditions for the reconstruction of symptoms: generally, the number of observations  $B$  of a system cannot be greater than the corresponding signal length  $M$ , so for signal  $Y = D^{CS}X$ , signal reconstruction is a difficult problem that requires solving the underdetermined equations  $Y = D^{CS}X$ . Generally speaking, it is very difficult to solve underdetermined equations, because the number of unknowns is more than the number of equations, and there are other constraints, it is difficult to solve. Through research in the compressed sensing theory, if the signal  $X$  can be guaranteed to be a sparse signal or can be compressed, starting from this hypothesis, we can draw a conclusion that the equation can be solved. In the compressed sensing theory, the observation matrix is required to have RIP properties, as long as this can accurately use the signal reconstruction algorithm to restore the signal in the  $B$  observation values, and ensure the effectiveness of the compressed sensing algorithm [25]. To study the signal reconstruction algorithm of compressed sensing theory, it is necessary to define the vector

$$X = \{X_1, X_2, \dots, X_m\}. \quad (8)$$

The  $P$  norm is

$$\|X\|_P = \left( \sum_{j=1}^N |x_j|^P \right)^{1/P}. \quad (9)$$

Among them, when  $P = 0$ , it is a norm, which is the number of nonzero items of  $X$ . If the signal  $X$  is sparse, or compression can be guaranteed, the underdetermined equations  $Y = D^{CS}X$  can be calculated as a minimum 0-norm problem:

$$\begin{cases} \min \|\psi^T X\|_0, \\ \text{s.t. } A^{CS}X = \varphi \psi^T X = Y. \end{cases} \quad (10)$$

This calculation method requires all permutations and combinations of the positions  $c$ :  $a$  of each nonzero item in

$M$  to be traversed, and finally, the optimal solution is solved. Proposing a new solution optimization method,

$$\begin{cases} \min \|\psi^T X\|_1, \\ \text{s.t. } A^{CS}X = \varphi \psi^T X = Y. \end{cases} \quad (11)$$

This kind of method has certain stability when used in sparse signal reconstruction [26]. Finally, it is concluded that the height of boys is in a period of rapid growth between the ages of 7-15, which is 2 years longer than that of girls. It may be that girls are quieter. Boys like to exercise, the amount of exercise is much greater than that of girls, bone stimulation is greater than that of girls, and bone growth will accelerate. Comprehensive analysis shows that the height change law of boys and girls basically meets the national testing standards, and there is no significant difference. In terms of weight, half of our classmates weighed slightly higher than the national standard compared with the average level of primary school students in China. The personal differences between classmates are very obvious. One reason may be genetic factors, and the other may be overeating or too little exercise.

Therefore, the following points need to be done: (1) strengthen nutrition, have a balanced diet, and ensure adequate intake of essential nutrients every day. (2) Persist in exercise and promote good physical development, persist in time for half an hour. (3) Pay close attention to own physical condition and understand relevant physical health knowledge. Young people are the future and hope of the motherland. Their physical fitness not only affects their current growth and education but also affects the future and destiny of the country. Therefore, the principals of primary and secondary schools should pay close attention to the health of students and take the necessary measures.

*4.2. Comparison of Male and Female Vital Capacity of College Students.* Cardiopulmonary function refers to the ability of the human heart to pump blood and the lungs to inhale oxygen, and the abilities of both directly affect the activities of the body's organs and muscles, which are essential. The whole process involves the function of the heart to make blood and pump blood, the lungs' ability to take oxygen and exchange gas, the efficiency of the blood circulation system to carry oxygen to all parts of the body, and the function of the muscles to use this oxygen. Therefore, cardiopulmonary function is the most important indicator of students' health. Basic strength usually reflects the strength and size of the respiratory muscles and is related to factors such as the amount of thoracic exercise, gender, age, height, weight, chest circumference, and physical activity. Normally, males are 3500 ml-4000 ml, and females are 2500 ml-3500 ml. The vital capacities before and after the first, second, third, and fourth year of the freshman year, sophomore year, junior year, and senior year are now researched and analyzed, as shown in Figure 8.

Studies have found that boys' lung capacity is generally much higher than that of girls, because boys often exercise their diaphragms, and their breathing is usually the abdomen; on the other hand, girls' breathing usually involves

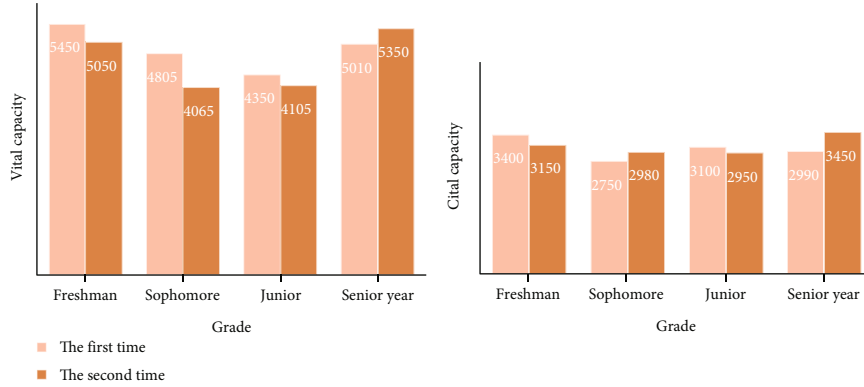


FIGURE 8: Comparison of vital capacity between men and women from freshman to sophomore year before and after half a year.

the joint muscles of the chest. In addition, the vital capacity of freshmen to junior college students generally showed a downward trend, and there was no sign of enhancement until the senior year. Schools must first establish the concept of health, take school physical exercise as an important work of school education, and organize fitness exercise programs scientifically.

**4.3. Junior High School Students 50 Meters.** Speed quality refers to the body's ability to perform fast movements or the ability to complete a certain movement in the shortest time. Speed quality is an important index to evaluate the human body's athletic ability, which is mainly related to the human body's muscle fiber type, muscle strength, and other factors. As a quality indicator of the student's physical fitness test, the 50 m run has an important reference value for evaluating students' speed ability.

Running projects can use network positioning algorithms, and the current positioning algorithms for wireless sensor networks mainly include DV. Hop positioning algorithm, Euclidean positioning algorithm, and Hop. Euclidean positioning algorithm.

V. The main working principle of the hop location algorithm is to first calculate the minimum number of hops from the node to the wireless sensor network beacon node for an unknown wireless sensor network node. At the same time, the average distance is calculated, and the average distance is multiplied by the minimum number of hops to obtain the distance from the wireless sensor network node to the beacon sensor node. When the unknown wireless sensor network node obtains the distance of more than three beacon nodes, the trilateral method is used to measure and locate, as shown in Figure 9.

The Euclidean location algorithm is an algorithm that calculates the location of an unknown sensor node that is two hops away from a wireless sensor network beacon node.

Supposing there is an unknown node in the wireless sensor network,  $E$ ,  $F$ , and  $G$ , let  $L$  be a beacon node. The Euclidean positioning algorithm can directly measure the distance  $FL$ ,  $FG$ , and  $GL$  between sensor nodes through RSSI technology. Sensor node  $E$  is adjacent to  $F$  and  $G$ . In this way, in the quadrilateral  $EFGL$ , by knowing the length of each side and the length of the diagonal  $FG$  of the quadrilat-

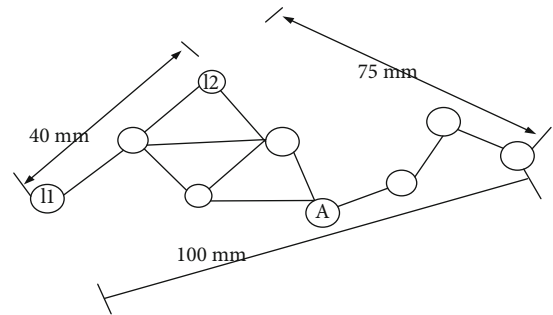


FIGURE 9: Wireless sensor network node.

eral, the length of the other diagonal  $EL$  of the quadrilateral can be calculated by the law of cosine of the trigonometric function. That is, the distance between the unknown sensor node  $E$  and the wireless sensor network beacon node  $L$ .

$$\cos \alpha = \frac{EF^2 - EG^2 - FG^2}{2EG \times FG}, \quad (12)$$

$$\cos \beta = \frac{FL^2 - EG^2 - GL^2}{2GL \times FG}, \quad (13)$$

$$EL^2 = EG^2 + GL^2 - 2EG \times GL \cos(\alpha + \beta). \quad (14)$$

The Euclidean positioning algorithm is a theoretically better positioning algorithm for wireless sensor networks. All unknown sensor nodes that are two hops apart from the beacon node of the wireless sensor network can be located. The 50-meter data monitoring of the second and third grade students in the study is shown in Figure 10.

Data research has found that the average score of students in the 50 m running test is  $807 + 124$  s for boys and  $914 \pm 108$  s for girls. The average scores for boys and girls are only maintained at the passing level of the National Physical Fitness and Health Standard and are at the lower limit of the passing range. All scores input through the wireless sensor will automatically form a student's 50-meter score evaluation according to the set program, as shown in Table 3.

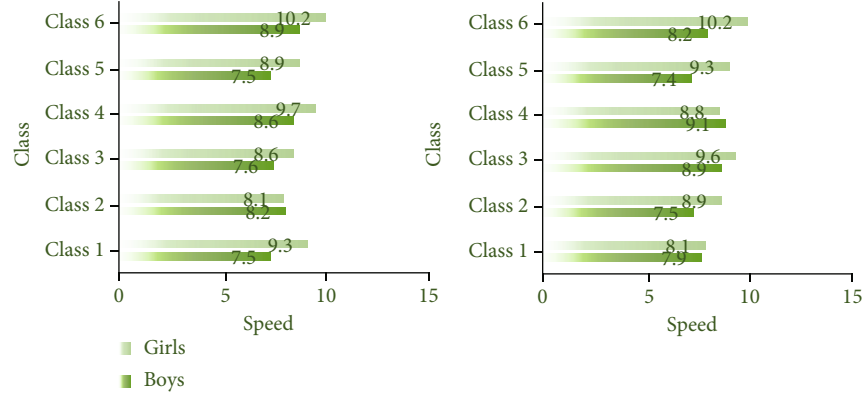


FIGURE 10: Men's and women's 50-meter scores in the second and third grades.

TABLE 3: Evaluation of the 50-meter test scores for all junior high school students.

Grade	First grade boys	First grade girl	Second grade boys	Second grade girl	Grade three boys	Grade three girls
Excellent	20.63%	25.31%	27.65%	29.36%	30.91%	32.19%
Good	36.25%	41.65%	45.99%	39.69%	45.98%	44.01%
Pass	43.12%	33.04%	26.36%	30.95%	23.11%	23.8%

The comprehensive evaluation from the two aspects of test scores and grade evaluation reflects the poor speed quality of students.

**4.4. Junior High School Students Bend Forward while Sitting.** Flexibility refers to the flexibility of different joints and muscles. Good flexibility can better reflect the beauty of the body. If the body lacks flexibility for a long time, it will cause mild heat around the joints, thereby limiting the range of joint motion.

How to calculate the forward bending distance of the sitting body? In the calculation distance section, calculate the average distance to each wireless sensor network reference node, and send the calculation result to each pending node of the wireless sensor network through broadcast. The node to be determined receives the information of the reference node and compares the received average hop distance with the minimum number of hops of each reference node previously obtained to calculate the distance of the node to be determined. The calculation method of the hop distance of the pending node is as follows:

$$L_n = \frac{\sum_{m \neq n} \sqrt{(x_n - x_m)^2 + (y_n - y_m)^2}}{\sum_{m \neq n} h_m}. \quad (15)$$

The reference node broadcasts the calculated average hop distance to the wireless sensor network where it is located, and the pending node retains the first average hop distance data received by the sensor node. At the same time, the hop count information is forwarded to the surrounding nodes to ensure that data can be received from the nearest reference node.

The coordinates of the undetermined node can be calculated by the above calculation to obtain the distance of more

than 3 reference nodes, and the position of the undetermined node can be calculated by the trilateral method. The coordinates of  $N$ ,  $M$ , and  $T$  are  $(x, y)$ ,  $(x_n, y_n)$ ,  $(x_m, y_m)$ , and  $(x_t, y_t)$ , respectively, and the distance from the node to be determined to the reference node is  $d_n$ ,  $d_m$ , and  $d_t$ . From the geometric relationship, the following relationship can be obtained:

$$\sqrt{(x - x_n)^2 + (y - y_n)^2} = d_n, \quad (16)$$

$$\sqrt{(x - x_m)^2 + (y - y_m)^2} = d_m, \quad (17)$$

$$\sqrt{(x - x_t)^2 + (y - y_t)^2} = d_t. \quad (18)$$

Through the above steps, the coordinates of the undetermined nodes are obtained, and the average positioning error index is used to compare the positioning algorithms of the wireless sensor network. Supposing the coordinate of the undetermined section  $i$  is  $x_i, y_i$ , the actual coordinate value is  $(x'_i, y'_i)$ , and the following formula calculates the error of the positioning algorithm:

$$\Delta d_i = \sqrt{(x_i - x'_i)^2 + (y_i - y'_i)^2}. \quad (19)$$

In a wireless sensor network including  $N$  undetermined nodes, the average positioning error is calculated using the following formula:

$$\Delta = \frac{1}{NR} \sum_{i=1}^N \Delta d_i \times 100\%. \quad (20)$$

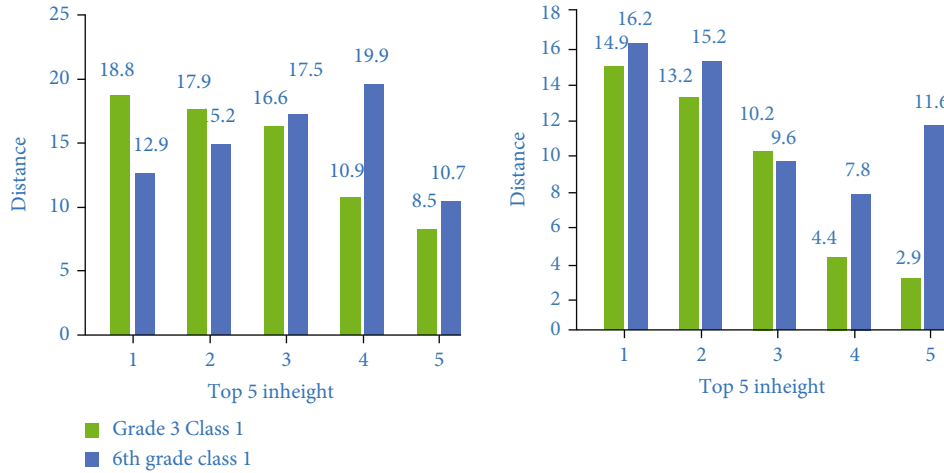


FIGURE 11: The five highest boys and girls in class 3 and class 6 are bent forward.

TABLE 4: Physical education curriculum intervention program.

Category	Intervention content		
	30 meters	60 meters	100 meters
Speed			
Strength	Raise your legs in place 10 seconds	15 m acceleration run	20 m forward run
Endurance	10 m lunge	Speed running	20 m trolley
Flexible	Kick	Yoga	Stretch

Inviting the highest five boys and girls in the first grade of third grade and the first grade of sixth grade to monitor the fixed-point distance statistics of sitting forward bending as shown in Figure 11.

The results of the seat bending test showed that the flexibility of girls is generally much better than that of boys, and the abovementioned students are within the scope of the national physical health standards. In addition to showing the flexibility of the human body, the results of the seat bending test also show the structural characteristics of the female body. Women’s muscles, ligaments, and joints are more flexible. In general, women are more flexible, while boys also have a good foundation for flexibility.

**4.5. Physical Fitness Intervention Program.** With the help of wireless sensor technology, it is detected that the physical health of students is generally low, which has a large relationship with the lack of a lot of physical exercise by students. Therefore, according to the analysis of the physical fitness of the students, it is recommended to draw an intervention plan for the basic physical fitness, as shown in Table 4.

At the same time, to help students better improve and improve their physical fitness, we propose an open extracurricular preplan for the experimental group students. The program mainly provides suggestions for students’ health awareness, extracurricular exercises, and lifestyle.

**4.5.1. Health Awareness.** Cultivating students’ health awareness and developing good health habits.

**4.5.2. Extracurricular Exercise.** The main form of exercise is aerobic exercise; daily walking is mainly brisk walking or

running at a constant speed; breaks between classes to do stretching exercises outdoors; interclass exercise time organizes extracurricular exercises in the unit of class.

The exercise intensity is mainly of medium intensity. It is recommended that 3-5 times a week, each time is about 05-1 hours. The frequency and time of exercise can be adjusted according to your own physical status, so as not to affect the next day of class.

**4.5.3. Lifestyle.** Diet-pay attention to the dietary rules, insist on eating breakfast, reasonably, match nutrition, pay attention to the intake of high-quality protein, diversify food as much as possible, and ensure a daily intake of 1500ml of drinking water. Sleep is in accordance with the school’s schedule. Go to bed at 22:00 in the evening, wake up at 5:30 in the morning, and take a lunch break at noon to ensure enough sleep.

**4.5.4. Matters Needing Attention.** Ensuring the intensity and time of each exercise.

If there are no special circumstances, work and rest on time.

Parents’ work cooperation is also essential, because children have no self-control, so parents need to help their children arrange reasonable time for physical exercise and develop good work and rest.

## 5. Conclusion

Physical fitness is an important foundation for students’ education and life. Without a healthy body, everything is impossible to talk about. Young students need not only

culture but also health knowledge. The continuous decline of students' physical fitness has become an inevitable topic. However, many students in physical health quality monitoring are not aware of their physical health, and it is difficult for schools to fully understand. Therefore, the student physical fitness test is a way for students and schools to better understand the physical condition of students and then promote the development of a physical education curriculum. It is an inevitable technology to apply scientific and accurate wireless sensors to physical health detection. Students are the pillars of the country and the body of the country. Students' education and life must be put first in order to maintain the country's strength forever, and sunshine always blooms.

### Data Availability

Data sharing not applicable to this article as no datasets were generated or analyzed during the current study.

### Conflicts of Interest

The author declares that she has no conflicts of interest.

### References

- [1] A. Musa, V. Gonzalez, and D. Barragan, "A new strategy to optimize the sensors placement in wireless sensor networks," *Journal of Ambient Intelligence and Humanized Computing*, vol. 10, no. 4, pp. 1389–1399, 2019.
- [2] Z. Kaleem and M. H. Rehmani, "Amateur drone monitoring: state-of-the-art architectures, key enabling technologies, and future research directions," *IEEE Wireless Communications*, vol. 25, no. 2, pp. 150–159, 2018.
- [3] D. Flores, I. Kristian, A. N. Bragado et al., "The role of parents in monitoring students academxxic performance in the new learning modality of their children," *International Journal of Multidisciplinary Studies*, vol. 5, no. 1, pp. 22–25, 2021.
- [4] V. Vituk, N. Skrypyuk, and I. Khomiak, "Test monitoring of the speech competence of students of modern higher education institutions," *ScienceRise*, vol. 2, no. 2, pp. 52–60, 2020.
- [5] S. Sugilar, "The role of service quality management in students' re-enrollment," *Turkish Online Journal of Distance Education*, vol. 21, no. 1, pp. 45–56, 2020.
- [6] C. C. Hsu, W. Y. Huang, and J. Y. Lee, "Research on the motivation and attitude of college students' physical education in Taiwan," *International Journal of Physical Education, Fitness and Sports*, vol. 8, no. 1, pp. 95–109, 2019.
- [7] T. Прошева, T. Grosheva, Г. Шелякина, and G. Shelyakina, "To the question of students' graphic training quality monitoring effectiveness," *Geometry & Graphics*, vol. 5, no. 4, pp. 75–82, 2017.
- [8] H. Lyu, "How are students immersed by providing virtual reality technology? The role of psychological distance in online flipped class," *International Journal of Information and Education Technology*, vol. 10, no. 1, pp. 79–83, 2020.
- [9] I. Jibreel and A. Al-Abbasi, "The relationship between translation strategies awareness and students' translation quality," *Journal of Applied Linguistics and Language Research*, vol. 4, no. 6, pp. 19–39, 2017.
- [10] V. Aryadoust, "Understanding the role of likeability in the peer assessments of university students' oral presentation skills: a latent variable approach," *Language Assessment Quarterly*, vol. 14, no. 4, pp. 398–419, 2017.
- [11] N. A. Zcan, M. E. Koak, and R. Arslan, "The role of aggression in the relationship between grandiose narcissistic traits and interpersonal style: university students in Turkey," *Journal of Clinical Psychiatry*, vol. 21, no. 4, pp. 341–350, 2018.
- [12] D. Abdelsamea and M. Shamrokh, "The role of E-learning in developing the skills of social work students in light of the total quality," *Egyptian Journal of Social Work*, vol. 10, no. 1, pp. 83–102, 2020.
- [13] Z. Sheng, C. Mahapatra, V. Leung, M. Chen, and P. K. Sahu, "Energy efficient cooperative computing in mobile wireless sensor networks," *IEEE Transactions on Cloud Computing*, vol. 6, no. 1, pp. 114–126, 2018.
- [14] P. Kumar, S. Kumari, V. Sharma, A. K. Sangaiah, J. Wei, and X. Li, "A certificateless aggregate signature scheme for healthcare wireless sensor network," *Sustainable Computing: Informatics and Systems*, vol. 18, pp. 80–89, 2018.
- [15] A. S. Makinde, A. O. Agbeyangi, and W. Nwankwo, "Predicting mobile portability across telecommunication networks using the integrated-KLR," *International Journal of Intelligent Information Technologies*, vol. 17, no. 3, pp. 50–62, 2021.
- [16] O. I. Khalaf and G. M. Abdulsahib, "Optimized dynamic storage of data (ODSD) in IoT based on blockchain for wireless sensor networks," *Peer-to-Peer Networking and Applications*, vol. 14, no. 5, pp. 2858–2873, 2021.
- [17] I. K. Osamh and G. M. Abdulsahib, "Energy efficient routing and reliable data transmission protocol in WSN," *International Journal of Advances in Soft Computing and its Application*, vol. 12, no. 3, pp. 45–53, 2020.
- [18] F. Wu, L. Xu, S. Kumari, and X. Li, "A privacy-preserving and provable user authentication scheme for wireless sensor networks based on internet of things security," *Journal of Ambient Intelligence & Humanized Computing*, vol. 8, no. 1, pp. 101–116, 2017.
- [19] M. Adil, H. Song, J. Ali et al., "EnhancedAODV: a robust three phase priority-based traffic load balancing scheme for internet of things," *IEEE Internet of Things Journal*, 2021.
- [20] J. Srinivas, S. Mukhopadhyay, and D. Mishra, "Secure and efficient user authentication scheme for multi-gateway wireless sensor networks," *Ad Hoc Networks*, vol. 54, pp. 147–169, 2017.
- [21] A. Hassani, J. Plata-Chaves, M. H. Bahari, M. Moonen, and A. Bertrand, "Multi-task wireless sensor network for joint distributed node-specific signal enhancement, LCMV beamforming and DOA estimation," *IEEE Journal of Selected Topics in Signal Processing*, vol. 11, no. 3, pp. 518–533, 2017.
- [22] A. Amin, X.-H. Liu, M. A. Saleem et al., "Collaborative wireless power transfer in wireless rechargeable sensor networks," *Wireless Communications and Mobile Computing*, vol. 2020, Article ID 9701531, 13 pages, 2020.
- [23] M. Guan, K. Wang, D. Xu, and W. H. Liao, "Design and experimental investigation of a low-voltage thermoelectric energy harvesting system for wireless sensor nodes," *Energy Conversion & Management*, vol. 138, pp. 30–37, 2017.
- [24] F. Gandino, R. Ferrero, and M. Rebaudengo, "A key distribution scheme for mobile wireless sensor networks: \$q\$ - \$s\$ - composite," *IEEE Transactions on Information Forensics and Security*, vol. 12, no. 1, pp. 34–47, 2017.

- [25] F. Xiao, "Multi-sensor data fusion based on the belief divergence measure of evidences and the belief entropy," *Information Fusion*, vol. 46, pp. 23–32, 2019.
- [26] S. S. Kim, S. McLoone, J. H. Byeon, S. Lee, and H. Liu, "Cognitively inspired artificial bee colony clustering for cognitive wireless sensor networks," *Cognitive Computation*, vol. 9, no. 2, pp. 207–224, 2017.

## Retraction

# Retracted: The Optimal Path of Cultivating and Promoting the Employment Ability of College Students Based on the Whole Process Management Mode of Construction Engineering Based on Computer Aided Technology

### Wireless Communications and Mobile Computing

Received 25 July 2023; Accepted 25 July 2023; Published 26 July 2023

Copyright © 2023 Wireless Communications and Mobile Computing. This is an open access article distributed under the Creative Commons Attribution License, which permits unrestricted use, distribution, and reproduction in any medium, provided the original work is properly cited.

This article has been retracted by Hindawi following an investigation undertaken by the publisher [1]. This investigation has uncovered evidence of one or more of the following indicators of systematic manipulation of the publication process:

- (1) Discrepancies in scope
- (2) Discrepancies in the description of the research reported
- (3) Discrepancies between the availability of data and the research described
- (4) Inappropriate citations
- (5) Incoherent, meaningless and/or irrelevant content included in the article
- (6) Peer-review manipulation

The presence of these indicators undermines our confidence in the integrity of the article's content and we cannot, therefore, vouch for its reliability. Please note that this notice is intended solely to alert readers that the content of this article is unreliable. We have not investigated whether authors were aware of or involved in the systematic manipulation of the publication process.

In addition, our investigation has also shown that one or more of the following human-subject reporting requirements has not been met in this article: ethical approval by an Institutional Review Board (IRB) committee or equivalent, patient/participant consent to participate, and/or agreement to publish patient/participant details (where relevant).

Wiley and Hindawi regrets that the usual quality checks did not identify these issues before publication and have since put additional measures in place to safeguard research integrity.

We wish to credit our own Research Integrity and Research Publishing teams and anonymous and named external researchers and research integrity experts for contributing to this investigation.

The corresponding author, as the representative of all authors, has been given the opportunity to register their agreement or disagreement to this retraction. We have kept a record of any response received.

### References

- [1] S. Chen, "The Optimal Path of Cultivating and Promoting the Employment Ability of College Students Based on the Whole Process Management Mode of Construction Engineering Based on Computer Aided Technology," *Wireless Communications and Mobile Computing*, vol. 2022, Article ID 4289413, 8 pages, 2022.



## Research Article

# The Optimal Path of Cultivating and Promoting the Employment Ability of College Students Based on the Whole Process Management Mode of Construction Engineering Based on Computer Aided Technology

Siyu Chen 

*School of Architecture and Civil Engineering, Xihua University, Chengdu 610039, Sichuan, China*

Correspondence should be addressed to Siyu Chen; [chensy@mail.xhu.edu.cn](mailto:chensy@mail.xhu.edu.cn)

Received 31 December 2021; Revised 11 February 2022; Accepted 17 February 2022; Published 5 March 2022

Academic Editor: Shalli Rani

Copyright © 2022 Siyu Chen. This is an open access article distributed under the Creative Commons Attribution License, which permits unrestricted use, distribution, and reproduction in any medium, provided the original work is properly cited.

The whole process management of construction project is to carry out all-round supervision and management of the whole stage of construction project implementation, which can realize the effective allocation of construction project (CP) funds and improve the construction quality at the same time. On this basis, this article analyzes the impact of the whole-process management (WPM) model on the employment ability (EA) of college students (CS), uses computer-aided technology to calculate the information of graduates in a construction company, and analyzes according to the work situation of the graduates in the enterprise and the evaluation of the EA of the graduates by the enterprise cultivation path of university students' EA. The experimental results of this paper show that the evaluation of the four structural elements of EA of CS by construction companies is higher than that of college students' self-evaluation, indicating that there is a difference between the EA of students and the needs of enterprise EA, which can be used as an entry point to train students EA.

## 1. Introduction

The employment problem of college students is a topic of social concern, and the demand of construction enterprises for the employability of college students is also increasing. In this context, how to make the employability of college students match the needs of construction enterprises and find a path to optimize the employability of college students from the actual talent requirements of enterprises are the focus of this paper.

Numerous students have conducted in-depth discussions on the study of the employment ability training path of CS based on the WPM mode of construction engineering based on computer-assisted technology. For example, a scholar believes that WPM can supervise construction projects, and letting CS learn this management model in advance will greatly help them to engage in construction industry-related work after graduation [1]. A scholar believes that EA is a kind of ability to make progress and

feedback and respond to the society. The concept of comprehensive EA is to expand on the main definition and does not include the ability to successfully engage in a certain job in the personality of the worker. Personal characteristics such as character and external environmental factors in addition to personal aspects are also included in the definition of EA [2]. There are also domestic scholars based on the perspective of ability structure composition, summarizing the EA of college students as a unified concept of all-round personal qualities of CS. In the field of psychology research, the EA of CS has a larger scope of research, and it is the key ability behavior to obtain a career and achieve success [3]. Although the research results on the EA improvement path under the WPM mode of CE are good, the improvement of the EA of CS still requires the joint efforts of society, schools, families, and individuals to create a good employment environment for students.

This article describes the WPM theory of CP and lists the WPM methods. It analyzes the differences between the

employability of students under the WPM mode and the employability required by the enterprise according to the structural elements of the employability of CS and proposes improvements based on the current situation of the difference (advice on the employability of CS).

## 2. The Whole Process Management of Construction Project and the Analysis of the Employability of College Students

*2.1. The WPM Theory of Construction Project.* The development direction of the WPM of construction engineering should be the following: comply with the requirements of the innovative, open harmonious development concept, in line with the principle of lowest cost and highest efficiency, maintain the general structure of the existing information management system, and improve the functions, develop and add new functions, expand the scope of information management, expand the ways and channels for managers to obtain information, and ensure the timely and rapid transmission of information; realize the completeness and traceability of information in the whole process of CE, and improve work efficiency [4, 5].

### *2.2. The WPM Method of Construction Project*

*2.2.1. Reasonably Formulate Cost Plans and Refine Project Cost Estimates.* The accuracy of the estimated investment value in the project decision-making stage is a key indicator of whether the project can be successfully completed. It is also a key link in the approval of the competent authority and is of great significance to all project plans. Once the reasonable cost allocation of the project is completed, the project design and project implementation can be completed perfectly. Usually, only approved costing is the maximum amount of the project. Every link in the future shall not exceed this limit. Therefore, this means that the cost estimation must be detailed and accurate; otherwise, it will definitely affect the evaluation of investment decision management and future construction plans [6, 7].

*2.2.2. Formulate Construction Organization Design Scientifically and Reasonably.* In the preparatory work of the project, appropriate multidepartmental and multistage methods should be adopted to calculate as many relevant construction details as possible, strictly control the work quality of the construction personnel, and decentralize the work concept. Practice the work attitude of honesty, dedication, and integrity, based on the quality assurance requirements of shortening the construction period and improving economic benefits [8].

*2.2.3. Improve Project Information.* Prior to reviewing the plan, relevant personnel should provide all relevant information. Under normal circumstances, the estimated cost of the project is increased or decreased based on the design budget of the preliminary construction. However, a key part of the construction process will be handed over to the finance department for immediate follow-up. The project budget manager does not know this information, so it is easy to

make mistakes in the project. Therefore, the project personnel should conduct a detailed cost review after the project is completed to complete the project evaluation [9].

*2.2.4. Establish an Accounting System throughout the Entire Process of the Project.* In the project management link, we must ensure the integrity of the accounting system of the real estate company, in order to ensure the implementation of project cost control tasks and then project cost management throughout all aspects of construction projects. The real estate company must create a project accounting system through the company management system, calculate the specific cost of the construction project on a monthly basis, and compare it with the target price to obtain an intuitive project cost control status. You can check the delivery date with the quality control department in the last month. Take the target cost of the construction project as the standard, and fill in any actual cost report at the completion of the project. In addition, statistical surveys should be completed on the basis of the fair value of each cost of each project and should be formulated regularly. Finally, through the project cost completion table, the cost-benefit analysis of each project is carried out, and the project accounting engineering system is improved.

### *2.3. The Structural Elements of the Employability of CS*

*2.3.1. Elements of Professional Competence.* The requirements for CS are not limited to academic qualifications or literary works; they must also have professional knowledge and skills that are compatible with their academic qualifications or literary works. In the era of knowledge economy, the EA of college students is crucial to the success or failure of college job hunting. Economic globalization, industrial modernization, and knowledge-based economic reforms enable students to excel in meeting the needs of today's society. Simple measurable indicators alone cannot fully reveal the concept of work ability [10, 11]. The above definition ignores the acquisition of skills, knowledge, and learning ability in the process of university teaching. The professional knowledge and skills acquired by the university are not only a requirement for students, because employees can choose jobs that do not match their vocational skills by reducing their career pursuits or other reasons. Therefore, the research on the work ability of CS is not limited to the ability to find a job but also focuses on the comprehensive ability of students to keep their jobs and achieve professional success [12].

*2.3.2. Common Skill Elements.* General skills generally refer to the basic abilities that CS must have when they enter the society, as opposed to professional skills, which every CS must possess. The basic definition of general skills needs to match the basic needs of the company and society, so the definition of general skills needs to start from the true reflection of the company. According to the literature, many scholars define some basic skills required by enterprises as general skills. In their understanding of foreign enterprises, they most hope that university graduates have the following eight abilities: personal control ability, initiative ability,

adventurous spirit, teamwork collaboration ability, the ability to capture business opportunities, the ability to process and apply data, the ability to use information equipment, and the ability to identify and eliminate difficulties [13]. These eight abilities come from the real needs of the company and are the development capabilities most needed by the company.

**2.3.3. Personal Quality Factors.** Personal quality embodies the inner quality of the individual and is the true manifestation of the personal spiritual world. It is cultivated through the acquired environment, similar to the concept of emotional intelligence. Emotional intelligence research has just emerged in recent years. It is about how individuals deal with their own emotions, their attitude toward others, their ability to regulate emotions, and the performance of their inner world. EQ can also be cultivated in campus culture and family culture [14]. Research shows that those who can get the ideal job are those who are proactive and optimistic graduates. There are also surveys that show that people who are more confident and optimistic are more likely to have better advantages and prospects in job search and work. Employers with stronger internal drive also have a stronger sense of self-efficacy, which can make it easier to obtain a career and quickly adapt to changes in the workplace. On the contrary, those who are emotional, pessimistic, and lazy cannot achieve their own development or even get a satisfactory job [15, 16].

**2.3.4. Elements of Career Planning Ability.** Career planning capabilities include the ability to design and manage their own development, which has a great degree of guiding significance for being able to distinguish employment situations, identify job opportunities, and stimulate work motivation, and can help employees achieve high performance and complete work beyond. Career planning begins in colleges and universities and is continuously improved and practiced in life development. It is a guarantee factor for college graduates' success in job hunting and career success and an important branch of college students' EA [17].

Figure 1 shows the employment-related EA of college students to be analyzed in this article. Under the four structural elements, a total of 11 EA is included.

**2.4. Reliability and Validity Test.** Reliability test is to verify the consistency of expert scores, and this coefficient cannot be lower than 0.6. If the consistency coefficient is low, you should consult the experts. The content validity of the I-CVI evaluation scale is usually used, which reflects the degree of consistency between the evaluators.

$$P_c = \left[ \frac{n!}{A!(n-A)!} \right] \times 0.5^n, \quad (1)$$

$$K^* = \frac{I - CVI - P_c}{1 - P_c}. \quad (2)$$

Among them,  $P_c$  is the random consistency probability,  $A$  is the number of scoring experts,  $n$  is the total number

of expert consultations, and  $K^*$  is the revised random consistency.

### 3. Experimental Research

**3.1. Research Purpose.** The main purpose of this article is to analyze the evaluation of graduates' EA by the construction company when a large-scale construction company implements the WPM mode of CE, so as to provide a reference for what kind of EA the college students need to master.

**3.2. Research Content.** School-enterprise cooperation is not only conducive to the export of talents from schools to the society, but also to the introduction of talents from enterprises, which is a win-win situation. The data in this article comes from the information of students from a construction company cooperating with a university, and these students are currently employed in the construction company. Through the drafting of survey items, graduates can make corresponding item selections, survey of the working years of graduated students in the enterprise, the evaluation of the employment guidance courses carried out by the school, the financial support of the school for employment projects, and the level of students and construction The enterprise level analyzes the structural elements of the EA of CS and proposes countermeasures and suggestions to improve the EA of CS.

### 4. Analysis of Cultivation of Undergraduates' Employability

**4.1. Basic Situation of Construction Graduates.** Figure 2 shows the number of graduates recruited by the construction company in the construction major of colleges and universities. There are 92 men and 34 women who have worked in the company for less than one year, accounting for 51.01% of the graduates recruited. There are 44 men and 17 women who have worked for 2-3 years, accounting for 24.70% of the total. The number of people who have worked for 3-5 years accounts for 15.79% of the total graduates, including 28 men and 11 women who have worked for 5 years. Among the above graduates, 15 are males and 6 are females, accounting for 8.50% of the total.

#### 4.2. Analysis of the Development of School Employment Projects

**4.2.1. The Overall Evaluation of Graduates on the Employment Guidance Courses (EGC) Carried Out by the School.** Table 1 shows the results of graduates' evaluation of the school's EGC. From the data in the table, it can be seen that the number of people who have general evaluation of EGC is the largest, accounting for 32.79%, and the number of people who have good or better evaluations is 46.56%, which is less than half.

**4.2.2. Analysis of the School's Investment in Employment Support.** Figure 3 shows the school's funding support for employment-related projects from 2016 to 2020. It can be seen from the figure that the capital investment in the

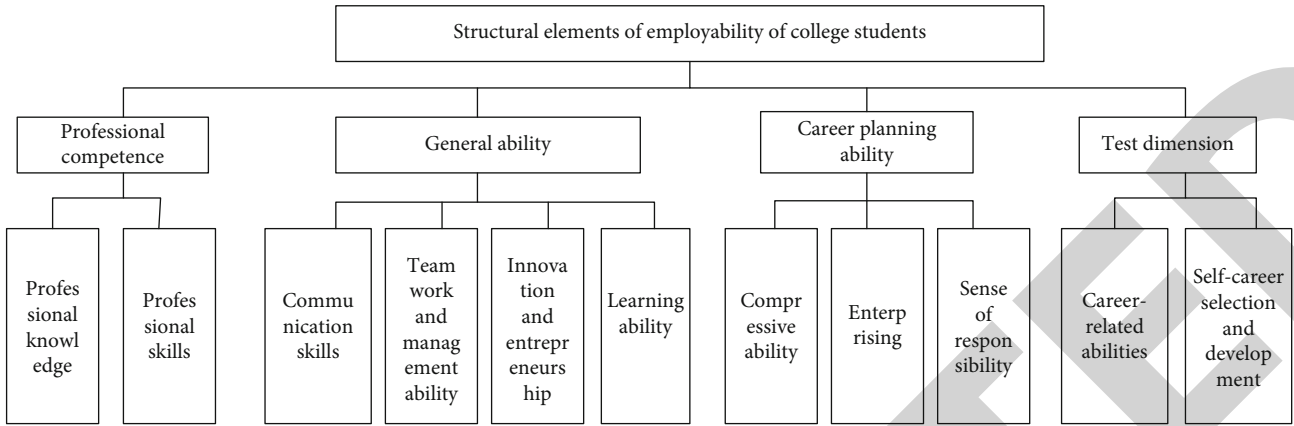


FIGURE 1: The structural elements and subitems of the employability of college students.

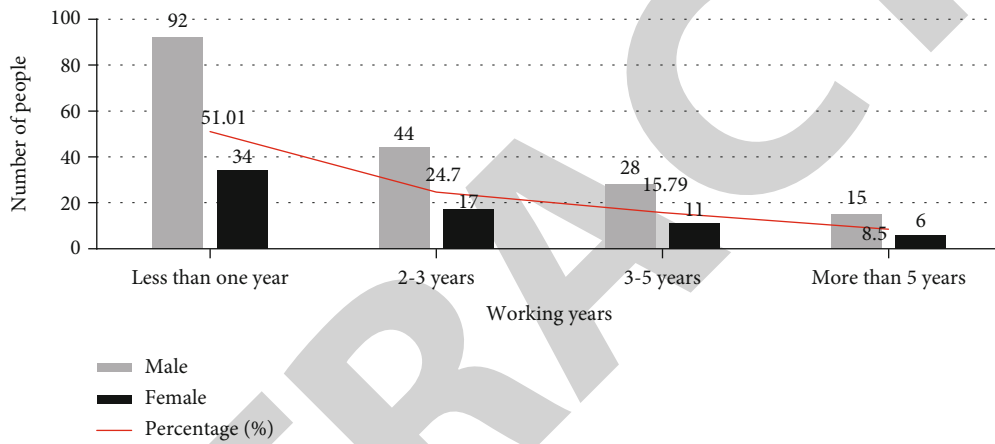


FIGURE 2: Distribution of the ratio of male to female graduates.

TABLE 1: Evaluation results of career guidance courses.

	Good	Better	Generally	Poor	Difference	Total
Number of people	53	62	81	24	27	247
Percentage	21.46%	25.10%	32.79%	9.72%	10.93%	100%

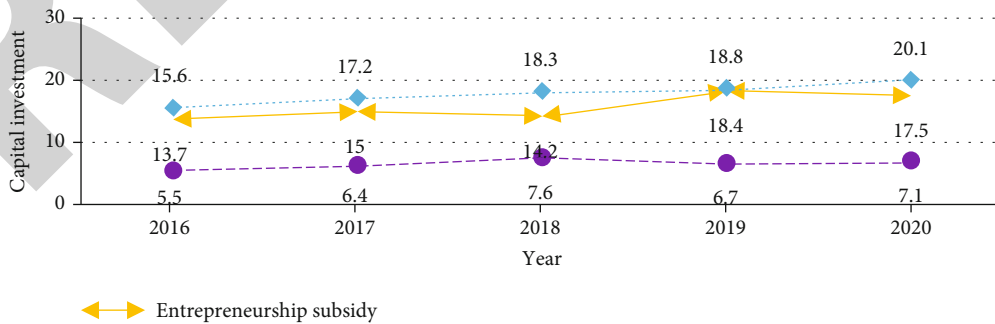


FIGURE 3: School employment support investment in recent years (ten thousand yuan).

entrepreneurship and employment project competition has increased year by year. Although the investment in entrepreneurship subsidies and grassroots employment subsidies have also shown an overall upward trend, the growth in capital investment has been unstable. To enhance the employability of CS, the school must still attach importance to the financial support of employment projects.

#### 4.3. Reliability and Validity Analysis of Dimensions Related to Employability

**4.3.1. Reliability Analysis.** Reliability is to test the consistency of data, and reliability testing is an indispensable link. In general research, reliability is expressed by correlation coefficient. The reliability test of this article is based on the four levels of college students' recognition A, construction company recognition B, college students' self-evaluation score C, and construction company evaluation score D. The corresponding reliability coefficients are shown in Table 2 and Figure 4. The minimum standard of the reliability coefficient is 0.6. The higher the coefficient, the better the data consistency. It can be seen from the data in the table that the coefficient values of the various employability components of the four levels are all greater than 0.7, indicating that the data in this survey is highly reliable.

### 5. Validity Analysis

Content validity is used to measure whether the listed questions can truly reflect the research content of the measurement. It is also called face validity or logical validity. The survey items in this study are all direct measurements. Other data that can be used as calibration standards cannot be found within a certain period of time, and it is difficult to conduct empirical validity analysis. Therefore, the analysis is selected from the perspective of construction validity and content validity. In order to satisfy the content validity of the survey items, based on the relevant research of employability structure theory, combined with the opinions given by relevant experts and teachers, this article continuously improves and improves the survey items, so as to make sure that the research data used in the article have considerable content validity.

**5.1. Comparison of Differences in the Degree of Attention Paid to Employability of College Students.** According to the basic principles of economics, the allocation of labor in the job market follows the principle of maximum utility. Enterprise recruitment is also inseparable from the goal of maximizing utility and striving to control the cost of human resources. The establishment of a selection and employment mechanism for enterprises based on their own characteristics and industry norms is an autonomous behavior that conforms to market economy guidelines. According to the current labor supply market, the employment requirements of enterprises are constantly increasing, but the reform of the training mode of students in colleges and universities is relatively lagging, resulting in significant differences between the EA of college students and the actual needs of enterprises in the following aspects. In the above, we extracted 4 impact

TABLE 2: Reliability coefficient table of four levels.

Test dimension	A	B	C	D
Professional competence	0.924	0.917	0.868	0.872
General ability	0.905	0.913	0.876	0.854
Career planning ability	0.776	0.824	0.791	0.783
Test dimension	0.760	0.752	0.788	0.733

factors as the structural elements of the EA of college students that can be explained. According to the four levels of A, B, C, and D above, the difference between the EA of college students and the social needs is judged, and then, the EA improvement path is proposed based on the difference. This paper uses the average value of various EA components at each level to express the score of this EA component, as shown in Table 3.

**5.1.1. Comparison of Differences in Professional Competence.** As the basic ability for college students to enter the workplace, professional ability is regarded as a very important EA by CS and construction companies. The professional competence in this article is defined as professional knowledge and professional skills. The data collected through the questionnaire survey shows that both college graduates and construction company executives recruited supervisors to regard professional knowledge and professional skills as the main components of college students' EA, with scores of 4.87 and 4.89 points, respectively. This shows that the training of professional ability cannot be ignored. However, the judgment of college students and construction companies on whether they have the ability and their importance cannot match. The average score of the self-evaluation of the professional ability of college students is 4.21 points, but the evaluation of the professional ability of college students by construction enterprises is only 3.74 points, which shows that the professional ability of college graduates has not reached the basic requirements of enterprises.

**5.1.2. Comparison of Differences in General Skills.** General skills are a necessary skill for college students to choose and acquire careers and achieve success in the workplace. The general skills defined in this article include communication skills, teamwork and management skills, innovation and entrepreneurship skills, and learning skills. In the survey of this skill, communication skills and teamwork and management skills were recognized by construction companies, with high scores of 4.33 and 4.19 points, respectively. The other two skills scores were generally low, and the innovation and entrepreneurship ability was only 2.66 points. Learning ability gets 3.56 points. In addition, the general skills possessed by college students themselves cannot basically meet the general skills required by society. The self-evaluation scores of the college students' communication skills and teamwork and management skills reached 4.51 and 4.35, and the self-evaluation scores of the other two abilities were also above 4 points. Construction companies' test scores for their employees are lower than those of college students, and

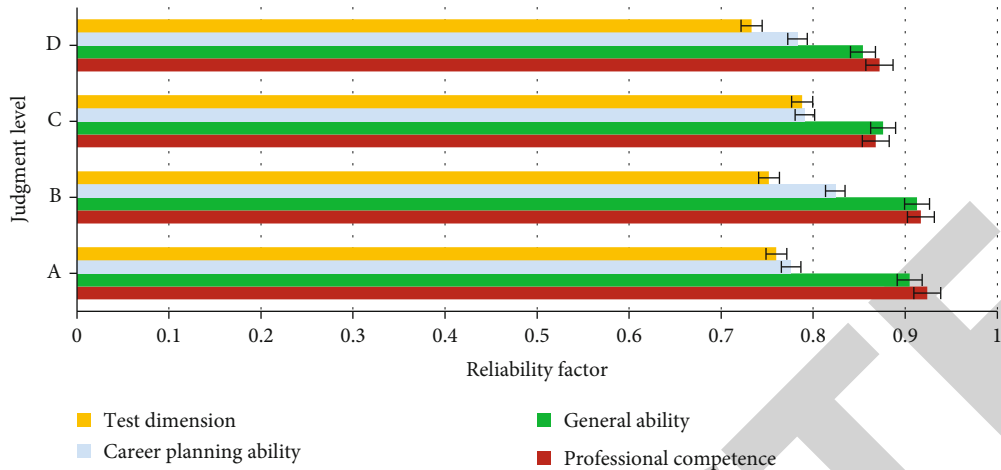


FIGURE 4: Distribution of reliability coefficients.

TABLE 3: Average value of employability components.

	A	B	C	D
Professional knowledge	4.36	4.87	4.21	3.74
Professional skills	4.75	4.89	3.62	2.78
Communication skills	4.23	4.33	4.51	3.76
Teamwork and management ability	4.41	4.19	4.35	3.52
Innovation and entrepreneurship	3.47	2.66	4.18	2.94
Learning ability	3.85	3.56	4.24	3.59
Compressive ability	4.06	4.37	3.62	2.13
Enterprising	4.29	4.61	4.14	3.54
Sense of responsibility	4.23	4.78	3.46	3.17
Career-related abilities	3.45	2.68	4.37	2.98
Self-career selection and development	3.64	2.90	3.75	3.31

they believe that the general skills of their employees need to be strengthened.

**5.1.3. Comparison of Differences in Personal Qualities.** Personal quality is a manifestation of the basic qualities of college students themselves and is a necessary guarantee for college students to obtain professional recognition and obtain professional promotion and development. The personal qualities defined in this article include the ability to withstand stress, enterprising spirit, and a sense of responsibility. College students and construction companies have expressed full recognition of these three skills, and their scores have reached 4.3 points or more. In the evaluation of college students themselves, the scores of the three abilities were 3.62 points, 4.14 points, and 3.86 points, respectively, which were in the middle level. However, in the evaluation of employees by construction companies, the scores of the three abilities were 2.13 points, 3.54 points, and 3.17 points are all around three points, especially the stress resistance is less than 3 points, which shows that college students have not really adapted to the graduation life and cannot handle the work pressure well. In addition, the score of responsibility in the evaluation of college students

by construction companies is only 3.17 points, which is basically similar to the 3.46 points of their own evaluation, generally low, and quite different from the degree of recognition.

**5.1.4. Comparison of Differences in Career Planning Ability.** Career planning ability is a developmental ability for college students to achieve success, which promotes college students' career recognition. The career planning ability of this article includes the basic skills of obtaining occupations, self-career selection, and career development ability. There is a big difference in recognition of this ability. College students value this ability because of their own development considerations. Relatively speaking, enterprises do not pay much attention to the employability of career planning ability. This is also due to the requirements of the market economy and the needs of construction companies. The company hopes to recruit employees who do their best for the company. Their career planning should follow the company's development path, so construction companies do not value career planning ability.

**5.2. Employability Training and Improvement Path**

**5.2.1. Establish a Support System for College Students' Employability Development.** The government has advantages in management, planning, economy, policy, and finance. These advantages can provide an effective platform for ensuring the employment of students and contribute to the overall development of schools and enterprises. In the process of cultivating the EA of college students, government actions play a programmatic role. Government policies are the political basis for employment, and government policies must adapt to the social employment situation and eliminate obstacles to student employment. The government uses policies to guide college students to choose employment positions reasonably, increase the tolerance for student talents, and jointly implement the student skill development mechanism to provide an effective support platform for the improvement of college students' employability and employment status.

**5.2.2. School-Enterprise Docking to Carry Out Corresponding Reforms.** In reality, some companies do not pay enough attention to school-enterprise cooperation. In the school-enterprise cooperation, they are eager to believe that the cooperation investment is large, the risk is high, the return period is long, and the cooperation with the school is easy to suffer. Some corporate human resource executives believe that the coeducation cycle is long and may not be able to retain people, so they are unwilling to participate in the training of students. They often recruit talents directly, and it is difficult to participate in vocational education. To achieve real cooperation in the teaching industry and the docking of schools and enterprises, it is necessary to clarify the real needs of both the school and the enterprise and establish a school-enterprise integration mechanism. Enterprises should participate in the professional setting of colleges and universities and guide colleges and universities to establish “teaching factories” that integrate theoretical teaching and practice.

**5.2.3. Strengthen the Cultivation of College Students' Innovative and Entrepreneurial Ability.** Colleges and universities should create a public platform for students' innovation and entrepreneurship internships, add innovation workshops, provide material guarantees for their innovation internships, and provide space for students' innovation and entrepreneurship training through cooperation with related enterprises. Colleges and universities should create an environment for student entrepreneurship development, encourage technological innovation, stimulate students' willingness to innovate, actively connect with venture capital institutions, and financially support college student innovation projects.

**5.2.4. Improve Interpersonal Skills.** After students complete the academic internship, they should complete the transition from student to social worker. They also need to regulate the different interpersonal relationships between partners, superiors, subordinates, and different age groups. But after all, most of the time when students study in school, they have relatively narrow social contact and lack of knowledge and experience, have not yet formed a systematic outlook on the world and life, and have weak cognitive abilities. For students who have just stepped into society, dealing with such complicated interpersonal relationships is often not handled well, which often leads to interpersonal tension, anxiety, and personal or even serious mental illness. It affects their happiness at work and life to varying degrees. Therefore, it is necessary for schools to organize appropriate courses for students and provide communication education to simulate social communication scenarios to analyze interpersonal relationships. Let students learn to improve interpersonal sensitivity, build self-confidence, and master interpersonal communication skills.

## 6. Conclusion

The employment of CS has attracted attention from all walks of life, and how to improve their EA has become a topic of

concern to schools and society. Based on the WPM of construction engineering, from the comparative analysis of the difference in the degree of attention of college students in construction enterprises, it can be seen that students' evaluation of their own professional skills, communication skills, innovation and entrepreneurship capabilities, and other related employability evaluations is about 0.5-1 higher than that of enterprises. This makes a certain gap between the EA that students consider themselves and that required by the enterprise, so that the EA of students does not match the actual talent demand of the enterprise. Therefore, the EA of college students can be improved by opening innovation and entrepreneurship training courses and enhancing students' interpersonal skills.

## Data Availability

The data underlying the results presented in the study are available within the manuscript.

## Conflicts of Interest

There is no potential conflict of interest in our paper.

## Authors' Contributions

All authors have seen the manuscript and approved to submit to your journal.

## References

- [1] N. Chhinzer and A. M. Russo, “An exploration of employer perceptions of graduate student employability,” *Education & Training*, vol. 60, no. 1, pp. 104–120, 2018.
- [2] A. A. Mackieh and F. Dlhin, “Evaluating the employability skills of industrial engineering graduates: a case study[J],” *International Journal of Engineering Education*, vol. 35, no. 3, pp. 925–937, 2019.
- [3] M. R. Hosseini, E. Zavadskas, B. Xia, N. Chileshe, and A. Mills, “Communications in hybrid arrangements: case of Australian construction project Teams,” *Engineering Economics*, vol. 28, no. 3, pp. 290–300, 2017.
- [4] H. Hjelmbrække, O. J. Klakegg, and J. Lohne, “Governing value creation in construction project: a new model,” *International Journal of Managing Projects in Business*, vol. 10, no. 1, pp. 60–83, 2017.
- [5] A. Mehreen, H. Yang, and Z. Ali, “A social network theory perspective on how social ties influence perceived employability and job insecurity: evidence from school teachers,” *Social Network Analysis and Mining*, vol. 9, no. 1, pp. 1–17, 2019.
- [6] X. Xue, R. Zhang, L. Wang, H. Fan, R. J. Yang, and J. Dai, “Collaborative innovation in construction project: a social network perspective,” *KSCE Journal of Civil Engineering*, vol. 22, no. 2, pp. 417–427, 2018.
- [7] R. Zhang, Z. Wang, Y. Tang, and Y. Zhang, “Collaborative innovation for sustainable construction: the case of an industrial construction project network,” *IEEE Access*, vol. 8, no. 99, pp. 41403–41417, 2020.
- [8] H. T. Nguyen and B. Hadikusumo, “Impacts of human resource development on engineering, procurement, and

## *Retraction*

# **Retracted: The Teaching Evaluation Index System and Intelligent Evaluation Methods of Vocational Undergraduate Pilot Colleges**

### **Wireless Communications and Mobile Computing**

Received 8 August 2023; Accepted 8 August 2023; Published 9 August 2023

Copyright © 2023 Wireless Communications and Mobile Computing. This is an open access article distributed under the Creative Commons Attribution License, which permits unrestricted use, distribution, and reproduction in any medium, provided the original work is properly cited.

This article has been retracted by Hindawi following an investigation undertaken by the publisher [1]. This investigation has uncovered evidence of one or more of the following indicators of systematic manipulation of the publication process:

- (1) Discrepancies in scope
- (2) Discrepancies in the description of the research reported
- (3) Discrepancies between the availability of data and the research described
- (4) Inappropriate citations
- (5) Incoherent, meaningless and/or irrelevant content included in the article
- (6) Peer-review manipulation

The presence of these indicators undermines our confidence in the integrity of the article's content and we cannot, therefore, vouch for its reliability. Please note that this notice is intended solely to alert readers that the content of this article is unreliable. We have not investigated whether authors were aware of or involved in the systematic manipulation of the publication process.

In addition, our investigation has also shown that one or more of the following human-subject reporting requirements has not been met in this article: ethical approval by an Institutional Review Board (IRB) committee or equivalent, patient/participant consent to participate, and/or agreement to publish patient/participant details (where relevant).

Wiley and Hindawi regrets that the usual quality checks did not identify these issues before publication and have since put additional measures in place to safeguard research integrity.

We wish to credit our own Research Integrity and Research Publishing teams and anonymous and named external researchers and research integrity experts for contributing to this investigation.

The corresponding author, as the representative of all authors, has been given the opportunity to register their agreement or disagreement to this retraction. We have kept a record of any response received.

### **References**

- [1] H. Wu, "The Teaching Evaluation Index System and Intelligent Evaluation Methods of Vocational Undergraduate Pilot Colleges," *Wireless Communications and Mobile Computing*, vol. 2022, Article ID 3485931, 8 pages, 2022.



## Research Article

# The Teaching Evaluation Index System and Intelligent Evaluation Methods of Vocational Undergraduate Pilot Colleges

Henan Wu 

Human Resources Department, Hainan Vocational University of Science and Technology, Haikou, 571126 Hainan, China

Correspondence should be addressed to Henan Wu; 1417421408@st.usst.edu.cn

Received 24 January 2022; Revised 15 February 2022; Accepted 18 February 2022; Published 5 March 2022

Academic Editor: Shalli Rani

Copyright © 2022 Henan Wu. This is an open access article distributed under the Creative Commons Attribution License, which permits unrestricted use, distribution, and reproduction in any medium, provided the original work is properly cited.

In recent years, with the popularization of higher education, quality problems have become increasingly prominent, and government documents often propose that the main task of education reform and development is to improve the quality of higher education. As a result, teaching evaluations have appeared one after another. Although various evaluation activities are carried out dynamically, expert evaluation has proven to be one of the most effective methods to ensure professional quality. This will help improve the quality of human resource development, promote regional economic development, improve the quality assurance system of higher education, and promote the formation of professional skills development mechanisms. This article studies the teaching evaluation index system and intelligent evaluation methods of vocational undergraduate pilot colleges, understands the relevant knowledge of the teaching evaluation index system on the basis of literature data, and then, constructs the teaching evaluation system of vocational undergraduate pilot colleges. The constructed system is tested, and the test results show that the error of the results of teacher self-evaluation and student evaluation is controlled within the two, which also verifies that the construction of the teaching ability evaluation index system this time is reasonable and scientific.

## 1. Introduction

The focus of our country's professional undergraduate pilot colleges has shifted from accelerating the construction of colleges and universities to strengthening the construction of colors [1, 2]. The professional assessment of the vocational undergraduate pilot college mainly assesses all aspects related to the profession. In addition, the existing professional undergraduate pilot colleges are mostly assessed at the macrolevel, including talent training, and lack mature microlevel assessments [3, 4]. Therefore, professional undergraduate pilot institutions should carry out microlevel assessments, focusing on the development model from quantity to quality. The reasons are as follows: first of all, the professional undergraduate pilot college is the most basic education unit and classifies students accordingly. Educational activities are carried out according to the field of specialization. Secondly, the evaluation always puts the improvement and improvement of the quality of education

in the first place, and according to the special needs of the society, the goal is to train experts in the field of specialization [5, 6]. Therefore, professional evaluation of vocational undergraduate pilot colleges can not only improve the quality of vocational undergraduate pilot colleges and shape the characteristics of vocational undergraduate pilot colleges but also promote the professional evaluation system of vocational undergraduate pilot colleges to a certain extent [7, 8].

In order to study education evaluation, some researchers have studied the existing professional index system of undergraduates and colleges, practical education, student employment, etc. [9]. Some researchers pointed out that an effective education evaluation and quality control mechanism is one of the key tools to ensure the quality of modern university education. Using scientific methods, adapting and promoting the characteristics of new undergraduate colleges and universities, establishing a scientific and fair education evaluation system, and evaluating education levels are effective means of guidance and supervision. Strengthen

educational activities, pay attention to the construction of “mechanical quality,” promote construction with evaluation, promote reform, promote management, and combine evaluation with construction [10]. Some scholars believe that the use of the same as traditional undergraduate colleges and recent higher education institutions The evaluation model of the evaluation system and methods cannot reflect the characteristics of the newly recruited faculty. New faculty and staff have distinctive characteristics in running schools. This is inevitable. It has led to the unification of the school model and the development direction of all universities. It is not only not suitable for the society of higher education development needs and has an adverse impact on the overall development of higher education, it is impossible to understand and guide the development of new departments through evaluation [11]. In summary, there are many research results on teaching evaluation, but in its evaluation system, the construction needs to be studied in depth.

This article studies the teaching evaluation system and intelligent evaluation methods of vocational undergraduate pilot colleges, analyzes the teaching evaluation and teaching evaluation system construction principles on the basis of literature data, and then, constructs the teaching evaluation system of vocational colleges, tests the constructed system, and draws relevant conclusions through the test results.

## 2. Research on Teaching Evaluation Index System

*2.1. Overview of Teaching Evaluation.* The doctrine evaluation in the narrow sense is mainly the evaluation of teacher’s specific teaching tasks, and the doctrine evaluation is mainly the development of teacher’s internal teaching activities, and it also depends on the content, methods, and other methods of teacher’s teaching, including all the requirements of teacher’s teaching [12], related to the activities of the school teaching system, courses, teaching plans, teaching conditions, etc. Therefore, the assessment is mainly based on the teaching system, and its scope continues to expand in the entire student education system and then extends to a broader national teaching system and various fields related to teaching. Teaching assessment is perfected and developed through the continuous development of its importance.

The degrees to which education meets social, political, economic, technological, and cultural needs are called political value, economic value, technical value, and cultural value, respectively. Therefore, research on teaching evaluation has practical significance. The sum of these values is the social value of educational activities. Therefore, the social value of the teaching profession is the degree to which it meets social needs, and the evaluation of the teaching profession is to judge the degree to which the teacher profession meets social needs. Facts have proved that the essential feature of the evaluation of doctrinal works is the value crisis, that is, the problem faced by the evaluation object: to what extent does the educational activity meet the needs of the body? So, the evaluation objects here are the organizers and managers of the evaluation. Today, in our country, the main organizers of higher education are governments and

education management departments at all levels representing the country and the country, so the object of teaching evaluation is the higher education institution being evaluated. Therefore, in the evaluation work, the evaluation model depends on the concept of value and the value model being evaluated. It cannot be simply said that the evaluation model is objective. In fact, the evaluation model has the duality of subjectivity and objectivity.

### 2.2. Principles for the Formulation of the Evaluation Index System

*2.2.1. Science.* Education is a systematic project with a wide range of content, including education and educational goals, educational content, teaching methods, and educational tools. Each element contains many elements. Therefore, there are many elements that need to scientifically determine the educational evaluation indicators. The definition of educational evaluation indicators should correctly reflect the ideas and concepts that guide educational activities, follow the basic laws of school human resource development, reflect the basic characteristics of the evaluation objectives as a model, and reflect the educational process. Therefore, the main aspects of evaluation need to be emphasized, but other aspects cannot be ignored. The education evaluation index system is the main content of the education evaluation work, which affects the evaluation results, and then affects the correct evaluation of schools, and its scientific nature must be ensured.

*2.2.2. Convenience.* All indicators strive to be measurable, comparable, convenient, and easy to apply. Through the review of the evaluation data, accurate information can be provided, targeted improvements can be made, and effective diagnosis of departmental education can be achieved. There are qualitative and quantitative methods for describing the importance of evaluation factors and scoring standards, and a combination of qualitative and quantitative methods is adopted according to the characteristics of evaluation factors. The qualitative explanation is as clear as possible so that experts can be trusted. Quantitatively expressing a high academic level and rich educational management experience can easily and accurately determine the degree of conformity between the actual state of the department-level education work and the required goals. For quantifiable factors, try to pass statistical analysis of some basic data to objectively reflect the basic state of educational activities. At the same time, remember that the indicators should be relatively intelligent, and the levels should not be too detailed, but not too general. The recognition is poor, which will affect the evaluation results. The indicator system needs to promote the self-monitoring and self-evaluation of the evaluated university to promote the development of evaluation projects.

*2.2.3. Direction.* The performance evaluation system will undoubtedly play the role of baton in university education activities. Therefore, the indicator system aims to play an objective leading role in college education and teaching, education reform, university construction, etc., highlight the characteristics of university application-oriented talent

training as much as possible, highlight the importance of the actual connection between colleges and universities, and attach importance to education the quality requirements of the team's "dual-teacher type" pay attention to the applicability and relevance of educational content. At the same time, the evaluation system should also guide departments and universities to properly handle the relationship between scale, quality, structure, and efficiency, handle the relationship between teaching and research, and promote innovation and create characteristics.

**2.2.4. Unity.** The task of educational evaluation of colleges and universities is, on the one hand, to evaluate, recognize, and summarize the work and achievements of colleges and universities. At the same time, guide and supervise the completed work. In the education field, whether it is designing a rating system or implementing a rating process, there is always a contradiction between the status quo and the growth trend. Unrealistic emphasis on the predictive index of the growth trend will definitely give people a feeling of impossibility and affect their confidence in university education. Based solely on the status quo, the index system has no incentive effect and is not conducive to improving education programs. Therefore, the model of the index system should not only be derived from the actual education system of the university but should also be able to adhere to higher standards, instill the spirit of reform, conform to the development direction, and link up with the curriculum, so that the standards established by the evaluation can be better integrated and the status quo keep consistent with the contradiction between development trends.

**2.2.5. Flexibility.** Although university education has similarities, different universities also have differences in specific training goals, disciplines and courses, and actual educational challenges. It is impossible to design an index system for the specific educational goals of each college, each type of discipline and curriculum, and the practical education of each university. It must be divided very carefully. Therefore, when designing the index system in this article, we need to consider as many common elements as possible so that the index covers the educational work of different colleges and universities. In the actual evaluation, if the educational activity data of individual universities is missing, the missing data can be processed.

The formulation of the teaching evaluation index system of vocational undergraduate pilot colleges must follow the above principles in order to play its role.

### **3. Construction of Teaching Evaluation Index System for Vocational Undergraduate Pilot Colleges**

**3.1. Construction of Specific Indicators.** On the basis of summarizing the experience and lessons of the construction of the education indicator system, this article will first add a self-evaluation item in the construction of the teacher education indicator system to facilitate the practical guidance

and development of evaluation. Based on the glacier structure theory, the personal qualities and characteristics of teachers are more decisive for their educational behavior, so the measurement system adds a measurement to this part; third, enrich the evaluation questions, enrich the classroom teaching, and emphasize the importance of teacher self-evaluation; fourth, self-selected index adjustment, distinguishing teacher leadership evaluation, and constructing an evaluation index system according to the principles of index system construction described in the previous section.

**3.2. Determining the Hierarchical Structure of the Evaluation Indicators for the Educational Ability of the Faculty and Staff in Colleges.** Combining the iceberg theory and the research topics of this article, one of the most obvious indicators of teachers' basic skills and scientific research innovation ability is the apparent quality of the upper part of the iceberg and the basic quality of the bottom of the iceberg personality to represent. Then, the first-level indicators are subdivided into second, third, or more subdivisions to comprehensively and scientifically reflect the comprehensive quality of teachers' educational ability. The index is shown in Table 1.

**3.3. The Teaching Ability Index System of College Teachers.** The design of a complete educational quality evaluation system for colleges and universities is based on the evaluation of the educational quality characteristics of all teachers, using thorough methods, questionnaire surveys, and other methods as indicators of key characteristics. Correspondingly, a model of the educational quality evaluation system as shown in Figure 1 was designed.

**3.4. Hierarchical Analysis Process Based on Data Mining.** Level division is a method of separating levels from top to bottom. It is often said that this is a method of summing first and then dividing. The principle of this method is simple. In other words, all data objects are placed in a cluster and gradually divided into smaller clusters (just like an image of an inverted tree, first with roots, then branches, and leaves). Even if the split is completed, the smallest cluster can perform certain functions relatively easily. For example, in the education quality evaluation system, the layered model constructed is a measurement system. The highest level of the rating system is separated at step 0. After separating these two steps, a hierarchical model with a two-level index structure is generated, as shown in Figure 2.

**3.5. Construction of the Judgment Matrix.** The figure clearly shows the subordination of the good and bad factors to the hierarchical structure model. If the target level of the upper-level factor is set to  $U$  and the reference level of the lower-level factor is set to  $U_1, U_2, \dots, U_3$ , then the corresponding weight  $W_1, W_2, \dots, W_n$  can be set according to the degree of dependence of each lower-level factor on the upper-level factor. If the dependence of each subordinate factor on the superior factor can be quantified in the design, the weight of each subordinate factor can be quickly

TABLE 1: The hierarchical structure of the evaluation index of the educational ability of university staff.

Iceberg capacity layer	Content	First level indicator
Skill	Such as: expression ability, organizational ability, decision-making ability, and learning ability	Basic teaching skills/teaching research ability
Knowledge	Such as: management knowledge, financial knowledge, and other professional knowledge	
Role positioning	Such as: managers, experts, and teachers	Basic teaching literacy/teacher's personal career planning and summary
Values	Such as: spirit of cooperation and dedication	
Self-awareness	Such as: self-confidence and optimism	
Quality	Such as: honesty, honesty, and sense of responsibility;	
Motivation	Such as: achievement needs and interpersonal communication needs	

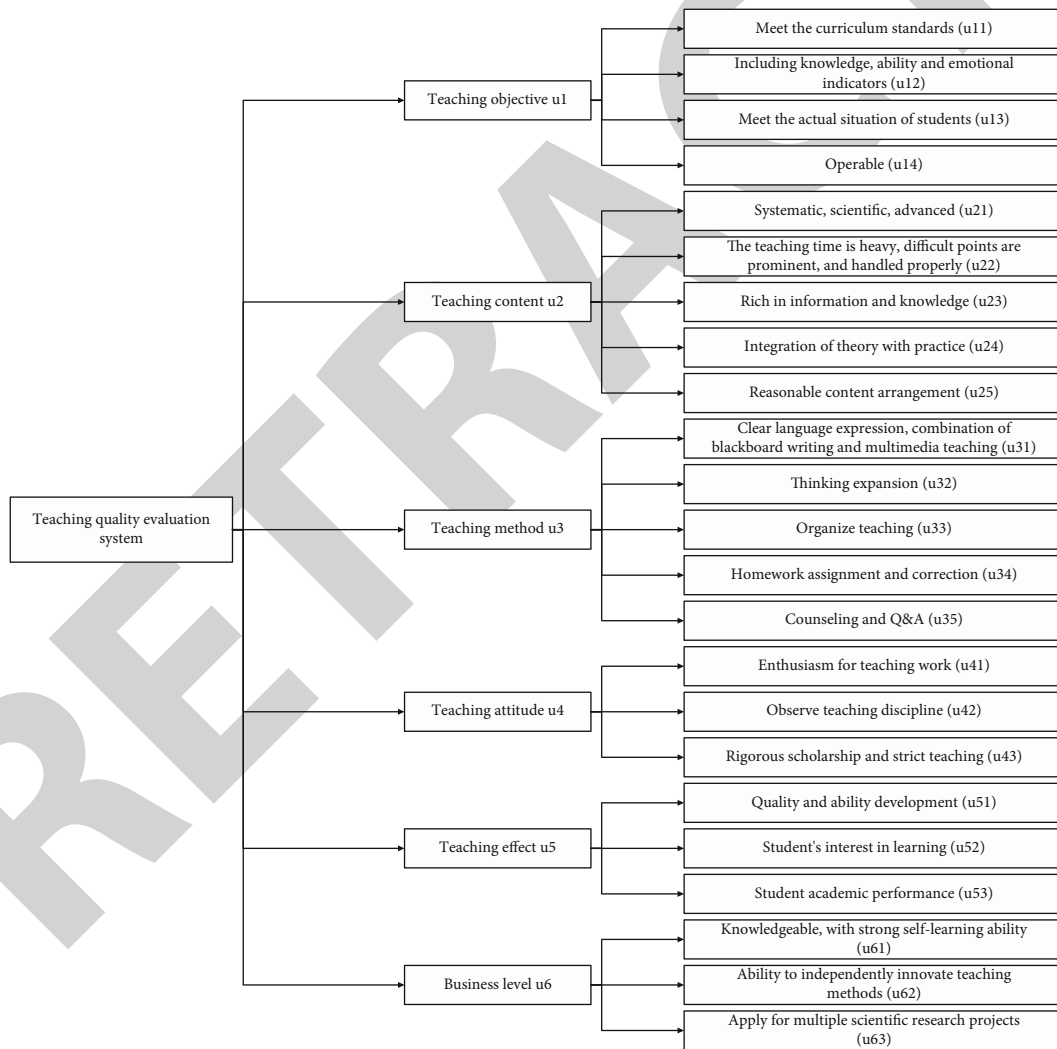


FIGURE 1: Educational quality evaluation system model.

determined, but it is difficult to judge the qualitative and subjective subordinate factors in decision-making. Once each weight is directly determined, the lower-level proxy weight can only be obtained through other calculation

methods. The main purpose here is to compare all the factors involved, that is, to compare the influence ratio of the two lower-level factors  $U_i$  and  $U_j$  to the target factor  $U$ , and the result is recorded as  $U_{ij}$ . Combine all comparison

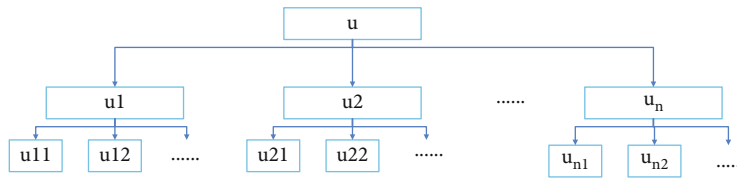


FIGURE 2: Hierarchical analysis process based on data mining.

TABLE 2: Scale table of judgment matrix.

Scale $U$	Definition
1	$i$ and $j$ have the same effect
3	$i$ is slightly stronger than $j$
5	$i$ is stronger than $j$
7	The effect of $i$ is significantly stronger than $j$
9	The effect of $i$ is definitely stronger than $j$
2, 4, 6, 8	$i$ and $j$ are in the middle value between two adjacent judgments

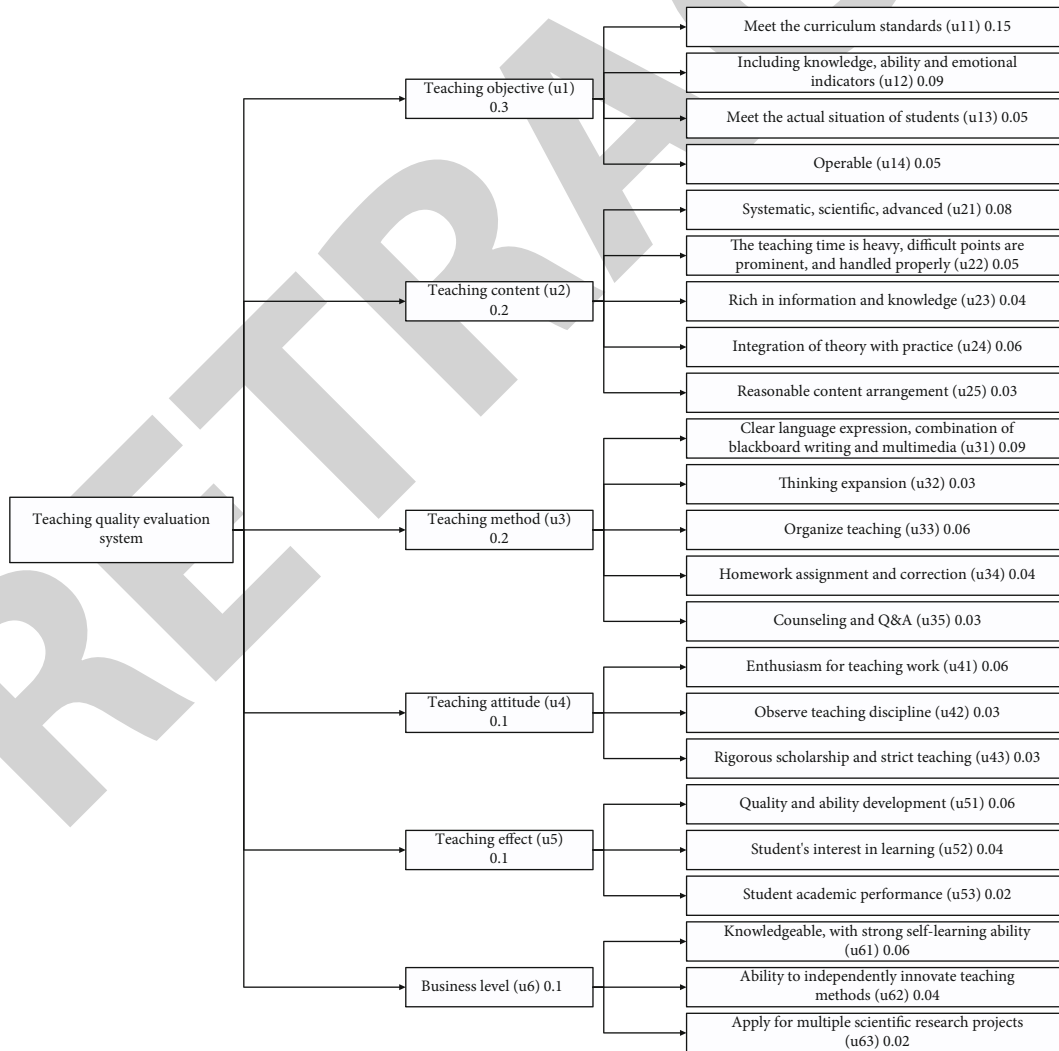


FIGURE 3: The hierarchical structure of college education quality evaluation system.

TABLE 3: Evaluation results of teacher education ability index system.

	Teacher	Student
Meet the curriculum standards (u11)	10.67	10.23
Including knowledge, ability, and emotional indicators (u12)	17.82	17.43
Meet the actual situation of students (u13)	2.22	2.04
Operable (u14)	3.32	3.34
Systematic, scientific, and advanced (u21)	4.23	4.12
The teaching time is heavy; difficult points are prominent, and handled properly (u22)	5.32	5.36
Rich in information and knowledge (u23)	2.57	2.73
Integration of theory with practice (u24)	1.35	1.24
Reasonable content arrangement (u25)	0.74	0.73
Clear language expression; combination of blackboard writing and multimedia teaching (u31)	3.12	3.25
Thinking expansion (u32)	1.12	1.13
Organize teaching (u33)	0.04	0.03
Homework assignment and correction (u34)	0.45	0.47
Counseling and Q&A (u35)	0.09	0.03
Enthusiasm for teaching work (u41)	0.34	0.33
Observe teaching discipline (u42)	5.71	5.73
Rigorous scholarship and strict teaching (u43)	7.34	7.32
Quality and ability development (u51)	0.53	0.55
Student interest in learning (u52)	1.15	1.05
Student academic performance (u53)	2.47	2.36
Knowledgeable, with strong self-learning ability (u61)	1.84	2.01

results to get a matrix. The expression is as follows.

$$U = (U_{ij})_{n \times n} = \begin{pmatrix} U_{11} & U_{12} & \cdots & U_{1n} \\ \cdots & \cdots & \cdots & \cdots \\ U_{n1} & U_{n2} & \cdots & U_{nn} \end{pmatrix}. \quad (1)$$

Based on the above properties, if  $U$  is a consistency matrix,  $\lambda_{\max} = n$ , then the eigenvector corresponding to  $\lambda_{\max}$  is normalized and recorded as  $W = (W_1, W_2, \dots, W_n)^T$  in

$$\sum_{i=1}^n W_i = 1. \quad (2)$$

In the expression,  $W$  is called the weight vector, which represents the weight of the target  $U$ . In the system, the weight of each element can be determined by pairing each element. Table 2 shows the size of the matrix.

**3.6. Weight Calculation.** The two levels of the standard, the first-level index and the corresponding second-level index, constitute the hierarchical structure of the college's education quality evaluation system. The same method described above is used to calculate the weights of all other subindices. The final result is shown in Figure 3.

#### 4. Example Test

In order to verify whether the teacher education ability indicator system constructed in this article is scientific and logical, this article designs a survey questionnaire based on various indicators of the teaching ability of professional undergraduate pilot teachers. The acceptance of undergraduate education ability is mainly aimed at professional pilot teachers and adopts a self-evaluation method. The evaluation method was adopted for 23 professors and 10 undergraduate pilot universities in the city, and professional students were selected to conduct a questionnaire survey. Finally, the survey results can be summarized and combined with the weights of various indicators to calculate the total score of the teacher's teaching ability (full score is 100 points). 40 questionnaires were distributed, and 40 were recovered, the efficiency was 100%, 50 student questionnaires were distributed, and 45 were recovered, and the recovery rate was 95%.

After the received survey is processed, the teacher and student surveys are handled separately. For student self-evaluation and evaluation, enter the score in the last column of the evaluation system, and then, perform the following data processing: find the average score of 40 teachers and 50 students, and then, multiply the value by the weight of the first-level indicator and then second weight of the first-level indicator, then the weight of the third-level indicator, and finally, the total score. The four indicators of basic education qualifications under the background of basic teaching skills can only be processed quantitatively, so when

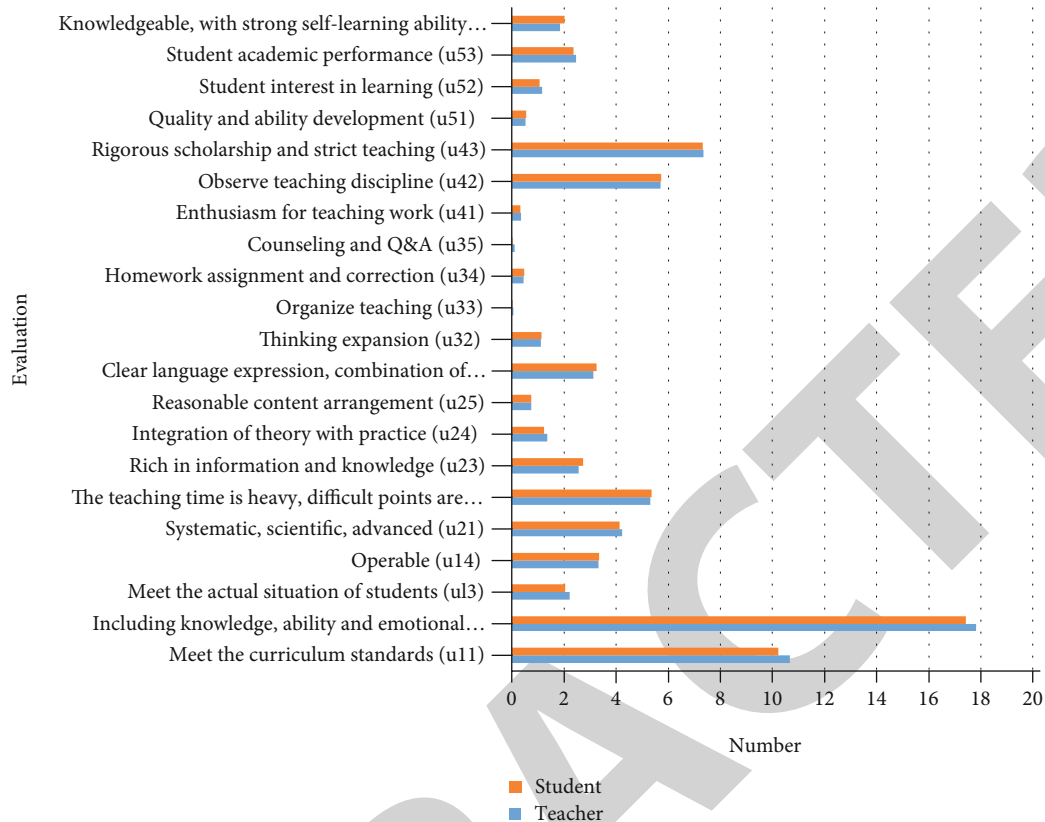


FIGURE 4: Evaluation results of teacher education ability index system.

calculating grades, only the data is calculated without processing. Due to the qualitative processing of these three levels of indicators, it can be estimated that the final average total score is within 10 points, that is, the average total score of teacher education ability assessment is about 90 points. Compare the difference between teacher self-evaluation and student evaluation scores, use the difference to judge whether the reconstructed teacher education evaluation system is reasonable. The results are shown in Table 3.

It can be concluded from Figure 4 that the error between teacher self-evaluation and student evaluation is within 2 points, so the construction of this educational ability evaluation index system is logical and scientific. First of all, from the first-level indicators, basic teaching skills account for the largest proportion, which also shows that general knowledge and professional skills represent the teaching ability of teachers to a large extent, and the proportion of education and scientific research is very small. Since the college is a professional pilot school, the ability of scientific research and innovation is considered to be an issue that university professors should pay attention to.

## 5. Conclusions

The teaching evaluation index system and intelligent evaluation of higher vocational undergraduate pilot colleges play an important role in the education of students. This paper takes the students of the pilot colleges and universities of higher vocational colleges as the research objects, and

through the analysis of relevant knowledge and theories, constructs the teaching evaluation system of the pilot colleges and universities of higher vocational colleges, tests the constructed system, and passes the test results. Get the results of teacher self-assessment and student assessment. It also verifies the rationality and scientificity of the construction of the teaching ability evaluation index system.

## Data Availability

The data underlying the results presented in the study are available within the manuscript.

## Conflicts of Interest

There is no potential conflict of interest in our paper, and the author has seen the manuscript and approved to submit to your journal. We confirm that the content of the manuscript has not been published or submitted for publication elsewhere.

## Acknowledgments

This work was supported by the Hainan Province Higher Education and Teaching Reform Research Project: project number: Hnjg2020-126; project name: Research on the Evaluation Index System of Teaching Work Level of Vocational Undergraduate Pilot Colleges-Taking Hainan Vocational University of Science and Technology, as an example.

## Retraction

# Retracted: Football Teaching Quality Evaluation and Promotion Strategy Based on Intelligent Algorithms in Higher Vocational Colleges

### Wireless Communications and Mobile Computing

Received 25 July 2023; Accepted 25 July 2023; Published 26 July 2023

Copyright © 2023 Wireless Communications and Mobile Computing. This is an open access article distributed under the Creative Commons Attribution License, which permits unrestricted use, distribution, and reproduction in any medium, provided the original work is properly cited.

This article has been retracted by Hindawi following an investigation undertaken by the publisher [1]. This investigation has uncovered evidence of one or more of the following indicators of systematic manipulation of the publication process:

- (1) Discrepancies in scope
- (2) Discrepancies in the description of the research reported
- (3) Discrepancies between the availability of data and the research described
- (4) Inappropriate citations
- (5) Incoherent, meaningless and/or irrelevant content included in the article
- (6) Peer-review manipulation

The presence of these indicators undermines our confidence in the integrity of the article's content and we cannot, therefore, vouch for its reliability. Please note that this notice is intended solely to alert readers that the content of this article is unreliable. We have not investigated whether authors were aware of or involved in the systematic manipulation of the publication process.

In addition, our investigation has also shown that one or more of the following human-subject reporting requirements has not been met in this article: ethical approval by an Institutional Review Board (IRB) committee or equivalent, patient/participant consent to participate, and/or agreement to publish patient/participant details (where relevant).

Wiley and Hindawi regrets that the usual quality checks did not identify these issues before publication and have since put additional measures in place to safeguard research integrity.

We wish to credit our own Research Integrity and Research Publishing teams and anonymous and named external researchers and research integrity experts for contributing to this investigation.

The corresponding author, as the representative of all authors, has been given the opportunity to register their agreement or disagreement to this retraction. We have kept a record of any response received.

### References

- [1] X. Jiao and Z. Li, "Football Teaching Quality Evaluation and Promotion Strategy Based on Intelligent Algorithms in Higher Vocational Colleges," *Wireless Communications and Mobile Computing*, vol. 2022, Article ID 9469553, 7 pages, 2022.



## Research Article

# Football Teaching Quality Evaluation and Promotion Strategy Based on Intelligent Algorithms in Higher Vocational Colleges

Xiance Jiao<sup>1</sup> and Zefeng Li<sup>2</sup> 

<sup>1</sup>College of Continuing Education, Henan Vocational College of Quality Engineering, Pingdingshan, 467000 Henan, China

<sup>2</sup>College of Artificial Intelligence, Chongqing Youth Vocational and Technical College, Chongqing 400712, China

Correspondence should be addressed to Zefeng Li; 41823047@xs.ustb.edu.cn

Received 20 January 2022; Revised 9 February 2022; Accepted 14 February 2022; Published 4 March 2022

Academic Editor: Shalli Rani

Copyright © 2022 Xiance Jiao and Zefeng Li. This is an open access article distributed under the Creative Commons Attribution License, which permits unrestricted use, distribution, and reproduction in any medium, provided the original work is properly cited.

With the continuous deepening of the education reform, the number of students in higher vocational college (HVC) has increased, which puts forward higher requirements for the overall development of talents. Football is a relatively common sport in HVC with a certain degree of regularity and difficulty. Therefore, how to improve the level and the quality of teaching through scientific and reasonable teaching methods has become one of the problems that need to be solved in HVC. This article mainly focuses on the analysis and research of the traditional teaching mode and students' learning situation based on the intelligent algorithm and puts forward effective improvement suggestions and strategies for reference. This article uses questionnaire surveys and data analysis methods to understand the evaluation results of the school's teachers and students on the teaching quality (TQ) of the football course and the necessity of implementing improvement strategies through questionnaire surveys. According to the survey results, most of the interviewees had a high evaluation of the TQ of the school's football course. 46 of the teachers and students who participated in the evaluation rated the school's football course teaching methods as excellent, and only 2 rated it as passing. In addition, 49 of the teachers and students interviewed believe that it is necessary to optimize the strength of teachers, followed by perfecting the equipment configuration of the venue.

## 1. Introduction

With the continuous advancement of educational reforms, the state's emphasis on HVC has gradually increased, and football as an important physical education course has also been valued. However, there are still many shortcomings at present. With the increasingly fierce social competition, the education of HVC is facing a severe situation. How to improve the quality of teaching has become a topic of research and discussion by many scholars. In the new era, it is very important to train students in football skills. In addition, intelligent algorithms also help people solve many problems. Therefore, it is a necessity to carry out research on the evaluation of football TQ and improvement strategies in HVC in combination with intelligent algorithms.

At present, many scholars have conducted research on TQ evaluation and improvement strategies and have obtained very rich research results. For example, Tang

pointed out that, at present, football courses in vocational colleges obviously cannot adapt to the new requirements and face new challenges. How to effectively improve the quality of football teaching in HVC is an important issue at present [1]. Ma believes that mathematics teaching is an important part of the elementary school education system. In order to better promote the improvement of students' learning quality and related basic literacy, people should pay attention to the evaluation of the quality of elementary school mathematics teaching [2]. Xu pointed out that education quality evaluation is a relatively important link in the education management process of universities and plays a vital role in improving the overall level of education [3]. Therefore, this article starts from a new perspective, combined with intelligent algorithms, to carry out research on the evaluation of football TQ and promotion strategies in HVC, which has important practical significance and research value to a certain extent.

This article mainly discusses these aspects. First, the intelligent algorithm and its related research are explained. Then, the status quo of football teaching in HVC is introduced. In addition, it also discusses the evaluation of football TQ in HVC and the research on promotion strategies. Finally, a questionnaire survey was launched, and the corresponding survey results and conclusions were drawn.

## 2. Related Theoretical Overview and Research

*2.1. Intelligent Algorithm and Related Research.* Intelligent computing, also known as “soft computing,” refers to algorithms designed to mimic the laws of nature inspired by the laws of nature when humans study the natural world. Most of the various intelligent algorithms are proposed by humans through the study of natural processes and biological survival competition and gene mutations.

In recent years, humans have successfully used intelligent computing methods to solve many problems. People have carried out related research on intelligent algorithms. The current popular intelligent algorithms mainly include neural network algorithm, genetic algorithm, particle swarm algorithm, simulated annealing algorithm, and gray wolf optimization algorithm.

*2.1.1. Neural Network Algorithm (NNA).* NNA is one of the most widely used intelligent algorithms. The structure of the neural network is based on the simulation of human brain nerve tissue, which is composed of a large number of neurons through a variety of connections.

An artificial neural network is a system composed of a large number of interconnected neurons. This structural feature means that artificial neural networks have extremely strong information processing capabilities. Although each neuron only performs simple processing and calculation of information, the efficiency of information transmission between neurons is low, but the elements of each neuron are connected to each other and processed in cooperation, which ultimately endows super processing capabilities. Since the artificial neural network contains many neurons and the network’s powerful information storage capabilities, this makes the neural network have a strong ability to process unsafe information. It is precisely because of this structural characteristic and the characteristic of distributed information storage that the artificial neural network has good robustness and will not lose the memory ability of the original model and its very powerful nonlinearity by destroying a “neuron” “capacity.”

*2.1.2. Genetic Algorithm.* GA is an intelligent optimization method inspired by biological evolution theory. GA does not need to calculate the gradient when searching for the optimal solution, and the group discovery strategy can share information with individuals. When the GA was originally designed, it was not used to solve optimization problems, but to assist the development of artificial intelligence. The characteristic of GA is based on the parallel search of chromosome groups and selection, crossover, and mutation operations according to probability. This special evolution

mode is not available in other search algorithms. In the evolution of each population, the GA can process several individuals in the population at the same time through its unique hybridization and mutation operations, which largely hinders the optimization of the population. The GA is adaptive and self-learning. The algorithm uses fitness functions to evaluate people without further auxiliary information.

The research process of GA involves three operations: selection, crossover, and mutation. The three operations of the GA involve a certain degree of contingency, but it is not just a simple random search; the search of this algorithm is an efficient directed search.

In the GA, many different individuals form a population, and the individuals in the population have multiple genetic codes corresponding to them, because only in this way can crossover and mutation operations be performed. After the initial population is established, the individuals in the population are continuously updated in nature until the optimal solution is found. In each iteration, the GA selects the best individual based on the fitness score of the individual in the population. Then, use crossover and mutation operations to generate a new population and iterate this process until the stopping criterion is met.

If there are only two selection and crossover operations in a GA without mutation operation, the evolution process will fall into a local optimal situation prematurely. Therefore, in order not to affect the quality of the output result, a crossover operation must be performed [4, 5].

*2.1.3. Particle Swarm Algorithm (PSA).* PSA is one of the most classic algorithms in intelligent algorithms. It is an optimization algorithm proposed on the basis of simulating the predation behavior of birds, and it is also an algorithm based on group iteration. The algorithm requires fewer parameters, and the function of the PSA is simple and easy to program.

In the PSA, each bird in the population is considered a particle, and the initial solution of the problem is the initial position of the particle. The distance between each particle and the food is determined by the fitness function of the problem. Through particle predation, the particles always fly around the current best particle closest to the food. Particles always move in two positions; one is called the individual optimal position, and the other is the overall optimal position. After a period of cyclic movement, the particles will finally find the optimal position, thereby achieving the optimal solution of the global optimization goal. The particle velocity and position update of this algorithm can be expressed by

$$W_u(r+1) = iW_u(r) + a_1e_1(Q_u(r) - Z_u(r)) + a_2e_2(Q_j(r) - Z_u(r)), \quad (1)$$

$$Z_u(r+1) = Z_u(r) + W_u(r+1). \quad (2)$$

Among them,  $W_u(r)$  represents the speed information of the  $u$ -th particle at time  $r$ ,  $Z_u(r)$  represents the position information of the  $u$ -th particle at time  $r$ ,  $Q_u(r)$  represents

the individual optimal position,  $Q_j(r)$  represents the global optimal position,  $i$  is the inertia factor,  $c_1$  and  $c_2$  are the learning factors, and  $e_1$  and  $e_2$  are random numbers with a value of  $[0, 1]$ .

The idea of PSA is simple and easy to implement, so it has been developed rapidly and widely used. According to the description of the algorithm, the particles contained in it all move in accordance with the path determined by the speed and position. Since their speed and position are limited, their search space is limited and cannot cover all possible solution spaces. In addition, the algorithm also has some shortcomings, such as slow convergence speed and simple local optimal solution, which requires further research and improvement. Later, some researchers combined the PSA with the quantum evolution algorithm and proposed the quantum PSA, which not only speeds up the convergence speed but also improves the overall optimization ability and efficiency of the algorithm [6, 7]. The optimization process of PSA is shown in Figure 1.

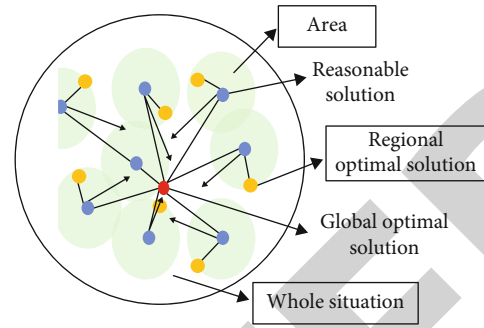


FIGURE 1: The optimization process of particle swarm optimization.

**2.1.4. Simulated Annealing Algorithm (SAA).** SAA is essentially a global optimization process. Once the algorithm falls into the local optimum, noise can be added in the process of simulated annealing to distract the algorithm from the local optimum, and then gradually reduce the noise, and finally find the overall optimum result. The algorithm can not only accept test points to improve the fitness score but also obtain a solution that has a certain probability of making the fitness score worse. All states in the iteration process are random. Secondly, a check function is introduced into the algorithm to divide the optimization process into different stages. The check function also determines the selection criteria for the random process at each stage. Finally, in the SAA, in order to obtain the next search area and search direction, the objective function must be converted into a fitness value.

**2.1.5. Gray Wolf Optimization Algorithm (GWOA).** GWOA is a new metaheuristic algorithm based on wolf predation principle. Gray wolves are considered predators, which means they are at the top of the food chain. Most gray wolves like to live with groups of 5 to 12 on average. They have a very strict hierarchy in the gray wolf family. The predation process of wolves can be roughly divided into three processes: hovering, summoning, and siege. Their leader is called the master wolf, and its main task is to control the predation activities of the wolf pack, where to sleep, when to wake up, etc., to master the activities of the entire wolf pack.

Although the gray wolf optimization algorithm appeared late, it has been successfully applied to solve various optimization problems. Compared with other intelligent algorithms, the main feature of the gray wolf optimization algorithm is to update the optimal overall solution according to the first three optimal solutions to determine where the wolf pack needs to be. In addition, whether the gray wolf optimization algorithm is in continuous space or discrete space, the algorithm has good robustness and global search ability [8, 9].

## 2.2. Evaluation and Promotion Strategy of Football TQ in HVC

**2.2.1. The Status Quo of Football Teaching in HVC.** From the current point of view, there are still some problems in the course of football in vocational colleges. Some schools lack effective campus football training methods and professional football teachers. There is still a gap between their skills and qualities and the development of campus football. Even some teachers do not have professional football experience, and the method of organizing football training lacks creativity. It is difficult to make students interested in football, and it is easier to affect the teaching effect.

In addition, some schools lack football venues and resources, professional football coaches, etc. This has also become a major obstacle to football teaching in HVC.

**2.2.2. Evaluation of Football TQ in HVC and Related Research.** The higher vocational TQ evaluation system (ES) is a set of systems composed of a group of closely related indicators of the evaluation target (higher vocational teachers).

The establishment of the TQ ES is conducive to improving the education management level and quality of HVC. It can be the basis for school leaders to improve their educational management capabilities. Problems found in the assessment process can also be reported back to relevant teachers in time, which also improves the quality of teachers. Therefore, certain principles should be followed when establishing an education quality ES.

**(1) Objective Principle.** The main construction principle of the football class quality evaluation index system is objectivity. The teaching evaluation process should be conducted in an open and transparent environment and based on the mutual understanding between the evaluator and the evaluated object. If the result of educational evaluation is unfair and unobjective, the evaluated object will question the evaluation result, which will greatly affect the enthusiasm of the evaluated object. When evaluating TQ itself, in order to comprehensively and objectively reflect the entire teaching style of the evaluated object, it is necessary to conduct an in-depth investigation of the evaluated object.

**(2) The Principle of Feasibility.** When establishing an education ES, attention should be paid to ensuring the feasibility

and appropriateness of the evaluation index to ensure that the establishment and implementation of the ES can be truly realized.

(3) *Systematic Principle*. The systematic principle refers to the use of holistic thinking in evaluation to evaluate the entire teaching process of teachers. The evaluation of the overall quality of football teaching is carried out on the basis of a full understanding of the internal and external factors that affect the evaluation results to better ensure the rationality of the evaluation results.

(4) *Guiding Principles*. The evaluation of educational quality refers to the evaluation of TQ, which can help teachers clarify the direction of their work and optimize the whole teaching process, so as to improve the quality of education. Of course, education quality evaluation can also make education managers make more flexible decisions. Therefore, education quality evaluation is an incentive system to improve education quality to a certain extent. This type of guidance usually uses the size of the index weight to influence the specific implementation process. Therefore, when establishing an education quality ES, people should pay attention to determining the weights of various indicators. This article also contains detailed applications.

(5) *Dynamic Principle*. The knowledge of the football class quality evaluation index system is not a summary evaluation, but a formative evaluation. This is a dynamic development process aimed at acquiring knowledge and improving teaching and teacher skills. It can flexibly reflect the changes of the curriculum. Therefore, the football TQ ES must be stable, dynamic, and developing.

(6) *The Principle of Integrity*. The overall principle of the football education quality evaluation index system structure is embodied in the combination of independence and integrity. The design of the indicator system should not only pay attention to the correlation between the various indicators but also avoid the overlap of the various indicators. The choice of indicators and their weights are the key to constructing the evaluation index system of football TQ. The selection of indicators for evaluating TQ should cover the entire teaching process, including the research and adaptation of content, the presentation of educational influence, the change of teaching conditions, and the innovation of teaching methods. Therefore, the establishment of the global education quality evaluation index system must consider the integrity and ensure the independence and the perfect combination of the whole and the part [10, 11].

In addition, the design of the comprehensive ES for the education quality of higher vocational schools should be based on the evaluation of teachers' TQ, and a relatively comprehensive TQ ES for HVC should be established. The ES should be established in strict accordance with the construction principles. When establishing the scientific ES of higher vocational TQ, another important aspect that needs to be considered is the evaluation index. The model of the TQ ES is shown in Figure 2.

The TQ evaluation work of various universities is based on the educational goals, in accordance with scientific standards, through the systematic collection of different information in the teaching process and the continuous improvement of the daily teaching process, effectively using various theories, means, technologies, and methods. And teaching influences the process of measuring and analyzing information and subsequent value judgments.

It is necessary to make a scientific and reasonable evaluation of the quality of education. The evaluation of the quality of football education in HVC has the function of diagnosis, regulation, and encouragement. TQ evaluation is an important part of education evaluation. Its guiding ideology is "promote teaching by evaluation, promote learning by evaluation, and promote reform by evaluation" [12, 13].

Educational quality evaluation has many functions, the focus is to promote the quality of education of football courses, and the evaluation is conducive to the optimization and upgrading of the teaching process. At the same time, the football TQ ES should combine actual education needs, play different functions, and highlight its role. Therefore, the role of football TQ ES should include the following content.

- (1) *Feedback function*: the feedback function of TQ evaluation has two meanings: on the one hand, it is feedback on teachers' teaching work; on the other hand, it is feedback on students' learning effects. Teachers can learn about students' learning conditions based on the results of the assessment, and they can also find themselves in the teaching process. Improve their teaching content and teaching methods
- (2) *Management function*: the results of TQ evaluation can reflect the degree of difference in teaching levels of different teachers and reveal the problems and gaps teachers face in the teaching process. On the one hand, it can assume the function of supervision; on the other hand, it can also be used as a reliable basis for evaluating teacher performance, maximizing strengths and avoiding weaknesses, and even providing theoretical basis for university decision-makers

All in all, the establishment of a scientific, reasonable, and standardized football education quality ES is a prerequisite for the normal performance of various educational evaluation functions and a fundamental guarantee for practical, complete, and efficient evaluation [14, 15].

*2.2.3. Strategies for Improving the Quality of Football Teaching in HVC and Related Research*. In order to further improve the quality of football education in vocational colleges, schools should adopt certain strategies and measures.

One is to improve the on-site equipment configuration. Some schools have small football fields, imperfect venue facilities, and insufficient training equipment. Strengthening the construction of infrastructure and establishing standardized training facilities and equipment are the basic prerequisites for improving the quality of football teaching in HVC.

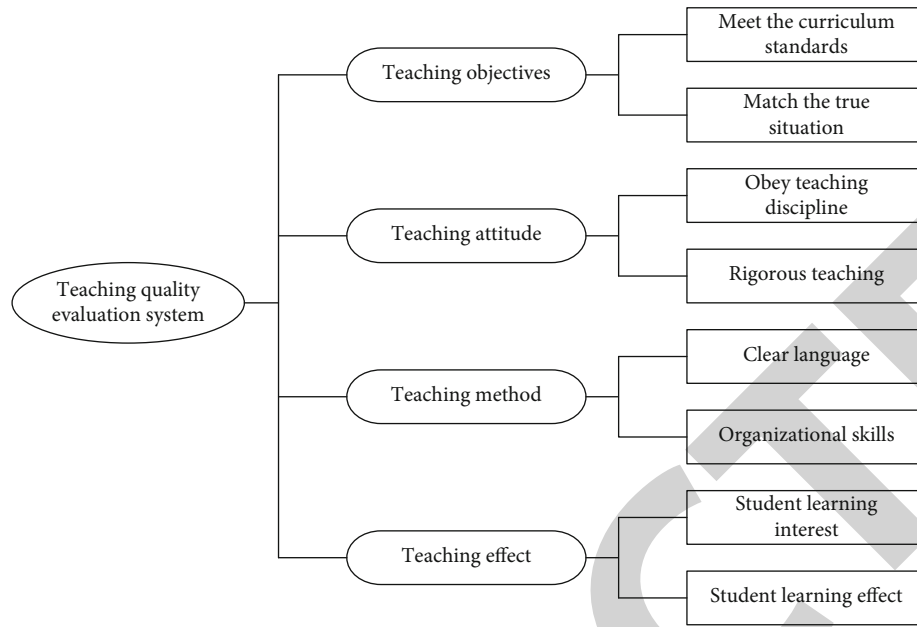


FIGURE 2: TQ ES model.

TABLE 1: Questionnaire distribution method and collection results.

Questionnaire distribution method	Number of questionnaires issued	Number of questionnaires returned	Recovery rate (%)
Internet questionnaire	25	20	80
On-site questionnaire	65	60	92.3
Email	30	20	66.7

TABLE 2: Evaluation and analysis of football TQ.

Evaluation index	Excellent	Good	Medium	Pass
TQ	45	39	12	4
Teaching content	41	40	14	5
Teaching method	46	42	10	2
Teaching effect	43	41	13	3

In addition, the school should hire competent staff to conduct regular inspections of the football field and facilities, conduct standardized planning and management, and avoid safety accidents.

The second is to attach importance to the combination of theory and practice. HVC should look for the connection between theory and practice in the development of college football. In this process, not only should focus on practical training but also on theoretical guidance. Relevant departments and schools actively develop and compile suitable football course materials to ensure the effectiveness and scientificity of football training and to achieve a perfect connection between theory and practice.

The third is to establish a scientific and reasonable curriculum system. In order to further improve the teaching level of football courses, schools should actively construct a scientific and reasonable teaching system and divide the relationship between football theory courses and football training. Before setting up courses, the time required for cultural classes should

be fully considered to ensure that students' participation in football classes will not interfere with cultural classes. During this period, the school should clarify the training objectives and training tasks of students, standardize training methods and assessment methods, and organically integrate ideological work, cultural research, and football.

The fourth is to optimize the teaching staff. At present, the professional level of football coaches in some schools is not high, and improvements can be made in the following aspects. First, the school should choose the professional instructor of football education and go to the school for training on a regular basis. In addition, exchanges and cooperation with football clubs can be strengthened, and teachers are encouraged to learn from the professional talents of football clubs. In this process, relevant government departments should take the initiative to broaden the training channels for football coaches and support them to learn the latest professional knowledge and football training methods. Second, hire a group of highly skilled football talents, retired football talents, experienced expert teachers, etc., to truly improve the overall professional level of high-level football coaches. Third, strengthen the connection with other schools and invite football majors to train in campus football schools. This not only provides practical opportunities for football majors but also adds vitality to the development of campus football. In this context, schools should establish an appropriate reward system for football teachers and coaches to increase the flow of talents and reduce the loss of talents [16, 17].

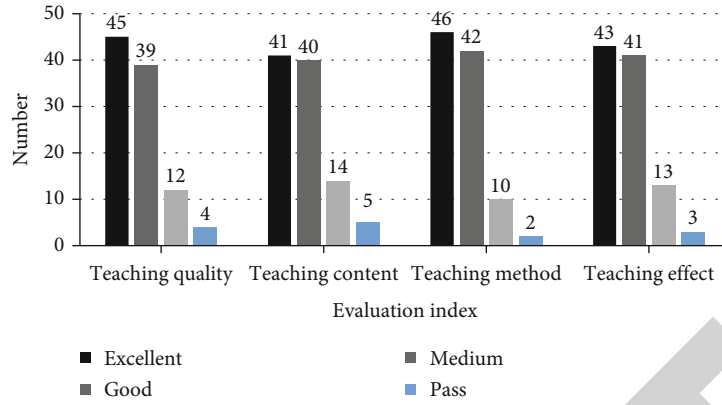


FIGURE 3: Evaluation and analysis of football TQ.

TABLE 3: The necessity of improving the quality of football teaching.

Promotion strategy	Very necessary	Necessary	General	Unnecessary
Improve venue equipment configuration	46	37	14	3
Combination of theory and practice	40	36	19	5
Improve the curriculum system	41	35	18	6
Optimize teachers' resources	49	36	12	3

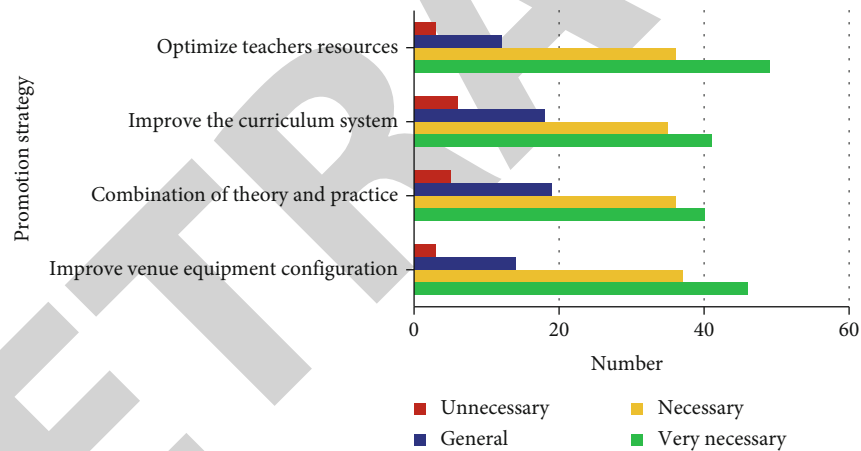


FIGURE 4: The necessity of improving the quality of football teaching.

### 3. Questionnaire and Research

3.1. *Questionnaire Design Process.* The subjects of the questionnaire survey are college leaders, fellow teachers, and students of a HVC in Q city. A total of 120 questionnaires were distributed and 100 valid questionnaires were returned. The questionnaire recovery rate was 83.3%. The questionnaire distribution method and the results of the collection are shown in Table 1.

The analysis results include the evaluation results of the TQ of the school's teachers and students on the football course and the necessity of implementing the promotion strategy.

3.2. *Questionnaire Survey Content.* The first part is to investigate the TQ evaluation of the school's teachers and students on football. The first-level indicators of TQ

evaluation include TQ, teaching content, teaching methods, and teaching effects. The evaluation grades include excellent, good, medium, and pass.

The second part is to organize the data collected in the questionnaire to understand the interviewee's need to implement improvement strategies.

### 4. Analysis and Discussion

4.1. *Evaluation and Analysis of Football TQ.* This questionnaire survey evaluates the TQ of the football course of the school. The first-level indicators of TQ evaluation include TQ, teaching content, teaching methods, and teaching effects. The evaluation grades include excellent, good, medium, and passing. The survey results are shown in Table 2.

## Research Article

# A Machine Learning Centered Approach for Uncovering Excavators' Last Known Location Using Bluetooth and Underground WSN

Sumit Kumari <sup>1</sup>, Vikas Siwach <sup>1</sup>, Yudhvir Singh <sup>1</sup>, Dheerdhvaj Barak <sup>2</sup>,  
and Rituraj Jain <sup>3</sup>

<sup>1</sup>CSE Department, UIET MDU Rohtak, Rohtak, Haryana, India

<sup>2</sup>Department of Computer Science & Engineering, Vaish College of Engineering, Rohtak, Haryana, India

<sup>3</sup>Department of Electrical and Computer Engineering, Wollega University, Nekemte, Ethiopia

Correspondence should be addressed to Sumit Kumari; [sumitmalik97@gmail.com](mailto:sumitmalik97@gmail.com) and Rituraj Jain; [jainrituraj@wollegauniversity.edu.et](mailto:jainrituraj@wollegauniversity.edu.et)

Received 9 January 2022; Revised 25 January 2022; Accepted 31 January 2022; Published 3 March 2022

Academic Editor: Shalli Rani

Copyright © 2022 Sumit Kumari et al. This is an open access article distributed under the Creative Commons Attribution License, which permits unrestricted use, distribution, and reproduction in any medium, provided the original work is properly cited.

Machine learning and data analytics are two of the most popular subdisciplines of modern computer science which have a variety of scopes in most of the industries ranging from hospitals to hotels, manufacturing to pharmaceuticals, mining to banking, etc. Additionally, mining and hospitals are two of the most critical industries where applications when deployed security, accuracy, and cost effectiveness are the major concerns, due to the huge involvement of man and machines. In this paper, the problem of finding out the location of man and machines has been focused on in case of an accident during the mining process. The primary scope of the research is to guarantee that the projected position is near to the real place so that the trained model's performance can be tested. The solution has been implemented by first proposing the MLAELD (Machine Learning Architecture for Excavators' Location Detection), in which Bluetooth Low Energy (BLE) beacons have been used for tracking the live locations of excavators preceded by collecting the data of the signal strength mapping from multiple beacons at each specific point in a closed area. Second, machine learning techniques are proposed to develop and train multioutput regression models using linear regression,  $K$ -nearest neighbor regression, decision tree regression, and random forest regression. These techniques can predict the live locations of the required persons and machines with a high level of precision from the last beacon strengths received.

## 1. Introduction

The mining industry constantly plays a vital role in the economic growth of a country due to its correlation with energy resources. Therefore, the engrossment of modern technology and its applications in this field have become very high. Machine learning technique has a comprehensive scope in almost all fields. It can be utilized to explore and experience fresh data for prediction. This allows corporations to develop effective business plans based on the forecasts of the ML algorithms. One of the remarkable achievements of this century is the deployment of

geolocation services which made it possible to navigate, and track and locate a person or an object. The primary goal of the research is to guarantee that the projected position is near to the real place so that the trained model's performance can be tested. On the other hand, these services have some limitations too; e.g., GPS has unequivocal limitations such as an error radius of about 10 meters and loss of signal strength at a height or deep down in Earth.

It is even more substantial when considering an indoor area and hence cannot be used to track people or objects in non-GPS visibility areas such as indoor or underground areas. GPS delivers the most accurate surveying and

mapping data available. GPS-based data collection is faster than traditional surveying and mapping procedures, requiring less equipment and personnel.

In addition to geolocation services like maps, navigation, and tracking applications, there is also a demand for indoor tracking and navigation systems. This includes navigation inside a large building, detecting the presence and movement of employees inside office spaces, tracking the movement of people inside stores to place various products strategically, and crowd control in hospitals and healthcare institutions. Therefore, there is an urgent requirement for the development of indoor positioning systems which can be very acute in workplaces like mines, where the risks of significant accidents always loom over. These excavation sites contain numerous hazardous zones. Due to the environmental situations, the safety and security of the excavators pose a problem for the staff overseeing the system. Even mild negligence in security and safety can result in worker fatalities and damage to costly equipment.

In this research work, a combination of Bluetooth technology and machine learning has been used for predicting the accurate locations of excavators (man and machines deployed on the mining site). The limitation of GPS has been overcome in underground areas by using Bluetooth Low Energy (BLE) beacons for exchanging the signals at the working site. BLE can work on low-power consumption and is designed to transmit a limited volume of data for the application of positioning systems. It plays an indispensable role in supporting IoT (Internet of Things) applications for wireless communication. One of the major obstacles of Bluetooth Low Energy is that it cannot be utilized for greater data rates such as those provided by wireless and cellular technology. BLE beacons can be installed at the suspected positions with man or machines at work, and the signal strength between the beacons can be measured using RSSI (Received Signal Strength Indicator). RSSI is a measurement of the relative level of power which is acquired by the RF client system which is an access point (AP) or a router. The signal strength is lower if the distance between the AP and the receiver is more; with the increase in the distance, the rates of wireless data transfer get reduced. The RSSI is used to show how much the remote attached client may hear a specific AP.

In this case, the beacons are placed inside a large indoor hall and act as data points. Additionally, the received signal strength is recorded from all these beacons at specific areas inside the room. Consequently, a database called *Beacons Database* (BDB) is created from these signal records. In this process, the next step is achieved by executing the popular machine learning algorithms including linear regression,  $K$ -nearest neighbor regression, decision tree regression, and random forest regression on BDB for predicting the locations of excavators. However, BDB is divided into train and test datasets; the train dataset is used to train the models of machine learning algorithms, and the test dataset is used to check the authenticity of the predicted outcome. The performance of these models is compared based on the Root Mean Square Error (RMSE) and  $R$ -Squared ( $R^2$ ) values. Subsequently, the model with the least error rate is chosen as the most suitable model.

## 2. Related Works

The mineral investigation is a very important assignment for a country and is very fruitful if it produces the expected outcome. However, it is so sensitive that a single point of failure can stop the process temporarily and sometimes destroy the project, which reflects in a huge loss of man and machine assets. Hence, companies try to provide the best resources for ensuring the successful completion of a mining project. The mining process has been improved as the era of technology begins; e.g., the struggle of deploying wireless communication technologies starts from the early 1970s, and the first VHF radio waves [1–5] were deployed; thereafter, UHF, WLAN, and RFID have been used. The applications based on UHF, WLAN, and RFID provide a potential boost to productivity and mining efficiency by providing better automation capabilities of machines, clear communication between deployed labor, and an easily approachable management information system [6, 7]. The increasing demand of the mining industry results in more involvement of costly machines and a huge amount of labor. Therefore, the requirement of reliable and accurate monitoring devices for underground lines [8], overhead, and WAMS [9] has increased tremendously.

Communication in underground mining can be done via three mechanisms, i.e., TTE (through the earth), TTW (through the wire), and TTA (through the air) transmission [10]. Because of the limitations of the first two methods, the third method, i.e., TTA, is the most popular one, in which ultrahigh frequency and super high frequency are used for wireless communication. In the evolution of wireless technologies, one of the most popular technologies, known for low-power consumption, reliability, security, and ease of operation, is ZigBee [11].

A lot of research has been presented for location detection in indoor environments using beacons, ZigBee, and other technologies which are focused on the progression of wireless data transmission in underground mines [12]. ZigBee technology is a wireless technology that was created as an open worldwide standard to meet the special requirements of low-cost, low-power wireless IoT networks. Therefore, the suggestion has been assessed for the reestablishment of applications and technology; modeling of digital, systematic, and metric-dependent propagation strategies; and wireless system designs by considering the immediate physical environment, antenna positioning, and patterns of radiation. Furthermore, a new study has been presented by introducing a magnetic induction based transmission technique [13] to resolve the different issues raised due to the conditions of the soil environment. This study exposed the possibility of MI-WUSNs (Wireless Underground Sensor Networks) and the implementation of wireless communication systems, including voice and data transmission for underground mines [14], and also addressed the development of wired, semi-cellular, and wireless networking services.

Additionally, the digital communication protocols for MI-WUSNs were proposed [15]; the effects of data communication parameters such as symbol rate and modulation



schemes have been evaluated for oil reservoirs. Suitable ranges for propagation linking nodes for specific water, crude oil, and soil formulations were explored.

The Wireless Network Sensor System was a suitable optimization technique. Later, a new model of communication channel was introduced [16]; it recognizes the transmission characteristics of EM waves (of terahertz) in the dynamic underground surroundings used in underground mines [17], which are used for the implementation of the systemic function of staff placement strategies in hazardous locations. It examines an economic and continuous monitoring strategy for the safety of excavators, which would help in an efficient and precise positioning of man and machines. In some other models, a mine quantitative approach [18] was used for calculating data and machinery (nodes) availability utilizing a Self-Encryption Program (SES) program that encrypts data until it is submitted to the cloud. As a continuation [19], a smart helmet which is capable of detecting dangerous situations during the mining process was designed. A miner removing the mining helmet was indicated to be in a hazardous situation. Air temperature, heart rate, and level of toxic gases (e.g., carbon monoxide, hydrogen sulfide, and methane) are the factors that are often used to classify the health situation of workers.

In some other cases [20], integrating on-channel signal booster strategies with the “daisy chain” repeater system was developed by utilizing wide-band linear amplifiers and selective filters to broaden the signals transmitted from base stations into subways across the ground. This technique satisfies the criteria for delivering radio communications that are multichannel, not just for subway stations, but also for paramedical, fire, police, and paging services etc., which are done at a much lower cost. In [21], different radio frequency communication strategies are used in underground mines through medium wave frequency (MF), very high frequency (VHF), and ultrahigh frequency (UHF) for electromagnetic transmission. Here, induction methods were also implemented to satisfy various types of mining conditions in both the laboratory and coal mines located underground. Another hybrid multimode model [22] for wireless communication in underground coal mines was proposed and evaluated for important parameters such as the size of the mine tunnel, operating frequency, and position of the transmitter/receiver. In this era of IoT, the development of Smart SAGES by utilizing the potential of IoT technologies was proposed [23]. As a result, a reliable and robust communication system would be set up for SAGES. This system ensures the confidentiality and durability of the SAGES data transmitted to the cloud, and details can be retrieved efficiently using a mobile application.

### 3. MLAELD (Machine Learning Architecture for Excavators’ Location Detection)

The problem of finding out the location of excavators by analyzing the database of RSSI values received from BLE beacons can be explained with the help of MLAELD as shown in Figure 1.

The MLAELD can be demonstrated by the following key terms.

*3.1. Bluetooth Beacons.* Bluetooth beacons can be used to determine precise locations of mobile devices using specific applications. A beacon transmits a Bluetooth Low Energy (BLE) signal within a distance of 50 meters (LOS) that can be detected by compatible devices. The signal is brief and does not change significantly; in fact, beacons are often very small and battery-powered. Bluetooth uses radio technology to carry the beacon broadcast which is relatively inexpensive for mass production. More specifically, Bluetooth Low Energy (BLE) beacons are used to work on low power by transmitting a signal that compatible applications can receive and detect. Effectively, it is a one-way broadcast where beacons transmit the signal with applications to receive them. In other words, an application can be used to detect the beacon and use the signal to regulate the location of a mobile device (excavators). Some beacon technologies used in India are given in Figure 2.

*3.2. Bluetooth-Based Localization.* BLE beacon generators are compact, affordable, battery-operated wireless transmitters, typically referred to as beacons, and possess several protocol modes. BLE transmits its identifier to local electronic devices like smartphones or single-board computers that can detect BLE signals. Consistently, beacons can send data packets to the receiver in a regular interval of 20 milliseconds to 10 seconds. The Bluetooth Special Interest Group (SIG) [25] adopted BLE as a Bluetooth subsystem to maintain device discovery that enables low-power consumption, and it is engineered for applications that do not require large volumes of data to be exchanged. The main difference between Bluetooth Low Energy (BLE) and classic Bluetooth is BLE’s low-power consumption which means that devices can run for years on a small battery. BLE is used in applications where periodic exchange of small amounts of data is needed with a broad connectivity spectrum; e.g., within reach of 60 meters, BLE 4.0 will achieve data transmission rates of 25 Mbps. These beacons are rather prevalent among IoT devices because of their affordability and low-power demands which make them one of the most promising technologies for localized location tracking while eliminating interference with other Wi-Fi devices.

*3.3. Triangulation.* The geometrical triangulation approach is the most widely employed positioning technique. Unlike the trilateration [26] approach of calculating distances, the geometrical triangulation process comprises over three sensors to perform the positioning operation, which is achieved by calculating the strength of the transmitted signal or the signal’s propagation period. The triangulation geometrical approach is not only quick but also simple, straightforward, and easy to build for the positioning algorithm. It works well in the absence of interference and barriers. However, in an indoor environment, as the signal

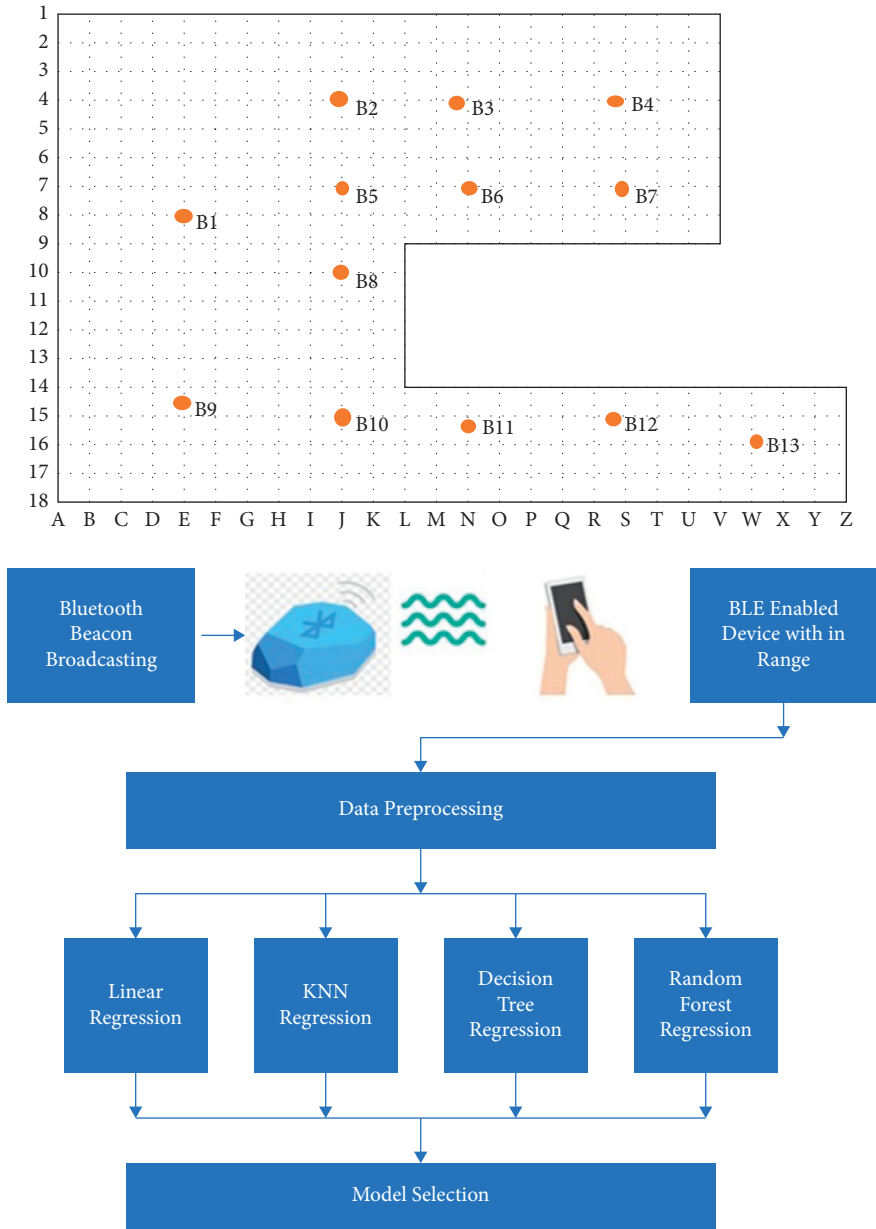


FIGURE 1: MLAELD (Machine Learning Architecture for Excavators' Location Detection).



FIGURE 2: Bluetooth Low Energy beacons in India [24].

gets reflected from the walls, floor, roof, and other obstacles in the room, the triangulation method does not yield good results in such scenarios.

**3.4. Android Support for BLE.** Android is one of the most widely used operating systems, so it has been selected to test the full solution, and Android apps are available on the Google play store for BLE support. However, other operating systems' apps are also available, e.g., CocoaPods for iOS. An Android smartphone is used in this research to detect the BLE strength at different locations using the BLE app to take RSSI readings from different beacons.

**3.5. Received Signal Strength Indicator (RSSI).** RSSI tests the intensity of a received radio signal, and a higher value indicates a stronger signal. RSSI is utilized in Bluetooth to determine that the signal transmitted is within the Golden Receiver Power Range (GRPR), which is used to describe the optimal spectrum of the strengths of the incoming signals. RSSI is calculated in dB, and the GRPR signal amplitude corresponding to a RSSI can be positive, negative, or zero dB depending upon whether the signal strength is above or below the GRPR.

**3.6. Data Collection and Preprocessing.** In this research work, the training data is collected in an indoor hall as given in Figure 1. The carpet area of the hall is divided into squares of 1 square foot each. Thereafter, 13 BLE beacons are placed at different locations inside the hall to send data packets to the receiver. The Bluetooth strength from these 13 beacons is measured at a few locations inside the hall to create a dataset. The position of the receiver and the RSSI for all the 13 beacons get recorded.

First, the data is transformed into a format compatible with classification algorithm to predict the location. Second, the data is split into two columns representing the  $x$  and  $y$  coordinates of the location, which are then used to train and develop regression models. Regression models are built with a predictive performance based on independent variables, and they are frequently used to figure out the relationship between variables and forecasts. It is observed that the beacon signal strength ranges from  $-40$  to  $-200$ . A value of  $-40$  indicates the strongest possible signal, and  $-200$  indicates the weakest possible signal.

In Figure 3, a correlation or heatmap is given among the values of beacons B1 to B13. A correlation map shows how closely related are the values in the different features. Illustratively, the correlation coefficient between b3001 (i.e., B1) and b3008 (i.e., B8) is 0.33, which reflects the positive behavior of both beacons concerning the receiver. Therefore, it can be said that both the beacons are present in the same direction from the receiver. On the other hand, the correlation coefficient between b3004 (i.e., B4) and b3002 (i.e., B2) is  $-0.41$ , which shows the negative behavior of both beacons for the receiver. Hence, it can be said that the receiver is present between both of the beacons.

**3.7. Model Training.** The next step for predicting the excavator's specific location is model training, in which supervised machine learning [27] techniques are used. Supervised learning techniques include the process of learning and developing a function that can map inputs to outputs based on similar input/output pairs. The function is inferred using training data that is labeled or has an assigned target variable. In supervised machine learning, every data point is a pair consisting of an input value and a corresponding output value. Learning algorithms generate an estimated function after following the study of the training data points, which can be used to predict the output vectors of different inputs once the function has been trained. In an optimal situation, the algorithm can determine the dependent variable or the class labels of data points to which the algorithm has never been exposed. For this, the algorithm generalizes its learning from the training data to unnoticeable circumstances. There is a wide range of supervised learning techniques which can be used. An algorithm that works well in a situation might not work the same in other circumstances. In this paper, different supervised learning algorithms are used and their performances, as well as precision, are compared.

**3.7.1. Multioutput Regression Techniques.** Regression analysis is a type of predictive modeling method which predicts a potential value based on subjective predictors. The interaction between a contingent (target) variable and an independent (predictor) variable is explored using regression analysis. Traditional machine learning predominantly uses just one output/target variable. In multioutput regression, the outputs are dependent not only upon the inputs but also upon one another. This dependency means that the outputs are often not independent of one another and may require a model which can predict both outputs together or each output contingent upon the different outputs. Some regression algorithms can be used to solve multioutput regression problems directly such as linear regression,  $K$ -nearest neighbor regression, and decision tree regression.

**3.7.2. Linear Regression.** Linear regression is a linear approach which is used to predict the interaction between an independent variable and a dependent variable response (or a scalar response). The scenario that operates for one explanatory variable is called simple linear regression. Regression models are designed with a predictive performance centered on independent variables, which is often used to work out the connection between variables and forecasting. Specific regression models differ based on the form of relationship that is assumed between the dependent and independent variables, and the number of independent variables used. In regression models,  $R$ -Squared ( $R^2$ ) and Root Mean Squared Error (RMSE) are the two accuracy metrics used to measure how well a regression model performs compared to other models.

$R$ -Squared calculates how much variation the model can identify in a dependent variable. It is the square of the

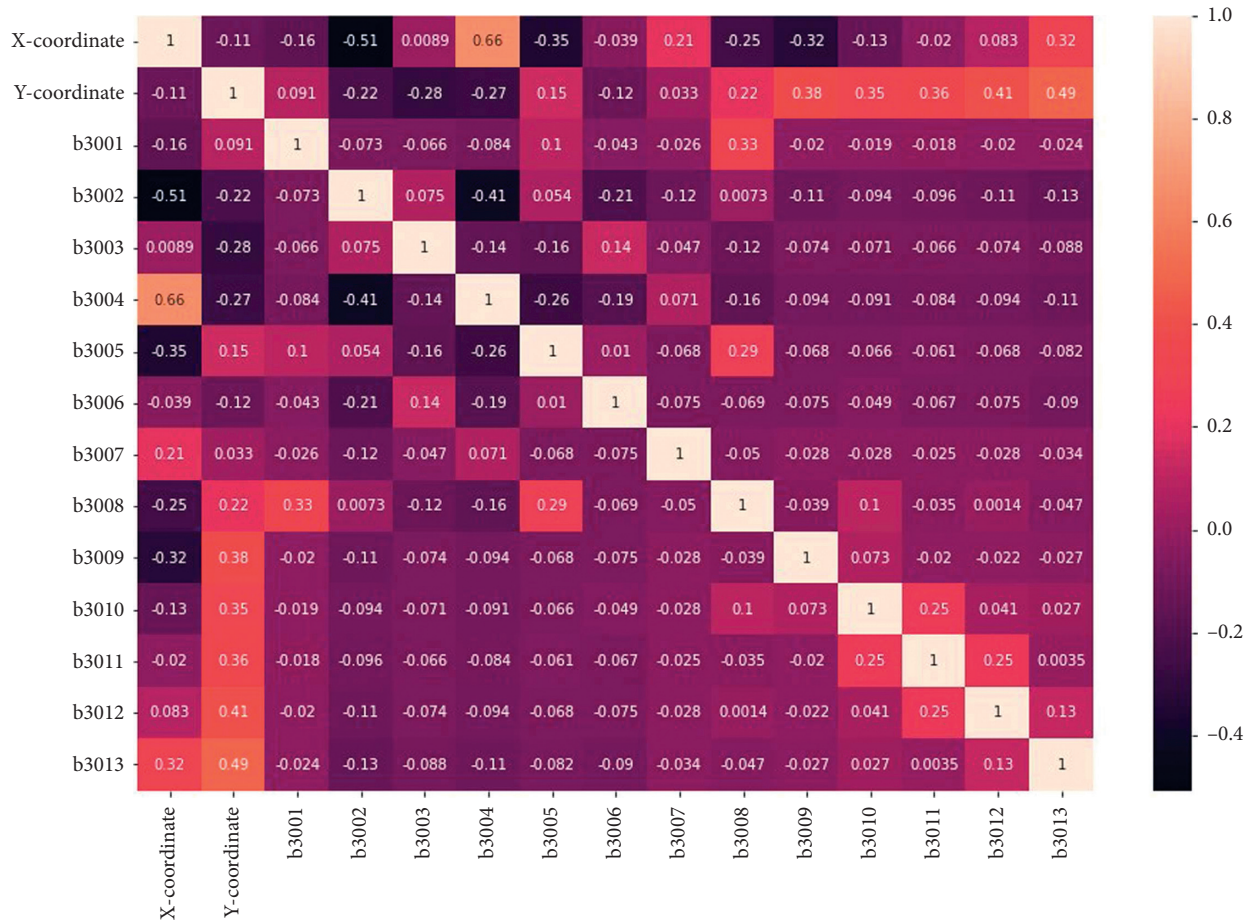


FIGURE 3: Correlation (heatmap) of different features.

correlation coefficient ( $R$ ). The value of  $R$ -Squared is between 0 and 1, so a higher value implies a closer match between the expected values and the real ones. This indication is a fair measure of how well the model matches the dependent factors. However, this does not take into consideration issues such as overfitting.  $R$ -Squared is a relative measure of how well the model conforms to dependent variables.

Mean Square Error (MSE) is an estimator of how well the model fits the exact solution. It is computed by the square sum of the prediction errors. Root Mean Square Error (RMSE) is MSE's square root value. It is used more often than MSE for two reasons: firstly, MSE values may often become too high for simple comparisons; secondly, the square of error determines MSE, and therefore the square root takes it up to the same degree of estimation error, making it easy to understand.

**3.7.3.  $K$ -Nearest Neighbors [27].**  $K$ -NN assumes a correlation between the current case data and the present cases and incorporates the new case into the category that is more identical to the available ones. The  $K$ -NN algorithm stores all the available information and classifies a new data point depending on its resemblance, which ensures that it will quickly be grouped into an appropriate group as new data arises. It is a nonparametric algorithm that requires no assumptions about the underlying data. In  $K$ -NN, a given

point is selected first using the distance method. There are many ways to calculate the distance between the given point and its closest location, which is called the Euclidean, Manhattan, or Hamming distance. The Euclidean distance metric is used by most machine learning algorithms, including  $K$ -Means, to assess the similarity of data. In this paper, the Euclidean distance has been considered.

**3.7.4. Decision Tree.** Decision tree [27] (Figure 4) splits down a dataset into further small subsets, thus constructing a correlated decision tree simultaneously. The result is a tree with decision nodes and leaf nodes, which includes two or more branches, each representing data for the evaluated attribute. The leaf node represents a decision made on the calculated numerical endpoint. The highest decision node of a graph that correlates to the strongest indicator is considered as the root node.

**3.7.5. Random Forest.** A random forest [27] (Figure 5) is an ensemble methodology that can implement both regression and classification tasks using several decision trees and by using the strategy referred to as bootstrap aggregation, which is widely recognized as bagging. The underlying principle behind this is to incorporate several decision trees

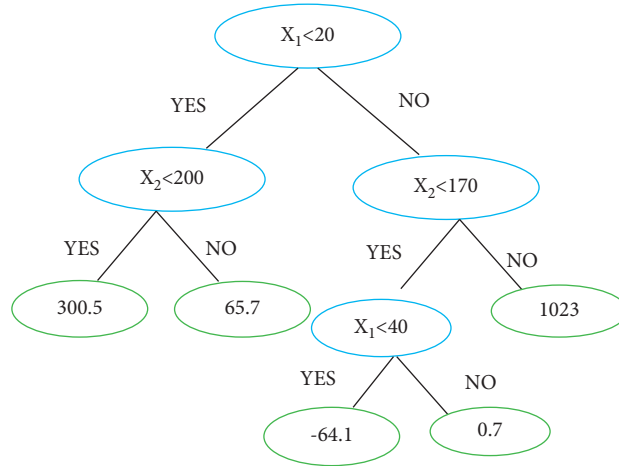


FIGURE 4: Decision tree.

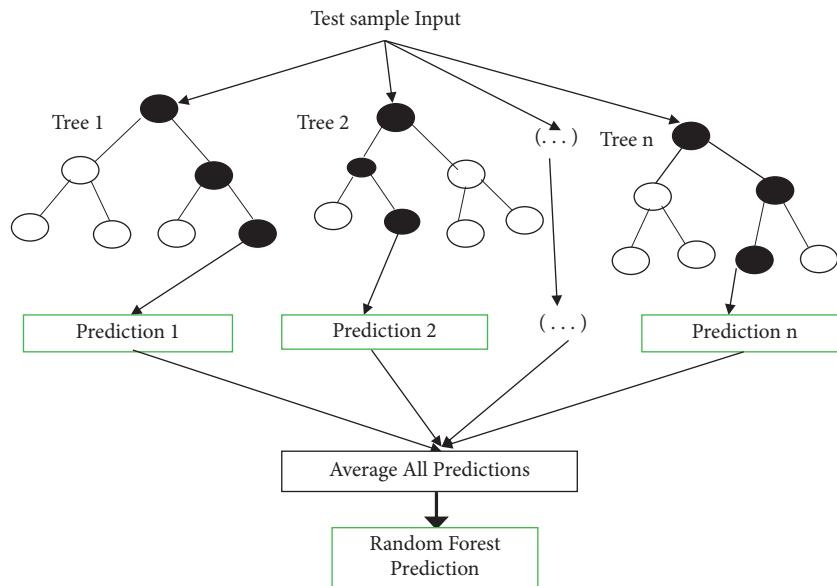


FIGURE 5: Random forest.

to assess the final version, rather than depending on individual decision trees. Random forest has several decision trees as its base learning models. The bootstrap method includes random row sampling, function dataset sampling, and generating sample datasets for each model. Each decision tree has a large variance, but when we add them all together concurrently, the resulting variance is small. Since each decision tree is appropriately trained on that specific sample data, the performance is not based on one decision tree but on several decision trees. In this method, the result is the mean of all the outputs referred to as aggregation.

#### 4. Result Analysis

In this research, thirteen Qualcomm CSR102x BLE modules are used as Bluetooth beacons. The data collected at different points are used to train multioutput machine learning

algorithms to develop models that can make precise predictions about the location of the Bluetooth signal receiver based on signal strength. The test results vary marginally from the training data due to the speculative variance of RSSI in indoor wireless networks, which degrades the position estimator efficiency. BLE support is offered to Android from version 4.3 (API level 18) to version 5.0 (API level 21).

The MLAELD has been used for implementing the machine learning algorithms (linear regression,  $K$ -NN, decision tree, and random forest), and the performances of all these algorithms have been compared using  $R^2$  and RMSE values. This step is divided into two different categories as follows.

*4.1. Comparison of Actual and Predicted Location of Beacons.* The main focus of the research work is to ensure that the predicted location is close to the actual location, so that the efficiency of the trained model can be measured.

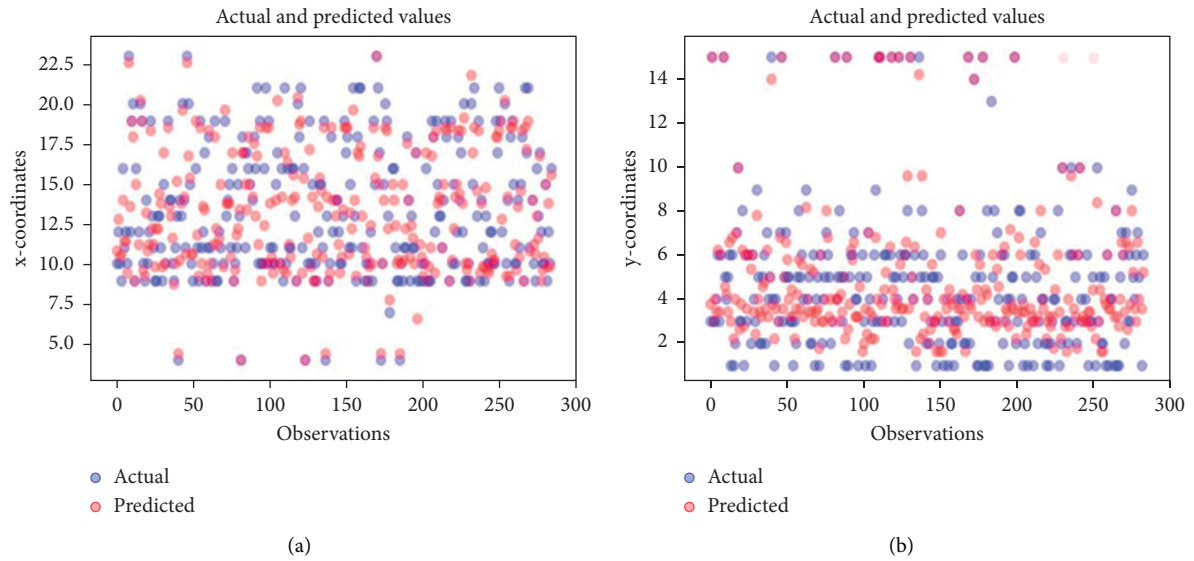


FIGURE 6: Scatter plot showing the actual and predicted values of  $x$  coordinate by a linear regression model (a) and the actual and predicted values of  $y$  coordinate by a linear regression model (b).

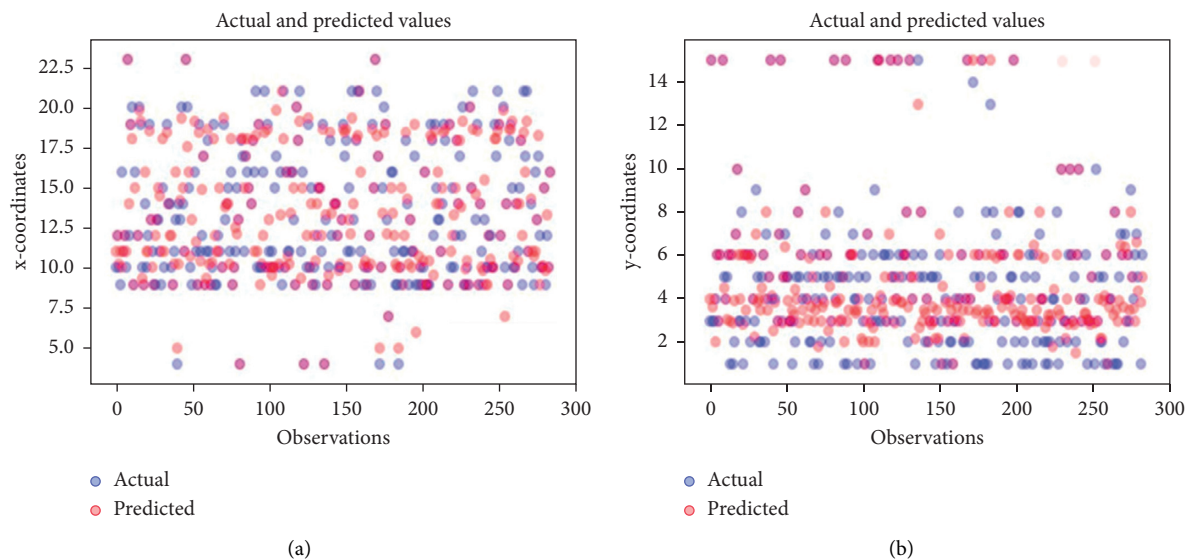


FIGURE 7: Scatter plot showing the actual and predicted values of  $x$  coordinate by a  $K$ -NN model (a) and the actual and predicted values of  $y$  coordinate by a  $K$ -NN model (b).

The *Beacons Database* (BDB) [28] provides the location of  $x$ ,  $y$  coordinates along with the signal strength. The models have been trained using this BDB by dividing it into train and test datasets using an 8:2 ratio. Training data is an extremely large dataset that is used to teach a machine learning model. Test dataset is a tertiary dataset in machine learning that is used to test a machine learning algorithm after it has been trained on an initial training dataset. The results of actual and predicted locations can be categorized based on selected machine learning algorithm as follows.

**4.1.1. Actual and Predicted Values by Linear Regression.** The actual and predicted values for  $x$  and  $y$  coordinates are depicted in Figure 6. The blue dots represent the actual values, and the red dots represent the predicted values. The scattering of these dots far from each other shows the difference between actual and predicted values. Overlapping shows that the actual and predicted values are very close to each other. In Figure 6, the values of  $x$  coordinates are scattered showing that the errors comparative to other methods are high.

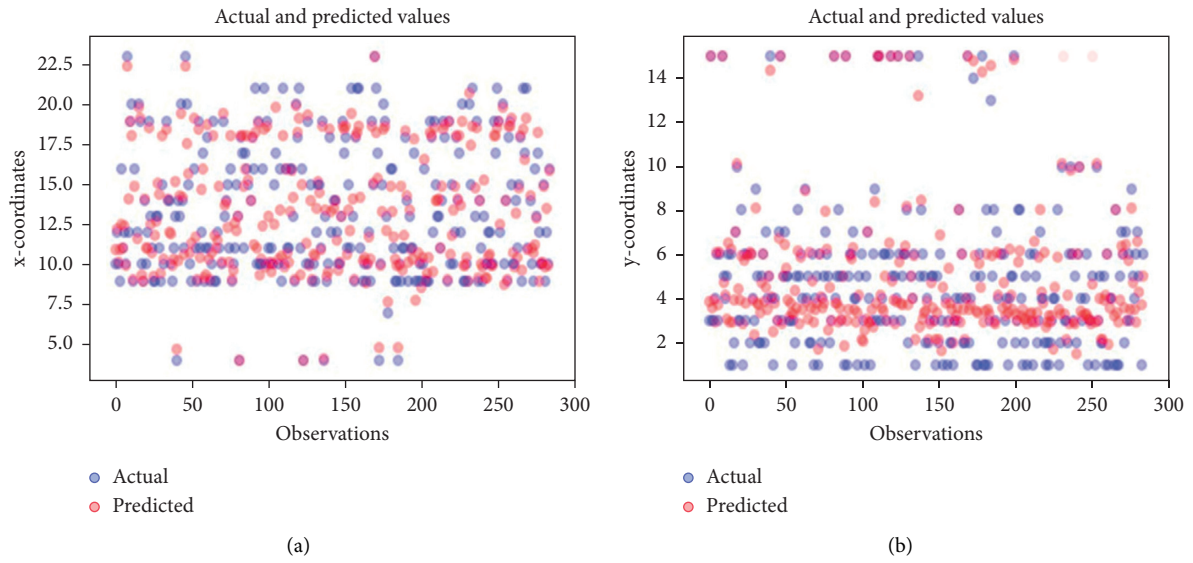


FIGURE 8: Scatter plot showing the actual and predicted values of  $x$  coordinate by a decision tree model (a) and the actual and predicted values of  $y$  coordinate by a decision tree model (b).

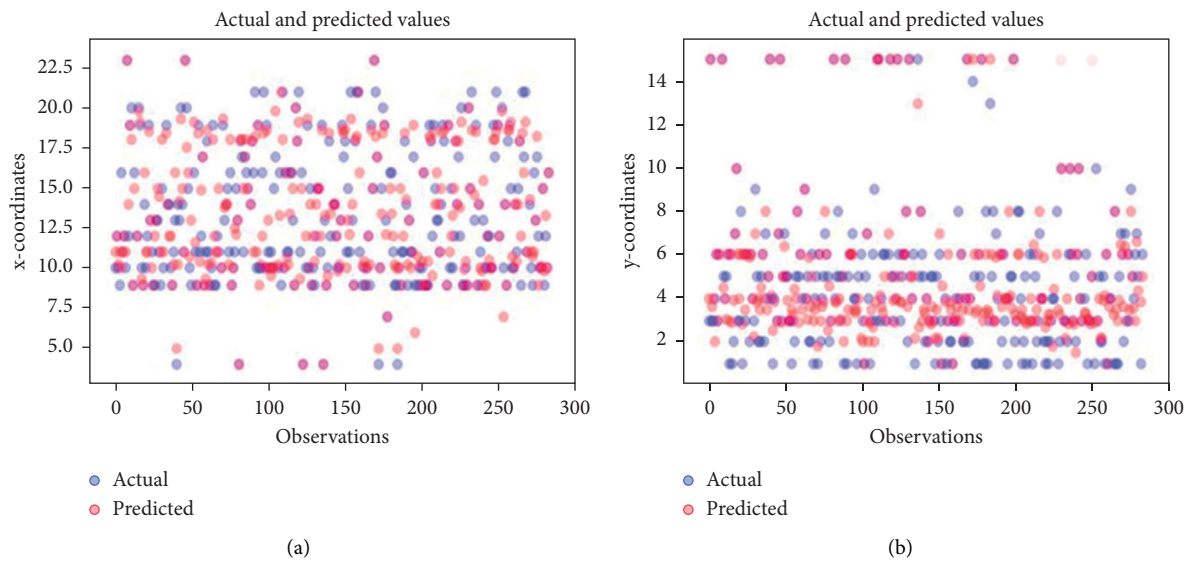


FIGURE 9: Scatter plot showing the actual and predicted values of  $x$  coordinate by a random forest model (a) and the actual and predicted values of  $y$  coordinate by a random forest model (b).

TABLE 1: RMSE and  $R^2$  values for different models on the training dataset.

Model	RMSE	$R^2$
Linear regression	1.79	0.79
$K$ -nearest neighbor	1.25	0.89
Decision tree	1.05	0.92
Random forest	1.07	0.92

4.1.2. *Actual and Predicted Values by K-NN.* The actual and predicted values of  $x$  and  $y$  coordinates by the  $K$ -nearest neighbor algorithms are shown in Figure 7.

In this case, the values are not saturated at one place as in Figure 6. Here, values are scattered, and most of the predicted

values overlap the actual values. Therefore, the accuracy increases, in this case, compared to linear regression.

4.1.3. *Actual and Predicted Values by Decision Tree.* The actual and predicted values of  $x$  and  $y$  coordinates by decision tree are given in Figure 8. In this case, the results are improved compared to linear regression but are almost similar to those of  $K$ -NN.

4.1.4. *Actual and Predicted Values by Random Forest.* The actual and predicted values of  $x$  and  $y$  coordinates by random forest are given in Figure 9. In this model, the results

TABLE 2: RMSE and  $R^2$  values for different models on the test dataset.

Model	RMSE	$R^2$
Linear regression	1.78	0.76
$K$ -nearest neighbor	1.45	0.84
Decision tree	1.62	0.81
Random forest	1.43	0.85

are improved compared to the other three methods. Extra white space on the figure indicates that most of the values are overlapped, which reflects a higher accuracy of prediction.

**4.2. Performance Comparison Using  $R^2$  and RMSE Values.** In this section, the numerical difference between actual and predicted values is discussed using  $R^2$  and RMSE values for training and testing data. If the main goal of the model is prediction, then the major criteria are to calculate the RMSE value, which gives the information of accurate prediction of response, and a lower value of RMSE shows a better fit.

However,  $R^2$  gives information about how two values are closely related. Therefore, a higher value or value closer to +1 of  $R^2$  indicates a good fit of values into the model.

The main focus of the research work is to ensure that the predicted location is close to the actual location.

Table 1 shows the comparison of the various RMSE and  $R^2$  values for the four algorithms implemented on the training dataset. The decision tree regression and the random forest regression provide considerably the best performance among the four models.

Table 2 shows the comparison of the various RMSE and  $R^2$  values for the four algorithms implemented on the test dataset. The random forest regression provides considerably the best performance among the four models.

## 5. Conclusion

In this work, a machine learning-based model has been designed to predict the location based on the RSSI values handled by a Bluetooth receiver. The model can be used for precisely locating trapped excavators or machines underground. Apart from that, it can be used at another place where similar requirements are found; e.g., it can be used in supermarkets where it can assist customers in locating shops and track the movement of customers, which can help in product placement. This study is limited to detecting the location of a receiver using a fixed number of BLE beacons inside an indoor hall. In the future, a similar study can be conducted inside a long tunnel with hundreds of beacons to detect precise locations by further leveraging a Wi-Fi setup in the area. This can help in developing a model which can be used to identify the location using Bluetooth, not just in a small indoor area but in a much larger space. Location detection and tracking using Bluetooth can also be used in monitoring the movement and flow of a crowd in a busy street or inside a busy supermarket.

As this technology can be used to track and detect a person's location in real time, it can be used in crowded fairs and shops to trace lost people or children with ease. It can also be used to detect the last known location of a person

stuck in a building during a fire or an earthquake, which can help fire fighters or disaster response teams track and rescue the person swiftly. Using indoor positioning in museums can be the best way to reduce expenditure on hiring staff and guides. It can assist tourists in navigating through the museum and in exploring various artifacts.

## Data Availability

The data shall be made available on request.

## Conflicts of Interest

The authors declare that they have no conflicts of interest.

## References

- [1] P. Delogne, "The INIEX mine communications systems," in *Proceedings of the Radio: Roads Tunnels Mines*, vol. 2, pp. 129–136, Liege, Belgium, April 1974.
- [2] J. N. Murphy and H. E. Parkinson, "Underground mine communications," *Proceedings of the IEEE*, vol. 66, no. 1, pp. 26–50, 1978.
- [3] D. J. R. Martin and R. Webster, "The use of radio in British coal mines," in *Proceedings of the Radio: Road Tunnels Mines*, vol. 2, pp. 110–128, Liege, Belgium, April 1974.
- [4] D. J. R. Martin, "Leaky-feeder radio communication: a historical review," in *Proceedings of the IEEE VTC*, pp. 25–30, Pittsburgh, PA, USA, May 1984.
- [5] P. Delogne, "EM propagation in tunnels," *IEEE Transactions on Antennas and Propagation*, vol. 39, no. 3, pp. 401–406, 1991.
- [6] L. K. Bandyopadhyay, S. K. Chaulya, P. K. Mishra, and A. Choure, "Wireless information and safety system for underground mines," in *Proceedings of the URSI*, pp. 9–16, Chicago, IL, USA, Aug 2008.
- [7] K. Srinivasan, M. Ndooh, and K. Kaluri, "Advanced wireless networks for underground mine communications," in *Proceedings of the IEEE ICWCUCA*, pp. 51–54, Mawii, Hawaii, USA, Jun 2005.
- [8] F. P. Mohamed, W. H. Siew, J. J. Soraghan, S. M. Strachan, and J. McWilliam, "The use of power frequency current transformers as partial discharge sensors for underground cables," *IEEE Transactions on Dielectrics and Electrical Insulation*, vol. 20, no. 3, pp. 814–824, 2013.
- [9] J. De La Ree, V. Centeno, J. S. Thorp, and A. G. Phadke, "Synchronized phasor measurement applications in power systems," *IEEE Transactions on Smart Grid*, vol. 1, no. 1, pp. 20–27, 2010.
- [10] W. H. Schiffbauer and J. F. Brune, *Coal Mine Communications*, American Longwall Mag., Chilhowie, VA, USA, 2006.
- [11] K.-L. Chen, Y.-Ru Chen, Y.-P. Tsai, and N. Chen, "A novel wireless multifunctional electronic current transformer based on ZigBee-based communication," *IEEE Transactions on Smart Grid*, vol. 8, no. 4, pp. 1888–1897, 2016.



- [12] A. E. Forooshani, S. Bashir, D. G. Michelson, and S. Noghianian, "A survey of wireless communications and propagation modeling in underground mines," *IEEE Communications Surveys & Tutorials*, vol. 15, no. 4, pp. 1524–1545, 2013.
- [13] S. Kisseleff, I. F. Akyildiz, and W. Gerstacker, "Interference polarization in magnetic induction based wireless underground sensor networks," in *Proceedings of the 2013 IEEE 24th International Symposium on Personal, Indoor and Mobile Radio Communications (PIMRC Workshops)*, pp. 71–75, IEEE, London, UK, September 2013.
- [14] A. Patri, A. Nayak, and S. Jayanthu, "Wireless communication systems for underground mines—a critical appraisal," *International Journal of Engineering Trends and Technology*, vol. 4, no. 7, pp. 3149–3153, 2013.
- [15] S. Kisseleff, I. F. Akyildiz, and W. Gerstacker, "On modulation for magnetic induction based transmission in wireless underground sensor networks," in *Proceedings of the 2014 IEEE International Conference on Communications (ICC)*, pp. 71–76, IEEE, Sydney, NSW, Australia, June 2014.
- [16] M. A. Akkaş and R. Sokullu, "Wireless underground sensor networks: channel modeling and operation analysis in the terahertz band," *International Journal of Antennas and Propagation*, vol. 2015, Article ID 780235, 2015.
- [17] S. Kataria, P. Singh, and P. Ahlawat, "Survey paper on wireless underground positioning system," *International Journal of Computer Applications*, vol. 975, p. 8887, 2015.
- [18] A. Mehbodniya, J. L. Webber, M. Shabaz, H. Mohafez, and K. Yadav, "Machine learning technique to detect sybil attack on IoT based sensor network," *IETE Journal of Research*, pp. 1–9, 2021.
- [19] A. M. Zungeru, M. M. MolamoganyiGorata, and C. Joseph, "Healthcare cloud computing for underground wireless sensor networks," in *Proceedings of the 2017 2nd International Conference on Frontiers of Sensors Technologies (ICFST)*, pp. 136–140, IEEE, Shenzhen, China, April 2017.
- [20] T. Nithya, M. Mohammed Ezak, K. Ranjith Kumar, V. Vignesh, and D. Vimala, "Rescue and protection system for underground mine workers based on Zigbee," *International Journal of Recent Research Aspects*, vol. 4, pp. 194–197, 2018.
- [21] C. Li, H. Niu, M. Shabaz, and K. Kajal, "Design and implementation of intelligent monitoring system for platform security gate based on wireless communication technology using ML," *International Journal of System Assurance Engineering and Management*, 2021.
- [22] L. K. Bandyopadhyay, P. K. Mishra, S. Kumar, and A. Narayan, "Radio frequency communications systems in underground mines," in *Proceedings of the International Seminar on 28th General Assembly of International Union of Radio Science*.
- [23] B. G. Anil Kumar, K. C. Bhagyalakshmi, K. Lavanya, and K. H. Gowranga, "A Bluetooth low energy based beacon system for smart short range surveillance," in *Proceedings of the IEEE International Conference on Recent Trends in Electronics, Information and Communication Technology (RTEICT)*, Venkateswara College of Engineering, Department of Electronics & Communication Engineering, Bengaluru, India, May 2016.
- [24] J. Bhola, M. Shabaz, G. Dhiman, S. Vimal, P. Subbulakshmi, and S. K. Soni, "Performance evaluation of multilayer clustering network using distributed energy efficient clustering with enhanced threshold protocol," *Wireless Personal Communications*, pp. 1–15, 2021.
- [25] F. Thomas and L. Ros, "Revisiting trilateration for robot localization," *IEEE Transactions on Robotics*, vol. 21, no. 1, pp. 93–101, 2005.
- [26] P. Cunningham, M. Cord, and S. Jane Delany, *Machine Learning Techniques for Multimedia*, Springer, Berlin, Heidelberg, 2008pp. 21–49, Supervised learning.
- [27] <https://www.kaggle.com/mehdimka/ble-rssi-dataset>.
- [28] R. Alok, P. Misra, and H. B. Sahu, "Experimental measurements and channel modeling for wireless communication networks in underground mine environments," in *Proceedings of the 2017 11th European Conference on Antennas and Propagation (EUCAP)*, pp. 1345–1349, IEEE, Paris, France, March 2017.

## Research Article

# A Novel Secure Authentication Protocol for IoT and Cloud Servers

Ummer Iqbal <sup>1</sup>, Aditya Tandon <sup>2</sup>, Sonali Gupta <sup>3</sup>, Arvind R. Yadav <sup>4</sup>,  
Rahul Neware <sup>5</sup> and Fraol Waldamichael Gelana <sup>6</sup>

<sup>1</sup>National Institute of Technology Srinagar, Jammu and Kashmir, India

<sup>2</sup>Krishna Engineering College, Ghaziabad, Uttar Pradesh, India

<sup>3</sup>Department of Computer Engineering, J C Bose University of Science and Technology, Faridabad, Haryana, India

<sup>4</sup>Parul Institute of Engineering & Technology, Parul University, Vadodara, India

<sup>5</sup>Department of Computing, Mathematics and Physics, Høgskulen På Vestlandet, Bergen, Norway

<sup>6</sup>Artificial Intelligence Centre, Addis Ababa, Ethiopia

Correspondence should be addressed to Ummer Iqbal; [drkhaniqbalummer@gmail.com](mailto:drkhaniqbalummer@gmail.com) and Fraol Waldamichael Gelana; [fraol.gelana@aic.et](mailto:fraol.gelana@aic.et)

Received 29 December 2021; Accepted 1 February 2022; Published 3 March 2022

Academic Editor: Shalli Rani

Copyright © 2022 Ummer Iqbal et al. This is an open access article distributed under the Creative Commons Attribution License, which permits unrestricted use, distribution, and reproduction in any medium, provided the original work is properly cited.

The integration of IoT with the cloud infrastructure is essential for designing smart applications. However, such integration may lead to security issues. Authentication and session key establishment is an essential security requirement for secure communication between IoT devices and cloud servers. For evaluating authentication key agreement schemes, the extended Canetti–Krawczyk (eCK) adversary model is regarded to be a more strict and relevant adversary model. Many schemes for authenticated key exchange between IoT devices and cloud servers have been proposed in the literature but have been assessed under Dolev and Yoa (DY) adversary model. Recently, Rostampour et al. introduced an ECC-based approach for enabling authentication between IoT devices and cloud servers that is secure and robust to various attacks under the Dolev and Yoa adversary model. In this paper, a detailed review and the automated security verification of the Rostampour et al. scheme are carried out under the eCK adversary model using Scyther-Compromise. The validation indicates that the scheme is not secure and is susceptible to various attacks under the eCK adversary model. To overcome the limitation of the Rostampour et al. scheme, a design of an ECC-based scheme for authentication between IoT devices and cloud servers under the eCK adversary model is proposed. The Scyther verification indicates that the scheme is safe under the eCK adversary model. The soundness of the correctness of the proposed scheme has been analyzed using BAN logic. Comparative analysis indicates that the scheme is resilient under the eCK adversary model with an energy overhead of 278.16 mJ for a resource constraint IoT device and a communication overhead of 1,408 bits.

## 1. Introduction

The internet of things (IoT) is a new network that provides numerous embedded devices to the Internet to share data. It is based on information and communication technologies. Embedded devices are becoming increasingly complicated as a result of the fast growth of technology, and they are employed in a broad variety of applications. The ability to relate such gadgets to huge resource pools, such as the cloud, is a significant advancement in modern technology. The integration of embedded devices and cloud servers enables the use of IoT in a wide range of commercial and

government applications. However addressing the security issues, such as authentication and data privacy is important for the efficient integration of these two systems [1–3]. IoT has grown significantly over the years because of its relevance in smart applications. The internet of things (IoT) market was valued at USD 250.72 billion in 2019 and is expected to grow to USD 1,463.19 billion by 2027 [4]. This exponential advancement of IoT is governed by its role in developing applications that include smart parking, smart building, smart health, smart environment, smart agriculture, and smart homes [5, 6]. Smart parking can be employed for effective monitoring of parking areas in the city, and

smart building applications can be used for monitoring the structural health of a building in terms of vibrations and material conditions. IoT can also be used for real-time monitoring the health and the hydraulic parameters of the water bodies and effective monitoring of road conditions in terms of climate conditions [5]. In terms of security and emergency applications, IoT nodes can be deployed for unauthorized perimeter access, detection of harmful chemical and radiation leaks, and detection of gas leaks in industrial surroundings [6]. For smart agriculture, the nodes can be employed for monitoring soil quality, climate control in the greenhouse, and smart irrigation. The various applications in smart homes include surveillance, remote monitoring of appliances, energy, and water conservation. In the medical field, IoT can be employed for developing applications that include wireless body area networks, geriatric assistance, and automatic monitoring of medical freezers [5].

A typical IoT-based smart application comprises a three-tier architecture that includes perception tier, network and server tier, and application tier [5, 7] as shown in Figure 1. The physical parameters are perceived in the perception layer using IoT devices, and the data perceived are further relayed to the server tier. The server tier serves as a communication backbone, employing different communication technologies [7]. As IoT applications generate a large volume of data, the server tier includes features for storing and processing it. A variety of servers, including mobile, web, and real-time communication servers, provide middleware support at the server tier. As the perception layer generates a very large volume of data, cloud servers can also be used at this layer for data storage and management. Various end-users connect to the server tier for offline and online data analysis in the user tier [8, 9]. The security of IoT-based smart applications is of paramount importance [10]. The communication between the server tier and client tier can be made secure using traditional security protocols. However, as IoT devices are resource-constrained, the communication between IoT devices in the perception tier and servers in the server tier becomes an emerging and active area of research [5].

Authentication and session key establishment are bedrock for all other security services between IoT nodes in the perception layer and the various servers in the server tier [11]. Many schemes have been suggested for securing communication between IoT devices and cloud servers. Liao and Hsiao [12] proposed a mutual authentication scheme with ID verifier protocol. However as indicated by [13], the scheme suffers from server impersonation attacks.

Kalra and Sood [14] presented a mutual authentication scheme based on ECC. The scheme is resilient to various attacks. However, the scheme has design issues in terms of mutual authentication, insider, and traceability attacks. Chang et al. [15] pointed out the limitations of Kalra and Sood and highlighted its weakness in terms of mutual authentication and mistress of the session key. Chang et al. suggested an improved scheme that overcame the limitations of Kalra and Sood. Kumari et al. [16] pointed out the deficiencies of Kalra and Sood in terms of insider attacks, device anonymity, session key agreement, and mutual

authentication. Kumari et al. also suggested an ECC-based scheme to overcome these limitations. Wang et al. [17] highlighted the deficiencies of the Chang et al. scheme in terms of impersonation attacks and suggested an improved scheme. Recently, Rostampour et al. [11] proposed an ECC-based scheme for authentication of IoT edge devices with the cloud server. Rostampour et al. made a detailed review of the schemes of Kalra and Sood, Chang et al., Kumari et al., and Wang et al. and highlighted their limitations. Rostampour et al. pointed out that all the existing schemes suffer from traceability attacks.

When connecting an embedded system to the cloud, security is the main consideration. Mutual authentication must also be established between the cloud server and the embedded devices. To address these security concerns, many authentication systems for IoT and cloud servers have been developed. However, there are several faults in the existing approaches that must be addressed. When memory and power are limited and greater security with a low key length is required, elliptic curve cryptography (ECC) is the best public-key cryptography solution [18, 19]. The existing schemes presented in the literature have been analyzed under Dolev and Yoa (DY) [20, 21]. However, the eCK [22] adversary model is a more stringent model for authentication key agreement schemes [23]. In this paper, a detailed review of the Rostampour et al. scheme has been made. The Rostampour et al. scheme has been formally validated using Scyther-Compromise [24] under the eCK adversary model. Scyther-Compromise validation depicts that the Rostampour et al. scheme is not secure under the eCK adversary model. Furthermore, an improved scheme for authentication and key agreement between IoT devices and the server under the eCK adversary model has also been proposed.

*1.1. Contributions.* The major highlights of the paper are as follows:

- (a) A review of the Rostampour et al. scheme has been made carried out. The scheme has been modeled on Scyther-Compromise and analyzed under the eCK adversary model.
- (b) An ECC-based authentication scheme for IoT and cloud servers has been designed. The designed scheme provides better functionality and security specifications.
- (c) The proposed scheme has been modeled on Scyther-Compromise. The results indicate that the scheme is safe under the eCK adversary model.
- (d) The soundness and correctness of the proposed protocol have also been evaluated using BAN [25] logic.

*1.2. Paper Organization.* The remainder of the paper is laid out as follows. The preliminaries are presented in Section 2. Section 3 reviews the Rostampour et al. scheme and discusses its formal security verification under the eCK adversary model. In Section 4, the design of the proposed

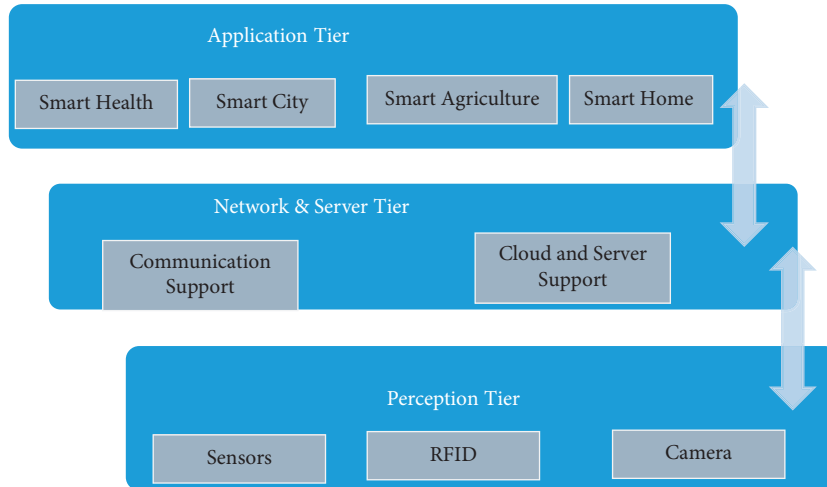


FIGURE 1: Three-tier architecture of IoT applications.

ECC-based scheme for authentication between IoT devices and cloud servers is presented. In Section 5, an informal security analysis has been carried out. Section 6 provides the simulation details of formal security analysis using the Scyther under the eCK adversary model. In Section 7, security analysis using BAN logic has been carried out. Finally, Section 8 presents the comparison of the proposed scheme with other relevant schemes in terms of functional and security specifications.

## 2. Preliminaries

**2.1. Notations.** The notations used in the paper are tabulated in Table 1.

**2.2. Adversary Model.** An adversary model formulates the potential capabilities an attacker can have. Various adversary models exist that include Dolev and Yoa (DY) [20, 21], Canetti–Krawczyk (CK), and extended Canetti–Krawczyk models (eCK) models [22]. In all the models, the communication channel is completely insecure; however, they differ in their adversary query capabilities. In DY threat model, the communication parties are considered to be honest and can run multiple sessions with each other. The communication channel is completely insecure and totally under the adversary’s control, with the ability to record, delete, replay, redirect, rearrange, and completely control message schedule. The adversary can act as an active adversary in the middle and lead various man-in-the-middle attacks. The CK and eCK models are the most widely accepted models for authentication and key agreement protocols. In this adversary model, an attacker has abilities to compromise PRNG and get access to the secret randomness of the session. It is also assumed that an adversary can compromise the session and get access to it. An attacker can also get access to the long-term keys [26]. The major difference between the CK model and the eCK model is that in the eCK model, the adversary is capable of accessing ephemeral secrets, thus leading to an ephemeral-secret-key-leakage attack. An

TABLE 1: Notations.

Notation	Meaning
$E_p(a, b)$	Elliptical curve
$S$	Server
$D_i$	$i$ -th IoT device
$ID_i$	Identity of $D_i$
$ID_s$	Identity of $S$
$R_i$	The random number at the server
$N_i$	Random number at the device
$X_S$	Private key of $S$
$K_i$	Private key of $D_i$
$S_i$	Ephemeral secret of $D_i$
$S_s$	Ephemeral secret of $S$
$ET$	Expiration time
$G(x, y)$	Generator point of $E_p(a, b)$
$SK$	Session key between $S$ and $D_i$
$H$	Collision resistant hash function
$\oplus$	Xor operation
$P + Q$	Point addition
$X.G$	Scalar multiplication

ephemeral key leakage indicates the weaknesses of a random number generator where the attacker can determine the randomness generated correctly with a high probability [26].

**2.3. Elliptical Curve Cryptography.** Koblitz [27] and Miller [28] introduced elliptical curve cryptography (ECC). ECC is a powerful cryptographic technology. It establishes security between key pairs for public-key encryption using elliptical curve mathematics. ECC has grown in popularity in recent years due to its smaller key size and ability to maintain security. This trend is expected to continue as the need for devices to be secure develops in response to the rising size of keys, putting pressure on limited mobile resources. This is why it is vital to understand elliptic curve cryptography in context of low power devices [29]. When compared to RSA, ECC is highly efficient with low overheads. With a key size of 160 bits, elliptical curve cryptography provides the same level of security as RSA with a key size of 1,024 bits, making it

ideal for devices with limited resources [29]. Over a finite prime field  $F_p$ , an elliptical curve  $E_p(a, b)$  is defined as follows [29]:

$$E_p(a, b): y^2 = x^3 + ax + b, \quad (1)$$

where  $\Delta = (4a^3 + 27b^2) \neq 0$ .

Some of the essential definitions related to elliptical curve cryptography are listed below [29]:

- (a) Point addition: point addition (+) between any two points  $[A(x_A, y_A), B(x_B, y_B)] \in E_p(a, b)$  is defined as follows:

$$C(x_R, y_R) = A(x_A, y_A) + B(x_B, y_B), \quad (2)$$

where  $C(x_R, y_R)$  is a reflection of the point at which the line joining  $A(x_A, y_A)$ , and  $B(x_B, y_B)$  intersects the curve  $E_p(a, b)$ . The algebraic computation is given as follows:

$$\begin{pmatrix} x_R = (\lambda^2 - x_A - x_B) \pmod{p} \\ y_R = (\lambda(x_A - x_B) - y_A) \pmod{p} \end{pmatrix},$$

Where,

$$\lambda = \begin{cases} \frac{(y_B - y_A)}{(x_B - x_A)} \pmod{p}, & \text{if } A \neq B, \\ \frac{3x_A^2 + a}{2y_A} \pmod{p}, & \text{if } A = B. \end{cases} \quad (3)$$

- (b) Scalar multiplication: for any scalar number  $X$  and  $A(x, y) \in E(a, b)$ , the scalar multiplication is defined as follows:

$$\begin{aligned} X.A(x, y) &= A(x, y) + A(x, y) + A(x, y) \\ &+ \dots + A(x, y), \end{aligned} \quad (4)$$

X times.

- (c) Elliptical discrete logarithmic property (ECDLP): given points  $R(x, y)G(x, y) \in E_p(a, b)$ , ECDLP is a computational problem to find a scalar  $n$  such that  $R(x, y) = n.G(x, y)$ . ECDLP has been a prominent field of research in cryptography over many decades, and it is the essential foundation for elliptic curve cryptography (ECC) and pairing-based cryptography. ECDLP has exponential time complexity.

**2.4. Scyther Simulation.** Scyther is a tool for validating and verifying security protocols that was created by Cremers [24]. It is a software that provides security risk assessments and attack simulation capabilities. Scyther uses an infinite number of sessions to verify security protocols. Scyther also allows multiprotocol assaults to be verified. Figure 2 depicts the Scyther Tool's design in its most basic form. To verify and validate a security protocol in Scyther, it is modeled using Scyther protocol description language

(SPDL). The tool accepts the SPDL model to be validated as well as simulation settings. As an output, the Scyther tool generates a summary report showing if the necessary security assertions are valid. If an attack is discovered, it generates a trace pattern in the form of a visual graph or an XML representation. An SPDL model of security protocol comprises roles that define the communication pattern of sender and receiver principals. The term claim is used to specify the various security requirements. Claim *secret* declares the parameters that must remain confidential from the adversary. The claim *alive* ensures that the claimant is executing events with the intended party. *Nisynch* ensures that all the intended messages in the session are sent and received in a synchronized manner, whereas *Niagree* indicates that the communicating parties agree on the messages exchanged. Finally, the *weakagree* ensures resilience against impersonation attacks. SKR claim indicates whether the session key designated using SKR can be revealed using the session key adversary rule. To verify this claim, the session key rule in the adversary model setting must be enabled. More details about Scyther are given in [24].

The adversary model by default in the Scyther standard version is Dolev and Yoa. The Scyther-Compromise provides extended support for various adversary models as compared to the standard Scyther version. In this paper, Scyther-Compromise version 0.9.2 has been used.

### 3. Review and Security Validation of Rostampour Et Al.'s Scheme

**3.1. Review of Rostampour Et Al.'s Scheme.** The Rostampour et al. scheme comprises two phases given as below:

- (1) Registration phase
- (2) Login and authentication phase

**3.1.1. Registration Phase.** The registration phase is carried out between the device and the server over a secure channel. The steps are given below:

- (i)  $D_i$  generates a random number  $X_i$  and computes  $PID_i$  as (4):

$$PID_i = X_i \oplus ID_i. \quad (5)$$

$D_i$  sends  $PID_i$  to the server Sas follows:

$$D_i \longrightarrow S: PID_i. \quad (6)$$

- (ii) The server generates a random number  $R_i$  and calculates (7) and (8):

$$CK_i = H(R_i \oplus X_i \oplus ET \oplus PID_i), \quad (7)$$

$$CK'_i = CK_i \cdot G. \quad (8)$$

Server stores  $PID_i, ET$ , and  $CK_i$  in a secure database.

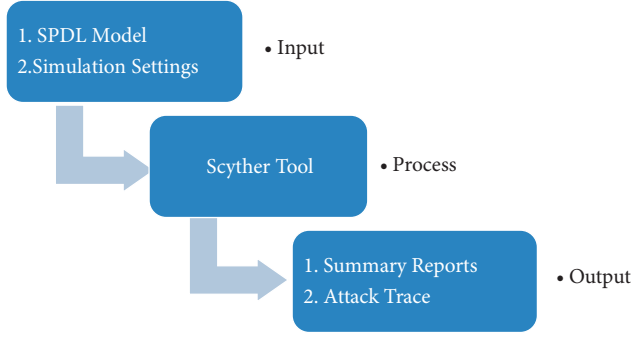


FIGURE 2: Basic architecture of Scyther.

- (iii) The server sends  $CK'_i$  to the device as follows:

$$S \longrightarrow Di : CK'_i. \quad (9)$$

The device  $Di$  stores  $CK_i$  along with generated  $PID_i$ .

### 3.1.2. Login and Authentication Phase

- (i)  $D_i$  generates a random number  $N_i$  and computes (10)–(12):

$$P_1 = N_1 \cdot G, \quad (10)$$

$$P_2 = N_1 \cdot CK'_i, \quad (11)$$

$$PPID_i = PID_i \cdot P_1. \quad (12)$$

And sends it to the server as follows:

$$D_i \longrightarrow S: P_1, P_2, PPID_i. \quad (13)$$

- (ii) The server finds the entry of  $D_i$  in its database and verifies  $P_2 \neq CK_i \cdot P_1$ . If the evaluation is false, then the process stops, and if true, then the device is authenticated.
- (iii) The server generates a random number  $N_2$  and computes (14) and (15):

$$P_3 = N_2 \cdot G, \quad (14)$$

$$P_4 = (CK'_i + PPID_i) + (N_2 \cdot P_1). \quad (15)$$

Also, it sends it to the device as follows:

$$S \longrightarrow D_i: P_3, P_4. \quad (16)$$

- (iv) Device verifies  $P_4 \stackrel{?}{=} (PPID_i \cdot CK'_i) + (N_1 \cdot P_2)$ . If the evaluation is false, then the process stops, and if true, then the device is authenticated. The device computes  $V_i$  as in the following equation and sends it to the server:

$$V_i = PPID_i \cdot P_3, \quad (17)$$

$$D_i \longrightarrow S: V_i. \quad (18)$$

- (v) The server receives  $V_i$  and verifies  $V_i \neq N_2 \cdot PPID_i$ . If the evaluation is false, then the process stops, and if true, then the device is authenticated.
- (vi) The server computes its session key:  $SK = N_2 \cdot P_1$ , and the device computes its session key:  $SK = N_1 \cdot P_3$ , such that  $SK = N_1, N_2, G$ .

The schematics of the Rostampour et al. scheme are given in Figure 3.

**3.2. Formal Validation of Rostampour Et Al.'s Scheme Using Scyther under the eCK Adversary Model.** The SPDL model of the Rostampour et al. protocol is shown in Figure 4. The SPDL modeling comprises two roles: role I and role R. role I models the communication of the  $D_i$ , and role R models the  $S$ .  $D_i$  sends  $P_1, P_2, PPID_i$  to the  $S$  using  $send\_1()$ . The  $S$  receives the  $P_1, P_2, PPID_i$  using  $recv\_1()$  function.  $S$  sends  $P_3, P_4$  to the  $D_i$  using  $send\_2()$ . The  $D_i$  receives the  $P_3, P_4$  using  $recv\_2()$  function. Finally,  $D_i$  sends  $V_i$  to the  $S$  using  $send\_3()$ . The  $S$  receives the  $V_i$  using  $recv\_3()$  function. The  $claim\_i1$  in role I and  $claim\_r1$  in role I and R indicates that the  $N_1, N_2$  must remain secret during the communication. The  $claim\_i2$  and  $claim\_r2$  in roles I and R indicate that  $SK = N_1, N_2, G$  can be revealed using the session key adversary rule.  $claim\_r3, claim\_r4, claim\_r3,$  and  $claim\_r4$  are to verify whether the authentication in terms of Nisynch and Niagree is maintained.

The SPDL model has been initially executed under Dolev and Yoa setting as shown in Figure 5. The Scyther-Compromise verification results of the Rostampour et al. scheme under the Dolev and Yoa setting indicate that the scheme is safe and does not have any attacks. Subsequently, the model was executed under the eCK adversary setting shown in Figure 6. The Scyther verification results under eCK are shown in Figure 7.

The results indicate that the scheme is not safe. The attack trace is shown in Figure 8. The attack trace indicates that the Rostampour et al. scheme under the eCK adversary model is not resilient to session key reveal attack; thus, the adversary can reveal the session key. This is primarily due to the design issue in the Rostampour et al. scheme for computing the session key. In the Rostampour et al. scheme, the session key is computed as  $SK = N_1 \cdot N_2 \cdot G$ . The session key (SK) depends only on short-term session secrets  $N_1$  and  $N_2$ . SK must also be dependent on long-term term secrets so that the reveal of short-term secrets does not reveal session key.

## 4. Proposed Scheme

The proposed scheme comprises two phases that include

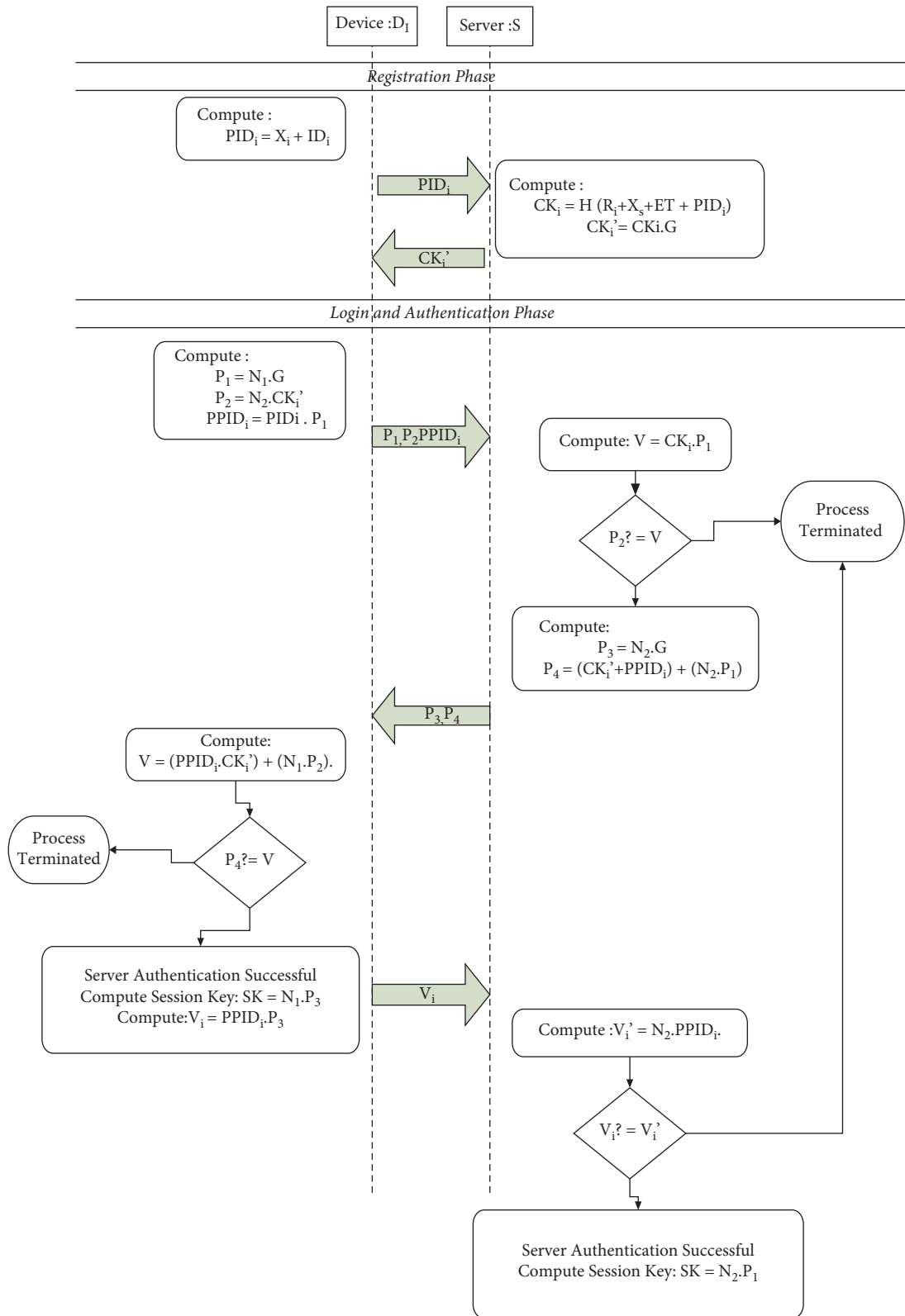


FIGURE 3: Schematics of the Rostampour et al. scheme.

Protocol description	Settings
1	hashfunction MUL;
2	hashfunction ADD;
3	Const G: Nonce;
4	secret PIDI,CKI-PRIME;
5	secret N1,N2;
6	macro P1=MUL (N1,G);
7	macro P2=MUL (N1,CKI-PRIME);
8	macro PPDI=MUL (PIDI,P1);
9	macro P3=MUL (N2,G);
10	macro P4=ADD (MUL (PPDI,CKI),MUL (N2,P1));
11	macro VI=MUL (PIDI,P3);
12	
13	protocol improved (I,R)
14	{
15	role I
16	{
17	var Message1:Nonce;
18	secret PIDI,CKI,CKI-PRIME;
19	send_1 (I,R, PPDI,P1,P2);
20	recv_2 (R,I,P3,P4);
21	send_3 (I,R, VI);
22	recv_4 (R,I, {Message} MUL (N1,N2,G));
23	Claim_i1 (I,Secret, N1);
24	Claim_i2 (I, SKR, MUL (N1,N2,G));
25	Claim_i3 (I,Niagree);
26	claim_i4 (I,Nisynch);
27	}
28	
29	role R
30	{
31	fresh Message1:Nonce;
32	secret PIDI,CKI,CKI-PRIME;
33	recv_1 (I,R, PPDI,P1,P2);
34	send_2 (R,I,P3,P4);
35	recv_3 (I,R, VI);
36	send_4 (R,I, {Message} MUL (N1,N2,G));
37	Claim_r1 (R,Secret,N2);
38	Claim_r2 (R, SKR, MUL (N1,N2,G));
39	Claim_r3 (R,Niagree);
40	Claim_r4 (R,Nisynch);
41	}
42	}

FIGURE 4: SPDL model of the Rostampour et al. Scheme.

Protocol description	Settings
<b>Verification parameters</b>	
Maximum number of runs (0 disables bound)	0
Matching type	typed matching
<b>Adversary compromise model</b>	
Long-term Key Reveal	<input checked="" type="checkbox"/> Others (DY)
Long-term Key Reveal	<input checked="" type="checkbox"/> Actor (KCI)
Long-term Key Reveal after claim	<input type="radio"/> None (DY) <input checked="" type="radio"/> aftercorrect (wPFS) <input type="radio"/> after (PFS)
Session-Key Reveal	<input checked="" type="checkbox"/>
Random Reveal	<input checked="" type="checkbox"/>
State Reveal	<input checked="" type="checkbox"/>
Automatically infer local state	<input checked="" type="checkbox"/>
<b>Advanced parameters</b>	
Search pruning	Find best attack
Maximum number of patterns per claim	10
Additional backend parameters	

FIGURE 5: Scyther settings for Dolev and Yoa adversary models.



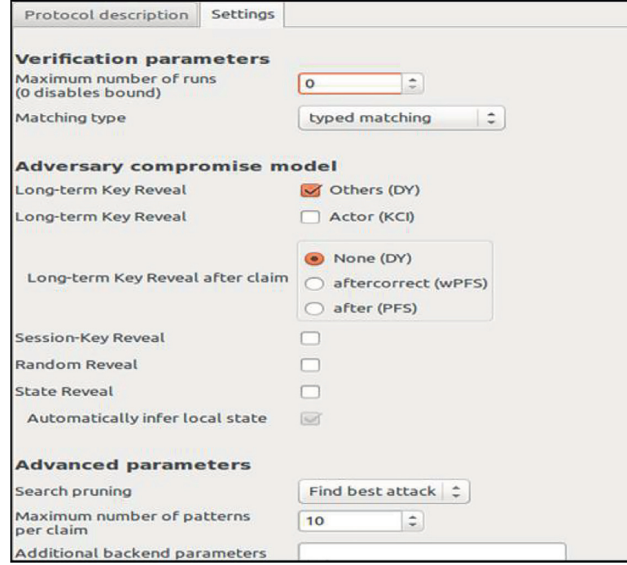


FIGURE 6: Scyther settings for the eCK adversary model.

Claim	Status	Comments	Patterns
improved I improved_i1 Secret N1	Ok	No attacks within bounds.	
improved_i2 SKR MUL(N1,N2,G)	Fail	Falsified At least 1 attack.	1 attack
improved_i3 Niagree	Fail	Falsified At least 1 attack.	1 attack
improved_i4 Nisynch	Fail	Falsified At least 1 attack.	1 attack
R improved_r1 Secret N2	Ok	No attacks within bounds.	
improved_r2 SKR MUL(N1,N2,G)	Ok	No attacks within bounds.	
improved_r3 Niagree	Ok	No attacks within bounds.	
improved_r4 Nisynch	Ok	No attacks within bounds.	

FIGURE 7: Scyther verification results of the Rostampour et al. scheme under the eCK model.

- (1) Registration phase
- (2) Login and authentication phase

**4.1. Registration Phase.** The registration phase includes the registration of an IoT device with the server. As with other schemes, the registration is performed on a secure channel [11]. The need for a secure channel for registration is highlighted as there is no preshared secret in the IoT device or any trusted third party is employed. The steps taken between the device and the server during the registration are listed as below:

- (i) Device  $D_i$  chooses its private key  $K_i$  and its identity  $ID_i$ .
- (ii) The device calculates  $PID_i$  as in (19) and sends  $PID_i$  it to the server:

$$PID_i = K_i \cdot ID_i \cdot G, \quad (19)$$

$$D_i \longrightarrow S: PID_i.$$

- (iii) The server calculates the hash of  $PID_i$  and splits its private key  $X_S$  into two unequal halves  $X_S^1, X_S^2$  such that  $X_S^1 \neq X_S^2$ . The server further computes (20) and (21):

$$CK_i^1 = PID_i \cdot X_S^1, \quad (20)$$

$$CK_i^2 = PID_i \cdot X_S^2. \quad (21)$$

The server stores  $PID_i, CK_i^1, CK_i^2$  and sends  $CK_i^1, CK_i^2$  to the device as follows:

$$S \longrightarrow D_i: CK_i^1, CK_i^2. \quad (22)$$

- (v) The device receives and stores the parameters  $CK_i^1, CK_i^2$  along with  $PID_i$  in its memory.

**4.2. Login and Authentication Phase.** During this phase, the device initiates to log in to the server. Subsequently, the server authenticates the device, and if the device is authenticated, a session key is subsequently established between the device and the server. The steps undertaken between the device and the server during the login and authentication phase is shown as below:

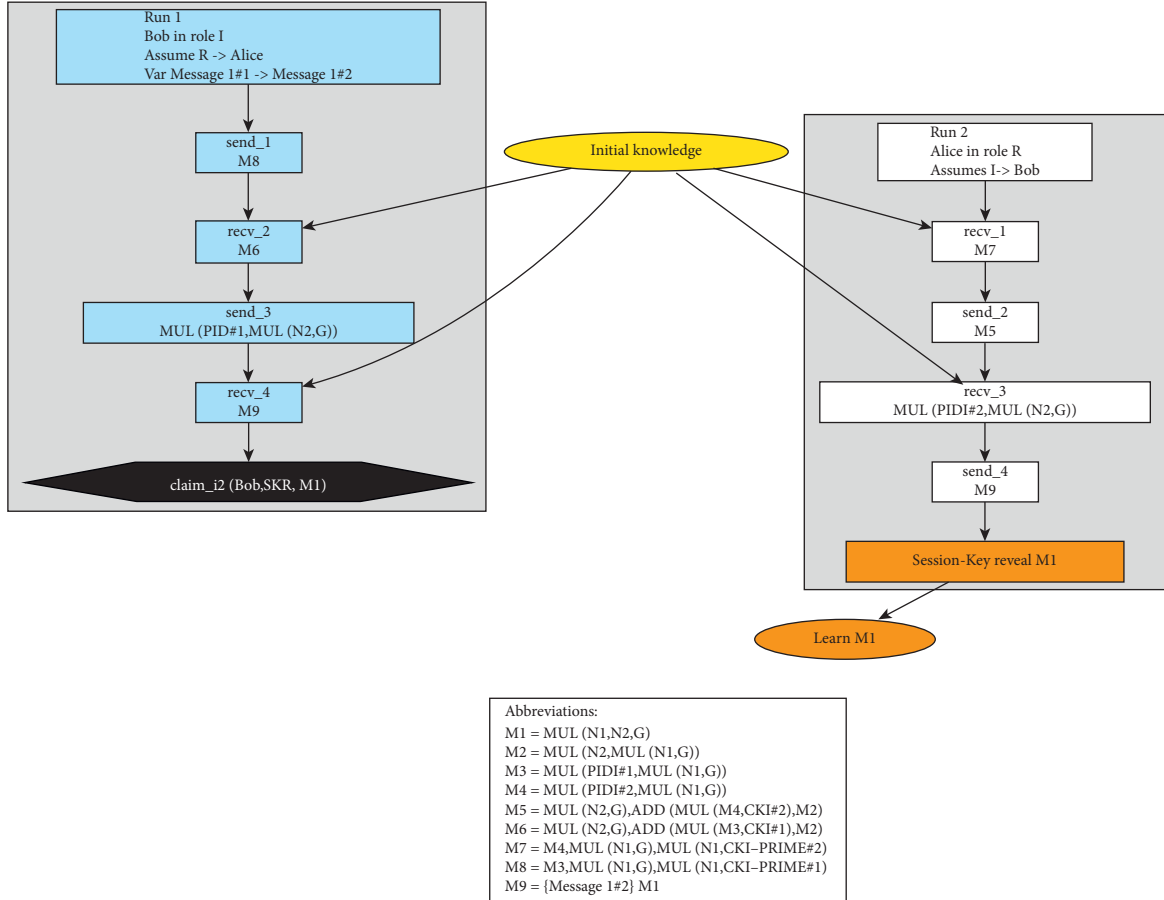
- (i) Device  $D_i$  chooses its ephemeral secret  $S_i$  and calculates  $P_1$  and  $P_2$  as (23) and (24):

$$P_1 = (CK_i^1 + CK_i^2) \cdot S_i \cdot H(PID_i), \quad (23)$$

$$P_2 = (CK_i^1 + CK_i^2) \cdot S_i. \quad (24)$$

The device sends  $P_1$  and  $P_2$  to the server as follows:

$$D_i \longrightarrow S: P_1, P_2. \quad (25)$$



Scyther pattern graph for the improved protocol, claim improved, i2 in role I

FIGURE 8: Attack trace under the eCK model for Rostampour et al.' scheme.

(ii) The server receives  $P_1, P_2$  from  $D_i$  and authenticates  $D_i$  as follows:

- The server finds the corresponding entry of  $D_i$  and calculates  $H(PID_i)$  from  $PID_i$  of the device stored in the database.
- The server calculates the multiplicative inverse of  $H(PID_i)$  as  $[H(PID_i)]^{-1}$  and computes  $P'_1$  as  $P'_1 = P_1 \cdot [H(PID_i)]^{-1}$ .
- The server compares  $P'_1 \neq P_2$ . If true, then Step 3 is performed; else, login request from  $D_i$  is rejected.

(iii) The server chooses its ephemeral secret  $S_s$  and calculates  $P_3$  and  $P_4$  as (26) and (27):

$$P_3 = P_1 \cdot S_s, \quad (26)$$

$$P_4 = (CK_i^1 + CK_i^2) \cdot S_s. \quad (27)$$

(iv) The server computes its session key ( $SK$ ) with  $D_i$  as follows:

$$SK = P_2 \cdot S_s, \quad (28)$$

$$\begin{aligned} SK &= (CK_i^1 + CK_i^2) S_i \cdot S_s, \\ SK &= (PID_i \cdot X_s^1 + PID_i \cdot X_s^2) S_i \cdot S_s, \\ SK &= (X_s^1 + X_s^2) \cdot PID_i \cdot S_i \cdot S_s, \\ SK &= X_s \cdot K_i \cdot ID_i \cdot G \cdot S_i \cdot S_s. \end{aligned} \quad (29)$$

(v) Server sends  $P_3, P_4$  to the device as follows:

$$S \longrightarrow D_i : P_3, P_4. \quad (30)$$

(vi) The device receives  $P_3, P_4$  from the server and authenticates it as follows:

- The device calculates the multiplicative inverse of  $H(PID_i)$  as  $[H(PID_i)]^{-1}$  and computes  $P'_3$  as  $P'_3 = P_3 \cdot [H(PID_i)]^{-1} \cdot S_i^{-1}$ .
- The device compares  $P'_3 \neq P_4$ . If true, then  $S$  is authenticated; else, login response from  $S$  is rejected.

- (vii) The device computes its session key with  $S$  as follows:

$$SK = P_4.S_i, \quad (31)$$

$$\begin{aligned} SK &= (CK_i^1 + CK_i^2)S_s.S_i, \\ SK &= (PID_i.X_S^1 + PID_i.X_S^2)S_s.S_i, \\ SK &= (X_S^1 + X_S^2).PID_i.S_i.S_s, \\ SK &= X_S.K_i.ID_i.G.S_i.S_s. \end{aligned} \quad (32)$$

- (viii) The device encrypts  $E_{SK}[H(SK)]$  and sends it to the server as follows:

$$D_i \longrightarrow S: E_{SK}[H(SK)]. \quad (33)$$

- (ix) The server decrypts  $E_{SK}[H(SK)]$  as  $V = D_{SK}[E_{SK}[SK]]$  and verifies that whether  $V \neq H[SK]$ . If true, then the login request is approved, and the device is authenticated.

The schematics of the proposed scheme are given in Figure 9.

## 5. Security Analysis

**5.1. Replay Attack.** In a replay attack, an adversary stores the messages exchanged between the communicating parties and retransmits them in the future to gain illegitimate access. In the proposed protocol, three messages are exchanged between the device and the server:

$$\begin{aligned} D_i &\longrightarrow S: P_1, P_2, \\ S &\longrightarrow D_i: P_3, P_4, \\ D_i &\longrightarrow S: E_{SK}[H(SK)]. \end{aligned} \quad (34)$$

Let us assume during the initiation of the login and authentication phase, an adversary can eavesdrop on the messages and stores  $(P_1, P_2, P_3, P_4)$  and  $E_{SK}[H(SK)]$  for a replay attack. Let an adversary (A) replay stored  $(P_1, P_2)$  of the previous session to gain illegitimate access as follows:

$$A \longrightarrow S: P_1, P_2. \quad (35)$$

When the server receives  $(P_1, P_2)$ , it validates the request and generates  $(P_3, P_4)$  with a new ephemeral random secret. The adversary receives  $(P_3, P_4)$  a new ephemeral secret. To validate  $(P_3, P_4)$  and subsequently generate a session key SK, the adversary needs to know  $PID_i$  and the ephemeral random secret previously used for computing  $(P_1, P_2)$ . The adversary does not have access to either due to the exponential time complexity of ECDLP [30–32]. As the adversary cannot generate a legitimate session key SK of the current session,  $E_{SK}[H(SK)]$  cannot be computed by the adversary. Moreover, if the adversary replays the old  $E_{SK}[H(SK)]$ , the server will not authenticate it as the current SK is based on the fresh ephemeral random secret of the server. Thus, the design of the scheme thwarts replay attacks.

**5.2. Impersonation Attack.** In an impersonation attack, an adversary tries to impersonate a legitimate device. The login and authentication phase starts by computing  $(P_1, P_2)$ . For computing  $(P_1, P_2)$ , an adversary must have access and knowledge of  $(CK_i^1, CK_i^2)$  and  $H(PID_i)$ . The  $(CK_i^1, CK_i^2)$  and  $H(PID_i)$  are shared between the device and the server over a secure channel. Moreover, even if the adversary eavesdrop on  $(P_1, P_2)$  of any previous login and authentication session between the device and the server, the  $(CK_i^1, CK_i^2)$  and  $H(PID_i)$  cannot be extracted from  $(P_1, P_2)$  due to the computational difficulty of ECDLP. Thus, without the knowledge of  $(CK_i^1, CK_i^2)$  and  $H(PID_i)$ , a valid  $(P_1, P_2)$  cannot be computed as such an adversary cannot impersonate any legitimate device by computing a malicious  $(P_1, P_2)$ .

**5.3. Traceability Attack.** In a traceability attack, the message with constant values may reveal the context of communication or the communication pattern. To avoid traceability attacks, messages exchanges must be randomized by incorporating pseudorandom numbers. In the proposed protocol, the ephemeral random secrets  $(S_i, S_s)$  induce the required randomness in the messages for each login session. Thus, the traceability attack is mitigated in the proposed scheme.

**5.4. Message Integrity Attack.** The message exchanged between the device and the server cannot be masqueraded. During the communication, the following messages are exchanged between the device and the server:  $P_1, P_2, P_3, P_4$  and  $E_{SK}[H(SK)]$ . Let us say an adversary intercepts the  $P_1, P_2, P_3, P_4$  and  $E_{SK}[H(SK)]$  and wants to create malicious:  $P_1^S, P_2^S, P_3^S, P_4^S$ . However, to create  $P_1^S, P_2^S, P_3^S, P_4^S$ , the adversary must have access to  $X_S$  and  $K_i$ . The adversary does not have access to  $X_S$  and  $K_i$ . Moreover, extraction of the private key of  $X_S$  from  $P_1, P_2, P_3, P_4$  is having exponential time complexity due to the computational complexity of ECDLP. Thus, the integrity of  $P_1, P_2, P_3, P_4$  is upheld by the computational infeasibility of ECDLP. Moreover, the message  $E_{SK}[H(SK)]$  can also not be altered as it is protected by a symmetric encryption technique and one-way hash.

**5.5. Man-in-the-Middle Attack.** In a man-in-the-middle attack, an attacker can eavesdrop, disguise, and change communication in the middle by forging the key established between the device and the server. An adversary would be successful in executing the man in the middle attack if the adversary in the middle of the communication can create malicious:  $P_1^S, P_2^S, P_3^S, P_4^S$ . However, to create malicious  $P_1^S, P_2^S, P_3^S, P_4^S$ , the adversary must be able to forge  $(CK_i^1, CK_i^2)$  as follows:

$$\begin{aligned} CK_i^1 &= PID_i.X_S^1, \\ CK_i^2 &= PID_i.X_S^2. \end{aligned} \quad (36)$$

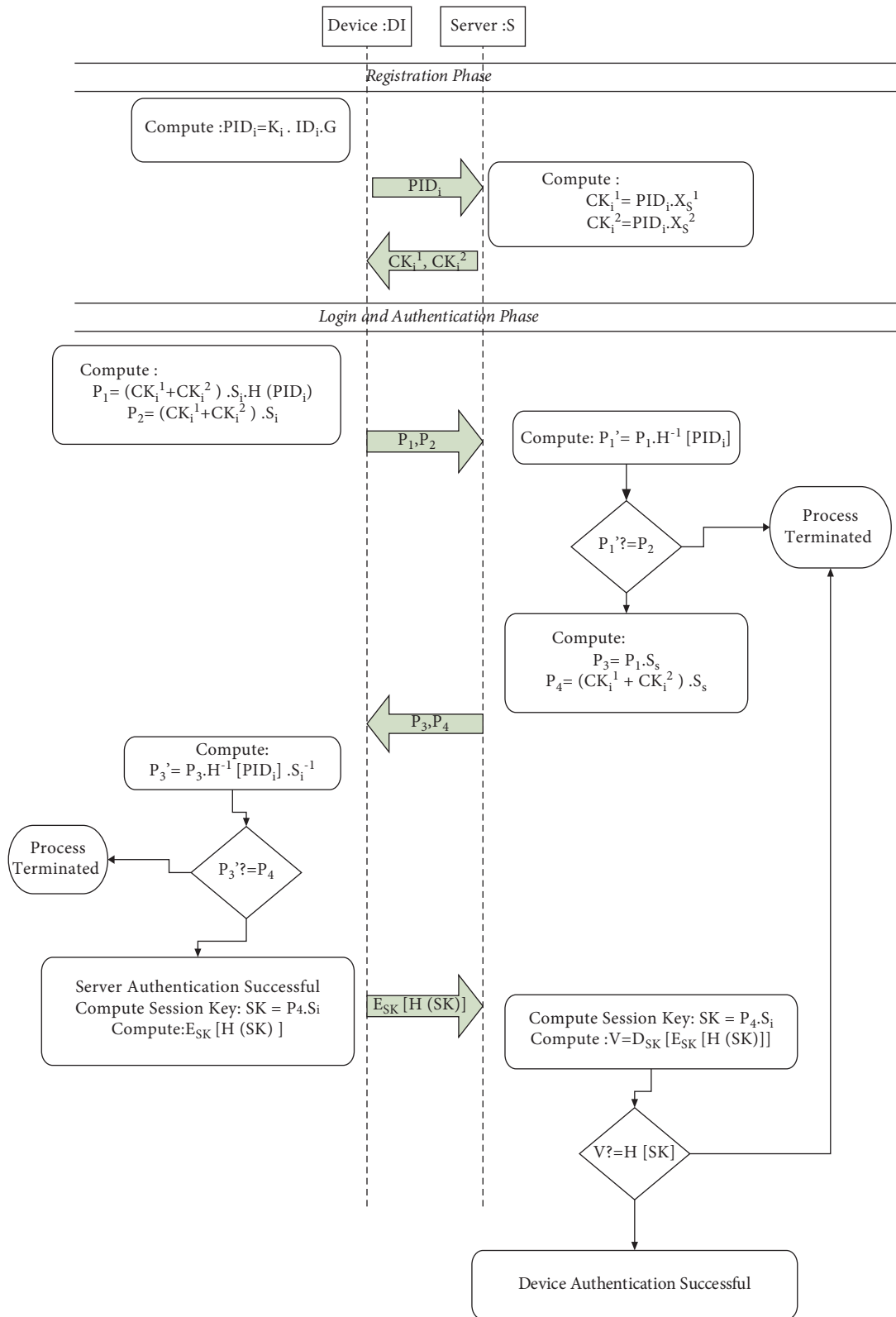


FIGURE 9: Schematics of the proposed scheme.

To forge  $(CK_i^1, CK_i^2)$ , adversary must have access to  $X_S$ . The adversary does not have access to  $X_S$ . Moreover, from  $P_1, P_2, P_3, P_4, X_S$  cannot be extracted due to the exponential complexity of ECDLP. As the adversary cannot forge  $P_1, P_2, P_3, P_4$  and proper authentication is employed prior to the key establishment, the man-in-the-middle attack is mitigated in the proposed scheme.

## 6. Formal Validation of the Proposed Protocol Using Scyther

The designed protocol has been modeled using SPDL to validate its security on Scyther-Compromise under the eCK adversary model. The SPDL model of the proposed protocol is shown in Figure 10. The role Device and role Server model the communication pattern of the  $D_i$  and  $S$ , respectively. The role Device initiates the login and authentication phase by sending  $(P_1, P_2)$  using the send\_1 function. On receiving  $(P_1, P_2)$  using the recv1 function, the role server sends  $(P_3, P_4)$  using send\_2 functions to the device. Finally, the device sends  $E_{SK}[H(SK)]$  to the server using the send\_3 function. The claim\_i1 in role Device and claim\_r1 in role Server indicate that the  $X_S$  and  $K_i$  must remain secret during the communication. The claim\_i2 in role Device and claim\_r2 in role Server indicate whether  $SK = X_S.K_i.ID_i.G.S_i.S_s$  can be revealed using the session key adversary rule. claim\_r3, claim\_r4, claim\_r3, and claim\_r4 is to verify whether the authentication in terms of Nisynch and Niagree is maintained.

The SPDL model of the designed protocol was simulated on the compromise 0.9 under the eCK adversary model as indicated in Figure 6. The verification results are shown in Figure 11. From Figure 11, we can infer that the protocol is safe and does not have any attack under the stringent eCK adversary model.

## 7. Formal Security Analysis Using BAN Logic

Burrows et al. proposed BAN logic to validate the soundness and correctness of a security protocol. This section employs BAN logic to determine the security validity of the proposed scheme.  $D$  and  $S$  denote the communicating principles, where  $K_I$  and  $X_S$  denote their private keys, respectively. The BAN notations are tabulated in Table 2 [31], and the BAN postulates are given in Table 3. Besides that, as derived in [33], synthesis rules are tabulated in Table 4.

### 7.1. Assumptions

- (A1)  $D| \equiv \longrightarrow CK_i^1, CK_i^2 S$
- (A2)  $S| \equiv \longrightarrow CK_i^1, CK_i^2 D$
- A3)  $D| \equiv \#(S_I)$
- (A2)  $S| \equiv \#(S_S)$
- A5)  $S| \equiv D| \longrightarrow S_I$
- (A6)  $D| \equiv S| \longrightarrow S_S$

### 7.2. Idealized Form

- $D \longrightarrow S; \{P_1, P_2\}_{K_I} \text{ MSG1}$
- $S \longrightarrow D; \{P_3, P_4\}_{X_S} \text{ MSG2}$

### 7.3. Goals

- G1)  $S| \equiv D \longrightarrow^S K S$  G2)  $S| \equiv D| \equiv D \longrightarrow^S K S$
- G3)  $D| \equiv D \longrightarrow^S K S$  G4)  $D| \equiv S| \equiv D \longrightarrow^S K S$

### 7.4. BAN Analysis. From (MSG1), we get that

- (1)  $D| \equiv \{P_1, P_2\}_{K_I}$
- (2)  $D \leftarrow \{P_1, P_2\}_{K_I}$   
From (2), (A1), and (R1), we get
- (3)  $D| \equiv S| \sim \{P_1, P_2\}_{K_I}$   
 $S_I$  is a part of  $P_1, P_2$ ; thus, as per (A3) and (R6), we get
- (4)  $D| \equiv \#(P_1, P_2)$   
From (3) and (5), we get
- (5)  $S| \equiv D| \sim P_1, P_2$   
From (7) and (S4), we get
- (6)  $S| \equiv \#(P_1, P_2)$   
From (3) and (6) on applying (R2), we get
- (7)  $S| \equiv D| \equiv P_1, P_2$   
 $S_I$  is the part of the  $P_1, P_2$ ; thus, on applying (R5), we get
- (8)  $S| \equiv D| \equiv S_I$   
Now as per (A5), (8), and (R3), we get
- (9)  $S| \equiv S_I$   
From (S3) and (3), we get
- (10)  $S| \equiv D| \sim S_I$   
From (A3) and (10), we get
- (11)  $S| \equiv D| \sim S_I$   
As per (R4) and (11), we get
- (12)  $S| \equiv \#(S_I)$   
 $S_I$  is a part of (SK); thus, as per (R6), we get
- (13)  $S| \equiv \#(SK)$   
From (13), (8), and (R7), we get
- (14)  $S| \equiv D \longrightarrow^S K S(\text{Goal G1})$   
Due to the symmetry of the protocol,
- (15)  $S| \equiv D| \equiv S \longrightarrow^S K D(\text{Goal G2})$   
From (MSG2), we infer that
- (16)  $S| \equiv \{P_3, P_4\}_{X_S}$
- (17)  $S \leftarrow \{P_3, P_4\}_{X_S}$   
From (17), (A2), (R1), we get
- (18)  $D| \equiv S| \sim \{P_3, P_4\}_{X_S}$   
 $S_s$  is a part of  $P_3, P_4$ ; thus, as per (A4) and (R6), we get
- (19)  $S| \equiv \#(P_3, P_4)$   
From (17) and (19), we get

Protocol description	Settings
1 hashfunction MUL;	
2 hashfunction H;	
3 hashfunction ADD;	
4 const G: Nonce;	
5 const KI,KS,KS1,KS2,SI,SS;	
6 secret N1,N2;	
7 macro PID=MUL (KI,Device,G);	
8 macro CK1=MUL (PID,KS1);	
9 macro CK2=MUL (PID,KS2);	
10 macro P1=MUL (ADD(CK1,CK2),SI,H (PID));	
11 macro P2=MUL (ADD(CK1,CK2),SI);	
12 macro P3=MUL (ADD(CK1,CK2),SS,H (PID));	
13 macro P4=MUL (ADD(CK1,CK2),SI);	
14	
15	
16 protocol improved(Devisе,Server)	
17 {	
18     role Device	
19     {	
20         freshSI,msg:Nonce;	
21         var SS: Nonce;	
22         secret KI,KS,KS1,KS2,SI,SS;	
23	
24         send_1 (Device,Server,P1,P2);	
25         recv_2 (Server ,Device,P3,P4);	
26         send_3 (Device,Server, {msg} msgMUL (KI,KS,SI,SS,Device,G));	
27	
28         claim_i1 (Device,Secret,SI);	
29         claim_i2 (Device,SKR,MUL(KI,KS,SI,SS,Device,G));	
30         claim_i3 (Device,Niagree);	
31         claim_i4 (Device,Nisynch);	
32     }	
33	
34     role Server	
35     {	
36         fresh SS: Nonce;	
37         var SI,msg: Nonce;	
38         fresh Message 1:Nonce;	
39         secret KI,KS,KS1,KS2,SI,SS;	
40	
41         recv_1 (Device,Server,P1,P2);	
42         send_2 (Server,Device,P3,P4);	
43         recv_3 (Device,Server, {msg} MUL(KI,KS,SI,SS,Device,G));	
44	
45         claim_r1 (Server,Secret,SS);	
46         claim_r2 (Server,SKR,MUL (KI,KS,SI,SS,Device,G));	
47         claim_r3 (Server,Niagree);	
48         claim_r4 (Server,Nisynch);	
49	
50     }	
51 }	
52	

FIGURE 10: SPDL model of the proposed scheme.

Scyther results : verify					
Claim				Status	Comments
improved	Device	improved,i1	Secret SI	OK	No attacks within bounds.
		improved,i2	SKR MUL(KI,KS,SI,SS,Device,G)	OK	No attacks within bounds.
		improved,i3	Niagree	OK	No attacks within bounds.
		improved,i4	Nisynch	OK	No attacks within bounds.
Server	Server	improved,r1	Secret SS	OK	No attacks within bounds.
		improved,r2	SKR MUL(KI,KS,SI,SS,Device,G)	OK	No attacks within bounds.
		improved,r3	Niagree	OK	No attacks within bounds.
		improved,r4	Nisynch	OK	No attacks within bounds.

Done.

FIGURE 11: Scyther verification results for the proposed scheme.

TABLE 2: BAN symbols.

Notation	Description
$D  \equiv MSG$	$D$ believes $M$
$D \leftarrow MSG$	$D$ receives the message $M$
$D  \sim MSG$	$D$ sent the message $M$ in past
$D   \sim MSG$	$D$ sent the message to $M$ currently
$D  \longrightarrow F$	$D$ has jurisdiction over $V$
$\#(MSG)$	$M$ is fresh
$\longrightarrow^P r D$	$P_r$ is the public parameter calculated using the private key of $D$
$D \longrightarrow^S K S$	SK is the key between $D$ and $S$
$\{X\}_{SK}$	SK is the key used to encrypt $X$
$(F1/F2)$	If $F1$ is true, then $F2$ is true

TABLE 3: BAN postulates.

Rule no.	Name	Representation
R1	Message-meaning rule	$(D  \equiv \longrightarrow^P S, D \leftarrow \{MSG\}XS/D  \equiv S  \sim MSG)$
R2	Nonce verification rule	$(D  \equiv \#(MSG), D \equiv S  \sim MSG/D  \equiv S  \equiv MSG)$
R3	Jurisdiction rule	$(D  \longrightarrow MSG, D  \equiv S  \equiv MSG/D  \equiv MSG)$
R4	Seeing rule	$(D \leftarrow MSG1, D \leftarrow MSG2/D \leftarrow (MSG1, MSG2))$
R5	Belief rule	$(D  \equiv MSG1, D  \equiv MSG2/D  \equiv (MSG1, MSG2))$
R6	Freshness rule	$(D  \equiv \#(MSG1)/D  \equiv \#(MSG1, MSG2))$
R7	Session key rule	$(D  \equiv \#(SK), D  \equiv S  \equiv X/D  \equiv D \longrightarrow^S K S) X$ is part of SK

TABLE 4: Synthesis rules.

Rule no.	Synthesis rule
S1	$D \leftarrow MSG1 \ D \leftarrow (MSG1, MSG2)$
S2	$D  \equiv S  \sim MSG1 \ D  \equiv S  \sim (MSG1, MSG2)$
S3	$D  \equiv S  \sim (MSG1, MSG2) \ D  \equiv S  \sim MSG1$
S4	$D  \equiv S  \sim MSG1 \ D  \equiv \#(MSG1)$

$$(20) \ D| \equiv S| \sim P_3, P_4$$

From (20) and (S4), we get

$$(21) \ D| \equiv \#(P_3, P_4)$$

From (18) and (21) on applying (R2), we get

$$(22) \ D| \equiv S| \equiv P_3, P_4$$

$S_S$  is the part of the formulae  $P_3, P_4$ ; thus, on applying (R5), we get

$$(23) \ D| \equiv S| \equiv S_S$$

Now, as per (A6) and (23) and (R3), we get

$$(24) \ D| \equiv S_S$$

From (SR3) and (18), we get

$$(25) \ D| \equiv S| \sim S_S$$

From (A4) and (25), we get

$$(26) \ D| \equiv S| \sim S_S$$

As per (R4) and (26), we get

$$(27) \ D| \equiv \#(S_S)$$

From (R6), we get

$$(28) \ D| \equiv \#(SK)$$

From (28) and (22) and on applying (R7), we get

$$(29) \ D| \equiv D \longrightarrow^S K S(\text{Goal } G3)$$

Due to the symmetry of the protocol,

$$(30) \ S| \equiv D| \equiv D \longrightarrow^S K S(\text{Goal } G4)$$

## 8. Comparison with Other Schemes

**8.1. Security Comparison.** The security comparison of the proposed scheme with relevant existing schemes is shown in Table 5. Kalra and Sood [14] do not support any security resistance. Chang et al. [15] are not resilient to traceability and impersonation attack. Kumari et al. [16] support only AK3 and AK4 features. Among the existing schemes, Rostampour et al.'s [11] scheme is the only scheme that supports AK1–AK5. However, from Table 5, we can infer that Kalra and Sood [14], Chang et al. [15], Kumari et al. [16], Wang et al. [17], and Rostampour et al. [11] have not been evaluated under the eCK adversary model. The formal validation of Rostampour et al. [11] under eCK adversary indicates that the scheme is not safe under the eCK model. The proposed scheme supports all the security requirements from AK1 to AK5 and is also safe under the eCK model.

**8.2. Computation and Communication Overhead.** The comparison in terms of computational and communication overhead is shown in Table 6. The time complexities of various critical operations considered include  $T_{ECM}$ : scalar multiplication,  $T_{EADD}$ : point addition,  $T_{HASH}$ : one-way hash,  $T_{SENC}/T_{SDEC}$ : symmetric encryption, and  $T_{inv}$ : multiplicative inverse.  $T_{ECM}$  is the most computationally intense operation. As IoT devices are resource constraints in nature, the computational overhead on these devices plays an important role in determining the efficiency of the scheme as the server is considered computationally more powerful. From Table 6, we can infer that a computational overhead of 4  $T_{ECM}$  for the IoT device and 8  $T_{ECM}$  in total is required in the proposed scheme. The highest device overhead is that of the

TABLE 5: Security comparison.

Scheme	AK1	AK2	AK3	AK4	AK5	eCK
Kalra and Sood [14]	✗	✗	✗	✗	✗	✗
Chang et al. [15]	✗	✗	✓	✓	✓	✗
Kumari et al. [16]	✗	✗	✓	✓	✗	✗
Wang et al. [17]	✗	✓	✓	✓	✗	✗
Rostampour et al. [11]	✓	✓	✓	✓	✓	✗
Proposed scheme	✓	✓	✓	✓	✓	✓

AK1: traceability attack; AK2: impersonation attack; AK3: replay attack; AK4: message integrity attack; and AK5: man-in-the-middle attack.

TABLE 6: Comparison of computational and communication overhead.

Scheme	Computation overhead			Communication overhead
	Device	Server	Total	
Kalra and sood [14]	$3 T_{ECM} + 4 T_{HASH}$	$4 T_{ECM} + 5 T_{HASH}$	$8 T_{ECM} + 9 T_{HASH}$	1,760
Chang et al. [15]	$4 T_{ECM} + 4 T_{HASH}$	$4 T_{ECM} + 4 T_{HASH}$	$8 T_{ECM} + 8 T_{HASH}$	1,632
Kumari et al. [16]	$4 T_{ECM} + 3 T_{HASH}$	$4 T_{ECM} + 4 T_{HASH}$	$8 T_{ECM} + 7 T_{HASH}$	1,760
Wang et al. [17]	$4 T_{ECM} + 5 T_{HASH}$	$4 T_{ECM} + 3 T_{HASH}$	$8 T_{ECM} + 8 T_{HASH}$	1,632
Rostampour et al. [11]	$7 T_{ECM} + T_{EADD}$	$6 T_{ECM} + T_{EADD}$	$13 T_{ECM} + 2 T_{EADD}$	1,920
Proposed scheme	$T_{ECM} + T_{EADD} + 2 T_{HASH} + T_{SENC}/T_{SDEC} + T_{inv}$	$4 T_{ECM} + T_{EADD} + 2 T_{HASH} + T_{SENC}/T_{SDEC} + T_{inv}$	$8 T_{ECM} + 2 T_{EADD} + 4 T_{HASH} + 2 T_{SENC}/T_{SDEC} + 2 T_{inv}$	1,408

TABLE 7: Time consumed for critical operations [34].

Operation	Seconds
$T_{ECM}$	2.82
$T_{SENC}/T_{SDEC}$	0.000029
$T_{HASH}$	0.0091
$T_{inv}$	0.14
$T_{EADD}$	0.16

Rostampour et al. scheme with  $7 T_{ECM}$  and the lowest is that of Kalra and Sood [14]. However, from Table 5, we can infer that none of the security specifications are supported by Kalra and Sood [14]. In terms of scalar multiplication ( $T_{ECM}$ ) overhead, the proposed scheme is required the same no of scalar multiplication as compared to other schemes considered for comparison. The communication cost is estimated based on the number of bits transmitted. We consider an elliptical curve  $E(a,b)$  of 160 bit. The size of an ECC point  $P(x,y)$  on the 160 bit curve is 320 bits ( $X[160], Y[160]$ ). The symmetric encryption considered generates a ciphertext of 128 bit. In the proposed scheme, 03 messages are exchanged that include  $(P_1, P_2)$ ,  $(P_3, P_4)$ , and  $E_{SK}[H(SK)]$ . The 03 messages requires  $[(320 + 320), (320 + 320) + 128] = 1,408$  bits.

**8.3. Energy Overhead.** To compare estimated energy consumed on an IoT device, the time consumed by various critical operations as indicated in [34] on a MicaZ mote [35] is shown in Table 7. The energy is consumed using  $E = V * I * T$ , where  $V$  is the voltage,  $I$  is the current drawn, and  $T$  is the time taken for the operation. For a MicaZ mote,  $V = 3 V$  and  $I = 8 mA$ . The proposed scheme has an energy

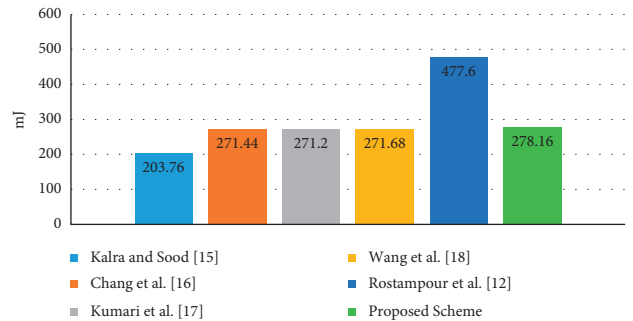


FIGURE 12: Energy overhead comparison.

overhead of 278.16 mJ for the IoT device. The comparison of the energy analysis of the proposed scheme with the relevant existing scheme is shown in Figure 12. The highest energy overhead is that of the Rostampour et al. scheme with 477.6 mJ. Rostampour et al. is not secure under the eCK adversary model. Though Kalra and Sood [12] have the lowest energy overhead for the IoT device, it has a high communication overhead and suffers from various security limitations that include AK1, AK2, AK3, AK4, and AK5. Kalra and Sood [12] have not been evaluated under the eCK model. Chang et al. [15], Kumari et al. [16], and Wang et al. [17] have the energy overheads of 271.44 mJ, 271.2 mJ, and 271.68 mJ, respectively. However, Chang et al. [15], Kumari et al. [16], and Wang et al. [17] do not suffice to all security requirements and have not been modeled under the eCK model. The designed scheme supports all the security specifications and is the only scheme that is formally validated under the eCK adversary model. Thus, with the computational requirement of 278.16 mJ and



communication overhead of 1,408 bits, the proposed scheme supports all the security requirements and is also safe under eCK adversary.

## 9. Conclusion

Authentication between IoT devices in the perception layer and the cloud server is critical for developing secure IoT-based smart applications. The existing schemes presented for authenticated key agreements between IoT devices and the cloud services have not been validated using the eCK adversary model. Recently, Rostampour et al. presented a scheme for authenticated key agreement between IoT devices and the cloud server that is secure under the Dolev and Yao model. A formal security validation of Rostampour et al. has been carried out using Scyther-Compromise under the eCK model. The verification indicates that the scheme susceptible to session key disclosure attacks under the eCK model. A lightweight ECC-based authentication technique for IoT devices and the cloud server has been presented in this paper. The Scyther-Compromise simulation indicates that the proposed scheme is secure under the eCK model. BAN logic analysis and evaluation indicate that the design of the proposed scheme is sound and correct. The overhead analysis indicates that the proposed scheme requires 199.44 mJ and 512 bits less in terms of energy and communication overhead as compared to the scheme presented by Rostampour et al.

## Data Availability

The data used to support the findings of this study are included within the article.

## Conflicts of Interest

The authors declare no conflicts of interest.

## References

- [1] S. Saxena, S. Vyas, B. Kumar, and S. Gupta, "Survey on online electronic payments security," in *Proceedings of the 2019 Amity International Conference on Artificial Intelligence (AICAI)*, Dubai, UAE, February 2019.
- [2] V. Hassija, V. Chamola, V. Saxena, D. Jain, P. Goyal, and B. Sikdar, "A survey on IoT security: Application areas, security threats, and solution architectures," *IEEE Access*, vol. 7, pp. 82721–82743, 2019.
- [3] J. Bhola, S. Soni, and G. K. Cheema, "Recent trends for security applications in wireless sensor networks—a technical review," in *Proceedings of the 6th IEEE International Conference on Computing for Sustainable Global Development (INDIACom)*, pp. 707–712, New Delhi, India, March 2019.
- [4] "Global IoT Market to be Worth USD 1,463.19 Billion by 2027 at 24.9% CAGR; Demand for Real-time Insights to Spur Growth, says Fortune Business Insights," <https://www.globenewswire.com/newsrelease/2021/04/08/2206579/0/en/Global-IoT-Market-to-be-Worth-USD-1-463-19-Billion-by-2027-at-24-9-CAGR-Demand-for-Real-time-Insights-to-Spur-Growth-says-Fortune-Business-Insights.html>.
- [5] V. Hassija, V. Chamola, V. Saxena, D. Jain, P. Goyal, and B. Sikdar, "A survey on IoT security: application areas, security threats, and solution architectures," *IEEE Access*, vol. 7, pp. 82721–82743, 2019.
- [6] R. Porkodi and V. Bhuvaneshwari, "The Internet of Things (IoT) applications and communication enabling technology standards: an overview," in *Proceedings of the 2014 International Conference on Intelligent Computing Applications*, pp. 324–329, Coimbatore, Tamilnadu, March 2014.
- [7] M. R. Abdmeziem, D. Tandjaoui, and I. Romdhani, "Architecting the internet of things: state of the art," *Robots and Sensor Clouds*, vol. 3, pp. 55–75, 2015.
- [8] U. Iqbal and A. H. Mir, "Secure and scalable access control protocol for IoT environment," *Internet of Things*, vol. 12, Article ID 100291, 2020.
- [9] G. Rastogi and R. Sushil, "Cloud Computing Implementation: Key Issues and Solutions," in *Proceedings of the 2nd IEEE International Conference on Computing for Sustainable Global Development (INDIACom)*, pp. 320–324, New Delhi, India, March 2015.
- [10] G. P. Gupta, "Security issues and its countermeasures in examining the cloud-assisted IoT," *Advances in Wireless Technologies and Telecommunication*, vol. 5, pp. 91–115, 2018.
- [11] S. Rostampour, M. Saffkhani, Y. Bendavid, and N. Bagheri, "ECCbAP: a secure ECC-based authentication protocol for IoT edge devices," *Pervasive and Mobile Computing*, vol. 67, 2020.
- [12] Y.-P. Liao and C.-M. Hsiao, "A secure ECC-BASED RFID authentication SCHEME integrated with Id-verifier transfer protocol," *Ad Hoc Networks*, vol. 18, pp. 133–146, 2014.
- [13] P. Roel and J. Hermans, "Attack on liao and Hsiao's secure ECC-based RFID authentication scheme integrated with ID-verifier transfer protocol," *IACR Cryptology*, vol. 399, 2013.
- [14] S. Kalra and S. K. Sood, "Secure authentication scheme for IoT and cloud servers," *Pervasive and Mobile Computing*, vol. 24, pp. 210–223, 2015.
- [15] C.-C. Chang, H.-L. Wu, and C.-Y. Sun, "Notes on "Secure authentication scheme for IoT and cloud servers"," *Pervasive and Mobile Computing*, vol. 38, pp. 275–278, 2017.
- [16] S. Kumari, M. Karuppiyah, A. K. Das, X. Li, F. Wu, and N. Kumar, "A secure authentication scheme based on elliptic curve cryptography for IoT and cloud servers," *The Journal of Supercomputing*, vol. 74, no. 12, pp. 6428–6453, 2017.
- [17] K.-H. Wang, C.-M. Chen, W. Fang, and T.-Y. Wu, "A secure authentication scheme for Internet of Things," *Pervasive and Mobile Computing*, vol. 42, pp. 15–26, 2017.
- [18] N. Saqib and U. Iqbal, "Security in wireless sensor networks using ECC," *IEEE International Conference on Advances in Computer Applications (ICACA)*, pp. 270–274, 2016.
- [19] Z. Zhao, C. Hsu, L. Harn, Q. Yang, and L. Ke, "Lightweight privacy-preserving data sharing scheme for Internet of medical Things," *Wireless Communications and Mobile Computing*, vol. 2021, Article ID 8402138, 13 pages, 2021.
- [20] D. Dolev and A. Yao, "On the security of public-key protocols," in *Proceedings of the IEEE 22nd Annual Symposium on Foundations of Computer Science*, pp. 350–357, Nashville, TN, USA, October 1981.
- [21] D. Dolev and A. Yao, "On the security of public-key protocols," *IEEE Transactions on Information Theory*, vol. 29, no. 2, pp. 198–208, 1983.
- [22] R. Canetti and H. Krawczyk, "Analysis of key-exchange protocols and their use for building secure channels," *Lecture Notes in Computer Science*, vol. 2045, pp. 453–474, 2001.
- [23] W. Wen, L. Wang, and J. Pan, "Unified security model of authenticated key exchange with specific adversarial capabilities," *IET Information Security*, vol. 10, no. 1, pp. 8–17, 2016.

- [24] C. J. Cremers, “The scyther tool: verification, falsification, and analysis of security protocols,” *Computer Aided Verification*, vol. 5123, pp. 414–418, 2008.
- [25] M. Burrows, M. Abadi, and R. M. Needham, “A logic of authentication,” *Proceedings of the Royal Society of London. A. Mathematical and Physical Sciences*, vol. 426, pp. 233–271, 1989.
- [26] Z. Clement Chan, C. Chuah, and J. Alawatugoda, “Review on leakage resilient key exchange security model,” *International Journal of Communication Networks and Information Security (IJCNIS)*, vol. 11, no. 1, 2019.
- [27] N. Koblitz, “Elliptic curve cryptosystems,” *Mathematics of Computation*, vol. 48, no. 177, pp. 203–209, 1987.
- [28] V. S. Miller, “Use of elliptic curves in cryptography,” *Lecture Notes in Computer Science Advances in Cryptology*, vol. 1985, pp. 417–426, 1986.
- [29] D. Hankerson and A. Menezes, “Elliptic curve cryptography,” *Encyclopedia of Cryptography and Security*, vol. 397, 2011.
- [30] N. Gura, A. Patel, A. Wander, H. Eberle, and S. C. Shantz, “Comparing elliptic curve cryptography and RSA on 8-bit CPUs,” *Lecture Notes in Computer Science*, vol. 3156, pp. 119–132, 2004.
- [31] S. H. Islam and G. P. Biswas, “A pairing-free identity-based two-party authenticated key agreement protocol for secure and efficient communication,” *Journal of King Saud University - Computer and Information Sciences*, vol. 29, no. 1, pp. 63–73, 2017.
- [32] D. J. Malan, M. Welsh, and M. D. Smith, “Implementing public-key infrastructure for sensor networks,” *ACM Transactions on Sensor Networks*, vol. 4, no. 4, pp. 1–23, 2008.
- [33] L. Buttyan, S. Staamann, and U. Wilhelm, “A simple logic for authentication protocol design,” in *Proceedings of the 11th IEEE Computer Security Foundations Workshop*, pp. 153–162, Rockport, MA, USA, June 1998.
- [34] U. Iqbal and A. Hussain Mir, “Secure and practical access control mechanism for WSN with node privacy,” *Journal of King Saud University-Computer and Information Scnces*, 2020.
- [35] Mote Works, *Getting Started Guide*, Memsic, Inc., 2013.

## Research Article

# Multiuser Computing Offload Algorithm Based on Mobile Edge Computing in the Internet of Things Environment

Xiao Chu  and Ze Leng

Changchun University of Finances and Economics, Changchun, Jilin 130122, China

Correspondence should be addressed to Xiao Chu; [chuxiao1983@ccufe.edu.cn](mailto:chuxiao1983@ccufe.edu.cn)

Received 5 January 2022; Revised 29 January 2022; Accepted 31 January 2022; Published 3 March 2022

Academic Editor: Shalli Rani

Copyright © 2022 Xiao Chu and Ze Leng. This is an open access article distributed under the Creative Commons Attribution License, which permits unrestricted use, distribution, and reproduction in any medium, provided the original work is properly cited.

As traditional cloud computing is not efficient enough to support large-scale computational task execution in IoT environments, a task offloading and resource allocation algorithm for mobile edge computing (MEC) is proposed in this paper. First, a multiuser computation offloading model is constructed, including a communication model and computation offloading model, which is transformed into the minimization of users' time delay and energy consumption (i.e., total system overhead) in the MEC system. Then, the task offloading model is formulated into a Markov decision process, and an offloading strategy based on a deep Q network (DQN) is designed to dynamically make fine tunings on the offloading proportion of each user so as to realize a low-cost MEC system. The proposed algorithm is analyzed based on the constructed simulation platform. The simulation results show that when the number of user terminals is 40, the average delay of the proposed algorithm does not exceed 0.9 s, and the average energy consumption tends to 65 J, which is better than the comparison method. Therefore, the proposed algorithm has certain application prospects.

## 1. Introduction

Nowadays, more and more mobile devices are emerging in people's lives, leading to the explosion in the population of smart network edge devices [1]. Subsequently, the data and computation tasks are also growing exponentially. In the context of massive data and large-scale computation tasks, mobile devices are required to process large amounts of application data quickly, which lays a high demand on their computing capacity. Due to the mismatch between data volume and transmission channel, traditional cloud computing brings huge pressure and ultrahigh delays to the crowded network and cannot efficiently support the execution of large-scale computing tasks [2]. Mobile edge computing (MEC) provides cloud computing capacity for mobile devices at the edge of networks via wireless access, which solves the problem of limited computation and energy resources for mobile devices. MEC has become a new paradigm for providing powerful computing and storage capabilities for mobile devices [3, 4]. In order to further

ameliorate the quality of services for users and the increase of resource utilization efficiency in MEC, complex computation task offloading strategies and the allocation of communication resources need to be addressed [5].

In early work on computation offloading, most researches considered single-user scenarios, such as low complexity dynamic computation offloading algorithms based on Markov decision processes and Lyapunov optimization, trying to achieve the load-balancing optimization through offloading strategies [6, 7]. Reference [8] proposed a low complexity heuristic algorithm to achieve load balancing by using fractional programming with the optimization goal of minimizing the energy consumption of task offloading. However, the multiscenario and multidimensional optimization for computational resource allocation is yet to be improved. Reference [9] realizes task unloading and efficient channel resource allocation based on the differential evolution algorithm. This scheme can significantly reduce energy consumption while ensuring convergence. However, the performance is poor for multiobjective optimization of

complex tasks. On the new cloud edge computing network designed by Reference [10], a joint optimization strategy based on a binary custom fireworks algorithm is proposed, which can ensure the rationality of system computing resources and response time. But the high occupancy of computational resources and the resource utilization need to be improved. Reference [11] proposed a joint distributed algorithm considering transmission power and unloading strategy and established a queue model with a separate capacity between different windows to optimize queue delay. However, with the massive number of network devices accessing the network in the 5G era, single-user scenarios are no longer able to meet people's daily needs.

Recently, deep learning techniques have been widely studied with the development of artificial intelligence. Since deep learning can solve some limitations in reinforcement learning, it is integrated into reinforcement learning to open a new era of deep reinforcement learning [12]. Deep reinforcement learning incorporates deep neural networks to optimize the process of reinforcement learning, thus improving the learning speed and performance of reinforcement learning algorithms. Therefore, deep reinforcement learning is widely used in the practice of reinforcement learning [13]. Reference [14] proposed a distributed optimization method based on an alternating direction multiplier, which decomposes the optimization problem into  $N$  subproblems and maximizes the weighted sum calculation rate through the optimal allocation of system resources and task calculation time. However, this method is weakly adaptable to new environments. An offloading strategy based on metareinforcement learning was proposed in Reference [15]. Mobile applications are modeled as directed acyclic graphs and offloading strategies via neural networks, and the collaboration of first-order approximation and tailoring of agent goals is applied for effective training. Although the adaptability is enhanced, the processing time for the strategy still needs to be improved. Reference [16] constructs a task unloading model based on multiagent deep reinforcement learning and uses the MEC model to better realize computing task unloading and resource allocation. Wang et al. proposed a reinforcement learning-based computing offloading strategy [17]. Although the aforementioned deep learning algorithms can achieve better performance in MEC, the training process and initial conditions are very complex, which means they need to be further optimized in practical applications.

Based on the above analysis, to alleviate the network load and reduce the risk of network congestion in traditional cloud computing of IoT, MEC is introduced to formulate the multiuser computing offloading problem. A task offloading and resource allocation algorithm for MEC in an IoT environment is proposed. Since user's tasks and the computation tasks in the edge server may be time-varying, a deep Q network (DQN) based computation offloading strategy is proposed to achieve the minimum operation overhead of the system by dynamically fine-tuning the ratio of time delay and energy consumption, which improves the robustness of the proposed algorithm.

## 2. System Model and Optimization Objectives

*2.1. System Model.* In the MEC system, in order to better serve users and improve system task processing capacity, computing tasks can be offloaded to the MEC server for execution via the wireless channel according to practical situations [18]. As shown in Figure 1, the number of mobile users is  $n = \{1, 2, \dots, N\}$ . The MEC server is deployed in the system, which is connected to the base station of this cell. Namely, in the process of task offloading, the computation task of each user cannot be split but can only be offloaded. Meanwhile, the offloading strategy cannot be changed.

Supposing that the number of wireless transmission channels between users and the base station is  $m = \{1, 2, \dots, M\}$ , users can choose one of the multiple wireless channels to offload tasks. The offloading strategy of the user  $n$  can be denoted as  $a_n = \{0, 1, \dots, M\}$ . When  $a_n = 0$ , it indicates that the user selects local computing, and when  $a_n > 0$ , it indicates that the user selects to uninstall the MEC server for execution.

Assume that the computation-intensive task is  $T_n = \{d_n, c_n\}$ . Where  $d_n$  and  $c_n$  denote the input data size of the task in K bits and the CPU cycles required to process the input data, respectively.

*2.2. Communication Model.* The communication model of the system includes the selection and assignment of the channel. When a user is connected  $n$  to the server  $\Omega$ , let  $S_{n,\Omega}^a = 1$ , then the user  $n$  can offload tasks  $T_n$  to the server through the high-speed network. At this point, if a task needs to be offloaded, the server is required to allocate a certain amount of network bandwidth to the user, which is denoted as  $B_{n,i}$ . Since the offloading time for a task is very short, we assume that the bandwidth obtained by the task is not grabbed during the offloading. When the task is offloaded, the occupied bandwidth will be released and the total bandwidth provided by the server  $\Omega$  is  $B_\Omega$ . The server can choose different bandwidth allocation methods  $\beta_\Omega^C$ , such as fixed percentage allocation, fixed amount allocation, or allocation based on user payment criteria.

As the channel selection and allocation strategy are not the focus of this work, the previously proposed communication model is adopted and the bandwidth allocation method is given when several users share a channel that is nonpreemptible. Namely, the bandwidth allocated to a user cannot be released until the user's data have been transmitted [19, 20]. In addition, unlike the strategy that requires waiting for the completion of a communication cycle before releasing the bandwidth, the occupied bandwidth is released immediately after the transmission is completed in this paper. And it is shown in this paper that immediate bandwidth release helps to improve the bandwidth utilization of the system.

Based on the above analysis, it is known that the remaining bandwidth of the current server is  $B_\Omega^a$ , and the offloading decision in each round offers  $n$  number of users to offload their tasks, then the bandwidth obtained by each user in this offloading process can be written as

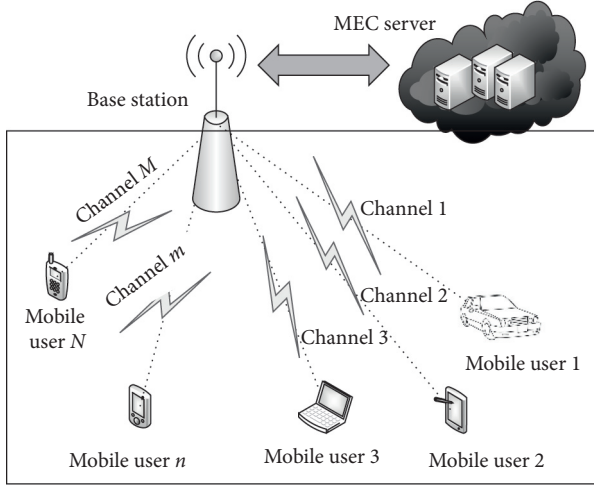


FIGURE 1: Multiuser MEC system model in single-cell.

$$B_{n,i} = \delta_0 \log_2 \left( 1 + \frac{p_n \times g_{n,\Omega}}{\delta_0 + \sum_{n \in N} (p_{m,n} \times g_{m,n,\Omega})} \right), \quad (1)$$

where  $\delta_0$  is the background noise,  $p$  represents the transmission power consumption, and  $g$  represents channel gain between the user equipment and the base station.

The model has the following features. If many users choose to offload tasks at the same moment, they will bring large interference among each other and reduce the transmission rate, which results in a challenge for the offloading algorithm when choosing the combination of offloading user devices. For a task with an uplink data volume of  $\widehat{d}_{n,i}$ , the relationship between the data volume and the transmission time can be calculated as

$$t_{n,i}^C = \frac{\widehat{d}_{n,i}}{B_{n,i}}. \quad (2)$$

Thus, the communication model  $C_\Omega$  of the server can be formulated as

$$C_\Omega = \langle B_\Omega, \beta_\Omega^C \rangle. \quad (3)$$

The communication model  $C_{n,i}$  of the user device can be formulated as

$$C_{n,i} = \langle t_{n,i}^C, \widehat{d}_{n,i} \rangle. \quad (4)$$

### 2.3. Computation Offloading Model

**2.3.1. Local Execution.** When  $a_n = 0$ , the user  $n$  chooses to execute the computation-intensive task  $T_n$  locally. Let  $f_n$  be the computing capacity of the user  $n$ , then the time delay  $t_1$  incurred by the task  $T_n$  when it is executed locally can be calculated as

$$t_1 = \frac{c_n}{f_n}. \quad (5)$$

The energy consumption  $e_1$  for local execution can be calculated as

$$e_1 = \chi_1 c_n (f_n)^2, \quad (6)$$

where  $\chi_1$  is a constant.

According to equations (5) and (6), the total overhead of local execution  $\Theta_1$  can be expressed as

$$\Theta_1 = \omega_t t_1 + \omega_e e_1, \quad (7)$$

where  $\omega_t$  is the weight of time delay,  $\omega_e$  is the weight of energy consumption,  $0 \leq \omega_t \leq 1$ , and  $0 \leq \omega_e \leq 1$ ,  $\omega_t + \omega_e = 1$ .

**2.3.2. MEC Offloading Computation.** When  $a_n > 0$ , the user selects to uninstall to the MEC server for execution, during the offloading process, the TD and EC are generated during the following three steps: (1) the computation task is transmitting data through the wireless channel; (2) the computation task is executed at the MEC server; and (3) the computation result is returned to the user.

When data are transmitted to the MEC, the user selects the wireless channel, and the resulting time delay can be written as

$$t_2 = \frac{d_n}{\widehat{v}_n(a)}, \quad (8)$$

where  $\widehat{v}_n(a)$  is the uplink data transmission rate.

The energy consumption incurred by the data transmission to the MEC can be expressed as

$$e_2 = p_n t_2 = \frac{p_n d_n}{\widehat{v}_n(a)}. \quad (9)$$

When the task is uploaded to the MEC server, it is computed using the computational resources of the server, at this point the resulting time delay can be calculated as

$$t_3 = \frac{c_n}{F_n}, \quad (10)$$

where  $F_n$  denotes the MEC server computing capacity.

The energy consumed when executing tasks at the MEC can be formulated as

$$e_3 = \chi_0 c_n (F_n)^2. \quad (11)$$

Generally, the size of the result calculated by the MEC server is very small compared with the input data, so the TD and EC when returning the calculation result to the user can be ignored [21]. Thus, the total overhead of offloading the computation task to the MEC for execution can be expressed as

$$\Theta_2 = \omega_t (t_2 + t_3) + \omega_e (e_2 + e_3). \quad (12)$$

Based on equations (7) and (11), the overhead of each user can be expressed as

$$\Theta_n(a) = \begin{cases} \Theta_1, & a_n = 0, \\ \Theta_2, & a_n > 0. \end{cases} \quad (13)$$

**2.4. Optimization Objectives.** The optimization objective of a multiuser MEC system is to minimize the TD and EC. Hence, it can be modeled as

$$\begin{aligned}
& \min \sum_{n \in N} \Theta_n(a) \\
& a_n \in \{0, 1, \dots, M\}, \forall n \in N \\
& \text{s.t. } p_n \in [p_{\min}, p_{\max}],
\end{aligned} \tag{14}$$

where  $p_{\min}$  is the minimum values of the transmission power and  $p_{\max}$  is the maximum values of the transmission power.

The above optimization problem involves the combinatorial optimization problem in multidimensional discrete space. We can consider using reinforcement learning technology and making use of the intelligent characteristics of mobile users so that mobile users can get mutually satisfactory unloading strategies.

### 3. Solutions

**3.1. Reinforcement Learning.** Reinforcement learning (RL) is an autonomous learning framework that implements experience-driven learning through interactions and is used to maximize the reward when intelligent agents are finding the optimal behavior at a given state. Reinforcement learning, as a part of machine learning, differs from supervised learning, where training is based on the right answer itself [22, 23]. In a standard RL model, the autonomous-learning agents interact with the environment. The process of reinforcement learning is shown in Figure 2. At each timestamp  $t$ , a state  $s(t)$  is first observed from the environment, then an action  $\varphi(t)$  is executed based on the current state, after which a reward/punishment  $r_t$  is fed back by the current environment. Thereafter, the environment will move to another state  $s(t+1)$ , where the probability of the environment moving to a state  $s(t+1)$  after performing an action  $\varphi(t)$  from the state  $s(t)$  can be represented by the state probability transfer function  $\sigma(s(t+1)|s(t), \varphi(t))$ .

The process described above is going to continue, which maximizes the desired reward in the long run. Mathematically, reinforcement learning can be described as a Markovian decision process in which the response of the environment to the state  $s(t+1)$  depends on  $s(t)$  and  $\varphi(t)$ . Furthermore, the key point of reinforcement learning is to learn without the knowledge of the underlying environment model. And the reinforcement learning that cannot compute rewards before actions are selected and cannot know the state probability transfer function is referred as model-free reinforcement learning [24]. Meanwhile, reinforcement learning uses a  $\varepsilon$ -greedy approach as the fundamental policy, where  $\varepsilon$  is a probability value between [0,1]. Each time an action is selected, there is a probability of  $\varepsilon$  being exploited in the Q-table and the action with the largest reward is expected, and there is a probability that an action is randomly performed in the exploitation.

**3.2. Systematic Action Transitions and Delayed Rewards.** Figure 3 demonstrates how the system states change over time. Assuming that at the moment  $t$ , the reinforcement learning algorithm, taking DQN as an example, obtains observation  $o_t$  from the server state, and makes offloading

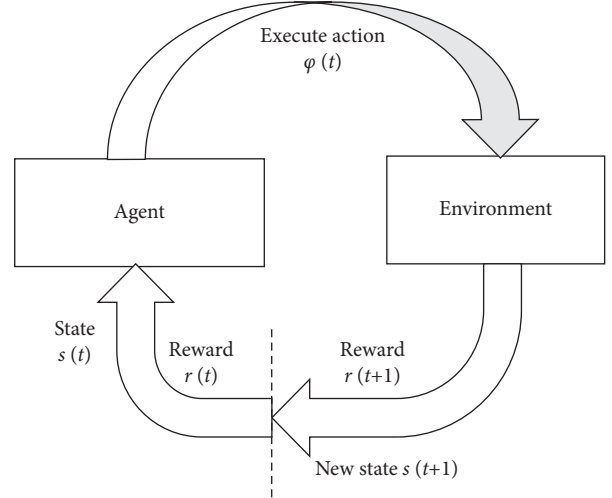


FIGURE 2: The process of reinforcement learning.

action  $\varphi_t$  based on the observation. Then the offloading action will affect the state of the user who receives the offloading permission, which in turn affects the state of the specific task to be offloaded. Once a task is in the offloading process, it undergoes state transitions such as transmission, arrival at the server cache, execution on the server, and execution completed, which have a continuous impact on the resources and state of the server throughout the transition process.

When the task is executed, the rewards  $r_t$  recorded by the system at this moment are returned to the decision-making algorithm for learning. It is clear from the description that at the moment  $t$ , the decision-making algorithm does not have access to the immediate rewards for this action but can only obtain the reward for the action at a previous moment. This is a distinctive feature of the incomplete observation system and is a key point for the offloading model to meet the conditions for asynchronous decision-making [25, 26]. Therefore, the cumulative reward of successive decisions constructed by the learning process is the key to determining whether the optimization objective of the system is satisfied.

Assuming that the cumulative positive rewards of reinforcement learning (excluding punitive rewards) are equal to the optimization objective  $\Psi$  of the system. Therefore, an upper bound on the cumulative reward is the optimization objective, which can be expressed as

$$\sum_{t \in T} |\bar{r}_t + r_t| \leq \Psi, \tag{15}$$

where  $\bar{r}_t$  is the punitive rewards.

The computation offloading in the edge environment is a complex process of continuous decision-making. And a model-free reinforcement learning method, i.e., temporal-difference (TD), is applied, which combines Monte Carlo sampling and bootstrapping in dynamic programming and usually leads to better learning performance and efficiency. Here, the loss function can be defined as

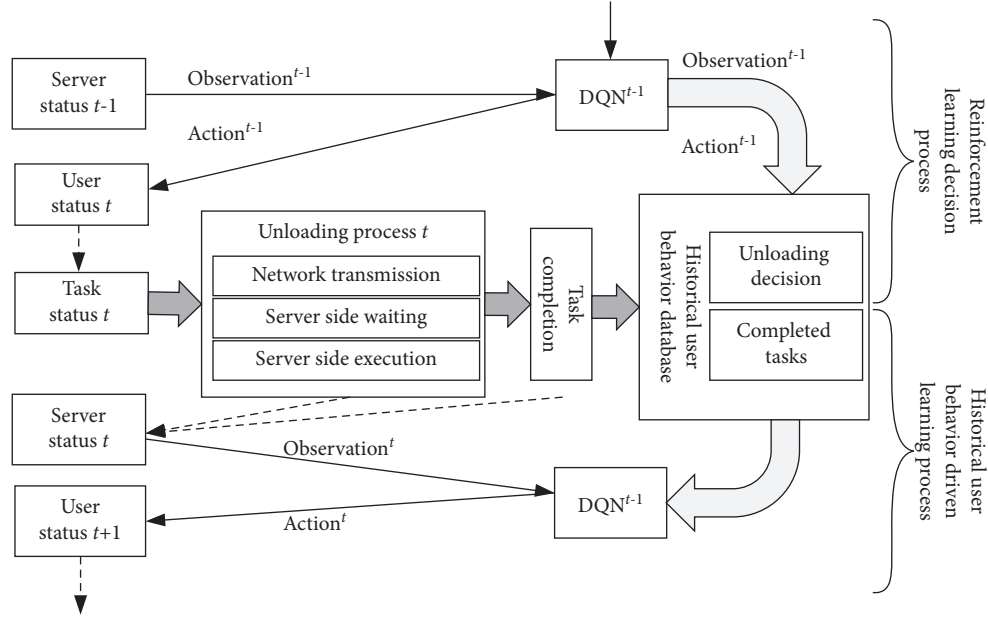


FIGURE 3: Learning process and delayed reward.

$$L(y, y') = \frac{\sum_{i=1}^n (y_i - y'_i)^2}{n}, \quad (16)$$

where  $y$  and  $y'$  are the real value and target value of the model output, respectively.

The proposed learning method runs on an offloading model on the edge server and is mainly as follows:

- (1) At the beginning of learning, the server starts the offloading process and updates the reward value  $r_t = (T_{n,i}^L / \varepsilon_{n,i})$  of the latest task for that user if the task has been executed
- (2) If the system is overloaded, it updates the reward value as  $r_t = -|r_{t-1}|$  of the latest task for that user
- (3) The server state  $s_{\Omega}^t$ , and the list of users  $\varphi_{\Omega}^t$  are obtained and can be offloaded in this decision from the action space. Then the offloading notifications are sent to the users in the list by the server
- (4) The server reads the latest reward value of the task and takes the triplet of state, action, and reward as the training input to the reinforcement learning algorithm

**3.3. DQN-based Offloading Strategy.** To better evaluate the effect of the policies on action selection, the value function about states and actions is converted into a recursive form, which can be denoted as

$$Q(s_t, \varphi_t) = \Phi_t + \zeta \min_{\varphi_{t+1}} Q(s_{t+1}, \varphi_{t+1}), \quad (17)$$

where  $\Phi_t$  is the value of cost and  $\zeta$  is the discount coefficient.

In conventional Q-learning algorithms, the number of states in the environment is generally assumed to be relatively small, and therefore a look-up table is used to record the state-action pairs  $(s, \varphi)$ . However, since the number of

states in the constructed MEC network is so large, it is computationally expensive to update the Q function in an iterative manner if the Q learning algorithm continues to be used. So DQN is proposed to address the problem. The DQN algorithm is a typical value-based policy algorithm that collects the state  $s_t$  of the current network environment as input data of the estimated value of the deep network. And the output of the estimated value network is  $Q(s_t, \varphi), \forall \varphi \in A$ , where Q values corresponds to all the actions. Then, a greedy algorithm, i.e.,  $\varepsilon$ -greedy, is used to select the actions  $\varphi_t$ . Next, the user performs the action  $\varphi_t$ , and the network environment turns to the next state  $s_{t+1}$ , while the value of cost  $\Phi_t$  is generated. Based on this value, the parameters of the estimated value network are updated, and after many iterations of update, the estimated value network has been trained to output the optimal Q function  $Q(s, \varphi)$ . The mean square error function is used to define the loss function of the estimated value network, which can be written as

$$L_t = E[(Y_t - Q(s_t, a_t | \theta))^2], \quad (18)$$

where  $\theta$  denotes the weight parameter of the estimated value network, and  $Y_t$  represents the value of optimization objective for the estimated value network. However, if an identical deep neural network is used to obtain the target value, the target output of the network also changes with the update of the parameters, that is, the label changes during the deep learning training, which is obviously unreasonable [27]. Therefore, it is necessary to introduce another neural network named as the target value network, whose network structure is exactly the same as the estimated value network. The only difference between them is that the parameter  $\theta$  of the target value network will not be updated at each timeslot but will be copied from the parameters of the estimated value network after every  $K$  steps of training. Namely, the

parameter of the target value network is updated  $K$  steps slower than the estimated value network. The target value can be expressed as

$$Y_t = \Phi_t + \zeta \min_{\varphi_{t+1}} Q(s_{t+1}, \varphi_{t+1} | \theta^-). \quad (19)$$

In addition, the samples of training data are independent of each other in supervised learning. But, it is noted that the states of the MEC network are continuous in time series, which affects the reliability of training to some extent. Therefore, an experience replay unit (ERU) is introduced in the DQN network and all the samples coming from the interaction between environments and agents are stored in the memory of the ERU in the form of quaternions  $(s_t, \varphi_t, \Phi_t, s_{t+1})$ , where  $s_{t+1}$  is the next state for the states  $s_t$ . In the training phase, one sample packet is randomly grabbed from the ERU at a time, and the size of the packet can be set arbitrarily within the maximum number of samples so that the temporal correlation between datasets can be broken, making the samples independent and increasing the generalization ability of deep learning. The pseudocode of the DQN-based offloading algorithm is shown in Algorithm 1.

## 4. Experiments and Analysis

The simulation experiment platform uses MATLAB mathematical software, and the version is 2016a. The computer hardware conditions used in the simulation are as follows: CPU is i7-7200U and the running memory size is 4GB. In the experiments, the simulation scenario is assumed as follows: the bandwidth  $B = 5$  MHz, and the computing capacity  $F = 12$  GHz/sec, and the computing capacity of each mobile user itself is  $f = 5$  GHz/sec. The transmission power of the mobile users is between  $p_{\min}$  and  $p_{\max}$ , where  $p_{\min} = 150$  mW and  $p_{\max} = 300$  mW. Assuming that the computation offloading follows a uniform distribution between 3000 and 5000 Kb. Besides, decision weights are set as  $\omega_t = \omega_e = 0.5$ .

**4.1. Convergence Procedure in Training DQN Strategy.** As shown in Figure 4, three different sets of variables are adopted in the experiments, which are as follows: (1) the number of users is the same as the number of edge servers  $(N, M) = (15, 15)$ ; (2)  $(N, M) = (15, 20)$ ; and (3)  $(N, M) = (20, 15)$ . And the number of iterations is 20,000.

As shown in Figure 4, in the DQN-based offloading strategy, the average system cost of these three curves decreases rapidly until convergence. When  $(N, M) = (15, 15)$ , the average cost converges to the lowest value after about 11,000 iterations; when  $(N, M) = (15, 20)$ , the average cost converges to a stable value after about 9,000 iterations, and this value approximates the value in the case of an equal number of users and edge servers. When  $(N, M) = (20, 15)$ , the average cost converges to a larger value than that in the other two cases after about 13,000 iterations. Hence, it is confirmed that the proposed strategy allows the system cost to gradually decrease and converge to a stable value regardless of the relationship between the number of users and the number of edge servers.

**4.2. Comparison with Other Algorithms.** Besides, it is compared with the algorithms in Reference [8], Reference [10], and Reference [15] in the simulation.

**4.2.1. Comparison of the Number of Terminals and Average Delay.** The relationship between the number of user terminals and the average delay for different algorithms is illustrated in Figure 5.

It can be seen in Figure 5 that since the algorithm proposed in Reference [8] does not consider the collaboration mechanism, the load on the computing server rises with the increase of the number of user terminals, leading to an overall rise in the user task delay. Therefore the average user delay is the biggest. The algorithm proposed in Reference [10] adopts side cloud collaboration, and when the number of user terminals increases, the MEC server can transmit the tasks that cannot be processed in time to the cloud server for execution. Although the side cloud collaboration can reduce the task delay, the average user delay is also relatively high because the cloud server is far away from the user, which increases the transmission delay. Algorithms proposed in this paper and Reference [15] both use reinforcement learning to design the offloading strategy. However, the proposed algorithm constructs a multiuser MEC model to offload computation tasks as quickly as possible or execute them locally, so the delay is the smallest and the average delay does not exceed 0.9 s when the number of terminals is 40.

**4.2.2. Relationship between Computing Capacity of MEC Servers and Maximum User Delay.** The effect of the computing capacity of MEC servers on the maximum user delay under different algorithms is shown in Figure 6.

From Figure 6, it is illustrated that the user task delay becomes smaller with the increase of the MEC computing capacity. Also, the proposed algorithm has a smaller delay compared to the other three algorithms, and its maximum user delay is about 0.6 s when the computing capacity of MEC servers reaches 16 GHz/sec. This is because when the computing capacity of MEC servers is low, the servers collaborate with each other to balance their load and reduce the task delay. Therefore, the advantages of edge-cloud collaboration will no longer be obvious, and the performance of the algorithm proposed in Reference [8] gradually approaches the curve of Reference [10].

**4.2.3. Relationship between Average System Overhead and the Number of Mobile Users.** Figure 7 illustrates the performance of the average system overhead with a different number of mobile users, where the number of channels is set to be 12 and the computing capacity of MEC servers is set as  $F = 12$  GHz/sec.

As shown in Figure 7, the average system overhead of all four algorithms increases with more and more users. In Reference [10], some of the computation tasks are offloaded to the cloud computing center for execution, and the cloud computing center is far away from users, thereby the TD and



```

Begin
(1) Emptying the storage area of the ERU
(2) Initialize the weight parameters of the estimated value network  $\theta$ , and make the parameters of the target value network  $\theta^- = \theta$ 
(3) Initialization status  $s$ 
(4) For  $t = 1 : T$ 
(5) do
(6) Under the greedy algorithm, an action is selected based on the state  $s_t \varphi_t$ 
(7) Execute the action  $\varphi_t$  and observe the system costs  $\Phi_t$  and  $s_{t+1}$ 
(8) Collecting samples  $(s_t, \varphi_t, \Phi_t, s_{t+1})$  and storing them in the ERU
(9) If the samples are larger than the size of the sample pack then grabbing a sample packet at ERU
(10) If  $s_t$  is the final state then  $Y_t = \Phi_t$ 
    Otherwise  $Y_t = \Phi_t + \zeta \min_{\varphi_{t+1}} Q(s_{t+1}, \varphi_{t+1} | \theta^-)$ 
(11) Execute RMSPropOptimizer, optimize  $(Y_t - Q(s, \varphi | \theta))^2$ 
(12) Every  $K$  time slots elapsed, so that  $\theta^- = \theta$ 
(13)  $s_t = s_{t+1}$ 
(14) End
    End
    
```

ALGORITHM 1: DQN-based offloading algorithm.

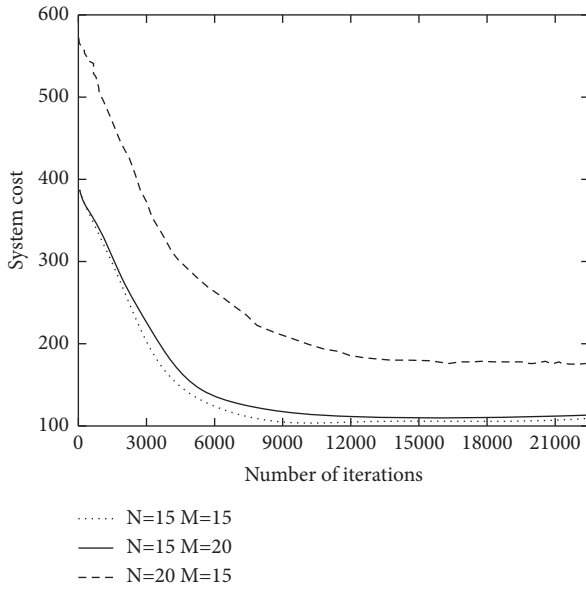


FIGURE 4: Convergence procedure in training the DQN strategy.

EC increases significantly and its computation overhead is the highest. Heuristic algorithms are applied in Reference [8] for system optimization, while its optimal solution searching performance is weaker compared to the learning results in deep learning networks. Meanwhile, as the number of mobile users increases, the resources that the system can provide in the process of task offloading are limited, so the competition for the limited resources in the system is intense, which can cause an increase in the system delay and energy consumption. In such an environment of intense competition for resources, the metareinforcement algorithm proposed in Reference [15] has a more obvious advantage over the DQN strategy of the proposed algorithm. The proposed algorithm realizes the optimal task unloading and resource allocation through the powerful data optimization ability of DQN. Its total system overhead is less than 120 and

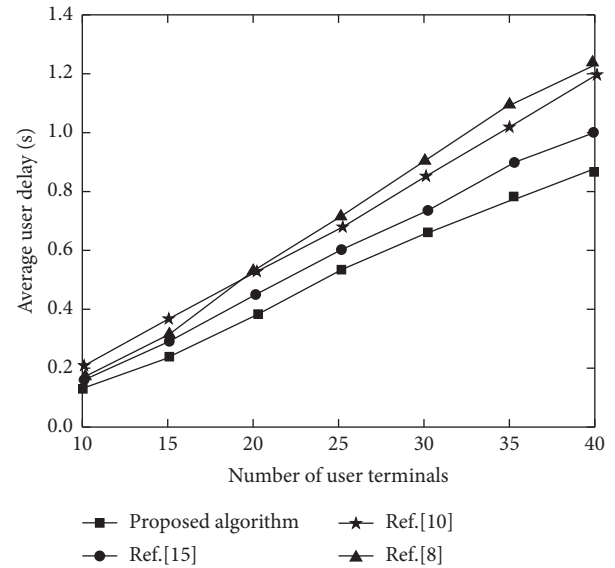


FIGURE 5: Comparison between the number of terminals and the average delay.

can dynamically fine-tune the delay and energy consumption according to the actual needs.

**4.2.4. Relationship between Average System Energy Consumption and Training Rounds.** When  $\omega_t = 0$  and  $\omega_e = 1$ , the optimization objective can only be concerned about the energy consumption of the whole system and neglect the system delay. Under such circumstances, the performance of energy consumption of the system is shown in Figure 8.

From Figure 8, it can be seen that the average system energy consumption of the four algorithms tends to be stable as the number of training rounds increases, but the proposed algorithm has the smallest average system energy consumption, which tends to be 65 J when the number of training rounds exceeds 19. The proposed algorithm uses

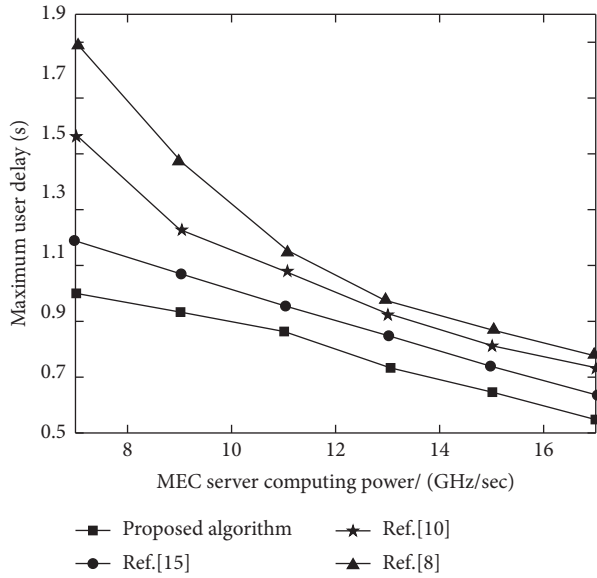


FIGURE 6: Relationship between computing capacity of MEC servers and maximum user delay.

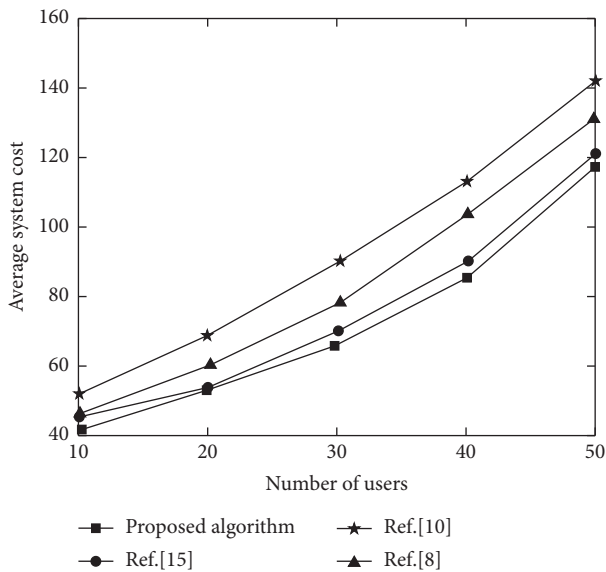


FIGURE 7: Relationship between average system overhead and the number of mobile users.

DQN to construct an offloading strategy in which the system optimization search is accelerated by system action transition with delayed reward and introduces the MEC system model, leading to smaller overall energy consumption. The meta-reinforcement strategy proposed in Reference [15] is computationally complex and lacks a reasonable system architecture, so the energy consumption increases. In Reference [10], the task offloading is executed based on the cloud edge collaborative architecture, but its stable energy consumption is more than 100 J due to the long distance between cloud computing centers and the users. Reference [8] has less computational overhead due to low complexity.

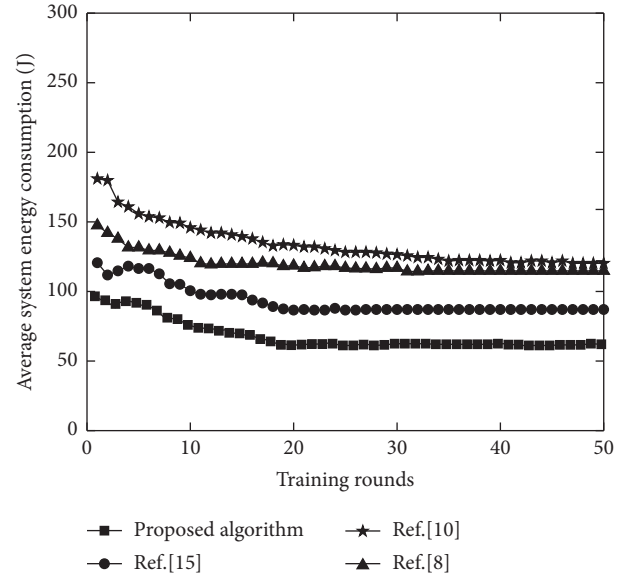


FIGURE 8: Relationship between average system energy consumption and training rounds.

However, the time delay is large, so the overall offloading is not effective.

## 5. Conclusion

To alleviate the network load and reduce the risk of network congestion in traditional cloud computing of IoT, MEC is introduced to formulate the multiuser computing offloading problem, where the optimization objective is set to minimize the total weighted overhead of time delay and energy consumption to ensure reasonable system resource allocation. Additionally, the optimization problem is solved using a DQN-based offloading strategy, obtaining the optimal scheme. The results based on the simulation platform show that:

- (1) The introduction of MEC, which enables the computation task in close proximity to the users, can reduce system time and energy consumption. The average delay of the proposed algorithm does not exceed 0.9 s, and the average energy consumption tends to be 65 J when the number of user terminals is 40.
- (2) The proposed algorithm can execute computational tasks as close as possible by adopting the MEC system, enabling it to reduce the total system overhead to a great extent. And the total overhead is lower than 120 when the number of users is 50.

As the mobile user devices have very limited resources and suffer from the problem of battery aging, the energy provided to the users is not enough for them to complete the whole offloading procedure in some cases. Therefore, how to renew the energy for mobile users to ensure that offloading will not be interrupted deserves deep study, which will also be the focus of our research in the future.

## Data Availability

The data included in this paper are available from the author upon request without any restriction.

## Conflicts of Interest

The authors declare that there are no conflicts of interest regarding the publication of this paper.

## References

- [1] J. Guo and N. Shah, "Internet of things based intelligent techniques in workable computing: an overview," *Scientific Programming*, vol. 2021, Article ID 6805104, 15 pages, 2021.
- [2] X. Wu, J. Gan, S. Chen, X. Zhao, and Y. Wu, "Optimization strategy of task offloading with wireless and computing resource management in mobile edge computing," *Wireless Communications and Mobile Computing*, vol. 2021, Article ID 8288836, 11 pages, 2021.
- [3] K. Wang, Z. Hu, Q. Ai et al., "Joint offloading and charge cost minimization in mobile edge computing," *IEEE Open Journal of the Communications Society*, vol. 1, no. 4, pp. 205–216, 2020.
- [4] W. Zhan, C. Luo, and G. Min, "Mobility-aware multi-user offloading optimization for mobile edge computing," *IEEE Transactions on Vehicular Technology*, vol. 69, no. 99, pp. 3341–3356, 2020.
- [5] Y. Fu, X. Yang, and P. Yang, "Energy-efficient offloading and resource allocation for mobile edge computing enabled mission-critical internet-of-things systems," *EURASIP Journal on Wireless Communications and Networking*, vol. 10, no. 1, pp. 1–16, 2021.
- [6] U. Saleem, Y. Liu, and S. Jangsher, "Latency minimization for d2d-enabled partial computation offloading in mobile edge computing," *IEEE Transactions on Vehicular Technology*, vol. 69, no. 99, pp. 4472–4486, 2020.
- [7] Z. Kuang, L. Li, and J. Gao, "Partial offloading scheduling and power allocation for mobile edge computing systems," *IEEE Internet of Things Journal*, vol. 6, no. 9, pp. 6774–6785, 2019.
- [8] L. I. Shulei, D. Zhai, and P. Du, "Energy-efficient task offloading, load balancing, and resource allocation in mobile edge computing enabled IoT networks," *Science China Information Sciences*, vol. 62, no. 2, pp. 1–3, 2019.
- [9] X. Chen, Z. Liu, Y. Chen, and Z. Li, "Mobile edge computing based task offloading and resource allocation in 5G ultradense networks," *IEEE Access*, vol. 7, no. 5, pp. 184172–184182, 2019.
- [10] C. Jiang, Y. Li, and J. Su, "Research on new edge computing network architecture and task offloading strategy for Internet of Things," *Wireless Networks*, vol. 5, no. 2, pp. 1–13, 2021.
- [11] Q. Wang, S. Guo, J. Liu, and Y. Yang, "Energy-efficient computation offloading and resource allocation for delay-sensitive mobile edge computing," *Sustainable Computing: Informatics and Systems*, vol. 21, no. 3, pp. 154–164, 2019.
- [12] L. Liu, X. Qin, Z. Zhang, and P. Zhang, "Joint task offloading and resource allocation for obtaining fresh status updates in multi-device MEC systems," *IEEE Access*, vol. 8, no. 5, pp. 38248–38261, 2020.
- [13] Z. Zhang, C. Li, and S. L. Peng, "A new task offloading algorithm in edge computing," *EURASIP Journal on Wireless Communications and Networking*, vol. 2, no. 1, pp. 1–21, 2021.
- [14] C. Li, M. Song, H. Tang, and Y. Luo, "Offloading and system resource allocation optimization in TDMA based wireless powered mobile edge computing," *Journal of Systems Architecture*, vol. 98, no. 7, pp. 221–230, 2019.
- [15] J. Wang, J. Hu, and G. Min, "Fast adaptive task offloading in edge computing based on meta reinforcement learning," *IEEE Transactions on Parallel and Distributed Systems*, vol. 32, no. 1, pp. 242–253, 2020.
- [16] H. Lu, C. Gu, F. Luo, W. Ding, S. Zheng, and Y. Shen, "Optimization of task offloading strategy for mobile edge computing based on multi-agent deep reinforcement learning," *IEEE Access*, vol. 8, no. 7, pp. 202573–202584, 2020.
- [17] K. Wang, X. Wang, X. Liu, and A. Jolfaei, "Task offloading strategy based on reinforcement learning computing in edge computing architecture of internet of vehicles," *IEEE Access*, vol. 8, no. 9, pp. 173779–173789, 2020.
- [18] C. Li, W. Chen, J. Tang, and Y. Luo, "Radio and computing resource allocation with energy harvesting devices in mobile edge computing environment," *Computer Communications*, vol. 145, no. 9, pp. 193–202, 2019.
- [19] P. Paymard, S. Rezvani, and N. Mokari, "Joint task scheduling and uplink/downlink radio resource allocation in PD-NOMA based mobile edge computing networks," *Physical Communication*, vol. 32, no. 1, pp. 160–171, 2019.
- [20] Y. He, L. Ma, R. Zhou, C. Huang, and Z. Li, "Online task allocation in mobile cloud computing with budget constraints," *Computer Networks*, vol. 151, no. 3, pp. 42–51, 2019.
- [21] F. Wang, J. Xu, and S. Cui, "Optimal energy allocation and task offloading policy for wireless powered mobile edge computing systems," *IEEE Transactions on Wireless Communications*, vol. 19, no. 4, pp. 2443–2459, 2020.
- [22] Y. Li and C. Jiang, "Distributed task offloading strategy to low load base stations in mobile edge computing environment," *Computer Communications*, vol. 164, no. 8, pp. 240–248, 2020.
- [23] K. Wang, Z. Xiong, L. Chen, P. Zhou, and H. Shin, "Joint time delay and energy optimization with intelligent overlocking in edge computing," *Science China (Information Sciences)*, vol. 63, no. 4, pp. 154–169, 2020.
- [24] C. Yang, Y. Liu, X. Chen, W. Zhong, and S. Xie, "Efficient mobility-aware task offloading for vehicular edge computing networks," *IEEE Access*, vol. 7, no. 7, pp. 26652–26664, 2019.
- [25] Z. Wang, P. Li, S. Shen, and K. Yang, "Task offloading scheduling in mobile edge computing networks," *Procedia Computer Science*, vol. 184, no. 4, pp. 322–329, 2021.
- [26] S. Hu and G. Li, "Dynamic request scheduling optimization in mobile edge computing for IoT applications," *IEEE Internet of Things Journal*, vol. 7, no. 2, pp. 1426–1437, 2020.
- [27] H. Guo, J. Zhang, J. Liu, and H. Zhang, "Energy-aware computation offloading and transmit power allocation in ultradense IoT networks," *IEEE Internet of Things Journal*, vol. 6, no. 3, pp. 4317–4329, 2019.

## Research Article

# Adorno's Cultural Industry Theory in the Environment of Internet Development

Fang Gao 

*School of Law, East China University of Political Science and Law, Shanghai 200042, China*

Correspondence should be addressed to Fang Gao; 172050039@ecupl.edu.cn

Received 17 January 2022; Revised 11 February 2022; Accepted 17 February 2022; Published 2 March 2022

Academic Editor: Shalli Rani

Copyright © 2022 Fang Gao. This is an open access article distributed under the Creative Commons Attribution License, which permits unrestricted use, distribution, and reproduction in any medium, provided the original work is properly cited.

Traditional cultural industry theory is confined to a specific historical context, and the theoretical level of simple denial and criticism of cultural industry phenomena has lost its historical significance. The development of the cultural industry is the inevitable result of the development of the market economy. It enables people to recover from their values in the spirit of humanism. This article was aimed at studying and evaluating Adorno's cultural industry theory based on the development environment of the Internet and using literature review techniques to obtain, collect, and summarize research related to Adorno's cultural industry and its subject critical theory, analyze, summarize, and classify their views and opinions, as well as data on gender significance and limitations, and compare and extract. In the research stage of the thesis, firstly, the background and conditions of Adorno's critical theory of cultural industry were systematically investigated with a complete historical and logical method. Then, it combines theory with practice and uses Adorno's critical theory of contemporary Chinese cultural industry to find problems and defects. Finally, based on the difference between Adorno's living environment and the current environment, it is logical to compare Adorno's theory with comparative research methods in modern China, but it needs to be improved and perfected.

## 1. Introduction

Adorno's cultural industry is Western Marxist ideology and culture, but Western Marxist ideology is essentially a beacon of my country's classical Marxism, which can be used as a reference to enhance my country's national experience [1, 2]. The Chinese cultural industry appeared for a short time in the 1990s, but it has successfully penetrated into modern society [3]. Its tremendous influence on Kannada-speaking society forces us to think about and explore cultural industries. The commercialization and popularity of music in modern Chinese society and the unification of TV and literary creation kitsch programs have also increased the awareness of cultural institutions in the fields of education and politics [4]. The cultural industry pushes culture and celebrities to the limit and opposes that culture affects people's lives and undermines public opinion. Therefore, it is very important to learn about the cultural industry on a regular basis. Revisiting Adorno's cultural industry and understanding the roots of his suspicion and important attitude towards

the cultural industry will certainly help our cultural research [5].

In today's world cultural trends, the highest level of cultural development is the cultural industry, which is an amazing historical fact [6]. Ada analytically reconstructed the rise of the Department of Art and Cultural Management, which was established in Istanbul about 20 years ago and has been training graduates in Turkey ever since. He believes that as a microcase, when trying to solve the problem of "cultural industry" as an education field, the knowledge provided by this experience is worthy of discussion and consideration [7]. Some scholars describe that in the view of Adorno's cultural industry theory, "popular culture" is generally a hodgepodge, imposed on the masses from the top down. But as far as the status quo of Chinese popular culture is concerned, Adorno's "denial of the cultural industry" has two states. On the one hand, in our real life, there are many phenomena that fit his description: contradictory situation [8]. In addition, some scholars believe that Adorno believes that modern culture and art in capitalist society have been

commercialized. Although this commercialized culture and art is popular and universal, in “popular culture,” art loses in “popular culture,” criticism, and negation function. The strong culture formed by popular culture has the social function of weakening people’s enterprising spirit and changing people’s souls [9]. Based on this fact, this article chooses to explore the cultural industry theory of the Frankfurt School from the development environment of the Internet.

There are two main innovations in this article: One is to classify and integrate Adorno’s critical theory of cultural industries based on understanding and knowledge and extract the basic framework of Adorno’s critical theory of cultural industries that the author understands. Previous work on the critical theory of Adorno’s cultural industry was largely based on a general explanation of his theory and lacked the core coupling and integration of the critical theory of Adorno’s cultural industry. This article tries to integrate Adorno’s critical theory of cultural industries from the author’s theory and understanding and reveals the profound colors behind Adorno’s critical theory of cultural industries. The second is to examine the critical theory of Adorno’s cultural industry in the context of the development of socialist culture with Chinese characteristics. At present, most domestic research on Adorno is purely theoretical. Some are just the combination of theory and Chinese reality, some focus on the shortcomings of Adorno’s theory in Chinese society, and some lack detailed research on the problem. This article broke the leg and fits mechanically, pushing the reality of Chinese society into Adorno’s theoretical framework. This article combines Adorno’s critical theory of cultural industries and at the same time combines Adorno’s critical theory of cultural industries with the actual situation of China’s sustainable development, based on the positive aspects of Adorno’s critical theory of cultural industries. It is used to study the reality of China and provide specific references for the construction of socialist culture with Chinese characteristics.

## 2. Research on the Theoretical Evaluation and Enlightenment of Adorno’s Cultural Industry in the Internet Development Environment

### 2.1. The Connotation of Cultural Industry

2.1.1. *Standardization.* Adorno believes that the term “industry” in the cultural industry means “not only the production process, but also the standardization of things and the reasonable and efficient allocation of technology.” With the development of media technology, cultural and artistic products are decorated with commodities with the same details, similar plots, and consistent styles. Such works can win the applause of the masses, but it is difficult to leave an indelible impression in their hearts. “Cultural industry technology realizes standardization and mass production by subtracting the two logical differences between social work and social system.” In order to make products attractive to consumers and occupy the market, producers “rationalize” according to consumers’ preferences. The choice is

more and more in line with the tastes of the vast majority of people, coupled with the so-called fashion trends, so the presented cultural works of art lose their individuality, and the manufacturer claims that the products are unique and each one cannot be replaced.

2.1.2. *Commercialization.* The industrial age enabled the mass production of cultural and artistic works, and technology accelerated the standardized production of cultural and artistic products. All of these are closely related to the basic characteristics of cultural industry products as commodities. “Art works that are products of the cultural industry are not real art, but are produced as products that can be sold immediately on the market.” The cultural industry is formed under the conditions of a developed capitalist market and has become a general law of the market economy. Adorno specifically pointed out that handicrafts are distributed as commodities in production and consumption activities. Now “people can replace the so-called use value in the structure of cultural commodities with exchange value.” When cultural and artistic works become popular as products, their use value, that is, aesthetic value, is replaced by exchange value. People consume cultural and artistic works to increase visibility and profit.

2.1.3. *Falsehood.* The standardization and commercialization of the cultural industry have led to the false personality of cultural and artistic works. This false personality became popular with the deliberate defense of the ruling class to guide public opinion to follow the trend and create public opinion. “A maverick movie star uses curly hair to cover his eyes and show his originality, etc.” Once the entire society is integrated into the cultural industry system, only when individuals reach a consensus with the general public can the industrial society tolerate the existence of individuals. Therefore, even if an individual knows the hypocrisy of this character, he will remain silent so as not to be rejected. Over time, the public loses the ability to distinguish between true and false. In this sense, “the personification of the cultural industry is nothing more than a marketing strategy, an era when consumers are deceived.”

2.2. *Evaluation of Adorno’s Cultural Industry Theory.* Adorno’s theory of cultural industry is the most representative theory of the Frankfurt School. Its influence lies in that it first proposed the concept of “cultural industry” and revealed that the existence and development of cultural industry is a sign of the decline of capitalist society, a serious phenomenon of alienation. Adorno was the first person in the Frankfurt School to pay attention to mass culture, and he was the first to bring mass culture and higher culture into the theoretical research field of modern culture at the same time.

During the Second World War, the American cultural industry was very prosperous, and the public can appreciate various forms of cultural products. In such a realistic context, Adorno’s pessimistic criticism of the industrialization of cultural products is undoubtedly like a “timely rain,” pouring out the consciousness of the public. Adorno pointed

out that the harmfulness of the cultural industry is manifested in the elimination of human personality, loss of the aesthetic value of art, domestication of public thoughts, and elimination of public judgment. When the public embraced the cultural industry and when the public wandered in the ocean of the cultural industry, he tried to use straightforward expressions and sharp comments to alert the public and prevent the public from being deceived by the cultural industry. He also worked hard to maintain elite culture. The authority and purity of art prevent the decline of culture.

In short, he warned cultural producers to produce cultural products with a sense of social responsibility and reminded the public to treat culture with a speculative perspective.

### 3. Investigation and Research on the Theoretical Evaluation and Enlightenment of Adorno's Cultural Industry in the Environment of Internet Development

*3.1. Research Methods.* This article adopts the online questionnaire survey method to conduct a questionnaire survey on the public's awareness of Adorno's cultural industry in the Internet environment. In the process of analyzing the characteristics of the cultural industry in the representative Internet environment, the characteristics of industrialization are interpreted through texts and raised to the level of theoretical understanding. On the basis of grasping the theory of cultural industry, sum up the industrialization characteristics of cultural industry under the Internet environment with universal laws.

*3.2. Data Collection.* This article mainly uses Questionnaire Star to distribute questionnaires online. A total of 255 questionnaires were distributed online. Because there will be a small reward after filling in the questionnaire, the effective rate of the questionnaire returned is 100%.

*3.3. Data Processing and Analysis.* This article uses SPSS 22.0 software to count and analyze the results of the questionnaire and conduct a *t*-test. The *t*-test formula used in this article is as follows:

$$t = \frac{\bar{X} - \mu}{(\sigma X)/(\sqrt{n})}, \quad (1)$$

$$t = \frac{\bar{X}_1 - \bar{X}_2}{\sqrt{((n_1 - 1)S_1^2 + (n_2 - 1)S_2^2)/(n_1 + n_2 - 2))(1/n_1 + 1/n_2)}}. \quad (2)$$

Among them, formula (1) is a single population test, *s* is the sample standard deviation, and *n* is the number of samples. Formula (2) is the double population test, and the sum is the sample size.

## 4. Investigation and Analysis of Adorno's Theoretical Evaluation and Enlightenment of Cultural Industry in the Environment of Internet Development

*4.1. Development of the Cultural Industry.* Different from Adorno's statement, Chinese scholars refer to the "cultural industry" as the cultural industry and believe that the cultural industry is a process of producing and composing cultural products and cultural services according to industrialization standards. The Chinese government attaches great importance to the development of the cultural industry and has taken it as a national policy to implement it. The development of technology will inevitably bring about the prosperity of culture. Only in this way can society achieve internal balance. The development of cultural industries is an unstoppable trend. When the level of productivity increases and material needs are met, people will naturally pursue spiritual satisfaction. Since the reform and opening up, China's economy has achieved unprecedented development, and the cultural industry has risen rapidly in the course of economic development, as shown in Figure 1. "Data shows that in 2020, the growth rate of residents' consumption of spiritual and cultural products is 9% higher than the growth of consumption of material products, as shown in Table 1. The cultural industry has undoubtedly become a new branch of China's economic growth." But today in this society where technology is taking off and commercialization is strong, the industrialization of culture has also brought some problems. Adorno's critical theory provides another reference for understanding the cultural significance of the cultural industry. We cannot but consider the convenience brought to mankind by the cultural industry.

Judging from the aesthetics of today's popular culture at that time, many works were full of entertainment and interest, and some were very mediocre, but they caused a strong shock to the Chinese people's psychology at that time. In fact, the entertainment and entertainment of popular culture itself, the personalized reading and singing of popular culture, and the innovation of expression methods brought by popular culture all contribute to the politicization, shaping, and grouping of culture and art. During the "Cultural Revolution," some people remember that they had sang "Everyone Has a Red Heart" and "The Great Proletarian Cultural Revolution is Good" before. After the ten-year catastrophe, they could only sing "Water" Jiaocheng and Jiaocheng Mountain. "He has hardened his heart and blood in his pale life, and then, whether he is a 20-year-old student or a student dragging children and girls, on the one hand, they are looking for the key to open the door of knowledge, on the other hand they are also looking for it," "Olive" and "Penghu Bay Grandma" in their dreams. Mass culture is essentially an entertaining and entertaining consumer culture and business culture, but there are a large number of Chinese who have just experienced the so-called "Cultural Revolution" for ten years I find myself lagging behind entertaining and

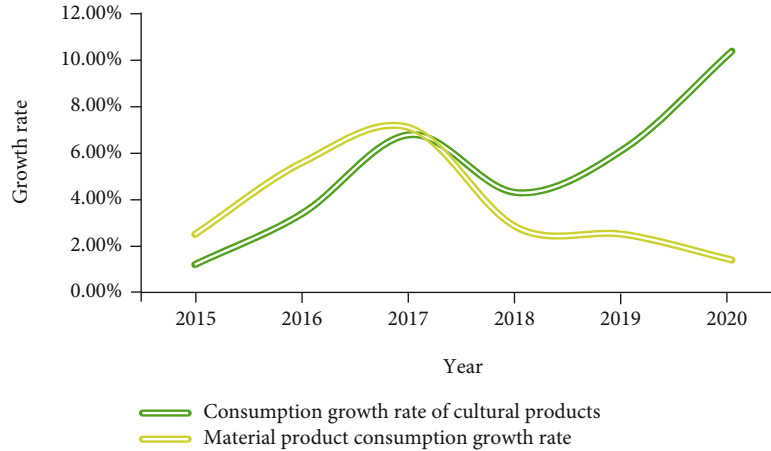


FIGURE 1: The growth rate of consumption of spiritual and cultural products compared with the growth rate of consumption of material products.

TABLE 1: The growth rate of consumption of spiritual and cultural products compared with the growth rate of consumption of material products.

Year	Consumption growth rate of cultural products	Material product consumption growth rate
2015	1.2%	2.5%
2016	3.4%	5.6%
2017	6.8%	7.1%
2018	4.3%	2.8%
2019	6.2%	2.5%
2020	10.4%	1.4%

TABLE 2: Proportion of application of cultural communication media in the Internet environment.

What kind of cultural communication medium do you usually use	Number of people	Percentage (%)
Press	22	8.6
Broadcast	23	9
Television	36	14.1
The Internet	57	22.3
Mobile phone	117	45.8

entertaining. Reading has a deeper meaning. Teresa Teng's soft voice and soothing melody have become, in a sense, people's dissatisfaction with integrated, politicized, and standardized culture and their yearning for secular life. The love story between Hong Kong's large-scale romantic novel and Taiwan not only provides an ideal love model but also provides an ideal state of transition from a rural society to an urban industrial society. It has all the material achievements of industrial civilization, and it retains the poetic and romantic feelings of rural society. This narrative method of dual opposition of good and evil, faith and betrayal, beauty and ugliness, and superiority and humility coincides with the efforts of the bourgeois Chinese to experience the indif-

ference and sense of justice in interpersonal relationships. The long-term class struggle requires warmth, justice and truth, kindness, and beauty.

*4.2. Diversification of Communication Media.* From the perspective of communication science, mass communication generally mainly passes through four media: newspapers, radio, television, and the Internet. Nowadays, mobile phones are sometimes classified as the fifth medium, as shown in Table 2. Each medium has its own characteristics. Newspapers and periodicals break through the limitations of time and space, their content is close to the masses, the readership is wide, and they are easy to collect and read carefully. Compared with newspapers and periodicals, broadcasting can release people's vision, and it also has the advantage of being able to transmit quickly and over long distances. Television and movies integrate audiovisual means to provide people with a wide range of information and entertainment. Figure 2 shows the application proportion of cultural communication media in the Internet environment.

The emergence of the network as the fourth medium has cross-media attributes and breaks through the framework of traditional mass communication. Since the network, information has changed from a linear transmission mode to a highly interactive communication mode. This mode makes the dissemination of information, and acceptance is more random and personal. Many newspapers, radio and television, and other physical media websites have appeared on the Internet. Most of these websites have opened audience feedback platforms. Using this platform, people can comment on news information or program columns, so the media can make timely adjustments to the audience. In this way, the active choice of the company acts on the development of the media. This realizes that the mass communication process described by Fiske is like dialogue and negotiation. It is an activity of exchange and interaction, which can perfectly show the main role of the audience.

The communication function of mobile phones is embodied in the form of short messages. In many cases, mobile phones and the Internet are connected with each

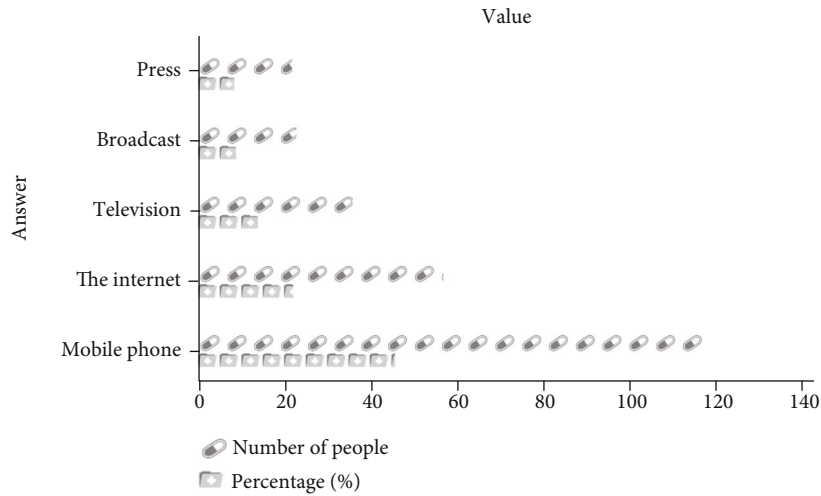


FIGURE 2: Proportion of the application of cultural communication media in the Internet environment.

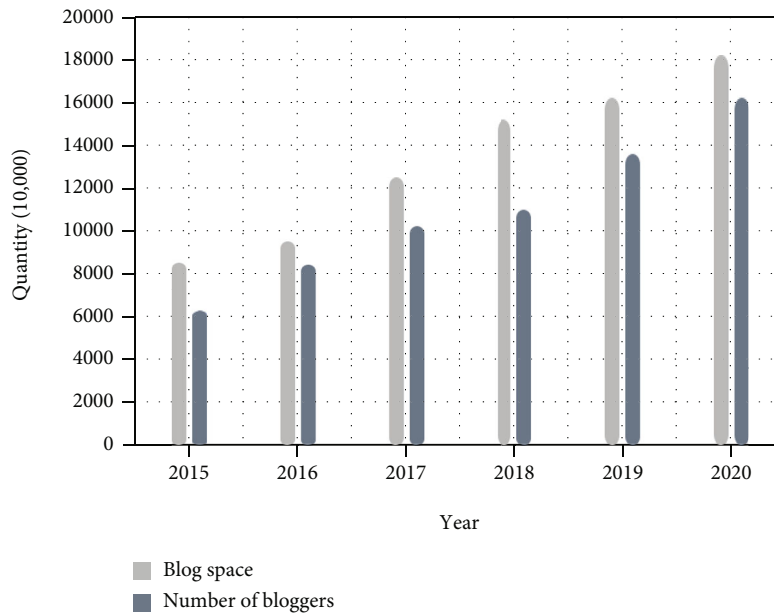


FIGURE 3: Changes in blog usage.

other. The popularization of mobile phones in life now makes this kind of message spreading information ubiquitous. In the event of natural disasters such as earthquakes, droughts, floods, and storms, the government will use text messages to remind the public to pay attention to disaster prevention. Like other media, mobile phone media has also been entertained, and the release of funny text messages has become one of the ways people express emotions. There will also be people with ulterior motives spreading rumors through text messages. For example, after the Wenchuan earthquake in 2008, mobile phone users in many areas received text messages claiming that there would be an earthquake, causing panic. While people enjoy the convenience and entertainment of short messages, they are often troubled by spam and fraudulent short messages. In any case, the diversity of media not only makes more people's

lives more colorful but also proves the value of the audience. Of course, we must also face up to the shortcomings in these media and give full play to their role.

The emergence and rapid promotion of blogs is another iconic phenomenon in the development of popular culture in 2005. Blog (Blog) is a simple way to publish personal information. Anyone can complete the creation, circulation, and update of a personal website through registration. In 2002, the concept of blog was introduced to China and developed rapidly. In 2005, the scale of blogs grew, and the number of blog sites registered by Chinese users exceeded 33 million. Blogs make full use of network interactive functions and timely updates, allowing people to access the most valuable information and resources at the fastest speed. They can also talk with friends, meet friends, and have in-depth exchanges. The blog has brought a great impact to the



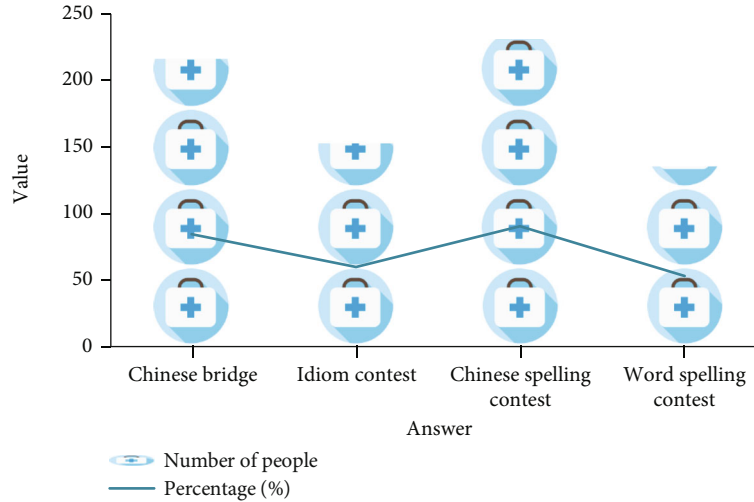


FIGURE 4: Proportion of watching programs with rich knowledge reserves.

TABLE 3: Percentage of watching programs with rich knowledge reserve.

The rich knowledge reserve programs you love to watch (multiple choices)	Number of people	Percentage (%)
Chinese Bridge	215	84.3
Idiom Contest	152	59.6
Chinese spelling contest	230	90.1
Word spelling contest	135	52.9

traditional Chinese writing concept. Its appearance marked the emergence of “civilian writing” and the expression of “civilian voice” in the era of popular culture. “Publishing” in China is the “discourse privilege” of a small number of people, and most of them are silent in front of “words.” The emergence of blogs allows everyone to display their own words instead of the previous writing skills. It must reach a certain level of sophistication and then be printed and published by the publishing agency. Therefore, for a while, blogs have become an ideal space for public expression. As of 2020, the number of blog spaces in China has reached 182.55 million, and the number of blog authors has reached 162.54 million, as shown in Figure 3.

With the increase in the number of subscribers, blogs are integrated into social life at an extremely fast speed and gradually become popular as a basic service based on the Internet, followed by a series of innovative business models such as blog advertising, blog search, corporate blogs, mobile blogs, blog publishing, and independent domain name blogs. In the next few years, as a new media phenomenon, the influence of blogs can surpass traditional media and become the most dazzling cultural phenomenon in popular culture.

*4.3. Ignorance of the Main Body Status of the Masses.* Adorno’s critical theory of cultural industry is too concentrated on the commercialization of culture and the nature of products. It has not done too much explanation and research for the purchasers of goods, that is, the general public, and has

ignored the subjectivity of the people. Almost all the masses are classified as passive receivers, which overemphasizes their passivity and degrades the subjective initiative of the masses. There is no doubt that there will be consumers if there are commodities. Therefore, in the process of consuming cultural industrial products, the role of the masses as consumers is also very important, and the dominant position of the masses cannot be ignored. Some scholars who are engaged in literary writing will still stick to their original intentions, will not be secularized due to the drive of interests, maintain the artistic quality of their works, and reject the commercial nature. Some excellent literary works cannot be bought with money, and writers are unwilling to sell their hard work, leaving them to enjoy with Bole who knows art. When watching a variety of TV dramas and TV programs, not all audiences will follow the plot, and people with discernment awareness are still common. No matter how true the advertising is or how superb the screenwriter’s skills are, there will always be some viewers who will turn off the TV dismissively or transfer to other TV stations. For example, CCTV produced Chinese Bridge, Idiom Contest, Chinese Characters Spelling contests, word spelling contests, and other programs. This type of program allows the audience to appreciate the talents of the contestants while enriching their knowledge reserves. While appreciating the wonderful performances of the contestants, more people are encouraged to participate in it, and also improved their cultural literacy as shown in Figure 4. Moreover, Adorno did not realize that in modern society, the needs of the masses are objective, but he has not clearly solved such problems. It is also impossible for the public’s cultural needs to be completely satisfied. Adorno clearly saw this point, but he did not conduct a more detailed study on this. Table 3 shows the watch ratio of rich knowledge reserve programs.

## 5. Conclusions

How to use scientific popular culture criticism to guide the development of popular culture and improve the aesthetic

connotation of serving the people is an urgent problem to be faced and solved in our country's popular culture criticism circles. This paper digs deep into the cultural connotation for aesthetic criticism and pays attention to the commercial criticism of popular elements of popular culture from the perspectives of economics and communication. It also conducts technical and media criticism of the high-tech technological connotations contained in popular culture. The research conforms to the humanistic orientation and cultural compatibility characteristics of popular cultural criticism and fully and effectively reveals the connotation of popular cultural texts.

### Data Availability

The data underlying the results presented in the study are available within the manuscript.

### Disclosure

The author confirms that the content of the manuscript has not been published or submitted for publication elsewhere.

### Conflicts of Interest

There is no potential conflict of interest in our paper.

### References

- [1] G. Vangelis, "The relevance of the theory of pseudo-culture," *Continental Philosophy Review*, vol. 52, no. 3, pp. 311–325, 2019.
- [2] A. S. Carvalhal, G. Costa, and M. Embirucu, "Evaluation of non-electrolyte hydrogel swelling and its pressure effects with simple equation of state and mechanical models using liquid–liquid equilibrium data," *Industrial and Engineering Chemistry Research*, vol. 59, no. 50, pp. 21969–21981, 2020.
- [3] C. H. Lee, X. Zhao, and Y. C. Lee, "Service quality driven approach for innovative retail service system design and evaluation: a case study," *Computers & Industrial Engineering*, vol. 135, pp. 275–285, 2019.
- [4] S. A. Tacey, T. Szilvási, J. J. Schauer, and M. Mavrikakis, "Computational chemistry-based evaluation of metal salts and metal oxides for application in mercury-capture technologies," *Industrial and Engineering Chemistry Research*, vol. 59, no. 19, pp. 9015–9022, 2020.
- [5] B. Sun, W. Ma, and X. Chen, "Variable precision multigranulation rough fuzzy set approach to multiple attribute group decision-making based on  $\lambda$ -similarity relation," *Computers & Industrial Engineering*, vol. 127, pp. 326–343, 2019.
- [6] H. Liang, D. Zou, Z. Li, M. J. Khan, and Y. Lu, "Dynamic evaluation of drilling leakage risk based on fuzzy theory and PSO-SVR algorithm," *Future Generation Computer Systems*, vol. 95, pp. 454–466, 2019.
- [7] S. Ada, "Creating critical mass in cultural management education: learning from an arts and cultural management programme in Turkey," *Arts and Humanities in Higher Education*, vol. 18, no. 2-3, pp. 159–177, 2019.
- [8] V. Giannakakis, "Neoliberalism and culture in higher education: on the loss of the humanistic character of the university

and the possibility of its reconstitution," *Studies in Philosophy and Education*, vol. 39, no. 4, pp. 365–382, 2020.

- [9] L. Zhao, Q. Shao, and J. Li, "Evaluation of urban comprehensive carrying capacity: case study of the Beijing–Tianjin–Hebei urban agglomeration, China," *Environmental Science and Pollution Research*, vol. 27, no. 16, pp. 19774–19782, 2020.

## Research Article

# The Influence of Wireless Network Communication and Edge Computing on the Performance of Aerobics Athletes

**Xiaoshuang Qi** 

*Department of Sports, Suzhou Industrial Park Institute of Service Outsourcing, Suzhou 215000, Jiangsu, China*

Correspondence should be addressed to Xiaoshuang Qi; [qixsh@siso.edu.cn](mailto:qixsh@siso.edu.cn)

Received 30 December 2021; Revised 19 January 2022; Accepted 26 January 2022; Published 24 February 2022

Academic Editor: Shalli Rani

Copyright © 2022 Xiaoshuang Qi. This is an open access article distributed under the Creative Commons Attribution License, which permits unrestricted use, distribution, and reproduction in any medium, provided the original work is properly cited.

As aerobics began to be included in one of the international sports competitions, China began to pay attention to it. How to improve the performance of aerobics athletes has become a top priority. This article aims to study how to improve the performance of aerobics athletes through some high-tech techniques. To this end, this article proposes a method of combining wireless network communication and edge computing algorithms to obtain aerobics athletes' bodybuilding actions through wireless network communication and use edge computing to conduct a comprehensive analysis of related data. At the same time, experiments were designed to explore its performance and actual use effects. The experimental results of this article show that the improved performance of the athletes has increased by 13%, which can help aerobics athletes to establish an advantage in terms of performance.

## 1. Introduction

Competitive bodybuilding operation is an international competitive sports project, which has a history of more than 30 years since it sprouted in the United States in the early 1980s and was introduced to my country in the late 1980s. Although competitive aerobics started late, it has developed rapidly. With the reform of the competition mechanism, the continuous reduction of the competition gap between athletes, the continuous improvement of the level of competition and the intensification of competition. For athletes of equal strength, the success or failure of the game is often determined by the athlete's competitive state during the game. Judging from the achievements of the Chinese aerobics team in the World Cup series held in this year in 2012, due to the lack of experience in major competitions among the young players born in the 90s in China, the cooperation between collective projects is insufficient, the completion of the new set is not skilled enough, and the completion of difficult skills is not stable enough. So the results of the competition are not satisfactory. This series of reasons can be attributed to the instability of the athletes' prematch

competitive state, especially the psychological competitive state, which affects their own performance in the competition.

Most experts, scholars, coaches, and athletes have recognized and valued the influence and role of athletes' competitive state in the competition. At present, most of the research on "competitive state" discusses its concept, content classification, characteristics, regulation, etc. from a qualitative perspective. The research on the competitive status of athletes in different sports is also mainly focused on the research of training, physical function or psychology, and the research on the competitive status of competitive aerobics is also limited to the psychological aspect. Moreover, these studies are basically the researcher's judgment on the broad sense of discussion and experience, lack of objective and unified standards, and there is no quantitative analysis of the precompetitive state of a specific sport, which will be more meaningful to guide practice.

After the use of the computing power of edge computing to help more aerobics athletes to enhance their liquidity was proposed, more and more people began to invest in this research. Ma proposed that when organizing aerobics, each

movement should be carefully designed to make the choreographed movements have a comfortable and pleasant feeling. The movements do not look too rigid, giving people an overall sense of beauty and aerobic exercise. The characteristics are expressed in the design of the action to achieve better results. His research found that the current aerobics combines the knowledge of dance and music, and its manifestations are diverse [1]. Cunha et al. proposed that water aerobic exercise is widely recommended to the elderly. Therefore, he evaluated the effect of water aerobic exercise on the blood pressure of elderly women with hypertension. A heart rate monitor is used to monitor the heart rate, and a semiautomatic monitor is used to measure systolic blood pressure (SBP) and diastolic blood pressure (DBP) before and after training and 10, 20, and 30 minutes after training [2]. Taleb et al. introduced the survey of MEC, focusing on basic key enabling technologies. He elaborated on the MEC orchestration, while considering a single service and the MEC platform network that supports mobility, bringing brilliance to different orchestration deployment options. In addition, he analyzed the MEC reference architecture and main deployment scenarios to provide multi-tenant support for application developers, content providers and third parties [3]. Ke et al. proposed a cloud-based mobile edge computing (MEC) offloading framework in vehicle networks. In this framework, he studied the effectiveness of the calculation transmission strategy for vehicle-to-infrastructure (V2I) and vehicle-to-vehicle (V2V) communication modes. Taking into account the time consumption of computing tasks and the mobility of vehicles, he proposed an effective predictive combination mode degradation scheme in which tasks are adaptively offloaded to the MEC server through direct upload or predictive relay transmission [4]. He et al. first introduced the deep learning of the Internet of Things to the edge computing environment. Due to the limited processing power of existing edge nodes, he also designed a novel offloading strategy to optimize the performance of IoT deep learning applications through edge computing. The evaluation results show that his method is superior to other optimization solutions in terms of deep learning of the Internet of Things [5]. Yu et al. proposed that the Internet of Things (IoT) now penetrates into our daily lives, providing important measurement and collection tools for every decision we make. Compared with the well-known cloud computing, edge computing migrates data computing or storage to the “edge” of the network, close to the end users. Therefore, multiple computing nodes distributed on the network can offload the computing pressure from the centralized data center and can significantly reduce the delay of message exchange [6]. Nastic et al. propose a novel method to implement cloud-supported real-time data analysis in edge computing applications. He introduced their serverless edge data analysis platform and application model, and discussed their main design requirements and challenges based on real healthcare use case scenarios [7]. Chen et al. designed a resource-efficient edge computing solution so that users of smart IoT devices can well support their computing-intensive tasks through proper task offloading of local devices, nearby auxiliary devices, and nearby

edge clouds. Performance evaluation confirmed the effectiveness and superior performance of the proposed resource-efficient edge computing scheme [8]. The abovementioned documents mainly introduced related edge computing algorithms, expressiveness of aerobics, and wireless communication networks. It is also very in place for their respective technical descriptions, and the depth of research on some technologies is also worth learning. However, there is no literature that discusses the combination of these types of research and conducts related research on them.

The innovation of this article is to use wireless network communication and edge computing as the technical support to conduct a comprehensive collection of aerobics athletes’ bodybuilding movements. And use the computing power of edge computing to analyze and guide it, helping aerobics athletes to improve related actions and enhance their performance. At the same time, experiments and analysis are designed to test the calculation performance and data acquisition ability and to explore the range of improving aerobics athletes.

## 2. Wireless Sensor Communication Method

### 2.1. Wireless Sensor Network

*2.1.1. The Overall Structure of the Wireless Communication System.* The overall structure of the system is mainly composed of three parts (ZigBee terminal node, gateway, and host computer) as shown in Figure 1 [9]. The terminal node can be connected with the workshop or factory area meter, the home appliance equipment in the smart home, and so on, and read and write the data of the meter or equipment through the serial port and upload it to the gateway through the ZigBee wireless network [10]. The gateway is the core controller of the entire ZigBee network, so as to realize the communication between the upper computer and the underlying equipment (mainly responsible for the network establishment and maintenance of the entire network and responsible for the protocol conversion between Ethernet and ZigBee networks). The gateway includes a ZigBee coordinator, a WiFi module, a wireless router, an Ethernet interface, and other modules [11]. Among them, the WiFi module and the Ethernet interface, respectively, provide wireless and wired modes to communicate with the host computer; the built-in wireless router in the gateway is responsible for establishing the WiFi network; the ZigBee coordinator is responsible for setting up a ZigBee network to realize data exchange with ZigBee terminal nodes. A BOA server is built in the gateway, and users can access the gateway through the Web and configure the network. The upper computer is used to configure and monitor the system and only supports three forms (desktop, notebook, and Android handheld terminal) [12].

*2.1.2. Wireless Sensor Network Protocol.* As shown in Figure 2, the communication protocol layer can be divided into the physical layer, the link layer, the network layer, the transport layer, and the application layer. The network management plane can be divided into the energy

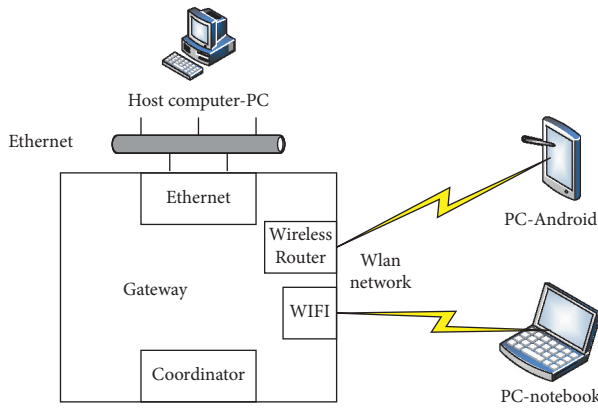


FIGURE 1: The overall structure of the system.

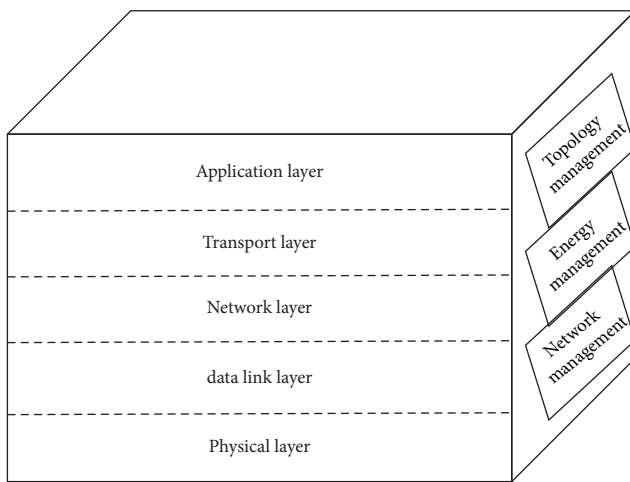


FIGURE 2: Wireless sensor network protocol stack structure diagram.

management plane, the mobility management plane, and the task management plane [13].

The wireless sensor network is divided into three structures (star, mesh, and hybrid networks). The star network is a single-hop network, and all terminal nodes can exchange data with routers and gateways. The mesh network is a multihop network, and all terminal sensor nodes can directly transmit data in both directions and can also communicate with the base station [14]. The hybrid network not only has the advantages of low power consumption and simplification of the star network but also has the advantages of long-distance transmission and automatic repair of the mesh network [15].

**2.1.3. Wireless Node Hardware Design.** The wireless node hardware structure includes a CPU part, a reset circuit part, a clock circuit part, a radio frequency antenna part, a power circuit part, and a data acquisition part. As shown in Figure 3, the data acquisition part provides a serial port to communicate with the test instrument [16]. The wireless node adopts the on-board antenna and reserves an external antenna interface. Also consider anti-interference issues in

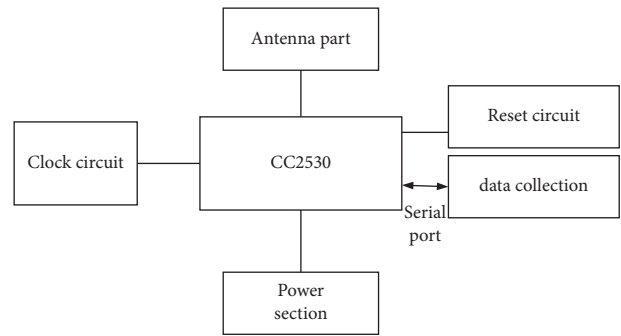


FIGURE 3: Wireless node hardware structure.

hardware design, and try to avoid interference between components and lines through reasonable layout and wiring [17].

**2.1.4. Wireless Gateway Hardware Design.** According to the application requirements of the wireless gateway, the hardware structure of the gateway is shown in Figure 4. Among them, the ZigBee wireless node adopts the same hardware design as the wireless gateway [18]. In view of the hardware and software functional requirements of this data server, the core controller adopts Samsung processors, and the hardware modularization is divided into two-layer board structures (core board and bottom board), which is convenient for design and maintenance [19].

The core controller uses Samsung processors, and the gateway uses ARM processors (compared with other 8-bit or 16-bit single-chip microcomputers, it has a faster processing speed and at the same time makes the entire system have better scalability) [20]. The ARM processor occupies a pivotal position in the embedded field with its high-speed data storage speed, flexible development tools, powerful instruction system, and a wide range of applications [21].

**2.2. Communication Model.** In the mobile edge computing system, communication mainly occurs between the mobile device and the MEC server. The MEC monthly server is a small data center deployed by cloud computing service providers or operators on wireless access points such as base stations and routers. Wireless access points not only provide wireless communication air interfaces for mobile devices and MEC servers, but also connect to large data centers located in the core network. It can help MEC servers to further offload computing tasks to large data centers or other MEC servers [22].

Some commercial wireless communication technologies mainly include NFC, Bluetooth, WiFi, and LTE. These wireless communication technologies can support the communication requirements of mobile devices and MEC servers at different transmission rates and different distances. The table lists the main characteristics of these typical wireless communication technologies [23]. For example, maximum coverage, frequency spectrum, and data transmission rate. NFC technology has a small coverage area and

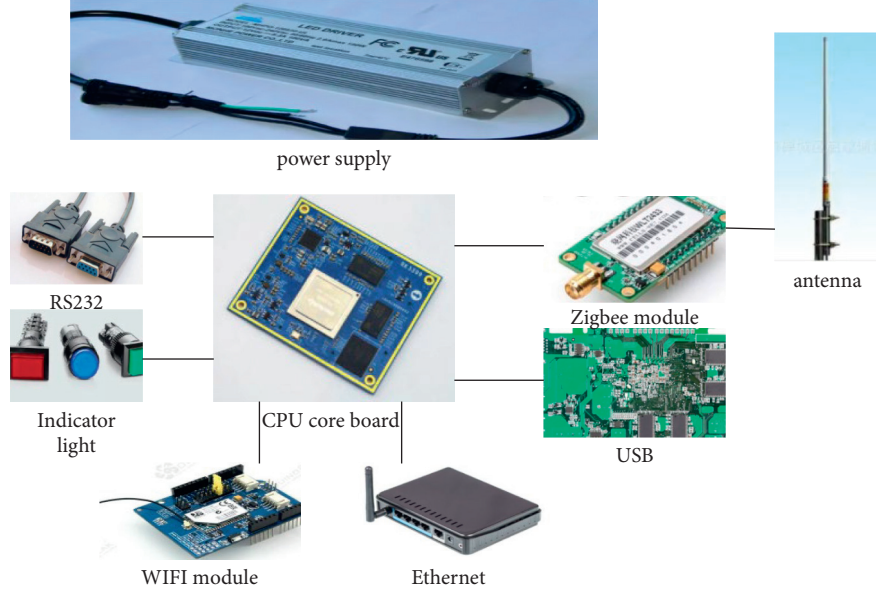


FIGURE 4: Wireless gateway hardware structure.

a low data transmission rate, which is suitable for services that require a small amount of information exchange, such as payment services [24]. RFID is similar to NFC, but only supports simplex communication. Compared with NFC and RFID, Bluetooth technology has a higher transmission rate, which can make the communication between mobile devices and MEC servers faster and more efficient in short-distance scenarios [25]. In long-distance scenarios, WiFi and LTE are two very effective communication methods. Related technical parameters are shown in Table 1.

Based on the several wireless communication methods listed in this section, according to Shannon's formula, the maximum data transmission rate at which the mobile device sends the data volume of the subtask to the MEC server is obtained, as shown in the following formula:

$$R = B * \log_2 \left( 1 + \frac{HP_{tr}^i}{\delta^2} \right). \quad (1)$$

For mobile devices, computing performance is determined by CPU performance, and CPU performance is controlled by CPU frequency. The locally calculated time is shown in the following formula:

$$t_{cp}^{iO} = \frac{D_i * X_i}{f_o}. \quad (2)$$

Mobile devices are battery-powered and energy-constrained devices. Therefore, when dealing with computationally intensive tasks, the battery energy consumed is a very important consideration. The energy consumed by the subtask calculation on the mobile device can be expressed as the following formula:

$$E_{cp}^{iO} = k_o D_i X_i f_o^2. \quad (3)$$

According to Shannon's formula, the maximum transfer rate from a mobile device to the MEC server is as follows:

$$R_j = B * \log_2 \left( 1 + \frac{HP_{tr}^i}{\delta^2} \right). \quad (4)$$

The transmission energy consumption is equal to the transmission power multiplied by the transmission time, as shown in the following formula:

$$t_{tr}^{ij} = \frac{D_i}{R_j}, \quad (5)$$

$$t_{tr}^{ij} = \frac{D_i}{B * \log_2 \left( 1 + \left( \frac{HP_{tr}^i}{\delta^2} \right) \right)}, \quad (6)$$

$$E_{tr}^{ij} = P_{tr}^i * t_{tr}^{ij}, \quad (7)$$

$$E_{tr}^{ij} = \frac{D_i}{B} * \frac{P_{tr}^i}{\log_2 \left( 1 + \left( \frac{HP_{tr}^i}{\delta^2} \right) \right)}. \quad (8)$$

The energy consumed is shown in the following two formulas:

$$t_{cp}^{ij} = \frac{D_i * X_i}{f_i}, \quad (9)$$

$$E_{cp}^{ij} = k_j D_i X_i f_j^2. \quad (10)$$

The optimization goal of this chapter is to find a solution for offloading decision-making and power allocation, which minimizes the system energy consumption of a certain separable computing task under a given time limit. The offloading decision and power allocation scheme refer to the MEC server to which several independent subtasks on the mobile device should be offloaded for execution or should be left on the local device for execution, and how much transmit power the mobile device should allocate for each subtask. The problem can be formulated as formulas:

TABLE 1: Comparison of wireless communication technologies.

	NFC	RFID	Bluetooth	WiFi	LTE
Coverage distance	10 cm	3 m	100 m	100 m	100 km
Frequency	13.56 MHz	13.56–960 MHz	2.4 GHz	2.4 GHz 5 GHz	700–2600 MHz
Rate	414	100–200 B/s	22 Mbps	135 Mbps	300 Mbps

$$\min_{a,p} \sum_{i=1}^N (E_{tr}^i + E_{cp}^i), \quad (11)$$

$$t_{tr}^i + t_{cp}^i \leq \tau, \quad \forall i \in \{1, 2, 3 \dots N\}, \quad (12)$$

$$\sum_{i=1}^N P_{tr}^i \leq P_{\max}. \quad (13)$$

Assigning subtasks to a device for calculation has a certain cost. The physical meaning of edge weight is the cost of energy consumption (transmission energy consumption + computing energy consumption). In particular, for a certain subtask, if the offloading decision is calculated locally on the mobile device, then the edge weight only includes the calculation energy consumption. It was shown as the formula for details.

$$\text{edge}[i][j] = E_{cp}^{i0}, \quad j = 0, \quad (14)$$

$$\text{edge}[i][j] = E_{tr}^{ij} + E_{cp}^{ij}, \quad j! = 0. \quad (15)$$

This algorithm is based on depth-first search or breadth-first search and has low computational complexity. In the simulation data, it is found that the transmission energy consumption is far less than the calculated energy consumption, and its order of magnitude is very small. Therefore, it can be approximated as follows:

$$\text{edge}[i][j] = E_{cp}^{ij}. \quad (16)$$

In the previous step, the calculation of total energy consumption has been minimized, and the problem becomes as follows:

$$\min \sum_{i=1}^N E_{tr}^i = \sum_{i=1}^N \frac{D_i}{B} * \frac{P_{tr}^i}{\log_2(1 + HP_{tr}^i/\delta^2)}. \quad (17)$$

The constraints remain unchanged.  
First, create the function as follows:

$$f(x) = \frac{x}{\log_2(1 + Ax)}. \quad (18)$$

The first derivative of  $f(x)$  is as follows:

$$f'(x) = \frac{\log_2(1 + Ax) - (Ax)/((1 + Ax)\ln 2)}{\log_2^2(1 + Ax)}. \quad (19)$$

It can be proved that when  $x > 0$ ,  $f'(x) > 0$ . Therefore,  $f(x)$  increases as  $x$  increases. Therefore, we can get the analytical solution as follows:

$$P_{tr}^i = \frac{\left(2^{D_i/(\tau - t_{cp}^i)} - 1\right) \sigma^2}{H_i}. \quad (20)$$

Among them,  $B$  is the line channel bandwidth,  $H$  is the channel gain, and  $P_{tr}^i$  is the transmit power allocated by the mobile device for the subtask.  $D_i$  and  $X_i$  represent the total number of time cycles required to process subtasks.  $f_0$  is the CPU frequency of the mobile device.  $\delta^2$  is the noise power.

**2.3. Mobile Edge Computing Network Design.** At present, most of the work related to mobile edge computing in the world is in the research stage. According to the future development trend of the access network and the basic needs of users for the access network, this paper mainly studies the mobile edge computing networking model. It designs a mobile edge computing platform architecture that integrates access networks and cloud computing capabilities and conducts related functional tests. This chapter will elaborate on these contents.

The application scenario of the mobile edge computing architecture is shown in Figure 5. Mobile users establish connections with the mobile edge network through base stations (such as LTE macro base stations, 3G wireless network controllers, and multitechnology convergence access points). The edge server is deployed at the location closest to the base station equipment and is physically connected to the base station equipment. The edge server has the ability to process and control user data traffic at the same time. The user's request and network message are sent to the local MEC server through the wireless access network. On the edge server, there are forwarding and filtering rules deployed by mobile network operators to control user traffic, as well as applications and services from third-party service providers. Therefore, at the edge of the mobile network, the edge server can both process and forward the user's request. After the edge server receives the user request from the wireless access network, it makes a corresponding response. When the local server can handle the user request, it can directly provide the corresponding cloud service. When the corresponding service is not used in the local edge server, the request can be forwarded to the edge server in the neighboring area, or the user request can be directly forwarded to the core network for processing.

In traditional mobile cloud computing, user requests and information are first transmitted to the central processing unit that provides mobile network access services. After being authenticated and authorized by the network operator, it is forwarded to the cloud data center via the mobile core network to obtain different services (such as databases, virtualized

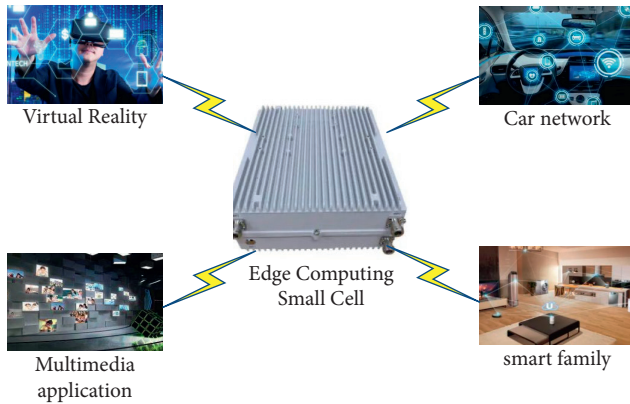


FIGURE 5: Schematic diagram of mobile edge computing application scenarios.

resources, computing resources, and storage services). Different from mobile cloud computing, in the mobile edge computing architecture, the functions of the cloud data center are migrated to the edge of the mobile network, and they directly process and respond to user requests on the wireless access network. Using distributed edge servers and wireless access networks, users can support a variety of applications, for example, high-definition video distribution, augmented reality, human-computer interaction, location services, data caching, mobile big data analysis, etc.

**2.3.1. MEC Platform Architecture.** With the continuous expansion of the influence of SDN and NFV, as well as the further development of cloud computing and edge computing, the softwareization of telecommunications and network systems has become a key promotion factor. In order to meet the user needs of next-generation networks and the basic requirements of ICT convergence, the software architecture of mobile computing and edge network convergence has been extensively studied in industry and academia.

The basic relational model of mobile edge computing proposed by ETSI is shown in Figure 6. In order to meet the needs of system management and scalability, the cloud platform adopts a layered structure to realize the virtualization of physical resources and the unified management of virtualized resources. At the same time, the mobile edge computing platform should also provide an interface to manage the entire platform. The operator manages the application platform, application life cycle, and other operations on the application through this interface. In addition, according to the requirements of mobile edge computing, the edge cloud platform also provides infrastructure services (communication services and service registration), wireless network information services, and traffic offloading services.

(1) *Communication Services.* Through a specially designed system interface, applications running on the platform can communicate with each other through infrastructure services. In addition, infrastructure services also support

communication between applications and platforms. The communication service module can achieve the purpose of one-to-many message publishing and application decoupling, and at the same time can provide a protection mechanism to defend against malicious applications.

(2) *Service Registration.* Provide a list of service types supported by the edge server, and provide flexible deployment strategies for applications through decoupling. In addition to the service list, the service registration module also provides related interfaces and their versions. Applications can use it to discover and locate required service locations and broadcast their own location to provide services to other applications.

(3) *Wireless Network Information Service.* Mobile edge computing allows applications running on edge servers to obtain real-time network and wireless information. The wireless network information service module in the platform can provide corresponding edge network information for certified applications. Third-party applications can perform high-level processing based on this open network information. The information provided by this module is mainly user equipment access-related information (such as QoS and cell ID), user-related measurement, and statistical information.

(4) *Traffic Offloading Module.* The traffic offloading module can control the traffic on the entire wireless access network at the data packet level. The traffic of those authenticated applications can be prioritized by setting rules. It plays an important role in the flow balance and QoS of the entire system.

**2.3.2. The Key Realization Technology of MEC Networking Scheme.** Network function virtualization, software-defined networking, and edge operating systems are key technologies in the implementation of mobile edge computing networking. Network function virtualization technology can realize the orchestration and management of computing and storage resources in mobile edge computing; software-defined network technology can realize the programming of edge network resources; and the edge operating system ensures the scalability of the entire mobile edge computing platform and speeds up the deployment of edge cloud.

Through the layered structure, the edge operating system can realize the abstraction and flexible allocation of physical resources such as computing, storage, and networking. At the same time, the recursive structure ensures the scalability and expansibility of the edge operating system and can flexibly control the scale and coordination of edge data centers.

### 3. Edge Computing Platform Performance Test Experiment

**3.1. Performance Test.** In this section, we will discuss and analyze the performance of the edge computing platform. It mainly includes network forwarding delay performance,



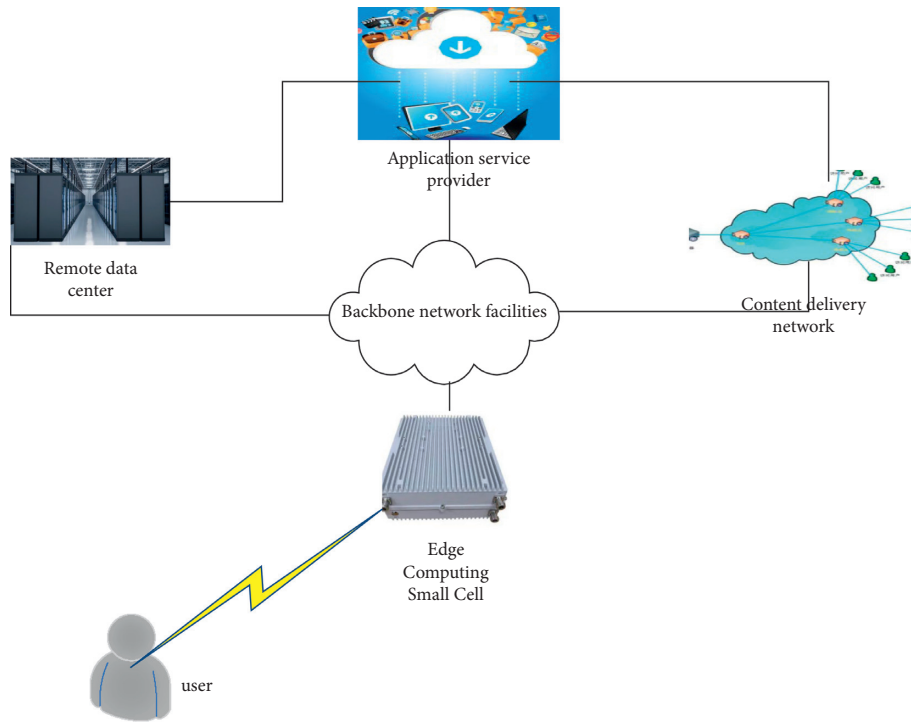


FIGURE 6: The basic relational model of mobile edge computing.

request processing capacity, power consumption performance, migration efficiency, and performance evaluation of container service orchestration. In each experiment, we introduced in detail the experiment preparation, the experiment process, and the experiment result analysis. In our experimental environment, the main equipment configurations used are shown in Table 2.

First of all, regarding the network forwarding delay, it will compare the network packet transmission round-trip time (RTT) of the EIS with that of the OvS installed with commercial SDN switches (CentecV350-8TS12X) and wireless routers. Two EIS devices with different hardware architectures were used during the experiment: the Raspberry3B single-board computer based on the ARM architecture and MinnowBoard Turbot single-board computer based on the x86 architecture. The prices of the two devices are about RMB280 and RMB2000, respectively. This comparison can not only analyze the performance pros and cons of platform EIS nodes compared to commercial switching equipment but also select node types within the platform cluster based on cost factors. It is worth pointing out that because DPDK running on Raspberry3B will bring equipment performance bottlenecks, we did not install DPDK on Raspberry, but instead only implemented OvS+DPDK practice on Turbo devices. In the experiment, we connect the two hosts through the abovementioned four different switching devices to form a single-hop network connection. Several experiments were performed during the measurement process, and the ping command of the Linux system was used to send five different data packet sizes from one host to another host for testing, recording the delay result, and calculating the average value. The specific values are shown in Table 3.

The results show that Turbot can reach the level of commercial SDN switches due to its own Gigabit Ethernet interface, combined with the optimization of DPDK technology. When the data packet size is increased from 64 bytes to 1024 bytes, it has better stability. When pursuing EIS nodes with high network performance in the edge network environment, Turbot will be the first choice. Although the network forwarding performance of Raspberry equipment is not as good as that of commercial switches, it is significantly better than ordinary routing and switching equipment. It is especially suitable as a low-cost network node pursuing high cost performance in the Internet of Things scenario. It cannot be ignored that the network switching nodes implemented by the platform all support the OpenFlow protocol, which can extract the control logic to the SDN controller for unified management. While EIS completes the network switching function, it can still carry the function of the service node at the same time, which is impossible for ordinary network equipment.

Request processing capacity due to the hardware difference between EIS and rack servers. The processing power of a single EIS is far inferior to that of rack servers. We designed experiments to compare the request processing capabilities of EIS single node, EIS cluster, and rack server (DELLR720) through service request response time. During the experiment, we used 8 EIS (Raspberry3B) devices to form a service cluster, and at the same time, we built a single-node service on one EIS and one rack server. We installed the ApacheBench stress test tool on the client to simulate 100 users to send 1000 data requests to single EIS, 8EIS clusters, and rack servers (request file size is 4 MB), and record the service response time.

TABLE 2: Test environment specific configuration.

Equipment	Model	Configuration	Price
Mobile terminal	Xiaomi Mix	4 GB RAM	\$3500
Edge intelligence server	Raspberry 3B	Broadcom BCM2837	\$250
SDN switch	Centec V350-8TS12X	8 * 1000Base-X	\$30000

TABLE 3: Comparison of network forwarding delay.

Bytes	Wireless router	Raspberry-EIS	Turbot-EIS	SDN switch
64	0.64	0.6	0.39	0.34
128	0.65	0.61	0.4	0.38
256	0.67	0.63	0.41	0.4
512	0.68	0.65	0.4	0.41
1024	0.85	0.65	0.47	0.58

The experimental results show that the response time of a single EIS is quite different from that of a rack server, and 10% of requests will not get a better quality of experience. However, using 8 EIS to process experimental requests in a distributed manner can achieve a response time similar to that of the rack server, and the overall difference is small. It is worth emphasizing that the price of a commercial server is about RMB 16000, and the cost of 8 EIS is about 1/7 of that of a commercial server. We achieved service request processing performance similar to that of commercial servers at a cost of 1/7. This shows that when processing computing tasks and requests similar to those found in the Internet of Things environment, the EIS platform can provide lightweight and cost-effective request processing capabilities at the user edge. The specific data are shown in Table 4.

**3.2. Power Performance.** Regarding power consumption performance, we compared EIS nodes with commercial servers (DELLR720), commercial SDN switches (CentecV350-8TS12X), and wireless routers (TP-LINKTL-WDR7500). During the experiment, we used a power tester (UNI-TUT230C) for testing, connected the abovementioned equipment with the tester, and modified the CPU load through the stress test tool, and recorded the test results after multiple measurements. The specific values are shown in Table 5.

It can be seen from the abovementioned table that the CPU is idle, the CPU usage rate is 50%, and the CPU usage rate is 100%. The power consumption of EIS nodes is lower than commercial servers and switches and even close to wireless routers. The experimental results fully verify the low power consumption characteristics of the EIS equipment in the platform when providing services.

## 4. Wireless Network Simulation Analysis

**4.1. Comparison of Average Data Packet Exchange Times of Intermediate Nodes.** In the case of a given network size ( $N=1200$ ), Figure 7 shows the average number of data packet exchanges of the intermediate nodes of the three mechanisms under different maximum replication times value  $Y_{max}$ , that is, the average energy consumption of the intermediate nodes. Since the COPE mechanism and the ER mechanism are not

TABLE 4: Comparison of request processing capabilities.

	Rack server	1-EIS	8-EIS
50%	0.38	0.42	3.21
75%	0.41	0.43	3.82
90%	0.62	0.67	4.48
98%	0.81	0.98	5.84
100%	0.91	1.12	7.01

TABLE 5: Power consumption comparison.

	CPU idle	50% CPU usage	100% CPU usage
EIS	4	6	9
Rack server	121	214	391
SDN switch	37	41	59
Wireless router	4	6	8

limited to the number of data packet replications, the average number of data packet exchanges at intermediate nodes will not change. When the maximum copy time value is low, the average data packet exchange times of the intermediate nodes of the CRNC mechanism are much lower than those of the ER mechanism and the COPE mechanism. Therefore, the energy consumption of the intermediate node is low as the limit of the maximum number of replications is approaching the minimum number of replications required to infect the entire network Ynet. The average number of data packet exchanges of the intermediate nodes of the mechanism also gradually rises and approaches the COPE mechanism. The CRNC mechanism based on network coding can complete the duplication of multiple source-code data packets in one data packet exchange process, which improves the transmission efficiency, and the energy consumption level can always be kept under the ER mechanism.

For the comparison of transmission delays, first analyze the performance comparison of the three mechanisms in the case of unlimited energy. As shown in Figure 8, when the maximum number of replications is close to the minimum number of replications required to infect the entire network, the transmission delay of the CRNC mechanism will gradually decrease, and its performance will approach the COPE mechanism. Compared with Figure 7, when the maximum copy time value is low, for example, from 1 to 6, compared to the COPE mechanism, the CRNC mechanism

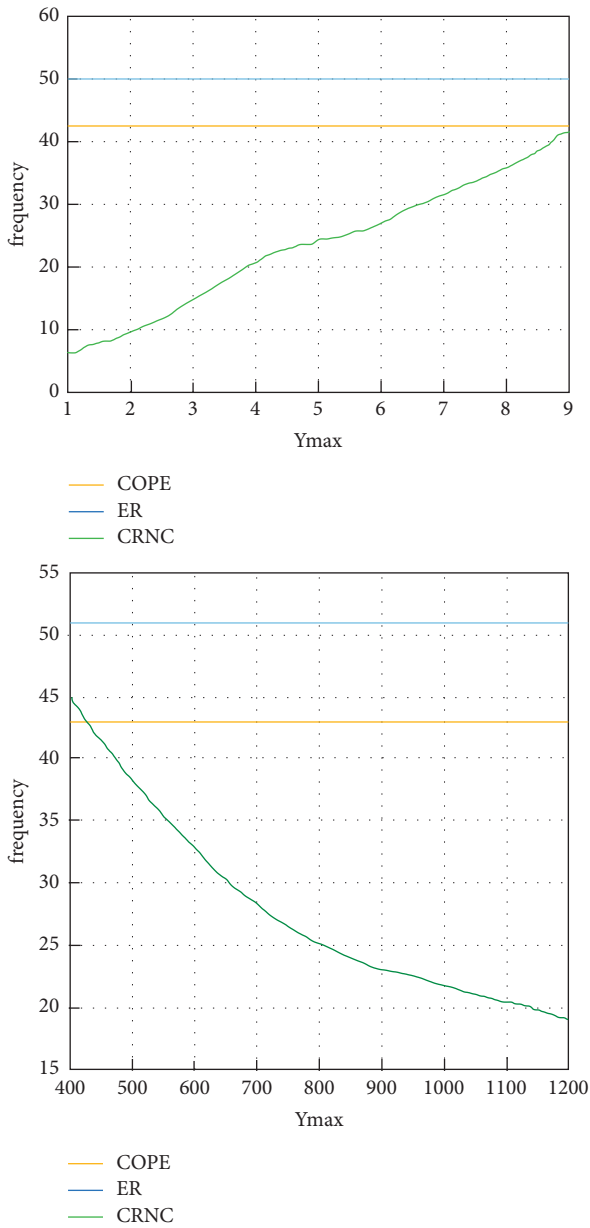


FIGURE 7: The relationship between different factors and the number of data packet replication.

greatly reduces the average number of data packet exchanges of the intermediate node. The cost of transmission delay is relatively low. Obviously, the performance of the CRNC mechanism in terms of transmission delay is always better than that of the ER mechanism.

The simulation experiments can show that if it is assumed that network resources such as transmission bandwidth, node cache, and node computing power are sufficient, compared with the ER mechanism and COPE mechanism based on flooding replication, the CRNC mechanism based on network coding will slightly increase the transmission delay. The purpose of simulation is to simulate the limited transmission bandwidth in practical applications. The CRNC mechanism can pay a lower transmission delay cost in exchange for greatly reducing the total number of transmissions required

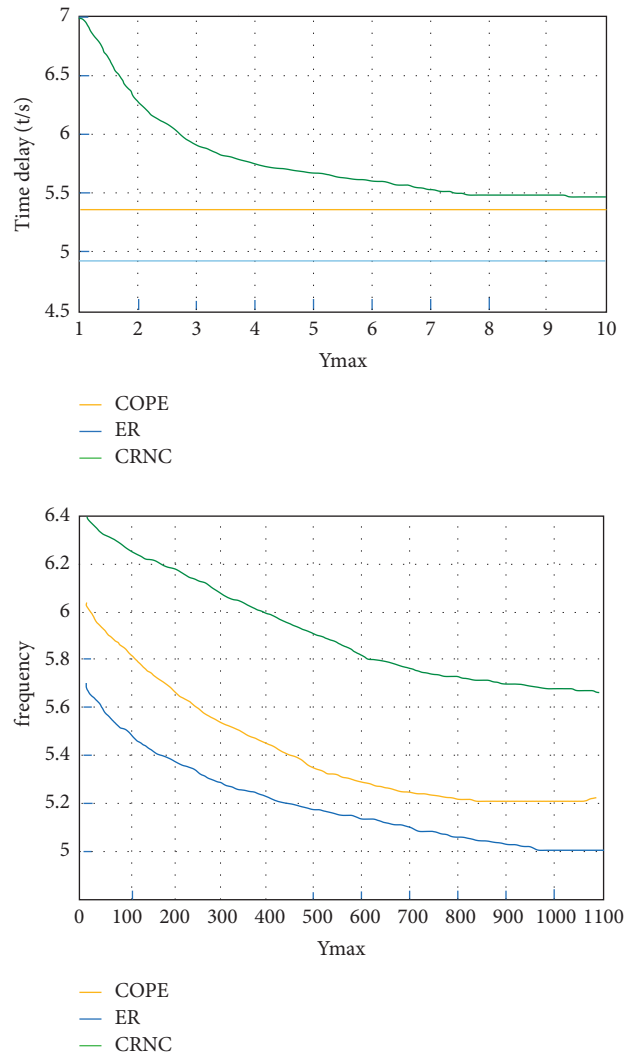


FIGURE 8: The relationship between different factors and transmission delay.

by the sink to receive complete source information, that is, the total energy overhead. Therefore, in a wireless ad hoc network with limited energy, network coding can achieve a balance between increasing network throughput gain and reducing energy consumption.

*4.2. Reasons for Choosing to Optimize the Sum of Distances within the Class First.* Separate the sum of intraclass distances from the sum of interclass distances for optimization, which is beneficial to treat the sum of intraclass distances and the sum of interclass distances equally. Because in the traditional feature extraction algorithm, optimizing the two at the same time, it is easy to cause the problem of unbalanced optimization. This is because in the data set, the sum of intraclass distances is generally much smaller than the sum of interclass distances. In this chapter, a series of verifications have been made to confirm the order of the sum of distances within the optimized class and the sum of distances between classes. Figure 9 shows the results on multiple data sets, and the accuracy varies by 30%.

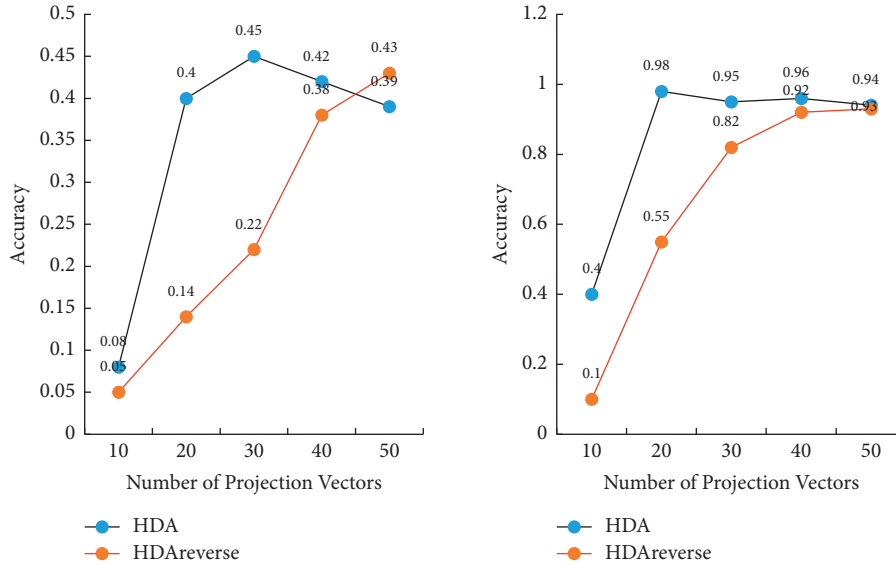


FIGURE 9: The accuracy of the two algorithms under different data sets.

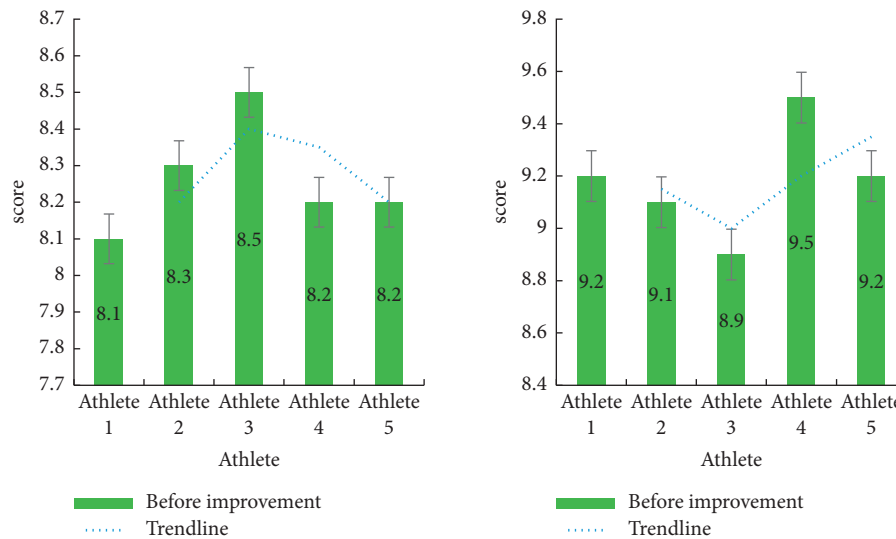


FIGURE 10: Comparison of performance scores of aerobics before and after improvement of athletes.

By comparing two different priority optimization strategies, comparing the recognition accuracy of the algorithm and the feature dimension selected at the best recognition rate, we found that the performance of minimizing the sum of intraclass distances first is far better than that of maximizing the sum of interclass distances first. We believe that the reason for this result is that the sum of distances between classes is much greater than the sum of distances within classes. After maximizing the sum of interclass distances, the new training sample set obtained according to the best projection matrix has been biased towards the optimal result of the sum of interclass distances. However, the sum of the distances within the class is not large enough, so it cannot play a good optimization role in optimization, which leads to a far drop in the recognition

rate. Therefore, we chose to first minimize the sum of the distances within the class as the first step of our hierarchical discriminant analysis algorithm.

*4.3. Before and after Performance Improvement.* In order to explore the improvement of the performance of aerobics athletes in the wireless communication network and edge computing, this paper is designed to calculate the performance scores of five athletes before and after the improvement. The specific statistics are shown in Figure 10.

From the abovementioned scores of aerobics performance before and after improvement, it can be seen that the scores of athletes before improvement are 8.1, 8.3, 8.5, 8.2, and 8.2, and the overall score is low. The improved athlete

scores are 9.2, 9.1, 8.9, 9.5, and 9.2, and the overall score has been greatly improved. The performance score of athletes has increased by an average of 13%, which can greatly improve the performance of aerobics athletes.

## 5. Conclusions

This article mainly studies how to improve the performance of aerobics athletes. Through the introduction of wireless communication network technology and edge computing, data acquisition of aerobics athletes is carried out. Accurate collection and use of the computing power of edge computing to analyze and summarize the collected data to improve the performance of aerobics athletes is carried out. Finally, in the experimental part, an experimental analysis is carried out on the accuracy of data collection and the related parameters of data collection, and the relevant data is summarized in the analysis part.

## Data Availability

No data were used to support this study.

## Conflicts of Interest

The author declares no conflicts of interest.

## References

- [1] Y. Ma, "Research on the arrangement and visual design of aerobics under the new situation," *International Core Journal of Engineering*, vol. 5, no. 9, pp. 170–173, 2019.
- [2] R. M. Cunha, J. Vilaça-Alves, M. V. Noleto et al., "Acute blood pressure response in hypertensive elderly women immediately after water aerobics exercise: a crossover study," *Clinical and experimental hypertension (New York, N.Y.: 1993)*, vol. 39, no. 1, pp. 17–22, 2017.
- [3] T. Taleb, K. Samdanis, B. Mada, H. Flinck, S. Dutta, and D. Sabella, "On multi-access edge computing: a survey of the emerging 5G network edge cloud architecture and orchestration," *IEEE Communications Surveys & Tutorials*, vol. 19, no. 3, pp. 1657–1681, 2017.
- [4] Z. Ke, Y. Mao, S. Leng, Y. He, and Y. Zhang, "Mobile-edge computing for vehicular networks: a promising network paradigm with predictive off-loading," *IEEE Vehicular Technology Magazine*, vol. 12, no. 2, pp. 36–44, 2017.
- [5] L. He, K. Ota, and M. Dong, "Learning IoT in edge: deep learning for the Internet of Things with edge computing," *IEEE Network*, vol. 32, no. 1, pp. 96–101, 2018.
- [6] W. Yu, F. Liang, X. He et al., "A survey on the edge computing for the Internet of Things," *IEEE Access*, vol. 6, no. 99, pp. 6900–6919, 2018.
- [7] S. Nastic, T. Rausch, O. Scekcic et al., "A serverless real-time data analytics platform for edge computing," *IEEE Internet Computing*, vol. 21, no. 4, pp. 64–71, 2017.
- [8] X. Chen, Q. Shi, L. Yang, and J. Xu, "ThriftyEdge: resource-efficient edge computing for intelligent IoT applications," *IEEE Network*, vol. 32, no. 1, pp. 61–65, 2018.
- [9] M. Ebrahimi, T. N. Guilan-Nejad, and A. F. Pordanjani, "Effect of yoga and aerobics exercise on sleep quality in women with Type 2 diabetes: a randomized controlled trial," *Sleep Science*, vol. 10, no. 2, pp. 68–72, 2017.
- [10] S. Tonstad, P. Herring, J. Lee, and J. D. Johnson, "Two physical activity measures: paffenbarger physical activity questionnaire versus aerobics center longitudinal study as predictors of adult-onset type 2 diabetes in a follow-up study," *American Journal of Health Promotion*, vol. 32, no. 4, pp. 1070–1077, 2018.
- [11] N. Le Chau, T.-P. Dao, and V. A. Dang, "An efficient hybrid approach of improved adaptive neural fuzzy inference system and teaching learning-based optimization for design optimization of a jet pump-based thermoacoustic-Stirling heat engine," *Neural Computing & Applications*, vol. 32, no. 11, pp. 7259–7273, 2020.
- [12] Y. Yan, X. Sun, B. Li, and X. Wang, "Construct a teaching system combining image linguistics and multimedia technology," *Wireless Communications and Mobile Computing*, vol. 2021, Article ID 6699010, 11 pages, 2021.
- [13] E. Ahmed, A. Ahmed, I. Yaqoob et al., "Bringing computation closer toward the user network: is edge computing the solution?" *IEEE Communications Magazine*, vol. 55, no. 11, pp. 138–144, 2017.
- [14] K. Kaur, S. Garg, G. S. Aujla, N. Kumar, J. J. P. C. Rodrigues, and M. Guizani, "Edge computing in the industrial Internet of Things environment: software-defined-networks-based edge-cloud interplay," *IEEE Communications Magazine*, vol. 56, no. 2, pp. 44–51, 2018.
- [15] L. Yang, C. Xu, Y. Zhan, Z. Liu, J. Guan, and H. Zhang, "Incentive mechanism for computation offloading using edge computing: a Stackelberg game approach," *Computer Networks*, vol. 129, pp. 399–409, 2017.
- [16] R. Wang, J. Yan, D. Wu, H. Wang, and Q. Yang, "Knowledge-centric edge computing based on virtualized D2D communication systems," *IEEE Communications Magazine*, vol. 56, no. 5, pp. 32–38, 2018.
- [17] B. P. Rimal, D. Pham Van, and M. Maier, "Mobile-edge computing versus centralized cloud computing over a converged FiWi access network," *IEEE Transactions on Network and Service Management*, vol. 14, no. 3, pp. 498–513, 2017.
- [18] S. Wang, Y. Zhao, L. Huang, J. Xu, and C.-H. Hsu, "QoS prediction for service recommendations in mobile edge computing," *Journal of Parallel and Distributed Computing*, vol. 127, pp. 134–144, 2017.
- [19] X. Lyu, H. Tian, L. Jiang et al., "Selective offloading in mobile edge computing for the green Internet of Things," *IEEE Network*, vol. 32, no. 1, pp. 54–60, 2018.
- [20] T. A. Simakova, A. A. Zharkikh, and N. Ankudinov, "Experimental study of the influence of self-realization of students in sports activities on the tendency to cyber dependence in University Education Context," *Psychology and Law*, vol. 10, no. 2, pp. 140–150, 2020.
- [21] Y. Cao, H. Song, O. Kaiwartya et al., "Mobile edge computing for big-data-enabled electric vehicle charging," *IEEE Communications Magazine*, vol. 56, no. 3, pp. 150–156, 2018.
- [22] M. Gusev and S. Dustdar, "Going back to the roots—the evolution of edge computing, an IoT perspective," *IEEE Internet Computing*, vol. 22, no. 2, pp. 5–15, 2018.
- [23] F. Qiang and N. Ansari, "Application aware workload allocation for edge computing based IoT," *IEEE Internet of Things Journal*, vol. 5, no. 3, pp. 2146–2153, 2018.
- [24] L. Hong, Y. Zhang, and Y. Tao, "Blockchain-enabled security in electric vehicles cloud and edge computing," *IEEE Network*, vol. 32, no. 3, pp. 78–83, 2018.
- [25] K. Zhang, S. Leng, Y. He, S. Maharjan, and Y. Zhang, "Co-operative content caching in 5G networks with mobile edge computing," *IEEE Wireless Communications*, vol. 25, no. 3, pp. 80–87, 2018.

## *Retraction*

# **Retracted: An Improved Orbit Model of Space Target Radar Based on Least Square Method and Its Program Implementation**

### **Wireless Communications and Mobile Computing**

Received 12 December 2023; Accepted 12 December 2023; Published 13 December 2023

Copyright © 2023 Wireless Communications and Mobile Computing. This is an open access article distributed under the Creative Commons Attribution License, which permits unrestricted use, distribution, and reproduction in any medium, provided the original work is properly cited.

This article has been retracted by Hindawi, as publisher, following an investigation undertaken by the publisher [1]. This investigation has uncovered evidence of systematic manipulation of the publication and peer-review process. We cannot, therefore, vouch for the reliability or integrity of this article.

Please note that this notice is intended solely to alert readers that the peer-review process of this article has been compromised.

Wiley and Hindawi regret that the usual quality checks did not identify these issues before publication and have since put additional measures in place to safeguard research integrity.

We wish to credit our Research Integrity and Research Publishing teams and anonymous and named external researchers and research integrity experts for contributing to this investigation.

The corresponding author, as the representative of all authors, has been given the opportunity to register their agreement or disagreement to this retraction. We have kept a record of any response received.

### **References**

- [1] Y. Zhang, X.-B. Huang, R. Xiao, L. Wang, and L. Lu, "An Improved Orbit Model of Space Target Radar Based on Least Square Method and Its Program Implementation," *Wireless Communications and Mobile Computing*, vol. 2022, Article ID 2341442, 10 pages, 2022.

## Research Article

# An Improved Orbit Model of Space Target Radar Based on Least Square Method and Its Program Implementation

Yan Zhang , Xiao-Bin Huang , Rui Xiao, Ling Wang, and Li Lu

*Air Force Early Warning Academy, Wuhan 430019, China*

Correspondence should be addressed to Xiao-Bin Huang; 532454132@qq.com

Received 12 November 2021; Accepted 26 January 2022; Published 24 February 2022

Academic Editor: Ali Kashif Bashir

Copyright © 2022 Yan Zhang et al. This is an open access article distributed under the Creative Commons Attribution License, which permits unrestricted use, distribution, and reproduction in any medium, provided the original work is properly cited.

Space target orbit determination module is an important component of the space target surveillance radar system. The development of this module requires very complex aerospace dynamics knowledge, which brings great difficulties to nonorbit mechanics researchers engaged in radar system design. Orbit improvement is a core content of orbit determination, and it is a necessary step to achieve high-precision orbit calculations. To this end, this paper focuses on the issue of batch processing orbit improvement of space target surveillance radar, introduces the principle of least-squares orbit improvement, the partial derivative of the model, and the main perturbation acceleration calculation methods, and gives the program design principle and implements the RadarOrbDet library. The developed library is compared and analyzed with STK and ODTK software, and the simulation results verify the effectiveness of the library. The library is also helpful for designers of space target surveillance radar systems to carry out a rapid demonstration of orbit determination indicators.

## 1. Introduction

The space target orbit determination module is an important component of the space target surveillance radar system. The development of this module requires a very complex knowledge of aerospace dynamics [1], which brings great difficulties to nonorbit mechanics researchers engaged in radar system design. To this end, this paper analyzes the basic orbit determination principles of space target radar and develops the RadarOrbDet open source library [2] to assist nonorbit mechanics engineers in the system design of space target surveillance radar.

According to different data processing methods, the orbit determination methods can be divided into dynamic orbit determination, geometric orbit determination, and reduced dynamic orbit determination. The dynamic orbit determination method uses a dynamic model of space target to establish motion equation and determines orbit based on the constraints of the dynamic equation. It can obtain a better orbit determination effect with fewer observation data, and it is widely used in navigation satellite orbit determination [3]. Geometric orbit determination method

does not consider the orbital dynamics model and obtains the orbital elements by fitting the observation data. This kind of method has been widely used in the orbit determination of low-orbit satellites [4], but the orbit extrapolation accuracy is relatively low. The reduced dynamic orbit determination method is based on orbital mechanics and combines geometric observation information for optimal weighting so as to achieve precise orbit determination. This method has also been widely used in satellite orbit determination and effectively alleviates the problem that the dynamic model is sensitive to observation errors [5, 6].

Modern orbit determination technology requires the measurement model to be expressed as a function of the orbit state. Usually, the measured value is a nonlinear function of the orbital position component, and then the weighted least-squares technique is used to minimize the residuals to solve the target state vector. This solving process requires repeated iterative corrections to the initial orbital state, so it is also called orbital improvement. Various types of measurement data can be used for orbit improvement, such as angle measurement data [7, 8], GPS measurement data [9, 10], doppler measurement data [11, 12], etc. The

calculation process involves various perturbation force analyses, such as the Earth's nonspherical gravitational perturbation [13, 14], atmospheric drag perturbation [15, 16], third-body perturbation [17, 18], solar radiation perturbation [19, 20], and so on. In order to speed up data analysis tasks, many open source orbit determination software [21–25] can be used by engineers to void complicated mathematical formula derivation, but these software is mainly used to process optical angle measurement data and are not suitable for processing radar measurement data.

This paper focuses on the batch orbit improvement in space target radar orbit determination, introduces the principle of least-squares orbit improvement, explains the calculation method of partial derivative and main perturbations in the model, describes the program design of the RadarOrbDet library, and finally compares the library with System Tool Kit (STK) and Orbit Determination Tool Kit (ODTK) software. The simulations verify the effectiveness of the RadarOrbDet library, which shows that the library is helpful for designers of space target surveillance radar systems to carry out a rapid demonstration of orbit determination indicators.

## 2. The Principle of Least-Squares Orbit Improvement

The basic principle of least-squares orbit determination is to find an orbit that minimizes the residual between theoretical measurements and actual measurements, which is, solving  $\mathbf{x}_0$  to minimize the value of the following equation:

$$J(\mathbf{x}_0) = [\mathbf{z} - \mathbf{h}(\mathbf{x}_0)]^T [\mathbf{z} - \mathbf{h}(\mathbf{x}_0)], \quad (1)$$

where  $\mathbf{x}_0 = [\mathbf{r}(t_0); \mathbf{v}(t_0)]$  is the state of a satellite at epoch  $t_0$ , and a reference trajectory can be predicted by this orbit state;  $\mathbf{z} = [\mathbf{z}_1; \mathbf{z}_2 \cdots; \mathbf{z}_N]$  is the actual measurement vector of radar, and each measurement contains three components, namely distance, azimuth, and elevation;  $\mathbf{h}(\mathbf{x}_0)$  is the calculated measurement obtained with reference trajectory.

Since  $\mathbf{h}$  is a nonlinear function, equation (1) describes a nonlinear least-squares problem, which is extremely difficult to solve. Usually, Taylor expansion is used to transform this nonlinear least-squares problem into a linear least-squares problem, and its solution can be approximately obtained using the following iterative equation:

$$\mathbf{x}_0^{(i+1)} = \mathbf{x}_0^{(i)} + (\mathbf{H}^{(i)T} \mathbf{H}^{(i)})^{-1} \mathbf{H}^{(i)T} (\mathbf{z} - \mathbf{h}(\mathbf{x}_0^{(i)})). \quad (2)$$

The initial value of the iteration is  $\mathbf{x}_0^{(0)} = \mathbf{x}_0^{\text{apr}}$ , which can be obtained by initial orbit determination. The iterative process terminates until the relative change of the error for two consecutive times is less than a given threshold.  $\mathbf{H}$  is Jacobian matrix described by the following equation:

$$\mathbf{H}^{(i)} = \left. \frac{\partial \mathbf{h}(\mathbf{x}_0)}{\partial \mathbf{x}_0} \right|_{\mathbf{x}_0 = \mathbf{x}_0^{(i)}}. \quad (3)$$

Taking into account the weight of different types of measurement, equation (2) can be modified as follows:

$$\mathbf{x}_0^{(i+1)} = \mathbf{x}_0^{(i)} + (\mathbf{H}^{(i)T} \mathbf{W} \mathbf{H}^{(i)})^{-1} \mathbf{H}^{(i)T} \mathbf{W} (\mathbf{z} - \mathbf{h}(\mathbf{x}_0^{(i)})), \quad (4)$$

where  $\mathbf{W} = \text{diag}(\sigma_\rho^{-2}, \sigma_\alpha^{-2}, \sigma_\beta^{-2})$  is a diagonal square matrix composed of radar measurement errors.

## 3. Computation of Model's Partial Derivatives

The key to the calculation of equation (4) lies in the computation of the matrix  $\mathbf{H}$ . Without loss of generality, take the once radar measurement as an example and omit the superscript  $i$ .

Using the derivative chain rule,  $\mathbf{H}$  is transformed into the following:

$$\mathbf{H} = \frac{\partial \mathbf{h}}{\partial \mathbf{x}} \cdot \frac{\partial \mathbf{x}}{\partial \mathbf{x}_0} = \mathbf{A} \Phi, \quad (5)$$

where matrix  $\mathbf{A}$  is the partial derivative matrix of the current measurement with respect to the current state, and  $\Phi$  is the partial derivative matrix of the current state with respect to the initial state, also called the error state transition matrix.

*3.1. Computation of Partial Derivative Matrix of Measurement with respect to the State Vector.* Ignoring the optical aberration and other minor factors, the radar measurement is only related to the current position of the satellite. Therefore, matrix  $\mathbf{A}$  can be split into the following:

$$\mathbf{A} = \frac{\partial \mathbf{h}}{\partial \mathbf{x}} = \begin{bmatrix} \frac{\partial \mathbf{h}}{\partial \mathbf{r}_{\text{ECI}}} & \mathbf{0}_{3 \times 3} \end{bmatrix}, \quad (6)$$

where  $\mathbf{r}_{\text{ECI}}$  is the position vector of the satellite in the inertial coordinate system (ECI coordinate system).

Radar measurement is based on the topocentric horizon coordinate system, such as SEZ (south-east-zenith) coordinate. It is difficult to directly calculate the partial derivative of the radar measurement with respect to the position vector in the ECI coordinate system. Therefore, the calculation of matrix  $\mathbf{A}$  needs to be further decomposed by derivation chain rule

$$\frac{\partial \mathbf{h}}{\partial \mathbf{r}_{\text{ECI}}} = \frac{\partial \mathbf{h}}{\partial \rho_{\text{SEZ}}} \cdot \frac{\partial \rho_{\text{SEZ}}}{\partial \rho_{\text{ECEF}}} \cdot \frac{\partial \rho_{\text{ECEF}}}{\partial \mathbf{r}_{\text{ECEF}}} \cdot \frac{\partial \mathbf{r}_{\text{ECEF}}}{\partial \mathbf{r}_{\text{ECI}}}, \quad (7)$$

where  $\rho_{\text{SEZ}}$  is the Cartesian position vector of the satellite in the SEZ coordinate system, represented by  $(\rho_S, \rho_E, \rho_Z)$ ;  $\rho_{\text{ECEF}}$  is a range vector from radar to satellite represented in the Earth-Fixed coordinate system (ECEF);  $\mathbf{r}_{\text{ECEF}}$  is the satellite's position vector in ECEF coordinate system.

Notice

$$\rho_{\text{ECEF}} = \mathbf{r}_{\text{ECEF}} - \mathbf{r}_{\text{siteECEF}}, \quad (8)$$

where  $\mathbf{r}_{\text{siteECEF}}$  is the radar position vector in ECEF coordinate system, which is a constant vector.

Therefore,

$$\frac{\partial \rho_{\text{ECEF}}}{\partial \mathbf{r}_{\text{ECEF}}} = \frac{\partial (\mathbf{r}_{\text{ECEF}} - \mathbf{r}_{\text{siteECEF}})}{\partial \mathbf{r}_{\text{ECEF}}} = \mathbf{I}. \quad (9)$$

According to the coordinate transformation



$$\mathbf{p}_{\text{SEZ}} = \begin{bmatrix} \text{SEZ} \\ \text{ECEF} \end{bmatrix} \mathbf{p}_{\text{ECEF}}, \quad (10)$$

where [SEZ/ECEF] is the transformation matrix from SEZ coordinate system to ECEF coordinate system.

According to equation (10),

$$\begin{aligned} \frac{\partial \mathbf{p}_{\text{SEZ}}}{\partial \mathbf{p}_{\text{ECEF}}} &= \frac{\partial}{\partial \mathbf{p}_{\text{ECEF}}} \left( \begin{bmatrix} \text{SEZ} \\ \text{ECEF} \end{bmatrix} \mathbf{p}_{\text{ECEF}} \right) \\ &= \frac{\partial}{\partial \mathbf{p}_{\text{ECEF}}} \begin{bmatrix} \text{SEZ} \\ \text{ECEF} \end{bmatrix} \mathbf{p}_{\text{ECEF}} + \begin{bmatrix} \text{SEZ} \\ \text{ECEF} \end{bmatrix} \frac{\partial \mathbf{p}_{\text{ECEF}}}{\partial \mathbf{p}_{\text{ECEF}}} \\ &= \begin{bmatrix} \text{SEZ} \\ \text{ECEF} \end{bmatrix}. \end{aligned} \quad (11)$$

It can be seen from equation (11) that the partial derivative matrix is actually a coordinate transformation matrix.

Similarly,

$$\frac{\partial \mathbf{r}_{\text{ECEF}}}{\partial \mathbf{r}_{\text{ECI}}} = \begin{bmatrix} \text{ECEF} \\ \text{ECI} \end{bmatrix}. \quad (12)$$

Substituting equations (9), (11), and (12) into equation (7), we have the following:

$$\frac{\partial \mathbf{h}}{\partial \mathbf{r}_{\text{ECI}}} = \frac{\partial \mathbf{h}}{\partial \mathbf{p}_{\text{SEZ}}} \cdot \begin{bmatrix} \text{SEZ} \\ \text{ECEF} \end{bmatrix} \cdot \begin{bmatrix} \text{ECEF} \\ \text{ECI} \end{bmatrix} = \frac{\partial \mathbf{h}}{\partial \mathbf{p}_{\text{SEZ}}} \cdot \begin{bmatrix} \text{SEZ} \\ \text{ECI} \end{bmatrix}, \quad (13)$$

where [SEZ/ECI] is the transformation matrix from SEZ coordinate system to ECI coordinate system.

In SEZ coordinate system, the relationship between Cartesian coordinate and polar coordinate is as follows:

$$\left\{ \begin{aligned} \rho &= \sqrt{\rho_S^2 + \rho_E^2 + \rho_Z^2}, \\ \alpha &= a \tan\left(\frac{-\rho_S}{\rho_E}\right), \\ \beta &= a \sin\left(\frac{\rho_Z}{\sqrt{\rho_S^2 + \rho_E^2 + \rho_Z^2}}\right). \end{aligned} \right. \quad (14)$$

So,

$$\frac{\partial \mathbf{h}}{\partial \mathbf{p}_{\text{SEZ}}} = \begin{bmatrix} \frac{\partial \rho}{\partial \rho_S} & \frac{\partial \rho}{\partial \rho_E} & \frac{\partial \rho}{\partial \rho_Z} \\ \frac{\partial \alpha}{\partial \rho_S} & \frac{\partial \alpha}{\partial \rho_E} & \frac{\partial \alpha}{\partial \rho_Z} \\ \frac{\partial \beta}{\partial \rho_S} & \frac{\partial \beta}{\partial \rho_E} & \frac{\partial \beta}{\partial \rho_Z} \end{bmatrix} = \begin{bmatrix} \frac{\rho_S}{\rho} & \frac{\rho_E}{\rho} & \frac{\rho_Z}{\rho} \\ \frac{\rho_E}{\rho_S^2 + \rho_E^2} & \frac{1}{\rho_S^2 + \rho_E^2} & 0 \\ \frac{-\rho_S \rho_Z}{\rho^2 \sqrt{\rho_S^2 + \rho_E^2 + \rho_Z^2}} & \frac{-\rho_E \rho_Z}{\rho^2 \sqrt{\rho_S^2 + \rho_E^2 + \rho_Z^2}} & \frac{\rho_S^2 + \rho_E^2}{\rho^2 \sqrt{\rho_S^2 + \rho_E^2 + \rho_Z^2}} \end{bmatrix}. \quad (15)$$

Substituting equation (15) into equation (13), we have the following:

$$\frac{\partial \mathbf{h}}{\partial \mathbf{r}_{\text{ECI}}} = \begin{bmatrix} \frac{\rho_S}{\rho} & \frac{\rho_E}{\rho} & \frac{\rho_Z}{\rho} \\ \frac{\rho_E}{\rho_S^2 + \rho_E^2} & \frac{1}{\rho_S^2 + \rho_E^2} & 0 \\ \frac{-\rho_S \rho_Z}{\rho^2 \sqrt{\rho_S^2 + \rho_E^2 + \rho_Z^2}} & \frac{-\rho_E \rho_Z}{\rho^2 \sqrt{\rho_S^2 + \rho_E^2 + \rho_Z^2}} & \frac{\rho_S^2 + \rho_E^2}{\rho^2 \sqrt{\rho_S^2 + \rho_E^2 + \rho_Z^2}} \end{bmatrix} \cdot \begin{bmatrix} \text{SEZ} \\ \text{ECI} \end{bmatrix}. \quad (16)$$

The calculation of the two matrices in equation (16) needs to be performed at the current observation time. Finally, substitute equation (16) into equation (6) to obtain matrix  $\mathbf{A}$ .

3.2. Computation of Error State Transition Matrix. Suppose the satellite's motion equation is as follows:

$$\frac{d\mathbf{x}(t)}{dt} = \dot{\mathbf{x}} = \mathbf{f}(t, \mathbf{x}) = \begin{bmatrix} \mathbf{v}(t) \\ \mathbf{a}(t, \mathbf{r}, \mathbf{v}) \end{bmatrix}. \quad (17)$$

Then,

$$\begin{aligned} \dot{\Phi} &= \frac{d}{dt} \left( \frac{\partial \mathbf{x}(t)}{\partial \mathbf{x}(t_0)} \right) = \frac{\partial}{\partial \mathbf{x}(t_0)} \left( \frac{d\mathbf{x}(t)}{dt} \right) = \frac{\partial \mathbf{f}(t, \mathbf{x}(t))}{\partial \mathbf{x}(t_0)} \\ &= \frac{\partial \mathbf{f}(t, \mathbf{x}(t))}{\partial \mathbf{x}(t)} \cdot \frac{\partial \mathbf{x}(t)}{\partial \mathbf{x}(t_0)} = \mathbf{F}\Phi, \end{aligned} \quad (18)$$

where the matrix  $\mathbf{F}$  is as follows:

$$\mathbf{F} = \begin{bmatrix} 0_{3 \times 3} & 1_{3 \times 3} \\ \frac{\partial \mathbf{a}(t, \mathbf{r}, \mathbf{v})}{\partial \mathbf{r}} & \frac{\partial \mathbf{a}(t, \mathbf{r}, \mathbf{v})}{\partial \mathbf{v}} \end{bmatrix}. \quad (19)$$

Due to the iterative mode being used to solve the least-squares problem, accuracy requirements for the partial derivatives  $\Phi$  and  $\mathbf{F}$  are generally more relaxed than those for the trajectory itself. It is common to apply a simplified force model in the solution of the equation (18). The incorporation of the lowest-order zonal gravity field perturbation ( $C_{2,0}$ ) already provides an acceptable minimum model.

When only the Earth's gravity is considered, the acceleration is only related to the position, and its calculation is usually carried out in the ECEF coordinate system. The specific expression can be found in reference [26].

Finally, the partial derivative matrix in the ECEF coordinate system needs to be converted to the ECI coordinate system. In the case of ignoring Coriolis force and centrifugal force, there is the following relationship:

$$\left( \frac{\partial \mathbf{a}}{\partial \mathbf{r}} \right)_{\text{ECI}} = \begin{bmatrix} \text{ECI} \\ \text{ECEF} \end{bmatrix}^{-1} \left( \frac{\partial \mathbf{a}}{\partial \mathbf{r}} \right)_{\text{ECEF}} \begin{bmatrix} \text{ECI} \\ \text{ECEF} \end{bmatrix}. \quad (20)$$

At the current time, after the matrix  $\mathbf{F}$  is calculated, the numerical differential equation method is used to solve matrix  $\Phi$ .

#### 4. Calculation of Main Perturbation Acceleration

In solving least-squares, a reference trajectory of the satellite needs to be calculated. So, it is necessary to appropriately select the perturbation force of the satellite according to the problem and the accuracy requirement. For LEO satellites, the Earth's nonspherical gravity and atmospheric drag perturbation are usually considered. The following describes

the satellite acceleration caused by these two perturbation forces.

*4.1. Gravitational Acceleration of the Earth.* Use  $\mathbf{r}_{\text{ECI}}$  and  $\mathbf{r}_{\text{ECEF}}$  to denote the position vectors of the satellite under the ECI and ECEF coordinate system, respectively. The acceleration can be obtained by calculating the gradient of the potential function  $U$ , namely,

$$\mathbf{a}_{\text{ECI}} = \nabla U(\mathbf{r}_{\text{ECEF}}) = \frac{\partial \mathbf{r}_{\text{ECI}}}{\partial \mathbf{r}_{\text{ECEF}}} \left[ \frac{\partial U}{\partial r_{\text{ECEF}}} \left( \frac{\partial \mathbf{r}_{\text{ECEF}}}{\partial \mathbf{r}_{\text{ECEF}}} \right)^T + \frac{\partial U}{\partial \varphi} \left( \frac{\partial \varphi}{\partial \mathbf{r}_{\text{ECEF}}} \right)^T + \frac{\partial U}{\partial \lambda} \left( \frac{\partial \lambda}{\partial \mathbf{r}_{\text{ECEF}}} \right)^T \right] = \begin{bmatrix} \text{ECI} \\ \text{ECEF} \end{bmatrix} \mathbf{a}_{\text{ECEF}}. \quad (21)$$

where  $\mathbf{a}_{\text{ECI}}$  and  $\mathbf{a}_{\text{ECEF}}$  are the accelerations of the satellite in the ECI and ECEF coordinates, respectively,  $r_{\text{ECEF}} = \sqrt{x_{\text{ECEF}}^2 + y_{\text{ECEF}}^2 + z_{\text{ECEF}}^2}$ ,  $(r_{\text{ECEF}}, \varphi, \lambda)$  is the altitude, latitude, and longitude of the satellite in the ECEF coordinate system;

$[\text{ECI/ECEF}]$  is the coordinate transformation matrix from ECI to ECEF coordinate system.

The three components of  $\mathbf{a}_{\text{ECEF}}$  can be calculated by the following equation:

$$\begin{cases} a_{x_{\text{ECEF}}} = \frac{x_{\text{ECEF}}}{r_{\text{ECEF}}} \frac{\partial U}{\partial r_{\text{ECEF}}} - \frac{x_{\text{ECEF}} z_{\text{ECEF}}}{r_{\text{ECEF}}^2 \sqrt{x_{\text{ECEF}}^2 + y_{\text{ECEF}}^2}} \frac{\partial U}{\partial \varphi} - \frac{y_{\text{ECEF}}}{x_{\text{ECEF}}^2 + y_{\text{ECEF}}^2} \frac{\partial U}{\partial \lambda}, \\ a_{y_{\text{ECEF}}} = \frac{y_{\text{ECEF}}}{r_{\text{ECEF}}} \frac{\partial U}{\partial r_{\text{ECEF}}} - \frac{y_b z}{r_{\text{ECEF}}^2 \sqrt{x_{\text{ECEF}}^2 + y_{\text{ECEF}}^2}} \frac{\partial U}{\partial \varphi} + \frac{x_b}{x_{\text{ECEF}}^2 + y_{\text{ECEF}}^2} \frac{\partial U}{\partial \lambda}, \\ a_{z_{\text{ECEF}}} = \frac{z_{\text{ECEF}}}{r_{\text{ECEF}}} \frac{\partial U}{\partial r_{\text{ECEF}}} + \frac{\sqrt{x_{\text{ECEF}}^2 + y_{\text{ECEF}}^2}}{r_{\text{ECEF}}^2} \frac{\partial U}{\partial \varphi}. \end{cases} \quad (22)$$

The partial derivative of the potential function  $U$  to  $(r_{\text{ECEF}}, \varphi, \lambda)$  is as follows:

$$\begin{cases} \frac{\partial U}{\partial r_{\text{ECEF}}} = -\frac{GM_e}{r_{\text{ECEF}}^2} \sum_{n=0}^{\infty} \sum_{m=0}^n (n+1) \left( \frac{R_e}{r_{\text{ECEF}}} \right)^n \bar{P}_n^m(\sin \varphi) [\bar{C}_{nm} \cos(m\lambda) + \bar{S}_{nm} \sin(m\lambda)], \\ \frac{\partial U}{\partial \varphi} = \frac{GM_e}{r_{\text{ECEF}}^2} \left\{ \sum_{n=0}^{\infty} \sum_{m=0}^n \left( \frac{R_e}{r_{\text{ECEF}}} \right)^n [P_n^{m+1}(\sin \varphi) - m \tan \varphi P_n^m(\sin \varphi)] [\bar{C}_{nm} \cos(m\lambda) + \bar{S}_{nm} \sin(m\lambda)] \right\}, \\ \frac{\partial U}{\partial \lambda} = \frac{GM_e}{r_{\text{ECEF}}^2} \sum_{n=0}^{\infty} \sum_{m=0}^n \left( \frac{R_e}{r_{\text{ECEF}}} \right)^n m \bar{P}_n^m(\sin \varphi) [\bar{S}_{nm} \cos(m\lambda) - \bar{C}_{nm} \sin(m\lambda)], \end{cases} \quad (23)$$

where  $G$  is the gravitational constant,  $M_e$  is the mass of the Earth,  $R_e$  is the average radius of the Earth's equator,  $\bar{P}_n^m(x)$  is the normalized Legendre polynomial, and  $\bar{C}_{nm}$  and  $\bar{S}_{nm}$  are the normalized gravitational potential coefficients, which can be read out directly from the Earth's gravity field model file.

*4.2. Atmospheric Drag Acceleration.* The satellite acceleration caused by atmospheric drag can be written as follows:

$$\mathbf{a}_{\text{drag}} = -\frac{1}{2} C_D \frac{A}{m} \rho v_r^2 \mathbf{e}_v, \quad (24)$$

where  $m$  is the satellite mass,  $C_D$  is the atmospheric drag coefficient, and its typical value ranges from 1.5 to 3.0. The relative velocity  $\mathbf{v}_r$  can be written approximately as follows:

$$\mathbf{v}_r = \mathbf{v} - \boldsymbol{\omega}_{\oplus} \times \mathbf{r}, \quad (25)$$

with the inertial satellite velocity vector  $\mathbf{v}$ , the position vector  $\mathbf{r}$ , and the Earth's angular velocity vector  $\boldsymbol{\omega}_{\oplus}$  of size  $0.7292 \times 10^{-4}$  rad/s. Note that the calculation of equations (24) and (25) is carried out in the true-of-date (TOD) coordinate system, and the corresponding value in the ECI coordinate system can be obtained after a coordinate transformation.

The drag depends on the atmospheric density  $\rho$  at the location of the satellite, and the atmospheric density is usually calculated by the semiempirical atmospheric density model. At present, the commonly used atmospheric model in orbit determination is NRLMSISE-00 atmospheric model, which plays an important role in satellite orbit determination and prediction.

The NRLMSISE-00 atmospheric model has 8 input items: The number of days from January 1 of the current year to the current day, the number of seconds from 00:00:00 to the calculating time, geographical longitude, latitude, altitude, the solar radiation flux of 10.7 cm on the previous day ( $F_{10.7}$ ), the average  $F_{10.7}$  for 81 days (3 solar rotation cycles, with the current day as the midpoint), average geomagnetic index (Ap) of current day and the twenty 3 h average values of Ap before the calculating time. The outputs include the number densities of  $N_2$ ,  $O_2$ , He, Ar, N, H, O, and  $O^+$ , the neutral atmospheric temperature, and the atmospheric density.

These space environment parameters are provided by the SpaceWeather.txt file. Each line in the file represents a spatial environment parameter record for the specified date. The record has 32 fields, as shown in Figure 1. The meanings of the fields related to atmospheric drag are shown in Table 1.

## 5. Programming Program Design

This section introduces the program design idea of perturbation acceleration calculation and least-squares orbit improvement.

Figure 2 shows the program design flow chart of the calculation of the Earth's gravitational acceleration. The input of the program is the position vector  $\mathbf{r}_{\text{ECI}}$ , the coordinate transformation matrix from ECI to ECEF coordinate system, and the order of the Earth's nonspherical gravity  $m$ ,  $n$ . The calculation process is as follows: firstly, calculate the satellite's coordinate  $\mathbf{r}_{\text{ECEF}}$ , and then convert it into geodetic coordinate ( $r_{\text{ECEF}}$ ,  $\varphi$ ,  $\lambda$ ), use the geodetic coordinate and the input nonspherical gravity order to calculate the value of the associated Legendre polynomial, then use the gravity potential coefficient file GGM03C.grv to calculate partial derivative according to equation (23), and finally use equation (21) to output  $\mathbf{a}_{\text{ECI}}$ .

Figure 3 is a program flow chart for calculating the perturbation acceleration of atmospheric drag. The main

calculation process in Figure 3 is as follows: the mean solar time, the number of seconds from 00:00:00 to the current time of the day, and the number of days from January 1 to the current day of the year are calculated using the input UTC time; the required Apgeo magnetic datum is obtained and calculated using the input space weather data document; the longitude and latitude of the satellite are calculated by the input satellite position vector. According to the above information, NRLMSISE-00 model is used to calculate the atmospheric density. Based on the position and velocity vectors of the satellite, the velocity of the satellite relative to the atmosphere is calculated according to the Earth's angular velocity vector. Finally, the atmospheric drag acceleration can be calculated from the relative velocity, atmospheric density, input area-to-mass ratio, and drag coefficient.

Figure 4 is a program design flow chart of the least-squares orbit improvement algorithm. The radar measurement data  $\mathbf{y}_i^o$  of each point in Figure 4 includes three components: range, azimuth, and elevation, namely ( $\rho$ ,  $\alpha$ ,  $\beta$ ); when using the numerical method to solve the reference trajectory, the perturbation factors should be considered as comprehensively as possible according to the accuracy requirement of the problem; while solving the error state transition matrix, only the center gravity of Earth and low-order nonspherical perturbation should be considered. The nonspherical perturbation of the Earth is introduced when solving the error state transition matrix, and the order is  $4 \times 4$ . When calculating the reference orbit, the order is  $21 \times 21$ .

The program is divided into three loops:

The first loop is the internal loop for solving the numerical differential equation. The program's inputs include Initial moment  $t_0$ ; Initial satellite orbit state  $\mathbf{x}_0^{(0)} = \mathbf{x}_0^{\text{aprt}}$ ;  $N$ -point radar measurement data  $\{\mathbf{y}_1^0, \mathbf{y}_2^0, \dots, \mathbf{y}_N^0\}$ ; least-squares convergence threshold  $\varepsilon$ ; number of iterations  $k=0$ ; measurement data index number  $i=1$ ; other relevant parameters, such as EOP files, atmospheric environment parameters, satellite surface-to-mass ratio, etc. The output results are the reference trajectory and error state transfer matrix at time  $i$ . The second loop is to traverse each measurement value and solve the single orbit improvement according to the least-squares principle. After iteration, update the orbital state at  $t_0$ :  $\mathbf{x}_0^{(k+1)} = \mathbf{x}_0^{(k)} + (\mathbf{H}^T \mathbf{W} \mathbf{H})^{-1} (\mathbf{H}^T \mathbf{W} \Delta \mathbf{z})$ . The third loop is to perform multiple least-squares orbit improvements to make the final result close to the actual orbit state. The output is the improvement orbit elements  $\mathbf{x}_0^{\text{lsq}}$  of  $t_0$  time.

Getting the time interval  $\Delta T$  and current orbit state of the satellite  $\mathbf{x}_{t_c} = [\mathbf{r}, \mathbf{v}]$  from the input parameters of the differential equation in the inner loop, we can follow these steps to solve the numerical differential equation:

- (1) Current time  $t_c = t_0 + \Delta t < t_i$
- (2) According to the force model and related parameters, calculate accelerations of two-body, nonspherical perturbation, planets, atmospheric drag, etc., so as to construct the vector  $\dot{\mathbf{x}}_{t_c} = [\mathbf{v}; \mathbf{a}]$

yyyy	mm	dd	BSRN	ND	Kp	Kp	Kp	Kp	Kp	Kp	Kp	Sum	Ap	Ap	Ap	Ap	Ap	Ap	Avg	Cp	C9	ISN	F10.7	Q	Adj	Adj	Adj	Obs	Obs	Obs		
yyyy	mm	dd	nnnn	nn	nn	nn	nn	nn	nn	nn	nn	nnn	nnn	nnn	nnn	nnn	nnn	nnn	nnn	n.n	n	nnn	nnn	n	nnn	nnn	nnn	nnn	nnn	nnn		
2000	01	01	2272	7	53	47	40	33	43	30	43	37	327	56	39	27	18	32	15	32	22	30	1.3	6	48	125.6	0	160.5	175.0	129.9	165.6	179.0

FIGURE 1: Parameter format of spatial environment parameter record.

TABLE 1: The meaning of space environment parameters.

Column	Name	Description
001-004	yyyy	Year
006-007	mm	Month
009-010	dd	Day
048-050	Ap0	Ap index (00:00-03:00)
052-054	Ap3	Ap index (03:00-06:00)
056-058	Ap6	Ap index (06:00-09:00)
060-062	Ap9	Ap index (09:00-12:00)
064-066	Ap12	Ap index (12:00-15:00)
068-070	Ap15	Ap index (15:00-18:00)
072-074	Ap18	Ap index (18:00-21:00)
076-078	Ap21	Ap index (21:00-24:00)
114-118	Obs F <sub>10.7</sub>	F <sub>10.7</sub> , previous day (observed)
126-130	Obs Lst81	F <sub>10.7</sub> , arithmetic mean for the previous 81 days (observed)

(3) Calculate  $\partial(\mathbf{a}_{\text{two-body}} + \mathbf{a}_{\text{non-spherical perturbation}})/\partial\mathbf{r}$  to construct matrix  $\mathbf{F}$ , then solve the differential equation  $\dot{\Phi}_{t_c} = \mathbf{F}\Phi_{t_c}$

### 6. Software Interface Call and Validity Verification

6.1. Earth's Nonspherical Gravitational Acceleration. The rodAccelHarmonic interface function for calculating the Earth's gravitational acceleration is realized by C language according to the programming principle of Part 5, and it is integrated into the RadarOrbDet library. The input and output of this function are shown in Figure 2.

A satellite is simulated in STK11.2, and its orbital elements are set as shown in Table 2. In order to compare STK with rodAccelHarmonic function under the same perturbation conditions, only the nonspherical gravitational perturbation of the Earth (21st order) is set in STK. The simulation time period is set from 2020-10-18 04:00:00 UTCG to 2020-10-19 04:00:00 UTCG. UTCG stands for Gregorian Universal Time Coordinated. Use STK's report function to output the satellite epoch time every 1 minute and the position and acceleration under ECI coordinate system. The epoch time is used to calculate the coordinate transformation matrix. The calculated matrix and the position in ECI coordinate system are used as the input parameters of the rodAccelHarmonic function. The acceleration output from the report is taken as the standard value and compared with the acceleration calculated by the rodAccelHarmonic function. The relative error described in equation (26) is used for quantitative analysis.

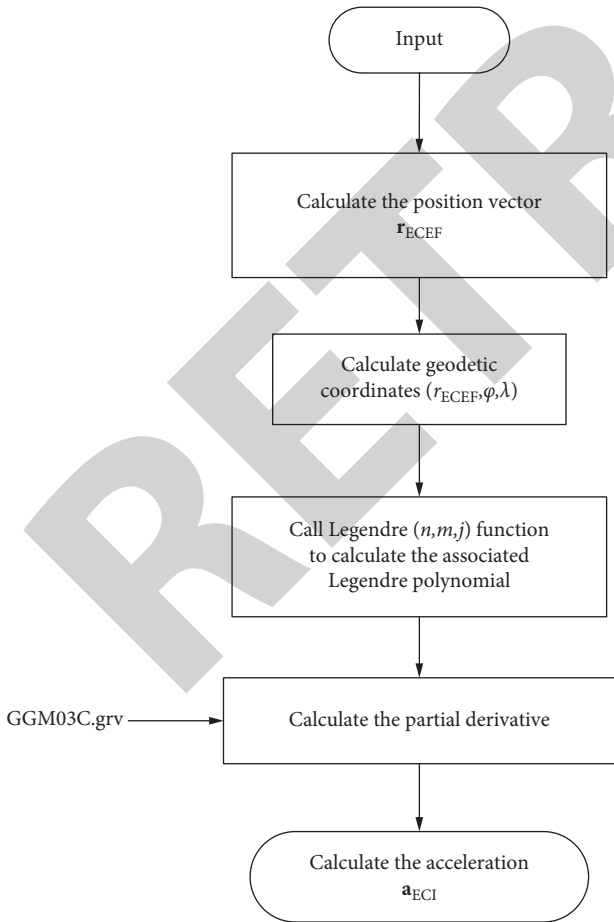


FIGURE 2: The flow chart of the program design for the calculation of the Earth's gravitational acceleration.

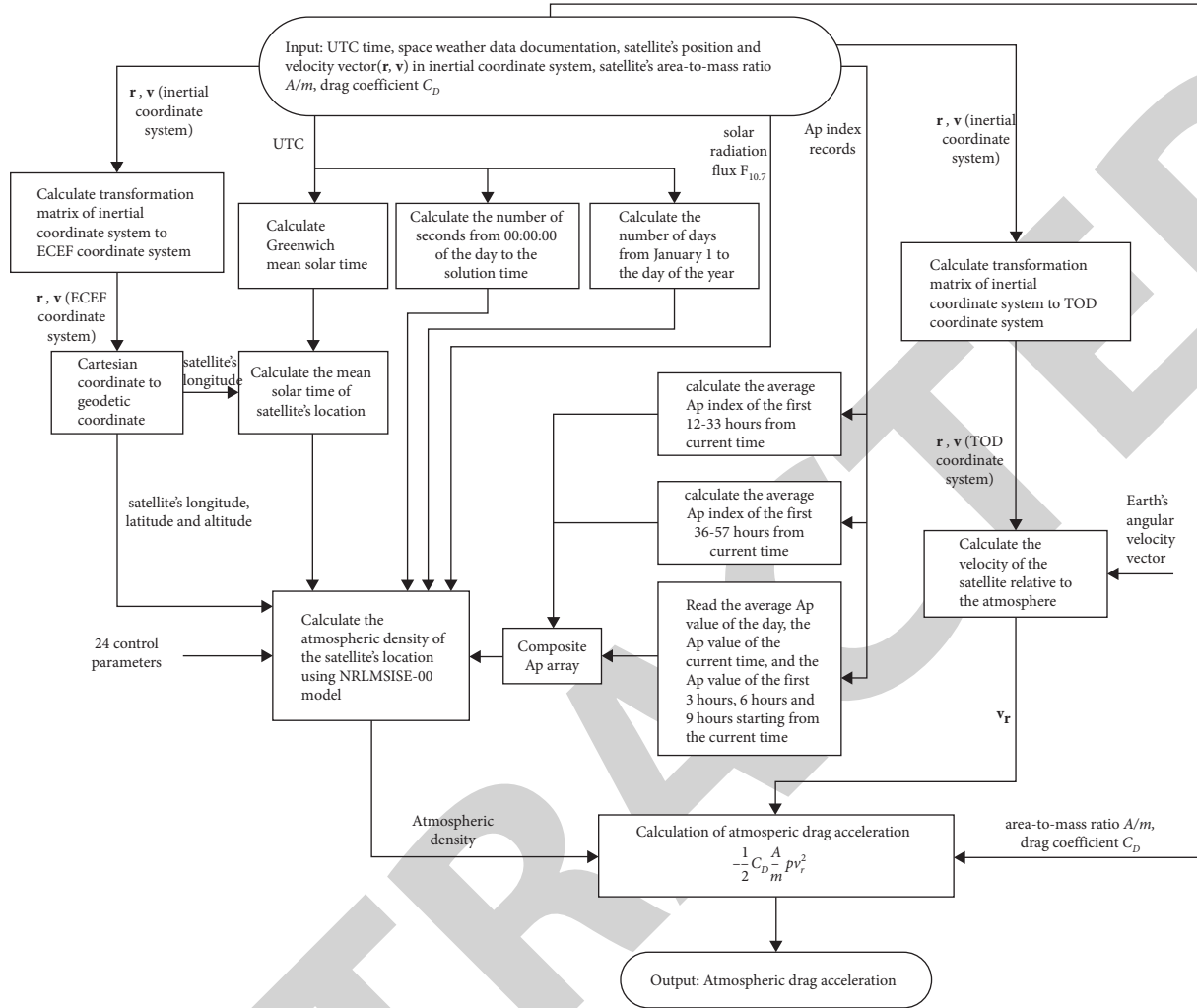


FIGURE 3: The flow chart of the program design for calculating the acceleration of atmospheric drag.

$$\text{relative error} = \frac{|\mathbf{a}_{\text{software}}| - |\mathbf{a}_{\text{STK}}|}{|\mathbf{a}_{\text{STK}}|} \quad (26)$$

There are 1441 data points in total. Figure 5 plots the acceleration (solid line) and relative error curve (dashed line) calculated by the rodAccelHarmonic function. It can be seen from the figure that the relative error is at the level of  $10^{-6}$ , which shows that the software algorithm is effective. The main source of error is the loss of accuracy due to the truncation of the text output of the STK report. In addition, the acceleration curve in the figure shows periodic changes because when the only nonspherical gravitational perturbation is considered, the semimajor axis of the satellite will change periodically.

**6.2. Atmospheric Drag Acceleration.** According to the program design principle in Part 5, the rodAccelAirDragPerturbation interface function for calculating the atmospheric drag perturbation acceleration is realized by using C language and integrated into RadaOrbDet library. The input and output of this function are shown in Figure 3.

Two satellites are simulated in STK11.2, and their initial orbital elements are set to be the same, as shown in Table 2, except that the epoch time is changed to 2016-06-16 04:00:00. The first satellite is set with a 21st order gravity model pulse atmospheric drag perturbation, and the second satellite is only set with a 21st order gravity model. Using the report function of STK, the accelerations of the two satellites at 2016-06-16 04:00:00 (STK11 does not contain the latest atmospheric model data, so use this time to ensure that our software and STK use the same atmospheric model data) are obtained respectively, and the atmospheric drag acceleration of the second satellite can be obtained by subtracting the two accelerations. In addition, another atmospheric drag acceleration can be calculated by calling the rodAccelAirDragPerturbation interface function. The calculation results of STK and our software are shown in Table 3, and the relative error described in equation (26) is used for quantitative comparison.

It can be seen from Table 3 that the error is 1.14%, indicating that the software algorithm in this paper is effective. The main sources of error are the coordinate and time conversion of the calculation program, and the calculation truncation error, etc.

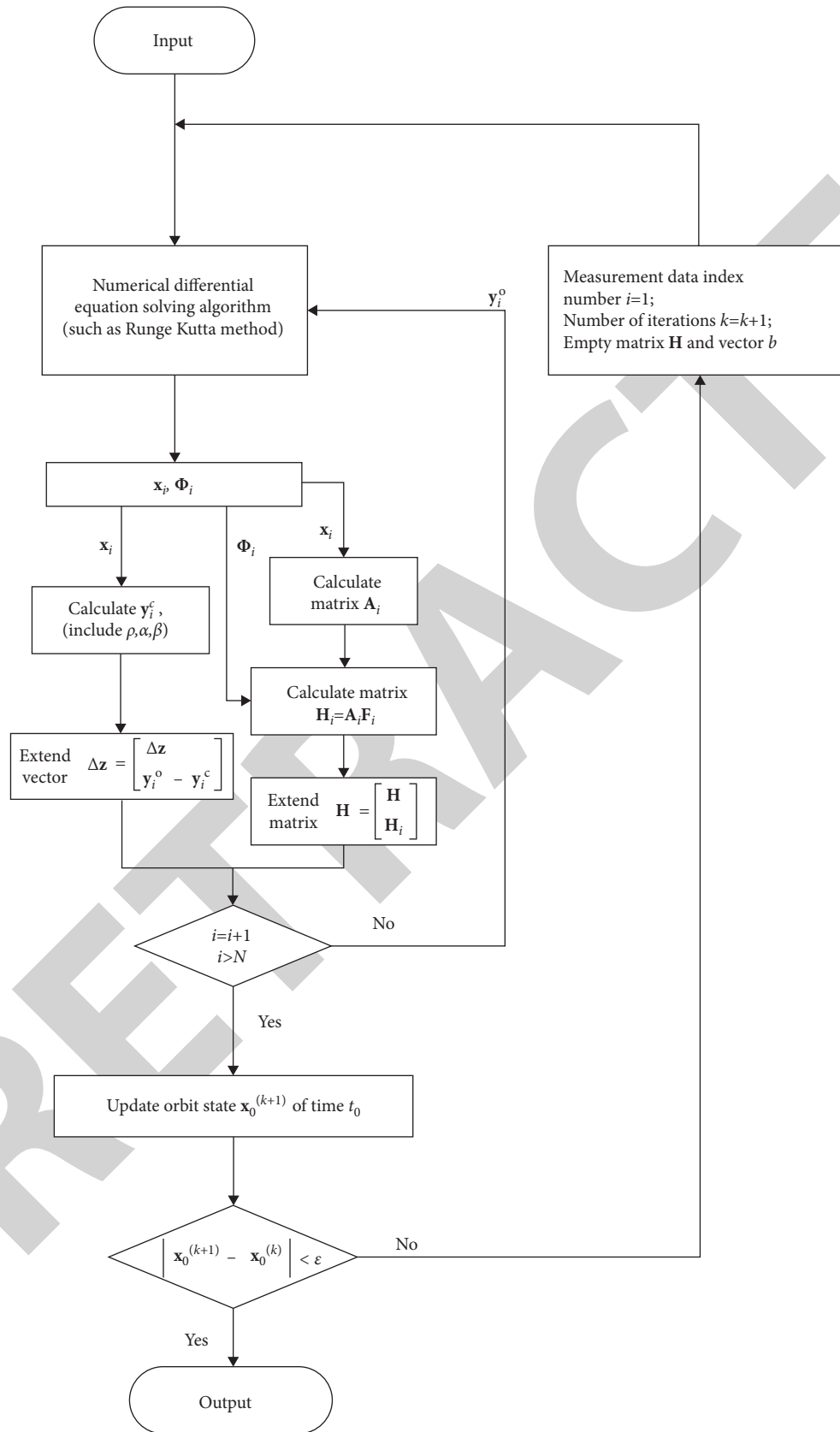


FIGURE 4: The flow chart of the program design for least-squares orbit improvement.

TABLE 2: Satellite orbit elements.

Epoch	Semimajor axis (km)	Eccentricity	Inclination	Argument of perigee	Ascension of ascending node	True anomaly
2020-10-08 04:00:00	6678.14	0	28.5°	0°	0°	0°

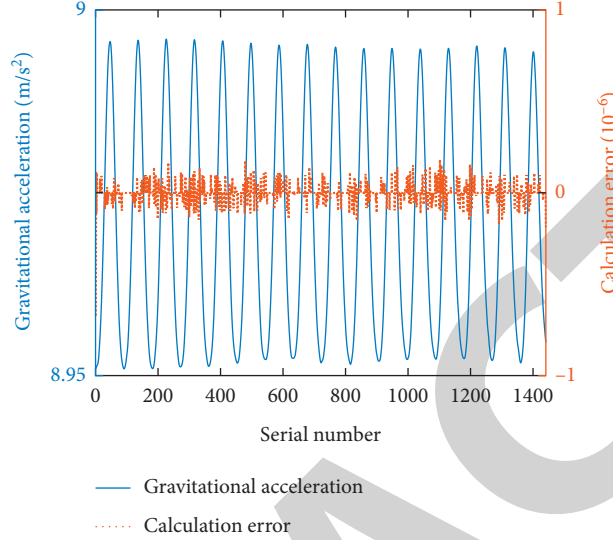


FIGURE 5: Earth's gravitational acceleration and its error.

TABLE 3: Comparison of atmospheric drag acceleration (STK and out software).

Category	Item	Acceleration (m/s <sup>2</sup> )		
		$x$	$y$	$z$
STK	Satellite 1	-8.9509556686	$-1.123596 \times 10^{-4}$	$-1.37593 \times 10^{-5}$
	Satellite 2	-8.9509556684	$-1.037988 \times 10^{-4}$	$-8.7521 \times 10^{-6}$
	Atmospheric drag perturbation	$-2 \times 10^{-10}$	$-8.5608 \times 10^{-6}$	$-5.0072 \times 10^{-6}$
Software	Atmospheric drag perturbation	$-6.6174 \times 10^{-24}$	$-8.4633 \times 10^{-6}$	$-4.9502 \times 10^{-6}$
Relative error		1.14%		

6.3. *Least Squares Orbit Improvement.* Using the programming principle in part 5, the least-squares orbit improvement interface function `rodLeadsquare` is realized and integrated into the `RadarOrbDet` library. The input and output of this function are shown in Figure 4.

A satellite is simulated in STK11.2 and its propagator `mod` is set to two-body. Its orbital elements settings are shown in Table 2. Only the epoch time is changed to 2021-09-07 04:00:00. The longitude, latitude, and altitude of the radar site are (120°, 30°, 0). Select 10 data points with an interval of 1 second from 19:15:01 to 19:15:10, and add measurement errors of 100 m, 0.1°, and 0.1° to the distance, azimuth, and elevation, respectively.

The software in this paper and the ODTK software are used to compare the orbit determination, respectively. The calculation results of ODTK and the software are shown in Table 4. The relative error of position and velocity described in equation (27) are used for quantitative comparison.

TABLE 4: Comparison of orbit determination results (ODTK and our software).

Category	Orbit determination results (epoch: 19:15:00; unit: km, km/s)					
	$x$	$y$	$z$	$v_x$	$v_y$	$v_z$
ODTK	5187.98	3690.77	2002.66	-4.84	5.29	2.88
Software	5190.66	3692.61	2004.97	-4.86	5.28	2.87
Relative error	0.06%			0.32%		

$$\text{relative position error} = \frac{|\mathbf{r}_{\text{software}} - \mathbf{r}_{\text{ODTK}}|}{|\mathbf{r}_{\text{ODTK}}|}, \quad (27)$$

$$\text{relative velocity error} = \frac{|\mathbf{v}_{\text{software}} - \mathbf{v}_{\text{ODTK}}|}{|\mathbf{v}_{\text{ODTK}}|}.$$

It can be seen from Table 4 that the position error of orbit determination is 0.06%, and the velocity error is 0.32%, indicating that the software algorithm in this paper is effective.

## Research Article

# Network Art Image Classification and Print Propagation Extraction Based on Depth Algorithm

Hao Zhang, Haimin Sun, and Tianyang Yuan 

*Department of Printmaking, Lu Xun Academy of Fine Arts, Shenyang 110004, Liaoning, China*

Correspondence should be addressed to Tianyang Yuan; [yuantianyang@lumei.edu.cn](mailto:yuantianyang@lumei.edu.cn)

Received 3 January 2022; Revised 24 January 2022; Accepted 4 February 2022; Published 23 February 2022

Academic Editor: Shalli Rani

Copyright © 2022 Hao Zhang et al. This is an open access article distributed under the Creative Commons Attribution License, which permits unrestricted use, distribution, and reproduction in any medium, provided the original work is properly cited.

In recent years, with the development of computer technology and the Internet, image databases have increased day by day, and the classification of image data has become one of the important research issues for obtaining image information. This article aims to study the role of depth algorithms in network art image classification and print propagation extraction. This article proposes a series of methods of image classification, print dissemination, and deep learning algorithms and also conducts corresponding experiments on the role of deep algorithms in image classification. The experimental results show that the neural network model based on the deep algorithm can effectively identify and classify network images, and its recognition accuracy is more than 80%. The image recognition method based on depth algorithm greatly improves the efficiency of image recognition.

## 1. Introduction

In order to efficiently manage and accurately classify image data, manual efficiency alone can no longer solve the problem. We hope to use computer computing power and efficient algorithms for quick and accurate classification. The problem of image classification can basically be studied from two aspects. One is quick and efficient classification from massive data, and the other is classification of subcategories from similar images. Mass data image classification is to classify images in terms of breadth. In the field of computer vision, this type of problem is a test of algorithm optimization capabilities. The content of the image is ever changing, and using only a few keywords to describe it obviously cannot meet the classification requirements.

Image classification is very common in life. The massive image data is messy and disorganized. How to extract the content that users are interested in has become a topic of great concern to industry and academia. Research on image classification can solve many practical problems in people's life or work, for example, the classification of items on Taobao shopping. The algorithm behind this supports the classification scenarios of hundreds of millions of products on Taobao, which efficiently allows users to find the products

they need and increases their desire to buy. This requires accurate and efficient classification of images.

On the basis of deep learning research, Lee et al. developed a computer-aided detection system based on CNN algorithm to evaluate the role of the system in the diagnosis and prediction of periodontal damaged teeth [1]. In Sudha and Priyadarshini's research, they proposed an advanced deep learning method, which uses an improved algorithm to detect multiple types and multiple vehicles in the input video [2]. The work by Farooq and Bazaz is different from that by Lee and Sudha in the research direction of deep learning. The former propose an online incremental learning technology based on artificial neural network (ANN). It is used to develop an adaptive and noninvasive analysis model of the COVID-19 pandemic to analyze the time dynamics of the spread of the disease. The model was validated with historical data, and a 30-day forecast of disease transmission was given in the five most severely affected states in India [3]. With the continuous in-depth study of deep learning algorithms by researchers, people have begun to conduct a lot of research on the application of deep algorithms in image classification. In their research on in-depth learning algorithms in image classification, Yan et al. proposed an image classification framework, which surpassed the window



sampling of a fixed spatial pyramid and was supported by a new learning algorithm [4]. In recent years, methods based on deep learning have attracted widespread attention in the field of hyperspectral image classification. However, due to the large number of parameters and complex network structure, when there are only a few training samples, deep learning methods may perform poorly [5]. When it comes to hyperspectral image classification, Su et al.'s research in this area has to be introduced. In Su et al.'s research, in order to optimize the classification of hyperspectral images and the selection and optimization of frequency bands, they proposed an extreme learning machine (ELM) method based on the firefly algorithm (FA) trigger [6]. Although these researchers have done a lot of research on image classification and depth algorithms, they have neglected the related research on some problems existing in image classification and depth algorithms in their research.

The innovation of this article lies in the corresponding research on image classification, print dissemination, and deep learning algorithms. Through relevant demonstrations on the image classification process and the extraction of image features, certain experimental research is carried out on the practical application of depth algorithms in image classification. Corresponding research provides a certain theoretical basis for popularizing the application of depth algorithm in image classification.

## 2. Depth Algorithm and Image Classification

### 2.1. Image Classification

**2.1.1. Image Recognition.** In daily life, images can be seen anytime and anywhere, occupying an important position, and visual information exceeds 70% of the total information received. This phenomenon can be described by the sentence "hearing is not as good as seeing" [7]. In many scenarios, images can show us information more intuitively than text or other forms of information. Figure 1 shows the common image types in life.

**2.1.2. Image Classification Process.** The general process of image classification is mainly divided into the following steps: (1) image preprocessing; (2) establishment of a classification model; (3) feature extraction and output classification results [8]. Figure 2 shows the general process of image classification.

There are two main research methods for image classification [9, 10]. One is a method based on manual features. The core of this method is the design of features. The second is image classification. The core of this method based on deep features is to build a deep learning model. Compared with methods based on manual features, methods based on depth features have better classification results [11].

There are two types of image features: global features and local features [12]. Local features usually include color features and texture features [13]. Commonly used image feature extraction algorithms include SIFT, SURF, MSER, Harris-Laplace, and Hessian-Affine [14]. As shown in

Table 1, the statistical table of the local feature extraction method of the image is displayed.

**2.1.3. Summary of Commonly Used Depth Features in Image Classification.** A feature is a piece of information related to solving a computing task related to an application. Features are specific structures within the image [15].

Deep features are extracted through deep learning networks. Compared with traditional manual features, the deep features obtained through deep learning have better expression effects. The high-level depth features are equivalent to the combination of low-level features. They have better abstraction, can better express a certain object, and are more conducive to image recognition and classification. Now, very popular frameworks for extracting deep features include AlexNet, VGG, GoogLeNet, and ResNet.

**(1) ResNet Depth Features.** ResNet has more layers, a total of 152 layers, which is far more than the number of layers in the previous networks. ResNet is also the first network to exceed 100 layers. The biggest difference between this network and other networks is the use of a residual network; that is, the original fitting output becomes the residual of the output and input, as shown in the ResNet network structure in Figure 3.

It can be seen from Figure 3 that the input  $a$  can directly reach the output, and the residual function is  $G(a)$ , which is also a new optimization goal, where

$$G(a) = T(a) - a. \quad (1)$$

In the formula,  $T(a)$  represents the expected mapping output of a certain layer.

Due to the large number of layers in the network, in order to reduce the amount of calculations, the residuals are optimized accordingly. Figure 4 shows the optimized ResNet network structure.

**(2) Comparison of Models for Extracting Depth Features.** Table 2 shows the summary and comparison result table of several deep learning models.

From the data in Table 2, we can see that the numbers of layers of ResNet, GoogLeNet, VGG, and AlexNet are decreasing layer by layer, and the number of layers of ResNet exceeds 100, which is obviously more than that of other networks. The number and size of the fully connected layers of VGG and AlexNet are exactly the same.

**2.2. Depth Algorithm.** Deep learning algorithms are an important field in machine learning; they are algorithms that classify data by learning feature performance [16]. The deep learning algorithm is a multilayer processing mechanism that simulates the external information of the human brain and nervous system [17].

CNN is the most common type of deep algorithms. CNN and multilayer neural network combine feature extraction and classification into one process, and CNN has several advantages over multilayer neural network: (1) The structure



FIGURE 1: Common image types.

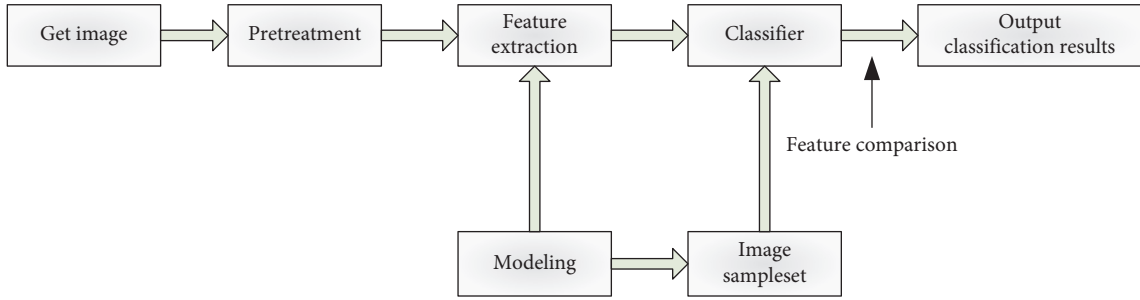


FIGURE 2: General process of image classification.

TABLE 1: Statistics of image local feature extraction methods.

	Corner	Spot	Area	Rotation invariance	Scale invariance	Radiological invariance	Accuracy	Timeliness
SIFT	Yes	Yes	No	Yes	Yes	No	Middle	Middle
SURF	Yes	Yes	No	Yes	Yes	No	Middle	High
MSER	No	No	Yes	Yes	Yes	Yes	High	High
Harris-Laplace	Yes	Yes	No	Yes	Yes	No	High	Low
Hessian-Affine	Yes	Yes	No	Yes	Yes	Yes	High	Middle

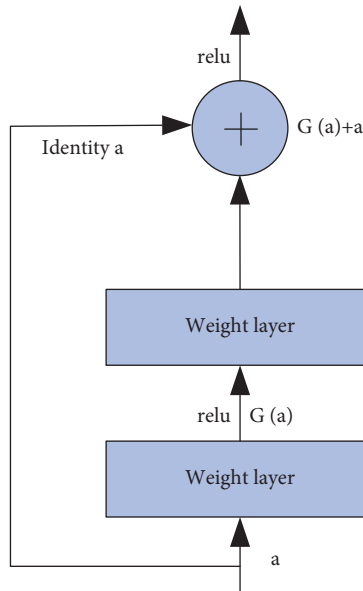


FIGURE 3: ResNet network structure diagram.

of CNN is more similar to the human visual processing system, and it is more suitable for 2D and 3D pictures. (2) CNN uses convolutional layers to implement convolution operations, and the convolution operation helps to obtain

the spatial structure relationship of the image, so it can extract features with stronger representation capabilities. (3) The pooling layer used by CNN can provide shape invariance characteristics, reduce network parameters, prevent overfitting, and improve the convergence speed of the network [18]. Figure 5 shows the structure of the CNN.

2.2.1. *Backpropagation of CNN.* The backpropagation algorithm is a learning algorithm suitable for multilayer neural networks, which is based on the gradient descent method. The input-output relationship of the backpropagation algorithm network is essentially a mapping relationship: the function completed by a BP neural network with  $n$  input and  $m$  output is a continuous mapping from  $n$ -dimensional Euclidean space to a finite field in  $m$ -dimensional Euclidean space, which is highly nonlinear. The backpropagation algorithm of CNN is based on gradient descent, and the iteration is divided into two steps [19]. For sample  $a$ , the error is

$$Z^a = \frac{1}{2} \sum_{m=1}^n (x_m^a - g_m^a)^2, \quad (2)$$

where  $x_m^a$  represents the target value of the  $m$ -th dimension of the corresponding  $a$ -th sample,  $n$  stands for gradient descent, and  $g_m^a$  represents the  $m$ -th dimension of the output

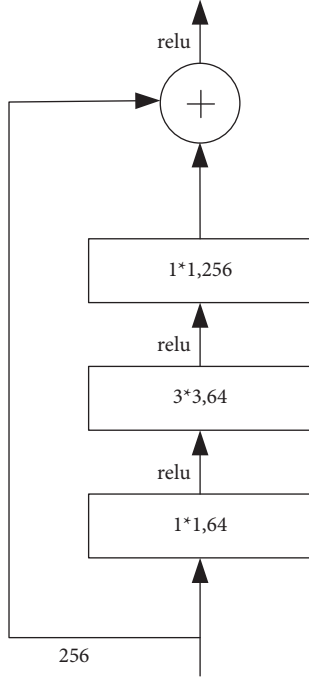


FIGURE 4: Optimized ResNet network structure diagram.

TABLE 2: Summary and comparison of several deep learning models.

Depth model	AlexNet	VGG	GoogLeNet	ResNet
Time	2012	2014	2014	2015
Number of layers	8	19	22	152
Convolutional layers	5	16	21	151
Convolution kernel size	11, 5, 3	3	6, 1, 3, 5	7, 1, 3, 5
Number of fully connected layers	3	3	3	1

of the corresponding  $a$ -th sample. In a fully connected network, the structure of the network is as follows.

$$r^s = f(w^s). \quad (3)$$

The activation function  $f$  generally uses the Sigmoid function.

Then, the partial derivative of the error to the network parameters is required; that is, the error is used to obtain the derivative of the bias and the weight.

$$\frac{\alpha Z}{\alpha q} = \frac{\alpha Z}{\alpha w} * \frac{\alpha w}{\alpha q} = \delta. \quad (4)$$

Since  $\alpha w/\alpha q = 1$ ,  $\alpha Z/\alpha q = \alpha Z/\alpha w = \delta$ ,  $\alpha Z/\alpha q = \alpha Z/\alpha w = \delta$ ; thus, the sensitivity of the hidden layer can be derived:

$$\delta^i = (T^{i+1})^R \delta^{i+1} \circ f'(w^i). \quad (5)$$

The sensitivity of the output layer is directly determined by the layer, which is expressed as follows:

$$\delta^I = f'(w^I) \circ (v^a - r^a). \quad (6)$$

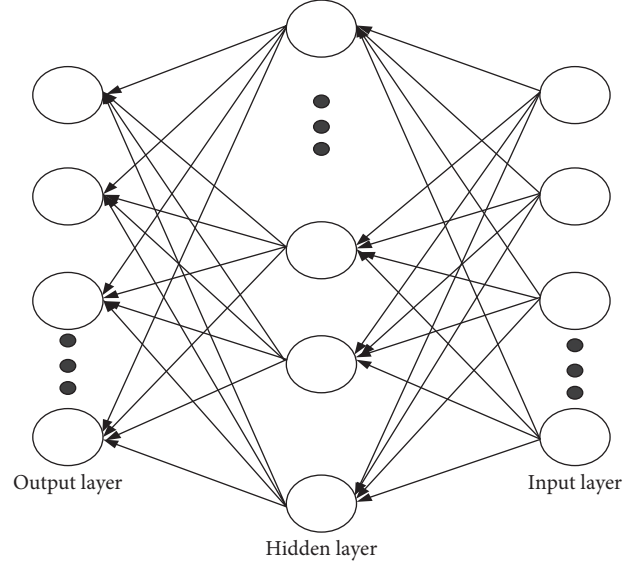


FIGURE 5: Structure diagram of CNN.

Since there is no error function that can be used directly in the hidden layer, the backpropagation algorithm uses the above formula to propagate the error to the front of each network layer [20]. Finally, the neuron weight is updated. The rule for updating the neuron weight is to multiply the input vector and the triangular array of the outer product neuron of the error signal vector. The specific operation process is as follows:

$$\frac{\alpha Z}{\alpha T^I} = n^{I-1} (\delta^I)^R, \quad (7)$$

$$\Delta T^I = -\ell \frac{\alpha Z}{\alpha T^I}. \quad (8)$$

2.2.2. CNN Gradient Descent. For the convolutional layer, the convolution process of the CNN can be expressed as

$$n_a^I = f \left( \sum_{i \in L_a} n_i^{I-1} * t_{ia}^I + y_i^I \right). \quad (9)$$

Like the backpropagation algorithm, the gradient descent process of the CNN is to multiply the deviation function of the activation function of the convolutional layer feature map with the error signal map obtained after downsampling. Since the weights in the downsampling layer are all  $\theta$ , here it needs to multiply another  $\theta$ :

$$\delta_a^I = \theta_a^{I+1} (f'(w_a^I) \circ wp(\delta_a^{I+1})). \quad (10)$$

Then, if the feature map is given, the deviation gradient can be found. The calculation method of the deviation gradient is

$$\frac{\alpha Z}{\alpha q_a} = \sum_{a,m} (\delta_a^I)_{am}. \quad (11)$$

Finally, the gradient of the kernel function can be calculated by post-attributes. Because the weights are shared, all gradients contained in the weights must be totaled:

$$\frac{\alpha Z}{\alpha R_{ia}^I} = \sum_{w,m} (\delta_a^I)_{wm} (Y_i^{I-1})_{wm}. \quad (12)$$

Among them,  $(Y_i^{I-1})_{wm}$  is the area in  $n_i^{I-1}$  that is multiplied by  $R_{ia}^I$  during convolution. The value of the  $(w, m)$  position of the output convolution graph is obtained by multiplying the patch at the position  $(w, m)$  of the previous layer by  $R_{ia}^I$ .

For the downsampling layer, there is no difference between the numbers of input and output feature maps, but the output content is the input downsampling result, so the size of the output map will change. The calculation formula for the change is

$$n_a^I = f(\theta_a^I \text{down}(Q_a^{I-1}) + \gamma_a^I). \quad (13)$$

To calculate the derived function, first calculate the error signal mapping of this layer. Because there will be a convolutional layer after the downsampling layer, it is necessary to clarify which area of the input image corresponds to the output pixel. Formula (14) shows the calculation method for a given pixel:

$$\delta_a^I = f'(w_a^I) \circ \text{conv}2(\delta_a^{I+1}, \text{rot}180(r_a^{I+1}), \text{full}'). \quad (14)$$

After calculating the given pixel size, after calculating the gradient of the multiplicative deviation  $\theta$  and the additional deviation  $\gamma$ , the gradient of the additional deviation  $\gamma$  is the sum of the elements in the error signal graph. The calculation method is

$$\frac{\delta Z}{\delta \gamma_a} = \sum_{w,m} (\delta_a^I)_{wm}. \quad (15)$$

The multiplication deviation  $\theta$  is associated with the sampling map. The original downsampling map refers to the feature map without additional deviation after downsampling. These feature maps are directly stored in the propagation sequence, so there is no need to calculate the multiplicative deviation during backpropagation.

$$d_a^I = \text{down}(n_a^{I-1}). \quad (16)$$

Therefore, the gradient of the error to  $\theta$  can be expressed as

$$\frac{\alpha Z}{\alpha \theta_a} = \sum_{w,m} (\delta_a^I \circ d_a^I)_{wm}. \quad (17)$$

### 2.2.3. Image Recognition Based on Deep Neural Network

(1) *The Method of Initializing Weights in Neural Network and the Existing Problems.* In deep learning, the weight initialization method of neural network has a crucial impact on the convergence speed and performance of the model [21–23]. In a deep neural network, as the number of

layers increases, gradient disappearance or gradient explosion is very easy to occur in the process of gradient descent. Therefore, the initialization of weights is very important. Although a good weight initialization cannot completely solve the problems of gradient disappearance and gradient explosion, it is very helpful in dealing with these two problems and is very beneficial to model performance and convergence speed. In the deep neural network, the initialization of the weight  $w$  is generated by following a standard normal distribution with a mean of 0 and a standard deviation of 1 [24].

(2) *Improved Initialization Weight Method.* The improved method is to initialize the weight value according to a normal distribution with a mean value of 0 and a standard deviation of  $1/\sqrt{r}$ , where  $r$  represents the number of neurons in the input layer. It is known that

$$M(g) = M\left(\sum_{n=1}^r w_n a_n + y\right). \quad (18)$$

Expanding formula (18), we get

$$M(g) = \sum_{n=1}^r M(w_n a_n) + M(y). \quad (19)$$

Transforming formula (19) based on the nature of variance, we get the result of the change as follows:

$$M(g) = \sum_{n=1}^r T\{[w_n a_n - T(w_n a_n)]^2\} + M(y). \quad (20)$$

If the variances of  $g$  and input data  $a$  are to be similar, that is, the degree of dispersion of data  $g$  and input data  $a$  is similar, then the weight  $w$  must be initialized to obey a normal distribution with a variance of  $I$ .

2.3. *Print Dissemination.* Printmaking is a kind of painting with strong artistic expression, and printmaking has a variety of painting languages and reproducibility [25]. Compared with other types of paintings, prints are not as direct as traditional Chinese paintings and oil paintings. Prints must be created with the help of wood panels, copperplates, slates, silk screens, etc. Figure 6 shows the common types of prints.

Communication media is different from communication forms. Communication forms refer to the specific ways that the communicators use to act on the audience when they carry out communication activities, such as oral communication, letter communication, image communication, and comprehensive communication.

The transformation of modern printmaking's communication function is mainly due to the development of modern printmaking, which has changed the development direction of modern printmaking. The art of printmaking has been strengthened, and the works present different forms, richness, and variety, breaking through the nature of printmaking itself. For modern printmaking, its full value lies not only in the spirit embodied in the picture, but also



FIGURE 6: Common types of prints.

TABLE 3: Classification accuracy of a single feature under different classification methods.

	SVM (%)	RF (%)	Bayes (%)	KNN (%)
DSIFT	76.58	70.11	74.69	60.36
HSV	84.37	85.99	83.22	71.04
HOG	55.68	48.57	48.62	41.90
SURF	77.49	66.41	78.15	66.38
LBP	25.14	21.51	24.61	21.93
Gabor	23.69	25.19	15.06	11.27

in the individuality of the printing techniques and materials and the technical spirit revealed in the printing process. In some of the current exhibitions, we can easily find that the prints are already very rich and diverse. Printmaking has its unique pluralism, and the ability to communicate is particularly strong. This kind of communication can not only popularize printmaking, but also make it affordable for fans who like to keep printmaking at home, give it to friends, etc. This is conducive to the spread and development of prints.

### 3. Image Recognition and Classification Experiment

*3.1. Image Classification Feature Extraction Experiment.* Global features refer to the overall attributes of an image, and common global features include color features, texture features, and shape features, such as intensity histograms. Because they are low-level visual features at the pixel level, the global features have the characteristics of good invariance, simple calculation, and intuitive representation. Traditional feature extraction methods mainly use six features, namely, Dense SIFT (DSIFT), color histogram, SURF, HOG, LBP, and Gabor features. Four classifiers are used, namely, SVM, Random Forest, Naive Bayes, and KNN. In the experiment, a single feature and a combination of multiple features are mainly used, then the BoW

model is used for feature coding, and finally a variety of classification methods are used for comparison experiments.

For the CNN method, this experiment uses the classic AlexNet and ResNet-18 network models and uses two training modes: The first is direct training; that is, the network parameters are randomly generated. The second type is pretraining. The network parameters are loaded by the parameters of the pretrained model, which is usually trained on the ImageNet database.

#### 3.1.1. Experimental Results of Single-Feature Classification.

Table 3 shows the experimental results of a single-feature classification method, where Bayes represents the Naive Bayes classification method. Except for the HSV color histogram, all features are extracted using the BoW method for feature coding, and the HSV color histogram is directly classified after normalizing the features, without the need for BoW feature coding.

It can be seen from Table 3 that the direct use of HSV color histogram features can get the best classification accuracy, with an average classification accuracy of 80%, followed by DSIFT features, and the worst is the use of Gabor and LBP features. As can be seen from the data in Table 3, the use of Gabor and LBP features achieved classification accuracy between 20% and 25%, which is too low.

TABLE 4: Classification accuracy of two-feature combinations.

	SVM (%)	RF (%)	Bayes (%)	KNN (%)
DSIFT + HSV	85.61	85.17	86.19	73.11
DSIFT + HOG	71.25	65.98	73.64	50.60
DSIFT + Gabor	63.98	69.31	65.12	55.81
DSIFT + LBP	62.66	65.87	62.67	56.92
SURF + HSV	89.03	88.15	89.70	80.10
SURF + Gabor	66.21	65.94	64.22	57.62
SURF + HOG	67.84	62.45	63.37	52.00
SURF + LBP	69.33	64.83	68.30	64.13

TABLE 5: Classification performance test results.

	Accuracy (%)	Recall rate (%)	F-measure (%)
Print	88.6	90.5	87.4
Chinese painting	91.3	86.8	89.2
Painting	87.7	85.1	85.9
Watercolor painting	87.2	85.4	86.0
Gouache	80.6	85.9	83.3

TABLE 6: Comparison of classification results of different network models.

	Parameter	Time	Accuracy (%)
ResNet-50	23.5M	61	84.2
Xception	20.1M	42	85.7
Inception-v4	42.6M	65	82.4
MobileNet-v1	3.0M	21	76.5
ShuffleNet	9.6M	19	80.3
Neural network model	8.8M	8	89.1

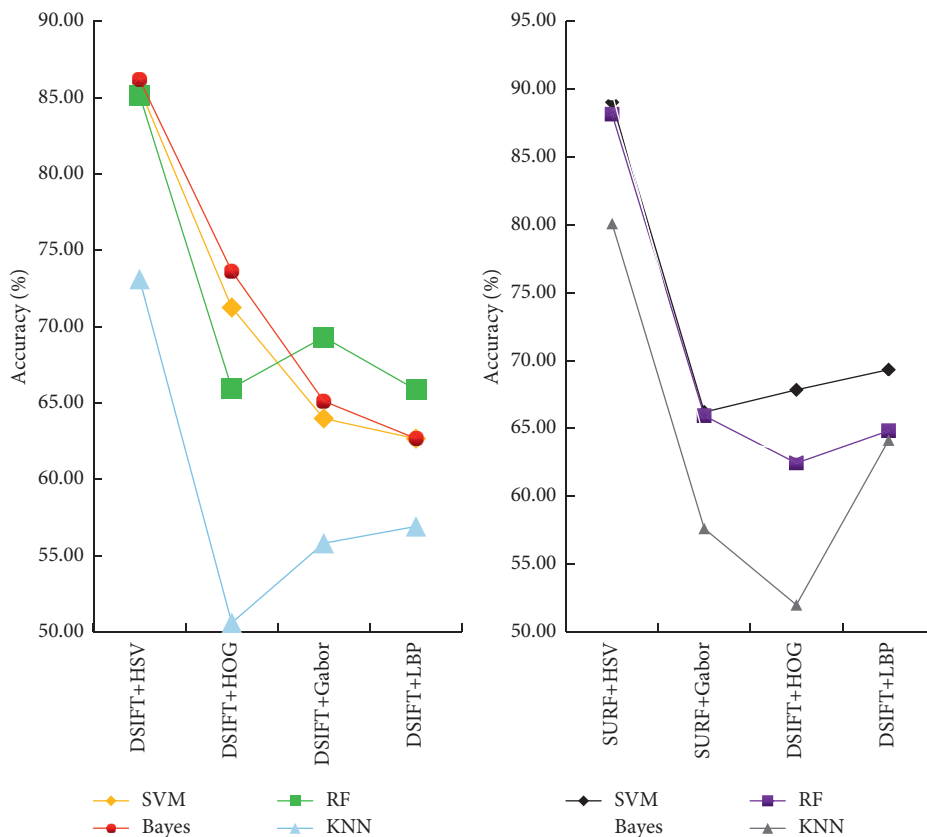


FIGURE 7: Multifeature combination classification results.

**3.1.2. Multiple-Feature Combination Experiment Results.** In single-feature classification, since DSIFT and SURF have better classification results, these two features are mainly used in combination with other features. Table 4 shows the classification results of the two-feature combinations.

**3.2. Image Recognition Experiment Based on Depth Algorithm.** In order to verify the role of the depth algorithm in the recognition of images and prints, in this experiment, various prints, Chinese paintings, oil paintings, watercolors, etc. from the network art images were randomly selected for recognition and classification. In the recognition process, different network models were used for many experiments, the purpose is to verify whether the neural network model based on the deep algorithm has more advantages in image recognition and classification than other network models. Tables 5 and 6 show the test results of image classification performance based on deep learning and the comparison table of classification results of different network models, respectively.

## 4. Results of Image Recognition and Classification Experiment

**4.1. Experimental Results of Feature Extraction Experiments Based on Image Classification.** In the experiment, the results of a single-feature classification experiment and multiple-feature combination experiments were recorded. In the current feature classification, it can be clearly seen that using the HSV color histogram feature can get the best classification accuracy. In the multifeature combination experiment, due to too much data, the experimental conclusion cannot be drawn directly. To this end, according to the data in Table 4, we can get the experimental results of the classification of DSIFT and SURF features with HSV color histograms, as shown in Figure 7:

According to Figure 7, it can be known that the HSV color histogram combined with DSIFT and SURF features has achieved better classification performance, especially when combined with SURF features to get the best classification accuracy, with an average accuracy rate of 80%.

In this experiment, two initialization methods are used to classify and recognize image features for the weight of CNN, namely, the initialization of Gaussian distribution and the Xavier initialization method. Figure 8 shows the experimental results of the two weight initialization methods.

According to Figure 8, it can be clearly seen that the accuracy of CNN image classification based on the Xavier initialization method is more suitable for image recognition. Its recognition accuracy can stabilize at 86% to 90% after a certain number of iterations. As the image layer increases, the Xavier initialization method has a higher recognition rate for the image. Figure 9 shows the comparison of the image recognition accuracy of the classic AlexNet and ResNet-18 network models in two different training modes.

It can be seen from Figure 9 that the accuracy of image recognition in the pretraining mode is greatly improved compared with the direct training mode. In the pretraining

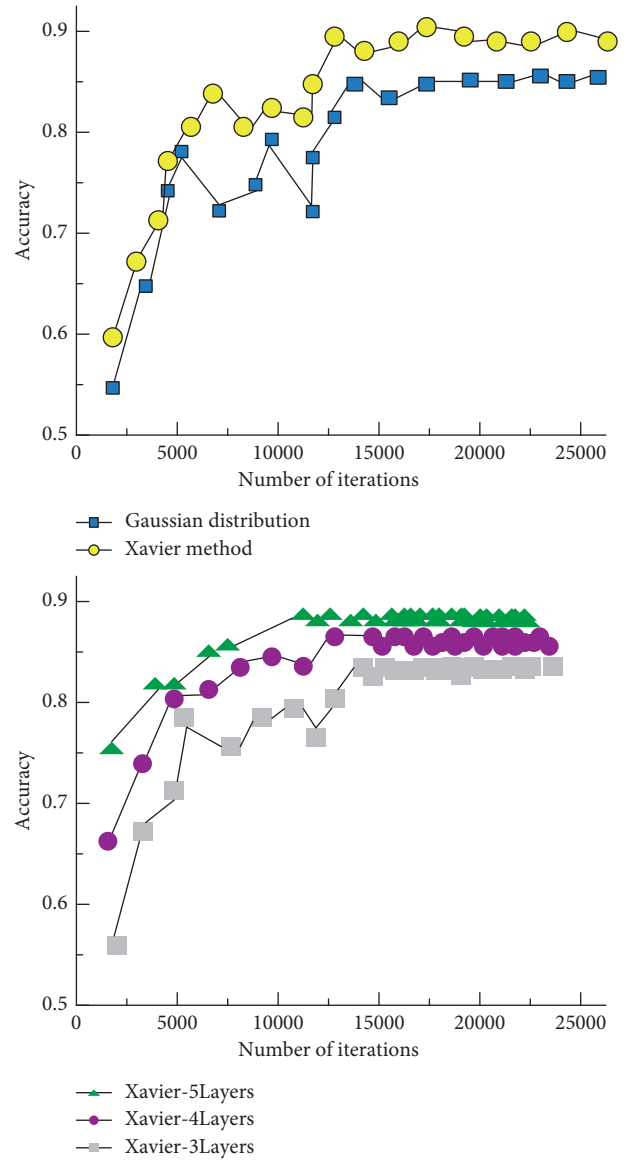


FIGURE 8: Classification accuracy.

mode, the accuracy of the AlexNet network model is maintained between 90% and 93%, while in the direct training mode, its recognition accuracy is only 87%.

**4.2. Results of Image Recognition Experiment Based on Depth Algorithm.** According to the experimental data in Tables 5 and 6, a comparison chart of the recognition rate accuracy of different images and the image recognition rate under different network models can be obtained, as shown in Figure 10.

According to Figure 10, the image recognition technology based on the depth algorithm maintains a high level of accuracy in the recognition of prints and web images. During the experiment, no matter what the type of the image is, the recognition accuracy rate can reach 80%. Moreover, the CNN image recognition model based on the depth algorithm is higher than other network models in image recognition rate, accuracy rate, and recognition speed.

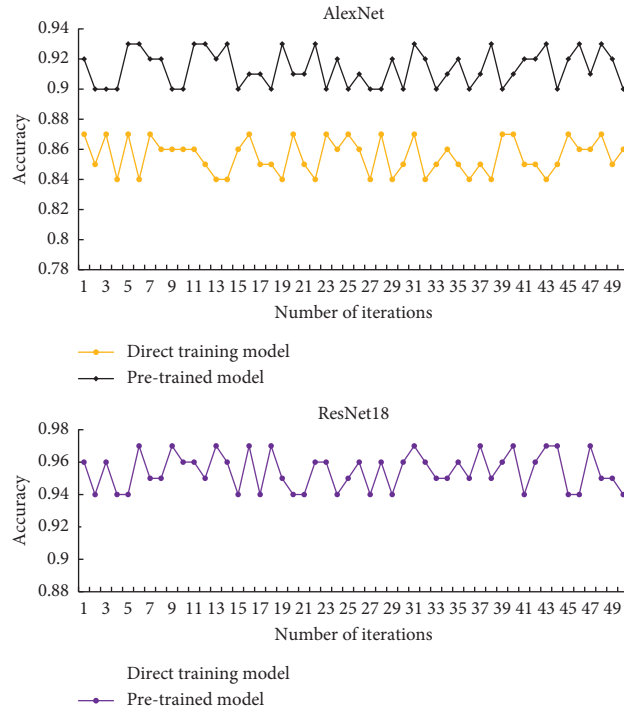


FIGURE 9: Comparison of image recognition accuracy rates in different training modes.

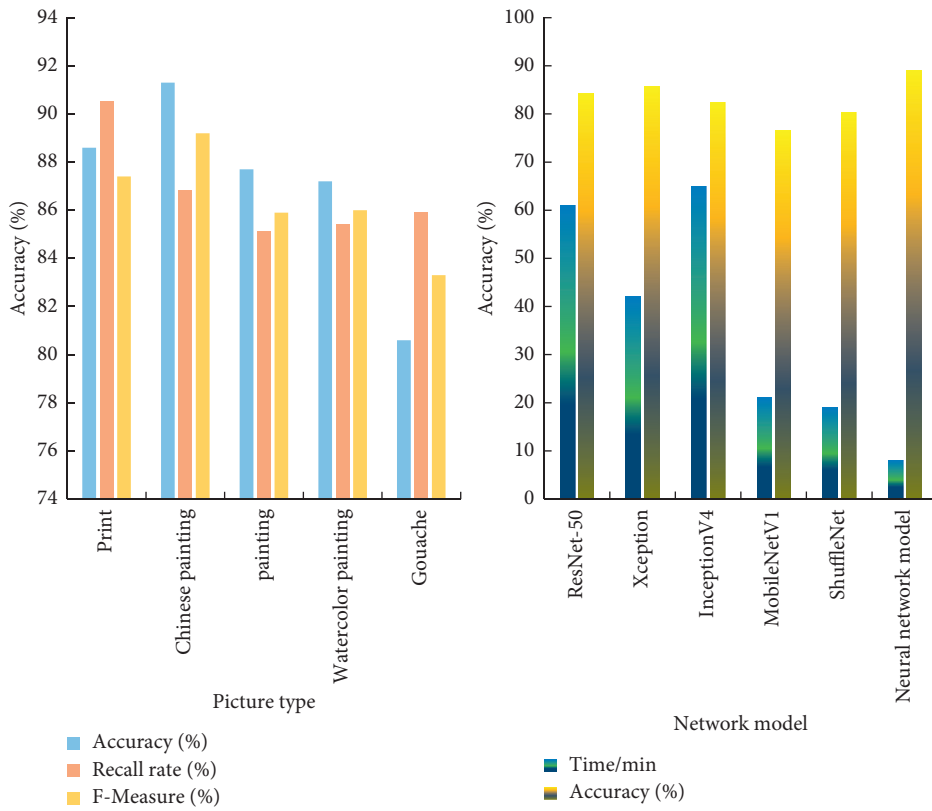


FIGURE 10: The recognition rate of different types of images.



## 5. Conclusions

With the continuous increase in the types and quantity of network images, traditional network image classification methods can no longer meet the needs of efficient management of network images. Network image classification management puts forward higher requirements for the professional knowledge and skills of classification personnel. The use of CNN has greatly improved the accuracy of image recognition and further improved the efficiency of network image recognition, classification, and organization. Its good feature extraction capabilities should also be widely used in more classification and retrieval tasks.

## Data Availability

No data were used to support this study.

## Conflicts of Interest

The authors declare that there are no conflicts of interest with any financial organizations regarding the material reported in this manuscript.

## Acknowledgments

This work was supported by the “Xing Liao Talents Plan” project of Liaoning Province (no. XLYC1907112).



## References

- [1] J.-H. Lee, D.-h. Kim, S.-N. Jeong, and S.-H. Choi, “Diagnosis and prediction of periodontally compromised teeth using a deep learning-based convolutional neural network algorithm,” *Journal of Periodontal & Implant Science*, vol. 48, no. 2, pp. 114–123, 2018.
- [2] D. Sudha and J. Priyadarshini, “An intelligent multiple vehicle detection and tracking using modified vibe algorithm and deep learning algorithm,” *Soft Computing*, vol. 24, no. 21, pp. 1–13, 2020.
- [3] J. Farooq and M. A. Bazaz, “A deep learning algorithm for modeling and forecasting of COVID-19 in five worst affected states of India,” *Alexandria Engineering Journal*, vol. 60, no. 1, pp. 587–596, 2021.
- [4] S. Yan, X. Xu, D. Xu, S. Lin, and X. Li, “Image classification with densely sampled image windows and generalized adaptive multiple kernel learning,” *IEEE Transactions on Cybernetics*, vol. 45, no. 45, pp. 381–390, 2017.
- [5] B. Pan, Z. Shi, and X. Xu, “MugNet: deep learning for hyperspectral image classification using limited samples,” *ISPRS Journal of Photogrammetry and Remote Sensing*, vol. 145, pp. 108–119, 2017.
- [6] H. Su, Y. Cai, and Q. Du, “Firefly-algorithm-inspired framework with band selection and extreme learning machine for hyperspectral image classification,” *IEEE Journal of Selected Topics in Applied Earth Observations and Remote Sensing*, vol. 10, no. 1, pp. 309–320, 2017.
- [7] C. Hu, Z. Yi, and M. K. Kalra, “Low-dose CT with a residual encoder-decoder convolutional neural network (RED-CNN),” *IEEE Transactions on Medical Imaging*, vol. 36, no. 99, pp. 2524–2535, 2017.
- [8] S. S. S. Kruthiventi, K. Ayush, and R. V. Babu, “DeepFix: a fully convolutional neural network for predicting human eye fixations,” *IEEE Transactions on Image Processing*, vol. 26, no. 9, pp. 4446–4456, 2017.
- [9] M. Abdolmaleky, M. Naseri, J. Batle, A. Farouk, and L.-H. Gong, “Red-Green-Blue multi-channel quantum representation of digital images,” *Optik*, vol. 128, pp. 121–132, 2017.
- [10] O. Ibrahim Khalaf, C. A. T. Romero, A. Azhagu Jaisudhan Pazhani, and G. Vinuja, “VLSI implementation of a high-performance nonlinear image scaling algorithm,” *Journal of Healthcare Engineering*, vol. 2021, Article ID 6297856, 10 pages, 2021.
- [11] M. Ye, Y. Qian, J. Zhou, and Y. Y. Tang, “Dictionary learning-based feature-level domain adaptation for cross-scene hyperspectral image classification,” *IEEE Transactions on Geoscience and Remote Sensing*, vol. 55, no. 3, pp. 1544–1562, 2017.
- [12] L. Ma, M. Li, X. Ma, L. Cheng, P. Du, and Y. Liu, “A review of supervised object-based land-cover image classification,” *ISPRS Journal of Photogrammetry and Remote Sensing*, vol. 130, pp. 277–293, 2017.
- [13] Y. Zhou, J. Peng, and C. Chen, “Extreme learning machine with composite kernels for hyperspectral image classification,” *IEEE Journal of Selected Topics in Applied Earth Observations and Remote Sensing*, vol. 8, no. 6, pp. 2351–2360, 2017.
- [14] L. Chang, M. Yong, and X. Mei, “Hyperspectral image classification with robust sparse representation,” *IEEE Geoscience and Remote Sensing Letters*, vol. 13, no. 5, pp. 641–645, 2017.
- [15] J. Xia, J. Chanussot, P. Du, and X. He, “(Semi-) supervised probabilistic principal component analysis for hyperspectral remote sensing image classification,” *IEEE Journal of Selected Topics in Applied Earth Observations and Remote Sensing*, vol. 7, no. 6, pp. 2224–2236, 2017.
- [16] J. Lin, H. Chen, and Z. J. Wang, “Structure preserving transfer learning for unsupervised hyperspectral image classification,” *IEEE Geoscience and Remote Sensing Letters*, vol. 14, no. 10, pp. 1–5, 2017.
- [17] S. S. Han, M. S. Kim, W. Lim, G. H. Park, I. Park, and S. E. Chang, “Classification of the clinical images for benign and malignant cutaneous tumors using a deep learning algorithm,” *Journal of Investigative Dermatology*, vol. 138, no. 7, pp. 1529–1538, 2018.
- [18] S. Khan, M. Khan, N. Iqbal, T. Hussain, S. A. Khan, and K.-C. Chou, “A two-level computation model based on deep learning algorithm for identification of piRNA and their functions via Chou’s 5-steps rule,” *International Journal of Peptide Research and Therapeutics*, vol. 26, no. 2, pp. 795–809, 2020.
- [19] C. Liu and X. Zheng, “Exploring resource management for innovation power network based on deep learning algorithm,” *Neural Computing & Applications*, vol. 33, no. 2, pp. 1–13, 2021.
- [20] X. Yan, Z. Jia, and L. B. Wang, “Large scale tissue histopathology image classification, segmentation, and visualization via deep convolutional activation features,” *BMC Bioinformatics*, vol. 18, no. 1, pp. 1–17, 2017.
- [21] W. Yin, Y. Cui, Q. Qian, G. Shen, C. Guo, and S. Li, “DI-AMOND: a structured coevolution feature optimization method for LDDoS detection in SDN-IoT,” *Wireless Communications and Mobile Computing*, vol. 2021, Article ID 9530274, 14 pages, 2021.
- [22] W. Wei, X. Hu, H. Liu, M. Zhou, and Y. Song, “Towards integration of domain knowledge-guided feature engineering

- and deep feature learning in surface electromyography-based hand movement recognition,” *Computational Intelligence and Neuroscience*, vol. 2021, Article ID 4454648, 13 pages, 2021.
- [23] Y. Zhao, H. Li, S. Wan et al., “Knowledge-aided convolutional neural network for small organ segmentation,” *IEEE journal of biomedical and health informatics*, vol. 23, no. 4, pp. 1363–1373, 2019.
- [24] S. Torres, “School-based body image intervention: overcoming challenges to dissemination,” *Journal of Adolescent Health*, vol. 68, no. 2, pp. 229–230, 2021.
- [25] Y. Huo, L. Ma, and Y. Zhong, “A big data privacy respecting dissemination method for social network,” *Journal of Signal Processing Systems*, vol. 90, no. 4, pp. 467–475, 2018.

## Research Article

# Lambertian Luminous Intensity Radiation Pattern Analysis in OLOS Indoor Propagation for Better Connectivity

Vaishali,<sup>1</sup> Sandeep Sancheti,<sup>2</sup> Arvind Dhaka ,<sup>3</sup> Amita Nandal,<sup>3</sup> Hamurabi Gamboa Rosales ,<sup>4</sup> Deepika Koundal,<sup>5</sup> Francisco Eneldo López Monteagudo,<sup>4</sup> Carlos Eric Galvan Tajada,<sup>4</sup> and Arpit Kumar Sharma<sup>3</sup>

<sup>1</sup>Tishitu Technology & Research Private Limited, Jaipur, Rajasthan 302017, India

<sup>2</sup>Department of Information & Communication Technology, Marwadi University, Rajkot, Gujarat 360003, India

<sup>3</sup>Department of Computer and Communication Engineering, Manipal University Jaipur, Jaipur, India

<sup>4</sup>Unidad Academica de Ingenieria Electrica, Universidad Autonoma de Zacatecas, Jardin Juarez 147, Centro Historico, ZA 98000, Mexico

<sup>5</sup>School of Computer Science, University of Petroleum & Energy Studies, Dehradun, India

Correspondence should be addressed to Arvind Dhaka; [arvind.neomatrix@gmail.com](mailto:arvind.neomatrix@gmail.com) and Hamurabi Gamboa Rosales; [hamurabigr@uaz.edu.mx](mailto:hamurabigr@uaz.edu.mx)

Received 11 October 2021; Accepted 17 January 2022; Published 22 February 2022

Academic Editor: Carles Gomez

Copyright © 2022 Vaishali et al. This is an open access article distributed under the Creative Commons Attribution License, which permits unrestricted use, distribution, and reproduction in any medium, provided the original work is properly cited.

This paper illustrates the impact of wavelength on the Optical Line of sight (OLOS) link working in the Visible Light Communication (VLC) spectrum. The extension of work is based on previous outcomes given by researchers. It has been elaborated with different determinants based on the color factor of LED available in the Visible Light (VL) spectrum. In the modern world, Light Emitting Diodes (LEDs) are prevailing the market as a light source, which is dominantly used at homes and workplaces. The designed VLC system includes LED as a transmitter, which is used as a higher source of brightness and provides both illuminations and data communication. Solid-state lighting characteristic shows the electroluminescence capability of high brightness LEDs. Within few years, the luminous efficacy of LED is exponentially increasing from the range of less than 0.1 lm/W to over 230 lm/W with a huge lifetime of around 100,000 h. MATLAB is used to simulate a VLC link between LEDs (operated at different wavelengths) and photodetector. We present here the performance analysis of Lambertian Luminous Intensity radiation pattern (LLIRP) generated by different colors of LED for a clear OLOS model with different Spectral Luminous Efficiency at photonic vision. A designed system model of VLC supports short links present in indoor room conditions with better connectivity.

## 1. Introduction

Optical wireless communication (OWC) has become a trending field among researchers because of the high capacity that it offers to solve last-mile applications [1, 2]. Visible light communication arises as to the latest research trend in indoor optical wireless communication (OWC), which contributes the most matured and robust solutions to many issues. Nowadays, VLC is not only limited to being a source of light in home networking but also provides high-speed communication networks via light links in offices, airplanes, traffic light signals, etc. [3, 4]. In the last few years,

growing research in VLC shows the reliability and power efficiency offered by LED, which is to date much more remarkable than any conventional incandescent source of light used for lighting. Recent research in VLC demonstrates successfully data transmission up to 3 Gbps over short links installed in indoor environments [5]. The main drivers of this technique include high bandwidth/data rate, longer lifetime LEDs as compared with incandescent bulbs, better brightness level, no health and physical hazards, data security, and low power consumption [6, 7]. Due to such advantages, LEDs show the potential for higher data communication with power-saving features on global platforms.

The main problem of indoor VLC links is only a requirement of precise alignment and pointing with perfect directionality of the source of light with the receiver.

The infrastructure of any commercial organization and office buildings offer light wave as optical light emitting diodes (OLED), which has a tremendous potential to deploy the several access points (AP) for light fidelity (Li-Fi) [8]. Li-Fi technology is also notable to many as an interference-free system with other existing technologies (e.g., Wi-Fi, Ethernet, WiMAX, etc.) due to the use of the terahertz spectrum. Rapid growth in multimedia communication needs a smart indoor wireless network for better connectivity with the number of portable appliances. Such technologies can be easily installed by just using inexpensive optoelectronic devices like OLED connected with silicon photodetectors [9]. Since the last decade, LEDs have been considered a general source of illumination only, but now it becomes an alternative source of high-speed communication. The first visible-light LEDs operated only at low intensity and were limited to wavelength of red color. Nevertheless, modern LEDs are available in vast ranges of visible, ultraviolet, and infrared wavelengths, with very high illuminance and low power consumption. As compared with other sources of illumination like traditional incandescent, luminous efficacy is limited to 52 lm/W only. While in the case of fluorescent lamps, it is limited to 90 lm/W [10]. Although, LEDs show their peak efficiency over 260 lm/W, which is much lower when compared with its theoretically predicted value that reaches up to 425 lm/W [11]. Coming years make us the witness of about rapid increase in performance level offered by illumination of OLEDs.

In recent times, visible light communication (VLC) has gained huge consideration from the academic community and industry. Indeed, the spectrum crunch of Wi-Fi is seeking the alternative of radiofrequency communication, and VLC becomes the front runner due to its simplicity, speed, full-duplex nature, license-free operation, and data security. Furthermore, VLC achieves several landmarks by offering new applications such as underwater communication, vehicle-to-vehicle communication, and indoor localization. VLC system plays a key role by selecting the accurate transmitter (TX) and receiver (RX) to attain and sustain high performance. The high performance majorly depends on the performance of the source, i.e., LEDs. The modulation needs a perfect source that can provide both the illumination and the communication channel. Numerous aspects such as the LED type, color, illumination power, and bandwidth can put a direct influence on performance. Therefore, the selection of exact LED is quite significant according to the VLC scenarios, particularly where the LEDs need to perform the bidirectional communication.

The bidirectional performance between LEDs can be affected by several factors and environmental circumstances. For example, the illumination of LED alters according to field-of-view and distance. The ambiance of light can also vary the LED communication and its performance. In brief, the selection of receiving mechanism is also critical due to the high sensitivity of photodiodes (PDs) for low-power LEDs. This paper elaborates the examination on accurate

usage of LEDs in VLC systems as trans-receiver. This work presents the evaluation of the LED impact on the VLC performance by varying the color under realistic environments. It becomes significant to understand the performance of LED (based on color), as it helps to understand the power losses with the change of distance. Our results validate that the color intensity of LED can greatly influence performance and communication quality. For instance, the green LED utilization can provide a high luminous intensity for the yellow, blue, and red LEDs. Such LEDs are very common in use and easily available. It is important to consider the fact that we need to work on such sources that are easily available. While prior research studies only target to assess physical properties of visible light or only work on a single parameter, our work opens new perspectives by considering the power losses. Different angles approach optical gain, modulation schemes, multiple access, and applications.

The proposed system offers several benefits as this model accurately predicts the intensity pattern of the source towards the receiver. LLIRP can estimate the received power distribution according to any room dimension. It helps in avoiding propagation losses and provides optimum efficiency. Furthermore, the mathematical derivations provide the precise calculation of the luminous intensity index based on radiant intensity and luminous intensity pattern. Such mathematical expressions can derive the received power of the room at any point. Further investigation is made on the calculation of transmitting LEDs' radiation pattern on the performance of received power. It becomes significant to measure the impact because it can help in transferring data at high speed. The proposed model has the potential to evaluate the performance of the receiver based on field of view and half power angle. Coordination between transmitter and receiver is important in order to develop an effective VLC system. The LLIRP model not only describes the characteristics of the source (wavelength dependent) but also focuses on the receiver's performance.

This paper deals with extensive work performed on the distribution of luminous intensity (LI) of light under various assumptions to set an optical line of sight link for VLC communication. The distribution of LIs has been analyzed in the form of Lambertian radiation pattern (LRP) that shows a clear variation in results when operated on different wavelengths in the visible spectrum. A radiation pattern describes the relative strength of light emitted in any direction from the light source, which is further related to Lambert's cosine law [12]. Based on practical results achieved as LLIRP on MATLAB simulations, additional work has been performed on the influence of LRP on the received power of photodetector.

## 2. Previous Work

In previous literature, researchers studied the color impact of LED on VLC in different manners. The primary methodologies focus on obtaining the correlation among several modulation schemes with different colors. For instance, IEEE 802.15.7.5 depicts the Color-Shift Keying approach. Furthermore, researchers proposed some other color-based

modulation mechanisms after the formation of this standard, such as generalized color modulation (GCM). This work has substantially used a different approach as several prior works utilized photodiodes (PDs) or cameras as receivers. At the same time, the present study focuses on the characteristics of LEDs that make them efficient trans-receiver for bidirectional communication. Full duplex communication among LEDs is conceivable as LEDs can work like photo sensors that have the potential to receive light even beyond the emitted frequency. Several studies have worked on defining and assessing the characteristics of LEDs. It starts with the assessment of the emission/reception spectrum of numerous LEDs based on their colors with their significant chemical applications as absorption sensors. Kowalczyk et al. suggested significant VLC application, however, restricted only in the selection of amber/red LEDs as transreceivers [13].

Since 2003, numerous research works have been performed on the efficient bidirectional utilization of LEDs under VLC conditions. Dietz et al. proposed the first experimental study that considered the utilization of LEDs as the transreceivers for the full-duplex channel [14]. Giustiano et al. have further designed the VLC system with low complexity considering the full-duplex transmission of data between LEDs [15]. The study depicted the primary concept of the different LED's impact on a VLC interface by conducting several experimentations under two scenarios, such as blue-to-blue and red-to-red LEDs to compare and attain superior performance. Afterward, Schmid et al. suggested another work on a full-duplex interface among LEDs and assessed the link performance by considering several aspects like energy consumption and communication range [16]. However, the outcomes were advanced to the prior studies as the link distances are greater than 2 m and the data transmission rate is 800 b/s. Further, the model operates only on the same color LEDs. Wang et al. used PDs/LEDs as the receivers by introducing a research platform as OpenVLC for full-duplex transmission [17]. This work only considers red LEDs for data transmission and made their evaluations. Although, our work provides the insights of several colors with their respective luminous intensities and their impact on data transmission in terms of power losses, this work is helping to gain better approaches while developing the full-duplex transmission by using LEDs.

VLC systems prove their worth by providing new perspectives for bidirectional communication using LEDs with their characteristics as highly efficient photosensors. For instance, Li et al. designed a novel model as a MIMO-VLC system utilizing LEDs. Such transreceivers worked on RGB wavelength and outlining the emission/reception potentials of LEDs while creating a system that has the potential to perform multiple communications [18]. The experts assessed the performance of data transmission regarding several color combinations. The authors concluded that blue-green and red-red interfaces do not experience interferences from each other.

Bhalerao et al. suggested a line of site model by using Lambertian pattern of LED in which they analyzed power distribution of white LED source with a photodiode as a

receiver in a room. This investigation completely depends upon the half-power angle of the LED source with the field of view of photodetector and mode number of radiation lobe [19]. Wang et al. developed a new theory for the analysis of received power distribution in a generalized indoor VLC system. The goal of their system is to develop a theory related to the location of LED, in which mathematical expressions of received power are derived for both wall-mounted and ceiling-mounted LED source layouts. Their model also explains the dependency of received power with illumination [20].

Chien et al. propose a novel and accurate analytical representation of radiation patterns, generated by an LED. Two major constraints as angular intensity distribution and the irradiance spatial pattern are taken into account during their analysis. A mathematical model is demonstrated, tested, and matched with datasheets of LEDs belonging to several major manufacturers [21]. In another work, Moreno explains about Spatial distribution of LED radiation. This model gives an analytical relationship between radiated patterns and the main constraints of LEDs, which are chip location, chip shape, chip radiance, encapsulant refractive index, encapsulant geometry, and cup reflector [22]. Our paper is the extended version of previous work in the form of analyzing the impact of change in wavelengths of light on Lambertian Luminous Intensity radiation pattern. There are some connections present between their work and the problems that encourage us to analyze the following issues in-depth but with different objectives.

This paper presents the expansion of several concepts considering the subsequent aspects as performing the work involving the LEDs diversity on a broader scale to widely explore the visible spectrum based on each color (red, green, yellow, and blue). Furthermore, this study illustrates the detailed experimental analysis by considering the most common colors (RGB) for full-duplex data transmission with the help of the Lambertian luminous intensity model, which is an accurate mathematical analysis with their respective simulation results. This work presents all the experimental assessments according to real-world VLC scenarios. In conclusion, this research study opens space for deliberations associated with recognizing the future aspects of VLC systems, e.g., medium access mechanisms and channel allocation depending on LED colors.

### 3. VLC System Model

A Clear Line of Sight model based on the light wave is designed under a free-space optical channel for indoor room dimensions, as shown in Figure 1. This design is applicable with some assumptions that all LED sources are placed at the center of the room and on the ceiling, i.e., at the top level, but in practicality, it may be possible that the position of source places is at horizontal plane like nearby windows. Another one is that there is a uniform distribution of luminance over the small active area of the receiver at receiving plane. Consideration of this assumption is due to the fact of using a solar panel as a photodetector (PD) in many VLC systems that consist of an active area of several hundred  $\text{cm}^2$ . The last

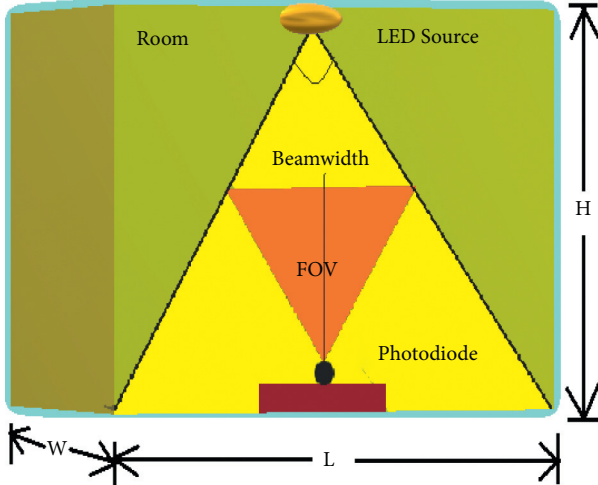


FIGURE 1: System model of LOS link.

one is LED sources completely work under the Lambertian radiation Pattern phenomenon. Practically, it is not a compulsion that LEDs follow LRP, e.g., Phosphor-coated multichip LED does not pursue the Lambertian model for the reproduction of luminous intensity pattern [19].

**3.1. Signal Transmission.** VLC is relatively a safe technology when it comes to eavesdropping because optical radiations do not permeate through walls which makes them well confined. Switching properties of LEDs in the visible spectrum are considered as the most important constraint that has a rapid capability to be switched on and off because of which it makes it possible to analyze data through impression on the human eye with their radiated power and optical intensity [23, 24]. A human eye can easily observe and detect ultrahigh-speed switching, which is not possible in other technologies. LEDs are considered as an excellent transmission source because of their energy-efficient phenomenon. The Color of LED plays an important role during the setting of the average luminous flux of the source, which is directly proportional to the relative width of the dimming signal [25]. The minimum illumination level for a typical office environment demands illuminance in between 200–1000 lx [26]. Colors that are considered for the OLOS link model during comparative analysis are red (665 nm), green (550 nm), blue (470 nm), and yellow (600 nm).

Luminance, hue, and saturation are three primary major attributes for the selection of color during conscious sensation. Luminous (often called brightness) is the most preferred one among these attributes, which is based upon luminous and radiant intensities. The second major attribute is the hue, which is related directly to the wavelength. It indicates the separation between color levels, like the distinction between redness, greenness, blueness, etc. The third attribute is saturation chroma, which is used to distinguish the strong colors from faint ones [27]. On the other hand, saturation level shows the freedom from dilution caused by white color, also known as the physical purity of the signal. Therefore, LRP is

analyzed here on the performance level of color/wavelength of the source having rotational symmetry.

Mathematical calculations of LRP symmetry rely on Spectral Luminous Efficacy and Spectral Luminous Efficiency. Luminosity factor or Spectral luminous efficacy of radiant flux  $K(\lambda)$  is defined as the quotient of the luminous flux at a certain wavelength by the radiant flux [27].

$$K(\lambda) = \frac{\Phi_{v\lambda}}{\Phi_{e\lambda}} \quad (\text{in lm W}^{-1}). \quad (1)$$

The optimum value of the  $K(\lambda)$  function is  $673 \text{ lm W}^{-1}$  achieved at a wavelength of about 555 nm [19]. Related to Spectral Luminous Efficacy, Spectral Luminous Efficiency of radiant flux  $V(\lambda)$  is defined as the ratio of luminous efficacy at a certain wavelength with the value of the maximum luminous efficacy.

$$V(\lambda) = \frac{K(\lambda)}{673}. \quad (2)$$

Luminous intensity (LI), as discussed earlier, shows the level of brightness represents the overall energy radiated from source and is defined as Luminous Flux per unit solid angle,

$$I = \frac{d\phi}{d\Omega}, \quad (3)$$

where  $\phi$  is the luminous flux and  $\Omega$  is the spatial/solid angle.

Lambertian distribution pattern for a typical room environment is defined in terms of radiation intensity, that is,

$$I(\varnothing) = I(0)\cos^{m_1}(\varnothing), \quad (4)$$

where  $\varnothing$  is denoting the angle of irradiance relative to the normal axis of the transmitter surface,  $I(0)$  represents the central luminous intensity, and  $m_1$  is the order of radiation lobe in Lambertian emission defined as follows [13]:

$$m_1 = \frac{\ln(2)}{\ln(\cos\varnothing_{(1/2)})}, \quad (5)$$

where  $\varnothing_{(1/2)}$  is the half-power/semiangle with  $\varnothing_{(1/2)} \in [-\pi/2, \pi/2]$  at half illuminance of source provided by the manufacturers of the LED product in their datasheet. Half power angle has a direct influence on the directivity of the transmitter by showing the maximum value of the lobe that contains 50% of radiant energy in a plane.

The radiation pattern is given by the following:

$$\mathcal{R}\mathcal{E}(\varphi, m_1) = \frac{(m_1 + 1)}{2\pi} \cdot \text{PE} \cdot \cos^{m_1}(\varphi), \quad (6)$$

where PE is the transmitting power and  $m_1$  gives the direction of the source, also known as mode number of radiation lobe.

**3.2. Reception.** The PIN photodiode is used here as a receptor to collect the light wave. Modeling was performed for luminous intensity distribution pattern at receiving plane in an OLOS path (assumption as neglecting the reflection of walls). The photodiode is used here to convert the optical

signal as a light wave into an electrical signal which is further enhanced and conditioned by filters. The effective area of receiver or operative signal collection area ( $A_{\text{eff}}$ ) is directly correlated with Field of View (FOV) as follows:

$$A_{\text{eff}}(\sigma) = A_d \cdot \cos(\sigma) \quad |\sigma| < \text{FOV} \quad \text{otherwise } 0, \quad (7)$$

where  $A_d$  denotes the physical area of the detector that is considered as small as one of the assumptions and  $\sigma$  indicates the direction of the angle between receiver axis at receiving plane and incident light ray as shown in Figure 2. The maximum value of  $\sigma$  is directly called FOV of detection of light. The detection capability of the photodiode can be increased by decreasing the FOV value that directly cuts off unwanted reflections through walls and noise at the receiver.

A large area of photodetector causes several problems, such as junction capacitance increases with a reduction in receiver bandwidth. Receiver noise also increases, which will hike the manufacturing cost of the photodetector. Therefore, a nonimaging concentrator is attached as a solution to increase the overall effective area of the receiver. Optical gain of concentrator having a refractive index is considered as follows:

$$G(\psi) = \frac{n^2}{\sin^2(\psi)}, \quad (8)$$

where  $\psi$  is the Field of View angle of the photodetector.

Radiant flux falling over the receiver also affects the channel gain of the link in which the receiver is located at the distance of  $d$  and with an angle of  $\phi$  with the OLED. Channel gain calculation for LLIRP requires a receiver connected with a bandpass filter of transmission value  $T_s(\psi)$  and the gain value of nonimaging concentrator [19],

$$H = \frac{A_{\text{eff}}(m_1 + 1)}{2\pi d^2} \cos^{m_1} \phi T_s(\psi) G(\psi) \cos(\psi). \quad (9)$$

Received power of OLOS link based on illuminance or intensity at a point  $(x, y)$ , can be measured with the following:

$$I_{(x,y)} = I(0) \frac{\cos^{m_1}(\varnothing)}{d^2} \cos\psi, \quad (10)$$

$$P_r = P_t \frac{(m_1 + 1)}{2\pi d^2} \cos^{m_1}(\varnothing) \cdot T_s(\psi) \cdot G(\psi) \cdot \cos(\psi). \quad (11)$$

By using equation (10) in equation (11), we obtain a new factor for LLIRP analysis:

$$P_r = P_t \frac{(m_1 + 1)}{2\pi} \frac{I_{(x,y)}}{I(0)} \cdot T_s(\psi) \cdot G(\psi). \quad (12)$$

Equation (12) illustrates the dependency of received power on the ratio of radiant intensity ( $I(x, y)$ ) in the direction of viewing angle with the luminous intensity pattern ( $I(0)$ ) of the LED transmitter. Let us consider a Luminous Intensity Index  $S(x, y)$  that can be expressed as follows:

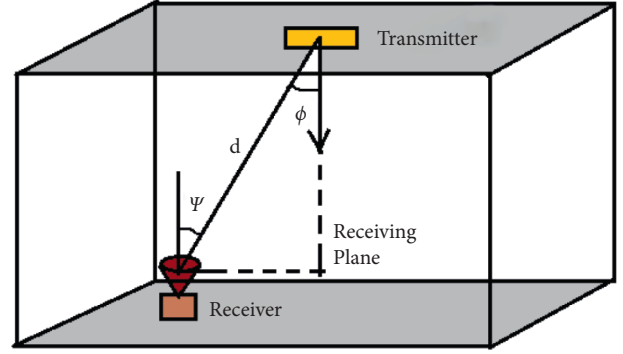


FIGURE 2: Geometry of OLOS propagation model.

$$\frac{I_{(x,y)}}{I(0)} = S(x, y). \quad (13)$$

## 4. Simulation Results

Simulation of results on OLOS model performed experimentally for short link communication under an indoor environment with certain room dimensions. In a room, for the analysis of LLIRP, some of the assumptions are considered here as the position of the LED source is located at the top level and in the center of the room while photodiode is situated at ground level, perfectly aligned with the source. Analysis of results completed at different values of the wavelength of light in visible spectrum showing variable colors when detected with human photopic [21] vision. The selection of color process is based on the availability of LED sources in the market. In general, red, green, blue, and yellow LEDs are easily available and very frequently used during most of the research and technical work. Wavelengths severely affect the factor of Spectral Luminous Efficiency of the beam of light, which has been observed during the simulation process while at the same time other parameters are kept constant. Table 1 shows the details of technical specifications being considered simulation process on MATLAB.

Plots indicate the LLIRP of OLED having different colors with the room dimensions. Direction angle relative with transmitter normal axis or half-power angle ( $\varnothing$ ) =  $60^\circ$ , height between photodetector and transmitter,  $h = 2.15$  m. Field of view =  $60^\circ$ , which is assumed as the half-power angle of the source. The peak value of Luminous intensity is placed at the center of the room for each wavelength but with the variation in brightness level. The wavelength of green light shows the best performance (4000 cd) under the same conditions when it comes to the illuminance of light, while the wavelength of red (250 cd) shows a minimum. LLIRP indicates that the performance level in luminous intensity of Green LED is around 16 times more than Red LED.

As shown in Figure 3, the LLIRP of green LED represents the maximum potential in terms of luminous intensity, which is measured in Candela (cd). This plot indicates a range that varies from 2000 cd to 4000 cd in particular room dimensions. On the other hand, the yellow LED in Figure 4 shows the next best performance for the same parameters

TABLE 1: Parameters of modeling LOS link.

Parameters	Values
Room dimensions	$5 \times 5 \times 3 \text{ m}^3$
Beam width	$60^\circ, 33^\circ, 27^\circ, 22^\circ$
Mode number of radiation lobe, m	1, 4, 6, 10
Field of view ( $\psi$ )	$60^\circ$
Color of LED	Green, yellow, blue, red
Wavelength (nm)	550, 600, 470, 665
Spectral luminous efficacy [27]	0.9950, 0.6310, 0.0910, 0.0610
Active area of photodiode	$10^{-4} \text{ mm}^2$
Refractive index of lens placed at PD	1.5
Transmitted optical power by LED	20 mW
Optical filter gain, $T(\psi)$	1
Receiver height ( $h_R$ )	2.15 m

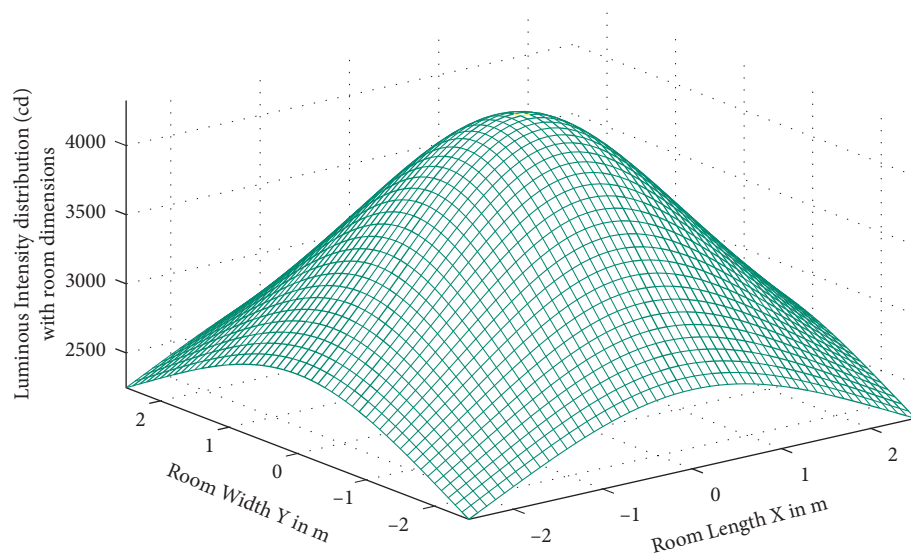


FIGURE 3: Lambertian radiation pattern for luminous intensity distribution at 550 nm (green LED).

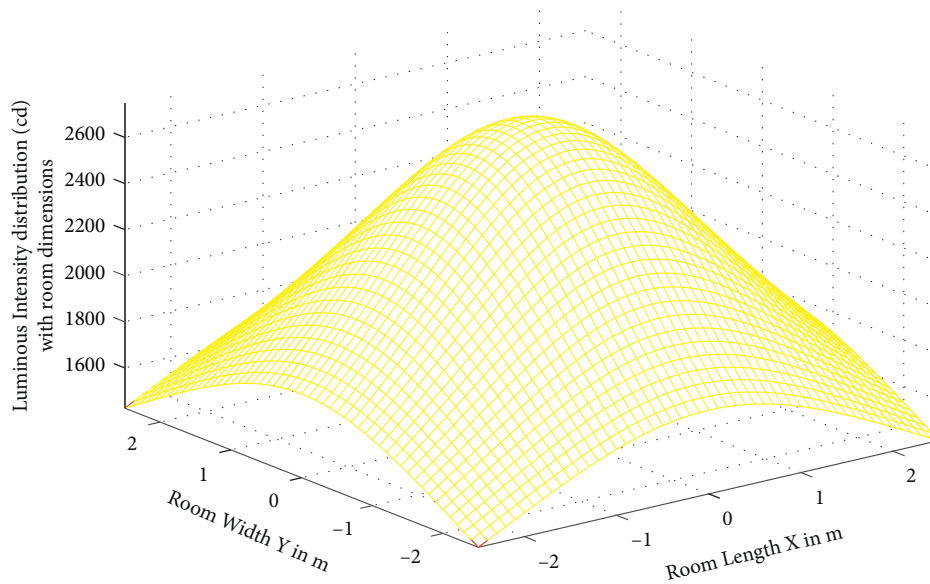


FIGURE 4: Lambertian radiation pattern for luminous intensity distribution at 600 nm (yellow LED).



but with different luminous efficacy that is fixed for a certain wavelength, as shown in Table 1. Its luminous intensity varies between 1400 cd to 2600 cd for the same dimensions of the room. Blue LED in Figure 5 illustrates a low brightness level as less energy radiates in the range of 200 cd to 350 cd. Minimum performance of LLIRP if given by red LED radiates lower energy than others shown in Figure 6 that ranges in between 100 cd and 250 cd.

Figure 7 shows a 2D analysis between LLIRPs of OLED at different wavelengths. Comparative analysis has been presented here that reveals a huge difference in Luminous Intensity of OLEDs that clearly affects the radiation patterns. Peak values of luminous intensity for different cases under the same conditions are shown in the form of a ratio as follows:

$$G : Y : B : R = 80 : 52 : 7 : 5. \quad (14)$$

Equation (14) indicates the level of difference between LIs of four different cases. The left-hand side of the equation stands for the color of LED, while the right hand signifies the amount of variation in the peak level of LIs. Now, the impact of these performances of Luminous Intensities can be analyzed on other important constraints to increase the credibility of the OLOS link in VLC for more reliable communication.

Based on LLIRP of OLED, analysis of received power distribution has been performed at different wavelengths. Equation (13) shows luminous intensity index,  $S(x, y)$ , plays a major role in estimating received power at photodetector, which is operated under the impact of various luminous intensity values. In addition, variation in the values of half-power angle of transmitting OLED have been made, that are set on  $\phi = 60^\circ, 33^\circ, 27^\circ$ , and  $22^\circ$ . Half power angle corresponds to the mode numbers of radiation lobe, which are  $m = 1, 4, 6$ , and  $10$ , respectively.

Figure 8 illustrates the outcomes achieved at four different wavelengths as Green, Yellow, Blue, and Red light are the same. Based on the location of the photodetector (in Figure 2) with the source of light, Figure 8 explains that amount of received power is maximum at near about 1m of light source, which has been dropped drastically for each case with the increase in distance. General expressions of received power indicate the variation in received power with Luminous Intensity of light, but when the simulation is performed, it shows a different scenario. A new conspiracy is generated, which explains that experimentally color of light does not affect the value of received power when it is operated at the same transmitting power with equivalent mode number of radiation lobe. In other words,  $S(x, y)$  does not alter the value of received power if the half power angle of source with its generated power is the same for all LEDs. We obtain the same results as Figure 8, when the LLIRP of the system varies with the wavelength of light due to the complete dependency on the values of  $\phi$  and  $m$ , respectively. For all cases that deals with different colors of OLED, the peak value of received power at the distance of 1 m as shown in Figure 8, is the same as follows:  $0.39 \times 10^{-3}$  at  $m = 1$ ,  $0.48 \times 10^{-3}$  at  $m = 4$ ,  $0.7 \times 10^{-3}$  at  $m = 6$  and  $1.1 \times 10^{-3}$  at  $m = 10$ , respectively.

This work presents the analysis of radiation patterns by using commonly available LEDs. It becomes significant to understand numerous physical properties and characteristics such as LED color, luminous intensity, power gain, transmission/reception power, and peak intensity before developing an efficient interface. The peak intensity of every color (whether it is red or green) is located optimum at  $60^\circ$  to  $70^\circ$ , whereas the half value of peak intensity shows center intensity. An angle range of  $65^\circ$ – $75^\circ$  is beyond center intensity that is symmetric to the normal axis. Uniform illumination intensity can be obtained from the difference between peak and center intensity onto the target area. Such a study also helps in eliminating the further glare effect via cut-off emitting light whose emitting angle is greater than  $80^\circ$ .

We tried to find out the best possible results by considering the specifications mentioned in Table 1 by using the far-field patterns of LEDs and developing the secondary optics element for multiple propagations. As the imprinted structure of LED can generate the flat far-flied pattern for the center intensity ratio under a superior circumstance. It also delivers the consistent intensity at the  $0$ – $40^\circ$  distributive angles. In last, the designed secondary optics element can attain the 50% intensity angle and peak intensity in order to eliminate the glare effect. This work also considers the reflective surface for one reflection in order to avoid the flux loss at the time of interface transmission. VLC transmitters generally utilize LEDs where several LEDs are present in off-the-shelf LED light bulbs. Such light bulbs also involve a driver to maintain the photocurrent that directly affects the Lambertian pattern or luminous intensity. In other words, one can easily manipulate LEDs at a high frequency as transistors control the current arriving at LEDs, conducting communication that is untraceable by human eyes. Normally, VLC works with receivers using PDs. Although, PDs are highly sensitive for human eyes and can handle the waves outside the visible light spectrum like infrared and ultraviolet. Therefore, PD often fails to obtain the data in an outdoor condition exposed to sunlight due to high interference. Some experiments suggest substitutions in order to sort out this challenge. For instance, LEDs have photo sensor characteristics that make them efficient receivers. The LEDs utilization as trans-receiver provides greater flexibility in the applications of VLC models.

LEDs have the property of photocurrent that also make them a good sensor. When LED receives the light, it can produce a small current. This current has magnitude related to the intensity of received light. LEDs can be considered a selective PD, as PD has a wider spectral response. Generally, an LED of a definite color can recognize the signals coming from the same color LED or greater frequencies as they detect a narrower wavelength range. For instance, a blue LED is only capable of recognizing the signals coming from the same color, while a red LED identifies signals from RGB LEDs. We consider multiple LEDs in this work in order to develop an inclusive and comprehensive examination of LED characteristics as sensors, ranging from lesser frequencies (red and yellow) to greater frequencies (blue and green). This work can be further extended to assess the LED

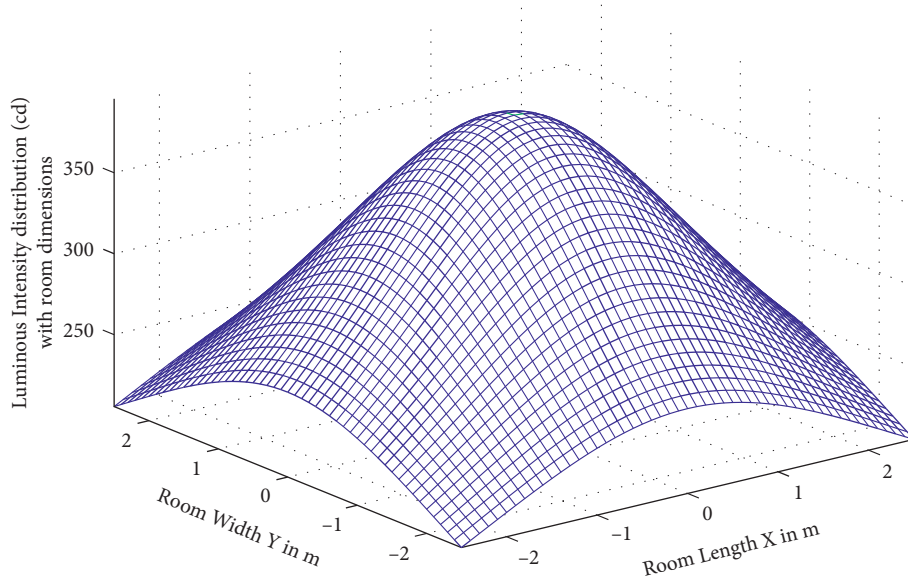


FIGURE 5: Lambertian radiation pattern for luminous intensity distribution at 470 nm (blue LED).

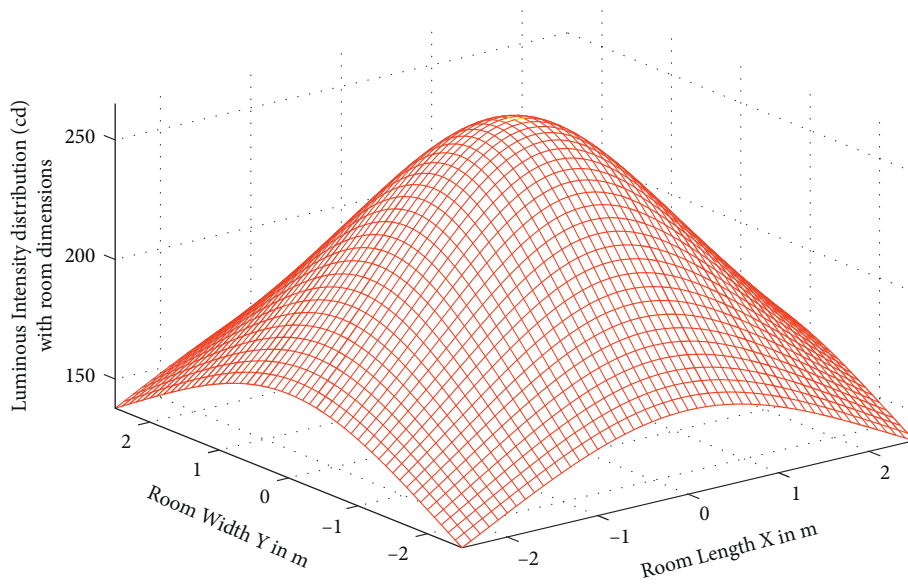


FIGURE 6: Lambertian radiation pattern for luminous intensity distribution at 665 nm (red LED).

characteristics by studying several color compositions such as white LED. Further, it helps analyze the materials that can emit radiation, having a mixture of yellow and blue colors. This work considers the experimental studies with the evaluations under practical environment dimensions appropriate for offices, rooms, and labs, etc., that are inclined to forthcoming VLC models because of the existing infrastructure.

## 5. Discussion on Work Novelty

Modeling and simulation of VLC links for OLOS propagation under indoor OWC are highly dependent on key characteristics of the transmitter, receiver, and channel. The objective of conducted work is to present one mathematical

model that connects all the variable constraints. The simulation results explain the consequences and dependency between the transmitter and receiver parameters. The various experiments demonstrated in this chapter are discussed as follows:

- (i) Color/wavelength is a very important constraint to attain the optimum performance of the link under the same scenario. Comparative results explain that the performance of green color LED in terms of LLIRP is much more effective than other color LEDs. These outcomes help during wavelength selection and support WDM. The impact of wavelength in the visible spectrum has been checked on LLIRP for the VLC link. Results show a clear and

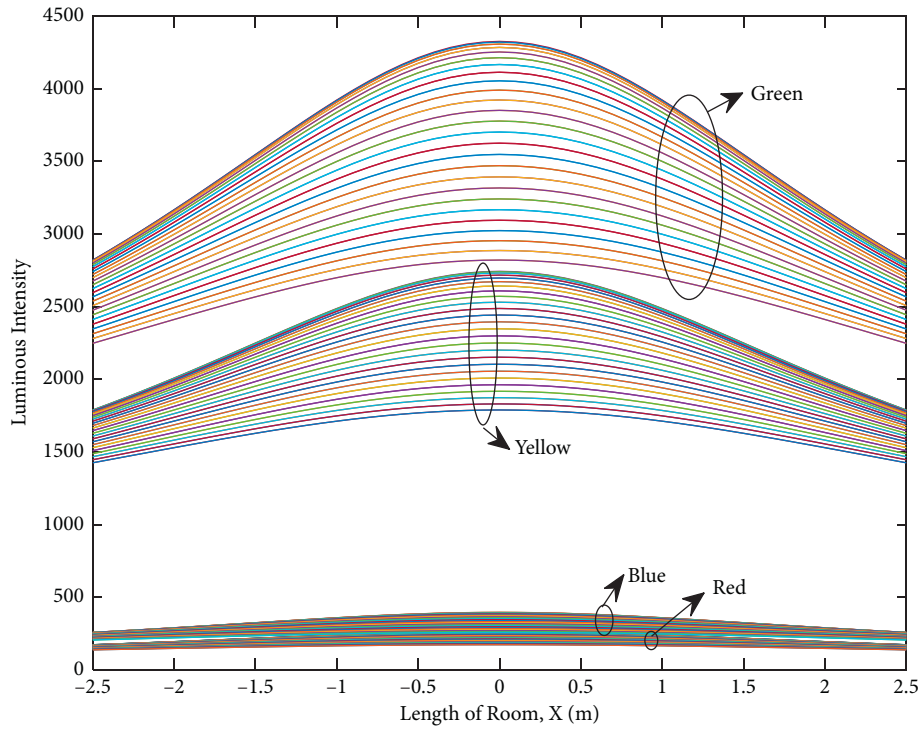


FIGURE 7: Comparative analysis between LLIRP of various wavelengths in 2D plot.

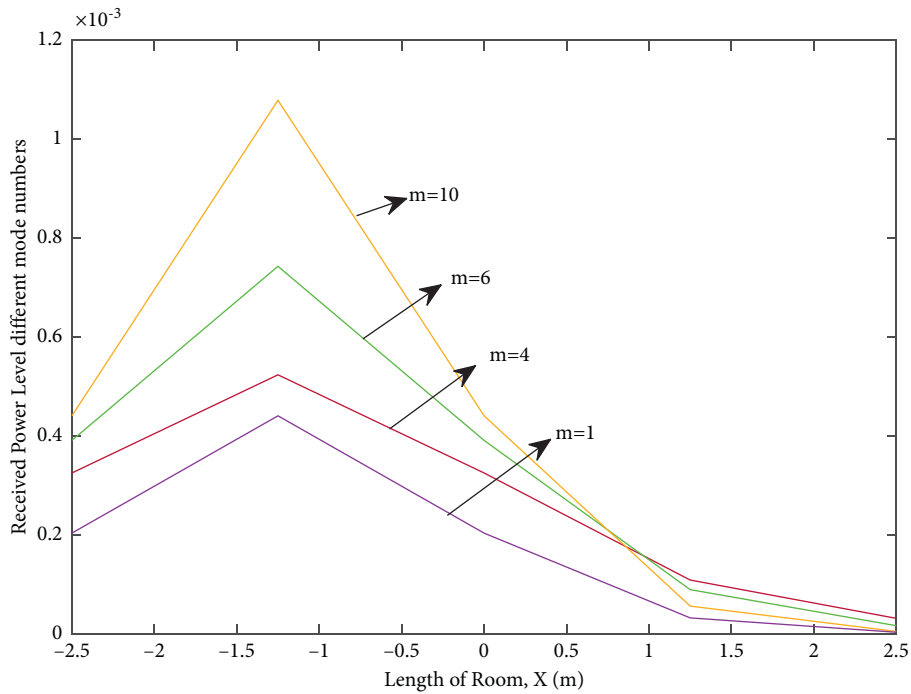


FIGURE 8: Received power distribution of green, yellow, blue, and red LEDs at different mode numbers,  $m = 1, 4, 6, 10$ .

notable variation in the levels of luminous intensity with the room dimensions when the color of light or wavelength varies. Therefore, the selection of light is also an important criterion while creating a reliable OLOS communication link.

(ii) Transmitting end depends on two factors: half power angle and the mode number of radiation lobe. Variation in arrival angle represents different mode numbers. Here, the results of four cases have been explained at the HPA of  $60^\circ, 33^\circ, 27^\circ,$  and  $23^\circ$ .

Mode number,  $m_1 = 1$  at  $60^\circ$  HPA represents an ideal Lambertian source that explains the direction where the radiated signal strength reaches the maximum. This work also compares the outcomes generated due to the impact of different mode numbers on the VLC system.

- (iii) Receiving section included the FOV and effective area of the photodetector as the main constraints to attain optimum performance.
- (iv) Coordinates of transmitter and receiver with rotational symmetry are also important parameters during the investigation of mathematical models.
- (v) In addition, the influence of luminous intensity has been noted on the further impact of brightness and optical received power. It displays that the color of light does not influence the received power of the photodetector. The behavior of spectral luminous efficacy, radiation flux, and luminous intensity of the source has been checked with the receiving section, including a nonimaging concentrator and a bandpass filter.  $S(x, y)$  found constant for all colors, whether it is green, yellow, blue, or red; each wavelength gives the same plot in case of received power. The only change is detected because of the variations in values of the number of modes caused by the half-power angle of transmitting source LED.

## 6. Conclusion

In this investigation, a new model of OLOS for indoor VLC systems has been proposed. It is widely applicable for the further analysis of LLIRP. Several parameters can affect the whole OLOS system with a minute change in values. It can include the coordinates of the transmitting source with the location of the photodetector or the half-power angle of OLED with their respective mode number of radiation lobe. This extension of work analyzes a new model that is created by changing the luminous intensity of light. The wavelength impact of light in the visible spectrum has been checked on the Lambertian radiation pattern of the lobe in a VLC link. Results show a clear variation in Luminous intensity levels with the room dimensions when wavelength varies. Therefore, the selection of light is also an important criterion while creating a reliable OLOS communication link. In addition, the luminous intensity factor is used to check the further impact of brightness on the factor of received power. It shows that the color of light does not influence the factor of the received power of the photodetector. The behavior of radiation flux, Spectral luminous Efficacy, and luminous intensity of source have been checked with the receiver connected with a nonimaging concentrator and a bandpass filter.  $S(x, y)$  found constant for all colors, whether it is green, yellow, blue, or red. Each wavelength gives the same plot in case of received power. The only change is observed due to changes in values of half-power angle and the number of modes of the transmitter.

Future work will be executed on other parameters that are linked with LLIRP. Parameters like bit error rate (BER)

or signal to noise ratio (SNR) will be investigated and further efforts will be made to find out a relation between the impacts of luminous intensity or OLED radiation patterns with these factors.

## Data Availability

The authors confirm that all relevant data are included in the article and its information files. Additionally, the derived data supporting the findings of this study are available from the corresponding author upon request.

## Conflicts of Interest

The authors declare that they have no conflicts of interest.

## Acknowledgments

This work was supported by Universidad Autonoma de Zacatecas, Mexico and CONACyT, Mexico.

## References

- [1] D. K. Borah, A. C. Boucouvalas, C. C. Davis, S. Hranilovic, and K. Yiannopoulos, "A review of communication-oriented optical wireless systems," *EURASIP Journal on Wireless Communications and Networking*, vol. 1, pp. 1–28, 2012.
- [2] M. A. Khalighi and M. Uysal, "Survey on free space optical communication: a communication theory perspective," *IEEE Communications Surveys & Tutorials*, vol. 16, no. 4, pp. 2231–2258, 2014.
- [3] D. Tsonev, S. Videv, and H. Haas, "Light fidelity (Li-Fi): towards all-optical networking," in *Broadband Access Communication Technologies VIII*, International Society for Optics and Photonics, Bellingham, WA, USA, 2014.
- [4] R. Sharma, A. Charan Kumari, M. Aggarwal, and S. Ahuja, "Optimal LED deployment for mobile indoor visible light communication system: performance analysis," *AEU-International Journal of Electronics and Communications*, vol. 83, pp. 427–432, 2018.
- [5] R. X. G. Ferreira, E. Xie, J. J. D. McKendry et al., "High bandwidth GaN-based micro-LEDs for multi-Gb/s visible light communications," *IEEE Photonics Technology Letters*, vol. 28, no. 19, pp. 2023–2026, 2016.
- [6] H. Hoa Le Minh, D. O'Brien, G. Faulkner et al., "100-Mb/s NRZ visible light communications using a postequalized white LED," *IEEE Photonics Technology Letters*, vol. 21, no. 15, pp. 1063–1065, 2009.
- [7] H. Elgala, R. Mesleh, H. Haas, and B. Pricope, "OFDM visible light wireless communication based on white LEDs," in *Proceedings of the 2007 IEEE 65th Vehicular Technology Conference-VTC2007-Spring*, pp. 2185–2189, IEEE, Dublin, Ireland, April 2007.
- [8] Y. Wang and H. Haas, "Dynamic load balancing with handover in hybrid Li-Fi and Wi-Fi networks," *Journal of Lightwave Technology*, vol. 33, no. 22, pp. 4671–4682, 2015.
- [9] C.-L. Tsai and Z.-F. Xu, "Line-of-sight visible light communications with InGaN-based resonant cavity LEDs," *IEEE Photonics Technology Letters*, vol. 25, no. 18, pp. 1793–1796, 2013.
- [10] M. C. Al Naboulsi, H. Sizun, and F. de Fornel, "Wavelength selection for the free space optical telecommunication technology," in *Reliability of Optical Fiber Components, Devices*,

- Systems, and Networks II*, pp. 168–179, International Society for Optics and Photonics, Bellingham, WA, USA, 2004.
- [11] O. Bouchet, M. El Tabach, M. Wolf et al., “Hybrid wireless optics (HWO): building the next-generation home network,” in *Proceedings of the 2008 6th International Symposium on Communication Systems, Networks and Digital Signal Processing*, pp. 283–287, IEEE, Graz, Austria, July 2008.
  - [12] I. Moreno and C.-C. Sun, “Modeling the radiation pattern of LEDs,” *Optics Express*, vol. 16, no. 3, pp. 1808–1819, 2008.
  - [13] G. Stepniak, M. Kowalczyk, L. Maksymiuk, and J. Siuzdak, “Transmission beyond 100 Mbit/s using LED both as a transmitter and receiver,” *IEEE Photonics Technology Letters*, vol. 27, no. 19, pp. 2067–2070, 2015.
  - [14] P. Dietz, W. Yerazunis, and D. Leigh, “Very low-cost sensing and communication using bidirectional LEDs,” in *Proceedings of the International Conference on Ubiquitous Computing*, pp. 175–191, Springer, Berlin, Heidelberg, October 2003.
  - [15] D. Giustiniano, N. O. Tippenhauer, and S. Mangold, “Low-complexity visible light networking with LED-to-LED communication,” in *Proceedings of the 2012 IFIP Wireless Days*, pp. 1–8, Dublin, Ireland, November 2012.
  - [16] S. Li, B. Huang, and Z. Xu, “Experimental MIMO VLC systems using tricolor LED transmitters and receivers,” in *Proceedings of the 2017 IEEE Globecom Workshops (GC Wkshps)*, pp. 1–6, Singapore, December 2017.
  - [17] Z. Ahmad, S. Rajbhandari, O. Salih, and R. Green, “Demonstration of a multi-hop underwater visible light communication system,” in *Proceedings of the 2017 19th International Conference on Transparent Optical Networks (ICTON)*, pp. 1–4, Girona, Spain, July 2017.
  - [18] M. Heydariaan, S. Yin, O. Gnawali, D. Puccinelli, and D. Giustiniano, “Embedded visible light communication: link measurements and interpretation,” in *Proceedings of the 2016 International Conference on Embedded Wireless Systems and Networks (EWSN 2016)*, Graz, Austria, February 2016.
  - [19] M. V. Bhalerao, M. Sumathi, and S. S. Sonavane, “Line of sight model for visible light communication using Lambertian radiation pattern of LED,” *International Journal of Communication Systems*, vol. 30, no. 11, p. e3250, 2017.
  - [20] Y. Wang, M. Chen, J.-Y. Wang et al., “Impact of LED transmitters’ radiation pattern on received power distribution in a generalized indoor VLC system,” *Optics Express*, vol. 25, no. 19, pp. 22805–22819, 2017.
  - [21] W.-T. Chien, C.-C. Sun, and I. Moreno, “Precise optical model of multi-chip white LEDs,” *Optics Express*, vol. 15, no. 12, pp. 7572–7577, 2007.
  - [22] I. Moreno, “Spatial distribution of LED radiation,” in *Proceedings of the International Optical Design Conference 2006*, International Society for Optics and Photonics, Vancouver, Canada, July 2006.
  - [23] D. O’Brien, L. Zeng, H. Le-Minh et al., *Visible Light Communication, Short-Range Wireless Communications: Emerging Technologies and Applications*, Wiley Publishing, Hoboken, NJ, USA, 2009.
  - [24] H. Le Minh, D. O’Brien, G. Faulkner et al., “High-speed visible light communications using multiple-resonant equalization,” *IEEE Photonics Technology Letters*, vol. 20, no. 14, pp. 1243–1245, 2008.
  - [25] S. Rajbhandari, *Optical Wireless Communications: System and Channel Modelling with MATLAB®*, CRC Press, Boca Raton, FL, USA, 2019.
  - [26] F. R. Gfeller and U. Bapst, “Wireless in-house data communication via diffuse infrared radiation,” *Proceedings of the IEEE*, vol. 67, no. 11, pp. 1474–1486, 1979.
  - [27] R. W. Waynant and M. N. Ediger, *Electro-Optics Handbook*, McGraw-Hill Education, New York, NY, USA, 2000.

## Research Article

# An Efficient Multidocument Blind Signcryption Scheme for Smart Grid-Enabled Industrial Internet of Things

Ako Muhammad Abdullah <sup>1</sup>, Insaf Ullah,<sup>2</sup> Muhammad Asghar Khan <sup>2</sup>,  
Mohammed H. Alsharif <sup>3</sup>, Samih M. Mostafa <sup>4</sup>, and Jimmy Ming-Tai Wu <sup>5</sup>

<sup>1</sup>University of Sulaimani, College of Basic Education, Computer Science Department, Sulaimaniyah, Kurdistan Region, Iraq

<sup>2</sup>Hamdard Institute of Engineering & Technology, Islamabad 44000, Pakistan

<sup>3</sup>Department of Electrical Engineering, College of Electronics and Information Engineering, Sejong University, Seoul 05006, Republic of Korea

<sup>4</sup>Faculty of Computers and Information, South Valley University, Qena 83523, Egypt

<sup>5</sup>College of Computer Science and Technology, Shandong University of Science and Technology, Shandong, China

Correspondence should be addressed to Jimmy Ming-Tai Wu; [wmt@wmt35.idv.tw](mailto:wmt@wmt35.idv.tw)

Received 29 November 2021; Accepted 5 January 2022; Published 21 February 2022

Academic Editor: Shalli Rani

Copyright © 2022 Ako Muhammad Abdullah et al. This is an open access article distributed under the Creative Commons Attribution License, which permits unrestricted use, distribution, and reproduction in any medium, provided the original work is properly cited.

The smart grid-enabled industrial Internet of Things (SG-IIoT) is a hybrid data communication network connected with the power grid that collects and analyzes data from transmission lines, distribution substations, and consumers. In the IIoT setting, SG provides predictive information to its supplier and customers on how to effectively manage the power based on this aggregated data. To achieve this goal, every virtual or physical entity in the SG-IIoT must be linked and accessible over the Internet, which can be susceptible to numerous cyberattacks. In this paper, we propose a multidocument blind signcryption scheme to simultaneously resolve the security and efficiency issues. The proposed scheme performs the blind signature and encryption operation on multiple digital documents in one step because SG-IIoT outputs a large amount of data that needs to be blind signed and encrypted in a batch. The proposed scheme employs the concept of hyperelliptic curve cryptography (HECC), which is lightweight owing to the smaller key size. The comparative analysis in both security and efficiency with the relevant existing scheme authenticates the viability of the proposed scheme.

## 1. Introduction

The electrical network that serves every residence, company, and infrastructure service in a city is known as the “grid.” The “smart grid” is the next generation of energy infrastructure that has been upgraded with communications technology and connectivity to enable more efficient utilization of resources [1]. Wireless equipment such as sensors, radio modules, gateways, and routers are among the technologies that make today’s IoT-enabled electricity grid “smart.” These devices provide the advanced connection and communications that enable customers to make smarter energy consumption decisions, communities to save energy and

money, and power authorities to restore power more rapidly after a blackout. Similar to distributed energy resources, real-time smart meter readings, rapid reaction through reliable communication and information exchange, and monitoring systems, it can manage the responsibilities of various applications across industrial processes [2]. The industrial Internet of Things (IIoT), also known as SG-enabled industrial Internet of Things, is growing popularity, and it includes a variety of IoT devices and technology that make smart grid (SG) for Industry 4.0 simpler [3], also known as SG-enabled industrial Internet of Things (SG-IIoT). The SG-IIoT infrastructure is built on faster and more reliable communication technologies that connect intelligent information systems,

the current power grid, and other IIoT devices. Furthermore, because industry 4.0 gadgets consume so much electricity, smart meters linked to them may need to request energy from power stations via substations and control centers (CC) [4]. Therefore, every virtual or physical thing in SG-IIoT can be interconnected, identified, and accessed through the Internet [5]. When evaluating the communication scenario of the SG-IIoT environment, authentication, confidentiality, and anonymity are the three key cybersecurity issues [6]. It is important to highlight that digital signatures can ensure authenticity, and anonymous encryption can ensure both confidentiality and anonymity. Blind signcryption [7] allows the sender to combine the concepts of blind signing and encryption on a message in a single step, achieving authenticity, confidentiality, and anonymity in one step. Further, making a blind signature and encryption on multiple digital documents is better than signcrypting a single document because SG-IIoT generates a huge amount of data that need to be blindly signcrypted in a bunch [8]. Most of the blindly signcryption, which is presented either for a single document or multi-digital documents is built upon the working strategy of old public key infrastructure (PKC) that can be poor in the view of the certificate renewal process. In contrast to PKC, identity-based cryptography (IBC) will be the best choice when the private key generation center is fully trusted, and further, IBC can enjoy the feature of certificate renewing and revocation-free features. Recently, several blind signcryptions are contributed to multi-digital documents; unfortunately, these schemes are not suitable for resource-hungry SG-IIoT devices due to higher computational cost and certificate renewing and revocation [8–10]. Thus, to neglect such types of flaws, we design a new scheme with the following advantages.

- (i) The proposed scheme is based on the notion of blind signcryption with IBC for multi-digital documents utilizing hyperelliptic curve concepts for power requests in SG-IIoT
- (ii) The proposed scheme ensures the integrity of multi-digital documents, nonrepudiation of blind signature, unlinkability of the signer to the multi-digital documents, untraceability of the signer to an original signature, confidentiality, and forward secrecy, respectively
- (iii) When comparing the proposed scheme to three recently published relevant schemes, we observed that our scheme is more efficient in terms of computation and communication costs.

This paper is organized in the following way. In Section 2, we present the related work of existing blind signcryption and multidocument blind signcryption. In Section 3, we provide the proposed network model for power requests. Section 4 presents the construction of the proposed scheme. In Section 5, correctness is provided. Sections 6 and 7 provide security analysis and costs analysis in terms of computational cost, respectively. Lastly, in Section 8, conclusions are presented.

## 2. Related Work

The SG-IIoT configuration relies entirely on faster and more reliable communication technologies to connect intelligent information systems, existing power grids, and other IIoT devices. Every device in the SG-IIoT can be networked, identified, and connected to the Internet in this manner. Thus, during communications, the three key concerns of the SG-IIoT environment are anonymity, privacy, and validation. It is critical to understand that signatures can provide authentication and anonymity, while encryption can provide confidentiality to SG-IIoT data. Awasthi and Lal [7] devised a blind signcryption employing a discrete logarithm problem to meet authentication, confidentiality, and anonymity requirements in one step. This scheme does not provide forward secrecy and has a longer processing time as a result. Using the discrete logarithm problem, Xiuying and Dake [11] proposed a blind signcryption with public verifiability. More processing time is a problem for this scheme once again. Riaz et al. [12] developed an elliptic curve discrete logarithm problem for blind signcryption. Unforgeability, authentication, integrity, and signer nonrepudiation are all vulnerabilities in the scheme [13]. Furthermore, the authors in [13] presented an improved blind signcryption scheme, although when considering resource-hungry devices, this scheme suffers from higher processing CPU time owing to the elliptic curve. Mohib et al. [14] proposed an elliptic curve-based blind signcryption to allow anonymous communication to mobile voting systems. Waheed et al. [15] presented blind signcryption utilizing the elliptic curve discrete logarithm problem for the use of electronic voting. However, both schemes [14, 15] suffer from increased processing CPU time and are hence unsuitable for resource-intensive devices. Ullah and Din [16] presented blind signcryption using a hyperelliptic curve discrete logarithm problem; however, the approach does not ensure that numerous digital documents are encrypted and signed. Tsai et al. [8] suggested multidocument blind signcryption based on elliptic curve cryptography to offer encryption and blind signing in one step. They did not, however, provide forward security and did not benefit from the reduced computational cost. Blind signcryption using a hyperelliptic curve discrete logarithm issue was presented by Fazlullah et al. [9]. However, in terms of authentication and integrity, this technique is weak [10]. Furthermore, the authors of [10] suggested an enhanced multidocument blind signcryption system; nevertheless, when considering resource-hungry devices, this scheme suffers from increased processing CPU time needs due to more main operations of the hyperelliptic curve. Although, because they are all built on ancient public key infrastructure cryptography, all of the aforementioned blind signcryption techniques are prone to certificate revocation and renewal issues.

## 3. Network Model

Figure 1 depicts the flow of our proposed blind signcryption for multiple digital documents' scheme, which includes entities such as the industrial Internet of Things (IIoT), smart meters (SMs), substation (SS), private key generator (PKG),

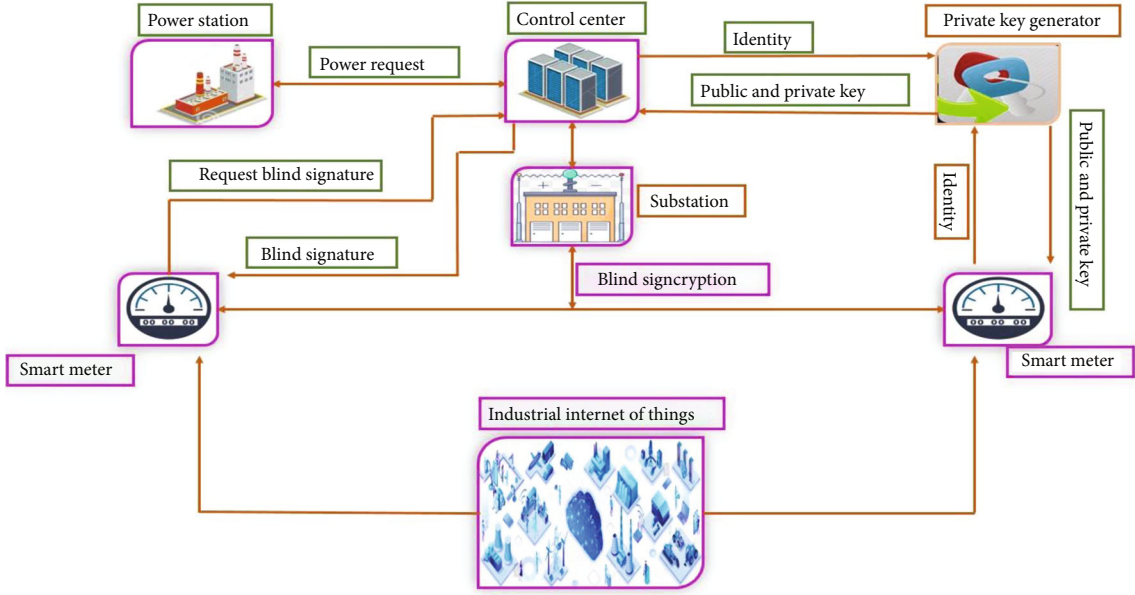


FIGURE 1: Network model of proposed SG-IIoT power request scheme [4].

TABLE 1: Symbols used in the constructions of the proposed algorithm.

No.	Symbol	Descriptions
1	$H_1, H_2, H_3$	One-way hash functions
2	$\ell$	The private key of PKG
3	$\mathcal{D}$	Divisor of a hyperelliptic curve
4	$n$	The order of finite field of a hyper elliptic curve and normally greater or equals 80 bits
5	$\eta$	The public key of PKG
6	$\Delta$	Published parameter set
7	$m_i$	Multi-digital documents
8	$U_s$	Signer private key
9	$V_s$	Signer public key
10	$U_v$	Verifier private key
11	$V_v$	Verifier public key
12	$\varphi$	Alice signature
13	$\mathcal{S}$	Signer signature
14	$K$	The secret key used for encryption and decryption

and power station (PS). When IIoT requires more power or some other utility, SMs seek a blind signature from CC, after which CC sends its identity to PKG for a private and public key, and PKG generates a public and private key for CC after receiving the CC identity. After that, CC generates a blind signature for SMs using his private key and returns it. When SMs obtain a blind signature, they transmit their identification to PKG for a private and public key. When PKG receives the SMs' identity, it generates a public and private key for them. After that, SMs produce and submit blind signcryption on many papers, including power requests and other utilities to

CC, using his private numbers and secret key. After receiving blind signcryption on numerous papers, CC can verify them using the verification method, then decode the ciphertext and supply power or other desired utilities to SMs if they are legitimate. Because all this information transmission is often in the range of a few bytes, LPWANs (low-power wide-area networks) are appropriate for interoperability of local micro-power grids. The low-power wide-area network (LPWAN) is a wide-area wireless communication network designed for long-range communications with low data rates and low power consumption.

#### 4. Proposed Multidocument Blind Signcryption

The proposed multidocuments blind signcryption can continue with the following phases and the symbols used in construction is available in Table 1.

**4.1. Setup.** In private key generator (PKG), pick three one-way hash functions  $(H_1, H_2, H_3)$ , hyperelliptic curve with genus 2, a divisor  $(\mathcal{D})$ , and a finite field of order  $n$ ; then, PKG selects  $\ell \in \{1, 2, 3, \dots, n-1\}$  as the private key of the signer and computes the corresponding master public key as  $\eta = \ell \cdot \mathcal{D}$ . In the end, PKG published  $\Delta = \{n, \mathcal{D}, H_1, H_2, H_3, \eta\}$  to the network

**4.2. Key Generation.** Here, PKG selects  $U_i \in \{1, 2, 3, \dots, n-1\}$  as the private key and computes the corresponding public key as  $V_i = U_i \cdot G$  for the user with identity  $(ID_i)$ . Then, PKG dispatched  $(U_i, V_i)$  to the user with  $ID_i$  using an open network

**4.3. Alice.** It can proceed with the following steps:

- Choose a random number  $\ell \in \{1, 2, 3, \dots, n-1\}$
- Compute  $V_h = H_1(\ell)$



TABLE 2: Major operations in proposed and existing schemes.

Schemes	Blind signcryption	Verifications and decryption	Total
Tsai et al. [8]	8 EM + 2 EA	4 EM	12 EM + 2 EA
Fazlullah et al. [9]	5 HEDM + 6 HEDA	3 HEDM + 2 HEDA	8 HEDM + 8 HEDA
Bashir and Ali [10]	8 HEDM + 6 HEDA	4 HEDM + 2 HEDA	12 HEDM + 8 HEDA
Proposed scheme	4 HEDM + 3 HEDA	3 HEDM + 3 HEDA	7 HEDM + 6 HEDA

TABLE 3: Computational cost comparison of proposed and existing scheme for a single message in milliseconds (ms).

Schemes	Blind signcryption	Verifications and decryption	Total
Tsai et al.[8]	$8 \times 2.226 + 2 \times 0.0288 = 17.8656$	$4 \times 2.226 = 8.904$	$12 \times 0.0288 + 2 \times 0.0288 = 26.7696$
Fazlullah et al. [9]	$5 \times 1.113 + 6 \times 0.0144 = 5.6514$	$3 \times 1.113 + 2 \times 0.0144 = 3.3678$	$8 \times 1.113 + 8 \times 0.0144 = 9.0192$
Bashir and Ali [10]	$8 \times 1.113 + 6 \times 0.0144 = 8.9904$	$4 \times 1.113 + 2 \times 0.0144 = 4.4808$	$12 \times 1.113 + 8 \times 0.0144 = 13.4712$
Proposed scheme	$4 \times 1.113 + 3 \times 0.0144 = 4.4952$	$3 \times 1.113 + 3 \times 0.0144 = 3.339$	$7 \times 1.113 + 6 \times 0.0144 = 7.8774$

TABLE 4: Computational cost comparison of proposed and existing scheme for a single message in milliseconds (ms).

Number of messages	Tsai et al. [8]	Fazlullah et al. [9]	Bashir and Ali [10]	Proposed scheme
50	1338.48	450.96	673.56	393.87
100	2676.96	901.92	1347.12	787.74
150	4015.44	1352.88	2020.68	1181.61

(c) Compute  $\mathcal{R} = H_2(m_i, V_h)$

(d) Send  $\mathcal{R}$  to the signer.

4.4. *Signer*. It can proceed with the following steps:

(a) Choose a random number  $\mathcal{L} \in \{1, 2, 3, \dots, n-1\}$

(b) Compute  $T = \mathcal{L} \cdot \mathcal{D}$

(c) Compute  $\mathcal{S} = (U_s + \mathcal{R} \cdot \mathcal{L}) \bmod n$

(d) Sends  $(T, \mathcal{S})$  to signer.

4.5. *Alice*. It can proceed with the following steps:

(a) Select random number  $\zeta \in \{1, 2, 3, \dots, n-1\}$

(b) Compute  $Z = \zeta \cdot \mathcal{D}$

(c) Choose a random number  $\mathcal{T} \in \{1, 2, 3, \dots, n-1\}$ , compute  $K = H_3(\mathcal{T} \cdot V_v)$

(d) Compute  $C = E_K(m_i, V_h)$

(e) Compute  $\varphi = \mathcal{T} / (\zeta + \mathcal{R} + \mathcal{S}) \bmod n$

(f) Send  $\mathfrak{A} = (C, T, \varphi, Z, \mathcal{R})$ .

4.6. *Verifications and Decryption*. It can proceed with the following steps:

(a) Compute  $K = H_3(\varphi \cdot U_v \cdot (V_s + \mathcal{R} \cdot (T + \mathcal{D}) + Z))$

(b) Compute  $m_i, V_h = D_K(C)$

(c) Compute  $P = H_2(m_i, V_h)$

(d) Accept if  $P = \mathcal{R}$ .

## 5. Correctness

The blind signcryption scheme can be correct if it holds the below equation.

$$H_3(\varphi \cdot U_i \cdot (V_s + \mathcal{R} \cdot (T + \mathcal{D}) + Z)) = \mathcal{T} \cdot V_i \quad (1)$$

Proof:

$$\begin{aligned}
&= H_3(\varphi \cdot U_v \cdot (U_s \cdot \mathcal{D} + \mathcal{R} \cdot (T + \mathcal{D}) + Z)) \\
&= H_3(\varphi \cdot U_v \cdot (U_s \cdot \mathcal{D} + \mathcal{R} \cdot (\mathcal{L} \cdot \mathcal{D} + \mathcal{D}) + Z)) \\
&= H_3(\varphi \cdot U_v \cdot (U_s \cdot \mathcal{D} + \mathcal{R} \cdot \mathcal{L} \cdot \mathcal{D} + \mathcal{R} \cdot \mathcal{D} + \mathcal{R} \cdot \mathcal{D})) \\
&= H_3\left(\frac{\mathcal{T}}{\zeta + \mathcal{R} + \mathcal{S}} \cdot U_v \cdot (U_s \cdot \mathcal{D} + \mathcal{R} \cdot \mathcal{L} \cdot \mathcal{D} + \mathcal{R} \cdot \mathcal{D} + \zeta \cdot \mathcal{D})\right) \\
&= H_3\left(\frac{\mathcal{T}}{\zeta + \mathcal{R} + U_s + \mathcal{R} \cdot \mathcal{L}} \cdot U_v \cdot (U_s + \mathcal{R} \cdot \mathcal{L} + \mathcal{R} + \zeta) \cdot \mathcal{D}\right) \\
&= H_3(\mathcal{T} \cdot U_v \cdot \mathcal{D}) = H_4(\mathcal{T} \cdot V_v) = K \quad (2)
\end{aligned}$$

## 6. Security Analysis

This phase includes detailed security analysis of the proposed scheme, which are based on the following hard problem: suppose  $P \& \mathcal{D}$  is given two divisors on the hyperelliptic curve of order  $n$ : hence, to find a unique integer  $\alpha$  from equation  $P = \alpha \cdot \mathcal{D}$  is called hyperelliptic curve discrete logarithm problem ( $\mathcal{H}\mathcal{E}\mathcal{C}\mathcal{D}\mathcal{L}\mathcal{P}$ ). So, in the following subphases of this section, we are going to explain each security requirement fulfilled by the proposed scheme in detail.

6.1. *Confidentiality*. Suppose an adversary  $\mathcal{A}$  attacked the proposed scheme for gaining the contents of ciphertext (C); then it must successfully be passed through the following subphases.

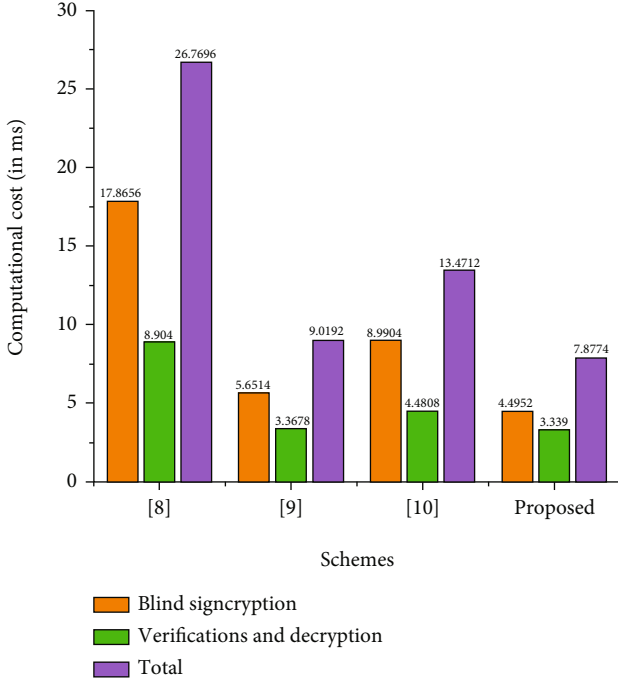


FIGURE 2: Computational cost comparisons for a single message.

- (i) Here, the first attempt of  $\mathcal{A}$  as it needs to process  $K_s = H_3(\varphi \cdot U_v \cdot (V_s + \mathcal{R} \cdot (T + \mathcal{D}) + Z))$  further requires  $U_v$  from  $V_v = U_v \cdot \mathcal{D}$  that can be clues towards the solution of  $\mathcal{H}\mathcal{E}\mathcal{C}\mathcal{D}\mathcal{L}\mathcal{P}$
- (ii) The second attempt of  $\mathcal{A}$  needs to process  $K_s = H_3(\mathcal{T} \cdot V_v)$ , so it requires  $\mathcal{T}$  that can be clues towards the solution of  $\mathcal{H}\mathcal{E}\mathcal{C}\mathcal{D}\mathcal{L}\mathcal{P}$
- (iii) The third attempt of  $\mathcal{A}$  needs  $\mathcal{T}$  from  $\varphi = \mathcal{T}/(\zeta + \mathcal{R} + \mathcal{S})$  to process  $K_s = H_3(\mathcal{T} \cdot V_v)$ , so  $\varphi$  contains two unknown hyperelliptic curve variables which are infeasible for  $\mathcal{A}$ .

The above three subphases indicate that the proposed scheme is secured from the content-stealing attack (confidentiality) against  $\mathcal{A}$ .

**6.2. Unforgeability.** Assume that  $\mathcal{A}$  attacked the proposed scheme for forging the original signature; then  $\mathcal{A}$  must effectively solve  $\varphi = \mathcal{T}/(\zeta + \mathcal{R} + \mathcal{S})$  for this; it passed through the following subphases.

- (i) Here, the first thing is that  $\mathcal{A}$  can require  $\mathcal{T}$ , and for this,  $\mathcal{A}$  must process  $K_s = H_3(\mathcal{T} \cdot V_v)$ , so it requires  $\mathcal{T}$  that can be clues towards the solution of  $\mathcal{H}\mathcal{E}\mathcal{C}\mathcal{D}\mathcal{L}\mathcal{P}$
- (ii) The second thing is that  $\mathcal{A}$  requires  $\zeta$ , and for this, it process  $Z = \zeta \cdot \mathcal{D}$ , so it requires  $\zeta$  that can be clues towards the solution of  $\mathcal{H}\mathcal{E}\mathcal{C}\mathcal{D}\mathcal{L}\mathcal{P}$
- (iii) The third attempt of  $\mathcal{A}$  needs  $\mathcal{S}$  from  $\varphi = \mathcal{T}/(\zeta + \mathcal{R} + \mathcal{S})$ , where  $\mathcal{S} = (U_s + \mathcal{R} \cdot \mathcal{L}) \bmod n$ , so  $\mathcal{S}$  con-

tains two unknown hyperelliptic curve variables which are infeasible for  $\mathcal{A}$ .

The above three subphases indicate that the proposed scheme is secured from forging attack (unforgeability) against  $\mathcal{A}$ .

**6.3. Message Integrity.** In our designed scheme, with ciphertext, the sender appends and computes  $\mathcal{R} = H_2(m_i, V_h)$  as a hash value and is dispatched to the receiver. After the reception, the receiver can verify using the following steps.

- (i) It computes the new hash value after decrypting the ciphertext as  $P = H_2(m_i, V_h)$
- (ii) Then compare  $P = \mathcal{R}$ , if it equals then accept the ciphertext; otherwise it returns a null value.

The above two steps indicate that the proposed scheme is secured from the content modifying attack (message integrity) against  $\mathcal{A}$ .

**6.4. Blindness.** In our designed scheme, when the signer acts as  $\mathcal{A}$ , then he just failed to get  $m_i$ , from  $\mathcal{R} = H_2(m_i, V_h)$ , because of the one-way nature of the hash function. Also,  $\mathcal{A}$  requires to proceed first the blind factor  $V_h = H_1(\ell)$ , and for this,  $\mathcal{A}$  needs  $\ell$  which is the private number of Alice, so we can say that the proposed scheme is secure from unfair signer attack (blindness).

**6.5. Untraceability.** Suppose the signer acts as  $\mathcal{A}$  when it received  $\mathfrak{A} = (C, T, \varphi, Z, \mathcal{R})$  and tries to gain the contents of ciphertext ( $C$ ), forging the original signature  $\varphi = \mathcal{T}/(\zeta + \mathcal{R} + \mathcal{S}) \bmod n$ . Therefore, for gaining the contents of the ciphertext ( $C$ ), it must be successfully passed through the following subphases.

- (i) Here, the first attempt of  $\mathcal{A}$  needs to process  $K_s = H_3(\varphi \cdot U_v \cdot (V_s + \mathcal{R} \cdot (T + \mathcal{D}) + Z))$ ; further, it requires  $U_v$  from  $V_v = U_v \cdot \mathcal{D}$  that can be clues towards the solution of  $\mathcal{H}\mathcal{E}\mathcal{C}\mathcal{D}\mathcal{L}\mathcal{P}$
- (ii) The second attempt of  $\mathcal{A}$  needs to process  $K_s = H_3(\mathcal{T} \cdot V_v)$ , so it requires  $\mathcal{T}$  that can be clues towards the solution of  $\mathcal{H}\mathcal{E}\mathcal{C}\mathcal{D}\mathcal{L}\mathcal{P}$
- (iii) The third attempt of  $\mathcal{A}$  needs  $\mathcal{T}$  from  $\varphi = \mathcal{T}/(\zeta + \mathcal{R} + \mathcal{S})$  to process  $K_s = H_3(\mathcal{T} \cdot V_v)$ , so  $\varphi$  contains two unknown hyperelliptic curve variables which are infeasible for  $\mathcal{A}$ .

The above three subphases indicate that the proposed scheme is secured from the signer to get access to the content of an original text.

Also, forging the original signature  $\varphi = \mathcal{T}/(\zeta + \mathcal{R} + \mathcal{S}) \bmod n$ , it must successfully be passed through the following subphases.

- (i) Here, the first thing is that  $\mathcal{A}$  can require  $\mathcal{T}$ , and for this,  $\mathcal{A}$  must process  $K_s = H_3(\mathcal{T} \cdot V_v)$ , so it requires  $\mathcal{T}$  that can be clues towards the solution of  $\mathcal{H}\mathcal{E}\mathcal{C}\mathcal{D}\mathcal{L}\mathcal{P}$

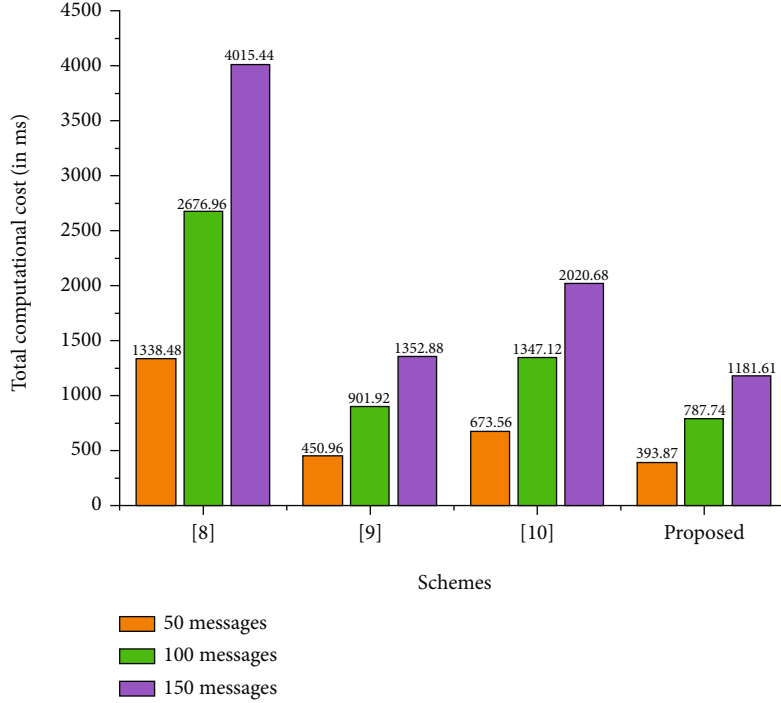


FIGURE 3: Computational cost comparisons for 50, 100, and 150 messages.

- (ii) The second thing is that  $\mathcal{A}$  requires  $\zeta$ , and for this, it processes  $Z = \zeta \cdot \mathcal{D}$ , so it requires  $\zeta$  that can be clues towards the solution of  $\mathcal{H}\mathcal{E}\mathcal{C}\mathcal{D}\mathcal{L}\mathcal{P}$ .

The above two subphases indicate that the proposed scheme is secured from forging attacks against the signer. Further, the above discussion indicates that the proposed scheme is secured from an untraceable attack against the signer.

**6.6. Forward Secrecy.** The designed scheme assures the property of message forward secrecy. Suppose an adversary  $\mathcal{A}$  attacked the proposed scheme for gaining the contents of ciphertext ( $C$ ); then it must successfully be passed through the following subphases.

- (i) The first attempt of  $\mathcal{A}$  needs to process  $K_s = H_3(\mathcal{T} \cdot V_v)$ , so it requires  $\mathcal{T}$  that can be clues towards the solution of  $\mathcal{H}\mathcal{E}\mathcal{C}\mathcal{D}\mathcal{L}\mathcal{P}$
- (ii) The second attempt of  $\mathcal{A}$  needs  $\mathcal{T}$  from  $\varphi = \mathcal{T} / (\zeta + \mathcal{R} + \mathcal{S})$  to process  $K_s = H_3(\mathcal{T} \cdot V_v)$ , so  $\varphi$  contains two unknown hyperelliptic curve variables which are infeasible for  $\mathcal{A}$ .

The above three subphases indicate that if the private key signer or Alice is compromised, then the proposed scheme is still secured from the content-stealing attack (forward secrecy) against  $\mathcal{A}$ .

**6.7. Authentication.** Upon reception of  $\mathfrak{A} = (C, T, \varphi, Z, \mathcal{R})$ , the receiver can proceed with it compute  $K = H_3(\varphi \cdot U_v \cdot (V_s + \mathcal{R} \cdot (T + \mathcal{D}) + Z))$ ,  $m_i, V_h = D_K(C)$ ,  $P = H_2(m_i, V_h)$ , and

accept if  $P = \mathcal{R}$ . So, the authentication will be done in this way in our proposed scheme.

**6.8. Nonrepudiation.** The blinded signature  $\mathcal{S} = (U_s + \mathcal{R} \cdot \mathcal{L}) \bmod n$  which is processed by the signer contains the signer's private key which is directly associated with its public key; that is why in our scheme, the signer cannot deny his generated signature.

## 7. Computational Cost

For the computational cost comparisons, we first introduce some notations that are EM, EA, HEDM, and HEDA representing elliptic curve point multiplication, elliptic curve point addition, hyperelliptic curve divisor multiplication, and hyperelliptic curve divisor addition. The experiment is done for the running time of a single EM and EA, with the help of a personal computer containing DUAL CPU E2200, 2.20 gigahertz processor, 2048 megabyte primary memory; EM consumes 2.226 ms and EA takes 0.0288 ms [17, 18]. Therefore, for HEDM and HEDA, we assume the half running time of EM and EA are 1.113 ms and 0.0144 ms, because the hyperelliptic curve consumes half of the elliptic curve [19]. The major operations proposed and those of Tsai et al. [8], Fazlullah et al. [9], and Bashir and Ali [10] are presented in Table 2. Then, based on the above major operations running time, in Tables 3 and 4, we present the running time comparison between the proposed scheme and Tsai et al. [8], Fazlullah et al. [9], and Bashir and Ali [10], for single message and a varying number of messages. In the end, Figures 2 and 3 clearly show that our scheme is efficient in requiring the processing time.

## 8. Conclusions

In this article, we proposed a multidocument blind signcryption scheme to concurrently address security concerns such as untraceability, confidentiality, and forward secrecy, as well as efficiency challenges such as high computation cost. Because SG-IIoT generates a considerable quantity of data that has to be blind signed and encrypted in a batch, the proposed scheme executes the blind signature and encryption operation on numerous digital documents in one step. The proposed scheme makes use of the hyperelliptic curve cryptography (HECC) idea, which is lightweight because of its lower key size. We performed a security analysis study for the proposed scheme, confirming our view that our scheme is more secure and capable of meeting data exchange security requirements such as untraceability, confidentiality, and forward secrecy. Furthermore, an efficiency study of the proposed scheme in terms of computational cost reveals that our scheme is more efficient than the relevant existing schemes.

## Data Availability

All data generated or analyzed during this study are included in this published article.

## Conflicts of Interest

The authors declare no conflict of interest.

## Authors' Contributions


Conceptualization and supervision are by Ako Muhammad Abdullah and Muhammad Asghar Khan. Original draft writing and methodology are by Insaf Ullah. Formal analysis is by Mohammed H. Alsharif. Validation is by Samih M. Mostafa. Software is by Ako Muhammad Abdullah. Conceptualization and review and editing are by Jimmy Ming-Tai Wu.

## References

- [1] S. M. A. A. Abir, A. Anwar, J. Choi, and A. S. M. Kayes, "IoT-enabled smart energy grid: applications and challenges," *IEEE Access*, vol. 9, pp. 50961–50981, 2021.
- [2] J. L. Gallardo, M. A. Ahmed, and N. Jara, "LoRa IoT-based architecture for advanced metering infrastructure in residential smart grid," *IEEE Access*, vol. 9, pp. 124295–124312, 2021.
- [3] A. Ghasempour, "Internet of things in smart grid: architecture, applications, services, key technologies, and challenges," *Inventions*, vol. 4, no. 1, p. 22, 2019.
- [4] W. Zhang, Z. Guo, N. Li, M. Li, Q. Fan, and M. Luo, "A blind signature-aided privacy-preserving power request scheme for smart grid," *Wireless Communications and Mobile Computing*, vol. 2021, Article ID 9988170, 10 pages, 2021.
- [5] I. Ullah, N. Ul Amin, M. Zareei et al., "A lightweight and provable secured certificateless signcryption approach for crowd sourced IIoT applications," *Symmetry*, vol. 11, no. 11, p. 1386, 2019.
- [6] M. Kaveh, S. Aghapour, D. Martin, and M. R. Mosavi, "A secure lightweight signcryption scheme for smart grid communications using reliable physically unclonable function," *2020 IEEE International Conference on Environment and Electrical Engineering and 2020 IEEE Industrial and Commercial Power Systems Europe*, 2020, pp. 1–6, Madrid, Spain, June 2020.
- [7] A. K. Awasthi and S. Lal, "Efficient scheme for sensitive message transmission using blind signcryption," in *Proceedings of the International Conference on Communication*, Kumabakonom India, December 2004.
- [8] C.-H. Tsai and P.-C. Su, "An ECC-based blind signcryption scheme for multiple digital documents," *Security and Communication Networks*, vol. 2017, Article ID 8981606, 14 pages, 2017.
- [9] N. U. Fazlullah, J. Amin, A. Iqbal, I. Umar, and M. Shahid, "Secure and efficient protocol for transmission of multi digital documents using blind signcryption," *International Journal of Computer Science and Network Security*, vol. 18, no. 6, pp. 68–78, 2018.
- [10] M. Z. U. Bashir and R. Ali, "Cryptanalysis and improvement of a blind multi-document signcryption scheme," *Cryptologia*, vol. 45, no. 5, pp. 450–464, 2021.
- [11] Y. Xiuying and H. Dake, "A new efficient blind signcryption," *Wuhan University Journal of Natural Sciences*, vol. 13, no. 6, pp. 662–664, 2008.
- [12] R. Ullah, A. I. Umar, and N. Ul Amin, "Blind signcryption scheme based on elliptic curves," *2014 Conference on Information Assurance and Cyber Security*, 2014, pp. 51–54, Rawalpindi, Pakistan, June 2014.
- [13] M. Zia and R. Ali, "Cryptanalysis and improvement of blind signcryption scheme based on elliptic curve," *Electronics Letters*, vol. 55, no. 8, pp. 457–459, 2019.
- [14] A. Waheed, N. Din, A. I. Umar, R. Ullah, and N. -u. Amin, "Novel blind signcryption scheme for E-voting system based on elliptic curves," *Mehran University Research Journal of Engineering and Technology*, vol. 40, no. 2, pp. 314–322, 2021.
- [15] M. Ullah, A. I. U. Nizamuddin, N. Amin, and S. Amin, "An efficient mobile phone voting system based on blind signcryption," in *4th International Conference on Computer and Emerging Technologies*, Shah Abdul Latif University, Khairpur Mirs, Pakistan, March 2014.
- [16] S. Ullah and N. Din, "Blind signcryption scheme based on hyper elliptic curves cryptosystem," *Peer-to-Peer Networking and Applications*, vol. 14, no. 2, pp. 917–932, 2021.
- [17] H. H. Kilinc and T. Yanik, "A survey of SIP authentication and key agreement schemes," *Ieee Communications Surveys & Tutorials*, vol. 16, no. 2, pp. 1005–1023, 2014.
- [18] S. A. Chaudhry, H. Alhakami, A. Baz, and F. Al-Turjman, "Securing demand response management: a certificate-based access control in smart grid edge computing infrastructure," *IEEE Access*, vol. 8, pp. 101235–101243, 2020.
- [19] M. A. Khan, I. Ullah, A. Alkhalifah et al., "A provable and privacy-preserving authentication scheme for UAV-enabled intelligent transportation systems," *IEEE Transactions on Industrial Informatics*, vol. 18, no. 5, 2020.

## Research Article

# AI-Based Equipment Optimization of the Design on Intelligent Education Curriculum System

Tu Peng,<sup>1</sup> Yipin Luo,<sup>2</sup> and Yanjin Liu <sup>2,3</sup>

<sup>1</sup>School of Cyberspace Science and Technology, Beijing Institute of Technology, Beijing 100081, China

<sup>2</sup>Chengdu Normal University, Chengdu 611130, Sichuan, China

<sup>3</sup>College of Educational Sciences, Xinjiang Normal University, Urumqi 830017, Xinjiang, China

Correspondence should be addressed to Yanjin Liu; 021019@cdnu.edu.cn

Received 30 December 2021; Revised 24 January 2022; Accepted 31 January 2022; Published 21 February 2022

Academic Editor: Shalli Rani

Copyright © 2022 Tu Peng et al. This is an open access article distributed under the Creative Commons Attribution License, which permits unrestricted use, distribution, and reproduction in any medium, provided the original work is properly cited.

With the rapid development of artificial intelligence-related technologies, especially the use of big data, an intelligent world is coming. In the era of intelligence, the traditional trading teaching work model is no longer adaptable. If it wants to survive the new wave of technological development, it must carry out a self-revolution in science and technology. This article aims to study the improvement and optimization of the current college education curriculum system by artificial intelligence equipment under the use of big data technology. To this end, this paper proposes a clustering algorithm for data analysis. Through the improvement of the clustering algorithm and using it in the reform of the education system of colleges and universities, the relevant education data is calculated with high performance and fed back to the teacher to improve the teaching method. At the same time, experiments are designed to analyze the performance of the algorithm and the feasibility of the teaching mode. The experimental analysis results in this paper show that the improved data analysis clustering algorithm has improved the data analysis ability in the teaching process by 37%, and the use of big data has increased the teaching quality score of colleges and universities by nearly 1 point. It can well promote the popularization of education informatization in the country and the improvement of teaching quality.

## 1. Introduction

In today's world, big data has penetrated all aspects of human society, not only changing people's ways of thinking, working, and lifestyles but also changing society's productivity and production relations, and it has also become the future "new oil", "new gold mine", "new resource", and "new engine" for innovation. After years of deliberation, the 5th Congress of the 18th Central Committee held in China in 2015 clearly advocated the "implementation of the national big data strategy". In order to deal with the issues of the big data era, the government is required to cooperate with enterprises, universities, and scientific research institutions. And universities are undoubtedly participants and promoters of this wave of big data. There are also "work problems" confusion in the field of domestic education big data, but universities have unique conditions for studying

big data, and the research and application of big data in education management have broad prospects.

Big data education management is a new stage in the development of university education management, and everything in the past is a prelude. According to big data, universities can use smarter methods to stimulate and generate new wisdom. There is a fundamental difference between the use of big data in the education management of school graduates and big data in the business field. The big data of the university will eventually find a special relationship. Using big data, cloud computing, the Internet of Things, and other technologies to optimize the structure of school operation elements and improve management is an important tool and foundation for universities to improve school operation efficiency and promote the transformation of higher education institutions. Nowadays, there are few research results on the integration of big data and university

education management in academia, the depth and scope are not enough, and the specific empirical research is insufficient. This part of the research is also urgent.

In the context of big data, people can more and more easily improve existing problems through a large amount of data acquisition and analysis, and the use of artificial intelligence equipment has accelerated this pace. As these technologies are being used more and more frequently, more and more people are involved in this research. Rongpeng tries to emphasize one of the most basic characteristics of the revolutionary technology in the 5G era. However, in the face of increasingly complex configuration problems and emerging new business needs, if there is a lack of complete artificial intelligence functions, 5G cellular networks are still not enough [1]. Lu H. proposed that underwater cameras are widely used to observe the seabed. They are usually included in autonomous underwater vehicles, unmanned underwater vehicles, and in situ ocean sensor networks. Although it is an important sensor for monitoring underwater scenes, recent underwater camera sensors have many problems [2]. Hasbabis D. believes that a better understanding of biological brains can play a vital role in building intelligent machines. He investigated the historical interaction between AI and neuroscience and emphasized the current advances in AI inspired by neural computing research in humans and other animals. Finally, he emphasized common themes that may be crucial to advancing future research in these two fields [3]. Raedt L. D. studied the basis of combining logic and probability into a so-called relational probability model. He introduced the representation, reasoning, and learning techniques of probability, logic, and their combinations. And it pays close attention to two representations in detail: the relationship between Markov logic network, undirected graph model, and weighted first-order predicate calculus formula is extended, the probability extension of the logic program, and it can also be regarded as the extension of Turing complete relational Bayesian network [4]. Goyache F. developed a method of using artificial intelligence to improve the design and implementation of linear morphological systems for beef cattle. The proposed process involves an iterative mechanism, in which type features are continuously defined and calculated using knowledge engineering methods, scored by a group of well-trained human experts, and finally analyzed by four well-known machine learning algorithms. The results obtained in this way can be used as feedback for the next iteration to improve the accuracy and effectiveness of the proposed evaluation system [5]. Makridakis S., by studying similar inventions in industrial, digital, and artificial intelligence revolutions, claims that the latter is targeted; it will bring about extensive changes and will also affect all aspects of our society and life. In addition, its impact on enterprises and employment will be considerable, leading to highly interconnected organizations that make decisions based on the analysis and use of “big” data and intensified global competition among enterprises [6]. Liu R. tried to conduct a comprehensive review of artificial intelligence algorithms in the fault diagnosis of rotating machinery from the perspective of theoretical background and industrial applications. First, the different

artificial intelligence algorithms are briefly introduced. Finally, the advantages, limitations, and practical significance of different artificial intelligence algorithms are discussed, as well as some new research trends [7]. Price S. proposed that the most advanced tools from machine learning and artificial intelligence are automating part of the peer-review process. However, there are still many opportunities for further improvement. Such simplification tools also provide perspective improvements on how the peer review process might be carried out. In particular, analytical ideas will naturally lead to peer review perspectives aimed at finding the best publishing location for the submitted papers [8]. The above-mentioned documents provide an explanation of big data artificial intelligence and related technology introduction. And the use of this part of the technology is also very good, but it is still a bit flawed because it does not make good use of the experimental area to verify its own conclusions.

The innovation of this article lies in the research and analysis of the intelligent education curriculum system in colleges and universities from the perspective of data analysis. Through the improvement of the big data data analysis clustering algorithm, the data analysis ability of the algorithm is greatly improved, and it is effectively applied to new teaching methods, which solves the current problem of insufficient teaching informatization. The experimental analysis part creatively uses three different data sets to verify the performance of the algorithm and conducts research and analysis on it in the analysis part to ensure the stable operation of the later big data analysis capabilities.

## 2. Methods of Optimizing the Education System

### 2.1. Conception of “Artificial Intelligence + Education”

*2.1.1. Changes in the Connotation of Higher Education.* The changes brought about by various technologies of artificial intelligence to the connotation of higher education will be described in detail from the following aspects: the purpose of the university, the reform of the education system, the change of teacher training, and student training.

First of all, with regard to the purpose of university education, that is, what kind of people to train, opinions vary from person to person. We must know that the future education in the artificial intelligence environment is to cultivate students’ ability to create and destroy knowledge. How should university education accept future topics? The first question is what kind of person to train. Of course, it is necessary to cultivate research skills and design skills, and the humanities will return strongly [9].

Second, for the reform of the education system, some people believe that the application of artificial intelligence technology will have a greater impact on the education system. After a large-scale discussion at Tsinghua University, it came to the conclusion that it is the so-called “Trinity” teaching model. In other words, the school’s values are not only “transmitting knowledge” or “cultivating competence” but also “formation of values”. The formation of values and the cultivation of abilities are often impossible to achieve in

the classroom. The purpose of education is to cultivate a sound personality, innovative thinking, a global outlook, and a new generation of talents with a sense of social responsibility. Regarding such a purpose, AI may not form an opposition but provide services and support to us. Therefore, the positioning must be correct. Under the background of artificial intelligence, the Bayesian model is strengthened. The Bayesian prediction model is a kind of prediction using Bayesian statistics. Yess statistics is different from general statistical methods. It not only uses model information and data information but also makes full use of prior information. Through the method of empirical analysis, the prediction results of the Bayesian prediction model and the ordinary regression prediction model are compared, so that course evaluation can be obtained, the learning style of students can be inferred, and the accuracy of data prediction can be improved [10].

An intelligent decision support system is a decision system that combines artificial intelligence and education proposed by American scholars. It is mainly composed of a database, model library, method library, and intelligent components. Its structural composition is shown in Figure 1.

At present, the intelligent decision support system has become the direction of the development of the decision support system DSS, and it has strong development potential and prospects in the application of online education. For example, the Intelligent Decision Support System (IDSS) is widely used in digital databases. The system provides decision-makers with data, information, and background information needed for decision-making, clarifies decision-making goals, and determines problems. This helps to establish or change the decision-making model and provide a variety of options, evaluations, and selection of various options to prepare. Through the interactive function of humans and computers (Multitouch, Gesture Sensing, Voice Recognition, Visual Tracking, and Other Interactive Functions), it provides the support needed for analysis, comparison, judgment, and correct and effective decision-making, adapting to the times to improve teacher training, and supporting teachers before service and teachers in service. Teachers should continue to learn, learn the use of artificial intelligence equipment, and apply it to the actual teaching process to help improve the quality of education and grow by themselves, reform the role of teachers, change the methods of education and evaluation, and learn to cooperate [11], using AI to integrate the role of professional dignity and professional role as a teacher to meet the educational requirements of the AI era [12]. The professional development model of future teachers in the "AI" era is shown in Figure 2.

*2.1.2. The Formation Process of "Smart Education".* In 2008, the then President of IBM promoted the concept of an intelligent platform for the first time in his report "Smart Planet: Next Generation Leadership Agenda" [13]. With the strong support of a new generation of information technology, almost everything on the Earth can be identified, connected to each other, and made intelligent [14].

The concept of "smart Earth" continues to penetrate into society, resulting in many new concepts such as smart medical care, smart elderly care, smart transportation, and smart cities [15]. In September 2009, Dubuque in the Midwestern United States and IBM jointly announced the construction of the first "smart city" in the United States. With the widespread use of smart devices, smart education has emerged. At the same time, IBM promotes five main ways of smart education: students' technological immersion; individualized and diverse learning paths; service-oriented economic knowledge and skills; the global integration of systems, culture, and resources; and the role of education in the 21st-century economy [16]. The research framework of smart education is shown in Figure 3.

Intelligent education is a new educational concept. In order to realize this concept, information technology needs to be used to build an intelligent learning environment (technical innovation: mainly through technology such as big data, data mining technology, clustering algorithm, neural network learning, etc.). In an intelligent environment, it is necessary to construct intelligent education methods and intelligent evaluation (methods) to apply innovation (innovation mainly refers to educational innovations such as teaching models, teaching methods, and student learning methods.), promote learners to implement intelligent learning (practical innovation), and cultivate the ability to hide and intelligently develop potential. They must be good at learning, good at cooperation, good at communication, research, and judgment requiring excellent creativity, and good at solving complex problems [17]. In the new era, smart education is open to the public in the form of reversal teaching. Inverted teaching, as the name suggests, is to transform the traditional learning model of "teaching first and then learning" into "learning first and then teaching", and the main body of the classroom is transformed from teachers to students, creating a worksheet first, then watching some microvideos before leaving the class, and then conducting some targeted questions and answers. Therefore, due to ample classroom time, students can concentrate on exercises, projects, and discussions, and teachers can also concentrate on explaining the knowledge structure [18]. Therefore, only by answering the object's question and solving the question, the reverse innovation of the education process can be implemented.

As shown in Figure 4, when most interviewees are studying professional courses, courses related to artificial intelligence are mainly concentrated in science and engineering, while liberal arts majors are relatively few or not [19]. Liberal arts majors should embrace technological development through dialogue with advanced science and technology (such as artificial intelligence) on the basis of preserving tradition.

*2.2. Cluster Analysis under Big Data.* In cluster analysis, how to define the similarity between samples is very important and determines the performance of the clustering algorithm to a large extent. The similarity between samples is generally expressed by a distance function (or similarity function).

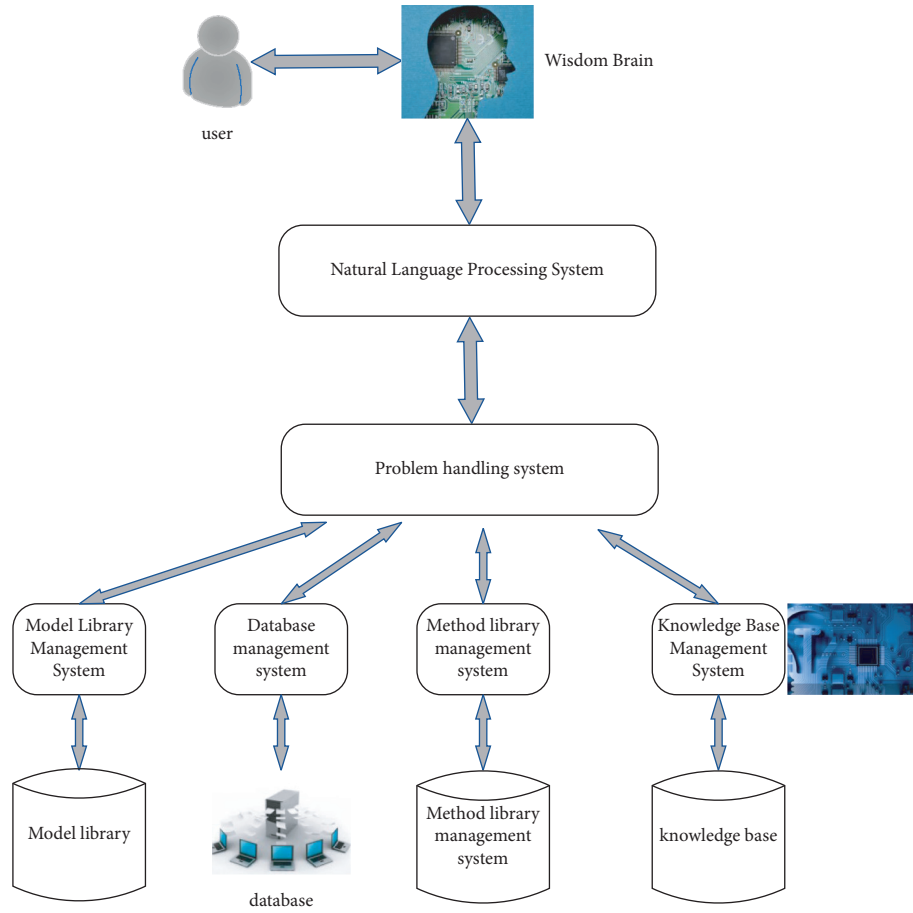


FIGURE 1: Composition diagram of intelligent decision support system.

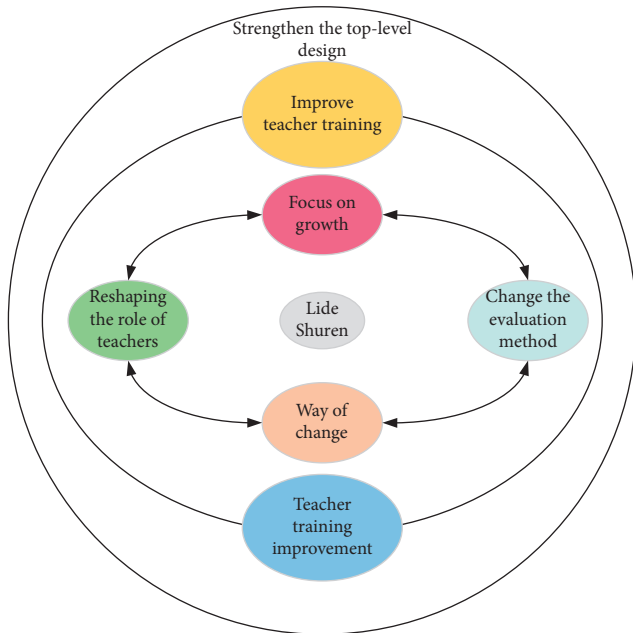


FIGURE 2: The professional development model of future teachers in the “AI” era.

Distance is not only the distance in space but also the gap caused by time, state, semantics, and density. So far, there is no distance function that can be applied to all clustering tasks. Different similarity measures should be designed in different clustering problems [20]. Here, we give two samples:

$$W_i = (w_{i1}, w_{i2}, \dots, w_{iD})^T, \tag{1}$$

$$W_j = (w_{j1}, w_{j2}, \dots, w_{jD})^T.$$

Based on these two samples, several common example functions are introduced.

2.2.1. *Euclidean Distance.* Euclidean distance is the most popular kind of distance measurement function, derived from the distance formula between two points in Euclidean space, which is defined as follows:

$$X_{ij} = \sqrt{\sum_{k=1}^x (w_{ik} - w_{jk})^2}. \tag{2}$$

It can also be represented by vector operations:



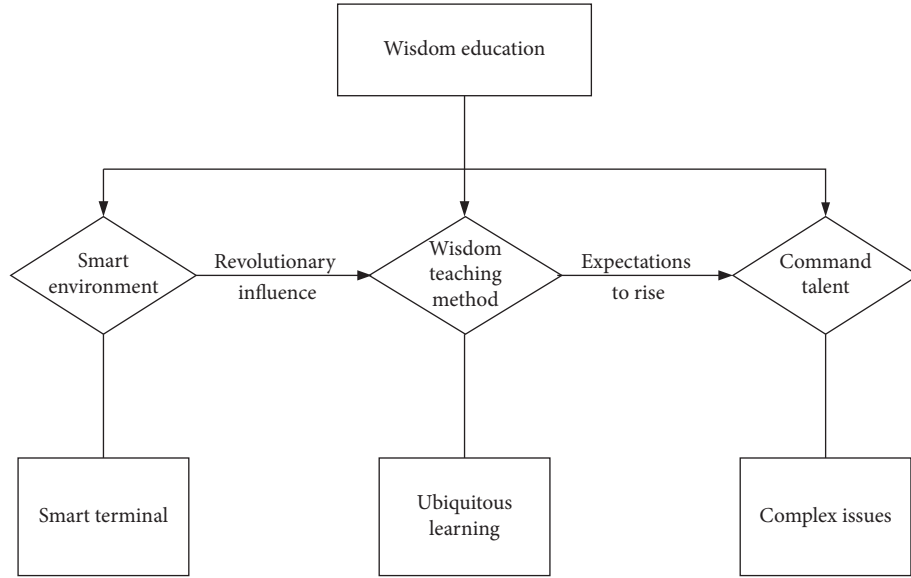


FIGURE 3: “Smart Education” research framework.

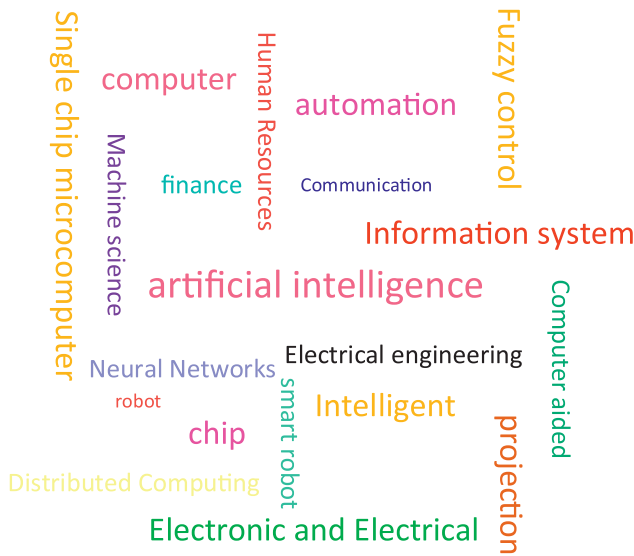


FIGURE 4: Professional word cloud diagram related to artificial intelligence.

$$X_{ij} = \sqrt{(w_i - w_j)^T (w_i - w_j)}. \quad (3)$$

2.2.2. *Harmanton Distance.* The definition of Manhattan distance is as follows:

$$X_{ij} = \sum_{k=1}^x |w_{ik} - w_{jk}|. \quad (4)$$

2.2.3. *Chebyshev Distance.* The Chebyshev distance is defined as follows:

$$X_{ij} = \max_k (|w_{ik} - w_{jk}|). \quad (5)$$

There is another form of expression for Chebyshev distance:

$$X_{ij} = \lim_{p \rightarrow \infty} \left( \sum_{k=1}^x |w_{ik} - w_{jk}|^p \right)^{1/p}. \quad (6)$$

2.2.4. *Minkowski Distance.* Minkowski distance is a set of distance functions, which is defined as

$$X_{ij} = \sqrt[p]{\sum_{k=1}^x |w_{ik} - w_{jk}|^p}, \quad (7)$$

where  $p$  only represents one parameter. When  $p$  is equal to 1, the formula is the representation of the Harmanton distance; when  $p$  is equal to 2, the formula is a representation of Euclidean distance.

2.2.5. *Mahalanobis Distance.* The Mahalanobis distance was proposed by Indian statisticians and is defined as

$$X_{ij} = \sqrt{(w_i - w_j)^T S^{-1} (w_i - w_j)}. \quad (8)$$

2.2.6. *Cosine Distance of Included Angle.* The angle cosine is defined as

$$X_{ij} = \cos(\theta) = \frac{w_i \cdot w_j}{\|w_i\| \|w_j\|}, \quad (9)$$

$$X_{ij} = \frac{\sum_{k=1}^x w_{ik} w_{jk}}{\sqrt{\sum_{k=1}^x w_{ik}^2} \sqrt{\sum_{k=1}^x w_{jk}^2}}.$$

**2.2.7. One-Time Sample Weighting Method.** Boosting is a supervised technique that uses multiple weak learners to get one strong learner. Adaptive Boosting is the most popular method of boosting. It iteratively generates a distribution of data and uses it to train the next weak classifier. In each iteration, the samples that are difficult to divide (misclassified) get more weight, while the weights of the samples that are easy to divide are reduced. The new classifier pays more attention to those samples that have significant weight. When the algorithm stops, Adaboost combines all the weak classifiers in the iterative process to get a strong classifier.

The effectiveness of boosting technology has been proven theoretically and experimentally. It uses the sample information of the training data to iteratively update the weight of the sample. This also explains to a certain extent why the application of sample weight information to the ensemble clustering problem has not been studied yet. This chapter proposes a one-time sample weighting method to make up for this gap, and its purpose is to make those samples that are difficult to divide play a more important role in the process of ensemble clustering. This method uses the basic clustering results to construct a co-joining matrix and assigns higher weights to difficult-to-divide samples at one time. The difference with boosting is that the method in this chapter is one-off while boosting is an iterative process. The specific details are described below.

First, the co-join matrix  $A$  is constructed by collecting the basic clustering result set  $C$  as follows:

$$A_{ij} = \frac{V_{ij}}{R}. \quad (10)$$

Among them,  $V_{ij}$  is the number of times that samples  $W_i$  and  $W_j$  appear in the same cluster.  $R$  is the total number of clustering results. Then, we divide the uncertainty of the samples  $W_i$  and  $W_j$  according to the definition as

$$\text{confusion}(w_i, w_j) = A_{ij}(1 - A_{ij}). \quad (11)$$

Next, we use the indicator confusion to define the weight of each sample:

$$\omega'_i = \frac{4}{n} \sum_{j=1}^n \text{confusion}(w_i, w_j). \quad (12)$$

In order to avoid the instability caused by the weight being 0, we added a smoothing term:

$$\omega_i = \frac{\omega'_i + e}{1 + e}, \quad (13)$$

where  $e$  represents a small positive number. This is similar to the idea of the boosting algorithm, which assigns larger weights to samples that are difficult to cluster; conversely, it assigns smaller weights to samples that are easy to cluster.

**2.2.8. Sample-Weighted Graph Division.** The sample-weighted clustering algorithm is to find a better single clustering result, and we aim to find a more effective consistent clustering result. In order to achieve this goal, we first calculate the corresponding weighted class center for each cluster in the base cluster:

Base cluster:

$$C^r \quad (r = 1, 2, \dots, R). \quad (14)$$

We calculate the weighted class center as shown in formula (15):

$$m_l^r = \frac{\sum_{w_i \in C_l^r} \omega_i w_i}{\sum_{w_i \in C_l^r} \omega_i}. \quad (15)$$

At the same time, we use an exponential function to measure the similarity of the sample to the center of the weighted class:

$$X(w_i, m_l^r) = \exp \left\{ -\frac{\|w_i - m_l^r\|^2}{t} \right\}. \quad (16)$$

Among them,  $t > 0$  is a parameter. Then, the probability that the sample  $W_i$  belongs to the cluster is given by

$$P(C_l^r | w_i) = \frac{X(w_i, m_l^r)}{\sum_{l'=1}^{k_r} X(w_i, m_{l'}^r)}. \quad (17)$$

Now, we can define the posterior probability vector of the sample in the base cluster as

$$P_i^r = (P(C_1^r | w_i), P(C_2^r | w_i), \dots, P(C_{k_r}^r | w_i)). \quad (18)$$

This process uses raw data and integrated clustering information. Based on the new expression of samples in base clustering, we use cosine similarity to define the similarity of two samples  $x_i$  and  $x_j$ :

$$S_{ij}^r = \frac{P_i^r (P_j^r)^T}{\|P_i^r\| \|P_j^r\|}. \quad (19)$$

$T$  represents the transpose of a matrix or vector. For  $R$  basis clusters,  $R$  similarity matrices can be generated. We merge all the similarity matrices and get a final similarity matrix  $S$ :

$$S = \frac{1}{R} \sum_{r=1}^R S^r. \quad (20)$$

The weight of the edge  $E_{ij}$  connecting nodes  $V_i$  and  $V_j$  is defined as follows:

$$S_{ij} = \begin{cases} S_{ji} = 0, \\ S_{ji} = P(C_j|w_i). \end{cases} \quad (21)$$

The similarity matrix  $S$  can be rewritten as

$$S = \begin{bmatrix} 0 & B^T \\ B & 0 \end{bmatrix}. \quad (22)$$

$n \times n_c$  matrix  $B$  is defined as

$$B = \begin{bmatrix} P_1^1 & P_1^2 & \dots & P_1^R \\ P_2^1 & P_2^2 & \dots & P_2^R \\ \dots & \dots & \dots & \dots \\ P_n^1 & P_n^2 & \dots & P_n^R \end{bmatrix}. \quad (23)$$

The graph segmentation algorithm can be used to segment the resulting mixed graph, where the division of samples is the final clustering result.

**2.3. Artificial Intelligence.** Recently, artificial intelligence has risen again in 2006 due to the success of deep learning algorithms. According to the strength of artificial intelligence, it can be divided into three categories: weak artificial intelligence, strong artificial intelligence, and super artificial intelligence. Weak artificial intelligence refers to artificial intelligence that is only good at a certain aspect, mainly human explicit intelligence. The current research on artificial intelligence is concentrated on this type. Strong artificial intelligence is a human-level artificial intelligence that can be compared with humans, possessing and demonstrating explicit wisdom. Super artificial intelligence is the intelligence that leads humans, and the degree of intelligence can cover almost all fields. Figure 5 shows the development history of artificial intelligence.

In the education field, in addition to assisting teachers in teaching work through traditional image, speech recognition, and semantic analysis technologies, artificial intelligence has its unique applications and promising prospects. The most representative ones are intelligent knowledge graph analysis and virtual learning assistants. The teaching object is often expressed as a chaotic collection, and there are obvious differences between each sample. Intelligent map analysis can independently extract the characteristics of the knowledge map of the sample, as well as the objective existence and subjective initiative characteristics of the sample knowledge map, formulate the most reasonable teaching content, and plan the most effective learning path for each sample. The intended learning assistant not only reduces the workload of teachers in teaching activities but also realizes “1 to 1” assisted learning and guidance. The biggest difference between virtual learning assistants and traditional computer-assisted teaching is that virtual learning assistants can learn flexibly and independently. Through constant contact with the teaching object, the virtual learning assistant can adjust its own relevant parameters through the feedback information of the teaching object and improve the ability of assisted learning.

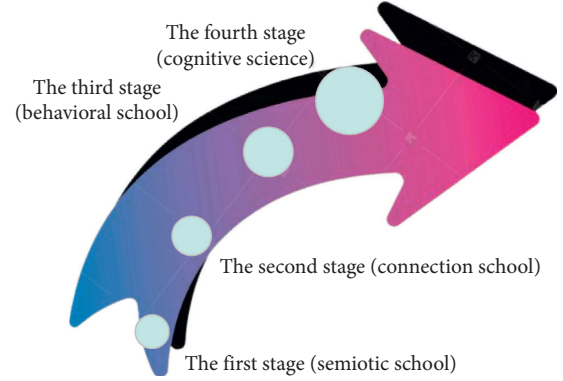


FIGURE 5: The development history of artificial intelligence.

Some scholars divide artificial intelligence into four application forms: intelligent tutor system, automated evaluation system, educational game, and educational robot. Combining the above classification of application forms, based on the integration mode of artificial intelligence technology and education and the support form of technology in the framework of instructional design, the application form of artificial intelligence in education is divided into two forms of subjectivity and auxiliary form, such as shown in Figure 6.

The subjective application form refers to the integration of artificial intelligence technology into the traditional teaching subject and object in the role of the teaching subject, such as educational robots and intelligent teaching systems, which mainly assume the roles of tutors, students, assistants, and learning companions; auxiliary application form refers to the integration of artificial intelligence into teaching content, teaching environment, and teaching evaluation or transformation into teaching media tools, which affect the teaching system, and assume the role of teaching aids, learning tools, resources, and scenarios.

Although the application of artificial intelligence technology in education is at the beginning stage, artificial intelligence technology is the most revolutionary technology at this stage. Technology is a tool of education and teaching, and it is also a revolutionary factor that subverts education and teaching. But not all technological revolutions will completely change education, only some revolutionary technologies will have such an impact. With the maturity of artificial intelligence technology, the learning ability of machines is getting stronger and stronger, and its application in the field of education will become more and more in-depth. Humanity’s long-standing educational philosophy will be realized on the basis of artificial intelligence-based big data, cloud computing, deep learning, and adaptive technology.

The cornerstone of artificial intelligence’s rapid and prosperous development again is cloud computing, new algorithms, and big data. Only the comprehensive application of revolutionary technologies will have an impact on the teaching system. Therefore, this article will explore the paradigm shift of instructional design in the context of the era of comprehensive technical support such as artificial

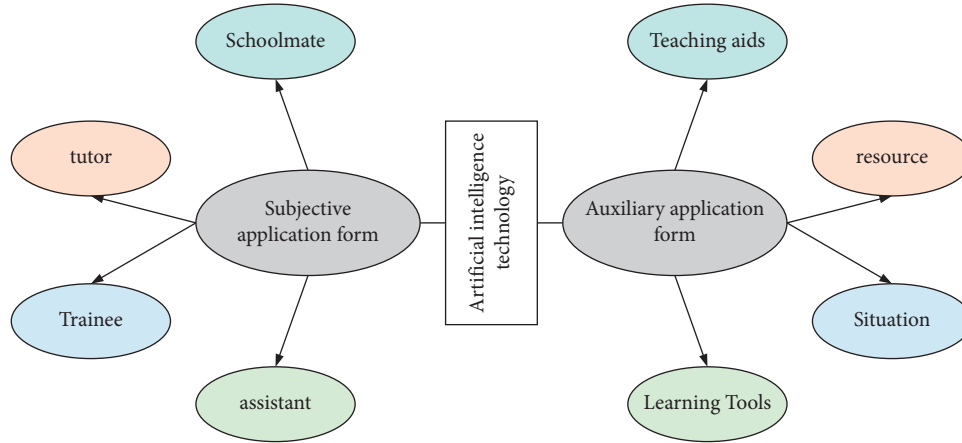


FIGURE 6: The application form of artificial intelligence in the teaching system.

intelligence, cloud computing, big data, learning analysis, and machine learning.

### 3. Simulation Data and Experiments

**3.1. Experimental Results of Algorithm Simulation Data.** The experiment uses three simulation data sets One, Two, and Three, which contain 3, 4, and 5 circular clusters, respectively. The center point and radius are shown in Tables 1–3. The method of generating each data cluster set is basically based on the center point and the radius.

Three data sets One, Two, and Three are randomly generated according to the table simulation. One is divided into 3 clusters, containing 300, 100, and 200 pieces of data, respectively. Two is divided into 4 clusters, containing 400, 100, 300, and 200 pieces of data, respectively. Three is divided into 5 clusters, containing 80, 40, 150, 80, and 120 pieces of data, respectively. We can see from the observations of the above three data sets that the data of the first two data sets are basically round, but the third one is different. The state of his data set is elliptical. To this end, we calculate the accuracy of his method and the sum of squares of internal errors for each data set, and the calculated values are shown in Table 4.

It can be seen from the above table that the accuracy of the TR-KMC method and the ID-KMC method in the One, Two, and Three datasets is not much different. However, in contrast, the latter clustering effect is more obvious, and it can better analyze the memory of intelligent education data in colleges and universities.

#### 3.2. Personalized Service Teaching Experiment Based on Big Data

**3.2.1. Personalized Learning Module Based on Big Data Mining, Analysis, and Aggregation.** There should be identity authentication and unique student number to achieve lifelong learning tracking. In the personalized teaching mode, students first need to register and establish each individual's own dynamic teaching electronic file. Future education is supported by Internet education, using a new

TABLE 1: One simulation data set.

Cluster	Center point	Radius	Number of data objects
One (cluster1)	(0.5, 0.5)	0.5	300
One (cluster2)	(2.8, 2.0)	2.0	100
One (cluster3)	(4.1, 4.0)	4.0	200

TABLE 2: One simulation data set.

Cluster	Center point	Radius	Number of data objects
Two (cluster1)	(0.5, 1.5)	0.5	400
Two (cluster2)	(2.4, 1.5)	1.3	100
Two (cluster3)	(4.1, 1.5)	0.3	300
Two (cluster4)	(5.6, 1.5)	1.5	200

TABLE 3: One simulation data set.

Cluster	Center point	Radius	Number of data objects
Three (cluster1)	(0.5, 1.5)	0.5	80
Three (cluster2)	(3.1, 2.0)	2.1	40
Three (cluster3)	(5.9, 2.5)	0.8	150
Three (cluster4)	(8.7, 2.5)	2.0	80
Three (cluster5)	(10.3, 3.0)	2.3	120

TABLE 4: Experimental results of the simulation data set.

Data set	Accuracy (%)		SSE		Reduction rate (%)
	TR-KMC	ID-KMC	TR-KMC	ID-KMC	
One	98.31	97.16	159.36	55.019	65.436
Two	98.4	98.642	94.361	19.399	78.259
Three	76.1295	98.1684	548.264	32.4	94.336

system on the basis of big data to certify personal qualifications, starting from a unique student number, and accompanying individuals for life. The dynamic electronic file records personal basic information, learning experience, educational level, and other necessary information. This basic information is a basic guarantee for the realization of personal lifelong learning.

*3.2.2. Use the Scale to Conduct Personalized Tests and Character Characteristics Analysis.* When the learner's learning characteristics match the learning environment, a benign interaction will be realized and the best learning effect will be produced. For this reason, before starting personalized learning, it is necessary to understand the individual characteristics and individual differences of each learner. Before implementing personalized and comprehensive teaching, it is necessary to consider the learner's previous experience, learning motivation, metacognitive ability, learning style, and learner's personality characteristics. Internet education can be used for the occupational personality test, occupational personality test, psychological test, and ability test.

*3.2.3. Establish Electronic Files for Dynamic Learning.* Construct an electronic file of student growth with the main contents of students' quality literacy, study foundation, study habits, academic achievement, physical and mental health, learning difficulties, task goals, etc. Accumulate and improve learner information big data, build a comprehensive learning electronic file with learner personality analysis as the main content, and change the static evaluation and single evaluation in traditional education into multiple evaluation and dynamic evaluation.

*3.2.4. Using Big Data Mining Technology to Realize the Aggregation and Generation of Personalized Information.* Under the vision of Internet thinking, learning pays more attention to providing personalized learning support services. This personalized learning support service is based on big data mining. The core link of personalized learning services in the context of Internet education is data. The use of big data to achieve personalized learning includes data collection, data generation, data mining, data analysis, data aggregation, and other data recycling. For example, a batch of data can be collected through the learner's dynamic learning of the learning trajectory, learning difficulties, and learning habits in the electronic file; and on the basis of data collection, generation, and mining, a database based on the learning object is generated, which includes all the important information of the learning object. Teachers can extract and analyze information in any dimension according to the database of the learning object and then use statistical analysis software for statistical analysis. It can also build a model of the learning object and realize personalized content recommendation based on the basic information of the learning task and the learning object, and the system automatically generates a dynamic learning path map based on the learner.

## 4. Data Analysis Ability and Teaching Improvement Analysis

*4.1. Model Analysis Based on BIC Criteria.* In the case of clustering, there are many cluster variables that can be selected, and the method of selecting cluster variables is called model selection. The benchmarks generally used in the

selection model are as follows: AIC standard, BIC standard, and HQ standard. This chapter adopts BIC guidelines. Figure 7 shows a specific BIC curve, including the number of variables, that is, the number of models and clusters.

By observing Figure 7 we can see the following. (1) As the number of clusters increases, BIC increases monotonously, and there is no obvious peak phenomenon. Explaining that on this issue, the BIC standard is a cluster. (2) When the number of clusters is greater than 4, BIC will increase more steadily. In other words, the increase in the number of clusters has no great impact on the interpretation of the model. This cluster should be close to 4, but this method cannot get an accurate value.

At the same time, in the calculation process of the predicted strength, the training set and the test set are randomly divided, so some accidental factors may have a great influence on the calculation result of the predicted strength. In order to reduce the influence of accidental factors, this paper adopts an improved method for calculating the intensity of prediction. The specific method is as follows. First, the data set is randomly divided into several equal parts, and the equal parts are obtained, respectively, and then the test set is executed. Finally, the average value is obtained as the predicted strength under this number of clusters. Figure 8 shows the predicted intensity change curve under various variable numbers and cluster numbers.

*4.2. Simulation Experiment Based on Clustering Analysis Algorithm.* In order to verify the effectiveness and feasibility of the clustering analysis algorithm, simulation experiments are used to verify the effectiveness of the algorithm.

*4.2.1. Simulation Experiment Data Set.* The first simulation experiment is based on an unbalanced data set for testing: the simulation sample set is composed of two two-dimensional Gaussian random distribution sample sets. The class centers of the two types are (5, 5) and (10, 10), respectively. The number of samples in the first type is 300, and the covariance matrix is taken as  $\begin{bmatrix} 6 & 0 \\ 0 & 6 \end{bmatrix}$ . The number of samples in the second type is 50, The covariance matrix is taken as  $\begin{bmatrix} 1 & 0 \\ 0 & 1 \end{bmatrix}$ . The distribution of the samples is shown in Figure 9.

In actual calculations, particle swarm optimization calculations tend to fall into local optimal solutions, resulting in poor clustering effects. The FCM algorithm is used to cluster the data, and the geometric average of various precisions is selected as the comparison standard to examine the effectiveness of each algorithm. The test results based on simulation data sets 1 and 2 are shown in Table 5.

When PCM is tested based on an unbalanced data set, it is very easy to fall into consistency, making the test result tend to 0, resulting in invalid test results.

The results of simulation experiment 1 and simulation experiment 2 show that the sample size of the data set has an impact on the algorithm clustering results. The test results based on balanced data are better than unbalanced data sets, which shows that the sample size interferes with the performance of the algorithm. Moreover, in the test of

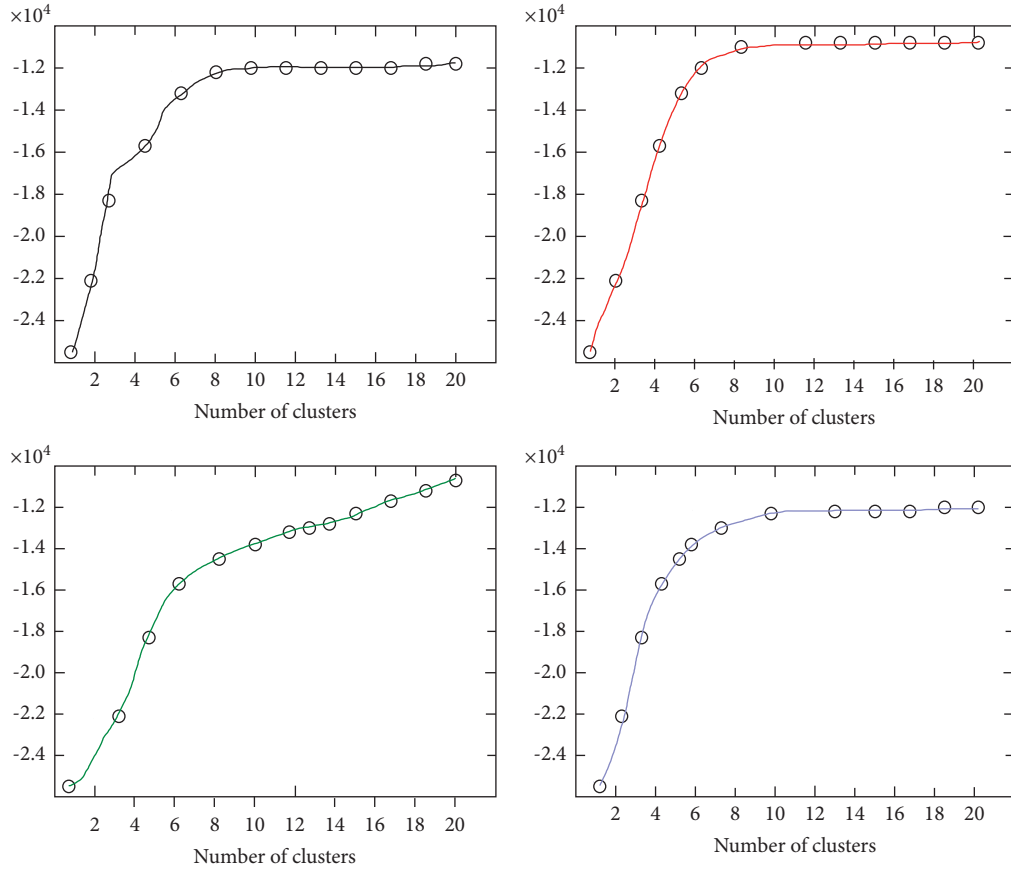


FIGURE 7: BIC varies with the number of variables, namely, the model and the number of clusters.

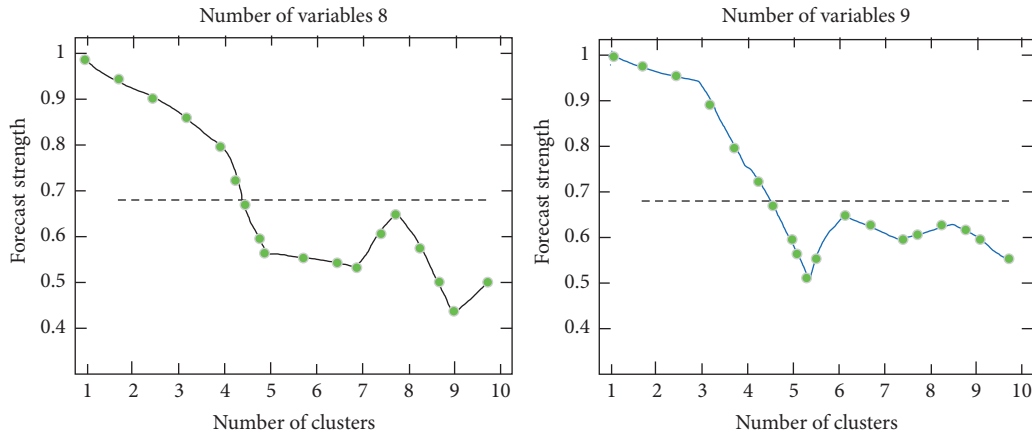


FIGURE 8: The change curve of prediction intensity under different variable numbers and cluster numbers.

unbalanced data sets, there are almost no errors in the test results of the positive class (small sample class) and the clustering error. Basically, they come from the negative class. This reflects that fuzzy cluster classification judgments tend to be positive, which is the opposite of supervised classification which tends to negative classes. It also shows that for balanced and unbalanced data sets, supervised classification and fuzzy clustering are two independent research problems.

According to the results of two simulation experiments, it can be explained that, compared with PCM, EPCM is not

only effective for balanced data sets but also can maintain good classification performance for unbalanced data sets. In contrast, because PCM does not contain sample size information, it only performs well for balanced data but performs very poorly for unbalanced data sets.

4.3. *The Degree of Education Informatization and Teaching Development in Colleges and Universities.* As a special form of education, ideological and political education in colleges

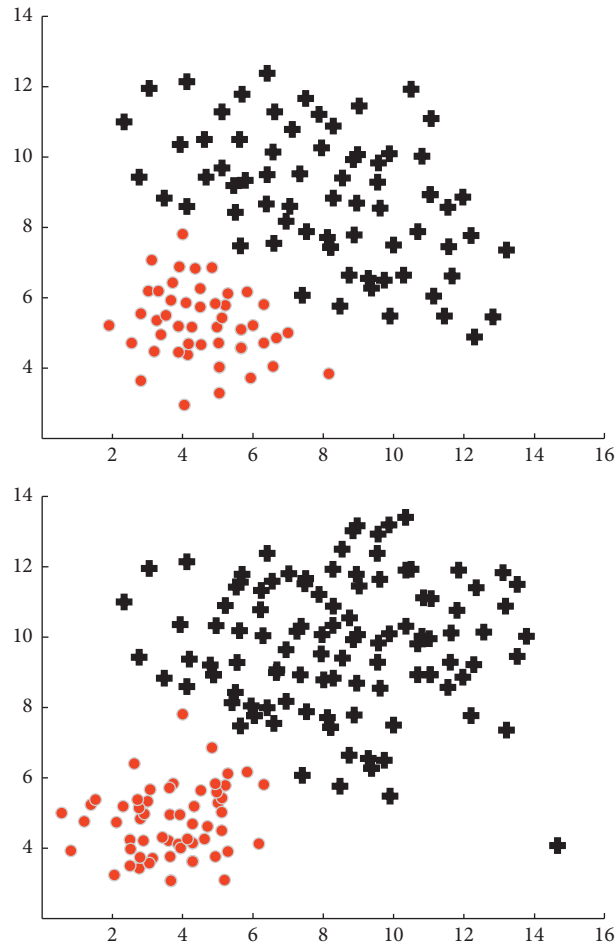


FIGURE 9: The spatial distribution of the two types of samples corresponding to the two simulation experiments.

TABLE 5: Simulation test results of two data sets.

Clustering model	Average value of various precisions	Clustering model	Average value of various precisions
EPCM (%) $m = 2$	95.38	EPCM (%) $m = 2$	99.41
EPCM (%) $m = 3$	93.11	EPCM (%) $m = 3$	99.34
PCM (%) $m = 2$	0	PCM (%) $m = 2$	100
PCM (%) $m = 3$	0	PCM (%) $m = 3$	100

and universities, with the help of big data, its informatization level has been significantly improved. The most obvious is that the construction of smart campuses boosted by big data provides an important support and platform for the informatization of ideological and political education in colleges and universities. Smart campuses have demonstrated significant advantages in providing fast, massive, multisource heterogeneous information. However, the domestic emphasis on this aspect is still far from enough. This article selects a mature foreign university teaching system

based on big data to compare and analyze with a current domestic university. The statistical data is shown in Figure 10.

From the figure, we can see that foreign countries pay more attention to related informatization. The use of artificial intelligence equipment in colleges and universities is very common, and the degree of informatization is far away from the domestic teaching model, and the quality of teaching is also higher than that in China. It is mainly through the use of big data, statistical analysis of school data



FIGURE 10: Comparison of the degree of informatization and teaching quality scores at home and abroad.

through big data. Statistics about students' habits and other related elements and feedback to teachers will help teachers teach symptomatically according to students' conditions and improve the problems they encounter in the learning process.

## 5. Conclusions

The main research content of this paper is the improvement of the intelligent education curriculum system of colleges and universities by artificial intelligence equipment under the background of big data. Through the research and analysis of the data analysis and clustering algorithm of big data, the data processing ability under the new teaching mode is improved, and the application of artificial intelligence equipment is discussed on the improvement of the memory of the teaching system. At the same time, we design experiments to investigate and analyze the improved data analysis clustering algorithm, and the final results are as follows: in the teaching process, the improved data analysis clustering algorithm has increased the data analysis ability by 37%, and the teaching quality score of colleges and universities has increased by about 1 point under the action of big data, which effectively improves the degree of informatization of colleges and universities and at the same time improved the quality of teaching.

## Data Availability

Data sharing is not applicable to this article as no new data were created or analyzed in this study.

## Conflicts of Interest

The authors state that this article has no conflicts of interest.

## Acknowledgments

This work was supported by the special scientific research project of on-the-job doctoral students of Chengdu Normal University in 2020" Research on the Framework of Teaching

Knowledge System under the Background of Artificial Intelligence" (ZZBS2020-10); The innovation training program for College Students "Research on the Development of Characteristic Curriculum of Sex Education in Primary School: Based on the Investigation and Analysis of Several Primary Schools in Chengdu"; Key Research Base of Philosophy and Social Sciences in Sichuan Province: key project of Sichuan Primary and secondary school teachers' Professional Development Research Center "Research on the Social Support System for Rural Teachers' Professional Development from the Perspective of Excellent Teachers (PDTR2020-02)"; and Key Research Base of Humanities and Social Sciences in Colleges and Universities in Sichuan Province: the key project of Sichuan Primary and secondary school teachers' Ethics Research Center "Research on the Realization of Primary and Secondary School Teachers' Fair Virtue from the Perspective of Socialist Core Values"(CJSD20-28).

## References

- [1] R. Li, Z. Zhao, X. Zhou et al., "Intelligent 5G: when cellular networks meet artificial intelligence," *IEEE Wireless Communications*, vol. 24, no. 5, pp. 175–183, 2017.
- [2] H. Lu, Y. Li, M. Chen, H. Kim, and S. Serikawa, "Brain intelligence: go beyond artificial intelligence," *Mobile Networks and Applications*, vol. 23, no. 7553, pp. 368–375, 2017.
- [3] D. Hassabis, D. Kumaran, C. Summerfield, and M. Botvinick, "Neuroscience-inspired artificial intelligence," *Neuron*, vol. 95, no. 2, pp. 245–258, 2017.
- [4] L. D. Raedt, K. Kersting, S. Natarajan, and D. Poole, "Statistical relational artificial intelligence: logic, probability, and computation," *Synthesis Lectures on Artificial Intelligence and Machine Learning*, vol. 10, no. 2, pp. 1–189, 2016.
- [5] F. Goyache, J. J. Del Coz, J. R. Quevedo et al., "Using artificial intelligence to design and implement a morphological assessment system in beef cattle," *Animal Science*, vol. 73, no. 01, pp. 49–60, 2016.
- [6] S. Makridakis, "The forthcoming artificial intelligence (AI) revolution: its impact on society and firms," *Futures*, vol. 90, pp. 46–60, 2017.



- [7] R. Liu, B. Yang, E. Zio, and X. Chen, "Artificial intelligence for fault diagnosis of rotating machinery: a review," *Mechanical Systems and Signal Processing*, vol. 108, pp. 33–47, 2018.
- [8] K. W. Kow, Y. W. Wong, R. K. Rajkumar, and R. K. Rajkumar, "A review on performance of artificial intelligence and conventional method in mitigating PV grid-tied related power quality events," *Renewable and Sustainable Energy Reviews*, vol. 56, pp. 334–346, 2016.
- [9] S. Jha and E. J. Topol, "Adapting to artificial intelligence: radiologists and pathologists as information specialists," *JAMA*, vol. 316, no. 22, pp. 2353–2354, 2016.
- [10] J. H. Thrall, X. Li, Q. Li et al., "Artificial intelligence and machine learning in radiology: opportunities, challenges, pitfalls, and criteria for success," *Journal of the American College of Radiology*, vol. 15, no. 3, pp. 504–508, 2018.
- [11] P. Glauner, J. A. Meira, P. Valtchev, R. State, and F. Bettinger, "The challenge of non-technical loss detection using artificial intelligence: a survey," *International Journal of Computational Intelligence Systems*, vol. 10, no. 1, pp. 760–775, 2017.
- [12] M. Seyedmahmoudian, B. Horan, T. K. Soon et al., "State of the art artificial intelligence-based MPPT techniques for mitigating partial shading effects on PV systems-a review," *Renewable and Sustainable Energy Reviews*, vol. 64, pp. 435–455, 2016.
- [13] R. Barzegar, J. Adamowski, and A. A. Moghaddam, "Application of wavelet-artificial intelligence hybrid models for water quality prediction: a case study in Aji-Chay River, Iran," *Stochastic Environmental Research and Risk Assessment*, vol. 30, no. 7, pp. 1797–1819, 2016.
- [14] L. Caviglione, M. Gaggero, J. F. Lalande, W. Mazurczyk, and M. Urbanski, "Seeing the unseen: revealing mobile malware hidden communications via energy consumption and artificial intelligence," *IEEE Transactions on Information Forensics and Security*, vol. 11, no. 4, pp. 799–810, 2017.
- [15] Z. Wang and R. S. Srinivasan, "A review of AI based building energy use prediction: contrasting the capabilities of single and ensemble prediction models," *Renewable and Sustainable Energy Reviews*, vol. 75, pp. 796–808, 2016.
- [16] C. Cath, S. Wachter, B. Mittelstadt, M. Taddeo, and L. Floridi, "Artificial intelligence and the 'good society': the US, EU, and UK approach," *Science and Engineering Ethics*, vol. 24, no. 7625, pp. 1–24, 2017.
- [17] M. Hutson, "Artificial intelligence faces reproducibility crisis," *Science*, vol. 359, no. 6377, pp. 725–726, 2018.
- [18] D. Tien Bui, Q.-T. Bui, Q.-P. Nguyen, B. Pradhan, H. Nampak, and P. T. Trinh, "A hybrid artificial intelligence approach using GIS-based neural-fuzzy inference system and particle swarm optimization for forest fire susceptibility modeling at a tropical area," *Agricultural and Forest Meteorology*, vol. 233, pp. 32–44, 2017.
- [19] J. Lemley, S. Bazrafkan, and P. Corcoran, "Deep learning for consumer devices and services: pushing the limits for machine learning, artificial intelligence, and computer vision," *IEEE Consumer Electronics Magazine*, vol. 6, no. 2, pp. 48–56, 2017.
- [20] C. Modongo, J. G. Pasipanodya, B. T. Magazi et al., "Artificial intelligence and amikacin exposures predictive of outcomes in multidrug-resistant tuberculosis patients," *Antimicrobial Agents and Chemotherapy*, vol. 60, no. 10, pp. 5928–5932, 2016.

## *Retraction*

# **Retracted: A Novel Strategy for Waste Prediction Using Machine Learning Algorithm with IoT Based Intelligent Waste Management System**

### **Wireless Communications and Mobile Computing**

Received 12 December 2023; Accepted 12 December 2023; Published 13 December 2023

Copyright © 2023 Wireless Communications and Mobile Computing. This is an open access article distributed under the Creative Commons Attribution License, which permits unrestricted use, distribution, and reproduction in any medium, provided the original work is properly cited.

This article has been retracted by Hindawi, as publisher, following an investigation undertaken by the publisher [1]. This investigation has uncovered evidence of systematic manipulation of the publication and peer-review process. We cannot, therefore, vouch for the reliability or integrity of this article.

Please note that this notice is intended solely to alert readers that the peer-review process of this article has been compromised.

Wiley and Hindawi regret that the usual quality checks did not identify these issues before publication and have since put additional measures in place to safeguard research integrity.

We wish to credit our Research Integrity and Research Publishing teams and anonymous and named external researchers and research integrity experts for contributing to this investigation.

The corresponding author, as the representative of all authors, has been given the opportunity to register their agreement or disagreement to this retraction. We have kept a record of any response received.

### **References**

- [1] G. Uganya, D. Rajalakshmi, Y. Teekaraman, R. Kuppasamy, and A. Radhakrishnan, "A Novel Strategy for Waste Prediction Using Machine Learning Algorithm with IoT Based Intelligent Waste Management System," *Wireless Communications and Mobile Computing*, vol. 2022, Article ID 2063372, 15 pages, 2022.

## Research Article

# A Novel Strategy for Waste Prediction Using Machine Learning Algorithm with IoT Based Intelligent Waste Management System

G. Uganya,<sup>1</sup> D. Rajalakshmi,<sup>2,3</sup> Yuvaraja Teekaraman <sup>4</sup>, Ramya Kuppusamy <sup>5</sup>,  
and Arun Radhakrishnan <sup>6</sup>

<sup>1</sup>Department of Electronics and Communication, Saveetha School of Engineering, SIMATS, Chennai 602 105, India

<sup>2</sup>Department of Computer Science and Engineering, Sri Sairam Institute of Technology, Chennai 600044, India

<sup>3</sup>CSE, Vel Tech Rangarajan Dr.Sagunthala R&D Institute of Science and Technology, Chennai, India

<sup>4</sup>Department of Electronic and Electrical Engineering, The University of Sheffield, Sheffield S1 3JD, UK

<sup>5</sup>Department of Electrical and Electronics Engineering, Sri Sairam College of Engineering, Bangalore 562 106, India

<sup>6</sup>Faculty of Electrical & Computer Engineering, Jimma Institute of Technology, Jimma University, Jimma, Ethiopia

Correspondence should be addressed to Yuvaraja Teekaraman; [yuvarajastr@ieee.org](mailto:yuvarajastr@ieee.org) and Arun Radhakrishnan; [arun.radhakrishnan@ju.edu.et](mailto:arun.radhakrishnan@ju.edu.et)

Received 13 October 2021; Revised 21 January 2022; Accepted 26 January 2022; Published 10 February 2022

Academic Editor: Ali Kashif Bashir

Copyright © 2022 G. Uganya et al. This is an open access article distributed under the Creative Commons Attribution License, which permits unrestricted use, distribution, and reproduction in any medium, provided the original work is properly cited.

Internet of Things (IoT) has now become an embryonic technology to elevate the whole sphere into smart cities. Hasty enlargement of smart cities and industries leads to the proliferation of waste generation. Waste can be pigeon-holed as materials-based waste, hazard potential based waste, and origin-based waste. These waste categories must be coped thoroughly to make certain of the ecological finest run-throughs irrespective of the origin or hazard potential or content. Waste management should be incorporated into ecological preparation since it is a grave piece of natural cleanliness. The most important goalmouth of waste management is to maintain the pecuniary growth and snootier excellence of life by plummeting and exterminating adversative repercussions of waste materials on environment and human health. Disposing of unused things is a significant issue, and this ought to be done in the best manner by deflecting waste development and keeping hold of cost, and it involves countless human resources to deal with the waste. These current techniques predominantly focus on cost-effective monitoring of waste management, and results are not imprecise, so that it could not be developed in real time or practically applications such as in educational organizations, hospitals, and smart cities. Internet of things-based waste management system provides a real-time monitoring system for collecting the garbage waste, and it does not control the dispersion of overspill and blowout gases with poor odor. Consequently, it leads to the emission of radiation and toxic gases and affects the environment and social well-being and induces global warming. Motivated by these points, in this research work, we proposed an automatic method to achieve an effective and intelligent waste management system using Internet of things by predicting the possibility of waste things. The wastage capacity, gas level, and metal level can be monitored continuously using IoT based dustbins, which can be placed everywhere in city. Then, our proposed method can be tested by machine learning classification techniques such as linear regression, logistic regression, support vector machine, decision tree, and random forest algorithm. The proposed method is investigated with machine learning classification techniques in terms of accuracy and time analysis. Random forest algorithm gives the accuracy of 92.15% and time consumption of 0.2 milli seconds. From this analysis, our proposed method with random forest algorithm is significantly better compared to other classification techniques.

## 1. Introduction

IoT is the latest developing technology for connecting various things, which will communicate with each other by using sensors and embedded and wireless technologies. The

wireless technologies may be mobile or wireless fidelity networks. This technology makes our live and habits easy and automatic. Some examples of IoT devices are automatically driving cars and smart wearable devices and machines. It does not need social interaction and computer

to human communication. The usage of IoT devices in industries and cities is speedily increasing due to its special features like rapid decision-making skills and efficient service. It has special key characteristics including connectivity, intelligence, enormous scaling, sensing, dynamic nature, and heterogeneity structure [1]. It can be used in enormous number of applications. These are smart household, wearables, grid, connected healthcare, traffic management, smart farming, connected vehicles, industrial Internet, and smart city.

The IoT structure can be developed in three layers. These are device, access, and platform layer. These layers are accessed by the steps of sensing, acquisition, edge information technology, and cloud storage. It can be shown in Figure 1. In the first stage, the information will be continuously collected from the environment. This unreadable information is converted to useable knowledge by using acquisition in second stage [2]. Then, this useable knowledge is transferred to information technology world in third stage. In the last stage, the collected data are stored in cloud.

Nowadays, smart city applications are developing by using Internet of things. Because this technology used to make the cities more intelligent by integrating the various approaches of transference, it is used for effective urban area furniture management, and smart efficiency enhancement. IoT can be used in many application areas like traffic and vehicle parking management, street lighting, safety management, and waste management system to achieve an efficient and intelligent smart city.

The intelligent smart city should have the features like sufficient water resource, guarantee electrical supply, urban flexibility, reasonably priced housing, digitalization, worthy governance, education, health, and sanitation of wastages. Due to this rapid development of smart city, the waste things also increased. Discarding unusable wastages is a major challenge in IoT based smart cities. It is a regular duty to get clean city, but it needs large human resources and energy. Figure 2 shows the features of IoT to develop the smart city. These are scalability, activity, security, connectivity control, data analytics, and management of IoT devices. The scalability feature considers the number of buildings, organization, and devices being used. The activity-based feature reflects the heterogeneity of the various devices and its development schemes. The connectivity feature manages the latency and movement of things. The data analytics feature considers the size and data collection in city [3]. Then, these data are continuously monitored and collected by the management ability of IoT devices. The feature of security is divided into object and data level security. It considers the cryptanalyses techniques and advanced attacks and tools. Here, the calculations are performed, in view of heuristic models or diagram hypothesis, from which we can track down ways of limiting the distance of waste assortment. The basic role is to lessen the all cost of transport, move, save work, and diminish the reliance on utilized vehicles, while expanding administration quality, just as working on broad personal satisfaction.

IoT with machine learning algorithm provides effective result in waste management system to develop the smart

city. Mainly, the following machine learning algorithms are used in waste management system. These are linear regression, logistics regression, support vector machine, and decision tree. These algorithms are used in collection and prediction of waste in smart city. But still, it has many issues and challenges to collect and dispose waste in accurate manner. This work is to introduce the intelligent waste management system with machine learning algorithms to classify the waste prediction.

The major contribution of the paper is summarized as follows:

- (i) Review on the smart city IoT applications and its key factors.
- (ii) A detailed explanation of existing waste management solutions and its drawbacks.
- (iii) A classification of different machine learning algorithms in smart city waste management system and its countermeasures.
- (iv) We present intelligent based waste management system with machine learning algorithm to collect and predict the waste accurately.
- (v) The proposed method can be analyzed with different machine learning algorithm in terms of accuracy and time consumption.

The paper is organized as follows: Section 2 discusses the overview of smart city in IoT including key elements and application area of smart city. Section 3 summarizes the related works in waste management system. In section 4, materials and methods of proposed method with machine learning algorithms and its issues are discussed. Section 5 presents the proposed method results and performance analysis of classification algorithms. Finally, section 7 concludes the paper.

## 2. Overview of Smart City IoT Applications

*2.1. Definition of Smart City.* Smart city is developing community to enhance the sustainability, livability, and achievability by using the key factor of IoT technology. Washburn et al. proposed SC architecture that has the domains like city organization, medical services, real estate, social safety, learning, and traffic management [4]. Giffinger et al. proposed an intelligent based smart city that has been defined in terms of features including economical social, human being, authority, movement of things, environment, and lifestyle [5]. Similarly, Neuroti et al. discussed the smart city in the major domain of hardware and software. The hardware domain provides the resource management and safety to enhance the sustainability. The software domain considers the learning and authority process [6]. Liu et al. proposed smart cities into three major areas. These are rich lifestyle, which considers the education, living place, and medical services, social management, which includes safety on food, society, and traffic, and resource management, which includes the water service, electricity service, and farming [7]. Similarly, many authors discussed the definition of smart cities with descriptions. But still it has many issues

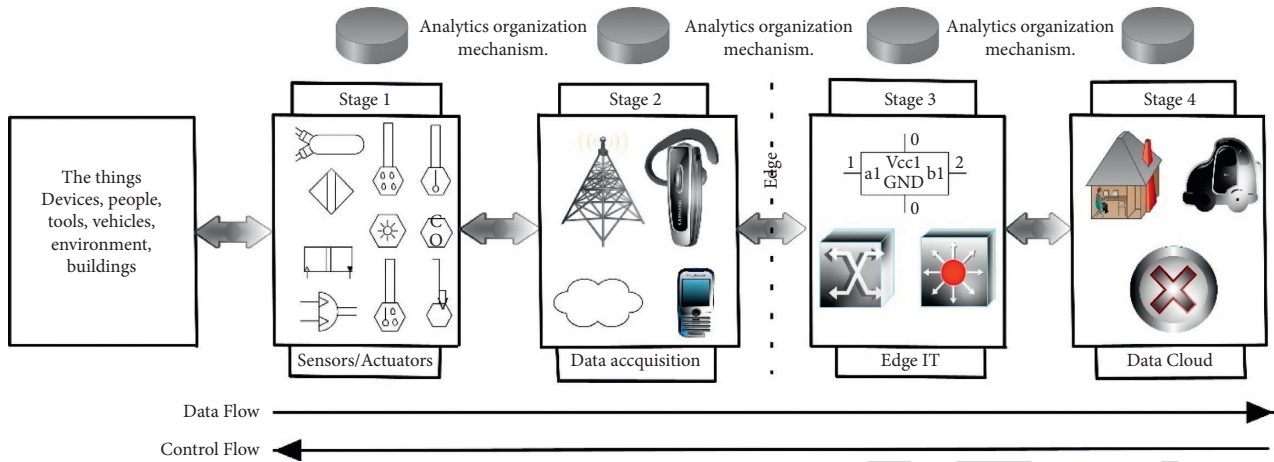


FIGURE 1: The four stages of IoT Architecture.

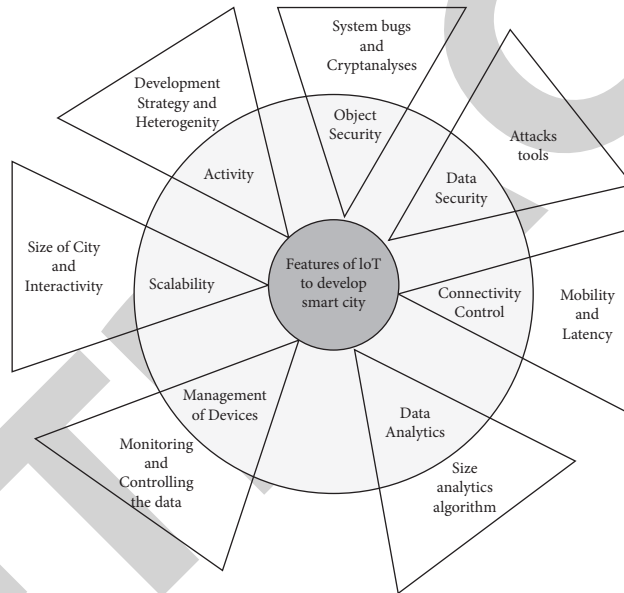


FIGURE 2: Features of IoT to develop the Smart City.

to develop the smartness and intelligent with security based smart city. However, the smart city is a developing technology in world. Figure 3 shows the Indian cities with most web searches for smart city, and Figure 4 shows the number of hits of smart city web searches between 2010 and 2020 from the source of Google trends explore. From this graph, we understand that the development of SC has been increased across the world like China, India, and UAE.

2.2. *Key Elements of Smart City.* Numerous authors discussed the key elements to enhance the smart city in IoT applications. Figure 5 shows the key elements of smart city. These key elements are security, medical services, smart learning, structure, mobility, environment, lifestyle, economical services, society, governance, and waste management. Table 1 shows the different key elements of smart city

analysis for various structures. Nam et al. discussed the SC, but it does not provide smart medical care, education, and waste management [8]. Similarly, Chourabi et al. discussed the smart city but did not consider the medical, education, security, and waste management system [9]. Dameri et al. discussed the SC with well-defined architecture and production of energy [10]. Neirotti et al. proposed the technique and mainly focused on smart social with human resources [6]. From this analysis, we understand that many frameworks are developed to obtain the smart city, but the researcher wants to concentrate more on waste management system.

2.3. *Application Scenarios for Smart Cities with IoT.* Smart city with IoT scenarios uses numerous areas to achieve a healthy atmosphere, to enhance the safety and traffic, to

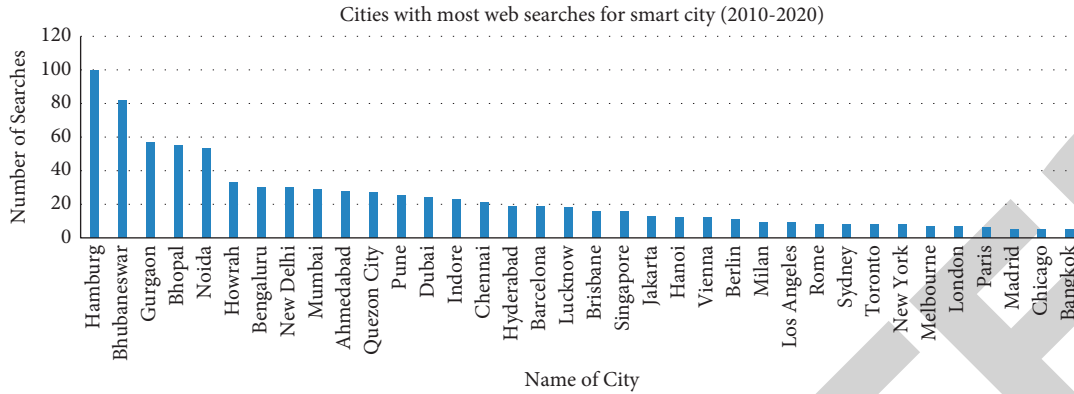


FIGURE 3: Cities with most Web Searches for Smart City from 2010 to 2020.

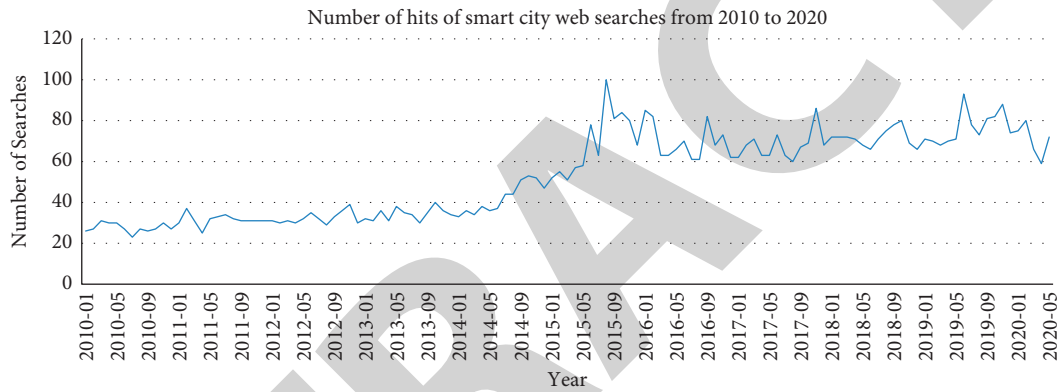


FIGURE 4: Number of hits of Smart City Web searches from 2010 to 2020.

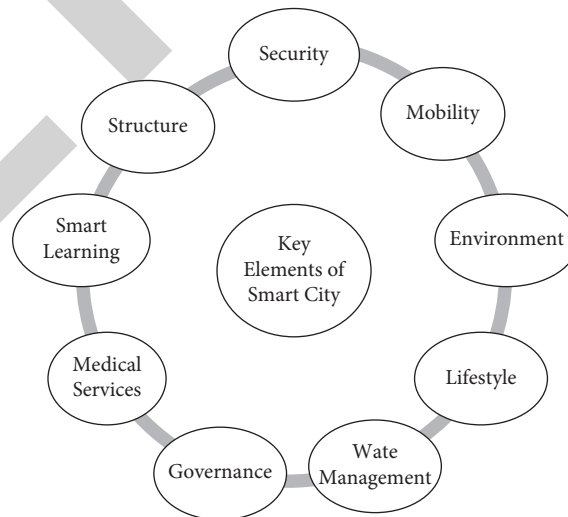


FIGURE 5: Key elements of Smart City.

improve the street lighting, and to manage the waste. Some applications of smart cities with IoT are traffic management, smart parking, transportation, home utilities, street lighting, environment safety, and waste management.

2.3.1. *Traffic Management.* It can be widely used in intelligent traffic management by the way of controlling the vehicles and extrapolation systems. It is used to enhance the security by collecting and investigating the actual data from



social. Nellore and Hancke proposed a technique to investigate the blockage in street traffic by controlling the lights in traffic signals [14]. Traffic jam is the main issue in traffic management system. It can be discussed by Knorr et al. There are many technologies developed to improve the traffic management [15]. These are analyzing the information from videos, usage of IR sensor, and remote sensor system. But these techniques have the limitations of time and cost. So, RFID based traffic organization techniques are developed by Miz et al. This technique is mainly recommended for traffic blockages with less time and less expenses [16]. Arbabi and Weigle proposed Dynamic Traffic Monitoring System (DTMon), which continuously gathers time and speed information [17]. Similarly, Mazloumi et al. proposed automobile tracing system based on global positioning system to minimize the distance limitations [18]. Chao et al. discussed the intelligent traffic management system based on RFID, which is used to control the minimize the accidents and regulate the traffic flow [19].

**2.3.2. Smart Parking.** IoT based smart parking management system is used to minimize the parking space and enhance the efficiency. Mainly, IoT based parking applications are used many sensors, which have the features including detection of speed, multilane, invasive, count, and climate sensitive. Table 2 shows comparison of various sensors used in smart parking system.

It can be categorized as booking system, direction system, crowdsourcing system, and agent-based system. Booking system is used to provide the spacing for vehicles automatically. But some methods are used to reserve the slots and not for place. Drivers can choose the place by using IoT techniques that are costlier and difficulty. And the verification of position is difficult in parking system. Pham et al. addressed this issue in parking management system [20]. Similarly, Zhang et al. proposed the technique of reservation payment system based on fog computing. In this technique, the driver can book the parking place by paying money [21].

In direction systems, the parking slots and positions can be chosen with the help of guide, whose purpose is to reduce the time for searching for free places. Geng et al. proposed smart parking with efficient resource allocation. It can be developed mainly for street or city parking in smart way [22]. It has the benefits of exact data with correct time and more decision-making choices. Crowdsourcing is mainly combined with cell phones to get exact real time data from parking place. Chen and Liu. proposed smart parking system with continuous monitoring system by using mobile. In this technique, smart parkers are used to send the information to the user in the way of answering the questions [23]. In agent-based system, software modules are used as agent. But these methods are costly and have scalability issues.

**2.3.3. Street Lighting.** Normally, we use the physical system to operate the street lights. But it needs more energy and human source. Street lighting is a major area to obtain smart city. It limits the usage of man power and wastage of

electricity. And it has been mainly developed to detect the crimes, reduce the preservation cost, and enhance the safety. Dheena et al. proposed smart street light system to save the power and minimize the human manual work [24]. But this system has high maintenance cost. Arkade et al. proposed the same energy in domestic and industrial applications. But it consumes more energy to develop this technique [25]. Parkash and Rajendra proposed the intelligent based smart lighting system, but it takes more initial cost [26]. Patil et al. discussed smart lighting system by using pollution detecting sensors to enhance the efficiency and to minimize the cost. But it will be work in independent way [27]. Similarly, Kokilavani et al. discussed the IoT based smart lighting system by using the LDR sensor, which has covered a small distance [28].

**2.3.4. Waste Management System.** The wastage can be generated by various environment as different characteristics. Based on this characteristic it can be collected and recycled to convert into useable things. IoT based waste management system concentrates on classification techniques and development of special containers. Table 3 shows the different types of waste and its definition.

Waste management system is the recent growing technology to develop IoT based smart cities. But still, it has many issues in collecting and disposing waste. Because it is daily routine process and needs more human source to complete the process. Many researches are already proposed for waste management system. Its related works can be discussed in next section.

### 3. Related Works

IoT with machine learning-based waste management system mainly focuses on dispersion of waste and enhances the environment to healthier. The collection and decomposition of waste things in intelligent way are the major issue in smart city application. Because rapid development of smart city and population increases the wastages in every day, in a traditional way, the decomposition of waste requires more human resources and more time. And it spoils the environment, social life, and atmosphere. Abdullah et al. and Talari et al. discussed the review of waste management system based on Internet of things [37, 38]. Monika et al. proposed the smart dustbin system to collect the waste with Arduino UNO board with GSM module. But it has limitations like difficult to maintenance, and more time to collect [39]. Similarly, Kumar et al. proposed dustbin by using ultrasonic sensor to continuously monitor the garbage level. And it ensures immediate disposal of waste after reaching the certain level of waste in dustbin [40]. In India, Shyam et al. proposed the intelligent based dustbin in Pune by using IoT prototype [41]. It analyzes the IoT-based waste administration, for example, the closest neighbor search, province advancement, hereditary calculation, and molecule swarm enhancement strategies.

Pardini et al. proposed the solid waste management system to collect the waste information from other



TABLE 2: Comparison of various sensors used in smart parking system.

Sensor Types	Detection of Speed	Detection of Multilane	Invasive	Count	Climate Sensitive
Acoustic	×	×	—	×	×
LDR	—	—	—	×	×
RFID	—	—	—	—	—
CCTV	×	×	—	×	×
Microwave	×	×	—	×	—
WIM	—	×	×	—	—
Pneumatic tube	×	—	×	×	—
Piezoelectric	×	—	×	×	×
Magnetometer	×	—	×	×	—
Inductive loop	×	—	×	×	×
Ultrasonic	—	—	—	×	×
Active IR	×	×	×	×	—
Passive IR	—	—	—	×	×

TABLE 3: Different types of waste and its definition.

Type of waste	Reference	Definition
Organic	[29]	It can be produced by restaurants, and areas related to work with food. And it is separated from other waste and used in landfills
Decomposable	[30]	It can be generated by companies or industries. This type of waste can be transformed to other forms through recycling process
Industrial	[31]	It can be produced by industries in the form of solid. This waste reused by the same industries
Medical	[32]	It can be produced by hospitals or clinics. But it is dangerous compared to other waste. Because it transfers the disease
Commercial	[33]	It can be generated by textiles, toy companies. These wastes are recycled easily
Green	[34]	These wastes are produced by trees which fall in street. But it can be used for organic purpose
Electronics	[35]	This type of waste produced by electronic companies. It can be transferred to recycling process without any cautions
Nuclear	[36]	It is radioactive elements produced by nuclear plants. As well as it is very dangerous to be treated carefully

companies. This existing work only focused on collection of data [42]. Similarly, Bueno-Delgado et al. proposed waste collection system using optimization in smart cities. It is mainly used to improve the rural areas. But it does not provide clarity results [43]. Lozano et al. discussed the linear regression and genetic algorithm-based waste management system to collect the waste and check the status of bins. But it has limitation to change the waste from bins to other devices. So, it is difficult to achieve waste transformation system [44]. Hannan et al. proposed garbage waste management system by using line following robot to collect the waste, but it is not developed for optimization of waste [45].

Popa et al. discussed the method to collect the food waste by using RFID technology and transferred through wireless networks. But this method is not suitable for huge distance area to obtain smart city. And practically, it cannot be applied for real time applications [46]. Cerchecci et al. discussed the sensor-based waste management system. But this work can be tested only in board but not in real time applications for waste management system [47].

Existing methods mainly focused on to predict the solid and nonhazardous waste. But these techniques do not concentrate on hazardous waste control that overspill and blowout gases with poor odor. And it leads to the emission of radiation and toxic gases and affects the environment. The main aim of this work is to introduce the intelligent waste management system in Internet of things to predict the

hazardous waste that produces toxic gases. Then, our proposed method can be tested by different machine learning classification algorithms for better waste prediction.

## 4. Materials and Methods

*4.1. Intelligent Waste Management System.* This section introduces the intelligent waste management system that contains combinations of Internet of things and machine learning. Internet of things can be used for real time monitoring and collecting the waste. The waste can be collected by placing sensor-based dustbins in different places. Arduino and microcontroller-based dustbins can collect the waste within small area, and it cannot be classified based on its characteristics. So, IoT based waste management system can be selected for continuously collecting and monitoring the waste. But existing systems did not give concentration on hazardous waste that produces poor odor and poisonous gas. So, intelligent based waste management system can be proposed to monitor the hazardous waste and nonhazardous waste. Sensor based dustbins can be placed in different places that contain sensors like ultrasonic sensor, MQ4 sensor, HX711 sensor, and metal oxide sensor. The collected information from sensors and actuators can be stored in cloud, which is used to process the data and stored as database. Machine Learning can be utilized to simply decide and research the enormous measure of data from

sensor IoT gadgets. It is a fundamental device to choose activities relying upon the information assortment.

Sensor based dustbins can be designed by raspberry pi and Wi-Fi module with sensors. Nonhazardous waste like metal and wood can be monitored by ultrasonic sensors from lower part of the dustbins. When the dustbin filled above 60%, the alert message can be sent to central waste management cloud center. MQ4 sensor can be used to monitor the methane asphyxiates gas that are produced in rainy seasons and cause the displacement of oxygen level in blood. It can be used to detect the methane gas in the range of 300 ppm to 10000 ppm. HX711 sensor is used as weight sensor that monitors the load in dustbins; once it reached above 60%, it sends an alert message to the central server. QS-01 can be used as an odor sensor to detect toxic gases, and metal oxide sensor can be used to sense the various gases with changes of metal oxide by absorbing the gases. Based on this sensor information, the waste can be classified in CSV file. Figure 6 represents the intelligent waste management system with sensor-based dustbin.

The database can be created by classification and prediction of waste in the file of comma separated file. The CSV file is used to collect and store large amount of information and transfer this information from machine to machine. Python based application can be used for classification and prediction of waste using machine learning algorithms. In our proposed method, the waste can be classified as organic, hazardous, and nonhazardous waste, and it can be predicted by machine learning algorithms. Finally, it analyzes the linear regression, logistic regression, support vector machine, decision tree, and random forest algorithm in terms of accuracy and time consumption.

**4.2. Machine Learning Algorithms.** IoT with machine learning algorithm can be used in waste management system to develop the smart city in effective manner. The waste can be classified depending on its characteristics by using ML classifier algorithm. ML algorithm can be classified into three major types. These are supervised learning, unsupervised learning, and reinforcement algorithm, which are shown in Figure 7.

Mainly, supervised learning algorithm is used for waste collection and management to develop the efficient smart city. Because it provides better output and to solve classification and regression challenge. So, this work mainly focuses on supervised learning-based waste management system. Applications of Machine learning algorithms send the monitored data through an android application, and these kinds of android application are well suited for deep learning approach, and they collect the real time data with the help of Bluetooth technologies.

The supervised learning is divided into linear regression, logistics regression, decision tree, support vector machine, and random forest algorithm.

**4.2.1. Linear Regression.** It is the numerical model that investigates the dependent variable with given independent variable. The data will be continuously predicted and

increased to get constant slope. This algorithm mainly concentrates on prediction of data and not the classification of data. If the dependent and given variables are positive, it can be called as positive relationship [48]. Otherwise, it can be called as negative relationship. The simple linear regression can be written as

$$A = nB + C, \quad (1)$$

where  $A$ -Predicted output,  $B$ & $C$ -Variables, and  $n$ -Given Input data.

Similarly, multivariable regression equation can be written as

$$F(a, b, c) = X_1a + X_2b + X_3c + e, \quad (2)$$

where  $X_1, X_2, X_3$  represent the weights or coefficients of the model,  $a, b, c$  represent the characteristics of the model, and  $e$  represents the error present in the data. The data can be predicted by using the considerations including multiple collinearities, auto connection, and variable relationship. In linear regression algorithm, there is no multiple collinearity and auto connection in data and its information. And the data response and its characteristics must have feature of linear.

**4.2.2. Logistics Regression.** Logistic regression is mainly focused on classification and prediction of data depending on its characteristics. Here, the dependent variable is denoted as binary forms. It can be classified into binomial, multinomial, and ordinal. Figure 8 shows the types of logistics regression. In binomial regression, the two types of dependent variables are possible, for example, pass and fail, win and loss, etc. In multinomial regression, the dependent variable must have the three or more possible values in unordered manner [49].

In ordinal regression, the dependent variable must have three or more possible values in ordered manner. The following assumptions are considered in logistics regression. These are binomial regressions representing the target values in terms of binary values. It does not have multiple collinearity, which means that the variables are independent of each other. These variables must have proper meaning. It can be used in huge model. Here, the input is linear function, and it can be related with another function  $G$ . The relationship can be written as

$$H\theta(y) = G(\theta^t y), \quad (3)$$

where  $H_\theta(y)$  can be denoted as binomial logistics regression, and it has the values between 0 and 1. Then, the performance of the algorithm can be found by loss function. It can be written by

$$H = G(y\theta). \quad (4)$$

**4.2.3. Support Vector Machine.** Support vector machines can be used in both regression and classification of data. But mainly, it can be used in data classification issues. This

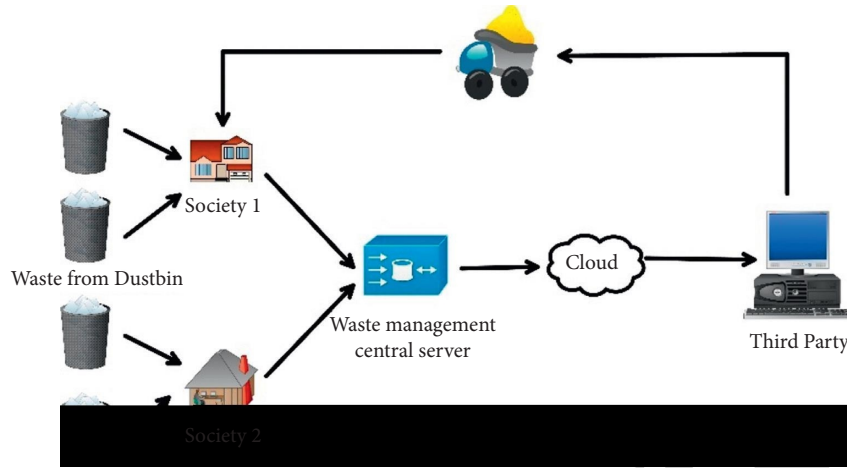


FIGURE 6: Intelligent waste management system.

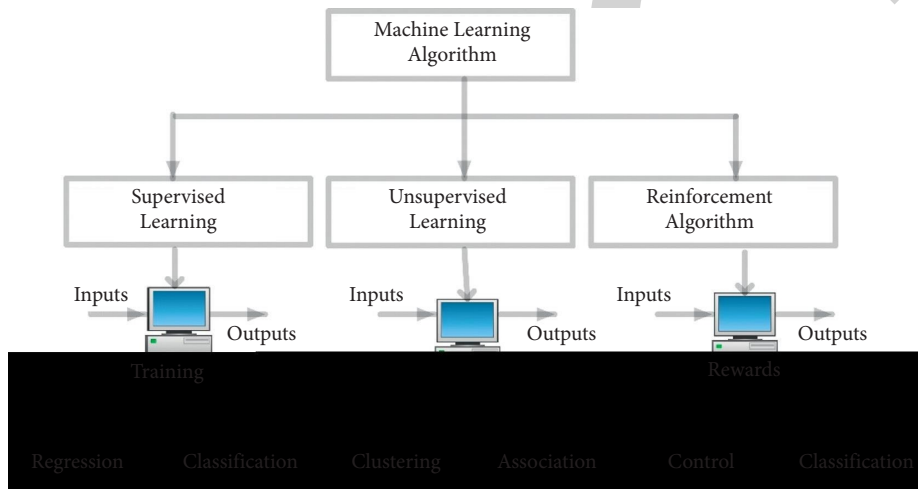


FIGURE 7: Types of machine learning algorithm.

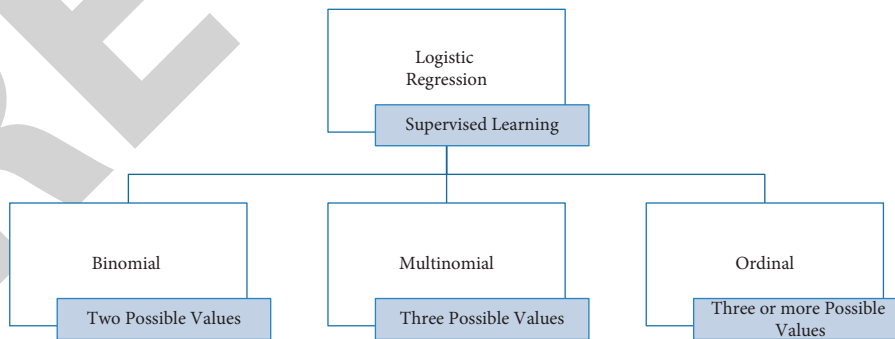


FIGURE 8: Types of logistics regression.

algorithm is very famous due to its capability to handle the multiple and continuous variables. The main of the SVM is to classify the data based on characteristics and to enhance the marginal hyperplane. It uses the models of hyperplane, margins, and support vectors. Hyperplane is a method of space that can be divided between objects and different

classes. Some data points are nearer to hyperplane, which are called as support vectors [50]. Margins are denoted by gap of two lines that is nearer to data points. And it can be measured by perpendicular distance to the support vector. The good margin has the large size, and the bad margin has small size.

Practically, it can be implemented with kernel, which is used to transfer the input space to essential form. This kernel makes the SVM more accurate and flexible by converting the nonseparable higher space into lower and separable data space. It can be classified into linear, polynomial, and RBF kernel that is shown in Figure 9.

Linear kernel is obtained by product of any two observations, and it can be written as two vectors by using the following equation:

$$K(x, y) = \text{sum}(x * y). \quad (5)$$

Polynomial kernel is distinguishing curve input space, and it can be written as

$$K(x, y) = 1 + \text{sum}(x * y)^{d_e}, \quad (6)$$

where  $d_e$  is polynomial degree, which is used to identify the learning algorithm.

Radial basis function can be used to map the input space the unspecified space, and it can be used by following equation:

$$K(x, y) = \exp(-\text{gamma} * \text{sum}((x - y)^2)), \quad (7)$$

where the gamma ranges from 0 to 1, and it can be separable data as linear.

**4.2.4. Decision Tree.** Decision tree is an algorithm to predict the values and to classify the data based on its features. So, it can be used for both regression and classification. It has the two main entities including data split and data leave. It can be classified into regression and classification decision tree. In classification decision tree, the decision variable is definite. In regression decision tree, the decision variable is continuous. A tree consists of root node and terminal node. First, the root node was created; then, the remaining nodes were formed by the following steps including creation of terminal node and recursive splitting [51]. The creation of terminal node is done by concentrated depth of tree and slightest records of the node. The prediction of data using decision tree is considering the following assumptions. The training data can be considered as root node. Then, the data feature values will be definite and recursively dispersed.

Many existing methods are based on machine learning algorithm including linear, logistic, decision tree, and support vector machine algorithm. But still, it has many issues in collecting of data. Existing methods are not effectively collecting the data in accurate manner [52]. Still, it needs efficient method to collect the waste in waste management system to develop smart city. The related works of waste management system are discussed in the next section.

**4.2.5. Random Forest Algorithm.** This work is to introduce the novel method of random forest algorithm to collect and predict the waste information depending on its features. It is a combination of huge number of decision tree and created from training dataset. It can be developed by using the constructions including the construction of discrete tree, generation of altered data set, and prediction of discrete tree.

Figure 10 shows the flowchart of random forest algorithm. It is used to create the forest by different way randomly. It gives the more accurate result compared with other classification algorithm by the relationship of number of trees and its results because randomly it finds the root node and split the feature of data. It has the following benefits compared to other algorithms. These are suitable for both classification and regression, fitting with model, handling the missed values, and definite data modelling.

In random forest algorithm, the certain features can be selected from total features. From those features, the root node can be calculating by using of split point. Similarly, the calculated node is divided into daughter nodes. The process was repeated until the specific tree number is obtained. Then, repeat the process until obtaining the  $n$  number of trees. In this way, the random forest classifier algorithm is developed. In data prediction, the test features can be processed to predict the target. Then, the votes are calculated by using predicted result. It creates the multiple trees and combines them together to enhance accuracy and to obtain an established prediction. In this algorithm, hyperparameters are used to enhance the speed and predictive power. These hyperparameters are  $n$ -number of estimators, maximized features, minimized leaf,  $n$ -number of jobs, random states, and sampling. First, three parameters are used to increase the predictive power. The last three parameters are used to increase the speed. This work is mainly focused on collecting and predicting of waste data based on its characteristics. This work is to enhance the security with less time compared with other algorithms.

## 5. Results and Discussions

The intelligent based waste management system provides accurate waste collection and prediction compared with another classifier algorithm. Figure 11 shows the waste collection and prediction using intelligent waste management system. It collects the data for each month and compares with other classifier algorithm. It collects the waste based on its characteristics like rubbish, organics, and recycling waste. The increasing strength of tree leads to reducing of forest error. This method is more efficient and robust due to its less error. In random forest algorithm, two parameters are considered as important. These are number of trees and random variables in forest. Based on these parameters, the classification and regression of waste data are developed. So, it does not have the problem of over fitting.

Figure 12 shows the proposed method regression and its heat map. The proposed work with random forest relies on good accuracy compared with other classifier algorithm including linear regression, logistics regression, support vector machine, and decision tree algorithm. In the next subsection, the performance analysis of various classifier algorithm was discussed.

**5.1. Performance Analysis.** Table 4 shows the performance analysis of various machine learning classifier algorithm. The performance of each and every algorithm is verified in terms

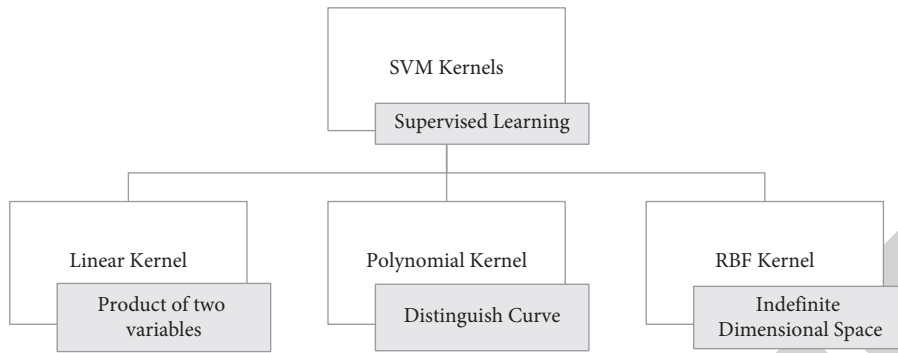


FIGURE 9: Types of SVM kernels.

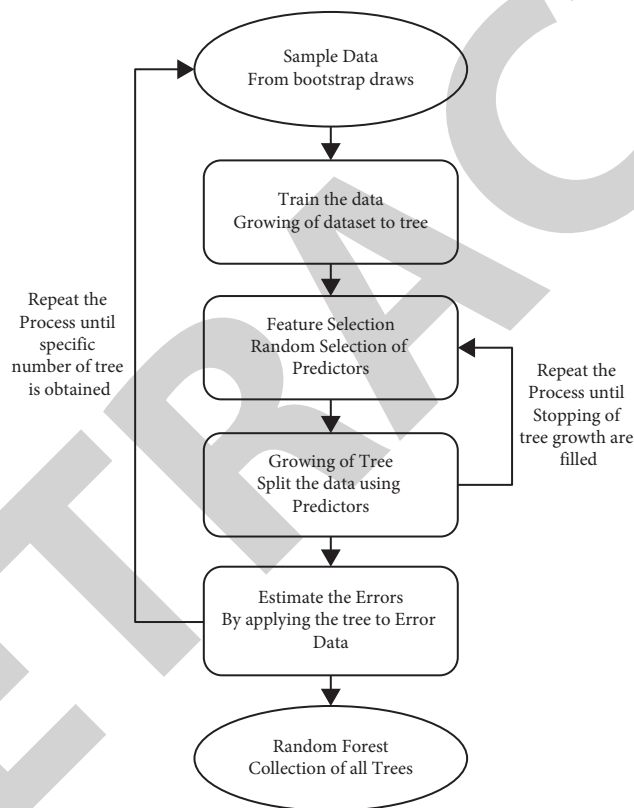


FIGURE 10: Flowchart of random forest algorithm.

of accuracy and time consumption to collect and predict the waste. In this work, accuracy can be measured by calculating predicted value and total predictions. It is the representation of correct prediction in testing the data, which can be denoted in percentage. It can be written as

$$\text{Accuracy} = \frac{\text{correct predictions}}{\text{All predictions}} \quad (8)$$

The average accuracy is obtained by calculating the waste collection from every month. In this work, time represents the period for testing and classification of data. Figure 12 represents the performance analysis various machine learning algorithm based on accuracy and time analysis.

From Figure 13 we understand that the random forest algorithm (RFA) provides good accuracy of 92.15% compared with another classifier algorithm. Similarly, decision tree provides the accuracy of 89.43%, and it is near the random forest algorithm, because the RFA escapes from overfitting. From that work, it is clear that our proposed work with RFA algorithm gives better accuracy with less time consumption compared with other algorithm. It has accuracy of 92.15% and time consumption of 0.2 milliseconds.

From above analysis, random forest algorithm has significantly higher accuracy, taking less time for classification of waste. The reason is that random forest algorithm is avoiding the overfitting data. It performs well by applying random split of waste in the form of possible best waste

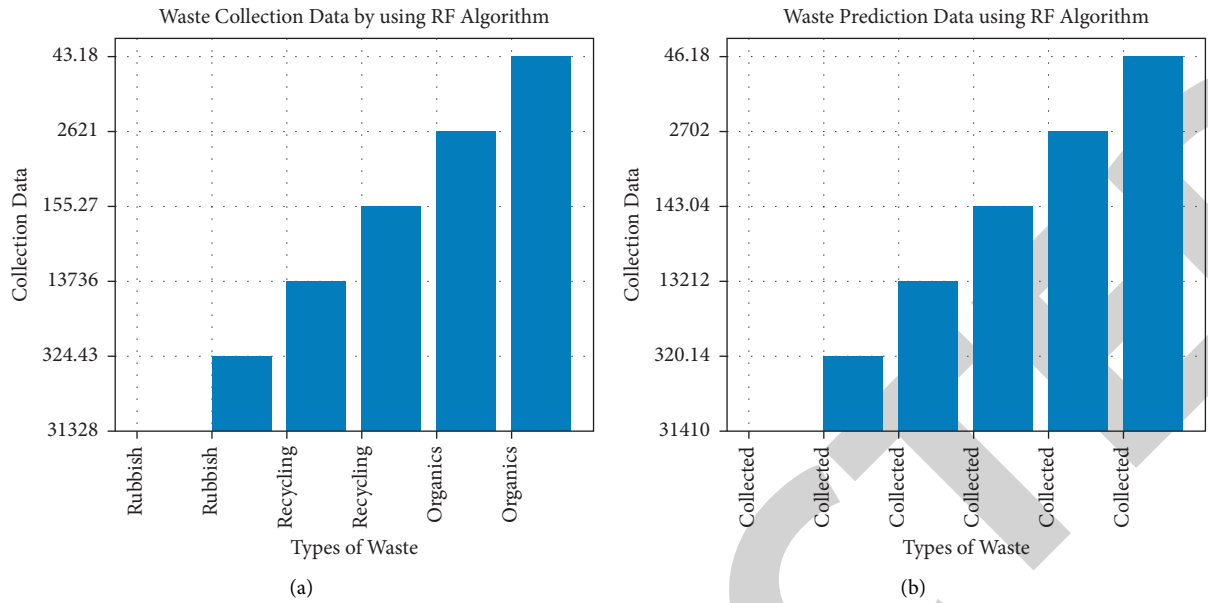


FIGURE 11: Proposed method. (a) Waste Collection. (b) Waste Prediction.

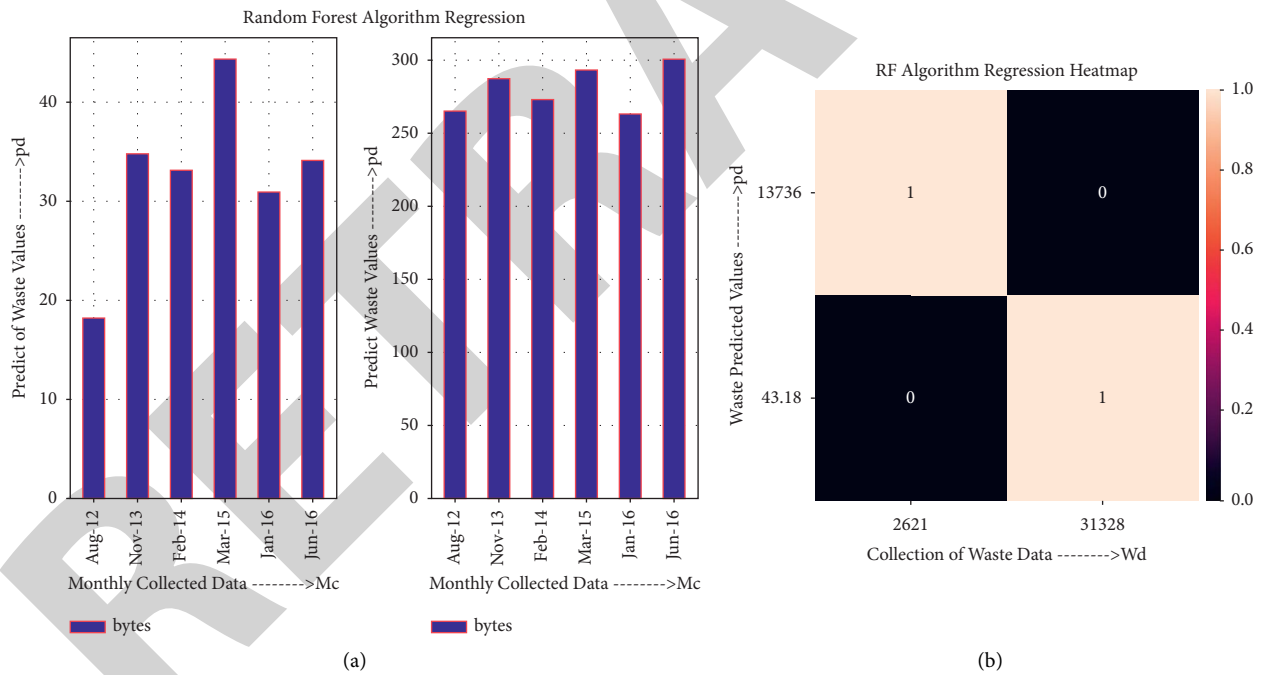


FIGURE 12: Proposed method. (a) Regression. (b) Regression Heat map.

TABLE 4: Performance analysis of machine learning algorithm.

Algorithm	Accuracy (%)	Time (ms)
Linear regression	73.12	2.5 ms
Logistics regression	78.38	1.4 ms
Support vector machine	85.27	0.7 ms
Decision tree	89.43	0.4 ms
Proposed work with RFA	92.15	0.2 ms

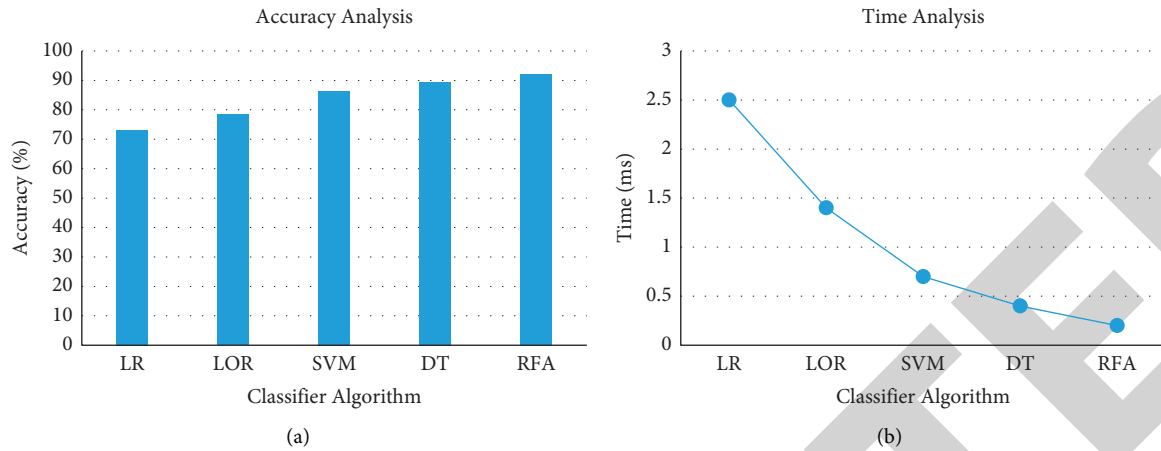


FIGURE 13: Performance analysis of machine learning algorithm: (a) accuracy analysis; (b) time analysis.

classification. And it has been done by random selection of subset of features for growing each tree.

## 6. Conclusion

IoT with machine learning is an emergent technology to upgrade the entire world into smart cities. Due to these rapid developments of smart cities and industries, the generation of waste is also increasing. Discarding unused things is a major issue in IoT. It is a regular and traditional duty in cities, but it requires a huge number of human resources to manage the waste. And it spoils nature, social characteristics, and efficient growth. In related works, many methods will be discussed about the waste management system for the disposal of unusable things. These existing methods mainly focused on giving the cost-effective monitoring of wastage. It provides a real-time monitoring system for collecting the garbage waste, but it does not control the dispersion of overspill and blowout gases with poor odor. So, in this work, we propose an intelligent waste management system by predicting the possibility of waste things in Internet of things. This work can be proposed to monitor hazardous and nonhazardous waste by sensor-based dustbins. Then, this work can be tested by classification algorithms like linear regression, logistic regression, support vector machine, decision tree, and random forest algorithm with normal parameters. From this analysis, random forest algorithm has an accuracy of 92.15% with less time of 0.2 milliseconds. When compared to existing approaches, our proposed method is working well with RF algorithm to effectively collect and predict the waste. In future, it can be extended to classify the waste based on its image and analyze it with various machine learning algorithms.

## Data Availability

The data used to support the findings of this study are available from the corresponding author upon request.

## Conflicts of Interest

The authors declare that they have no conflicts of interest.

## References

- [1] G. Uganya, Radhika, and N. Vijayaraj, "A survey on internet of things: applications, recent issues, attacks, and security mechanisms," *Journal of Circuits, Systems, and Computers*, vol. 30, no. 5, Article ID 2130006, 2021.
- [2] K. Yelamarthi, M. S. Aman, and A. Abdelgawad, "An application-driven modular IoT architecture," *Wireless Communications and Mobile Computing*, vol. 2017, Article ID 1350929, 16 pages, 2017.
- [3] T. Anh Khoa, C. H. Phuc, P. D. Lam et al., "Waste management system using IoT-based machine learning in university," *Wireless Communications and Mobile Computing*, vol. 2020, Article ID 6138637, 13 pages, 2020.
- [4] D. Washburn, U. Sindhu, S. Balaouras, R. A. Dines, N. Hayes, and L. E. Nelson, "Helping CIOs understand "smart city" initiatives," *Growth*, vol. 17, no. 2, pp. 1–17, 2009.
- [5] R. Giffinger and H. Gudrun, "Smart cities ranking: an effective instrument for the positioning of the cities?" *ACE - Architecture, City and Environment*, vol. 4, no. 12, pp. 7–26, 2010.
- [6] P. Neirotti, A. De Marco, A. C. Cagliano, G. Mangano, and F. Scorrano, "Current trends in Smart City initiatives: some stylised facts," *Cities*, vol. 38, pp. 25–36, 2014.
- [7] P. Liu and Z. Peng, "China's smart city pilots: a progress report," *Computer*, vol. 47, no. 10, pp. 72–81, 2013.
- [8] T. Nam and T. A. Pardo, "June. Conceptualizing smart city with dimensions of technology, people, and institutions," in *Proceedings of the 12th Annual International Digital Government Research Conference: Digital Government Innovation in Challenging Times*, pp. 282–291, College Park, MA, USA, June 2011.
- [9] H. Chourabi, T. Nam, S. Walker et al., "January. Understanding smart cities: an integrative framework," in *Proceedings of the 2012 45th Hawaii International Conference on System Sciences*, pp. 2289–2297, IEEE, Maui, HA, USA, January 2012.

- [10] R. P. Dameri, "Searching for smart city definition: a comprehensive proposal," *International Journal of Computers & Technology*, vol. 11, no. 5, pp. 2544–2551, 2013.
- [11] C. Balakrishna, "September. Enabling technologies for smart city services and applications," in *Proceedings of the 2012 Sixth International Conference on Next Generation Mobile Applications, Services and Technologies*, pp. 223–227, IEEE, Washington, DC, USA, September 2012.
- [12] F. Mosannenzadeh and D. Vettorato, "Defining smart city. A conceptual framework based on keyword analysis," *TeMA-Journal of Land Use, Mobility and Environment*, 2014.
- [13] R. Petrolo, V. Loscri, and N. Mitton, "Towards a smart city based on cloud of things, a survey on the smart city vision and paradigms," *Transactions on Emerging Telecommunications Technologies*, vol. 28, no. 1, p. e2931, 2017.
- [14] K. Nellore and G. Hancke, "A survey on urban traffic management system using wireless sensor networks," *Sensors*, vol. 16, no. 2, p. 157, 2016.
- [15] F. Knorr, D. Baselt, M. Schreckenberger, and M. Mauve, "Reducing traffic jams via VANETs," *IEEE Transactions on Vehicular Technology*, vol. 61, no. 8, pp. 3490–3498, 2012.
- [16] V. Miz and V. Hahanov, "Smart traffic light in terms of the cognitive road traffic management system (CTMS) based on the Internet of Things," in *Proceedings of the IEEE East-West Design & Test Symposium (EWDTS 2014)*, pp. 1–5, IEEE, Kiev, Ukraine, September 2014.
- [17] H. Arbabi and M. C. Weigle, "Using DTMon to monitor transient flow traffic," in *Proceedings of the 2010 IEEE Vehicular Networking Conference*, pp. 110–117, IEEE, Jersey City, NJ, USA, December 2010.
- [18] E. Mazloumi, G. Currie, and G. Rose, "Using GPS data to gain insight into public transport travel time variability," *Journal of Transportation Engineering*, vol. 136, no. 7, pp. 623–631, 2010.
- [19] K.-H. Chao and P.-Y. Chen, "An intelligent traffic flow control system based on radio frequency identification and wireless sensor networks," *International Journal of Distributed Sensor Networks*, vol. 10, no. 5, Article ID 694545, 2014.
- [20] T. N. Pham, M.-F. Tsai, D. B. Nguyen, C.-R. Dow, and D.-J. Deng, "A cloud-based smart-parking system based on Internet-of-Things technologies," *IEEE Access*, vol. 3, pp. 1581–1591, 2015.
- [21] Y. Zhang, C.-Y. Wang, and H.-Y. Wei, "Parking reservation auction for parked vehicle assistance in vehicular fog computing," *IEEE Transactions on Vehicular Technology*, vol. 68, no. 4, pp. 3126–3139, 2019.
- [22] Y. Geng and C. G. Cassandras, "New "smart parking" system based on resource allocation and reservations," *IEEE Transactions on Intelligent Transportation Systems*, vol. 14, no. 3, pp. 1129–1139, 2013.
- [23] X. Chen and N. Liu, "Smart parking by mobile crowdsensing," *International Journal of Smart Home*, vol. 10, no. 2, pp. 219–234, 2016.
- [24] P. F. Dheena, G. S. Raj, G. Dutt, and S. V. Jinny, "December. IOT based smart street light management system," in *Proceedings of the 2017 IEEE International Conference on Circuits and Systems (ICCS)*, pp. 368–371, IEEE, Thiruvananthapuram, India, December 2017.
- [25] S. Arkade, A. Mohite, S. Joshi, R. Sonawane, and V. Patil, "IoT based street lights for smart city," *International Journal for Research in Applied Science and Engineering Technology*, vol. 4, pp. 178–181, 2016.
- [26] P. V. Parkash and D. Rajendra, "Internet of things based intelligent street lighting system for smart city," *International journal of innovative research in science, engineering and technology*, vol. 5, no. 5, 2016.
- [27] S. Patil, G. Rudresh and K. Kallendrachari, "Design and implementation of automatic street light control using sensors and solar pane," *Int. Journal of Engineering Research and Applications*, vol. 5, no. 6, pp. 97–100, 2015.
- [28] M. Kokilavani and A. Malathi, "Smart street lighting system using IoT," *International Journal of Advanced Research in Science, Engineering and Technology*, vol. 3, no. 11, pp. 08–11, 2017.
- [29] K. Kawai and L. T. M. Huong, "Key parameters for behaviour related to source separation of household organic waste: a case study in Hanoi, Vietnam," *Waste Management & Research: The Journal for a Sustainable Circular Economy*, vol. 35, no. 3, pp. 246–252, 2017.
- [30] N. Seyring, M. Dollhofer, J. Weißenbacher, I. Bakas, and D. McKinnon, "Assessment of collection schemes for packaging and other recyclable waste in European Union-28 Member States and capital cities," *Waste Management & Research: The Journal for a Sustainable Circular Economy*, vol. 34, no. 9, pp. 947–956, 2016.
- [31] T. Zobel, "ISO 14001 adoption and industrial waste generation: the case of Swedish manufacturing firms," *Waste Management & Research: The Journal for a Sustainable Circular Economy*, vol. 33, no. 2, pp. 107–113, 2015.
- [32] M. Ali, W. Wang, N. Chaudhry, and Y. Geng, "Hospital waste management in developing countries: a mini review," *Waste Management & Research: The Journal for a Sustainable Circular Economy*, vol. 35, no. 6, pp. 581–592, 2017.
- [33] H. Bacot, B. McCoy, and J. Plagman-Galvin, "Municipal commercial recycling," *The American Review of Public Administration*, vol. 32, no. 2, pp. 145–165, 2002.
- [34] A. Krzywoszynska, "'Waste? You mean by-products!' from bio-waste management to agro-ecology in Italian winemaking and beyond," *The Sociological Review*, vol. 60, no. 2, pp. 47–65, 2012.
- [35] B. R. Balakrishnan Ramesh Babu, A. K. Anand Kuber Parande, and C. A. Chiya Ahmed Basha, "Electrical and electronic waste: a global environmental problem," *Waste Management & Research: The Journal for a Sustainable Circular Economy*, vol. 25, no. 4, pp. 307–318, 2007.
- [36] L. Gan and S. Yang, "Legal context of high level radioactive waste disposal in China and its further improvement," *Energy & Environment*, vol. 28, no. 4, pp. 484–498, 2017.
- [37] N. Abdullah, O. A. Alwesabi, and R. Abdullah, "IoT-based smart waste management system in a smart city," *Advances in Intelligent Systems and Computing*, vol. 843, pp. 364–371, 2018.
- [38] S. Talari, "A review of smart cities based on the internet of things concept," *Energies*, vol. 10, no. 4, pp. 1–23, 2017.
- [39] K. A. Monika, "Smart dustbin-an efficient garbage monitoring system," *International Journal of engineering science and computing*, vol. 6, no. 6, pp. 7113–7116, 2016.
- [40] N. S. Kumar, "IOT based smart garbage alert system using Arduino UNO," in *Proceedings of the 2016 IEEE Region 10 Conference (TENCON)*, pp. 1028–1034, Singapore, November 2016.
- [41] G. K. Shyam, S. S. Manvi, and P. Bharti, "Smart waste management using Internet-of-Things (IoT)," in *Proceedings of the 2nd International Conference on Computing and Communications Technologies IEEE*, pp. 199–203, Chennai, India, February 2017.
- [42] K. Pardini, J. J. P. C. Rodrigues, S. A. Kozlov, N. Kumar, and V. Furtado, "IoT-based solid waste management solutions: a survey," *Journal of Sensor and Actuator Networks*, vol. 8, no. 1, p. 5, 2019.



## Research Article

# An Improved Authentication Scheme for Digital Rights Management System

Sajid Hussain <sup>1</sup>, Yousaf Bin Zikria <sup>2</sup>, Ghulam Ali Mallah <sup>3</sup>, Chien-Ming Chen <sup>4</sup>,  
Mohammad Dahman Alshehri <sup>5</sup>, Farruh Ishmanov <sup>6</sup>, and Shehzad Ashraf Chaudhry <sup>7</sup>

<sup>1</sup>Department of Cyber Security, Air University, Islamabad, Pakistan

<sup>2</sup>Department of Information and Communication Engineering, Yeungnam University, Gyeongsan 38541, Republic of Korea

<sup>3</sup>Department of Computer Science, Shah Abdul Latif University, Khairpur, Sindh 66020, Pakistan

<sup>4</sup>College of Computer Science and Engineering, Shandong University of Science and Technology, Shandong, China

<sup>5</sup>Department of Computer Science, College of Computers and Information Technology, Taif University, P.O. Box 11099, Taif 21944, Saudi Arabia

<sup>6</sup>Department of Electronics and Communication Engineering, Kwangwoon University, Seoul 01897, Republic of Korea

<sup>7</sup>Department of Computer Engineering, Faculty of Engineering and Architecture, Istanbul Gelisim University, Istanbul, Turkey

Correspondence should be addressed to Farruh Ishmanov; [farruh@kw.ac.kr](mailto:farruh@kw.ac.kr)  
and Shehzad Ashraf Chaudhry; [sashraf@gelisim.edu.tr](mailto:sashraf@gelisim.edu.tr)

Received 13 October 2021; Accepted 29 December 2021; Published 27 January 2022

Academic Editor: Vinayakumar Ravi

Copyright © 2022 Sajid Hussain et al. This is an open access article distributed under the Creative Commons Attribution License, which permits unrestricted use, distribution, and reproduction in any medium, provided the original work is properly cited.

With the increasing number and popularity of digital content, the management of digital access rights has become an utmost important field. Through digital rights management systems (DRM-S), access to digital contents can be defined and for this, an efficient and secure authentication scheme is required. The DRM authentication schemes can be used to give access or restrict access to digital content. Very recently in 2020, Yu et al. proposed a symmetric hash and xor-based DRM and termed their system to achieve both security and performance efficiency. Contrarily, in this study, we argue that their scheme has several issues including nonresistance to privileged insider and impersonation attacks. Moreover, it is also shown in this study that their scheme has an incorrect authentication phase and due to this incorrectness, the scheme of Yu et al. lacks user scalability. An improved scheme is then proposed to counter the insecurities and incorrectness of the scheme of Yu et al. We prove the security of the proposed scheme using BAN logic. For a clear picture of the security properties, we also provide a textual discussion on the robustness of the proposed scheme. Moreover, due to the usage of symmetric key-based hash functions, the proposed scheme has a comparable performance efficiency.

## 1. Introduction

The rapid expansion of computer technology and media of various types such as software, music services, videos, photos, documents, and e-books is combined and manipulated as digital contents. With the invention of the low power devices, the distribution of such digital content along the globe is increased rapidly [1]. This rapid distribution demands an efficient digital rights management system to be utilized to preserve the digital rights associated with the content. A serious concern is the downloading of the contents by unauthorized users, which is a big problem

and deprivation for the copyright owners. Thus, the protection of the digital contents is the major issue, and authentication is a very necessary security requirement for the prevention of unauthorized access and making the availability of the digital contents to the only legitimate users. Digital right management (DRM) systems are specifically designed environments that include some access control mechanism for the use of the digital content [2, 3]. The main purpose of the DRM system is to provide protection to the digital contents and to make sure these are only accessible to valid users. Digital content services that include important data are conveyed through the public channels, which are fully

accessible to malicious users. Hence, for the sake of secure transmission of the digital contents to the valid user through the public channel, strong authentication and key agreement schemes are needed [4–6].

In the immediate past, various authentication schemes have been proposed to make sure the privacy of the digital content and user. In 2008, Chen [7] proposed a biometric-based authentication scheme based on biometric for DRM environment. Later on, Chang et al. [8] pointed weaknesses such as attackers can steal keys and can access digital content without any permission and proposed an improved system. Later on, Chang et al. [9] pointed that [8] is insecure against stolen device attacks and proposed an improved scheme for DRM. Mishra et al. [10] proved that the scheme of Zhang et al. [11] was vulnerable to password guessing attacks and insider attacks and proposed an improved biometric-based scheme for DRM. In 2015, Jung et al. [12] proposed an ECC-based authentication scheme for DRM. In 2017, Jung et al. [12] presented a biometric-based authentication scheme for the DRM system. Later in 2018, Lee et al. [13] proved that the protocol of [10] is suspected to the secret key disclosure which leads to anonymity violation. Yu et al. [14] claimed that the method presented in [13] is insecure against user impersonation and device theft attack and proposed an improved scheme to overcome the flaws of [13].

**1.1. Adversarial Model.** The main purpose of authentication schemes for DRM systems is to provide a scalable solution for remote user successful authentication. However, the authentication protocols should oppose many active/passive attacks [15–17]. The analysis of attacks is based on the CK adversarial model [18], which is an extension of the DY model [19] with the following features:

- (1) A valid user can possess the login credentials, namely, identity, password, biometric, etc. The server keeps the master key [20, 21]
- (2) A public communication channel is in full control of the adversary
- (3) A legal user can be dishonest [22, 23]
- (4) Any malicious user can extract saved credentials in the smart card by applying a stolen attack

**1.2. System Model of DRM.** DRM system is a verification and access control method to access digital content. Figure 1 shows the DRMS common architecture comprising of four major entities: (1) the content writer/owner, (2) content server, (3) the user, and (4) license sever.

- (1) The user who wants to obtain digital content transmits an authentication ask to the content and license servers. As soon as mutual authentication with the license server is successfully completed, reach to the encrypted digital content is issued with the help of a secret key

- (2) The content server saves the encrypted digital content in its database receive by the digital content creator and after that abstract of the content is accessible to the users on the internet
- (3) The content generator/provider provides content generation services. The digital content is generated and encrypted by the secret key. This key is transmitted to the license server using the public channel, and also encrypted digital content is also sent to the content server using a tunneled channel
- (4) The license server receives the secret key and stores it in its database. When a user requires the secret key of the encrypted digital content, the license server first authenticates that user and then sends the secret key of the content

## 2. The Scheme of Yu et al.: A Review

The scheme of Yu et al. [14] is reviewed and briefly explained in this section and the notation guide which is used in this paper is depicted in Table 1.

**2.1. User Registration Phase.** The process to register a user  $U_m$  with the license server  $LS_j$  is depicted in Figure 2 and explained through the following steps:

- (RG1) user  $U_m$  chooses his/her identity  $ID_m$ , password  $PW_m$ , and marks biometrics  $BIO_m$ . After that  $U_m$  calculates  $Gen(BIO_m) = R_m, P_m$ , and  $RPW_m = h(PW_m || R_m)$  and dispatches  $\{ID_m, RPW_m\}$  to  $LS_j$ -license server via private channel
- (RG2) license server  $LS_j$  on receiving request containing  $\{ID_m, RPW_m\}$  by  $U_m$  calculates  $X_m = h(ID_m || X_{LS})$ ,  $d_m = X_m \oplus h(ID_m || RPW_m)$ , and  $f_m = h(RPW_m || X_m)$ .  $LS_j$  saves  $ID_m$  and  $X_m$  within its database and replies the registration request message  $\langle d_m, f_m \text{ to } U_m \rangle$  via private channel
- (RG3)  $U_m$  receives the message from  $LS_j$  saves  $\{d_m, f_m\}$  in its mobile device memory

**2.2. Login and Authentication Phase.** A registered user  $U_m$  who wants to utilize the digital content  $DC$  initiates a mutual authentication request with  $LS_j$  with an aim to attain mutual authentication and obtain the secret key  $K_C$  of the  $DC$ . The steps involved in the login and authentication procedure are detailed in Figure 3 and explained as follows:

- (LAA 1)  $U_m$  enters his/her  $\{ID_m, PW_m\}$  apir and submits  $BIO_m$ . After that,  $U_m$  calculates  $R_m = Rep(BIO_m, P_m)$ ,  $RPW_m = h(PW_m || R_m)$ ,  $X_m = d_m \oplus h(ID_m || RPW_m)$ , and  $f_m^* = h(RPW_m || X_m)$  and compare if  $f_m^* = ? f_m$ . If the condition is true,  $U_m$  creates  $R_1$  randomly and calculates  $Z_1 = X_m \oplus R_1$ ,  $Z_2 = ID_m \oplus R_1$ ,  $Z_3 = ID_c \oplus R_1$ , and  $Z_{US} = h(ID_m || ID_c || X_m || R_1)$ . Then, the user

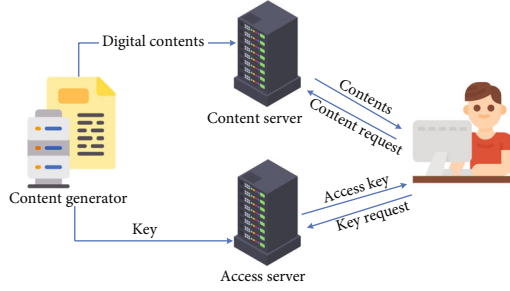


FIGURE 1: DRM-system-architecture.

TABLE 1: Symbol guide.

Symbols	Explanations
$U_m, LS_j$	Mobile user, license server
$ID_m, ID_c$	Identities of $U_m, LS_j$
$PW_m, BIO_m$	Password and biometric of $U_m$
$X_{LS}, K_C$	Secret keys $LS_j, ID_c$
$h(\cdot), H(\cdot)$	Hash and biohash functions
$R_1, R_2$	Random nonces
$PID_m$	Unique random nonce for each user
$T_m, T_{cs}$	Current timestamps
$KEY_{DC}$	Secret key of digital content
$X_{LS}$	Master key of license server
$\Delta T$	Allowed transmission delay
$\ , \oplus$	Concatenation and XOR operations

User ( $U_m$ )	License server ( $LS_j$ )
$U_m$ inputs $\{ID_m, PW_m\}$	
Imprints biometric $BIO_m$	
$Gen(BIO_m) = \langle R_m, P_m \rangle$	
$RPW_m = h(PW_m \  R_m)$	
$\langle ID_m, RPW_m \rangle$	
$\xrightarrow{\text{(via secure channel)}}$	
	$X_m = h(ID_m \  X_{LS})$
	$d_m = X_m \oplus h(ID_m \  RPW_m)$
	$f_m = h(RPW_m \  X_m)$
	Saves $X_m$ and $ID_m$
	$\langle d_m, f_m \rangle$
	$\xleftarrow{\text{(via secure channel)}}$
Saves $\{d_m, f_m\}$ in the memory	

FIGURE 2: Yu et al.'s user registration.

$U_m$  initiates the request message  $\{Z_1, Z_2, Z_3, Z_{US}\}$  through public channel to  $LS_j$

(LAA 2)  $LS_j$  receives the request message sent by  $U_m$  and calculates  $R_1 = Z_1 \oplus X_m$ ,  $ID_m = Z_2 \oplus R_1$ ,  $ID_c = Z_3 \oplus R_1$ , and  $M_{US}^* = h(ID \| ID_c \| X_m \| R_1)$  and verifies if  $M_{US}^* = ? Z_{US}$ . If the condition is true,  $LS_j$  picks relevant  $K_C$ , creates random nonce  $R_2$ , and calculates  $Z_4 = R_2 \oplus X_m$ ,  $Z_5 =$

User ( $U_m$ )	License server ( $LS_j$ )
$U_m$ inputs $ID_m$ , password $PW_m$	
Imprints biometric $BIO_m$	
Calculates	
$R_{CC} = Rep(BIO_m, P_m)$	
$RPW_m = h(PW_m \  R_m)$	
$X_m = d_m \oplus h(ID_m \  RPW_m)$	
$f_m^* = h(RPW_m \  X_m)$	
check if $f_m^* = f_m$	
Creates random nonce $R_1$	
$Z_1 = X_m \oplus R_1$	
$Z_2 = ID_m \oplus R_1$	
$Z_3 = ID_c \oplus R_1$	
$Z_{US} = h(ID_m \  ID_c \  X_m \  R_1)$	
$\langle Z_1, Z_2, Z_3, Z_{US} \rangle$	
$\xrightarrow{\text{(via public channel)}}$	
	$R_1 = Z_1 \oplus X_m$
	$ID_m = Z_2 \oplus R_1$
	$ID_c = Z_3 \oplus R_1$
	$M_{US}^* = h(ID \  ID_c \  X_m \  R_1)$
	Check if $M_{US}^* = ? Z_{US}$
	Retrieves $K_C$
	Generate random nonce $R_2$
	Calculate
	$Z_4 = R_2 \oplus X_m$
	$Z_5 = K_C \oplus X_m$
	$Z_{SU} = h(ID_m \  X_m \  K_C \  R_2)$
	$\langle Z_4, Z_5, Z_{SU} \rangle$
	$\xleftarrow{\text{(via public channel)}}$
Calculates	
$R_2 = Z_4 \oplus X_m$	
$K_C = Z_5 \oplus X_m$	
$M_{SU}^* = h(ID_m \  X_m \  K_C \  R_2)$	
Check if $M_{SU}^* = ? Z_{SU}$	
Saves $K_C$	

FIGURE 3: Yu et al.'s login and authentication scheme.

$K_C \oplus X_m$  and  $Z_{SU} = h(ID_m \| X_m \| K_C \| R_2)$ . At the end,  $LS_j$  sends the message  $\{Z_4, Z_5, Z_{SU}\}$  to user  $U_m$  directly through public channel

(LAA 3)  $U_m$  receives the response message from  $LS_j$  and calculates  $R_2 = Z_4 \oplus X_m$ ,  $K_C = Z_5 \oplus X_m$ , and  $M_{SU}^* = h(ID_m \| X_m \| K_C \| R_2)$ . At the end user,  $U_m$  verifies if  $M_{SU}^* = ? Z_{SU}$  and saves  $K_{DC}$  in the device

### 3. Cryptanalysis of Yu et al.'s Scheme

In this section, through the informal analysis of Yu et al.'s scheme [14], it is affirmed that their scheme is secure against well-known attacks. However, the following subsections demonstrate that the scheme presented in [14] is having correctness issues, is weak against ephemeral secret leakage attacks, and does not provide anonymity.

3.1. *Incorrectness.* The authentication phase of Yu et al.'s scheme cannot end normally, and the license server and user may be unable to share any key at all. The user in the Yu et al. scheme after initiating an authentication message to the license server may never receive an acknowledgment,

and the license server may never create a session key. Hence, their scheme lacks the property of authentication and key agreement. The depiction of incorrectness case is as follows:

- (Inc 1) user  $U_m$  sends a login request by entering password, identity, and biometric, and transmits  $Z_1, Z_2, Z_3, Z_{US}$  to  $LS_j$  (the license server)
- (Inc 2) license server ( $LS_j$ ) receives the request message and computes

$$R_1 = Z_1 \oplus X_m. \quad (1)$$

The computation of the above equation requires the  $X_m$  corresponding requesting user identity  $ID_m$ , which the license server does not know. Also, the request message sent by the user  $U_m$  does not include the identity of the requesting user. The license server computes the request without the information of any designated user. In the same way, the license server sends the acknowledgment message without knowing to whom this message is to be sent.

The only case in which Yu et al.'s scheme can achieve the authentication and key agreement in the view is if the system has only one registered user. Hence, systems with a single registered user are not preferable in the real world. Therefore, Yu et al.'s scheme for facilitating digital rights management systems is incorrect, and this incorrectness shows that their system is not preferable for real-world deployments.

**3.2. Privileged Insider Attack.** Yu et al.'s scheme stores the sensitive information in the database of the license server. Due to which it is susceptible to user impersonation, server impersonation attacks, and secret key leakage attacks. The attacks can be simulated in the following methods.

**3.2.1. User Impersonation Attack.** The internal adversary  $\mathcal{A}$  gets  $IS_m$  and  $X_m$  from the database of the license server. Now the adversary  $\mathcal{A}$  can impersonate as  $U_m$  by adopting the following steps:

- (IUA 1)  $\mathcal{A}$  picks a random number  $R_{UA}$
- (IUA 2) computes  $Z_1 = X_m \oplus R_{UA}$ ,  $Z_2 = ID_m \oplus R_{UA}$ ,  $Z_3 = ID_c \oplus UA$ , and  $Z_{AUS} = h(ID_m || ID_c || X_m || UA)$
- (IUA 3) transmits the message  $\langle Z_1, Z_2, Z_3, Z_{AUS} \rangle$  to license server  $LS_j$
- (IUA 4) license server  $LS_j$  accepts the message  $\langle Z_1, Z_2, Z_3, Z_{AUS} \rangle$  and verifies the message legitimacy and verification will be successful as user verification on license server  $LS_j$  is not taking place
- (IUA 5)  $LS_j$  will fetch relevant  $K_C$  and computes  $Z_4 = R_2 \oplus X_m$ ,  $Z_5 = K_C \oplus X_m$  and  $Z_{SU} = h(ID_m || X_m || K_C || R_2)$ .  $LS_j$  sends the message  $\{Z_4, Z_5, Z_{SU}\}$  to  $\mathcal{A}$
- (IUA 6)  $\mathcal{A}$  receives the message sent by  $LS_j$  and computes  $R_2 = Z_4 \oplus X_m$ ,  $K_C = Z_5 \oplus X_m$ , and  $M_{SU}^* =$

$h(ID_m || X_m || K_C || R_2)$ . Adversary gets successfully the secret key  $K_C$

**3.2.2. License Server Impersonation Attack.** The privileged adversary  $\mathcal{S}\mathcal{A}$  steals the  $\langle ID_m, X_m \rangle$  from the database of the  $LS_j$ . When  $U_m$  sends the the message  $\langle Z_1, Z_2, Z_3, Z_{AUS} \rangle$  to  $LS_j$  through public channel; then,  $\mathcal{S}\mathcal{A}$  will intercept the message and and impersonate as a valid license server in the following ways.

- (ISA 1)  $\mathcal{S}\mathcal{A}$  will compute  $R_1 = Z_1 \oplus X_m$ ,  $ID_m = Z_2 \oplus R_1$ ,  $ID_c = Z_3 \oplus R_1$ , and  $M_{US}^* = h(ID || ID_c || X_m || R_1)$
- (ISA 2) verify if  $M_{US}^* = ? Z_{US}$ . If the condition is true,  $LS_j$  picks relevant  $K_C$  and creates random nonce  $R_{US}$
- (ISA 3) calculate  $Z_4 = R_{US} \oplus X_m$ ,  $Z_5 = KEY_{ADC} \oplus X_m$ , and  $Z_{ASU} = h(ID_m || X_m || KEY_{ADC} || R_{US})$ .
- (ISA 4)  $\mathcal{S}\mathcal{A}$  sends the message  $\{Z_4, Z_5, Z_{ASU}\}$  to user  $U_m$
- (ISA 5)  $U_m$  will verify the message and verification will be successful and as a result, get secret key  $K_{EY_{ADC}}$  which is in real a forged key and will not work

**3.2.3. No Secret Key Secrecy.** Only those users who have the secret key can access the digital content in the digital rights management system. But, as shown in Section 3.2.1, an adversary  $\mathcal{A}$  can acquire the secret key by impersonating as a valid user  $U_m$ . Hence, Yu et al.'s scheme does not ensure the security of the secret key.

## 4. Proposed Scheme

To ensure privacy, security, and to remove the incorrectness in the scheme of Yu et al. [14], a new scheme is proposed in this section. The proposed scheme comprises three main phases, which are further divided into subphases. The detail of the scheme is given in the following subsections.

**4.1. Registration Phase.** To get access to the digital contents, a user must register himself/herself to be a legitimate user. Following are the steps as mentioned in Figure 4 to be followed:

RGD 3: the user  $U_m$  picks the pair  $\{ID_m, PW_m\}$  and engraves  $BIO_m$ . Now  $U_m$  computes  $Gen(BIO_m) = \langle R_m, P_m \rangle$ , and  $RPW_m = h(PW_m || R_m)$  and dispatches  $\{ID_m, RPW_m\}$  to license server  $LS_j$  by using secure channel

RGD 3: license server  $LS_j$  receiving the registration request by  $U_m$  computes  $X_m = h(ID_m || X_{LS})$ ,  $d_m = X_m \oplus h(ID_m || RPW_m)$ , and saves  $ID_m$  and  $PID_m$  in its database and reply the registration request message  $\langle X_m \text{ to } PID_m \rangle$  by using channel

RGD 3:  $U_m$  receives the message from  $LS_j$  and computes  $PID'_m = PID_m \oplus h(PW_m || R_m)$ ,  $X'_m = X_m \oplus h(PW_m || R_m)$ ,  $Z_m = h(ID_m || PW_m || R_m)$  and stores  $\{X'_m, PID'_m, Z_m\}$  in the mobile device memory

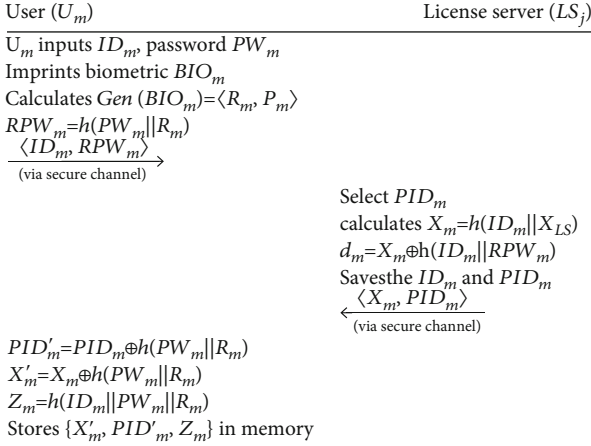


FIGURE 4: Proposed user registration.

**4.2. Login and Authentication.** Following steps as mentioned in Figure 5 are executed to furnish login and authentication phase of the proposed scheme:

- (LAAuth 1)  $U_m$  inputs  $ID_m$ , password  $PW_m$ , imprints biometric  $BIO_m$ , calculates  $R_m = Rep(BIO_m, P_m)$ , and checks if  $Z_m = ? h(ID_m || PW_m || R_m)$ , and if the condition is true, then, select  $R_1$  and  $T_m$  and compute  $X_m = X'_m \oplus h(R_m || PW_m)$ ,  $Z_1 = ID_m \oplus R_1 \oplus h(X_m \oplus T_m)$ ,  $Z_2 = ID_c \oplus R_1 \oplus h(X_m \oplus T_m)$ ,  $Z_{US} = h(ID_m || ID_c || h(X_m || T_m) || R_1 || T_m)$  and send the message containing  $\langle Z_1, Z_2, Z_{US}, PID_m, T_m \rangle$  to the  $LS_j$
- (LAAuth 2) after receiving the message  $LS_j$  verifies if  $|T_m - T_c| < \Delta T?$ , if the condition is true then fetch  $ID_m$  corresponding to  $PID_m$  and compute  $X_m^* = h(ID_m || X_{LS})$ ,  $R_1 = Z_1 \oplus ID_m \oplus h(X_m^* || T_m)$ ,  $ID_c = Z_2 \oplus R_1 \oplus ID_m \oplus h(X_m^* || T_m)$ ,  $M_{US}^* = h(ID_m || ID_c || h(X_m^* || T_m) || R_1 || T_m)$  and check if  $M_{US}^* = ? Z_{US}$  is true. If true pick  $R_2$ ,  $T_{CS}$ , and  $PID_m^{new}$ , fetches  $K_C$  and calculate  $TEMP1 = h(ID_m \oplus R_1)$ ,  $Z_3 = R_2 \oplus h(X_m^* || T_{cs}) \oplus TEMP1$ ,  $Z_4 = PID_m^{new} \oplus h(X_m^* || T_{cs}) \oplus TEMP1$ ,  $Z_5 = K_C \oplus h(X_m^* || T_{cs}) \oplus R_2 \oplus TEMP1$ ,  $Z_{SU} = h(ID_m || h(X_m^* || T_{cs}) || K_C || R_2, || TEMP1 || T_{cs})$ . Replace  $PID_m$  with  $PID_m^{new}$ , and send the message containing  $\langle Z_3, Z_4, Z_5, Z_{SU}, T_{cs} \rangle$  to  $U_m$
- (LAAuth 3) after receiving the message from  $LS_j$ ,  $U_m$  check if  $|T_{cs} - T_c| < \Delta T?$  the condition is true then calculates  $TEMP2 = h(ID_m \oplus R_1)$ ,  $R_2 = Z_3 \oplus h(X_m || T_{cs}) \oplus TEMP2$ ,  $PID_m^{new} = Z_4 \oplus h(X_m || T_{cs}) \oplus TEMP2$ ,  $K_C = Z_5 \oplus h(X_m || T_{cs}) \oplus R_2 \oplus TEMP2$ ,  $M_{SU}^* = h(ID_m || h(X_m || T_{cs}) || K_C || R_2 || TEMP2 || T_{cs})$ . Then, check if  $M_{SU}^* = ? Z_{SU}$ , if the condition is true, then, calculate  $KEY_{DC}^* = K_C \oplus h(PW_m || R_m)$  and save  $KEY_{DC}^*$

**4.3. Password Change.** If a valid user has lost/forgot his/her password then can change password by adopting the following steps:

- (PWD 1) user  $U_m$  enters new pair  $\{ID_m^*, PW_m^*\}$  and engraves  $BIO_m^*$ . Now,  $U_m$  computes  $Gen(BIO_m^*) = \langle R_m^*, P_m^* \rangle$ , and  $RPW_m^* = h(PW_m^* || R_m^*)$  and dispatches  $\{ID_m^*, RPW_m^*\}$  to the mobile device
- (PWD 2) upon receipt of the message mobile check if  $Z_m^* = ? h(ID_m^* || PW_m^* || R_m^*)$ , if true, it sends confirmation to the user  $U_m$
- (PWD 3)  $U_m$  chooses new password  $PW_m^{new}$  and biometric  $BIO_m^{new}$  and compute  $Gen(BIO_m^{new}) = \langle R_m^{new}, P_m^{new} \rangle$ , and  $RPW_m^{new} = h(PW_m^{new} || R_m^{new})$
- (PWD 4) Receiving the message mobile device calculates  $X_m = h(ID_m || X_{LS})$  and  $d_m^{new} = X_m^* \oplus h(ID_m || RPW_m^{new})$  and send  $X_m$  and  $PID_m^{new}$
- (PWD 5)  $U_m$  computes  $PID_m^{new'} = PID_m^{new} \oplus h(PW_m^{new} || R_m^{new})$ ,  $X_m^{new'} = X_m \oplus h(PW_m^{new} || R_m^{new})$ ,  $Z_m = h(ID_m || PW_m^{new} || R_m^{new})$  and update  $\{X_m^{new'}, PID_m^{new'}, Z_m\}$ .

## 5. The Security Analysis

To describe the security of the proposed scheme, we have scrutinized the scheme through formal and informal security analysis in the following subsections.

**5.1. Authentication Proof Based on the Burrows–Abadi–Needham Logic (BAN Logic).** The security of the proposed scheme is formally analyzed in the standard model using the widely accepted Burrows–Abadi–Needham logic [24].

**5.1.1. Postulates for BAN Logic.** Some of the logical postulates of BAN logic and the meaning related to the postulates are given below in Table 2.

**5.1.2. Security Goal Establishment.** Established security goals and logical notations of the BAN logic are given below in Table 3.

- $$G_1: LS_j | \equiv (R_1)$$
- $$G_2: LS_j | \equiv U_m | \equiv (R_1)$$
- $$G_3: U_m | \equiv (R_2)$$
- $$G_4: U_m | \equiv LS_j | \equiv (R_2)$$

**5.1.3. Proposed Schemes Idealized Form**

- $$(M1) U_m \longrightarrow LS_j: \langle ID_m, ID_c, R_1 \rangle_{X_m}$$
- $$(M2) LS_j \longrightarrow U_m: \langle ID_m, ID_c, K_C, R_2 \rangle_{X_m}$$

**5.1.4. Assumptions**

- $$(A1) LS_j | \equiv \#(R_1)$$
- $$(A2) U_m | \equiv \#(R_2)$$

User ( $U_m$ )	License server ( $LS_j$ )
$U_m$ inputs $ID_m$ , password $PW_m$ Imprints biometric $BIO_m$ $R_m = Rep(BIO_m, P_m)$ If $Z_m \stackrel{?}{=} h(ID_m    PW_m    R_m)$ Select $R_1$ and $T_m$ $X_m = X'_m \oplus h(R_m    PW_m)$ $Z_1 = ID_m \oplus R_1 \oplus h(X_m \oplus T_m)$ $Z_2 = ID_c \oplus R_1 \oplus h(X_m \oplus T_m)$ $Z_{US} = h(ID_m    ID_c    h(X_m    T_m)    R_1    T_m)$ $\langle Z_1, Z_2, Z_{US}, PID_m, T_m \rangle$ (via public channel) $\rightarrow$	Check if $ T_m - T_c  < \Delta T$ ? Fetch $ID_m$ corresponding to $PID_m$ Compute $X_m^* = h(ID_m    X_{LS})$ Compute $R_1 = Z_1 \oplus ID_m \oplus h(X_m^*    T_m)$ $ID_c = Z_2 \oplus R_1 \oplus ID_m \oplus h(X_m^*    T_m)$ $M_{US}^* = h(ID_m    ID_c    h(X_m^*    T_m)    R_1    T_m)$ Check if $M_{US}^* \stackrel{?}{=} Z_{US}$ If true Pick $R_2, T_{CS}$ and $PID_m^{new}$ Fetches $K_C$ Calculate $TEMP1 = h(ID_m \oplus R_1)$ $Z_3 = R_2 \oplus h(X_m^*    T_{CS}) \oplus TEMP1$ $Z_4 = PID_m^{new} \oplus h(X_m^*    T_{CS}) \oplus TEMP1$ $Z_5 = K_C \oplus h(X_m^*    T_{CS}) \oplus R_2 \oplus TEMP1$ $Z_{SU} = h(ID_m    h(X_m^*    T_{CS})    K_C    R_2    TEMP1    T_{CS})$ Replace $PID_m$ with $PID_m^{new}$ $\langle Z_3, Z_4, Z_5, Z_{SU}, T_{CS} \rangle$ (via public channel) $\leftarrow$
Check if $ T_{CS} - T_c  < \Delta T$ ? Calculates $TEMP2 = h(ID_m \oplus R_1)$ $R_2 = Z_3 \oplus h(X_m    T_{CS}) \oplus TEMP2$ $PID_m^{new} = Z_4 \oplus h(X_m    T_{CS}) \oplus TEMP2$ $K_C = Z_5 \oplus h(X_m    T_{CS}) \oplus R_2 \oplus TEMP2$ $M_{SU}^* = h(ID_m    h(X_m    T_{CS})    K_C    R_2    TEMP2    T_{CS})$ Check if $M_{SU}^* \stackrel{?}{=} Z_{SU}$ If true $KEY_{DC}^* = K_C \oplus h(PW_m    R_m)$ Saves $KEY_{DC}^*$	

FIGURE 5: Proposed login and authentication scheme.

TABLE 2: Postulates for BAN logic.

$A \mid \equiv A \xleftrightarrow{K} Y, A \triangleleft \langle B \rangle_K / A \mid \equiv Y \sim K$	Message-meaning rule
$A \mid \equiv \#B, A \mid \equiv Y \sim B / A \mid \equiv Y \sim K$	Nonce-verification rule
$A \mid \equiv B, A \mid \equiv C / A \mid \equiv (B, C)$	Belief rule
$A \mid \equiv \#B, A \mid \equiv C / A \mid \equiv \#(B, C)$	Fresh conjunction rule
$A \mid \equiv Y \implies B, A \mid \equiv Y \sim B / A \mid \equiv B$	Jurisdiction rule

TABLE 3: BAN logic notations.

$A \mid \equiv B$	$A$ believes a statement $B$
$A \xleftrightarrow{K} Y$	Share a key $K$ between $A$ and $Y$
$\#B$	$B$ is fresh
$A \triangleleft B$	$A$ sees $B$
$A \mid \sim B$	$A$ said $B$
$(B, C)_K$	$B, C$ is hashed by key $K$
$\{B\}_K$	$B$ is hashed with key $K$
$\langle B \rangle_K$	$B$ is encrypted with key $K$

$$(A3) \quad LS_j \mid \equiv (LS_j \xleftrightarrow{X_m} U_m)$$

$$(A4) \quad U_m \mid \equiv (LS_j \xleftrightarrow{X_m} U_m)$$

$$(A5) \quad LS_j \mid \equiv U_m \implies (R_1)$$

$$(A6) \quad U_m \mid \equiv (LS_j \longrightarrow R_2)$$

Step 1. According to message 1:

$$P1 : LS_j \triangleleft \{ID_m, ID_c, R_1\}_{X_m}. \quad (2)$$

Step 2. From the message meaning rule according to P1 and A3:

$$P2 : LS_j \mid \equiv \{U_m\}. \quad (3)$$

Step 3. According to the freshness rule with A1, we get

$$P3 : LS_j \mid \equiv U_m \mid \equiv \#\{ID_m, ID_c, R_1\}_{X_m}. \quad (4)$$

Step 4. From the nonce verification rule with P2 and P3, we get

$$P4 : LS_j \mid \equiv U_m \mid \equiv \{ID_m, ID_c, R_1\}_{X_m}. \quad (5)$$

Step 5. According to the belief rule with P4, we get

$$P5 : LS_j \mid \equiv U_m \mid \equiv \{R_1\} \text{Goal} - X2. \quad (6)$$

Step 6. From the jurisdiction rule with P5 and A5, we get

$$P6 : LS_j \mid \equiv \{R_1\} \text{Goal} - X1. \quad (7)$$

Step 7. According to M2, we obtain

$$P7 : U_m \triangleleft \{ID_m, ID_c, K_C R_2\}_{X_m}. \quad (8)$$

Step 8. From the message meaning rule with P7 and A4, we get

$$P8 : U_m \mid \equiv LS_j \mid \equiv \{ID_m, ID_c, K_C R_2\}_{X_m}. \quad (9)$$

Step 9. According to the freshness rule with A2, we get

$$P9 : U_m \mid \equiv LS_j \mid \equiv \#\{ID_m, ID_c, K_C R_2\}_{X_m}. \quad (10)$$

Step 10. From the nonce verification rule with P9 and P10, we get

$$P10 : U_m \mid \equiv LS_j \mid \equiv \{ID_m, ID_c, K_C R_2\}_{X_m}. \quad (11)$$

Step 11. According to the belief rule with P10, we get

$$P11 : U_m \mid \equiv LS_j \mid \equiv \{R_2\} \text{Goal} - X4. \quad (12)$$

Step 12. From the jurisdiction rule with P11 and A6, we get

$$P12 : U_m \mid \equiv \{R_2\} \text{Goal} - X3. \quad (13)$$

According to Goal - X1 to Goal - X4, we proved that our scheme attains secure mutual authentication among  $U_m$  and  $LS_j$ .

5.2. Informal Security Analysis. To assess the security of the introduced scheme, also we have inspected the scheme through informal security analysis procedures.

5.2.1. Mutual Authentication. Our proposed scheme provides mutual authentication by making verification on both sides of participating entities. License server  $LS_j$  receives the login request messages  $Msg_1 = (Z_1, Z_2, Z_{US}, PID_m, T_m)$  from  $U_m$ , license server  $LS_j$  verifies the authenticity of the user by verifying the  $M'US = ? Z_{US}$ . If the condition is true,  $LS_j$  authenticates  $U_m$  and sends  $Z_3, Z_4, M5, Z_{SU}, T_{cs}$  to  $U_m$ .  $U_m$  receives the response messages from  $LS_j$ ,  $U_m$  verifies whether  $M'_{SU} = ? Z_{SU}$ . If the condition is true, then,  $U_m$  authenticates  $S_j$ ; otherwise, terminates the request. Hence, the proposed scheme successfully achieves mutual authentication property.

5.2.2. Replay Attack. Suppose that  $\mathcal{A}$  hijacks the messages  $Msg_1 = (Z_1, Z_2, Z_{US}, PID_m, T_m)$  and  $Msg_2 = (Z_3, Z_4, Z_5, Z_{US}, T_{cs})$  in a selective session and tries to replay these hijacked messages after a while. As it is evident that the all message contains current timestamps  $T_m$  and  $T_{cs}$ , the acceptance of the timeliness  $T_m$  and  $T_{cs}$  will be declined at the  $U_m$  and  $LS_j$ . Furthermore,  $\Delta T$  value is fixed very small and due to which it will be very difficult for the attacker  $\mathcal{A}$  to replay the hijacked messages within limit of the  $\Delta T$ . Hence, the proposed scheme is stealth against the replay attack.

**5.2.3. Stolen Mobile Device Attack.** Suppose that  $\mathcal{A}$  has stolen mobile device [25, 26] of user  $U_m$  or  $U_m$  has lost the mobile device due to some reason. Then,  $\mathcal{A}$  can extract the credentials  $\{X'_m, PID'_m, Z_m\}$  from mobile device memory using the power analysis attacks. After getting all these parameters, the attacker  $\mathcal{A}$  will not be able to get useful parameters  $ID_m$  and  $PW_m$ , as these are protected through a collision-resistant hash function. Therefore, if any mobile device will be lost/stolen will not affect the proposed authentication mechanism.

**5.2.4. Anonymity and Untraceability.** In the proposed scheme, all the messages  $Msg_1 = (Z_1, Z_2, Z_{US}, PID_m, T_m)$  and  $Msg_2 = (Z_3, Z_4, Z_5, Z_{US}, T_{cs})$  in each session are explicit and nonrepeated, also all the message includes current timestamps  $T_m$  and  $T_{cs}$ , and random nonces  $R_1$  and  $R_2$ . Hence,  $\mathcal{A}$  will not be able to trace  $U_m$  and  $LS_j$ . Moreover, even any single message does not contain identities  $ID_m$  and  $ID_c$ . Hence, the anonymity [27, 28] is guaranteed in the proposed scheme.

**5.2.5. Denial-of-Service Attack.** In the login and authentication phase, when a valid user  $U_m$  inputs his/her identity  $ID_m$ , password  $PW_m$ , and imprints biometric  $BIO_m$  into the mobile device. Mobile device retrieves the saved secret biometric key corresponding to  $BIO_m$  as  $R_m = Rep(BIO_m, P_m)$ . Further mobile device computes  $Z_m = h(ID_m || PW_m || R_m)$  and checks if  $Z_m$  values are the same or not. If the condition is not met, the session is terminated immediately, and in case of success, the session proceeds normally. Therefore, in case of denial-of-service attack [29, 30], the proposed scheme will resist it.

**5.2.6. Man-in-the-Middle Attack.** In this type of attack,  $\mathcal{A}$  grabs the messages being exchanged when the communication is taking place and tries to alter those messages to make other valid messages, to deceive the recipient from guessing the altered messages, and he/she considered these altered messages as normal as other original messages. Suppose  $\mathcal{A}$  grabs the messages  $Msg_1$  and  $Msg_2$ . Due to lack of the some parameters knowledge such as  $ID_m, ID_c, X_m$ , and  $K_C$ , the attacker  $\mathcal{A}$  will be unable to forge these messages  $Msg_1$  and  $Msg_2$ . Hence, the proposed scheme opposes man-in-the-middle attack [31].

**5.2.7. User Impersonation Attack.** Assume an attacker  $\mathcal{A}$  tries to impersonate a message on behalf of a user  $U_m$  to license server  $LS_j$ .  $\mathcal{A}$  gets  $\{X'_m, PID'_m, Z_m, h(\cdot)\}$  from mobile device and  $\{Z_1, Z_2, Z_{US}, PID_m, T_m\}$  during the communication. At the moment, if  $\mathcal{A}$  tries to construct message, but it will not possible as he/she does not know these parameters  $ID_c, ID_m$ , and  $X_m$ , due to which it will be hard to produce these for attacker.

**5.2.8. License Server Impersonation Attack.** Assume an attacker  $\mathcal{A}$  tries to impersonate a message on behalf of a license server  $LS_j$  to user  $U_m$ .  $\mathcal{A}$  gets  $\{X'_m, PID'_m, Z_m, h(\cdot)\}$  from mobile device and  $\{Z_3, Z_4, Z_5, Z_{US}, T_{cs}\}$  during the communication. At the moment, if  $\mathcal{A}$  tries to construct a

reply message on the behalf of the license server  $LS_j$ , but it will not possible as he/she does not know these parameters  $K_C, ID_m$ , and  $X_m$ , due to which it will be hard to produce these for an attacker. Hence, the proposed scheme is secure against impersonation attacks.

**5.3. Automated Security Verification through ProVerif.** The ProVerif is an automated security verification tool utilized to visualize the key agreement scheme to check mutual authentication and confidentiality of the session key among the participant entities of the authentication scheme [32–34]. To verify the security of the proposed scheme, we have simulated and verified it through ProVerif. For the sake of the experiment, we have used two events  $Ui$  and  $LS_j$  to check the authentication codes of each entity, respectively. The participant  $U_m$  uses two events, which are beginUi(bitstring) and endUi(bitstring) to authenticate the license server  $LS_j$ . Similarly, the beginSj(bitstring) and endSj(bitstring) events are used by the license server to authenticate the user  $U_m$ . The outcomes of the queries executed show that both participants are successfully communicating with each other. The simulation results are shown in Figure 6, which exhibits that the mutual authentication is successful and communication between the valid participants is secure from the reach of any potential attacker  $\mathcal{A}$ .

## 6. The Comparisons

This section provides security attributes and performance comparisons among proposed and relevant schemes [10, 13, 14], in the corresponding subsections produced below.

**6.1. Security Attributes.** This subsection provides the security attribute comparisons of the proposed with relevant schemes presented in [10, 13, 14]. The comparisons of the proposed with recent, related, and compared schemes [10, 13, 14] are depicted in Table 4. Referring to Table 4, all the compared proposals [10, 13, 14] are deficient of at least one security attribute. As per Table 4, the scheme of Mishra et al. [10] is already argued in [14] that it does not provide mutual authentication and resistance to impersonation. Moreover, the scheme of [10] is prone to theft/stolen mobile device attacks. The scheme of Yu et al. [14] does not provide anonymity of the mobile/user. Similarly, in this paper, we proved that the scheme of Yu et al. [14] has incorrect login and authentication phase, which can work with only one user, and it has weaknesses against privileged insider and impersonation attacks and due to these crucial issues, it cannot extend mutual authentication among a user and a license server.

**6.2. Computation Cost.** For computation cost, we consider the experiment executed through the MIRACL library over a mobile phone Redmo-Note-v8 with 4 GB RAM and octacore  $\mu$  processor with 2.01 GHz. The operating system underlying Redmo-Note-v8 is v-9-Android-MIUI-V:11.0.7. Moreover, to simulate a license server, we consider the running time computed over an HP:Elite-Book: P-8460  $\mu$  processor with 2.7 GHz Intel-R-Core TM with 4 GB RAM



---

Verification summary:

Query inj-event (end\_Ui (Ui[]))=>inj-event (start\_Ui (Ui[])) is true.  
 Query inj-event (end\_Sj (Sj[]))=>inj-event (start\_Sj (Sj[])) is true.  
 Query not attacker (KEYdc[]) is true

---

FIGURE 6: ProVerif simulations.

TABLE 4: Security features.

Schemes → ↓attributes	Our	[13]	[10]	
PMA	✓	✗	✓	✗
PUA	✓	✓	✗	✓
PUS	✓	✗	✓	✓
RRA	✓	✓	✓	✓
RSD	✓	✓	✓	✗
RIA	✓	✗	✓	✗
RMA	✓	✓	✓	✓
PPF	✓	✓	✓	✓
ROP	✓	✓	✓	✓
RPI	✓	✗	✓	✓

Note: PMA: provides mutual authentication; PUA: provides user anonymity/untrability; PSU: provides user scalability; RRA: resists replay attack; RSD: resists stolen mobile device; RIA: resists impersonation attack; RMA: resists man in middle attack; PPF: provides perfect forward secrecy; ROP: resists offline password guessing; RPI: resists privileged insider attack; ✓: provides; ✗: not provides.

and over LTS-16 Ubuntu-OS. Here, we denote  $T_h$  for the execution time of a hash operation and  $T_{bh}$  for computation of a biohash/fuzzy extraction operation. The  $T_h \approx 0.009$  for mobile device and  $T_h \approx 0.004$  for license server. Likewise,  $T_f \approx 0.16$  over the mobile device. To complete a round of authentication in the proposed DRM scheme, the user  $U_m$  executes  $\{9T_h + 1T_f\}$  operations, the server  $LS_j$  executes  $\{6T_h\}$ , and the whole process completes in  $\approx 0.265$  ms. The scheme of Yu et al. [14] completes the same in  $\approx 0.213$  ms. Likewise, in the scheme of Lee et al. [13], the  $U_m$  and  $LS_j$  compute execution of a round in  $\approx 0.216$  ms, and the scheme of Mishra et al. [10] completes the process in  $\approx 0.243$  ms. The proposed scheme has a slightly higher computation cost. However, only the proposed scheme provides the required security features.

**6.3. Communication Cost.** The proposed and the relevant scheme are mainly based on hash functions in addition to an exclusive-or. We adopted SHA-1 whose length is 160 bits, all other parameters including identities, pseudoidentities, timestamps, and passwords are fixed at 32 bit-size. In proposed, the user initiates the request by sending  $\langle Z_1, Z_2, Z_{US}, PID_m, T_m \rangle$ , and the size of request message is  $\{160 + 160 + 160 + 32 + 32\} = 544$  bits. The response message sent by server  $\langle Z_3, Z_4, Z_5, Z_{US}, T_{cs} \rangle$  has the size  $\{160 + 160 + 160 + 160 + 32\} = 672$ . Therefore, the total communication cost of the proposed scheme is 1216 bits. The communication costs of the schemes of Yu et al. [14], Lee et al. [13], and Mishra et al. [10] are 1120 bits, 1120 bits, and 832 bits, respectively. The computation and com-

TABLE 5: Performance comparisons.

Protocol	$U_m$	$LS_j$	RT-ms	B.E
Mishra et al. [10]	$7T_h + 1T_f$	$5T_h$	$\approx 0.243$	832
Lee et al. [13]	$4T_h + 1T_f$	$5T_h$	$\approx 0.216$	1120
Yu et al. [14]	$5T_h + 1T_f$	$2T_h$	$\approx 0.213$	1120
Proposed	$9T_h + 1T_f$	$6T_h$	$\approx 0.265$	1216

Note: RT: running time in milliseconds; B.E: bit exchanges.

munication costs along with running times of each of the proposed and schemes of Yu et al., Lee et al., and Mishra et al. are also depicted in Table 5.

## 7. Conclusion

In this paper, we first reviewed and then cryptanalyzed a recent authentication scheme presented by Yu et al. for digital rights management systems (DRM-S). We have proven that the scheme of Yu et al. lacks scalability due to faulty design and is prone to privileged insiders and impersonation attacks. Based on the only symmetric hash function and xor, an improved scheme of DRM-S is then proposed. The proposed scheme can cope with the changing security requirements of the DRM-S, which is proved through formal BAN and informal textual explanations. The proposed DRM-S authentication scheme completes the process of authentication among a user and a license server in 0.265 ms and by exchanging 1216 bits among a user and a license server.

## Data Availability

No data is available for this study

## Conflicts of Interest

The authors declare that they have no conflicts of interest.

## Authors' Contributions

Sajid Hussain and Yousaf Bin Zikria are the co-first authors. Farruh Ishmanov and Shehzad Ashraf Chaudhry are the corresponding authors.

## Acknowledgments

This research was conducted by the Research Grant of Kwangwoon University, Seoul, Korea, in 2021 and in part by Taif University Researchers Supporting Project number (TURSP-2020/126), Taif University, Taif, Saudi Arabia.

## References

- [1] L. L. Win, T. Thomas, and S. Emmanuel, "Privacy enabled digital rights management without trusted third party assumption," *IEEE Transactions on Multimedia*, vol. 14, no. 3, pp. 546–554, 2012.

- [2] E. H. Wu, S. Chuang, C.-Y. Shih, H.-C. Hsueh, S.-S. Huang, and H.-P. Huang, "A flexible and lightweight user-demand drm system for multimedia contents over multiple portable device platforms," *Software: Practice and Experience*, vol. 47, no. 10, pp. 1417–1441, 2017.
- [3] Z. Ma, M. Jiang, H. Gao, and Z. Wang, "Blockchain for digital rights management," *Future Generation Computer Systems*, vol. 89, pp. 746–764, 2018.
- [4] C.-C. Lee, C.-T. Li, Z.-W. Chen, S.-D. Chen, and Y.-M. Lai, "A novel authentication scheme for anonymity and digital rights management based on elliptic curve cryptography," *International Journal of Electronic Security and Digital Forensics*, vol. 11, no. 1, pp. 96–117, 2019.
- [5] D. Mishra, M. S. Obaidat, S. Rana, D. Dharminder, A. Mishra, and B. Sadoun, "Chaos-based content distribution framework for digital rights management system," *IEEE Systems Journal*, vol. 15, no. 1, pp. 570–576, 2021.
- [6] T. Gaber, A. Ahmed, and A. Mostafa, "Privdrm: a privacy-preserving secure digital right management system," in *Proceedings of the Evaluation and Assessment in Software Engineering*, pp. 481–486, Trondheim, Norway, 2020.
- [7] C.-L. Chen, "A secure and traceable e-drm system based on mobile device," *Expert Systems with Applications*, vol. 35, no. 3, pp. 878–886, 2008.
- [8] C.-C. Chang, J.-H. Yang, and D.-W. Wang, "An efficient and reliable e-drm scheme for mobile environments," *Expert Systems with Applications*, vol. 37, no. 9, pp. 6176–6181, 2010.
- [9] C.-C. Chang, S.-C. Chang, and J.-H. Yang, "A practical secure and efficient enterprise digital rights management mechanism suitable for mobile environment," *Security and Communication Networks*, vol. 6, no. 8, 984 pages, 2013.
- [10] D. Mishra, A. K. Das, and S. Mukhopadhyay, "An anonymous and secure biometric-based enterprise digital rights management system for mobile environment," *Security and Communication Networks*, vol. 8, no. 18, 3404 pages, 2015.
- [11] Y. Zhang, M. K. Khan, J. Chen, and D. He, "Provable secure and efficient digital rights management authentication scheme using smart card based on elliptic curve cryptography," *Mathematical Problems in Engineering*, vol. 2015, Article ID 807213, 16 pages, 2015.
- [12] J. Jung, D. Kang, D. Lee, and D. Won, "An improved and secure anonymous biometric-based user authentication with key agreement scheme for the integrated epr information system," *PLoS One*, vol. 12, no. 1, article e0169414, 2017.
- [13] C.-C. Lee, C.-T. Li, Z.-W. Chen, and Y.-M. Lai, "A biometric-based authentication and anonymity scheme for digital rights management system," *Information Technology and Control*, vol. 47, no. 2, pp. 262–274, 2018.
- [14] S. J. Yu, K. S. Park, Y. H. Park, H. P. Kim, and Y. H. Park, "A lightweight threefactor authentication protocol for digital rights management system," *Peer-to-Peer Networking and Applications*, vol. 13, no. 5, p. 1340, 2020.
- [15] M. Tanveer, G. Abbas, Z. H. Abbas, M. Bilal, A. Mukherjee, and K. S. Kwak, "Lake-6sh: lightweight user authenticated key exchange for 6lowpan-based smart homes," *IEEE Internet of Things Journal*, vol. 1, 2021.
- [16] Z. Ali, S. A. Chaudhry, K. Mahmood, S. Garg, Z. Lv, and Y. B. Zikria, "A clogging resistant secure authentication scheme for fog computing services," *Computer Networks*, vol. 185, article 107731, 2021.
- [17] M. A. Saleem, S. K. H. Islam, S. Ahmed, K. Mahmood, and M. Hussain, "Provably secure biometric-based client-server secure communication over unreliable networks," *Journal of Information Security and Applications*, vol. 58, article 102769, 2021.
- [18] R. Canetti and H. Krawczyk, "Analysis of key-exchange protocols and their use for building secure channels," in *International Conference on the Theory and Applications of Cryptographic Techniques*, pp. 453–474, Innsbruck, Austria, 2001.
- [19] D. Dolev and A. C. Yao, "On the security of public key protocols," *IEEE Transactions on Information Theory*, vol. 29, no. 2, pp. 198–208, 1983.
- [20] M. F. Ayub, S. Shamshad, K. Mahmood, S. K. H. Islam, R. M. Parizi, and K.-K. R. Choo, "A provably secure twofactor authentication scheme for usb storage devices," *IEEE Transactions on Consumer Electronics*, vol. 66, no. 4, pp. 396–405, 2020.
- [21] S. A. Chaudhry, A. Irshad, K. Yahya, N. Kumar, M. Alazab, and Y. B. Zikria, "Rotating behind privacy: an improved lightweight authentication scheme for cloud-based iot environment," *ACM Transactions on Internet Technology*, vol. 21, no. 3, pp. 1–19, 2021.
- [22] M. Tanveer, A. U. Khan, N. Kumar, and M. M. Hassan, "Ramp-iod: a robust authenticated key management protocol for the internet of drones," *IEEE Internet of Things Journal*, vol. 1, 2022.
- [23] S. A. Chaudhry, "Designing an efficient and secure message exchange protocol for internet of vehicles," *Networks*, vol. 2021, article 5554318, pp. 1–9, 2021.
- [24] M. Burrows, M. Abadi, and R. M. Needham, "A logic of authentication," *Proceedings of the Royal Society of London. A. Mathematical and Physical Sciences*, vol. 426, no. 1871, pp. 233–271, 1989.
- [25] K. Mahmood, J. Arshad, S. A. Chaudhry, and S. Kumari, "An enhanced anonymous identity-based key agreement protocol for smart grid advanced metering infrastructure," *International Journal of Communication Systems*, vol. 32, no. 16, article e4137, 2019.
- [26] T. Maitra, M. S. Obaidat, R. Amin, S. K. H. Islam, S. A. Chaudhry, and D. Giri, "A robust elgamal-based password-authentication protocol using smart card for client-server communication," *International Journal of Communication Systems*, vol. 30, no. 11, article e3242, 2017.
- [27] F. Wu, X. Li, L. Xu, P. Vijayakumar, and N. Kumar, "A novel three-factor authentication protocol for wireless sensor networks with iot notion," *IEEE Systems Journal*, vol. 15, no. 1, pp. 1120–1129, 2021.
- [28] X. Li, J. Tan, A. Liu, P. Vijayakumar, N. Kumar, and M. Alazab, "A novel uav-enabled data collection scheme for intelligent transportation system through uav speed control," *IEEE Transactions on Intelligent Transportation Systems*, vol. 22, no. 4, pp. 2100–2110, 2021.
- [29] T. Liu, F. Wu, X. Li, and C. Chen, "A new authentication and key agreement protocol for 5g wireless networks," *Telecommunication Systems*, vol. 78, no. 3, pp. 317–329, 2021.
- [30] T. Y. Wu, L. Yang, Q. Meng, X. Guo, and C.-M. Chen, "Fog-driven secure authentication and key exchange scheme for wearable health monitoring system," *Security and Communication Networks*, vol. 2021, Article ID 8368646, 14 pages, 2021.

- [31] T.-Y. Wu, Y. Q. Lee, C. M. Chen, Y. Tian, and N. A. Al-Nabhan, "An enhanced pairing-based authentication scheme for smart grid communications," *Journal of Ambient Intelligence and Humanized Computing*, pp. 1–13, 2021.
- [32] B. Blanchet, B. Smyth, V. Cheval, and M. Sylvestre, "Proverif 2.00: automatic cryptographic protocol verifier, user manual and tutorial," January 2022, <https://bblanche.gitlabpages.inria.fr/proverif/manual.pdf>.
- [33] S. A. Chaudhry, "Correcting "PALK: password-based anonymous lightweight key agreement framework for smart grid"," *International Journal of Electrical Power & Energy Systems*, vol. 125, article 106529, 2021.
- [34] Q. Xie, B. Hu, N. Dong, and D. S. Wong, "Anonymous three-party password-authenticated key exchange scheme for tele-care medical information systems," *PLoS One*, vol. 9, no. 7, article e102747, 2014.

## *Retraction*

# **Retracted: An Automatic Driving Control Method Based on Deep Deterministic Policy Gradient**

### **Wireless Communications and Mobile Computing**

Received 12 December 2023; Accepted 12 December 2023; Published 13 December 2023

Copyright © 2023 Wireless Communications and Mobile Computing. This is an open access article distributed under the Creative Commons Attribution License, which permits unrestricted use, distribution, and reproduction in any medium, provided the original work is properly cited.

This article has been retracted by Hindawi, as publisher, following an investigation undertaken by the publisher [1]. This investigation has uncovered evidence of systematic manipulation of the publication and peer-review process. We cannot, therefore, vouch for the reliability or integrity of this article.

Please note that this notice is intended solely to alert readers that the peer-review process of this article has been compromised.

Wiley and Hindawi regret that the usual quality checks did not identify these issues before publication and have since put additional measures in place to safeguard research integrity.

We wish to credit our Research Integrity and Research Publishing teams and anonymous and named external researchers and research integrity experts for contributing to this investigation.

The corresponding author, as the representative of all authors, has been given the opportunity to register their agreement or disagreement to this retraction. We have kept a record of any response received.

### **References**

- [1] H. Zhang, J. Xu, and J. Qiu, "An Automatic Driving Control Method Based on Deep Deterministic Policy Gradient," *Wireless Communications and Mobile Computing*, vol. 2022, Article ID 7739440, 9 pages, 2022.

## Research Article

# An Automatic Driving Control Method Based on Deep Deterministic Policy Gradient

Haifei Zhang <sup>1</sup>, Jian Xu,<sup>2</sup> and Jianlin Qiu<sup>1,2</sup>

<sup>1</sup>School of Computer and Information Engineering, Nantong Institute of Technology, Yongxing Road 211, Nantong 226002, China

<sup>2</sup>School of Information Science and Technology, Nantong University, Seyuan Road 9, Nantong 226019, China

Correspondence should be addressed to Haifei Zhang; 46462490@qq.com

Received 15 November 2021; Accepted 24 December 2021; Published 24 January 2022

Academic Editor: Ali Kashif Bashir

Copyright © 2022 Haifei Zhang et al. This is an open access article distributed under the Creative Commons Attribution License, which permits unrestricted use, distribution, and reproduction in any medium, provided the original work is properly cited.

The traditional automatic driving behavior decision algorithm needs to manually set complex rules, resulting in long vehicle decision-making time, poor decision-making effect, and no adaptability to the new environment. As one of the main methods in the field of machine learning and intelligent control in recent years, reinforcement learning can learn reasonable and effective policies only by interacting with the environment. Firstly, this paper introduces the current research status of automatic driving technology and the current mainstream automatic driving control methods. Then, it analyzes the characteristics of convolutional neural network, reinforcement learning method (Q-learning), and deep Q network (DQN) and deep deterministic policy gradient (DDPG). Compared with the DQN algorithm based on value function, the DDPG algorithm based on action policy can well solve the continuity problem of action space. Finally, the DDPG algorithm is used to solve the control problem of automatic driving. By designing a reasonable reward function, deep convolution network, and exploration policy, the intelligent vehicle can avoid obstacles and, finally, achieve the purpose of avoiding obstacles and running the whole process in a 2D environment.

## 1. Introduction

The traditional automatic driving technology involves the composition of perception, planning, decision-making, control, and other modules. Through the perception module, the relevant information of the road and environment is obtained, the overall driving route is planned, and then, the planning and perceived information are continued to be used for future driving goals. Such a design may be associated with many task modules. For some complex task systems, the number of modules will be particularly large, and the maintenance cost will be relatively high. At present, some supervised learning methods can achieve their goals through learning and training, but such learning methods need a large amount of learning data as the basis of network training. Through the historical data, some feature points are obtained to act on the experience pool of target decision-making. Such methods need a large amount of labeled data, which cannot achieve the goal of self-help learning and online decision-making. This paper uses the technology of

the deep reinforcement learning-deep deterministic policy gradient method to train the policy network, so that the network can control the intelligent vehicle to avoid obstacles and, finally, achieve the purpose of avoiding obstacles and running the whole process in the 2D environment.

## 2. Related Work

The automatic driving technology in China started later than in other countries. In the real sense, the automatic driving vehicle equipped with some sensors is the beginning of the study of automatic driving in China. After entering the 21st century, the emergence of autonomous driving of unmanned vehicles has created the highest driving speed record in China, reaching 76 kilometers per hour. After that, some other scientific research institutions developed an automatic driving vehicle platform, which has a certain impact in China. The domestic Baidu company is a leader in the IT field and has invested a lot of money and R&D strength in automatic driving. In terms of automatic driving,

fully automatic driving under mixed road conditions has been perfectly realized, and relevant research and development tests are further promoted [1, 2]. By the end of November 2016, the number of patent applications for Baidu automatic driving technology had reached 605. Relying mainly on the accumulation of artificial intelligence and deep learning, Baidu is engaged in the development of ten technologies related to driverless vehicles, including ten technologies of environmental perception, behavior prediction, planning and control, operating system, intelligent interconnection, on-board hardware, human-computer interaction, high-precision positioning, high-precision map, and system security [3]. The methods based on reinforcement learning and deep reinforcement learning have achieved good results in automatic driving and have great application significance in training efficiency and driving strategies. However, further research and development are still needed in complex problems and considering pedestrians [4–7]. In terms of deep learning automatic driving, scholars from Tsinghua University have improved the robustness and accuracy of algorithm recognition through the research on CNN-related algorithms and achieved good results in multitarget recognition, but there are too many redundant results and low efficiency [8]. The automatic driving technology using machine learning mainly studies how computers acquire knowledge or optimize their own skills through experience or exploring the environment to improve learning and computing efficiency. This is a technical field used to solve automatic driving in the current development [9]. Transfer trajectory planning, reinforcement learning, deep reinforcement learning, and machine learning are widely used to solve the problem of automatic driving [10–12]. At present, although some research results have been achieved in automatic driving technology, there are still some problems in many aspects. Therefore, it is very meaningful to use the deep deterministic policy gradient method to study automatic driving technology.

Foreign automatic driving technology, from the beginning of the unmanned carrier, automatic driving handling equipment first appeared in the United States. It was used to transport goods in the grocery warehouse with arranged wires [3]. After that, someone successfully developed an autonomous robot, which can drive automatically on low speed and flat roads. Some automatic driving competitions abroad have also promoted the development of automatic driving technology. The foreign Google company is a leader in the technology of automatic driving in the industry. Since the preparation, it participated in the driving test on time urban roads with the developed automatic driving vehicle in 2010 [13–15]. Bojarski et al. [16] proposed an end-to-end learning automatic driving mode, which can learn the steering wheel control policy from the data captured by the vehicle camera through the convolutional neural network. However, this method needs to input the data of human driving into the training network, and the cost of data acquisition and annotation is large. Chae et al. [17] proposed a brake control system based on deep reinforcement learning. Based on the DQN algorithm, the system judges whether braking is required and the braking force through the data

captured by the sensor, so as to avoid hitting obstacles and pedestrians. However, this method only applies deep reinforcement learning to the brake control system, which has great limitations. Sallab et al. proposed an end-to-end reinforcement learning policy [18] for lane auxiliary maintenance, comparing the DQN algorithm of discrete policy with the DDAC algorithm of discrete policy, and achieved good results. Sallab et al. proposed a deep reinforcement learning framework for automatic driving [19], which divides automatic driving into three stages: identification, prediction, and planning. The framework uses a deep neural network for identification and a cyclic neural network for prediction and uses the method of deep reinforcement learning to train the planning network segment. Chen et al. [20] proposed a new autonomous driving mode based on direct perception, which uses the deep ConvNet architecture to estimate the enlightenment of driving behavior, rather than analyzing the whole scene (intermediary perception method) or blindly mapping the image directly to driving commands (behavior reflection method). In May 2016, Google announced its cooperation with Fiat Chrysler Automobiles (FCA). FCA produced 100 Pacifica hybrid vans for Google, equipped with a complete set of sensors, telematics, and computing units. In October, the test vehicle equipped with the new automatic driving system was tested in many places with extreme weather in the United States. At the same time, automobile enterprises including Japan and Germany have also joined the research of automatic driving and are jointly committed to the research of automatic driving technology.

### 3. Reinforcement Learning

*3.1. Principles of Reinforcement Learning.* Reinforcement learning is a process in which agents learn how to take a series of actions in the environment, so as to maximize the cumulative reward. The basic framework of reinforcement learning algorithm is shown in Figure 1. The agent in the algorithm represents the subject of problem solving. For example, the agent in this study is an autonomous vehicle. The agent tries to make an action in the environment, which will lead to the environment being updated, and the agent will transition to a new state. In such a process, the agent can get the reward corresponding to the previous action at the same time. Repeating this process will produce a large number of training sample sets. Using these data to continuously optimize the behavior of the agent, after a long time of training, we will get an optimal policy to complete the task.

The theoretical basis of reinforcement learning is the Markov decision process (MDP). The most basic form of MDP is the Markov chain, which must conform to the Markov property, that is, the conditional probability distribution  $P$  of the future state  $S$  of the system only depends on the current state and has nothing to do with the past state, which will make the observed state conditionally independent.

The Markov decision process includes the following steps: give the agent the initial state  $s_1$ , the agent is in the

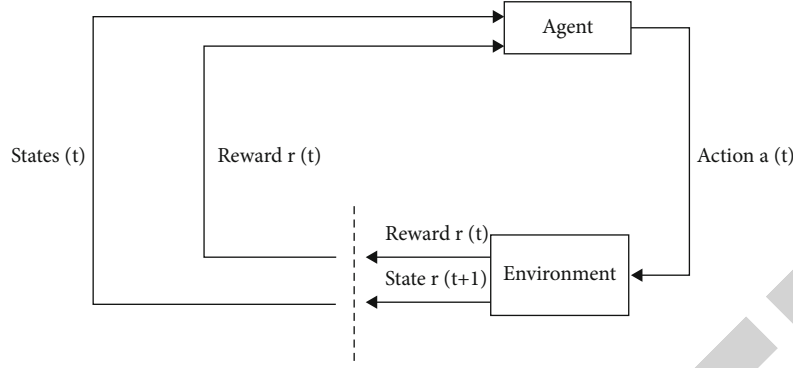


FIGURE 1: Basic framework of reinforcement learning.

$s_1$  state, select the action  $a_1$  from the action space  $A$ , reach the next state  $s_2$ , get the reward  $r_1$ , continue to select the action  $a_2$ , get the reward  $r_2$ , and enter the state  $s_3$ , and so on until the agent reaches the maximum number of iterative steps  $T$ . The process from any time  $t$  to the ending state is called an episode, and the reward obtained in the episode is expressed as the following equation:

$$G_t = r_{t+1} + \gamma r_{t+2} + \gamma^2 r_{t+3} + \dots + \gamma^T r_{t+T+1} = \sum_{k=0}^T \gamma^k r_{t+k+1}. \quad (1)$$

Among them,  $\gamma$  is a number between  $[0, 1]$ ;  $\gamma^k$  means that the larger the time step  $t$  is, the less influence the reward will have on the current action. Since the reward obtained fluctuates greatly, the expectation of reward is introduced as the state-value in the following equation:

$$V(s) = E[G | S_t = s]. \quad (2)$$

The learning process of reinforcement learning is the process of optimizing the policy by maximizing the state value function. The policy is the control rule of the agent, which can be expressed as the probability distribution function of the actions that can be taken in a certain state. That is,

$$\pi(a | s) = P[A_t = a | S_t = s]. \quad (3)$$

If you want to maximize the reward in the whole stage, you can achieve it by selecting the maximum reward action in each state in the agent and introducing the Bellman equation to define the state value in the following equation:

$$\begin{aligned} V(s) &= \max_{a \in A} E_{s' \in S} [r_{s,a} + \gamma V_{s'}] \\ &= \max_{a \in A} \sum_{s' \in S} p_{a,s \rightarrow s'} (r_{s,a} + \gamma V(s')), \end{aligned} \quad (4)$$

where  $V(s)$  and  $V(s')$  represent the value of the current state and the target state, respectively;  $p_{a,s \rightarrow s'}$  represents the probability that the agent reaches the target state  $s'$  after an action  $a$  is selected in the state  $s$ . According to this formula, the value

expression of the action can be extracted as the following equation:

$$Q(s, a) = E_{s' \in S} [r_{s,a} + \gamma V_{s'}] = \sum_{s' \in S} p_{a,s \rightarrow s'} (r_{s,a} + \gamma V(s')). \quad (5)$$

Thus, the theoretical basis of Q-learning is obtained as the following equation:

$$Q(s, a) = r_{s,a} + \gamma \max_{a' \in A} Q(s', a'). \quad (6)$$

**3.2. Q-Learning Algorithm.** The Q-learning algorithm is an algorithm based on value function, which belongs to the model-free learning method. The learning algorithm establishes a “state action” Q table, learns the value of a specific state and a specific action, records the action value function obtained by the action taken in the current state, and updates the Q table through the reward brought by each action. The update method is expressed in the following equation:

$$Q(s, a) = (1 - \lambda_t) Q(s, a) + \lambda_t [r + \gamma \max_{a' \in A} Q(s', a')], \quad (7)$$

where  $A$  is the collection of a series of actions,  $a$  is the action taken in the current state,  $s'$  is the next state, and  $a'$  is the next predicted action.  $\gamma$  is the discount factor, and  $\lambda$  is the learning rate. The larger the  $\lambda$  value, the faster the learning convergence. If it is too large, it is easier to overconverge rather than to arrive at the optimal solution. The flow chart of the Q-learning algorithm is shown in Figure 2.

## 4. Deep Reinforcement Learning

Deep reinforcement learning is the combination of deep learning and reinforcement learning. Classical algorithms include the DQN algorithm and DDPG algorithm. The DDPG algorithm is further developed on the basis of the DQN algorithm. It is a model-free and off-policy algorithm.

**4.1. DQN Algorithm.** The traditional DQN [21] is a method combining Q-learning and the deep neural network. Deep Q network has advantages in dealing with continuous state space, but it cannot solve the problem of continuous action

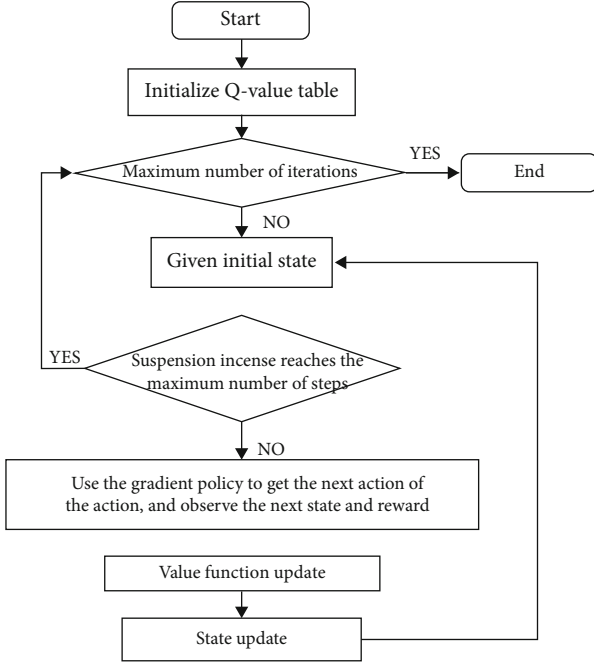


FIGURE 2: Flow chart of Q-learning algorithm.

space. Figure 3 shows the structure of the DQN algorithm, and Figure 4 shows the flow chart of the DQN algorithm.

**4.2. DDPG Algorithm.** The DDPG algorithm [22] is an off-policy and model-free deep reinforcement learning algorithm, combining deep learning and reinforcement learning, integrating the advantages of the DQN algorithm and Actor-Critic (AC) algorithm. The DDPG algorithm is the same as the AC algorithm framework, but its neural network division is finer. The DQN algorithm has good performance in discrete problems. The DDPG algorithm uses the experience of DQN for reference to solve the problem of continuous control and realize end-to-end learning. The algorithm flow of DDPG is shown in Figure 5, in which the actor network accepts the input state, makes action selection, and outputs action variables; the critic network evaluates the quality of the selected action and calculates the reward value. The detailed steps of the DDPG algorithm are as follows:

- (1) Initialize the parameters of the neural network. The actor selects an action according to the behavior policy, adds noise  $N_t$  to the action output by the policy network to increase exploration, and transmits it to the environment to execute the action  $a_t$ :

$$a_t = \mu(s_t | \theta^\mu) + N_t. \quad (8)$$

- (2) After the environment is executed  $a_t$ , return to reward  $r_t$  and new state  $s_{t+1}$
- (3) Actor stores the state transition  $(s_t, a_t, r_t, s_{t+1})$  into the replay memory as the training set of the online network

- (4) DDPG creates two copies of neural networks for the policy network and the Q network, respectively, the online network and the target network. The update method of the policy network is as follows:

$$\begin{cases} \text{online : } Q(s, a | \theta^\mu), & \text{gradient update } \theta^\mu, \\ \text{target : } Q(s, a | \theta^{\mu'}), & \text{soft update } \theta^{\mu'}. \end{cases} \quad (9)$$

The Q network update method is as follows:

$$\begin{cases} \text{online : } Q(s, a | \theta^Q), & \text{gradient update } \theta^Q, \\ \text{target : } Q(s, a | \theta^{Q'}), & \text{soft update } \theta^{Q'}. \end{cases} \quad (10)$$

$N$  transition data are randomly sampled from replay memory as minibatch training data of the online policy network and online Q network. Single transition data in minibatch is represented by  $(s_i, a_i, r_i, s_{i+1})$ .

- (5) In critical, calculate the Q gradient of the online Q network:

The loss of the Q network is defined as

$$L = \frac{1}{N} \sum_i (y_i - Q(s_i, a_i | \theta^Q))^2, \quad (11)$$

$$y_i = r_i + \gamma Q'(s_{i+1}, \mu'(s_{i+1} | \theta^{\mu'}) | \theta^{Q'}).$$

The gradient for  $L$  and  $\theta^Q$  can be obtained:  $\nabla_{\theta^Q} L$ , where the calculation uses the target policy network  $\mu'$  and target Q network  $Q'$ .

- (6) Update online Q: update  $\theta^Q$  with the Adam optimizer
- (7) In the actor, calculate the policy gradient of the policy network:

$$\nabla_{\theta^\mu} J_\beta(\mu) \approx \frac{1}{N} \cdot \left( \nabla_\alpha Q(s, a | \theta^Q) \Big|_{s=s_i, a=w(s_i)} \cdot \nabla_{\theta^\mu} \mu(s | \theta^\mu) \Big|_{s=s_i} \right). \quad (12)$$

- (8) Update online policy network: update  $\theta^\mu$  with the Adam optimizer
- (9) The parameters of the target network adopt the method of soft update:

$$\begin{cases} \theta^{Q'} \leftarrow \tau \theta^Q + (1 - \tau) \theta^{Q'}, \\ \theta^{\mu'} \leftarrow \tau \theta^\mu + (1 - \tau) \theta^{\mu'}. \end{cases} \quad (13)$$



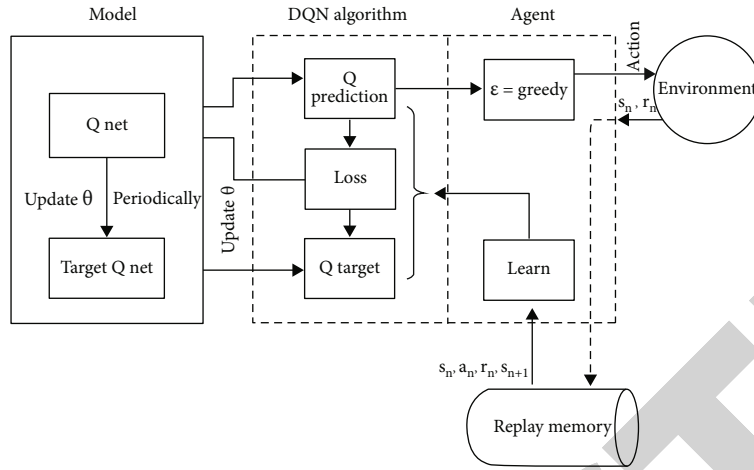


FIGURE 3: DQN algorithm flow structure.

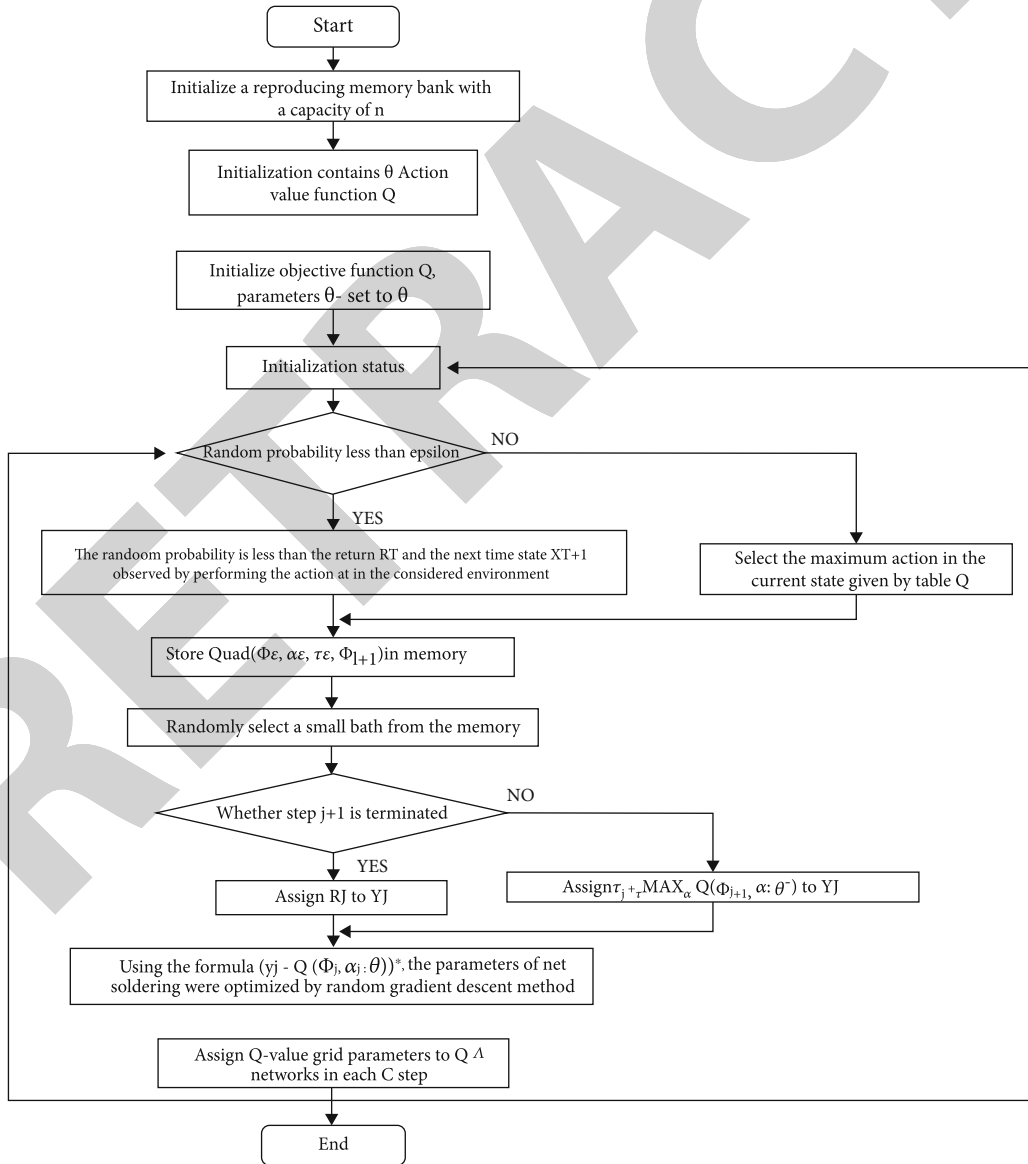


FIGURE 4: The flow chart of DQN algorithm.

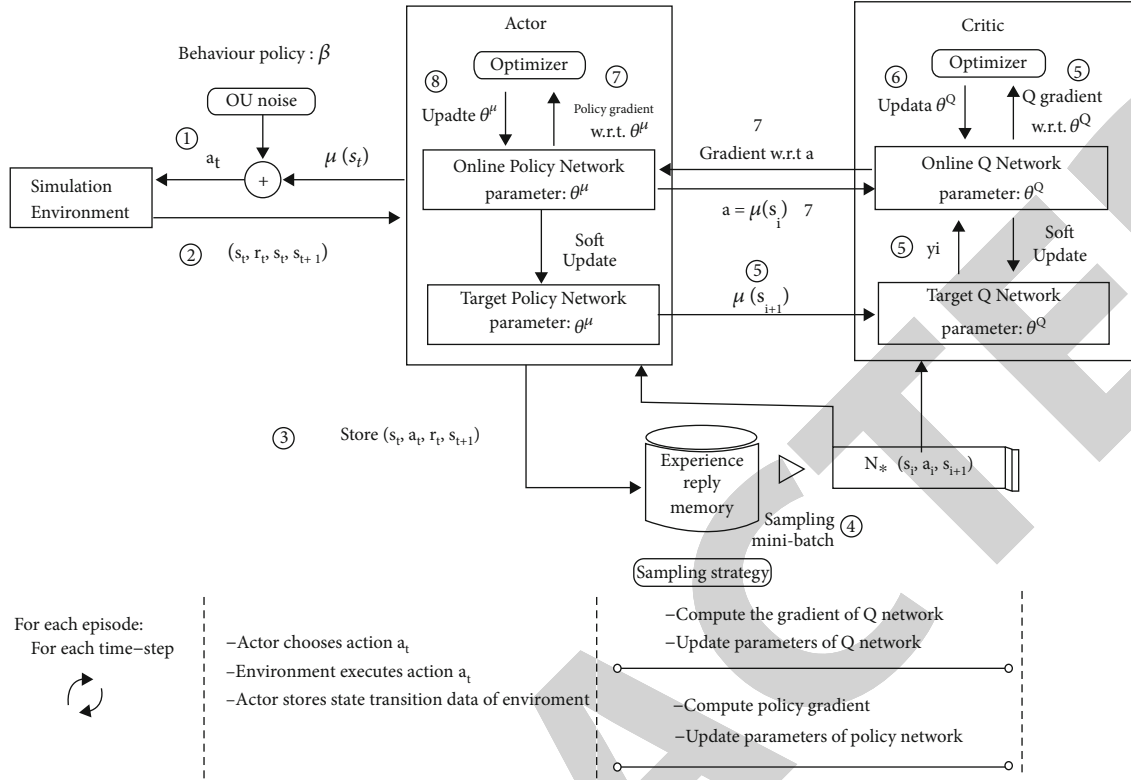


FIGURE 5: The algorithm flow chart of DDPG.

In general, the DDPG algorithm uses the Actor-Critic framework to iterate the training of the policy network and Q network through the interaction among the environment, actor, and critic.

## 5. Automatic Driving Control Method Based on DDPG

**5.1. System Structure.** The model of automatic driving is mainly divided into two parts, including the DDPG algorithm and the experimental simulation. By using the DDPG algorithm to train the neural network of the automatic driving model, the network can control the motor vehicle to avoid obstacles and drive normally on the road.

The experimental simulation part mainly includes the motor vehicle and the environment of the motor vehicle. After receiving the control sensor, the information of the environment is continuously transmitted to the DDPG algorithm, so that the algorithm can obtain the state variables and reward values. Through the continuous training of the network and the continuous updating of network parameters, the target reward value is also continuously improved. The structure diagram of the automatic driving control system model is shown in Figure 6. It mainly reflects that in the motor vehicle motion model, according to the control command action execution of the environment, the new state value is obtained and then the obtained reward value; the relevant parameters of this motion are trained in the neural network; and the trained network is continuously updated

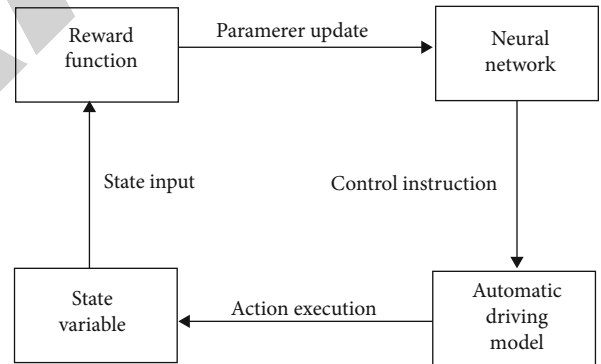


FIGURE 6: Structure of automatic driving control system.

until the end. Such a process ends with the maximum number of iterations.

**5.2. Automatic Driving Control Model.** The automatic driving model involved in this design uses the two-dimensional  $500 \times 500$  pixel space to control the automatic driving motor vehicle, in which the range of obstacles is the pixel space of the middle area  $260 \times 260$ , and the parts  $(120, 120)$ ,  $(380, 120)$ ,  $(380, 380)$ , and  $(120, 380)$  surrounded by the following four points and the areas beyond  $500 \times 500$  are the range of obstacles. The motor vehicle adopts the mode of fixed speed, with 5 sensors; the farthest detectable distance is 150; and the position coordinate of the motor vehicle starting training is  $(450, 300)$ . The sensors are located in the middle and front of both sides of the vehicle, 45 degrees in front of the left and

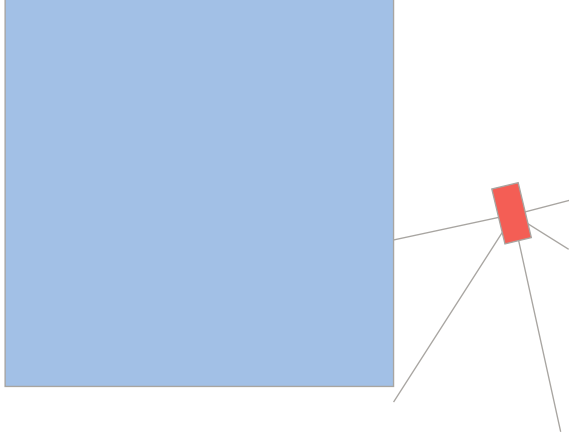


FIGURE 7: Automatic driving model.

45 degrees in front of the right. A total of five sensors are used to detect the operation of the current vehicle. The automatic driving control model is shown in Figure 7. The unmanned vehicle is marked as a  $20 \times 40$  pixel coordinate area. The sensor data mainly includes the distance from the obstacle and its coordinates. During the training process, the straight and turning directions of the agent are controlled by the network.

### 5.3. Automatic Driving Control Method

**5.3.1. Reward.** The design of the reward function of the unmanned vehicle under this model is relatively simple. It mainly detects whether the unmanned vehicle encounters obstacles during each movement. If the target is -1, otherwise it is 0.

$$r = \begin{cases} 0, & \text{No\_collision,} \\ -1, & \text{Have\_collision.} \end{cases} \quad (14)$$

**5.3.2. State.** According to the current model design, the relevant parameters of the unmanned vehicle are selected as the training parameters of the DDPG algorithm, which mainly includes the five distance parameters detected by the sensor. When the minimum distance between the motion sensor and the obstacle is less than half of the unmanned vehicle, it means that the unmanned vehicle has a collision, and the reward is -1.

## 6. Simulation Experiment and Result Analysis

**6.1. Experimental Setup.** The parameters for solving the automatic driving problem using the DDPG algorithm are as follows: the maximum number of iterations is 500, the maximum number of steps per iteration is 600; the reward discount factor is 0.9; the learning rate of the actor and critic is 0.0001; batch-size, that is, the number of samples obtained in one training, is 16; and the number of neurons is 120. Simulation training for this problem was done in Python language and observation on the model training

was done according to the model diagram, which can better reflect the current training degree of the model.

**6.2. Result Analysis.** The training of the algorithm at the beginning of model training is randomly intercepted. Through the visual diagram and the training process, it can be seen that the learning ability of the model at the beginning of training is not strong, the model can only be explored at will, and it is easy to collide at the beginning. Occasionally, automatic driving can be carried out briefly in a single direction. According to the diagram, we can only learn at the initial stage, mainly to explore some movement directions, and the uncertainty in the movement direction is not high.

In the middle of model training, a model diagram in the training process is randomly intercepted. As can be seen from the figure, the automatic driving model of the unmanned vehicle has been able to avoid obstacles for turning or straight operation and can better avoid obstacles in the process of turning. The process of quickly avoiding obstacles and driving forward has been basically realized. The automatic driving control model can still gradually find a better motion planning direction through random straight or turning. In the process of this training, when encountering some places that have not been explored, there is still the possibility of collision, but with the continuation of the iteration, the driving can be basically completed.

In the later stage of model training, a model diagram in the training process is randomly intercepted. As can be seen from the figure, the unmanned vehicle has been able to drive better in the control model, avoid obstacles perfectly, and hardly encounter obstacles. In the later stage of training, the network has basically been trained and formed, which can quickly judge whether the next action is straight or turning, and basically reaches the maximum steps of each iteration. From this aspect, it also reflects that the learning ability of the model is very good in the later stage and can well control the movement of the unmanned vehicle. The agent driverless model already has a relatively formed network model. The network parameters are optimized and the loss value is low, so this good effect can be achieved. Through this training, it is more fully explained that the DDPG algorithm is feasible and effective in solving the unmanned control problem.

In this model simulation experiment, the change of reward value in each iteration is shown in Figure 8. It can be seen from the figure that after about 300 iterations, the reward value obtained can basically be stable at 0, indicating that collision-free motion has been basically realized at this time. The 500 iterations set in this simulation basically converge to about 300 times, and the relative number of times to reach convergence is still relatively small. This shows that the DDPG method based on the deep deterministic policy gradient has fast convergence speed and obvious effect in solving the unmanned vehicle automatic driving problem, which shows that the depth reinforcement learning algorithm has better advantages in this problem. Through this experiment, we can know that the method based on deep reinforcement learning makes the model have better self-

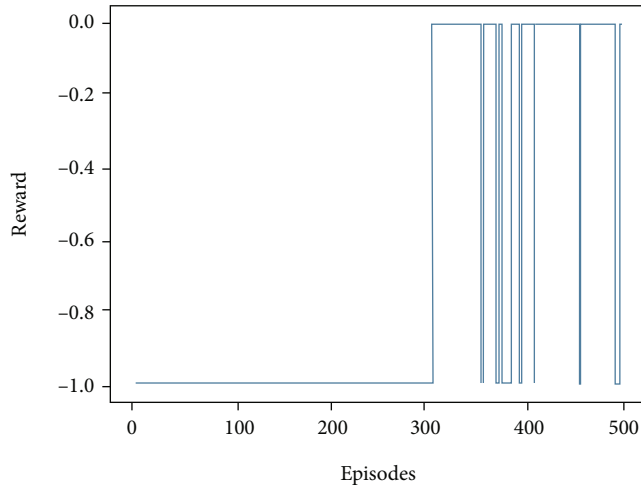


FIGURE 8: The reward value of each iteration of automatic driving model.

learning ability. Compared with the general supervised learning method, the trained model agent has obvious advantages. The agents in the model generate a large number of training data to train the network according to the environmental changes, which is flexible and convenient for network training. The network can be trained and analyzed without too much label data.

It can be seen from Figure 9 that at the initial stage of iteration, the unmanned vehicle automatic driving model performs fewer steps, and the model easily collides with obstacles. After 300 iterations, the model can basically achieve the maximum number of steps each time. It can also be seen that due to the continuous training and the continuous optimization of the network, the network can better judge the selection decision of execution action. At the later stage of training, the collision-free driving in the model can be basically realized. This better shows that the agent algorithm model has strong applicability, strong robustness, and high stability. At the same time, the test mode is used to test the network. The trained network can well control the automatic driving of the unmanned vehicle and avoid obstacles.

## 7. Conclusions

This paper introduces the current research status of automatic driving technology and analyzes the current mainstream automatic driving control methods. Then, it analyzes the characteristics of the convolutional neural network, reinforcement learning method (Q-learning), and deep Q network (DQN) and deep deterministic policy gradient (DDPG). Compared with the DQN algorithm based on value function, the DDPG algorithm based on action policy can well solve the continuity problem of action space. Finally, the DDPG algorithm is used to solve the control problem of automatic driving. Data are collected through training, and the neural network training is carried out on the automatic driving model, so that the network can control the intelligent vehicle to avoid obstacles and finally achieve the goal that the intelligent vehicle can avoid obstacles and

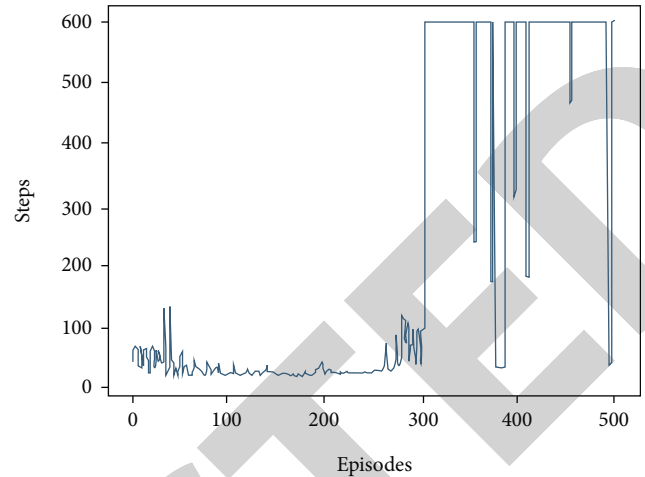


FIGURE 9: The number of steps of each episode of automatic driving model.

run the whole process in 2D environment. In terms of automatic driving model design, this design simply uses the unmanned vehicle driving in two-dimensional space for control, and the driving action considered is only limited to straight ahead and turning. It contains less automatic driving control information and does not carry out training and testing in real three-dimensional space or mature automatic driving model. After that, the automatic vehicle control of three-dimensional and multidimensional model can be considered for training simulation test.

## Data Availability

The experiments involved in this paper do not require any raw/processed data. The model is automatically trained by the DDPG algorithm.

## Conflicts of Interest

The authors declare that they have no conflicts of interest to report regarding the present study.

## Acknowledgments

This work is sponsored by the following: (1) the Training Project of Top Scientific Research Talents of Nantong Institute of Technology under Grant No. XBJRC2021005; (2) the Science and Technology Planning Project of Nantong City under Grant Nos. JC2021132, JCZ20172, JCZ20151, JCZ20148, and MS22021028; (3) the Scientific Research Backbone Training Project of Nantong Institute of Technology under Grant No. ZQNGG109; (4) the Key Projects of Innovation and Entrepreneurship Training Program for College Students in Jiangsu Province in 2021 under Grant No. 202112056003Z; and (5) the Innovation and Entrepreneurship Training Program of Nantong Institute of Technology in 2021 under Grant No. XDC2021036.

## Research Article

# CUCKOO-ANN Based Novel Energy-Efficient Optimization Technique for IoT Sensor Node Modelling

Deepshikha Bhargava <sup>1</sup>, B. Prasanalakshmi <sup>2</sup>, Thavavel Vaiyapuri <sup>3</sup>,  
Hemaid Alsulami <sup>4</sup>, Suhail H. Serbaya <sup>5</sup>, and Abdul Wahab Rahmani <sup>6</sup>

<sup>1</sup>DIT University, Dehradun, India

<sup>2</sup>Department of Computer Science, Center for Artificial Intelligence, King Khalid University, Saudi Arabia

<sup>3</sup>College of Computer Engineering and Sciences, Prince Sattam Bin Abdulaziz University, Saudi Arabia

<sup>4</sup>Department of Industrial Engineering, King Abdulaziz University, Jeddah 21589, Saudi Arabia

<sup>5</sup>Department of Industrial Engineering, Faculty of Engineering, King Abdul Aziz University, Jeddah 21589, Saudi Arabia

<sup>6</sup>Isteqlal Institute of Higher Education, Kabul, Afghanistan

Correspondence should be addressed to B. Prasanalakshmi; prengaraj@kku.edu.sa  
and Abdul Wahab Rahmani; ab.wahab.professor@isteqlal.edu.af

Received 3 December 2021; Revised 22 December 2021; Accepted 30 December 2021; Published 17 January 2022

Academic Editor: Shalli Rani

Copyright © 2022 Deepshikha Bhargava et al. This is an open access article distributed under the Creative Commons Attribution License, which permits unrestricted use, distribution, and reproduction in any medium, provided the original work is properly cited.

Wireless sensor networks (WSNs) based on the Internet of Things (IoT) are now one of the most prominent wireless sensor communication technologies. WSNs are often developed for particular applications such as monitoring or tracking in either indoor or outdoor environments, where battery power is a critical consideration. To overcome this issue, several routing approaches have been presented in recent years. Nonetheless, the extension of the network lifetime in light of the sensor capabilities remains an open subject. In this research, a CUCKOO-ANN based optimization technique is applied to obtain a more efficient and dependable energy efficient solution in IoT-WSN. The proposed method uses time constraints to minimize the distance between sources and sink with the objective of a low-cost path. Using the property of CUCKOO method for solving nonlinear problem and utilizing the ANN parallel handling capability, this method is formulated. The resented model holds significant promise since it reduces average execution time, has a high potential for enhancing data centre energy efficiency, and can effectively meet customer service level agreements. By considering the mobility of the nodes, the technique outperformed with an efficiency of 98% compared with other methods. The MATLAB software is used to simulate the proposed model.

## 1. Introduction

Sensor nodes serve as the main backbone in wireless sensor networks (WSNs), which are among the most common wireless communication networks [1, 2]. In terms of sensor designs, WSNs can have either homogeneous or heterogeneous sensors, with numbers ranging from hundreds to thousands [3, 4]. Most WSNs are tailored to a specific use case, and their sensor nodes typically offer fundamental functions including sensing, processing, computation, and communication [5]. The communication is mostly done with neighboring nodes using radio frequency electromagnetic pulses [6].

Wireless sensor networks (WSNs) based on the Internet of Things (IoT) have recently opened up a new exciting arena for novel and new sorts of applications [7–10]. The small and active sensor nodes are the basic structure of WSNs that monitor their surroundings, analyses data (in few cases), and send/receive refine/processed data to/from other neighboring sensor nodes. In the centralized network, these sensing nodes are spread across the defined area connecting base node with sink node [11]. In centralized networks, the sink collects sensor data for end-user use. In certain situations, the sink can also send network pol to sensor nodes to activate them [12, 13]. Figure 1 depicts the basic general architecture of the WSNs encountered in this

investigation. The message is sent from the source sensor to the sink sensor via the most efficient way feasible, which includes the use of other random sensors [14–16].

In contrast to most existing research, which focuses on a specific element of WSNs [17], we define an Energy Driven Architecture (EDA) as a new architecture for decreasing the total energy consumption of WSNs. The architecture specifies the network's generic and important energy-consuming parts. WSNs are deployed using EDA as a constituent-based architecture based on energy dissipation through their components. This perspective on overall energy use in WSNs can be used to optimize and balance energy utilization while also extending network lifetime. The main objective of this research is as follows:

- (1) To find the best possible routes to transfer message from source sensor node to sink sensor node
- (2) To reduce the route cost for transferring the message

After extensive literature survey, it was found that CUCKOO method is very effective in solving nonlinear problems and when combines with ANN which have advantage of parallel processing make CUCKOO-ANN a best combination for this research work. The presented model's goal is to provide a high-performance, low-power computer infrastructure that also meets an energy-efficient and secure service mode.

The following contributions are highlighted in this paper in this regard:

- (1) Using CUCKOO-ANN based optimization technique for reducing total cost of the path
- (2) The IoT-WSN is placed optimally to transfer message from sink to source with minimum time constraints

## 2. IoT-WSN Background and Problem Formulation

*2.1. IoT-WSN Architecture.* Installing IoT technology in residential and commercial buildings enables businesses and individuals to measure their energy use and make changes to reduce demand and boost efficiency. Buildings, whether commercial, residential, or industrial, have a substantial influence on the environment as well as the overall cost of energy use. IoT sensors may be installed throughout a building and send real-time energy use data to a data centre for analysis. Organizations may utilize IoT to monitor important assets such as equipment, air conditioning systems, water heating systems, large refrigerating units, and lighting systems on an individual basis [18, 19]. Small batteries and power harvesting techniques power IoT-WSN sensors, which are often put in inaccessible places; replacing batteries is not an option [20]. Not only does using a battery shorten the sensor's lifespan, but it also makes WSN design and management more challenging. However, energy scarcity has prompted extensive study into WSNs at all layers of the protocol stack. The OSI model and the Internet, for

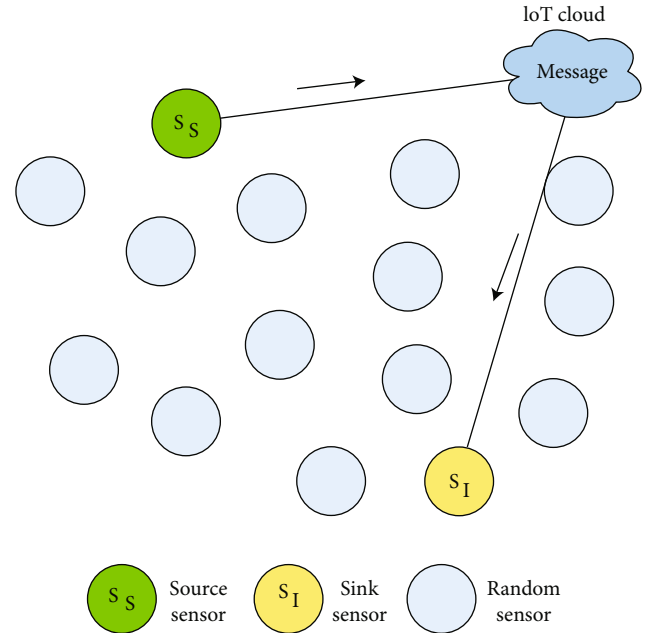


FIGURE 1: IoT-WSN architecture.

example, are functional models arranged as layers, with each layer offering services to the layer above it (for example, the application layer delivers services to end users) [21, 22]. The quality of a network's service parameters is routinely evaluated, including availability, delay, throughput, jitter, dependability, and even security [23]. However, there are various issues when it comes to energy consumption (EC), because there is no comprehensive model for analyzing and optimizing the network that includes EC. Most current energy minimization models [24] focus on sending and receiving data, while other parameters are ignored. The power consumption model in [25, 26] focused on the cost of sending and receiving data and calculated the upper limit of single hop distance energy efficiency [27]. This method proposes an intermediate node between the source and the destination in order to conserve energy during retransmission. Other ways use the power consumption model described in [25] to assess the energy efficiency of wireless sensor networks.

In the physical layer of WSN, a radio connection communication system is implemented which consume energy whenever the signal is transmitted with in the sensor network. The physical layer modulates and codes data in the transmitter, and it must optimally decode data in the receiver. Idle, sleep, and active are the three modes of the radio channel. The time and energy required to switch between different modes and transmit and receive states must be reduced in order to save energy.

Furthermore, a low-power listening method may also be utilized at the physical layer, with the key idea being to turn on the receiver periodically to sample the incoming data. This duty-cycle method decreases the network's idle listening overhead [28]. Furthermore, sending and receiving data consume the same amount of energy on the radio channel; energy-efficient MAC protocols must maximize sensor sleep time [29]. Due to real-time monitoring and interaction with

different aspects of a sensing node, the operating system (OS) is probably the ideal place to optimize and manage energy usage of a WSN at the node level. Clustering is another strategy for reducing energy consumption while ensuring that deadlines are met. Clustering, on the other hand, has a technical limitation: it can only be employed in wireless sensor clusters with DVS processors and compute capability [30–32]. To overcome this problem, the paper suggests a new approach as stated in next sections.

**2.2. Problem Formulation for Energy Module.** The goal of this research is to reduce and conserve energy in WSNs. CUCKOO search is used in the initial phase to construct static clusters to reduce the use of energy sensor nodes. According to [33], the radio model used is the most commonly used assumptions, and models in sensor network simulation and analysis are listed below.

Nodes are spread in a 2-dimensional space at random in a uniform distribution, and all sensors are aware of the location of the Base Station (BS). Depending on the distance to the receiver, the nodes can transmit at different power levels. The nodes have no idea where they are. If the transmit power level is known, the nodes may estimate the approximate distance using the received signal intensity, and communication between nodes is not affected by multipath fading. Here, a network operating model based on rounds is used, similar to that of LEACH and HEED [34, 35]. A clustering phase precedes the data collection phase in each round.

$$E_{ms} = \{1E_{eng} + E_a \cdot d^2\} \text{ for } 0 \leq d \leq d_1, \quad (1)$$

$$E_{ms} = \{1E_{eng} + E_a \cdot d^4\} \text{ for } d \geq d_1. \quad (2)$$

Equations (1) and (2) give the amount of energy consumed for transmission  $E_{ms}$  (Watts) of a 1-bit message across a distance  $d$  (meters). The energy expended per bit during the execution of the transmitter, or receiver circuit is represented by the  $E_{eng}$ .  $E_a$  (Watts) is energy consumed by the amplifier. The main aim of this research is to minimize the  $E_{ms}$ .

### 3. Proposed CUCKOO-ANN Optimization Modeling for IoT-WSN

The energy consumption of IoT-WSN depends on the distance and the message bit. To have the efficient system CUCKOO-ANN based model is proposed as shown in Figure 2. The CUCKOO search has three stage as described below:

- (1) *Stage 1.* Random placement of eggs
- (2) *Stage 2.* The finest nest having good quality of eggs is selected and carried over for next generation
- (3) *Stage 3.* Probability of getting discovered by the host bird nest

Taking into account these three stages of CUCKOO search, it increases the system effectiveness for global opti-

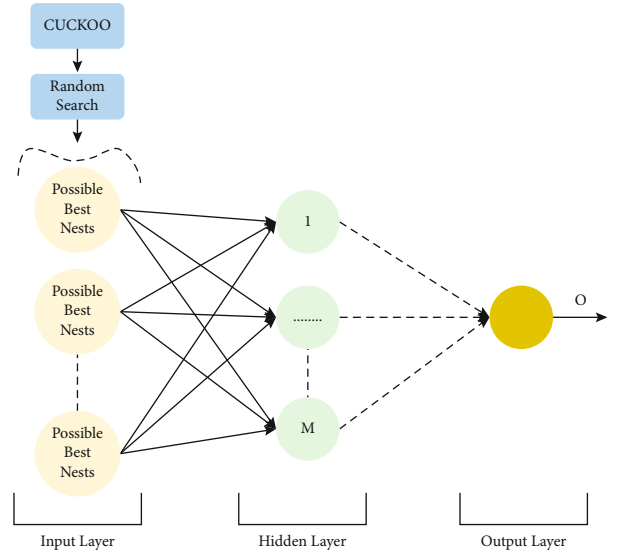


FIGURE 2: Proposed CUCKOO-ANN basic diagram.

mizations by maintaining a balance between global random walk and local random walk. The output of CUCKOO search regarding to possible best nests is used as input for the ANN. The output of ANN is the best efficient path having the lowest cost in terms of path from source to sink leads to energy efficient system.

**3.1. Proposed CUCKOO Search Modeling for Possible Best Nests.** The aim of the CUCKOO search in IoT-WSN is to find all the best possible path to send the message from the source sensor to the sink sensor by using the random sensors present in the vicinity. This is achieved using the nature of the CUCKOO which lay eggs in the range of 2-10, which can be used as lower and upper limit of egg dedication to each CUCKOO involved. The second habit is they try to lay eggs at maximum distance from their source habitat. The flow chart in Figure 3 shows the use of CUCKOO search for finding the best possible route from source sensors to base/sink sensor. For selecting best sensor nodes for message transfer, the fitness function of each random node must be calculated using the equation:

$$\begin{aligned} f_n &= \alpha_1 f_1 + \alpha_2 f_2 + \alpha_3 f_3, \\ \alpha_1 + \alpha_2 + \alpha_3 &= 1, \end{aligned} \quad (3)$$

where  $\alpha$  are the constants and having a value range from 0 to 1. The fitness ( $f$ ) 1, 2, and 3 is calculated using the equations:

$$\begin{aligned} f_1 &= \frac{1}{m} \times \sum_{n=1}^m \left( \frac{\text{dist}(S_s, S_T)}{m} \right), \\ f_2 &= \frac{E_{ms}}{E_t}, \\ f_3 &= \frac{CK}{m}. \end{aligned} \quad (4)$$

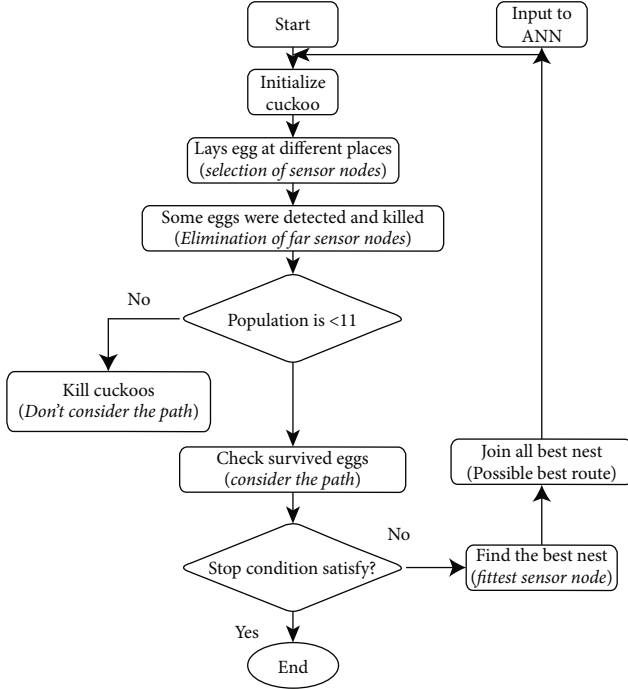


FIGURE 3: CUCKOO search for best sensor nodes.

TABLE 1: Simulation parameters.

Parameters	Value
Area	800 m * 800 m
No. of sensors	80
Initial energy	4 Watts
Data packet size	2 Mb/sec
No. of rounds	200
Motion coefficient (constant)	20
No. of possible nest	80
No. of CUCKOOS	5
Max. No. of CUCKOOS	20
No. of eggs in each nest	2
Radius coefficient (constant)	0.05
Cuckoo population variation	1e-10

Here,  $m$  is the number of nodes in the system,  $S_s$  and  $S_t$  are the source node and sink/base node,  $E_t$  (Watts) is the total energy of the node in watts, and  $CK$  is the number of CUCKOOS assigned. After calculating the fitness function of each node, the best nodes having high fitness values nodes are chosen for sending the message. For the selection of the best route, cost of each route is evaluated using the equation:

$$\text{cost} = d_1 \times \gamma + d_2 \times (1 + \gamma). \quad (5)$$

The  $d_1$  is the function of distance between the random nodes present in the system, and  $d_2$  is the function of

energy consumption of the nodes. The expression for  $d_1$  and  $d_2$  is given in equations (6) and (7).

$$d_1 = \max \left\{ \sum \frac{x(m, S_s, S_t)}{CK} \right\}, \quad (6)$$

$$d_2 = \sum_{n=1}^m \frac{E(m_n)}{E_t}. \quad (7)$$

Minimum value of  $d_1$  and  $d_2$  helps to obtain the best cost and subsequently best possible routes. The possible best route is served as input to the ANN network as shown in Figure 2. The next section gives the details about the ANN modeling regarding the best route and minimum time to send the message from source to base/sink sensor node.

**3.2. Proposed ANN Modeling for Possible Best Solution.** The best possible nodes are identified by the CUCKOO search in the previous section. Using the best nodes and possibility of best path is used as input for the ANN model. In this model, the best 3 possible input is considered from CUCKOO search. A total of 30 hidden layer neurons is used to get the best output. The steps required to get the best solution consist of low cost, and low energy use using ANN is given below:

*Step 1.* Find the best possible routes using the fittest sensor nodes.

*Step 2.* Which route has minimum number of sensor nodes involvement.

*Step 3.* Train the neural network for minimum cost leads to minimum energy consumption.

*Step 4.* If simulation round over stop, otherwise simulate for possible solution.

*Step 5.* Compute the performance of the different parameters required.

## 4. Result and Discussion

**4.1. Simulation Results.** The following result is obtained from the proposed CUCKOO-ANN method. The simulation parameters required for the proposed method are given in Table 1. First, the IoT-WSN is placed in two-dimension coordinates as shown in the simulation (Figure 4). The green color indicates the sensor with their sensor number. The CUCKOO search gives the fitness parameters for different rounds of simulation. Figure 5 shows the last 10 best fitness parameters of simulation. The range of fitness parameters are well in ranged for best results.

The CUCKOO search finds the best sensor nodes which help the ANN to form the possible routes. The best possible routes find after the simulation is given in Table 2. The ANN estimate the cost of the route and find route 3 as the best route to transfer message from source to base/sink sensor.



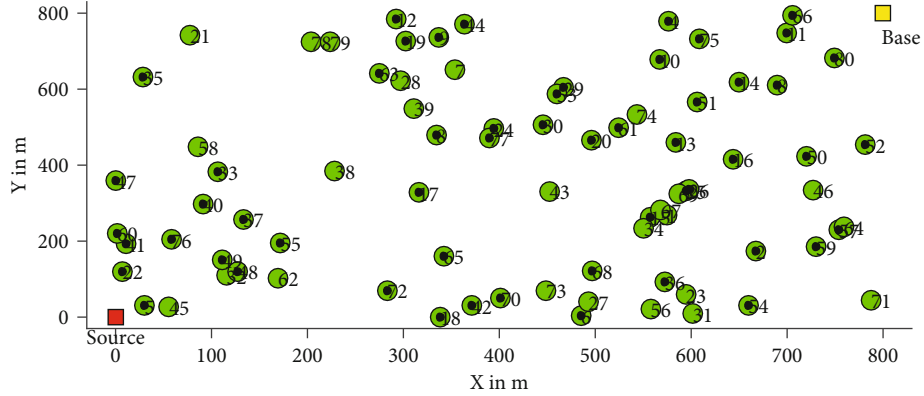


FIGURE 4: Random placement of IoT-WSN in two-dimensional coordinates.

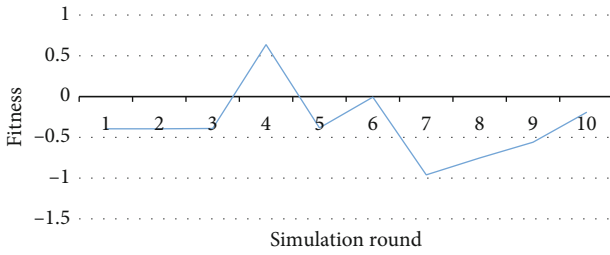


FIGURE 5: Best fitness for last 10 rounds of simulation.

Through MATLAB simulation, the cost of route 3 is found to be 2.145.

The route cost of other four are as follow: for route 1, it is 3.897; for route 2, it is 2.892; for route 4, it is 3.110; and for route 5, it is 3.776. Although the method finds 28 best routes out of which only five best is mentioned. Figure 6 shows the simulation result for the cost for 201 iterations, and Figure 7 shows the best path selected by the CUCKOO-ANN based model. Just to verify, the saturation 201 simulation is done. The energy consumption for each round of simulation is showed in Figure 8. From simulation 196 to 201, the energy consumption is almost constant with very small deviation.

This highlights that the proposed algorithm learns from the previous errors and updates entire algorithm so that minimum energy path can be obtained. Figure 9 shows the predicted best nodes and route compare with the real data. The error % is almost 2% which indicate the proposed model is very effective in nature. The red dot shows the CUCKOO ANN predicted energy data for sensors, and blue dots show the real energy data of sensors.

**4.2. Comparison with Existing Techniques.** Table 3 shows the comparisons of several strategies, with parameters such as routing type, overhead, delay, scalability, and efficiency taken into account. The routing type indicates either the technique can be used for single-hop (SH) or multihop (MH). The overhead, sometimes known as overhead costs, is a recurring cost for the system. Scalability refers to ability to perform well as one or more of the network's fundamental parameters rise in value. Delay defines the time required to pass message from source to base/sink.

So, from Table 3, it is clear that CUCKOO-ANN perform well compared to the other existing techniques. Proposed model has low delay and good scalability with efficiency of 98%.

The fitness functions in the proposed model are Root Mean Squared Error (RMSE) and Mean Magnitude of Relative Error (MMRE). The RMSE indicates the clustering of data sets around the best fitness function defining the objectives of the system. In similar manner, MMRE is used to estimate the error difference between the estimated data and actual data [39]. The RMSE identifies the large errors by giving them relatively high weights, while MMRE indicates the relative error in relation with correct value. Both help to find the errors in the system with respect to the correct value. In the literature, MMRE is the most extensively used performance metric for software cost estimation. The goal is to keep these numbers as low as possible. Equation (8) defines the RMSE function, and equation (9) defines the function MMRE.

$$\text{RMSE} = \sqrt{\sum_{i=1}^n \frac{((\vartheta - \theta)^2)}{n}}, \quad (8)$$

$$\text{MMRE} = \sum_{i=1}^n \frac{((\vartheta - \theta)^2)}{n}, \quad (9)$$

where  $\vartheta$  is estimated time series and  $\theta$  represents actual observations time series. Table 4 compares the RMSE and MMRE values for different techniques.

**4.3. Performance Assessment of Proposed Model.** To evaluate the performance of the proposed CUCKOO-ANN model, the confusion matrix is used. Table 5 indicates the parameters obtained from the confusion matrix. Table 6 shows the results obtained from the confusion matrix and compared with the technique stated in Table 3; it can be seen that the proposed model performance is high.

For high accuracy, the system must predict the true positive response and true negative response of the technique. Out of four parameters defined in Table 4, accuracy is considered as most important in case of WSN.

TABLE 2: Possible routes for transferring the message.

Nodes for route 1	Nodes for route 2	Nodes for route 3	Nodes for route 4	Nodes for route 5	Remarks
44	32	60	45	32	
22	76	55	62	76	
40	37	70	65	37	
33	17	49	38	17	
38	3	67	43	3	These five are the best route provided by the proposed algorithm. Out of these five, the best is route 2 as it has low nodes which indicate low energy consumption.
3	74	56	13	74	
30	20	20	61	20	
29	10	69	14	61	
10	11	13	10	14	
11	66	44	11	8	
66			66	60	

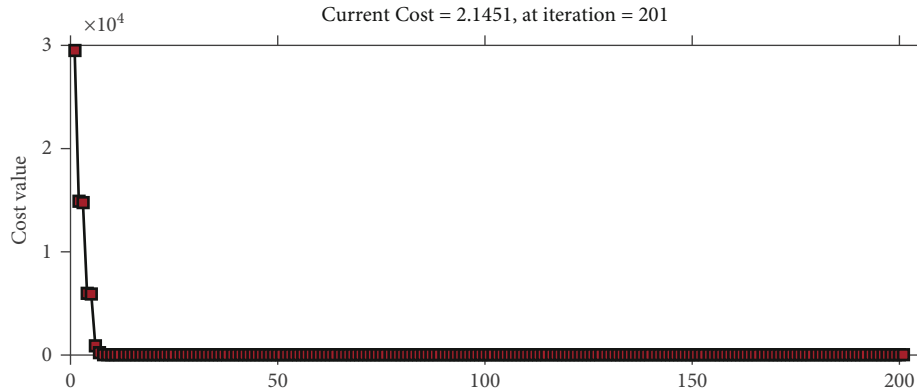


FIGURE 6: Best cost for simulation round.

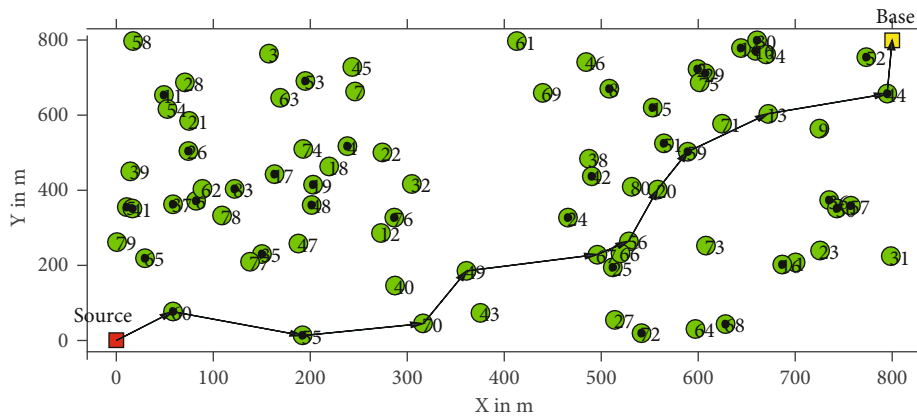


FIGURE 7: Best route found using CUCKOO-ANN based model.

4.4. Discussion. From the simulation results, it can be concluded that the proposed CUCKOO-ANN technique is the most suitable for IoT-WSN in terms of energy efficiency. The CUCKOO optimization plays a vital role in selecting the best sensors for message transfer, and the ANN module helps the system obtain the best suitable path for message transfer from source to base sensors. By combining these two features, the overall cost of the system decreases, which directly indi-

cates the superiority of the model with respect to other models discussed in the literature review. Although the technique is better than other existing technique but for large size network, the method needs more computation space and fast processor.

For future work, keeping security and efficiency as key points in the block chain can be a useful tool for future IoT-WSN routing and safety. The following are possible future goals for using block chain:

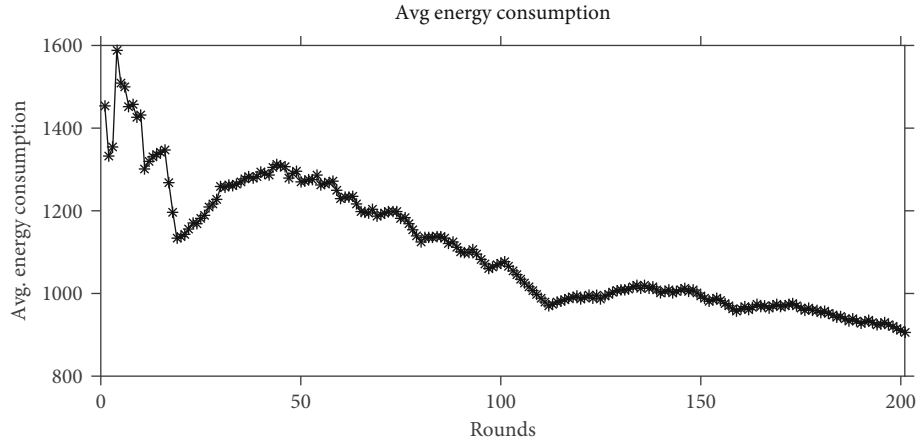


FIGURE 8: Average energy consumption (in watts) of nodes during simulation.

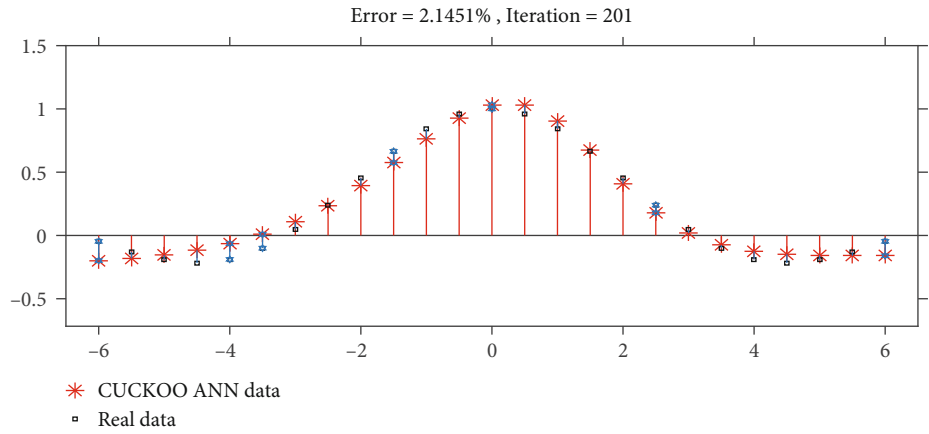


FIGURE 9: Error in predicted data set.

TABLE 3: Comparison with existing technique.

Techniques	Routing	Overhead	Scalability	Delay	Efficiency
ANNR [36]	MH	High	Limited	Medium	90%
QLRR-WA [37]	MH	Low	Good	Low	87%
WL-DCNN [38]	MH	High	Good	Low	89%
CUCKOO-ANN	MH/SH	Low	Good	Low	98%

TABLE 4: RMSE and MMRE comparison [40].

Parameters	Technique	Values	Remarks
RMSE	ANNR	0.052	Model having small RMSE value performs well.
	QLRR-WA	0.045	
	WL-DCNN	0.480	
	CUCKOO-ANN	0.035	
MMRE	ANNR	0.750	Model having small MMRE value shows less deviations in terms of error.
	QLRR-WA	0.670	
	WL-DCNN	0.490	
	CUCKOO-ANN	0.140	

TABLE 5: Parameters for performance assessment.

Parameters	Description	Formula
Sensitivity	The percentage of positive cases that were correctly predicted	$\frac{TP}{FN + TP}$
Accuracy	The percentage of observations that were successfully categorized	$\frac{TP + TN}{FN + TN + FP + TP}$
PPV	The percentage of true positive forecasts in the overall number of positive predictions	$\frac{TP}{FP + TP}$
NPV	The percentage of true negative predictions in the overall number of negative forecasts	$\frac{TN}{FN + TN}$

PPV: positive predicted value; NPV: negative predicted value; TP: true positive; FP: false positive; FN: false negative; TN: true negative.

TABLE 6: Confusion matrix parameters comparison with existing techniques.

Parameters	ANNR	QLRR-WA	WL-DCNN	CUCKOO-ANN
Sensitivity	62%	49%	35%	97%
Accuracy	92%	97%	96%	98%
PPV	60%	65%	48%	82%
NPV	89%	94%	87%	93%

- (i) Improving network performance
- (ii) Minimizing the random deployment cost
- (iii) Enhancing the security of sensors

## 5. Conclusion

IoT-WSNs are commonly installed in dense clusters in certain fields to monitor required parameter values. Any wireless sensor network's main goal is to extend the network's overall lifetime as much as feasible. As a result, energy efficiency is a critical parameter for every sensor network, and any effective management must emphasize it. In this research paper, a novel CUCKOO-ANN based optimization technique is used to achieve a more efficient and reliable energy efficient solution. First, the CUCKOO method finds the suitable/possible nodes which can help for fast message transfer. Then, the ANN system finds out all the possible paths and then chooses the three best paths, those having the smallest number of nodes, and calculates the cost of the possible routes.

The simulation results show that the cost of the best route is 2.14. Route 3 consists of 10 nodes and is the most suitable for message transfer from source node to sink node. The RMSE and MMRE values are 0.035 and 0.14, which indicate the best results. In contrast to other strategies used in the literature, we discovered that the CUCKOO-ANN model outperformed the majority of them. As compared with other technique, CUCKOO-ANN have very good sensitivity with efficiency of 97% and accuracy of 98%. This makes it more suitable where a large network is required. Using data structure and analytics, the computation time and computa-

tion burden can be reduced in future. In the future, one can improve the proposed technique by considering various operators and computing complexity in order to make future work more feasible for the proposed technology.

## Data Availability

The data used to support the findings of this study are available from the corresponding author upon request.

## Conflicts of Interest

The authors declare that there is no conflict of interest regarding the publication of this paper.

## References

- [1] R. N. Jadoon, A. A. Awan, M. A. Khan, W. Zhou, and A. N. Malik, "PACR: position-aware protocol for connectivity restoration in mobile sensor networks," *Wireless Communications and Mobile Computing*, vol. 2020, Article ID 8859256, 15 pages, 2020.
- [2] N. K. Singh and V. Mahajan, "Detection of cyber cascade failure in smart grid substation using advance grey wolf optimization," *Journal of Interdisciplinary Mathematics*, vol. 23, no. 1, pp. 69–79, 2020.
- [3] G. Rastogi and R. Sushil, "Cloud computing implementation: key issues and solutions," in *2nd International Conference on Computing for Sustainable Global Development (INDIACom)*, New Delhi, India, 2015.
- [4] R. K. Garg, J. Bhola, and S. K. Soni, "Healthcare monitoring of mountaineers by low power wireless sensor networks," *Informatics in Medicine Unlocked*, vol. 27, article 100775, 2021.
- [5] N. K. Pour, *Energy Efficiency in Wireless Sensor Networks. [Ph.D. thesis]*, Department of Engineering and Information Technology at The University of Technology Sydney, 2015.
- [6] L. U. Khan, "Visible light communication: applications, architecture, standardization and research challenges," *Digital Communications and Networks*, vol. 3, no. 2, pp. 78–88, 2017.
- [7] N. K. Singh and V. Mahajan, "End-user privacy protection scheme from cyber intrusion in smart grid advanced metering infrastructure," *International Journal of Critical Infrastructure Protection*, vol. 34, article 100410, 2021.
- [8] J. Bhola, S. Soni, and G. K. Cheema, "Recent trends for security applications in wireless sensor networks – a technical review," in *2019 6th International Conference on Computing for Sustainable Global Development (INDIACom)*, New Delhi, India, 2019.
- [9] V. Bhatia, S. Kaur, K. Sharma, P. Rattan, V. Jagota, and M. A. Kemal, "Design and simulation of capacitive MEMS switch for Ka band application," *Wireless Communications and Mobile Computing*, vol. 2021, Article ID 2021513, 8 pages, 2021.
- [10] A. Kumar, V. Jagota, R. Q. Shawl et al., "Wire EDM process parameter optimization for D2 steel," *Materials Today: Proceedings*, vol. 37, no. 2, pp. 2478–2482, 2021.
- [11] S. F. Suhel, V. K. Shukla, S. Vyas, and V. P. Mishra, "Conversion to automation in banking through Chatbot using artificial machine intelligence language," in *2020 8th International Conference on Reliability, Infocom Technologies and Optimization (Trends and Future Directions) (ICRITO)*, Noida, India, 2020.

- [12] M. Carlos-Mancilla, E. López-Mellado, and M. Siller, "Wireless sensor networks formation: approaches and techniques," *Journal of Sensors*, vol. 2016, 2016.
- [13] S. Deshmukh, K. Thirupathi Rao, and M. Shabaz, "Collaborative learning based straggler prevention in large-scale distributed computing framework," *Security and Communication Networks*, vol. 2021, Article ID 8340925, 9 pages, 2021.
- [14] J. H. Ryu, M. Irfan, and A. Reyaz, "A review on sensor network issues and robotics," *Journal of Sensors*, vol. 2015, Article ID 140217, 14 pages, 2015.
- [15] T. Nandy, M. Y. I. B. Idris, R. Md Noor et al., "Review on security of Internet of Things authentication mechanism," *IEEE Access*, vol. 7, pp. 151054–151089, 2019.
- [16] K. Singh and A. Awasthi, *Quality, Reliability, Security and Robustness in Heterogeneous Networks*, Springer, Berlin, Germany, 2013.
- [17] D. B. Hoang and N. Kamyabpour, "An energy driven architecture for wireless sensor networks," in *2012 13th International Conference on Parallel and Distributed Computing, Applications and Technologies*, pp. 10–15, Beijing, China, 2012.
- [18] S. Gupta, S. Vyas, and K. P. Sharma, "A survey on security for IoT via machine learning," in *2020 International Conference on Computer Science, Engineering and Applications (ICCSEA)*, pp. 1–5, Gunupur, India, 2020.
- [19] K. Rajakumari, M. V. Kumar, G. Verma, S. Balu, D. Kumar Sharma, and S. Sengan, "Fuzzy based ant colony optimization scheduling in cloud computing," *Computer Systems Science and Engineering*, vol. 40, no. 2, pp. 581–592, 2022.
- [20] F. Mazunga and A. Nechibvute, "Ultra-low power techniques in energy harvesting wireless sensor networks: recent advances and issues," *Scientific African*, vol. 11, article e00720, 2021.
- [21] K. G. Knightson, T. Knowles, and J. Larmouth, *Standards for Open Systems Interconnection*, McGraw-Hill, Inc., 1987.
- [22] L. Chen, V. Jagota, and A. Kumar, "Research on optimization of scientific research performance management based on BP neural network," *International Journal of System Assurance Engineering and Management*, 2021.
- [23] S. M. Absi, A. H. Jabbar, S. O. Mezan, B. A. Al-Rawi, and S. T. Al Attabi, "An experimental test of the performance enhancement of a Savonius turbine by modifying the inner surface of a blade," *Materials Today: Proceedings*, vol. 42, pp. 2233–2240, 2021.
- [24] Q. Wang, M. Hempstead, and W. Yang, "A realistic power consumption model for wireless sensor network devices," in *2006 3rd annual IEEE communications society on sensor and ad hoc communications and networks*, pp. 286–295, Reston, VA, USA, 2006.
- [25] W. R. Heinzelman, A. Chandrakasan, and H. Balakrishnan, "Energy-efficient communication protocol for wireless microsensor networks," in *Proceedings of the 33rd annual Hawaii international conference on system sciences*, Maui, HI, USA, 2000.
- [26] W. B. Heinzelman, A. P. Chandrakasan, and H. Balakrishnan, "An application-specific protocol architecture for wireless microsensor networks," *IEEE Transactions on Wireless Communications*, vol. 1, no. 4, pp. 660–670, 2002.
- [27] G. Verma and R. Chakraborty, "A hybrid privacy preserving scheme using finger print detection in cloud environment," *Ingénierie des Systèmes d'Information*, vol. 24, no. 3, pp. 343–351, 2019.
- [28] K. Langendoen and G. Halkes, "Energy-efficient medium access control," *Embedded Systems Handbook*, vol. 6000, 2005.
- [29] V. Raghunathan, C. Schurgers, Sung Park, and M. B. Srivastava, "Energy-aware wireless microsensor networks," *IEEE Signal Processing Magazine*, vol. 19, no. 2, pp. 40–50, 2002.
- [30] I. Daanoune, B. Abdennaceur, and A. Ballouk, "A comprehensive survey on LEACH-based clustering routing protocols in wireless sensor networks," *Ad Hoc Networks*, vol. 114, article 102409, 2021.
- [31] G. Kirubasri, "A contemporary survey on clustering techniques for wireless sensor networks," *Turkish Journal of Computer and Mathematics Education (TURCOMAT)*, vol. 12, no. 11, pp. 5917–5927, 2021.
- [32] A. Srivastava and P. K. Mishra, "A survey on WSN issues with its heuristics and meta-heuristics solutions," *Wireless Personal Communications*, vol. 121, no. 1, pp. 745–814, 2021.
- [33] P. Kevin and D. Viely, "Critical evaluation on WSNs positioning methods," *International Journal of Innovative Research in Computer Science & Technology (IJIRCST)*, 2021.
- [34] A. A. Kazerooni, H. Jelodar, and J. Aramideh, "Leach and heed clustering algorithms in wireless sensor networks: a qualitative study," *Advances in Science and Technology. Research Journal*, vol. 9, no. 25, pp. 7–11, 2015.
- [35] J. Bhola, M. Shabaz, G. Dhiman, S. Vimal, P. Subbulakshmi, and S. K. Soni, "Performance evaluation of multilayer clustering network using distributed energy efficient clustering with enhanced threshold protocol," *Wireless Personal Communications*, 2021.
- [36] S. Ji, S. F. Yuan, and M. M. Cui, "Using self-organizing map in backbone formation for wireless sensor networks," in *2009 Fifth International Conference on Natural Computation*, pp. 468–472, Tianjian, China, 2009.
- [37] G. Künzel, L. S. Indrusiak, and C. E. Pereira, "Latency and lifetime enhancements in industrial wireless sensor networks: a q-learning approach for graph routing," *IEEE Transactions on Industrial Informatics*, vol. 16, no. 8, pp. 5617–5625, 2020.
- [38] R. Huang, L. Ma, G. Zhai, J. He, X. Chu, and H. Yan, "Resilient routing mechanism for wireless sensor networks with deep learning link reliability prediction," *IEEE Access*, vol. 8, pp. 64857–64872, 2020.
- [39] J. Bhola and S. Soni, "A study on research issues and challenges in WSN," in *2016 International Conference on Wireless Communications, Signal Processing and Networking (WiSPNET)*, pp. 1667–1671, Chennai, India, 2016.
- [40] V. S. Desai and R. Mohanty, "ANN-Cuckoo optimization technique to predict software cost estimation," in *2018 Conference on Information and Communication Technology (CICT)*, pp. 1–6, Jabalpur, India, 2018.

## Retraction

# Retracted: Applications of Big Data in Economic Information Analysis and Decision-Making under the Background of Wireless Communication Networks

### Wireless Communications and Mobile Computing

Received 25 July 2023; Accepted 25 July 2023; Published 26 July 2023

Copyright © 2023 Wireless Communications and Mobile Computing. This is an open access article distributed under the Creative Commons Attribution License, which permits unrestricted use, distribution, and reproduction in any medium, provided the original work is properly cited.

This article has been retracted by Hindawi following an investigation undertaken by the publisher [1]. This investigation has uncovered evidence of one or more of the following indicators of systematic manipulation of the publication process:

- (1) Discrepancies in scope
- (2) Discrepancies in the description of the research reported
- (3) Discrepancies between the availability of data and the research described
- (4) Inappropriate citations
- (5) Incoherent, meaningless and/or irrelevant content included in the article
- (6) Peer-review manipulation

The presence of these indicators undermines our confidence in the integrity of the article's content and we cannot, therefore, vouch for its reliability. Please note that this notice is intended solely to alert readers that the content of this article is unreliable. We have not investigated whether authors were aware of or involved in the systematic manipulation of the publication process.

Wiley and Hindawi regrets that the usual quality checks did not identify these issues before publication and have since put additional measures in place to safeguard research integrity.

We wish to credit our own Research Integrity and Research Publishing teams and anonymous and named external researchers and research integrity experts for contributing to this investigation.

The corresponding author, as the representative of all authors, has been given the opportunity to register their

agreement or disagreement to this retraction. We have kept a record of any response received.

### References

- [1] Y. Deng, H. Zheng, and J. Yan, "Applications of Big Data in Economic Information Analysis and Decision-Making under the Background of Wireless Communication Networks," *Wireless Communications and Mobile Computing*, vol. 2022, Article ID 7084969, 7 pages, 2022.

## Research Article

# Applications of Big Data in Economic Information Analysis and Decision-Making under the Background of Wireless Communication Networks

Yaotian Deng, Han Zheng , and Jingshi Yan 

*School of Accounting, Southwestern University of Finance and Economics, Chengdu, 611130 Sichuan, China*

Correspondence should be addressed to Han Zheng; 295161662@qq.com

Received 3 November 2021; Revised 11 December 2021; Accepted 17 December 2021; Published 17 January 2022

Academic Editor: Shalli Rani

Copyright © 2022 Yaotian Deng et al. This is an open access article distributed under the Creative Commons Attribution License, which permits unrestricted use, distribution, and reproduction in any medium, provided the original work is properly cited.

Owing to the growing volumes of mobile telecommunications customers, Internet websites, and digital services, there are more and more big data styles and types around the world. With the help of big data technology with high semantic information, this paper focuses on exploring the value and corresponding application of big data in finance. By comparing with the existing methods in terms of search speed and data volume, we can effectively see the effectiveness and superiority of the algorithm proposed in this paper. Furthermore, the algorithm proposed in this paper can provide some reference ideas for the follow-up-related research work.

## 1. Introduction

Systems produce bandwidth in a variety of methods, resulting in an estimated 17.5 exabyte of data generated each week. There exist numerous factors that contribute to data's growing volume. Technological investigations, for example, can produce a massive amount of data, for example, CERN's Large Hadron Collider (LHC), which produces about 39 terabytes annually (Table 1). Having more than 1 billion members on Facebook and Twitter, social media contributes largely where individuals allocate an equivalent of 2.5 hours per day liking, tweeting, publishing, and exchanging respective views. Without a question, leveraging interaction-produced data could have an impact on the economics field. Unfortunately, utilizing data's potential is a difficult undertaking. Storage facilities with large space and computational abilities are constantly getting created to manage the data boom, such as the National Security Agency (NSA) Utah facility, which can keep 0.5 to 1.5 yottabyte of data and has computing capacity exceeding 100 petaflops [1].

Frameworks which operated on multiple computers began to spring up as a result of the elevated demand to

broaden datasets to large datasets that surpassed operating and/or memory functionalities. Around June 1986, Tera-data Corporation utilized the foremost concurrent database framework with just 1-terabyte memory volume in the Kmart data center to preserve and make accessible everything about their company information for inter-actio-nal inquiries and organizational evaluation (Table 2). The University of Wisconsin's Gamma framework and the University of Tokyo's GRACE framework are two such illustrations.

The phrase "big data" was coined with respect from the theory below.

In Latin, "data" means "fact" or "knowledge." Big data relates to the massive amounts of information that cannot be acquired, handled, analyzed, or sorted into more action-able knowledge. Big data comprises not only explicit knowl-edge in the conventional manner but also implicit resourceful information [2]. Big data is also described as ele-vated-speed, and great-diversity data (Figure 1). Big data can furthermore be defined by that quantity of information that is surpassing conventional technology's ability to store, orga-nize, and compute [3].

TABLE 1: Company investments on big data.

Year	Enterprise software spending for specified submarkets	Forecast: social media revenue, worldwide, 2011-2016	Big data IT services spending	Total
2011	2,565	76	24,407	27,047
2012	2,918	1,384	23,476	27,778
2013	3,516	1,812	28,578	33,906
2014	4,240	2,827	37,404	44,472
2015	5,207	3,615	36,189	45,010
2016	6,461	4,411	43,713	54,586

Note: accuracy is to the nearest \$1 million and is derived from percentage-based algorithms. Research data does not provide total accuracy to the nearest \$1 million. Some rounding errors apply.

TABLE 2: Big data model.

Ad hoc analytics	Relational databases	Big data sets
Data volume	Megabytes-gigabytes	Terabytes-petabytes
Data velocity	Near-real-time updates (seconds)	Real-time updates (milliseconds)
Data variety	Structured data	Structured and unstructured data
Data model	10s of tables/variables	100s-1000s of tables/variables

Big data, in its utmost elementary meaning, references to a significant expanse of information collected. Big data is a phrase applied to define massive database volumes which are very huge that storing them in memory is almost impossible. Such data can be collected, saved, shared, processed, and consolidated. With the amount of data increasing, the necessity to update the technologies that are employed to analyze it also raises simultaneously. This data should not be organized in ordered spreadsheets as they were in the earlier times in order to be examined by present tech. Big data can be found in a variety of data types. They comprise a wide range of data across a variety of sources. They can be organized, semiorganized, or completely unorganized [4]. Big data is made up of numerical data, image data, speech, text, and discourse, to name a few categories. Radio frequency identification (RFID), global positioning system (GPS), point-of-sale (POS), call centers, and consumer blogs are all examples of these.

With present advanced analytical technology, we can retrieve insights from any type of information. Analytics is a combination of math and statistics applied to massive volumes of datasets. Big data analysis denotes the use of statistics and arithmetic to process enormous quantities of data. With the absence of analytics, big data is just a bunch of numbers. Over decades, the researchers have been compiling a large amount of data (Figure 2). With the omission of big data, analytics is just a set of arithmetic and statistical techniques and methods. Such massive quantities of information can be used to derive knowledge by companies. This is achieved by nowadays huge processing capacity that is further reasonably priced than earlier [1].

## 2. Characteristics of Big Data Are Shown in Table 3

*2.1. Volume.* It alludes to databases' huge magnitude. It is true that the Internet of Things (IoT) has played a role

towards the massive extraction of information (tally history, customer data, charts and graphs, files, and so on) via the advancement and proliferation of linked mobile devices, detectors, as well as other gadgets, in conjunction with quickly changing information and communication technologies (ICTs) such as artificial intelligence (AI). The amounts of information production have brought other metrics for information preservation, such as exabyte, zettabytes, and yottabytes, since the information transfer rate exceeds Moore's law [5].

*2.2. Variety.* It alludes to databases' huge magnitude. It is true that the Internet of Things (IoT) has played a role towards the massive extraction of information via the advancement and proliferation of linked mobile devices, detectors. The amounts of information production have brought other metrics for information preservation [5]. It exemplifies the growing wide range of information generating origins and styles. Web 3.0 encourages the development of Internet communication connections, resulting in the production of a variety of information kinds. Some of the most important origins of big data are relatively new [6].

*2.3. Variability.* It is frequently mistaken with diversity, while variability is linked to fast shifts in interpretation. Taking an example, phrases in a script would contain varied interpretations depending on the setting of the content; hence, for reliable viewpoint assessment, programs must determine the interpretation (impression) of a phrase while considering the entire setting in mind.

*2.4. Velocity.* The rapidity with which information is generated distinguishes big data. Information from linked gadgets and the online world is emerging instantaneously in businesses. That velocity is critical for businesses to take certain steps which allow them to become increasingly nimble and acquire a competitiveness benefit over their competing



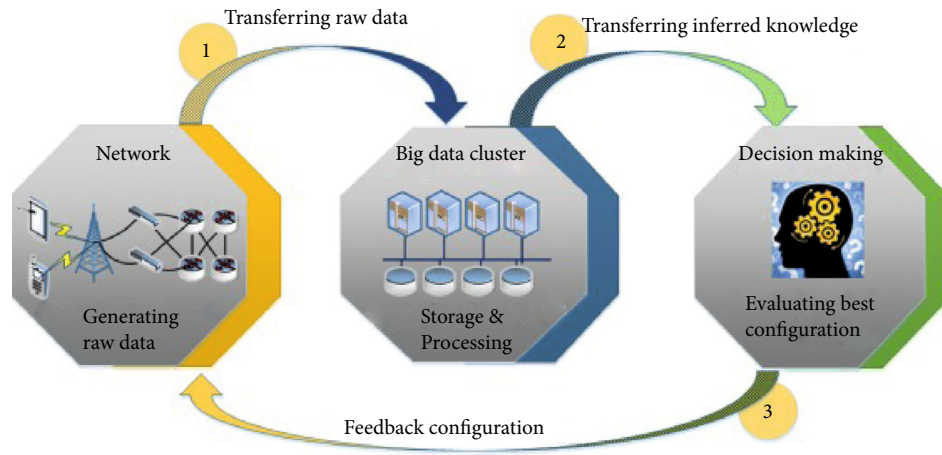


FIGURE 1: Big data network.

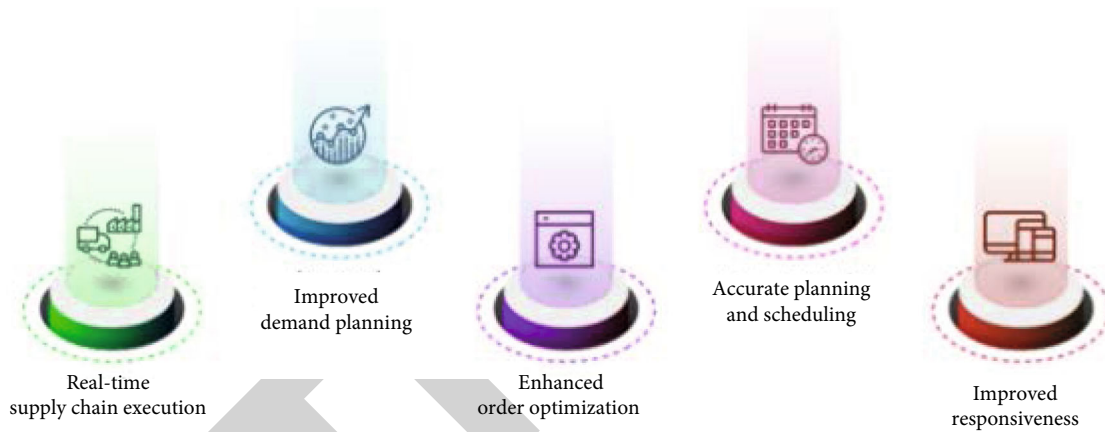


FIGURE 2: Some benefits of big data.

TABLE 3: Characteristics of big data.

No. of Vs	References	Dimensions (characteristics)							
		Volume	Velocity	Variety	Veracity	Value	Variability	Volatility	Validity
3Vs	[33-39]	✓	✓	✓					
4Vs	[11, 40-42]	✓	✓	✓	✓				
	[6, 29, 43-45]	✓	✓	✓		✓			
5Vs	[3,22, 26, 46, 47]	✓	✓	✓	✓	✓			
6Vs	[30, 48, 49]	✓	✓	✓	✓	✓		✓	
7Vs	[31, 32]	✓	✓	✓	✓	✓			✓

companies. Regardless of the reality that certain businesses previously used big data (click-stream data) to provide acquisition suggestions to their clients, today’s businesses can evaluate and comprehend data in real-time using big-data analytics.

2.5. *Veracity*. The term “data veracity” relates to the exactness and consistency of data. Because the information gathering contains data which is rarely safe and correct, data veracity relates to the quantity of information unpredict-

ability and dependability associated with a particular sort of data.

2.6. *Visualization*. The discipline of visualizing data and information is known as data visualization. It displays primary and secondary data sources in a diagrammatic manner, demonstrating structures, dynamics, abnormalities, consistency, and variety in methods which words as well as figures cannot (Table 4).

TABLE 4: Traditional and big data analysis.

	Traditional analytics	Big data analytics
Analytics type	Descriptive, predictive	Predictive, prescriptive
Analysis methods	Hypothesis-based	Machine learning
Primary objective	Internal decision support and performance management	Business process driver and data-driven products
Data type	Structured and defined (formatted in rows and columns)	Unstructured and undefined (unstructured formats)
Data age/flow	>24 h static pool of data	<min constant flow of data
Data volume	Tens of terabytes or less	100 terabytes to petabytes

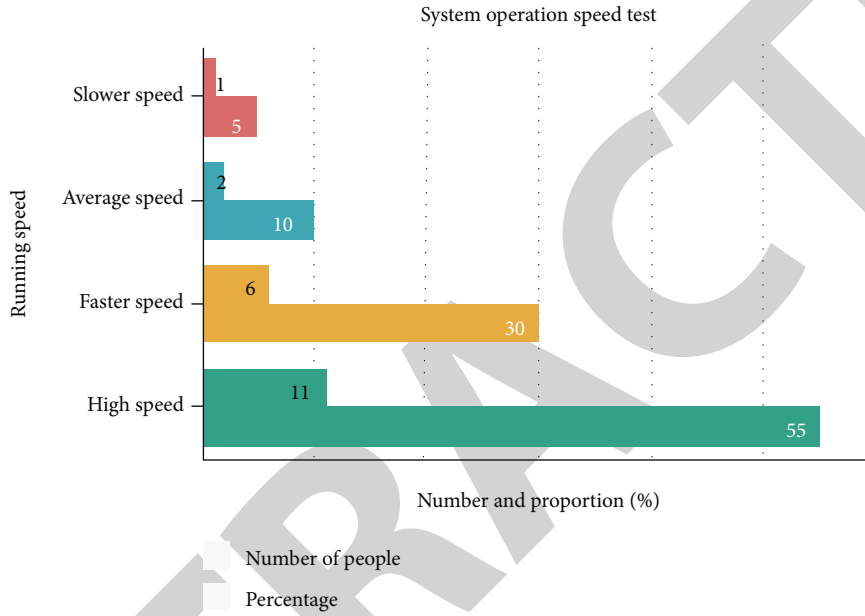


FIGURE 3: Sample model results.

### 3. Model

An example of a model that can be used is the industrial economic information model. This model uses the following formula in its creation process.

$$F(t) = \sum_{i=1}^k w_i f_i(t) + \varepsilon. \tag{1}$$

Sample results from a sample model (Figures 3 and 4). For analysis, the following formula is used:

$$Z = \lambda_1 v_1 + \lambda_2 v_2 + \dots + \lambda_n v_n. \tag{2}$$

### 4. Applications of Big Data

4.1. *Management of Supplier Interaction.* Vendor interaction administration is establishing proficiency in tactical strategy formulation and supervising all contacts with an organization’s vendors in attempt to minimize the likelihood of mistakes as well as increase the worth of such relationships. In SRM, developing tight connections among major vendors and improving engagement with them is critical to identifying and generating unique content and lowering the chance

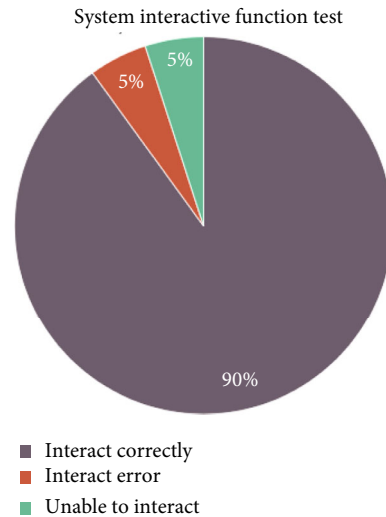


FIGURE 4: Sample result chart.

of loss. Companies that concentrate on connection managing and cooperation will benefit from organizational capabilities and supplier relationship management (SRM). Big data analysis methods can assist in regulating vendor interactions

by providing reliable knowledge and statistics on institutional consumption habits. Big data, for instance, may produce precise knowledge on the profitability (returns on investments) of every project as well as a detailed study of possible suppliers. Considering the great capability of big data computation among the examined elements, fuzzy artificial assessment and analytical hierarchy process (AHP) have been utilized in a research to assess and choose suppliers. The goal is to find a supplying company that can adjust to potential big data problems [7].

*4.2. Design of Physical Distribution Networks.* Logistics and operation network architecture is a calculated choice that encompasses all physical distribution partner sourcing choices as well as organizational regulations and initiatives aimed at achieving protracted planned goals. The logistics and operation network architecture design task include establishing the structural arrangement of the supply chain, which influences the majority of a corporation's functional departments or operational departments. It is critical to assess service quality and supply chain performance when constructing the supply chain network [8]. The goal of supply chain design is to create a system of individuals who can help the firm achieve its protracted performance goals. These essential stages should be observed while designing a supply chain:

- (1) Decide the protracted tactical aims
- (2) Identify the task domain
- (3) Define the type of analysis to be performed
- (4) Identify the instruments to be applied
- (5) Identify the optimal structure for program accomplishment

The organization will get a substantial competitive edge by choosing the best distribution network design and strategy. In a study, a method which used big data and arbitrarily produced large databases for logistics operations, client need, and transit was employed, and it was referred to as combined-integer nonlinear approach for describing transmission locations. It was supposed that marketing analytics techniques had been used to examine the attitudinal dataset. Big data, according to the results of the research, may supply all of the essential data on penalized cost data and service quality, making it a very valuable resource for complicated allocation network model [9].

*4.3. Commodity Design and Development.* Some of the primary worries of flexible item makers could be whether their items correspond to the demands of respective clients. Developers require devices to anticipate and evaluate client inclinations and desires as they evolve over the course of a commodity's life cycle. In the item development phase, a shortage of data regarding clients' tastes and desires is a significant challenge. Developers may create goods that satisfy client interests and desires if companies regularly observe client conduct and have exposure to updated infor-

mation on client inclinations. Client conduct, commodity creation, and production processes all produce large amounts of information, which are referred to as big data. It is possible to decrease unpredictability by gathering, monitoring, and using emerging methodological tools to acquire discoveries and relevant knowledge, which may then be applied to judgments. Technical design is the procedure of converting client requirements into design requirements. Data science (DS) is described as the act of converting visible global truth knowledge into understandable information that can be used to make decisions [10]. In as much as there are many techniques to commodity design which are accessible, all of these methodologies are basic from a DS standpoint. The design procedure is depicted schematically below Figure 5.

Big data will have significant influence over numerous businesses, including concept development. Designers will progressively incorporate electronics and wireless communications within their designs, which shall contribute to this trend. As a result, throughout the production distribution procedure, company's goods features should be addressed, and all supply chain stakeholders and limitations need to be included at the concept phase. Supply chain design that is based on commodity design gives the supply chain a competitive edge and adaptability. BDA approaches have lately been employed in item creation and production, resulting in the creation of new goods based on user interests. When big data analysis is used in commodity design, it allows the developer to be continually conscious of the interests and desires of the client, allowing them to create an item that meets their wants and inclinations [11]. Engineers can foresee and anticipate client wants by looking at virtual conduct and consumer acquisition records. Through continuously observing client activities as well as conveying clients' thoughts and wants, developers may uncover innovative attributes and forecast prospective market patterns.

The significance of big data in the automobile sector stems from the car, which displays vast amounts of efficiency statistics and consumer requirements. One of the eventual aims of industries producing durables for consumers is to preserve existing economic viability for as long as it is achievable. This has therefore made it easier to apply the idea of (operated) data-driven development. Current advances in data processing as well as overall use of data analytics technologies have paved the way for alternative ways to generate insights for item improvement and achievement of goals. As a result of this theory, item designers can continuously improve their goods and services depending on actual consumption, performance, and loss data. Despite the fact that several data analytic (software) applications and modules were established for gathering product-related information, item improvement using automated analysis methodologies and technologies is currently in its infancy. Developers nevertheless confront numerous obstacles and must address numerous constraints. Selecting the most appropriate data analytic tools (DATs) and incorporating them into creative concepts are said to be difficult for developers [12].

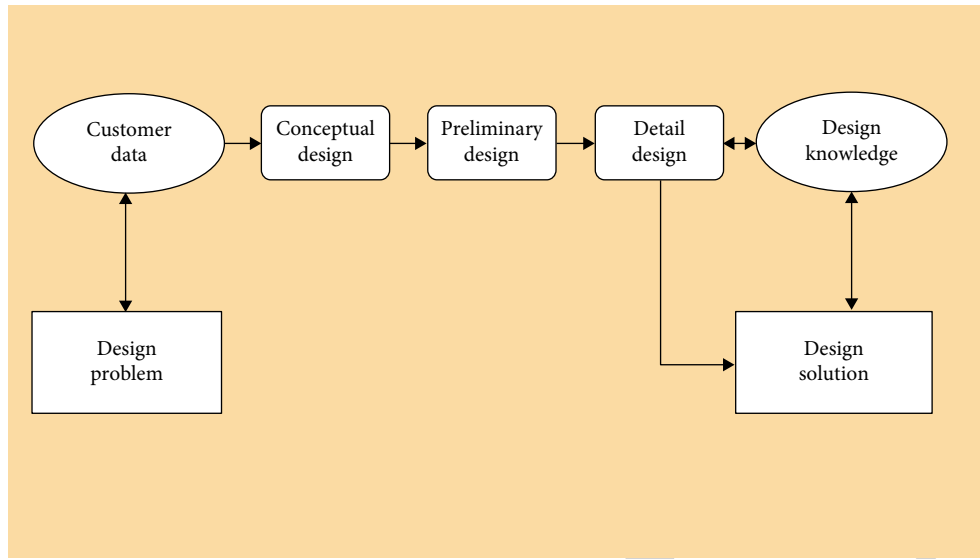


FIGURE 5: The process of design.

**4.4. Planning for Demand.** Several distribution network managers are eager to use big data to enhance market forecasts and manufacturing scheduling. Demand forecasting has traditionally proven to be a difficult task in SCM. Big data analysis can be used to track customer allegiance, market signals, and ideal cost statistics. The capacity to use modern electronics, program, and computational design is, nevertheless, one of the obstacles that the businesses encounter. Big data analysis allows for the detection of emerging economic changes as well as the identification of the core sources of problems, losses, and flaws. Through analyzing consumer activities, data analytics could forecast clients' interests and wants, allowing businesses to be more creative and innovative. Through estimating the operating demand, this framework allows developers to design generation identities and operations. Further in a different study, big data is used to assess air traveler need and proposes a methodology for anticipating demand for air passengers. This study's findings suggest a 5.3 percent forecasting inaccuracy [13].

**4.5. Monitoring of Procurement.** Procurement is made up of a number of implementation mechanisms and agreements as technical and practical judgments. Considering the huge amount of extensively scattered information produced all over various processes, frameworks, and different locations, operational institutions require improved technology to process this massive data, and highly competent people that can evaluate it and obtain useful information and ideas to use in their planning and decisions. Previously, gathering domestic and architectural data from the activities and exchanges of the organization and its affiliates was a time-consuming procedure that lasted a couple of days. However, nowadays, many different structural, procedural, interior, and exterior information recorded by intelligent automation is readily accessible to these companies at a great velocity, across several instances instantaneously [14]. SCA can be used to monitor the quality of vendors as well as supply chain risk.

Exterior and domestic big data were utilized to swiftly detect and control shortfalls in one study. For instance, alerting the public via social sites and the headlines regarding forex rate fluctuations and natural calamities has an impact on the distribution network. This paradigm may be used to detect distribution network danger in real time, allowing for actual risk monitoring, judgment assistance, and emergency preparedness [15].

**4.6. Customization of Production.** Industries can use big data to uncover significant knowledge and trends, allowing them to enhance operations, improve distribution network effectiveness, and detect manufacturing factors. Distribution channels as well as production methods are extensive and sophisticated in modern worldwide and interlinked economy; it should be feasible to evaluate all elements for every operation and connect distribution network in finer precision to modify the operations and maximize the distribution network [16]. Producers may accurately determine each individual's behaviors and duties via fast and reliable data assessment for every phase of the manufacturing procedure, as well as analyze the whole corporation, using data analytics. Producers can use this capability to discover constraints and uncover underperforming operations and equipment. Previously, consolidated manufacturing and large manufacturing were impractical since they were centered solely on the orders of a limited number of clients; however, today's BDA have made it feasible to precisely estimate consumer requests and tastes for personalized items [17].

## 5. Logistics

Owing to the introduction of vast numbers of information and gadgets, environmental worries, sophisticated regulatory rules, shifting industrial structures, personnel limits, equipment, and the emergence of digital technologies, the logistics sector has experienced a profound transition. Within that sector, normalization of data exchange framework and

## Research Article

# Internet of Things-Based Data Hiding Scheme for Wireless Communication

A. Shobanadevi <sup>1</sup>, G. Maragatham <sup>2</sup>, Syam Machinathu Parambil Gangadharan <sup>3</sup>,  
Mukesh Soni <sup>4</sup>, Rohit Kumar <sup>5</sup>, Tien Anh Tran <sup>6</sup>, and Bhupesh Kumar Singh <sup>7</sup>

<sup>1</sup>Department of Data Science and Business Systems, SRM Institute of Science and Technology, Chennai, India

<sup>2</sup>Department of Computational Intelligence, SRM Institute of Science and Technology, Chennai, India

<sup>3</sup>Sr General Mills, 1 General Mills Blvd, Golden Valley, Minnesota 55426, USA

<sup>4</sup>Senior IEEE Member, Bhopal, India

<sup>5</sup>Institute of Management Studies, Noida, Uttar Pradesh, India

<sup>6</sup>Vietnam Maritime University, Haiphong, Vietnam

<sup>7</sup>Arba Minch University, Ethiopia

Correspondence should be addressed to G. Maragatham; maragatg@srmist.edu.in  
and Bhupesh Kumar Singh; dr.bhupeshkumarsingh@amu.edu.et

Received 7 November 2021; Revised 6 December 2021; Accepted 11 December 2021; Published 17 January 2022

Academic Editor: Shalli Rani

Copyright © 2022 A. Shobanadevi et al. This is an open access article distributed under the Creative Commons Attribution License, which permits unrestricted use, distribution, and reproduction in any medium, provided the original work is properly cited.

The substantial rise of information technology has facilitated the methods of access to digital information and internet of things (IoT). Digital image processing handles the digital material to store and distribute more effectively with decreased time and space complexity. However, these tactics undermine the privacy of digital materials. A recent study focuses on shielding digital materials from illicit use and distribution by making reversible data strategies to tackle the risk of privacy breaches for digital content. In this study, a composite reversible data hiding (CRDH) approach is suggested. CRDH employed the integer wavelet transform (HAAR transform) with the HH band's eigenvalue decomposition. The suggested CRDH first performed the IWT transformation on the cover image (CI) and parsed it into four consecutive frequency subbands, namely, LL, HL, LH, and HH. Sensitive data of the proposed approach are incorporated by merging the HH band of the cover image's individual values with the encrypted eigenvalues of the confidential data. The choosing of casing art is such a method that values are within a range. The confidential data picture and HH band's frequency band are roughly the same; thus, modifying the individual values will not affect the quality of the confidential data image and the HH band's content. The suggested strategy's primary purpose is to design a data concealing technique that hinders the verification of digital information by maintaining a high rate of peak signal-to-noise ratio (PSNR). The PSNR of the existing technology is less than 50 per cent of the total accessible data set. The PSNR value shows the picture's visual quality, where the PSNR increases the better image quality. Therefore, concealing data is essential for the technique that inhibits authentication and keeps a high rate of PSNR. The suggested approach fulfils this aim, gets a PSNR rate of above 50 per cent, and hits 59 per cent for line.

## 1. Introduction

The internet of things (IoT) is aimed at connecting every device to the Internet so that these devices can be accessed anytime, anywhere, and from any path (i.e., any network). This concept has been defined as a new communication sys-

tem that connects the Internet with the physical world via wireless sensor devices. As a result, everyday devices have become a network component that collects information about their environment and generates reports. Thus, every object with wireless technology can provide data to a large number of applications and users. However, to realize this

potential, wireless devices with different communication standards and hardware limitations need to work in harmony with each other and with existing internet protocols.

Today, wireless sensor networks are used in smart home, health, agriculture, and industrial applications primarily work in local area networks to provide information to a certain number of users. Since application protocols running on TCP/IP stacks designed for traditional wired networks cannot be used directly on devices with limited hardware resources, these networks are connected to the Internet via a gateway between the user and the sensor devices. TCP/IP is also called the Internet protocol suite, which is a set of communication protocols used by the internet or the networks which are parallel to it. It allows large-distance communication by creating a virtual network. This situation is time-consuming and laborious since each new application requires modifications to the existing protocols defined on the wireless sensor network. Therefore, wireless sensor networks cannot be directly integrated into the internet infrastructure. In wireless sensor networks, CoAP, MQTT, STMP, etc., application protocols have been proposed. These application protocols work on the IP protocol as simplified versions of the HTTP protocol and require each device to have an IP address. Considering that the number of devices connected to the Internet will be over 29 billion in 2023 and IoT devices will manage the internet traffic (Cisco, 2020), needs such as addressing a large number of devices and supporting the traffic generated by the existing infrastructure arise.

In this context, the adaptation layer and IPv6/6LoWPAN protocol stack enable wireless sensor devices to connect to external IP networks using IPv6 addresses. However, since the IPv6 method supports end-to-end communication, unfortunately, different solutions are required against the traffic bottleneck caused by IoT devices. The second layer of TCP/IP model is a transport layer. This is an end-to-end layer which is used to deliver messages to the host. Moreover, it provides point-to-point connection between the source host and destination host for delivering services efficiently. In this context, the most striking solution proposal in recent years as an alternative to end-to-end communication is information-centered network architecture (ICN (information-centric networks)). This architecture proposes a network model that focuses on content/data instead of address-based communication between destination and source nodes. Therefore, methods such as naming, routing, caching, and securing ICN provide advantages for IoT applications. For example, the data is provided by the naming of the data, regardless of the address where it is located. In addition, fast and efficient content provision is ensured by caching data by wireless devices on the same network, regardless of the data source. Thus, the information-centered approach has become a strong candidate in incorporating wireless sensor networks into the Internet by eliminating the necessity of establishing and maintaining the end-to-end connection required by the traditional Internet architecture.

With the global expansion of the Internet, the Internet has become a powerful and accessible platform for data transmission. Unfortunately, sensitive information can be

stolen and tempered on the Internet. In recent times, information security has attracted the focus of the researcher as a data hiding scheme. Data hiding [1] plays a vital role in Internet and multimedia-based secure communication. The primary purpose of data hiding is to secure the confidentiality of the message and share the sensitive news safely. If there is any splash in the confidential message or its media during data transmission, the secret message cannot be reorganized entirely after receiving it. Data hiding schemes for sharing confidential data in intelligence, buro, paramilitary, military, and company financial reports would have played a significant role in recent times and lead to focus research in reversible data hiding schemes in recent years [1].

The reversible data hiding [2, 3] uses images as an input tool because of their easy access. Images can be downloaded with a scanner, digital camera, or directly online. Depending on the encryption method, the most recent algorithm data can be divided into three areas: location, currents, and pressure points. Encryption method offers various advantages. It is cheap to apply in algorithms. It increases the integrity factor of our data. Moreover, it allows sharing your files safely. Algorithms in the field section include encryption by changing the pixel value directly. However, algorithms in the network area begin to convert the image to coefficients [4, 5]. Then, the coefficient changes include individual messages [6, 7]. Pressure algorithms accept images generated by a series of compressed codes as their intervening medium. Inclusive details are achieved by modifying the computer code [8, 9].

This paper presents a composite reversible data hiding (CRDH) scheme that employs integer wavelet transform (HAAR transformation) with eigen decomposition over both cover and confidential data images [10]. The proposed data hiding scheme significantly improved the extracted hidden data measure as MSE and PSNR and acquired higher PSNR and lower MSE.

## 2. Internet of Things

IoT is a system that allows all objects in the ecosystem to connect to the Internet. In addition to the ability to communicate with each other, these tiny objects can send data directly to the Internet or act by taking commands on the data coming from the Internet. Therefore, IoT allows objects with different properties to be accessible from the Internet for data collection, resource sharing, analysis, and management. As a result, in transportation, health, environment, agriculture, etc. smart devices used in various business areas and having sensors and actuators have become intelligent internet components. IoT is aimed at transforming the data collected from these devices into information with methods used in application areas such as artificial intelligence and data mining and serve this information to many applications or users. In addition, standardization studies have been carried out so that wireless sensors with different hardware/communication sources can be used in large-scale applications.

Most applications carrying various information obtained from sensor devices to users with existing internet protocols

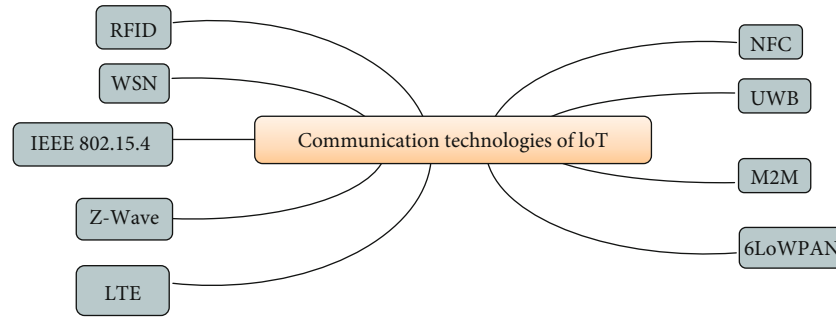


FIGURE 1: Internet of things: communication technologies and applications [5].

work in local area networks (LAN (local area networks)). On the other hand, IoT is aimed at providing information to many users and services by measuring the information obtained from sensor nodes depending on their application areas. In this direction, IoT applications and currently used technologies are examined in 5 different layers in Figure 1: object/device layer, connection layer, management layer, data processing and analysis layer, and application layer. With this architecture, the data provided by the sensor nodes over the internet in real-time or periodically can be used by many applications and users. The sharing of secret keys of nodes is provided by symmetric and asymmetric encryption mechanisms. The fundamental difference between these two types of encryption is that symmetric uses one key for both encryption and decryption, while the later one uses a public key for encryption and a private key for decryption.

In Figure 1, each layer represents the area of production and use of information. In the object layer, each device collects information about its environment. At the same time, the identification and tracking of objects in this layer are provided by RFID technology, proximity, smoke, temperature, light, etc. The information that needs to be measured can be identified with other sensing devices. The connection layer is where devices with different technologies are named, and the produced measurement data (temperature, light, etc.) is transmitted. In this layer, each device uses its communication technology (Zigbee (IEEE 802.15.4), 6LoWPAN, NFC, Bluetooth, etc.)

It carries the information it produces to the upper layers of management and data processing. Security, media access control, installation, and configuration of devices are done at the management layer. This layer is where the periodic operating times of wireless devices and discovery and configuration protocols are set in the local network area. The generated information can be used by end-users in the application layer, and it also provides information to different application areas in the data processing and analysis layer. At the application layer, the information obtained from the devices and meaningful information can be used for suspicious event detection, efficient energy consumption, occupational safety, etc. It can be used in many applications (Ersin & Öz, 2020), e.g., the electricity consumption information measured by the sensor nodes used in smart homes, and innovative grid applications can be used by electricity com-

panies to optimize supply and demand and make savings and consumption plans by the consumer.

Another application area emerging within the Internet of things with body area sensor nodes is intelligent health systems—physical measurement information obtained from body area sensor nodes, Bluetooth, etc. With the help of communication technology, it can be monitored in real time via a smartphone, or these measurements can be controlled by doctors with cloud technology. In addition, elderly surveillance systems can be given as an example. Remote real-time surveillance of the patient can be provided, and physical measurements such as blood value and heartbeat can be followed with the help of sensor nodes. As an application that can be used shortly, it can be used for smart homes, building, cities, etc. Any sensor node will transmit the values it produces to social networking sites periodically, and this information will be followed by many users and end systems. Along with applications such as smart houses and buildings, innovative agriculture/forest systems and transportation systems define new application areas that emerge within the Internet of Things.

### 3. Communication Features

Sensor devices used in various applications of IoT have different communication technologies such as IEEE 802.11, IEEE 802.15.4, IEEE ZigBee, IEEE Bluetooth, and RFID. In the IoT communication model, wireless sensor devices are connected to a gateway connected to the Internet. The gateway can query data from nodes at specific intervals or transmit data to nodes. Data generated in wireless devices are transmitted with IEEE 802.15.4 or a similar wireless technology standard with low data transmission capacity (kb/s). The data transmission capacity of the IoT environment is limited by the resource constraints (energy, computing power, and memory) of the sensor devices and the insecure nature of the transmission environment. For this reason, reliable communication protocols have taken into account the limited data rate and power capacity of the devices while minimizing energy consumption at the same time.

### 4. Data Security in IOT

The accessibility of data by many users and applications has made it more critical to ensure the security of devices that

collect sensitive information about almost every environment and this sensitive information. The processor power, storage space, and energy constraints of wireless sensor devices used in the IoT cause these devices to be inherently vulnerable. At the same time, problems such as the loss and corruption of packets containing sensitive information are frequently experienced in these environments. Therefore, ensuring security in a complex and dynamic system such as the IoT is critical. For this, in applications where wireless sensor networks are used, the security requirements are determined as data confidentiality, source authentication, data integrity, and availability of data.

Security models integrated with the data itself are not supported in IP-based Internet applications. Instead, in IP networks where end-to-end communication is established, the security of the communication channel between the two ends is provided with TLS/DTLS/SSL security protocols for the formation of a secure session. In addition, mechanisms such as content integrity and authentication were added to the upper layers later. The high messaging requirement of these protocols causes packet delay, reducing network and application performance. The energy consumed by wireless devices with limited resources to provide a secure communication channel is more than the energy spent for encryption algorithms. In this case, security methods integrated with the content itself can be an efficient solution for restricted devices. One mechanism that makes the knowledge-centric network approach a strong candidate for IoT applications and future internet architecture is providing the content itself. In ICN, the safety of the data is ensured by the control of integrity, accuracy, and privacy. Completeness check consists of the name–data pair. In this case, the information itself is accessed by the given word. Accessing the data with the signature-based naming method also provides the accuracy condition. Privacy control is provided at the transmission and application layers. In addition, the security of devices must be ensured in various IoT applications. In this case, authentication and authorization checks are required. For example, machines that send commands to an actuator may need to be authenticated. However, ICN focuses on the security of interest and data messages. Therefore, additional security mechanisms should be used for different service models using wireless devices. Cryptography is the study of secure communication techniques that allow only the sender and the intended recipient of a message to view its contents. The term is derived from the Greek word *kryptos*, which means hidden. If the message is intercepted, a third party has everything they need to decrypt and read the message.

In traditional ICN networks, the public critical cryptography method is used, and encryption information is added to the end of data/interest packets. Cryptography can be described as the study of secure communications which will allow only the sender and the intended recipient of a message to see the content. For example, if the message is being intercepted, then the third party will have anything they require to decrypt and to read the message. In wireless sensor networks, data confidentiality is provided with key-sharing AES, Blowfish, and Triple DES using various

encryption algorithms. However, key usage and encryption alone are not enough. In the wireless environment, suspicious nodes can quickly get into the communication scope of other nodes, eavesdropping on sensitive data and decrypting them. Source authentication is used by the sending and receiving nodes to distinguish between malicious fake packets and original packets. The sharing of secret keys of nodes is provided by symmetric and asymmetric encryption mechanisms. However, the increase in the use of the processor and the size of the communication packets by the encryption mechanisms reduces resource-constrained wireless sensor devices (Tourani et al., 2018). The elliptic curve encryption method provides security with lower processing power with the fundamental structure produced smaller than other methods and can be applied in limited IoT devices. However, this method requires the critical exchange and sharing keys between nodes which adds a burden on communication. Data integrity is essential in detecting data damage or loss caused by the conditions of the wireless transmission environment. However, malicious nodes can inject incorrect data or modify data inside communication packets.

For this reason, the integrity of the data is essential not only for error control mechanisms but also for ensuring security. Data availability is essential when wireless sensor nodes or a group of nodes in the network are exposed to a denial of service (DoS) attack. Security mechanisms have been developed for each type of attack in the literature. These mechanisms, which take attack-based security measures, should be designed specifically for application requirements.

## 5. Reversible Data Hiding

With the rapid advancement of communication through the Internet, the information exchanged could tamper intentionally or accidentally through unprivileged access. In recent years, reversible data hiding (RDH) has become an active research domain in data replication. In reversible data hiding, the bits hidden are embedded in the cover file (image) on the sender side. Confidential data and original cover media are extracted without distortion to the receiver. The data hiding technique is divided into immutable data hiding and reversible data hiding. In the immutable data hiding, the information in a database cannot be changed or deleted. One cannot overwrite the previous data when the new data is available. However, in the reversible data hiding technique, the data is embedded in the image in such fashion that the original data can be restored. The embedding ability to hide immutable data is high. However, while the original cover media is destroyed, the embedding capacity in RDH is low, but the original cover media can be recovered [11, 12].

Some of the present data hiding schemes are not invertible, the presence of truncation error and round-off error in spread spectrum technique makes it nonreversible, because of the bit replacement without memory, and the least significant bit plane scheme is taken into account to be non-reversible and because of the quantization error quantization-index-modulation rendered as invertible. RDH also links two data



sets, and a group belongs to the embedded information [13]. This reversible data handling technique has some advantages like the scheme offers the embedding capacity which is directly proportional to the number of pixel in image. Moreover, the reversible technique inherited from this scheme provides functionality that allows recovery of the cover image. Another set belongs to the cover media data such that the cover media will be lossless recovered once the hidden information has been extracted out. Confidential data is embedded by modifying the frequency coefficient of the cover image by using some standard methods like discrete Fourier transform (DFT), discrete cosine transform (DCT), discrete wavelet transform (DWT), and integer wavelet transform [14, 15]

**5.1. Proposed Work.** This paper presents a composite reversible data hiding (CRDH) scheme. CRDH competitively applied integer wavelet transform (HAAR transformation) with eigen decomposition over the cover image's cover image and brand of the cover image. CRDH decomposed the cover image (CI) into four subbands, namely, LL, HL, LH, and HH, and evaluated the HH band's eigen decomposition value for data hiding.

In the proposed reversible data hiding scheme, integer wavelets transform the cover image (CI) by decomposing, namely, into lower-lower (LL), higher-lower (HL), lower-higher (LH), and higher-higher (HH) frequency subband as shown in Figure 2.

In CRDH algorithm, the hidden data is integrated into the host image by changing the band of high-frequency coefficients described in Figure 3, that is, the HH subband. As shown in Figures 1, 2, and 4, the proposed reversible data hiding scheme is based on both integer wavelet transform and eigen decomposition with encryption [16, 17]. Initially, integer wavelet transform divides the host image into four frequency subfields as LL, HL, LH, and HH bands. The LL tape works with rough details, the HL band deals with horizontal elements, the LH provides vertical information, and the HH band contains diagonal image information. The HH band uses the HH band to embed sensitive data because you lose data on the image energy [18, 19]. In this way, an embedded confidential data will not affect the perception accuracy of the cover image. The proposed reversible data hiding scheme has two steps with hiding and sending and receiving as extraction steps.

**5.2. Hiding Phase of Composite Reversible Data Hiding (CRDH) Scheme.** Once the cover image decomposes into four subsequent frequency subbands, CRDH uses the HH band to hide confidential data (CDI), as its accounted minimum noise level. The proposed data hiding scheme evaluates the eigen decomposition of HH band confidential data followed by encryption [20]. Encrypted eigen decomposition then superimposes over HH band of IWT (CI) after applying inverse eigen decomposition operation. Finally, we apply the inverse integer wavelet transform to generate an embedded cover image (ECI).

**5.3. Extraction Phase of Composite Reversible Data Hiding (CRDH) Scheme.** The extracting phase of the proposed



FIGURE 2: IWT transform of cover image.

scheme uses exactly the inverse operation of the hiding phase; in extracting, the proposed scheme is used to apply integer wavelet transform over the embedded image (ECI) to get the HH band confidential data (CDI) is hidden, as shown in Figure 4. The CRDH scheme enforces eigen decomposition on HH frequency band of the received data. The retrieved eigen decomposition compositely contains eigen decomposition on the cover image's HH frequency band and confidential data. As the image dimension of covered data is already shared between the sender and receiver before the established data communication, the extracting phase compared the shared cover image with the received image. The received image contains both the cover image and confidential data. The extraction step's subtracting returns the eigenvalue of encrypted confidential data and subsequently applies all inverse operations to get confidential data at the receiver side.

## 6. Result Analysis

The proposed works have tested on various data set images of size  $512 \times 512$ . These entire data set images are gray scale. The gray scale is defined for digital images. It means the value of each pixel will represent information about the intensity of the light. In other words, the image which has only black, white, and gray colors than gray will have multiple levels. Here, the data set images are used as Fruits, Elaine, Lena, and Tiffany. The size of the confidential image is also the same as the original image. To simulate the proposed work, the implementation is done in MATLAB. The i3 processor is executed with 4GB RAM and 500 GB HDD.

**6.1. Performance Parameter.** PSNR is an image factor used to determine the quality of an image by comparing quality differences between the original image and the resulting image.

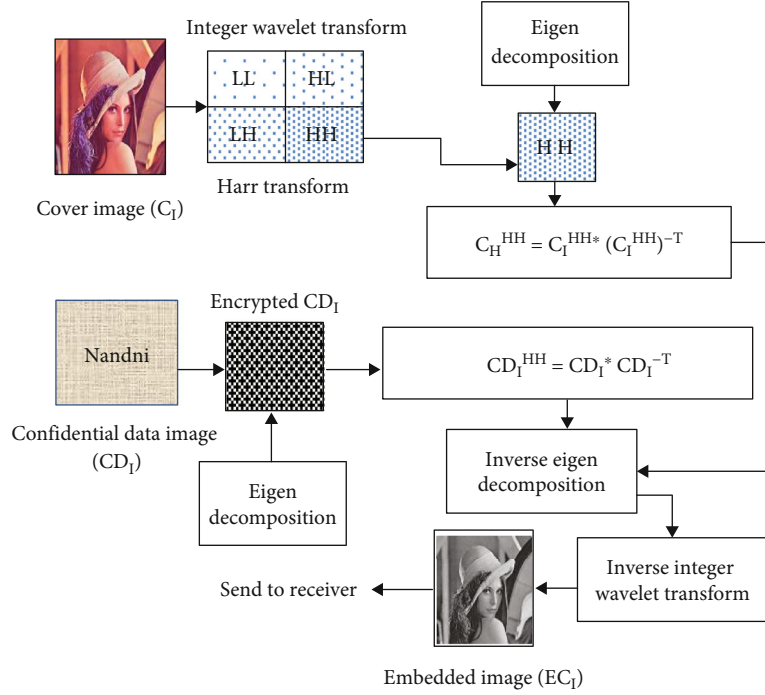


FIGURE 3: Reversible data hiding embedding procedure.

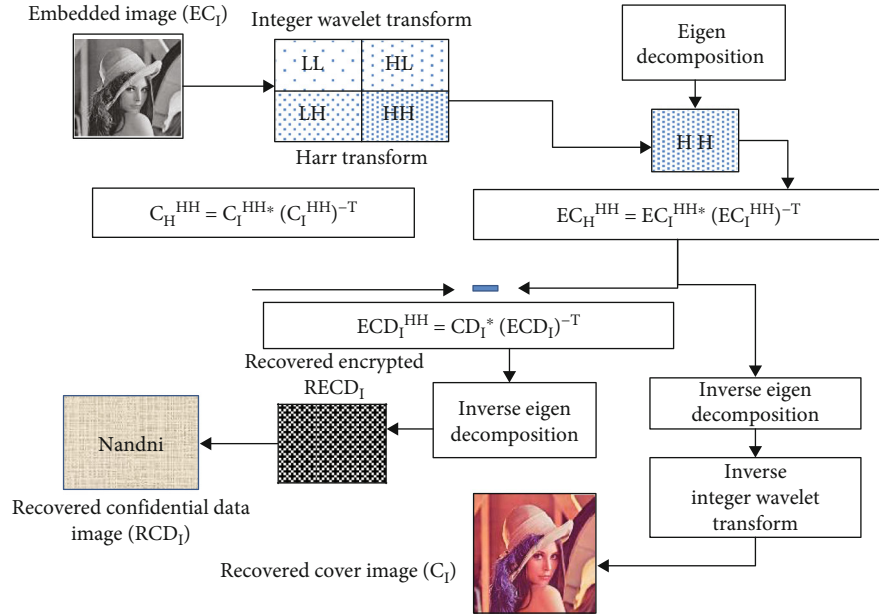


FIGURE 4: Reversible data hiding extraction procedure.

It is calculated using the mean square error (MSE). The following formula calculates both parameters:

$$PSNR = 10 \log_{10} \left( \frac{MAX^2}{MSE} \right), \quad (1)$$

$$MSE = \frac{\sum_{i,j} [I_1(i,j) - I_2(i,j)]^2}{i * j}. \quad (2)$$

TABLE 1: Mean square error vs. noise level ratio comparison over different data images.

Images	MSE	Noise level
Fruits	0.099007	0.45
Elaine	0.127639	0.29
Lena	0.05318	0.38
Tiffany	0.243832	0.41

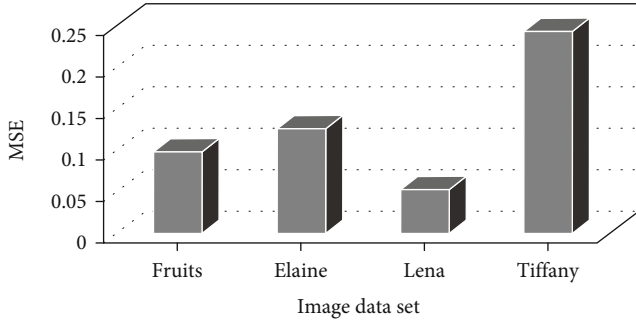


FIGURE 5: Comparative analysis of mean square error ratio.

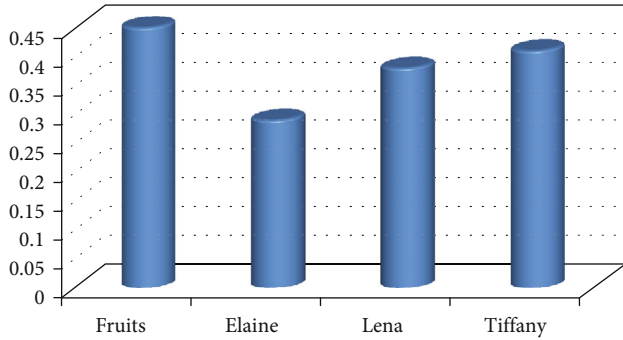


FIGURE 6: Comparative analysis of noise ratio.

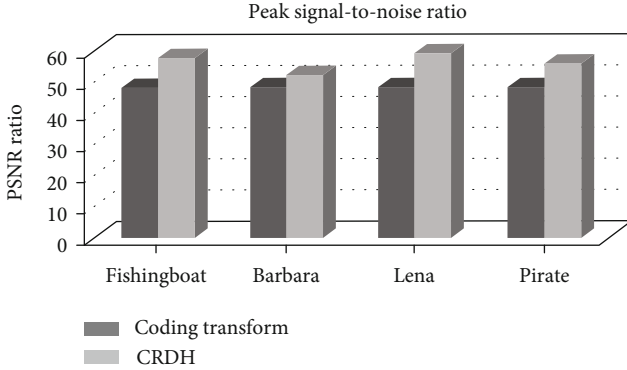


FIGURE 7: Comparative analysis of for PSNR.

This calculation has been gathering by the computer program. There are various testing images has been used. Some of them have been shown here with their results. Table 1 shows comparison of mean square error and noise level ratio over different data images.

For four different data sets, the mean square error is compared with noise level over the data range.

Figures 5 and 6 show the MSE and noise ratio, as the graph shows that there are some images has been used for as input. This input and the generated output image has been used for calculating the comparison ratio. The graph also shows the proposed approach shows the better results.

Figures 7 and 8 show the PSNR and SNR, as the graph shows that there are some images has been used for as input. This input and the generated output image has been used for

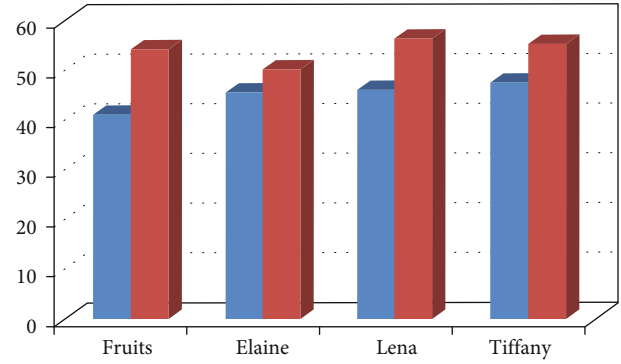


FIGURE 8: Comparative analysis of for SNR.

TABLE 2: PSNR comparison over different data images.

Images	Coding transform	CRDH
Fruits	48.36	57.85
Elaine	48.31	52.36
Lena	48.39	59.54
Tiffany	48.45	56.24

TABLE 3: SNR comparison over different data images.

Images	Coding transform	CRDH
Fruits	41.21	54.25
Elaine	45.63	50.26
Lena	46.35	56.54
Tiffany	47.52	55.41

calculating the PSNR. The graph also shows the proposed approach shows the batter results.

As shown in Tables 2 and 3, PSNR and SNR of existing technique for all the available data set describes in Figure 8 is less than 50%. The PSNR value indicates the image’s visual quality, where a higher PSNR and SNR value leads to better image quality. It is needed to develop a data hiding scheme that prevents authentication of digital information with maintaining a higher PSNR, whereas the proposed scheme significantly achieves this goal and gains PSNR greater than 50 and achieves up to 59% for Lena.

## 7. Conclusion

Confidential data exchange is virtually insecure in this era of wireless communication. Intentional or unintentional changes to the transmitted data are possible. Recently, researchers focused on hiding confidential data within the covered image via a reversible data hiding scheme. But the data hiding scheme still faces challenges to extract distortion less and noise-free confidential data at the receiver side. This paper presents a composite reversible data hiding (CRDH) scheme. CRDH competitively applied integer wavelet transform (HAAR transformation) with eigen decomposition

over the cover image and confidential data image. CRDH decomposed the cover image (CI) into four subbands, namely, LL, HL, LH, and HH, and evaluated the HH band's eigen decomposition value for data hiding. The discussed technique will help to design a data concealing method which impedes the verification of digital information by keeping the rate of PSNR high. The PSNR of the existing technology is less than 50 per cent for the total accessible data set. The proposed data hiding scheme significantly improved the extracted confidential data measure as the MSE and PSNR and acquired higher PSNR (up to 59%) and lower MSE. For the future researchers, it creates a gap to work on additional factors which do not directly relate to the performance of the proposed technique. It will also include reducing the size of the auxiliary file.

### Data Availability

The data shall be made available on request.

### Conflicts of Interest

The authors declare that they have no conflict of interest.

### References

- [1] G. Xuan, C. Yang, Y. Zhen, Y. Q. Shi, and Z. Ni, "Reversible data hiding using integer wavelet transform and companding technique," in *Digital Watermarking. IWDW 2005. Lecture Notes in Computer Science*, vol. 3304, I. J. Cox, T. Kalker, and H. K. Lee, Eds., Springer, Berlin, Heidelberg, 2005.
- [2] A. Shaik and V. Thanikaiselvan, "Comparative analysis of integer wavelet transforms in reversible data hiding using threshold based histogram modification," *Journal of King Saud University-Computer and Information Sciences*, vol. 33, no. 7, pp. 878–889, 2021.
- [3] J. Hou, O. Bo, H. Tian, and Z. Qin, "Reversible data hiding based on multiple histograms modification and deep neural networks," *Signal Processing: Image Communication*, vol. 92, p. 116118, 2021.
- [4] Y. Fei Peng, X. Z. Zhao, M. Long, and W.-q. Pan, "Reversible data hiding based on RSBEMD coding and adaptive multi-segment left and right histogram shifting," *Signal Processing: Image Communication*, vol. 81, p. 115715, 2020.
- [5] S. Weng, W. Tan, O. Bo, and J.-S. Pan, "Reversible data hiding method for multi-histogram point selection based on improved crisscross optimization algorithm," *Information Sciences*, vol. 549, pp. 13–33, 2021.
- [6] G. Xuan, X. Li, and Y.-Q. Shi, "Histogram-pair based reversible data hiding via searching for optimal four thresholds," *Journal of Information Security and Applications*, vol. 39, pp. 58–67, 2018.
- [7] J. Wang, N. Mao, X. Chen, J. Ni, C. Wang, and Y. Shi, "Multiple histograms based reversible data hiding by using FCM clustering," *Signal Processing*, vol. 159, pp. 193–203, 2019.
- [8] X. Gao, Z. Pan, E. Gao, and G. Fan, "Reversible data hiding for high dynamic range images using two-dimensional prediction-error histogram of the second time prediction," *Signal Processing*, vol. 173, p. 107579, 2020.
- [9] G. Gao, S. Tong, Z. Xia, W. Bin, X. Liya, and Z. Zhao, "Reversible data hiding with automatic contrast enhancement for medical images," *Signal Processing*, vol. 178, p. 107817, 2021.
- [10] T.-S. Nguyen, C.-C. Chang, and N.-T. Huynh, "A novel reversible data hiding scheme based on difference-histogram modification and optimal EMD algorithm," *Journal of Visual Communication and Image Representation, Volume*, vol. 33, pp. 389–397, 2015.
- [11] R. M. Rad, K. S. Wong, and J.-M. Guo, "Reversible data hiding by adaptive group modification on histogram of prediction errors," *Signal Processing*, vol. 125, pp. 315–328, 2016.
- [12] C.-C. Lin, W.-L. Tai, and C.-C. Chang, "Multilevel reversible data hiding based on histogram modification of difference images," *Pattern Recognition*, vol. 41, no. 12, pp. 3582–3591, 2008.
- [13] M. Xiao, X. Li, Y. Wang, Y. Zhao, and R. Ni, "Reversible data hiding based on pairwise embedding and optimal expansion path," *Signal Processing*, vol. 158, pp. 210–218, 2019.
- [14] E. Gao, Z. Pan, and X. Gao, "Reversible data hiding based on novel pairwise PVO and annular merging strategy," *Information Sciences*, vol. 505, pp. 549–561, 2019.
- [15] W. Hong, T.-S. Chen, and M.-C. Wu, "An improved human visual system based reversible data hiding method using adaptive histogram modification," *Optics Communications, Volume*, vol. 291, pp. 87–97, 2013.
- [16] Y. Shoji, K. Nakauchi, W. Liu, Y. Watanabe, K. Maruyama, and K. Okamoto, "A community-based IoT service platform to locally disseminate socially-valuable data: best effort local data sharing network with no conscious effort?," in *2019 IEEE 5th World Forum on Internet of Things (WF-IoT)*, pp. 724–728, 2019.
- [17] F. T. Jaigirdar, C. Rudolph, and C. Bain, "Prov-IoT: a security-aware IoT provenance model," in *2020 IEEE 19th International Conference on Trust, Security and Privacy in Computing and Communications (TrustCom)*, pp. 1360–1367, 2020.
- [18] J. H. Jeon, K. Kim, and J. Kim, "Block chain based data security enhanced IoT server platform," in *2018 International Conference on Information Networking (ICOIN)*, pp. 941–944, 2018.
- [19] W. Iqbal, H. Abbas, M. Daneshmand, B. Rauf, and Y. A. Bangash, "An in-depth analysis of IoT security requirements, challenges, and their countermeasures via software-defined security," *IEEE Internet of Things Journal*, vol. 7, no. 10, pp. 10250–10276, 2020.
- [20] M. A. López Peña and I. Muñoz Fernández, "SAT-IoT: an architectural model for a high-performance fog/edge/cloud IoT platform," in *2019 IEEE 5th World Forum on Internet of Things (WF-IoT)*, pp. 633–638, 2019.

## Research Article

# A Novel Framework of an IOT-Blockchain-Based Intelligent System

**Aliaa M. Alabdali** 

*Faculty of Computing and Information Technology, King Abdulaziz University, P. O. Box 411, Rabigh, Saudi Arabia*

Correspondence should be addressed to Aliaa M. Alabdali; [amalabdali@kau.edu.sa](mailto:amalabdali@kau.edu.sa)

Received 11 November 2021; Accepted 20 December 2021; Published 15 January 2022

Academic Editor: Shalli Rani

Copyright © 2022 Aliaa M. Alabdali. This is an open access article distributed under the Creative Commons Attribution License, which permits unrestricted use, distribution, and reproduction in any medium, provided the original work is properly cited.

With the growing need of technology into varied fields, dependency is getting directly proportional to ease of user-friendly smart systems. The advent of artificial intelligence in these smart systems has made our lives easier. Several Internet of Things- (IoT-) based smart refrigerator systems are emerging which support self-monitoring of contents, but the systems lack to achieve the optimized run time and data security. Therefore, in this research, a novel design is implemented with the hardware level of integration of equipment with a more sophisticated software design. It was attempted to design a new smart refrigerator system, which has the capability of automatic self-checking and self-purchasing, by integrating smart mobile device applications and IoT technology with minimal human intervention carried through Blynk application on a mobile phone. The proposed system automatically makes periodic checks and then waits for the owner's decision to either allow the system to repurchase these products via Ethernet or reject the purchase option. The paper also discussed the machine level integration with artificial intelligence by considering several features and implemented state-of-the-art machine learning classifiers to give automatic decisions. The blockchain technology is cohesively combined to store and propagate data for the sake of data security and privacy concerns. In combination with IoT devices, machine learning, and blockchain technology, the proposed model of the paper can provide a more comprehensive and valuable feedback-driven system. The experiments have been performed and evaluated using several information retrieval metrics using visualization tools. Therefore, our proposed intelligent system will save effort, time, and money which helps us to have an easier, faster, and healthier lifestyle.

## 1. Introduction

Over the past decade, the number of Internet users has increased rapidly [1], and the IoT is one of the latest and newest Internet technologies which is capable of providing great assistance to automated systems utilized daily everywhere around the world [2, 3]. The intelligent innovation that has enabled and connected the intelligent interaction of discrete constructs for elaborating the immense range of services to entities is IoT [4]. Referring to smart homes and sustainability, intelligent devices are different representative emerging technologies in the IoT era. Smart home is one of the leading development which has changed house equipment into being more intelligent [5–7]. Generally, a smart home consists of several smart appliances [8], which are able to collect and exchange data over the Internet and connect to each other through various protocols (like

Bluetooth, Wi-Fi, and Ethernet) that can work independently and interactively to perform specific functions [9, 10]. To this end, computers or applications are utilized in order to manage the functions and features of a main appliance remotely via the Internet [11]. At a smart home, the kitchen is the most likely place to house smart devices [12], and the refrigerator is one of the most important appliances in the kitchen [13–15].

In the past years, several works have been proposed to design IoT-based smart refrigerator systems [16–19]. An IoT-based low-cost smart refrigerator is presented in [20] which is designed in order to reduce the food loss and help in providing a more comfortable life. The application given by Android or Mac applications has given a real-time update even though the individual is not physically present at home. In such scheme, the data of the fresh food is inserted in the refrigerator by taking a picture of the food. In [21], a smart

refrigerator system is presented which suggests the recipe information as per availability of vegetables which includes inside the refrigerator and processes it to know about vegetable status, temperature, and vegetable items for the recipes that need to be purchased if not available inside the refrigerator. The suggested system is able to determine the weight of the vegetables and predict the dishes which can be cooked in available material. Moreover, the main goal of the system proposed in [18] was to warn the user when a food is over or a week before shelf life of the food. The invention continued to design and develop with features of sensing the quantity and quality of food items inside the fridge [22]. The main aim behind this work was to inform the user about the current status of food items through an android app on a mobile phone. The main achievement of that system was to save money and reduce the food wastage. In addition, the authors focused on developing a low-cost smart refrigerator system in [23] which is aimed at achieving a minimum number of intelligent decision making. Likewise, in order to detect the available items inside the refrigerator and make a decision, deep learning methods are used for training the model in this paper. Such scheme could improve the precision performance with better computational needs. People's lives are becoming ever busier, and few have time (or perhaps forget) to check the stock of food and beverages inside the household refrigerator. Visits to the supermarket to replenish the refrigerator are also time-consuming. This lack of available time may lead to changes in cooking habits, waste of a lot of food, or an inconvenient lack of a foodstuff when needed. Having a system that can periodically, automatically, and immediately check, order, and purchase depleted products may solve these problems. However, based on the literature review, most of the previous smart refrigerators can only inform the consumers about the available and required stocks in the refrigerator without being able to purchase the depleted products. Moreover, previous studies have not simultaneously considered all criteria of a high-quality smart refrigerator with the intelligent techniques and privacy concerns for security reasons. Even integration of varied techniques including combination of IoT, artificial intelligence (AI), and blockchain is lacking in the previously designed systems. This work attempts to combine the abovementioned technologies as they have the potential to improve supply and usage efficiency, information traceability, smart consumption, and domestic logistics, among other things. On each level of usage and consumption, the item/product will be well linked to the resources and products. AI can assess the conditions for ordering, cooling, etc., and machine level changes using IoT are also considered. This novel design, with the IOT-block, an intelligent refrigerator system, will overcome the previous limitations. Majority of time taken for running a machine learning model is taken in structuring and analysis of the data and features. Using the blockchain technology will ensure that the data is stored in separate blocks and when a particular dataset is required, respective machine learning model will call the data using functions from block chain. This method will significantly reduce the running time.

The proposed system has the capability of automatically self-checking and self-purchasing (after receiving owner confirmation), by integrating smart mobile device applications and IoT technology with minimal human intervention. It is smart enough to check the availability and quantity of foods and beverages stored inside the refrigerator. When the stock of a product reaches a half, a quarter, and then zero, it will automatically notify the owner by sending an SMS message, an email, and an alert to the system's application. To this end, the proposed smart refrigerator is connected via Ethernet module to Blynk, which is a platform in iOS and Android apps used to connect to Arduino, Raspberry Pi, etc. Blynk mediates all communications between the smartphone and the hardware. An Arduino is connected to the Internet and will be considered as the central server. An application programming interface (API) in the mobile device and website is used for obtaining live updates of the device's status.

The machine is also integrated with artificial intelligence (AI); by IOT hardware, it collects data from the refrigerator, and this collected data goes into the cloud database. The data is ingested into the preprocessing machine where data preprocess and feature selection are done. The automatic decision related to factors is done by experimenting with different machine learning and deep learning classifiers.

Moreover, our smart fridge uses a load cell sensor to record the weight of a product each time the product is taken, used, and then returned. The system gives the owner control of the purchase operation via an application on a mobile phone from anywhere in the world via the Internet. This electronic system can complete all tasks while people are busy with other activities, thereby saving effort, time, and money; minimizing food waste; and helping us to live an easier, faster, and healthier lifestyle. This will benefit in a number of ways such as periodically checking the availability and quantity of products such as foods and beverage; notifying the consumer immediately once the stock of a product has reached a half, a quarter, and zero via SMS, email, and its own application; and offering the consumer an opportunity to decide and control the purchase operation. This will save customer's effort, time, and money; minimize waste of food and beverages; and help people to live an easier, faster, and healthier lifestyle.

## 2. Motivation and Contributions

The development of IOT has given machines a way to communicate. IOT is used to get feedback from hardware and create a channel to make devices communicate among themselves. Here, the use of blockchain is envisaged to create a secure method of data transfer and an effective data retrieval process for our machine learning model. The main contributions of the paper are as follows:

- (i) To study the in-depth literature related to micro-processors and smart refrigerator systems
- (ii) To integrate the hardware technology with more sophisticated software using AI for automatic

decisions with different opportunities to decide and control the purchase operation

- (iii) To develop the system architecture underlying the hardware process
- (iv) To implement a blockchain architecture for storing data. This will work as a middleware between the hardware and ML layer, with integration of blockchain framework
- (v) To implement the system using machine learning methodologies and comparison is made using accuracy of the classifiers

The structure of this paper is as follows. Section 2 reviews related works. Section 3 illustrates the utilized material in this study. In Section 4, the proposed method is illustrated, followed by Section 5 which presents the system testing of this approach, while the conclusion is discussed in Section 6.

### 3. Background

In the past years, several smart refrigerator systems have been presented. In this section, current systems and the benefits of the proposed system will be analysed. Also, the criteria of the current systems and our proposed system will be compared, in terms of (i) sending notifications, email, and SMS; (ii) the methodology of knowing the status of foods and liquid products; (iii) checking the stock of products; (iv) the language being used; (v) the percentage of human intervention; (vi) the system platform (control unit), sensors, wireless, and server used; (vii) the ability to send orders to the supermarket; (viii) payment methods; (ix) the ability to control the system remotely; (x) the OS; and (xi) the technique that is used. The blockchain and AI are discussed in the next section.

*3.1. Related Work.* An I-Fridge using RFID technology is presented in [24] which enables the consumer to efficiently and accurately manage the products stored inside the refrigerator. It uses Radio-Frequency Identification (RFID) technology to collect and identify information about the products stored in the refrigerator, via attached RFID tags. In that system, detailed information and descriptions of the food products can be monitored. Moreover, the customer will be notified when a product is about to expire or to be depleted. The I-Fridge system consists of a normal fridge with an RFID system, a tablet PC, an Alien9900 reader, and two Alien-9611 circular polarized antennas inside the refrigerator. An RFID tag is attached to each item stored in the refrigerator, and this tag communicates with the other elements of the system. In I-Fridge, a tablet PC is placed on the door of the refrigerator and works as the user interface. The RFID reader scans the tags inside the refrigerator via the antennas each time the door is closed, collecting the information from the tags' IDs. This information is then transmitted from the reader to the tablet PC via the Wi-Fi channel. By making the comparison between the new results of scanned tags and the previous scanned tag set, the system

can monitor the items entering and leaving the refrigerator. The applications running on the tablet PC can locate the foods in the fridge effectively and accurately [24]. By investigating the I-Fridge system, we found that one basic problem is that the collected information needs to be checked by the consumer, with no alarm or notification system in place. This markedly reduces the usefulness of the system. That is, since the system only displays the collected information, the consumer needs to manually check the location of food and its expiry date by looking at the tablet PC personally and then must buy the food personally. The system can only be used for foods, and it does not support other languages, like Arabic.

In [25], an IoT-based intelligent home using smart devices (refrigerator) has been introduced which is comprised of different sensors, transceivers, a microcontroller, and a Raspberry Pi module which controls the system. This smart fridge system works on the actual quantity of daily required products in the refrigerator. It uses a load cell sensor to measure the quantity of products in refrigerator, and, when the quantity of current products (e.g., eggs and milk) falls below a set limit, it informs the consumer via an LCD display. When a product has completely run out, the auto mode is on, after which an automatic message of daily needs is submitted to the supermarket by SMS (Short Message Service). This smart device is connected via wireless, and a Raspberry Pi is utilized as a central server. This system can be controlled through a web browser to monitor, control, and manage. The information is submitted to and received from the central server via the Internet or the cloud. An Android application has been developed for remote control of the system (on/off) from anywhere across the globe that has Internet access. This system lacks many of the services provided by ours. For example, the system displays the quantity of a product on the LCD only when it has run out, the customer must check the stock of food and drinks by looking at the LCD personally, the customer must manually check the expiry dates, there is no customer control of purchase action, the system does not alert the user that a product has run out, the system does not inform the user that it is going to send an order to the supermarket, and it does not support other languages, like Arabic.

An IoT-based smart refrigerator system is presented in [22] which uses sensing technology to monitor the quantity and quality (expiry date) of the food products stored inside it. The complete system is controlled by an ARM microcontroller, where a load cell is used as an input to the microcontroller and Wi-Fi transmits all information to an Android phone via IoT. It uses the load cell sensor, to measure the quantity of a product in the refrigerator. When that product is about to run out, an alert notification is sent to the user's mobile. This system notifies the consumer about the current status of food products via an Android application and will remind the consumer before a product is about to expire. The Android app is used as a GUI for the user to see the status of the food products kept inside the refrigerator. Again, this system is missing many of the services provided by ours. For example, the customer buys the food personally and checks the quantity and quality of food (no liquids), and it does not support other languages, like Arabic.

Authors attempt to present an intelligent refrigerator with monitoring capability through the Internet which is able to automatically keep track items by detecting an empty space in the refrigerator [26]. This smart refrigerator uses three sensors. Each sensor represents a product (e.g., tomatoes, milk, strawberries). Each sensor contains an IR sensor. When the product is about to run out, the sensor sends a signal to the ARM processor which sends an order to the supermarket. The system consists of an LCD screen and a buzzer on the door of the refrigerator. When a product runs out, the LCD screen shows a message and the buzzer sounds to notify residents. Also, the system will automatically inform the owner by sending a Short Message Service (SMS) to the user. After that, the system sends an order to the supermarket via the fast Ethernet network. Once more, this system is missing many of the features provided by ours. The system monitors products but does not weigh them (the milk bottle may be empty), customer must check the expiry dates personally (the system does not monitor expiry dates), there is no user control of purchase action, IR cannot detect products that are transparent (like water), and the system does not inform the user that it is going to send an order to the supermarket.

A smart refrigerator using Internet of Things is presented in [27] which can sense and monitor the products stored inside it. It uses two kinds of sensors, a pressure sensor which triggers a notification to the user as soon as the applied pressure drops below 0.5 kg (so the consumer is notified every time three eggs are used) and light-dependent resistors (LDRs) which monitor and detect the level of milk or soft drink, for example, in a container. Each bottle has its own LDR. Also, LDR sensors are placed alongside a counter, which can be used to sense the number of eggs on a refrigerator shelf. The core functionality of this smart fridge is to provide a list of food products which might want to be purchased once they have run out. This system is also able to remotely notify the user when a product is about to run out, via SMS (Short Message Service) and email. The message contains information about the product which is about to run out and contains a link which facilitates online purchasing of that specific product. This system, too, is missing many of the services provided by ours. The system does monitor expiry dates, the customer must buy the food personally, and the system does not support other languages, like Arabic.

A typical Internet of Things- (IoT-) based refrigerator has been designed in [28] which features an in-built wide-angle camera that takes a picture of its shelves' contents every time its doors are opened and closed. While visiting a shop, the consumer can then check the latest photo they were sent, to check if they are missing a particular product. In order to keep an updated list of the products in the fridge, RFID is used.

In addition, this system uses "Freshness Tracker" software to track the expiry and by asking the user to enter details of the different features. Observation and monitoring occur when the door of the refrigerator is opened, and information is accessed via monitoring apps on smartphones (mobile devices). Again, this system lacks many of the services provided by ours. The system monitors products but

does not weigh them (milk may be empty), the customer buys the food personally, the system does not alert the user that a product has run out, and it does not support other languages, like Arabic. The authors [29] explained the basic fundamentals related to blockchain and IOT; a detailed review on the various aspects of interconnection, interoperability, reliability, and security needed in daily activities has been described. The researchers listed the challenges, future prospects, and the benefits incurred with the IOT by inculcating blockchain nodes in IOT devices [30]. The paper proposes a novel lightweight framework using blockchain that can be used in IOT devices, and experiments claim the effectiveness of the proposed research with significant reduced overhead and processing time and enhanced security aspect [31]. The authors emphasized on the blockchain as a service and how it can be utilized within IOT, and different case studies have been explored for experimentations and simulations with acceptable accuracies reported [32]. The architecture for arbitrating roles and permissions in realistic IOT scenarios has been explained in the paper [25]. The permissions needed in IOT with scalable architecture have been proposed underlying certain advantages.

#### 4. Comparison with Existing Systems

The comparisons of the selected systems against our proposed system are made, in terms of the problems of each system, the technique of each system, the connection type that each system uses, the services that each system provides, what services are lacking in each system, and a full comparison between these systems and our proposed system.

Based on the results demonstrated (see Table 1), some criteria have been considered in all of the systems studied: the status of food and liquids, checking the quantity of products, human intervention, product checking, utilizing sensors, using central server, employing system platform, and using a specific technique. However, using a proper computer or application issue has been taken into consideration in 86% of the studied systems. Moreover, sending notification (alert) buzzer about the status of food or liquids and checking expiry date of products (quality) in the future have been considered only in 57% of the studied systems. Likewise, only 42% of the related systems are able to do payment automatically and send order to the supermarket (refrigerator self-purchasing). Furthermore, only 28% of the studied systems have taken remote controlling issue into account and the Arabic language criterion has not been considered in previous related systems. Moreover, as can be observed (see Table 2), unlike previous works, all criteria are simultaneously considered in our proposed system, which leads to enhance the performance and save effort, time, and money.

#### 5. Hardware Required

This section presents the required hardware and software for completing the proposed refrigerator circuit. Based on the diagram (see Figure 1), in the circuit of our implemented system, a load cell sensor is utilized which calculates the weight of a product and transmits the data as signals. As



TABLE 1: Execution time representing five stages.

Task	Excellent	Acceptable	Unacceptable	Real time
Scaling product	<3 sec	4-5 sec	>9 sec	3 sec
Sending notification	<2 sec	3-4 sec	>6 sec	2 sec
Controlling purchase	<2 sec	3-4 sec	>7 sec	1 sec
Sending purchase order	<2 sec	3-4 sec	>5 sec	1 sec
Confirm order	<3 sec	6-7 sec	>8 sec	2 sec

TABLE 2: Comparison with previous systems.

Criterion	[24]	[2]	[22]	[26]	[27]	[28]	Our proposed system
Sending notifications about the status of foods	x	x	✓	✓	✓	x	✓
Knowing the status of food and liquid products	✓	✓	✓	✓	✓	✓	✓
Checking expiry date of products	✓	x	✓	x	x	✓	✓
Checking the quantity of products	✓	✓	✓	✓	✓	✓	✓
Arabic language	x	x	x	x	x	x	✓
Human intervention	✓	✓	✓	✓	✓	✓	✓
Product checking	✓	✓	✓	✓	✓	✓	✓
Sensors used	✓	✓	✓	✓	✓	✓	✓
Wireless used	✓	✓	✓	✓	✓	✓	✓
Automatic payment method	x	✓	x	✓	x	x	✓
Sending order to the supermarket	x	✓	x	✓	x	x	✓
Server	✓	✓	✓	✓	✓	✓	✓
Controlling the system remotely	x	✓	x	x	x	x	✓
System platform	✓	✓	✓	✓	✓	✓	✓
Using computer or application	✓	✓	✓	x	✓	✓	✓
Specific technique	✓	✓	✓	✓	✓	✓	✓
Artificial intelligence	✓	x	✓	x	✓	x	✓
Blockchain	X	X	X	X	x	x	✓

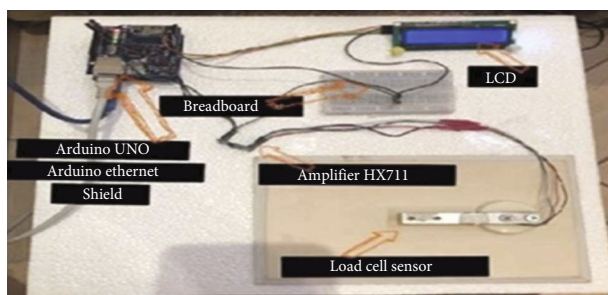


FIGURE 1: Refrigerator circuit.

its signals cannot be read by Arduino, an amplifier HX711 is used. The load cell reads the required information to amplify and further communicate for processing operation. The Liquid Crystal Display (LCD) is used to view the response of the weight. Breadboard is used as a port to collect, as an example, two wires needing the same port. The utilized materials are described in following subsections.

**5.1. Arduino UNO.** In the proposed system, we utilized Arduino UNO as an open-source microcontroller board, which comes with sets of digital and analogue input-output

pins that may be connected to different expansion shields and other circuits. It depends on the Microchip ATmega328P microcontroller and was developed by Arduino.cc [33].

**5.2. Arduino Ethernet Shield.** An Arduino Ethernet shield is employed in our proposed work. This is a microcontroller board based on the ATmega328, with a reset button [33]. The shield contains two informational LEDs: PWR and RX and TX. The first LED indicates that both the Arduino UNO board and the Arduino Ethernet shield are powered. In the second LED, RX flashes when data is received, while TX flashes when data is sent by the shield.

**5.3. Load Cell Sensor.** A load cell sensor is utilized to discover the presence of a food product and then to calculate its weight. The load cell weight depends on the application. In our system, we use 20 kg and the straight bar type. The load cell and the HX711 module should be connected.

**5.4. Load Cell Amplifier HX711 Module.** As the Arduino is not able to read the signal issued from the weight sensor, the HX711 is employed. HX711 is responsible to read the information from the load cell, amplify the signals received from the weight sensor, and then send it to the Arduino processor,

based on the ATmega328 microcontroller as digital for processing, which is connected to the Arduino Uno. The GND pins of the module and Arduino should be connected. DT and SCK and digital pins 2 and 3 of the Arduino should be connected. The remaining pins of the Arduino VCC and 3.3V should be connected. Figure 2 shows the diagram.

A breadboard is utilized which is aimed at building an Arduino-compatible circuit [34].

**5.5. LCM1602 Module.** The LCM1602 module is employed in order to display for the system. It requires a connection to the 5V pin. To divide the Arduino's 3.3V signal, a breadboard is placed in the middle. Both the SDA and SCL pins of the LCM1602 module are connected by connecting the pins. Moreover, the GND pins and one of the Arduino's GND pins should be connected, and the VCC pin and the 3.3V signal of the breadboard should be connected. In general, IOS OS is used to run the Blynk application. In addition, this application is used to inform the user of all product situations and for controlling purchase as well. The same has been shown in Figure 3.

**5.6. Blynk Application.** To control the Arduino, we decided to use Blynk. It is a platform designed for the IoT, with different applications for controlling the Arduino and other devices. The Blynk platform consists of three main components: Blynk app, where you can create a graphical interface using different widgets; the Blynk server, which is responsible for the process of communication between the smartphone and the hardware (Arduino); and the Blynk Library, which allows communication with the server and the processing of all incoming and outgoing commands. To start using the Blynk platform, you need only two things: the hardware (Arduino) and a smartphone. This makes it very easy, as seen (see Figure 4) [10]. Every time a button in the Blynk app is pressed, the message is submitted to the Blynk cloud, as the message knows its path to the Arduino, and in the opposite direction, it works the same [35].

**5.7. Proposed Methodology.** This section gives the system architecture of the proposed system in detail (see Figure 5); it depicts the architectural design of the proposed system. This system uses a few weight sensors, which monitor the weight of the product stored inside the refrigerator. Weighing the product is performed by interfacing the load cell sensor and the HX711 weight sensor with Arduino. When a product (e.g., milk) is placed on a load cell sensor, pressure (or "load") is applied. The electrical resistance of the sensor will respond to this pressure and will change to give accurate information of the weight as a signal. As the Arduino is not able to read the signal issued by the weight sensor, the HX711 reads the information from the load cell, then amplifies the signal and sends it to the Arduino processor (based on the ATmega328 microcontroller) for processing.

If the stock of the product has dropped to half, a quarter, or zero, the Arduino sends a notification to the Blynk app, via the Ethernet that is connected to the Arduino processor through the RS232 interface. In addition, in case any temporary problem has affected the application, the Arduino will

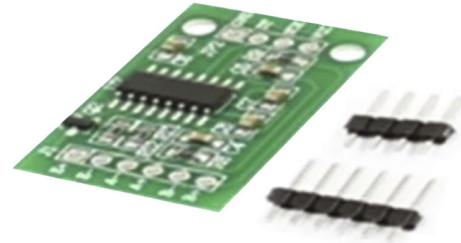


FIGURE 2: Load cell amplifier HX711 module.

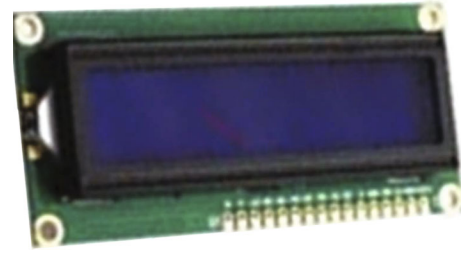


FIGURE 3: LCM1602 module.

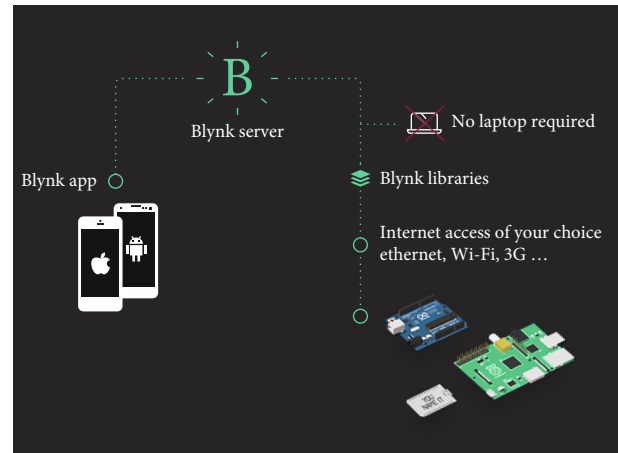


FIGURE 4: Blynk platform.

notify the owner via two methods: email or SMS when the owner does not access to the Internet. The notification includes a message about the current stock of the product, seeking permission from the owner to commence a purchase process with the shop that the owner has already registered with. Once the Arduino receives an acceptance from the owner, it sends the order to the shop via Ethernet.

In the shop's system, an appropriate software is installed. This system will be connected to refrigerators using generated IDs, unique to each owner for each refrigerator IP, and whenever a request is sent to the shop, a message will pop up, informing the shop that a request has been sent by a refrigerator. The unique code number (ID) will be given to the customer when he/she signs up with the shop online, on provision of home address and card details. This system will use online payment via credit/debit cards.



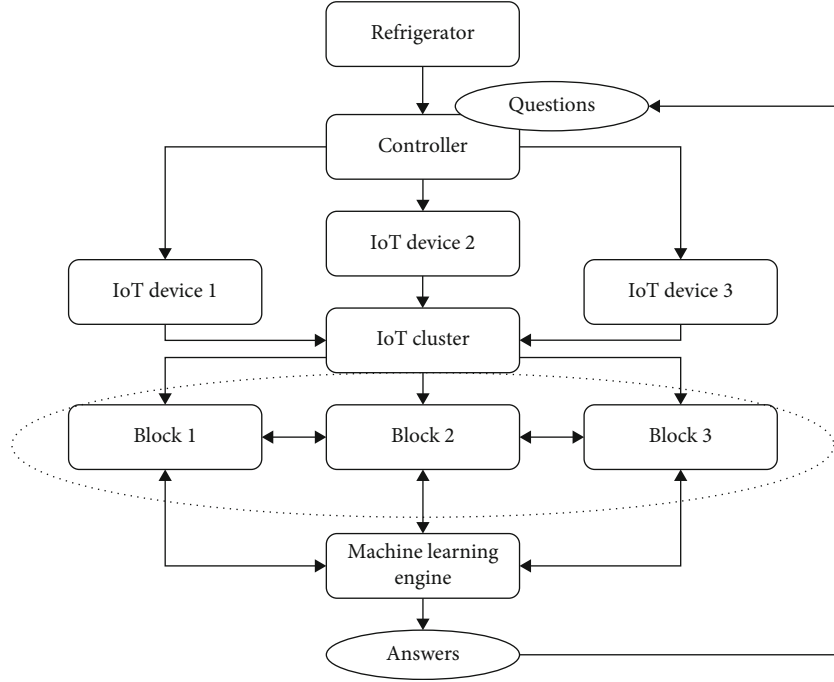


FIGURE 6: Data flow system.

blockchain needs to be diamantine for taking the data out, blockchain is mined using very complex machines; however, the underlying mathematics, for mining any blockchain two important factors, needs to be considered.

In the time frame ( $t$ ) of the blockchain and the nonce of the dataset, which is the number, both will act as public keys to extract the information from the block chain. The machine learning model will use this technique the get the right information. A hash function turns a numerical input value into another compressed numerical value. The input to the hash function can be any length, but the output is always the same. The other name of Merkle tree is hash tree which helps in verifying and synchronizing the data. In this, every nonleaf node is labelled with the hash of the labels or values of its child nodes. They allow efficient and secure verification of the contents of large data structures. Cryptographic accumulators allow you to compact arbitrarily many pieces of data into a constant amount of space. In other words, a Merkle tree represents arbitrarily many blocks while only transmitting a single hash across the wire. The explanation is given below:

**5.9.1. Basics. Hash function:** a deterministic function to transform data of any range into a fixed range.

**Merkle tree:** a way of storing a potentially huge amount of data, while providing the user with a simple way to check that the data has not been modified.

Say, the dataset is

$$D = \{d_1, d_2, d_3, \dots, d_n\}. \quad (1)$$

Hashed  $D$  is

$$D = \{H(d_1), H(d_2), H(d_3), \dots, H(d_n)\}, \quad (2)$$

where  $H$  is the hash function.

Merkle tree is a graphical relational tree between the dataset of hashed functions. A block is defined as a vector of entries. Say, we have  $n$  datasets. So, block  $B$  will be defined as

$$B = \{T_1, T_2, \dots, T_n\}. \quad (3)$$

Say, we have two blocks,  $B$  and  $B^{\text{prev}}$ ; in order to find the proof-of-work of the block chain, we need to find a number called “nonce.”

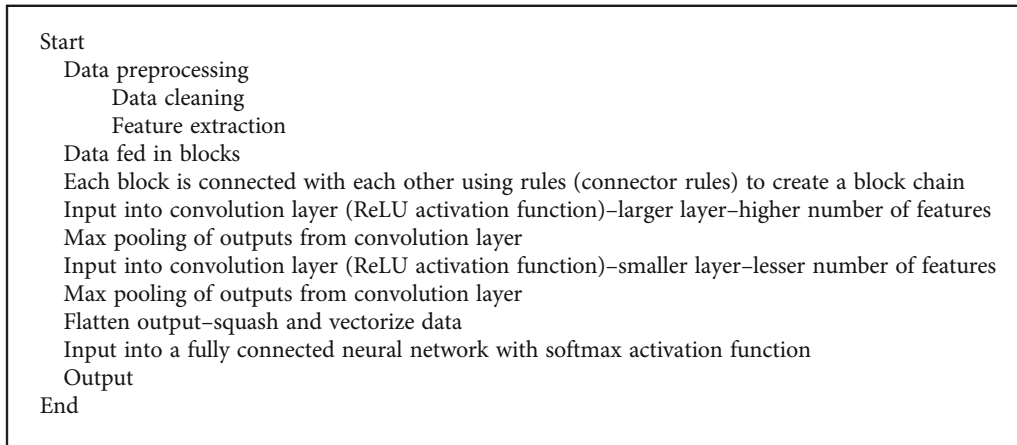
Mathematically, the relation is

$$(H(B^{\text{prev}}) \oplus R^{\#}(B) \oplus \text{timestamp}(t) \oplus b \oplus \text{nonce}) \leq \text{target}, \quad (4)$$

where  $\oplus$  is the concatenation operator and  $R^{\#}$  is the hash factor.

The nonce and timestamp explain the complexity and the ease of usage of the blockchain.

**5.10. Integration of AI Using Deep Learning Techniques.** AI is of great significance from economic, food safety, and public health points of views. Artificial intelligence is the art and science of creating intelligent machines, especially intelligent computer programs [37]. It is like the task of using computers to decode human intelligence and significantly to



ALGORITHM 1: Process showing integration of software into smart system.

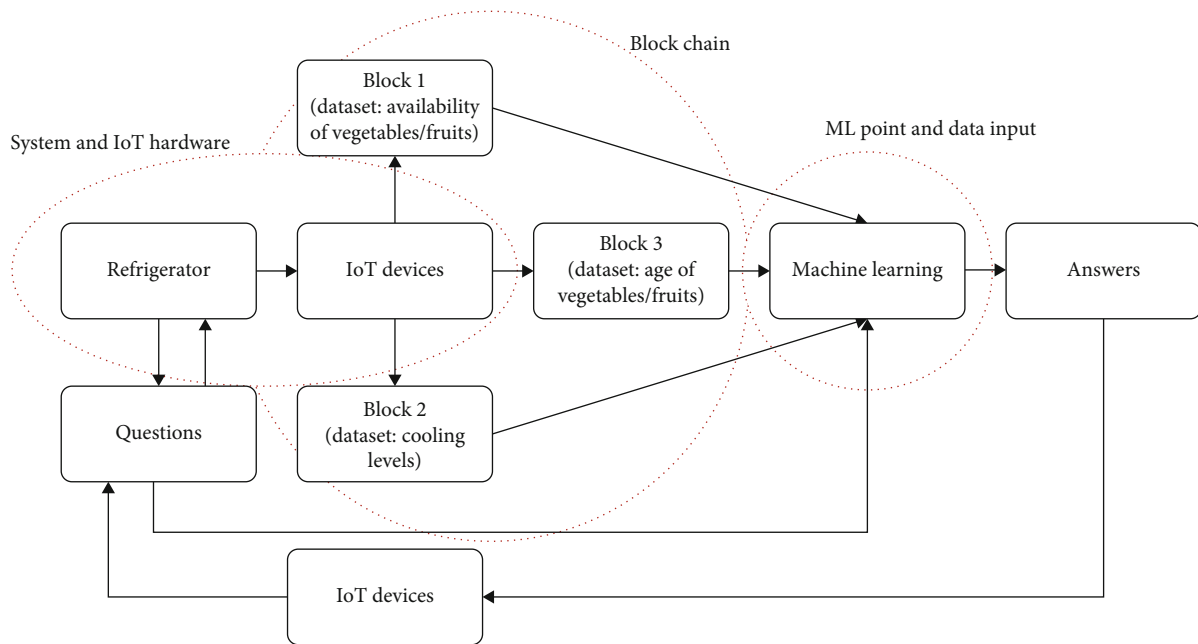


FIGURE 7: Pipeline showing the system architecture.

the economy. In the following phase of the pipeline, the IOT hardware is collecting data from the refrigerator and the collected data goes into the cloud database, like AWS and after the data is ingested into the data preprocessing machine where data cleaning, formatting, and feature selection are done. The data preprocessing is done; thereafter, the answer is needed for several answers are required. Should we reorder item A, is item B’s inventory less or more, cooling is less, and cooling is more? For getting the answers, we run the data into the CNN model. The CNN model is based on the convolution layer, pooling layer, and the softmax layer [38]. The convolution happens in two steps; the first step happens in more extensive number of features, from where we get the larger number of pool of data. Then, it is again max pooled into the smaller convolutional network which will pin point to the answers of the decision which we want. The algorithm of the whole process is shown (see Algorithm 1).

The hardware level of integration of equipment is achieved with a more sophisticated software level of integration of system. The microprocessors are gradually graduated to the level of algorithms and computing through cloud. The framework model outlining the process is shown (see Figure 7).

## 6. Results and Discussions

In this section, five stages of the proposed system are separately tested. The goal of this section is to realize how real users interact with the system and improve system based on the results. The proposed system consists of five stages as follows: (i) the refrigerator system scales the product, (ii) the refrigerator system sends product status notifications (email and alarm to mobile), (iii) the owner of refrigerator controls purchase order of products, (iv) the refrigerator system sends purchase order of product, and (v) the owner of

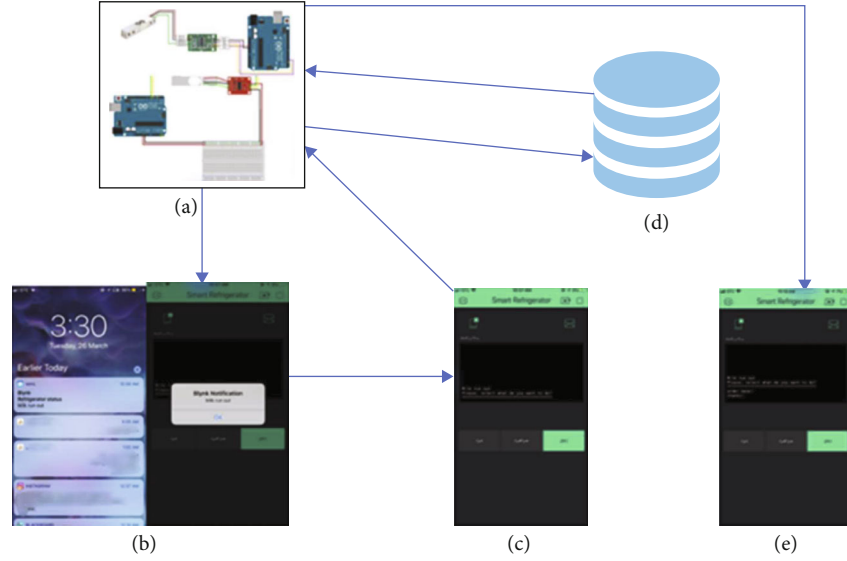


FIGURE 8: System testing.

TABLE 3: Results with precisions, recall, and accuracy.

Epoch	Accuracy	Precision	Recall	<i>F</i> -score
1	79	62	49	54
50	85.91	76	52	61
100	87.12	77	54	63
200	89.19	81	59	68
500	92.72	83	62	70
1000	97.66	86	67	75
2000	98.19	87	74	79
3000	99.01	89	77	82
4000	99.1	92	79	85
5000	99.17	93	82	87

refrigerator receives a confirmation message of sending product order (see Figure 8).

Table 1 shows the real time of execution of five stages. As can be observed, all five stages have been executed in excellent time, which shows high performance of the presented system.

*6.1. Experiments and Analysis.* This study has been experimented using Python where the different modules such as NumPy for analysis on the dataset, Seaborn for plotting operations, pandas for data ingestion, Matplotlib for basic plotting graphs, and machine learning classifiers sklearn and TensorFlow for performing the training and testing of the data [39] have been used. The results have been computed by using the Intel i5 8th Gen processor with 16 GB RAM and CentOS operating system. Secondly, the deep learning and machine classifiers are applied considering total 14 features. Blockchain is implemented using Hashlib library and Python 3.0. Table 3 shows the precision, recall, and accuracy of the deep learning classifiers.

Precision is defined as the ratio of recovered words that are appropriate to search [40].

$$\text{Precision rate} = \frac{PT}{(TP + FP)}. \quad (5)$$

Recall is defined as the ratio of words that are appropriate to that which is successfully recovered.

$$\text{Recall} = \frac{PT}{(TP + FN)}. \quad (6)$$

*F*-measure is defined as the harmonic mean of the above two defined.

$$F\text{-measure} = \frac{2 * \text{recall} * \text{precision}}{(\text{recall} * \text{precision})}. \quad (7)$$

In order to train the CNN, KNN, and SVM model, 5000

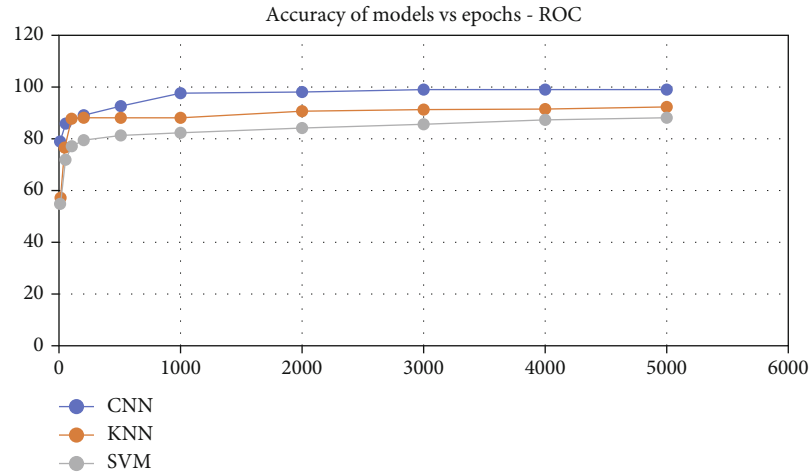


FIGURE 9: Accuracy comparison with machine learning classifiers.

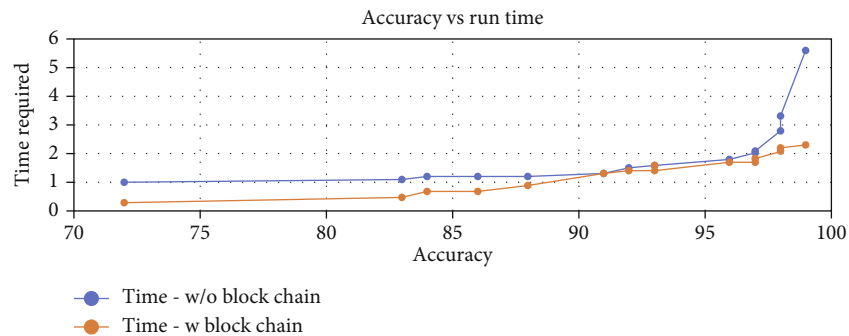


FIGURE 10: Experiments showing the computation time with and without integration of blockchain.

epochs have been run. The epoch vs. accuracy plot is given (see Figure 9) representing the accuracy at each iteration.

Figure 10 demonstrates the decreased run time with and without the implementation of block chain, which has been validated mathematically as well. The figure shows that the computation time increases by a factor of 25 to 30%.

## 7. Conclusions

In this paper, a smart refrigerator system using a Blynk platform has been introduced. The proposed system has been created to help users be immediately updated about the quantity of one product (milk) stored in the refrigerator, using IoT technology and Blynk. The AI-enabled system can automatically make the decisions which will help the users in efficient and productive purchasing of the product from a connected shop when it receives permission from the user. This hardware technology can be incorporated with the software level of integration to make unique decisions by cohesively combining cloud database for decreasing the computation complexities involved in the process. Unlike the previous systems, our designed system considers all criteria of a high-quality smart refrigerator, which leads to help us to live an easier, faster, and healthier lifestyle. A single refrigerator has to continuously run for a very long time for the ML module to have sufficient data to make precise

predictions. The accuracy with which the system works also depends on the hardware quality of the IoT Devices. Since IoT devices also interact among themselves, the signal attenuation in the process also affects the performance of the system.

Moreover, in the future studies, it is suggested to improve the proposed system in such a way that the customers can be updated about the expiry dates of all products stored inside their refrigerator, immediately and periodically, without human intervention. This paper is better because of an optimized run time and also in terms of providing better data security by using blockchain technology. This research can be extended to agricultural and medical fields.

## Data Availability

This is confidential and cannot be discussed at this stage, since the project is ongoing.

## Conflicts of Interest

The author declares that there are no conflicts of interest to report regarding the present study.

## Acknowledgments

This project was funded by the Deanship of Scientific Research (DSR) at King Abdulaziz University, Jeddah, under Grant No. J: 163-865-1440. The author, therefore, acknowledges with thanks DSR for the technical and financial support.

## References

- [1] L. Liu, Y. Guo, Y. Sun, Z. Wang, E. Sun, and Y. Sun, *Improved joint optimization design for wireless sensor and actuator networks with time delay*, Wireless Communications and Mobile Computing, 2021.
- [2] Y. Wang, S. Tang, X. Zhu, and Y. Xie, *A novel multitask scheduling and distributed collaborative computing method of edge nodes in the internet of things*, Wireless Communications and Mobile Computing, 2021.
- [3] N. Kakade and S. Lokhande, "IoT based intelligent home using smart devices," *International Journal of Innovation Research Computer Communication Engineering*, vol. 4, no. 6, pp. 12090–12097, 2016.
- [4] Y. Kim, Y. Park, and J. Choi, "A study on the adoption of IoT smart home service: using value-based adoption model," *Total Quality Management & Business Excellence*, vol. 28, no. 9-10, pp. 1149–1165, 2017.
- [5] H. Yang, W. Lee, and H. Lee, "IoT smart home adoption: the importance of proper level automation," *Journal of Sensors*, vol. 2018, Article ID 6464036, 11 pages, 2018.
- [6] E. Park, Y. Cho, J. Han, and S. J. Kwon, "Comprehensive approaches to user acceptance of Internet of Things in a smart home environment," *IEEE Internet of Things Journal*, vol. 4, no. 6, pp. 2342–2350, 2017.
- [7] A. Zielonka, M. Wozniak, S. Garg, G. Kaddoum, M. J. Piran, and G. Muhammad, "Smart homes: how much will they support us? A research on recent trends and advances," *IEEE Access*, vol. 9, pp. 26388–26419, 2021.
- [8] B. L. Risteska Stojkoska and K. V. Trivodaliev, "A review of Internet of Things for smart home: challenges and solutions," *Journal of Cleaner Production*, vol. 140, no. 3, pp. 1454–1464, 2017.
- [9] O. Vermesan and P. Friess, *Internet of Things—from Research and Innovation to Market Deployment*, vol. 29, River publishers Aalborg, Aalborg, Denmark, 2014.
- [10] K. Agarwal, A. Agarwal, and G. Misra, "Review and performance analysis on wireless smart home and home automation using IoT," in *2019 Third International conference on I-SMAC (IoT in Social, Mobile, Analytics and Cloud) (I-SMAC)*, Palladam, India, 2019.
- [11] M. Khan, B. N. Silva, and K. Han, "Internet of things based energy aware smart home control system," *IEEE Access*, vol. 4, pp. 7556–7566, 2016.
- [12] I. García-Magariño, R. Muttukrishnan, and J. Lloret, "Human-centric AI for trustworthy IoT systems with explainable multi-layer perceptrons," *IEEE Access*, vol. 7, pp. 125562–125574, 2019.
- [13] S. S. Hosseini, K. Agbossou, S. Kelouwani, A. Cardenas, N. Henao et al. et al., "A practical approach to residential appliances on-line anomaly detection: a case study of standard and smart refrigerators," *IEEE Access*, vol. 8, pp. 57905–57922, 2020.
- [14] X. Jiang and C. Xiao, "Household energy demand management strategy based on operating power by genetic algorithm," *IEEE Access*, vol. 7, pp. 96414–96423, 2019.
- [15] D. Serpanos and M. Wolf, *Internet-of-Things (IoT) Systems: Architectures, Algorithms, Methodologies*, Springer, Gewerbestrasse, Cham, Switzerland, 2019.
- [16] A. D. Floarea and V. Sgârciu, "Smart refrigerator: a next generation refrigerator connected to the IoT," in *2016 8th International Conference on Electronics, Computers and Artificial Intelligence (ECAI)*, Ploiesti, Romania, 2016.
- [17] D. Fakhri and K. Mutijarsa, "Secure IoT communication using blockchain technology," in *2018 International Symposium on Electronics and Smart Devices (ISESD)*, Bandung, Indonesia, 2018.
- [18] S. Qiao, H. Zhu, L. Zheng, and J. Ding, "Intelligent refrigerator based on internet of things," in *2017 IEEE International Conference on Computational Science and Engineering (CSE) and IEEE International Conference on Embedded and Ubiquitous Computing (EUC)*, Guangzhou, China, 2017.
- [19] M. A. Ahmed and R. Rajesh, "Implementation of smart refrigerator based on internet of things," *International Journal of Innovative Technology and Exploring Engineering*, vol. 9, no. 2, pp. 2278–3075, 2019.
- [20] H. H. Wu and Y. T. Chuang, "Low-cost smart refrigerator," in *2017 IEEE International Conference on Edge Computing (EDGE)*, Honolulu, HI, USA, 2017.
- [21] M. P. C. S. P. Harish and K. B. P. A. Sanghavi, "Smart refrigerator and vegetable identification system using image processing and IOT," *Open Access International Journal of Science and Engineering*, vol. 7, no. 4, 2021.
- [22] D. Singh and P. Jain, "IoT based smart refrigerator system," *International Journal of Advanced Research in Electronics and Communication Engineering*, vol. 5, no. 7, pp. 2080–2084, 2016.
- [23] I. Mohammad, M. S. I. Mazumder, E. K. Saha, S. T. Razzaque, and S. Chowdhury, "A deep learning approach to smart refrigerator system with the assistance of IOT," in *ICCA 2020: Proceedings of the International Conference on Computing Advancements*, pp. 1–7, New York, NY, USA, 2020.
- [24] L. Xie, Y. Yin, X. Lu, B. Sheng, and S. Lu, "iFridge: an intelligent fridge for food management based on RFID technology," in *Proceedings of UbiComp*, pp. 291–294, New York, NY, USA, 2013.
- [25] O. Novo, "Blockchain meets IoT: an architecture for scalable access management in IoT," *IEEE Internet of Things Journal*, vol. 5, no. 2, pp. 1184–1195, 2018.
- [26] G. S. Nayak and C. Puttamadappa, "Intelligent refrigerator with monitoring capability through internet," *International Journal of Computer Applications*, vol. 2, pp. 65–68, 2011.
- [27] S. Prapulla, G. Shobha, and T. Thanuja, "Smart refrigerator using internet of things," *Journal of Multidisciplinary Engineering Science and Technology*, vol. 2, no. 7, pp. 1795–1801, 2015.
- [28] F. Osisanwo, S. Kuyoro, and O. Awodele, "Internet refrigerator—a typical internet of things (IoT)," in *3rd International Conference on Advances in Engineering Sciences & Applied Mathematics (ICAESAM'2015)*, London (UK), 2015.
- [29] X. Zhu, Y. Ni, L. Gu, and H. Zhu, "Blockchain for the IoT and industrial IoT: a review," *Internet of Things*, vol. 10, pp. 100081–100095, 2020.
- [30] A. Reyna, C. Martín, J. Chen, E. Soler, M. Díaz et al., "On blockchain and its integration with IoT. Challenges and



- opportunities,” *Future Generation Computer Systems*, vol. 88, pp. 173–190, 2018.
- [31] A. Dorri, S. S. Kanhere, and R. Jurdak, “Towards an optimized blockchain for IoT,” in *2017 IEEE/ACM Second International Conference on Internet-of-Things Design and Implementation (IoTDI)*, pp. 173–178, Pittsburgh, PA, USA, 2017.
- [32] M. Samaniego, U. Jamsrandorj, and R. Deters, “Blockchain as a service for IoT,” in *2016 IEEE international conference on internet of things (iThings) and IEEE green computing and communications (GreenCom) and IEEE cyber, physical and social computing (CPSCom) and IEEE smart data (SmartData)*, pp. 433–436, Chengdu, China, 2016.
- [33] V. Phulphagar and R. Jaiswal, “Arduino controlled weight monitoring with dashboard analysis,” *International Journal of Research Applied Sciences and Engineering Technology*, vol. 5, pp. 1164–1167, 2017.
- [34] A. G. Smith, *Introduction to Arduino*, University in Cambridge, England, 2011.
- [35] T. Deshpande and N. Ahire, “Home automation using the concept of IoT,” *IJCSN International Journal of Computer Science and Network*, vol. 5, no. 3, p. 443, 2016.
- [36] S. Basheer, K. K. Nagwanshi, S. Bhatia, S. Dubey, G. R. Sinha et al., “FESD: an approach for biometric human footprint matching using fuzzy ensemble learning,” *IEEE Access*, vol. 9, pp. 26641–26663, 2021.
- [37] K. Nikhil, “Design and construction of an IOT based intelligent home using smart devices,” *International Journal of Innovative Research in Electrical Electronics and Instrumentation Engineering*, vol. 4, no. 6, pp. 12090–12097, 2016.
- [38] M. Alojail and S. Bhatia, “A novel technique for behavioral analytics using ensemble learning algorithms in E-commerce,” *IEEE Access*, vol. 8, pp. 150072–150080, 2020.
- [39] S. Bhatia, “A comparative study of opinion summarization techniques,” *IEEE Transactions on Computational Social Systems*, vol. 8, no. 1, pp. 110–117, 2021.
- [40] S. Bhatia, M. Sharma, and K. K. Bhatia, “Opinion score mining: an algorithmic approach,” *International Journal of Intelligent Systems and Applications*, vol. 9, no. 11, pp. 34–41, 2017.

## *Retraction*

# **Retracted: Graph Convolutional Networks for Cross-Modal Information Retrieval**

### **Wireless Communications and Mobile Computing**

Received 25 July 2023; Accepted 25 July 2023; Published 26 July 2023

Copyright © 2023 Wireless Communications and Mobile Computing. This is an open access article distributed under the Creative Commons Attribution License, which permits unrestricted use, distribution, and reproduction in any medium, provided the original work is properly cited.

This article has been retracted by Hindawi following an investigation undertaken by the publisher [1]. This investigation has uncovered evidence of one or more of the following indicators of systematic manipulation of the publication process:

- (1) Discrepancies in scope
- (2) Discrepancies in the description of the research reported
- (3) Discrepancies between the availability of data and the research described
- (4) Inappropriate citations
- (5) Incoherent, meaningless and/or irrelevant content included in the article
- (6) Peer-review manipulation

The presence of these indicators undermines our confidence in the integrity of the article's content and we cannot, therefore, vouch for its reliability. Please note that this notice is intended solely to alert readers that the content of this article is unreliable. We have not investigated whether authors were aware of or involved in the systematic manipulation of the publication process.

Wiley and Hindawi regrets that the usual quality checks did not identify these issues before publication and have since put additional measures in place to safeguard research integrity.

We wish to credit our own Research Integrity and Research Publishing teams and anonymous and named external researchers and research integrity experts for contributing to this investigation.

The corresponding author, as the representative of all authors, has been given the opportunity to register their agreement or disagreement to this retraction. We have kept a record of any response received.

### **References**

- [1] X. Yang and W. Zhang, "Graph Convolutional Networks for Cross-Modal Information Retrieval," *Wireless Communications and Mobile Computing*, vol. 2022, Article ID 6133142, 8 pages, 2022.

## Research Article

# Graph Convolutional Networks for Cross-Modal Information Retrieval

Xianben Yang and Wei Zhang 

College of Computer Science and Technology, Beihua University, Jilin, 132000 Jilin, China

Correspondence should be addressed to Wei Zhang; [allenlov@21cn.com](mailto:allenlov@21cn.com)

Received 3 November 2021; Revised 2 December 2021; Accepted 8 December 2021; Published 6 January 2022

Academic Editor: Shalli Rani

Copyright © 2022 Xianben Yang and Wei Zhang. This is an open access article distributed under the Creative Commons Attribution License, which permits unrestricted use, distribution, and reproduction in any medium, provided the original work is properly cited.

In recent years, due to the wide application of deep learning and more modal research, the corresponding image retrieval system has gradually extended from traditional text retrieval to visual retrieval combined with images and has become the field of computer vision and natural language understanding and one of the important cross-research hotspots. This paper focuses on the research of graph convolutional networks for cross-modal information retrieval and has a general understanding of cross-modal information retrieval and the related theories of convolutional networks on the basis of literature data. Modal information retrieval is designed to combine high-level semantics with low-level visual capabilities in cross-modal information retrieval to improve the accuracy of information retrieval and then use experiments to verify the designed network model, and the result is that the model designed in this paper is more accurate than the traditional retrieval model, which is up to 90%.

## 1. Introductions

With the development of image acquisition and sharing technology, the amount of image data that people experience has increased significantly, and the biggest problem facing today is how to effectively and accurately obtain the images that users are interested in [1, 2]. Cross-modal information retrieval technology has made great progress in recent years, but it still cannot meet human needs. The main reason is that due to the semantic gap between image visual features and high-level semantic concepts, the accuracy of cross-modal information retrieval cannot meet the demand, and the image feature vectors used in CBIR usually result in slow retrieval speed [3, 4]. TBIR uses only textual information to index and search images. Compared with visual information, text information basically uses low-dimensional and simple concepts to describe the content of images, which is easy for humans to understand, but TBIR often requires manual semantic annotation, which is only suitable for small special libraries [5, 6]. In recent years, the development of social networks has made image data grow exponentially, but this

kind of semantic information-based retrieval is very random, contains a lot of noise, and is incomplete [7, 8].

Regarding the research of image retrieval technology, some researchers believe that as people's demand for restoration continues to grow, content-based image retrieval systems may not be able to meet people's needs. At present, the derivation based on semantic image retrieval technology can better represent the local attributes of image semantic information. However, there are still some problems; that is, the complex image descriptors obtained by deep learning algorithms (such as mapping and grouping) may not be able to fully express the semantic information expressed by the complex graphics itself. Therefore, in real applications, the more complex the image structure, the worse the robustness of the semantic search method [9]. Some researchers derived the image mean and standard deviation as general color features in the YUV color space and obtained a binary image bitmap, thereby deriving its local color features. Then, the shape of the image is derived through more compact and instant Clauchuk feature variables, and then, the texture characteristics of the image are obtained through the

improved four-pixel concurrent matrix algorithm. Finally, multiple feature points are integrated to calculate the similarity between the inspected image and the image in the image library, thereby returning a highly similar image [10]. When studying deep learning technology, some researchers found that in traditional content-based image retrieval algorithms, the choice of predesigned image feature extraction algorithms is often a priori image content. Therefore, SIFT algorithm is usually more conducive to deriving characteristic scene images, while HOG algorithm is more able to measure pedestrian characteristics and behavior. The main disadvantages of this selection method are low efficiency and long debugging time. Deep learning technology overcomes these shortcomings. Deep learning is a feature extraction process that does not require human intervention at all. This is a deep framework using unsupervised learning algorithms. In-depth training automatically learns the low-level characteristics of the image in the original input image, gradually subtracts, maps, and combines this feature, and finally obtains the high-level semantic function and then analyzes or detects the real-time high-level semantic feature. Higher-order semantic features are more expressive than those obtained in traditional feature extraction algorithms and also help to improve search accuracy [11]. In summary, there are many research results on image retrieval technology, but there are few researches on the fusion of convolutional neural network technology and cross-modal image retrieval technology, and there are still some problems in the retrieval process.

This paper studies the graph convolutional network for cross-modal information retrieval. Based on the literature, it puts forward the basic ideas of cross-modal information retrieval in this paper and summarizes the application of convolutional neural networks. The cross-modal information retrieval of the neural network is designed, and then, the designed network model is verified, and conclusions are drawn through experiments.

## 2. Cross-Modal Information Retrieval and Convolutional Network Research

### 2.1. The Basic Idea of Cross-Modal Information Retrieval.

With the development of social networks in recent years, it is easier to obtain text information related to the image from the user, such as comments and tags, from users during the process of sharing pictures on the Internet [12]. Artificial annotation semantics technology allows the extraction of semantic concepts related to images from textual information. In fact, the traditional way of manually labeling semantics has been socialized through Internet technology. For example, photo sharing sites provide users with annotation and tagging functions. Users viewing photos can add descriptive text paragraphs to photos at any time and select one or more tags (birds, trees, sea, etc.) for the photos. However, due to the high randomness of comments and points, the generated text contains a lot of noise. Some tags may be assigned to images that are unrelated to them. In addition, some images may receive incomplete labels. This

means that some important semantic information described in the image has not been recorded.

Both content-based image search and text-based search have disadvantages, but they compensate for each other. For example, it is difficult to infer high-level semantics directly from image search features, but the semantics of text-based searches are more accurate, so they can use their complementarity to partially filter text semantic noise. In addition, some semantic thinking can be inferred more accurately from the content. In this case, the use of content-based editing technology to extract semantics can be used as a supplement to image semantics. Therefore, this article focuses on cross-graphic information retrieval. The main reason why images and texts can learn from each other is that they are related to each other at the semantic level, while the mutual search of images and text requires a high degree of generalization and content representation. The association of images and text requires the creation of a cross link between the two features of graphics and text. In-depth understanding is the key to crossing the two characteristics of graphics and text. For example, an image search system can search for images in a clear sky by assigning "1 blue dots," while a text search system can search for the sky in the text using the "sky" keyword. Therefore, the cross information retrieval system also needs to understand the correlation between the text "sky" and the visual feature "blue." Therefore, when editing images or text, you need to go through many hidden layers to remove semantic noise and extract features between different modes.

### 2.2. Application of Convolutional Network.

CNN has long been used in the field of image classification. Compared with other theories, convolutional neural networks achieve better classification accuracy on large data sets. Similarly, important discoveries have been made in reducing the size of the filter and increasing the depth of the filter. For many image sorting tasks in image classification, creating a hierarchical classifier structure is a common strategy of convolutional neural networks. By using a hierarchical structure to exchange information between related classes, classification performance can also be improved without many training examples. The strategy to improve the classification accuracy is to build a tree structure to more accurately record the detailed features in subcategory recognition. There is a theory that the development of convolutional networks is not only reflected in accuracy but also in layering. In this theory, different categories are grouped according to similarities and organized voluntarily to form different levels.

Image classification and image positioning methods are common techniques in cross-modal image analysis. But in fact, image target discovery also solves the semantic process of discovering the target first and then discovering the target with the idea of sorting. At the same time, in the entire convolution model, semantic extraction only needs to obtain the final semantic label, not the semantic label coordinates of the image or the covered area. For example, an image includes people, cars, and trees. The first thing to do is to extract features representing people, cars, and trees from the image, but you do not need to know the relationship between the

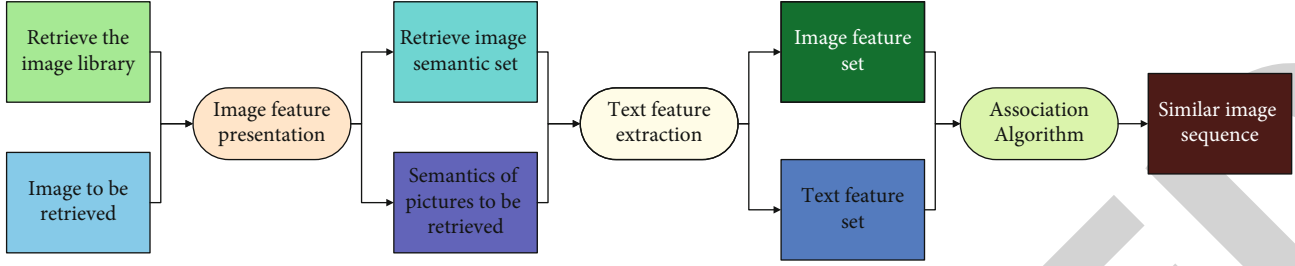


FIGURE 1: Cross-modal semantic information acquisition model.

coordinates and positions of people, cars, and trees. In addition, for some special tags, it is difficult to identify the areas covered by the tags, such as family and carnival tags.

**2.3. Convolutional Neural Network Algorithm.** The neural network model is mainly composed of the following three parts: the connection between the networks, the weighted summation of the input information, and the activation mapping function. Assuming that the input sample is composed of four elements  $(x_1, x_2, x_3, +1)$ , the output result of the neuron is expressed as:

$$h_{w,b}(x) = f(w^T x) = f\left(\sum_{i=1}^3 w_i x_i + b\right). \quad (1)$$

Among them,  $f$  is the activation mapping function of this neuron, and  $b$  is a bias.

CNN is a supervised learning network model with multiple hidden layers. The hidden layers include convolutional layers and downsampling layers. The two operations are performed alternately to complete the main part of extracting features. The network structure can be represented by the following function:

$$h_w(x) = f_1(\dots f_2(f_1(x, w_1), w_2) \dots, w_i). \quad (2)$$

Generally, a convolutional neural network includes three stages: convolution, nonlinear transformation, and downsampling. Each hidden layer of the convolutional neural network has an input  $x_i$  and a weight parameter  $w_i$ . The output  $x_{i+1}$  of each layer is the input of the next layer, and the parameter  $w = (w_1, w_2, \dots, w_i)$  is the weight of the convolution kernel of each layer.

### 3. Cross-Modal Information Retrieval Based on Convolutional Neural Network

**3.1. Cross-Modal Information Retrieval Analysis.** Combining high-level semantics with low-level visual capabilities to perform image search more accurately and efficiently is a hot spot in the current image search research field. At present, in view of the overall high-level semantics and low-level features of the image, there is no mature semantic information collection model, which is difficult to meet the needs of today's massive image information retrieval. This article constructs a basic semantic information acquisition model

to extract the semantics of the objects in the image from the basic features of the image information and conduct a series of exploratory research. Figure 1 is a schematic diagram of a cross-modal semantic information acquisition model.

#### 3.2. Data Collection

- (1) Through Baidu, Google, and Tencent three map software, in real-time street view, according to the operation of the time machine, obtain the street shop signs in this city. In fact, the main source of the screenshots here is Baidu Time Machine, because Google's time machine in mainland China is limited, and Tencent Maps captures a relatively small number of images while retaining the GPS location
- (2) Filter and clean up the collected data set. Before cleaning the image, this article first determines the main area of the image used in this article. The main areas of the logo mainly include main text (shop name), shop logo, and related main auxiliary explanatory text
- (3) After receiving the data set, the size of the data has a greater impact on the recognition of image semantics, in order to facilitate the continuation of the work of this paper. This article uses data improvement strategies to increase the amount of data. Common data expansion strategies include zooming, scaling the image according to a specific ratio, rotating, rotating the image at a specific angle or direct mirroring, and adding noise, such as adding specific noise or Gaussian motion blur

#### 3.3. Image Text Extraction

**3.3.1. Image Extraction.** For image processing, this article uses a convolutional neural network. The output network consists of 10 cohesive layers, 4 concentrated layers, and 3 fully connected layers. The size of the torsion core of the first rotating layer is  $5 \times 5$ . For a long time, the number of feature maps retrieved has been 64. The rest of the twist core size is  $3 \times 3$ , the feature map data gradually increases from 64, 128, 256, and 512, and the size of all concentrated layers is  $2 \times 2$ . The input image size is  $256 \times 256$  pixels, the spacing of all distortion layers is 1, the spacing of all concentrated layers is 2, the size of the feature map obtained after the first

TABLE 1: Comparison of model retrieval accuracy.

	Top 1	Top 2	Top 4	Top 6	MAP
LMNN (1)	47.41	51.12	55.56	58.34	53.401
LMNN (2)	50.52	56.01	60.12	63.80	57.721
NetVlad	65.56	67.21	71.00	76.11	70.136
Deephash	46.43	50.17	53.24	55.52	51.657
CNN (image)	77.35	79.56	80.10	82.24	79.931
CNN (full)	85.37	87.21	88.76	90.11	87.612

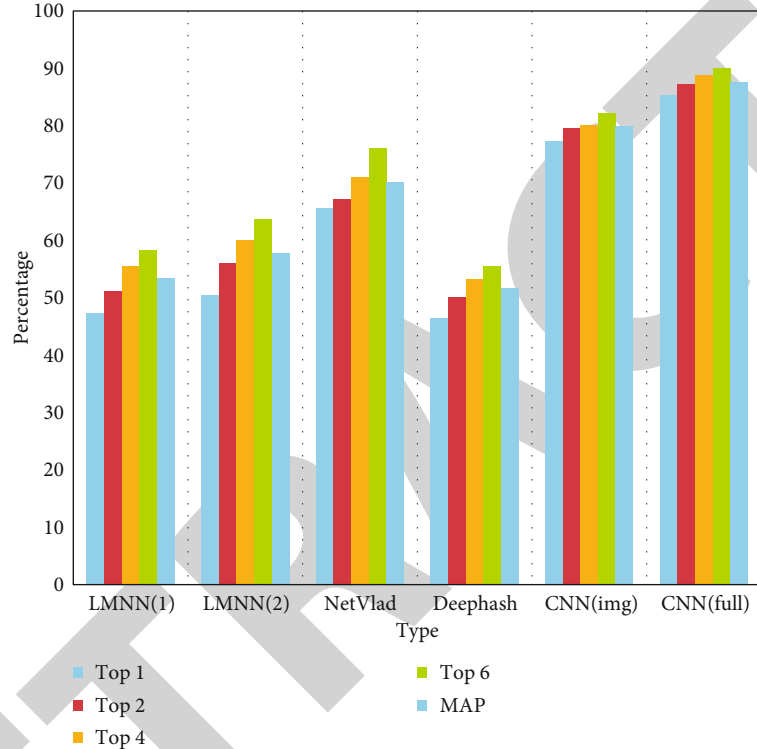


FIGURE 2: Comparison of model retrieval accuracy.

TABLE 2: Comparison of model retrieval accuracy.

	Top 1	Top 2	Top 4	Top 6	MAP
LMNN (1)	72.21	77.42	85.58	92.36	82.141
LMNN (2)	76.53	82.21	88.12	95.01	85.221
NetVlad	82.51	87.53	93.02	96.19	89.45
Deephash	71.41	77.01	83.45	89.74	80.342
CNN (image)	89.11	90.41	93.12	98.51	92.573
CNN (full)	96.01	97.0	98.76	99.38	97.423

rotation is  $261 * 261$ , the number is 64, and the number of sides is 64, so the size of the feature map will not be adjusted after the second rotation. The number of feature maps after sampling reduction is 128, the size is  $108 * 108$ , and the feature maps are rotated. They are all angular, the feature map does not adjust the image size, and the next two rotations do not fill the edges until the size becomes  $27 * 27$  after two samples. The fill edge becomes  $24 * 24$  after sampling. The feature map size before entering the fully connected

layer is  $12 * 12 * 512$ . The fully connected layer has three layers, the first layer has 4096 outputs, and the output of the last two layers is adjustable. The reason for the design of fully connected 3 layers here is that different sorted image data sets have different image types, that is, different numbers of image tags. When the number of layers is different and the corresponding pictures are the same, but the number of labels corresponds to the same, this requires a training set with different output numbers in the last fully connected

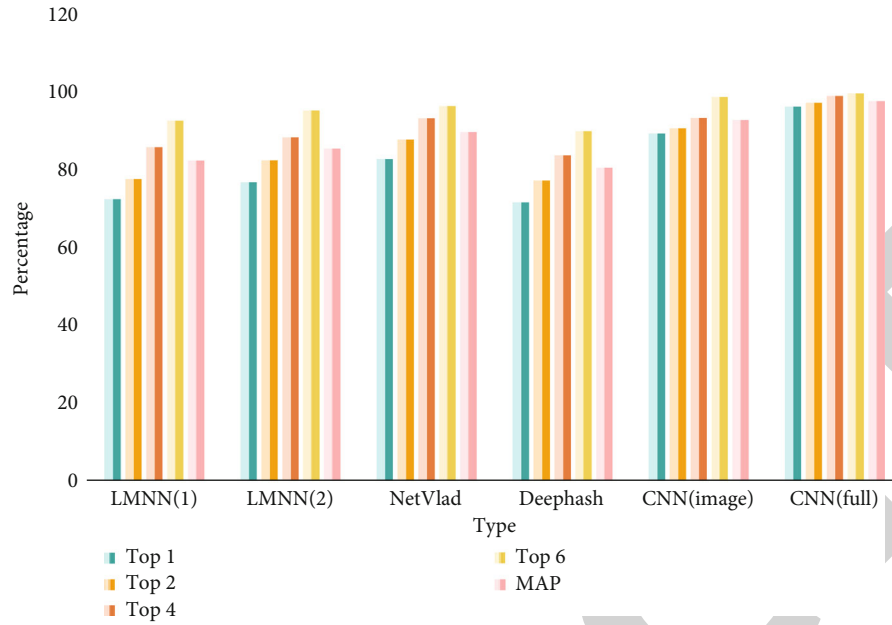


FIGURE 3: Comparison of model retrieval accuracy.

network layer, and there is a big gap in the number of labels between different data sets. The fully coupled layer ensures that the latter can smoothly adapt to different label numbers. Define the second fully connected layer and at the same time make the number of outputs of the second fully connected layer variable.

**3.3.2. Export Text.** The word segmentation tool used in this article will continue to use the stuttering word segmentation tool to segment the document. Then, use the LDA model to model the split words of each document in the data set. Finally, a word distribution can be realized in the topic, and then, a text topic distribution can be realized according to the topic distribution of the word.

**3.3.3. The Relevance of Images and Text.** Image and text information carriers are different in function, but both can express similar semantic information in content. Therefore, there is a correlation between information carriers in multiple formats and the characteristic data of each medium. This document uses the CCA algorithm to analyze the correlation of various data attributes and realizes the correlation analysis of vector graphics and text attribute tables.

## 4. Cross-Modal Information Retrieval Verification Based on Convolutional Neural Network

**4.1. Experimental Data.** The experiment in this paper is carried out on the Chinese signboard dataset. This paper selects the first 55 street signs of the Chinese signboard dataset for training and the last 15 street signs for testing. Because the data set is filtered, all the first 55 streets are finally obtained. The ratio of the total number of signs to the

TABLE 3: Test set error of different core network structures.

	Test set error rate\%	Time\s
16-16-16	2.56	65
16-16-32	2.12	76
32-32-32	1.21	123
32-32-64	1.31	132
64-64-64	1.1	211

total number of signs in the last 15 streets is 5: 4, which is relatively reasonable.

### 4.2. Experimental Design

- (1) After selecting some basic comparison models, this article will conduct experiments in the following situations (Top- $n$  represents the accuracy percentage of the results returned by the first  $n$  search results. MAP is the percentage of Top1-Top6 accuracy) to compare the recovery results of the CNN model in this article with the results of LMNN, NetVlad, and Deephash. First of all, since this article uses a complete data set (including Chinese and English license plates), the GPS information of each license plate is not considered. The experimental results are shown in Table 1

Top- $n$  in Figure 2 represents the accuracy percentage of the results returned by the first  $n$  search results. MAP is the percentage of Top1-Top6 accuracy. LMNN (1) means that LMNN is restored to 48 dimensions, and LMNN (2) means that LMNN is restored to 96 dimensions. CNN (image) only corresponds to the search results of the model image subnet features in this article, and CNN (full) corresponds to the

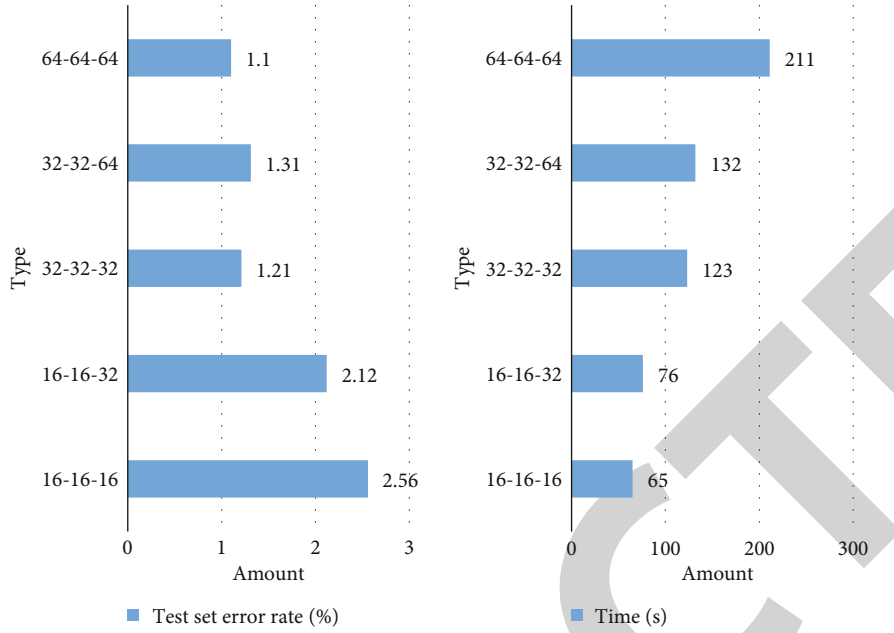


FIGURE 4: Test set error of different core network structures.

TABLE 4: Error comparison of different convolution kernel sizes.

	Training set error rate\%	Test set error rate\%
$3 \times 3$	0.31	1.12
$5 \times 5$	0.65	1.76
$7 \times 7$	0.73	2.02

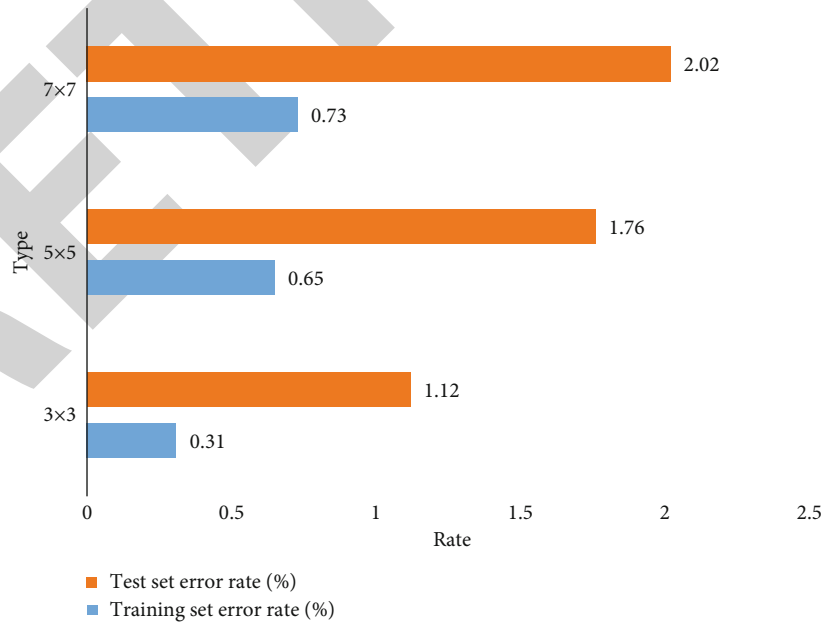


FIGURE 5: Error comparison of different convolution kernel sizes.

search results of the complete model in this article. In summary of the retrieval experiment results, the model in this article can achieve a good retrieval effect.

(2) This article also conducts experiments on the GPS information (1 km) combined with the signboard. The results are shown in Table 2



It can be seen from Figure 3 that when the GPS information is used to narrow the search range, the model data dimension is restored to 99, so the CNN (full) model in this article basically reaches the commercial level. In actual commercial use, only the general GPS range of the current query image is obtained, which greatly improves the speed and accuracy of the query.

**4.3. The Influence of the Choice of Convolution Parameters.** Based on the CNN convergence network model designed in this article, this article conducted various comparative experiments on the Caffe platform to determine the impact of different configuration settings on the performance of the convolutional neural network. The computer's CPU frequency is 5.6 GHz, and the memory is 8 G. The designed CNN model consists of three processes: sample assembly, activation, and execution; after inserting the complete combination layer into the softmax classifier, 10 categories are derived.

#### (1) Choice of audit

To see how the number of convolution cores in each twist layer affects network performance, just change the number of twist cores at each level according to the CNN network structure. The core number structure is 16-16-16, 16-16-32, 32-32-32, 32-32-64, and 64-64-64. In this paper, the converted core structure model is used to compare the test set errors of different core network structures. In the test, the training time batch size is 200, and the number of repetitions is 20. The results are shown in Table 3.

It can be seen from Figure 4 that the number of cores increases within a certain range, the performance is improved, and the time increases with the increase of the number of shrinking cores. Comparing the structure 32-32-32 with the 16-16-16 structure, the network time is more than twice the training time, and the test time is also increased. Therefore, different structures can be selected according to the actual needs of precision grading or time efficiency.

#### (2) Convolution kernel size

The size of the convolution kernel is used to extract image features into the rotation layer. Its size will definitely affect the quality of its functions. In order to study the impact of convolution kernel size on classification performance, in the structure of the CNN network designed in this article, the size of each convolution kernel is set to  $3 \times 3$ ,  $5 \times 5$ , and  $7 \times 7$ . The present study uses database 1 and 2 to run experiments. The experimental results are shown in Table 4.

It can be seen from Figure 5 that the smaller the core size, the lower the network error rate of the training set and test set, and the better the network performance. The larger the core size, the higher the network error rate of the training set and test set, and the lower the network performance. However, if the size is too small (for example,  $1 \times 1$ ), the performance will not be as good as  $3 \times 3$  due to increased noise.

## 5. Conclusions

This paper focuses on the research of graph convolutional network for cross-modal information retrieval. After understanding the relevant theories, the cross-modal information retrieval based on convolutional neural network is designed, and then, the designed network model is verified. Experimental results are concluded that the accuracy of the convolutional neural network model designed in this article is high, with the highest accuracy reaching 90% and the traditional model reaching 80%. Then, there are still shortcomings in the research process of this article, mainly due to the incomplete detection of the model.

## Data Availability

Data available on request from the authors.

## Conflicts of Interest

There is no potential conflict of interest in our paper.

## Authors' Contributions

All authors have seen the manuscript and approved to submit to your journal.

## References

- [1] G. Toliás, Y. Avrithis, and H. Jégou, "Erratum to: image search with selective match kernels: aggregation across single and multiple images," *International Journal of Computer Vision*, vol. 116, no. 3, pp. 262–262, 2016.
- [2] L. Dan, X. Liu, and X. Qian, "Tag-based image search by social re-ranking," *IEEE Transactions on Multimedia*, vol. 18, no. 8, pp. 1628–1639, 2016.
- [3] R. Liu, G. Lin, and C. Shen, "CRF learning with CNN features for image segmentation," *Pattern Recognition*, vol. 48, no. 10, pp. 2983–2992, 2015.
- [4] Z. Cheng and J. Shen, "On very large scale test collection for landmark image search benchmarking," *Signal Processing*, vol. 124, no. Jul., pp. 13–26, 2016.
- [5] Z. Ji, Y. Pang, Y. Yuan, and J. Pan, "Relevance and irrelevance graph based marginal Fisher analysis for image search reranking," *Signal Processing*, vol. 121, no. Apr., pp. 139–152, 2016.
- [6] M. Behrisch, B. Bach, M. Hund et al., "Magnostics: image-based search of interesting matrix views for guided network exploration," *IEEE Transactions on Visualization & Computer Graphics*, vol. 23, no. 1, pp. 31–40, 2017.
- [7] G. Toliás, Y. Avrithis, and H. Jégou, "Image search with selective match kernels: aggregation across single and multiple images," *International Journal of Computer Vision*, vol. 116, no. 3, pp. 247–261, 2016.
- [8] J. Lu, V. E. Liang, and Z. Jie, "Deep hashing for scalable image search," *IEEE Transactions on Image Processing*, vol. 26, no. 5, pp. 2352–2367, 2017.
- [9] F. Shen, Y. Yang, L. Liu, W. Liu, D. Tao, and H. T. Shen, "Asymmetric binary coding for image search," *IEEE Transactions on Multimedia*, vol. 19, no. 9, pp. 2022–2032, 2017.
- [10] J. Music, T. Marasovic, V. Papic, I. Orovic, and S. Stankovic, "Performance of compressive sensing image reconstruction

## Research Article

# New Trends and Advancement in Next Generation Mobile Wireless Communication (6G): A Survey

Sher Ali <sup>1</sup>, Muhammad Sohail <sup>2</sup>, Syed Bilal Hussain Shah <sup>3</sup>, Deepika Koundal <sup>4</sup>,  
Muhammad Abul Hassan <sup>5</sup>, Asrin Abdollahi <sup>6</sup> and Inam Ullah Khan <sup>7</sup>

<sup>1</sup>School of Computer Science and Communication Engineering, Jiangsu University, Zhenjiang, China

<sup>2</sup>Department of Computer Software Engineering, MCS, National University of Sciences and Technology (NUST), Pakistan

<sup>3</sup>Manchester Metropolitan University, UK

<sup>4</sup>Department of Systemics, School of Computer Science, University of Petroleum & Energy Studies, Dehradun, India

<sup>5</sup>Department of Computing and Technology, Abasyn University Peshawar Pakistan, Pakistan

<sup>6</sup>Department of Electrical Engineering, University of Kurdistan, Iran

<sup>7</sup>Department of Electronic Engineering, School of Engineering & Applied Sciences (SEAS), Islamabad, Pakistan

Correspondence should be addressed to Asrin Abdollahi; a.abdollahi@eng.uok.ac.ir

Received 5 October 2021; Revised 17 October 2021; Accepted 10 November 2021; Published 11 December 2021

Academic Editor: Abdul Basit

Copyright © 2021 Sher Ali et al. This is an open access article distributed under the Creative Commons Attribution License, which permits unrestricted use, distribution, and reproduction in any medium, provided the original work is properly cited.

As the commercial implementations of 5G networks have been initiated in different regions of the world, the focus of the researchers is bending towards the next generation of wireless communication. This research study intends to investigate the requisites of the fast establishment of the theoretical and practical measures for sixth generation (6G) wireless communication. To this end, this paper first outlined the existing research works that have considered different aspects of 6G, and then based on this existing works, the future vision is established. Then, the 6G vision is based on four types of connectivity and is summarized as “Wherever you think, everything follows your heart.” To fill the gap between the market requirements after one decade and the limited capabilities of 5G, different specifications of 6G that make it an appropriate replacement are discussed. Furthermore, different candidate technologies that can potentially realize the 6G communication are studied, followed by discussion on different challenges in the realization and possible research directions to cope with these challenges. By exploring the vision of future, its specification, and key candidate technologies, this paper attempts to summarize the general 6G framework. In addition, with mentioned challenges in realization of 6G, the aim of this paper is to guide the researcher and attract their interest to consider them.

## 1. Introduction

Though the deployment of fifth-generation (5G) wireless communication is in the early phase, i.e., the associated features should be more enhanced, it is also essential to uniformly set the communication requirements of the upcoming information society and initiate the theoretical and practical projects on future wireless system generation (henceforth mentioned as 6G). To this end, we intend to investigate the requisites for the establishment of the theoretical and practical works on 6G from three perspectives: (i) 10-year gap between successive generations [1]. More specifically, any generation takes a ten-year period to initiate

the theoretical research till the practical deployment; that is, when any generation moves in the practical deployment phase, the next generation initiates theoretical research. Therefore, research on 6G is now in theoretical phase since research on 5G was initiated ten years back. To better understand, the time gap and technology evolution from 4G to 6G are presented in Table 1. (ii) For catfish effect, different from the previous generations, 5G primarily targets the IoT application related to industry. With the commercial implementation of 5G on a large-scale, there will be numerous members from vertical industry involved in the ecology of 5G. As compared to the status quo controlled by operators, the thorough contribution of developing enterprises will

TABLE 1: The evolution of cellular communications from 4G to 6G and their comparison with respect to different key features.

Generation	4G	5G	6G
Time range	2010 to 2020	2020 to 2030	2030 to 2040
Maximum achievable rate	1 Gb/sec	35.46 Gb/sec	100 Gb/sec
Frequency	6 GHz	90 GHz	10 THz
Standards	LTE, LTE-A, WiMAX	5G NR, WWWW	Yet to be decide
Service	Video	3D VR/AR	Tactile
Architecture	MIMO	Massive MIMO	Intelligent surface
Multiplexing	OFDMA	OFDMA	Smart OFDMA plus IM
Core network	Internet	IoT	Internet of Everything

have a revolutionary effect on the telecommunication industry which is generally termed as “catfish effect.” (iii) For the IoT business model, the introduction of smartphones accelerated the usage of 3G services and prompted the 4G deployment demands; it is assumed that certain IoT business modes will encourage the 5G outbreak somewhere in the 5G period, thus boosting the need for the upcoming 6G networks. We must be prepared for the potential advent of the upcoming generation to lay an effective technical foundation. In short, it is the appropriate time to initiate the research on 6G. Recently, ever more individuals or organizations, including governments, industry, academia, and public [2–5], have initiated to implicate 5G/6G concepts. Federal Communications Commission in 2018 publicly expressed their expectation about 6G [5]. China and the United States (US) have already initiated research on 6G in 2018 [6]. Besides the US and China, the European Union, Japan, and Russia have also taken research initiatives towards 6G. It is obvious from the aforementioned points that there is a positive consent on initiating researches on 6G. To this end, the envision network for 6G is illustrated in Figure 1.

Major contribution points are as follows:

- (i) Research initiatives for 6G
- (ii) 6G vision
- (iii) 6G specification
- (iv) 6G technologies
- (v) Challenges and future directions

## 2. Research Initiatives for 6G

The 6G vision along with some other key research advancements has been the focused areas of researchers in last few years [2, 7–11]. To this end, the authors in [7] have given the 6G vision and summarized its requirements. They have mainly focused on the battery life of mobile unit and different 6G service classes, rather than the latency and data rate. In [8], it is proposed that the research in beyond 5G (5GB) period must be based on the manufacturing capabilities of network devices to develop a feedback loop of research undertakings. In [2], different communication scenarios for

6G are forecasted, which contains flying networks, tactile internet, tele-operated driving, and the holographic calls.

The future trends and applications and enabling 6G technologies are summarized in [9, 10]. Particularly, blockchain technology-based network decentralization is considered to be a foundation for network management and delivering convincing performance in 6G. Furthermore, the human-centric service model is presented and considered as the key aspect in 6G. In [11], key 6G metrics are specified, and a detailed comparison of 5G and 6G is presented.

Some recent studies are focused on real-world implementation including air interfaces [12], data centers [13], and multiple access techniques [14] for 6G communications. 6G network networking patterns are discussed in [15–17], where cell-less architecture, three-dimensional superconnectivity, and decentralized resource allocation are highly anticipated to be present in 6G networks. In [18], vertical-specific solutions and massive machine-type communications (mMTCs) for 6G networks are discussed, and it is predicted that 6G could simplify the leading wall-breaking standard to entirely substitute the current standards and offer a combined way out by allowing continuous connectivity for all the requirements of vertical industries.

In 6G-related works, reconfigurable intelligent, and surfaces, artificial intelligence (AI) and terahertz communications are highly attractive concepts. They are considered as game changer technologies in the field of wireless communications. A detailed survey on 6G based on terahertz communications is presented in [19], which summarizes different 6G technological advancements, design aspects of the transmitter-receiver, and several use cases. AI-enabled 6G is supposed to offer lots of advanced features, including auto-configuration, context awareness, opportunistic set-up, and self-aggregation [20]. Moreover, AI-enabled 6G would explore radio signal potentials and allow cognitive radio to shift to intelligent radio [21]. Particularly, machine learning (ML) is a key for recognizing AI-enabled 6G from the algorithmic angle, which has been studied in [22, 23]. In [24, 25], reconfigurable intelligent surfaces are envisioned as the massive MIMO 2.0 in 6G. These materials can also combine index modulation to result in an increase of 6G spectral efficiency [26]. Besides the above discussed individual initiatives, multiple 6G projects are in progress globally, which target to first start and specify 6G followed by framework

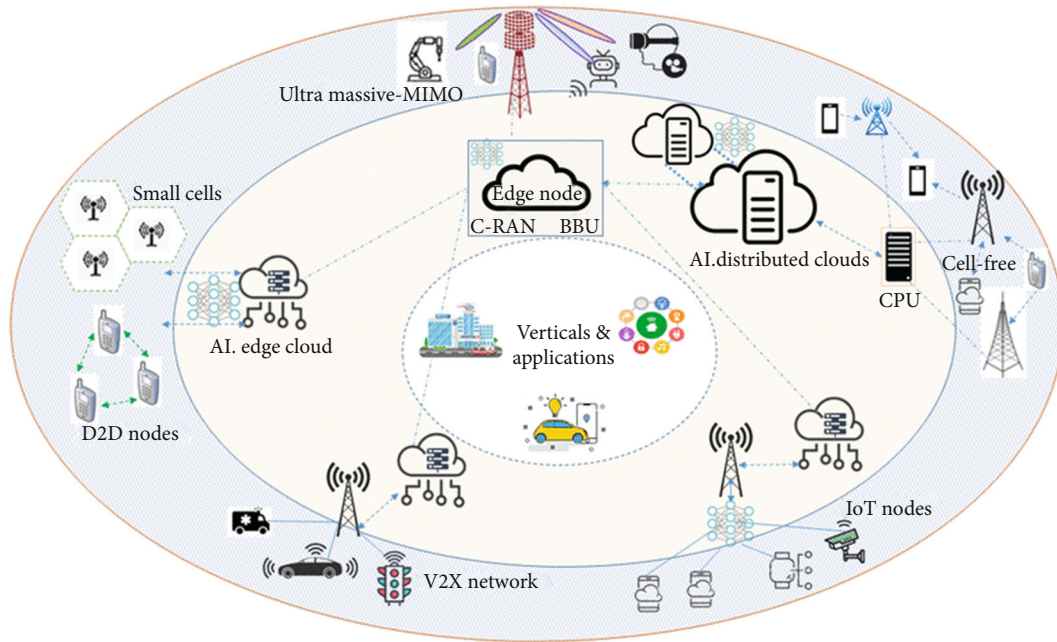


FIGURE 1: Illustration of the envisioned 6G architecture.

reshaping as well as setting wireless communication business model. To this end, 6Genesis Flagship Program was the first project followed by the Terabit Bidirectional Multiuser Optical Wireless System for 6G, which initiated in 2019. The first summit on 6G was held in March 2019 at Levi, Finland, and properly stimulated the launch of research race on 6G in academia. Many seminars and small-scale workshops were also arranged globally to discuss the 6G feasibility, for example, the Wi-UAV Globecom 2018, the Carleton 6G, and the Huawei 6G Workshops.

Beyond academia, future generations including 6G attract the attention of industrial and governments, organizations, and standardizing bodies. In August 2018, IEEE established Future Network program named “Enabling 5G and beyond” while ITU-T [27] established the Focus Group of ITU-T, namely, “Technologies for Network 2030” which aims at understanding the future network service requirements around 2030. Google triggered the Project Loon program which aims at offering consistent internet links to the 5 billion unconnected people. An EU’s Terranova project-based research group is currently leading on the way to reliable 6G communication links having transmission capability of 400 G bits/sec in the terahertz band. LG Electronics also established a 6G research center in South Korea. In 2019, Samsung started its 6G research program while SK Telecom and Nokia and Ericsson collaborated for the same purpose. Towards the end of 2018, China declared the determination that in 2030s, they will lead the wireless communication market by increasing investment in 6G research. The US has opened the 95 GHz-3 THz spectrum for 6G research. Moreover, an EU-Japan program called as “Networking Research beyond 5G” which is supported by the funding of Horizon 2020 ICT-09-2017 studies the possibility of utilizing the terahertz band in the range 100 GHz to 450 GHz.

As 5G has already been implemented on experimental basis in many countries and researchers have taken research initiatives towards 6G, therefore, it is the need of the day that the available literature on 6G should be systematically assembled in the form of a survey. To this end, in this paper, we present a detailed and systematic survey on 6G communication where we presented a brief literature review on the available literature on 6G followed by the detail vision of 6G. Then, different specification and requirements of the 6G are studied followed by the details of potential 6G technologies. Finally, some future research directions are discussed. The flow and contents of these topics are provided in Figure 2.

The remaining of this paper is structured as follows. Section 3 discuss the 6G visions while Section 4 contains different specifications and requirements for 6G. In Section 5, different candidate technologies for 6G are discussed. Different challenges to which 6G is faced and some future research directions in 6G are discussed in Section 6. Section 7 contains the conclusion.

### 3. 6G Vision

In the early period of 5G, its vision is set as “everything is at your fingertips, and information is at your disposal” [28]. Keeping in view this vision, the 5G technical requirements, key technologies, and standards are recommended. Now, the next stage is to put 5G systems on large-scale commercial use. At this stage, it is also essential to set the vision for 6G, and its corresponding technological requirements and challenges are required to be specified in order to start research on 6G so as to follow the 10-year generation shift rule. But, 5G is so sensational and will completely attract the society in every aspect of life. If so, then what is there to be done in future? To this end, this section will first

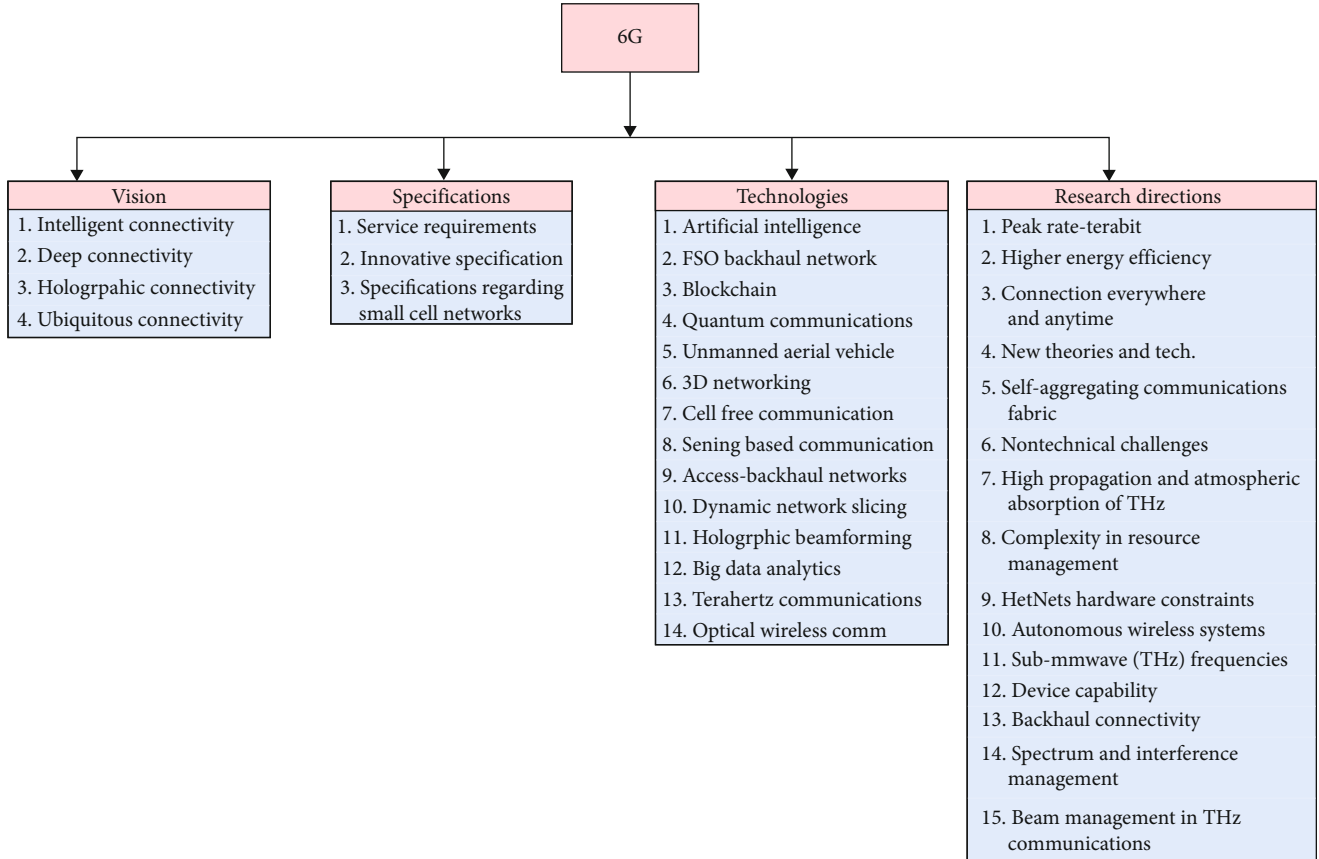


FIGURE 2: Skeleton of this paper.

provide the 6G vision establishment followed by analysis on the vision necessity, and then different technical requirements and issues in meeting this 6G vision will be discussed.

Currently, the main objective of 5G is to cover every aspect of human life and develop a user's centered information ecosystem. But, owing to immaturity of 5G standardization and associated technologies, still lots of deficiencies are there to overcome: the existing technologies are suitable to perform well in the limited space range, i.e., few kilometers above the surface of the land; while considering the IoT requirements, there is still a lot to do to achieve the real global IoT. Particularly, with the speedy growth of the human activities scope and advancement in various fields of technology, the demand for diverse information interaction is getting increase.

The 6G basic goal is to fulfil the information society requirements in 2030 ~; that is, the vision of 6G will be based on requirements that 5G is unable to fulfil and those services that 5G is unable to provide. Based on those requirements and services that 5G is unable to fulfil and provide, respectively, we believe that the vision of 6G should be categorized into the following four fundamental services: "Intelligent Connectivity," "Deep Connectivity," "Holographic Connectivity," and "Ubiquitous Connectivity." These different types of connectivity together set up the overall 6G vision. In contrast, the 5G vision puts emphasis on information exchange and IoT, while the communication range for connectivity is limited to 10 km space above the earth surface. Although 5G

is underway to standardize the nonterrestrial network (NTN) technical characteristics, the technical systems and standard of cellular, and satellite networks involved in the architecture of NTN are still independent of each other, and special gateway equipment is needed for their connectivity and interaction [29]. Its efficiency and communication capability can hardly fulfil the future ubiquitous connectivity requirements. To fulfil the future connectivity requirements, 6G will require to support the space-air-ground-sea (SAGS) integration network. This network will require a unified technical system and standard protocol architecture to realize the ubiquitous connectivity of SAGS integration in true sense. Besides, instead of real-time performance, the main emphasize of the 5G mMTC is on the number of communication links [30, 31], while Ultra-Reliable Low Latency Communications (URLLC) focuses on real-time performance and reliability but does not emphasize on throughput and connections count, which leads to a decrease in the connection count and spectral efficiency. To overcome these shortcomings in 5G, the 6G vision includes reliability, massive connectivity, high throughput, and real-time performance. The wireless tactile networks can be presented as a typical scenario which is described below. Therefore, though some of the fundamental ideas which are included in 6G vision are already parts of the 5G, 6G vision is based on advanced objectives to fulfil the requirements and cope with the challenges of new scenarios in the future.

*3.1. Intelligent Connectivity.* Nowadays, artificial intelligence (AI) has gained the interest of researchers and become the most active research topic. Therefore, almost every field is moving towards the utilization of AI technology. The AI enabled wireless communication network has become a foreseeable trend [32–48]. In recent times, people have started to attempt the utilization of AI in 5G system [49, 50]; however, the enabling of AI in 5G systems is possible only as optimization of conventional networks based on AI, instead of a new one. AI-enabled 5G will change the dynamics of the networks. Even though the initial 5G architecture is more flexible (software definable), but AI has not been considered in it, therefore, it is still considered to be conventional network architecture. Secondly, even though the development of AI technology is speedy enough, and in many areas, it has proven its performance efficiencies; still it is in the experimental phase in most of the other fields. The enabling of AI in wireless communication technology is in its early research phase, and a long-term research planning is desirable before the actual technology grows up to maturity.

The growing tendency towards AI indicates the high probability of technology growth in the upcoming decade. In addition, believing that the upcoming 6G networks will be growingly massive and heterogeneous, and different application scenarios will become growingly dynamic; the active use of AI is expected to cope with these challenges. It is envisioned that the upcoming 6G will bring a revolution in the applications scope of conventional cellular systems and turn into the main Internet supporting all the operations in every industry and society. If the upcoming generation networks still utilize the current unified communication models to handle the very complex and diverse applications in 6G era, it will be faced with many severe challenges [51]. Therefore, we consider that building the AI-based 6G network will be an unavoidable move, and “Intelligent” will be its essential feature, resulting in “Intelligent connectivity.”

The “Intelligent Connectivity” characteristic can be considered as an essential intellectualization of communication networks: intellectualization of connecting units (terminal devices) and intellectualization of network architecture and elements. In future, lots of issue will be faced in the realization of 6G networks: growingly massive and complex networks, massive densification of terminal devices, and complex business models. “Intelligent Connectivity” will simultaneously fulfil two demands: (1) all the connected network devices need to be intelligent and (2) the need of intelligent management for the growingly massive network.

*3.2. Deep Connectivity.* Conventional cellular systems (including 5G) are based on the vision of deep coverage, basically for the optimization of deep coverage of indoor access requirements. Deep coverage in indoor can be attain through macro base stations (BS) deployed in outdoor or wireless nodes deployed in indoor. 4G and prior cellular network generations were focused on people-cantered communication. In contrast, from 5G and onward, this focus has been shifted to the simultaneous and real-time communication of things, which is called Internet of Everything. Therefore, the architecture and implementation of 5G and onward

generations require considering of deep coverage requirements for both the users as well as objects.

As the human productions and living space are increasing, the scenarios and categories of information exchange are turning growingly complex. From 5G and onward, the Internet of Everything will encourage the speedy growth of IoT communications, and it is expected that this growth will keep increasing in coming few years. Furthermore, the requirements for the Internet of Everything will drastically rise in the following four perspectives: (i) the deep expansion of the activity space of connecting objects, (ii) deeper perceptual interaction, (iii) deep data mining in physical world, and (iv) in-depth nerve interaction [52]. Thus, from deep coverage, the access requirements will change to “Deep connectivity,” and its main features will include telepathy, AI, and deep sensing.

*3.3. Holographic Connectivity.* Virtual and augmented reality (AR/VR) is supposed to be among the most significant 5G requirements, specifically for high throughput applications. 5G will have the capability to allow the transformation of AR/VR of existing stationary wireless access into mobile wireless AR/VR. Once the utilization of AR/VR becomes convenient without location constraint, it will speed up the growth of AR/VR services, followed by speeding up the maturity and growth of AR/VR itself. After one decade, most of the media communication are generally imagined as planar multimedia, and holographic information interaction, high fidelity AR/VR-based communication, and holographic interaction will turn into realization. Holographic communication will be ubiquitous to allow people for making full advantage of the holographic interactive capability anywhere, which is the real purpose of “holographic connectivity.” To achieve holographic connectivity, lots of challenges will be faced [53]. A number of articles have been focusing on the utilization of AI technology to cope with these challenges [54–56].

*3.4. Ubiquitous Connectivity.* Anywhere, anytime type of wireless access is the need of conventional cellular networks also. However, as per the communication needs of people, 5G will significantly expand the scope of space and information exchange types in IoT. The equipment activity range will significantly increase the geographic range of communication, comprising detectors installed in deep sea, human/unmanned aerial vehicle (UAV) in the medium and high altitude, intelligent remote-control equipment, autonomous robots in the harsh environment, and so on. Besides, human activity space is also increasing quickly due to the speedy improvements of technology in the areas of deep-sea exploration, astronautics, and the enhancement of survival ability in specific natural situations. For example, there may be high chances for people in 2030–2040, to approach the outer space. Consequently, the needs for satellite-ground communication and satellite-space craft’s communication will be more common than that of conventional communication. The abovementioned communication scenarios will stimulate the needs for “anytime, anywhere” connections in 2030 ~ and beyond; that is, by achieving “Ubiquitous connectivity” in real sense, a vast world will turn into

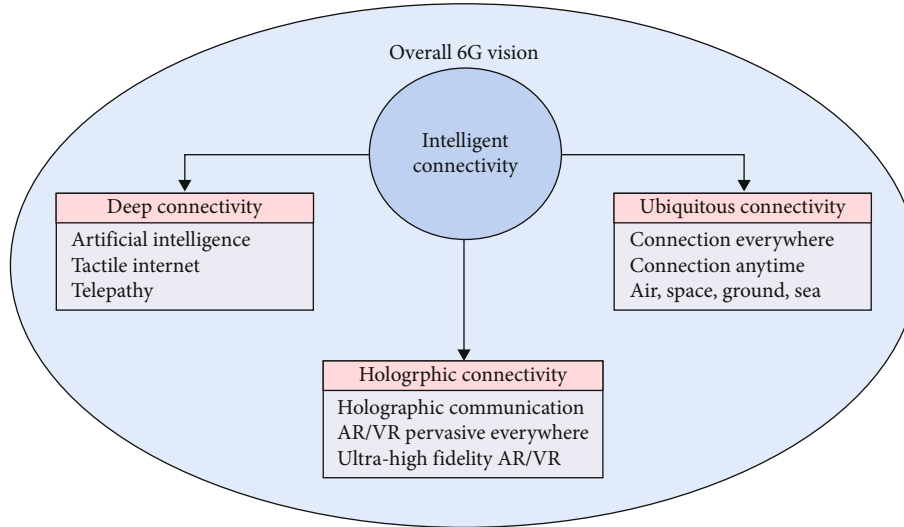


FIGURE 3: Sixth generation vision.

easily accessible place. The ubiquitous connectivity main feature is the integration of SAGS communication. In comparison with deep connectivity which focuses on the depth of the connected object, the focus of ubiquitous connectivity is on the breadth of the distributed area of the connected object [57].

Summarizing the above discussion on the four visions of upcoming 6G, intelligent connectivity performs as a nerve and brain of the 6G, while the remaining three features constitute the of 6G trunk as shown Figure 3. When these four features combine, the communication system will be more improved, the information will break through the time as well as space constraints, the distance between network devices will be minimized, the uninterrupted integration of human and everything will become reality, and finally the overall 6G vision will be realized.

## 4. 6G Specifications

It is highly expected that 5G will be unable to deal with the market requirements after one decade as it is faced with many challenges, for example, latency, throughput, deployment costs, energy efficiency, hardware complexity, and reliability. To fill the gap between the market requirements and the capabilities of 5G, 6G will be an appropriate choice. Based on the previously discussed 6 visions, the basic 6G goals are (a) latency minimization, (b) global connectivity, (c) massive connectivity, (d) enormously high data rates, (e) energy efficiency of network devices, (f) connection reliability, and (g) machine learning-based connected intelligence [58].

**4.1. Service Requirements.** The main services that 6G systems will provide contain mMTC, URLLC, IoT, tactile internet, AI-based communication, and Enhanced Mobile Broadband (eMBB). In addition, high network sum-rate, capacity, energy efficiency, and data security are also among the main services of 6G.

It is envisioned that the number of simultaneous wireless connections provided by 6G will be 1000 times more than

that of 5G system. One of the main features of 5G named URLLC will also be part of the 6G. URLLC will provide less than 1 ms end-to-end delay [11]. In comparison with the area spectral efficiency, volume spectral efficiency is expected to better outcome in 6G [28]. In addition, 6G will support advanced improved technology which in turn will result in ultralong battery life. Furthermore, mobile units will not require to get charged alone.

### 4.2. Different Innovative Specification

**4.2.1. Satellite Integrated Network.** To realize worldwide connectivity, 6G is envisioned to combine satellite, airborne, and terrestrial networks. This way, the 6G vision of Connect Anywhere Anytime will be addressed [59].

**4.2.2. Connected Intelligence.** In comparison with the previous wireless network generations, 6G will support the shift from “connected things” to “connected intelligence” [21]. Consequently, AI will be utilized in every phase of the communication procedure. The ubiquitous utilization of AI will develop a new model of communication systems.

**4.2.3. Smooth Combination of Wireless-Information and Energy-Transfer (WIET).** 6G will also provide the wireless transfer of power to support wireless charging of battery units, for example, sensors and smartphones. It utilizes the same waves and fields as wireless communication systems. It will make the sensors and smartphones able to charge during communication through wireless power transfer. In addition, increasing the lifetime of wireless charging systems for batteries is also the potential capability of WIET [60]. Therefore, battery less devices are envisioned in 6G systems.

**4.2.4. Universal 3D Connectivity.** Controlling the functionalities of core networks through aerial vehicles and satellites will lead to the Universal Connectivity in 6G era [61].

**4.3. General Specifications regarding Small Cell Networks.** The concept of small cells in cellular systems is presented

to enhance the quality of received signals as a consequence of enhancement in the network spectral and energy efficiencies [62] and sum-rate [63–65]. Thus, small cell networks is an important consideration for 5G. Therefore, like 5G, 6G will also include this type of network model.

**4.3.1. Dense Heterogeneous Networks (HetNets).** Dense HetNets [66, 67] is another vital 6G feature. Multitier networks comprising different types of access points will enhance the network quality-of-service and decrease the cost [68].

**4.3.2. High-Capacity Backhaul.** The backhaul communication must be featured by high-capacity backhaul networks to allow a massive traffic. Free space optical (FSO) communication systems and high-speed optical fiber are potential solutions to this issue [69].

**4.3.3. Virtualization and Softwarization.** Virtualization and softwarization are two main features of 5G and beyond that are foundations for the design process to guarantee reconfigurability, flexibility, and programmability. Besides, they will make possible the sharing of same physical infrastructure among billions of network devices [70].

## 5. 6G Technologies

6G is the combination of several technologies, few of which are briefly discussed in the following.

**5.1. Artificial Intelligence (AI).** Among all the envisioned for 6G, AI is the most significant and advanced [14, 18, 20, 71, 72]. In 4G systems, AI was not included while the forthcoming 5G will support a limited use of AI. However, there will be full support for AI in 6G. The rapid developments in machine learning will result in efficient intelligent networks in 6G which will lead to achievement of real-time communication. Through different analytics, AI will be able to find the method for execution of complex target tasks [73]. Improving the energy efficiency, decreasing the communication and processing delays, time efficient network selection, and handover efficiency [74] will also be the salient features of AI. In addition, AI will play a vibrant part in intermachine, human-to-machine, and machine-to-human communications. Communication systems based on AI will be supported by meta-materials, intelligent networks, intelligent devices, machine learning, and self-sustaining wireless networks.

**5.2. FSO Backhaul Network.** Owing distant geographical situations, it is not always feasible to achieve fiber backhaul connectivity. FSO is a new trending technology to achieve efficient backhaul connectivity. The properties of FSO transmitter and receiver are comparable to that of optical fiber-based system. Hence, the data transfer of both, i.e., the FSO and optical fiber systems, are also comparable. Keeping this in view, in addition to the optical fiber networks, the FSO backhaul network is considered to be a capable technology for backhaul connectivity in 6G systems [75–77]. FSO can potentially support a long-range communication in more than 10,000 km range. Furthermore, it allows cellular BS connectivity as well as high-capacity backhaul connectiv-

ity everywhere such as underwater, outer space, sea, and isolated islands.

**5.3. Blockchain.** Another vital technology to handle the 6G massive traffic is blockchain [78–80]. Blockchains are a type of the distributed ledger technology which is a database spread over multiple processing units. Each processing unit keeps a duplicate version of the ledger. As it is controlled by peer-to-peer networks, so, there is no need of centralized server for its existence. The blockchain data is assembled and organized in blocks which are linked with each other and protected via cryptography. It is principally a suitable counterpart to the mMTC with enhanced security, scalability, and reliability [81]. Thus, it will offer many services, like traceability of data, self-regulating of IoT communications, and reliability of mMTC in 6G.

**5.4. Quantum Communications.** Unsupervised reinforcement learning is an efficient technique to achieve the envision goals of 6G. In contrast, the supervised learning technique will not be able to deal with the labeling of massive data produced in 6G. As labeling is not required in unsupervised learning, so, it can be utilized to develop complex networks. Furthermore, when reinforcement and unsupervised learnings are combined, it can lead to the possibility of network operation in a real autonomous way [82].

**5.5. Unmanned Aerial Vehicle (UAV).** UAVs or drone BSs are supposed to be significant components of the upcoming 6G. In various cases, efficient wireless connectivity will be achieved with the help of UAV technology. To this end, the BS units will be deployed in UAVs. There are certain features of a UAV which a fixed BS does not provide, for example, easy placement and strict line-of-sight. In case of emergency circumstances such as natural disasters, the implementation of conventional terrestrial infrastructure-based network will not be feasible economically and impossible sometimes to deliver any service in such an unstable environments. In contrast, the UAVs can conveniently cope with this kind of situations as it can fulfil the important 6G requirements that are mMTC, eMBB, and URLLC. In addition, UAVs can also provide several other services such as the fire detection, network connectivity enhancement, security, pollution monitoring, accident monitoring, and surveillance [83].

**5.6. 3D Networking.** The envisioned integration of different networks in 6G will allow users to communicate in vertical extension. In addition, UAVs will be utilized to realize the 3D BSs [84, 85]. The introduction of new dimensions with respect to altitude will turn the 3D connectivity substantially changed from the existing 2D networks.

**5.7. Communications without the Limitations of Cells.** The combination of heterogeneous technologies and multiple frequencies will be another potential method to achieve the envision goals of 6G because, this will allow the seamlessly internetwork mobility of the users without any physical change in the device configurations. The suitable network will be chosen spontaneously among the accessible



networks. Thus, the limitation of cell-based wireless communications is overcome. Currently, the user intercell mobility in dense networks results in frequent handovers which may cause an increase in handover failures, data losses, and handover delays. The cell-free model of 6G will deal with all these issues. This type of communication model can be attained by adopting multitier communication architecture and associated techniques and mMTC [86].

*5.8. Sensing-Based Communication.* An important move towards autonomous systems is the potential to uninterruptedly sense the frequent and random variations in environments and the information communication amid multiple device units [87]. In 6G, the strict integration of sensing with communication is proposed to achieve autonomous systems.

*5.9. Integration of Access-Backhaul Networks.* The 6G networks will be massively dense in terms of access networks. Every access network will be coupled with backhaul connectivity networks, such as FSO and optical fiber. To deal with this massive densification of access networks, strict integration of the access network with backhaul network is proposed in 6G [88].

*5.10. Dynamic Network Slicing (DNS).* DNS makes the network operators capable of dedicating virtual networks for the optimized distribution of services to different types of industries, machines, vehicles, and users. Among the potential 6G technologies, DNS is the most significant as it can manage the situation where a huge number of users is associated with a huge number of HetNets [89].

*5.11. Holographic Beamforming.* Beamforming is a common technique for signal processing where an antenna array is used for the directive transmission of radio signals. It is a group of smart and advanced antennas and has multiple benefits, such as improved network efficiency and low interference. Holographic beamforming (HBF) is an advanced technique to achieve beamforming and is substantially different from the MIMO [90, 91] systems as it utilizes software-defined antennas. It is supposed to be an efficient and effective technique in 6G to achieve the efficient communication in multiantenna communication network units.

*5.12. Big Data Analytics.* To investigate a range of large data sets also known as big data, Big Data Analytics technique is used. This technique reveals information, for example, customer inclinations, hidden patterns, and unknown correlations to guarantee the seamless data management. The big data is collected from a range of sources, such as social networks, videos, sensors, and images. It is supposed that this technology has the capability to deal with massive data in 6G systems [92].

*5.13. New Spectrum-Based Technologies.* Spectrum is a limited resource and foundation for any wireless communication. The rising wireless traffic needs the future wireless systems to increase their spectrum resources. For 6G, the terahertz spectrum and visible light spectrum are envisioned as two capable spectrums. The use of terahertz frequencies in

wireless communication has been appreciated by Japan and many European and American countries. In addition, it has also gained strong interest of the ITU. Visible light-based technology is a modern development which is a potential alternate for short-range wireless communication in 6G. In the following, these two technologies are briefly discussed.

*5.13.1. Terahertz Communications.* Spectral efficiency is among the most important objectives of every cellular generation and can be further improved by increasing the bandwidth. In 6G, spectral efficiency can be attained using THz communication technology. The RF band is now insufficient as it is not able to meet the growing 6G demands. To cover this deficiency in 6G, the THz band is an appropriate choice [93, 94] as it is envisioned as the future spectrum for data hungry applications. THz waves generally have frequency and wavelengths in 0.1-10 THz and 0.03-3 mm ranges, respectively [95]. As per recommendations of ITU-R, the band ranging from 275 GHz to 3 THz is supposed to be the suitable portion for cellular communications because this band is not specified for any other purpose globally, and it can provide high data rates. This proposed portion of THz band when added with the mmWave band ranging from 30 to 300 GHz and can improve the overall 6G cellular communication capacity. More specifically, this addition results in at least 11.11 times increase in the total band capacity. Of the THz band, the specified cellular band lies on the mmWave, while the band ranging from 300 GHz to 3 THz lies on the far infrared band. Furthermore, the band ranging from 300 GHz to 3 THz is located at the border of optical band and sharply next to the RF band, thus, resembles to the RF. The THz communication core features comprise ultralarge bandwidth and high path-loss [96].

*5.13.2. Optical Wireless Communications.* Optical Wireless Communications (OWC), which involves ultraviolet, visible, and infrared bands, is an expected replacement of the current RF technology. Among the three mentioned bands, the most useful is the visible band which is discussed in the following.

OWC system in 390 to 700 nanometer range is typically known as Visible Light Communications (VLC), which utilizes the potentials of LEDs to attain high data rates along with illumination. In contrast to the RF-based communication, VLC is more advantageous from the following four perspectives. Primarily, VLC allows the utilization of unassigned large THz bandwidth, which can be utilized without any bounds and authorization of spectrum regulators. In addition, VLC does not lead to electromagnetic (EM) radiation nor is it prone to interference from other EM radiation, so it is suitable to be utilized in different places, such as aircraft, hospitals, chemical plants, and gas stations which are usually sensitive to EM interference. Furthermore, the VLC network security is higher, because it utilizes the visible light as transmission medium, which is unable to penetrate the wall like obstructions, and the transmission remains restricted to the visual range of users only. Consequently, the transmitted information remains restricted to a building, which guarantees the information security from the outer

malicious interception. Finally, VLC allows the speedy establishment of wireless networks. In case of RF-based communication, the BS deployment and their maintenance costs are significantly high. The indoor VLC technology can utilize its indoor illumination source as the BS, to allow users to conveniently utilize the indoor wireless services. The common use cases of OWC include submarine communication (to cope with attenuation and EM interference), short-range communication, and optical hotspots (especially in indoor case) [97–100].

## 6. Challenges and Future Research Directions

Several technical problems need to be solved to successfully deploy 6G communication systems. A few of possible concerns are briefly discussed below.

**6.1. Peak Rate-Terabit.** In previously mobile communication era, the users were really concerned about peak rate, which is one of the key technical indicators that the first generation of wireless mobile communication systems have been pursuing since its inception. In fact, 6G further enhances the peak rate. According to an idea, 6G peak rate will increase up to Tera (bits/sec). Here, we quantitatively predict the peak rate in next decade up to 2030. Secondly, from 6G vision, two applications need significant increased peak rate, (1) intelligent applications and (2) big-data-based application, and analytics requires massive data transmission. Intelligence systems can be driven force for next generation communication technology. Also, high fidelity augmented/virtual reality (AR/VR) and holographic communication will be imminent applications carry by 6G, with the promise of providing higher data rate than existing wireless communication systems and also to provide high fidelity not only higher data required but with minimum latencies. It will increase throughput and minimize delay. Moreover, by AR/VR mean, we need communication anytime anywhere with high data rate, which would be another challenge for 6G.

**6.2. Higher Energy Efficiency.** Ultrascale mobile communication system becomes necessary part of world's energy utilization. It occupies considerable operating system costs with production of large carbon emissions. As proposed, future 6G technology will be capable to produce ultrahigh bandwidth, throughput, and with large number of wireless nodes, which results in extra challenges to energy consumption. Compared to spectrum efficiency and bandwidth, energy consumption is more serious issue as it will increase user cost. Therefore, we have to reduce this energy consumption as much as possible in per bit (J/bit). Further, the pervasive deployment of wireless sensors nodes along with human production and living space will trigger two important energy consumption issues; first pervasive deployed sensors will result in huge energy consumption, and second, the energy supply for largely placed sensors effectively would be a challenge. Also, the connected devices in 6G technology will bring mega data processing with power consumption of huge number of installed antennas for 6G technology oper-

ations. Due to these important energy consumption problems, Green communication can be suitable solution [101].

**6.3. Connection Everywhere and Anytime.** We are living in the world where technology changing second by second, which makes human life more advance and comfortable. With the rapid growth of information and communication technology, the space of human connections will be expanded where active area will have no boundary. In this 6G communicating, nodes like nodes in IoT will be spread over large area, which makes the communication unbounded. The future communication should be truly capable of providing efficient connection to Internet of Everything (covering deep sea, air, large geographic areas), multipurpose communication and computing (covering artificial intelligence, deep learning, SDN, Internet of Vehicles, big data, etc.). In short, the fundamental phenomenon of future technology should be that anyone can communication and connect to anything at any time efficiently [102].

**6.4. New Theories and Technologies.** In fact, to fully incorporate 6G technology, we need to push-up available spectrum resources for use and implement. Also, some basic theories need to be aligned with the need of future 6G technology. Further, refereeing to the 6G vision, we require break thoughts in several key areas, which will include improved channel coding and modulation schemes, millimeter wave solutions, Tera Hz communication, AI supported advance technology mechanism, etc.

**6.5. Self-Aggregating Communication Fabric.** The previously used technology standards like 3GPP or 4G claimed to integrate variety of technical standards, but after passage of time, these becomes self-enclosed standard systems. At first, the 3GPP standard tried to solve many challenges by itself, but with time passage, the integration of multiple devices and system becomes harder due to latest industrial and technology advancement. Therefore, to better provide interconnectivity of all things, 6G should be able to dynamically integrate different technology systems and networks, although 5G capable to integrate different networks but only combined or semistatic mode. Further, 6G needs to integrate different technologies with devices in a more efficient and intelligent way so dynamically and adaptively meet new complex and diverse technology standards and professional needs.

**6.6. Nontechnical Challenges.** For smooth transition of 6G, there are many nontechnical challenges along with the abovementioned technical challenges. In nontechnical challenges, we have to overcome different aspects like marketing factor, trade barriers, customer desires, rules, and regulations by the authorities. Compared to 5G, 6G will boost almost every aspect of socialism and life more adequately and will be closely integrated with other vertical industries. Also, the spectrum allocation and restrictions by authorities are also not-technical issues. For example, the use of terahertz spectrum in 6G requires different countries and region collaboration interim of coordinated allocation across the world to agree upon on a uniform band range as much as possible. Also, coordination with users in other spectrum

like meteorological radar or satellite communication will be more restricted in policies. As there should a central policy with consensus of different countries and region for the solution of orbit and satellite communication spectrum resources. Besides, compared with existing ground communication, satellite communication will face more issue in facing global roaming handover. Presently, different countries and commercial industry working to build coordinated satellite communication systems; however, to make this communication independently deployed system would be very complex and challenging. Further soon after the mobile communication emerged many vertical industries have different characteristics, it has to deal with user habits with huge differences. It would be great challenge to change user habits and inherent ways of things among diverse industries to adapt new rules and policies more quickly and efficiently.

The 6G vision is interesting along with numerous challenges from integrated key technologies in 6G. According to an idea, 6G will provide Tera bits/sec and be able to support 1000+ communicating nodes per person in 10 years (up to 2030) with smooth connectivity anytime anywhere. The future belongs to completely data-oriented society, which bring users and thing are connected universally as small technology hub and things going to have instantaneously in milliseconds in this universal connected world.

*6.7. High Propagation and Atmospheric Absorption of THz.* In fact, the high terahertz frequencies provide huge data rates. However, THz need to overcome the challenge of data transfer over long distances due to different atmospheric absorption and propagation-path loss [103]. This demands an updated design of transceiver for THz communicating systems. This transceiver would be able to operate on fully avail be high bandwidths and frequencies. Communication issues must be addressed properly. Health and safety measures using THz also be kept in mind, and problems emerged from it need to addressed.

*6.8. Complexity in Resource Management for 3D Networking.* With emergence of 3D networking, a new dimension added. Also, numerous malicious actions may legitimate the desired information and results in degrading the system performance. Therefore, new improved techniques for 6G resource management, optimization for handover-mobility, multiple access, and routing protocol are urgent priorities.

*6.9. Heterogeneous Hardware Constraints.* In 6G, a very large of numerous and heterogeneous communication including high frequency bands, different network topologies, service delivery, and many more will be involved. The existing hardware settings will be changed for access points and mobile terminals in 6G. Furthermore, MIMO techniques will be updated in transition from 5G to 6G; hence, it requires complex architecture. The routing protocols and algorithm will be more complex. Similarly, the hardware design is different for several communication systems. Also, the emerging needs to use AI, unsupervised, and reinforcement learning would be challenging in terms of complex hardware design

and implementation, while integration of all these communicating and intelligent systems is also a big issue to solve.

*6.10. Autonomous Wireless Systems.* 6G industry will also able to provide services to automation systems such as intelligent transportation, unmanned vesicle, wireless drone, and Industry 4.0 using AI. To make intelligent autonomous wireless systems, we need convergence of subsystems, e.g., AI, machine learning, autonomous computing, and heterogeneous wireless systems [104]. Due to these integrations, overall system complexity and developing model become more complex. For example, to deploy fully intelligent vehicle system for unmanned vehicle would become more challenging for researchers and industry to overcome all aspect and complexity design of intelligent vehicle systems.

*6.11. Modelling of Sub-mmWave (THz) Frequencies.* Due to the propagation characteristics, the mmWave and sub-mmWave (THz) are dependent on atmospheric conditions: therefore, dispersive and absorptive effects are seen [105]. As atmospheric condition is changeable and hence unpredictable, the channel modelling of this band would be very complex, and it is quite possible that this band does match perfect channel modelling.

*6.12. Device Capability.* The 6G technology will support new features and device capabilities. However, it would be challenging to get 1 Tbps throughput, compatible AI, and integrated sensing features using the existing devices. Also, 5G devices need to be upgraded as they may not be fully compatible to 6G features. No doubt, it will increase the overall cost. As there are numerous devices connected to 5G technologies, so urgent need is to ensure the compatibility with 6G technology.

*6.13. High-Capacity Backhaul Connectivity.* The density of access networks will be increase in new 6G networks, as access networks diverse in nature and will cover large geographic area. Each of these access networks requires high data rate connection for diverse applications. The backhaul in 6G technology will be capable to provide high data rate connections between access networks and core network to support high data-driven applications at user end. One solution can be optical fiber and FSO for the high capacity backhaul system. However, how to improve the capacity of existing networks would be a challenge in 6G.

*6.14. Spectrum and Interference Management.* Managing 6G spectrum resources and interference problems is not easy and requires effective handling of spectrum sharing policies and updated spectrum management solutions. As effective spectrum handling is important for efficient resource utilization with high QoS. Researchers and industrial expert need to look issues such like how to manage and share spectrum in heterogeneous networks that synchronize the transmission at same frequencies. Also, they need to investigate the interference cancellation techniques, such as parallel interference cancellation and successive interference cancelation.

6.15. *Beam Management in THz Communications.* Beamforming using MIMO is promising candidate to provide high data-driven communications. However, its management in sub-mmWave or THz is very challenging due to wave propagation characteristics. Hence, effective beamforming management in terms of unfavorable propagation characteristics is a big issue to solve in MIMO [75]. While for smooth handover, it is important to select optimal beam efficiently in high mobility networks.

## 7. Conclusion

In this research paper, we have provided a detail and systematic survey on 6G wireless communication. This survey is carried out in such a way that initially, the literature on 6G and different practical research initiatives taken by different organizations are presented followed by the 6G vision, specifications, challenges, different candidate technologies, and future research directions. The vision of 6G is based on requirements that 5G is unable to fulfil and those services that 5G is unable to provide. To this end, the vision of 6G is categorized into four fundamental services: “Intelligent Connectivity,” “Deep Connectivity,” “Holographic Connectivity,” and “Ubiquitous Connectivity.” Based on discussed 6 visions, the achievable 6G goals are specified which are (a) latency minimization, (b) global connectivity, (c) massive connectivity, (d) enormously high data rates, (e) energy efficiency of network devices, (f) connection reliability, and (g) machine learning-based connected intelligence. To achieve these specified 6G goals, many potential technologies are proposed which include AI, FSO backhaul network, blockchain, UAVs, 3D networking, DNS, sensing-based communication, big data analytics, and some new spectrum-based technologies, e.g., terahertz spectrum and Optical Wireless Communications. To realize the vision of 6G and implementation of the potential candidate technologies to achieve the specified 6G goals, a lot of challenges will be faced which require intense research. These challenges include Peak Rate-Terabit, higher energy efficiency, connection everywhere and anytime, self-aggregating, high propagation and atmospheric absorption of THz, complexity in resource management for 3D networking, heterogeneous hardware constraints, autonomous wireless systems, modelling of sub-mmWave (THz) frequencies, and spectrum and interference management.

## Data Availability

This research is survey based; therefore, no dataset is used in this research.

## Conflicts of Interest

The authors declare that they have no conflicts of interest.

## References

[1] T. Wild, V. Braun, and H. Viswanathan, “Joint design of communication and sensing for beyond 5G and 6G systems,” *IEEE Access*, vol. 9, pp. 30845–30857, 2021.

[2] A. Yastrebova, R. Kirichek, Y. Koucheryavy, A. Borodin, and A. Koucheryavy, “Future networks 2030: architecture & requirements,” in *2018 10th International Congress on Ultra Modern Telecommunications and Control Systems and Workshops (ICUMT)*, pp. 1–8, Moscow, Russia, 2018.

[3] K. Rikkinen, P. Kyosti, M. E. Leinonen, M. Berg, and A. Parssinen, “THz radio communication: link budget analysis toward 6G,” *IEEE Communications Magazine*, vol. 58, no. 11, pp. 22–27, 2020.

[4] K. Sheth, K. Patel, H. Shah, S. Tanwar, R. Gupta, and N. Kumar, “A taxonomy of AI techniques for 6G communication networks,” *Computer Communications*, vol. 161, pp. 279–303, 2020.

[5] T. Hewa, G. Gür, A. Kalla, M. Ylianttila, A. Bracken, and M. Liyanage, “The role of blockchain in 6G: challenges, opportunities and research directions,” in *2020 2nd 6G Wireless Summit (6G SUMMIT)*, pp. 1–5, Levi, Finland, 2020.

[6] A. Chaoub, M. Giordani, B. Lall et al., “6G for bridging the digital divide: wireless connectivity to remote areas,” *IEEE Wireless Communications*, pp. 1–9, 2021.

[7] K. David and H. Berndt, “6G vision and requirements: is there any need for beyond 5G?,” *IEEE Vehicular Technology Magazine*, vol. 13, no. 3, pp. 72–80, 2018.

[8] V. Raghavan and J. Li, “Evolution of physical-layer communications research in the post-5G era,” *IEEE Access*, vol. 7, pp. 10392–10401, 2019.

[9] W. Saad, M. Bennis, and M. Chen, “A vision of 6G wireless systems: applications, trends, technologies, and open research problems,” *IEEE Network*, vol. 34, no. 3, pp. 134–142, 2020.

[10] E. Calvanese Strinati, S. Barbarossa, J. L. Gonzalez-Jimenez et al., “6G: The next frontier: from holographic messaging to artificial intelligence using subterahertz and visible light communication,” *IEEE Vehicular Technology Magazine*, vol. 14, no. 3, pp. 42–50, 2019.

[11] F. Tariq, M. R. A. Khandaker, K.-K. Wong, M. A. Imran, M. Bennis, and M. Debbah, “A speculative study on 6G,” *IEEE Wireless Communications*, vol. 27, no. 4, pp. 118–125, 2020.

[12] Z. Zhang, Y. Xiao, Z. Ma et al., “6G wireless networks: vision, requirements, architecture, and key technologies,” *IEEE Vehicular Technology Magazine*, vol. 14, no. 3, pp. 28–41, 2019.

[13] S. Rommel, T. R. Raddo, and I. T. Monroy, “Data center connectivity by 6G wireless systems,” in *2018 Photonics in switching and computing (PSC)*, pp. 1–3, Limassol, Cyprus, 2018.

[14] F. Clazzer, A. Munari, G. Liva, F. Lazaro, C. Stefanovic, and P. Popovski, “From 5G to 6G: has the time for modern random access come?,” 2019, <https://arxiv.org/abs/1903.03063>.

[15] M. Giordani, M. Polese, M. Mezzavilla, S. Rangan, and M. Zorzi, “Toward 6G networks: use cases and technologies,” *IEEE Communications Magazine*, vol. 58, no. 3, pp. 55–61, 2020.

[16] H. Yanikomeroglu, “Integrated terrestrial/non-terrestrial 6G networks for ubiquitous 3D super-connectivity,” in *Proceedings of the 21st ACM International Conference on Modeling, Analysis and Simulation of Wireless and Mobile Systems*, pp. 3–4, 2018.

[17] E. Yaacoub and M.-S. Alouini, “A key 6G challenge and opportunity—connecting the remaining 4 billions: a survey on rural connectivity,” in *Qatar University*, 2019, <https://arxiv.org/abs/1906.11541>.

- [18] N. H. Mahmood, H. Alves, O. A. López, M. Shehab, D. P. Moya Osorio, and M. Latva-aho, "Six key enablers for machine type communication in 6G," 2019, <https://arxiv.org/abs/1903.05406>.
- [19] T. S. Rappaport, Y. Xing, O. Kanhere et al., "Wireless communications and applications above 100 GHz: opportunities and challenges for 6G and beyond," *IEEE access*, vol. 7, pp. 78729–78757, 2019.
- [20] R.-A. Stoica and G. T. F. de Abreu, "6G: the wireless communications network for collaborative and AI applications," 2019, <https://arxiv.org/abs/1904.03413>.
- [21] K. B. Letaief, W. Chen, Y. Shi, J. Zhang, and Y.-J. A. Zhang, "The roadmap to 6G: AI empowered wireless networks," *IEEE Communications Magazine*, vol. 57, no. 8, pp. 84–90, 2019.
- [22] S. J. Nawaz, S. K. Sharma, S. Wyne, M. N. Patwary, and M. Asaduzzaman, "Quantum machine learning for 6G communication networks: state-of-the-art and vision for the future," *Access*, vol. 7, pp. 46317–46350, 2019.
- [23] M. Di Renzo, M. Debbah, D.-T. Phan-Huy et al., "Smart radio environments empowered by reconfigurable AI meta-surfaces: an idea whose time has come," *EURASIP Journal on Wireless Communications and Networking*, vol. 2019, 2019.
- [24] J. Zhao, "A survey of intelligent reflecting surfaces (IRSs): towards 6G wireless communication networks," 2019, <https://arxiv.org/abs/1907.04789>.
- [25] Q.-U.-A. Nadeem, A. Kammoun, A. Chaaban, M. Debbah, and M.-S. Alouini, "Asymptotic max-min SINR analysis of reconfigurable intelligent surface assisted MISO systems," *IEEE Transactions on Wireless Communications*, vol. 19, no. 12, pp. 7748–7764, 2020.
- [26] E. Basar, "Reconfigurable intelligent surface-based index modulation: a new beyond MIMO paradigm for 6G," *IEEE Transactions on Communications*, vol. 68, no. 5, pp. 3187–3196, 2020.
- [27] Q.-U.-A. Nadeem, A. Kammoun, A. Chaaban, M. Debbah, and M.-S. Alouini, "Intelligent reflecting surface assisted wireless communication: modeling and channel estimation," 2019, <https://arxiv.org/abs/1906.02360>.
- [28] P. T. Dat, A. Kanno, K. Inagaki, T. Umezawa, N. Yamamoto, and T. Kawanishi, "Hybrid optical wireless-mmWave: ultra high-speed indoor communications for beyond 5G," in *IEEE INFOCOM 2019-IEEE Conference on Computer Communications Workshops (INFOCOM WKSHPs)*, pp. 1003–1004, Paris, France, 2019.
- [29] A. Vanelli-Coralli, A. Guidotti, T. Foggi, G. Colavolpe, and G. Montorsi, "5G and beyond 5G non-terrestrial networks: trends and research challenges," in *2020 IEEE 3rd 5G World Forum (5GWF)*, pp. 163–169, Bangalore, India, 2020.
- [30] S. Ali and A. Ahmad, "Resource allocation, interference management, and mode selection in device-to-device communication: a survey," *Transactions on Emerging Telecommunications Technologies*, vol. 28, no. 7, article e3148, 2017.
- [31] S. Ali, A. Ahmad, Y. Faheem, M. Altaf, and H. Ullah, "Energy-efficient RRH-association and resource allocation in D2D enabled multi-tier 5G C-RAN," *Telecommunication Systems*, vol. 74, no. 2, pp. 129–143, 2020.
- [32] N. C. Luong, D. T. Hoang, P. Wang, D. Niyato, D. In Kim, and Z. Han, "Data collection and wireless communication in Internet of Things (IoT) using economic analysis and pricing models: a survey," *IEEE Communications Surveys & Tutorials*, vol. 18, no. 4, pp. 2546–2590, 2016.
- [33] T. Park, N. Abuzainab, and W. Saad, "Learning how to communicate in the Internet of Things: finite resources and heterogeneity," *IEEE Access*, vol. 4, pp. 7063–7073, 2016.
- [34] T. J. O'Shea and J. Hoydis, "An introduction to machine learning communications systems," 2017, <https://arxiv.org/abs/1702.00832>.
- [35] H. Sun, X. Chen, Q. Shi, M. Hong, F. Xiao, and N. D. Sidiropoulos, "Learning to optimize: training deep neural networks for wireless resource management," in *2017 IEEE 18th International Workshop on Signal Processing Advances in Wireless Communications (SPAWC)*, pp. 1–6, Sapporo, Japan, 2017.
- [36] C. Jiang, H. Zhang, Y. Ren, Z. Han, K.-C. Chen, and L. Hanzo, "Machine learning paradigms for next-generation wireless networks," *IEEE Wireless Communications*, vol. 24, no. 2, pp. 98–105, 2017.
- [37] M. Bkassiny, Y. Li, and S. K. Jayaweera, "A survey on machine-learning techniques in cognitive radios," *IEEE Communications Surveys & Tutorials*, vol. 15, no. 3, pp. 1136–1159, 2013.
- [38] N. Kato, Z. M. Fadlullah, B. Mao et al., "The deep learning vision for heterogeneous network traffic control: proposal, challenges, and future perspective," *IEEE Wireless Communications*, vol. 24, no. 3, pp. 146–153, 2017.
- [39] D. Praveen Kumar, T. Amgoth, and C. S. R. Annavarapu, "Machine learning algorithms for wireless sensor networks: a survey," *Information Fusion*, vol. 49, pp. 1–25, 2019.
- [40] Yang Zhang, N. Meratnia, and P. Havinga, "Outlier detection techniques for wireless sensor networks: a survey," *IEEE Communications Surveys & Tutorials*, vol. 12, no. 2, pp. 159–170, 2010.
- [41] A. Mehta, J. K. Sandhu, and L. Sapra, "Machine learning in wireless sensor networks: a retrospective," in *2020 Sixth International Conference on Parallel, Distributed and Grid Computing (PDGC)*, pp. 328–331, Wagnaghat, India, 2020.
- [42] R. M. Neal, *Bayesian Learning for Neural Networks*, vol. 118, Springer Science & Business Media, 2012.
- [43] R. Rojas, *Neural Networks: A Systematic Introduction*, Springer Science & Business Media, 2013.
- [44] K. Hwang and W. Sung, "Fixed-point feedforward deep neural network design using weights+1, 0, and-1," in *2014 IEEE Workshop on Signal Processing Systems (SiPS)*, pp. 1–6, Belfast, UK, 2014.
- [45] J. Schmidhuber, "Deep learning in neural networks: an overview," *Neural Networks*, vol. 61, pp. 85–117, 2015.
- [46] F. Maleki, K. Ovens, K. Najafian, B. Forghani, C. Reinhold, and R. Forghani, "Overview of machine learning part 1: fundamentals and classic approaches," *Neuroimaging Clinics of North America*, vol. 30, no. 4, pp. e17–e32, 2020.
- [47] R. E. Schapire, "The boosting approach to machine learning: an overview," in *Nonlinear estimation and classification*, pp. 149–171, Springer, 2003.
- [48] E. Basesmez, "The next generation neural networks: deep learning and spiking neural networks," *Advanced Seminar in Technical University of Munich*, pp. 1–40, 2014.
- [49] X. You, C. Zhang, X. Tan, S. Jin, and H. Wu, "AI for 5G: research directions and paradigms," *Science China Information Sciences*, vol. 62, no. 2, pp. 1–13, 2019.
- [50] M. G. Kibria, K. Nguyen, G. P. Villardi, O. Zhao, K. Ishizu, and F. Kojima, "Big data analytics, machine learning, and

- artificial intelligence in next-generation wireless networks,” *IEEE Access*, vol. 6, pp. 32328–32338, 2018.
- [51] S. Bi, R. Zhang, Z. Ding, and S. Cui, “Wireless communications in the era of big data,” *IEEE Communications Magazine*, vol. 53, no. 10, pp. 190–199, 2015.
- [52] E. Abu-Taieh, I. H. Al Hadid, and A. Zolait, “5G road map to communication revolution,” in *Cyberspace*, pp. 3–12, IntechOpen, 2020.
- [53] M. Torres Vega, C. Liaskos, S. Abadal et al., “Immersive interconnected virtual and augmented reality: a 5g and IoT perspective,” *Journal of Network and Systems Management*, vol. 28, no. 4, pp. 796–826, 2020.
- [54] E. Baştuğ, M. Bennis, M. Médard, and M. Debbah, “Towards interconnected virtual reality: opportunities, challenges and enablers,” *IEEE Communications Magazine*, vol. 55, 2016.
- [55] D. Xu, “A neural network approach for hand gesture recognition in virtual reality driving training system of SPG,” in *18th International Conference on Pattern Recognition (ICPR’06)*, pp. 519–522, Hong Kong, China, 2006.
- [56] R. Hambli, A. Chamekh, and H. Bel Hadj Salah, “Real-time deformation of structure using finite element and neural networks in virtual reality applications,” *Finite Elements in Analysis and Design*, vol. 42, no. 11, pp. 985–991, 2006.
- [57] P. Zhang, X. Xiaodong, X. Qin, Y. Liu, N. Ma, and S. Han, “Evolution toward artificial intelligence of things under 6G ubiquitous-X,” *Journal of Harbin Institute of Technology (New Series)*, vol. 27, no. 3, pp. 116–135, 2020.
- [58] M. Indoounon, “6G ultra-low latency communication in future mobile XR applications,” in *Advances in Signal Processing and Intelligent Recognition Systems: 6th International Symposium, SIRS 2020*, pp. 302–312, Springer, 2021.
- [59] N. Saeed, H. Almorad, H. Dahrouj, T. Y. Al-Naffouri, J. S. Shamma, and M.-S. Alouini, “Point-to-point communication in integrated satellite-aerial 6G networks: state-of-the-art and future challenges,” *IEEE Open Journal of the Communications Society*, vol. 2, pp. 1505–1525, 2021.
- [60] H. Wang, W. Wang, X. Chen, and Z. Zhang, “Wireless information and energy transfer in interference aware massive MIMO systems,” in *2014 IEEE Global Communications Conference*, pp. 2556–2561, Austin, TX, USA, 2014.
- [61] K. M. Huq, J. Rodriguez, and I. E. Otung, “3D network modeling for THz-enabled ultra-fast dense networks: a 6G perspective,” *IEEE Communications Standards Magazine*, vol. 5, no. 2, pp. 84–90, 2021.
- [62] S. Ali, A. Ahmad, and A. Khan, “Energy-efficient resource allocation and RRH association in multitier 5G H-CRANs,” *Transactions on Emerging Telecommunications Technologies*, vol. 30, no. 1, article e3521, 2019.
- [63] M. Z. Chowdhury, M. T. Hossain, and Y. M. Jang, “Interference management based on RT/nRT traffic classification for FFR-aided small cell/macrosell heterogeneous networks,” *Access*, vol. 6, pp. 31340–31358, 2018.
- [64] A. S. M. Z. Shifat, M. Z. Chowdhury, and Y. M. Jang, “Game-based approach for QoS provisioning and interference management in heterogeneous networks,” *Access*, vol. 6, pp. 10208–10220, 2018.
- [65] A. J. Mahbas, H. Zhu, and J. Wang, “Impact of small cells overlapping on mobility management,” *IEEE Transactions on Wireless Communications*, vol. 18, no. 2, pp. 1054–1068, 2019.
- [66] T. Zhou, N. Jiang, Z. Liu, and C. Li, “Joint cell activation and selection for green communications in ultra-dense heterogeneous networks,” *IEEE Access*, vol. 6, pp. 1894–1904, 2018.
- [67] S. Andreev, V. Petrov, M. Dohler, and H. Yanikomeroglu, “Future of ultra-dense networks beyond 5G: harnessing heterogeneous moving cells,” *IEEE Communications Magazine*, vol. 57, no. 6, pp. 86–92, 2019.
- [68] S. Ali, A. Ahmad, R. Iqbal, S. Saleem, and T. Umer, “Joint RRH-association, sub-channel assignment and power allocation in multi-tier 5G C-RANs,” *IEEE Access*, vol. 6, pp. 34393–34402, 2018.
- [69] T. Sharma, A. Chehri, and P. Fortier, “Review of optical and wireless backhaul networks and emerging trends of next generation 5G and 6G technologies,” *Transactions on Emerging Telecommunications Technologies*, vol. 32, no. 3, article e4155, 2021.
- [70] P. Carbone, G. Dan, J. Gross, B. Goeransson, and M. Petrova, “NeuroRAN: rethinking virtualization for AI-native radio access networks in 6G,” 2021, <https://arxiv.org/abs/2104.08111>.
- [71] L. Lovén, T. Leppänen, E. Peltonen, J. Partala, E. Harjula, P. Porambage, M. Ylianttila, and J. Rieki, Eds., “EdgeAI: a vision for distributed, edge-native artificial intelligence in future 6G networks,” in *The 1st 6G Wireless Summit*, pp. 1–2, 2019.
- [72] J. Zhao, “A survey of reconfigurable intelligent surfaces: towards 6G wireless communication networks with massive MIMO 2.0,” 1907, <https://arxiv.org/abs/1907.04789>.
- [73] S. Ali, A. Haider, M. Rahman, M. Sohail, and Y. B. Zikria, “Deep learning (DL) based joint resource allocation and RRH association in 5G-multi-tier networks,” *Access*, vol. 9, pp. 118357–118366, 2021.
- [74] S. Ali, N. Saleem, and T. Tareen, “Measuring the performance of handover mechanisms in UMTS for diverse traffic services classes to improve QoS,” *International Journal of Computer Applications*, vol. 55, no. 11, pp. 14–19, 2012.
- [75] Z. Gu, J. Zhang, Y. Ji, L. Bai, and X. Sun, “Network topology reconfiguration for FSO-based fronthaul/backhaul in 5G+ wireless networks,” *IEEE Access*, vol. 6, pp. 69426–69437, 2018.
- [76] A. Douik, H. Dahrouj, T. Y. Al-Naffouri, and M.-S. Alouini, “Hybrid radio/free-space optical design for next generation backhaul systems,” *IEEE Transactions on Communications*, vol. 64, no. 6, pp. 2563–2577, 2016.
- [77] B. Bag, A. Das, I. S. Ansari, A. Prokes, C. Bose, and A. Chandra, “Performance analysis of hybrid FSO systems using FSO/RF-FSO link adaptation,” *IEEE Photonics Journal*, vol. 10, no. 3, pp. 1–17, 2018.
- [78] R. Henry, A. Herzberg, and A. Kate, “Blockchain access privacy: challenges and directions,” *IEEE Security & Privacy*, vol. 16, no. 4, pp. 38–45, 2018.
- [79] T. Aste, P. Tasca, and T. Di Matteo, “Blockchain Technologies: The Foreseeable Impact on Society and Industry,” *Computer*, vol. 50, no. 9, pp. 18–28, 2017.
- [80] D. Miller, “Blockchain and the Internet of Things in the industrial sector,” *IT Professional*, vol. 20, no. 3, pp. 15–18, 2018.
- [81] H.-N. Dai, Z. Zheng, and Y. Zhang, “Blockchain for Internet of Things: a survey,” *IEEE Internet of Things Journal*, vol. 6, no. 5, pp. 8076–8094, 2019.
- [82] A. Manzalini, “Quantum communications in future networks and services,” *Quantum Reports*, vol. 2, no. 1, pp. 221–232, 2020.

- [83] R. Shrestha, R. Bajracharya, and S. Kim, "6G enabled unmanned aerial vehicle traffic management: a perspective," *IEEE Access*, vol. 9, pp. 91119–91136, 2021.
- [84] C. Pan, J. Yi, C. Yin, J. Yu, and X. Li, "Joint 3D UAV placement and resource allocation in software-defined cellular networks with wireless backhaul," *IEEE Access*, vol. 7, pp. 104279–104293, 2019.
- [85] M. Mozaffari, A. Taleb Zadeh Kasgari, W. Saad, M. Bennis, and M. Debbah, "Beyond 5G with UAVs: foundations of a 3D wireless cellular network," *IEEE Transactions on Wireless Communications*, vol. 18, no. 1, pp. 357–372, 2019.
- [86] C. Liu, W. Feng, Y. Chen, C.-X. Wang, and N. Ge, "Cell-free satellite-UAV networks for 6G wide-area Internet of Things," *IEEE Journal on Selected Areas in Communications*, vol. 39, no. 4, pp. 1116–1131, 2021.
- [87] M. Kobayashi, G. Caire, and G. Kramer, "Joint state sensing and communication: optimal tradeoff for a memoryless case," in *2018 IEEE International Symposium on Information Theory (ISIT)*, pp. 111–115, Vail, CO, USA, 2018.
- [88] Y. Zhang, M. A. Kishk, and M.-S. Alouini, "A survey on integrated access and backhaul networks," 2021, <https://arxiv.org/abs/2101.01286>.
- [89] W. Wu, C. Zhou, M. Li, W. Huaqing, H. Zhou, N. Zhang, and W. Zhuang, Eds., "AI-native network slicing for 6G networks," 2021, <https://arxiv.org/abs/2105.08576>.
- [90] H. Gao, S. Yumeng, S. Zhang, and M. Diao, "MassiveMIMOAntenna designs," *China Communications*, vol. 16, no. 4, pp. 1–15, 2020.
- [91] M. Attarifar, A. Abbasfar, and A. Lozano, "Modified conjugate beamforming for cell-free massive MIMO," *IEEE Wireless Communications Letters*, vol. 8, no. 2, pp. 616–619, 2019.
- [92] Z. Lv, R. Lou, J. Li, A. K. Singh, and H. Song, "Big data analytics for 6G-enabled massive Internet of Things," *IEEE Internet of Things Journal*, vol. 8, no. 7, pp. 5350–5359, 2021.
- [93] I. F. Akyildiz, J. M. Jornet, and C. Han, "Terahertz band: next frontier for wireless communications," *Physical Communication*, vol. 12, pp. 16–32, 2014.
- [94] K. Tekbiyik, A. R. Ekti, G. K. Kurt, and A. Görçin, "Terahertz band communication systems: challenges, novelties and standardization efforts," *Physical Communication*, vol. 35, article 100700, 2019.
- [95] I. Siaud and A.-M. Ulmer-Moll, *THz Communications: An Overview and Challenges*, 2019.
- [96] J. Wells, "Faster than fiber: the future of multi-G/s wireless," *IEEE Microwave Magazine*, vol. 10, no. 3, pp. 104–112, 2009.
- [97] M. Z. Chowdhury, M. T. Hossan, A. Islam, and Y. M. Jang, "A comparative survey of optical wireless technologies: architectures and applications," *IEEE Access*, vol. 6, pp. 9819–9840, 2018.
- [98] M. Z. Chowdhury, M. T. Hossan, M. K. Hasan, and Y. M. Jang, "Integrated RF/optical wireless networks for improving QoS in indoor and transportation applications," *Wireless Personal Communications*, vol. 107, no. 3, pp. 1401–1430, 2019.
- [99] M. Hossan, M. Z. Chowdhury, M. Hasan et al., "A new vehicle localization scheme based on combined optical camera communication and photogrammetry," *Mobile Information Systems*, vol. 2018, Article ID 8501898, 14 pages, 2018.
- [100] M. T. Hossan, M. Z. Chowdhury, M. Shahjalal, and Y. M. Jang, "Human bond communication with head-mounted displays: scope, challenges, solutions, and applications," *IEEE Communications Magazine*, vol. 57, no. 2, pp. 26–32, 2019.
- [101] Z. Ma, Z. Q. Zhang, Z. G. Ding, P. Z. Fan, and H. C. Li, "Key techniques for 5G wireless communications: network architecture, physical layer, and MAC layer perspectives," *Science China information sciences*, vol. 58, no. 4, pp. 1–20, 2015.
- [102] M. E. Morocho-Cayamcela, H. Lee, and W. Lim, "Machine learning for 5G/B5G mobile and wireless communications: potential, limitations, and future directions," *Access*, vol. 7, pp. 137184–137206, 2019.
- [103] S. Mumtaz, J. Miquel Jornet, J. Aulin, W. H. Gerstaecker, X. Dong, and B. Ai, "Terahertz communication for vehicular networks," *IEEE Transactions on Vehicular Technology*, vol. 66, no. 7, pp. 5617–5625, 2017.
- [104] D. Elliott, W. Keen, and L. Miao, "Recent advances in connected and automated vehicles," *Journal of Traffic and Transportation Engineering (English Edition)*, vol. 6, no. 2, pp. 109–131, 2019.
- [105] Y. Golovachev, A. Etinger, G. A. Pinhasi, and Y. Pinhasi, "Propagation properties of sub-millimeter waves in foggy conditions," *Journal of Applied Physics*, vol. 125, no. 15, article 151612, 2019.

## Retraction

# Retracted: A Novel Smart Healthcare Monitoring System Using Machine Learning and the Internet of Things

### Wireless Communications and Mobile Computing

Received 8 August 2023; Accepted 8 August 2023; Published 9 August 2023

Copyright © 2023 Wireless Communications and Mobile Computing. This is an open access article distributed under the Creative Commons Attribution License, which permits unrestricted use, distribution, and reproduction in any medium, provided the original work is properly cited.

This article has been retracted by Hindawi following an investigation undertaken by the publisher [1]. This investigation has uncovered evidence of one or more of the following indicators of systematic manipulation of the publication process:

- (1) Discrepancies in scope
- (2) Discrepancies in the description of the research reported
- (3) Discrepancies between the availability of data and the research described
- (4) Inappropriate citations
- (5) Incoherent, meaningless and/or irrelevant content included in the article
- (6) Peer-review manipulation

The presence of these indicators undermines our confidence in the integrity of the article's content and we cannot, therefore, vouch for its reliability. Please note that this notice is intended solely to alert readers that the content of this article is unreliable. We have not investigated whether authors were aware of or involved in the systematic manipulation of the publication process.

In addition, our investigation has also shown that one or more of the following human-subject reporting requirements has not been met in this article: ethical approval by an Institutional Review Board (IRB) committee or equivalent, patient/participant consent to participate, and/or agreement to publish patient/participant details (where relevant).

Wiley and Hindawi regrets that the usual quality checks did not identify these issues before publication and have since put additional measures in place to safeguard research integrity.

We wish to credit our own Research Integrity and Research Publishing teams and anonymous and named external

researchers and research integrity experts for contributing to this investigation.

The corresponding author, as the representative of all authors, has been given the opportunity to register their agreement or disagreement to this retraction. We have kept a record of any response received.

### References

- [1] M. B. Alazzam, F. Alassery, and A. Almulih, "A Novel Smart Healthcare Monitoring System Using Machine Learning and the Internet of Things," *Wireless Communications and Mobile Computing*, vol. 2021, Article ID 5078799, 7 pages, 2021.



## Research Article

# A Novel Smart Healthcare Monitoring System Using Machine Learning and the Internet of Things

Malik Bader Alazzam <sup>1</sup>, Fawaz Alassery <sup>2</sup>, and Ahmed Almulihi<sup>3</sup>

<sup>1</sup>Faculty of Computer Science and Informatics, Amman Arab University, Jordan

<sup>2</sup>Department of Computer Engineering, College of Computers and Information Technology, Taif University, Taif, Saudi Arabia

<sup>3</sup>Department of Computer Science, College of Computers and Information Technology, Taif University, Taif, Saudi Arabia

Correspondence should be addressed to Malik Bader Alazzam; [m.alazzam@aau.edu.jo](mailto:m.alazzam@aau.edu.jo)

Received 31 October 2021; Revised 6 November 2021; Accepted 16 November 2021; Published 8 December 2021

Academic Editor: Shalli Rani

Copyright © 2021 Malik Bader Alazzam et al. This is an open access article distributed under the Creative Commons Attribution License, which permits unrestricted use, distribution, and reproduction in any medium, provided the original work is properly cited.

The Internet of Things (IoT) has enabled the invention of smart health monitoring systems. These health monitoring systems can track a person's mental and physical wellness. Stress, anxiety, and hypertension are key causes of many physical and mental disorders. Age-related problems such as stress, anxiety, and hypertension necessitate specific attention in this setting. Stress, anxiety, and blood pressure monitoring can prevent long-term damage by detecting problems early. This will increase the quality of life and reduce caregiver stress and healthcare costs. Determine fresh technology solutions for real-time stress, anxiety, and blood pressure monitoring using discreet wearable sensors and machine learning approaches. This study created an automated artefact detection method for BP and PPG signals. It was proposed to automatically remove outlier points generated by movement artefacts from the blood pressure signal. Next, eleven features taken from the oscillometric waveform envelope were utilised to analyse the relationship between diastolic blood pressure (SBP) and systolic blood pressure (DBP). This paper validates a proposed computational method for estimating blood pressure. The proposed architecture leverages sophisticated regression to predict systolic and diastolic blood pressure values from PPG signal characteristics.

## 1. Introduction

The Internet of Things (IoT) is a rapidly evolving technology. The Internet of Things (IoT) is about connecting computing devices, mechanical and digital machines, objects, animals, and people with sensors and actuators to collect data and improve wellness, productivity, and efficiency [1]. Smart home, smart grid, and smart city are well-known concepts that are revolutionising our lives.

Using IoT-based remote patient health monitoring is one of the most promising technological interventions emerging to bridge the global health equity gap. These IoT technologies are also known as the Internet of Medical Things (IoMT). Throughout this dissertation, we will use IoT and IoMT interchangeably, though we will focus on the healthcare domain. The Internet of Things can also improve healthcare and safety. We can get information about our lifestyle, physical and mental performance, living

environments, etc., by connecting our bodies to the Internet. This allows healthcare providers to monitor human subjects' health remotely and continuously [2]. The measured data may also support evidence-based solutions for disease, injury, safety prevention, early diagnosis, and treatment.

However, unlike mechanical or digital technologies, the human body cannot be easily connected to the Internet. It is possible to connect a digital gadget to the Internet by including a sensing and networking system. However, having a sensing system built in the human body will not allow us to connect it to the Internet. Large sensing or measurement equipment is typically utilised to carry out the measurement in order to learn about the health state of the subject. Large measurement equipment, on the other hand, has a constraint in that it can only be used in controlled situations for a short period of time. It is therefore impossible to connect a person's body to the Internet everywhere at any time using conventionally employed massive sensing and

measurement equipment [3]. The inability to connect the human body to the Internet severely restricts the application of IoT in the fields of healthcare and security.

Another component and its linked intricate factors may evolve as the result of an initial health concern caused by one aspect. The concept map in Figure 1 helps to show the relationship between the three aspects. Figure 1 depicts some of the symptoms of stress, such as headaches and dizziness suffering can be classified as either distress or eustress, with distress being the more detrimental of the two. It is important to remember that the length of stress is likewise divided into three categories: short term, episodic, and long term. Acute stress is characterised by being short and sharp in duration, while episodic acute stress is characterised by recurrence. Stress can lead to a lack of adaptation, which can have serious consequences on relationships, employment, health, and even on one's personal well-being in the form of emotional breakdowns [4]. It is critical to be able to develop a self-monitoring strategy for dealing with stress. A way for consumers to adapt is created by incorporating these approaches into the Internet of Medical Things (IoMT).

Studies have shown that stress contributes significantly to the development of anxiety and hypertension. Anxiety has also been linked to hypertension in some research. Figure 1 uses arrows to show this idea. Aside from that, stress-related illnesses including cognitive decline and heart disease can be triggered by worry as well. High blood pressure can potentially lead to heart disease.

By keeping tabs on and controlling stress and its side effects like anxiety and high blood pressure, people are less likely to suffer from long term and often irreversible health problems in the future [4]. Furthermore, keeping track of a patient's stress, anxiety, and blood pressure levels might assist the caregiver in establishing an informed diagnosis and initiating early intervention to prevent long-term damage.

## 2. Background

It is possible to obtain precise information about body posture and force exertions using direct methods that make use of instruments like inertial measurement units (IMUs) and electromyography (EMG) sensors, among other things. For example, Vignais et al. used an IMU in conjunction with goniometers to measure upper-body movement and angle. The magneto-resistive angle sensors developed by Alwasel et al. were proposed to measure the kinematics of shoulder movement. The use of accelerometers to detect the movement of subjects was also common [5]. These methods, however, are limited to posture recognition and do not capture information on force exertion, a significant risk factor for WMSDs60. They should be improved. Force exertion data could be recorded using EMG sensors. Due to the limited use of EMG sensors, it was difficult to obtain information on the total amount of force being exerted by the body as a whole. Additionally, these methods required the use of additional instruments or electrodes on the head, truck, or upper limbs, which was uncomfortable and inconvenient for the user [6].

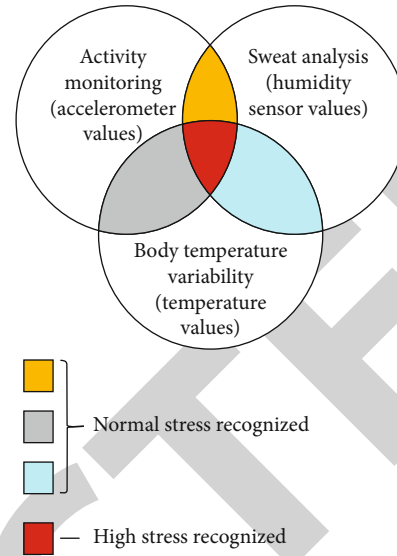


FIGURE 1: Logical analysis for stress detection.

**2.1. Stress Detection.** The scientific community has recently placed a high value on detecting stress levels from physiological signals. However, the majority of previously published works have either utilised adolescents or failed to mention a specific target audience. The use of cortisol as a stress reference for stress detection is another area that has received relatively little attention. As the ground truth, most studies have used stress levels calculated from self-reporting questionnaires such as the DASS 21 [7]. Because of erroneous stress perceptions, low objectivity, and inconsistent assessment, the results obtained using this method may be skewed.

As shown in Figure 2, we used real-time stress detection (such as programmers and testers). Physical data is collected by E4-wristband6 sensors. In this first version, the stress detector only uses electrodermal activity as an input (EDA). A brief increase in the EDA signal is linked to increased sweating and stress. The stress detector's main job is to assess the user's stress level [7–9]. The detector will label your body if you are stressed. We used Bakker et al.'s preprocessing steps to allow real-time processing (see Figure 2 for the involved preprocessing steps). Then, we will look at how stress is detected.

**2.2. Blood Pressure Estimation Models.** There is a lot of research on calculating blood pressure from physiological cues (PWV). Repeated sensing or a dual element probe is required. Calculate PWV using a dual element PPG probe. And here, used three signals (ECG, PCG, and PP) to calculate pulse transit and arrival time to predict blood pressure (PPG). Using a Ballistocardiogram, blood pressure is calculated in [10] (BCG). We developed a new method for measuring blood pressure using a PPG-based single sensor and single probe.

The current study examined two new Adobos models (MLP and DT) as well as the traditional Maximum Amplitude Algorithm (MAA) method based on predefined characteristic ratios. The classic MAA approach depends on a constant characteristic ratio to determine SBP and DBP.

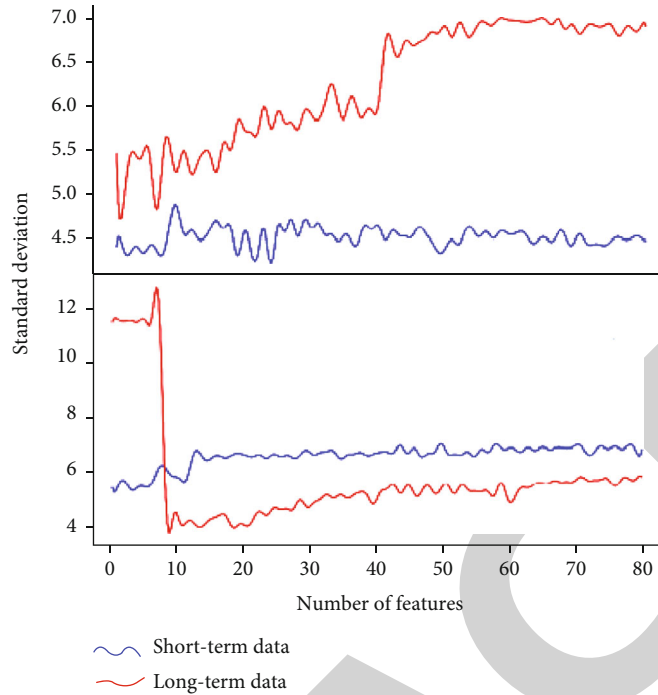


FIGURE 2: Graph between the systolic short-term blood pressure.

The SBPR and DBPR fixed values were calculated using our Reference Scoring averages (RSs).

### 3. Methodology

To collect, process, and analyse the massive amounts of data generated by medical sensors, the proposed framework makes use of three key steps. In the first step, a large volume of data is collected. In the second step, data storage is discussed. In this step, Hbase is the database used to store the data. Step 3 is all about making a prediction.

**3.1. Data Collection.** There are three layers to the proposed health monitoring systems. Data collection is done at the top layer, followed by storage and analysis at the bottom. Using a wearable device that is implanted in a patient, the first layer collects medical data from the patient and continuously transfers it to the second layer [11]. It records data when a value exceeds a preset limit, then issues a warning, and sends a message to family members and caregivers. An alert message would be sent via wireless networks in the framework. Data is stored on Amazon S3 in an algorithmic representation of the observed clinical values.

**3.2. Storage of Medical Data.** Because smart devices generate a lot of data, traditional query-structured databases cannot handle it. That is why I used big data in this study. The medical data is stored in a distributed fashion using Apache and Hbase in this paper [12]. There is not enough room in devices and computer memory to store all of the data that is generated. Stability and elasticity are provided by the proposed method, which makes use of the cloud. An Amazon account is created for data storage, and clinical data

can be stored using Amazon's simple storage service S3. Monitoring systems send alert messages to Amazon S3 when observed values go above threshold values, which are then forwarded to doctors along with the patient's health records.

**3.3. Analysis of Medical Data.** The data is analysed using the decision tree algorithm, which is built on a mining algorithm for heart disease prediction [13]. There are three steps in this model. Medical data must first be collected, and then, that data must be remotely diagnosed as the second step.

A system level flow chart explains the design methodologies used to develop stress-lysis, while the following subsections discuss machine learning modelling techniques for stress-level detection.

**3.4. Logical Stress Analysis.** Truth table analysis of sensor values in system determines logical relationships. Logic 0 indicates that the output stress is minimal when the sensor values are low. Logic 1 indicates that the stress level is high when all of the inputs are high [14]. It is possible that not all sensor values, no matter how low they are, will be indicative of stress.

Using a truth table, the sensor values of the system can be logically analysed (see Figure 2). There is less output stress when the sensor values are low. It is easy to get stressed out when everything is going well [15]. In situations where both of the inputs are high, stress levels will be high as well. For in-between values, a Sum of Product (SOP) analysis is performed:

$$SL = TSR.(ASR + HSR) + (ASR.HSR), \quad (1)$$

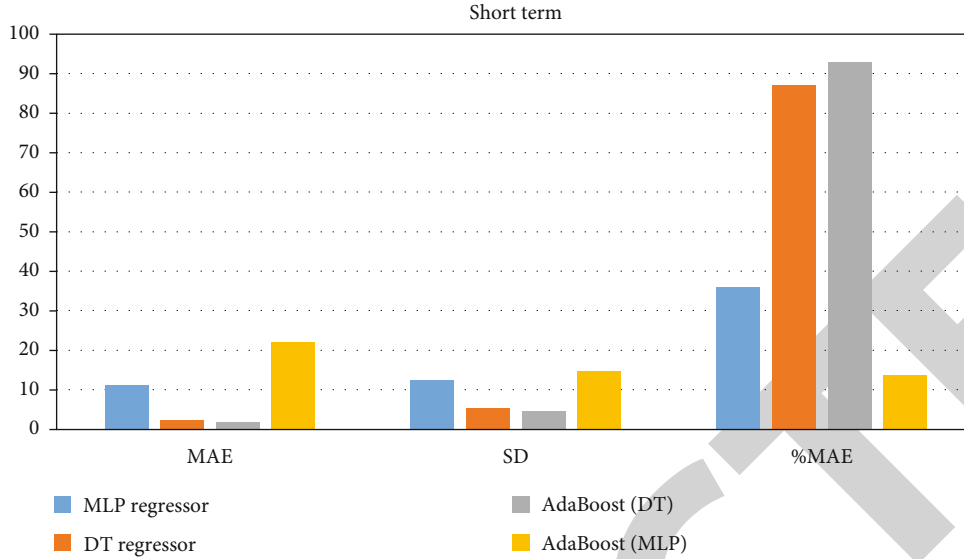


FIGURE 3: Graph between short- and long-term standard deviation vs. number of features.

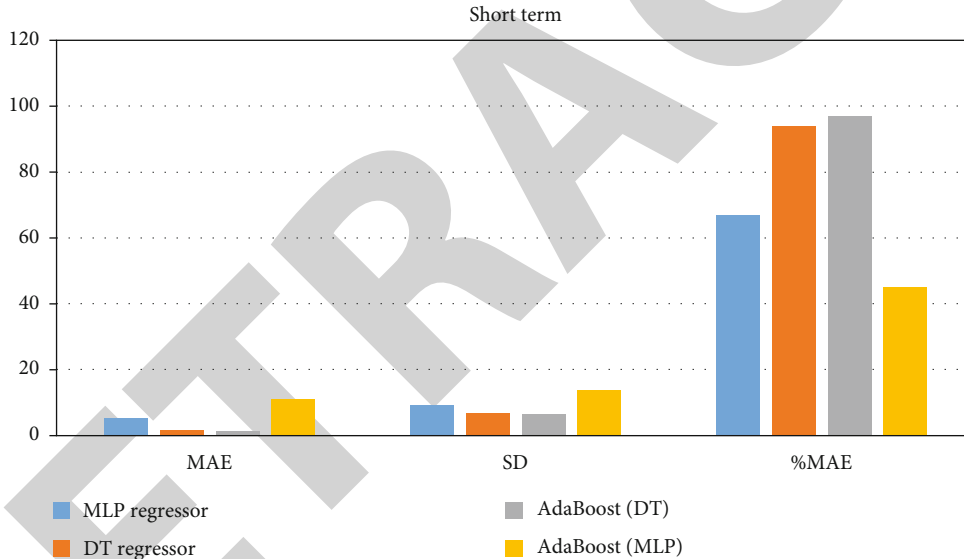


FIGURE 4: Graph between the diastolic short-term blood pressure.

where TSR is the temperature sensor reading, ASR is the accelerometer sensor reading, and HSR is the humidity sensor reading. A pictorial representation, representing the detailed explanation of the fuzzy operation, is represented through Figure 3.

## 4. Implementation

**4.1. Data Extraction.** We built and validated our model using the MIMIC database in this study. The MIMIC database is made up of ICU patient recordings with multiple parameters. A total of 72 complete records were downloaded from the Physio Bank database, varying in length and sampling rate from 500 Hz. For the sake of thoroughness, we will only be looking at the first 20 records of each album [16]. Subjects for this study were chosen based on two main selection cri-

teria. To begin, we only included patients whose records included data from both their PPG and arterial blood pressure (ABP) sensors. Second, only subjects with missing PPG data totalling more than 10% of the total length of the data were included in the analysis. Additionally, the value 0 was used to replace any missing PPG signal values.

The first, middle, and end of each record's three hours of data were chosen at random. The final dataset combines PPG and ABP signals. The ground truth is derived from ABP data. The next part discusses data preprocessing in depth.

**4.1.1. Feature Extraction.** Lee et al. previously proposed amplitude class features. Amp1 was inspired by the findings of Baker's theoretical analysis showing that MAA estimates are dependent on arterial mechanical properties, BP pulse

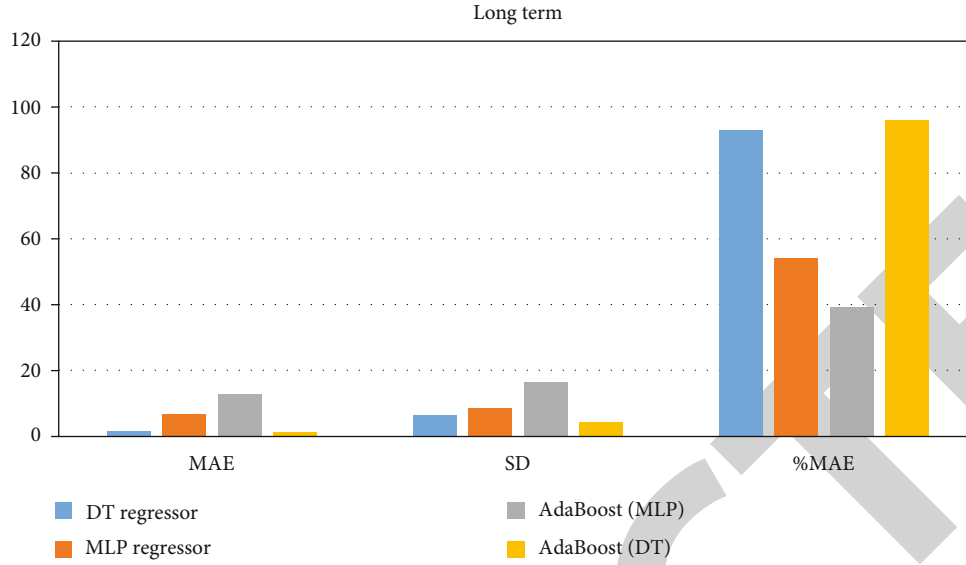


FIGURE 5: Graph between the diastolic long-term blood pressure.

TABLE 1: Performance analysis of systolic term blood pressure prediction.

	DT regressor		MLP regressor		AdaBoost (DT)		AdaBoost (MLP)	
	Short term	Long term	Short term	Long term	Short term	Long term	Short term	Long term
MAE	2.34	2.56	11.29	16.20	1.69	2.07	22.05	19.59
SD	5.42	6.00	12.35	15.51	4.52	5.97	14.85	15.66
%MAE	87	86	36	23	93	91	13.8	17

TABLE 2: Performance analysis of diastolic blood pressure prediction.

	DT regressor		MLP regressor		AdaBoost (MLP)		AdaBoost (DT)	
	Short term	Long term	Short term	Long term	Long term	Long term	Short term	Long term
MAE	1.69	1.55	5.23	6.6	11.01	12.77	1.32	1.15
SD	6.74	6.41	9.12	8.51	13.89	16.38	6.40	4.05
%MAE	94	93	67	54	45	39	97	96

shape, and BP pressure using duration as a basis, and a second set of features was created. Researchers Dur1 and Dur2 were inspired by their previous work, which showed that new relationships between mean cuff pressure and pseudo-envelopes linking the duration of the MA's position to OMWE improved SBP and DBP estimates. Area measurements were used to derive the third category of features.

**4.1.2. Feature Selection.** It is the feature extraction phase's extracted feature that gets sent to the feature selection unit. To map features from one dimension to another, they must first be scalar converted. This helps find features with lots of interdependencies. Multicollinearity features are turned into features with a comparable look in a lower dimension, making it easy to locate and eliminate duplicates. One set of features is used for training and the other for testing after being scalar transformed (30 percent). The data is used to create the training programme, including the training feature set and the training objective data.

## 5. Results

**5.1. Results Based on Feature Analysis.** This section evaluated the performance of machine learning algorithms trained on the training set to estimate continuous blood pressure. Machine learning algorithms are trained and tested on historical data. The predictive model's performance will be evaluated using two metrics: MAE and SD. The result is analysed in two stages:

- (i) *Feature Analysis.* The mean absolute error and standard deviation of the top 80 features' predictions will be examined in this study. Short-term and long-term data will be used for this analysis.
- (ii) *Model Performance Evaluation by Selected Feature.* We will estimate the predictive model's performance based on the chosen feature combination in this study.

The Adobos Regress is used to train and test the short- and long-term data. Figures 4 and 5 show the mean absolute

error for diastolic prediction for the 80 feature combination. The standard deviation variation is calculated using the 80 feature combination. Figures 5 and 4 reveal the following.

- (i) On the other hand, long-term MAE and SD for diastolic prediction are not affected by feature count
- (ii) The MAE and SD for systolic prediction increase with feature count. After a steep initial fall, the MAE and SD for diastolic prediction stay stable with feature count
- (iii) The MAE and SD function best with 10 or more factors in diastolic prediction

Based on the above, we need at least ten features to optimise systolic and diastolic prediction. A selection technique was utilised to prioritise the most critical features, which were then evaluated for systolic and diastolic prediction. The PPG signal's spectral characteristic was ranked 8th out of 20 features. Consider the peak amplitude's maximum and minimum, skewness and kurtosis, frequencies' arithmetic mean, and root mean square. 12 characteristics were obtained from PPG signal and statistical measurements. Standard deviation, variance, maximum, and lowest were all present. The Fourier transform or its derivatives produced no significant selection statistics.

The maximum and minimum PPGs, as well as their first and second derivatives, were the highest and minimum frequencies of the 8 distinctive traits. Our feature set consists of ten features obtained from the PPG signal. This provides us a ten-feature set.

**5.2. Model Performance Evaluation by Selected Feature.** In this section, we will look at the four regression models we created using the ten features we selected. We use metrics like mean absolute error, Tables 1 and 2 variance, and percentage error less than or equal to 5 mmHg to evaluate the work.

## 6. Conclusion

The major goal of this work is to automatically detect motion distortions in BP and PPG signals. The algorithms were tested on a publicly available ICU database, healthy patients, elderly patients, and arrhythmia patients. That is, the Adobos Regress or with decision tree as a foundation outperformed all others in estimating blood pressure values. Based on this research, the suggested model's single signal (PPG) and single probe approach are highly accurate in measuring SBP and DBP. Wearable devices benefit from PPG signal monitoring with a single sensor and probe. This method allows for discreet blood pressure monitoring, which is useful for long-term in-home care. The current study only provided a healthy people BP estimation technique. However, the algorithm's efficacy across patient populations is unknown. Moreover, studies show that estimating BP in obese patients is inaccurate. The PPG algorithm was only tested on five older arrhythmia patients ( $N = 5$ ). Atrial

fibrillation and ventricular arrhythmia (including fibrillation and T-waves) patients have yet to be studied.

## Data Availability

The data used to support the findings of this study are included within the article.

## Disclosure

It was performed as a part of the Employment of Institutions.

## Conflicts of Interest

The authors declare that they have no conflicts of interest regarding the publication of this paper.

## Acknowledgments

We deeply acknowledge Taif University for supporting this study through Taif University Researchers Supporting Project Number (TURSP-2020/344), Taif University, Taif, Saudi Arabia.

## References

- [1] T. Pereira, N. Tran, K. Gadhoumi et al., "Photoplethysmography based atrial fibrillation detection: a review," *NPJ Digital Medicine*, vol. 3, no. 1, pp. 1–12, 2020.
- [2] H. Pandey and S. Prabha, "Smart health monitoring system using IOT and machine learning techniques," in *2020 Sixth International Conference on Bio Signals, Images, and Instrumentation (ICBSII)*, pp. 1–4, Chennai, India, 2020.
- [3] S. Sengan, O. I. Khalaf, G. R. K. Rao, D. K. Sharma, K. Amarendra, and A. A. Hamad, "Security-aware routing on wireless communication for E-health records monitoring using machine learning," *International Journal of Reliable and Quality E-Healthcare*, vol. 11, no. 3, pp. 1–10, 2022.
- [4] W. N. Ismail, M. M. Hassan, H. A. Alsalamah, and G. Fortino, "CNN-based health model for regular health factors analysis in Internet-of-Medical Things environment," *IEEE Access*, vol. 8, pp. 52541–52549, 2020.
- [5] S. Sengan, O. I. Khalaf, S. Priyadarsini, D. K. Sharma, K. Amarendra, and A. A. Hamad, "Smart healthcare security device on medical IoT using Raspberry Pi," *International Journal of Reliable and Quality E-Healthcare*, vol. 11, no. 3, pp. 1–11, 2022.
- [6] F. Piccialli, S. Cuomo, D. Crisci, E. Prezioso, and G. Mei, "A deep learning approach for facility patient attendance prediction based on medical booking data," *Scientific Reports*, vol. 10, no. 1, pp. 1–11, 2020.
- [7] A. Akbari, R. Solis Castilla, R. Jafari, and B. J. Mortazavi, "Using intelligent personal annotations to improve human activity recognition for movements in natural environments," in *IEEE Journal of Biomedical and Health Informatics*, vol. 24, no. 9, pp. 2639–2650, 2020.
- [8] G. Zhang, Z. Guo, Q. Cheng, I. Sanz, and A. A. Hamad, "Multi-level integrated health management model for empty nest elderly people's to strengthen their lives," *Aggression and Violent Behavior*, 2021.

## Research Article

# Applications of Deep Learning on Topographic Images to Improve the Diagnosis for Dynamic Systems and Unconstrained Optimization

Gharbi Alshammari <sup>1</sup>, Abdulsattar Abdullah Hamad <sup>2</sup>, Zeyad M. Abdullah,<sup>3</sup>  
Abdulrhman M. Alshareef <sup>4</sup>, Nawaf Alhebaishi <sup>4</sup>, Abdullah Alshammari <sup>1</sup>  
and Assaye Belay <sup>5</sup>

<sup>1</sup>College of Computer Science and Engineering, Department of Computer Science and Information, University of Ha'il, Saudi Arabia

<sup>2</sup>College of Sciences, Tikrit University, Iraq

<sup>3</sup>College of Computer Science and Mathematics, Department of Mathematics, University of Tikrit, Iraq

<sup>4</sup>Department of Information Systems, Faculty of Computing and Information Technology, King Abdulaziz University, Jeddah, Saudi Arabia

<sup>5</sup>Department of Statistics, Mizan-Tepi University, Ethiopia

Correspondence should be addressed to Assaye Belay; [assaye@mtu.edu.et](mailto:assaye@mtu.edu.et)

Received 8 November 2021; Revised 16 November 2021; Accepted 26 November 2021; Published 7 December 2021

Academic Editor: Shalli Rani

Copyright © 2021 Gharbi Alshammari et al. This is an open access article distributed under the Creative Commons Attribution License, which permits unrestricted use, distribution, and reproduction in any medium, provided the original work is properly cited.

Studies carried out by researchers show that data growth can be exploited in such a way that the use of deep learning algorithms allow predictions with a high level of precision based on the data, which is why the latest studies are focused on the use of convolutional neural networks as the optimal algorithm for image classification. The present research work has focused on making the diagnosis of a disease that affects the cornea called keratoconus through the use of deep learning algorithms to detect patterns that will later be used to carry out preventive detections. The algorithm used to perform the classifications has been convolutional neural networks as well as image preprocessing to remove noise that can limit neural network learning, resulting in more than 1900 classified images out of a total of >2000 images distributed between normal eyes and those with keratoconus, which is equivalent to 92%.

## 1. Introduction

Artificial intelligence (AI) is associated with simulating human reasoning through machines that are programmed to think and imitate their actions, which is associated with learning and problem solving to achieve a specific objective with the best opportunity that presents itself [1]. It is a branch of artificial intelligence that seeks to develop techniques or algorithms, which allow a system or machine to learn patterns from the data provided to predict future behaviour [2]. Machine learning (ML) has two main areas to predict events based on data: supervised learning and unsupervised learning. The basis for each of the previously mentioned areas starts from human intervention, such as

supervised learning, where human intervention can make predictions [3]. In contrast, in unsupervised learning, there is no human intervention for predictions [2, 3]. Deep learning (DL) is a subfield of machine learning that seeks to use algorithms that mimic the brain's functioning, which would allow machines to become intelligent [4]. Shanthi et al. (2021) explain that keratoconus is an atypical disease that affects the cornea, thinning its thickness and deforming it into a cone shape, thus generating a gradual decrease in vision, blurred or distorted vision. The causes of this disease have not yet been identified, so there are several factors. [5–8] indicate that the computerized corneal topographer and video kera to scope have been the most used methods for detecting keratoconus. They also mention the various

treatments to control the progression of this disease and, in extreme cases, eliminate it.

The purpose of this research work is to promote the knowledge of deep learning, which uses artificial neural networks to perform text processing, image, object, and voice recognition; the particularity of the application of these systems is that the algorithm that is used learns by itself, thus simulating the decisions made by human beings, which is why the more data there is, the higher the precision. The main topic of the research work is focused on making diagnoses using deep learning to analyze the images generated by the corneal topographer OPD-Scan III. The main objective of this study is to design and analyze a computer solution through the application of deep learning on topographic images to improve the precision of the diagnosis of keratoconus in the teaching hospital, Baghdad, Iraq. This work is limited to the specialist's availability for data collection because sensitive data will be treated in the research work—the number of images generated by the OPD-Scan III corneal topographer. Deep learning research work related to the health sector is scarce, so it is an emerging technology. Based on the Fundamental Methodology for Data Science, the deep learning application will be developed until the evaluation stage of the proposed model since the implementation analysis will not be carried out in the teaching hospital (BTH), Baghdad, Iraq.

## 2. Materials and Methodology

*2.1. Methodology.* The research work is a quantitative work to study the variables for their subsequent analysis; a correlational scope will be considered because it will analyze how the proposal of “deep learning application on topographic images” (independent variable) will behave on the “precision of the diagnosis of keratoconus” (dependent variable). Similarly, the Fundamental Methodology for Data Science will be used since it will provide strategies to solve data science problems in technology, data, or approaches in an agnostic way [9].

*Paradigm.* The paradigm is positivist. It pursues the rigorous verification of general propositions (hypotheses) through empirical observation and experiment in wide-ranging samples and from a quantitative approach to verify and perfect laws related to education. Its purpose is to verify and control the phenomena.

*Focus.* The focus of the research work is quantitative. It uses data collection to test hypotheses based on the numerical measurement and statistical analysis, to establish behavioural guidelines and test theories.

*2.2. Variables. Independent.* Application of deep learning on topographic images because it is the phenomenon that will condition the result of the dependent variable through actions that will be carried out to comply with what is proposed in the research work.

*Dependent.* Accuracy of the diagnosis of keratoconus because it is the phenomenon that will be affected by the actions of the independent variable.

*2.2.1. Population and Sample. Population.* This research focuses on the number of topographic images that the BTH has, where 456 images were identified, which are distributed in 228 healthy eyes and 228 with keratoconus.

*Sample.* The sample will be intentional since the entire population is needed to obtain better results in the analysis of the images.

*Analysis Unit.* The unit of analysis of the present research work will be the topographic images since the diagnoses of keratoconus will be carried out from them.

*2.2.2. Analysis Method.* Continuing with the use of the Fundamental Methodology for Data Science [10, 11], the modelling stage is where the data sets defined in the previous stage will be used. That is why this research work will propose five designs with different neural network architectures as well as the dimension that each image will have to validate which of them will provide the highest level of precision concerning learning and testing of the neural network, the designs proposed for this research work are the following (Table 1).

### 2.3. Instruments and Techniques

*2.3.1. Instruments.* The instruments are related to the tools that will be used to make the diagnosis of keratoconus; therefore, in this research work, the tools to be used are as follows:

- (i) Keras: it is a high-level neural network library designed under the rapid development approach, where it automatically detects the availability of a GPU and tries to use it; otherwise, it uses the CPU to continue with the correct operation; this library supports both network convolutional and recurrent [4]
- (ii) OpenCV: it is an open-source library that supports real-time computer vision applications and improves the computer's performance concerning its perception of images (OpenCV, s. F.)
- (iii) Python: it is a programming language oriented to object-oriented programming, which allows rapid development of web or server applications due to the simplicity of its syntax (Python, s. F.)
- (iv) Jupyter Notebook: it is an open-source web application that allows you to compile code from different programming languages; within the same work document or book, you can integrate texts, images, or graphics shared by different means (Jupyter Notebook, s. F.)

*2.3.2. Techniques.* In the present investigation, the techniques to be used are associated with the interpretation of the images through the program that will be implemented as well as the generation of more images because the number of images is small, and this may affect the learning of the convolutional neural network, the libraries that will allow applying the aforementioned are the following:



TABLE 1: Results of proposed models.

	Test data	Execution time	Number of layers
Design 1	92.04%	97 minutes	17
Design 2	89.00%	43 minutes	13
Design 3	84.90%	18 minutes	14
Design 4	73.85%	4 minutes	13
Design 5	78.19%	7 minutes	22

- (i) Keras: one of the various functionalities that will be used in this library is the one that allows generating a great variety of images with different filters from an image as a sample, so the size of the sample can be increased substantially
- (ii) OpenCL: it will interpret the images through the pixels and the intensity of each one of them. The pixel values range from 0 to 255, and the channel that presents the image will significantly influence the program

**2.4. Procedures.** Fundamental Methodology for Data Science provides strategies divided into ten stages, adapted from Fundamental Methodology for Data Science [12]. The first step of the methodology is understanding the business, which seeks to define what the problem is and how it can be solved. The next stage is the analytical approach, which seeks to adapt the solution using machine learning techniques. One of the techniques that will be used is convolutional neural networks, which is part of deep learning, part of machine learning, to perform keratoconus detection with a high level of precision and early detection.

The data requirements define what type of data is necessary for the solution, including multimedia files and flat files. The type of data needed for the deep learning solution is images, so the files generated by the OPD-Scan III equipment are needed. The data collection stage is focused on obtaining the necessary data for the algorithm; on the other hand, in the data understanding stage, techniques are used to evaluate the quality of the data, so if errors are found in the data collected, they can return to the previous stage mentioned. In the stages mentioned earlier, a Python program was developed that allows the necessary information to be extracted from what was obtained by the OPD-Scan III equipment since the equipment generated multiple reports in a single file. The files exported from the specialized equipment contain multiple reports, so only those that contain "EY" in the name were considered since within that file are the necessary images. When executing the file extraction, it generates a new folder where the images to be used in the research work will be stored. The next process was to list the cases of healthy eyes and those with keratoconus for another process to be in charge of distributing and classifying images to the respective category. The next stage is that of data preparation, in which it is sought to perform image treatments with the objective that the most valuable sections can be used, as well as the definition of the data set to be used in the modelling stage. In this way, the techniques

mentioned in the previous sections were implemented to generate various cases since the sample is small. Therefore, a process will be carried out to increase the number of images. As a first step, the program must obtain the path of the folder where the images are located since the OpenCV (Figure 1) library needs it to interpret it as a matrix of  $n$  by  $m$ , referring to the width and height, respectively, of the image.

Next, the Keras library was used to increase the data, where a random rotation of 45 degrees was carried out as well as the horizontal rotation of the image. By making use of the data augmentation technique, it generated a significant increase resulting in a total of 6609 images that will be distributed in 3 data sets so that the algorithm can learn correctly, which are as follows:

- (i) Training: set of data that will be used to learn the proposed model
- (ii) Validation: data set that will be used to validate what the model has learned based on the training data set, thus making the model learn to classify incorrectly
- (iii) Tests: data set that will be used to evaluate the performance of the model in order to validate whether it has been classified correctly or not based on the data provided

The distribution of the training and validation categories is part of a single group of data since the number of images they count is too high to make a manual adjustment, so the distribution of 70% and 30%, respectively, has been made. While the test data set is independent, the number of images for each data set to be used in the convolutional neural network is as follows: in this way, by having a more significant number of images to process, a comparison will be made of convolutional neural network designs to measure image classification performance and accuracy. When generating images, the images were preprocessed using the OpenCV library, since it allows applying filters to reduce noise or segments of the image that are not useful, which leads to causing the model not to obtain a good performance; the filters to apply are the following:

- (i) Gaussian blur: this allows you to apply a blur to the image in order to reduce noise so that a later process can continue with the treatment
- (ii) Edge detection: this allows you to identify the edges of the image in order only to treat the most significant parts

The images are processed in their original size since they are subsequently resized according to the input parameter of the designs.

### 3. Results

**3.1. Current Situation.** In the Baghdad Teaching Hospital, Iraq, the specialized equipment OPD-Scan III is used to identify different diseases, one of them being keratoconus

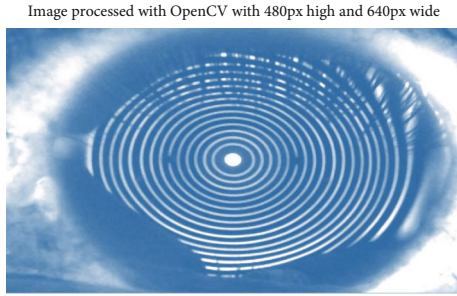


FIGURE 1: Demonstration of image processing using OpenCV.

through the corneal topographer functionality that the team has; the procedure to identify the disease consists of measuring the thickness of the cornea. The main reason why this procedure is chosen is that keratoconus degrades the thickness, so it tends to deform into a cone shape. One of the peculiarities of the OPD-Scan III equipment is that it allows identifying the most significant parts of the rings and regions where deformities occur, resulting in a value expressed as a percentage value that must exceed the minimum threshold of 70% to consider that the eye presents keratoconus.

**3.2. Development of the Proposal.** This research work is aimed at carrying out a correct classification of keratoconus disease that leads to an early detection based on the history of patients who present the disease to carry out treatments in an initial stage. That is why various designs have been proposed executed in Amazon Elastic Compute Cloud (EC2). This platform provides computational resources in the cloud, allowing the implementation to be carried out more efficiently than its computer.

The characteristics acquired in EC2 are sufficient to carry out the processing of the images according to the dimension established for each design in Table 1. Using a GPU instead of a CPU makes a significant difference in terms of learning execution time. Validation and testing of the proposed designs because a GPU allows multiple tasks to be carried out simultaneously. At the same time, a CPU handles the tasks sequentially, and this can generate that a model that runs in 2 hours using a GPU becomes in 20 hours on a CPU. Due to the scalability it offers regarding the construction of the virtual machine that one needs, the characteristics of the acquired virtual machine.

To configure the virtual machine purchased from Amazon EC2, the following components must first be configured:

- (i) *Key Pair.* Component that generates a public key hosted on Amazon Web Service and a private key that will allow communication to the virtual machine through the SSH protocol
- (ii) *Security Group.* Component that allows or denies access to the virtual machine performs the work of a virtual firewall

Once the components have been configured, give read-only permission to the generated private key using the “chmod 400” command.

Only if the private key has read permissions can the SSH connection to the virtual machine be made. The exposure of remote port 8888 through port 8888 of the machine where the connection was made is because the Jupyter Notebook application will be used to compile Python code. The default port the application uses to run is 8888. This is followed by the execution of the “source activate tensorflow\_p36” command, which installs the base configurations provided by Amazon EC2. An outstanding feature of the base installations that were previously made is the use of “tmux,” which is a program that allows multiple virtual sessions through a single terminal, resulting in the ability to activate Jupyter Notebook, view consumption from the GPU, and run Linux-related or Python-related commands. After running the Jupyter Notebook application, a URL is generated with an access code, which allows access to the application that was exposed locally when starting the SSH connection. We proceed to load the file where the Python code will be executed as well as the compressed file that contains the previously generated images. To complete the environment configuration, the following libraries must be installed through the terminal or Jupyter Notebook in order not to generate errors due to dependency failures. On this occasion, Jupyter Notebook was used for the installation, which requests a reboot of the Kernel, which is responsible for executing the codes by the user.

The workflow of this research work can be represented in Figure 2.

Table 1 will present the results obtained from the models when validating the test data as well as the execution time.

Based on the results presented, it is evident that the convolutional neural network algorithm has correctly classified the images due to the adequate use of layers in the design of architecture, thus achieving a result of 92.04% when performing the classification of healthy eyes and those suffering from keratoconus; one of the most significant parts of the results presented is the execution time, which in design 1 is not. It has been affected during the total of defined periods, thus achieving differentiation from the results of the other designs. Regarding the use of the Fundamental Methodology for Data Science, the result obtained refers to the evaluation stage where the test data set is used to validate the performance of the proposed model, in this case being design 1, the one that met the expected approach.

The architecture of design 1 will be presented graphically to visualize the processing through each implemented layer and the size associated with each of them. As can be seen, the decrease in size is carried out progressively when the “maximum grouping” layer is executed, in the same way in the use of the “totally connected layer,” which are in the final part of the architecture since they allow to connect all the neurons and result in a new neuron, where the classification that is being carried out will be indicated. The last layers related to “totally connect” are not shown in Figure 3 because they are in charge of classifying them based on the neurons assigned to them. Understanding how image processing is done will present the result of design 1 with test images.

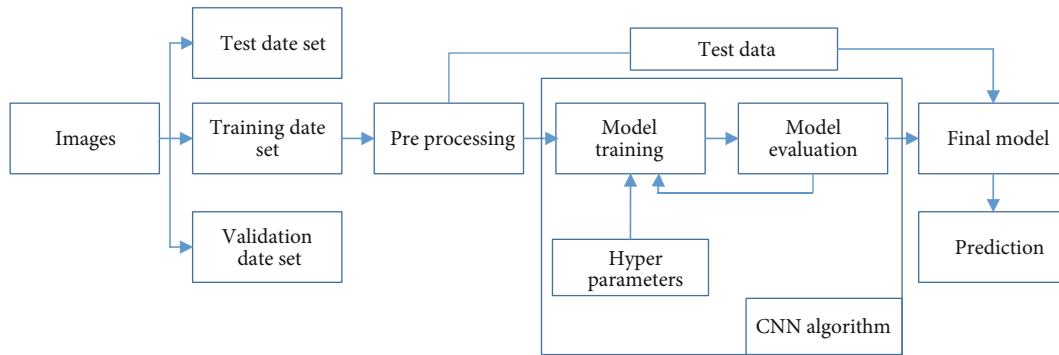


FIGURE 2: Workflow of the proposed designs.

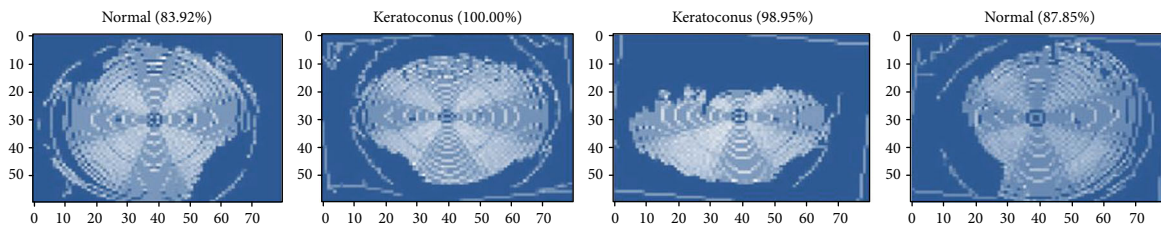


FIGURE 3: Results of predicting the test data.

Design 1 made the correct classification of 1908 images out of a total of 2073; the detail of each number of eyes with keratoconus and normal is detailed in Table 2.

Next, the confusion matrix will be made to evaluate the implemented algorithm (Figure 4).

Based on what is presented in Table 2, the following statements are disclosed:

- (i) Positive + Positive = True Positive (VP)
- (ii) Positive + Negative = False Negative (FN)
- (iii) Negative + Positive = False Positive (FP)
- (iv) Negative + Negative = True Negative (VN)

Knowing the combinations generated by the confusion matrix, the algorithm metrics will be generated:

- (i) Accuracy value here calculated as 92.04% indicates the number of correct classifications made

The value generated in this metric is the same obtained in Table 3.

- (i) The sensitivity value of 90.56% indicates the number of true positives that the algorithm has classified
- (ii) F1 score of 91.29% indicates the overall value obtained for sensitivity and accuracy shown in Figure 4

In relation to the problem presented on the diagnosis of keratoconus applying deep learning, firstly, in conjunction with the expert, healthy eyes and those suffering from kera-

toconus were identified to obtain 100% of cases correctly classified. Subsequently, it seeks to achieve that the evaluations of the proposed solution are carried out. In this way, the established acceptance criteria can be met, which was 90% of cases correctly classified.

The results are presented in Table 2, and the indicators serve as support to reject the general null hypothesis because it is shown that the application of deep learning classifies correctly and with a high level of precision the cases of keratoconus as well as overcome the proposed acceptance criteria threshold.

The last stages of the Fundamental Methodology for Data Science, implementation and feedback, are associated with starting up the production environment and compiling the results obtained from the model to reinforce learning. These two stages have not been contemplated in the present research work; however, it could be implemented in a future work, where you could choose to expose the model through an API to be consumed by web applications or mobile devices with the purpose of that the user can provide comments on whether the classification has been correct or not.

#### 4. Discussion

Implemented has been a convolutional neural network for the classification of X-ray images, stating that the use of this algorithm can perform the classification of images correctly, resulting in acceptable values, but that can be improved if more images were obtained. In the same way, in this present research work, techniques were used to increase the number of images and obtain high values in the classification of the various proposed models; for this reason, I agree with

TABLE 2: Confusion matrix.

	Keratoconus (positive)	Normal (negative)	Total
Keratoconus (positive)	940	98	1038
Normal (negative)	67	968	1035
Total	1007	1066	2073

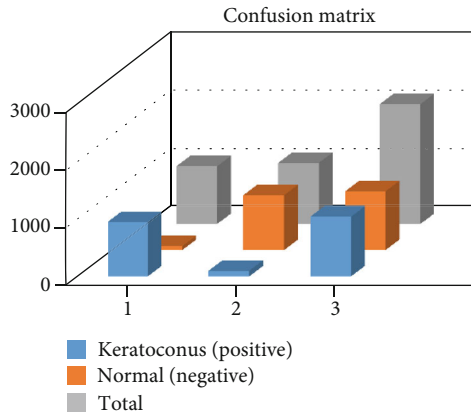


FIGURE 4: Confusion matrix.

TABLE 3: Number of images classified by category.

Category	Images classified correctly	Total images
Normal	968	1035
Keratoconus	940	1038

Thivagar et al. [12] if a large number of images are necessary to process in the world.

In the research work by Kuo et al. [1], it is indicated that the learning transfer method is used to perform a pretraining of the neural network, which leads to better results and also the use of hyperparameters that can improve neural network performance, based on the results obtained in this research [1, 13–17] on the use of hyperparameters that allow the algorithm to make the necessary adjustments to improve performance and even precision.

Accardo and Pensiero [16] explain that the proper use of filters can improve the neural network’s performance during the training phase since there is a case of suffering from overfitting or overfitting, which limits learning and can generate results with a value low. I agree with Accardo’s correct use of filters in a neural network since it can limit learning. In the present research work, the dropout layer was used to avoid overfitting during training learning.

According to Cao et al. [17], who performed image classification tests using various algorithms to validate performance, one of them being the  $K$ -nearest neighbor algorithm applied to computed tomography scans, resulting in low precision and handwritten digits, where a high percentage was obtained; based on this, Seeböck emphasizes the proper use of the algorithms as well as the hyperpara-

eters to be used. For this reason, in the present research work, a comparative analysis of the algorithms was carried out to choose the one that best suited the need to classify images, which is why Seeböck is in agreement with what was indicated.

## 5. Conclusions

The proposed objectives, as well as the results obtained, allowed us to reach the following conclusions:

- (i) The use of convolutional neural networks allowed validating the correct classification of eyes that present keratoconus, which can be seen in Table 2, where 940 of 1038 images have been correctly classified. In this way, it can be concluded that the diagnosis of keratoconus using deep learning or deep learning has been satisfactory, managing to comply with what is proposed in the present research work
- (ii) Based on the research works presented in the theoretical framework as well as in state of the art, it can be concluded that the preferred algorithm to perform a classification of images is that of convolutional neural networks; in the same way, in the present research work, it was carried out a comparative analysis of the algorithms to be used, resulting in the application of the convolutional neural network algorithm
- (iii) It is concluded that the designs presented in the research work have generated mixed results, of which design one was built taking into account the mitigation of overfitting as well as a correct preprocessing that allowed the algorithm to continue learning without being stopped during the defined times
- (iv) Based on the results obtained, it has been shown that the execution time of design 1 presents a longer time compared to the other designs since the learning process has not stopped by maintaining constant improvement in the value of the activation function of the validation data set

## Data Availability

The data underlying the results presented in the study are available within the manuscript.

## Conflicts of Interest

The authors declare that they have no conflicts of interest regarding the publication of this paper.

## References

- [1] B.-I. Kuo, W.-Y. Chang, T.-S. Liao et al., “Keratoconus screening based on deep learning approach of corneal topography,” *Translational Vision Science & Technology*, vol. 9, no. 2, p. 53, 2020.

- [2] S. Shanthi, L. Aruljyothi, M. Balasundaram, A. Janakiraman, K. Nirmaladevi, and M. Pyingkodi, "Artificial intelligence applications in different imaging modalities for corneal topography," *Survey of Ophthalmology*, vol. 6, no. 4, 2021.
- [3] A. A. Hamad, A. S. Al-Obeidi, E. H. Al-Taiy, and D. Le, "Synchronization phenomena investigation of a new nonlinear dynamical system 4d by Gardano's and Lyapunov's methods," *Computers, Materials & Continua*, vol. 66, no. 3, pp. 3311–3327, 2021.
- [4] K. Kamiya, Y. Ayatsuka, Y. Kato et al., "Keratoconus detection using deep learning of colour-coded maps with anterior segment optical coherence tomography: a diagnostic accuracy study," *BMJ Open*, vol. 9, article E031313, 2019.
- [5] A. Al-Timemy, N. Hussein, Z. Musa, and J. Escudero, "Deep transfer learning for improved detection of keratoconus using corneal topographic maps," *Cognitive Computation*, vol. 13, no. 4, 2021.
- [6] J. Vazirani and S. Basu, "Keratoconus: current perspectives," *Clinical Ophthalmology*, vol. 7, pp. 2019–2030, 2013.
- [7] M. Souza, F. Medeiros, D. Souza, R. Garcia, and M. Alves, "Evaluation of machine learning classifiers in keratoconus detection from orbscan II examinations," *Clinics*, vol. 65, pp. 1223–1228, 2010.
- [8] G. Zhang, Z. Guo, Q. Cheng, I. Sanz, and A. A. Hamad, "Multi-level integrated health management model for empty nest elderly people's to strengthen their lives," *Aggression and Violent Behavior*, vol. 13, article 101542, 2021.
- [9] S. Shanthi, K. Nirmaladevi, M. Pyingkodi, K. Dharanesh, T. Gowthaman, and B. Harsavardan, "Machine learning approach for detection of keratoconus," *IOP Conference Series: Materials Science and Engineering*, vol. 1055, article 012112, 2021.
- [10] A. Lavric and P. Valentin, "KeratoDetect: keratoconus detection algorithm using convolutional neural networks," *Computational Intelligence and Neuroscience*, vol. 2019, Article ID 8162567, 2019.9 pages, 2019.
- [11] S. R. Gandhi, J. Satani, K. Bhuvu, and P. Patadiya, "Evaluation of deep learning networks for keratoconus detection using corneal topographic images," in *International Conference on Computer Vision and Image Processing*, Singapore, 2021.
- [12] L. M. Thivagar, A. A. Hamad, and S. G. Ahmed, "Conforming dynamics in the metric spaces," *Journal of Information Science and Engineering*, vol. 36, no. 2, pp. 279–291, 2020.
- [13] M. Tahvildari, R. Singh, and H. Saeed, "Application of artificial intelligence in the diagnosis and management of corneal diseases," *Seminars in Ophthalmology*, vol. 36, 2021.
- [14] J. B. Rollins, *IBM, Fundamental Methodology for Data Science*, 2015, <https://ibm.co/2V1fLER>.
- [15] M. Sorić, D. Pongrac, and I. Inza, "Using convolutional neural network for chest X-ray image classification," in *2020 43rd International Convention on Information, Communication and Electronic Technology (MIPRO)*, pp. 1771–1776, Opatija, Croatia, 2020.
- [16] P. Agostino Accardo and S. Pensiero, "Neural network-based system for early keratoconus detection from corneal topography," *Journal of Biomedical Informatics*, vol. 35, no. 3, pp. 151–159, 2002.
- [17] K. Cao, K. Verspoor, S. Sahebjada, and P. Baird, "Evaluating the performance of various machine learning algorithms to detect subclinical keratoconus," *Translational Vision Science & Technology*, vol. 9, no. 2, p. 24, 2020.

## Research Article

# Named Data Networking-Based On-Demand Secure Vehicle-To-Vehicle Communications

Qudsia Saleem <sup>1</sup>, Ikram Ud Din <sup>1</sup>, Ahmad Almogren <sup>2</sup>, Ibrahim Alkhalifa <sup>2</sup>,  
Hasan Ali Khattak <sup>3</sup> and Joel J. P. C. Rodrigues <sup>4,5</sup>

<sup>1</sup>Department of Information Technology, The University of Haripur, Pakistan

<sup>2</sup>Chair of Cyber Security, Department of Computer Science, College of Computer and Information Sciences, King Saud University, Riyadh 11633, Saudi Arabia

<sup>3</sup>School of Electrical Engineering and Computer Science, National University of Sciences and Technology, Islamabad, Pakistan

<sup>4</sup>Senac Faculty of Ceará, 60160-194 Fortaleza CE, Brazil

<sup>5</sup>Instituto de Telecomunicações, Portugal

Correspondence should be addressed to Ikram Ud Din; ikramuddin205@yahoo.com, Ahmad Almogren; ahalmogren@ksu.edu.sa, and Hasan Ali Khattak; hasan.alikhattak@seecs.edu.pk

Received 16 September 2021; Revised 22 October 2021; Accepted 30 October 2021; Published 26 November 2021

Academic Editor: Shalli Rani

Copyright © 2021 Qudsia Saleem et al. This is an open access article distributed under the Creative Commons Attribution License, which permits unrestricted use, distribution, and reproduction in any medium, provided the original work is properly cited.

The detection of secure vehicles for content placement in vehicle to vehicle (V2V) communications makes a challenging situation for a well-organized dynamic nature of vehicular ad hoc networks (VANET). With the increase in the demand of efficient and adoptable content delivery, information-centric networking (ICN) can be a promising solution for the future needs of the network. ICN provides a direct retrieval of content through its unique name, which is independent of locations. It also performs better in content retrieval with its in-network caching and named-based routing capabilities. Since vehicles are mobile devices, it is very crucial to select a caching node, which is secure and reliable. The security of data is quite important in the vehicular named data networking (VNDN) environment due to its vital importance in saving the life of drivers and pedestrians. To overcome the issue of security and reduce network load in addition to detect a malicious activity, we define a blockchain-based distributive trust model to achieve security, trust, and privacy of the communicating entities in VNDN, named secure vehicle communication caching (SVC-caching) mechanism for the placement of on-demand data. The proposed trust management mechanism is decentralized in nature, which is used to select a trustworthy node for cluster-based V2V communications in the VNDN environment. The SVC-caching strategy is simulated in the NS-2 simulator. The results are evaluated based on one-hop count, delivery ratio, cache hit ratio, and malicious node detection. The results demonstrate that the proposed technique improves the performance based on the selected parameters.

## 1. Introduction

Transmissions nowadays become necessary among devices, communication servers, and more specifically among vehicles [1]. Vehicle communication leads us towards the new type of network called vehicular ad hoc network (VANET). VANET is a special type of network in which one vehicle communicates with other vehicles and roadside communications towers. This network contains two types of nodes, i.e., roadside units (RSU) and on-board units (OBU). Vehicles are moving objects, and the installed equipment is fixed

on roadsides [2]. Communications in VANETs take place in three categories, i.e., vehicle-to-roadside infrastructure (V2I), vehicle-to-vehicle (V2V), and infrastructure-to-infrastructure (I2I) communications. The communication is possible through the installed wireless communications infrastructures. Multiple RSUs are installed on roadsides, which may effectively provide access to content inside vehicular communications infrastructures. A single base station (BS) that controls the entire communications is possible inside and outside the communication infrastructure. The infrastructure-based communication is only possible when

everything is in the control of RSU and BS. The proposed framework only considers communications between vehicles, i.e., V2V communications. The basic concept is to provide communications among vehicles in a secure communication environment. VANET enhances road safety, reduces traffic congestion, and controls traffic information sharing. In addition to all this information, VANET can provide weather information and multimedia content.

Traditional IP-based VANET communications make the quality of service (QoS) task more complex on the provision of the services. On the other hand, VANET can provide benefits in terms of safety applications. Information-centric networking (ICN) converts content requests from host-centric networking to content-centric networking [3], where all requests are handled based on the content names rather than communication channels. The proposed framework uses content-based instead of IP-based communications, which make the system more secure for infrastructure-based communications. Various architectures have been proposed, where named data networking (NDN) has gained higher popularity due to its most effective communication features in terms of security [4], reliability, and efficiency [2]. Typically, NDN contains three data structures, i.e., forward information base (FIB), pending interest table (PIT), and content store (CS) [5].

This research was conducted based on VNDN secure communications among vehicles. Content is stored on selected vehicles that can handle requests of other vehicles inside the communication range. The CS caches content coming from RSUs without any security policy. The PIT stores the incoming interfaces and pending requests from vehicles. Another responsibility of the PIT is to create back link paths from one hop to another inside the request tables. Finally, the FIB maps the content with the attached prefixes to arrange content requests of the vehicles. Figure 1 shows the data exchange in the ICN-based VANET communications. The NDN routers are fixed, whereas in the VNDN, the routers are vehicles with high mobility [5, 6]. Since there is no mobility support in NDN, it results in a frequent data retrieval failure [7].

The cluster-based network architecture can enhance the network performance by reducing the number of vehicles involved in the forwarding. Thus, it enhances network stability [6, 8]. However, the selection of clusters and cluster head (CH) in VANETs is challenging due to trust management issues. In the highly dynamic nature of VANETs, the selection of CH is a critical issue. The problem found in this approach is the detection of compromised requests coming from malicious nodes. Besides, some malicious vehicles transfer wrong information, compromise the VANET trustable environment, and alter the messages broadcast in the V2V environment, which can cause serious traffic accidents and some other critical issues in the VNDN. To improve the security in VANETs, several schemes have been proposed in the literature. However, these techniques are not sure to provide the current V2V security in the on-demand environment. Since users in the vehicular environment do not know each other, there should be a mechanism that can provide trust and secure communications among the partic-

ipating vehicles to avoid miss behaviors. Here, centralized trust management does not provide better solution due to communication delay [9]. Therefore, a distributed trust mechanism is needed for secure VANET communications.

In the proposed solution, the blockchain mechanism is used for secure V2V communications. The SVC-caching strategy has been introduced to cache content in the VNDN environment. The SVC-caching provides a secure placement of NDN content on vehicles after the selection of a CH. The content may be traffic information and popular data with a high dynamic nature. The proposed strategy is aimed at providing a secure environment for the selection of the cache node and content placement. The SVC-caching can also detect malicious requests received from infected vehicles. The main contributions of this study are listed below:

- (1) proposes a novel strategy for blockchain-based trustable V2V communications in a highly dynamic vehicular environment
- (2) selects cluster nodes and CH using a customized  $K$ -Means dynamic clustering algorithm
- (3) presents a strategy to place content using an NDN approach for intervehicle communications in clusters
- (4) provides secure V2V communications for reliable and stable content placement, where vehicles request entertainment better than other VANET caching placement strategies

The rest of the paper is organized as follows. Section 2 reviews the previous researches. Section 3 presents the proposed SVC-caching strategy, clustering transformation, and a secure placement of NDN content. Research evaluation and discussion on results are presented in Section 4. The presentation of the feasibility of the SVC-caching and its contributions are presented in Section 5. At last, the conclusion and future directions are presented in Section 6.

## 2. Literature Review

Various strategies have been proposed by the research community for solving security issues in content caching and sharing [10, 11]. Each strategy has its own advantages and limitations. The existing techniques designed for caching and security of data in the VANET environment are discussed here in detail.

In [5], the idea of ICN was proposed wherein the leave copy everywhere (LCE) was supposed to be deployed. LCE is a reactive caching strategy that cache content on all on-path nodes lies between the publisher and subscribers. The beauty of this strategy is such that if a content is accessed once, its copy would be available for all future requests. Therefore, the content delay is reduced, and the cache hit ratio is increased. However, the availability of content on all nodes increases redundancy, which may fill the node cache soon, and the new arriving content would not have space to be stored. In the remaining of the paper, LCE will be referred to as *reactive caching*.

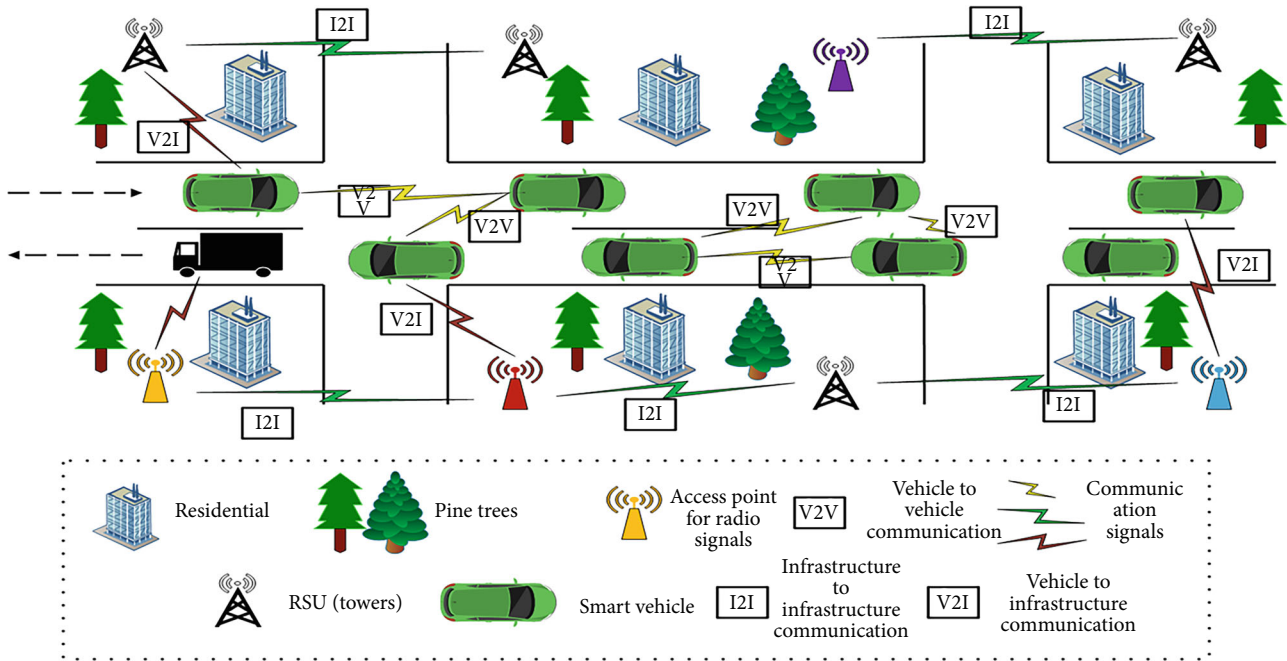


FIGURE 1: Communications in the VANET environment.

In [12], the authors identify that the current host-centric vehicular model does not support the new device registration and handling capabilities in a large number. Their scheme, named PeRCeIVE, is proposed for mobile node delivery problems. PeRCeIVE is a proactive caching approach for data placement at right network elements. A hierarchical namespace is used to name the address for each chunk of the data packet. The first algorithm calculates the chunk lists for requested data, and the second one examines the chunk distribution. The simulation results show that the PeRCeIVE approach improves the one-hop ratio and resolves interest ratios in a limited/average number of cached copies inside the network with a comparable threshold. However, this approach seems to be unsuitable for large cache sizes because it is better for a limited number of content cached in a node's cache.

In [13], a content name-based addressing mechanism, named neighbor cache explore routing based on trajectory prediction (PNCE), is proposed that works efficiently in a dynamic VANET environment. Due to dynamic and weak network connections among vehicles, it is important to adopt a routing protocol for message broadcasting in an emergency situation. With the use of an in-centering cache strategy, the proposed mechanism works well for reducing redundant packet traffic and choosing an optimal path for forwarding information. The PNCE claims to improve the round-trip delivery ratio. However, periodically broadcasting beacon messages may cause packet congestion in a network.

With the intention of settling in to VANET scenarios, a few routing protocols are determined by geographical locations in the VND environment. For instance, name/ID-based routing protocol (we will call it IR protocol throughout the article) [14] judges the next hop by measuring the path between the publisher and subscribers. The main

theme is to get to the destination with a minimum number of hops. Nevertheless, the IR protocol seems to be imprecise because of the mobility option. Moreover, IR may not be deployed in the VNDN since it does not support the in-network caching capabilities in addition to caching unnecessary content on the path [13].

In [15], the authors proposed a group leader and group members' strategy for secure V2V communications. In the proposed methodology, a secure connection is established between the group leader and member vehicles in a network by broadcasting asymmetric keys to all member vehicles, whereas the message is encrypted with a symmetric key. To manage overlapping vehicles in a network, the authors proposed a multihop communication mechanism. Moreover, for the authentication of vehicles, the group-based hybrid model is utilized and malicious vehicles are detected by comparing the trust score to a threshold value. Based on the network of vehicles, the paper also discusses the revocation process, which reduces the certificate revocation list (CRL) size and increases the network performance. For evaluation, the scheme combines direct trust calculation and feedback from neighbor vehicles. The proposed mechanism achieves successful results for trust management. However, there are maximum chances of content retrieval delay because of encryption and decryption of keys at each node.

Security credential management system (SCMS) is presented in [16]. This system is in the transition phase and develops a dynamic identifier (ID) virtualization method. Moreover, the method makes difficult for attackers to generate valid messages in addition to preventing controller area network (CAN) logs from being analyzed. In [17], a secure caching mechanism is proposed for VNDN wherein the reputation of nodes is calculated using a blockchain mechanism to achieve privacy and security. In the NDN environment,



each node serves as a cache store, forwarder, and consumer of the data at the same time. Therefore, there should be a mechanism that can protect the cache content in the VNDN, which is based on three roles, i.e., forwarder, consumer, and content store. The authors propose the reputation-based trust mechanism to calculate the trustworthiness of the cache store in order to make the communications secure and reliable. This is achieved by taking the experience of consumers to give the reputation value to the content store, i.e., intermediate node on data consumption that provides the requested content. The requested content is stored in the blockchain network based on the validation of the content by consumers. The reputation of each content is updated after validating it from the blockchain. The same mechanism will be followed for the content that will be received by consumers. If the reputation is greater than the threshold value, then the data will be consumed. In case of false data received, the consumer will issue a new interest for the same content. The consumer will create a new block to send the reputation value to the blockchain network. The results are compared with the normal NDN approach, which shows that the proposed mechanism stores zero nontrusted content irrespective of the caching policy. However, due to generation of new requests for the same content in the case of false data received, the redundancy is increased.

A blockchain-based IoT system is developed in [18, 19] wherein IoT nodes store the private key, whereas the Ethereum public keys are stored to perform data provenance in the IoT network. Many algorithms are presented for IoT ecosystems, which can be studied in [20, 21]. However, there are only few solely blockchain-based algorithms. The authors in [22] deliberate the challenges related to electric vehicles (EVs) and present a registration and authorization mechanism for various scenarios. The presented model is a decentralized security model, which is smart contract and lightning network in the blockchain ecosystem.

In [23], the authors propose a solution for secure message dissemination in VANET using blockchain technology. In addition, the authors assume that the vehicle is a full node having the capabilities to mine new blocks and the normal node helps in the message verification and forwarding process. The RSUs and vehicles use asymmetric keys and digital signature technology for the validation and verification process. The miner will be able to mine the block if it solves the proof-of-work puzzle and gets a nonce value, which is generated periodically according to the difficulty target of the vehicle. The authors check the validity of critical messages through blockchain, which are not encrypted and have local region of interest (ROI). The validity of the message is verified by at least 15 vehicles on the basis of proof-of-location. The mining vehicle will validate the message and calculate the new trust value of the vehicle's broadcasting message. The location certificate is issued by RSU with a time stamp, which makes the verification process more trustworthy [24]. The session ID will be assigned to the vehicle. The vehicle will send back its session ID signed with a digital signature. If the vehicle response is less than the threshold time, then, the certificate will be issued to the vehicle; otherwise, it may be rejected. The proof-of-location check will prevent

the denial-of-service, spamming, or other hassle attacks. The simulation shows that the proposed solution works well for trusted emergency message dissemination in the VANET environment. However, several certificates may be rejected if the vehicle response is less than the threshold time.

In [13], on the basis of cache and geographical parameters, a mechanism, named neighbor cache explore routing based on trajectory prediction (PNCE), is proposed. Vehicles are categorized as providers, containing the actual content of data, and consumer vehicles that request the data. Moreover, the packets are divided into three categories, namely, beacon packets, interest packets, and data packets. A forwarding model that contains four components, i.e., CS, FIB, neighbor table (NT), and neighbor cache table (NCT), is proposed. The actual content is stored in the CS, whereas the FIB table contains the record of the reverse path and each entry has three associated fields, i.e., node ID, next hop ID, and timestamp. Geographical location's information is cached in the NT, and neighbor's cached content is stored in the NCT. Moreover, the NT is updated on the basis of timestamp and NCT is updated on the basis of content cached in neighbor's node. To access information from an unknown destination for the first time, the interest packets are broadcast until the provider sends the requested data to consumers. Each vehicle upon receiving the interest packet either delivers the requested data or calculates the next hop in the network, whereas the FIB table is utilized to finding the closest source by using the distance prediction method. With the use of an in-centering cache strategy, the proposed mechanism works efficiently for reducing redundant packet traffic and choosing an optimal path for forwarding information. However, the response latency may increase because of the interest packet broadcast in the network until the consumer receives the data sent by the publisher.

In [25], a cluster-based cooperative caching approach is introduced with the prediction mechanism of the mobility of vehicles in VNDN. The proposed clustering algorithm groups similar mobility pattern vehicles within the same cluster through a prediction technique. After grouping, the cooperative caching technique based on intercluster and intraclustering communications for clusters is applied. Furthermore, the most popular caching data and least popular caching data are handled separately based on the frequency of access rates. At the end, multiple cache placement and cache transmission schemes are proposed for VNDN. The proposed strategy has the advantage of enhancing cache and network performance for communications. However, the performance degrades for different types of vehicles and large cache sizes. In [26], a secure trust model for autonomous vehicles is proposed for the authentication of information and protection of vehicle tracking in VNDN. The proposed model contains four entities, i.e., autonomous vehicle organization, manufacturer, vehicle, and data. A hierarchical naming for the key generation process is adopted. The manufacturer assigns a unique vehicular ID to all vehicles when manufactured. The trust anchor in this approach is the autonomous vehicle authority who validates the data by a unique ID assigned to the manufacturer. The technique stops false data dissemination in the network.

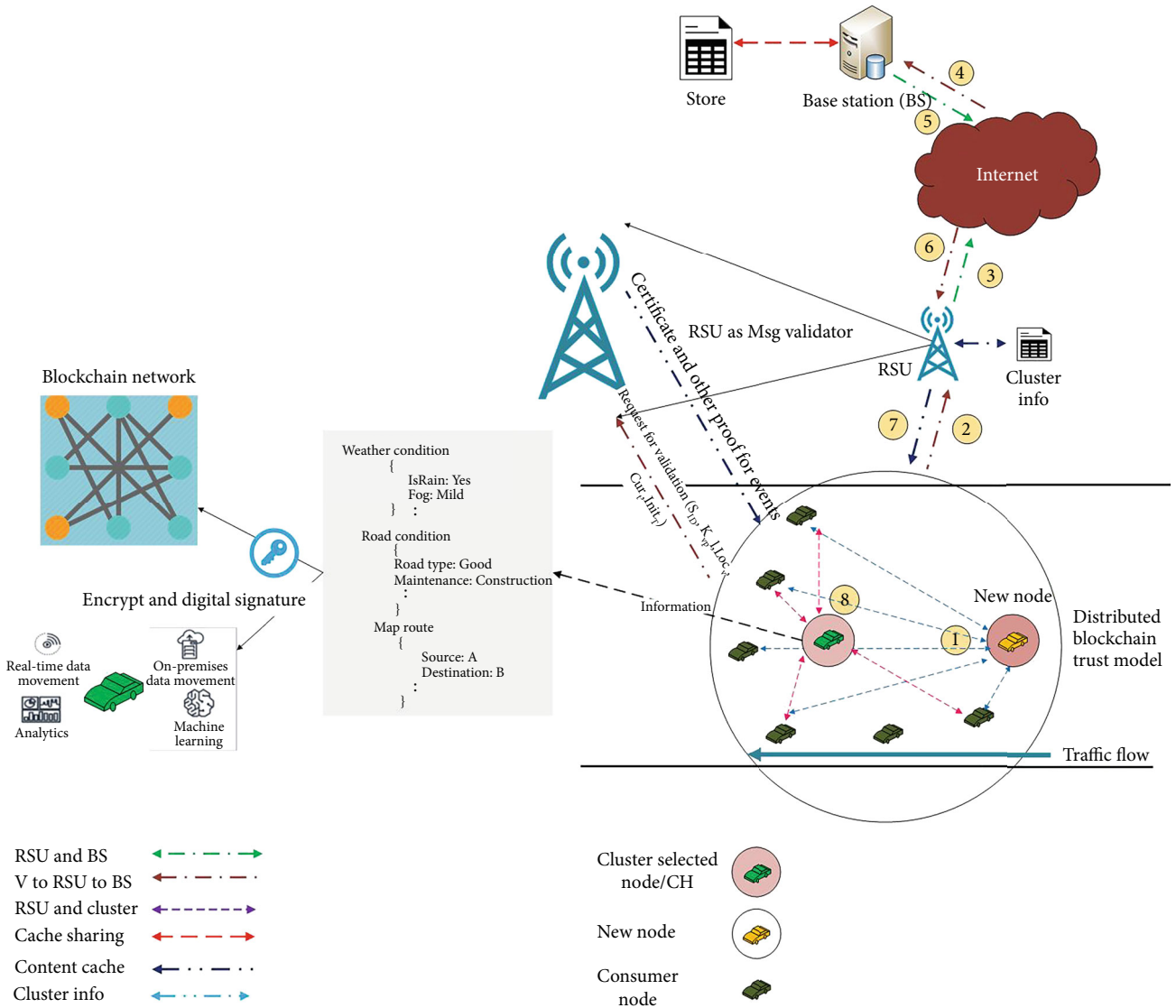


FIGURE 2: Architecture of the blockchain-based V2X.

```

Steps:
1. Start
2.  $V_{PreviousT} \leftarrow V_{NDNB}$ 
3.
if ( $RSU_{POL} \leftarrow issue()$ ) then
     $V_{RSU_{SessID}} \leftarrow TRUE$ 
     $T_{V_{res}} \leftarrow Threshold$ 
    add-message()
  else
    reject-message()
4. End

```

ALGORITHM 1: Message verification policy (MVP) adopted by each normal node.

The second contribution is the protection of vehicle tracking, which is achieved by introducing a pseudonym instead of the vehicle ID, which is used in the certification process and hides the actual identity of the vehicle. However, this

approach may increase content retrieval delay due to checking the certificates for several times for the content validity.

In [27], a mechanism is proposed to detect various kinds of attacks and the attack table is updated to record the

```

Steps:
1. Start
2. Nonce-value-check()  $\leftarrow$  Bi
3.  $N \leftarrow (H(M_i) \| H(B_i - 1) \| N)$ 
4. check-trust()  $\leftarrow$  (check(LOC)
&& check-time()) &&  $M_{IDsg}$ )
5. check( $N < D_t$ )
6.
if ( $M_{VNDN} \leftarrow$  check-trust()) then
    if (check( $M_{IDsg}, V_{info}$ )  $M_{IDsg}$ )
         $B_{new_i} V_{currentTrust}$ 
        update TL  $\leftarrow V_{currentT} + V_{previousT}$ 
        m= True Message ++
        n= False Message ++
         $V_{currenttrust} ++ \leftarrow V_{m+n/mtrust}$ 
        update TL  $\leftarrow V_{currentT} + V_{previousT}$ 
7. add-new()  $\leftarrow B_{new_i}$ 
8. End

```

ALGORITHM 2: Policy for the message verification of minor nodes and proof-of-work (Pow) consensus.

```

Steps:
1. Start
2. RSU  $\leftarrow$  send-Msg(VPK)
3. VNDN  $\leftarrow$  send(RSU, sessionID)
4. RSU  $\leftarrow$  send-signedID(VNDN, sessionID)
5. SessionID  $\leftarrow$  check(VPK, Vthreshold)
6.
if (time < threshold) then
    LOC  $\leftarrow$  publish-LOC (LOC, time, VPK, RSUpK)
    else
        !published()
7. End

```

ALGORITHM 3: Proof of location certification issued by RSU.

abnormal requests. By this way, the unnecessary filling of cache can be prohibited. To meet the challenges of unnecessary filling of cache, the detection and defense cache pollution based on clustering (DDCPC) is proposed for NDN. The DDCPC uses three algorithms to calculate the total number of requests, compute the Euclidean distance between all data points, and detect CPAs. The simulation results prove that this is better caching approach in ICN to avoid filling storage and CPAs. In order to track the target, i.e., suspicious vehicle, the authors in [28] proposed a strategy based on pertinence zone having a maximum probability of the presence of the target. The proposed mechanism is divided into two phases, namely, the discovery phase—involving tracking request broadcast, informing entering vehicles about the target, etc., and the tracking phase—involving the detection of target and forwarding reply packets to RSUs. Moreover, for continuous monitoring tracking target, the authors proposed the concept of virtual RSU in the region where real RSU is missing. Virtual RSU is selected on the basis of partitioning of the infrastructure-less region into

different clustering zones. Each intermediate vehicle cooperates in tracking a target by broadcasting a message containing detailed information about the target. The vehicle closer to the target acts as virtual RSU for forwarding reply packets to the real RSU. The network architecture is divided into different zones having starting and arrival points. For initiating a tracking process, the central server is a node that acts as an intermediate point between the participating vehicles and an authoritative entity. The proposed strategy has shown an effective way to solve security issues, but the response time is decreased because of checking the content in different tracking zones.

In [29], the authors have proposed a strategy, named blockchain-based anonymous reputation system (BARS), which describes its function, i.e., blockchain, certificate transparency, and components while making assumptions. During system initialization, each vehicle submits its private information including a public key and other legal identification information to law enforcement authority (LEA), which passes the signed warrant to the certificate authority

```

Steps:
1. Start
2.
if ( $T_v < 0.5$ ) then  $\&\& (PRR < threshold) \&\& (V < threshold)$  cluster-member(VNDN)
3.
if (TRUE) then
cluster-member()  $\leftarrow$  Cn
 $V_{PID} \leftarrow$  allocate( $V_{pk}, V_{prk}$ )
else
!cluster-member()  $\leftarrow$  Cn
 $M_{NTrust} ++$  //Malicious node
4.
if  $CH_j > V_{PID}$  then
CH  $\leftarrow$  trustable()
CHj++
broadcast(RSU, BS)
RSU  $\leftarrow$  save-info()
6. broadcast()
7. End
    
```

ALGORITHM 4: Trust evaluation for cluster head (CH) selection.

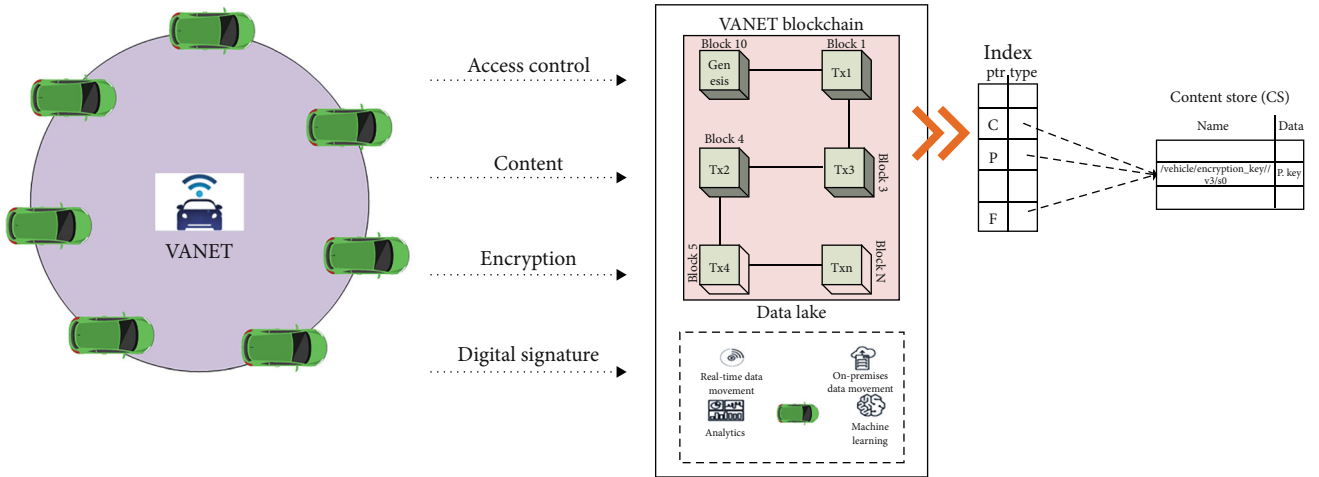


FIGURE 3: CS for vehicular identification and VANET information retrieval.

(CA) and the CA issues an initial certificate to the vehicle. On the other hand, the LEA receives certificate updating requests from vehicles in one of the three cases, i.e., certificate expiry, threat to private key, or replacement of public key. Next, the updated public key is inserted into revocation blockchain (RevBC) after the verification of RSU based on information broadcast by the CA and LEA during public key revocation. However, the authentication process is used for checking certificate expiry and finding proof of present or proof of absence of a vehicle by matching the root hash value and blockchain for certificate (CerBC) records. This technique provides content security with the expense of content retrieval delay.

### 3. Proposed Methodology

In this section, different elements of the proposed mechanism for providing security to content based on blockchain

```

Steps:
1. Start
2. CH  $\leftarrow$  Algorithm 4
3.  $V_{CacheFinal} \leftarrow V_{NewTrust}$ 
4.
if ( $V_{contentFinal} \geq CH_{CS}$ ) then
eviction-policy()
else
accommodate()
5. End
    
```

ALGORITHM 5: Cache content on cluster head (CH).

is discussed. The proposed technique provides the mechanism for secure V2V communications through blockchain equipped vehicles in VANETs. We define the *K*-Mean

```

Steps:
1. Interest(CH←Cn)
2. Cn←CHData
3.
if ( $P_{SignPK} = CH_{PKData}$ ) then
  Cn←consume()
  else
  discard()
  new-interest()
4. Stop

```

ALGORITHM 6: Placement of on-demand data for cluster members ( $C_n$ ).

cluster head-based minor node selection with push-based and on-demand content placement strategies in the VNDN environment [30]. The SVC-caching strategy provides complete V2V communications in the NDN environment. The proposed approach focuses on the detection of malicious node's intranode trust evaluation policy.

Initially, the vehicle needs to join VNDN by sending vehicle identification (Vid), vehicle public key (Vpk), vehicle private key (Vprk), electronic licence (EL), and trust level (TL).

All the upcoming nodes provide the significance of data and content placement for the vehicle identification authority (BS). Inside the VNDN environment, the vehicles continuously change their positions and the RSU is responsible for tracking the vehicles' location. Due to this, all the above information is stored through RSUs.

The RSU sends data to the BS, which generates the mapping log assigns the Pseudo ID (Pid) and the public and private keys to the Vid. The mapping between the real identity of the vehicle and the Vid was stored in the BS cache [31] for future references in case of a dispute. The TL of the vehicle is set to 0.5. Figure 2 shows the joining of new vehicle and validation process through RSUs. An RSU acts as a validator and provides the validation after the request issued by the vehicle with SID, Kvp1, Locv, CurT, and InitT. The architecture of the proposed strategy is described as follows:

- (i) A distributed blockchain trust model is used to add the trustable blockchain in VNDN
- (ii) The public key cryptography is used in to provide security for both data and trust evaluation mechanism through blockchain. The emergency messages are kept unencrypted, whereas the infotainment-related messages are encrypted [32]
- (iii) At the initial joining, the vehicle normal and minor node selection policy is implemented through a consensus technique, as presented in Algorithms 1, IV-A, and IV-A
- (iv) The RSU receives the required VID
- (v) The RSU initially checks the joined vehicle's pre-stored values through vehicle identification VID, vehicle public key and private Key (Vpk, Vprk), EL, CID, and TL

- (vi) The BS checks the vehicle identification through a distributed network of VNDN environment and provides a secure message delivery through blockchain
- (vii) The RSU also works as a message validator for vehicular nodes (see Algorithm 4.1)
- (viii) The RSU issues a proof of location certificate after initial consensus from the vehicular identification and vehicular nodes message validations
- (ix) Figure 3 defines the CS Cardenas, an NDN-based secure validation scheme for on-demand content storage (see Algorithm 4-3)
- (x) On-demand/infotainment message data requirements inside VNDN are added inside the blockchain on minor nodes and vehicle public and private keys (Vpk, Vprk), which are shared among the VNDN trusted node on-demand
- (xi) The Vprk is kept private, and Vpk is shared among all other trustable nodes
- (xii) After the final selection of the nodes to become part of VNDN, the content placement is identified [Algorithm 6]

Furthermore, different components involved in the proposed mechanism are discussed in the following subsections.

**3.1. Base Station.** The BS is a fixed entity in the VNDN environment that maintains the RSUs of a certain area and provides the vehicles' required content. It is responsible for the provision of the keys. Besides, it records the mapping between the real ID and Pseudo ID of the vehicle [33].

**3.2. Road Side Unit.** The RSU is responsible for the provision of on-demand data from the BS. The legitimate RSU provides the genesis block based on local emergency messages and provides proof of the vehicle's location certificate. It also maintains the log of cluster information. All RSUs (i.e.,  $RSU_{pk}$  and  $RSU_{prk}$ ) have a pair of keys that performs validation [34].

**3.3. Vehicle.** The vehicle has two types in the proposed model, i.e., full node and normal node. The full node has

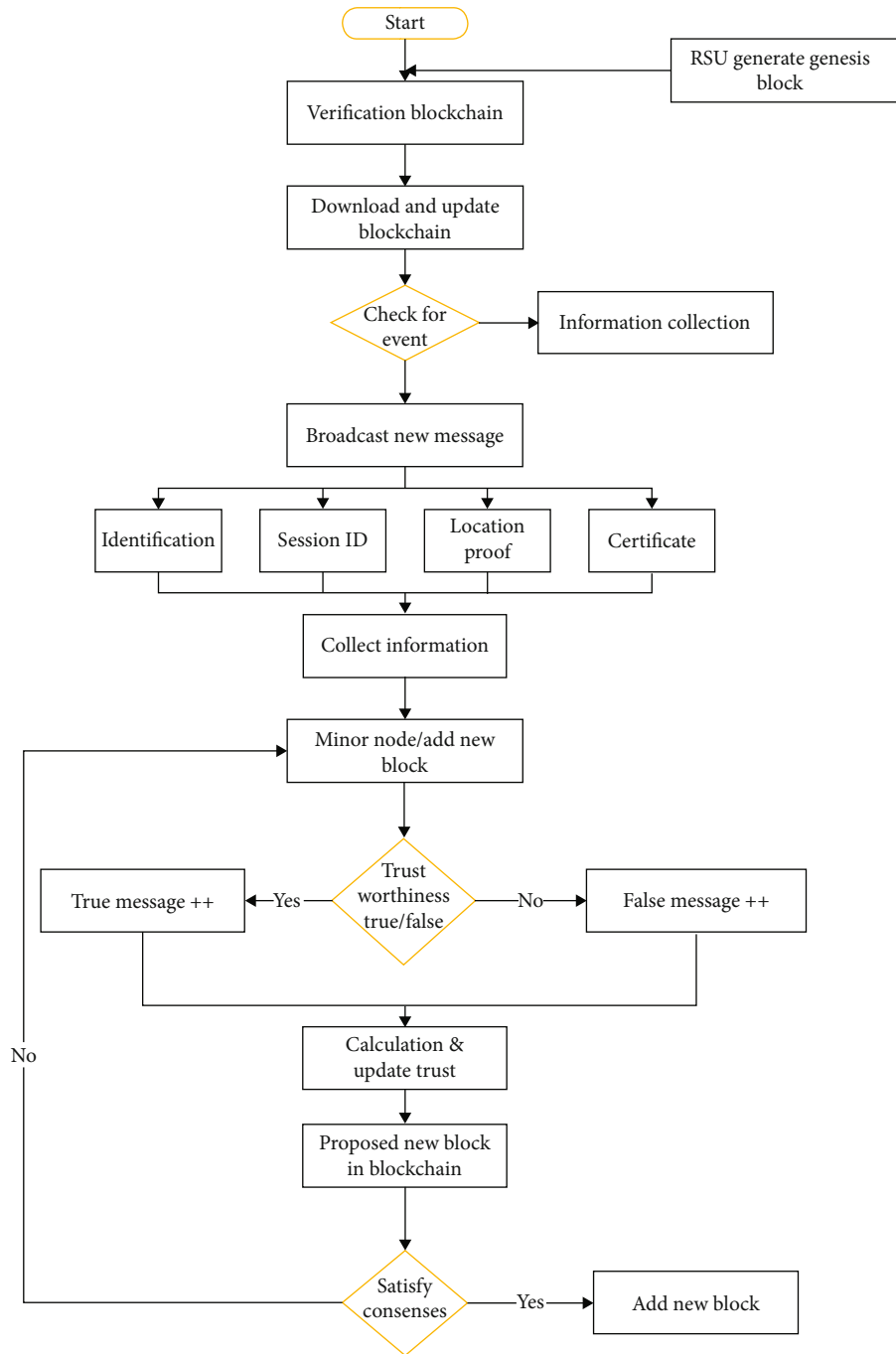


FIGURE 4: SVC-caching working mechanism.

more computing power and trust than the normal node and mines the new block in the blockchain network. At the same time, the normal node helps in the verification and creation of the event [35].

3.4. *Vehicular Named Data Network.* In VNDN, there are two types of messages, i.e., emergency/push-based messages and infotainment/on-demand messages.

Since the severity of emergency messages is more, we calculate the vehicle’s trust based on emergency messages. The infotainment messages are placed encrypted through a

digital signature mechanism of NDN, which is provided on demand of the vehicle.

3.5. *Block.* Block consists of a block header, which contains information of the previous block hash, timestamp, difficulty target, Merkel root, and a Block body that consists of the event messages as a digital transaction stored on blockchain, added in the main blockchain through the consensus process.

3.6. *Proof of Location Certificate.* The proof of location certificate is assigned to the vehicle by the respective RSU at a

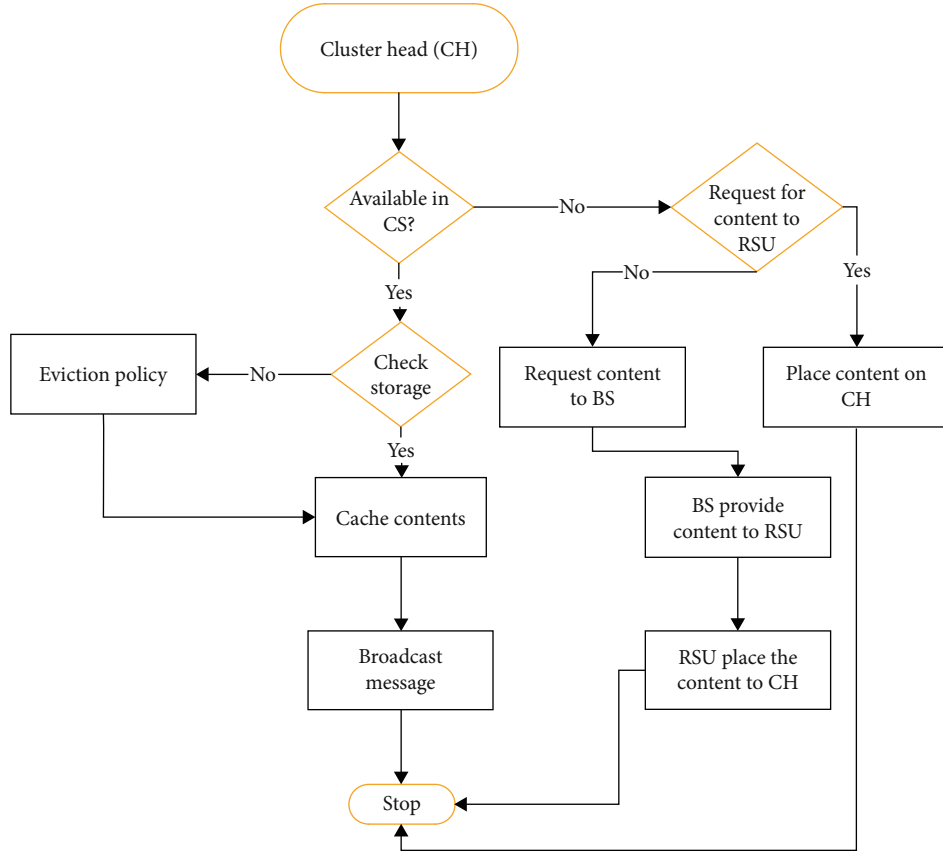


FIGURE 5: Cache content placement for VNDN SVC-caching.

given time. The RSU acts as a data validator for the vehicle's proof of presence in a particular event.

#### 4. Steps in the Proposed Scheme

All RSUs, i.e.,  $RSU_{pk}$  and  $RSU_{prk}$ , and vehicles have their public and private key pairs ( $V_{pk}$ ,  $V_{prk}$ ). The vehicle sends a message signed by its public key ( $V_{pk}$ ). In reply, the RSU sends a random session ID (SID). The vehicle sends the signed session ID back to RSU [ $sign(SID)$ ]. The RSU validates the message through ( $V_{pk}$ ).

**4.1. Threshold Time.** The threshold time of response (few milliseconds) is set by the RSU to validate the message. The RSU publishes a LOC to the vehicle including location, time, and public-key ( $V_{pk}$ ) signed by the RSU private key ( $RSU_{prk}$ ). The POL is used instead of GPS so that the message trustworthiness; therefore, the blockchain mechanism is used.

**4.2. SVC-Caching.** SVC-caching works the same as that of the NDN caching environment with a security feature embedded to secure minor vehicles' secure content placement. In this approach, we work with two main vehicles, where one is normal node (after verification from RSU through trust threshold values of greater than 0.5 issued by the RSU validation policy) and minor node (for the content

placement, which is aimed at controlling the whole verification policy for the efficient management of these nodes with a high level of vehicular trust development). Normal and minor node data are stored in either RSU or BS for the vehicles' future verification. Figure 4 demonstrates the workflow of SVC-caching technique.

Initially, the RSU generates the genesis block to add inside the blockchain. The genesis block is the first block of the blockchain network to secure the blockchain technique. The RSU verifies the blockchain, and then every VNDN verifies, downloads, and updates the existing blockchain. After the initial verification of the blockchain, the VNDN checks for any new event that happens, e.g., a *Request* for the content or content placement in the VNDN environment. The information is collected from the VNDN environment, which is part of the network automation.

The time to select the new node for the normal and minor nodes according to the POL, there is a technique to collect the information. A message is broadcast to all the vehicular nodes to become normal or minor ones. Besides, the threshold values are set to verify the vehicles to add or remove from the blockchain network. The information collected from the vehicles includes  $MsgID$ , Session ID, and POL. After the initial validation, the RSU/validator validates and provides the certificate. The whole process continues until it provides the information. After the collection of certification verification, the minor node is selected and added inside the blockchain.

TABLE 1: Different symbols used in algorithms.

S. No	Legend	Description
1	$V_T^{\text{Previous}}$	Previous trust value of the vehicle
2	$RSU_{\text{POL}}$	Check for RSU's proof of location (POL) certificate
3	$V_{\text{Sess ID}}^{\text{RSU}}$	Session ID assigned by RSU to vehicle
4	$T_{\text{respond}}^V$	Response time of the vehicle assigned by RSU
5	$B_i^{\text{New}}$	New blockchain
6	H#	Hash of all under event messages
7	$B_{i-1}$	Hash of the previous blockchain
8	$D_t \leftarrow \text{coefficient} * 2^{(8 * ((\text{exp}^{-3})))}$	Target difficulty
9	$M_{\text{VNDN}}$	Messages in the VNDN environment
10	$V_{\text{LOC}}$	Vehicle location
11	$M_{\text{sg}}^{\text{ID}}$	Instructions/second (job/task execution speed)
12	$V_T^{\text{current}}$	Current trust of the vehicle
13	R	RAM required on memory (in bytes)
14	$V_{\text{info}}$	Vehicle information
15	V	Vehicle velocity threshold: average speed: 30 km/h, urban trunk road: 60 km/h, urban secondary roads: 40 km/h
16	$V_{\text{CID}}$	Vehicular cluster identification
17	$V_{\text{s}}^{\text{Cache}}$	Storage of the vehicular caching
18	CH	Cluster head
19	$V_{\text{d}}$	Vehicle direction
20	$V_{(\text{Clusters})n}$	Vehicular clusters
21	BS	Base station
22	Threshold	Range (0.1–1.0)
23	trustable-Node	$\geq 0.5$
24	malicious-Node	$\leq 5$
25	$M_v^{(N)}$	Malicious node
26	$V_{\text{Trust}}^{(\text{New})}$	Trustable nodes
27	$V_{\text{NODE}}$	Vehicular node
28	$CH_{\text{DATA}}$	Data on the cluster head
29	$P_{\text{PK}}^{\text{Sign}}$	Matches the signature of the public key
30	PRR	Previous request rate threshold: 10 interest/sec
31	$CH^j$	Number of times selected as cluster head

4.3. *Trustworthiness.* The trustworthiness is checked and is shared with all vehicles after the complete validation process, as described in Algorithm 4-1. The values are updated if the trust is true as True Message++ and updated if the trustworthiness is false and calculated as false verification as False message++. The values are updated and the trust computations are calculated according to the suggested values. The new blockchain is proposed in the whole new process. In the next step, a consensus is checked according to the blockchain values. All the consensus is satisfied and provides considerable details to conduct the analysis; i.e., at least 15 vehicles should verify the event message. If it is satisfied, a new block is added inside the blockchain network. If not satisfied, the new minor node is selected for the blockchain validation process.

The process in Figure 5 is used to place the content for the normal and on-demand secure content placement. Till

now, we have selected the normal and minor nodes as trustable nodes for the VNDN environment (see Algorithm 4-1). The trustable minor node is selected as the CH, which provides the mechanism to support a temporary adjustment of these nodes because their trustworthiness is calculated, which finally provides the content placement mechanism (see Algorithm 4-3). The CS is used to store on-demand and normal content to provide the content to requested vehicles. After initial requests, if the content is available in the CS, then, the CH storage is checked. The eviction policy [36] is applied in case of insufficient storage; otherwise, the content is placed.

During the checking of the content at the NDN's CS, if the content is not found, then, the request is made for the RSU to store the content. If the content is not found on the RSU's CS, then, content placement does happen. Otherwise, the content request is made through the BS, and the BS



provides the content to the RSU to place over the CH for content delivery in VNDN, as presented in Algorithm 4-3. After successful placement of the content, a broadcast message is sent, which contains the public key of the node selected as CH to gather the selected vehicles' content, as demonstrated by Algorithm 6. Based on the policies of the selection of trustable normal nodes, minor nodes, proof of location certification, trust evaluation, and content placement, separate algorithms are proposed for every task to be accomplished in the SVC-caching technique. This technique provides the mechanism for data security through trust and content placement on these trustable vehicles. Table 1 defines all special symbols used inside the content placement technique and provides a complete mechanism to control all these operations. We have provided the security of both on-demand and push-based data in the VNDN environment for secure V2V communications through privacy and trust, which are the main requirements of VANET security.

## 5. Results and Discussion

The simulations have been performed in the NS-2 simulator to measure the performance of SVC-caching and other strategies, i.e., PNCE, IR, Reactive, and PeRCeIVE. The input parameters for simulations are presented in Table 2. The SVC-caching is a very effective approach to achieve the security and cache placement in the VNDN environment. In addition, it is suitable for the applications of VANET caching schemes. This section elaborates the simulation environment and simulated parameters, which are cache hit, content delivery, one hop ratio, and malicious node detection.

The number of tests is performed to obtain reasonable results. The performance of SVC-caching shows major contributions to the VNDN environment.

**5.1. Cache Hit Ratio.** The cache hit ratio is set as one parameter explaining the number of cache content found inside the minor nodes' memory. To find the cache hit ratio, the formula presented in Equation (1) is used.

$$\text{Cache hit ratio} = \frac{\text{Total}_{\text{cache}}}{\text{Cache}_{\text{hit}} + \text{Cache}_{\text{miss}}}. \quad (1)$$

Figures 6 and 7 show the cache hit ratios of the proposed scheme in comparison with PNCE and IR techniques with the cache size of 50 and 100 MB. The performance of all techniques increases with the increase of cache size, where the SVC-caching has 15% higher cache hit as compared to PNCE and 60% higher than IR. When the node size reaches 100, the performance of SVC-caching is still stable, as shown in Figure 7. Shortly, SVC-caching has 13% higher cache hit ratio than PNCE and 55% than IR.

**5.2. Delivery Ratio.** The delivery ratio is linked with the round-trip time. The round-trip time is the total time from data request submission to data received. To calculate the delivery ratio, Equation (2) is used.

TABLE 2: Simulation environment parameters.

S. No	Parameter	Value
1.	Simulation time	1000 s
2.	Simulation area size	Region 1    Region 2 250 * 250 m    500 * 500 m
3.	Number of vehicles	50 in Region 1 100 in Region 2
4.	Vehicle time for a drive	150 s
5.	Wireless area (single RSU)	200 m
6.	Cache values	0 s to 200 s
7.	Road condition	New entry (one-way road)
8.	RSUs	10
9.	RSU broadcast time interval	50 s
10.	Breakdown duration for vehicles	120 s
11.	Number of simulation runs	200

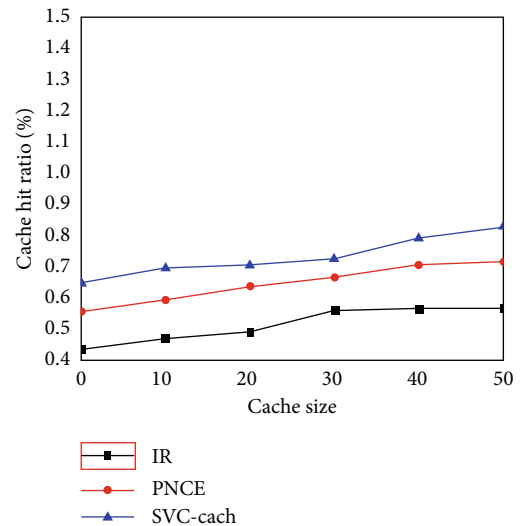


FIGURE 6: Cache hit ratio for cache size 50 MB.

$$\text{Delivery ratio} = \frac{\text{Packet}_{\text{Receive}}}{\text{Packet}_{\text{sent}}}. \quad (2)$$

Figures 8 and 9 show the delivery ratios under different conditions. It is clear that when the node size increases, the delivery ratio for all techniques increases.

The SVC-caching strategy guarantees higher increase in the delivery ratio with the node size increase because SVC-caching has greater neighbour cache information for vehicles due to CHs. The cache size growth at the IR and PNCE is not increased, whereas in the SVC-caching, the efficiency of the algorithm increases with the increase of cache size.

**5.3. One Hop Ratio.** The hop count is an essential parameter in the VNDN environment. The hop count illustrates that how many intermediate nodes are involved in the content

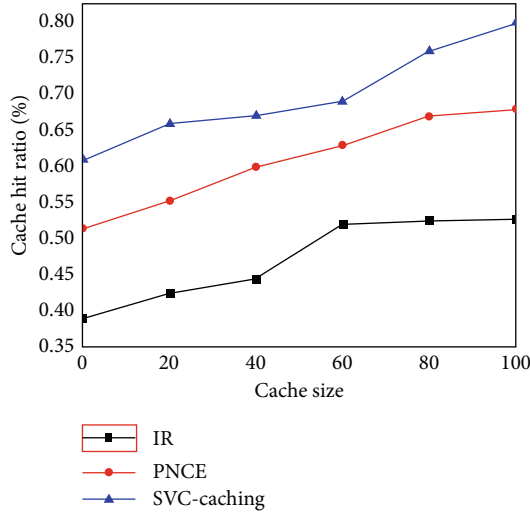


FIGURE 7: Cache hit ratio for cache size 100 MB.

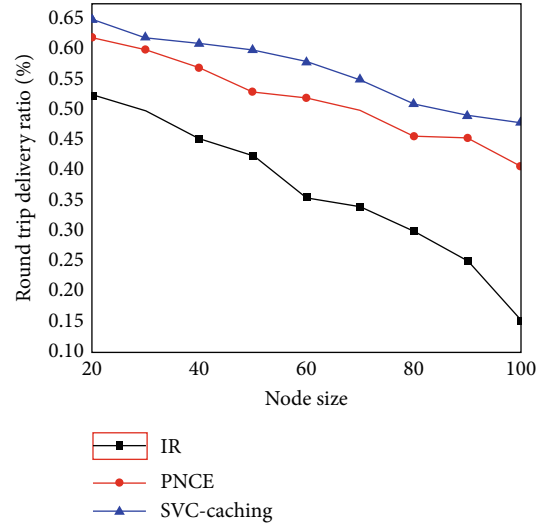


FIGURE 9: Delivery ratio for node size 100 MB.

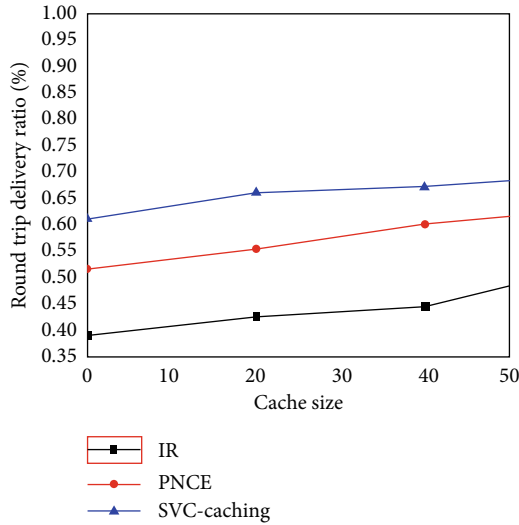


FIGURE 8: Delivery ratio for node size 50 MB.

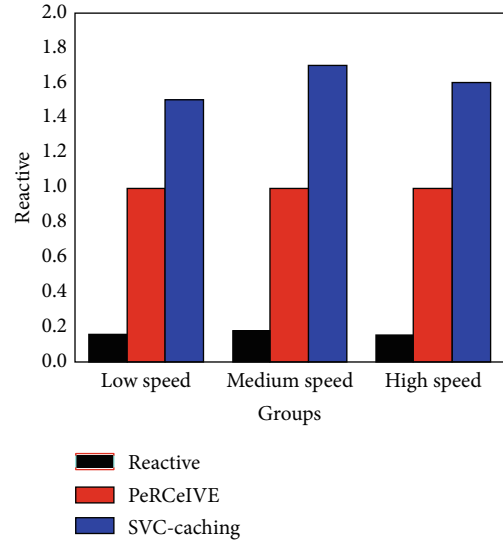


FIGURE 10: One hop ratio.

request response of vehicles. There is a limited number of nodes linked to provide the necessary details for controlling these parameters. The hope count is calculated through

$$\text{One hop count} = \frac{\text{Request}_{\text{sent}}}{\text{Request}_{\text{respons}} + \text{Responses}_{\text{all}}} \quad (3)$$

One hop ratio is the comparison of requests sent by vehicles and response between the first hop and all hop responses. The SVC-caching strategy is compared with the PeRCeIVE and reactive caching strategies for the one hop count. To place the cache data on particular selected vehicles based on RSU selection criteria, SVC-caching places higher data rates than other caching techniques based on three vehicle speed parameters, i.e., low speed vehicles, medium speed vehicles, and high speed vehicles. Figure 10 shows the comparison results on the basis of multiple data caching techniques.

At low speed, Reactive shows 0.16, while PeRCeIVE and SVC-caching exhibit 1 and 1.5 ratios, respectively. At medium speed, Reactive, PeRCeIVE, and SVC-caching demonstrate 0.18, 1, and 1.7 ratios, respectively, whereas, at higher speed, the ratios of Reactive, PeRCeIVE, and SVC-caching are 0.15, 1, and 1.5, respectively. At the end, an average of 60% improvement in the one hop ratio of SVC-caching strategy is achieved.

**5.4. Malicious Node Detection.** Throughout simulations, two regions were selected, i.e., Region 1 and Region 2. Region 1 contains a total of 50 vehicles and Region 2 consists of 100 vehicles. A blockchain-based message validation technique is applied to detect malicious nodes. Malicious nodes are the ones that do not satisfy the criteria to become a member of the cluster. Figure 11 shows a total of 50 vehicles out of which 5 do not pass the RSU's validation criteria to become members of the cluster. Again, the simulations are run in a

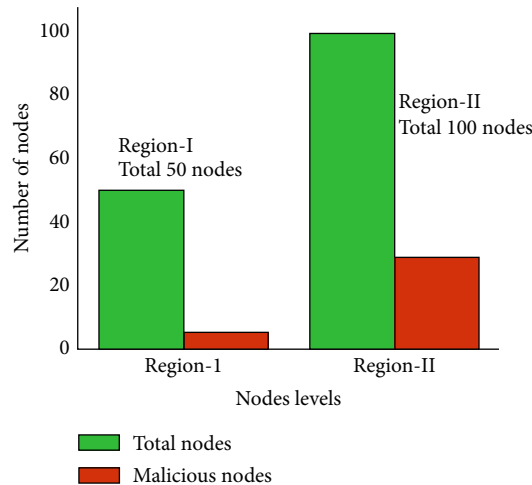


FIGURE 11: Region 1 and Region 2 malicious node detection.

larger environment, like 100 vehicles, passing through trust management criteria. Out of 100, only 29 vehicles are detected as malicious nodes.

## 6. Conclusion

A new model for cache placement is proposed, which is well suited for the VNDN environment. Using the blockchain-based distributive trust model is achieved for the eviction of malicious nodes to provide security and reliability of the data. The trust management strategy is adopted for gaining security while placing content on selected nodes. Furthermore, the NDN environment is used for V2V communications, which has multiple advantages over traditional IP-based communications. VANET provides a very effective way for passengers, drivers, and vehicles to exchange content with proper security. The proposed SVC-caching shows superior performance over other caching placement techniques. The results are evaluated based on the following parameters: one-hop count, delivery ratio, cache hit ratio, and malicious node detection. In addition, the proposed mechanism provides an effective way for vehicular communications. Moreover, this technique improves the performance on the basis of selected parameters. In the future, the proposed work can be extended to cloud/fog computing-based VANET environment wherein the communication has a wider range over the simple VANET environment.

## Data Availability

This paper is based on simulations, which does not need any dataset.

## Conflicts of Interest

The authors declare that they have no conflicts of interest.

## Acknowledgments

This work was supported in part by the Deanship of Scientific Research at King Saud University, Riyadh, Saudi Arabia, through the Vice Deanship of Scientific Research Chairs: Chair of Cyber Security; in part by FCT/MCTES through national funds and when applicable cofunded EU funds under the project UIDB/50008/2020; and in part by Brazilian National Council for Scientific and Technological Development (CNPq) via Grant No. 313036/2020-9.

## References

- [1] C. Chen, C. Wang, T. Qiu, M. Atiquzzaman, and D. O. Wu, "Caching in vehicular named data networking: architecture, schemes and future directions," *IEEE Communications Surveys & Tutorials*, vol. 22, no. 4, pp. 2378–2407, 2020.
- [2] G. Ma, Z. Chen, J. Cao, Z. Guo, Y. Jiang, and X. Guo, "A tentative comparison on cdn and ndn," in *2014 IEEE International Conference on Systems, Man, and Cybernetics (SMC)*, pp. 2893–2898, San Diego, CA, USA, October 2014.
- [3] I. U. Din, S. Hassan, A. Almogren, F. Ayub, and M. Guizani, "PUC: Packet Update Caching for energy efficient IoT-based information-centric networking," *Future Generation Computer Systems*, vol. 111, pp. 634–643, 2020.
- [4] S. Hassan, I. U. Din, A. Habbal, and N. H. Zakaria, "A popularity based caching strategy for the future internet," in *2016 ITU Kaleidoscope: ICTs for a Sustainable World (ITU WT)*, pp. 1–8, Bangkok, Thailand, November 2016.
- [5] V. Jacobson, D. K. Smetters, J. D. Thornton, M. F. Plass, N. H. Briggs, and R. L. Braynard, "Networking named content," in *Proceedings of the 5th international conference on Emerging networking experiments and technologies - CoNEXT '09*, pp. 1–12, Rome, Italy, December 2009.
- [6] C. Cooper, D. Franklin, M. Ros, F. Safaei, and M. Abolhasan, "A comparative survey of VANET clustering techniques," *IEEE Communications Surveys & Tutorials*, vol. 19, no. 1, pp. 657–681, 2016.
- [7] J. M. Duarte, T. Braun, and L. A. Villas, "Source mobility in vehicular named-data networking: an overview," in *Ad Hoc Networks*, pp. 83–93, Springer, 2018.
- [8] X. Wang and H. Qian, "Constructing a 6lowpan wireless sensor network based on a cluster tree," *IEEE Transactions on Vehicular Technology*, vol. 61, no. 3, pp. 1398–1405, 2012.
- [9] J. Y. Kim and H. K. Choi, "An enhanced security protocol for VANET-based entertainment services," *IEICE Transactions on Communications*, vol. E95.B, no. 7, pp. 2245–2256, 2012.
- [10] O. A. Khan, M. A. Shah, I. Ud Din et al., "Leveraging named data networking for fragmented networks in smart metropolitan cities," *IEEE Access*, vol. 6, pp. 75899–75911, 2018.
- [11] S. Ul Islam, H. A. Khattak, J. M. Pierson et al., "Leveraging utilization as performance metric for CDN enabled energy efficient internet of things," *Measurement*, vol. 147, article 106814, 2019.
- [12] D. Grewe, M. Wagner, and H. Frey, "PeRcEIVE: proactive caching in ICN-based VANETs," in *2016 IEEE Vehicular Networking Conference (VNC)*, pp. 1–8, Columbus, OH, USA, December 2016.
- [13] M. Duan, C. Zhang, Y. Li, W. Xu, X. Ji, and B. Liu, "Neighbor cache explore routing protocol for VANET based on trajectory prediction," in *2018 IEEE 3rd Advanced Information*

- Technology, Electronic and Automation Control Conference (IAEAC)*, pp. 771–776, Chongqing, China, October 2018.
- [14] W. Xu, X. Ji, C. Zhang, and B. Liu, “Nih: name/id hybrid routing in information-centric VANET,” in *2020 IEEE Wireless Communications and Networking Conference (WCNC)*, pp. 1–7, Seoul, Korea (South), May 2020.
- [15] H. Hasrouny, A. E. Samhat, C. Bassil, and A. Laouiti, “A security solution for v2v communication within VANETs,” in *2018 Wireless Days (WD)*, pp. 181–183, Dubai, United Arab Emirates, April 2018.
- [16] H. Sun, S. Y. Lee, K. Joo, H. Jin, and D. H. Lee, “Catch id if you can: dynamic id virtualization mechanism for the controller area network,” *IEEE Access*, vol. 7, pp. 158237–158249, 2019.
- [17] H. Khelifi, S. Luo, B. Nour, H. Mounqila, and S. H. Ahmed, “Reputation-based blockchain for secure ndn caching in vehicular networks,” in *2018 IEEE Conference on Standards for Communications and Networking (CSCN)*, pp. 1–6, Paris, France, October 2018.
- [18] S. Huh, S. Cho, and S. Kim, “Managing iot devices using blockchain platform,” in *2017 19th International Conference on Advanced Communication Technology (ICACT)*, pp. 464–467, PyeongChang, Korea (South), February 2017.
- [19] H. A. Khattak, K. Tehreem, A. Almogren, Z. Ameer, I. U. Din, and M. Adnan, “Dynamic pricing in industrial internet of things: blockchain application for energy management in smart cities,” *Journal of Information Security and Applications*, vol. 55, article 102615, 2020.
- [20] A. Almogren, I. Mohiuddin, I. U. Din, H. Almajed, and N. Guizani, “Ftm-iomt: fuzzy-based trust management for preventing Sybil attacks in internet of medical things,” *IEEE Internet of Things Journal*, vol. 8, no. 6, pp. 4485–4497, 2020.
- [21] M. A. Judge, A. Manzoor, H. A. Khattak, I. Ud Din, A. Almogren, and M. Adnan, “Secure transmission lines monitoring and efficient electricity management in ultra-reliable low latency industrial Internet of Things,” *Computer Standards & Interfaces*, vol. 77, article 103500, 2021.
- [22] X. Huang, C. Xu, P. Wang, and H. Liu, “Lnscc: a security model for electric vehicle and charging pile management based on blockchain ecosystem,” *IEEE Access*, vol. 6, pp. 13565–13574, 2018.
- [23] R. Shrestha, R. Bajracharya, A. P. Shrestha, and S. Y. Nam, “A new type of blockchain for secure message exchange in VANET,” *Digital Communications and Networks*, vol. 6, no. 2, pp. 177–186, 2020.
- [24] I. U. Din, A. Bano, K. A. Awan, A. Almogren, A. Altameem, and M. Guizani, “LightTrust: lightweight trust management for edge devices in industrial internet of things,” *IEEE Internet of Things Journal*, 2021.
- [25] W. Huang, T. Song, Y. Yang, and Y. Zhang, “Cluster-based cooperative caching with mobility prediction in vehicular named data networking,” *IEEE Access*, vol. 7, pp. 23442–23458, 2019.
- [26] M. Chowdhury, A. Gawande, and L. Wang, “Secure information sharing among autonomous vehicles in ndn,” in *Proceedings of the Second International Conference on Internet-of-Things Design and Implementation*, pp. 15–25, New York, NY, USA, April 2017.
- [27] L. Yao, Z. Fan, J. Deng, X. Fan, and G. Wu, “Detection and defense of cache pollution attacks using clustering in named data networks,” *IEEE Transactions on Dependable and Secure Computing*, vol. 17, no. 6, 2020.
- [28] A. Derder, S. Moussaoui, Z. Doukha, and A. Boualouache, “An online target tracking protocol for vehicular ad hoc networks,” *Peer-to-Peer Networking and Applications*, vol. 12, no. 4, pp. 969–988, 2019.
- [29] Z. Lu, Q. Wang, G. Qu, and Z. Liu, “Bars: a blockchain-based anonymous reputation system for trust management in VANETs,” in *2018 17th IEEE International Conference on Trust, Security and Privacy In Computing And Communications/ 12th IEEE International Conference On Big Data Science And Engineering (TrustCom/BigDataSE)*, pp. 98–103, New York, NY, USA, April 2018.
- [30] I. Hussain and C. Bingcai, “Cluster formation and cluster head selection approach for vehicle ad-hoc network (VANETs) using k-means and Floyd-Warshall technique,” *International Journal of Advanced Computer Science and Applications*, vol. 8, no. 12, p. 01, 2017.
- [31] L. Cárdenas-Robledo and A. Peña-Ayala, “Ubiquitous learning: a systematic review,” *Telematics and Informatics*, vol. 35, no. 5, pp. 1097–1132, 2018.
- [32] D. S. P. K. Nirmala, “Probabilistic mceliece public-key cryptography based identity authentication for secured communication in VANET,” *Solid State Technology*, vol. 63, no. 6, 2020.
- [33] A. R. Abdellah, A. Muthanna, and A. Koucheryavy, “Robust estimation of VANET performance-based robust neural networks learning,” *Learning*, vol. 11660, pp. 402–414, 2019.
- [34] R. Zhang, F. Yan, W. Xia, S. Xing, Y. Wu, and L. Shen, “An optimal roadside unit placement method for VANET localization,” in *GLOBECOM 2017 - 2017 IEEE Global Communications Conference*, pp. 1–6, Singapore, December 2017.
- [35] M. H. Alwan, K. N. Ramli, Y. A. al-Jawher, A. Z. Sameen, and H. F. Mahdi, “Performance comparison between 802.11 and 802.11p for high speed vehicle in VANET,” *International Journal of Electrical and Computer Engineering (IJECE)*, vol. 9, no. 5, pp. 3687–3694, 2019.
- [36] Y.-T. Yu and M. Gerla, “Information-centric VANETs: a study of content routing design alternatives,” in *2016 International Conference on Computing, Networking and Communications (ICNC)*, Kauai, HI, USA, February 2016.

## Research Article

# Augmentation of Contextualized Concatenated Word Representation and Dilated Convolution Neural Network for Sentiment Analysis

Fazeel Abid,<sup>1,2</sup> Ikram Ud Din ,<sup>3</sup> Ahmad Almogren ,<sup>4</sup> Hasan Ali Khattak ,<sup>5</sup> and Mirza Waqar Baig<sup>6</sup>

<sup>1</sup>Department of Information Systems, School of Business and Economics, University of Management and Technology, Lahore, Pakistan

<sup>2</sup>School of Information Science and Technology, Northwest University, Xi'an, China

<sup>3</sup>Department of Information Technology, The University of Haripur, Pakistan

<sup>4</sup>Department of Computer Science, College of Computer and Information Sciences, King Saud University, Riyadh 11633, Saudi Arabia

<sup>5</sup>School of Electrical Engineering and Computer Science, National University of Sciences and Technology (NUST), Islamabad, Pakistan

<sup>6</sup>Department of Electrical Engineering, FAST National University of Computer and Emerging Sciences, CFD Campus, Faisalabad, Pakistan

Correspondence should be addressed to Ikram Ud Din; [ikramuddin205@yahoo.com](mailto:ikramuddin205@yahoo.com), Ahmad Almogren; [ahalmogren@ksu.edu.pk](mailto:ahalmogren@ksu.edu.pk), and Hasan Ali Khattak; [hasan.alikhattak@seecs.edu.pk](mailto:hasan.alikhattak@seecs.edu.pk)

Received 13 October 2021; Revised 26 October 2021; Accepted 29 October 2021; Published 25 November 2021

Academic Editor: Shalli Rani

Copyright © 2021 Fazeel Abid et al. This is an open access article distributed under the Creative Commons Attribution License, which permits unrestricted use, distribution, and reproduction in any medium, provided the original work is properly cited.

Deep learning-based methodologies are significant to perform sentiment analysis on social media data. The valuable insights of social media data through sentiment analysis can be employed to develop intelligent applications. Among many networks, convolution neural networks (CNNs) are widely used in many conventional text classification tasks and perform a significant role. However, to capture long-term contextual information and address the detail loss problem, CNNs require stacking multiple convolutional layers. Also, the stacking of convolutional layers has issues requiring massive computations and the tuning of additional parameters. To solve these problems, in this paper, a contextualized concatenated word representation (CCWRs) is initialized from social media data based on text which is essential to misspelled and out of vocabulary words (OOV). In CCWRs, different word representation models, for example, Word2Vec, its optimized version FastText and Global Vectors, and GloVe, collectively create contextualized representations upon the sequence of input. Second, a three-layered dilated convolutional neural network (3D-CNN) is proposed that places dilated convolution kernels instead of conventional CNN kernels. Incorporating the extension in the receptive field's size successfully solves the detail loss problem and achieves long-term context information with different dilation rates. Experiments on datasets demonstrate that the proposed framework achieves reliable results with the selection of numerous hyperparameter tuning and configurations for improved optimization leads to reduced computational resources and reliable accuracy.

## 1. Introduction

In topical years, progress towards intelligent applications showed excellent technological developments through social media data analytics [1]. These advancements are regulated

mainly and decently using social networks like Twitter, Facebook, and Instagram [2]. These social networks now transformed into a potential origin for mining social information to prevail over people's sentiments. The enormous opinions over social media comprise simple word sentences

and hold helpful information in several aspects. Consequently, social media data can be engaged to determine valued insights. Development in the pattern of social media data mining algorithms must focus on textual data. Sentiment analysis based on social media data is a rapidly evolving field to understand people's opinions, attitudes, and behaviors. An intelligent application can benefit social media sentiment analysis as these attitudes, feelings, and reactions can be correlated to the disasters, epidemic situations, government policies, and people perception, which is a substantial source of assessing the polarity: positive, negative, and neutral.

These applications concentrate on improvements in multiple aspects such as technological and legislative measures with social media data mining. It could also raise people's perspectives and cognition and endue them to acquire a viable environment [3]. The social media data on social networks consider a principal source of reviews against the events, disasters, and current epidemic situations though the challenge is a sizable social data that concerns efficient and scalable techniques to work on noise. The requirement for cleaning the noisy data requires automatic techniques for the classification of worthy information. It also goes through various issues, such as sentences written in short length, notations, and typos mistakes. In this regard, semantic exploration can adapt excessive social media data for syntactic regularities towards advancements through incorporation and scalability [4]. Thus, social media data mining algorithms consider gathering and handling social data effectively on Instagram, Facebook, and Twitter. We decide on twitter, which incorporates various posts and comprises 280 characters [5] for sentiment analysis.

Nowadays, machine learning methods are leveraged to augment services by mining social media data [6]. Among numerous methods of machine learning towards the classification of sentiments, Naive Bayes (NB) is exploited for topic detection [7], sentiment analysis [8], recommendation systems [9], and spam detection [10]. Further, a support vector machine that is a preferred technique in social media data has been applied [11]. However, due to the varying size of sequence composition, the stated methods are problematic towards extracting the features, which is significant. A sub-field of machine learning stated that deep learning incorporates neural architectures to extract expeditious high-level features while considering social media data classification. Also, techniques based on neural networks are increasingly utilized to solve the problems associated with supervised as well as unsupervised learning [12–14].

Deep learning methodologies assure researchers that the use of neural networks empowers extracting features devoid of involving the complex engineering of features [15, 16]. Feature extraction and classification are carried out through a sequence of words by multiplying with related weight as a one-hot vector or matrix [17]. The succession of a respective word is interpreted by way of continuous vector space initializing to neural architecture using several layers for prediction. This impacts the learning set to increase the classification evaluation metrics such as accuracy defined in [18]. Among neural architectures, convolutional neural

networks have attained adequate results to classify sentences obtained from social media [19, 20]. Multiple distributed word representations such as Word2Vec [21], GloVe [22], and FastText [23] can learn through mapping the words upon lower dimensions. A technique for extracting features using handcrafted features to classify sentences featuring convolutional neural networks introduced in [24] cannot hold long-term dependencies. Relatively, the employment of the CNN variant as dilated convolution removes the consequences containing information loss owing to traditional approaches of down sampling in conventional pooling operations and the stride convolution. Additionally, it scales receptive fields significantly, devoid of more parameters that make dilated convolution feasible to hold long-term dependencies and semantics.

Though many research works inadequately coupled relations regarding social media data ought to be intensified, this study modifies a deep neural network technique that automatically specifies social media data engaging a dilated convolutional neural network architecture in the parallel mechanism. From our best evaluation, a parallel mechanism in a dilated convolutional neural network can efficiently predict appropriate information by learning features from a contextualized concatenated word representational model using different embeddings. Beyond the developments, various hyperparameters employing dilated convolutional neural networks to analyze social media data sentiments are reasoned. This paper sets up a new approach for sentiment analysis and is utilizable to improve many services. The following are the contributions of this work:

- (i) Contextualized concatenated word representational (CCWRs) model is utilized to get classifier's improved exhibition features compared with many state-of-the-art techniques
- (ii) A parallel mechanism in three dilated convolution pooling layers featured different dilation rates, and two fully connected layers in a novel approach are considered
- (iii) Lastly, the work undertakes a deep learning approach using multiple parameters and hyperparameters to offer intelligent applications using Twitter data for sentiment analysis to enhance people's behavior

The rest of the paper is organized as follows. Section 2 continued with related work. The proposed framework for sentiment analysis is accessible in Section 3. Section 4 covers experimental setups and results, while the discussion is in Section 5. Finally, the paper is concluded in Section 6.

## 2. Related Work

The continuous social media data maturation has incited an advanced degree in scientific and sustainable smart urban explorations. Plenty of tasks have been performed over sustainability toward smart applications by social media networks [25, 26]. Still, the collective signification is not yet

entirely considered and admired [27]. Social media users now appreciate the accessibility and necessity of smart services that imply smart applications' requirements by concentrating on social media contexts [28, 29]. These smart applications activate the combination of social media networks and a smart environment for the social user's opinions, and prospects possess a sound impact, as explained in [30, 31]. By concentrating on social media networks with associated information, like hashtags, time, location, and name, the present work intends to explore how these networks fundamentally contribute to elevating the importance of smart applications. Therefore, social media network users regarded as smart application sensors together with associated metainformation can be utilized in many research works as described by [32–34].

Moreover, the data composed by social users tend to be syntactically unique and ubiquitous using smartphones, which can be appropriately collected and analyzed the information in a short textual framework [35]. Numerous multiple perspectives, from event detection to disease tracking and monitoring employing small textual content on social media, have been proposed in [35–37]. This short textual content of social media networks such as Twitter is semantically essential and extensively utilized in heterogeneous applications related to text classification [38, 39].

A methodology using features (metalevel) considering emotions from Twitter data for the polarity classification has been offered [40]. Many methodologies of manual tagging data gathered from Twitter with metainformation similar to location and social user for training based on conditional random fields as presented in [41, 42]. Similarly, multiple techniques categorize different topics like joy, fear, anger, love, and surprise by tagging on Twitter proposed in [43, 44], to accomplish emotional analysis. To originate smart applications, Twitter can identify numerous aspects such as people inferring and trends. However, these aspects are bound toward noise from nonassociative contents, which are crucial, as clarified in [45]. Therefore, a filter should be considered to attain adequate associative information on mentions, URLs, slang words, and numbers. A set of features as the evaluation metrics rely on features class.

Machine and deep learning-centered techniques employing social media data must be essential to mine valuable insights as presented in [46, 47]. The mining process, such as social media data, intends to assess people's opinions in many prospects, such as gathering data linked to the user and observing interactions [47]. Overall representation starts from unstructured to structured data; deep learning performs better than machine learning methods, which are time-consuming and require complex manual feature engineering processes. These positive aspects in deep learning methods to mine opinions from enormous social networks in streaming, multimedia, and textual framework provoked researchers in numerous works [48–52]. Therefore, extracting opinions from social networks such as Twitter in text form using unsupervised learning is significantly regarded for appropriate representation in this work.

Among many neural networks, traditional convolutional and recurrent neural networks have prominently accom-

plished higher outcomes from social networks for capturing long-term dependencies and extracting the opinions, such as sentiment analysis. An optimized version of recurrent neural network, long-short-term memory utilized to improve the semantics, is proposed in [53], but the training of mentioned version was computationally difficult. To extract syntactic features and perform faster training for text classification based on social media, convolutional neural networks testified to be more suitable [54, 55]. Further, a convolutional neural network as a joint trained task can substantially extract features as well as classification [56]. Many researchers are progressively employing convolutional in recent works with pooling layers for morphological modeling [57, 58].

Similarly, to cope with contextual data in character and sentence-level, two convolutional layers of deep architecture for the classification of short texts are offered in [59]. However, conventional convolutional architecture requires multiple layers stacking with the length of text. An improved form referred to as dilated convolution neural network; comparatively, a more sensible choice capable of the increased size of receptive field size adequately overcomes the issues and utilized in many works [60–62].

Distributed word representation in deep learning transforms words into a continuous vector; likewise, pretrained learning representation makes an essential impact while classifying the social data for sentiment analysis. It is also observed that social data classification augments the learning toward syntactical, phonological, and sentimental information; some of the works attempt to combine pretrained vectors. But the syntactical and phonological issues are demanding relationships between the words for the sufficient and actual classification as explained in [63–65], although the concept of combining varied pretrained representations is of significant results concerning different channels towards the classification of multiple sentences as presented in [66]. However, the dimensions of combined representations should be the same, restricting the scope and usage of pretrained representations due to multiple dimensions.

Furthermore, CNN has been employed to identify the actual word events from sentence-level social data by considering position along with entity explained in [67]. A more in-depth work focused on social media data pursuance of sentence-level classification confirms the ubiquity of multiple opinions or events in [68]. In this work, a dynamic multipooling layer is introduced to extract opinions about events for improved information. Although CNNs have been in continuous considerations among researchers, long-term dependencies regarding semantic features toward input sequence remain challenging. Also, it has been observed that CNNs tend to depend on stacking various layers together with the convolution-pooling to adapt long-term semantic dependencies. From the best of our knowledge, a dilated convolution network that adjusts dimension and encompasses addition in the receptive field's size devoid of loss of detailed information and the problem of long contextual and semantic dependencies is addressed effectively through varied dilation rates.

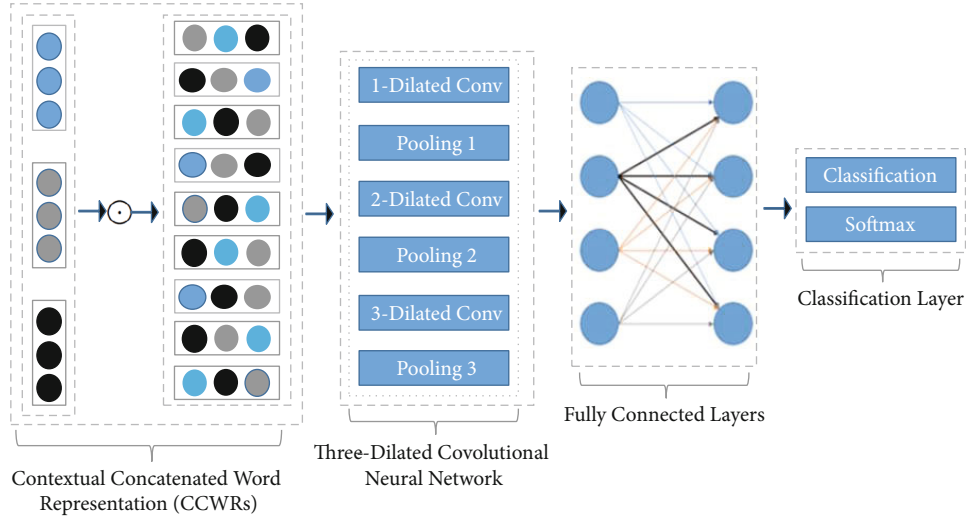


FIGURE 1: Structure 3D-CNN with 2 fully connected layers followed by contextualized concatenated word representations.

### 3. The Proposed Architecture for Sentiment Analysis Based on CCWRs and 3D-CNN

This section contributes a theoretical model regarding a potential approach for social media data considering Twitter for sentiment analysis based on COVID's perspective. Initially, different word representational models are concatenated, referred to as contextualized concatenated word representation (CCWRs). Second, the 3D-CNN architecture in this work is made by utilizing three dilated convolution kernels and two fully connected layers to seize long-term contextual dependencies concerning semantic features. We utilized multiple dimensional convolution processes to manage additional complexities toward enhanced performance by initializing the words to the 3D-CNN as a matrix to extract sufficient features through corresponding weights. Our proposed architecture has subsequent portions: concatenated word representations, three dilated convolution-pooling layers, two fully connected layers, and Softmax (as shown in Figure 1).

*3.1. Contextualized Concatenated Word Representations (CCWRs).* To represent the words as dense vectors, word representation models are regarded as essentials for feature extraction. These word representations are effective and result in advances toward the execution of social media data sentiment analysis as described in [69–71]. Many recent works have considered improved word and feature representations by way of different word embedding models [65, 72, 73]. Though these models diversify in architecture and pretraining, they still encode the input according to the surroundings. Words are represented utilizing only a single pretrained language model.

Further, these representations are unfeasible as a result of slow training and evaluation. Using pretrained models trained on multiple datasets exploits the biasness in different datasets, leading to numerous representations associated with the same word. On the other hand, the concatenation

of multiple word representational model can produce better representations devoid of computational complexities compared to a single model nearer to contextualized embeddings.

In this work, different pretrained word representational models such as Word2vec [21], fastText [23], and GloVe [22] are concatenated to deal with sentiments regarding contextualized and semantic information through the weighted mechanism. We leverage multiple word representations to produce a single table for every pretrained model in which the token of related input is embedded into a single vector space. Then, the subsequent vectors tend to be concatenated toward a single vector. Such weighted concatenation sufficiently upgrades the semantics and can handle the most recent problems identified with the misspelled and out of vocabulary words. The process of concatenation using associated weights assists in exploring better representations and functionally helps for sentence encoding in pursuance of feature selection. We utilize GloVe trained on Twitter, having 2 billion tweets, 27 billion tokens, and 1.2 million vocabulary, Word2vec 30 million tweets, and google news. In contrast, fastText on 1-million-word vectors, 16 billion tokens with subword information on Wikipedia, UMBC web-based corpus, and <http://statmt.org> news dataset considering dimensions range from 100 to 200.

We discard words that lie less than ten times and convert the characters to lowercase, and the most acceptable size corresponding to context window size selection is 5. In the training of CCWRs, we proportionately dropped the learning rate with the improvement in training. It has been observed that early regarded text does have an overall impact on the precession of the model. In this work, we train the concatenated representations on multiple datasets associated with different anomalies in the world. The first dataset is congregated by the use of TAGS and streaming API as described in [74]. The variety of keywords seemed to be evolving incessantly over social media. However, to stream the tweets of contextual perspective, the rational filtering keywords of our work exhibited in the table accumulated



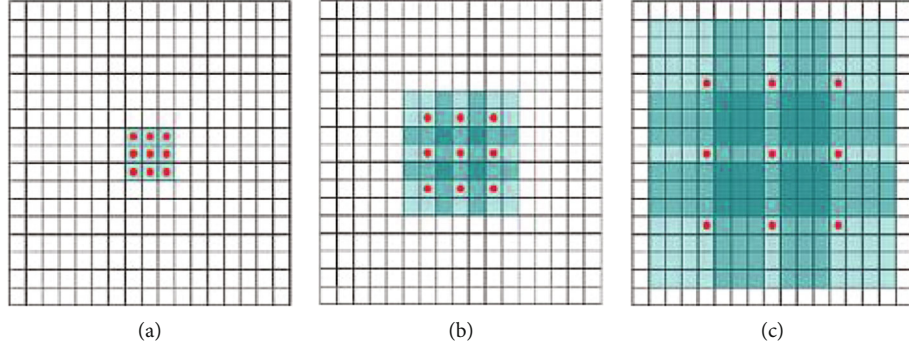


FIGURE 2: The process of stacking and its effect of dilated convolution kernel [60].

from September 2020 to March 2021 are still in use. The other dataset considers the anomalies in the real world based on Twitter as utilized in [75].

### 3.2. Three Dilated Convolutional Neural Network (3D-CNN).

In sentiment analysis based on the textual framework, the conventional CNN, due to the pooling layer, some significant text features are missed during calculation, ending in the adverse effect in overall network precision. Similarly, to acquire significant features, CNN architecture is deepened by stacking more layers, which concerns more parameters and additional computational resources. Also, the backpropagation of gradient may lead to vanishing gradient while increasing layers in network, causing performance to reduce significantly. Further, the limited size of convolutional kernels causes classical CNN only to hold short-term dependencies of text. To handle stated issues, a process that places zeros into the primary convolution kernel formed the dilated convolution kernel as introduced in [60]. This placement by way of intensifying receptive field size enables capturing more information and uplifting network's entire performance, for example, Figure 2 by which conventional convolution kernel of  $3 \times 3$  size, a point upon 0 weight placed on each point in a matrix in Figure 2(a) and then develop in Figure 2(b); equally, Figure 2(c) exhibits as receptive field size  $3 \times 3$ ,  $7 \times 7$ ,  $15 \times 15$  concerning convolution kernel.

The receptive field size tends to increase as the placed holes increase. However, it is observed that the parameters are the same as shown in Figures 2(a)–2(c). The dilated convolution kernel seems to process the text enabling the convolution kernel to obtain additional information without additional computational resources. Therefore, the increase in receptive field size is essential for many tasks such as prediction and classification. A three dilated convolutional layers model is presented in Figure 3 showing the significant rise in dilation rate at each layer. The model with a specific feature map as  $(F_1, F_2, F_3, F_4)$  of dilation convolution  $(1, 2, 3, 4)$  together with the receptive field size of each element as  $((3 \times 3), (2^3 - 1) \times (2^3 - 1), (2^4 - 1) \times (2^4 - 1))$  where receptive field size of each element in  $F_{i+1}$  by way of  $(2^{i+2} - 1) \times (2^{i+2} - 1)$  can be seen.

To maximize the performance of the dilated CNN over the traditional CNN model, a novel architecture 3D-CNN following CCWRs containing three dilated convolution

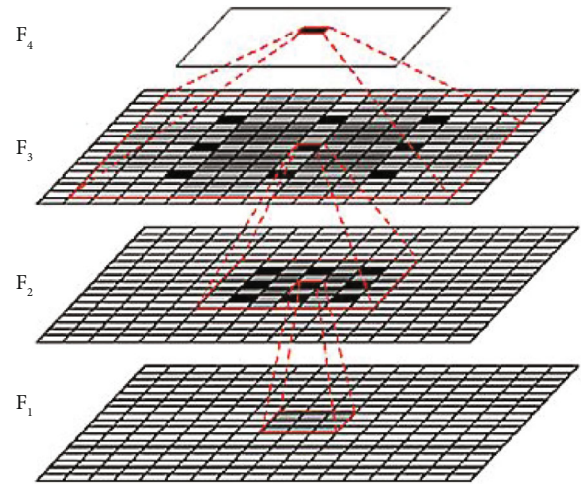


FIGURE 3: Three dilated convolution layers [76].

and pooling layers via two fully connected layers is proposed. The increase in the receptive field size extracts sufficient linguistics and contextual information without affecting and extending dimensions and parameters. This implementation efficiently increases the convolution kernel considering multiple scales with the aid of dilated operation while applying distinctive dilation rates as described in [77] and shown in Figure 4.

The choice of these dilation rates is significant when designing the structure of 3D-CNN as mentioned in [21] depends upon:

$$D_i = \max [D_{i+1} - 2d_i, D_{i+1} - 2(D_{i+1} - d_i), d_i]. \quad (1)$$

Here,  $i = 1, 2, \dots, n$ ;  $d_i$  as dilation rate toward the  $i^{\text{th}}$  layer, whereas  $D_i$  being foremost  $d_i$  in the prescribed layer. Figure 5(a) has three dilated convolution kernels utilizing  $3 \times 3$  as size with  $d_i = 2$ , similarly, Figure 5(b) using  $d_i = 1, 2$ , and 3.

The considered dilated convolution kernels  $(1, 2, 4)$  over several dilation rates  $(1, 2, 4)$  ensure the extraction of each semantics and not obstinate contextual information while extracting the feature maps. Our model significantly extracts the semantics and contextual information for sentiment

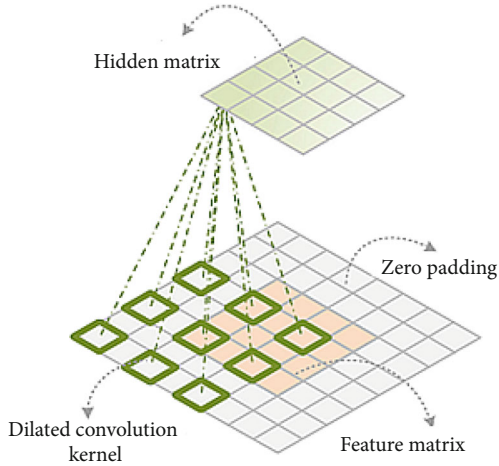


FIGURE 4: The dilated convolution operations over multiple dilated rates  $(2 * 2)$  [77].

words and sentences by considering multiple dilation rates. The three dilated convolution-pooling layer calculation for the extraction of long semantics and contextual information following CCWRs is presented in the following articulations:

$$D_c^1 = \text{RRELU}(F *_{d_1} X_t^x), \quad (2)$$

$$D_c^i = \text{RRELU}(F *_{d_i} D_c^{i-1}), \quad (3)$$

$$D_c^l = \text{RRELU}(F *_{d_l} D_c^{l-1}), \quad (4)$$

where the dilated convolution is  $F *_{d_i}$  in the particular layer.

## 4. Experiments

This section initially incorporates the datasets, experimentation, and analysis of the results via different methodologies compared with multiple datasets. The main goal is to evaluate the proposed novel technique; this work presents an appropriate classifier including three dilated convolutional layers accompanied through CCWRs.

**4.1. Datasets.** To precisely evaluate, we test the proposed model on two datasets towards suitability, adaptability, and reliability. The first dataset encompasses various 27 events in real-world life, such as disasters, emergencies, and incidents that are publicly accessible [78]. The second dataset is congregated by streaming and TAGS [79]. These API are considered as interface Twitter search interface, which utilizes the keywords and terms specified by the user. The user places a query, and TAGS retains the results through a free google sheet and offers setup tags to update the sheet whenever needed. The keywords selected for tweets gathered from September 2020 to March 2021 are mentioned in Table 1 as search terms accumulate to 18920. Social media data like Twitter carry a lot of noise, such as numbers, URL, and user mentions, to normalize the data and handle redundancy; some preprocessing techniques, tokenization, and lemmatization are considered described in [80]. Further, tweets fea-

turing only five words as well as the stop words decided to eliminate. A shuffling in both datasets is determined for reliable outcomes, applicability, and appropriate analysis since all datasets are equal for better performance [81]. Four sets from the shuffling of selected datasets are acquired in which each fuses a comparable amount of tweets alluded to ESD1, ESD2, ESD3, and ESD4 as equally shuffled data.

**4.2. Experimental Setup.** The experimentations accumulated using diverse datasets coupled with multiple word representations language models to provide contextual concatenated word representation by considering suitable parameters. The activation functions, optimization algorithm, training, mini-batch size, filter size, number of hidden layers, the receptive field size, and the number of epochs incorporated are presented in Table 1. To deal with the issue of vanishing gradient in training, the rectified linear unit (Relu) and hyperbolic tangent (Tanh) are taken into consideration, which generally sets the output and serves input to neurons in the subsequent layer as explained in [82]. For the regular distribution and to reduce overfitting, a variant of Relu, a randomized (RRelu), is also considered through which the parameters with regard to negative impacts are sampled randomly [83].

For training, optimization algorithms such as stochastic gradient descent SGD, a 0.01 learning rate, and a stochastic optimization ADAM learning rate of 0.001 are utilized. Further, to improve training performance, the root mean squared propagation (Rmprop) optimizer that calculates the gradients upon a fixed window is regarded. There is no conceptualization for a specific choice of neurons in hidden layers; similarly, the wrong choice of neurons results in underfitting and overfitting due to few or more neurons that ultimately influence model's training [84]. Keeping in mind the nature of this work, the different choices of neurons 150, 300, and 400 in hidden layers are adequate to evaluate.

Moreover, training in neural architectures is reasonable using minibatches to split the large datasets into smaller sets. The minibatch gradient descent is taken into account with batch sizes of 64, 128, and 256, respectively. On the other hand, considering 10, 15, and 20 widths of the model since model's width is determined by the choices of hidden layers that impact the entire complexity of the neural network architecture. Similarly, for generalization, epochs refer to the number of times a dataset tends to pass through the network and cause the model to under or overfit due to selected epochs number. The selected number of epochs continues to be 10 to 100 for best critical analysis by considering mentioned hyperparameters. Lastly, varied filter size incorporates  $(2, 2, 3)$ ,  $(2, 2, 4)$ ,  $(2, 2, 5)$ , as well as the dilation width is set to  $(1, 2, 4)$ .

**4.3. Results and Analysis.** We completed experimentations on numerous assessment metrics on equally shuffled datasets by way of baseline and proposed methods. Precision, recall, classical metric accuracy, and  $f1$ -score to inspect the symmetry in recall and precision are considered to deal with the imbalanced data. A 16 core processor of 3000 MHZ and 32 GB RAM is used to accomplish all the experimentation. Additionally, ML library "TensorFlow," an open-sourced

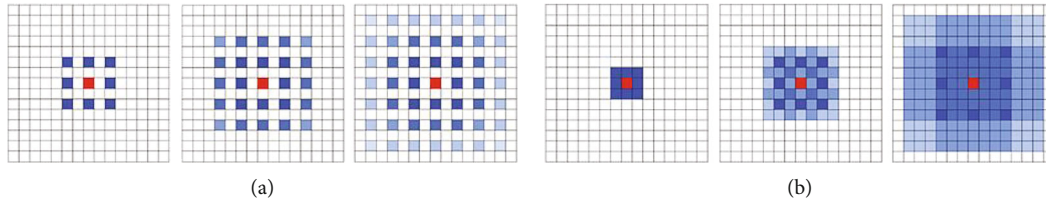


FIGURE 5: The stacking effect of dilated convolution kernels [21].

TABLE 1: Selected keywords for data selection and gathering.

Period	Filtered keywords
September 2020 to March 2021	#corona, #coronavirus, #first wave of Coronavirus, #firstwaveofCoronavirus, #pandemic, pandemic, #epidemic, epidemic, #handsanitizer, #covid, #covid19, #sarscov2, #ncov2019, #2019-ncov, #vaccination trials
	#lockdown, #quarantine, #Socialdistance, #Social Distance, #flattencurve, #flatteningcurve #working from home, #workfromhome, #second wave of Coronavirus, #secondwave of coronavirus, #huge number of deaths, #deadly virus, #deadly wave, #againlock down #n95, #K95, #N95, #k95, #Govt Polices on Covid, #Govt relied on Covid.
	#Covid Vaccine, #Covid Vaccination, #Pfizer, #Astrazenca, #Astra Zeneca, #side effects of vaccinations, #price of vaccination # availability of Pfizer, #chinese vaccine #sinopharm
	#new variant of Covid, #third wave # third wave of covid #more mutation #Moremutation, # relaxation in lockdown, #immunity in covid, #vaccination started

[85], is involved in the training and comparing the proposed framework [85]. We settled the evaluation by including baseline models, which contained each model and pre-trained word vectors compared with the proposed framework, with each pretrained vector on similar architecture involving hyperparameters for the comparative analysis carried out.

The evaluation metrics for baseline models are accuracy together with  $F1$ -score. The most elevated accuracy accomplished in baseline models is 74.04% and  $F1$ -score 70.42% by utilizing FastText and 73.65% and  $F1$ -score 70.64% through GloVe ESD-1, which are presented in Tables 2 and 3 and displayed in Figures 4 and 5.

The accuracy achieved on the proposed model is mentioned in Tables 4, 5, 6, and 7, along with hyperparameter settings selected and shown in Table 8. The employment of hidden layers seems to have a significant impact on the improvement of network tuning. Astonishingly, the optimization algorithm Rmprop attains dependable accuracy of 77.92% on ESD-4 with a batch size of 256, 20 hidden layers, and 300 neurons using randomized rectified linear units (RRelu), whereas the selection of other parameters accomplished slightly closer accuracy 77.80% on ESD-3 with a batch size of 256, 15 number of hidden layers, and 150 neurons using rectified linear unit (Relu) through SGD and 76.84% on ESD-4 with a batch size of 128, 15 number of hidden layers, and 150 neurons using tanh through ADAM, respectively. Further, the batch sizes from 64, 128, and 256, in our architecture achieved the best accuracy on the equally shuffled dataset denying many works claiming the best performance with 2 to 32 batch size. The other evaluation metrics for handling imbalanced data are precision,  $F1$ -score, and recall (as shown in Tables 9, 10, 11, and 12).

TABLE 2: Accuracy on baseline models.

Methods	ESD-1	ESD-2	ESD-3	ESD-4
GloVe-3D-CNN	73.65%	71.98%	70.91%	69.89%
Word2Vec-3D-CNN	71.52%	69.82%	72.47%	70.93%
FastText-3D-CNN	74.04%	73.97%	72.84%	72.76%

TABLE 3:  $F1$ -score on baseline methods.

Methods	ESD-1	ESD-2	ESD-3	ESD-4
GloVe-3D-CNN	70.64%	66.80%	69.57%	56.51%
Word2Vec-3D-CNN	71.52%	68.67%	68.49%	60.38%
FastText-3D-CNN	70.42%	69.25%	71.57%	67.2%

The most efficient results in consideration of precession are 79.21% on ESD-1, and recall is 79.08%, while  $f1$ -score is 76.82%, shown in Figures 6, 7, 8, and 9, which reveals proposed archieture's significance.

## 5. Discussion

Deep learning-based methodologies promoted the significant availability of word representations models such as Word2Vev, GloVe, and Fasttext. This work investigates the quality of the different word representation models to perform social media sentiment analysis for intelligent applications. Our work referred to the collection, selection, and evaluation of multiple standard metrics and appropriate hyperparameters mentioned in Table 8. The foremost challenge during this work is related to dimensions of multiple word representation models by way of weighted

TABLE 4: Proposed method accuracy on ESD-1.

Datasets	Optimization algorithm	Epochs	Activation function	Neurons	Hidden layers	Accuracy	Batch size
ESD-1	RMprop	10-100	RRelu	300	20	77.34%	256
ESD-1	SGD	10-100	Relu	75	10	76.96%	64
ESD-1	ADAM	10-100	Tanh	150	15	76.35%	128

TABLE 5: Proposed method accuracy on ESD-2.

Datasets	Optimization algorithm	Epochs	Activation function	Neurons	Hidden layers	Accuracy	Batch size
ESD-2	SGD	10-100	Relu	75	10	77.69%	64
ESD-2	RMprop	10-100	RRelu	300	20	75.91%	256
ESD-2	ADAM	10-100	Tanh	150	15	76.46%	128

TABLE 6: Proposed method accuracy on ESD-3.

Datasets	Optimization algorithm	Epochs	Activation function	Neurons	Hidden layers	Accuracy	Batch size
ESD-3	ADAM	10-100	RRelu	300	20	76.77%	64
ESD-3	RMprop	10-100	Tanh	75	10	76.27%	128
ESD-3	SGD	10-100	Relu	150	15	77.80%	256

TABLE 7: Proposed method accuracy on ESD-4.

Datasets	Optimization algorithm	Epochs	Activation function	Neurons	Hidden layers	Accuracy	Batch size
ESD-4	ADAM	10-100	Tanh	150	15	76.84%	128
ESD-4	RMprop	10-100	RRelu	300	20	77.92%	256
ESD-4	SGD	10-100	Relu	75	10	76.98%	64

TABLE 8: Selected parameters and hyperparameters.

Activation function	Optimization algorithm	Neurons in hidden layer	Minibatch	Hidden layers	Epochs	Dilation filter size	Dilation width
Relu	Rmprop	150	64	10		2,2,3	
Tanh	ADAM	300	128	15	10	2,2,4	1,2,4
RRelu	SGD	400	256	20	100	2,2,5	

TABLE 9: Proposed method performance metrics on ESD-1.

Datasets	F1-score	Recall	Precision
ESD-1	76.22%	73.67%	79.21%
ESD-1	76.82%	75.98%	76.37%
ESD-1	76.59%	76.28%	76.91%

TABLE 11: Proposed method performance metrics on ESD-3.

Datasets	F1-score	Recall	Precision
ESD-3	75.72%	72.59%	77.10%
ESD-3	75.28%	76.64%	76.39%
ESD-3	76.81%	73.01%	77.24%

TABLE 10: Proposed method performance metrics on ESD-2.

Datasets	F1-score	Recall	Precision
ESD-2	74.26%	71.90%	76.50%
ESD-2	73.36%	71.88%	75.63%
ESD-2	73.61%	72.41%	77.46%

TABLE 12: Proposed method performance metrics on ESD-4.

Datasets	F1-score	Recall	Precision
ESD-4	75.07%	72.60%	77.84%
ESD-4	76.38%	76.64%	75.93%
ESD-4	75.19%	79.08%	76.14%

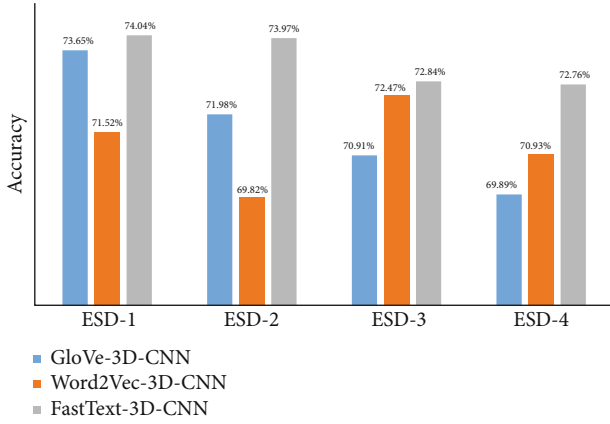


FIGURE 6: Baseline models accuracy on ESD-1, ESD-2, ESD-3, and ESD-4.

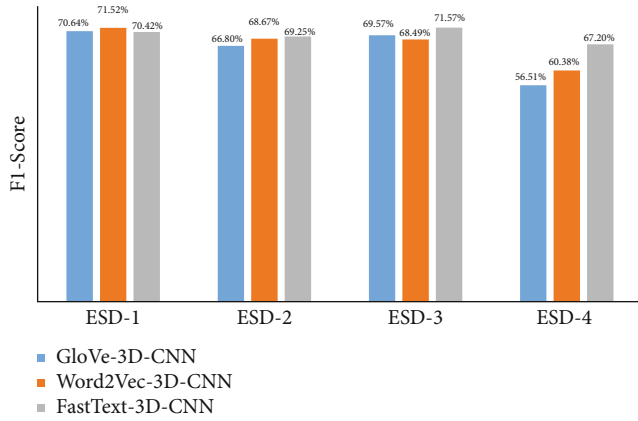


FIGURE 7: Baseline models on F1-score on ESD-1, ESD-2, ESD-3, and ESD-4.

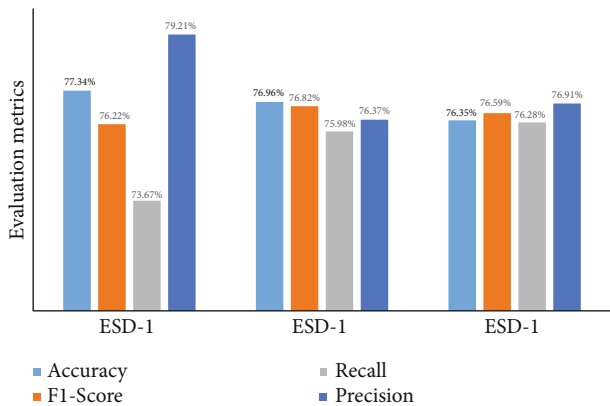


FIGURE 8: Evaluation metrics on proposed method on ESD-1.

concatenation to produce novel contextual concatenated word representation (CCWRs). The maturation of dilated convolution neural network architecture referred to as 3D-CNN is employed to increase the scale of receptive fields with different dilation rates to attain long-term contextual

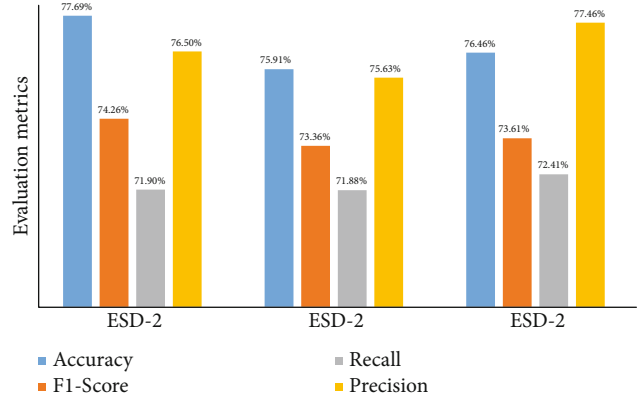


FIGURE 9: Evaluation metrics on proposed method on ESD-2.

regularities. The 3D-CNN architecture incorporates three dilated convolutional layers and a pair of fully connected layers. Following CCWRs, the processing of successive textual data and the computational time is spatially regulated by a succession of text [62].

Throughout this work as evident from Figures 10 and 11, it is observed that merely the stacking process of dilated convolution kernels effectively reduces training time and raises training accuracy to a definite level; however, not satisfactory enough to enhance the testing accuracy. This happens due to discontinuation between the dilated convolutions kernels, which captures minor information causes to neglect the constancy of information. Also, fixed-rate size during the extraction of feature maps, the big and little size information, cannot be considered simultaneously. These issues influence the training as well as testing accuracy of the fixed dilated convolutional model. In our work, novel CCWRs with 3D-CNN dilated varying dilation rates in the multiple layers utilize convolution operations series to capture complete information devoid of holes or missing. This successfully avoids information loss and the problem of testing accuracy using different dilated convolution kernels by increasing receptive field size.

By correlating the multiple distributed word representation model and contextual concatenated word representation model, we acknowledge that the development of CCWRs is significant despite including the small size of the corpus. Our experimentation provides the implementation of 3D-CNN in terms of important revelations such as (i) multiple word representation models by way of weighted concatenation for the generation of contextual representation along with two fully connected layers to classify social media data utilizing the linguistics regarding social media for intelligent applications and (ii) comparing and analyzing the optimization, preference, selection, tuning, and configuration of multiple parameters indicates the significant effect on the entire structure.

Nowadays, data available on social platforms, such as Twitter, is frequently used and has exceptional impacts on making intelligent and informed decisions marking which can be analyzed concerning people’s opinions toward real-world events. Though many methodologies have been examined, it is still unable to mine out of vocabulary, misspelled,

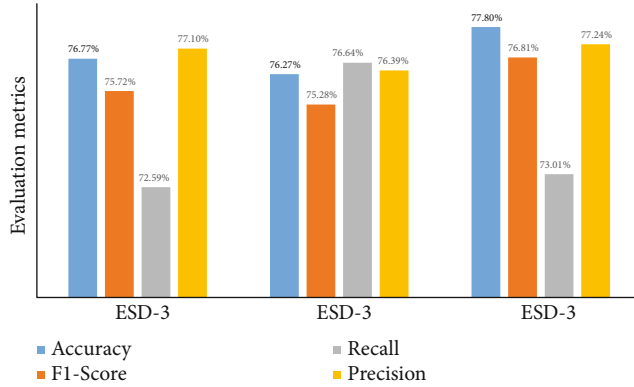


FIGURE 10: Evaluation metrics on proposed method on ESD-3.

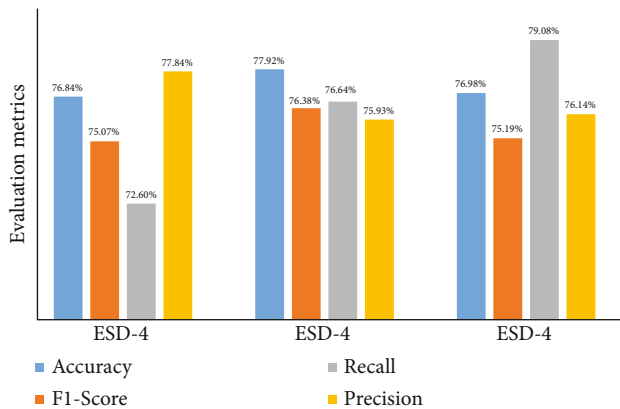


FIGURE 11: Evaluation metrics on proposed method on ESD-4.

and simple words to analyze social insights and the utilization of new neural architectures for intelligent applications. This work is also essential to social media textual data mining algorithm to consider real-world situations like disasters and current COVID-19 that entails well-timed effective techniques by observing people's impulses to assist the government in policy and strategic decisions.

Further, this paper is a significant source of accessibility of authentic, powerful, and evolving techniques concerning authorities necessary to consider the varying situation of the world with multiple variants of COVID-19. More in-depth, the idea can also extend to empower smart cities by contributing new methods through professionals by developing intelligent applications in epidemic situations towards the robustness of techniques and interpretations. To institutionalize intelligent applications regarded as an essential means, there is a need for propositions to use social media textual data mining algorithms in an intelligent environment involving a rapidly increasing social media textual data size. We can say that the development of the proactive, responsive, and cost-effective intelligent application will remain inadequate while performing without inheriting the significance of deep learning approaches and, more importantly, mining of insights of social media data.

## 6. Conclusion

The significance of social media data established an essential mean to realize people's attitudes to improve service. This paper uniquely formulates several hyperparameter tuning, selection, and configurations towards maximum model optimization on different valuation metrics. Proposing contextual concatenated word representations (CCWRs) trained on streamed social media data effectively surpasses various word representation models and overcomes out of vocabulary (OOV) words problem to some extent. Also, a novel proposition of three dilated convolution layers (3D-CNN) upon different dilated convolution kernels at each layer instead of stacking convolutional layers is utilized via a series of experimentations and verifications on multiple datasets. The proposed architecture as the augmentation of CCWRs and (3D-CNN) in the manner above accurately performs with many views such as avoiding loss of detailed, informative messages and capturing the long contextual information. However, it has been concluded that specific extensive training social media data can be helpful to extend evaluation metrics. Further, in our method, the imbalanced training data and subject-based collection of social media data from Twitter through relevant keywords is still a challenge that can be diluted in future work.

## Data Availability

The data used to support the findings of this study are included in the article.

## Conflicts of Interest

The authors declare that they have no conflicts of interest.

## Acknowledgments

This work was supported by the King Saud University, Riyadh, Saudi Arabia, through researchers supporting project number RSP-2021/184.

## References

- [1] P. B. Anand and J. Navío-Marco, "Governance and economics of smart cities: opportunities and challenges," *Telecommunications Policy*, vol. 42, no. 10, pp. 795–799, 2018.
- [2] A. Mainka, S. Hartmann, W. G. Stock, and I. Peters, "Looking for friends and followers: a global investigation of governmental social media use," *Transforming Government: People, Process and Policy*, vol. 9, no. 2, pp. 237–254, 2015.
- [3] C. T. Yin, Z. Xiong, H. Chen, J. Y. Wang, D. Cooper, and B. David, "A literature survey on smart cities," *Science China Information Sciences*, vol. 58, no. 10, pp. 1–18, 2015.
- [4] J. F. F. Pereira, "Social media text processing and semantic analysis for smart cities," 2017, <http://arxiv.org/abs/1709.03406>.
- [5] R. Passonneau, "Sentiment analysis of Twitter data," in *Proceedings of the Workshop on Language in Social Media (LSM 2011)*, pp. 30–38, Portland, Oregon, 2011.

- [6] J. Chin, V. Callaghan, and I. Lam, "Understanding and personalising smart city services using machine learning, the Internet-of-Things and Big Data," in *2017 IEEE 26th International Symposium on Industrial Electronics (ISIE)*, pp. 2050–2055, Edinburgh, UK, 2017.
- [7] K. Lee, D. Palsetia, R. Narayanan, M. M. A. Patwary, A. Agrawal, and A. Choudhary, "Twitter trending topic classification," in *2011 IEEE 11th International Conference on Data Mining Workshops*, pp. 251–258, Vancouver, BC, Canada, 2011.
- [8] B. O'Connor, R. Balasubramanyan, B. R. Routledge, and N. A. Smith, "From tweets to polls: linking text sentiment to public opinion time series," in *ICWSM 2010 - Proceedings of the 4th International AAAI Conference on Weblogs and Social Media*, pp. 122–129, Washington, DC, USA, 2010.
- [9] A. I. Schein, A. Popescul, L. H. Ungar, and D. M. Pennock, "DNA extraction from plant leaves with Minilyis," in *Proceedings of the 25th annual international ACM SIGIR conference on Research and development in information retrieval - SIGIR '02*, pp. 253–260, Tampere, Finland, 2002.
- [10] C. Shekar, S. Wakade, K. J. Liszka, and C. C. Chan, "Mining pharmaceutical spam from Twitter," in *2010 10th International Conference on Intelligent Systems Design and Applications*, pp. 813–817, Cairo, Egypt, 2010.
- [11] A. Zubiaga, D. Spina, V. Fresno, and R. Martínez, "Classifying trending topics: a typology of conversation triggers on Twitter," in *Proceedings of the 20th ACM international conference on Information and knowledge management*, pp. 2461–2464, Glasgow, Scotland, UK, 2011.
- [12] X. Peng, J. Feng, S. Xiao, W.-Y. Yau, J. T. Zhou, and S. Yang, "Structured autoencoders for subspace clustering," *IEEE Transactions on Image Processing*, vol. 27, no. 10, pp. 5076–5086, 2018.
- [13] X. Peng, Z. Yu, Z. Yi, and H. Tang, "Constructing the L2-graph for robust subspace learning and subspace clustering," *IEEE Transactions on Cybernetics*, vol. 47, no. 4, pp. 1053–1066, 2017.
- [14] F. Karim, S. Majumdar, H. Darabi, and S. Chen, "LSTM fully convolutional networks for time series classification," *IEEE Access*, vol. 6, pp. 1662–1669, 2017.
- [15] D. A. Shamma, L. Kennedy, and E. F. Churchill, "Peaks and persistence: modeling the shape of microblog conversations," in *Proceedings of the ACM Conference on Computer Supported Cooperative Work, CSCW*, pp. 355–358, Hangzhou, China, 2011.
- [16] J. Yang and J. Leskovec, "Patterns of temporal variation in online media," in *Proceedings of the 4th ACM International Conference on Web Search and Data Mining, WSDM 2011*, pp. 177–186, Hong Kong, China, 2011.
- [17] A. Conneau, H. Schwenk, L. Barrault, and Y. Lecun, "Very deep convolutional networks for text classification," in *15th Conference of the European Chapter of the Association for Computational Linguistics, EACL 2017 - Proceedings of Conference*, vol. 1, pp. 1107–1116, Valencia, Spain, 2016.
- [18] X. Zhang, J. Zhao, and Y. Lecun, "Character-level convolutional networks for text classification," *Advances in neural information processing systems*, vol. 28, pp. 649–657, 2015.
- [19] Y. Kim, "Convolutional neural networks for sentence classification," in *Proceedings of the 2014 Conference on Empirical Methods in Natural Language Processing (EMNLP)*, pp. 1746–1751, Doha, Qatar, 2014.
- [20] Y. Zhang and B. Wallace, "A sensitivity analysis of (and practitioners' guide to) convolutional neural networks for sentence classification," in *Proceedings of the Eighth International Joint Conference on Natural Language Processing (Volume 1: Long Papers)*, Taipei, Taiwan, 2015.
- [21] T. Mikolov, K. Chen, G. Corrado, and J. Dean, "Efficient estimation of word representations in vector space," in *1st International Conference on Learning Representations, ICLR 2013 - Workshop Track Proceedings*, pp. 1–12, Scottsdale, AZ, USA, 2013.
- [22] J. Pennington, R. Socher, and C. D. Manning, "Glove: global vectors for word representation," in *Proceedings of the 2014 Conference on Empirical Methods in Natural Language Processing (EMNLP)*, pp. 1532–1543, Doha, Qatar, 2014.
- [23] P. Bojanowski, E. Grave, A. Joulin, and T. Mikolov, "Enriching word vectors with subword information," *Transactions of the Association for Computational Linguistics*, vol. 5, pp. 135–146, 2017.
- [24] D. Zeng, K. Liu, S. Lai, G. Zhou, and J. Zhao, "Relation classification via convolutional deep neural network," in *Proceedings of COLING 2014, the 25th International Conference on Computational Linguistics: Technical Papers*, Dublin, Ireland, 2014.
- [25] A. Visvizi, M. D. Lytras, E. Damiani, and H. Mathkour, "Policy making for smart cities: innovation and social inclusive economic growth for sustainability," *Journal of Science and Technology Policy Management*, vol. 9, no. 2, pp. 126–133, 2018.
- [26] E. P. Trindade, M. P. F. Hinnig, E. M. da Costa, J. S. Marques, R. C. Bastos, and T. Yigitcanlar, "Sustainable development of smart cities: a systematic review of the literature," *Journal of Open Innovation: Technology, Market, and Complexity*, vol. 3, no. 1, 2017.
- [27] N. Komninos, "Intelligent cities: towards interactive and global innovation environments," *International Journal of Innovation and regional development*, vol. 1, no. 4, p. 337, 2009.
- [28] M. Lytras, N. R. Aljohani, A. Hussain, J. Luo, and J. X. Zhang, *Cognitive Computing Track Chairs' Welcome & Organization*, pp. 247–250, 2018.
- [29] H. Mora, R. Pérez-delHoyo, J. F. Paredes-Pérez, and R. A. Mollá-Sirvent, "Analysis of social networking service data for smart urban planning," *Sustainability*, vol. 10, no. 12, p. 4732, 2018.
- [30] M. D. Lytras, H. I. Mathkour, H. Abdalla, W. Al-Halabi, C. Yanez-Marquez, and S. W. M. Siqueira, "An emerging - social and emerging computing enabled philosophical paradigm for collaborative learning systems: toward high effective next generation learning systems for the knowledge society," *Computers in Human Behavior*, vol. 51, pp. 557–561, 2015.
- [31] M. D. Lytras, W. Al-Halabi, J. X. Zhang, R. A. Haraty, and M. Masud, "Enabling technologies and business infrastructures for next generation social media: Big Data, cloud computing, Internet of Things and virtual reality," *The Journal of Universal Computer Science*, vol. 21, no. 11, pp. 1379–1384, 2015.
- [32] T. Sakaki, M. Okazaki, and Y. Matsuo, "Tweet analysis for real-time event detection and earthquake reporting system development," *IEEE Transactions on Knowledge and Data Engineering*, vol. 25, no. 4, pp. 919–931, 2013.
- [33] A. Rosi, M. Mamei, F. Zambonelli, S. Dobson, G. Stevenson, and J. Ye, "Social sensors and pervasive services: approaches and perspectives," in *2011 IEEE International Conference on Pervasive Computing and Communications Workshops*,

- PERCOM Workshops 2011, pp. 525–530, Seattle, WA, USA, 2011.
- [34] G. Anastasi, M. Antonelli, A. Bechini et al., “Urban and social sensing for sustainable mobility in smart cities,” in *2013 Sustainable internet and ICT for sustainability, SustainIT 2013*, Palermo, Italy, 2013.
- [35] A. Crooks, A. Croitoru, A. Stefanidis, and J. Radzikowski, “Earthquake: twitter as a distributed sensor system,” *Transactions in GIS*, vol. 17, no. 1, pp. 124–147, 2013.
- [36] E. D’Andrea, P. Ducange, B. Lazzerini, and F. Marcelloni, “Real-time detection of traffic from twitter stream analysis,” *IEEE Transactions on Intelligent Transportation Systems*, vol. 16, no. 4, pp. 2269–2283, 2015.
- [37] A. Signorini, A. M. Segre, and P. M. Polgreen, “The use of Twitter to track levels of disease activity and public concern in the U.S. during the influenza A H1N1 pandemic,” *PLoS One*, vol. 6, no. 5, article e19467, 2011.
- [38] M. Al-Ghalibi, A. Al-Azzawi, and K. Lawonn, “NLP based sentiment analysis for Twitter’s opinion mining and visualization,” in *Eleventh International Conference on Machine Vision (ICMV 2018)*, p. 6, Munich, Germany, 2019.
- [39] F. Abid, M. Alam, M. Yasir, and C. Li, “Sentiment analysis through recurrent variants latterly on convolutional neural network of Twitter,” *Future Generation Computer Systems*, vol. 95, pp. 292–308, 2019.
- [40] F. Bravo-Marquez, M. Mendoza, and B. Poblete, “Combining strengths, emotions and polarities for boosting Twitter sentiment analysis,” in *Proceedings of the second international workshop on issues of sentiment discovery and opinion mining*, pp. 1–9, Chicago, IL, USA, 2013.
- [41] T. Finin, W. Murnane, A. Karandikar, N. Keller, J. Martineau, and M. Dredze, “Annotating named entities in Twitter data with crowdsourcing,” in *Proceedings of the NAACL HLT 2010 Workshop on Creating Speech and Language Data with Amazon’s Mechanical Turk*, vol. 2010, pp. 80–88, Los Angeles, CA, USA, 2010.
- [42] S. Collovini, B. Pereira, H. D. P. dos Santos, and R. Vieira, “Annotating relations between named entities with crowdsourcing,” *Lecture Notes in Computer Science (including subseries Lecture Notes in Artificial Intelligence and Lecture Notes in Bioinformatics)*, vol. 10859 LNCS, pp. 290–297, 2018.
- [43] K. Roberts, M. A. Roach, J. Johnson, J. Guthrie, and S. M. Harabagiu, “EmpaTweet: annotating and detecting emotions on twitter,” in *Proceedings of the 8th International Conference on Language Resources and Evaluation, LREC 2012*, pp. 3806–3813, Istanbul, Turkey, 2012.
- [44] L. Barbosa and J. Feng, “Robust sentiment detection on twitter from biased and noisy data,” *Coling 2010: Posters*, vol. 2, pp. 36–44, 2010.
- [45] M. Avvenuti, S. Cresci, M. N. La Polla, A. Marchetti, and M. Tesconi, “Earthquake emergency management by social sensing,” in *2014 IEEE International Conference on Pervasive Computing and Communication Workshops, PERCOM WORKSHOPS 2014*, pp. 587–592, Budapest, Hungary, 2014.
- [46] S. M. Weiss, N. Indurkha, T. Zhang, and F. J. Damerau, *Text Mining: Predictive Methods for Analyzing Unstructured Information*, Springer New York, 2005.
- [47] R. Zafarani, M. A. Abbasi, and H. Liu, *Social Media Mining: An Introduction*, vol. 9781107018, Cambridge University Press, Cambridge, 2014.
- [48] B. Ait Hammou, A. Ait Lahcen, and S. Mouline, “Towards a real-time processing framework based on improved distributed recurrent neural network variants with fastText for social big data analytics,” *Information Processing & Management*, vol. 57, no. 1, article 102122, 2020.
- [49] A. S. M. Alharbi and E. de Doncker, “Twitter sentiment analysis with a deep neural network: an enhanced approach using user behavioral information,” *Cognitive Systems Research*, vol. 54, pp. 50–61, 2019.
- [50] L. M. Ang, K. P. Seng, A. M. Zungeru, and G. K. Ijamaru, “Big sensor data systems for smart cities,” *IEEE Internet of Things Journal*, vol. 4, no. 5, pp. 1259–1271, 2017.
- [51] L. M. Ang and K. P. Seng, “Big sensor data applications in urban environments,” *Big Data Research*, vol. 4, pp. 1–12, 2016.
- [52] Y. Zheng, L. Capra, O. Wolfson, and H. Yang, “Urban computing: concepts, methodologies, and applications,” *ACM Transactions on Intelligent Systems and Technology (TIST)*, vol. 5, no. 3, 2014.
- [53] K. S. Tai, R. Socher, and C. D. Manning, “Improved semantic representations from tree-structured long short-term memory networks,” in *ACL-IJCNLP 2015 - 53rd Annual Meeting of the Association for Computational Linguistics and the 7th International Joint Conference on Natural Language Processing of the Asian Federation of Natural Language Processing, Proceedings of the Conference*, vol. 1, pp. 1556–1566, Beijing, China, 2015.
- [54] B. Liu, “Sentiment analysis and subjectivity,” *Handbook of Natural Language Processing*, 627–666, 2010.
- [55] A. M. Popescu and O. Etzioni, “Extracting product features and opinions from reviews,” in *HLT/EMNLP 2005 - Human Language Technology Conference and Conference on Empirical Methods in Natural Language Processing, Proceedings of the Conference*, pp. 339–346, Vancouver, British Columbia, Canada, 2005.
- [56] R. Collobert and J. Weston, “A unified architecture for natural language processing,” in *Proceedings of the 25th international conference on Machine learning - ICML ’08*, pp. 160–167, Helsinki, Finland, 2008.
- [57] L. Flekova, O. Ferschke, and I. Gurevych, “UKPDIPF: lexical semantic approach to sentiment polarity prediction in Twitter data,” in *Proceedings of the 8th International Workshop on Semantic Evaluation (SemEval 2014)*, pp. 704–710, Dublin, Ireland, 2014.
- [58] J. Serrano-Guerrero, J. A. Olivas, F. P. Romero, and E. Herrera-Viedma, “Sentiment analysis: a review and comparative analysis of web services,” *Information Sciences*, vol. 311, pp. 18–38, 2015.
- [59] C. N. Dos Santos and M. Gatti, “Deep convolutional neural networks for sentiment analysis of short texts,” in *COLING 2014 - 25th International Conference on Computational Linguistics, Proceedings of COLING 2014: Technical Papers*, pp. 69–78, Dublin, Ireland, 2014.
- [60] F. Yu and V. Koltun, *Multi-Scale Context Aggregation by Dilated Convolutions*, 2015.
- [61] N. Kalchbrenner, L. Espeholt, K. Simonyan, A. van den Oord, A. Graves, and K. Kavukcuoglu, *Neural Machine Translation in Linear Time*, 2016.
- [62] A. V. Oord, S. Dieleman, H. Zen et al., *WaveNet: A Generative Model for Raw Audio*, 2016.
- [63] R. Jozefowicz, O. Vinyals, M. Schuster, N. Shazeer, and Y. Wu, *Exploring the Limits of Language Modeling*, 2016.



- [64] M. E. Peters, W. Ammar, C. Bhagavatula, and R. Power, "Semi-supervised sequence tagging with bidirectional language models," in *ACL 2017 - 55th Annual Meeting of the Association for Computational Linguistics, Proceedings of the Conference (Long Papers)*, vol. 1, pp. 1756–1765, Sanya, China, 2017.
- [65] M. E. Peters, M. Neumann, M. Iyyer et al., "Deep contextualized word representations," in *Proceedings of the 2018 Conference of the North American Chapter of the Association for Computational Linguistics: Human Language Technologies, Volume 1 (Long Papers)*, pp. 2227–2237, New Orleans, LA, USA, 2018.
- [66] W. Yin and H. Schütze, *Multichannel Variable-Size Convolution for Sentence Classification*, 2016.
- [67] T. H. Nguyen and R. Grishman, "Event detection and domain adaptation with convolutional neural networks," in *ACL-IJCNLP 2015 - 53rd Annual Meeting of the Association for Computational Linguistics and the 7th International Joint Conference on Natural Language Processing of the Asian Federation of Natural Language Processing, Proceedings of the Conference*, vol. 2, pp. 365–371, Beijing, China, 2015.
- [68] Y. Chen, L. Xu, K. Liu, D. Zeng, and J. Zhao, *Event Extraction via Dynamic Multi-Pooling Convolutional Neural Networks*, 2015.
- [69] W. Lei, K. Khine, N. Thwet, and T. Aung, *Sentiment Aware Word Embedding Approach for Sentiment Analysis*, 2018.
- [70] J. Acosta, N. Lamaute, M. Luo, E. Finkelstein, and A. Cotoranu, "Sentiment analysis of Twitter messages using Word2Vec," in *Proceedings of Student-Faculty Research Day, CSIS, Pace University*, pp. 1–7, Pleasantville, NY, USA, 2017.
- [71] R. Petrolito and F. Dell'orletta, *Word Embeddings in Sentiment Analysis*, 2018.
- [72] A. Akbik, D. Blythe, and R. Vollgraf, *Contextual String Embeddings for Sequence Labeling*, 2018.
- [73] J. Devlin, M. W. Chang, K. Lee, and K. Toutanova, "BERT: pre-training of deep bidirectional transformers for language understanding," in *Proceedings of the 2019 Conference of the North American Chapter of the Association for Computational Linguistics: Human Language Technologies, Volume 1 (Long and Short Papers)*, pp. 4171–4186, Minneapolis, MN, USA, 2019.
- [74] E. H. Alkhamash, J. Jussila, M. D. Lytras, and A. Visvizi, "Annotation of smart cities twitter micro-contents for enhanced citizen's engagement," *IEEE Access*, vol. 7, pp. 116267–116276, 2019.
- [75] A. Zubiaga, "A longitudinal assessment of the persistence of twitter datasets," *Journal of the Association for Information Science and Technology*, vol. 69, no. 8, pp. 974–984, 2018.
- [76] J. Gu, Z. Wang, J. Kuen et al., "Recent advances in convolutional neural networks," *Pattern Recognition*, vol. 77, pp. 354–377, 2018.
- [77] C. Gan, L. Wang, Z. Zhang, and Z. Wang, "Sparse attention based separable dilated convolutional neural network for targeted sentiment analysis," *Knowledge-Based Systems*, vol. 188, 2019.
- [78] *Twitter event datasets (2012-2016)*, November 2019, [https://figshare.com/articles/Twitter\\_event\\_datasets\\_2012-2016\\_/5100460](https://figshare.com/articles/Twitter_event_datasets_2012-2016_/5100460).
- [79] *TAGS Twitter Archiving Google Sheet*, November 2019, <https://tags.hawksey.info/>.
- [80] C. Manning, M. Surdeanu, J. Bauer, J. Finkel, S. Bethard, and D. McClosky, *The Stanford CoreNLP Natural Language Processing Toolkit*, pp. 55–60, 2015.
- [81] B. Chiu, G. Crichton, A. Korhonen, and S. Pyysalo, "How to train good word embeddings for biomedical NLP," in *Proceedings of the 15th Workshop on Biomedical Natural Language Processing*, pp. 166–174, Berlin, Germany, 2016.
- [82] A. C. Ian Goodfellow and Y. Bengio, "Deep learning," *Genetic Programming and Evolvable Machines*, vol. 19, no. 1–2, pp. 305–307, 2017.
- [83] B. Xu, N. Wang, T. Chen, and M. Li, *Empirical Evaluation of Rectified Activations in Convolutional Network*, 2015.
- [84] J. Heaton, "The number of hidden layers," in *Introduction to Neural Networks for Java*, pp. 157–158, Heaton Research, Inc., 2008.
- [85] *TensorFlow*, 2016, November 2019, <https://www.tensorflow.org/>.

## Research Article

# Mobile Edge Computing Enabled Efficient Communication Based on Federated Learning in Internet of Medical Things

Xiao Zheng,<sup>1</sup> Syed Bilal Hussain Shah ,<sup>2</sup> Xiaojun Ren,<sup>3</sup> Fengqi Li,<sup>2</sup> Liqaa Nawaf ,<sup>4</sup> Chinmay Chakraborty ,<sup>5</sup> and Muhammad Fayaz <sup>6</sup>

<sup>1</sup>School of Computer Science and Technology, Shandong University of Technology, Zibo, Shandong, China

<sup>2</sup>School of Mechanical and Electronic Engineering, Dalian Jiaotong University, Dalian, China

<sup>3</sup>Blockchain Laboratory of Agricultural Vegetables, Weifang University of Science and Technology, Weifang, Shandong, China

<sup>4</sup>Computer Science School of Technologies, Cardiff Metropolitan University, UK

<sup>5</sup>Birla Institute of Technology Ranchi Jharkhand, Jharkhand, India

<sup>6</sup>Department of Computer Science, University of Central Asia, Naryn, Kyrgyzstan

Correspondence should be addressed to Muhammad Fayaz; [muhammad.fayaz@ucentralasia.org](mailto:muhammad.fayaz@ucentralasia.org)

Received 23 September 2021; Accepted 14 October 2021; Published 27 October 2021

Academic Editor: Shalli Rani

Copyright © 2021 Xiao Zheng et al. This is an open access article distributed under the Creative Commons Attribution License, which permits unrestricted use, distribution, and reproduction in any medium, provided the original work is properly cited.

The rapid growth of the Internet of Medical Things (IoMT) has led to the ubiquitous home health diagnostic network. Excessive demand from patients leads to high cost, low latency, and communication overload. However, in the process of parameter updating, the communication cost of the system or network becomes very large due to iteration and many participants. Although edge computing can reduce latency to some extent, there are significant challenges in further reducing system latency. Federated learning is an emerging paradigm that has recently attracted great interest in academia and industry. The basic idea is to train a globally optimal machine learning model among all participating collaborators. In this paper, a gradient reduction algorithm based on federated random variance is proposed to reduce the number of iterations between the participant and the server from the perspective of the system while ensuring the accuracy, and the corresponding convergence analysis is given. Finally, the method is verified by linear regression and logistic regression. Experimental results show that the proposed method can significantly reduce the communication cost compared with the general stochastic gradient descent federated learning.

## 1. Introduction

The Internet of Medical Things (IoMT) is using a variety of communication systems to connect many devices to form best-in-class systems that can detect, collect, exchange, analyze, and transmit valuable communications [1, 2], helping companies manage smarter and deliver faster business solutions. IoMT can build a large number of applications through various “smart” sensors such as artificial intelligence and machine learning (ML) technology, thereby revolutionizing the ubiquitous computing system [3, 4]. Secure communications and sensing technologies can leverage a participatory approach to implement integrated solutions

while establishing new applications relevant to the industry, particularly healthcare. One of the key applications of 5G-based IoMT is healthcare, which is aimed at maintaining patients’ medical information in electronic environments (such as cloud and edge cloud) systems through the latest telecom paradigm [5, 6]. For healthcare applications, ML models are typically trained on enough user data to track health status information. Traditional machine learning methods such as support vector machine (SVM), decision tree (DT), and hidden Markov model (HMM) can be used in a variety of healthcare applications [7]. Patterns are analyzed and classified based on the construction of explicit or implicit models, and its ML method has been used to

improve the detection rate of malicious data [8]. However, they still have many problems in detecting new or evolving malicious data, and the accuracy of unsupervised anomaly detection used to detect new security is low [9]. As the number of variants grew, this became a major bottleneck, mainly because of the amount of work required to gather enough datasets. In addition, when new features from different network layers need to be combined to deal with the evolving malicious data, the learned classifier cannot be directly used to test the data with different feature spaces [10]. This paper attempts to overcome these challenges, which involve data aggregation with security and privacy protection. First, in the real world, data often exists in separate, decentralized forms. Although there is a lot of data in different sensors, it is not shared due to privacy and security concerns [11]. If the same user uses data from two different sensors, the data stored in different clouds cannot be exchanged, making it difficult to train powerful models with valuable data. Another important issue is personalization based on feature data, most of which are based on a common server model for almost all users. After capturing enough user data, train a satisfactory machine learning model, which itself is distributed to all user devices that can track health information on a daily basis, but the program lacks personalization. It can be seen that different users have different characteristics and daily behavior models. As a result, general models cannot deliver personalized healthcare. Based on this idea, a federated transfer learning algorithm is proposed, which is an IoMT-enabled intelligent healthcare framework named FT-IoMT Health [12]. FT-IoMT Health can solve the problem of data decentralization and model personalization through federated learning and homomorphic multiparty encryption methods [13]. FT-IoMT Health aggregates data from different systems to build powerful machine learning models and appropriately protect user privacy. After building the cloud model, FT-IoMT Health utilizes migration learning to implement a personalized model for each network entity [14]. Transfer learning is a novel machine learning technology, which utilizes knowledge learned from related training (source) sets to improve the prediction accuracy of test (target) sets with almost no label data [15] and enables the framework to update gradually. FT-IoMT Health is scalable and used in many healthcare applications, enabling them to constantly update their learning capabilities every day.

In short, the main contributions of the paper are as follows:

- (1) This paper proposes an algorithm, FT-IoMT Health, which is the first federated migration learning mechanism based on IoMT. This mechanism aggregates data from different entities without compromising privacy and security and obtains relatively personalized models by means of transfer learning
- (2) On the basis of known data analysis, transfer learning technique is used to detect new unknown data analysis. The use of transfer learning itself is the

main advantage of enhancing the adaptability of the detection model

- (3) This paper validates FT-IoMT Health's superior performance in identifying human activity on UCI smartphones. The experimental results show that FT-IoMT Health greatly improves the recognition accuracy compared with traditional ML methods

## 2. Related Work

In traditional healthcare applications, it is important to note that models are typically built by aggregating all user data. In practice, however, data is often separated and difficult to share due to privacy issues, and the models built by applications lack the characteristics of model personalities. A well-known network data detection technique is signature-based detection, which is based on the deep information of the specific characteristics of each detection. Another technique used for network data detection is supervised learning [16, 17]. Both studies were less accurate in detecting new data because they typically relied on known cases of detection. Federated machine learning was first proposed by Google [18]; since the phone is distributed throughout its life cycle, Google trains the machine learning model on this machine, with the primary purpose of protecting user data in the program. Federated learning is a technical approach to solve the problem of data discreteness through the training of privacy models in networks. The goal of transfer learning is to transfer information from known related fields to new fields, so as to achieve the purpose of analogical reasoning, and the main goal is to reduce the distribution differences between different fields. Therefore, there are two main implementation methods: instance reweighting [19] and feature matching [20]. Recently, deep transfer learning technology has made great achievements in many applications. FT-IoMT Health mostly involves deep transfer learning. Many methods assume the feasibility of training data, which is obviously unrealistic. FT-IoMT Health builds deep migration learning into a federated learning framework, eliminating the need to access raw user data. Therefore, this achieves the goal of greater security.

The point of federated transfer learning here is that samples or features do not have more in common. In recent years, a number of researchers have begun to dabble in the field. In [12], Liu et al. put forward a secure federated transfer learning algorithm in a two-party privacy protection environment, which paid more attention to data security. Most studies also propose a federated domain adaptive approach, which extends the domain adaptive approach to federated setting constraints to achieve data privacy and domain transformation. Although a great deal of research work continues to develop rapidly, there are still many challenges in the practical application of federated transfer learning. The work in this paper is the first federated transfer learning mechanism designed specifically for IoMT applications and will therefore be extended by a variety of transfer learning technologies.

### 3. System Model

**3.1. Problem Definition.** Take data from  $N$  different users, the user is represented as  $\{U_1, U_2, \dots, U_N\}$ , and the reading value of the sensor providing the data is defined as  $\{\mathcal{D}_1, \mathcal{D}_2, \dots, \mathcal{D}_N\}$ . The conventional method trains the general model  $\mathcal{M}_{\text{GEN}}$  by combining all the data  $\mathcal{D} = \{\mathcal{D}_1 \cup \mathcal{D}_2 \dots \cup \mathcal{D}_N\}$ . All data should have different distributions. In response to our proposed problem, we aim to gather on all data to train the federated model  $\mathcal{M}_{\text{FED}}$ , in which no user  $U_i$  will disclose these data  $\mathcal{D}_i$  to each other. If we define the accuracy as  $\mathcal{A}$ , the goal of FT-IoMT Health is to guarantee that the accuracy of federated learning is approximately or better than the accuracy of the following conventional learning:  $\mathcal{A}_{\text{FED}} - \mathcal{A}_{\text{GEN}} > \delta$ , where  $\delta$  is a very small positive real number.

FT-IoMT Health is aimed at leveraging joint transfer learning technology to obtain accurate personal healthcare information without compromising user privacy. Figure 1 shows a profile of the mechanism. Suppose there exist  $N$  users (network data) and one server, and then, expand them to a more general situation. The main components of the framework are described below. First, train the cloud model on the server based on a common dataset. Therefore, the cloud model is distributed to all users so that each user will train his model on his own dataset. The user model is then uploaded to the cloud for training the new cloud model using model aggregation. Finally, each user will implement personalized models to train users based on cloud models, network data, and predictive future data. In this process, due to the large distribution difference between server data and user data, the transfer learning method is adopted to make the model more suitable for users, as shown on the right end of Figure 1. It is important to note that none of the parameter sharing processes will include user data leaked through homomorphic encryption.

The federated learning model is an important computation model for the entire FT-IoMT Health mechanism. Its role in the whole process is to deal with model construction and parameter sharing. The server model will be directly applied to users after the learning and training process. This is exactly a way based on traditional healthcare applications applied to model learning. Obviously, the probability distribution of the samples in the server and the data generated by each user is very different. Therefore, it is difficult for the general model to achieve personalized settings of the data model. In addition, due to privacy security issues, the user model cannot easily achieve continuous model updates.

**3.2. Federated Learning.** FT-IoMT Health uses the federated learning paradigm to implement training and sharing of encryption models, and its steps mainly involve the following two key parts: namely, cloud and user model learning. For FT-IoMT Health, deep neural networks are used to learn cloud and user models. The deep neural network uses the original input of user data as the network input for end-to-end feature learning and classifier training, where  $f$  represents the server model to be learned, and the learning goal is

$$\underset{\theta}{\operatorname{argmin}} L = \sum_{i=1}^N L(y_i, f(x_i)), \quad (1)$$

where  $L(*, *)$  indicates network loss function such as cross-entropy loss for classification tasks,  $\{x_i, y_i\}$  is a sample of server data, and its size is  $N$ .  $\theta$  represents all the parameters to be learned, namely, weights and bias.

After obtaining the cloud model, distribute it to all users. From the obstacle in Figure 1, direct sharing of user info will be prohibited. The process exploits homomorphic encryption to prevent info leakage. Due to the fact that encryption is not a subject to be considered, only the procedure of homomorphic encryption applying the addition of real numbers is explained. Therefore, this can complete parameter sharing without leaking any user information. We apply federated learning to aggregate user data without compromising privacy and security. Therefore, the learning goal for user  $u$  is defined as

$$\underset{\theta^u}{\operatorname{argmin}} L_u = \sum_{i=1}^N y_i^u, f_u(x_i^u). \quad (2)$$

After completing the training of all user models  $f_u$  according to the shared cloud model, upload them to the server for aggregation. It can be seen from the evaluation that in the case of shared initialization, the method of federated averaging [21] can be adopted to average the model to achieve good performance in reducing loss. Therefore, following [21], align the user model by the model average value, and then, perform the cloud model update average value on  $b$  user models in each training round. The updated cloud model is expressed as

$$f(\bar{w}) = \frac{1}{B} \sum_{b=1}^B f_{u_b}(w), \quad (3)$$

where  $w$  is the parameter of the network and  $B$  is the number of users. After enough iterations, the updated server model  $\bar{f}$  has better generalization capabilities. Then, new users can join the next round of server model training. Therefore, FT-IoMT Health has incremental learning functions.

**3.3. Transfer Learning.** Apply transfer learning technology to improve the detection of new network data analysis by transferring the information learned from known network data analysis, so as to distinguish between the common coarse feature model for all users and the fine-grained feature model for personalized user. The expression source and target are used to define the training and test datasets in the machine learning task, respectively. Both source and target data are represented by normal flow records and abnormal flow records. The purpose of this transfer learning is to adapt source data to assist distinguish new detections from the target, thereby building a personalized model for each user.

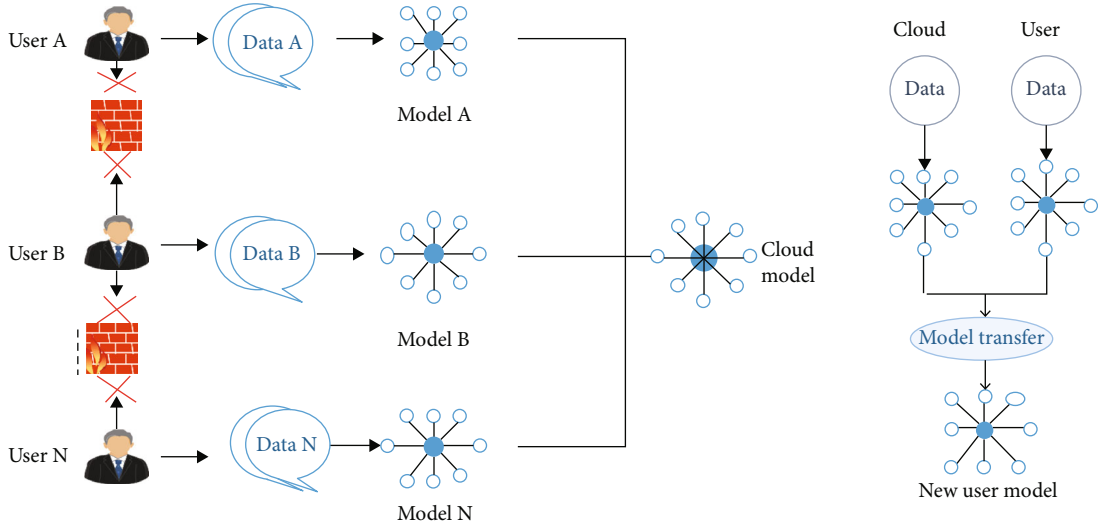


FIGURE 1: Overview of FT-IoMT Health framework.

The transfer learning mechanism is composed of the following three major processes: (1) feature extraction process (obtained from the original network), (2) feature-based learning process, and (3) supervised classification process. The first step is to perform data tracking on the original network to extract features based on the statistical calculation of network traffic. In the second step, a feature-based transfer learning algorithm is used to learn the new feature representation from both the source data and the target data, and the new representation will be fed to the general basic classifier.

The data detection is modeled as a binary classification problem, i.e., the data state is classified as malicious or normal. Assume a source training instance  $S = \{X | x_i\}$ ,  $X \in R^m$  with label  $L_S = y_i$ , and target data  $T = \{Z | z_i\}$ ,  $Z \in R^n$ , where  $X$  and  $Z$  are both users' data extracted from the network.  $X$  and  $Z$  come from different distributions  $P_S(X) \neq P_T(X)$ ,  $X$  and  $Z$  have different dimensions,  $R^m \neq R^n$ . Our goal is to accurately predict the label on  $T$ .

The method is to apply new public latent space through spectrum transformation, in which the distribution of malicious examples is similar, but the distance between discriminatory ones is still very different. The ultimate purpose is to learn a new representation of the original data and target data in the  $k$ -dimensional latent semantic space, namely,  $V_S \in R^k$ ,  $V_T \in R^k$ , so that it can use  $V_S$  and  $V_T$  instead of the original  $S$  and  $T$  better against malicious data sort. Its key purpose is given in Figure 2, because in the new projected public latent space (Figure 2(c)), the distribution of malicious A and malicious B are indistinguishable, even though they are in their original 2D and 3D spaces.

The following discusses how to search the public latent subspace. The optimal subspace is described in the following.

**3.3.1. Optimization.** Based on the given source data  $S$  and target data  $T$ , find the best projection of  $S$  and  $T$  on the best

subspace  $V_S$  and  $V_T$  on the basis of the optimization goals given below:

$$\min_{V_S, V_T} L(V_S, S) + L(V_T, T) + \gamma \cdot D(V_S, V_T), \quad (4)$$

where  $L(*, *)$  is a distortion function used to evaluate the difference between the original data and the projection data and  $D(V_S, V_T)$  indicates the projection difference between the source data and the target data.  $\gamma$  is a trade-off parameter used to control the resemblance between two datasets.

Therefore, the first two components of (4) can assure that the projection data is as consistent as possible with the original data structure. Define  $L(*, *)$  as follows:

$$L(S, V_S) = \|S - P_S * V_S\|, L(T, V_T) = \|T - P_T * V_T\|, \quad (5)$$

where  $V_S$  and  $V_T$  are realized via a linear transformation with linear mapping matrices expressed as  $R_S \in R^{k \times m}$  and  $P_T \in R^{k \times n}$  to the source data and target data.  $\|X\|^2$  indicates the Frobenius norm, which is also denoted as the matrix trace norm. In another point of view,  $P'_S \in R^{k \times m}$  and  $P'_T \in R^{k \times n}$  project the original data  $S$  and  $T$  into a  $k$ -dimensional space, in which the projected data are equivalent ( $L(S, V_S) = \|SP'_S - V_S\|^2$ ). But it can produce trivial solutions  $P_S = 0$ ,  $V_S = 0$ . Therefore, Equation (5) will be applied. It is regarded as matrix factorization, which is a well-known advantageous tool for extracting latent subspaces while maintaining the original data structure.

According to  $L(*, *)$  to define  $\Delta(V_S, V_T)$  as

$$\Delta(V_S, V_T) = L(V_S, V_T), \quad (6)$$

which represents the difference between the projection target data and the source data. Therefore, based on the minimized

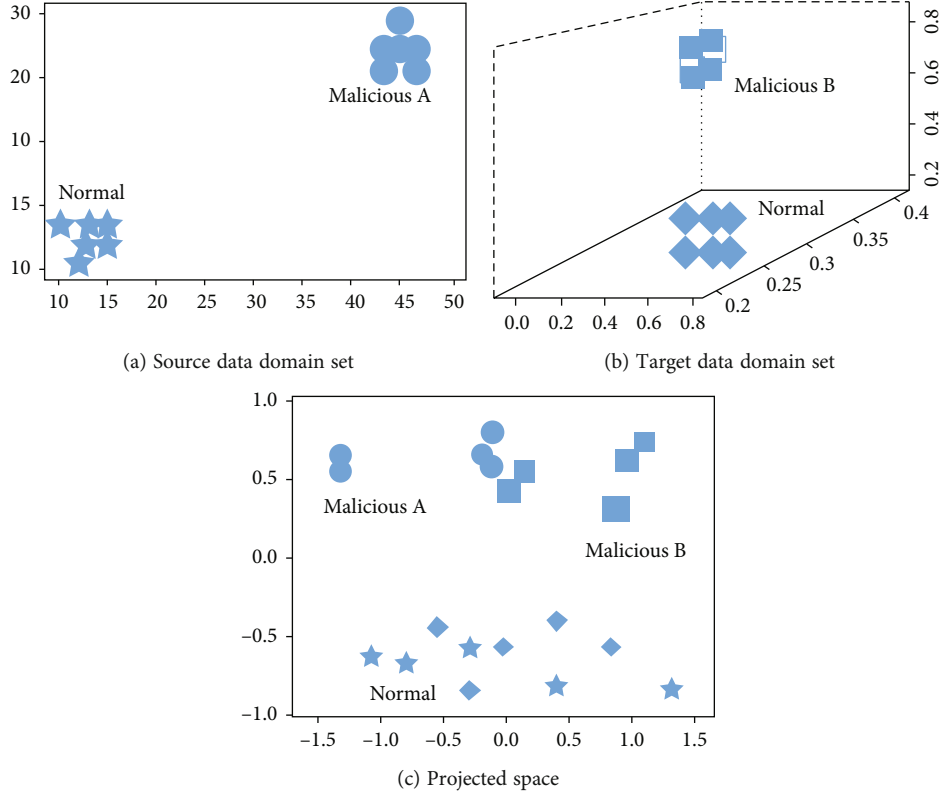


FIGURE 2: Overview of the proposed feature space transformation form.

difference function (6), the source data and target data constraints of the projection are similar.

Substituting (5) and (6) into (4), the following optimization goals to minimize with respect to  $V_S$ ,  $V_T$ ,  $P_S$ , and  $P_T$  are as follows:

$$\begin{aligned} \min_{V'_S V_S = I, V'_T V_T = I} \nabla(V_S, V_T, P_S, P_T) &= \min_{V'_S V_S = I, V'_T V_T} \\ &= I \|S - V_S P_S\|^2 + \|T - V_T P_T\|^2 + \gamma \cdot (\|V_T - V_S\|^2). \end{aligned} \quad (7)$$

Therefore, the loss function of the user model can be calculated by the following formula:

$$\begin{aligned} \operatorname{argmin}_{\theta^s} L_s &= \sum_{i=1}^N L(y_i, f(x_i)) + \sum_{i=1}^{N_s} L(y_i^s, f_s(x_i^s)) + \|S - V_S P_S\|^2 \\ &\quad + \|T - V_T P_T\|^2 + \gamma \cdot (\|V_T - V_S\|^2). \end{aligned} \quad (8)$$

The learning process of FT-IoMT Health is given in Algorithm 1. The framework will work continuously with newly emerging user data. When faced with new user data, FT-IoMT Health can simultaneously update the user model and the network-based cloud model. Thus, the longer the user spends data, the more personalize the model. In addition to transfer learning, other common methods

(e.g., incremental learning) are also implanted in FT-IoMT Health for personalized settings.

## 4. Experiments

**4.1. Datasets.** We employ a public human action recognition dataset named UCI smartwatch. The dataset involves 6 actions gathered from 35 users who use smartwatch around their wristband. 10 accelerometer and gyroscope data channels are gathered at a constant rate of 50 Hz. There exist 10,300 cases. To construct the subject status in FT-IoMT Health, five relevant topic features (content IDS 31-35) are extracted from them, and they are regarded as independent users, who will not share data because of privacy security. The data of the remaining 30 users is used to train the cloud model. Then, the goal is to use the cloud model and all 5 independent objects to improve the accuracy of the activity recognition of these 5 objects without compromising privacy. Consider it is a simplification of the framework in Figure 2, where there are 5 users.

For the feature transfer learning used in the construction of the personalized model, we mainly analyze from the network data detection. The network functions that contains can be summarized into three groups: here, we focus on studying the traffic data features, which are generally extracted by flow analysis tools, and content features, which need to deal with grouping content.

**4.2. Specific Implementation Steps.** Both the server and the user side use CNN for training and testing. The cyber

- 1: **Input:**  $T, S, \gamma, k, \{\mathcal{D}_1, \mathcal{D}_2, \dots, \mathcal{D}_N\}$ , learning rate  $\alpha$ , steps = 500
- 2: **Output:**  $f_u, V_S, V_T$
- 3: Construct an initial cloud model  $f$  with common datasets applying Equation (1)
- 4: Distribute  $f$  to all users
- 5: Train user model by Equation (2)
- 6: All user models are updated to the server through homomorphic multiparty encryption. Perform aggregation on the model employing Equation (3). Then, the server treats the aggregation model as the updated cloud model  $\bar{f}$ .
- 7: Distribute  $\bar{f}$  to all users and then execute transfer learning on each user to obtain their model  $f_u$  Applying Equation (8)
- 8: **while** optimized function Equation (7) not converge **do**
- 9:     Update  $V_T$  by gradient descent with  $V_T = V_T - \alpha(\partial\nabla/\partial V_T)$
- 10:    Update  $V_S$  by gradient descent with  $V_S = V_S - \alpha(\partial\nabla/\partial V_S)$
- 11:    Update  $P_T$  by gradient descent with  $P_T = P_T - \alpha(\partial\nabla/\partial P_T)$
- 12:    Update  $P_S$  by gradient descent with  $P_S = P_S - \alpha(\partial\nabla/\partial P_S)$
- 13:    step++
- 14: **end**
- 15: Repeat the above process for new user data constantly appearing

ALGORITHM 1: The learning process of FT-IoMT Health.

consisted of the following 2 convolutional layers, 2 pooling layers and 3 fully connected layers, which employ a  $1 \times 9$  convolution size. It is optimized using small batch stochastic gradient descent (SGD). In the training process, 80% of the training data is used for model training, and the remaining 20% is used for assessment. Set user  $B = 5$  and fixed. When the batch size is 64 and the training period is set to 80, the learning rate  $\alpha$  is set to 0.01. Model network data detection as a binary classification issue to differentiate malicious traffic from normal one.

To effectively assess the transfer learning method, source and target datasets will be generated as follows. To assess the performance of the transfer learning method in detecting unknown model variants in the cloud, so as to construct personal model, the problem is regarded as a detection that only exists in the target network but is not visible in the source network. Suppose there is one data detection in the source and another detection in the target. Therefore, the distribution of detection feature value between the source and the target is different. Therefore, three datasets are reconstructed, each of which includes a series of randomly chosen normal cases and a set of detections from one category. Here, one of the datasets is set as the target, and the other dataset is set as the source. Therefore, there are mainly the following three detection tasks: Seen  $\rightarrow$  Unseen (i.e., source Seen data for training, target Unseen data (new network) for testing), Seen  $\rightarrow$  Detection, and Detection  $\rightarrow$  Unseen. It is presumed that the feature space between the source and target is the identical. The accuracy of user  $u$  is computed by the following formula:  $\mathcal{A}_u = |X : X \in \mathcal{D}_u \wedge \tilde{y}(X) = y(X)| / |X : X \in \mathcal{D}_u|$ , where  $y(X)$  and  $\tilde{y}(X)$  define the true and predicted labels on  $X$ , respectively. Perform federated learning according to homomorphic encryption. During the transfer learning period, all convolution and pooling layers in the network are frozen, and only the parameters of the fully connected layer are updated using SGD. To verify the validity of FT-IoMT Health, its performance was compared with conventional deep learning

(DL). In traditional deep learning, we only use the primary server model and other conventional machine learning modes to record each the performance of each subject. The hyperparameters used in all comparison methods are adjusted by cross-validation. To achieve a fair study, all experiments were performed 5 times to record the average accuracy. Table 1 shows the performance comparison between the detection technologies proposed based on FT-IoMT and the benchmark method. Table 2 shows the accuracy of activity classification for each topic. Figure 3 indicates the ROC curve. Figure 4 compares FT-IoMT with other transfer learning methods. Figure 5 shows the results of extending FT-IoMT through other transfer learning methods.

**4.3. Evaluation.** FT-IoMT achieves the best classification accuracy for all users. From the outcomes in Tables 1 and 2, it can be concluded that FT-IoMT Health has importantly enhanced performance in all examples. Compared with DL, it slightly increases the average result by 5.6%. Mainly due to the fact that federated learning can be used indirectly for more info from distributed data model to train better and applying transfer learning, the model can be more personalized for each user's features. Compared with traditional methods such as KNN, SVM, and RF, FT-IoMT Health also significantly enhances the recognition outcomes. Overall, it proves the validity of the FT-IoMT Health mechanism. For activity recognition, the results also show that deep learning methods (DL and TL-IoMT) attain better outcomes than conventional modus.

It is controlled by the representation capabilities of deep neural networks, while conventional modus depend on manual feature learning. Deep learning also has another advantage of enabling the online update model to be incrementally updated without retraining, while conventional modus need further incremental algorithms. The performance is very valuable in model reuse and federated transfer learning. In view of the unseen new network data detection

TABLE 1: Classification accuracy of the test objective.

Subject	KNN	SVM	RF	DL	FT-IoMT Health
$P_1$	82.6	80.8	86.7	93.4	97.6
$P_2$	87.4	95.7	94.6	94.1	97.8
$P_3$	91.8	96.8	87.5	92.6	99.7
$P_4$	84.5	94.8	90.3	94.8	98.9
$P_5$	91.3	97.9	92.1	91.9	99.8
AVG	87.5	93.2	90.2	93.2	99.1

TABLE 2: Accuracy of unprediction network detection.

Datasets	Method	SVM	KNN	RF
Seen→Unseen	No-TL	0.51	0.52	0.54
	TL-IoMT	0.82	0.81	0.80
Seen→Detection	No-TL	0.76	0.75	0.65
	TL-IoMT	0.87	0.82	0.80
Detection→Unseen	No-TL	0.50	0.52	0.53
	TL-IoMT	0.84	0.82	0.81

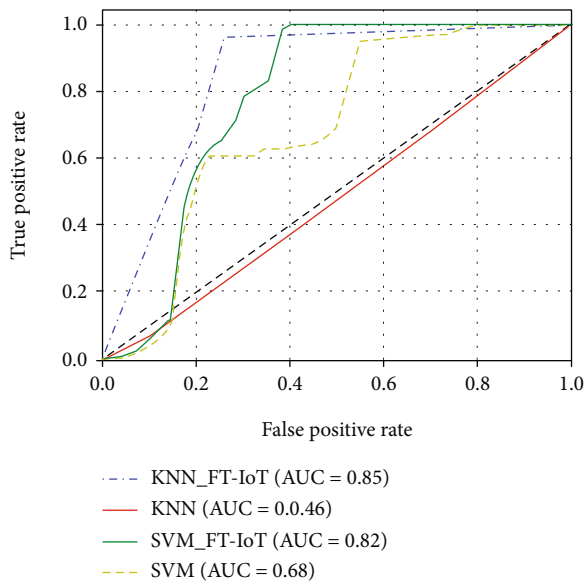


FIGURE 3: ROC curve on Seen→Unseen.

environment, we will compare the performance of FT-IoMT Health with common basic classifiers, instead of using the transfer learning method for the three detection tasks. We chose random forest (RF), SVM, and KNN as common basic classifiers. From the ROC curve illustrated in Figure 3, it will be seen that FT-IoMT Health has improved the detection rate compared to the baseline. Comparison of IoT-based transfer learning methods: we have used other feature-based transfer learning methods (such as HeMap [22] and CORrelation ALignment (CORAL) [23]) to evaluate FT-IoMT network data detection tasks. From the outcomes

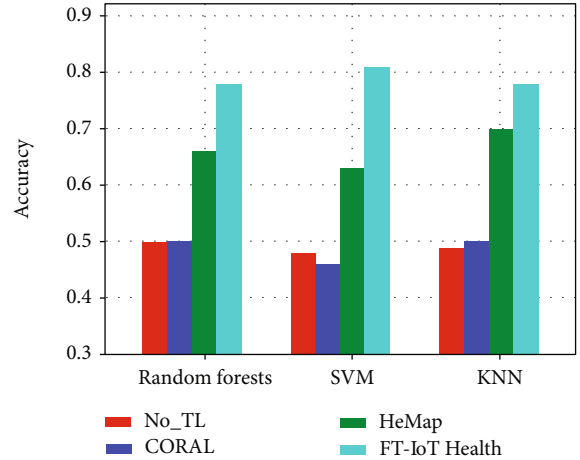


FIGURE 4: Performance comparison of feature-based transfer learning on Seen→Unseen.

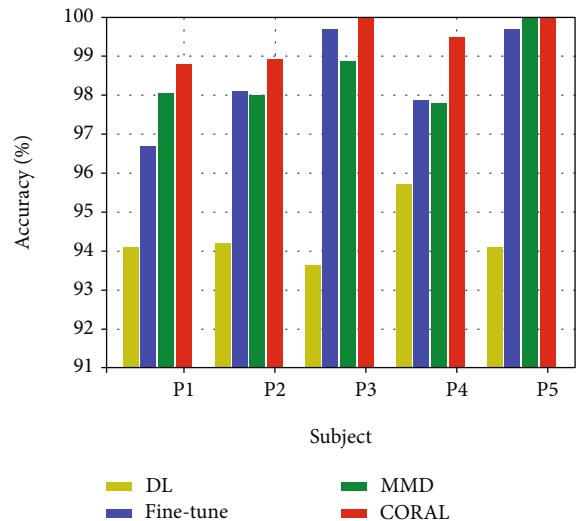


FIGURE 5: Extending FT-IoMT with other transfer learning approaches.

illustrated as Figure 4, it can be achieved that the performance of FT-IoMT is better than other feature-based methods in all classifiers for network data detection tasks. There exist two adjustable parameters, the similarity confidence parameter  $\gamma$  and the size of the new feature space  $k$ , which will be set manually or automatically by experiential research. There are methods for automatically determining the best parameters, for example, by calculating the similarity degree between the source and the target data to determine the similarity confidence parameter  $\gamma$ . In this work, a small labeled dataset (300 labeled) is used in the test set to search the best parameters.

For the use of other transfer learning methods to expand FT-IoMT Health, using different transfer learning methods to analyze the scalability of FT-IoMT Health, it uses two methods to compare its performance: (1) fine-tune, by only fine-tune the network on each subject, it will not significantly reduce the distribution difference between sets; (2)



TABLE 3: Classification accuracy of every subject in arm swing and postural normal tremor.

Subject	KNN	SVM	RF	DL	FT-IoMT Health	Upper bound
Arm swing						
$P_1$	37.2	41.5	45.1	50.2	74.7	87.9
$P_2$	45.3	47.6	49.2	58.5	91.2	99.4
$P_3$	56.2	55.7	53.4	63.6	86.4	87.5
$P_4$	63.8	62.0	56.7	69.4	94.6	100
$P_5$	84.9	73.6	66.6	71.3	85.7	88.4
AVG	57.5	56.0	54.2	62.6	86.5	92.6
Postural tremor						
$P_1$	51.3	46.5	58.3	46.2	84.3	86.2
$P_2$	52.5	58.7	56.9	60.4	75.8	85.9
$P_3$	64.8	54.1	56.1	58.7	68.6	75.6
$P_4$	58.6	59.2	52.7	62.8	71.4	86.8
$P_5$	65.2	53.6	52.0	59.2	69.1	76.4
AVG	58.4	54.5	55.2	57.4	73.8	82.4

MMD (Maximum Mean Difference) is used for transfer, and MMD loss is used instead of alignment loss. The comparison outcome is shown in Figure 5. It will be seen from the figure that in addition to alignment loss, FT-IoMT Health can also attain desirable outcomes through fine-tuning or MMD.

The outcomes of transfer learning are greatly better than no transfer in average accuracy. It shows that the transfer learning process of FT-IoMT Health is very valid and scalable. Thus, FT-IoMT Health is universal and will be expanded in many fields by merging other transfer learning algorithms. In addition, other encryption algorithms can also be used to extend the federated learning, which may be a future research direction.

## 5. Application of Assistance in Diagnosis and Treatment of Neurological Diseases

Parkinson's disease is generally a neurological disease characterized by some motor symptoms, so biosensors can be used in IoMT to help diagnose [24]. In addition, patient data is also a privacy-sensitive problem and must be resolved through federated learning. Therefore, FT-IoMT Health is applied to assist in diagnosis and treatment of Parkinson's disease and is arranged in hospitals. After training the user model on the user side, the patient downloads it to the biosensor and connects to the network to update it during the next access. This allows users to detect and obtain real-time feedback on their own, so as to more easily obtain disease status.

Based on this, a biosensing application was developed to collect the patient's acceleration and gyroscope signals at a frequency of 80 Hz for symptom testing. The symptom condition test is designed in the following states: arm swing, balance, walking, postural normal tremor, and resting tremor. For each test set, each symptom is divided into five levels from normal to severe. The treating doctor evaluated the

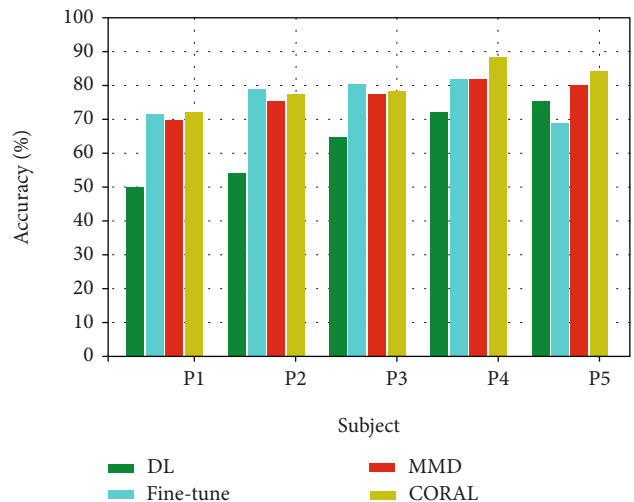


FIGURE 6: Extending on arm swing test.

collected symptoms. We collected sensor data from 150 patients aged 18 to 85 years. In the following evaluation process, the test data of arm swing and postural normal tremor are evaluated, and two categories with quite sufficient data are chosen as references.

Evaluate the classification accuracy of the collected dataset. The data is gathered from three hospitals, 80% of each hospital is randomly chosen as the public dataset, the remaining 20% are randomly selected as 5 users, and  $K = 5$ .

Table 3 shows the comparison results. In addition, the proposed method gives the result of the ideal scheme. Due to all the data is preserved in one location, it is easier to view the upper bound of the model performance. From the outcomes, it will be seen that FT-IoMT Health has achieved the best classification accuracy, which obviously exceeds the best comparison means, and has narrowed the gap with the perfect case. It is fully proved that using federated

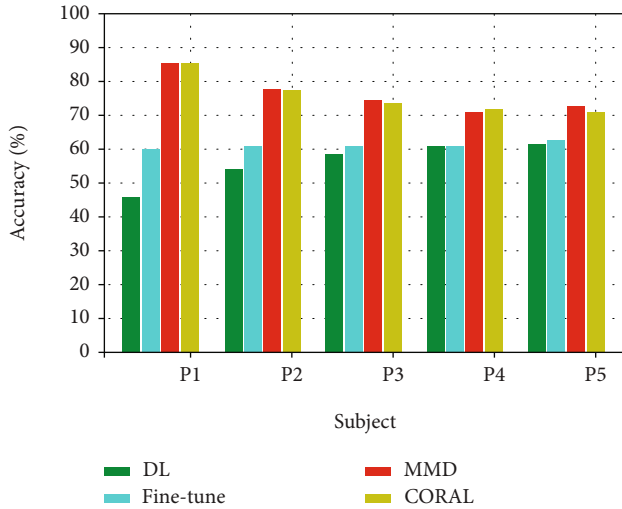


FIGURE 7: Extending on normal posture tremor test.

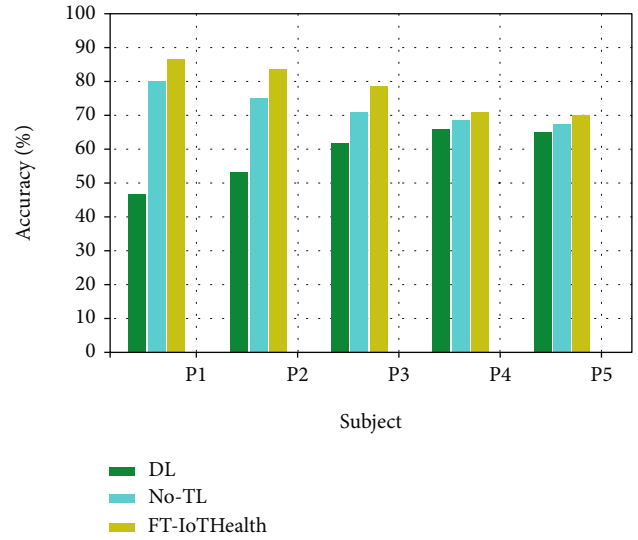


FIGURE 9: Ablation analysis on normal posture tremor test.

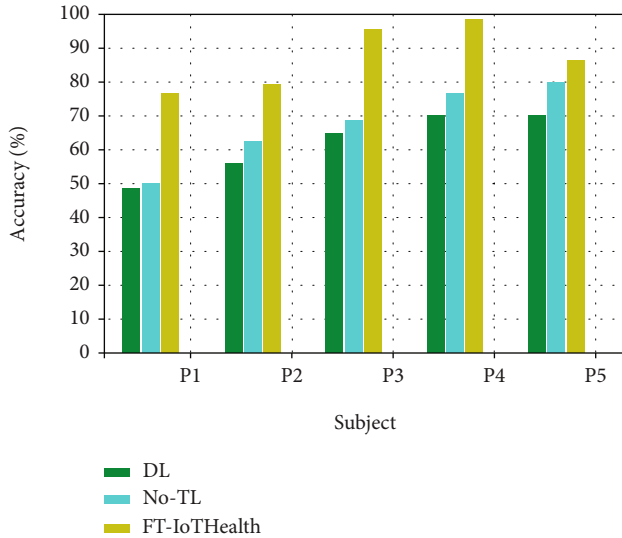


FIGURE 8: Ablation analysis on arm swing test.

transfer learning technology, the FT-IoMT Health mechanism can achieve effective symptom classification in practical applications.

Consistent with the experimental setup mentioned above, Figures 6 and 7 show the scalability results of the arm swing and normal posture tremor test data, respectively. It can be shown that in most cases, FT-IoMT Health can achieve satisfactory results using fine-tuning or MMD, which also shows that FT-IoMT Health and other transfer learning algorithms are as effective and scalable in practical applications.

For the performance of the given model, we further study ablation analysis (also called sensitivity analysis) to evaluate the two components of joint learning and transfer learning. We apply No-TL to mean an average model without personalized transfer learning. The outcomes are

indicated in Figures 8 and 9. It can be seen from the results that both federated learning and transfer learning have made significant achievements to the performance of FT-IoMT Health. Comparing No-TL with DL, it can be seen that the model with federated conditions will increase the classification accuracy, which shows the effectiveness of federated learning. By further comparing No-TL with our federated transfer learning mechanism FT-IoMT Health, it can be seen that integrated with transfer learning technology, each user model will attain better performance in classification. The reasons are as follows. (1) Using federated learning, the server can indirectly aggregate more communication from multiple users to obtain a more general network cloud model. (2) Using transfer learning, users will obtain a more personalized user data model based on the cyber cloud model.

## 6. Conclusion

In the paper, we propose FT-IoMT Health, which is a federated transfer learning mechanism based on IoMT healthcare. FT-IoMT Health aggregates data from different network users without affecting privacy and security and realizes the user's relatively personalized model learning through transfer learning. The key is feature-based transfer learning technology to overcome various detection methods that lead to variants in network performance. Experiments and applications have verified the validity and accuracy of the mechanism compared to other benchmark methods. Meanwhile, the experimental outcomes also indicate that the transfer learning method enhances the performance of detecting unseen new network malicious data compared with the baseline and proves that FT-IoMT Health can support the detection of new data in different feature spaces. In the future, we will plan to expand FT-IoMT Health through incremental learning to achieve a more personalized, flexible, and efficient healthcare system.

## Data Availability

All the data is available in the paper.

## Conflicts of Interest

The authors declare that they have no conflicts of interest.

## Acknowledgments

The authors gratefully acknowledge the support from the Shandong National Science Foundation of China (Grant No. ZR202103040468).

## References

- [1] L. Lyu, C. Chen, J. Yan, F. Lin, and X. Guan, "State estimation oriented wireless transmission for ubiquitous monitoring in industrial cyberphysical systems," *IEEE Transactions on Emerging Topics in Computing*, vol. 7, no. 99, pp. 12–23, 2016.
- [2] S. Kurt, H. U. Yildiz, M. Yigit, B. Tavli, and V. C. Gungor, "Packet size optimization in wireless sensor networks for smart grid applications," *IEEE Transactions on Industrial Electronics*, vol. 64, no. 3, pp. 2392–2401, 2017.
- [3] Q. Chi, H. Yan, C. Zhang, Z. Pang, and L. D. Xu, "A reconfigurable smart sensor interface for industrial WSN in IoT environment," *IEEE Transactions on Industrial Informatics*, vol. 10, no. 2, pp. 1417–1425, 2014.
- [4] R. Zhu, X. Zhang, X. Liu, W. Shu, T. Mao, and B. Jalaian, "ERDT: energy-efficient reliable decision transmission for intelligent cooperative spectrum sensing in industrial iot," *IEEE Access*, vol. 3, pp. 2366–2378, 2015.
- [5] B. Holfeld, D. Wieruch, T. Wirth et al., "Wireless communication for factory automation: an opportunity for LTE and 5g systems," *IEEE Communications Magazine*, vol. 54, no. 6, pp. 36–43, 2016.
- [6] H. Shariatmadari, R. Ratasuk, S. Irajii et al., "Machine-type communications: current status and future perspectives toward 5g systems," *IEEE Communications Magazine*, vol. 53, no. 9, pp. 10–17, 2015.
- [7] A. J. Ward, G. Pirkel, P. Hevesi, and P. Lukowicz, *Towards recognising collaborative activities using multiple on-body sensors*, UbiComp Adjunct, 2016.
- [8] D. Bekerman, B. Shapira, L. Rokach, and A. Bar, "Unknown malware detection using network traffic classification," in *2015 IEEE Conference on Communications and Network Security (CNS)*, pp. 134–142, Florence, Italy, 2015.
- [9] K. Bartos, M. Sofka, and V. Franc, "Optimized invariant representation of network traffic for detecting unseen malware variants," in *25th {USENIX} Security Symposium ({USENIX} Security 16)*, pp. 807–822, USA: USENIX Association, 2016.
- [10] N. Inkster, *China's Cyber Power*, Routledge, 2016.
- [11] M. Goddard, "The eu general data protection regulation (gdpr): European regulation that has a global impact," *International Journal of Market Research*, vol. 59, no. 6, pp. 703–705, 2017.
- [12] Q. Yang, Y. Liu, T. Chen, and Y. Tong, "Federated machine learning," *ACM Transactions on Intelligent Systems and Technology*, vol. 10, no. 2, pp. 1–19, 2019.
- [13] R. L. Rivest, L. Adleman, and M. L. Dertouzos, "On data banks and privacy homomorphisms," in *Foundations of Secure Computation*, pp. 169–179, Academia Press, 1978.
- [14] S. J. Pan and Q. Yang, "A survey on transfer learning," *IEEE Transactions on Knowledge and Data Engineering*, vol. 22, no. 10, pp. 1345–1359, 2010.
- [15] K. D. Feuz and D. J. Cook, "Transfer learning across feature-rich heterogeneous feature spaces via feature-space remapping (fsr)," *Acm Transactions on Intelligent Systems & Technology*, vol. 6, no. 1, pp. 1–27, 2015.
- [16] R. Perdisci, W. Lee, and N. Feamster, "Behavioral clustering of httpbased malware and signature generation using malicious network traces," in *ser. NSDI'10*, p. 26, USENIX Association, USA, 2010.
- [17] A. Valdes and D. Zamboni, *Recent Advances in Intrusion Detection*, Springer, Berlin Heidelberg, 2006.
- [18] J. Konen, H. B. McMahan, D. Ramage, and P. Richtarik, "Federated optimization: distributed machine learning for on-device intelligence," 2016, <http://arxiv.org/abs/1610.02527>.
- [19] P. Huang, G. Wang, and S. Qin, "Boosting for transfer learning from multiple data sources," *Pattern Recognition Letters*, vol. 33, no. 5, pp. 568–579, 2012.
- [20] X. Qin, Y. Chen, J. Wang, and C. Yu, "Cross-dataset activity recognition via adaptive spatial-temporal transfer learning," *Proceedings of the ACM on Interactive, Mobile, Wearable and Ubiquitous Technologies*, vol. 3, no. 4, pp. 1–25, 2019.
- [21] H. B. McMahan, E. Moore, D. Ramage, S. Hampson, and B. Arcas, *Communication-efficient learning of deep networks from decentralized data*, arXiv e-prints, 2016.
- [22] X. Shi, Q. Liu, W. Fan, P. S. Yu, and R. Zhu, "Transfer learning on heterogenous feature spaces via spectral transformation," in *Proceeding of the IEEE International Conference on Data Mining*, pp. 1049–1054, Sydney, NSW, Australia, 2010.
- [23] B. Sun, J. Feng, and K. Saenko, "Return of frustratingly easy domain adaptation," 2015, <http://arxiv.org/abs/1511.05547>.
- [24] Y. Chen, X. Yang, B. Chen, C. Miao, and H. Yu, "Pdassit: objective and quantified symptom assessment of Parkinson's disease via smartphone," in *2017 IEEE International Conference on Bioinformatics and Biomedicine (BIBM)*, Kansas City, MO, USA, 2017.